**UNIVERSIDAD AUTÓNOMA DE MADRID**
**DOCTORADO EN BIOCIENCIAS MOLECULARES**


# Orchestration of the neural stem cell fate by NRF2 and TAZ

**Natalia Robledinos Antón**
**Madrid, 2019**

**UNIVERSIDAD AUTÓNOMA DE MADRID**
**DEPARTAMENTO DE BIOQUÍMICA**
**FACULTAD DE MEDICINA**

# Orchestration of the neural stem cell fate by NRF2 and TAZ

Memoria de la Tesis para optar al grado de Doctor
Presentada por la graduada en Biotecnología
**NATALIA ROBLEDINOS ANTÓN**

Director de tesis:
**Prof. ANTONIO CUADRADO PASTOR**
Catedrático de Bioquímica y Biología Molecular

Departamento de Bioquímica, Facultad de Medicina
Instituto de Investigaciones Biomédicas "Albertos Sols"
UAM-CSIC

Este trabajo ha sido realizado en el Departamento de Bioquímica de la Facultad de Medicina e Instituto de Investigaciones Biomédicas “Alberto Sols” (UAM-CSIC) gracias a un contrato predoctoral para Formación de Profesorado Universitario concedida por el Ministerio de Educación, Cultura y Deporte (FPU14/01073) y con subvención del Ministerio de Ciencia e Innovación (SAF2013-43271-R y SAF2016-76520-R) así como financiación internacional (Organización: Centres of Excellence in Neurodegeneration (JPND); Call: 2013 COEN initiative on international research “pathfinder” projects; European Cooperation in Science and Technology (COST) Action BM1203 (EU-ROS)).

*"Life is not easy for any of us. But what of that? We must have perseverance and above all confidence in ourselves. We must believe that we are gifted for something and that this thing must be attained".*

*"I was taught that the way of progress was neither swift nor easy".*

Marie Curie

*"Above all, don't fear difficult moments. The best comes from them".*

Rita Levi-Montalcini

*"Y si el sueño finge muros*
*en la llanura del tiempo,*
*el tiempo le hace creer*
*que nace en aquel momento".*

Federico García Lorca.

# ACKNOWLEDGEMENTS

La consecución de esta tesis ha sido resultado del esfuerzo conjunto durante años de la gente que me ha rodeado, me ha enseñado y, sobre todo, ha tenido paciencia conmigo.

Desde que comencé a trabajar en ciencia, hace ya casi diez años, he trabajado en diversos laboratorios, con distintos jefes y compañeros que me han ido enseñando no sólo cómo enfrentar el reto científico, sino también la vida.

En primer lugar, dar las gracias a mi director de tesis, el Profesor Antonio Cuadrado Pastor, por darme la oportunidad de llevar a cabo este trabajo y depositar en mí la confianza necesaria para la realización de este proyecto. Durante estos años has sido un fuerte apoyo, me has permitido desarrollarme como científica y como persona. Me has facilitado el acceso a todos los medios posibles para llevar a cabo el proyecto y, lo más importante, has sabido valorar mi esfuerzo. Muchas gracias por tu ayuda, tanto a nivel científico como personal.

En segundo lugar, quiero dar las gracias a mis compañeros de laboratorio. En Analand, a la Dra. Ana Rojo, fuente de sabiduría y seguridad, todo un ejemplo como científica y como persona, en definitiva, todo un referente. A Martini, que durante este tiempo ha sabido comprender y compartir el sufrimiento predoctoral, además de ser una gran ayuda en todo momento y más en el mundo del ChIP: al fin en septiembre nos vamos juntas de congreso. Al otro lado de la poyata, con su risa siempre, dar las gracias a Ángel, que ha sabido aguantar mis locuras. A la nueva incorporación, Raquel, que ha traído una dosis extra de cariño al laboratorio: todo va a salir bien. A María, que se ha atrevido a unirse a esta locura. A Ruth, esperando que le esté yendo bien. Y en Mariland, dar las gracias a Diego, en el que he tenido un apoyo para que mis bromas no cayesen en saco roto.

Dar las gracias a Maribel, a mi Mari, que se ha convertido en una de las personas más importantes de mi vida. Gracias, no sólo por la ayuda científica, sino por la humana. Por ayudarme a entender los sentimientos de los demás y los míos propios. Por no haberme dejado sola. La mitad de esta tesis no hubiera sido posible sin ti, y una parte de lo que soy como persona tampoco hubiera sido posible.

Agradecer también a la Dra. Isabel Lastres el tiempo compartido y, aunque ya no estemos en el mismo laboratorio, sigues teniendo un huequito en él.

Agradecer a Lola Morales toda la confianza depositada en mí para poder usar a horas intempestivas el microscopio confocal. Sin esa ayuda esta tesis no hubiera sido posible. Dar las gracias al resto de servicios de la UAM y del IIB, que con su trabajo han facilitado el logro de los objetivos de este trabajo.

Asimismo, agradecer a los integrantes del IIB y del Departamento de Bioquímica su soporte, en especial a mi tutor, el Prof. Francisco Portillo Pérez.

Durante esta tesis he tenido la suerte de conocer a científicos de gran valía. Entre ellos, quisiera destacar a la Dra. Elisabete Ferreiro: gracias por toda tu ayuda prestada para el cultivo de neuroesferas y por enseñarme qué es lo realmente importante en esta vida. Te debo una visita a Coimbra.

No he de olvidar de dónde vengo y dónde comencé a formarme como científica. Muchas gracias al Prof. José María Luengo, por abrirme las puertas de mi primer laboratorio. A Irena, por ese verano de

aprendizaje. Y, sobre todo, al laboratorio de la Prof. Carmen Marín y Dra. Margot Marqués, por iniciarme en el mundo de la investigación en cáncer y mostrarme por primera vez la belleza de la neurogénesis. A Sandra, Marta, Laura González-Cano, Rosalía, Sara y Laura Gallego, por ayudarme en esas primeras fases de la vida científica y enseñarme que *la paciencia es la madre de la ciencia*. Por mucho que pasen los años, sigo siendo la Yogu.

Durante el desarrollo de esta tesis he tenido la gran oportunidad de trabajar en el laboratorio del Prof. Karl-Heinz Krause. Muchas gracias por toda la ayuda y el gran aprendizaje científico. Gracias al Dr. Vincent Jaquet y al resto de mis compañeros de Ginebra, por aceptarme con toda naturalidad y por las tardes de voleibol y barbacoa. Ese lago vale toda la plata a la que se parece.

A Pancho y Pepi, sus hijas Christelle y Jess y sus familias, por abrirme las puertas de su casa y hacerme sentir una más. Hicisteis que estar lejos de casa no fuese tan duro.

No quiero dejar atrás a mis amigas. A las Pelicas, las de toda la vida, por el apoyo durante estos años. En especial a Moni y Cris, mis compañeras en Madrid, por todo lo que hemos compartido y lo que nos queda aún por delante. A Carmen, que se ha unido a esta aventura en la capital. Dar las gracias a los Pulpos: nos vemos en el siguiente Sonorama. No cabe en estas páginas todo lo que os debo y he aprendido de vosotras.

Quisiera dar las gracias también a todos aquellos que, aunque ahora ya no estén en mi vida, han formado parte de ella durante esta tesis doctoral y me han apoyado en el trayecto.

Nada de esto hubiera sido posible sin la ayuda de mi familia. Mis padres, por haberme dado la oportunidad que ellos no pudieron tener y me enseñaron que el éxito depende de la inteligencia, pero sobre todo de la constancia en el trabajo. A mis hermanos, Edu, Antonio y Alba, que han sabido perdonar a esta hermana mayor desaparecida y aguantarme cuando ni yo misma me soportaba.

He tenido la suerte de haberme criado con mujeres muy fuertes. Mi abuela, que me ha enseñado lo que es el amor de verdad, lo que significa seguirse emocionando por una sonrisa en medio del Alzhéimer y seguir hacia delante en mitad de la adversidad. Eres mi referente. A mis tías, por su fortaleza haciendo frente al cáncer. Es por todas vosotras por las que inicié este camino en la investigación. Si algo he aprendido durante esta tesis es que el ser humano es superviviente, y ante los peores momentos seguimos fortaleciéndonos.

Dar las gracias a todas aquellas mujeres que durante años han ido rompiendo los muros del mundo de la ciencia y con su lucha han permitido que más mujeres accedamos a él.

Dar las gracias a Borja. Muchas gracias por este tiempo, por cuidar de nuestro hogar y seguir ahí. Gracias a tu familia, por haberme hecho un hueco entre ellos y hacerme formar parte de ella.

Por último, quiero pedir perdón por los errores que he cometido en este tiempo y por los momentos en lo que prácticamente he desaparecido. Y dar las gracias a todos los que supieron esperar a que volviese. Soy afortunada por poder contar con todos vosotros.

# SUMMARY/RESUMEN

Neurogenesis is a multiple step process that must be tightly regulated or otherwise results in pathological events. Therefore, a deep characterization of the molecular mechanisms that control the biology of neural stem/progenitor cells (NSPCs) will provide a better understanding of the role of neurogenic niches and new therapeutic strategies for neurodegenerative diseases and brain tumours.

In this thesis we have analyzed the regulation of NSCs fate by the transcription factor Nuclear factor (erythroid-derived 2)-like 2 (NRF2), which is considered a master regulator of cellular homeostasis, and the Transcriptional co-activator with PDZ-binding motif (TAZ), a major effector of the Hippo pathway. NRF2 controls the expression of a wide battery of cytoprotective genes that have a tremendous impact on physiological responses such as inflammation, senescence or metabolism. However, its relevance in neurogenesis is just starting to be unveiled. On the other hand, TAZ is a major effector of the Hippo pathway, which plays a key role in tissue homeostasis and organ size control by regulating tissue-specific stem cells. However, the implication of TAZ in neurogenesis has not been analyzed.

In this study, we have identified NRF2 as a regulator of hippocampal NSCs self-renewal and differentiation. We show that genetic manipulation of NRF2 results in the modulation of NSPCs differentiation and proliferation capacity. To assess the functional relevance of NRF2 in neurogenesis under pathological conditions, we analyzed the impact of NRF2 deficiency in neurogenesis of the subgranular zone (SGZ) of the hippocampus in a mouse model of Alzheimer´s Disease (AD). We found that NRF2 deficiency results in an accelerated loss of NSCs, loss of synaptic plasticity measured as long term potentiation (LTP) and impaired the execution of cognitive tasks.

At the molecular level, we have identified NRF2 enhancer sequences, termed Antioxidant Response Elements (AREs), in the promoter region of the TAZ coding gene. Consequently, we show that genetic and pharmacological manipulation of NRF2 results in the modulation of TAZ gene expression in NSPCs. These findings open a new window to understand the molecular mechanisms underlying NRF2 function in stemness.

We have also established a novel role of TAZ as repressor of neuronal differentiation, based on the transcriptional repression of SOX2 and the basic helix-loop-helix (bHLH) factors ASCL1, NEUROG2 and NEUROD1. Data mining of The Cancer Genome Atlas showed a negative correlation between TAZ and the expression of these proneurogenic factors in lower grade gliomas and glioblastomas. We found that TAZ favours glioblastoma CSCs tumorigenic capacity and that genetic modulation of TAZ in these cells inversely correlated with proneurogenic genes expression. Due to the relevance of these proneurogenic factors in the ablation of glioblastoma cancer stem cells (CSCs), this novel TAZ/proneurogenic factors axis may have important implications in the development of this type of brain tumours.

The characterization of molecular mechanism governing NSPCs fate provides new insights to harness these cells for brain repair. Overall, this thesis describes a novel role of NRF2 and TAZ in the control of neural stem cell fate, suggesting a new strategy to combat brain pathology.

La neurogénesis es un proceso con varias etapas que debe estar estrictamente regulado, en caso contrario, conllevaría una serie de procesos patológicos. De esta manera, una caracterización profunda de los mecanismos moleculares que controlan la biología de las células troncales/progenitores neurales (NSPCs) nos permitirá conocer mejor el papel de los nichos neurogénicos y las implicaciones en el desarrollo de nuevas terapias en enfermedades neurodegenerativas y tumores cerebrales.

En esta tesis, hemos estudiado el papel del *Nuclear factor (erythroid-derived 2)-like 2* (NRF2), considerado el maestro regulador de la homeostasis celular, y del *Transcriptional co-activator with PDZ-binding motif* (TAZ), uno de los mayores efectores de la vía Hippo, en el destino de las NSPCs. NRF2 controla la expresión de genes citoprotectores con un enorme impacto en respuestas fisiológicas como inflamación, senescencia o metabolismo. Sin embargo, su importancia en neurogénesis está empezando a ser estudiada. Por su parte, TAZ es uno de los mayores efectores de la vía Hippo, con un papel fundamental en la homeostasis tisular y en el control del crecimiento de los órganos, mediante la regulación de las células mesenquimales específicas de tejido. Sin embargo, ningún estudio previo ha abordado la importancia de TAZ en neurogénesis.

En este estudio, identificamos a NRF2 como un regulador de la capacidad de auto-renovación y diferenciación de las NSPCs hipocampales. Mostramos cómo la manipulación genética de NRF2 conduce a una modulación estas capacidades en las NSPCs. Para abordar la relevancia funcional del papel que NRF2 juega en neurogénesis en condiciones patológicas, analizamos el impacto de NRF2 en la neurogénesis hipocampal del giro dentado en modelos murinos de la enfermedad de Alzhéimer. La ausencia de NRF2 conlleva una pérdida acelerada de NSPCs y a un deterioro de la plasticidad sináptica y las capacidades cognitivas. A nivel molecular, hemos identificado elementos de respuesta a NRF2, llamados elementos de respuesta antioxidante (AREs), en la región promotora del gen que codifica a TAZ. Además, la manipulación genética y farmacológica de NRF2 modula la expresión génica de TAZ en NSPCs. Estas observaciones abren una nueva vía para entender los mecanismos moleculares que se encuentran tras la función de NRF2 en el control de las células troncales. También hemos establecido un nuevo papel del TAZ como represor de la diferenciación neuronal, basada en la represión transcripcional de SOX2 y los factores hélice-bucle-hélice básica (bHLH) ASCL1, NEUROG2 y NEUROD1. Los datos de *The Cancer Genome Atlas*, muestran una correlación negativa entre TAZ y la expresión de estos factores proneurogénicos en gliomas de bajo grado y glioblastomas. Encontramos que TAZ favorece la capacidad tumorigénica en las células mesenquimales de cáncer (CSCs) en glioblastoma y que la modulación genética de TAZ correlaciona inversamente con la expresión de los factores proneurogénicos. Debido a la relevancia de estos factores proneurogénicos en la supresión de las CSCs, este nuevo eje TAZ/factores proneurogénicos puede tener importantes implicaciones en el desarrollo de estos tumores cerebrales. La caracterización de los mecanismos moleculares que gobiernan el destino de las NSPCs ofrece nuevas posibilidades para sacar partido a estas células en la reparación cerebral. De manera global, esta tesis describe un nuevo papel de NRF2 y TAZ en el control del destino de las NSPCs, ofreciendo una nueva estrategia para combatir la patología cerebral.

# TABLE OF CONTENTS

# LIST OF FIGURES

# LIST OF TABLES

# ABBREVIATIONS

| | |
|---|---|
| AcH3 | Acetylated lysine 9 in histone 3. |
| ACTB | Actin beta. |
| AD | Alzheimer´s disease. |
| Akt | Protein kinase B. |
| APC | Adenomatous Polyposis Coli. |
| ApoE4 | Apolipoprotein E4. |
| APP | Amyloid precursor protein. |
| ARE | Antioxidant response element. |
| ASCL1 | Achaete-scute like 1. |
| *ASCL1* | Human gene encoding ASCL1. |
| AT | $APP^{V717I}/TAU^{P301L}$. |
| Aβ | Amyloid beta. |
| BACH1 | Bric-a-brac homodimerization domain and cap ‘n’ collar homolog 1. |
| BDNF | Brain-derived neurotrophic factor. |
| bFGF | Basic fibroblast growth factor. |
| bHLH | Basic helix-loop-helix. |
| BIRC5 | Baculoviral IAP Repeat Containing 5, also known as Survivin. |
| *BIRC5* | Human gene encoding BIRC5. |
| BLBP | Brain lipid-binding protein. |
| BMP | Bone morphogenetic protein. |
| β-TrCP | β-Transducing repeat-containing protein. |
| BrdU | 5-bromo-2'-deoxyuridine. |
| Brg1 | Brahma-related gene-1. |
| BSA | Bovine serum albumin. |
| BTB | Bric-a-brac homodimerization domain. |
| bZIP | Basic-leucine-zipper. |
| CA1 | Area 1 of the *Cornu Ammonis*. |
| CA3 | Area 3 of the *Cornu Ammonis.* |
| CHD4 | Chromodomain-helicase-DNA-binding protein 4. |
| ChIP | Chromatin immunoprecipitation assay. |
| CK1 | Casein kinase 1. |
| CNC | Cap ‘n’ collar. |
| CNS | Central nervous system. |
| CSC | Cancer stem cell. |
| CSF | Cerebral spinal fluid. |
| CT | Control. |
| CTGF | Connective tissue growth factor. |
| *CTGF* | Human gene encoding CTGF. |
| *Ctgf* | Murine gene encoding CTGF. |
| CUL3 | Cullin3. |
| CYR61 | Cysteine-rich, angiogenic inducer 61. |

| | |
|---|---|
| *CYR61* | Human gene encoding CYR61. |
| DAB | 3´-3´-diaminobenzidine tetrahydrochloride. |
| DAPI | 4',6-diamidino-2-phenylindole. |
| DCX | Doublecortin. |
| DDIT4 | DNA damage inducible transcript 4. |
| DG | Dentate gyrus. |
| Dll1 | Delta-like protein 1. |
| DMEM | Dulbecco's modified Eagle medium. |
| DNA | Deoxyribonucleic acid. |
| EC | Entorhinal cortex. |
| ECL | Enhanced chemiluminiscence. |
| EDTA | Ethylene diamine tetraacetic acid. |
| EdU | 5-ethynyl-2'-deoxyuridine. |
| EGF | Epidermal growth factor. |
| EGTA | Ethylene glycol tetraacetic acid. |
| EMT | Epithelial–mesenchymal transition. |
| ENCODE | Encyclopedia of DNA elements at the University of California Santa Cruz. |
| ER | Endoplasmic reticulum. |
| ESC | Embryonic stem cell. |
| FBS | Fetal bovine serum. |
| fEPSP | Field excitatory post-synaptic potential. |
| FGF-2 | Fibroblast growth factor-2. |
| GABA | Gamma-Aminobutyric acid. |
| GAPDH | Glyceraldehyde 3-phosphate dehydrogenase. |
| GB | Glioblastoma. |
| GBM | Glioblastoma multiforme. |
| GBMLGG | Lower grade glioma and glioblastoma. |
| GC | Granular cell. |
| GCL | Granular cell layer. |
| GCLC | Glutamate-cysteine ligase catalytic subunit. |
| GCLM | Glutamate-cysteine ligase modifier subunit. |
| GFAP | Glial-fibrillary acidic protein. |
| GFP | Green fluorescent protein. |
| GLAST | Astrocytic glutamate aspartate transporter. |
| GLI | Glioma-associated oncogene homolog (Zinc Finger Protein). |
| GSH | Glutathione. |
| GSK-3β | Glycogen-synthetase-kinase-3 beta. |
| H3 | Histone 3. |
| H3K27ac | Acetylation at lysine 27 of histone 3. |
| HBSS | Hank's balanced salt solution. |
| hEGF | Human epidermal growth factor. |

| | |
|---|---|
| HEPES | N-2-hydroxyethylpiperazine-N'-2-ethanesulfonic acid. |
| Hes | Hairy enhancer of split. |
| hFGF | Human fibroblast growth factor. |
| HMG | High-mobility group. |
| *HMOX1* | Human gene encoding HO1. |
| HO1 | Heme oxygenase 1. |
| HRD1 | Inositol requiring enzyme/E3 ubiquitin ligase synoviolin. |
| HRP | Horseradish peroxidase. |
| ICC | Immunocytochemistry. |
| IF | Immunofluorescence. |
| IGF-1 | Insulin-like growth factor-1. |
| IHC-Fr | Immunohistochemistry on frozen slices. |
| IHC-p | Immunohistochemistry on paraffin slices. |
| IPC | Intermediate progenitor cell. |
| IRE1 | Inositol requiring enzyme. |
| KDM3A | Lysine demethylase 3A. |
| KEAP1 | Kelch-like ECH-associated protein 1. |
| LATS1/2 | Large tumour suppressor kinase 1/2. |
| LB | Luria-Bertani medium. |
| LRP5/6 | Low-density lipoprotein receptor related protein 5/6. |
| LTP | Long-term potentiation. |
| MAF | Small muscle aponeurosis fibromatosis. |
| MAP2 | Microtubule associated protein- 2. |
| MOB1 | Mps one binder 1. |
| MPP | Medial perforant path. |
| MPTP | 1-methyl-4-phenyl-1,2,3,6-tetrahydropyridine. |
| MST1/2 | Serine/threonine kinases mammalian Ste20-like kinases. |
| MWM | Morris water maze. |
| NADP | Nicotinamide adenine dinucleotide phosphate. |
| NDP52 | Nuclear dot protein 52 kDa. |
| Neh | NRF2 − ECH homology. |
| Nestin | Neuroectodermal stem cell marker. |
| NeuN | Neuron nuclear protein. |
| NEUROD1 | Neuronal differentiation 1. |
| *NEUROD1* | Human gene encoding NEUROD1. |
| NEUROG2 | Neurogenin 2. |
| *NEUROG2* | Human gene encoding NEUROG2. |
| NF2 | Neurofibromin 2. |
| *NFE2L2* | Human gene encoding NRF2. |
| *Nfe2l2* | Murine gene encoding NRF2. |
| NICD | Notch intracellular domain. |

| | |
|---|---|
| NPC | Neural progenitor cell. |
| NQO1 | NAD(P)H quinone dehydrogenase 1. |
| *NQO1* | Human gene encoding NQO1. |
| *Nqo1* | Murine gene encoding NQO1. |
| NRF2 | Nuclear factor (erythroid-derived 2)-like 2. |
| NSC | Neural stem cell. |
| NSPC | Neural stem/progenitor cell. |
| NuRD | Nucleosome remodelling and histone deacetylase. |
| OB | Olfactory bulb. |
| PAX3 | Paired box protein 3. |
| PAX6 | Paired box protein 6. |
| PBS | Phosphate buffered saline. |
| PCR | Polymerase chain reaction. |
| PCR2 | Polycomb repressive complex 2. |
| PDGF-β | Platelet-derived growth factor β. |
| PFA | Paraformaldehyde. |
| PI3K | Phosphoinositide 3-kinase. |
| PMSF | Phenylmethylsulfonyl fluoride. |
| PROX1 | Prospero homeobox protein 1. |
| PS | Presenilin. |
| PSA-NCAM | Polysialylated neural cell adhesion molecule. |
| PSSM | Position-specific scoring matrix. |
| QNP | Quiescent neural progenitor. |
| qRT-PCR | Quantitative real time polymerase chain reaction. |
| RA | Retinoic acid. |
| RBPJ | Recombining binding protein suppressor of hairless. |
| RBX1 | RING-box protein 1. |
| RG | Radial glia. |
| RGL | Radial glial-like cell. |
| RMS | Rostral migratory stream. |
| RMST | Rhabdomyosarcoma 2-associated transcript. |
| RNA | Ribonucleic acid. |
| RNA Pol II | RNA polymerase II. |
| ROS | Reactive oxygen species. |
| RUNX2 | Runt-related transcription factor 2. |
| RXR | Retinoid X receptor. |
| S100β | S100 calcium-binding protein B. |
| SAV1 | Salvador family WW domain containing protein 1. |
| SCF | S-phase kinase-associated protein 1–CUL1–F box containing complex. |
| S.D. | Standard deviation. |
| SDS | Sodium dodecyl sulfate. |

| | |
|---|---|
| SDS-PAGE | Sodium dodecyl sulfate polyacrylamide gel electrophoresis. |
| SEM | Standard error of the mean. |
| SFN | R,S-sulforaphane. |
| SGZ | Subgranular zone. |
| Shh | Sonic hedgehog. |
| SKP1 | S-phase kinase-associated protein. |
| SMAD2/3/4 | Mothers against decapentaplegic homolog 2, 3 and 4. |
| SOD | Superoxide dismutase. |
| SOX2 | Sex determining region Y (SRY)-Box 2. |
| *SOX2* | Human gene encoding SOX2. |
| SV40 | Simian virus 40. |
| SVZ | Subventricular zone. |
| TAE | Tris base, acetic acid and EDTA buffer. |
| TAP | Transit-amplifying precursor. |
| TAU | Neuronal microtubule associated protein. |
| TAZ | Transcriptional co-activator with PDZ-binding motif. |
| TBP | TATA box binding protein. |
| TBS | Tris buffered saline. |
| TBX5 | T-box transcription factor 5. |
| TCF/LEF | T-cell factor/lymphoid enhancer-binding factor. |
| TCGA | The cancer genome atlas. |
| TE | Tris-EDTA buffer. |
| TEAD | Transcriptional enhancer factor TEF-1. |
| TEMED | N N N′N′-Tetramethylethylenediamine. |
| TF | Transcription factor. |
| TGF-β | Transforming growth factor β. |
| TIR | TAZ interacting region. |
| Trb2 | T-box brain protein 2. |
| TTBS | Tris buffered saline with Tween 20. |
| TUBB3 | β-III-tubulin. |
| UCSC | University of California, Santa Cruz. |
| VEGF | Vascular endothelial growth factor. |
| V-SVZ | Ventricular-subventricular zone. |
| VZ | Ventricular zone. |
| WB | Western blot. |
| Wnt | *Wingless* and *integrated* or *int-1*. |
| WWTR1 | WW-domain containing transcriptional regulator 1. |
| *WWTR1* | Human gene encoding TAZ. |
| *Wwtr1* | Murine gene encoding TAZ. |
| YAP | Yes-associated protein. |

# INTRODUCTION

## 1. Neurogenesis.

Neurogenesis is the formation of newborn neurons derived from neural stem cells (NSCs). NSCs are multipotent cells with self-renewal capacity which give rise to several cell types in the central nervous system (CNS): astrocytes, oligodendrocytes and neurons (Kriegstein and Alvarez-Buylla, 2009). Although initially it was postulated that the CNS lacks regenerative capacity in adults, during the last decades, this idea has been questioned by several studies. In the 60s, it was probed that the formation of newborn neurons occurs in distinct region of the brain as the hippocampus, olfactory bulb (OB) and cortex in mammals (Altman, 1962; Altman J Fau - Das and Das, 1965), and songbirds (Paton and Nottebohm, 1984; Burd and Nottebohm, 1985). During the 90s, NSCs from adult mammalian brains were isolated, propagated *in vitro* and differentiated into neurons and glia (Reynolds and Weiss, 1992; Richards et al., 1992; Gage et al., 1995).

## 2. Neurogenic niches.

In the adult mammalian brain, NSCs are restricted to specialized brain regions known as neurogenic niches. The main neurogenic niches are the subventricular zone (SVZ) of the lateral walls of the I and II ventricles (Alvarez-Buylla and Garcia-Verdugo, 2002) and the subgranular zone (SGZ) of the dentate gyrus (DG) of the hippocampus (Doetsch et al., 1997). The presence of NSCs in other regions of the adult brain, such the neocortex and the hypothalamus, is still under controversy (Ernst et al., 2014; Ernst and Frisen, 2015; Magnusson and Frisen, 2016; Gould, 2007) (Fig. 1).

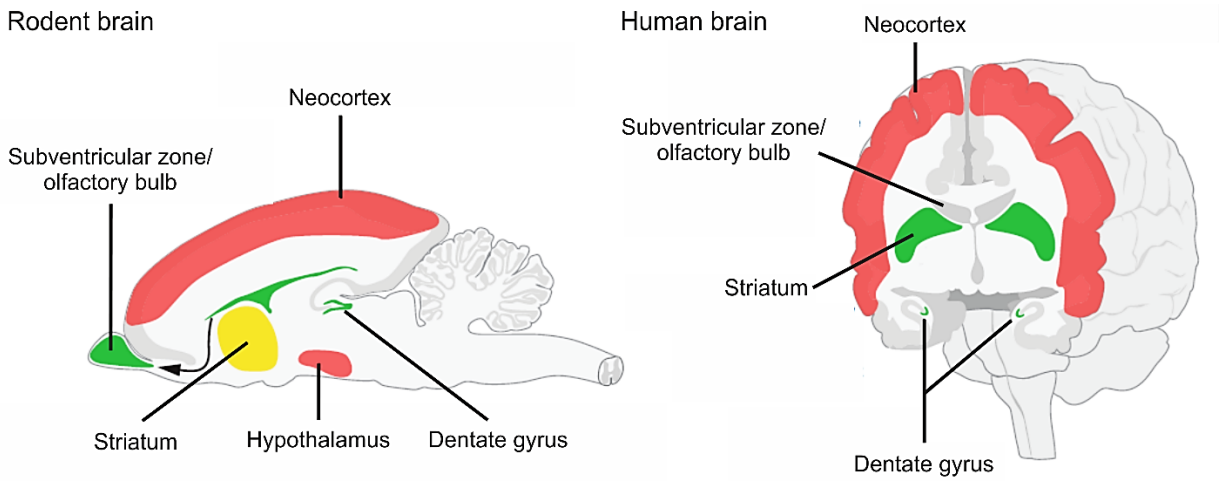


**Figure 1. Neurogenic regions in the adult murine and human brain.** Green areas correspond to the best-characterized neurogenic niches. Yellow areas indicate regions that respond to injury. Red areas indicate regions with weak evidence of neurogenic activity (modified from Magnusson and Frisen, 2016).

## 2.1. Subventricular zone (SVZ).

In the adult mouse brain, the largest germinal niche is the subventricular zone (SVZ), also known as ventricular-subventricular zone (V-SVZ). This neurogenic niche comprises several cell types. First, the NSCs named B1 cells are largely quiescent with astrocytic properties, expressing glial-fibrillary acidic protein (GFAP), astrocytic glutamate aspartate transporter (GLAST) and brain lipid-binding protein (BLBP) and possess an end-feet on blood vessels (Hartfuss et al., 2001; Malatesta et al., 2000). Type B1 cells could be in activated or inactivated state (Codega et al., 2014; Mich et al., 2014). Active B1 cells express Nestin and the transcription factor Sex Determining Region Y (SRY)-Box 2 (SOX2) and divide asymmetrically to generate one B1 daughter cell and a transit-amplifying precursor (TAP, type C cell or neural progenitor cell (NPC)) (Ortega et al., 2013b; Ortega et al., 2013a). Type C cells are more committed neuronal progenitors that express transcription factors such as proneural basic-helix loop helix (bHLH) Achaete-scute like 1 (Ascl1), and Neurogenin 2 (Neurog2) (Brill et al., 2009), and are more proliferative than B1 cells, dividing several times symmetrically before finally converting into neuroblasts (type A cells) (Ponti et al., 2013). Type A cells express basic helix-loop-helix (bHLH) factors Neurog2 (Brill et al., 2009), Neuronal Differentiation 1 (NeuroD1), ß-III-tubulin (Tubb3), doublecortin (DCX) and polysialylated neural cell adhesion molecule (PSA-NCAM) (Hsieh, 2012; Brown et al., 2003) and form a network of migrating neurons within an astrocytic sheath that coalesces to form the rostral migratory stream (RMS) towards the olfactory bulb (OB) (Doetsch and Alvarez-Buylla, 1996) (Fig. 2). In the OB, A cells migrate radially outward from the RMS, integrate into the existing circuitry and mature into gamma-aminobutyric acid (GABA)-ergic and dopaminergic interneurons. The newborn neurons express the neuron nuclear protein NeuN and the microtubule associated protein- 2 (MAP2). Newborn neurons have several functions facilitating fine-odor discrimination (Li et al., 2018; Lledo and Saghatelyan, 2005; Cecchi et al., 2001) and odor-reward association during adaptive learning (Grelat et al., 2018).

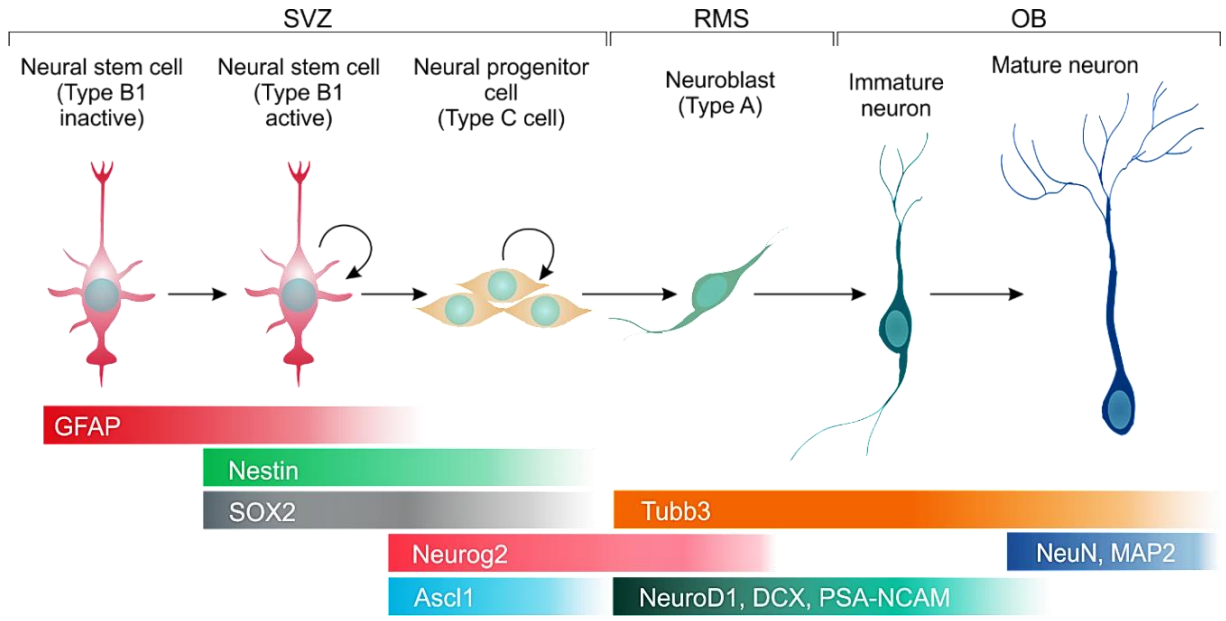


**Figure 2. Schematic overview of the cells types in the SVZ neurogenic niche.** Adult neural stem cells in the SVZ (B1 cells) differentiate into mature neurons in the OB. Specific markers and transcription factors are indicated below each cell type. SVZ: subventricular zone; RMS: rostral migratory stream; OB: olfactory bulb.

B1 cells generate neurons and, to a lesser extent, new oligodendrocytes (Menn et al., 2006; Nait-Oumesmar et al., 1999; Picard-Riera et al., 2002) and astrocytes (Benner et al., 2013).

The SVZ presents a specific cytoarchitecture: B1 cells have their small apical surface in contact with the cerebrospinal fluid (CSF) in the ventricle, surrounding the ependymal cells in a pinwheel-like architecture (Mirzadeh et al., 2008). The contact with the CSF, which contains soluble factors related to bone morphogenetic proteins (BMPs), Wnts, Sonic hedgehog (Shh) and retinoic acid (RA), and the basal contact with the blood vessels modulates B1 cells responses (Huang et al., 2010; Lehtinen and Walsh, 2011; Lehtinen et al., 2011). C cells are located at the SVZ and close to their progenitors and the blood vessels (Tavazoie et al., 2008).

Here, we have described the SVZ in rodents, but this region presents anatomical and proliferative differences between species (Perez-Martin et al., 2000; Kornack and Rakic, 2001; Luzzati et al., 2006; Sawamoto et al., 2011). In humans, NSCs can be isolated from the SVZ and proliferate *in vitro* forming clonal aggregates named "neurospheres" (Kukekov et al., 1999; Sanai et al., 2004), but their proliferative capacity is significantly lower than the rates observed in mice, and there has been an extensive debate about the levels of newborn neurons incorporated into the human OB (Sanai et al., 2007; Sanai et al., 2004; Quinones-Hinojosa et al., 2006; Curtis et al., 2007). Some studies suggest that the highest neuronal production takes place in the fetal brain (Guerrero-Cazares et al., 2011), while in the adult, low numbers of neurons are born in the OB under physiological conditions (Kempermann, 2013; Sanai et al., 2004; Ihrie and Alvarez-Buylla, 2011).

## 2.2. Subgranular zone of the dentate gyrus (SGZ).

Active neurogenesis in the adult subgranular zone (SGZ) of the DG of the hippocampus in rodents has been described by several studies (Kempermann et al., 1997; Kuhn et al., 1996; Seki and Arai, 1999). Here, the NSCs are known as Type 1 cells, Radial glial-like cells (RGLs), radial astrocytes, or quiescent neural progenitors (QNPs). In this study, we refer them as neural stem cells (NSCs). NSCs are a heterogenic population (Jhaveri et al., 2015; Lacar et al., 2016; Shin et al., 2015) which express the astrocytic markers GFAP and vimentin, and the transcription factor SOX2, but contrary to astrocytes, also Nestin (Kempermann et al., 2004; Kriegstein and Alvarez-Buylla, 2009). NSCs have a low proliferative rate and present a long process that crosses the granular cell layer (GCL) towards the molecular layer and is in contact with the basal vasculature of the SGZ.

When NSCs undergo asymmetric division, they generate transient amplifying progenitors (type 2a and 2b cells, also known as intermediate progenitor cells (IPCs)), positive for Nestin, Ascl1, Neurog2 and SOX2 (Hsieh, 2012), but not for GFAP (Gebara et al., 2016). In this study, these cells are named neural progenitor cells (NPCs). NPCs cells are highly proliferative, lack ramifications (Suh et al., 2007; Steiner et al., 2006) and remain in the SGZ (Encinas et al., 2011) until they turn into neuroblasts (type 3) (Kempermann et al., 2004) expressing DCX, PSA-NCAM, and NeuroD1. Neuroblasts finally differentiate into glutamatergic excitatory granular cell (GC) neurons that integrate into the GCL (Bonaguidi et al., 2011; Bonaguidi et al., 2012; Lugert et al., 2010; Suh et al., 2007; Sun et al., 2013). Immature neurons express DCX and PSA-NCAM and undergo a phase of increased synaptic plasticity, being responsible for inducing long-term potentiation (LTP) rather than the mature granule cells (Wang et al., 2000; Schmidt-Hieber et al., 2004). In fact, the only LTP measurable from the DG under normal conditions originates from the immature neurons (Saxe et al., 2006; Garthe et al., 2009). Mature GCs express NeuN, MAP2 and the calcium-binding protein calbindin. GCs project out a large dendritic tree into the adjacent molecular layer and axons that innervate target cells in the hilus and area 3 of the *cornu Ammonis* (CA3). These cells receive GABAergic inputs from the entorhinal cortex (Zhao et al., 2006; Toni et al., 2008) (Fig. 3).

Hippocampal neurogenesis has been associated to learning and memory (Deng et al., 2010). Increased levels of neurogenesis correlate with improved performance in hippocampus-dependent learning and memory tasks, such as the Morris water maze (MWM) (Kempermann et al., 1997; van Praag et al., 1999). Other studies relate hippocampal neurogenesis to spatial and object recognition memory (Jessberger et al., 2009), fear conditioning and synaptic plasticity (Saxe et al., 2006) and pattern discrimination (Clelland et al., 2009; Sahay et al., 2011; Nakashiba et al., 2012; Danielson et al., 2016; Aizawa et al., 2009).

In addition to neurons, adult NSCs in the rodent SGZ give rise to a small population of astrocytes (Encinas et al., 2011; van Praag et al., 1999), but apparently they do not form oligodendrocytes (Steiner et al., 2004).

In humans, the existence of hippocampal neurogenesis is still under controversy. Although several studies describe the existence of lifelong hippocampal neurogenesis in humans (Bergmann et al., 2015; Eriksson et al., 1998; Knoth et al., 2010; Roy et al., 2000; Spalding et al., 2013; Boldrini et al., 2018; Moreno-Jimenez et al., 2019; Tobin et al., 2019), recently, some studies concluded that hippocampal neurogenesis drops to undetectable amounts during childhood (Sorrells et al., 2018). The inability to reach a consensus is due, at least in part, to the lack of standardized protocols in tissue processing and the reduced number of marker studies. The development of methods to follow the hippocampal neurogenesis *in vivo* would help to assess the impact of lifelong neurogenesis in humans.

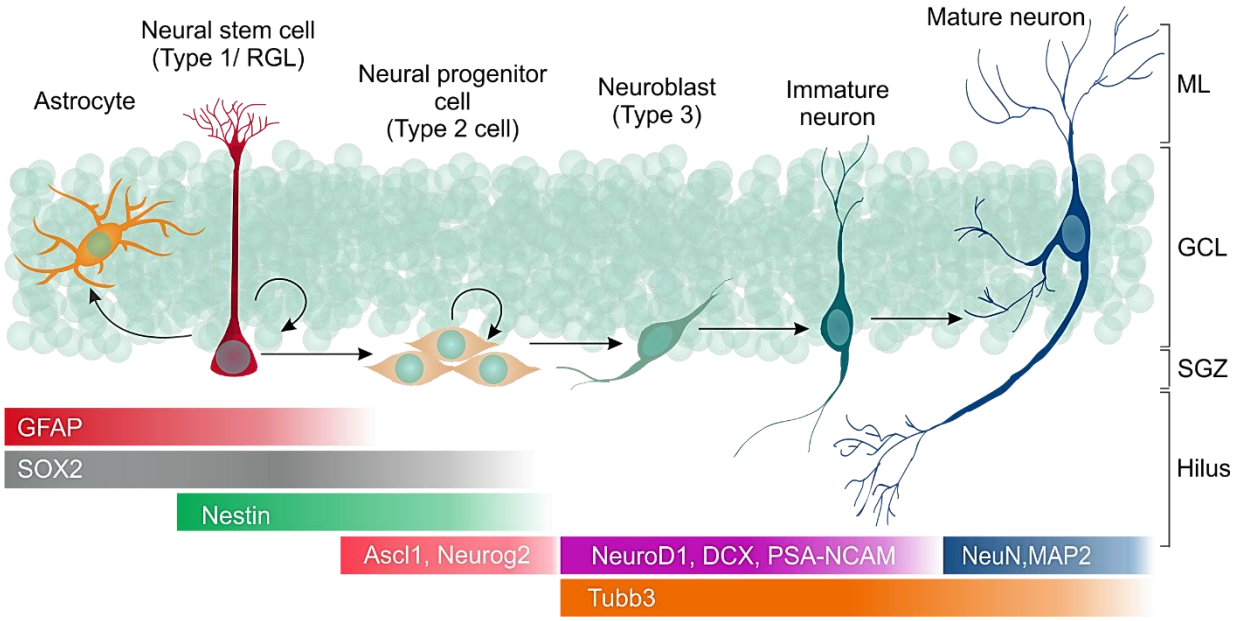


**Figure 3. Schematic overview of the hippocampal neurogenic niche.** Adult NSCs in the hippocampus (radial glia-like cells, type 1 cells) and their differentiation in the SGZ of the DG. Below each cell type it is indicated its specific cell markers and transcription factors. ML: molecular layer; GCL: granular cell layer; SGZ: subgranular zone.

In this thesis, we will refer sometimes, to simplify, altogether to the population of neural stem cells and neural progenitor cells as neural stem/progenitor cells (NSPCs).

## 3. Regulation of adult neurogenesis.

Adult neurogenesis is an orchestrated multistep process, which comprises: 1) maintenance and proliferation of NSCs, 2) fate specification, 3) differentiation, maturation, and survival of neurons and 4) integration into existing brain circuits. The progression of neurogenesis is dynamically coordinated by extrinsic as well as intrinsic factors, such as microenvironment-derived signals and coordinated by precise changes in the pattern of gene expression (Zhao et al., 2008b; Suh et al., 2009; Ming and Song, 2011; Beckervordersandforth et al., 2015).

### 3.1. Signaling pathways.

A variety of signaling pathways triggered at the plasma membrane are known to act during the process of neurogenesis by the control of different key transcription factors. Many of the signaling pathways have an effect on NSC proliferation and undergo considerable crosstalk.

**Notch.** - The Notch signaling pathway, maintains the proliferative and undifferentiated stages of both embryonic and adult NPCs (Pleasure et al., 2000; Breunig et al., 2007; Lavado and Oliver, 2014). Upon Notch signaling, the expression of bHLH transcription factors, such as Hairy enhancer of split (Hes), is induced (Bray and Bernard, 2010). Hes represses the expression of proneural genes, such as *Ascl1* and *Neurog2*, thus enabling maintenance of the NSCs pool (Hatakeyama et al., 2004; Imayoshi et al., 2008). The specific context in which Notch signaling is activated dictates the particular downstream process that is triggered: proliferation, fate specification, or apoptosis.

**Wnt.** - Wnt/β-catenin signaling is important for proliferation and differentiation in the developing cortex and hippocampus (Zechner et al., 2003), but also in postnatal and adult neurogenesis (Zhang et al., 2011; Ortiz-Matamoros et al., 2013; Varela-Nallar and Inestrosa, 2013). Wnt ligands are a family of auto- and paracrine glycoproteins secreted by astrocytes and NSCs (Lie et al., 2005; Qu et al., 2010; Okamoto et al., 2011). After Wnt signaling activation, cytoplasmic β-catenin is stabilized and translocates to the nucleus where it binds T-cell factor/lymphoid enhancer-binding factor (TCF/LEF) transcription factor and drives the expression of neurogenic genes such as *Neurog2* and *Neurod1* (Gao et al., 2009; Kuwabara et al., 2009; Lavado et al., 2010). In the absence of Wnt ligand, glycogen-synthetase-kinase-3 beta (GSK3β), a key modulator of the Wnt pathway, forms a degradation complex, comprising Axin, Adenomatous Polyposis Coli (APC), and β-Transducing repeat- Containing Protein (β-TrCP), that leads to phosphorylation and ubiquitination of β-catenin and subsequent degradation by the proteasome (Chen et al., 2000).

Wnt plays dual roles during neurogenesis. On one hand, it promotes self-renewal and maintains RG during early neurogenesis (Wrobel et al., 2007; Zhou et al., 2004). On the other, it induces the proliferation of hippocampal progenitors (Varela-Nallar and Inestrosa, 2013) and neuronal differentiation during mid and late neurogenesis (Kuwabara et al., 2009; Lie et al., 2005) through epigenetic modification of targeted genes by context- and cell-type-dependent mechanisms.

**Shh.** - The Sonic hedgehog (Shh) signaling cascade is essential for the expansion and establishment of postnatal hippocampal progenitors (Breunig et al., 2008; Amador-Arjona et al., 2011; Han et al., 2008). During neurogenesis, active Shh signaling decreases, whereas the activity of the zinc finger protein GLI repressor increases (Fuccillo et al., 2006; Philipp and Caron, 2009), being necessary for production of progenitors and for neuronal differentiation (Wang et al., 2011).

### 3.2. Neurotrophic and growth factors.

Neurotrophic factors are extracellular signaling proteins that play important roles in both the developing and the adult CNS (Glebova and Ginty, 2005; Lu et al., 2005). One neurotrophic factor is brain-derived neurotrophic factor (BDNF), which favours neurogenesis both in the SGZ and the SVZ (Scharfman et al., 2005; Zigova et al., 1998; Benraiss et al., 2001).

Growth factors are extracellular proteins that promote cell growth and maintenance on the neurogenic niches (Bottcher and Niehrs, 2005; Guillemot and Zimmer, 2011). Regarding neurogenesis, fibroblast growth factor-2 (FGF-2), also known as basic FGF (bFGF), is related with an increase in the number of newly born cells in the adult rat hippocampus (Rai et al., 2007). Another cytokine implicated in neurogenesis is the epidermal growth factor (EGF). EGF administration into lateral ventricles leads to significant upregulation of cell proliferation within the SVZ (Morshead et al., 2003; Okano et al., 1996). Moreover, NPCs express receptors for FGF-2 and EGF (Gritti et al., 1999). Thus, FGF-2 and EGF are used to promote cell proliferation and survival of NSPCs grown in culture as neurospheres (Pincus et al., 1998; Tropepe et al., 1999) and are used in this study to maintain stem cells *in vitro*. Other trophic factors important in neurogenesis are vascular endothelial growth factor (VEGF), insulin-like growth factor-1 (IGF-1) and transforming growth factor β (TGF-β) (Brooker et al., 2000; Aberg et al., 2003; Aberg et al., 2000; Yasuhara et al., 2004; Khaibullina et al., 2004; Cao et al., 2004; Funa and Sasahara, 2014).

### 3.3. Redox control of neurogenesis.

Changes in environmental and intracellular redox status are crucial for the fate of NSPCs (Madhavan, 2015; Dickinson et al., 2011; Tsatmali et al., 2005; Yuan et al., 2015). Recent studies indicate that a reducing environment favours cell proliferation, whereas an oxidizing environment favours cell differentiation (Schafer and Buettner, 2001). Furthermore, a more oxidized environment favours differentiation towards astroglia, whereas a more reduced environment favours the neuronal lineage (Prozorovski et al., 2008). At the intracellular level, as the stem cells are stimulated, either by tissue injury, inflammation, or growth factors, low levels of reactive oxygen species (ROS) are produced, which activate redox-sensitive signaling pathways such as phosphoinositide 3-kinase (PI3K)/Akt signaling that favours cell proliferation (Smith et al., 2000; Yoneyama et al., 2010; Le Belle et al., 2011). When ROS levels increase, the rate of proliferation slows down and in turn the intracellular environment favours differentiation (Smith et al., 2000; Yoneyama et al., 2010; Le Belle et al., 2011). Thus, a delicate redox balance needs to be achieved in neurogenesis because its perturbation in NSPCs or within the neurogenic microenvironment can lead to changes in the production, functional integration, and long-term survival of new neurons.

## 3.4. Transcriptional regulation of neurogenesis.

The changes in gene expression point transcriptions factors as central coordinators of the development of new functional neurons from NSCs.

### 3.4.1. SOX2.

Sex determining region Y (SRY)-box 2 (SOX2) is a homeobox transcription factor of the SOX family characterized by a highly conserved DNA binding domain known as high-mobility group (HMG). SOX2 is highly expressed in NSCs and NPCs (Steiner et al., 2006) and controls their multipotency and proliferative capacities (Favaro et al., 2009; Steiner et al., 2006; Ferri et al., 2004) as well as proper neuronal differentiation and maturation (Cavallaro et al., 2008). SOX2 is regulated by Notch signaling (Ehm et al., 2010) and is able to modulate Shh signaling by controlling the expression of Shh (Favaro et al., 2009). Recently, SOX2 has been described as an epigenetic regulator of the bHLH genes *Neurog2* and *Neurod1*, preventing excessive activity of Polycomb Repressive Complex 2 (PRC2). Thus, SOX2 favours a permissive epigenetic state in NPCs, appropriate for the activation of the differentiation program upon exposure to a neurogenic stimulus (Amador-Arjona et al., 2015) (Fig. 4A). SOX2 interacts with the long non-coding RNA RMST (rhabdomyosarcoma 2-associated transcript). In the onset of neurogenesis in human NSCs, the complex RMST-SOX2 regulates a large pool of downstream genes including *ASCL1* and *NEUROG2* (Ng et al., 2013) (Fig. 4B). The implication of SOX2 in neurogenesis has also been described in the acquisition of neuronal fates in sensory ganglia (Cimadamore et al., 2011).

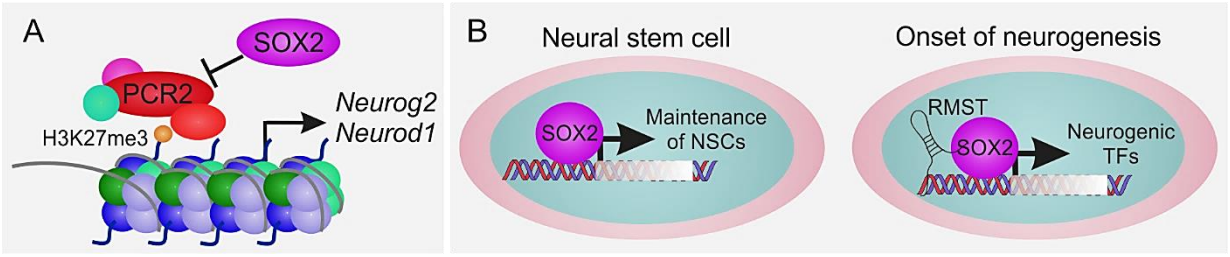


**Figure 4. Schematic view of SOX2 mechanisms involved in the regulation of neurogenesis. (A)** SOX2 inhibits PCR2 activity favouring a permissive epigenetic state of NPCs for neuronal differentiation. **(B)** SOX2 interacts with RMST in the onset of neurogenesis driving the expression of proneural factors.

*SOX2* gene expression is activated by several signaling pathways, including Shh, Wnt, FGF and TGF-β (Manoranjan et al., 2012), but few studies have analyzed which transcription factors are involved. For example, *SOX2* is positively regulated in NSPCs by transcription factors that are expressed at considerably high levels during early neural development and differentiation such as prospero homeobox protein 1 (PROX1) and paired box protein 6 (PAX6) (Lengler et al., 2005; Chen et al., 2008b).

### 3.4.2. Basic helix-loop-helix (bHLH) transcription factors.

The basic helix-loop-helix (bHLH) transcription factors are essential regulators of NSCs fate specification and differentiation in embryonic development and adult neurogenesis (Bertrand et al., 2002; Ross et al., 2003; Imayoshi and Kageyama, 2014) and have emerged as potential candidates for transcription factor-based neural cell reprogramming.

The structure of bHLH transcription factors is comprised by two alpha-helices connected by a non-conserved loop region for dimerization and a basic domain for DNA binding (Fig. 5A). After dimerization with ubiquitously expressed bHLH E proteins, bHLH transcription factors bind the consensus E-box sequence (CANNTG) (Bertrand et al., 2002). bHLH are classified based on their pattern of expression. In this section, we will focus on the Class II proneural factors that are expressed in the CNS, such as Ascl1, Neurog2 and NeuroD1. These factors regulate the expression of neuron-specific genes and those encoding Notch ligands, such as Delta-like protein 1 (Dll1), which activates Notch signaling in neighbouring cells contributing to NPC maintenance (Castro et al., 2006; Henke et al., 2009).

Achaete-scute like 1 (Ascl1) is expressed in NPCs (Uda et al., 2007) and has several roles, regulating the expression of genes related to cell-cycle exit, neuronal components of the cytoskeleton (as *Dcx* and *Tubb3*), neurotransmitter biosynthesis, and neurite outgrowth, but also other genes related with cell-cycle progression (Castro et al., 2011). In the SVZ, Ascl1 expression is restricted to TAPs destined to differentiate into GABAergic interneurons of the OB. In the adult hippocampus, Ascl1 is transiently expressed by NPCs that subsequently develop into glutamatergic granule cell neurons (Kim et al., 2007). During neuronal differentiation, Ascl1 promotes chromatin accessibility, which may be important to allow subsequent regulation by other transcription factors. Thus, Aslc1 acts as a pioneer factor during neuronal fate (Raposo et al., 2015) (Fig. 5B).

Neurogenin 2 (Neurog2) is another proneural bHLH factor expressed in NPCs. In the adult SVZ, in contrast to Ascl1, Neurog2 is expressed by a subset of NPCs that differentiate into glutamatergic interneurons (Brill et al., 2009). Neurog2 is also expressed transiently by NPCs in the SGZ (Hodge et al., 2008). Neurog2 remodels the closed chromatin of its target genes by binding to histone acetyltransferases, such as the H3K9 demethylase known as KDM3A (lysine demethylase 3A) (Lin et al., 2017) or the chromatin remodelling protein Brahma-related gene-1 (Brg1) (Seo et al., 2005). These interactions facilitate Neurog2 binding to the regulatory regions of neuronal differentiation genes such as *Neurod1* and *Tubb3* (Ma et al., 1996; Sommer et al., 1996; Lin et al., 2017) (Fig. 5C).

Neurogenic Differentiation 1 (NeuroD1) is a bHLH factor which plays an important role during neuronal differentiation and is expressed transiently in committed progenitors and neuroblasts and declines in immature neurons (Gao et al., 2009; Hevner et al., 2006; Aprea et al., 2014). NeuroD1 is crucial for the survival and differentiation of newborn neurons in the adult SGZ and SVZ (Gao et al., 2009; Schwab et al., 2000). NeuroD1 confers transcriptional competence, acting as a precursor factor

during neuronal differentiation and favouring chromatin accessibility, which is epigenetically maintained even after NeuroD1 disappearance during neurogenesis (Pataskar et al., 2016) (Fig. 6).

The general mode of proneural gene function has thus been elucidated. However, the regulatory mechanisms that spatially and temporally control proneural gene function are only beginning to be deciphered.

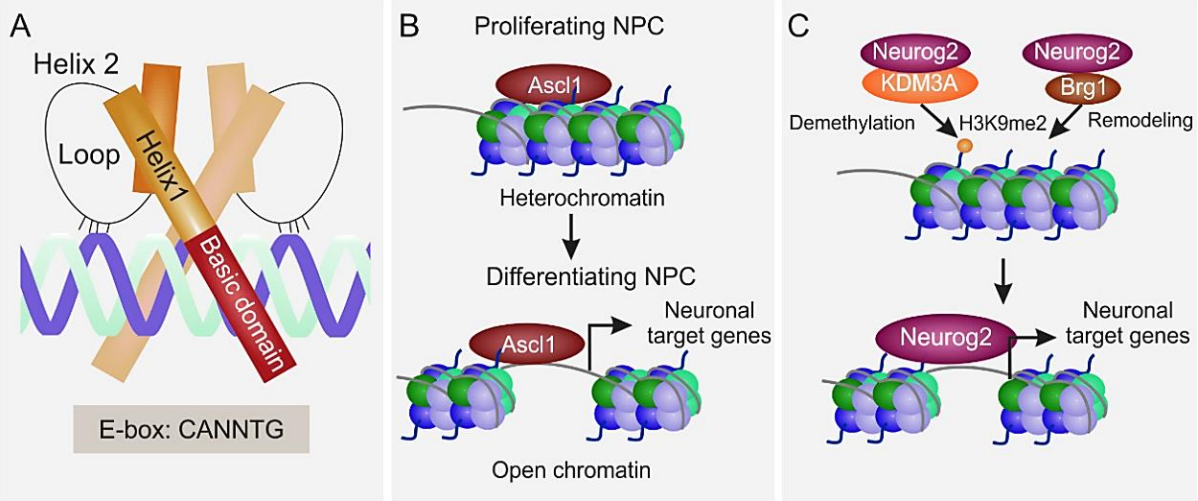


**Figure 5. Proneural basic helix-loop-helix structure and epigenetic mechanism. (A)** Structure of basic helix-loop-helix (bHLH) factors. bHLH transcription factors present two alpha-helices connected by a non-conserved loop region for dimerization and a basic domain to bind E-box sequence in the DNA. **(B)** Ascl1 is a pioneer transcription factor which induces chromatin opening of target neuronal genes**. (C)** Neurog2 binds lysine demethylase 3A (KDM3A) to demethylate H3K9me2 at repressive sites, allowing for new chromatin modifications that open the chromatin (eg. H3K37ac3). Neurog2 also binds Brg1, a chromatin remodeler, to directly open the chromatin.

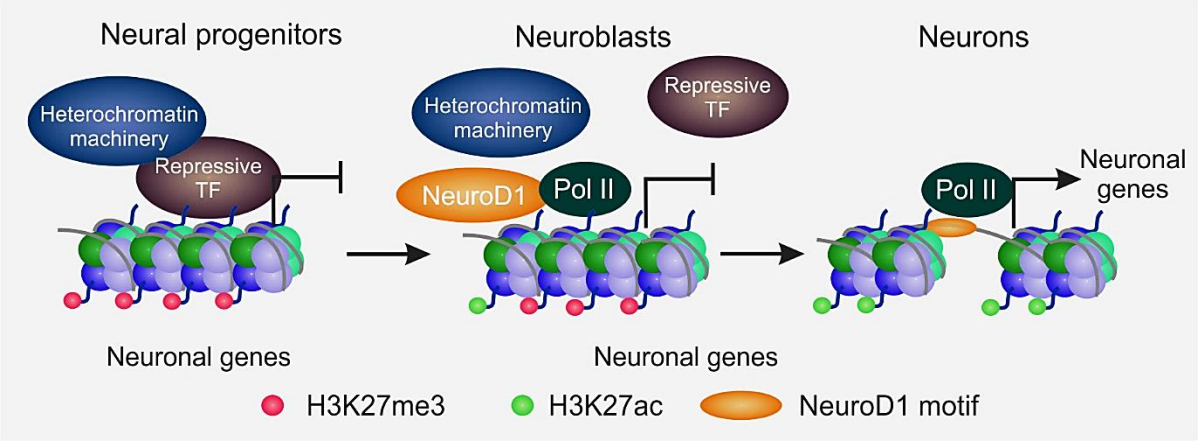


**Figure 6. NeuroD1 acts as a pioneer factor during neuronal program.** NeuroD1 reprograms chromatin by loss of inactive (H3K27me3) and gain of active (H3K27Ac) histone marks, leading to increased chromatin acessibility for RNA polymerase II (Pol II) recruitment, followed by neuronal gene expression.

Due to their neurogenic functions, proneural bHLH factors are key players in the neuronal reprogramming of somatic cells. Ascl1 directly reprogram fibroblasts, astrocytes and pericytes (combined with SOX2) to induce neuronal differentiation (Chanda et al., 2014; Wapinski et al., 2013; Karow et al., 2012; Vierbuchen et al., 2010). Neurog2 can induce glutamatergic neurons from postnatal astrocytes (Berninger et al., 2007; Heinrich et al., 2010) and motor neurons from fibroblasts (Liu et al., 2013). Forced NeuroD1 expression reprograms astrocytes towards functional neurons (Guo et al., 2014). Recently, neuronal conversion from mouse microglia by NeuroD1 has been reported (Matsuda et al., 2019). Despite these intensive studies, the generation of induced neurons nowadays is still little efficient.

In this thesis, we will simplify the way to refer altogether to SOX2 and proneural bHLH factors ASCL1, NEUROG2 and NEUROD1 as proneurogenic factors, based on their implication in the neuronal differentiation of NSPCs (Colasante et al., 2019). A better understanding of how proneurogenic genes are regulated will allow a more efficient use in regenerative medicine based on neuronal reprogramming.

There are other factors related with regulation of neurogenesis that will not be addressed in the present study. These include intrinsic factors which can modulate neurogenesis as inflammation state, hormones and neurotransmitters (Kohman and Rhodes, 2013; Trivino-Paredes et al., 2016), and extrinsic factors such as enriched environment (Kempermann et al., 1997), calorie restriction (Murphy et al., 2014) and exercise (Trivino-Paredes et al., 2016; van Praag et al., 1999).

## 4. Deregulation of neurogenesis.

Adult neurogenesis is emerging as an important player in brain homeostasis. Alterations in the proper course of neurogenesis have been described in aging and several CNS diseases, such as major depression, epilepsy, Alzheimer´s disease (AD) and glioblastomas (GB) (Sahay and Hen, 2007; Parent and Murphy, 2008; Alcantara Llaguno and Parada, 2016). Aging, AD and cancer are analyzed in this work as three examples of deregulation of neurogenesis.

### 4.1. Aging.

Aging is one of the most significant risk factors for cognitive decline and neurodegenerative disorders and leads to a progressive decay in adult neurogenesis. During aging, neurogenesis declines both the DG and the SVZ of rodents, non-human primates and humans (Apple et al., 2017; Luo et al., 2006; Kuhn et al., 1996; Spalding et al., 2013; Encinas et al., 2011; Aizawa et al., 2009; Amrein et al., 2011; Dennis et al., 2016). Furthermore, the age-related decline in neurogenesis has been correlated with cognitive impairment. In the SVZ, the decrease in newborn neurons in the OB is observed behaviourally by olfactory deficits in aged rodents (Enwere et al., 2004; Rochefort et al., 2002). On the other hand, the progressive loss of hippocampal neurogenesis correlates with deficits in hippocampal functions of

learning and spatial memory in old rats as measured by the MWM and visual pattern discrimination tests (Drapeau et al., 2003; Driscoll et al., 2006). Identifying the mechanisms involved in the depletion of the NSPCs pool with aging may reveal therapeutic targets for increasing the neurogenic response and improving the cognitive functions of the elderly.

### 4.2. Alzheimer´s disease (AD).

Aging is the main risk factor for AD. AD is characterized by progressive neuronal loss, followed by memory loss and cognitive impairment (Goedert and Spillantini, 2006). The main neuropathological hallmarks of AD are the neurofibrillary tangles of hyperphosphorylated neuronal microtubule associated TAU protein (Geschwind, 2003) and senile plaques formed by the deposition of β-amyloid (Aβ) (Selkoe, 2001; Nicolas and Hassan, 2014). $A\beta_{1–40}$ and $A\beta_{1–42}$ are released from amyloid precursor protein (APP) by β and γ secretases, the presenilins 1 and 2 (PS1 and PS2, respectively) (Selkoe, 2001; Nicolas and Hassan, 2014). The genes encoding APP, PS1 and PS2 are involved in familiar AD, and mutations in these genes can increase the production of $A\beta_{1–42}$ (Lithner et al., 2011). Furthermore, PS1 is expressed in the adult hippocampus (Page et al., 1996; Boissiere et al., 1996), including the NPCs of the SGZ (Wen et al., 2002). Indeed, PS1 plays a role in regulating Notch signaling, and is responsible for maturation of glia and neurons (Gaiano and Fishell, 2002) by cleavage of Notch intracellular domain (NICD) (Kojro and Fahrenholz, 2005). On the other hand, hyperphosphorilation of TAU has been related with an over activation of GSK3β in AD (Leroy et al., 2007; Blalock et al., 2004; Hooper et al., 2008). GSK3 was identified as a master regulator of NSCs homeostasis with impact in Wnt, Shh and Notch signaling in the mammalian brain development (Kim et al., 2009). Even more, small GSK3 inhibitors elicit an increase of NPCs (Lange et al., 2011).

The relevance of neurogenesis in AD differs among several mouse models (Lazarov and Marr, 2010; Mu and Gage, 2011). For example, transgenic mice with mutant APP/PS1 exhibit impaired neurogenesis at both the SVZ and SGZ even earlier than the appearance of Aβ deposits and memory loss, suggesting that impaired neurogenesis may partly initiate the neuropathology of AD (Demars et al., 2010). The double knockout of PS1 and PS2 apparently enhances neurogenesis at first steps but in term leads to exhaustion of the neurogenic niche (Chen et al., 2008a). Moreover, transgenic mice with mutant APP exhibit increased proliferation and differentiation of NPCs in the SGZ (Jin et al., 2004). The triple transgenic mice (3xTg-AD) harbouring three mutant genes ($APP^{K595N/M596L}$, $PS1^{M146V}$ and $TAU^{P301L}$) show temporal and region-specific Aβ and TAU pathology, accompanied by cognitive deficits, including reduced LTP (Oddo et al., 2003a; Oddo et al., 2003b). The neurogenic niches of these mice present an accelerated age-related reduction in proliferating cells, committed progenitors and newborn neurons prior to the development of amyloid plaques or neurofibrillary tangles, thus, indicating again that loss of adult neurogenesis may be partly the cause of the premature cognitive decline in AD (Rodriguez et al., 2008b; Rodriguez et al., 2009; Hamilton et al., 2010). In addition, apolipoprotein E4 (ApoE4), the major known

risk factor for AD, inhibits hippocampal neurogenesis by impairing the functions of GABAergic interneurons (Li et al., 2009). As it happens with AD animal models, hippocampal neurogenesis is controversial in AD patients. Some studies have reported that adult hippocampal neurogenesis is inhibited in AD patients, whereas gliogenesis is increased (Boekhoorn et al., 2006; Crews and Masliah, 2010; Moreno-Jimenez et al., 2019; Tobin et al., 2019), meanwhile other studies have reported an increase in adult hippocampal neurogenesis in AD patients (Jin et al., 2004). These discrepancies may reflect different stages of AD or the heterogeneous nature of AD pathology.

The characterization of factors that modulate NSPCs will allow us to understand the implication of neurogenesis in AD and its therapeutic implication.

### 4.3. Glioblastomas.

Glioblastoma multiforme (GBM) is a highly aggressive grade IV tumour based on the criteria of The World Health Organisation. GBM is the most prevalent glial tumour, with the worst prognosis, lowest rate of patient's survival and with a poor response to current therapies (Wen and Kesari, 2008; Stupp et al., 2009). One of the most significant questions in GBM research is its cellular origin. GBM comprises a heterogeneous population of cells ranging from highly tumorigenic stem-like cells to more differentiated cancerous cells (Singh et al., 2004). The cancer stem cell (CSC) model suggests that only a small group of cells have quiescence and self-renewal capacity within the tumour bulk, and that those are responsible for tumour maintenance and recurrence (Pattabiraman and Weinberg, 2014). Although there is controversy about which cell types in the CNS contribute to GBM formation, recent studies suggest that deregulation of proliferation or oncogenic mutations within NSPCs could lead to brain tumour formation, pointing to the transformation of NSPCs to CSCs in gliomas (Swartling et al., 2014; Zheng et al., 2008; Alcantara Llaguno et al., 2009; Jacques et al., 2010; Sanai et al., 2005; Lee et al., 2018; Altmann et al., 2019; Chen et al., 2012; Holland et al., 2000). Indeed, NSPCs harbouring driver mutations have been highlighted as potential targets for preventing the recurrence of GBM (Zong et al., 2015; Chen et al., 2013; Khalifa et al., 2017; Visvader, 2011).

In GBM, the limited therapeutic options increase the pressure to discover new genetic and molecular targets. Recent studies based on the forced expression of the proneurogenic bHLH factors, as NEUROG2 (Su et al., 2014), ASCL1 (Park et al., 2017) and NEUROD1 (Guichet et al., 2013) showed a reduction in the tumorigenic properties of GBM cells and enhanced neuronal differentiation. Thus, identification of factors that could control the expression of these proneurogenic factors opens a new window in the therapeutic treatment of GBM.

## 5. Transcription factor NRF2.

Nuclear factor (erythroid-derived 2)-like 2 (NRF2) is a protein that belongs to the cap 'n' collar (CNC) family of transcription factors, encoded by the *NFE2L2* gene. At the C-terminus, NRF2 contains a basic leucine-zipper (bZip) domain that participates in the formation of heterodimers with other bZip proteins, like small muscle aponeurosis fibromatosis (MAF) K, G and F (Ma, 2013; Hayes and Dinkova-Kostova, 2014). These heterodimers bind to the regulatory enhancer sequence termed Antioxidant Response Element (ARE; 5′-TGACNNNGC-3′) (Moi et al., 1994; Venugopal and Jaiswal, 1996). NRF2 regulates more than 250 genes that participate in multiple homeostatic functions including regulation of inflammation, redox metabolism, cell survival and proteostasis (Wild et al., 1999; Rushmore et al., 1991, Rushmore and Pickett, 1990; Lee et al., 2005; Thimmulappa et al., 2002; Pajares et al., 2017; Pajares et al., 2016; Rojo de la Vega et al., 2018; Rojo de la Vega et al., 2016). Thus, NRF2 is considered a master regulator of cellular homeostasis.

### 5.1. NRF2 structure and regulation.

Human NRF2 comprises 605 aminoacids (597 in the mouse) organized in seven regions, called NRF2 − ECH homology (Neh) domains 1–7 (Fig. 7). Neh1, Neh3, Neh4 and Neh5 regions are required for transactivation activity (Hayes and McMahon, 2009; Hirotsu et al., 2012; Kim et al., 2013). The Neh1 domain comprises the CNC-bZIP region that dimerizes with the small MAF proteins and binds DNA (Hirotsu et al., 2012).

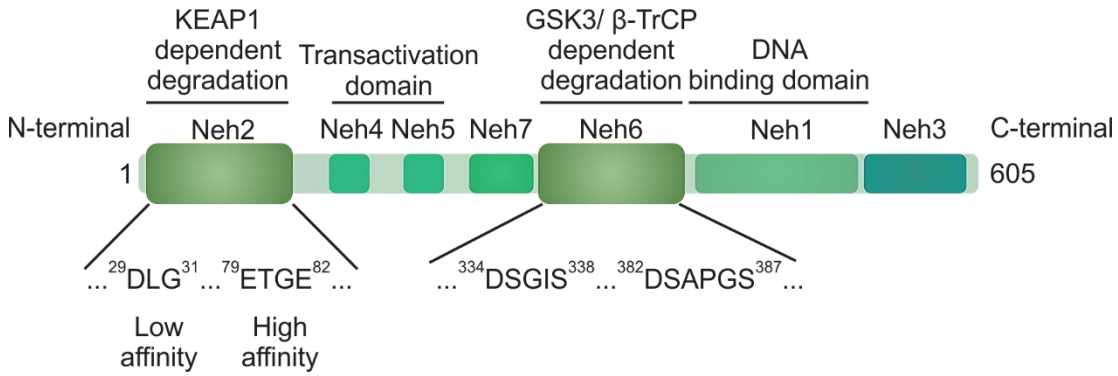


**Figure 7. NRF2 structure.** NRF2 possesses seven regions called NRF2-ECH homology (Neh) domains. The functional role of the main Neh domains is specified. Residue numbers are shown for the human protein.

Neh2 and Neh6 regions contain several destruction motifs and are related with NRF2 instability. The Neh2 region comprises the DLG and ETGE motifs which recruit Kelch-like ECH-associated protein (KEAP1) (Tong et al., 2006; McMahon et al., 2006). KEAP1 presents NRF2 for ubiquitination to the E3 ligase complex formed by Cullin3 and RING-box protein 1 (CUL3/RBX1) (Tong et al., 2007), resulting in subsequent NRF2 degradation by the proteasome 26S (Suzuki et al., 2013; Hayes and Dinkova-

Kostova, 2014). ROS, electrophiles or many xenobiotics induce NRF2 accumulation through modifications of key cysteine residues in KEAP1. They cause a conformational change in the NRF2-KEAP1 complex by promoting the formation of adducts or oxidation of sulfhydryl groups in some of the Cys residues of KEAP1 (mainly Cys-151, Cys-273 and Cys-288). This conformational change prevents NRF2 ubiquitination and subsequent proteasomal degradation (Zhang and Hannink, 2003) and results in NRF2 stabilization, translocation to the nucleus and activation of its transcriptional activity (Itoh et al., 1997) (Fig. 8).

The Neh6 region comprises the DSGIS and DSAPGS motifs. DSGIS is phosphorylated by the serine/threonine protein kinase GSK3β. This phosphodomain recruits β-TrCP (Rada et al., 2011; Rada et al., 2012), a substrate adaptor for the S-phase kinase-associated protein 1 (SKP1)–CUL1–F box containing complex (SCF) (SCF/β-TrCP) (Suzuki et al., 2000; Wu et al., 2003). Thus, GSK3/β-TrCP targets NRF2 for ubiquitin-proteasome degradation and links NRF2 regulation with signaling responses such as Wnt and Shh (Cuadrado, 2015). β-TrCP also recognizes the DSAPGS motif in the Neh6 which seems to be constitutively phosphorylated (Chowdhry et al., 2013) (Fig. 8).

The Neh7 domain mediates repression of NRF2 by the retinoid X receptor (RXR)α through physical association of the two proteins (Wang et al., 2013). Additional degradative systems regulate NRF2 at post-transcriptional level, such as the inositol requiring enzyme (IRE1)/E3 ubiquitin ligase synoviolin (HRD1) under endoplasmic reticulum (ER) stress (Wu et al., 2014) (Fig. 8).

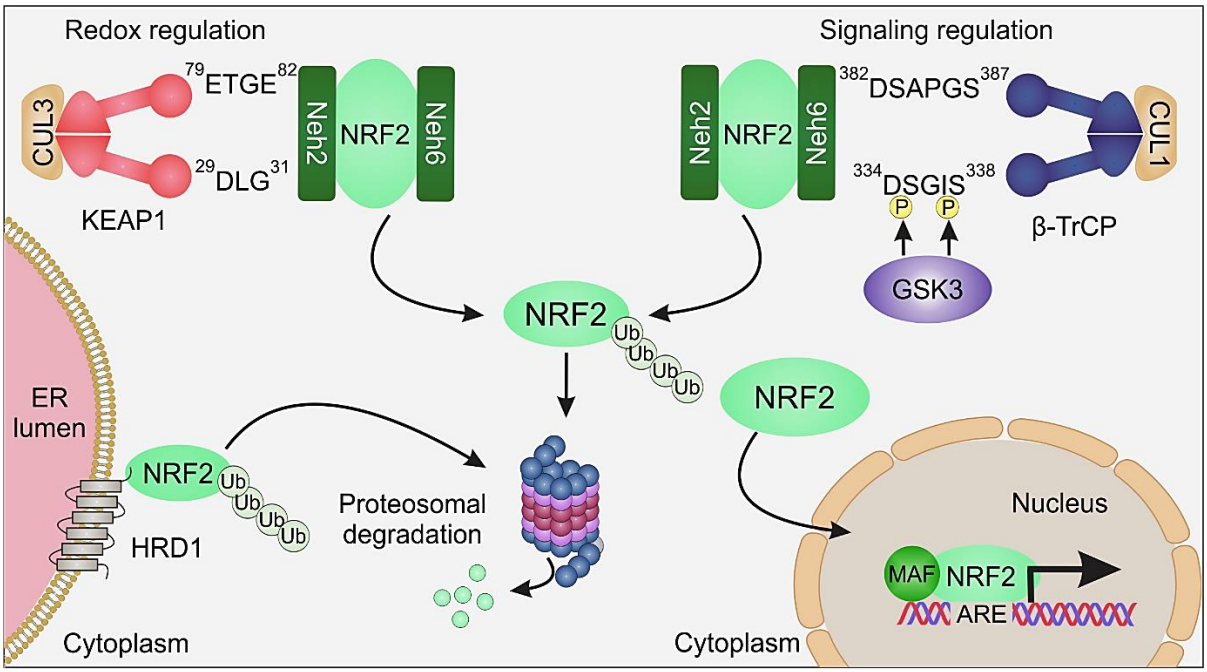


**Figure 8. Molecular mechanisms of NRF2 regulation.** Under basal conditions, NRF2 is bound to KEAP1 and undergoes rapid proteasomal degradation. Upon induction, cysteine residues in KEAP1 are modified, the E3 ubiquitin ligase activity is suppressed, and NRF2 levels increase. NRF2 can be also regulated by its Neh6 region (right): DSGIS motif is phosphorylated by GSK3β and recruits ubiquitin ligase adapter β-TrCP for proteasome degradation by a Cullin1/Rbx1 (CUL1) complex (SCF). Another mechanism for NRF2 degradation is the E3 ubiquitin ligase HRD1. Activated NRF2 enters the nucleus and dimerizes with MAFs to promote transcription of ARE-dependent genes.

### 5.2. Function of NRF2 in neurogenesis.

NRF2 modulates a global cellular response to promote cell survival, cell growth, self-renewal, differentiation, and increased lifespan, all of which are relevant to the function of the NSCs (Zhu et al., 2013; Ryoo et al., 2016; Murakami and Motohashi, 2015; Murakami et al., 2017; Gurusamy et al., 2010; Cai et al., 2012; Gambari et al., 2014). Particularly, Wakabayashi and colleagues described how NRF2 regulates Notch1 expression through an ARE in its promoter region, thus impacting on cell proliferation (Wakabayashi et al., 2010). Furthermore, NRF2 has been linked to the activity of trophic factors, including VEGF, IGF-1 and TGF-β, which are also important for NSCs (Kweider et al., 2011; Lee et al., 2005). Another mechanism by which NRF2 controls cell proliferation and differentiation is the regulation of redox signaling by the control of antioxidant molecules, such as superoxide dismutase (SOD), glutathione (GSH), glutamate-cysteine ligase (GCL) catalytic subunit (GCLC) and modifier subunit (GCLM) and the detoxification enzyme heme oxygenase 1 (HO1) (Wild et al., 1999; He et al., 2001; Venugopal and Jaiswal, 1998). The intracellular redox state is emerging as a critical aspect of NSC physiology (Noble et al., 2003; Smith et al., 2000). Thus, NRF2 emerges as a key factor for the proper functioning of NSCs.

### 5.3. NRF2 in aging and AD.

In this study, we will focus in the impact of NRF2 in neurogenesis during aging and AD. Given the impact of inflammation and oxidative stress in aging and neurodegenerative disease (Jo et al., 2010; Liu et al., 2017; Smith et al., 2012), and the role of NRF2 as a master regulator of anti-inflammatory and antioxidant response, it is important to elucidate the impact of NRF2 in age-related disorders. As it has been described for neurogenesis, during aging NRF2 activity also declines, parallel to increased activity of its negative regulators (KEAP1, GSK3 and HRD1) and an epigenetic silencing of its promoter (Zhang et al., 2015; Silva-Palacios et al., 2018; Suh et al., 2004). In the major age-related neurodegenerative disease, AD, NRF2 activity also decreased, probably due to the hyperactivation of its inhibitor GSK3β (Leroy et al., 2007; Blalock et al., 2004; Hooper et al., 2008). NRF2 has been shown to be a protective factor against AD pathology, and NRF2 expression is low in aged AD animal models and AD patient brains (Kanninen et al., 2008; Ramsey et al., 2007; Johnson and Johnson, 2015; Rojo et al., 2017). For example, NRF2 reduces the levels of phosphorylated TAU by inducting autophagy adaptor protein nuclear dot protein 52 kDa (NDP52) (Jo et al., 2014). Interestingly, one haplotype allele in the promoter of NRF2 encoding gene (*NFE2L2)* was associated with an earlier onset of AD, implying that common variants of the *NFE2L2* gene might affect AD progression (von Otter et al., 2010).

All these studies suggest the potential of NRF2 activation to optimally modulate NSCs function with age and to attenuate the progression of neurodegeneration and cognitive impairment (Bahn and Jo, 2019; Cuadrado et al., 2019; Cuadrado et al., 2018).

## 6. NRF2 and Hippo pathway in stemness.

It is generally accepted that the stemness promoting activity of NRF2 is due to its homeostatic functions. However, high NRF2 expression is observed in embryonic, pluripotent and cancer stem cells (Jia et al., 2015; Wu et al., 2015; Zhu et al., 2014), suggesting additional functions in stem cells maintenance. As described previously, NRF2 controls the expression of the stemness associated protein Notch1 (Wakabayashi et al., 2010), while NRF2 inactivation affects stem cell renewal (Zhu et al., 2013). However, a mechanistic connection between stemness and NRF2 has not been demonstrated yet. Here, we focused on the Hippo pathway effector Transcriptional co-activator with PDZ-binding motif (TAZ) that is described in the following section as a possible target of NRF2 in stem cells.

## 7. Transcriptional cofactor TAZ.

Transcriptional co-activator with PDZ-binding motif (TAZ) is a transcriptional cofactor also known as WWTR1 (WW-domain containing transcriptional regulator 1) that was initially described as a 14-3-3 binding protein (Kanai et al., 2000). TAZ is, together with Yes-associated protein (YAP), one of the major effectors of the Hippo signaling pathway. The Hippo pathway involves a highly conserved cascade of serine/threonine protein kinases which comprises the mammalian Ste20-like kinases (MST1/2) and large tumour suppressor kinase 1/2 (LATS1/2) (Chan et al., 2005; Callus et al., 2006). The Hippo pathway regulates organ size during development, cell proliferation, apoptosis, cell-cell contact inhibition, stem cell self-renewal, and tissue regeneration (Yang and Xu, 2011; Varelas, 2014).

### 7.1. Structure and regulation of TAZ.

TAZ comprises 400 amino acids organized in several motifs and domains (Fig. 9). First, the protein-interaction domain WW, comprises two tryptophan (W) residues separated by 20-23 amino acids and recognizes a PPxY motif (proline/proline/any amino acid/tyrosine) related to control of TAZ subcellular localization (Salah et al., 2012).

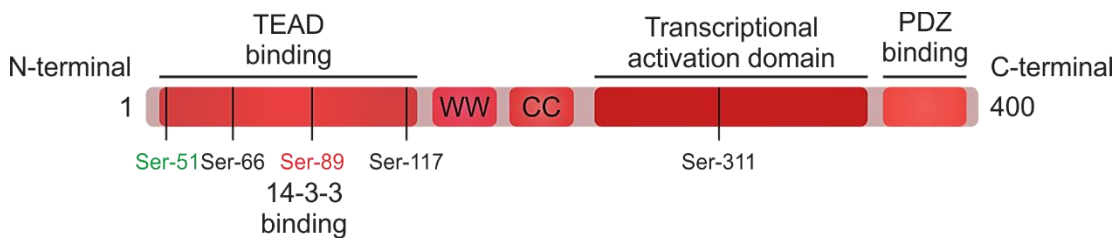


**Figure 9. TAZ structure.** TAZ possesses several domains and motifs that regulate its function: a 14-3-3 binding motif and TEAD binding-domain in the N-terminal, a WW domain, a coiled-coiled (CC) motif and a transcriptional activation domain and a PDZ binding motif and in the C-terminal. Some key posttranslational modifications are also shown. Ser-51 indicates the main residue implicated in TEAD-binding. Residue numbers are shown for the human protein.

The N-terminal region of TAZ mediates binding to the Transcriptional enhancer factor TEF-1 (TEAD) transcription factors, the main cofactors of TAZ (Chan et al., 2009). The TEAD-binding region of TAZ is in very close proximity (possibly overlapping) with that required for 14-3-3 binding (Varelas, 2014). The main residue implicated in TAZ-TEAD interaction is the Ser-51, as replacement of this Ser-51 by an alanine ($TAZ^{S51A}$) abolishes the interaction between TAZ and TEADs (Zhang et al., 2009). When the Hippo pathway is activated, for example in response to cell density, polarity signals, or mechanical cues (Bae and Luo, 2018), phosphorylated MST1/2, complexed with its regulatory subunit Salvador family WW domain containing protein 1 (SAV1), phosphorylates and activates LATS1/2, in complex with its regulatory subunit Mps One Binder 1 (MOB1). Activated LATS phosphorylates TAZ at Ser-89 to enhance cytoplasmic retention of TAZ by increasing the interaction between TAZ and 14-3-3 (Lei et al., 2008). This events result in separation of TAZ from its transcription factor, therefore inhibiting transcription of TAZ-target genes (Basu et al., 2003; Kanai et al., 2000) (Fig. 10).

The C-terminal region mediates interactions with PDZ domains by a PDZ-binding motif. PDZ domains are found in transmembrane and cytoskeleton associated proteins (Ye and Zhang, 2013; Kanai et al., 2000). Near this C-terminal region, TAZ presents a transcriptional activation domain.

TAZ contains four consensuses serine-rich phosphodegron motifs (HxRxxS). Besides Ser-89, LATS kinase also phosphorylates TAZ at Ser-66, Ser-117 and Ser-311. The replacement of these four serines with alanines ($TAZ^{4SA}$) conducts to TAZ resistance to the mobility shift caused by MST1/2 and LATS1/2 and leads to TAZ accumulation (Lei et al., 2008). LATS phosphorylation of TAZ in Ser-311 confers a prime phosphorylation site for sequential phosphorylation Ser-314 by another kinase, Casein Kinase 1 (CK1). This cooperative phosphorylation recruits SCF/β-TrCP E3 ligase and leads to ubiquitination and proteasomal degradation of TAZ (Liu et al., 2010) (Fig. 10). Other regions are also important for TAZ regulation. Phosphorylation of TAZ by GSK3β on Ser-58 and Ser-62 in human TAZ also recruits β-TrCP, leading to TAZ degradation (Huang et al., 2012).

Hippo pathway deactivation leads to the accumulation of non-phosphorylated TAZ and its translocation to the nucleus. There, TAZ interacts with a variety of transcription factors, not only TEAD, but also Runt-related transcription factor 2 (RUNX2) (Cui et al., 2003), T-box transcription factor 5 (TBX5) (Murakami et al., 2005), paired box protein 3 (PAX3) (Murakami et al., 2006) and Mothers against decapentaplegic homolog 2, 3 and 4 (SMAD2/3/4) (Varelas et al., 2010; Varelas et al., 2008; Mo et al., 2014), among others (Liu et al., 2011). By binding to these factors, TAZ regulates the expression of genes involved in organ development, stem cell proliferation and development of human cancer (Cui et al., 2003; Murakami et al., 2005).

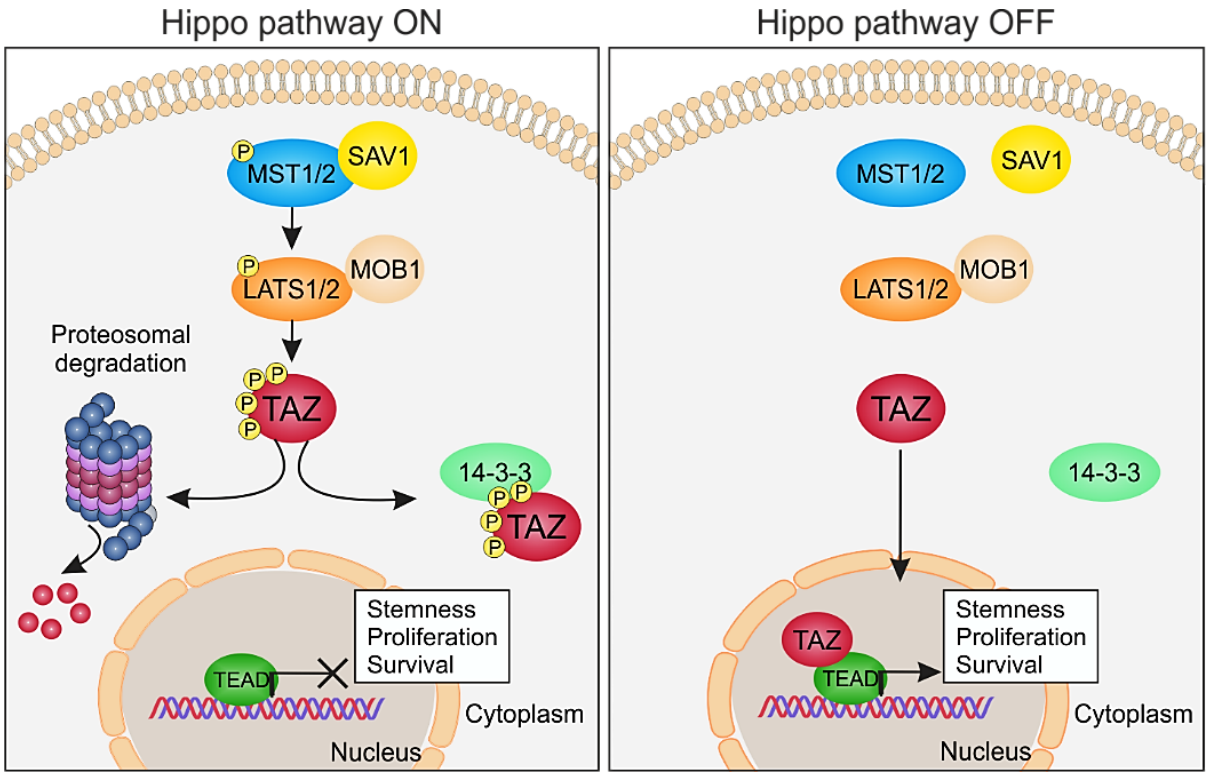


**Figure 10. TAZ regulation by the Hippo pathway.** When Hippo signaling is active the phosphorylated MST1/2 kinase, in complex with SAV1, phosphorylates and activates LATS1/2 in complex with its regulatory protein MOB1. In turn, LATS1/2 phosphorylates TAZ on highly conserved residues located within a consensus sequence (HxRxxS). The phosphorylation of TAZ promotes its cytoplasmic retention by 14-3-3, or its degradation. When the Hippo pathway is off, unphosphorylated TAZ goes to the nucleus, where it binds and activates the TEAD transcription factors and stimulates the expression of genes related to stemness, proliferation and survival.

### 7.2. TAZ function in neurogenesis.

The importance of Hippo signaling is illustrated in early animal development, as precise changes in TAZ/YAP localization are essential for determining some of the first cell fate events between trophectoderm or inner cell mass (Nishioka et al., 2009). Moreover, the Hippo pathway cross-talks with Wnt, BMPs, Notch, and Shh, as these signals also modulate the activities of YAP and TAZ (Hansen et al., 2015). In embryonic stem cells (ESCs), TAZ controls the localization of SMAD2/3-4 proteins in the nucleus which are required for maintenance of self-renewal markers. Furthermore, TAZ loss, but not YAP, results in neuroectoderm differentiation (Varelas et al., 2008). Regarding neurogenesis, most studies have focused in Hippo signaling and YAP, and little is known about the implication of TAZ. For example, reduced YAP levels result in a decreased number of neuroepithelial cells in the developing chick neural tube and *Xenopus laevis* embryo, whereas increased nuclear YAP-TEAD activity drives the expansion of these cells (Cao et al., 2008; Gee et al., 2011). The expression of dominant-negative MST2 or knockdown of LATS1/2 activity was similarly found to drive proliferation of neuroepithelial cells. Additionally, neurofibromin 2 (NF2) has been shown to suppress mouse NPCs expansion by inhibiting YAP activity (Lavado et al., 2013). The same group has recently found that inhibition of Hippo pathway

by LATS1/2 ablation, accompanied by YAP activation, in apical NPCs results in their transient expansion, quickly followed by massive apoptosis (Lavado et al., 2018). All this data point YAP as a "stemness" factor, but the specific role of its paralog TAZ in NSC function and neuronal differentiation is yet to be identified.

### 7.3. TAZ function in glioblastoma.

The Hippo pathway controls organ size and prevents tumorigenesis by inhibiting cell proliferation and promoting apoptosis (Pan, 2010). Therefore, lack of Hippo signaling is associated with tumour progression, and elevated expression and activity of YAP and TAZ co-activators is found in various human cancers (Zender et al., 2006; Chan et al., 2008). The implication of TAZ in cancer has been further analyzed in tumorigenesis, metastasis, and drug resistance (Pan, 2010; Barron and Kagey, 2014; Gomez et al., 2014). One of the main TAZ/TEAD targets is connective tissue growth factor (CTGF), a cytokine important for cell growth and development, which is significant for TAZ function in promoting cell proliferation (Zhang et al., 2009; Zhao et al., 2008a). TAZ sustains proliferation and tumorigenicity of neuroblastomas by targeting CTGF and platelet-derived growth factor β (PDGF-β) (Wang et al., 2015a). Additionally, another direct target of TAZ/TEAD, cysteine-rich, angiogenic inducer 61 (CYR61), cooperatively acts with CTGF to render taxol resistance to TAZ overexpressing breast cancer cells (Lai et al., 2011). Higher expression of another TAZ target, baculoviral inhibitor of apoptosis repeat containing 5 (BIRC5), was associated with worse overall survival in patients with glioma (Zhang et al., 2018).

Regarding GBM, TAZ expression is upregulated in gliomas and correlates with tumour grade (Li et al., 2016b). Yang and colleagues showed that TAZ can promote proliferation and tumour formation in glioblastoma CSCs (Yang et al., 2016). Even more, overexpression of TAZ promoted resistance to the cytotoxic agent temozolomide in the human glioblastoma CSC cell line U87-MG, whereas knockdown of TAZ expression sensitized GBM U251-MG cells to temozolomide (Tian et al., 2015). Altogether, this data suggests that TAZ silencing serves as a potential target for the treatment of GBM. Determining the mechanisms used by TAZ to drive tumour growth and progression will clarify its value in cancer therapy.

# OBJECTIVES

Neurogenesis is a multiple step process that must be tightly orchestrated by multiple extrinsic and intrinsic factors. In this thesis we will explore the relevance of NRF2 and TAZ in the regulation of neurogenesis under physiological and pathological conditions. Our specific objectives are the following:

**1. Analysis of NRF2-mediated regulation of neurogenesis.**

1.1. Impact of NRF2 deficiency in hippocampus-related cognition.
1.2. Role of NRF2 in the proliferative capacity of NSPCs.
1.3. Implication of NRF2 in NSPCs differentiation.
1.4. Relevance of NRF2 deficiency in neurogenesis in an AD mouse model.

**2. Analysis of the molecular connection between NRF2 and TAZ.**

2.1. *In silico* identification and further validation of putative Antioxidant Response Elements (AREs) in the *WWTR1* gene.
2.2. Validation of the NRF2/TAZ axis modulation in NSPCs.

**3. Analysis of the role of TAZ in neural stem cell fate.**

3.1. Characterization of TAZ expression in the neurogenic niche cell types.
3.2. Impact of TAZ activity on neuronal differentiation.
3.3. *In silico* identification and further validation of putative TAZ interaction regions in proneurogenic genes.
3.4. Identification of TAZ as a transcriptional corepressor of proneurogenic genes.
3.5. Pathophysiological significance of the TAZ/proneurogenic factors axis in glioblastoma.

# MATERIAL AND METHODS

# 1. Materials.

## 1.1. Reagents.

**Cell culture**: DMEM (Dulbecco's Modified Eagle Medium) and PBS (Phosphate Buffered Saline) were prepared by the Culture Media Preparation Facility at the *Instituto de Investigaciones Biomédicas "Alberto Sols" (UAM-CSIC)*; DMEM: F12 (1:1), DMEM/F-12 GlutaMAX™ Supplement, neurobasal medium, fetal bovine serum (FBS), B27 supplement, B27 supplement minus vitamin A, glutamine, sodium pyruvate, non-essential aminoacids (L-Ala 44 mM, L-Asn 45 mM, L-Asp 40 mM, L-Glu 40 mM, L-Pro 30 mM), trypsin, trypsin- ethylenediaminetetraacetic acid (EDTA) (0.05%) phenol red, epidermal growth factor (EGF), mouse protein native, basic fibroblast growth factor (bFGF) recombinant human protein, Opti-MEM, N-2-hydroxyethylpiperazine-N'-2-ethanesulfonic acid (HEPES), Penicillin-Streptomycin, $Ca^{2+}$/$Mg^{2+}$-free Hank's balanced salt solution (HBSS) (Gibco, Thermo Fisher Scientific, Grand Island, NY, USA); accutase (StemCell Technologies); gentamicin (Laboratorios Normon, Madrid, Spain); amphotericin B (Lonza, Hopkinton, MA, USA); heparin, polybrene, puromycin, poly-D-lysine hydrobromide (Sigma-Aldrich, St. Louis, Missouri, USA); human fibroblast growth factor and epidermal growth factor (hFGF-2 and hEGF) (Peprotech, NJ, USA); Matrigel hESC-Qualified Matrix (Corning, Bedford, MA, USA); plastic material (Falcon, Thermo Fisher Scientific and BD Biosciences, San Jose, CA, USA); coverslips (VWR, Lutterworth, UK).

**Pharmacological activators, inhibitors and other compounds**: R, S-sulforaphane (SFN) (LKT Laboratories, St Paul, USA).

**DNA manipulation and extraction**: Antibiotics: ampicillin (Sigma-Aldrich). Plasmid DNA preparation: Genopure Plasmid Maxi Kit (Roche Applied Science, Penzberg, Germany), Speedtools Plasmid DNA Purification Kit (mini preps) (Biotools, Madrid, Spain). Plasmid digestions: restriction enzymes (Thermo Fisher Scientific and New England Biolabs). DNA cloning: alkaline phosphatase (Roche), T4 polynucleotide kinase and T4 DNA ligase (Promega). DNA electrophoresis: agarose (CONDA laboratories, Madrid, Spain) and low melting temperature agarose (Nusieve, agarose, Lonza). SYBR Safe DNA Gel Stain (Thermo Fisher Scientific). DNA molecular weight markers: DNAλ HindIII (Thermo Fisher Scientific). DNA purification from band in agarose gel: "Geneclean® Kit" (MP Biomedicals).

**Transfection reagents:** TransFectin™ Lipid Reagent (BioRad, Hercules, California, USA), Lipofectamine 2000 Reagent, Lipofectamine Transfection Reagent and PLUS Reagent (Invitrogen).

**Protein electrophoresis, transfer and immunoblotting**: Protein quantification DC Protein Assay (BioRad). Molecular weight markers: "Bench protein ladder" (Invitrogen). Cuvettes, TEMED (N

N N′N′-Tetramethylethylenediamine), ammonium persulfate, acrylamide/bys-acrylamide (BioRad), Immobilon-P membranes (Millipore), enhanced chemiluminescence substrate (Amersham™ ECL™ Select Western Blotting Detection Reagent, GE Healthcare).

**RNA extraction and qRT-PCR**: TRIzol® Plus RNA Purification Kit (Thermo Fisher Scientific). DNase I, amplification grade (Thermo Fisher Scientific). Retrotranscriptase (High Capacity RNA-to-cDNA Kit, Applied Biosystems). SYBR green, PCR plates (Applied Biosystems), chloroform, isopropanol, ethanol (Merck).

**RNA and DNA quantification:** NanoDrop™ spectrophotometer (Thermo Fisher Scientific).

**Luciferase activity**: Dual-Luciferase® Reporter Assay System (Promega).

**Live assay:** Calcein (#C3099, Molecular Probes/ Thermo Fisher Scientific).

**Proliferation assay:** Click-iT™ 5-ethynyl-2'-deoxyuridine (EdU) Alexa Fluor™ 488 Imaging Kit (C10337, Thermo Fisher Scientific).

**Brain dissection and sectioning:** scissors, scalpels, forceps (Fine Science Tools).

**Immunofluorescence and immunohistochemistry**: paraformaldehyde, formic acid, Triton X-100, 3´-3´-diaminobenzidine tetrahydrochloride (DAB), bovine serum albumin (BSA), xylol, cresyl violet acetate (Sigma-Aldrich); DEPEX mounting media, ProLong™ Gold antifade mountant, horse serum (Thermo Fisher Scientific).

**Chromatin Immunoprecipitation assay (ChIP)**: formaldehyde (Fluka, 47630), glycine (Bio-Rad, 161–0718), protein G Sepharose (GE Healthcare, 17-0618-01), Glycogen (Invitrogen, 10814-010), proteinase K (Sigma-Aldrich, P2308), Triton X-100 (Sigma-Aldrich, T8787), phenylmethylsulfonyl fluoride (PMSF) (Sigma-Aldrich, P7626), leupeptin (Sigma-Aldrich, L8511), phenol: chloroform: isoamyl alcohol 25:24:1 (Sigma-Aldrich, P2069).

### 1.2. Antibodies.

#### 1.2.1. Primary antibodies.

Primary antibodies used in this study are indicated in Table 1. The specificity of TAZ antibody is showed in Fig. 11.

| Antibody | Reference | Clonality | Isotype | Dilution and application |
|---|---|---|---|---|
| Acetyl-Histone H3 | Sigma Aldrich. 06-599. | Polyclonal | Rabbit | 1.5 µg/$10^6$ cells (ChIP) |
| ACTB | Santa Cruz Biotechnology. Sc-1616. | Polyclonal | Goat | 1/5000 (WB) |
| APP/Aβ (6E10) | Covance. 803001. | Monoclonal | Mouse | 1/2000 (WB)<br>1/500 (IHC-Fr/p) |
| Caspase-3 | Cell Signaling Technology. 9662. | Polyclonal | Rabbit | 1/1000 (WB) |
| CHD4 | Abcam. Ab72418. | Polyclonal | Rabbit | 3 µg/$10^6$ cells (ChIP) |
| CTGF (L-20) | Santa Cruz Biotechnology. Sc-14939. | Polyclonal | Goat | 1/2000 (WB) |
| Doublecortin (DCX) | Santa Cruz Biotechnology. Sc-8066. | Polyclonal | Goat | 1/250 (IHC-Fr; ICC/IF) |
| GAPDH | Millipore. CB1001. | Monoclonal | Mouse | 1/15000 (WB) |
| GFAP | Dako. Z0334. | Polyclonal | Rabbit | 1/200 (IHC-Fr; ICC/IF) |
| GFAP | Sigma-Aldrich. G3893. | Monoclonal | Mouse | 1/200 (IHC-Fr; ICC/IF) |
| hNRF2 | Abyntek. Abgent#AJ1555a. | Polyclonal | Rabbit | 1/2000 (WB) |
| IgG2a | Abcam. Ab18413. | Monoclonal | Mouse | 3 µg/$10^6$ cells (ChIP) |
| Ki67 (SP6) | Abcam. Ab16667. | Monoclonal | Rabbit | 1/2000 (IHC-Fr; ICC/IF) |
| Lamin B | Santa Cruz Biotechnology. Sc-6217. | Polyclonal | Goat | 1/2000 (WB) |
| MAP2 | Sigma-Aldrich. M9942. | Monoclonal | Mouse | 1/200 (ICC/IF) |
| Nestin | Abcam. Ab11306. | Monoclonal | Mouse | 1/200 (IHC-Fr; ICC/IF) |
| Nestin | Novus Biologicals. NB100-1604. | Polyclonal | Chicken | 1/500 (IHC-Fr; ICC/IF) |
| Nestin (10c2) | Santa Cruz Biotechnology. Sc-23927. | Monoclonal | Mouse | 1/200 (IHC-Fr; ICC/IF) |
| NEUROD (A-10) | Santa Cruz Biotechnology. Sc-46684. | Monoclonal | Mouse | 1/500 (WB) |
| NQO1 | Abcam. Ab34173. | Polyclonal | Rabbit | 1/2000 (WB) |
| NQO1 | Abcam. Ab2346. | Polyclonal | Goat | 1/2000 (WB) |
| NRF2 | Homemade (Cuadrado´s Lab). | Polyclonal | Rabbit | 1/2000 (WB) |
| RNA Pol II (A-10) | Santa Cruz Biotechnology. Sc-17798. | Monoclonal | Mouse | 3 µg/$10^6$ cells (ChIP) |
| p-Tau (Ser202, Thr205) (AT-8) | Thermo Scientific. MN1020. | Monoclonal | Mouse | 1/200 (IHC-Fr/p; ICC/IF) |
| Rabbit IgG Control | Abcam. Ab37415. | Polyclonal | Rabbit | 1.5 µg/$10^6$ cells (ChIP) |
| SOX2 | R&D Systems. AF2018. | Polyclonal | Goat | 1/500 (IHC-Fr; ICC/IF)<br>1/2000 (WB) |
| Tau (H-150) | Santa Cruz Biotech. Sc-5587. | Polyclonal | Rabbit | 1/200 (IHC-Fr/p; ICC/IF) |
| TAU (HT7) | Thermo Scientific. MN1000B. | Monoclonal | Mouse | 1/2000 (WB)<br>1/250 (IHC-Fr/p; ICC/IF;IHC-P) |
| TAZ | Sigma Aldrich. HPA007415. | Polyclonal | Rabbit | 1/2000 (WB)<br>1/200 (IHC-Fr; ICC/IF)<br>1/100 (ChIP) |
| Tubulin β class III (TUBB3) | Sigma-Aldrich. T2200. | Polyclonal | Rabbit | 1/200 (ICC/IF) |
| V5 | Life Technologies. 37-7500. | Monoclonal | Mouse | 1/2000 (WB) |
| YAP/TAZ (D24E4) | Cell Signaling Technology. 8418. | Monoclonal | Rabbit | 1/2000 (WB)<br>1/250 (IHC-Fr; ICC/IF; IHC-P) |

**Table 1. Primary antibodies** used in immunoblots, immunofluorescence and ChIP, indicating their reference, clonality, isotype and application. ICC/IF: immunocytochemistry/immunofluorescence; IHC-Fr, immunohistochemistry on floating slices; IHC-p, immunohistochemistry on paraffin slices; WB, western blot; ChIP, chromatin immunoprecipitation.

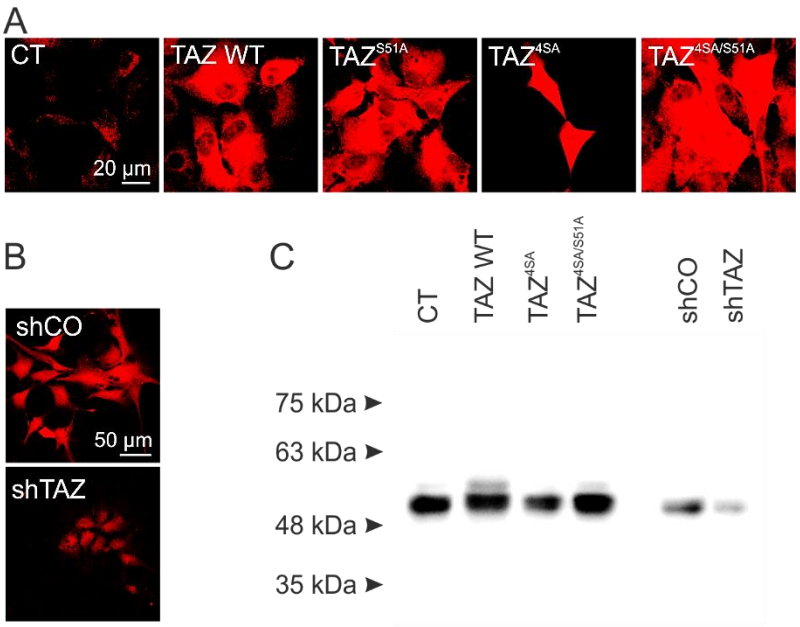


**Figure 11. Characterization of the TAZ antibody. (A)** Representative confocal images of TAZ immunostaining in untransfected cells (CT), or cells expressing wild type (TAZ-WT), or mutant $TAZ^{S51A}$, $TAZ^{4SA}$ and $TAZ^{4SA+S51A}$, after 5 days of retroviral transduction. **(B)** Representative confocal images of TAZ immunostaining in shCO and shTAZ in ReNcells after 5 days of lentiviral transduction. **(C)** Representative immunoblot analysis of TAZ in ReNcells CT, TAZ-WT, $TAZ^{4SA}$ and $TAZ^{4SA+S51A}$, shCO and shTAZ after 5 days of viral transduction, showing a specific band around 50 kDa.

### 1.2.2. Secondary antibodies.

The secondary antibodies conjugated to horseradish peroxidase (HRP) used in WB and the secondary antibodies conjugated to Alexa Fluor® for immunofluorescence are described in Table 2.

| Antibody | Reference | Clonality | Isotype | Dilution and application |
|---|---|---|---|---|
| Alexa Fluor 647 Donkey anti-Goat | Abcam. Ab150131. | Polyclonal | Donkey | 1/500 (IHC-Fr; ICC/IF) |
| Alexa Fluor 647 Donkey anti-Mouse | Thermo Fisher. A-31571. | Polyclonal | Donkey | 1/500 (IHC-Fr; ICC/IF) |
| Alexa Fluor 488 Donkey anti-Mouse | Thermo Fisher. A-21202. | Polyclonal | Donkey | 1/500 (IHC-Fr; ICC/IF) |
| Alexa Fluor 555 Donkey anti-Rabbit | Thermo Fisher. A-31572. | Polyclonal | Donkey | 1/500 (IHC-Fr; ICC/IF) |
| Alexa Fluor 647 Donkey anti-Rabbit | Thermo Fisher. A-31573. | Polyclonal | Donkey | 1/500 (IHC-Fr; ICC/IF) |
| Alexa Fluor 555 Donkey anti-Rat | Abcam. Ab150154. | Polyclonal | Donkey | 1/500 (IHC-Fr; ICC/IF) |
| ECL™ Anti-Rabbit IgG HRP | GE Healthcare. NA934V. | Polyclonal | Donkey | 1/1000 (WB) |
| ECL™ Anti-Mouse IgG HRP | GE Healthcare. NA931V. | Polyclonal | Donkey | 1/1000 (WB) |
| Anti-Goat IgG HRP | Novex Life Technologies. A15999. | Polyclonal | Donkey | 1/1000 (WB) |

**Table 2. Secondary antibodies** used in immunoblots and immunofluorescence. ICC/IF: immunocytochemistry/immunofluorescence; IHC-Fr, immunohistochemistry on floating slices; WB, western blot.

### 1.3. Plasmids.

**pcDNA3.1-mNrf2-V5/HisB:** plasmid encoding the wild type sequence of murine NRF2, with a V5 tag (GKPIPNPLLGLDST) in the C-terminus. This plasmid was originally provided by Dr. John D. Hayes (Division of Cancer Research, School of Medicine, Ninewells Hospital and Medical School, University of Dundee, Dundee).

**pcDNA3.1-mNrf2-ΔETGE-V5/HisB:** plasmid encoding the KEAP1-insensitive version of murine NRF2, with a V5 tag in the C-terminus. This construct lacks residues 79- ETGE-82, responsible for the high affinity binding to KEAP1. This plasmid was originally provided by Dr. John D. Hayes.

**pTK-Renilla:** plasmid used as an internal control in the luciferase assays. It contains the sea pansy (*Renilla reniformis*) luciferase gene under the control of the thymidine kinase promoter from Herpes Simplex Virus for its constitutive expression in mammalian cells.

**p29SOD1:** luciferase reporter pGL3-basic with a modified version of firefly (*Photinus pyralis*) luciferase under the control of the 29 bp-long minimal promoter from the human SOD1 gene (Rojo et al., 2004). This vector has been optimized for monitoring transcriptional activity in transfected eukaryotic cells.

***WWTR1*-ARE2-LUC reporter and *WWTR1*-ARE-mutated-LUC reporter:** oligonucleotides with three tandem repetitions of ARE2 or ARE2-mutated of the *WWTR1* gene promoter (Sigma-Aldrich) were subcloned into the NheI and XhoI sites of a p29SOD1 vector described above. Artificial oligonucleotides are indicated below: ARE sequence is indicated in red, separated with a BamHI site (underlined) and a random separating-sequence (bold letters). Asterisk indicates mutated NheI site to facilitate re-ligated vectors exclusion with NheI digestion prior to transformation. Bold and red letters in *WWTR1* ARE2-mutated indicate nucleotide site mutation.

*WWTR1* ARE2:

5′- CTAGT*GTGACTCAGCTGGATCCGTGACTCAGCT**ACGTGA**GTGACTCAGCTC -3′

3′- A*CACTGAGTCGACCTAGGCACTGAGTCGA**TGCACT**CACTGAGTCGAGAGCT-5′

*WWTR1* ARE2-mutated:

5′- CTAGT*G**C**GACTCAACTGGATCCG**C**GACTCAACT**ACGTGA**G**C**GACTCAACTC -3′

3′- A*C**G**CTGAGTTGACCTAGGC**G**CTGAGTTGA**TGCACT**C**G**CTGAGTTGAGAGCT-5′

***SOX2*-TEAD1(a)-LUC reporter:** oligonucleotides with three tandem repetitions of TEAD1(a) sequence in the promoter of *SOX2* (Sigma-Aldrich) were subcloned into the NheI and XhoI sites of a p29SOD1 vector described above. Artificial oligonucleotides are indicated below: TEAD-recognized

sequence is indicated in red, separated with a BamHI site (underlined) and a random separating-sequence (bold letters). Asterisk indicates mutated NheI site to facilitate re-ligated vectors exclusion with NheI digestion prior to transformation.

5´- CTAGT*CCCCATTCCCATCGGATCCCCCCATTCCCATC**ACGTGA**CCCCATTCCCATCC-3´

3´- A*GGGGTAAGGGTAGCCTAGGGGGGTAAGGGTAG**TGCACT**GGGGTAAGGGTAGGAGCT-5´

**pMD2.G:** plasmid that encodes the G protein from the envelope of the Vesicular Stomatitis Virus used for lentiviral production (Addgene, #12259).

**pSPAX2:** packaging plasmid that encodes the Gag and Pol proteins from the Human Immunodeficiency Virus necessary for lentiviral production (Addgene, #12260).

**pLKO.1-TRC control:** plasmid used for the generation of lentiviral particles with the sequence CCGCAGGTATGCACGCGT to be used as a non-hairpin control (Addgene, #10879).

**pLKO.1-puro shNRF2** (mouse): plasmid used for the generation of lentiviral particles with the sequence CCAAAGCTAGTATAGCAATAA transcribed into a short hairpin RNA (shRNA) sequence against murine *Nfe2l2* gene (MISSION shRNA, Sigma- Aldrich).

**pLKO.1-puro shNRF2** (human): several plasmids have been used to knockdown human *NFE2L2* gene, used for the generation of lentiviral particles (MISSION© shRNA, Sigma-Aldrich, SHCLNG-NM_006164) and are indicated below with their targeting sequence:

- TRCN0000007555: AGTTTGGGAGGAGCTATTATC.
- TRCN0000007556: GCACCTTATATCTCGAAGTTT.
- TRCN0000007557: CCCTGTTGATTTAGACGGTAT.
- TRCN0000007558: CCGGCATTTCACTAAACACAA.
- TRCN0000273494: AGTTTGGGAGGAGCTATTATC.

**pLKO.1-puro shTAZ** (human): plasmid used for the generation of lentiviral particles with the sequence GCGTTCTTGTGACAGATTATA transcribed into a shRNA sequence against human *WWTR1* gene (shRNA WWTR1 SHCLNG-NM_015472 TRCN0000370007) (MISSION© shRNA, Sigma-Aldrich).

**pLKO.1-puro shTEAD2** (human): plasmid used for the generation of lentiviral particles with the sequence ATGACCTGTGAGATCACAAAG transcribed into a shRNA sequence against human *TEAD2* gene (shRNA TEAD2 SHCLNG-NM_003598, TRCN0000426430) (MISSION© shRNA, Sigma-Aldrich).

**pLKO.1-puro shTEAD1/3/4** (human): plasmid used for the generation of lentiviral particles with the sequence ATGATCAACTTCATCCACAAG transcribed a shRNA sequence targeting an identical region in TEAD1, TEAD3 and TEAD4. This plasmid was a generous gift from Prof. Zengqiang Yuan.

**pWPXL**: plasmid generated from pWPXL-GFP, a plasmid for the generation of lentiviral particles expressing the green fluorescence protein (GFP) under the control of the Elongation Factor 1α promoter. This plasmid was originally provided by Dr. Didier Trono (School of Life Sciences, École Polytechnique Fédérale de Lausanne, Switzerland). In the pWPXL plasmid, the GFP encoding sequence has been removed.

**pWPXL-mNrf2-V5/HisB**: plasmid for the generation of lentiviral particles expressing the murine NRF2 and with a V5 tag in the C-terminus. The mNrf2-V5/HisB insert from pcDNA3.1-mNrf2-V5/HisB was subcloned into the BstEII and SmaI/PmeI restriction sites of the pWPXL vector.

**pWPXL-mNrf2-ΔETGE-V5/HisB**: plasmid for the generation of lentiviral particles expressing the murine version of NRF2 lacking residues 79-ETGE-82 and with a V5 tag in the C-terminus. The mNrf2-ΔETGE-V5/HisB insert from pcDNA3.1-mNrf2-ΔETGE-V5/HisB was subcloned into the BsteII and SmaI/PmeI restriction sites of the pWPXL vector.

**pCMV-Gag-Pol**: retroviral packaging vector which encodes for retroviral genes *Gag* and *Pol* (Cell Biolabs, RV-111).

**pCMV-VSV-G**: plasmid encoding the envelope protein for producing retroviral particles (Addgene, #8454).

**pCL-Ampho**: packaging vector designed to maximize recombinant-retrovirus titers (Novusbio, NBP2-29541).

**pBABE-puro**: control retroviral vector for the overexpression of TAZ mutants. This plasmid presents puromycin selection (Addgene, #1764).

**pBABE-puro-TAZ-WT**: retroviral vector encoding the wild type sequence of human TAZ protein. This plasmid was a generous gift from Dr. Kun-Liang Guan (Department of Pharmacology and Moores Cancer Center, University of California, San Diego, USA) (Fig. 12).

**pBABE-puro-TAZ-S51A**: retroviral vector encoding the TEAD-binding-defective mutant form of human TAZ. Serine 51 has been replaced to alanine which selectively abolishes TAZ ability to activate TEAD (Zhang et al., 2009). This plasmid was a generous gift from Dr. Kun-Liang Guan (Fig. 12).

**pBABE-puro-TAZ-4SA**: retroviral vector encoding constitutively active mutant form of human TAZ, resistant to inhibition by LATS kinases. All putative phosphorylation sites, the four serine residues in the HxRxxS motifs, have been replaced to alanine residues (S66A, S89A, S117A, and S311A) (Lei et al., 2008). This plasmid was a generous gift from Dr. Kun-Liang Guan (Fig. 12).

**pBABE-puro-TAZ-4SA-S51A**: retroviral vector encoding constitutively active and TEAD-defective mutant of human TAZ. This plasmid was a generous gift from Dr. Kun-Liang Guan (Fig. 12).

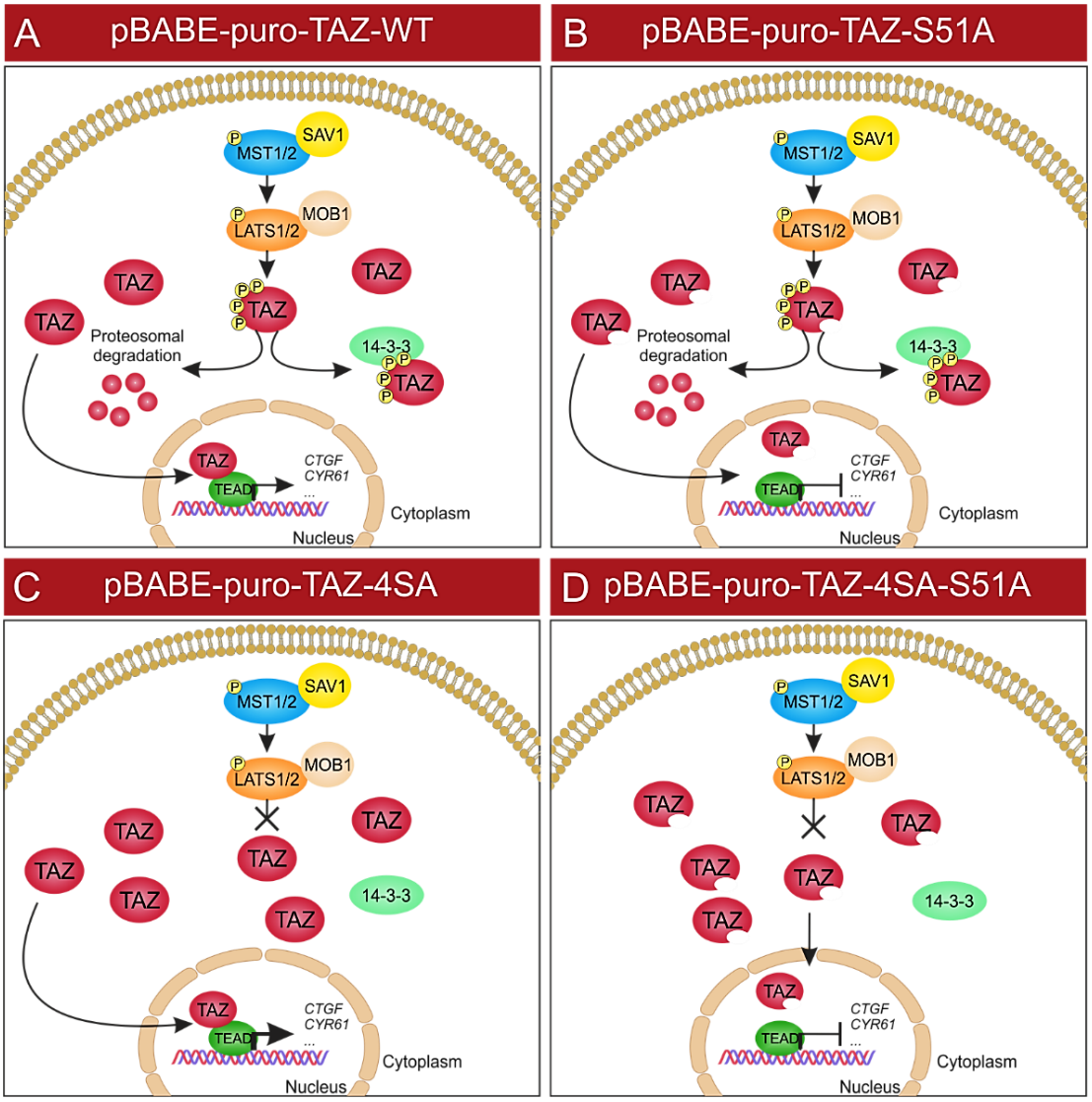


**Figure 12. Graphical overview of the different TAZ mutants used in this study. (A)** Wild type TAZ is phosphorylated by LATS kinases leading to sequestration in the cytosol with 14-3-3 proteins and its proteasomal degradation. **(B)** Mutant TAZ-51A cannot bind TEAD and competes with endogenous TAZ for phosphorylation (dominant negative). **(C)** Mutant TAZ-4SA is not phosphorylated by LATS kinases and therefore is constitutively active. **(D)** Mutant TAZ-4SA-51A combines constitutive activation with lack of TEAD binding.

### 1.4. Buffers and solutions.

**General buffers**: Luria-Bertani medium (LB) for the growth of bacteria, LB agar plates, phosphate saline buffer (PBS), 1 M Tris-HCl pH 7.5, 1 M Tris-HCl pH 8.8, 1 M Tris- HCl pH 6.6, 1 M HEPES pH 7.5, 10% sodium dodecyl sulfate (SDS), 0.5 M EDTA pH 8.0 and 0.5 M EGTA pH 7.5 were provided by the Culture Media Preparation Facility at the *Instituto de Investigaciones Biomédicas "Alberto Sols" (UAM-CSIC).*

**Cellular lysis buffer**: 50 mM Tris pH 7.6, 400 mM NaCl, 1 mM EDTA, 1 mM EGTA, 1% SDS.

**Protein loading buffer for SDS-PAGE (5X)**: 50 mM Tris-HCl pH 6.8, 2% SDS, 0.1% bromophenol blue, 10% glycerol, 150 mM β-mercaptoethanol.

**Electrophoresis running buffer**: 0.37% EDTA, 191 mM glycine, 0.1% SDS and 25 mM Tris-HCl pH 7.4.

**Transfer buffer**: 25 mM Tris-HCL pH 7.4, 191 mM glycine and 20% methanol.

**Tris buffered saline with Tween 20 (TTBS)**: 50 mM Tris-HCl pH 7.5, 150 mM NaCl and 0.1% Tween-20.

**DNA loading buffer**: DNA Gel Loading Dye (6X) (Thermo Scientific), consisting on 10 mM Tris-HCl (pH 7.6), 0.03% bromophenol blue, 0.03% xylene cyanol, 60% glycerol and 60 mM EDTA.

**Tris buffered saline (TBS)**: 100 mM Tris-HCl pH 7.5 and 225 mM NaCl.

**Tris-EDTA buffer (TE)**: 10 mM Tris-HCl pH 7.5 and 1 mM EDTA.

**Tris base, acetic acid and EDTA buffer (TAE)**: 40 mM Tris-HCl pH 7.5, 20 mM acetic acid and 1mM EDTA.

**ChIP assay buffers**: PBS, Elution Buffer (1% SDS, 0.1 M $NaHCO_3$), SDS Lysis Buffer (1% SDS, 10 mM EDTA, 50 mM Tris-HCl pH 8.0), Dilution Buffer (0.01% SDS, 1.1% Triton X-100, 1.2 mM EDTA, 16.7 mM Tris-HCl (pH 8.0), 167 mM NaCl), Low Salt Washing Buffer (0.1% SDS, 1% Triton X-100, 2 mM EDTA, 20 mM Tris-HCl pH 8.0, 150 mM NaCl), High Salt Washing Buffer (0.1% SDS, 1% Triton X-100, 2 mM EDTA, 20 mM Tris-HCl pH 8.0, 500 mM NaCl), LiCl Washing Buffer (0.25 mM LiCl, 1% NP-40, 1% sodiumdesoxycholate, 1 mM EDTA, 10 mM Tris-HCl pH 8.0) and TE buffer (10 mM Tris-HCl pH 8.0, 1 mM EDTA).

### 1.5. Bacterial stocks.

The high efficiency competent strain DH5-α of *Escherichia coli* was provided by the Culture Media Preparation Facility from the *Instituto de Investigaciones Biomédicas "Alberto Sols" (UAM-CSIC)*.

### 1.6. Cell lines.

**HEK293T:** cell line derived from human embryonic kidney cells, generated in 1987 in Dr. Michele P. Calos (Standford University, USA) by stable insertion of the simian virus 40 (SV40) large T antigen in the HEK293 cell line. This allows a very efficient replication of vectors carrying the SV40 region of replication, achieving remarkable expression levels.

**HEK293T/17:** specific clone (clone 17) from HEK293T cells that was selected for its high transfectability (Rockefeller University, USA), which makes them especially suitable for lentiviral and retroviral production.

**Murine Neural Stem/Progenitor Cells:** primary neural stem/progenitor cell cultures were generated from the neurogenic niches of postnatal and adult *Nrf2*-WT, *Nrf2*-KO, APP-TAU-*Nrf2*-WT and APP-TAU-*Nrf2*-KO with the method described in section 2.2.1.

**Human Neural Progenitor Cell line ReNcell VM:** The immortalized neural progenitor cell line derived from ventral mesencephalon of human fetal brain were purchased from EMD Millipore (Billerica, MA, USA, Ref. SCC008). ReNcell VM cell line was developed by the ReNeuron Group plc. Cells were immortalized using retroviral transduction with the v-myc oncogene and are able to generate neurons and glia cells under differentiation conditions. In this study ReNcell VM will be abbreviated to ReNcell.

**U87-MG** (ATCC® HTB-14™): Human primary glioblastoma/astrocytoma cell line derived by explant technique from a male patient (Ponten and Macintyre, 1968; Westermark et al., 1973).

### 1.7. Animals.

Animals were housed under a 12 h light-dark cycle. Food and water were provided *ad libitum* and mice were cared according to protocols approved by the Ethics Committee for Research of the Universidad Autónoma de Madrid following institutional, Spanish and European guidelines (RD 53/2013, and ECC 566/2015, 2010/63/UE European Council Directives).

C57/BL6J-*Nrf2*$^{-/-}$ (*Nrf2*$^{-/-}$) mice and their wild type counterparts were kindly provided by Dr. Masayuki Yamamoto (Tohoku University Graduate School of Medicine, Sendai, Japan) (Itoh et al.,

1997). C57/BL6J-*Nrf2*$^{-/-}$ mice bear a lacZ-neo cassette replacing a 1.2 kb long segment from the fifth exon of *Nrf2*.

APP-TAU-*Nrf2*$^{+/+}$ (AT-*Nrf2*$^{+/+}$) and APP-TAU-*Nrf2*$^{-/-}$ (AT-*Nrf2*$^{-/-}$) mice were obtained by crossing the proper founder mice. APP$^{V717I}$ mice expressing in heterozygosis the human APP isoform 695 carrying the V717I (London) mutation under the control of neuron specific mouse *Thy1* promoter (Vidal et al., 1990; Moechars et al., 1999), were backcrossed with C57/BL6J-*Nrf2*$^{+/+}$ or C57/BL6J-*Nrf2*$^{-/-}$ mice for over five generations. TAU$^{P301L}$ mice, expressing in homozygosis human TAU isoform of 441 aminoacids containing four repeats, with 2 N-terminal inserts, and carrying P301L mutation (Tg(Thy1-MAPT*P301L)2Vln) under control of the neuron-specific mouse *Thy1* gene promoter (Terwel et al., 2005), were backcrossed with C57/BL6J-*Nrf2*$^{+/+}$ or C57/BL6J-*Nrf2*$^{-/-}$ mice for over five generations. APP$^{V717I}$ (*Nrf2*$^{+/+}$ or *Nrf2*$^{-/-}$) mice and TAU$^{P301L}$ (*Nrf2*$^{+/+}$ or *Nrf2*$^{-/-}$) mice were backcrossed for over five generations to obtain offspring APP-TAU-*Nrf2*$^{+/+}$ (AT-*Nrf2*$^{+/+}$) and APP-TAU-*Nrf2*$^{-/-}$ (AT-*Nrf2*$^{-/-}$), respectively.

Nude mice (*Foxn1*$^{nu}$) are athymic and lack cell-mediated immunity (The Jackson Laboratory, stock #002019) (Kaushik et al., 1995).

### 1.8. Human material.

Human glioblastomas (GB) were derived from brain surgery biopsies in the Hospital Ramón y Cajal (Madrid, Spain). These cells were kindly supplied by Dr. Marta Izquierdo (*Centro de Biología Molecular "Severo Ochoa" - UAM*), with the approval of the Ethic Committees of UAM and Hospital Ramón y Cajal.

## 2. Methods.

### 2.1. *In silico* assays.

#### 2.1.1. *In silico* analysis of putative binding sequences of transcription factors.

The putative elements recognized by the transcription factors of interest were identified based on the data available in the Encyclopedia of DNA Elements at UCSC (ENCODE) (https://genome.ucsc.edu/encode/) for human genome (Feb. 2009). This database contains chromatin immunoprecipitation (ChIP) information available for several transcription factors. Regarding NRF2, there is not data available, but there is for other ARE-binding factors such as MAFF, MAFK and Bric-a-brac homodimerization domain and cap 'n' collar homolog 1 (BACH1). For transcription cofactor TAZ studies, data are available for several TAZ-binding partners as TEADs, SMADs and RUNX. These sequences were localized in DNase hypersensitive and H3K27Ac-enriched regions, often found near regulatory elements and, in particular, in promoters. The selected sequences from ENCODE where next compared with the consensus sequence recognized by each transcription factor based on the position frequency matrix from the JASPAR database (http://jaspar.genereg.net/) derived from published and experimentally defined transcription factor binding sites for eukaryotes, which is converted to a PSSM (Position Specific Scoring Matrix) (PSSM for each transcription factor analyzed are available in Tables 3 to 9) using $\log_2$(odd-ratio) (Sandelin et al., 2004; Khan et al., 2018). The robustness of these PSSMs depends on the amount of data available for each transcription factor in the JASPAR database. For analysis, a script was generated with Python 3.4 (Appendix I). The relative score for each putative site was calculated with the following formula:

$$Score\ relative = \frac{Score\ of\ the\ sequence\ max - Score \min possible}{Score \max possible - Score \min possible}$$

where score of the sequence max is the addition of the score of each pair base of the selected sequence based on the PSSM, the score min possible is the summation of all negative values of the PSSM, so the lowest possible score able to obtain for a sequence, and the score max possible is the addition of all the positive values from the PSSM, so the highest possible score able to obtain. The Python script for NRF2 and its PSSM were a courtesy of Natalia Jiménez-Moreno (present address: University of Bristol, UK). The script was modified for TEADs, SMADs and RUNX2 to obtain their PSSM. The data of the relative scores for the putative binding sites are available in Results.

| | 1 | 2 | 3 | 4 | 5 | 6 | 7 | 8 | 9 | 10 | 11 |
|---|---|---|---|---|---|---|---|---|---|---|---|
| **A** | 1.1375 | -2.3219 | -2.3219 | 2.0704 | -2.3219 | 0.4854 | 0.2630 | 1.7655 | -2.3219 | -2.3219 | 1.6781 |
| **C** | -1.3219 | -2.3219 | -2.3219 | -2.3219 | 1.8480 | -0.7370 | 1.1375 | -2.3219 | -2.3219 | 2.0704 | -0.7370 |
| **G** | 1.0000 | -2.3219 | 2.0000 | -2.3219 | -1.3219 | -1.3219 | -1.3219 | -0.7370 | 2.0704 | -2.3219 | -0.7370 |
| **T** | -2.3219 | 2.0704 | -1.3219 | -2.3219 | -0.7370 | 1.2630 | 0.0000 | -0.7370 | -2.3219 | -2.3219 | -1.3219 |

**Table 3. Position specific scoring matrix (PSSM) for NRF2** and its motif from JASPAR database. PSSM is derived from the frequency matrix available in JASPAR database.

| | 1 | 2 | 3 | 4 | 5 | 6 | 7 | 8 | 9 | 10 | 11 | 12 |
|---|---|---|---|---|---|---|---|---|---|---|---|---|
| **A** | -0.58496 | 1.73697 | -1.58496 | 2.11548 | -1.58496 | -1.58496 | -1.58496 | -1.58496 | 1.00000 | -0.58496 | 0.00000 | -1.58496 |
| **C** | 1.22239 | -1.58496 | 2.11548 | -1.58496 | -1.58496 | -1.58496 | 2.11548 | 2.00000 | -1.58496 | 1.41504 | 0.73697 | 0.00000 |
| **G** | -0.58496 | 0.41504 | -1.58496 | -1.58496 | -1.58496 | -1.58496 | -1.58496 | -1.58496 | -1.58496 | 0.73697 | 0.41504 | 1.58496 |
| **T** | 0.73697 | -1.58496 | -1.58496 | -1.58496 | 2.11548 | 2.11548 | -1.58496 | -0.58496 | 1.41504 | -1.58496 | 0.41504 | 0.00000 |

**Table 4. Position specific scoring matrix (PSSM) for TEAD1** and its motif from JASPAR database. PSSM is derived from the frequency matrix available in JASPAR database.

| | 1 | 2 | 3 | 4 | 5 | 6 | 7 | 8 | 9 | 10 | 11 | 12 | 13 |
|---|---|---|---|---|---|---|---|---|---|---|---|---|---|
| **A** | 0.0264 | -0.6064 | 1.7058 | -1.7602 | 1.9347 | -5.4972 | -3.0821 | -3.9122 | -3.9122 | 0.9622 | -0.2620 | -0.2748 | -0.3008 |
| **C** | 0.1077 | 0.8187 | -2.9122 | 1.8217 | -4.4972 | -3.6227 | -3.9122 | 1.8865 | 1.9235 | -1.1514 | -0.2748 | 0.3525 | 0.7123 |
| **G** | -0.2620 | -0.7246 | -0.9324 | -3.1753 | -3.4972 | -4.2748 | -3.7602 | -3.6227 | -5.0821 | -1.2493 | 0.6183 | 0.1273 | -0.1995 |
| **T** | 0.1370 | 0.0053 | -3.1753 | -3.4972 | -3.7602 | 1.9540 | 1.9150 | -2.4383 | -2.8342 | 0.2754 | -0.2620 | -0.2620 | -0.4972 |

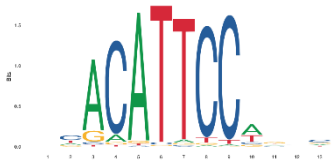

**Table 5. Position specific scoring matrix (PSSM) for TEAD2** and its motif from JASPAR database. PSSM is derived from the frequency matrix available in JASPAR database.

| | 1 | 2 | 3 | 4 | 5 | 6 | 7 | 8 |
|---|---|---|---|---|---|---|---|---|
| **A** | 1.14803 | -1.16312 | 1.92317 | -12.46518 | -0.30815 | -12.46518 | -12.46518 | 1.92317 |
| **C** | -6.39909 | 1.74252 | -12.46518 | -12.46518 | -7.88022 | 1.92317 | 1.92317 | -2.44282 |
| **G** | 0.65667 | -3.67728 | -12.46518 | -12.46518 | -2.54334 | -12.46518 | -12.46518 | 0.61413 |
| **T** | -2.34884 | -12.46518 | -12.46518 | 1.92317 | 1.57776 | -12.46518 | -10.14326 | 1.27291 |

**Table 6. Position specific scoring matrix (PSSM) for TEAD3** and its motif from JASPAR database. PSSM is derived from the frequency matrix available in JASPAR database.

| | 1 | 2 | 3 | 4 | 5 | 6 | 7 | 8 | 9 | 10 |
|---|---|---|---|---|---|---|---|---|---|---|
| **A** | -0.18715 | 1.35382 | 0.78330 | 2.00143 | -3.52214 | -0.24010 | -7.98157 | -2.33771 | 1.18082 | -0.20021 |
| **C** | 0.51429 | -3.45801 | 2.00143 | -4.28113 | -7.98157 | -7.98157 | 2.00143 | 2.00143 | -1.60653 | 0.19834 |
| **G** | -0.22668 | 0.53807 | -2.85228 | -3.52214 | -7.98157 | -3.89410 | -3.65964 | -6.98157 | -0.15502 | -0.33771 |
| **T** | -0.22668 | -3.02737 | -3.73364 | -3.22668 | 2.00143 | 2.00143 | -3.17421 | 0.46552 | 0.79979 | 0.27110 |

**Table 7. Position specific scoring matrix (PSSM) for TEAD4** and its motif from JASPAR database. PSSM is derived from the frequency matrix available in JASPAR database.

| | 1 | 2 | 3 | 4 | 5 | 6 | 7 | 8 | 9 | 10 | 11 | 12 | 13 |
|---|---|---|---|---|---|---|---|---|---|---|---|---|---|
| **A** | -0.4285 | -0.1901 | -3.9053 | -2.7247 | -7.8122 | -7.8122 | -1.0707 | -0.0843 | -7.8122 | 1.7690 | -2.8580 | -0.9295 | -1.0178 |
| **C** | 0.9460 | -1.5642 | -4.6423 | -2.2886 | 2.0016 | -7.8122 | 0.0458 | -0.8349 | 1.9968 | -3.4902 | 1.7133 | 1.3776 | -0.0640 |
| **G** | -0.4113 | -2.6829 | 1.9659 | -1.1117 | -7.8122 | -7.8122 | 1.2646 | 0.3222 | -5.8122 | -3.5642 | -0.7461 | -2.2272 | -2.6423 |
| **T** | -0.7461 | 1.4046 | -7.8122 | 1.6777 | -7.8122 | 2.0016 | -3.2272 | 0.3376 | -7.8122 | -1.1975 | -7.8122 | -0.5548 | 1.2673 |

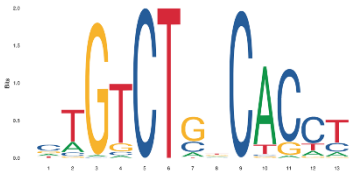

**Table 8. Position specific scoring matrix (PSSM) for SMAD2/3/4** and its motif from JASPAR database. PSSM is derived from the frequency matrix available in JASPAR database.

| | 1 | 2 | 3 | 4 | 5 | 6 | 7 | 8 | 9 |
|---|---|---|---|---|---|---|---|---|---|
| **A** | 0.9466 | 1.7204 | 1.7204 | -10.9726 | -10.9726 | -0.0695 | -10.9726 | 1.7204 | 1.0646 |
| **C** | -0.8785 | -1.8511 | -2.6239 | 1.7204 | 1.7204 | -5.7632 | 1.7204 | -2.0748 | -1.5675 |
| **G** | -2.6195 | -0.7247 | -10.9726 | -10.9726 | -10.9726 | 1.2283 | -10.9726 | -2.1303 | -0.8241 |
| **T** | 0.4521 | -1.7853 | -10.9726 | -10.9726 | -10.9726 | -4.0538 | -10.9726 | -3.3877 | -1.7247 |

**Table 9. Position specific scoring matrix (PSSM) for RUNX2** and its motif from JASPAR database. PSSM is derived from the frequency matrix available in JASPAR database.

### 2.1.2. Brain RNA-seq data.

The Brain RNA-seq database from Stanford University, Stanford, CA, USA (http://www.brainrnaseq.org/) was analyzed for TAZ encoding-gene expression in astrocytes, neurons and endothelial cells both in human and murine tissue. This database contains transcriptome data from purified populations of the main cell types present in the brain, but not for neural stem cells. Murine data was obtained by RNA sequencing of cell types derived from the cerebral cortex (Zhang et al., 2014). Transcriptome profiles for humans were obtained from purified cell cultures derived from juvenile and adult temporal lobe cortex tissue and brain fetal tissue (Zhang et al., 2016).

### 2.1.3. UCSC Xena platform.

UCSC Xena system is an analysis tool which hosts datasets from several landmark cancer genomics resources as TCGA (The Cancer Genome Atlas) (https://xenabrowser.net/). This platform was examined to obtain the survival rate and the correlation between different proteins based on the data available in TCGA for low-grade glioma and glioblastoma (Goyal, 2019).

## 2.2. *In vitro* assays.

### 2.2.1. Cell lines.

**HEK293T and HEK237T/17** cells were grown in DMEM supplemented with 10% FBS, 4 mM L-glutamine and 80 µg/ml gentamicin.

**U87-MG and GB from human explant** were grown in adhesion conditions in DMEM supplemented with 10% FBS, 4 mM L-glutamine, 5 mM HEPES, 80 µg/ml gentamicin and 1 µg/ml amphotericin B. When maintained in stem cell culture conditions, cells were plated on uncoated 10 cm dishes in DMEM: F12 (1:1) supplemented with 2 mM L-glutamine, 5 mg/ml albumax I, 6 mg/ml glucose, B27 supplement (without vitamin A), 15 ng/ml hFGF-2, 20 ng/ml hEGF, 2 µg/ml heparin, 80 µg/ml gentamicin and 1 µg/ml amphotericin B, and allowed to grow forming spheres in an incubator with 5% $CO_2$ and 95% atmospheric air at 37°C.

**Human neural progenitor ReNcells** were grown in neurobasal medium supplemented with 1X B27 supplement, 2 mM L-glutamine, 1X non-essential aminoacids, 1 mM sodium pyruvate, 20 ng/ml hEGF, 20 ng/ml hFGF-2, 100 U/ml penicillin/streptomycin and 1 µg/ml amphotericin B. ReNcells were plated onto Corning Matrigel hESC-Qualified Matrix-coated T75 cell culture flasks and maintained in an incubator with 5% $CO_2$ and 95% atmospheric air at 37°C.

**Primary neural stem/progenitor cell (NSPCs) cultures** were stablished from the neurogenic niches of the SGZ and SVZ of mice from postnatal day 0-4 and 3-month-old mice of *Nrf2*$^{+/+}$, *Nrf2*$^{-/-}$, AT-*Nrf2*$^{+/+}$ and AT-*Nrf2*$^{-/-}$ genotypes following the protocol described in (Bernardino et al., 2008). Briefly, after the mice were euthanized by decapitation, brains were removed and chopped in 450 µm sections. Under the magnifier, neurogenic niches were isolated in each section with ultrafine forceps and put in dissection media ($Ca^{2+}$/$Mg^{2+}$- free HBSS supplemented with 100 U/ml penicillin/streptomycin). Then, tissue pieces were digested in 0.025% trypsin and 0.265 mM EDTA during 10 min at 37°C.Cells were washed twice in dissection media and the pellet was dissociated in the proliferation medium (DMEM/F12/Glutamax supplemented with 1x B27 without vitamin A, 10 ng/ml EGF, 5 ng/ml bFGF, 2

µg/ml heparin and 100 U/ml penicillin/streptomycin) by gentle trituration with a P1000 pipette. For adult-derived cultures, the medium was the same as for neonatal-derived cultures but using 20 ng/ml EGF, 20 ng/ml bFGF and 4 µg/ml heparin. Single cells were then plated on uncoated 10-cm dishes at a concentration of 200,000 cell/ml and were allowed to grow in an incubator with 5% $CO_2$ and 95% atmospheric air at 37°C. In culture, the progenitor cells proliferate and form neurospheres (Fig. 13).

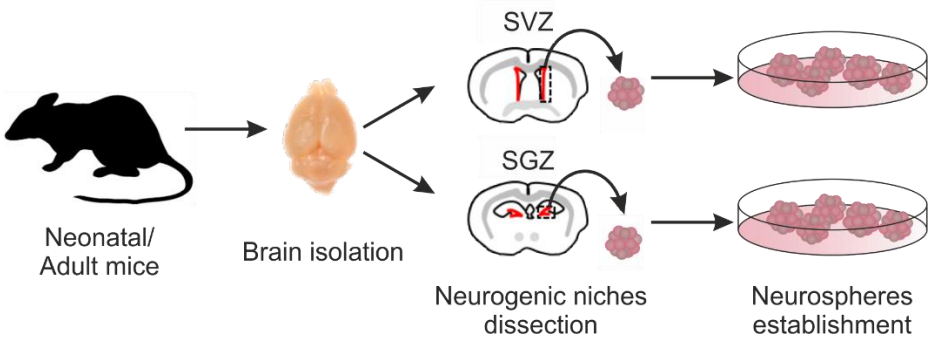


**Figure 13. Primary neural stem/progenitor cells cultures establishment.** Neural stem/progenitor cells were isolated from the neurogenic niches (subventricular zone (SVZ) and subgranular zone (SGZ)) of neonatal and adult mice.

### 2.2.2. Proliferation assays of primary cultures of NSPCs.

**Neurosphere quantification:** Primary neurospheres were dissociated with 1X accutase for 5 min at 37°C and cultured at low density (20,000 cells/ml) in proliferation media to obtain the secondary neurospheres. Secondary neurospheres were quantified by counting 16 distinct fields in each culture dish (three dishes per condition) under 4X magnification (AxioPhot, Carl Zeiss). Similar protocol was followed for the quantification of neurospheres from U87-MG and GB cultures, but using Trypsin-EDTA to dissociate the neurospheres.

**Cell number quantification:** neurospheres were disaggregated with accutase to quantify cell number using a Neubauer chamber. This protocol was followed for the quantification of cell number in U87-MG and GB cultures.

**Serial dilution assay:** secondary neurospheres were disaggregated with accutase and seeded into a 96-well plate in an amount of 5, 25, 125, 250, 500 and 1000 cells/well. Five wells per condition were plated. Cells were incubated in 5% $CO_2$ and 95% atmospheric air at 37°C in proliferation media during 7 days allowing the formation of tertiary neurospheres. Formed neurospheres were quantified under 4x magnification in each well (Corenblum et al., 2016).

**Cell pair assay:** primary neurospheres were disaggregated with accutase and plated on poly- D-lysine-coated coverslips at low density (10,000 cells/$cm^2$) for 24 h with proliferation media containing

half concentration of EGF and bFGF and immunostained for SOX2 and Nestin following the protocol described in section 2.2.9. This assay allows for the quantification of the number of symmetric cell divisions (self-renewal potential, both cells in the pair are $SOX2^{+}/Nestin^{+}$) and asymmetric divisions (differentiation of neural stem/progenitor cells, $SOX2^{+}/Nestin^{+}$ and $SOX2^{-}/Nestin^{-}$ cells present in the cell pair (Fig. 14). Divisions were quantified under 40X magnification (Leica TCS SP5 Confocal Laser Scanning Microscope) and using FiJi (ImageJ Software).

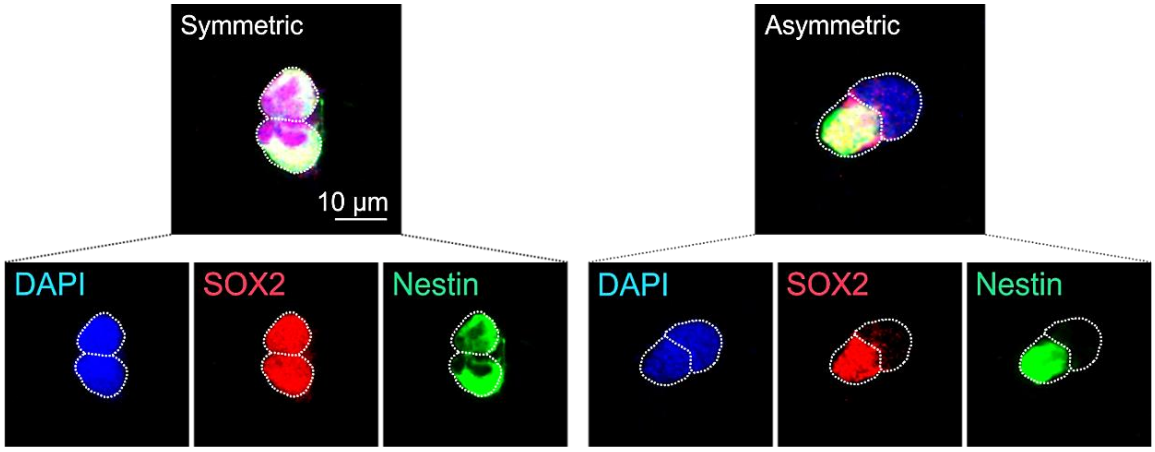


**Figure 14. Cell pair assay.** Neural progenitor cells could undergo symmetric divisions (left) giving rise to two progenitors siblings, positive for SOX2 and Nestin. Neural progenitor cells could also give rise to a progenitor cell and a differentiated cell (asymmetric division, right).

**EdU assay:** Neurospheres were plated on poly- D- lysine- coated glass coverslips in proliferation media and treated with 10 µM 5-ethynyl-2'-deoxyuridine (EdU) (Click-iT® EdU Imaging Kits, Invitrogen) during 8 h and allow to differentiate for 5 days in differentiation media (DMEM/F12/Glutamax, 1X B27 without vitamin A and 100 U/mL penicillin/streptomycin). Finally, cells were fixed with 4% paraformaldehyde (PFA) and immunostained for EdU following the manufacturer´s instructions. Immunolabeling with the primary antibodies detailed in the Table 1 was performed as described in section 2.2.9. Nuclei were counterstained with Hoestcht 33342. At least 20 neurospheres per condition were analyzed under 40X magnification (Leica TCS SP5 Confocal Laser Scanning Microscope).

### 2.2.3. Calcein-AM Cell Viability Assay.

Neurospheres were plated in poly- D- lysine covered glass coverslips and treated in proliferation media with 3 µM Calcein-AM (acetoxymethyl ester of calcein) (#C3099, Molecular Probes/Invitrogen) during 30 min at 37°C, and fixed with 4% PFA. Nuclei were counterstained with 4',6-diamidino-2-fenilindol (DAPI). Calcein-AM is a non-fluorescent and membrane permeable compound. In live cells, Calcein-AM is converted by cytoplasmatic esterases to calcein, a green fluorescent (excitation at 488 nm

and emission at 520 nm), and non-permeable membrane compound which is retained in the cytoplasm of live cells, giving them a green fluorescent labelling. In death cells, the absence of active esterases impedes Calcein-AM conversion to calcein, not acquiring green fluorescence (Fig. 15). Live cells were quantified under 40X magnification (Leica TCS SP5 Confocal Laser Scanning Microscope) and using FiJi (ImageJ Software).

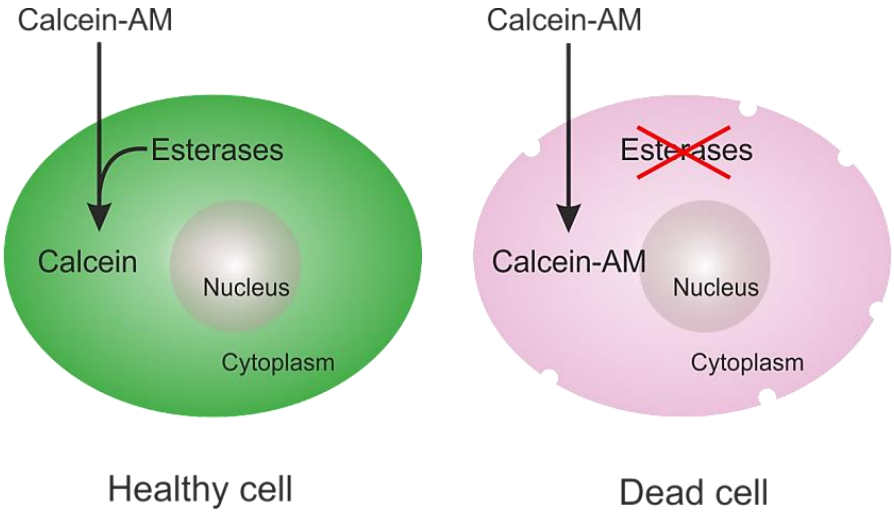


**Figure 15. Graphic overview of Calcein-AM cell viability assay.** Calcein-AM is membrane-permeable and non-fluorescent. In healthy cells, cytoplasmatic esterases cleave it into calcein, a green fluorescent dye that is retained in the cell. In dead cells esterase activity is missing and Calcein-AM does to convert into the green fluorescent Calcein

### 2.2.4. Differentiation assays of primary culture of NSPCs.

Five-day-old secondary neurospheres were plated on poly- D- lysine- coated coverslips, at approximately 30 neurospheres per coverslips, and incubated for 7 days in differentiation medium (DMEM: F12-Glutamax, B27 without vitamin A and 100 U/ml penicillin/streptomycin). After fixation in 4% PFA, cells were immunolabelled as described below and quantified under 40x magnification (Leica TCS SP5 Confocal Laser Scanning Microscope) and using FiJi (ImageJ Software).

### 2.2.5. Differentiation assays of ReNcells.

ReNcells were plated on Corning Matrigel hESC-Qualified Matrix coated coverslips, at a density of 30,000 cells/cm$^2$, and incubated for 30 days in differentiation medium: neurobasal medium supplemented with 1X B27 supplement, 2 mM L-glutamine, 1X non-essential aminoacids, 1 mM sodium pyruvate, 100 U/ml penicillin/streptomycin and 1 µg/ml amphotericin B solution. Media were changed twice a week.

### 2.2.6. Transient transfections.

Transient transfections in HEK293T were performed with TransFectin™ Lipid Reagent according to the manufacturer's instructions.

### 2.2.7. Production of lentiviral stocks and transduction of cell lines.

Recombinant lentiviral stocks were produced in HEK293T/17 cells at 80% cell density by co-transfecting 10 µg of transfer vector, 6 µg of envelope plasmid pMD2.G and 6 µg of packaging plasmid pSPAX2, using 24 µl PLUS Reagent and 36 µl Lipofectamine Transfection Reagent for each 10-cm plate. Cells were incubated in transfection mix and Opti-MEM during 6 h at 37°C. Then, the medium was replaced with fresh DMEM supplemented with 10% FBS, 4 mM L-glutamine and 80 µg/ml gentamicin. Virus particles were harvested at 24 h and 48 h post-transfection after filtration with 45-µm filter.

Lentiviral transduction of primary cultures of NSPCs: 3.6 ml of lentiviral suspension with 4 µg/ml polybrene were added to cells in adhesion condition in dishes coated with poly- D-lysine in DMEM supplemented with 10% FBS and 80 µg/ml gentamicin. After 16 h, the media was replaced by proliferation media and 12 h later, cells were plated in suspension in proliferation media and the different assays were performed as described above.

Lentiviral transduction of glioblastoma cell lines: U87-MG and GB cells were incubated with 3.6 ml of lentiviral suspension plus 4 µg/ml polybrene in adhesion conditions in DMEM supplemented with 10% FBS, 4 mM L-glutamine, 5 mM HEPES, 80 µg/ml gentamicin and 1 µg/ml amphotericin B. After 16 h, the following day, cells were seeded in stem cell conditions in uncoated 10 cm dishes in DMEM: F12 (1:1) supplemented with 2 mM glutamine, 5 mg/ml Albumax I, 6 mg/ml glucose, B27 supplement (without vitamin A), 15 ng/ml hFGF-2, 20 ng/ml hEGF, 2 µg/ml heparin, 80 µg/ml gentamicin and 1 µg/ml amphotericin B. Infected cells were selected using 1 mg/ml puromycin when necessary.

Lentiviral transduction of ReNcells: 3.6 ml lentiviral suspension with 4 µg/ml polybrene per T75 flask were added to ReNcells incubated in neurobasal medium supplemented with 1X B27 supplement, 2 mM L-glutamine, 1X non-essential aminoacids, 1 mM sodium pyruvate, 20 ng/ml hEGF, 20 ng/ml hFGF-2, 100 U/ml penicillin/streptomycin and 1 µg/ml amphotericin B solution. The following day, medium was replaced by fresh media and infected cells were selected using 0.5 mg/ml puromycin when necessary.

### 2.2.8. Production of retroviral stocks and transduction of cell lines.

Retroviral stocks were produced in HEK293T/17 cells by co-transfecting 10 µg of transfer vector, 6 µg of pCMV-Gag-Pol, 5 µg of pCMV-VSV-G and 6 µg of pCL-Ampho, using 24 µl PLUS Reagent and 36 µl Lipofectamine Transfection Reagent for each 10 cm plate. Cells were incubated in transfection mix and Opti-MEM during 6 h at 37°C. After 6 h at 37°C the medium was replaced with fresh specific medium for each cell line. For each p100, virus particles were harvested at 24 h and 48 h post-transfection after filtration with 45 µm filter. Retroviral particles cannot be frozen and retroviral transduction has to be performed immediately.

Retroviral transduction of cell lines: cells were seeded at low density (for retroviral transduction cells have to be proliferating) and incubated with 6 ml of the specific retroviral suspensions with 4 µg/ml polybrene for each T75 during 16 h. Then, medium was changed by fresh medium. Infected cells were selected using 0.5 µg/ml (ReNcells) or 1 µg/ml (U87-MG and GB) puromycin.

### 2.2.9. Immunofluorescence analysis of cell cultures.

Cells were seeded on sterile coverslips in 24-well plates as specified for each cell type. For secondary neurospheres, plates were centrifuged 5 min at 112 g. Then, cells were washed twice with PBS to remove cell media and fixed with 4% PFA during 15 min at room temperature. Coverslips were washed three times during 5 min/each with PBS and blocked in PBS containing 0.5% Triton X-100 and 3% bovine serum albumin during one hour. Coverslips where then incubated during 2 h at room temperature and overnight at 4°C with relevant primary antibodies (Table 1). Next, coverslips were washed gently with PBS and incubated 2 h at room temperature with appropriate secondary antibodies coupled to fluorochromes Alexa Fluor 488, 594, or 647 (Table 2) and nuclei were counterstained with DAPI for 10 min at room temperature. After washing with PBS and sterile water to remove salts, coverslips were mounted in slides using ProLong. Images were acquired using Leica TCS SP5 Confocal Laser Scanning Microscope and cells were quantified using FiJi (ImageJ Software).

### 2.2.10. Analysis of neuron complexity.

After differentiation of primary NSPCs and ReNcells, immunostaining with specific neuronal markers was performed as described in section 2.2.9. To quantify neuronal complexity, Sholl analysis was performed using the Simple neurite tracer plugin (http://homepages.inf.ed.ac.uk/s9808248/imagej/tracer/); total axonal, dendrite or neurite lengths were determined using NeuronJ (https://imagescience.org/meijering/software/neuronj/) and the image processing package Fiji (http://pacific.mpicbg.de/wiki/index.php/Main_Page). At least 60 neurons were analyzed per assay.

### 2.2.11. Cell lysis, electrophoresis and immunoblotting.

Cells were homogenized in cellular lysis buffer (50 mM Tris pH 7.6, 400 mM NaCl, 1 mM EDTA, 1 mM EGTA, 1% SDS.), followed by an incubation 15 min at 95ºC, sonicated with the ultrasonic processor UP100H (100W, 30kHz) (Hielscher Ultrasonics GmbH, Teltow, Germany) 10 times at 60% of amplitude and 0.5 cycles, and centrifuged 10 min at 19,000 g. Samples were quantified with the Bradford method (Pierce TM BCA Protein Assay Kit) and 1X protein loading buffer (6.5 mM Tris-HCl pH 6.8, 25% glycerol, 10% SDS, 0.5% bromophenol blue and 5% β-mercaptoethanol) was added per sample. Samples were incubated 5 min at 95ºC and centrifugated at 19,000 g for 5 min. Equal amounts of samples were resolved by SDS-PAGE together with molecular weight markers. After electrophoresis, proteins were transferred to 0.45 µm pore size Immobilon-P membranes at 100V for 2 h.

For immunoblotting, membranes were hydrated in methanol and incubated 5 min in TTBS buffer. Membranes were blocked with 4% bovine serum albumin (BSA) or 5% non-fat dry milk in TTBS. After washing, membranes were incubated overnight with indicated primary antibodies diluted in 0.4% BSA in TTBS in the conditions indicated in Table 1. Membranes were washed with TTBS and incubated with the appropriate HRP-conjugated secondary antibodies (Table 2) at 1:10,000. After gentle washing, proteins were detected by enhanced chemiluminescence (GE Healthcare, RPN2232).

### 2.2.12. Analysis of mRNA levels by quantitative real-time polymerase chain reaction.

Total RNA extraction was performed with TRIzol® Plus RNA Purification Kit following the manufacturer´s instructions. DNase I, Amplification Grade, was applied to 1 µg of RNA after its quantification with NanoDropTM spectrophotometer (Thermo Fisher Scientific) following the manufacturer´s instructions to eliminate possible genomic DNA contaminations. cDNA was then obtained with Retrotranscriptase High Capacity RNA-to-cDNA Kit.

Sybr Green Master Mix was used for the quantitative real time polymerase chain reaction (qRT-PCR). For each reaction, 5 pmol of forward- and reverse-specific oligonucleotides for each transcript were utilized (Table 10 and 11). Reactions took place in a StepOne thermocycler. Reaction conditions were 10 min denaturation at 95°C followed by 40 cycles [15 s at 95°C (denaturation), 30 s at 60 °C (annealing) and 30 s at 60 °C (elongation)]. The amplification specificity of oligonucleotides was analyzed by their melting curve. Messenger RNA (mRNA) levels were estimated with the ΔΔCt method, using the geometric media of *ACTB (Actb)*, *GAPDH* (*Gapdh*) and *TBP (Tbp)* house-keeping genes as reference. Samples were analyzed in quadruplicate.

| GENE PRODUCT | FORWARD PRIMER (5´- 3´) | REVERSE PRIMER (5´- 3´) |
|---|---|---|
| ***ACTB*** | TCCTTCCTGGGCATGGAG | AGGAGGAGCAATGATCTTGATCTT |
| ***ASCL1*** | CATCTCCCCCAACTACTCCA | GAAAGCCATGTCTCTCAGGC |
| ***BIRC5*** | ACCCCGGAGCGGATGG | GCAACCGGACGAATGCTTTT |
| ***CD44*** | ACAAGCACAATCCAGGCAAC | GCTGGTATGAGCTGAGGCTG |
| ***CTGF*** | CTTCTGTGACTTCGGCTCCC | GATGCAGGGAGCACCATCTT |
| ***CYR61*** | CCAAGAAATCCCCCGAACCA | CGGAACCGCATCTTCACAGT |
| ***GAPDH*** | CTCTCTGCTCCTCCTGTTCGAC | TGAGCGATGTGGCTCGGCT |
| ***NEUROD1*** | GGTGCCTTGCTATTCTAAGACGC | GCAAAGCGTCTGAACGAAGGAG |
| ***NEUROG2*** | ATCCGAGCAGCACTAACACG | GCTGAGGCACAGTTAGAGCC |
| ***NFE2L2*** | AAACCAGTGGATCTGCCAAC | GTGACTGAAACGTAGCCGAAGA |
| ***NQO1*** | GTTCATAGGAGAGTTTGCTT | CCTTGCAGAGAGTACATGGA |
| ***SOX2*** | GAGCTTTGCAGGAAGTTTGC | GCAAGAAGCCTCTCCTTGAA |
| ***TBP*** | TGCACAGGAGCCAAGAGTGAA | CACATCACAGCTCCCCACCA |
| ***TEAD1*** | CTGAGTCGCAGTTACCACCA | AGCCTGGAGCCTTTTCAAG |
| ***TEAD2*** | ACATGATGAACAGCGTCCTG | CAGCAGTTCCTGGGTGTCTC |
| ***TEAD3*** | CATCGAGCAGAGCTTCCAG | CGTGCAATCAACTCATTTCG |
| ***TEAD4*** | GCCTTCCACAGTAGCATGG | AAAGCTCCTTGCCAAAACC |
| ***WWTR1*** | TTTCCTCAATGGAGGGCCA | GGGTGTTTGTCCTGCGTTTT |

**Table 10. Human primers used for quantitative real time polymerase chain reaction (qRT-PCR).**

| GENE PRODUCT | FORWARD PRIMER (5´- 3´) | REVERSE PRIMER (5´- 3´) |
|---|---|---|
| ***Actb*** | TCCTTCCTGGGCATGGAG | AGGAGGAGCAATGATCTTGATCTT |
| ***Gapdh*** | CGACTTCAACAGCAACTCCCACTCTTCC | TGGGTGGTCCAGGGTTTCTTACTCCTT |
| ***Ctgf*** | CCTGCCATTACAACTGTCCT | GTTCGTGTCCCTTACTTCCTG |
| ***Nqo1*** | GGTAGCGGCTCCATGTACTC | CATCCTTCCAGGATCTGCAT |
| ***Nrf2*** | CCCGAAGCACGCTGAAGGCA | CCAGGCGGTGGGTCTCCGTA |
| ***Tbp*** | TGCACAGGAGCCAAGAGTGAA | CACATCACAGCTCCCCACCA |
| ***Wwtr1*** | GAGAGGATTAGGATGCGTCAAG | GGATCTGAGCTACTGTTGGTG |

**Table 11. Mouse primers used for quantitative real time polymerase chain reaction (qRT-PCR).**

### 2.2.13. Chromatin immunoprecipitation (ChIP) assays.

ReNcells were transduced with pBABE-puro (control) and pBABE-puro-TAZ-4SA retroviral particles and grown on T75 flasks. After 5 days-post-transduction, cells were fixed with 1% PFA for 12 min on ice and the reaction was neutralized with 125 mM glycine. Cells were then washed twice with cold PBS and lysed. Cells were sonicated twice for 4 min at highest power to obtain 200-800 bp DNA fragments. Supernatant was diluted 10-fold with ChIP dilution buffer and pre-cleared with Protein G Sepharose. Supernatant was incubated with primary antibodies overnight at 4ºC. Anti-IgG antibodies were used as a negative control. DNA was eluted and purified, analyzing the presence of previously identified putative binding sites by qRT-PCR with specific primers (Table 12 and Table 13). Samples from at least four independent ChIPs were analyzed.

| GENE PRODUCT | FORWARD PRIMER (5´- 3´) | REVERSE PRIMER (5´- 3´) |
|---|---|---|
| ***WWTR1* ARE1** | GCACCAGAGGGCATACATCT | AACCACACCATCAGGAAAGC |
| ***WWTR1* ARE2** | AATCCTGTGGGGTGGGTACT | CAGGTACTGCCCGTAAGAGG |
| ***WWTR1* ARE3** | TTCCAGGAAAAACAGGATGG | GAGGCTCCAGAACCTCAATG |
| ***WWTR1* ARE4** | AATGAAGGCTGGGTGTTCAG | TCAAAAACACACCCTCAGCA |
| ***WWTR1* ARE5** | CCTGATTTGGCTCATCTGCT | AGCAGCCATGTGAAAGGTCT |
| ***WWTR1* ARE6** | AGTGAAGCCAGGAAGGAGGT | CACTTCCCAAACCCAGGATA |
| ***WWTR1* ARE7** | TTCCAGCTGTAGGTGCCTTT | CATGAGTCCCTGTGAGCAAA |
| ***WWTR1* ARE8** | ATTCAGCCCTGCTTTTACCC | CCCTCTTTTCTCGTCCCTGT |
| ***WWTR1* ARE9** | CGCGGAGAAATTATCTGCTT | CTTTCTCCTTCCCCCTTCAG |
| ***ACTB*** | CACCCAGCACATTTAGCTAGCTGA | TTCAGAGCAACTGCCCTGAAAGCA |
| ***NQO1**** | TCTCAGTTTTTGCCCTTATTTAA | TAAAAAGTAGAGTGGTTGGAGTGATGACG |
| ***HMOX1*** | CCCTGCTGAGTAATCCTTTCCCGA | ATGTCCCGACTCCAGACTCCA |
| ***NQO1*** | TGCACCCAGGGAAGTGTGTTGTAT | CCCTTTTAGCCTTGGCACGAAA |

**Table 12. Oligonucleotides used for chromatin immunoprecipitation (ChIP) analysis.** ARE: Antioxidant Response Element.

| GENE PRODUCT | FORWARD PRIMER (5´- 3´) | REVERSE PRIMER (5´- 3´) |
|---|---|---|
| ***CTGF 3´UTR*** | GGTTTGGCCTAGCACTCCA | TCTGGTGACCTGCTCAATTT |
| ***CTGF*** | TCAGACGGAGGAATGCTGAG | CGAGGCTTTTATACGCTCCG |
| ***CMYC Enh. 4*** | GGGGAACTCTCACTCTCCTTTGA | CCAGGGGGTCTTTACACAGC |
| ***CMYC Enh. 6*** | AGGGTCCTGGGCTTTTTCAG | GGGCCATTCGTCACCTTTTC |
| ***CYR61*** | AGCAAACAGCTCACTGCCTT | ATGGTAGTTGGAGGGTCGTG |
| ***SOX2* TIR-a (1)** | CATTTGAAAGCCGCACGACC | ATGCTTCTACTGTCTGCCCC |
| ***SOX2* TIR-a (2)** | ACCGAAACCCTTCTTACGGG | AACCGTAGCAAAGGGGATGC |
| ***SOX2* TIR-a (3)** | GCACGACCGAAACCCTTCTT | TCAACCGTAGCAAAGGGGAT |
| ***SOX2* TIR-b (1)** | AGAGAAAACCTGGGGAGGGT | GCAAAGCTCCTACCGTACCA |
| ***SOX2* TIR-b (2)** | CTGGACTTCTTTTTGGGGGACT | GCAAAGCTCCTACCGTACCA |
| ***SOX2* TIR-c (1)** | ATTACCCTCTTGGGTCCTGG | CAGCGCACACTGGGAGAA |
| ***SOX2* TIR-c (2)** | AAATTACCCTCTTGGGTCCTGG | CACACTGGGAGAAGGCGG |
| ***ASCL1* TIR-a (1)** | TGGGTGCTCACCTCCTATACT | GTGGGATTCACACCTCAGGC |
| ***ASCL1* TIR-a (2)** | TTTGGGTGCTCACCTCCTAT | GGATTCACACCTCAGGCCTTT |
| ***ASCL1* TIR-b** | CGTCATTACTGCCCACCATC | TAAAGGGCCAAGGGGATGAC |
| ***ASCL1* TIR-c (1)** | AGGCCACCAGTTGTACTTCA | TGCCACTTTGAGTTTGGACAG |
| ***ASCL1* TIR-c (2)** | GCCACCAGTTGTACTTCAGCA | GCCACTTTGAGTTTGGACAGTA |
| ***NEUROG2* TIR-a (1)** | TGCAACTGGTTCCTGTGATCT | GCCAGCCATTGCAAATCTGT |
| ***NEUROG2* TIR-a (2)** | TGGTTCCTGTGATCTCTTCACC | CAGCCATTGCAAATCTGTGGA |
| ***NEUROG2* TIR-a (3)** | GGGGAATGCAACTGGTTCCT | ACCAGCAAAATCATTCAGATGC |
| ***NEUROG2* TIR-a (4)** | GCAACTGGTTCCTGTGATCT | TTACCAGCAAAATCATTCAGATGC |
| ***NEUROG2* TIR-b (1)** | AGAGGGGCAGGTTAGAAGTCA | AGCCTAAATTTCCACGCTTGC |
| ***NEUROG2* TIR-b (2)** | TGTTTTGTTAGAGGGGCAGGT | GCCTAAATTTCCACGCTTGCAT |
| ***NEUROD1* TIR-a (1)** | GTCCGCGGAGTCTCTAACTG | ATGCGCCATATGGTCTTCCC |
| ***NEUROD1* TIR-a (2)** | CTAACTGGCGACAGATGGGC | CATTTGTATGCCGCGGAGC |
| ***NEUROD1* TIR-a (3)** | CTGCGGGTAAAAACAGGTCC | ACGTGACCTGCCCATTTGTAT |
| ***NEUROD1* TIR-b (1)** | CCTTGAGTATTCACACCATGGAA | GAGCGGTAACAGGTAGCAGG |
| ***NEUROD1* TIR-b (2)** | TGGATACCTTGAGTATTCACACCA | GGAGCGGTAACAGGTAGCAG |
| ***NEUROD1* TIR-c** | AGCCAGGACAGAAATGGAAGT | TGCCCGACAGGATAATGTGT |

**Table 13. Oligonucleotides used for chromatin immunoprecipitation (ChIP) analysis.** TIR: TAZ interacting region.

### 2.2.14. Measurement of luciferase activity.

For ARE-LUC luciferase assay, HEK293T cells were seeded in 24-well (75,000 cells per well) plates and transiently transfected with Tranfectin according to the manufacturer's instructions with the expression vectors *WWTR1* ARE2-WT, *WWTR1* ARE2-mutated or positive control *HMOX1*-ARE-Luc. pTK-Renilla was also transfected to be used as an internal control. After 24 h after transfection, cells were lysed in 100 µl lysis buffer (Promega) and 40 µl of this lysate was used for the luciferase assay, performed according to the manufacturer's instructions.

For *SOX2*-TEAD1(a)-LUC luciferase assay, HEK293T cells were seeded in 24-well (75,000 cells per well) plates and transiently transfected with Tranfectin according to the manufacturer's instructions with *SOX2*-TEAD1(a)-luc vector, Renilla vector and increasing amounts of pBABE-puro-TAZ-4SA vector. For ReNcells luciferase assays, cells were previously infected with retrovirus encoding $TAZ^{4SA}$ and 24 h later they were plated on 24-multiwell (60,000 cells per well) and transfected with Lipofectamin 2000 Reagent with *SOX2*-TEAD1(a)-luc plasmid and Renilla following manufacturer´s instructions. After 24 h, cells were lysed in 100 µl lysis buffer (Promega) and 40 µl of this lysate was employed for the luciferase assay, performed according to the manufacturer's instructions. Luciferase expression was quantified as luminol oxidation with a GloMax 96 microplate luminometer with dual injectors (Promega). Each sample was measured in quadruplicate and normalized by the levels of Renilla.

## 2.3. *In vivo* assays.

### 2.3.1. Morris water maze test (MWM).

This test was conducted as double blind at the Animal Facility of Instituto Cajal. Animals performed 1 day of habituation trial in which animals with preferences between quadrants in the different experimental groups were discarded. After habituation, animals were trained to find the hidden platform for the following 5 days, doing 4 trials/day. Prior to the test, we confirmed that the mice to be analyzed exhibited similar motor competence, not detecting any inter-group differences in the average swim speed and travelled distance. Each animal spent 60 s in each trial, plus 20 s in the platform. On the $6^{th}$ day, the animals were subjected to two trials, the first without the platform to assess possible differences in swimming speed between the animals and their preference for the platform quadrant. In the second trial, a visible platform was used to determine sensorimotor and motivational status of the animals.

### 2.3.2. Electrophysiological recordings.

These experiments were done double blind in collaboration with Prof. Ángel Nuñez (Department of Anatomy, Histology and Neuroscience, Medical College, UAM). Animals were anaesthetized by intraperitoneal injection of 1.6 g/ kg urethane and local 1% lidocaine. During the procedure, body temperature was maintained at 37°C with the help of a thermal blanket. Field potentials were recorded through tungsten microelectrodes (1 MΩ; World Precision Instruments) stereotaxically implanted in the DG (A: -2,3; L: 2; H: 1.5 mm from bregma) according to the Paxinos and Watson Atlas. Twisted bipolar electrodes for electrical stimulation were aimed at the medial perforant path (MPP) (A: -2.5; L: 0.5; H: 1.5 mm from bregma) (Fig. 16). Baseline recordings were taken with test stimuli (10-50 mA, 0.3 ms, 0.5 Hz) during 15 min before tetanic stimulation consisting of 3 pulse trains of 10-50 mA, lasting each pulse 0.3 ms and at 50 Hz. Trains lasted 500 ms and the inter-train interval was 2 s. Recording was maintained for 30 min after tetanic stimulation. Field potentials were 0.1 Hz–1 kHz band-pass filtered, amplified (P15 Amplifier, Grass Co., USA), and digitized at 10 kHz (CED 1401; Cambridge Electronic Design). Signals were stored and off-line analysis was carried out with Spike 2 software (Cambridge Electronic Design, Cambridge, UK). Field potential segments of 5 min were analyzed to obtain the response average. The mean average response during the 15 min period before the tetanic stimulation was considered as 100%. Recordings were accepted for analysis when baseline variability was less than 10%.

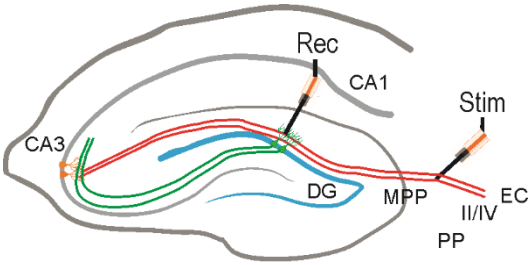


**Figure 16. Graphic overview of electrophysiological recordings in the DG**, indicating the positions of the stimulating electrode (Stim) on the medial perforant pathway (MPP) and recording electrode (Rec) in the dentate gyrus (DG). CA1 and CA3: *Cornu Ammonis* areas 1 and 3, respectively, EC: entorhinal cortex.

### 2.3.3. Immunofluorescence on mouse tissues.

Animals were anesthetized with 8 mg/kg ketamine and 1.2 mg/kg xylazine and perfused with phosphate-buffered saline, followed by fixation in 4% PFA and cryoprotected by soaking in 30% sucrose solution in phosphate buffer until they sank. The immunofluorescence was performed in 30 µm-thick sections. Briefly, free-floating sections were washed 3 times with PBS during 5 min each before blocking. Sections were blocked for 2 h at room temperature with PBS with 3% horse serum and 1% Triton X-100. Incubation with primary antibodies (Table 1) was performed for 2 h at room temperature and overnight at 4ºC in 10% blocking solution. Next day, sections were washed gently three times with PBS (5 min/each) and incubated with the secondary antibodies (Table 2) in blocking solution. Nuclei were counterstained with a 15 min incubation in DAPI at room temperature. Sections were washed twice in PBS for 10 min/each and 0.03 M PB. Sections were mounted in gelatin coated glass slides with ProLong. Control sections were treated by following identical protocols but omitting the primary antibody.

### 2.3.4. Immunohistochemistry.

Immunohistochemistry was performed on 30 µm-thick coronal brain sections with a standard avidin- biotin immunohistochemical protocol. Briefly, free-floating sections were washed 3 times with 1X PBS for 5 min/each and incubated with 0.5% $H_2O_2$ in PBS for 30 min at room temperature to block endogenous peroxidase activity. Antigen retrieval was performed with 10 mM citrate buffer pH 6 for 20 min at 90ºC, or formic acid for 5 min at room temperature for APP/Aβ. Sections were incubated with blocking solution (3% BSA and 0.2% Triton X-100 in PBS) for 2 h. Incubation with the appropriate dilutions of the primary antibodies (Table 1) was done overnight at 4ºC. After washing several times with 1X PBS, free floating sections were incubated with biotinylated secondary antibodies and the avidin/biotin system with the VectastainR ABC Kit (Vector Laboratories) according to manufacturer's instructions. Labeling was developed with 0.009% $H_2O_2$, 0.025% 3-3'diaminobenzidine tetrahydrochloride (DAB) in PBS until the appearance of the desired intensity. Staining was stopped with washes with TBS. Sections were washed twice in 1X PBS for 10 min/each and 0.03 M PB. Sections were mounted on gelatin-coated glass slides, and de-hydrated by increasing concentrations of ethanol until absolute ethanol and finally, rinsed in xylol 6 times for 5 min/each. Slides were coversliped with DePeX (Serva).

### 2.3.5. Nissl staining.

Nissl staining is based on cresyl violet (basic dye) which binds to negatively charged molecules like RNA and DNA. Brain sections were attached in gelatin- coated slides and washed quickly with $H_2O$ and incubated with 0.1% cresyl violet and 0.025% acetic acid in $H_2O$ for 20 min at room temperature. After washing with $H_2O$, sections were de-hydrated by sequential immersion in 70%; 80% and 96% ethanol solutions. Sections were washed with 2% acetic acid in 96% ethanol for few seconds and de-hydrated in absolute ethanol and xylol. Sections were coversliped with DePeX.

### 2.3.6. Cell counting in immunofluorescence of brain sections.

Cell counts were performed every 8 sections (30 µm-thick) through the DG and SVZ by using FiJi Software (ImageJ) under 40X magnification (Leica TCS SP5 Confocal Laser Scanning Microscope) for each cell type. Five adjacent sections per animal were quantified.

### 2.3.7. Tumour induction in immunodeficient mice.

Eight-week-old nude (*Foxn1*$^{nu}$) male mice were used for xenograft. U87-MG cells ($10^6$ cells in 0.1 ml PBS) were inoculated subcutaneously for tumour growth analysis. Tumour growth was examined every 5 days for up to 65 days. Tumour volume = $\pi/6 \times (\text{mean diameter})^3$. For intracranial tumour assays, U87-MG cells ($2x10^5$ cells) were stereotaxically inoculated into the corpus striatum of the right brain hemisphere (1 mm anterior and 1.8 mm lateral to the bregma; 2.5 mm intraparenchymal) of mice under isoflurane gas anaesthesia. Mice were euthanized when they presented neurological symptoms or significant weight loss. Tumours were obtained surgically and fixed with 4% PFA.

## 2.4. Statistical analysis.

Unless otherwise indicated, all experiments were performed at least 3 times and all data are the mean of at least 3 independent samples ± standard error of the mean (SEM). A Student's *t*-test was used to assess differences between groups with Graph Pad Prism 5.0. and $p<0.05$ was considered significant.

# RESULTS

# I. NRF2 regulates hippocampal neural stem cell fate.

## 1. NRF2 deficiency impairs long-term potentiation.

Adult wild type (*Nrf2*$^{+/+}$) and *Nrf2*-deficient (*Nrf2*$^{-/-}$) mice (6-month-old) were examined electrophysiologically for long-term potentiation (LTP) in the DG. The synaptic transmission in the DG was recorded in response to stimulation of the medial perforant path (MPP) (Fig. 16). High frequency stimulation increased the field excitatory post-synaptic potential (fEPSP) in control *Nrf2*$^{+/+}$ mice, but these values were strongly diminished in *Nrf2*$^{-/-}$ mice (Fig. 17A and B), indicating that NRF2 is required for normal LTP. Under physiological conditions, LTP is inhibited in mature GCs by GABAergic interneurons. By contrast, newborn neurons are more plastic and less prone to GABAergic inhibition than the mature ones. Thus, the measurable LTP in the DG under physiological conditions is mainly derived from the newborn neurons (Wang et al., 2000; Schmidt-Hieber et al., 2004; Snyder et al., 2001; Saxe et al., 2006; Garthe et al., 2009). For this reason, in the following experiments, we analyzed if the LTP impairment found in *Nrf2*$^{-/-}$ mice could be related, at least in part, to abnormal hippocampal neurogenesis in adult mice.

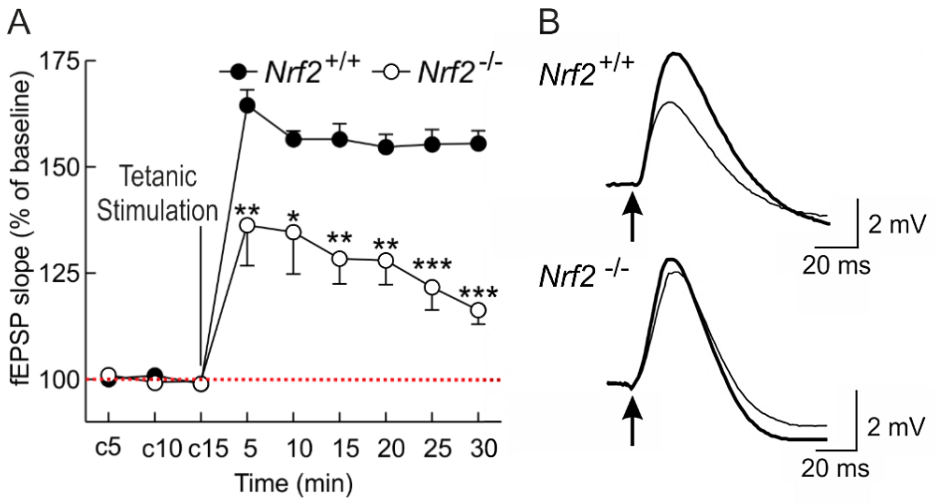


**Figure 17. NRF2 deficiency impairs LTP. (A)** LTP of field Excitatory Postsynaptic Potential (fEPSP) in 6-month-old animals before and after tetanic stimulation of the MPP. c5, c10, c15: control baseline recordings before tetanic stimulation. **(B)** Representative responses recorded from *Nrf2*$^{+/+}$ and *Nrf2*$^{-/-}$ mice before (thin line) and after (thick line) high-frequency trains of tetanic stimulation. Calibration: 2 mV, 20 ms. Data are mean ± SEM (n = 6). Statistical analysis was performed with a Student's *t*-test. **p<0.01, and ***p<0.001 *vs.* the *Nrf2*$^{+/+}$ group.

## 2. The clonogenic and proliferative capacity of NSPCs from the SGZ is impaired in *Nrf2*$^{-/-}$ mice.

First, we investigated the proliferative capacity of neural stem/progenitor cells (NSPCs) in the SGZ hippocampal neurogenic niche of *Nrf2*$^{+/+}$ and *Nrf2*$^{-/-}$ mice at 3, 6 and 12 months of age. We performed immunostaining with the proliferative marker Ki67 in combination with the NSPC marker Nestin (Fig. 18A and B). As expected, both *Nrf2*$^{+/+}$ and *Nrf2*$^{-/-}$ mice exhibited a drastic reduction in proliferating cells with aging. However, the number of proliferating NSPCs was ~50% lower in *Nrf2*$^{-/-}$ mice at all age points.

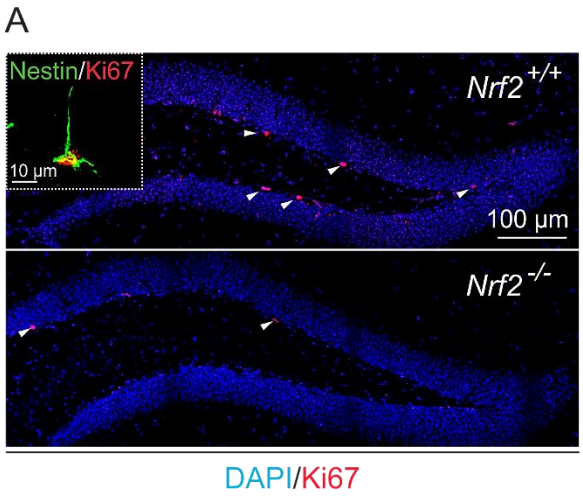


**Figure 18. Reduction of proliferative NSPCs in the SGZ of *Nrf2*$^{-/-}$ mice. (A)** Representative confocal microscope images of Ki67 staining in the SGZ of 3-month-old *Nrf2*$^{+/+}$ and *Nrf2*$^{-/-}$ mice. The green channel for Nestin staining has been removed except in the inset to allow easier visualization of proliferating cells. Nuclei were counterstained with DAPI. White arrowheads point to Ki67$^{+}$ cells. **(B)** Quantification of Ki67$^{+}$ NSPCs in 3-, 6- and 12-month-old mice of the indicated genotypes. Data represent mean ± SEM (n = 5). Statistical analysis was performed with a Student's *t*-test. ***$p \leqslant 0.001$ *vs.* the *Nrf2*$^{+/+}$ group.

In order to compare proliferative and clonogenic capacities of NSPCs, we performed a neurosphere assay on NSPCs derived from the SGZ of newborn and 3-month-old *Nrf2*$^{+/+}$ and *Nrf2*$^{-/-}$ mice. As expected, NSPCs derived from the SGZ of *Nrf2*$^{+/+}$ mice expressed NRF2 protein and messenger RNA (mRNA), while NSPCs derived from the SGZ of *Nrf2*$^{-/-}$ did not (Fig. 19A, B and C). Moreover, *Nrf2*$^{-/-}$-isolated NSPCs presented a reduced gene expression of the *bona fide* NRF2 target *Nqo1*, indicating an impairment in the NRF2-dependent transcriptional activity of these cells (Fig. 19C).

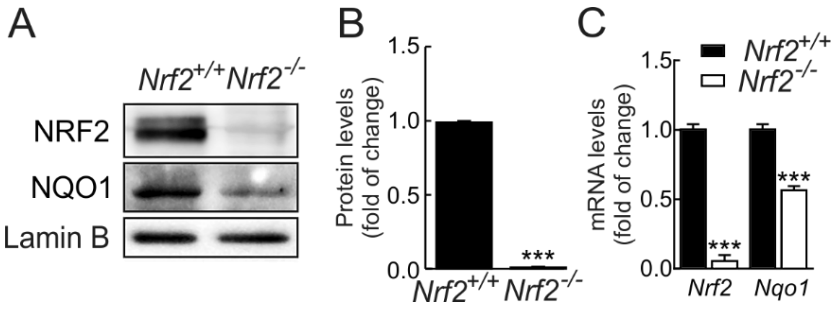


**Figure 19. Expression of NRF2 and NQO1 in NSPCs derived from the SGZ. (A)** Representative immunoblot of NRF2 and NQO1 from *Nrf2*$^{+/+}$ and *Nrf2*$^{-/-}$ neurospheres derived from the SGZ of 3-month-old mice, with Lamin B as a loading control. **(B)** Densitometric quantification of representative blots from A. Data are mean ± SEM (n = 4). **(C)** Relative expression of mRNA encoding NRF2 in *Nrf2*$^{+/+}$ and *Nrf2*$^{-/-}$ neurospheres normalized by the geometric mean of *Actb*, *Gapdh* and *Tbp* levels. Data are mean ± S.D. (n = 4). In **B** and **C**, the statistical analysis was performed with a Student's *t*-test. ***$p \leqslant 0.001$ *vs.* the *Nrf2*$^{+/+}$ group.

To analyze their clonogenic capacity, first NSPCs were seeded them at low density (20,000 cells/ml), so that only the self-renewing cells would be capable of forming new neurospheres. After 5 days in culture under proliferation conditions, the cell number in the *Nrf2*$^{-/-}$-derived neurospheres was about 50% lower compared to *Nrf2*$^{+/+}$, in neurospheres of both newborn and 3-month-old mice (Fig. 20A and G). Additionally, we found that NSPCs from *Nrf2*$^{-/-}$ mice had a lower clonogenic capacity as determined by the number of neurospheres formed after seeding equal amounts of *Nrf2*$^{-/-}$ and *Nrf2*$^{+/+}$ NSPCs in a serial dilution assay (Fig. 20B, C and H, I). Ki67 immunostaining (Fig. 20D, E and J, K) and

Ki67 protein levels (Fig. 20F and L) also demonstrated a reduction in the number of proliferating cells in *Nrf2*$^{-/-}$-derived neurospheres.

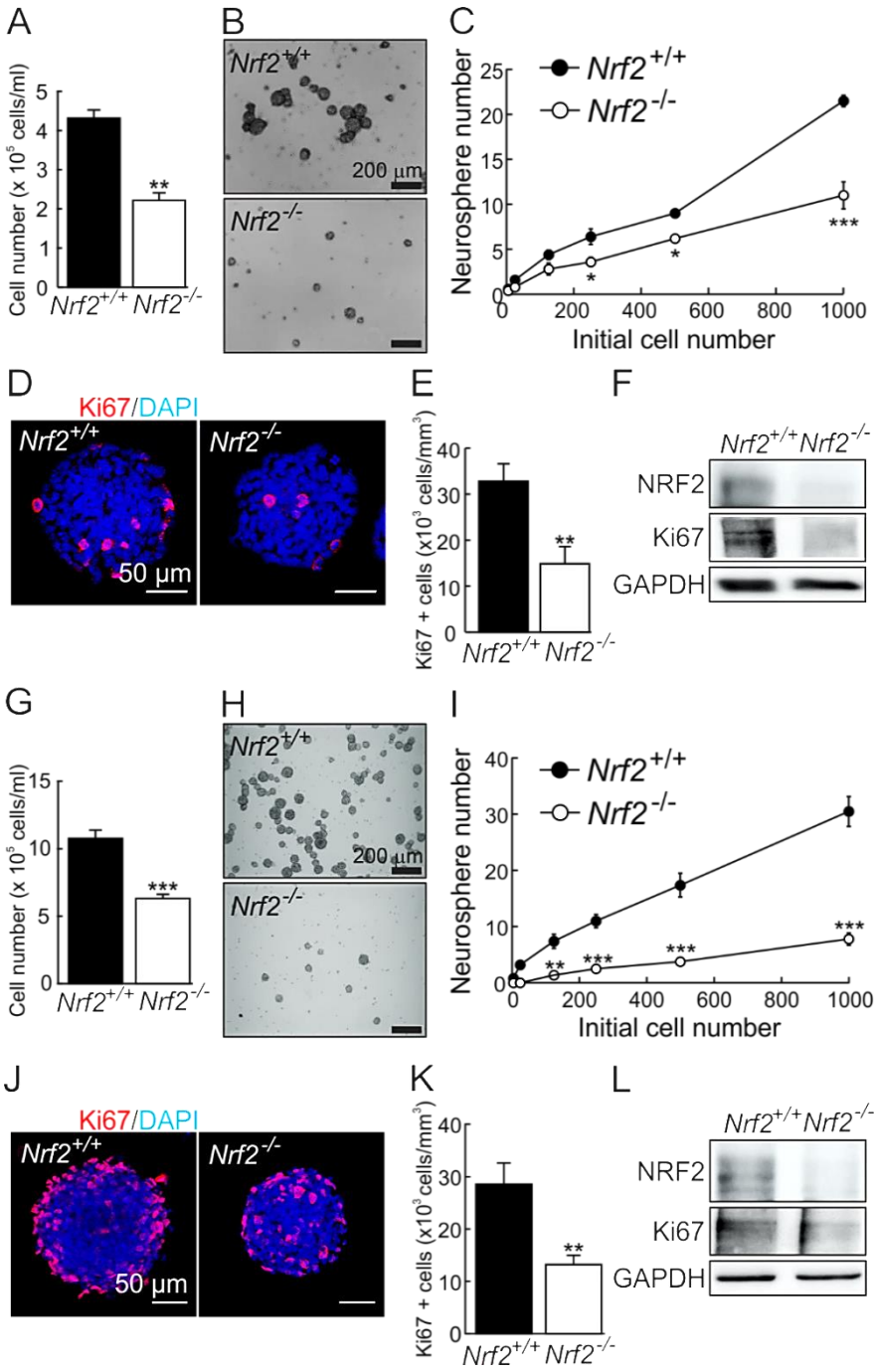


**Figure 20. Impaired clonogenic and proliferative capacity of NSPCs from *Nrf2*$^{-/-}$ mice. (A)** Determination of cell number after 5 days in culture from an initial seeding of 20,000 NSPCs/ml derived from newborn *Nrf2*$^{-/-}$ *vs.* *Nrf2*$^{+/+}$ mice. **(B)** Representative images of the neurospheres formed under these conditions. **(C)** Serial dilution assay of *Nrf2*$^{+/+}$ and *Nrf2*$^{-/-}$ NSPCs from newborn mice showing the number of neurospheres formed after 7 days. Data are mean ± S.D. (n = 10). **(D)** Representative confocal images of the proliferative marker Ki67 in neurospheres derived from the SGZ of newborn mice of the indicated genotypes after 5 days *in vitro*. Nuclei were counterstained with DAPI. **(E)** Quantification of Ki67$^+$ cells in 150-200 µm-diameter neurospheres from **D**. Data are mean ± SEM (n ≥ 10). **(F)** Representative immunoblots of NRF2 and Ki67 from *Nrf2*$^{+/+}$ and *Nrf2*$^{-/-}$ neurospheres with GAPDH as a loading control. **(G)** Determination of cell number after 5 days in culture from an initial seeding of 20,000 NSPCs/ml derived from 3-month-old *Nrf2*$^{-/-}$ *vs.* *Nrf2*$^{+/+}$ mice. **(H)** Representative images of neurospheres formed under these conditions. **(I)** Serial dilution assay of NSPCs derived from 3-month-old *Nrf2*$^{+/+}$ and *Nrf2*$^{-/-}$, showing the number of neurospheres formed after 7 days. Data are mean ± S.D. (n = 10). **(J)** Representative confocal image of the proliferative marker Ki67 in neurospheres derived from the SGZ of 3-month-old mice of the indicated genotypes after 5 days *in vitro*. Nuclei were counterstained with DAPI. **(K)** Quantification of Ki67$^+$ cells in 150-200 µm-diameter neurospheres from **J**. Data are mean ± SEM (n ≥ 10). **(L)** Representative immunoblots of NRF2 and Ki67 in *Nrf2*$^{+/+}$ and *Nrf2*$^{-/-}$ neurospheres with GAPDH as a loading control. Statistical analysis were performed with a Student's *t*-test. *$p \leqslant 0.05$; **$p \leqslant 0.01$, ***$p \leqslant 0.001$ *vs.* the *Nrf2*$^{+/+}$ group.

In additional experiments, we tested caspase-3 cleavage as a measurement of cell death in the DG of 3-month-old *Nrf2*$^{+/+}$ and *Nrf2*$^{-/-}$ mice (Fig. 21A) and in neurospheres from both genotypes (Fig. 21B and C). *In vivo*, we did not detect significant differences in cleaved caspase-3. In the established neurospheres from the DG of these mice, we detected very low levels of cleaved caspase-3 by immunoblot, suggesting that NSPCs are not undergoing apoptosis or they do it at undetectable levels. Furthermore, we determined the cell viability by Calcein staining. Calcein AM is a non-fluorescent, hydrophobic compound that easily permeates intact, live cells. The hydrolysis of Calcein AM by intracellular esterases produces Calcein, a hydrophilic, strongly fluorescent compound that is retained in the cell cytoplasm and emits green fluorescence. This assay did not show significant differences between *Nrf2*$^{+/+}$ and *Nrf2*$^{-/-}$-derived neurospheres (Fig. 21D and E). Thus, the differences observed in clonogenic capacity between the both genotypes did not derive from changes in the viability of NSPCs.

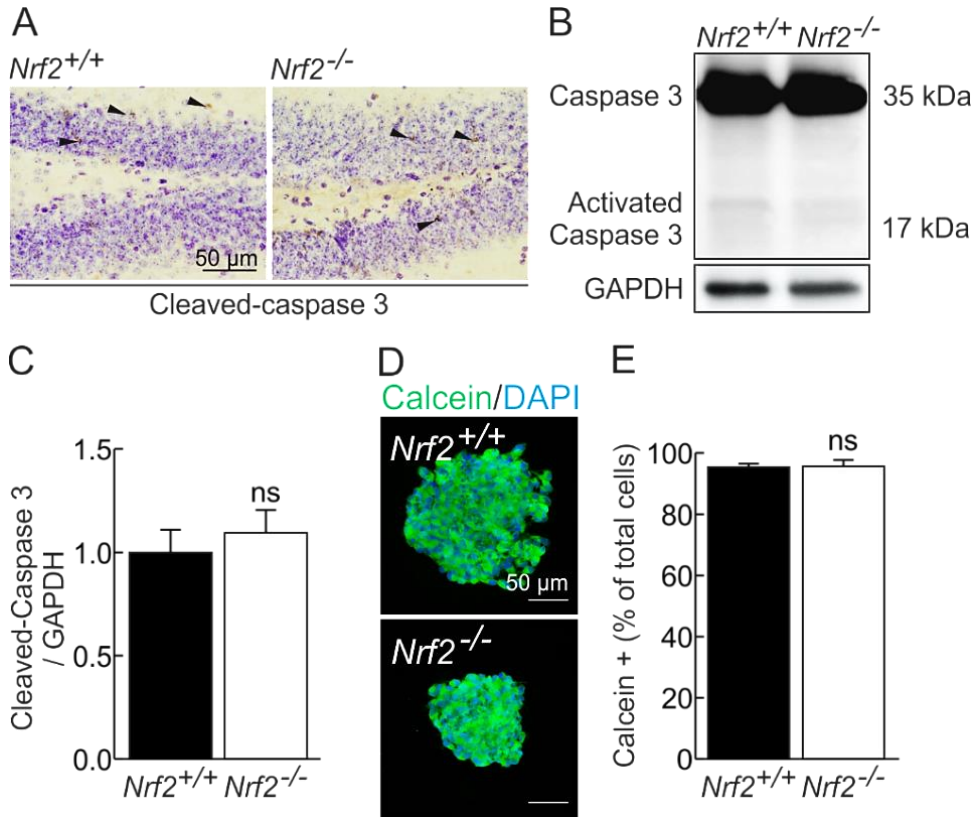


**Figure 21. NRF2 deficiency does not increase apoptosis or affect cell viability. (A)** Representative images of Nissl and cleaved- Caspase 3 immunohistochemistry in the DG of 3-month-old *Nrf2*$^{+/+}$ and *Nrf2*$^{-/-}$ mice. **(B)** Representative immunoblot of Caspase 3 (35 kDa) and cleaved-Caspase 3 (17 kDa) in *Nrf2*$^{+/+}$ and *Nrf2*$^{-/-}$ -derived neurospheres with GAPDH as loading control. **(C)** Densitometric quantification of cleaved Caspase 3 in representative blots from **B**. Data are mean ± SEM (n = 3). Statistical analysis with a Student's t-test indicated non-significant differences (ns). **(D)** Representative confocal images of Calcein staining in *Nrf2*$^{+/+}$- and *Nrf2*$^{-/-}$-derived neurospheres. Nuclei were counterstained with DAPI. **(E)** Quantification of Calcein$^{+}$ cells in C. Data are mean ± SEM (n = 20). Statistical analysis with Student's *t*-test indicated non-significant differences (ns).

Next, we conducted genetic modulation of NRF2 levels to further analyze its implication in NSPCs proliferation. On the one hand, we conducted rescue experiments by ectopic expression of NRF2 in *Nrf2*$^{-/-}$ NSPCs with a lentiviral vector expressing a constitutively active mutant of NRF2. This mutant lacks residues 79-ETGE-82 (NRF2$^{\Delta ETGE}$), being insensitive for KEAP1-mediated degradation, and resulting in NRF2 protein accumulation and increased transcriptional activity (Rada et al., 2011; Higgins and Hayes, 2011). We measured mRNA and protein levels after 5 days of transduction and found NRF2 expression (Fig. 22A and B) accompanied by an increase in the protein and mRNA levels of its well-known target NQO1 (Fig. 22A and C).

When we quantified the number of cells in the secondary neurospheres after 5 days of lentiviral transduction, we found that ectopic expression of NRF2 led to an increase in the number of *Nrf2*$^{-/-}$-NRF2$^{\Delta ETGE}$ NSPCs compared to the *Nrf2*$^{-/-}$-CT NSPCs (Fig.23A). In the serial dilution assay, the *Nrf2*$^{-/-}$-NRF2$^{\Delta ETGE}$ NSPCs produced a significantly greater number of neurospheres at every dilution tested compared to *Nrf2*$^{-/-}$-Control NSPCs (Fig. 23B and C). Furthermore, ectopic expression of NRF2 led to an increase in the number of Ki67$^{+}$ cells as determined by immunofluorescence (Fig. 23D and E) and immunoblot (Fig. 23F) Thus, ectopic expression of NRF2 partially rescued the clonogenic and proliferative capacity of *Nrf2*$^{-/-}$-derived NSPCs.

On the other hand, we silenced NRF2 using shRNA against murine *Nrf2* (shNRF2) in *Nrf2*$^{+/+}$ NSPCs. A reduction at protein and mRNA levels of NRF2 and NQO1 was observed in NSPCs where NRF2 was knocked-down (Fig. 22D and E). To ensure that NRF2 was silenced, we used the NRF2 activator sulforaphane (SFN) at a concentration of 15 µM during 6 h (Fig. 22F, G and H). SFN is an electrophilic NRF2-inducer which forms an adduct with KEAP1-Cys$^{151}$ and disrupts the union between KEAP1 and CUL3, preventing NRF2 ubiquitination and subsequent proteasomal degradation and allowing NRF2 to accumulate, translocate to the nucleus and exert its transcriptional function (Takaya et al., 2012). SFN induced an increase in NRF2 protein levels in the control NSPCs transduced with mock lentivirus (shCO), but not with shNRF2, indicating the efficient NRF2-knockdown (Fig. 22F and G). The NRF2-encoding gene promoter presents two ARE-like sequences, which allow NRF2 auto-regulation (Kwak et al., 2002). In this regard, when we determined by qRT-PCR the transcriptional level of NRF2, we found that this increment in NRF2 protein levels was accompanied by an increase in NRF2 transcript upon SFN treatment in *Nrf2*$^{+/+}$-shCO NSPCs, but not in *Nrf2*$^{+/+}$-shNRF2 NSPCs. This observation indicates that NRF2 accumulation leads to an increase in its transcriptional activity (Fig. 22H).

Knockdown of NRF2 led to a reduction in the number of cells in the derived neurospheres (Fig. 23G). In the serial dilution assay, *Nrf2*$^{+/+}$-shNRF2 NSPCs produced a significantly lower number of neurospheres in each dilution compared to *Nrf2*$^{+/+}$-shCO NSPCs (Fig. 23H and I). Additionally, the number of Ki67$^{+}$ cells was significantly lower in neurospheres derived from *Nrf2*$^{+/+}$-shNRF2 NSPCs (Fig.23J and K). This reduction in Ki67 was observed also at protein level (Fig. 23L). Thus, NRF2-knockdown led to the impairment of clonogenic and proliferating capacity of NSPCs. Taken together,

these results suggest a cell autonomous need of NRF2 to maintain the clonogenic and proliferative capacity of NSPC pool.

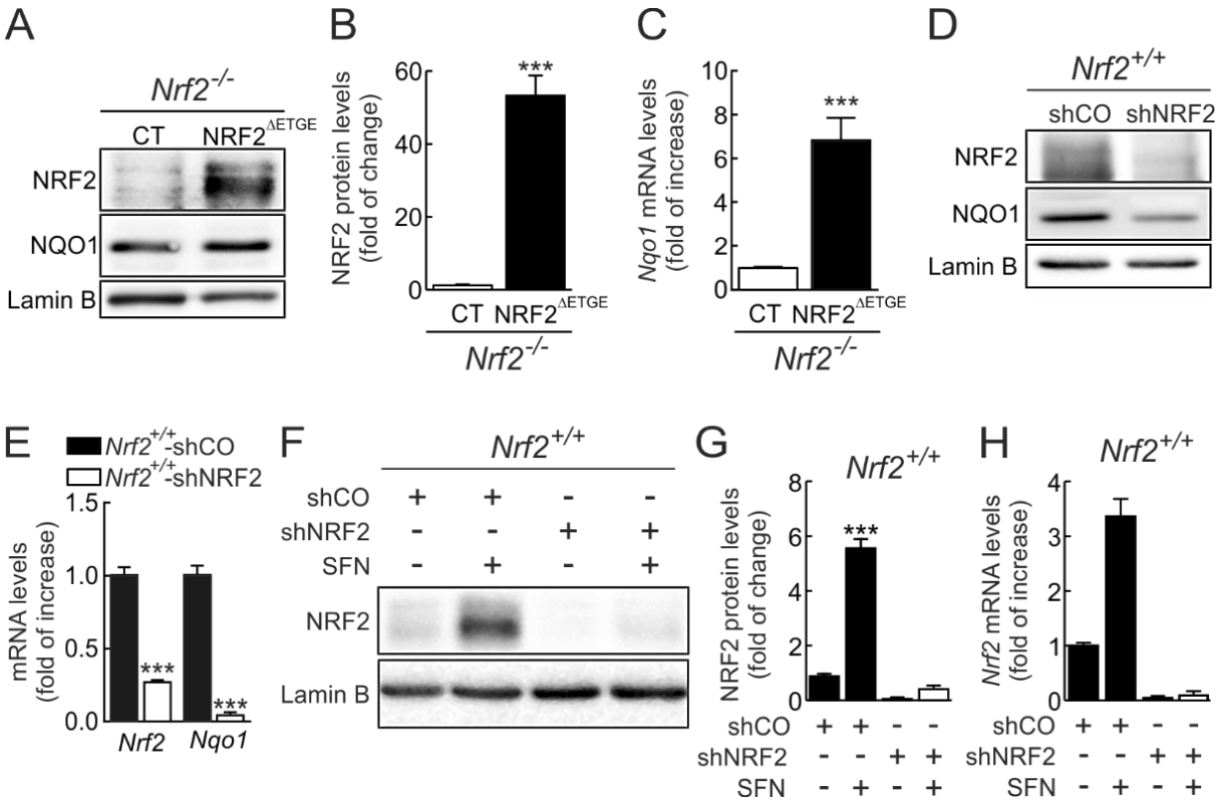


**Figure 22. Modulation of NRF2 protein levels by its ectopic expression or shRNA knockdown. (A)** Representative immunoblots of NRF2, NQO1, and Lamin B as a loading control in *Nrf2*$^{-/-}$-derived NSPCs transduced with a lentivirus control (CT) or encoding active NRF2$^{\Delta ETGE}$ after 5 days of lentiviral transduction. **(B)** Densitometric quantification of NRF2 protein levels from A. Data are mean ± SEM (n = 3). **(C)** Relative expression of mRNA encoding *Nqo1* in *Nrf2*$^{-/-}$-CT and *Nrf2*$^{-/-}$-NRF2$^{\Delta ETGE}$ after 5 days from lentiviral transduction. Data are mean ± S.D. (n = 4). **(D)** Representative immunoblots of NRF2, NQO1 and Lamin B as a loading control in *Nrf2*$^{+/+}$ NSPCs transduced with a lentivirus control (shCO) or mouse shNRF2 after 5 days of lentiviral transduction. **(E)** Relative expression of mRNA encoding *Nrf2* and *Nqo1* in *Nrf2*$^{+/+}$-shCO and shNRF2 after 5 days of lentiviral transduction determined by qRT-PCR. Data are mean ± S.D. (n = 4). **(F)** Representative immunoblots of NRF2, NQO1 and Lamin B as a loading control in *Nrf2*$^{+/+}$ NSPCs transduced with lentivirus control (shCO) or mouse shNRF2 after 5 days and treated with vehicle or sulforaphane (SFN, 15 µM, 6 h). **(G)** Densitometric quantification of representative blots from F. Data are mean ± SEM (n = 3). **(H)** Relative expression of mRNA encoding NRF2 in *Nrf2*$^{+/+}$-shCO and shNRF2 after 6 h of SFN treatment. In **C**, **E**, and **H**, mRNA levels are normalized by the geometric mean of *Actb*, *Gapdh* and *Tbp* levels. Data are mean ± S.D. (n = 4). Statistical analysis was performed with a Student's *t*-test. *$p \leqslant 0.05$; **$p \leqslant 0.01$; ***$p \leqslant 0.001$ *vs.* control group.

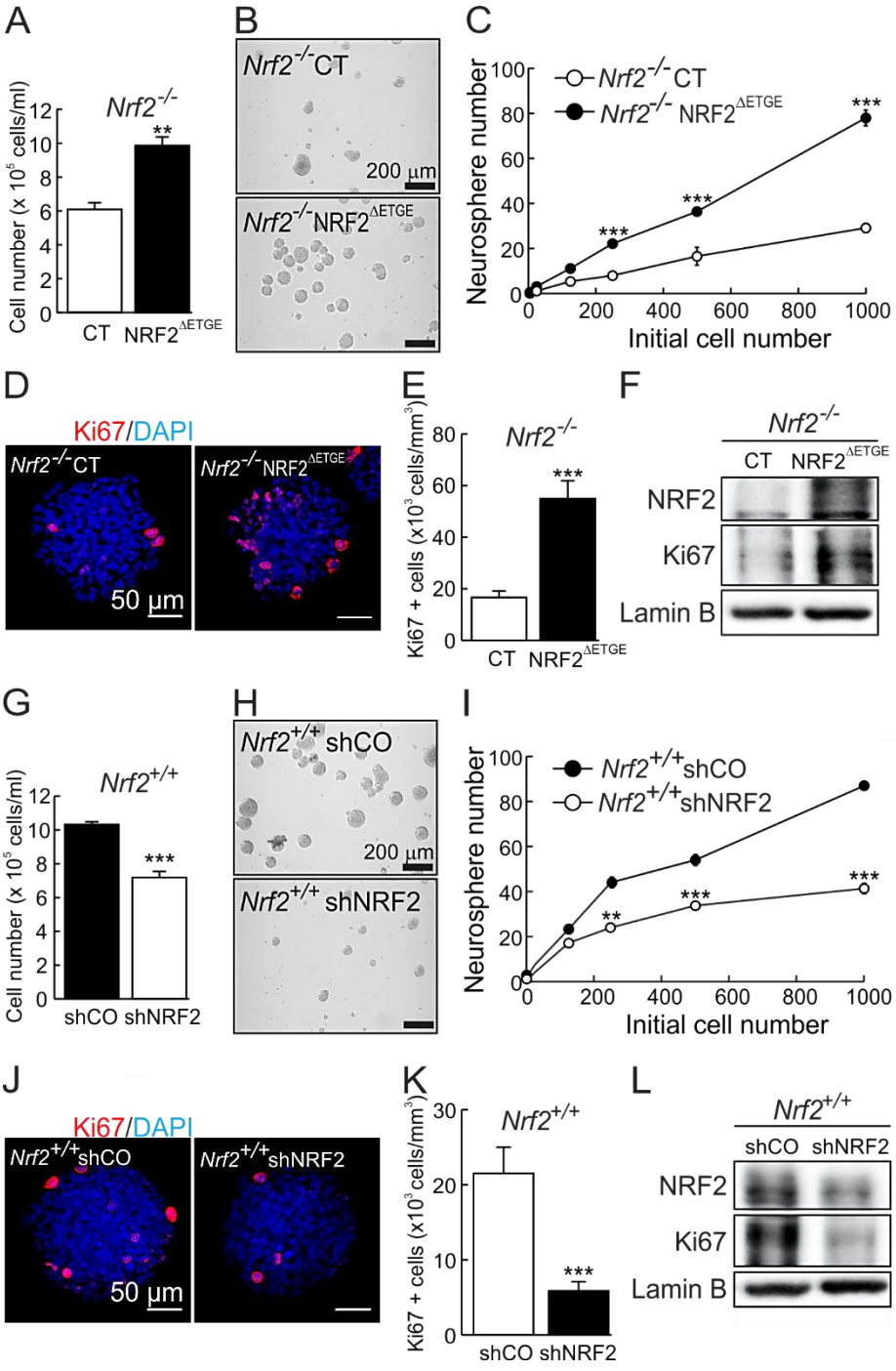


**Figure 23. Impaired proliferative and clonogenic capacity of NSPCs from *Nrf2*$^{-/-}$ mice.** **(A)** Cell number determination from an initial seeding of 20,000 cells/ml of *Nrf2*$^{-/-}$-NSPCs transduced with lentivirus encoding control (CT) or active NRF2$^{\Delta ETGE}$ after 5 days of lentiviral transduction. Data are mean ± S.D. (n = 10). **(B)** Representative images of neurosphere formation under these conditions. **(C)** Serial dilution assay of *Nrf2*$^{-/-}$-CT and *Nrf2*$^{-/-}$-NRF2$^{\Delta ETGE}$ NSPCs showing the number of neurospheres formed after 7 days. Data are mean ± S.D. (n = 10). **(D)** Representative confocal image of proliferative marker Ki67. Nuclei were counterstained with DAPI. **(E)** Quantification of Ki67$^{+}$ cells in 150-200 µm-diameter neurospheres from **D**. Data are mean ± SEM (n ≥ 10). **(F)** Representative immunoblots of NRF2, Ki67 and Lamin B as loading control in *Nrf2*$^{-/-}$-CT and *Nrf2*$^{-/-}$-NRF2$^{\Delta ETGE}$ neurospheres after 5 days of lentiviral transduction. **(G)** Cell number determination from an initial seeding of 20,000 cells/ml of NSPCs *Nrf2*$^{+/+}$ transduced with lentivirus encoding shcontrol (shCO) or mouse shNRF2 and after 5 days of lentiviral transduction. Data are mean ± S.D. (n = 10). **(H)** Representative images of neurosphere formed under these conditions. **(I)** Serial dilution assay of *Nrf2*$^{+/+}$-shCO and *Nrf2*$^{+/+}$-shNRF2 NSPCs showing the number of neurospheres formed after 7 days. Data are mean ± S.D. (n = 10). **(J)** Representative confocal image of proliferative marker Ki67 of neurospheres *Nrf2*$^{+/+}$-shCO and *Nrf2*$^{+/+}$-shNRF2 after 5 days *in vitro*. Nuclei were counterstained with DAPI. **(K)** Quantification of Ki67$^{+}$ cells in 150-200 µm-diameter neurospheres from **J**. Data are mean ± SEM (n ≥ 10). **(L)** Representative immunoblot analysis of NRF2, Ki67 and Lamin B as a loading control in *Nrf2*$^{+/+}$-shCO and *Nrf2*$^{+/+}$-shNRF2 neurospheres after 5 days of lentiviral transduction. Statistical analysis was performed with the Student's *t*-test. **p* ⩽ 0.05; ***p* ⩽ 0.01, ****p* ⩽ 0.001 *vs.* control group.

### 3. Age-related decline of the NSPCs pool from the SGZ is exacerbated in NRF2-deficient mice.

Next, we assessed the NSPCs pool in the SGZ. For this, we first performed immunostaining with Nestin, SOX2 and GFAP antibodies to determine the number of NSCs and NPCs, as these cell populations drive NSPCs towards mobilization and differentiation of neural lineages. NSCs were identified as Nestin$^{+}$/SOX2$^{+}$/GFAP$^{+}$ cells and NPCs as Nestin$^{+}$/SOX2$^{+}$/GFAP$^{-}$ cells, and were distinguished morphologically: NSCs exhibit a non-branched long neurite across the GCL while NPCs are located at the basis of the granular layer and do not present long neurites (Fig. 24A) (Encinas et al., 2011). The number of NSCs and NPCs in *Nrf2*$^{+/+}$ mice decreased with aging (Fig. 24B, C and D). Thus at 12 months of age the number of NSCs and NPCs had decreased to ~50% compared to 3 months of age. Importantly, in 3-month-old *Nrf2*$^{-/-}$ mice the amount of these cells was already substantially decreased to ~50%. This suggests that NRF2 deficiency accelerates aging-dependent decline of NSCs and NPCs in the hippocampal neurogenic niche.

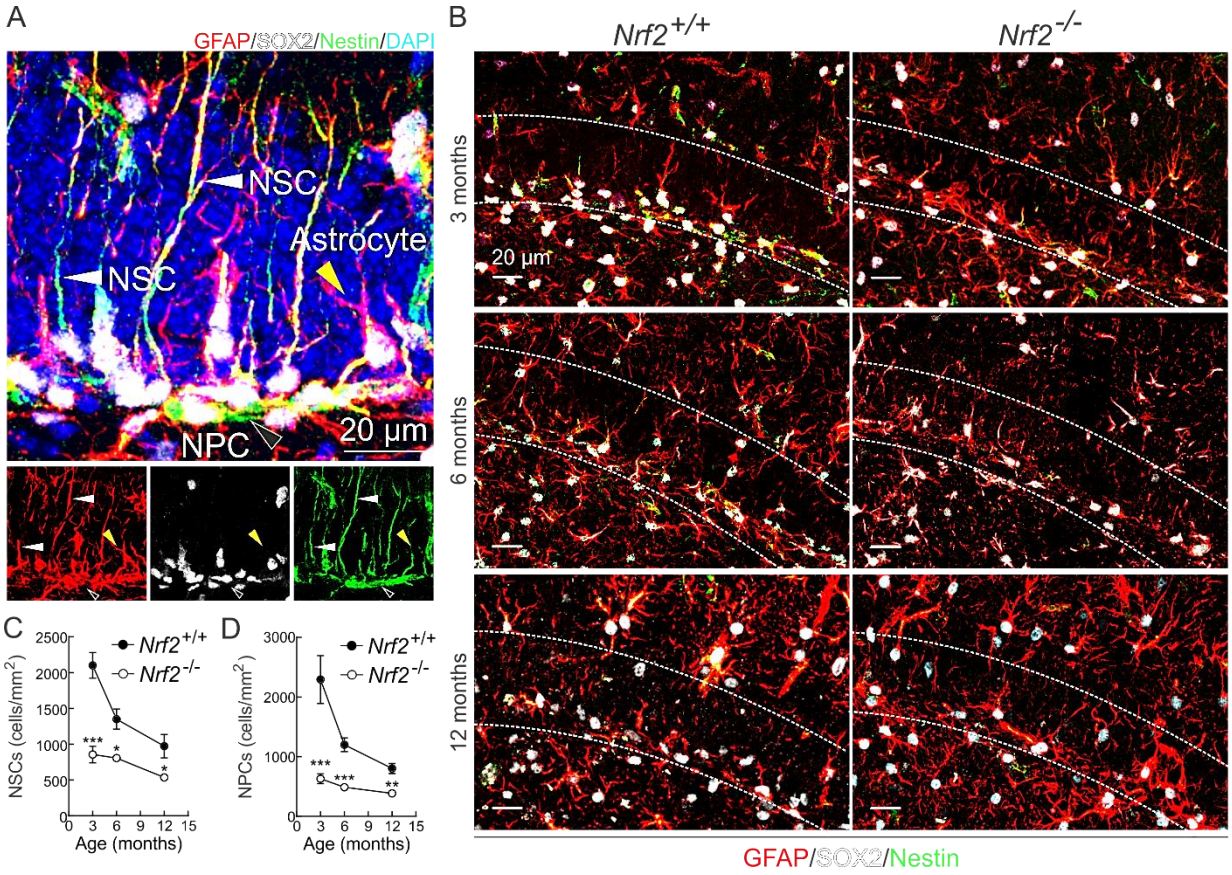


**Figure 24. NRF2 deficiency provokes a drop in the pool of NSCs and NPCs. (A)** Representative confocal image of the SGZ immunostained with GFAP, SOX2 and Nestin. White, black and yellow arrowheads point a typical NSC, NPC and astrocyte, respectively. Nuclei were counterstained with DAPI. **(B)** Representative confocal images of GFAP, SOX2 and Nestin in the SGZ of 3- (Upper panel), 6- (middle panel) and 12- (lower panel) month-old mice of the indicated genotypes. Dotted lines delimit the GCL and SGZ. **(C)** and **(D)** quantification of NSCs and NPCs, respectively, in 3-, 6- and 12-month-old mice of the indicated genotypes. Data represent mean ± SEM (n = 5). Statistical analysis was performed with a Student's *t*-test. *$p \leqslant 0.05$; **$p \leqslant 0.01$, ***$p \leqslant 0.001$ *vs.* *Nrf2*$^{+/+}$ mice.

Accordingly, the number of Nestin$^{+}$ cells, evaluated by immunostaining, was decreased in *Nrf2*$^{-/-}$ neurospheres from newborn (Fig. 25A and B) and 3-month-old (Fig. 25D and E) mice, even at the protein level (Fig. 25C and F).

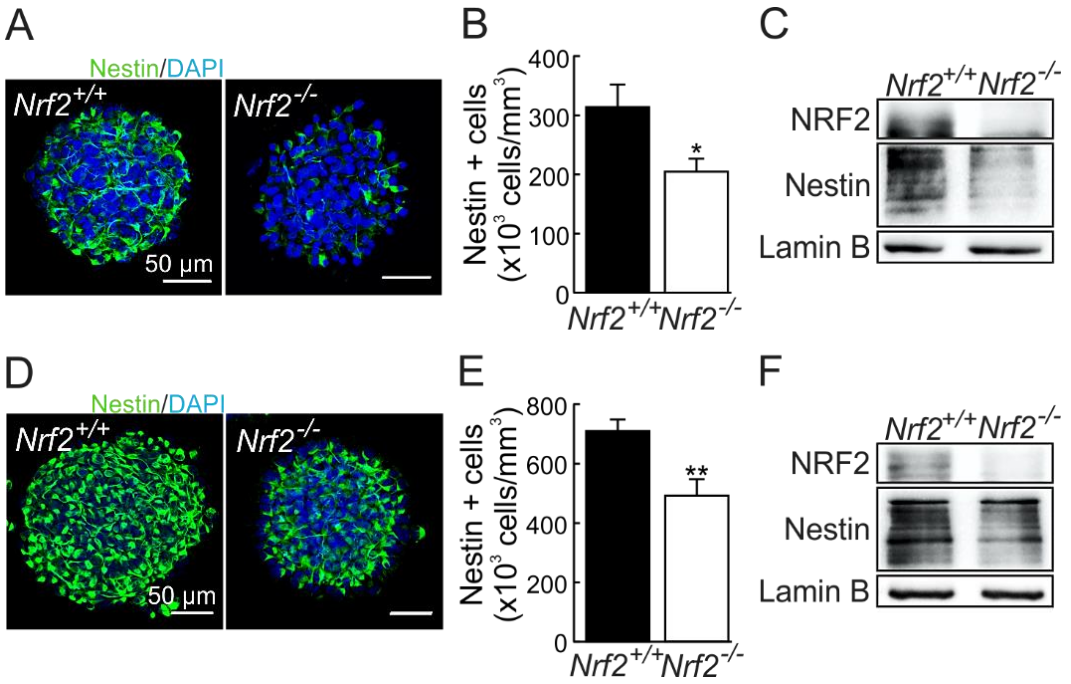


**Figure 25. NRF2 deficiency leads to a decreased of Nestin$^{+}$ cells in neurospheres.** **(A)** Representative confocal images of Nestin immunofluorescence on neurospheres derived from newborn mice of the indicated genotypes. **(B)** Quantification of Nestin$^{+}$ cells in these neurospheres Data show mean ± SEM (n ≥ 10). **(C)** Representative immunoblots of NRF2, Nestin and Lamin B as a loading control in *Nrf2*$^{+/+}$ and *Nrf2*$^{-/-}$ neurospheres derived from the SGZ of newborn mice. **(D)** Representative confocal images of Nestin immunofluorescence on neurospheres derived from 3-month-old mice of the indicated genotypes. **(E)** Quantification of Nestin$^{+}$ cells in these neurospheres (n = 10). Data show mean ± SEM (n ≥ 10). **(F)** Representative immunoblot analysis of NRF2, Nestin and Lamin B as a loading control in *Nrf2*$^{+/+}$ and *Nrf2*$^{-/-}$ neurospheres derived from the SGZ of 3-month-old mice. *$p \leqslant 0.05$; **$p \leqslant 0.01$, ***$p \leqslant 0.001$ *vs.* *Nrf2*$^{+/+}$ according to a Student's *t*-test.

These results suggested an impaired self-renewal capacity of NSCs and NPCs. Therefore, we evaluated the number of symmetric and asymmetric divisions in cell culture based on SOX2 and Nestin immunostaining. Cells derived from symmetric divisions express SOX2 and Nestin in both siblings, while in asymmetric divisions only one sibling expresses SOX2 and Nestin (Fig. 26A). In *Nrf2*$^{+/+}$ NSPCs cultures, ~60% (in newborn isolated NSPCs) or ~75% (in adult isolated NSPCs) of the cells underwent symmetric divisions (Fig. 26B and C). However, in the *Nrf2*$^{-/-}$ NSPCs symmetric divisions accounted for only ~25%, thus inversely increasing the percentage of asymmetric divisions (Fig. 26B and C). These observations were further analyzed by rescuing *Nrf2*$^{-/-}$ NSPCs by lentivirus-mediated expression of NRF2$^{\Delta ETGE}$. Ectopic expression of NRF2 led to an increase in symmetric divisions compared to the control (Fig. 26D). By contrast, lentiviral knockdown of NRF2 in *Nrf2*$^{+/+}$ NSPCs resulted in a reduction of symmetric divisions (Fig. 26E). Taken together, these results suggest that NRF2 deficiency limits the self-renewal capacity of the NSPCs in the neurogenic niche of the SGZ.

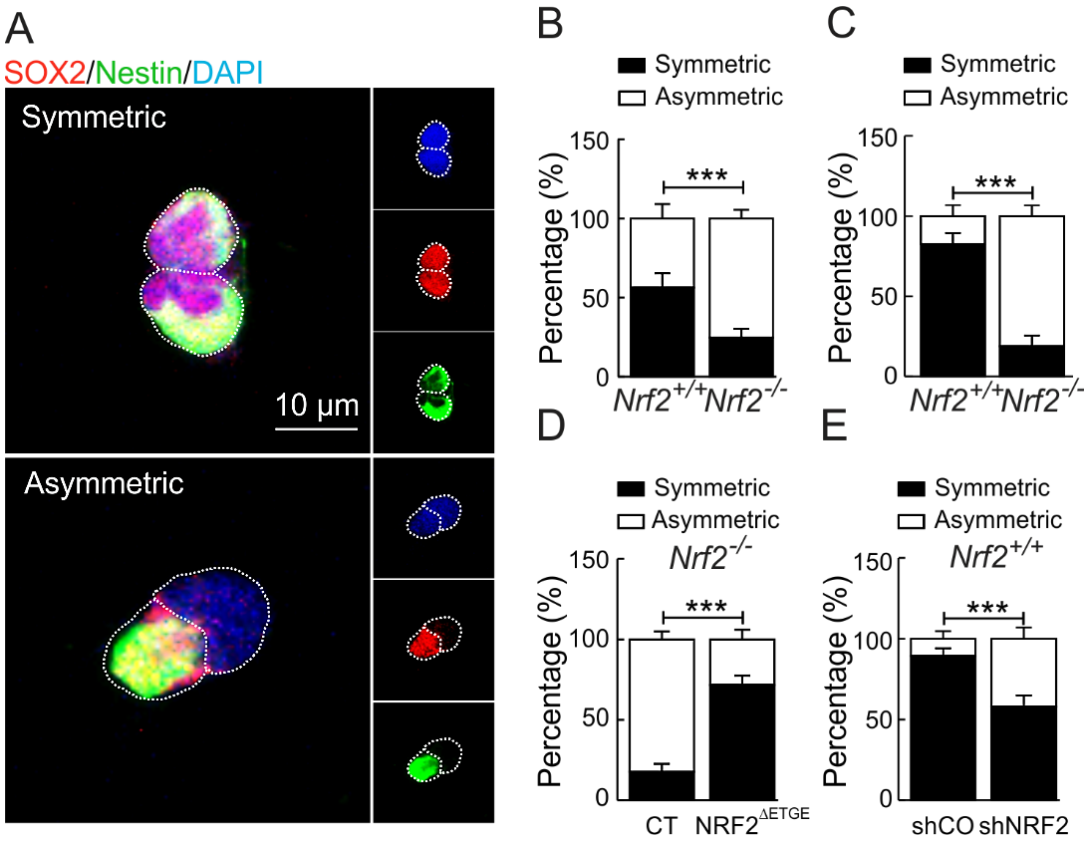


**Figure 26. NRF2 participates in self-renewal of NSPCs. (A)** Representative confocal images of symmetric (upper panel) and asymmetric (lower panel) divisions by immunofluorescence of SOX2 and Nestin. Nuclei were counterstained with DAPI. **(B)** Quantification of symmetric and asymmetric divisions in cultures of NSPCs isolated from the SGZ of newborn mice. **(C)** Quantification of symmetric and asymmetric divisions in cultures of NSPCs isolated from the SGZ of 3-month-old mice. **(D)** Cell pair assay in cultures of *Nrf2*$^{-/-}$-CT and *Nrf2*$^{-/-}$- NRF2$^{\Delta ETGE}$ NSPCs. **(E)** Quantification of symmetric and asymmetric divisions in cultures of *Nrf2*$^{+/+}$ NSPCs transduced with control (shCO) or shRNA lentivirus to knockdown NRF2 (shNRF2). Data show mean ± S.D. (n = 60 pairs). ***$p \leqslant 0.001$ *vs.* experimental controls according to Student's *t*-test.

### 4. Neuronal differentiation of NSPCs from the SGZ is impaired in *Nrf2*$^{-/-}$ mice.

We evaluated the capacity of the SGZ to produce new neurons using Doublecortin (DCX) staining that specifically labels neuroblasts and immature neurons (Fig. 27A and B). In both *Nrf2*$^{+/+}$ and *Nrf2*$^{-/-}$ mice the amount of DCX$^{+}$ cells decreased gradually to 10% at 12 months of age, but the SGZ of *Nrf2*$^{-/-}$ mice presented a lower capacity to generate these adult-born neurons already at 3 and 6 months of age. These data correlate with the impairment of LTP response in *Nrf2*$^{-/-}$ mice (Fig. 17).

These results were also analyzed in neurospheres after removal of growth factors during 2 days in non-adherent conditions, allowing partial NSPCs differentiation. The amount of DCX$^{+}$ cells in the neurospheres was substantially decreased to ~20% in newborn (Fig. 28A and B) and ~50% in 3-month-old *Nrf2*$^{-/-}$ mice (Fig. 28C and D).

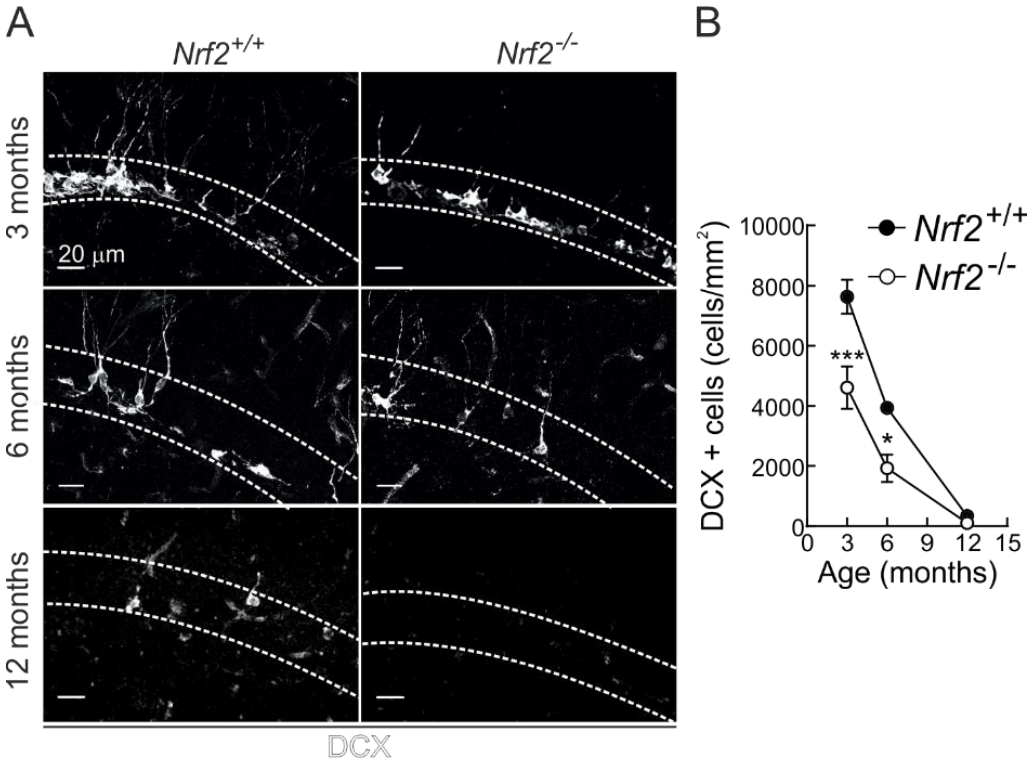


**Figure 27. NRF2 deficiency leads to a reduction of adult-born neurons. (A)** Representative images of DCX immunostaining in the SGZ of 3-, 6- and 12-month-old mice of the indicated genotypes. The white dotted line delimits the GCL. **(B)** Quantification of $DCX^+$ cells of the indicated genotypes. Data represent mean ± SEM (n = 5). Statistical analysis was performed with a Student's *t*-test. $*p \leqslant 0.05$; $***p \leqslant 0.001$ *vs.* *Nrf2*$^{+/+}$ mice.

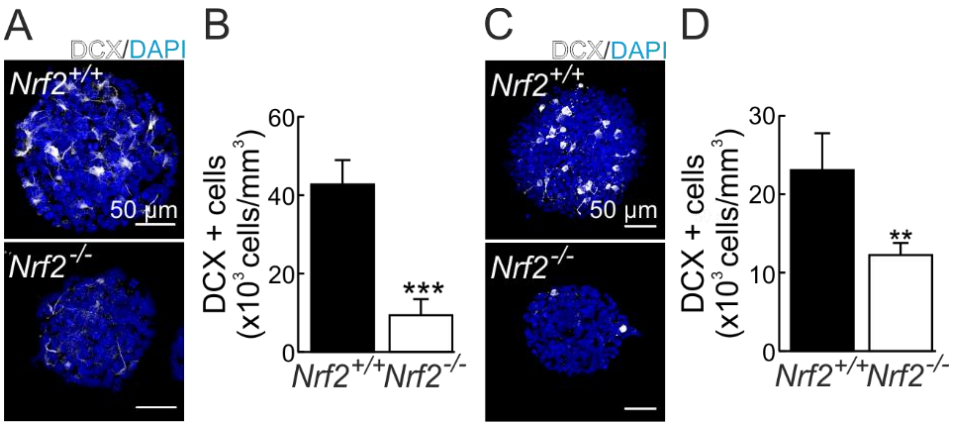


**Figure 28. NRF2 deficiency leads to a decreased number of $DCX^+$ cells in neurospheres. (A)** Representative confocal images of DCX immunofluorescence on neurospheres derived from newborn mice of the indicated genotypes after two days without growth factors. **(B)** Quantification of $DCX^+$ cells of in neurospheres of A ($n \geq 10$). **(C)** Representative confocal images of DCX immunofluorescence on neurospheres derived from 3-month-old mice of the indicated genotypes after two days without growth factors. **(D)** Quantification of $DCX^+$ cells in neurospheres of C ($n \geq 10$). Data show mean ± SEM. $**p \leqslant 0.01$, $***p \leqslant 0.001$ *vs.* *Nrf2*$^{+/+}$ according to a Student's *t*-test.

Next, we examined the differentiation potential of the NSPCs. When neurospheres are plated under adherent conditions on poly-D-lysine and grown in the absence of growth factors, NSPCs migrate away from the neurosphere core and spread around forming a carpet of cells differentiating to neurons, astrocytes and oligodendrocytes (Reynolds and Weiss, 1992; Reynolds and Weiss, 1996). First, following DCX and DAPI immunostaining, we observed a decrease in the migration distance of cells from newborn

(Fig.29A and B) and, more notoriously, from 3-month-old (Fig. 29F and G) *Nrf2*$^{-/-}$ mice. DCX immunostaining in the differentiating cultures indicated impairment in the neuronal differentiation of *Nrf2*$^{-/-}$ neurospheres at birth (Fig. 29A and C) and at 3 months of age (Fig. 29F and H) measured as the percentage of DCX$^{+}$ cells in the differentiation carpet. To analyze the maturation of these cells and their capacity to interact with other neurons, we performed Sholl analysis in DCX$^{+}$ cells after 7 days of differentiation. This analysis measures the branching complexity in newborn (Fig. 29D and E) and 3-month-old (Fig. 29I and J) derived cultures. DCX$^{+}$ cells from *Nrf2*$^{-/-}$ mice showed a decrease in the number of neurite crossings suggesting a reduced maturation compared to those of *Nrf2*$^{+/+}$ mice.

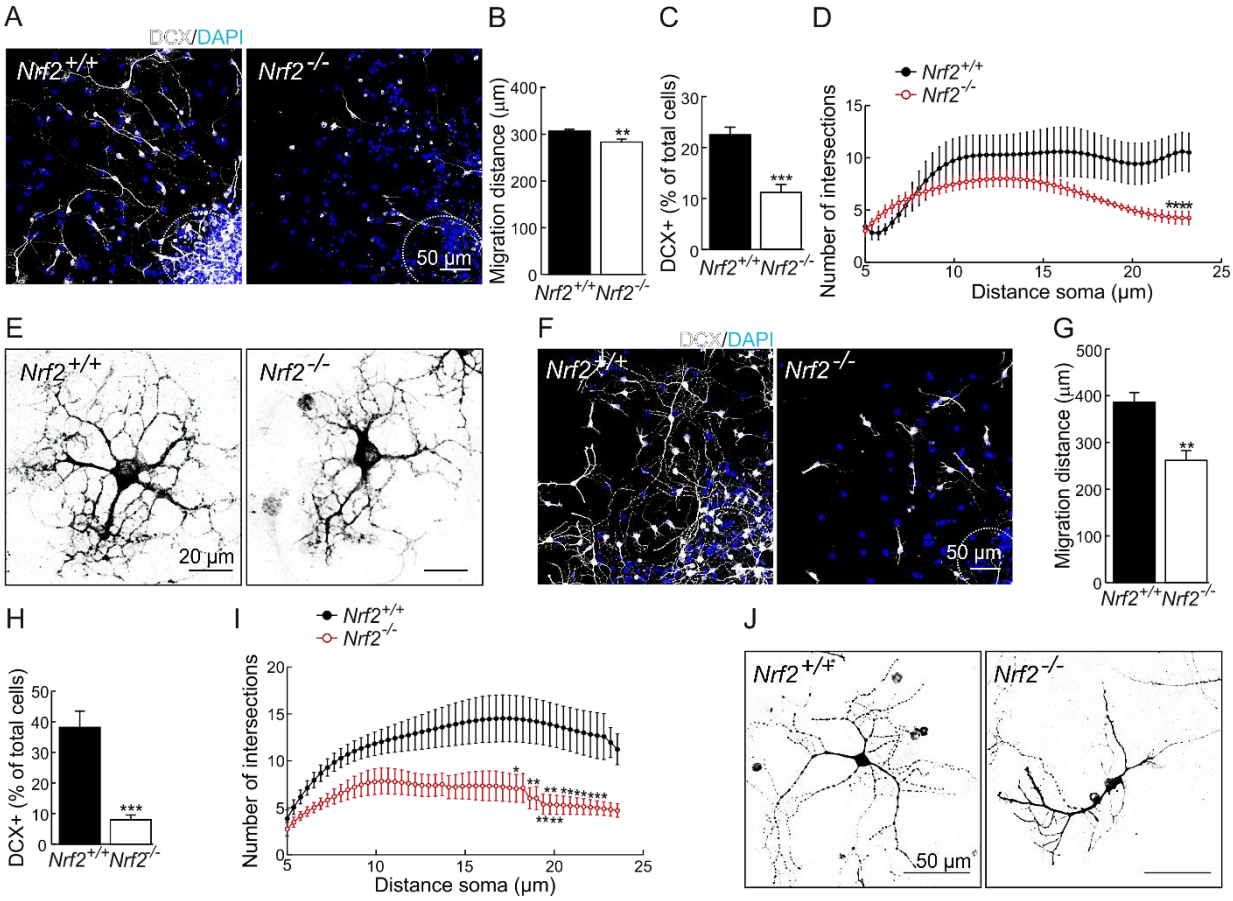


**Figure 29. Role of NRF2 in the differentiation of NSPCs *in vitro*. (A)** Representative confocal images of DCX immunostaining of neurospheres from newborn mice grown after 7 days in differentiation conditions. Nuclei were counterstained with DAPI. **(B)** Measurement of the migration distance as determined by distance from the neurosphere edge (dotted line in **A**) to DAPI stained nuclei (n = 40). **(C)** Quantification of DCX$^{+}$ cells from neurospheres shown in **A** (n = 12). **(D)** Sholl analysis of the neurons in the differentiated neurospheres derived from 3-month-old mice (n = 24). **(E)** Representative images of DCX$^{+}$ cells in the *Nrf2*$^{+/+}$ and *Nrf2*$^{-/-}$ cultures derived from newborn mice. **(F)** Representative confocal images of DCX immunostaining of neurospheres from 3-month-old mice grown after 7 days in differentiation conditions. Nuclei were counterstained with DAPI. **(G)** Measurement of migration distance as determined by distance from the neurosphere edge (dotted line in **F**) to DAPI stained nuclei (n = 40). **(H)** Quantification of DCX$^{+}$ cells from neurospheres shown in **F** (n = 12). **(I)** Sholl analysis of the neurons in the differentiated neurospheres derived from 3-month-old mice (n = 24). **(J)** Representative images of DCX$^{+}$ cells in the *Nrf2*$^{+/+}$ and *Nrf2*$^{-/-}$ cultures derived from 3-month-old mice. Data represent mean ± SEM. *$p \leqslant 0.05$; **$p \leqslant 0.01$, ***$p \leqslant 0.001$ *vs.* the *Nrf2*$^{+/+}$ group according to a Student's *t*-test.

Genetic manipulation by lentiviral expression of NRF2 was also analyzed in differentiation assays. Neurospheres were seeded after 5 days of lentiviral transduction in differentiation conditions during 7 additional days (Fig. 30A). The migration distance was partially recovered by reintroduction of NRF2 expression in *Nrf2*$^{-/-}$ cultures (Fig. 30B and C), and reduced by knockdown of NRF2 in *Nrf2*$^{+/+}$ cultures (Fig. 30E and F). Moreover, rescue of NRF2 expression in *Nrf2*$^{-/-}$ cultures led to enhanced neuronal differentiation quantified as DCX$^{+}$ cells in the differentiation carpet (Fig. 30D). By contrast, silencing NRF2 in *Nrf2*$^{+/+}$ neurospheres reduced significantly the percentage of DCX$^{+}$ cells (Fig. 30G). All these data suggest that NRF2 is not only important for maintaining the NSPCs pool but also for supporting a proper neuronal differentiation.

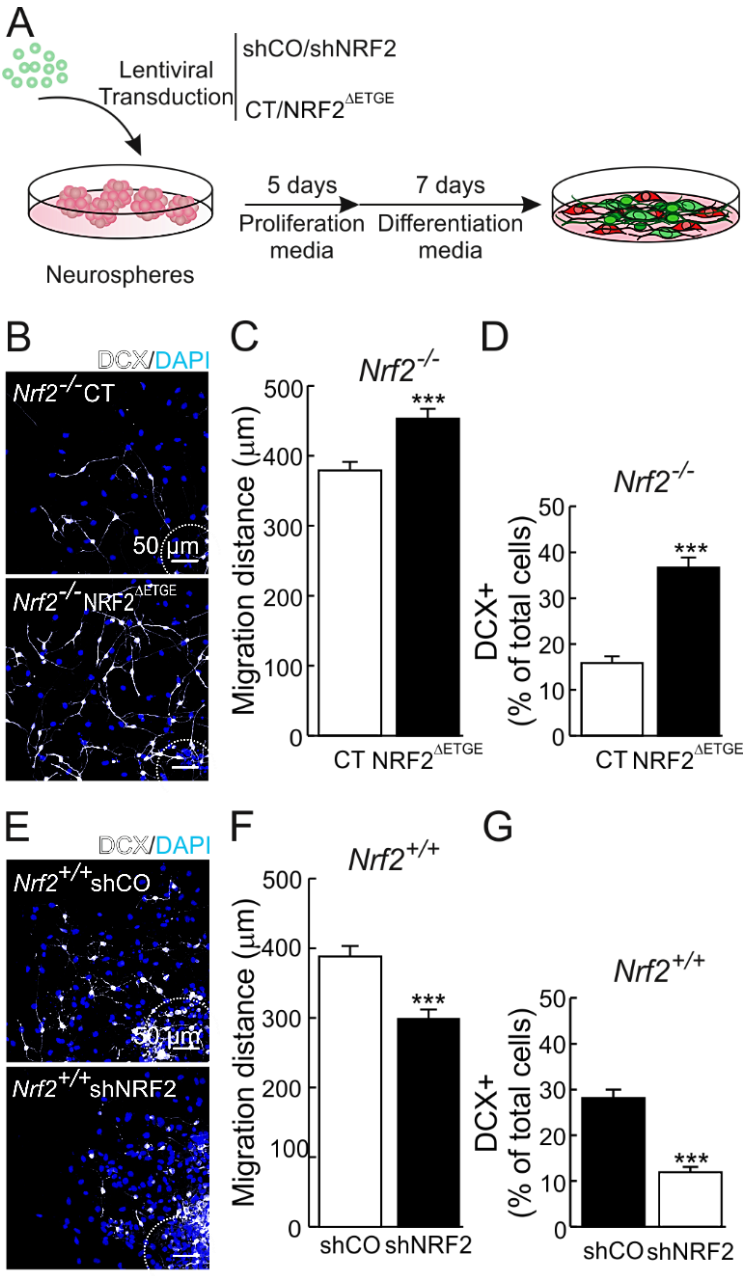


**Figure 30. Impact of genetic modulation of NRF2 levels on neuronal differentiation of NSPCs. (A)** Schematic overview of experimental procedure. **(B)** Representative confocal images of DCX immunostaining of control *Nrf2*$^{-/-}$ neurospheres (CT) or rescued by lentiviral expression of NRF2$^{\Delta ETGE}$ after 7 days in differentiation conditions. Nuclei were counterstained with DAPI. **(C)** Measurement of the cell migration distance from the neurosphere edge (dotted line in **B**) (n = 40). **(D)** Quantification of DCX$^{+}$ cells in the differentiation carpet of *Nrf2*$^{-/-}$-CT and *Nrf2*$^{-/-}$-NRF2$^{\Delta ETGE}$ cultures (n = 12). **(E)** Representative confocal images of DCX immunostaining of *Nrf2*$^{+/+}$ neurospheres transduced with lentiviral control vector (shCO) or NRF2-knockdown (shNRF2) after 7 days in differentiation conditions. Nuclei were counterstained with DAPI. **(F)** Measurement of the cell migration distance from the neurosphere edge (dotted line in **E**) (n = 40). **(G)** Quantification of DCX$^{+}$ cells in the differentiation carpet of *Nrf2*$^{+/+}$-shCO and *Nrf2*$^{+/+}$-shNRF2 cultures (n = 12). Data represent mean ± SEM. ***$p \leqslant 0.001$ *vs.* control$^{-}$ group according to a Student's *t*-test.

## 5. NRF2 deficiency impairs the balance in neuron/glia differentiation.

Our previous data suggest that NRF2 participates in the fate of NSPCs. To determine the role of NRF2 in this process, we performed a differentiation assay after incubation of *Nrf2*$^{+/+}$ and *Nrf2*$^{-/-}$ isolated neurospheres during 8 h with EdU, a nucleoside analogue of thymidine which is incorporated into DNA of proliferating cells during active DNA synthesis (Fig. 31A). Thus, we can mark NSPCs with EdU and monitor their differentiation dynamics. The rate of differentiation of EdU$^+$ cells towards astrocytes (GFAP$^+$ cells) and neurons (DCX$^+$ cells) in *Nrf2*$^{+/+}$ cultures was similar (Fig. 31B, C and D). By contrast, in *Nrf2*$^{-/-}$-derived-cultures, this ratio favoured astroglial differentiation, with an ~80% of EdU$^+$ cells being GFAP$^+$, while only ~20% were DCX$^+$ (Fig. 31B, C and D). Thus, NRF2 deficiency affects the differentiation rate of NSPCs, favouring astroglial differentiation.

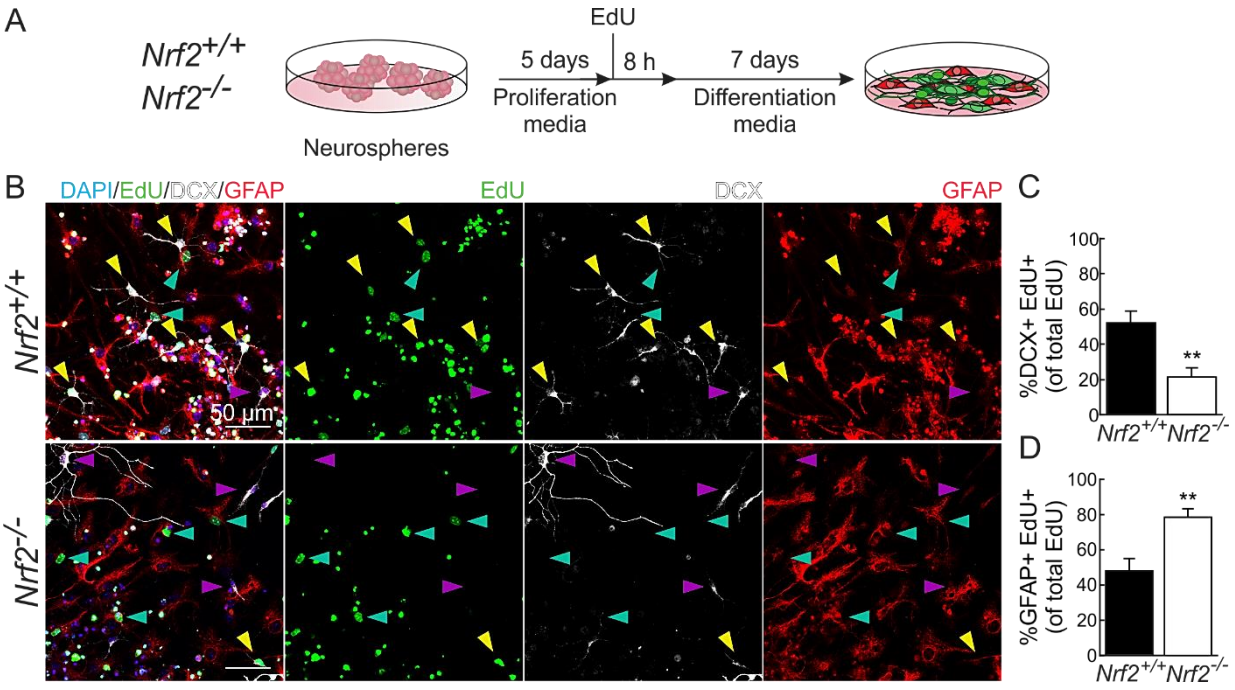


**Figure 31. NRF2 influences the fate of NSPCs. (A)** Schematic overview of experimental procedures: *Nrf2*$^{+/+}$ and *Nrf2*$^{-/-}$ formed neurospheres where incubated during 8 h with EdU and allowed to differentiate during 7 days. **(B)** Representative confocal images of EdU, DCX and GFAP immunostaining in *Nrf2*$^{+/+}$ and *Nrf2*$^{-/-}$ cultures of NSPCs after 7 days in differentiation conditions. Yellow arrowhead: DCX$^+$/EdU$^+$ cells; Purple arrowhead: DCX$^+$/EdU$^-$ cells; Green arrowhead: GFAP$^+$/EdU$^+$ cells. Nuclei were counterstained with Hoestcht 33342. **(C)** Quantification of DCX$^+$/EdU$^+$ cells. **(D)** Quantification of GFAP$^+$/EdU$^+$ cells. Data represent mean ± SEM (n = 20). $^{**}p \leqslant 0.01$ *vs.* control group according to a Student's *t*-test.

Astrocyte differentiation of NSCs *in vivo* in the SGZ was analyzed in 3, 6 and 12-month-old *Nrf2*$^{+/+}$ and *Nrf2*$^{-/-}$ mice by GFAP and SOX2 immunostaining, using co-labelling with Nestin (not showed in the figure to facilitate the view of astrocytes) to distinguish between astrocytes and NSPCs (Fig. 32A and B). The amount of astrocytes in the SGZ and GCL increased during aging, but more importantly, the *Nrf2*$^{-/-}$ mice exhibited higher abundance of astrocytes at all ages (Fig. 32A and B). Then, we evaluated the astroglial differentiation *in vitro*, using GFAP staining in neurospheres *Nrf2*$^{+/+}$ and *Nrf2*$^{-/-}$ after 7 days in differentiation conditions. We detected an increase in the number of astrocytes in *Nrf2*$^{-/-}$ vs *Nrf2*$^{+/+}$ cultures, being ~20% higher in newborn (Fig. 33A and B) and ~40% higher in 3-month-old derived neurospheres (Fig. 33C and D). Furthermore, rescuing NRF2 expression in *Nrf2*$^{-/-}$ cultures resulted in a reduction to ~20% of GFAP$^{+}$ cells (Fig. 33E and F). When we silenced NRF2 expression in *Nrf2*$^{+/+}$ cultures, we observed an increase in astrocytes (Fig. 33G and H).

All these experiments indicate that NRF2 is required not only for the proliferation of NSPCs, but also to keep the balance between neuronal and glial differentiation.

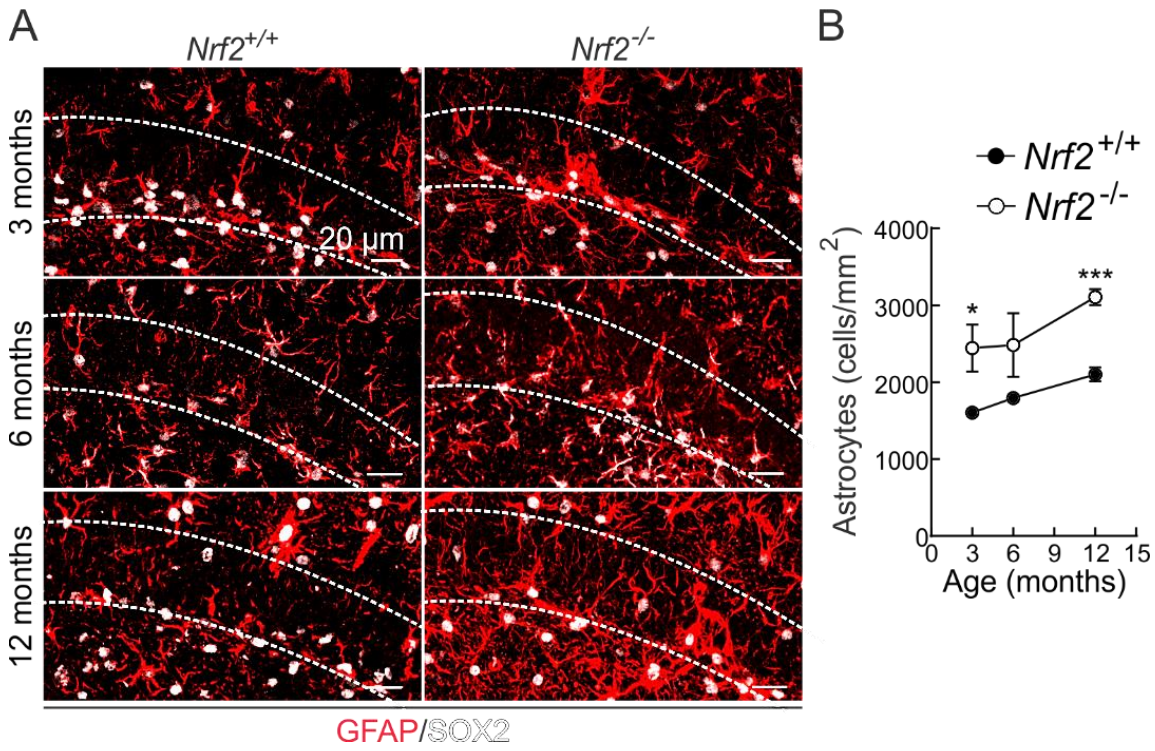


**Figure 32. NRF2 deficiency leads to an increase in astroglial differentiation. (A)** Representative confocal images of astrocytes immunostained with GFAP and SOX2 in the SGZ of 3-, 6- and 12-month-old mice of the indicated genotypes. Dotted lines limit SGZ and GCL. **(B)** Quantification of astrocytes in the SGZ and GCL of the indicated mice. Data represent mean ± SEM (n = 5). Statistical analysis was performed with a Student's *t*-test. *$p \leqslant 0.05$, ***$p \leqslant 0.001$ *vs.* *Nrf2*$^{+/+}$ mice.

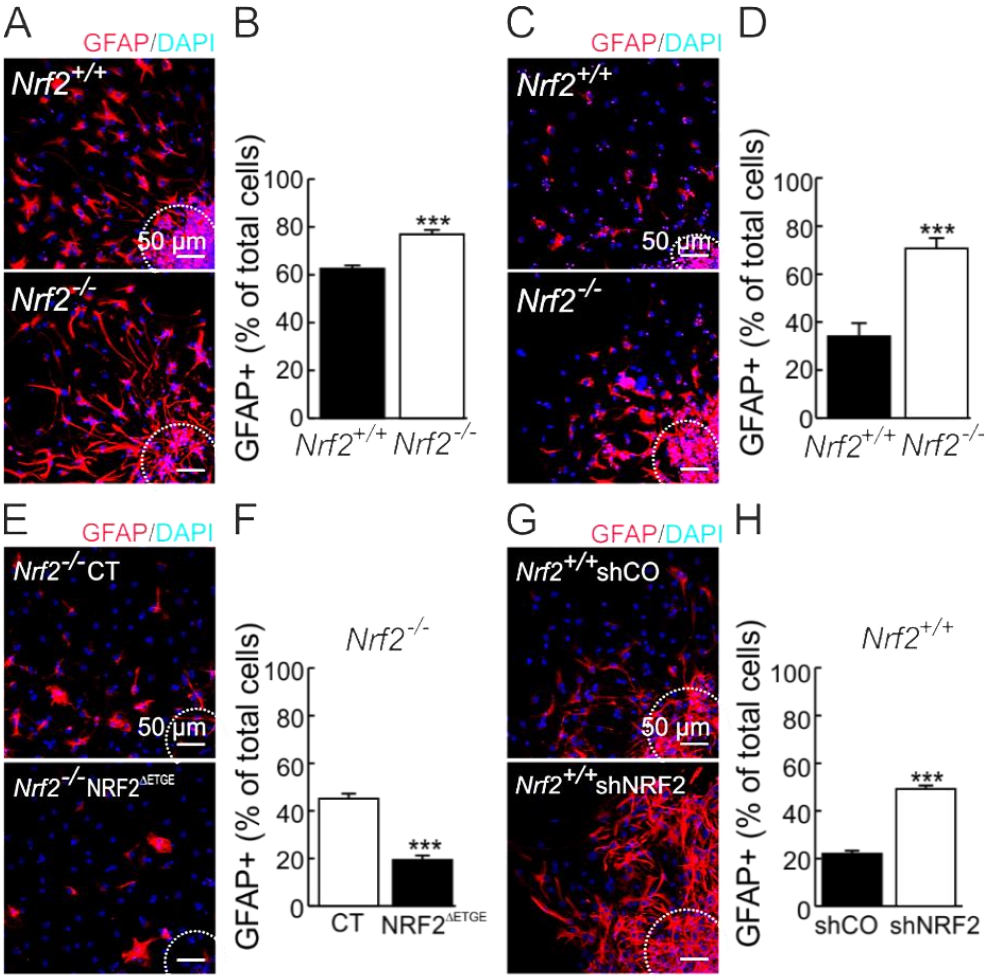


**Figure 33. NRF2 deficiency favours astroglial differentiation of NSPCs. A)** Representative confocal images of GFAP immunostaining of neurospheres from newborn mice grown after 7 days in differentiation conditions. Nuclei were counterstained with DAPI. **(B)** Quantification of GFAP$^+$ cells from neurospheres shown in **A** (n = 12). **(C)** Representative confocal images of GFAP immunostaining of neurospheres from 3-month-old mice grown after 7 days in differentiation conditions. Nuclei were counterstained with DAPI. **(D)** Quantification of GFAP$^+$ cells from neurospheres shown in **C** (n = 12). **(E)** Representative confocal images of GFAP immunostaining of control *Nrf2*$^{-/-}$ neurospheres (CT) or rescued by lentiviral expression of NRF2$^{\Delta ETGE}$ after 7 days in differentiation conditions. Nuclei were counterstained with DAPI. **(F)** Quantification of GFAP$^+$ cells in the differentiation carpet of *Nrf2*$^{-/-}$-CT and *Nrf2*$^{-/-}$-NRF2$^{\Delta ETGE}$ cultures (n = 12). **(G)** Representative confocal images of GFAP immunostaining of *Nrf2*$^{+/+}$ neurospheres transduced with lentiviral control vector (shCO) or NRF2-knockdown (shNRF2) after 7 days in differentiation conditions. Nuclei were counterstained with DAPI. **(H)** Quantification of GFAP$^+$ cells in the differentiation carpet of *Nrf2*$^{+/+}$-shCO and *Nrf2*$^{+/+}$-shNRF2 cultures (n = 12). Data represent mean ± SEM. ***$p \leqslant 0.001$ *vs.* control group according to a Student's *t*-test.

# II. Relevance of NRF2 in neurogenesis in a mouse model of AD.

## 1. Characteristics of the AD mouse model.

The role of NRF2 in maintenance of the SGZ neurogenic niche under the proteinopathy associated with AD has not been explored. We sought to determine if NRF2 deficiency, a typical hallmark of aging, might affect the neurogenic niche of the SGZ under conditions of amyloidopathy and tauopathy. To this purpose, we used a transgenic mouse expressing the human mutant proteins $APP^{V717I}$ and $TAU^{P301L}$ under the control of *Thy1* promoter in a genetic background with (AT-*Nrf2*$^{+/+}$) and without NRF2 (AT-*Nrf2*$^{-/-}$) (Rojo et al., 2017) (extended description is provided in Material and Methods). These mice develop amyloidopathy and tauopathy over time (Rojo et al., 2017) that correlate with disrupted autophagic degradation of APP and TAU (Pajares et al., 2016), exacerbated microglial activation (Rojo et al., 2018) and a low-grade persistent oxidative stress as determined by a drop in reduced glutathione levels, and an increase in protein carbonyls and peroxidised lipids (Rojo et al., 2017).

First, we characterized the expression of the human $APP^{V717I}$ or $TAU^{P301L}$ transgenes in the DG of 3, 6 and 12-month-old AT-*Nrf2*$^{+/+}$ and AT-*Nrf2*$^{-/-}$ mice (Fig. 34A and B). NSPCs did not express human $APP^{V717I}$ or $TAU^{P301L}$ transgenes (data not shown), consistent with previous reports indicating that transgenes under the control of the *Thy1* promoter co-localize with neuronal markers as MAP2 and Tubb3, but not with the NSPCs marker Nestin (Alic et al., 2016; Vidal et al., 1990; Hirrlinger et al., 2005; Lim et al., 2001). By immunohistochemistry, we determined the presence of neurons expressing human TAU and APP in the SGZ already at 3 months and also at 6 and 12 months of age. Furthermore, the expression of human TAU and APP in the SGZ was similar in both mouse types (Fig. 34A and B).

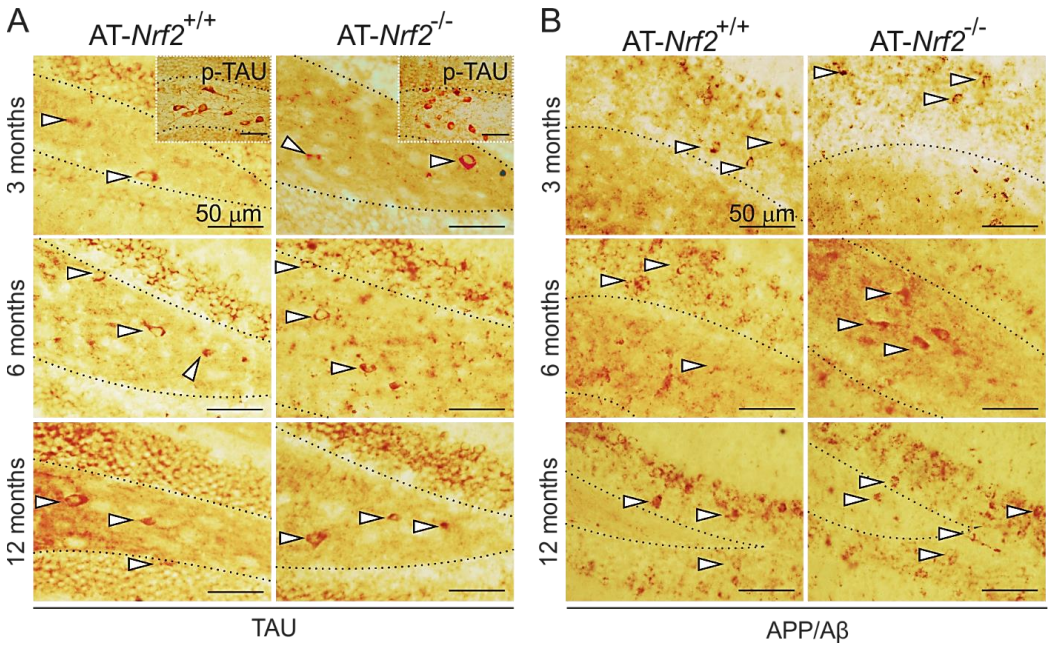


**Figure 34. Distribution of human TAU$^{+}$ and APP$^{+}$ neurons in the DG of the indicated genotypes. (A)** Representative images of TAU$^{+}$ neurons (HT7 clone) in the DG of 3, 6 and 12-month-old AT-*Nrf2*$^{+/+}$ and AT-*Nrf2*$^{-/-}$ mice. White arrowheads indicate TAU$^{+}$ neurons. Dotted lines delimit the DG. Insets are representative images of phosphorylated TAU$^{+}$ neurons (AT-8 clone). **(B)** Representative images of APP/Aβ (6E10 clone) in 3, 6 and 12-month-old AT-*Nrf2*$^{+/+}$ and AT-*Nrf2*$^{-/-}$ mice. White arrowheads indicate APP/Aβ$^{+}$ neurons. Dotted lines delimit the DG.

## 2. NRF2 deficiency aggravates the cognitive impairment of AD mice.

We tested the cognitive function related with the hippocampus. The Morris water maze (MWM) test is a widely used method to assess hippocampal spatial learning and memory in rodents (Morris, 1984; Morris et al., 1982). Thus, we evaluated the learning performance of 6-month-old AT-*Nrf2*$^{+/+}$ and AT-*Nrf2*$^{-/-}$ mice using this test (Fig. 35A and B) and measured the time necessary for the mice to find a submerged hidden platform (acquisition time) over 5 days (Fig. 35A). While the acquisition time of AT-*Nrf2*$^{+/+}$ mice decreased over training from 60 s to 20 s, indicating a normal learning performance, AT-*Nrf2*$^{-/-}$ mice still needed almost 40 s on the fifth day. Additionally, on the sixth day the hidden platform was removed to estimate spatial-memory, indicated as the tropism of the animals to remain at the haunt quadrant (Fig. 35B). AT-*Nrf2*$^{+/+}$ mice spent significantly more time in the target quadrant compared to AT-*Nrf2*$^{-/-}$, indicating that NRF2-absence correlated with impaired spatial memory already at 6 months of age in these AD mice.

In order to further analyze hippocampal function, we measured LTP in medial perforant path-to-DG synapses in 6-month-old AT-*Nrf2*$^{+/+}$ and AT-*Nrf2*$^{-/-}$ mice (Fig 35C and D). The recordings in the DG showed that the fEPSP was significantly lower after the administration of high-frequency stimuli in the AT-*Nrf2*$^{-/-}$ mice compared to AT-*Nrf2*$^{+/+}$ mice. Considering that, under normal conditions, the only measurable LTP in the DG is derived from adult-newborn neurons (Wang et al., 2000; Schmidt-Hieber et al., 2004; Snyder et al., 2001; Saxe et al., 2006; Garthe et al., 2009), these results indicate that NRF2 deficiency worsens the cognitive function related with adult hippocampal neurogenesis.

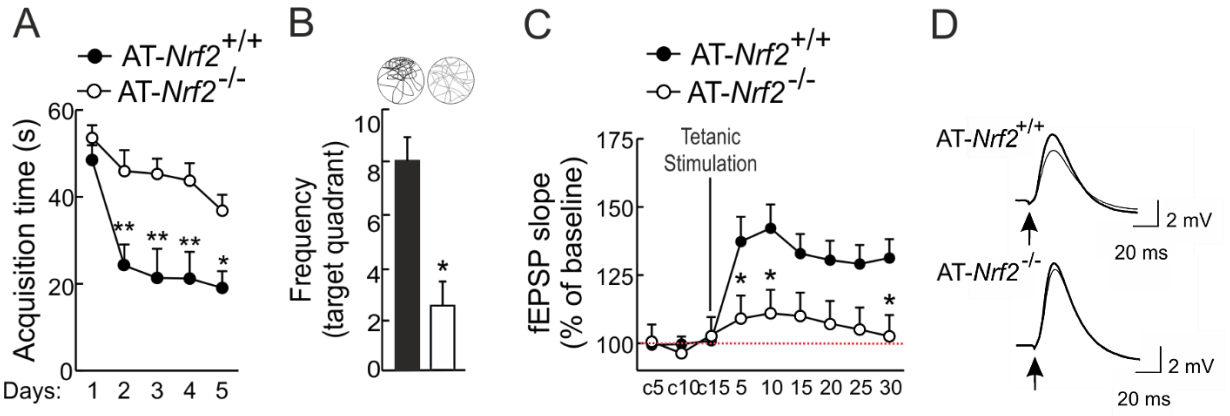


**Figure 35. NRF2 deficiency impairs spatial learning memory and LTP in AD mice. (A)** MWM performance indicated as acquisition time in the 5 trials for 6-month-old mice of the indicated genotypes. Data represent mean ± SEM (n = 10). **(B)** Top circles, representative swimming tracks of mice when the hidden platform had been removed. Lower graph, quantification of time spent in the target quadrant. Data represent mean ± SEM (n = 10). **(C)** LTP recordings for 6-month-old mice of the indicated genotypes. Data represent mean ± SEM (n = 6). **(D)** Illustrative responses recorded from the indicated mice before (thin line) and after (thick line) high-frequency trains of stimulation. Statistical analysis was performed with a Student's *t*-test *$p \leqslant 0.05$; **$p \leqslant 0.01$ *vs.* AT-*Nrf2*$^{+/+}$.

### 3. NRF2 deficiency correlates with a decrease in NSPCs in the SGZ of AD mice.

To analyze the dynamics of the NSPC pool under proteinopathic conditions, we immunostained dividing NSPCs with the NSPC marker Nestin and the proliferative marker Ki67 in the SGZ of 3, 6 and 12-month-old AT-*Nrf2*$^{+/+}$ and AT-*Nrf2*$^{-/-}$ mice and found that the proliferative rate declined with time, reaching almost undetectable levels at 12 months (Fig. 36A and B). Importantly, AT-*Nrf2*$^{-/-}$ mice exhibited a drastic reduction in the pool of proliferative NSPCs (Ki67$^{+}$/Nestin$^{+}$ cells) already at 3 months compared to AT-*Nrf2*$^{+/+}$ mice (Fig. 36A and B). Since at this age we did not find significant differences in APP/TAU expression in neurons (Fig. 34A and B), these results suggest that the disruption of the neurogenic niche is a very early event in the proteinopathy-associated neuronal damage.

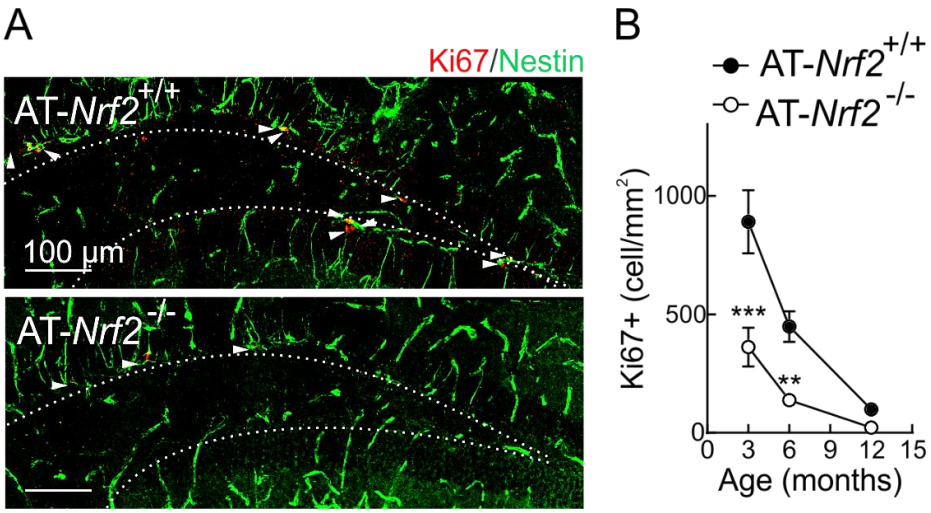


**Figure 36. NRF2 deficiency correlates with a decrease in proliferative NSPCs in the SGZ of AD mice. (A)** Representative confocal images of the NSPCs marker Nestin and the proliferative marker Ki67 in the SGZ of 3-month-old mice of the indicated genotypes. White arrowheads point to Ki67$^{+}$/Nestin$^{+}$ cells. **(B)** Quantification of Ki67$^{+}$ cells in 3-, 6- and 12-month-old mice of the indicated genotypes. Data represent mean ± SEM (n = 5). $^{**}p \leqslant 0.01$; $^{***}p \leqslant 0.001$ *vs.* AT-*Nrf2*$^{+/+}$ according to a Student's *t*-test.

We also monitored the pool of NSCs and NPCs by triple labelling with GFAP, SOX2 and Nestin. NSCs and NPCs were identified by their morphology: NSCs, in contrast to NPCs, present a long process crossing the GCL and are Nestin$^{+}$/SOX2$^{+}$/GFAP$^{+}$ (Encinas et al., 2011). As shown in Fig. 37, although the NSC and NPC pools decline in both genotypes during aging, they were ~3 folds lower in AT-*Nrf2*$^{-/-}$ compared to AT-*Nrf2*$^{+/+}$ mice already at 3 months. Therefore, the proteinopathy in the hippocampus induces a dependence of NRF2 in order to maintain this pool.

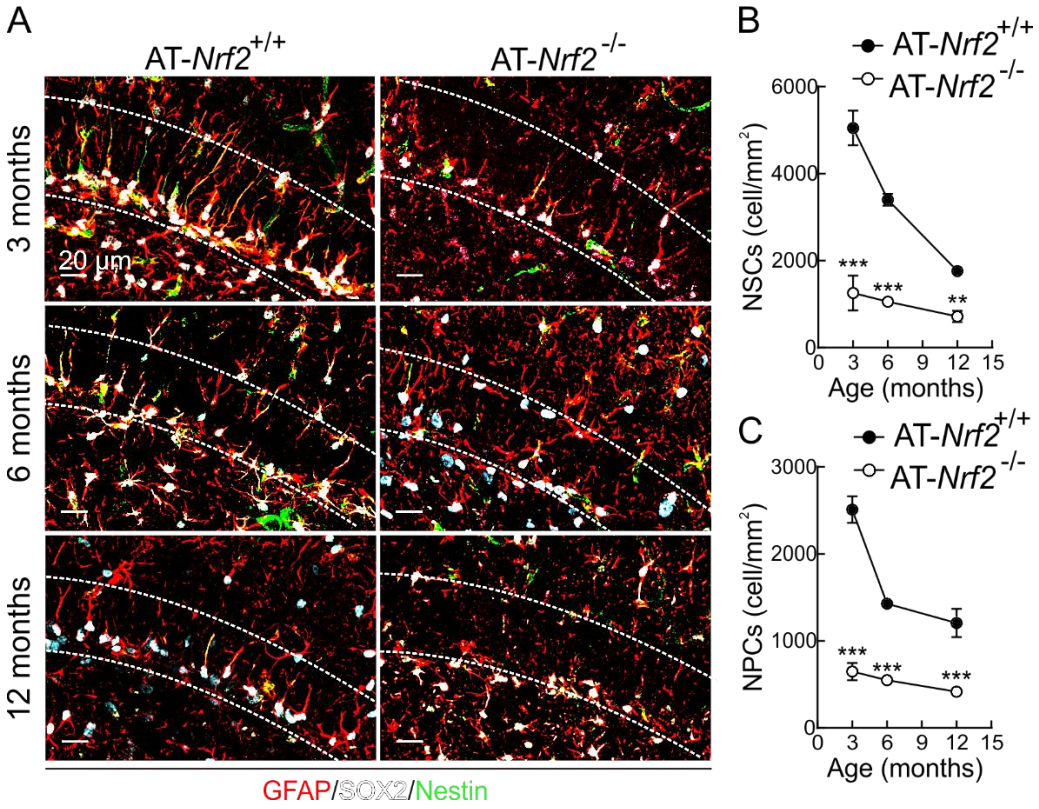


**Figure 37. NRF2 deficiency leads to a strong reduction in the number of NSCs and NPCs in the hippocampus. (A)** Representative confocal image of GFAP, SOX2 and Nestin immunofluorescence in 3-, 6- and 12-month-old mice of the indicated genotypes. Dotted lines delimit the SGZ and the GCL. **(B)** Quantification of NSCs in 3-, 6- and 12-month-old mice of the indicated genotypes. **(C)** Quantification of NPCs in 3-, 6- and 12-month-old mice of the indicated genotypes based on the immunostaining showed in (A). Data show mean ± SEM (n = 4). $^{**}p \leqslant 0.01$; $^{***}p \leqslant 0.001$ *vs.* AT-*Nrf2*$^{+/+}$ according to a Student's *t*-test.

## 4. NRF2 deficiency in AD mice favours astroglial vs. neuronal differentiation.

We performed immunostaining with the marker of neuroblasts and immature neurons, DCX in the SGZ of 3, 6 and 12-month-old AT-*Nrf2*$^{+/+}$ and AT-*Nrf2*$^{-/-}$ mice (Fig 38A and B). As expected, during aging, the cell density of DCX$^{+}$ cells was decreasing, but its cell number was lower in AT-*Nrf2*$^{-/-}$ even at 3-months of age (Fig. 38A and B), suggesting an accelerated loss of neurogenic capacity under NRF2-deficient conditions.

Next, we determined the astrocyte differentiation of NSCs in the SGZ by immunostaining with GFAP, accompanied by Nestin (not seen in the figure to facilitate the view of GFAP staining) to distinguish astrocytes from NSCs. The population of astrocytes was enriched in AT-*Nrf2*$^{-/-}$ at all ages studied (Fig. 39A and B). These results suggest that loss of NRF2 favours NSPCs differentiation to astrocytes at the expense of neuronal differentiation and exhaustion of NSPCs pool.

Our findings point NRF2 as a factor required for hippocampal NSPCs to undergo proper proliferation and differentiation under AD pathological conditions, and suggest that NRF2 up-regulation might provide a mechanism to preserve the neurogenic functionality of the hippocampus.

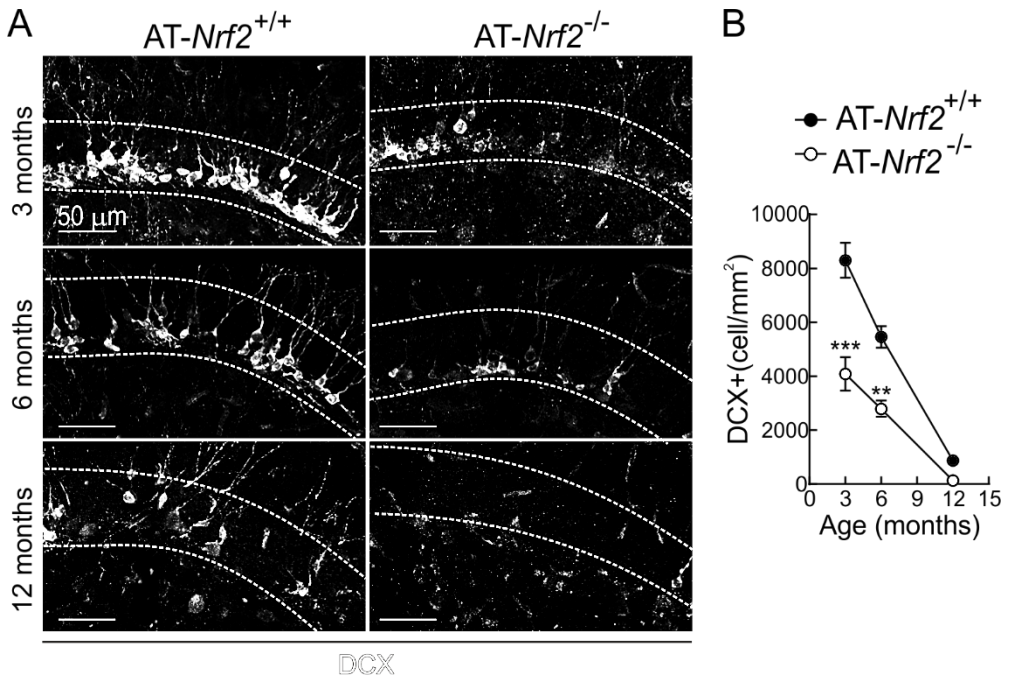


**Figure 38. Lack of NRF2 impairs neuronal differentiation in AD mice. (A)** Illustrative confocal images of the immature neuron marker DCX in the SGZ of 3-, 6- and 12-month-old mice of the indicated genotypes. Dotted lines delimit the SGZ and the GCL. **(B)** Quantification of $DCX^+$ cells under the conditions detailed in (A). Data show mean ± SEM (n = 4). $^{**}p \leqslant 0.01$; $^{***}p \leqslant 0.001$ *vs.* AT-$Nrf2^{+/+}$ according to a Student's *t*-test.

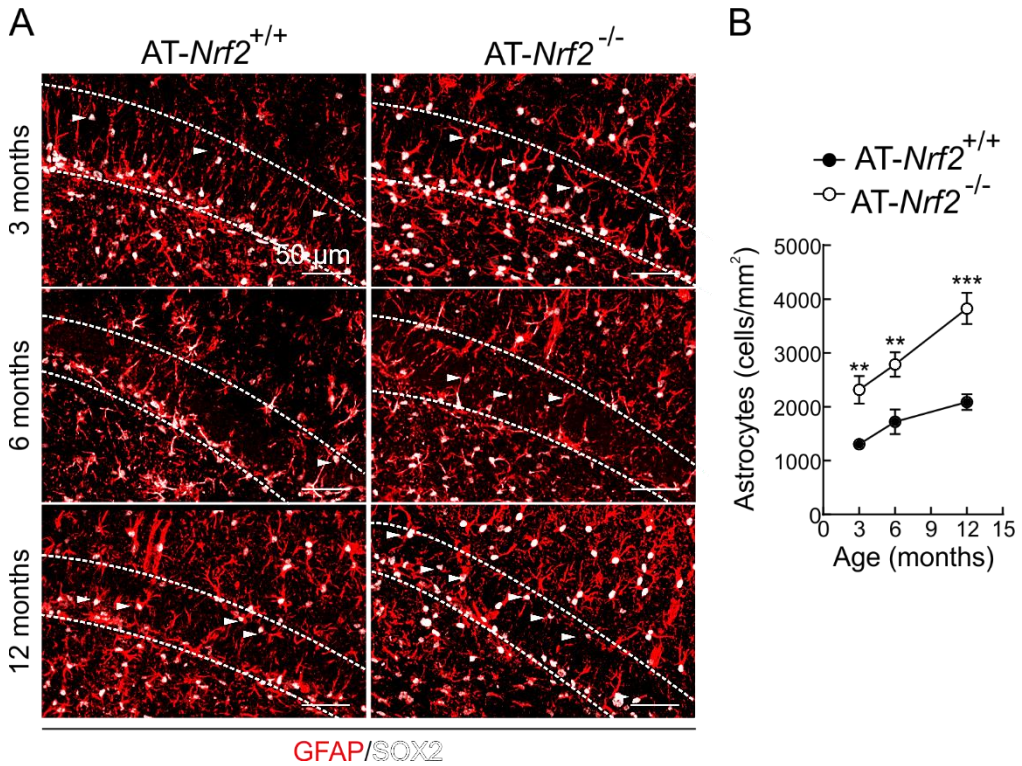


**Figure 39. Lack of NRF2 favours astrogliogenesis in AD mice. (A)** Representative confocal images of astrocyte marker GFAP and SOX2 immunostaining in the SGZ of 3-, 6- and 12-month-old mice of the indicated genotypes. Dotted lines delimit the SGZ and the GCL. **(B)** Quantification of astrocytes based on (A). Data show mean ± SEM (n = 4). $^{**}p \leqslant 0.01$; $^{***}p \leqslant 0.001$ *vs.* AT-$Nrf2^{+/+}$ according to a Student's *t*-test.

# III. The transcription factor NRF2 is a regulator of *WWTR1*/TAZ gene expression.

## 1. The *WWTR1* promoter has functional NRF2-binding sites.

We looked for putative NRF2-regulated AREs (Antioxidant Response Elements) in the TAZ-encoding gene (*WWTR1)* by using the ENCODE (https://genome.ucsc.edu/encode/) of the human genome (Feb. 2009). This database contains experimental data from chromatin immunoprecipitation (ChIP) studies of several transcription factors. Although NRF2 is not included, we examined three other ARE-binding factors, MAFK, MAFF and BACH1, for which information is available, in DNase sensitive regions (Keene et al., 1981; McGhee et al., 1981) and enriched in acetylation in $Lys^{27}$ of histone H3 (H3K27Ac), regions which are related to active enhancers (Creyghton et al., 2010) (Fig. 40A). We compared this information with the position specific scoring matrix (PSSM) for the consensus sequence recognized by NRF2, depicted at the JASPAR database (http://jaspar.genereg.net/) using a Python 3.4-script (Appendix I).We obtained a relative score for each sequence and considered those with a threshold value over 80%. We retrieved 9 putative ARE candidates in regulatory regions of TAZ with this bioinformatics approach (Table 14). Sequences in the regulatory regions of the *bona fide* NRF2-targets *HMOX1* and *NQO1* were analyzed as positive controls (Table 14).

| GENE (HUMAN) | LOCALIZATION IN THE HUMAN GENOME | MAX SCORE | RELATIVE SCORE (%) | ARE PUTATIVE BINDING SEQUENCE |
|---|---|---|---|---|
| ***HMOX1*** | chr22:35773158- 35773147 | 18.97 | 99.7 | G**TGA**CTCA**GC**A |
| ***NQO1*** | chr16:69760919-69760908 | 18.97 | 99.7 | G**TGA**CTCA**GC**A |
| ***WWTR1* ARE1** | chr3: 149435325-149435336 | 11.34 | 81.4 | G**TGC**CAGA**GC**A |
| ***WWTR1* ARE2** | chr3: 149378461-149378450 | 15.97 | 92.5 | G**TGA**CTCA**GC**T |
| ***WWTR1* ARE3** | chr3: 149365723-149365712 | 13.15 | 85.7 | A**TGA**TTAT**GC**A |
| ***WWTR1* ARE4** | chr3: 149365892-149365903 | 13.84 | 87.4 | A**TGT**CTAA**GC**A |
| ***WWTR1* ARE5** | chr3: 149299667-149299656 | 13.44 | 86.4 | A**TGA**GTCT**GC**A |
| ***WWTR1* ARE6** | chr3: 149294176-149294165 | 15.16 | 90.5 | A**TGA**GACA**GC**A |
| ***WWTR1* ARE7** | chr3: 149258004-149258015 | 13.94 | 87.6 | A**TGA**TGCA**GC**A |
| ***WWTR1* ARE8** | chr3: 149254494-149254483 | 13.36 | 86.2 | C**TGA**CTAA**GC**C |
| ***WWTR1* ARE9** | chr3: 149230221-149230232 | 15.04 | 90.2 | C**TGA**GTGA**GC**G |

**Table 14. Putative Antioxidant Response Elements (AREs) for MAFK/MAFF/BACH1 in the *WWTR1* gene** found in the ENCODE database by a bioinformatics analysis, taking a threshold of relative score higher than the 80%. The table also shows the max score and the chromosomic localization in the human genome. The most relevant bases for NRF2/MAF binding are shown in bold.

## 2. Validation of putative AREs in the TAZ promoter by ChIP and luciferase assays.

These putative AREs were further analyzed in ChIP assays (Fig. 40B) in HEK293T cells transfected with an expression vector for V5-tagged NRF2 (pcDNA3.1-mNRF2$^{\Delta ETGE}$-V5). ChIPs were performed with anti-V5 antibody and with anti-IgG as negative control. Immunoprecipitated DNA was analyzed by qRT-PCR with specific primers surrounding the putative AREs (Table 11). At least 1 of the 9 putative AREs analyzed, ARE2, exhibited significantly high enrichment although not as strong as the

positive controls *HMOX1* and *NQO1* (Fig. 40B). No enrichment was detected with specific primers for ACTB as a negative control, or for an upstream region of *NQO1* that does not contain an ARE (*NQO1**) (Pajares et al., 2016). In additional experiments, three tandem nucleotide sequences of ARE2 were cloned in the promoter region of a luciferase reporter in a non-modified form (ARE2-WT) or with the most conserved T and G residues mutated (ARE2-mutated) (Fig. 40C). HEK293T cells were transiently co-transfected with these reporters and the positive control *HMOX1*-ARE plus increasing amounts of the activated NRF2$^{\Delta ETGE}$-V5. We found that NRF2 induced luciferase expression in the ARE2-WT and the positive control *HMOX1*-ARE, but not in the ARE2-mutated reporter (Fig. 40D). Altogether, these results indicate that NRF2 binds and activates at least one specific ARE enhancer in the *WWTR1* gene promoter.

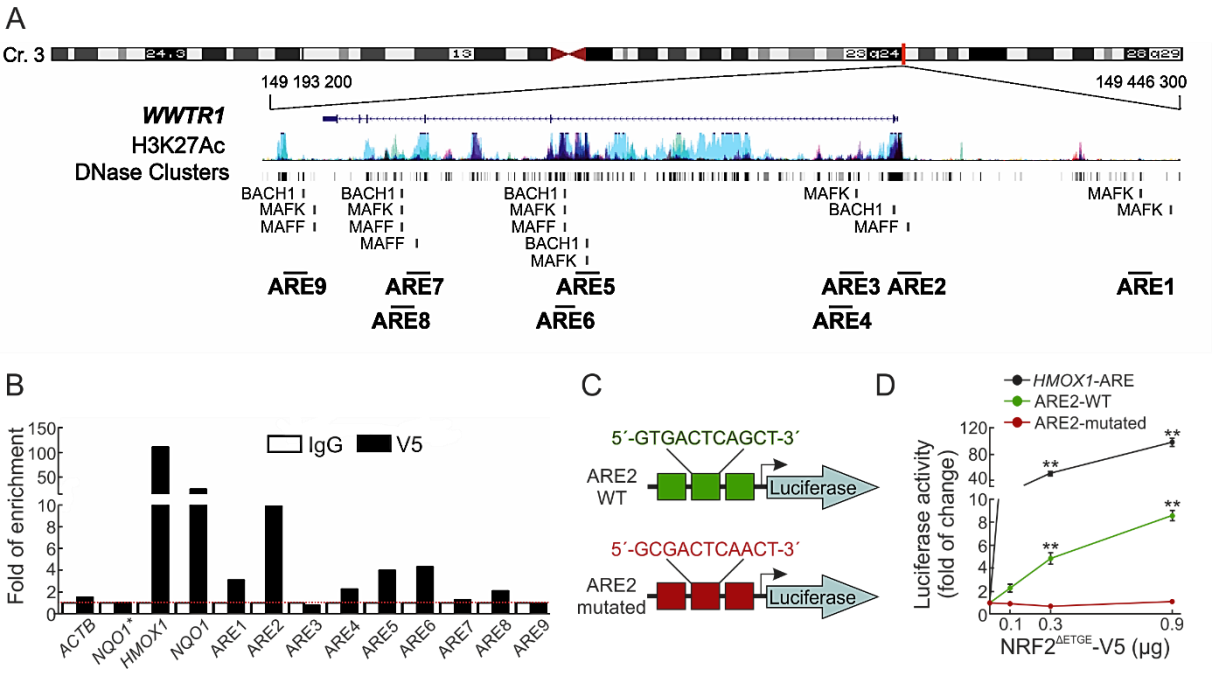


**Figure 40. The *WWTR1* promoter has at least one functional NRF2-binding site. (A)** Representative scheme of the gene *WWTR1* encoding TAZ. Regions enriched in acetylated histone H3 lysine 27 (H3K27ac) are shown in blue. Regions sensitive to DNase are represented as dark boxes. Experimental sequences reported to bind MAFK, MAFF and BACH1 were analyzed of the presence of AREs (ARE 1-9). **(B)** ChIP analysis of putative AREs found in **(A)** using the anti-V5 antibody *vs.* a control IgG in HEK293T cells overexpressing NRF2$^{\Delta ETGE}$-V5. **(C)** Luciferase reporter constructs used for assessment of wild type or mutated ARE2 functionality in pGL3basic vector. **(D)** HEK293T cells were transfected with wild type or mutated ARE2 reporter plus increasing amounts of NRF2$^{\Delta ETGE}$-V5. Luciferase activity was measured 24 h after transfection. The reporter construct carrying an ARE from *HMOX1* was used as control. Luciferase activities were normalized to renilla activity. Results are shown relative to control and are mean ± S.D. (n = 3). **$p \leqslant 0.01$ according to a Student's *t*-test.

### 3. Changes in NRF2 expression modify TAZ levels in NSPCs.

Next, we further extended these observations to the NSPCs isolated from the SGZ of 3-month-old *Nrf2*$^{+/+}$ and *Nrf2*$^{-/-}$ mice. In agreement with the results obtained in the previous assays, NRF2 deficiency in the neurospheres led to a reduction of protein levels of NQO1, as a positive control, as well as TAZ and its target CTGF (Fig. 41A). This reduction was also observed at transcriptional level by qRT-PCR (Fig. 41B).

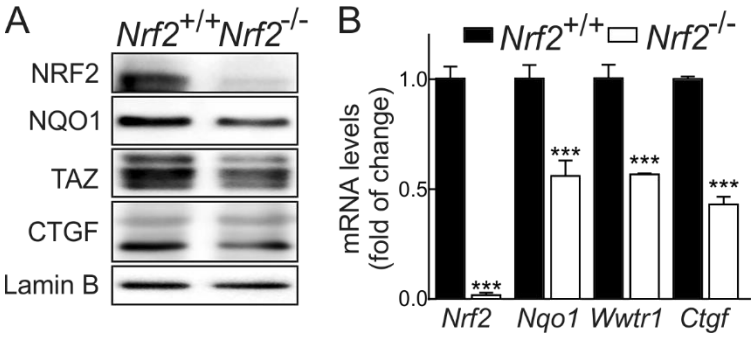


**Figure 41. NRF2 deficiency is accompanied with a reduction in TAZ levels and its targets in NSPCs. (A)** Representative immunoblot of NRF2, NQO1, TAZ, CTGF and Lamin B as a loading control of NSPCs isolated from the DG of 3-month-old mice. **(B)** mRNA levels of *Nrf2*, *Nqo1*, *Wwtr1* and *Ctgf* were determined by qRT-PCR and normalized by the geometric mean of *Actb*, *Gapdh* and *Tbp* levels. Data are presented as mean ± S.D. (n = 6). ***$p \leqslant 0.001$ *vs.* *Nrf2*$^{+/+}$ according to a Student's *t*-test.

To get further insight into these results, we down-regulated NRF2 in the human NSPCs immortalized cell line ReNcells. NRF2-knockdown reduced the protein levels of NQO1 and provoked a slight reduction in TAZ determined by immunoblot analysis (Fig. 42A). At transcriptional level, NRF2-knockdown triggered a reduction in *NQO1* and subtle reduction in *WWTR1* transcripts (Fig. 42A and B).

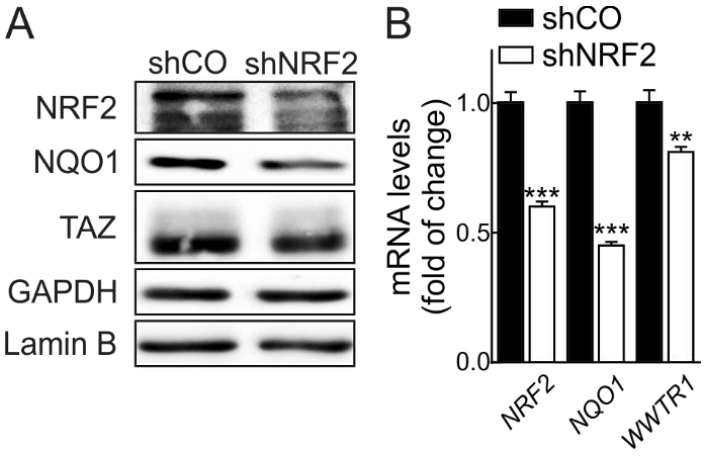


**Figure 42. Genetic down-regulation of NRF2 decreases TAZ levels in ReNcells. (A)** Representative immunoblot analysis of NRF2, TAZ, NQO1 and GAPDH and Lamin B as a loading controls (n = 3) of ReNcells transduced with empty vector or lentiviral vector for NRF2 knockdown (shNRF2). **(B)** mRNA levels of *NRF2*, *NQO1*, and *WWTR1* were determined by qRT-PCR and normalized by the geometric mean of *ACTB*, *GAPDH* and *TBP* levels. Data are presented as mean ± S.D. (n = 4). **$p \leqslant 0.01$, ***$p \leqslant 0.001$ *vs.* shCO according to a Student's *t*-test.

Then, we used genetic and chemical strategies to upregulate NRF2 in ReNcells. Ectopic overexpression of NRF2 led to increased levels of control NQO1 protein and mRNA but also TAZ and its target CTGF (Fig. 43A and B). In additional experiments, ReNcells were treated with the NRF2 activator sulforaphane (SFN, 15 μM) for different times (Fig 43C-F). SFN led to the accumulation of

NRF2 protein within the first 3 h and then slowly decreased to basal levels at 48 h (Fig. 43C). The increase in NRF2 also correlated with a gradual increase in NQO1, TAZ and CTGF proteins and transcripts (Fig. 43C-F). Although the effect at the transcript level for TAZ was more transient than for NQO1, both proteins remained elevated for at least 12- 48 h. By contrast, CTGF increased more slowly reaching maximal protein and transcript levels at 48 h. These results are consistent with a first wave of NRF2-dependent transcriptional activation that includes NQO1 and TAZ, followed by a second wave when TAZ levels are high enough to induce expression of the CTGF gene.

Altogether, these results indicate a link between NRF2 and TAZ expression in murine and human NSPCs.

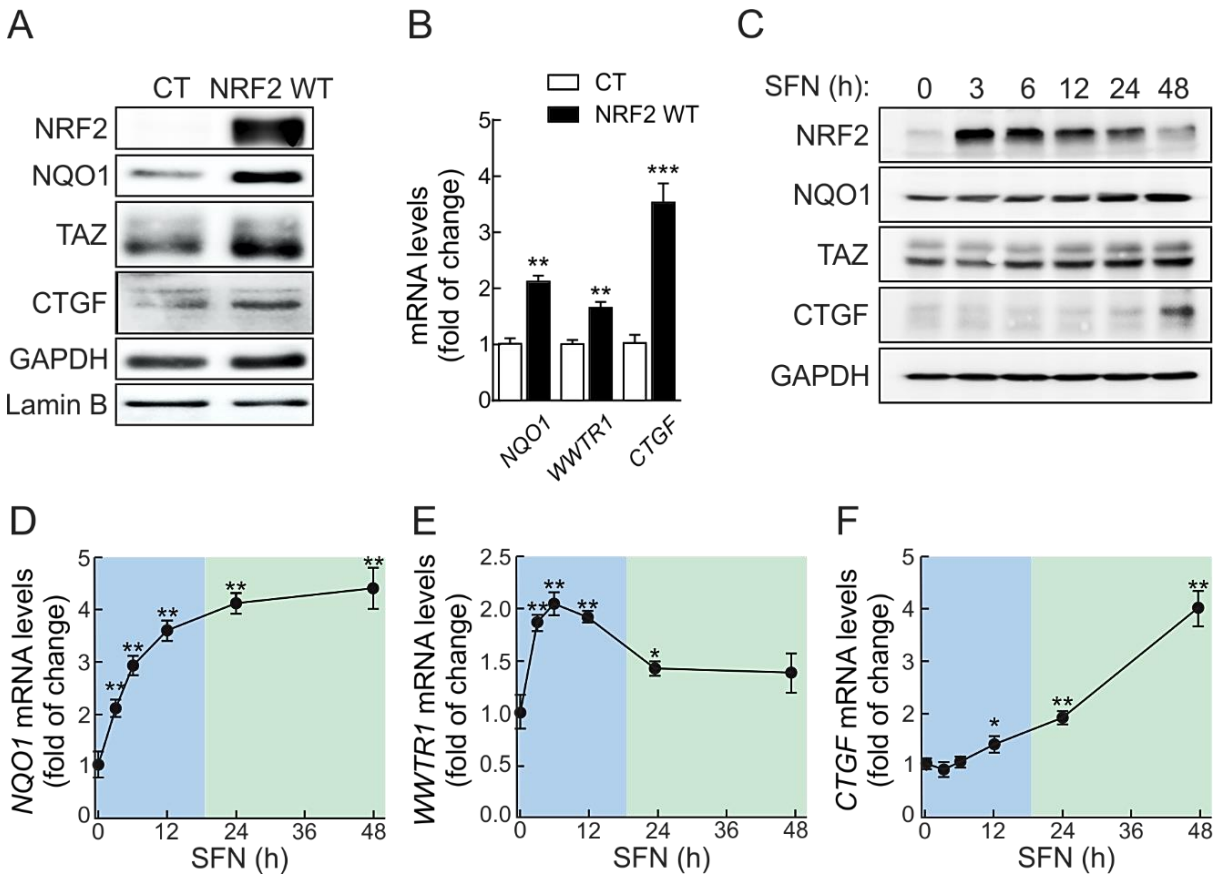


**Figure 43. Genetic and pharmacological up-regulation of NRF2 increases TAZ levels in ReNcells. (A)** Representative immunoblot analysis of NRF2, TAZ, NQO1, CTGF and GAPDH and Lamin B as a loading controls (n = 3) of ReNcells transduced with empty vector or lentiviral vector for overexpression of NRF2. **(B)** mRNA levels of *NQO1*, *WWTR1* and *CTGF* were determined by qRT-PCR and normalized by the geometric mean of *ACTB, GAPDH* and *TBP* levels. Data are presented as mean ± S.D. (n = 4). $^{**}p \leqslant 0.01$, $^{***}p \leqslant 0.001$ *vs.* CT according to a Student's *t*-test. **(C)** ReNcells were treated with sulforaphane (SFN) (15 μM) for the indicated times. **(C)** Representative immunoblot analysis of NRF2, TAZ, NQO1, CTGF and GAPDH as a loading control (n = 3). **(D, E, F)** mRNA levels of *NQO1* **(D)**, *WWTR1* **(E)** and *CTGF* **(F)** were determined by qRT-PCR and normalized by the geometric mean of *ACTB, GAPDH* and *TBP* levels. Data are presented as mean ± S.D. (n = 4). $^{*}p \leqslant 0.05$, $^{**}p \leqslant 0.01$ according to a Student's *t*-test. The blue area represents the wave of NRF2 dependent transcription and the green area depicts a second wave that involves NRF2 and also TAZ-dependent transcription. The time for transition from one wave to the other was chosen arbitrarily.

# IV. The transcription cofactor TAZ regulates proneurogenic genes expression.

## 1. TAZ expression is absent in mature neurons.

To study the function of TAZ in neurogenesis, we first consulted the Brain RNA-seq database. This database provides the expression levels of numerous genes in the main cell types of human (Zhang et al., 2016) and murine brain (Zhang et al., 2014). We found that *WWTR1* expression, encoding TAZ, is mostly limited to astroglia and endothelial cells but is low in neurons of either humans (Fig. 44A) or mice (Fig. 44B).

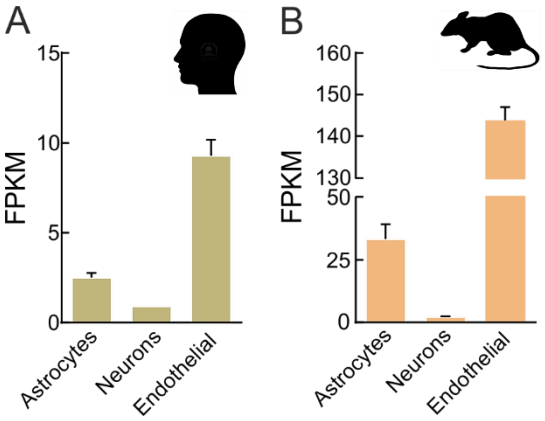


**Figure 44. *WWTR1* expression in the human and murine brain.** **(A)** Distribution of *WWTR1* mRNA in cell types isolated from human grey matter from mature brain specimens after removal of meninges and blood clots. For details of human data see (Zhang et al., 2016). **(B)** Analysis of *WWTR1* mRNA expression in glia, neurons and vascular cells isolated from mouse cerebral cortex. For details of mouse data see (Zhang et al., 2014). Data show mean ± SEM. Data were obtained from the Brain RNA-seq database. FPKM: fragments per kilobase million.

These differences prompted us to analyze *WWTR1* expression during differentiation of NSPCs in the two main murine neurogenic niches: the SGZ of the DG and the SVZ of the striatum, in newborn and 3-, 6-, and 12-months-old mice. We combined TAZ immunostaining with Nestin to identify NSPCs, and with DCX to identify neuroblasts and immature neurons. The specificity of anti-TAZ antibody was validated in Figure 11. As expected, the pool of progenitors (Nestin$^+$ cells) declined with aging, both in the SVZ (Fig. 45A and C) and the SGZ (Fig. 46A and C). The number of neuroblasts and immature neurons (DCX$^+$ cells) also declined in the SVZ (Fig. 45B and C) and the SGZ (Fig. 46B and C). More importantly, we detected that TAZ-expressing cells also decayed parallel to the exhaustion of the pool of progenitors (Fig 45C and Fig 46C). Furthermore, in double immunofluorescence assays we found that TAZ is expressed in Nestin$^+$ cells but not in DCX$^+$ cells, both in the SVZ (Fig. 45D) and the SGZ (Fig. 46D) and the pool of double Nestin$^+$/TAZ$^+$ cells (NSPCs expressing TAZ) dramatically declined after 3 months of age in both locations. Furthermore, measuring the distribution of TAZ$^+$ cells between the different populations, almost all TAZ$^+$ cells were Nestin$^+$, and no one DCX$^+$, indicating that TAZ expression is limited to NSPCs in the murine neurogenic niches (Fig. 45E and 46E). Even more, a small proportion of TAZ$^+$ cells were GFAP$^+$, which is expressed in astrocytes and NSCs. These results indicate that TAZ expression in murine neurogenic niches is mostly limited to NSPCs and astrocytes, and is absent in neurons already from immature stages.

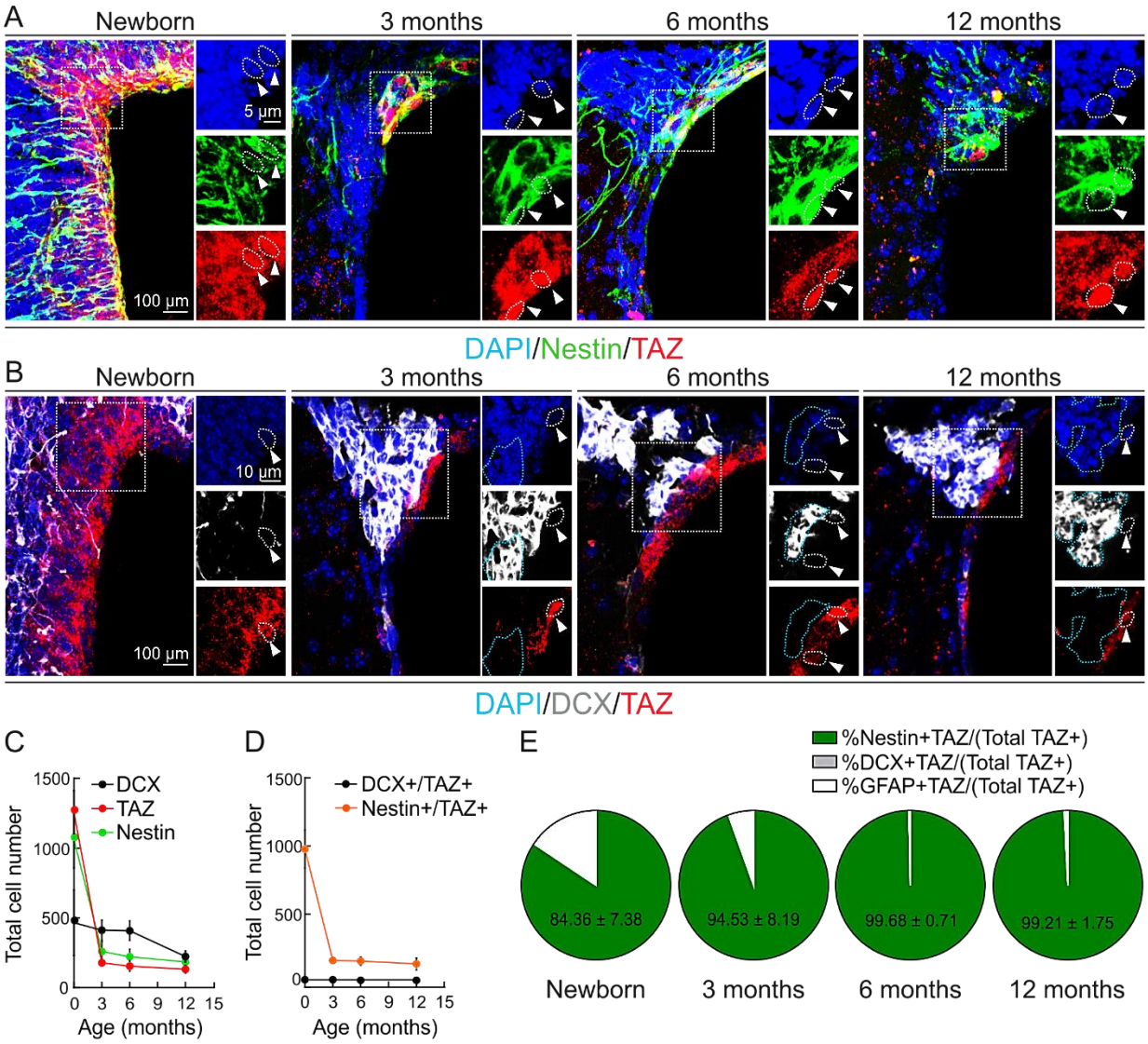


**Figure 45. TAZ distribution in the subventricular zone (SVZ). (A)** Representative confocal immunofluorescence of Nestin and TAZ. **(B)** Representative confocal immunofluorescence DCX and TAZ. Nuclei were counterstained with DAPI. White arrowheads indicate $TAZ^+$ cells also delineated with white dotted lines. Blue dotted lines delimit $DCX^+$/ $TAZ^-$ cells. **(C)** Quantification of total $Nestin^+$, $DCX^+$ or $TAZ^+$ cells in the SVZ of newborn, 3-, 6- and 12-month-old mice. Data represent mean ± SEM (n = 5). **(D)** Quantification of the total number of $Nestin^+/TAZ^+$ or $DCX^+/TAZ^+$ in the SVZ of newborn, 3-, 6- and 12-month-old mice. Data represent mean ± SEM (n = 5). **(E)** Pie charts represent the distribution of $TAZ^+$ cells as the percentage of TAZ cells that are $Nestin^+$, $DCX^+$ or $GFAP^+$, ± SEM in the SVZ of newborn, 3-, 6- and 12-month-old mice (n = 5).

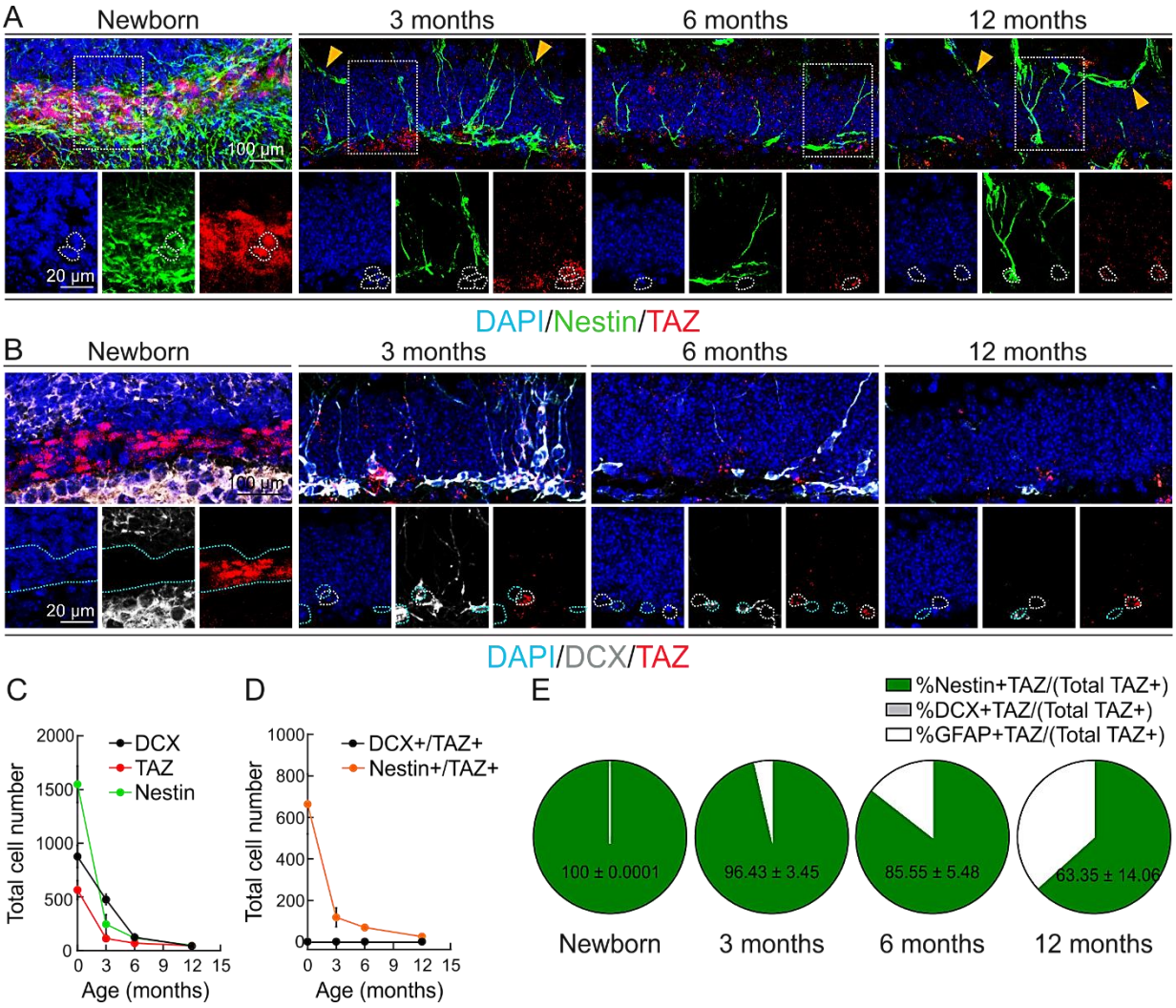


**Figure 46. TAZ distribution in the murine SGZ. (A)** Representative confocal immunofluorescence of Nestin and TAZ. **(B)** Representative confocal immunofluorescence of DCX and TAZ. Nuclei were counterstained with DAPI. White arrowheads indicate $TAZ^+$ cells also delineated with white dotted lines. Blue dotted lines point $DCX^+$/ $TAZ^-$ cells. Yellow arrowheads in A indicate $Nestin^+$ blood vessels, which have not been quantified in this study. **(C)** Quantification of total $Nestin^+$, $DCX^+$ or $TAZ^+$ cells in the SGZ of newborn, 3-, 6- and 12-month-old mice. Data represents mean ± SEM (n = 5). **(D)** Quantification of the total cell number co-expressing $Nestin^+/TAZ^+$ cells or $DCX^+/TAZ^+$ cells in the SGZ of newborn, 3-, 6- and 12-month-old mice. Data represent mean ± SEM (n = 5). **(E)** Pie charts represent the distribution of $TAZ^+$ cells as the percentage of TAZ cells that are $Nestin^+$, $DCX^+$ or $GFAP^+$, ± SEM in the SGZ of newborn, 3-, 6- and 12-month-old mice (n = 5).

## 2. TAZ expression declines during neuronal differentiation.

Then, we analyzed the expression of TAZ during differentiation of the human immortalized NSPC line ReNcell. As shown in Fig. 47A, under stem growth conditions (in the presence of growth factors) these cells exhibited the Nestin marker of NSPCs but also expressed TAZ both in the nucleus and cytoplasm (white arrowheads), consistent with our observations in the neurogenic niches. After 7 days in differentiation medium (in the absence of growth factors), many NSPCs were differentiating to immature neurons ($DCX^+$), while others retained the expression of GFAP, marker of both NSPCs and

astrocytes. Importantly, $DCX^+$ cells did not express TAZ (Fig. 47B, blue arrowheads) in agreement with our observations in the murine neurogenic niches (Fig. 45 and 46). We also determined a progressive loss of $Nestin^+$ NSPCs to ~50%, a progressive increase of $DCX^+$ immature neurons to ~40%, and, more relevant, a decrease in TAZ expression to ~70% that paralleled the loss of NSPCs (Fig. 47C). Additionally, the loss of $TAZ^+$ cells was further correlated with neuronal differentiation because the fraction of $Nestin^+/TAZ^+$ cells remained constant while that of $DCX^+/TAZ^+$ cells declined (Fig. 47D). This decay was parallel to neuronal maturation, analyzed as neurite length (Fig. 47E and F). Moreover, TAZ nuclear expression decreased as neural maturation proceeded (Fig. 47F). These results demonstrate a negative correlation between TAZ expression and exit of stemness towards neuronal differentiation.

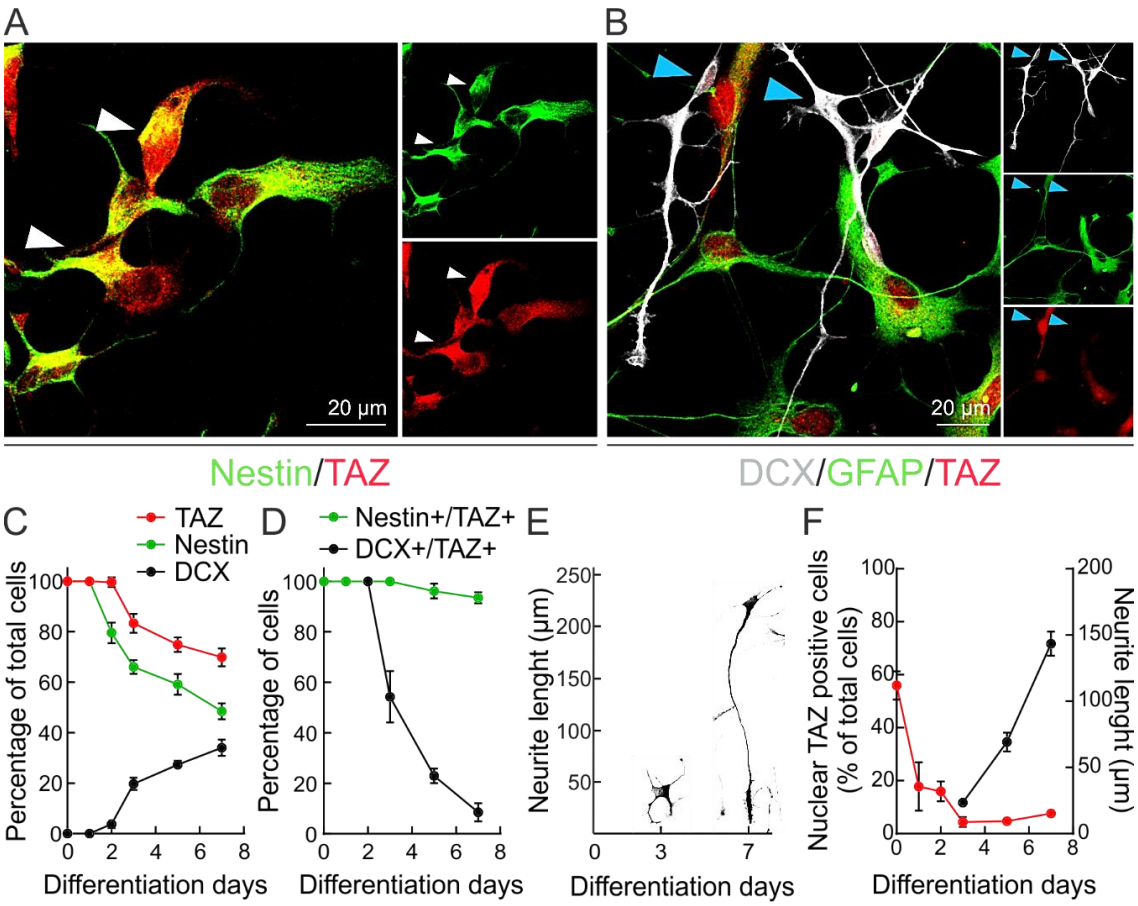


**Figure 47. TAZ expression declines during neuronal differentiation. (A)** Representative confocal images of ReNcells immunostained with Nestin and TAZ under proliferative conditions. White arrows indicate $TAZ^+$ cells**. (B)** Representative confocal images of specific neuronal marker DCX, astrocyte and NSPCs marker GFAP with TAZ immunostaining of ReNcells after 7 days of *in vitro* differentiation. Blue arrows indicate $TAZ^-$ cells. **(C)** Quantification of $Nestin^+$, $DCX^+$ and $TAZ^+$ ReNcells during differentiation. **(D)** Percentage of $Nestin^+/TAZ^+$ of total $Nestin^+$ cells and $DCX^+/TAZ^+$ of total $DCX^+$ ReNcells during differentiation. **(E)** Representative images of $DCX^+$ cells after 3 and 7 days of differentiation. **(F)** Percentage of cells expressing nuclear TAZ (left Y axis) and neurite length (right Y axis) of $DCX^+$ cells during neuronal differentiation, indicating neuronal maturation. Data are mean ± SEM ($n \geq 50$).

### 3. TAZ depletion in neural progenitors favours neuronal differentiation.

In order to determine if this negative correlation was evidencing a role of TAZ in the control of stemness *vs.* neuronal differentiation, ReNcells were infected with a control lentivirus (shCO) or with a lentivirus for human TAZ-knockdown (shTAZ), allowed to growth 5 days under proliferative conditions and them grown in differentiation medium for 30 days (Fig. 48A). Neuronal differentiation was analyzed with the specific markers DCX (neuroblasts and immature neurons), MAP2 (dendrite marker), TUBB3 (neuronal marker) and TAU (axon marker) (Fig. 48B, C, D). We detected that TAZ silencing resulted in an increase in the number neurons as determined by the quantification of $DCX^+$ (Fig. 48B and E), $MAP2^+$ (Fig. 48B and F), $TUBB3^+$ (Fig. 48C and G) and $TAU^+$ (Fig. 48D and H) cells. We next evaluated neuronal complexity and maturation as determined by dendrite length, based on MAP2 staining, and axonal length, based on TAU staining. TAZ-knocked-down cells presented longer dendrites (Fig. 48I) and axons (Fig. 48J) than shCO-infected cells. These results indicate that loss of TAZ favours neuronal differentiation.

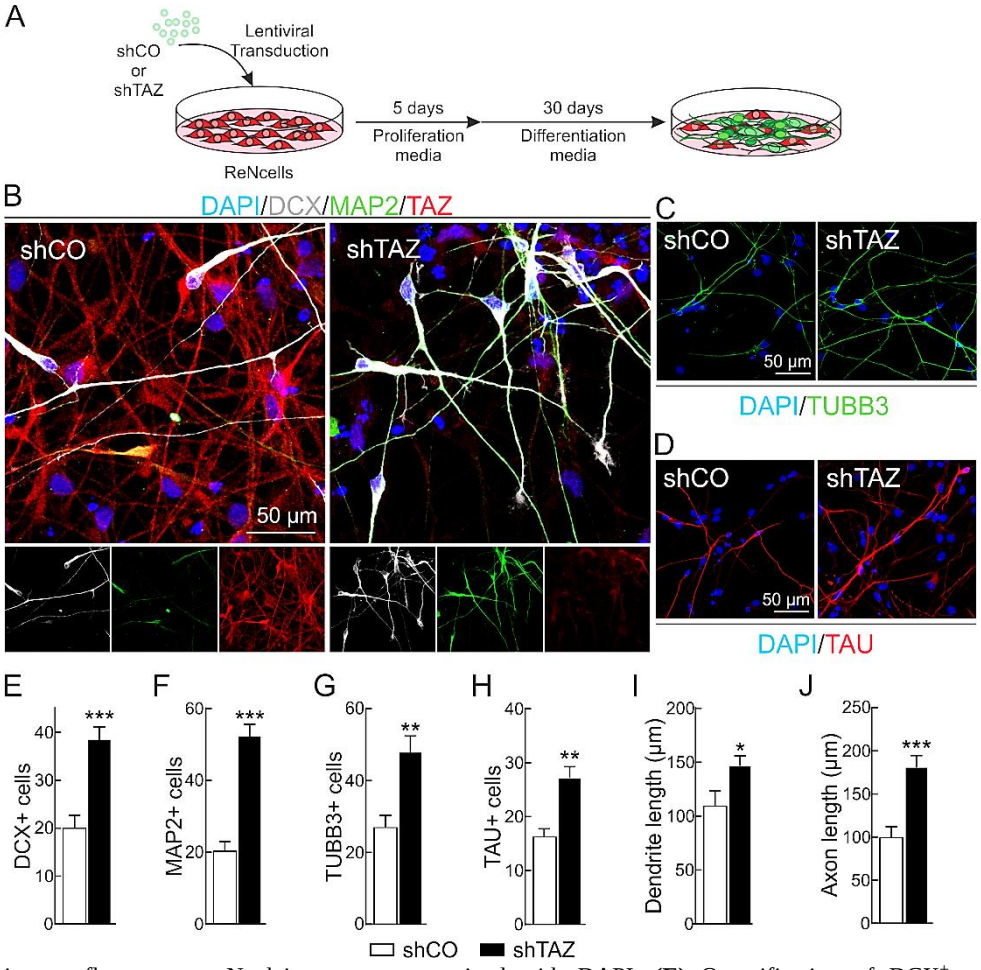


**Figure 48. Loss of TAZ favours neuronal differentiation. (A)** Schematic overview of the experimental procedure: ReNcells were transduced with lentivirus encoding shcontrol (shCO) or human shTAZ and after 5 days were plated under differentiation conditions for 30 days. **(B)** Representative confocal images of neuronal markers DCX and MAP2 with TAZ. **(C)** Representative images of TUBB3 immunofluorescence staining. **(D)** Representative image of TAU immunofluorescence. Nuclei were counterstained with DAPI. **(E)** Quantification of $DCX^+$ cells described in B. **(F)** Quantification of $MAP2^+$ cells described in B. **(G)** Quantification of $TUBB3^+$ cells described in C. **(H)** Quantification of $TAU^+$ cells described in D. **(I)** Dendrite length based on MAP2 staining. **(J)** Axon length based on TAU staining. Data are mean ± SEM ($n \geq 20$). Statistical analysis was performed with the Student's *t*-test. $*p \leqslant 0.05$; $**p \leqslant 0.01$, $***p \leqslant 0.001$ *vs.* shCO.

## 4. TAZ inhibits neuronal commitment partially in a TEAD-dependent manner.

As an additional approach, we overexpressed several mutant TAZ versions during 5 days in proliferation medium and analyzed ReNcells differentiation after 30 days in differentiation medium, without growth factors (Fig. 49A). Expression of *wild type* TAZ (TAZ-WT) reduced the neuronal differentiation as determined with the DCX (Fig. 49B and C), MAP2 (Fig. 49B and D) and TAU (Fig.49B and E) markers. Moreover, expression of the constitutively stable mutant of TAZ ($TAZ^{4SA}$) abolished completely neuronal differentiation (Fig. 49B, C, D and E). Regarding neuronal maturation, we observed an impairment in dendrite (MAP2 staining) and axon (TAU) length in TAZ-overexpressing cells, indicating that TAZ not only diminishes neuronal differentiation, but also affects further stages of neuronal maturation (Fig. 49F and G).

TEAD transcription factors are the main transcriptional co-partners of TAZ. To gain more insight into the implication of TEADs in neuronal commitment, we expressed mutant forms of TAZ defective in the binding to TEAD, were the Ser-51 has been mutated to alanine ($TAZ^{S51A}$) and the constitutively active TAZ ($TAZ^{4SA+S51A}$) (Zhang et al., 2009) (Fig. 12). Expression of $TAZ^{S51A}$ partially restored neuronal differentiation as determined with DCX (Fig. 49B and C), MAP2 (Fig. 49B and D) and TAU (Fig.49B and E) immunostaining. Moreover, $TAZ^{4SA+S51A}$, that is not degradable and does not bind TEAD, partially restored neuronal differentiation despite harbouring high TAZ levels (Fig. 49B to E). These findings indicate that TAZ repression of neuronal differentiation is partially TEAD-dependent. These observations were further extended to study the neuronal complexity as described previously. In line with the data on neuronal differentiation, we found that overexpression of TEAD-binding defective TAZ mutants partially restored the dendrite and axonal length (Fig. 49F and G).

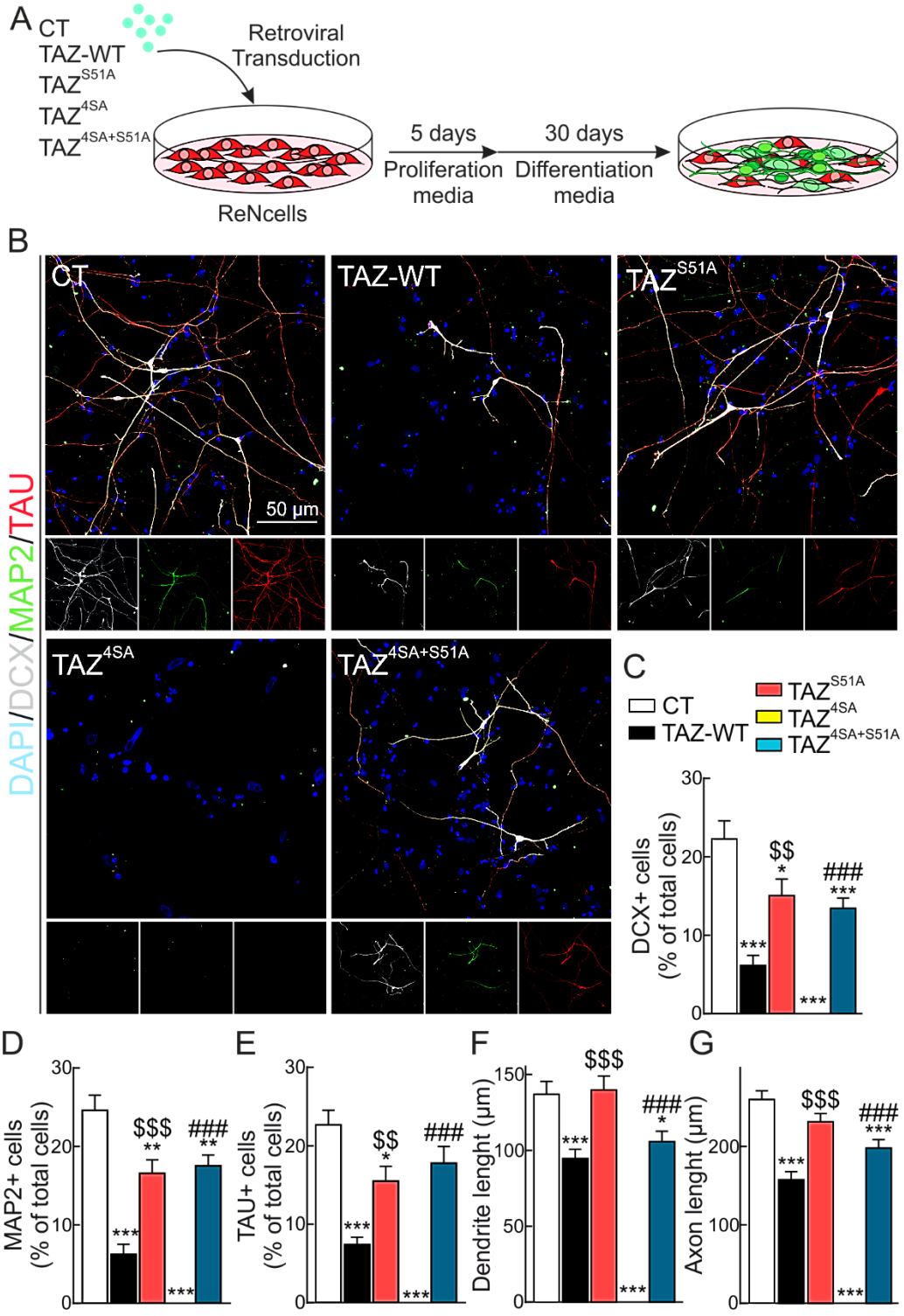


**Figure 49. TAZ impairment of neuronal differentiation is partially TEAD-dependent. (A)** Schematic overview of experimental design: ReNcells were transduced with empty vector (CT) or retroviral vector for overexpression of TAZ-WT and TAZ mutants $TAZ^{S51A}$, $TAZ^{4SA}$ and $TAZ^{4SA+S51A}$ and, after 5 days of retroviral transduction, plated under differentiation conditions during 30 days. **(B)** Immunostaining of neuronal markers DCX, MAP2 and TAU. Nuclei were counterstained with DAPI. **(C, D, E)** Quantification of $DCX^+$ **(C),** $MAP2^+$ **(D)** and $TAU^+$ **(E)**. **(F)** Measurement of dendrite length based on MAP2 staining. **(G)** Measurement of axonal length based on TAU staining. Data are mean ± SEM (n ≥ 20). Statistical analysis was performed with the Student's *t*-test. $^*p \leqslant 0.05$; $^{**}p \leqslant 0.01$, $^{***}p \leqslant 0.001$ *vs.* CT. $^{\#}p \leqslant 0.05$; $^{\#\#}p \leqslant 0.01$, $^{\#\#\#}p \leqslant 0.001$ comparing $TAZ^{S51A}$ *vs.* TAZ-WT. $^{\$}p \leqslant 0.05$; $^{\$\$}p \leqslant 0.01$, $^{\$\$\$}p \leqslant 0.001$ comparing $TAZ^{4SA+S51A}$ *vs.* $TAZ^{4SA}$.

## 5. Identification of putative TAZ interacting regions in proneurogenic genes.

To assess why TAZ represses neurogenesis, we first analyzed the possible link between TAZ and transcription factors known to be positive regulators of neurogenesis, such as SOX2 (Panaliappan et al., 2018; Lim et al., 2017; Steevens et al., 2017; Ng et al., 2013; Amador-Arjona et al., 2015) and proneural basic helix-loop-helix factors (bHLH) ASCL1 (Castro et al., 2011; Memic et al., 2016), NEUROG2 (Lacomme et al., 2012; Hufnagel et al., 2010; Heng et al., 2008) and NEUROD1 (Pataskar et al., 2016; Kuwabara et al., 2009). First, we surveyed the ENCODE of the human genome (Feb. 2009) in search for TAZ-regulated elements. Although TAZ does not bind directly to gene regulatory elements, ENCODE includes information about TAZ co-partners TEAD4 (Zhang et al., 2009), SMAD2 (Varelas et al., 2008) and RUNX (Kim et al., 2018). Furthermore, this database also gathers information of DNase hypersensitive areas and H3K27Ac, which correlates with open chromatin that characterizes regulatory regions. In addition, we obtained the PSSM for the consensus sequence recognize by TAZ co-partners TEAD1, TEAD2 (Fig. 50B and C), TEAD3, TEAD4, SMAD2/3/4 and RUNX2 (Tables 4 to 9) based on the frequency matrix depicted at the JASPAR database. We then compared the regulatory regions retrieved from ENCODE for each gene with the PSSM of the consensus sequence for each transcription factors using a Python-based bioinformatics analysis (Appendix I).

Using this script, we obtained a relative score for each sequence and considered those with a relative score higher than 80%. We identified several putative TEADs, SMADs and RUNX binding sites in the gene regulatory regions of *SOX2* and bHLH factors *ASCL1*, *NEUROG2* and *NEUROD1* (Table 15 to 20). Sequences in the regulatory regions of the *bona fide* TAZ-targets *CTGF* and *CYR61* were analyzed as positive controls (Table 15 to 20). As it is shown in Table 15 to 20, the proneurogenic genes presented several putative binding sequences for TAZ co-transcriptional partners with relative scores similar or even higher to those found in *bona fide* TAZ targets.

| GENE (HUMAN) | LOCALIZATION IN THE HUMAN GENOME | MAX SCORE | RELATIVE SCORE (%) | TEAD1 PUTATIVE BINDING SEQUENCE |
|---|---|---|---|---|
| *CTGF* | chr6:132269288-132269276 | 13.77 | 82.8 | AACATTTCTGAG |
| | chr6:132269659-132269671 | 15.62 | 85.8 | TACATTCTACCT |
| | chr6:132270157-132270169 | 13.62 | 82.5 | TACATTCTGGTG |
| | chr6:132270884-132270872 | 12.97 | 81.5 | GACATTCCAAGA |
| | chr6:132270949-132270961 | 13.1 | 81.7 | CTCATTCCAGCA |
| | chr6:132272609-132272621 | 17.78 | 89.3 | CGCATTCCTCCC |
| *CYR61* | chr1:86046332-86046344 | 16.14 | 86.6 | AGCATTCCTGAG |
| | chr1:86047219-86047207 | 16.2 | 86.7 | TGCATTCCAGCC |
| | chr1:86047721-86047733 | 18.56 | 90.5 | TGCATTCCTCTG |
| | chr1:86048360-86048348 | 14.99 | 84.8 | CACATCCCACCC |
| *SOX2* | chr3:181431413-181431401 | 13.88 | 83 | TCCATTCCCCCG (b) |
| | chr3:181428382-181428394 | 13.77 | 82.8 | AAGATTCCTGAG (c) |
| *ASCL1* | chr12:103349554-103349542 | 13.99 | 83.1 | CACATCCCTGAC (b) |
| *NEUROG2* | chr4:113435415-113435427 | 14.3 | 83.6 | TGCATTCCCCCT (a) |
| *NEUROD1* | chr2:182543940-182543952 | 15.41 | 85.4 | TACATTTCAGCG (c) |
| | chr2:182544023-182544035 | 15.78 | 86 | CACATTCTACTT (c) |

**Table 15. Putative TEAD1 binding sequences in the promoter regions** of *SOX2* and bHLH factors genes with a relative score higher than 80%. The table also shows the max score and the localization in the human genome.

| GENE (HUMAN) | LOCALIZATION IN THE HUMAN GENOME | MAX SCORE | RELATIVE SCORE (%) | TEAD2 PUTATIVE BINDING SEQUENCE |
|---|---|---|---|---|
| *CTGF* | chr6:132269289-132269276 | 8.66 | 91.1 | AAACATTTCTGAG |
| | chr6:132269658-132269671 | 9.07 | 91.5 | TTACATTCTACCT |
| | chr6:132270885-132270872 | 12.97 | 95.5 | AGACATTCCAAGA |
| | chr6:132270948-132270961 | 10.85 | 93.3 | TCTCATTCCAGCA |
| | chr6:132272599-132272612 | 12.99 | 95.6 | GGACATTCCTCGC |
| *CYR61* | chr1:86046331-86046344 | 10.42 | 92.9 | CAGCATTCCTGAG |
| | chr1:86047220-86047207 | 13.29 | 95.9 | TTGCATTCCAGCC |
| | chr1:86047720-86047733 | 10.16 | 92.6 | CTGCATTCCTCTG |
| | chr1:86048153-86048140 | 10.58 | 93.1 | ATACATTTCTGGC |
| | chr1:86048573-86048560 | 8.39 | 90.8 | TCACAGTCCTGGT |
| | chr1:86049144-86049157 | 11.28 | 93.8 | GGGCATTCCATCC |
| *SOX2* | chr3:181431414-181431401 | 6.99 | 89.3 | GTCCATTCCCCCG (b) |
| | chr3:181428381-181428394 | 8.06 | 90.5 | CAAGATTCCTGAG (c) |
| | chr3:181428844-181428831 | 8.49 | 90.9 | CCCCATTCCCATC (a) |
| *ASCL1* | chr12:103349820-103349833 | 9.6 | 92 | CCACATACCAAGA (a) |
| | chr12:103349555-103349542 | 9.57 | 92 | CCACATCCCTGAC (b) |
| | chr12:103354060-103354047 | 7.77 | 90.1 | CAACATTTCTATA (c) |
| *NEUROG2* | chr4:113435031-113435044 | 5.56 | 87.9 | TTGCATTCAATCA (b) |
| | chr4:113438807-113438794 | 7.65 | 90 | TAACACTCCAACT |
| | chr4:113435345-113435358 | 9.31 | 91.8 | ATACATTTCTTTC (a) |
| *NEUROD1* | chr2:182543939-182543952 | 10.29 | 92.8 | GTACATTTCAGCG (c) |
| | chr2:182544022-182544035 | 9.16 | 91.6 | ACACATTCTACTT (c) |
| | chr2:182544640-182544653 | 8.01 | 90.4 | CCACTTTCCCCCC (b) |
| | chr2:182545564-182545577 | 9.07 | 91.5 | CTCCATTCCGGCC (a) |

**Table 16. Putative TEAD2 binding sequences in the promoter regions** of *SOX2* and bHLH factors genes with a relative score higher than 85%. The table also shows the max score and the localization in the human genome.

| GENE (HUMAN) | LOCALIZATION IN THE HUMAN GENOME | MAX SCORE | RELATIVE SCORE (%) | TEAD3 PUTATIVE BINDING SEQUENCE |
|---|---|---|---|---|
| *CTGF* | chr6:132270622-132270614 | 10.89 | 97.2 | ACATACCG |
| | chr6:132269884-132269892 | 6.86 | 95.2 | GGATTCCG |
| | chr6:132270883-132270875 | 14.08 | 98.7 | ACATTCCA |
| | chr6:132270950-132270958 | 10.59 | 97 | TCATTCCA |
| | chr6:132271352-132271344 | 8.64 | 96.1 | AAATACCT |
| | chr6:132272601-132272609 | 13.43 | 98.4 | ACATTCCT |
| *CYR61* | chr1:86046333-86046341 | 12.94 | 98.2 | GCATTCCT |
| | chr1:86047218-86047210 | 13.59 | 98.5 | GCATTCCA |
| | chr1:86047722-86047730 | 12.94 | 98.2 | GCATTCCT |
| | chr1:86048065-86048057 | 10.4 | 96.9 | GCATACCG |
| | chr1:86048501-86048509 | 7.98 | 95.7 | AAATACCG |
| | chr1:86049146-86049154 | 13.59 | 98.5 | GCATTCCA |
| | chr1:86048877-86048869 | 8.64 | 96.1 | AAATACCT |
| *SOX2* | chr3:181430473-181430481 | 7.98 | 95.7 | AAATACCG |
| | chr3:181431412-181431404 | 2.17 | 92.9 | CCATTCCC (b) |
| | chr3:181430283-181430291 | 5.92 | 94.7 | GAATGCCT |
| | chr3:181428383-181428391 | 8.01 | 95.8 | AGATTCCT (c) |
| | chr3:181428711-181428703 | 4.13 | 93.8 | GCATCCCA |
| *ASCL1* | chr12:103349822-103349830 | 12.2 | 97.8 | ACATACCA (a) |
| | chr12:103350367-103350359 | 7.52 | 95.5 | GGATTCCT |
| *NEUROG2* | chr4:113434627-113434619 | 4.54 | 94.1 | AGATGCCA |
| | chr4:113439907-113439899 | 8.17 | 95.8 | GGATTCCA |
| | chr4:113435416-113435424 | 9.23 | 96.4 | GCATTCCC (a) |
| *NEUROD1* | chr2:182542983-182542975 | 5.6 | 94.6 | ACATGCCC |
| | chr2:182543732-182543740 | 5.92 | 94.7 | GAATGCCT |
| | chr2:182544713-182544705 | 5.64 | 94.6 | GGATACCT (b) |
| | chr2:182545492-182545484 | 8.16 | 95.8 | GCATGCCG (a) |
| | chr2:182545234-182545242 | 10.04 | 96.8 | GAATTCCT |

**Table 17. Putative TEAD3 binding sequences in the promoter regions** of *SOX2* and bHLH factors genes with a relative score higher than 90%. The table also shows the max score and the localization in the human genome.

| GENE (HUMAN) | LOCALIZATION IN THE HUMAN GENOME | MAX SCORE | RELATIVE SCORE (%) | TEAD4 PUTATIVE BINDING SEQUENCE |
|---|---|---|---|---|
| *CTGF* | chr6:132269659-132269669 | 12.98 | 94.9 | TACATTCTAC |
| | chr6:132270202-132270212 | 12.64 | 94.6 | AACATTCTTC |
| | chr6:132270884-132270874 | 14.12 | 96 | GACATTCCAA |
| | chr6:132272600-132272610 | 14.13 | 96.1 | GACATTCCTC |
| | chr6:132272772-132272762 | 11.87 | 93.8 | AAAATTCTAT |
| *CYR61* | chr1:86046332-86046342 | 12.82 | 94.8 | AGCATTCCTG |
| | chr1:86047293-86047303 | 9.02 | 91 | AAAATACTAG |
| | chr1:86047219-86047209 | 13.16 | 95.1 | TGCATTCCAG |
| | chr1:86048500-86048510 | 9.18 | 91.1 | GAAATACCGG |
| | chr1:86049145-86049155 | 13.77 | 95.7 | GGCATTCCAT |
| | chr1:86048878-86048868 | 10.75 | 92.7 | GAAATACCTT |
| *SOX2* | chr3:181430472-181430482 | 9.18 | 91.1 | TAAATACCGG |
| | chr3:181431587-181431577 | 8.26 | 0.90.2 | TAAATACTGT |
| | chr3:181430289-181430279 | 8.44 | 90.4 | GGCATTCATG |
| | chr3:181428382-181428392 | 8.78 | 90.8 | AAGATTCCTG (c) |
| *ASCL1* | chr12:103349821-103349831 | 12.62 | 94.6 | CACATACCAA (a) |
| | chr12:103353739-103353729 | 12.28 | 94.2 | AGCATTCTAT |
| *NEUROG2* | chr4:113434601-113434591 | 11.38 | 93.3 | GAAATTCTTC |
| | chr4:113439588-113439578 | 11.24 | 93.2 | CAAATTCTGT |
| | chr4:113435415-113435425 | 10.91 | 92.9 | TGCATTCCCC (a) |
| *NEUROD1* | chr2:182543738-182543728 | 9.05 | 91 | GGCATTCATT |
| | chr2:182543940-182543950 | 8.8 | 90.8 | TACATTTCAG (c) |
| | chr2:182544023-182544033 | 13.72 | 95.6 | CACATTCTAC (c) |
| | chr2:182545233-182545243 | 12.84 | 94.8 | CGAATTCCTC |

**Table 18. Putative TEAD4 binding sequences in the promoter regions** of *SOX2* and bHLH factors genes with a relative score higher than 90%. The table also shows the max score and the localization in the human genome.

| GENE (HUMAN) | LOCALIZATION IN THE HUMAN GENOME | MAX SCORE | RELATIVE SCORE (%) | SMAD2/3/4 PUTATIVE BINDING SEQUENCE |
|---|---|---|---|---|
| *CTGF* | chr6:132269508-132269521 | 8.17 | 92 | GAGGCTACCACAT |
| | chr6:132270238-132270225 | 8.2 | 92 | TAGTCTATCAACC |
| | chr6:132270384-132270397 | 13.87 | 95.8 | ATGTCTCTCACTC |
| | chr6:132270796-132270809 | 5.12 | 90 | TTGTCTGACTTCT |
| | chr6:132272476-132272489 | 13.97 | 95.9 | CTGGCTGTCTCCT |
| *CYR61* | chr1:86046219-86046206 | 14.07 | 96 | GTGTCTGTCTCCC |
| | chr1:86047067-86047080 | 8.74 | 92.4 | CTGCCTGCCACTG |
| | chr1:86048336-86048349 | 7.99 | 91.9 | TTGCCTGGCAGGT |
| | chr1:86049198-86049185 | 8.32 | 92.1 | CTGCCTCTCACA |
| *SOX2* | chr3:181431086-181431099 | 6.2 | 90.7 | CCCTCTCACACAT |
| | chr3:181429502-181429515 | 8.17 | 92 | GTGGCTGGCAGGC |
| | chr3:181428859-181428846 | 11.01 | 93.9 | CTGTCTGCCCCCA (a) |
| *ASCL1* | chr12:103351454-103351467 | 8.37 | 92.1 | CACTCTCTCACTT |
| | chr12:103350931-103350918 | 7.24 | 91.4 | TTCTCTCTCTCCT |
| *NEUROG2* | chr4:113435134-113435121 | 5.98 | 90.5 | CCATCTGTCTCTT |
| | chr4:113436841-113436828 | 10.56 | 93.6 | CTGACTGGCAGCA |
| | chr4:113437328-113437341 | 14.71 | 96.4 | GTGTCTGGCACAC |
| *NEUROD1* | chr2:182542551-182542564 | 7.44 | 91.5 | ATGACTCGCTCAT |
| | chr2:182542875-182542862 | 9.08 | 92.6 | ATGTCTTCCACGT |
| | chr2:182543475-182543488 | 10.29 | 93.4 | TTGTCTGCCTCGT |
| | chr2:182544227-182544240 | 7.28 | 91.4 | GGGTCTTCCACCC |
| | chr2:182544628-182544615 | 5.27 | 90.1 | GGGACTCACTCCT (b) |
| | chr2:182545412-182545425 | 6.01 | 90.6 | TCGTCTCCCGCCC |

**Table 19. Putative SMAD2/3/4 binding sequences in the promoter regions** of *SOX2* and bHLH factors genes with a relative score higher than 90%. The table also shows the max score and the localization in the human genome.

| GENE (HUMAN) | LOCALIZATION IN THE HUMAN GENOME | MAX SCORE | RELATIVE SCORE (%) | RUNX2 PUTATIVE BINDING SEQUENCE |
|---|---|---|---|---|
| *CTGF* | chr6: 132269512-132269521 | 4.14 | 94.1 | CTACCACAT |
| | chr6: 132270934-132270925 | 6.64 | 95.6 | CAACCACCA |
| | chr6: 132271935-132271926 | 11.74 | 98.6 | CAACCGCAA |
| *CYR61* | chr1: 86046444-86046453 | 7.27 | 96 | AGACCGCGA |
| | chr1: 86047194-86047203 | 5.36 | 94.8 | CGACCACAC |
| | chr1: 86047279-86047270 | 12.26 | 99 | AAACCACAA |
| | chr1: 86048526-86048517 | 8.11 | 96.5 | GAACCGCAG |
| *SOX2* | chr3: 181430686-181430695 | 6.83 | 95.7 | TACCCGCAG |
| | chr3: 181430914-181430905 | 9.88 | 97.5 | TAACCACAG |
| | chr3: 181431302-181431311 | 9.71 | 97.4 | AAACCGCGA |
| | chr3: 181431473-181431464 | 0.08 | 91.6 | GTACCACTA |
| | chr3: 181430222-181430231 | 2.43 | 93.1 | CCACCGCGG |
| | chr3: 181430304-181430295 | 3.62 | 93.8 | GGACCACAC |
| | chr3: 181428582-181428591 | 6.87 | 95.7 | CCACCACAA |
| | chr3: 181429469-181429460 | 6.06 | 95.2 | ACACCACAC |
| *ASCL1* | chr12: 103349919-103349928 | 8.2 | 96.5 | TCACCACAA |
| | chr12:103350513-103350504 | 4.44 | 94.3 | CTACCGCCA |
| | chr12: 103353685-103353694 | 3.78 | 93.9 | AAACCCCAT |
| | chr12: 103353976-103353967 | 9.48 | 97.3 | AAACCACAT |
| *NEUROG2* | chr4: 113436266-113436257 | 10.77 | 98.1 | AAACCGCAT |
| | chr4: 113439955-113439964 | 6.08 | 95.2 | TAACCCCAA |
| *NEUROD1* | chr2: 182542264-182542255 | 4.84 | 94.5 | ACACCACGA |
| | chr2: 182542484-182542475 | 0.92 | 92.2 | AACCCACTG |
| | chr2: 182543055-182543046 | 4.12 | 94.1 | AACCCACCA |
| | chr2: 182543029-182543038 | 6.77 | 95.7 | AGCCCGCAA |
| | chr2: 182543908-182543899 | 6.64 | 95.6 | CAACCACCA |
| | chr2: 182543847-182543856 | 0.95 | 92.2 | ACACCACTC |
| | chr2: 182544607-182544598 | 1.82 | 92.7 | TTACCGCTC |
| | chr2: 182545639-182545648 | 6.83 | 95.7 | TACCCGCAG |

**Table 20. Putative RUNX2 binding sequences in the promoter regions** of *SOX2* and bHLH factors genes with a relative score higher than 90%. The table also shows the max score and the localization in the human genome.

## 6. Validation of putative TAZ interacting regions in proneurogenic genes.

In order to validate the TAZ-interacting regions with highest scores, we first determined which TEADs are expressed in ReNcells by qRT-PCR analysis. We determined that TEAD2 and TEAD1 were the most highly expressed TEADs (Fig. 50A). Therefore, we evaluated the putative binding sequence for TEAD1 and TEAD2, although some of these regions also included other TEADs and SMADs-binding sequences. For this reason, we called these regions TAZ-interacting regions (TIR) (Table 15 to 20, indicated as (a), (b) and (c)). In Fig. 51, TIR regions are showed in the proneurogenic genes accompanied by the data from ENCODE database for DNase sensitive regions, H3K27Ac areas and RNA Pol II enriched regions.

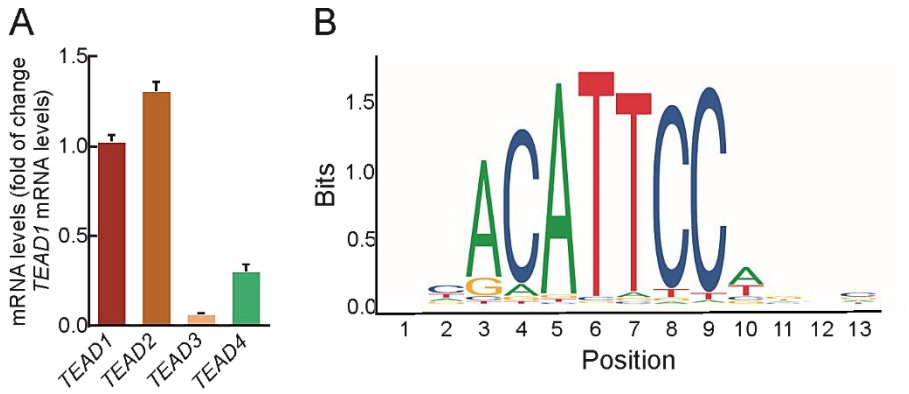


C

| | 1 | 2 | 3 | 4 | 5 | 6 | 7 | 8 | 9 | 10 | 11 | 12 | 13 |
|---|---|---|---|---|---|---|---|---|---|---|---|---|---|
| A | 0.0264 | -0.6064 | 1.7058 | -1.7602 | 1.9347 | -5.4972 | -3.0821 | -3.9122 | -3.9122 | 0.9622 | -0.2620 | -0.2748 | -0.3008 |
| C | 0.1077 | 0.8187 | -2.9122 | 1.8217 | -4.4972 | -3.6227 | -3.9122 | 1.8865 | 1.9235 | -1.1514 | -0.2748 | 0.3525 | 0.7123 |
| G | -0.2620 | -0.7246 | -0.9324 | -3.1753 | -3.4972 | -4.2748 | -3.7602 | -3.6227 | -5.0821 | -1.2493 | 0.6183 | 0.1273 | -0.1995 |
| T | 0.1370 | 0.0053 | -3.1753 | -3.4972 | -3.7602 | 1.9540 | 1.9150 | -2.4383 | -2.8342 | 0.2754 | -0.2620 | -0.2620 | -0.4972 |

**Figure 50. Expression of TEADs transcripts in ReNcells. (A)** mRNA levels of the TEADs 1 to 4 were determined by qRT-PCR and normalized to the levels of *TEAD1*. Data represent mean ± S.D. (n ≥ 8). **(B)** TEAD2 motif from JASPAR database indicating its consensus binding profile. **(C)** Position specific scoring matrix (PSSM) for TEAD2 PSSM derived from the frequency matrix available in JASPAR database.

To validate the TIRs with the highest score in each proneurogenic gene, TAZ interaction to these sequences was determined by ChIP analysis. ReNcells were transduced with a retroviral vector expressing the constitutively stable mutant TAZ$^{4SA}$ (Lei et al., 2008). TAZ was immunoprecipitated with an anti-TAZ antibody and an anti-IgG antibody was used as a negative control. TAZ binding was analyzed by qRT-PCR employing as template the immunoprecipitated DNA and primers designed to specifically amplify TIRs (Table 13). We detected TAZ enrichment to the well-known positive control TIRs in *CTGF*, *MYC* and *CYR61*, whereas TAZ did not bind to a region of *CTGF* that does not contain any TIR (*CTGF* 3´UTR) (Fig. 52). Immunoprecipitation with TAZ showed enrichment of several TIRs in *SOX2*, *ASCL1*, *NEUROG2* and *NEUROD1* genes (Fig. 52). Therefore, TAZ binds regulatory regions of proneurogenic genes.

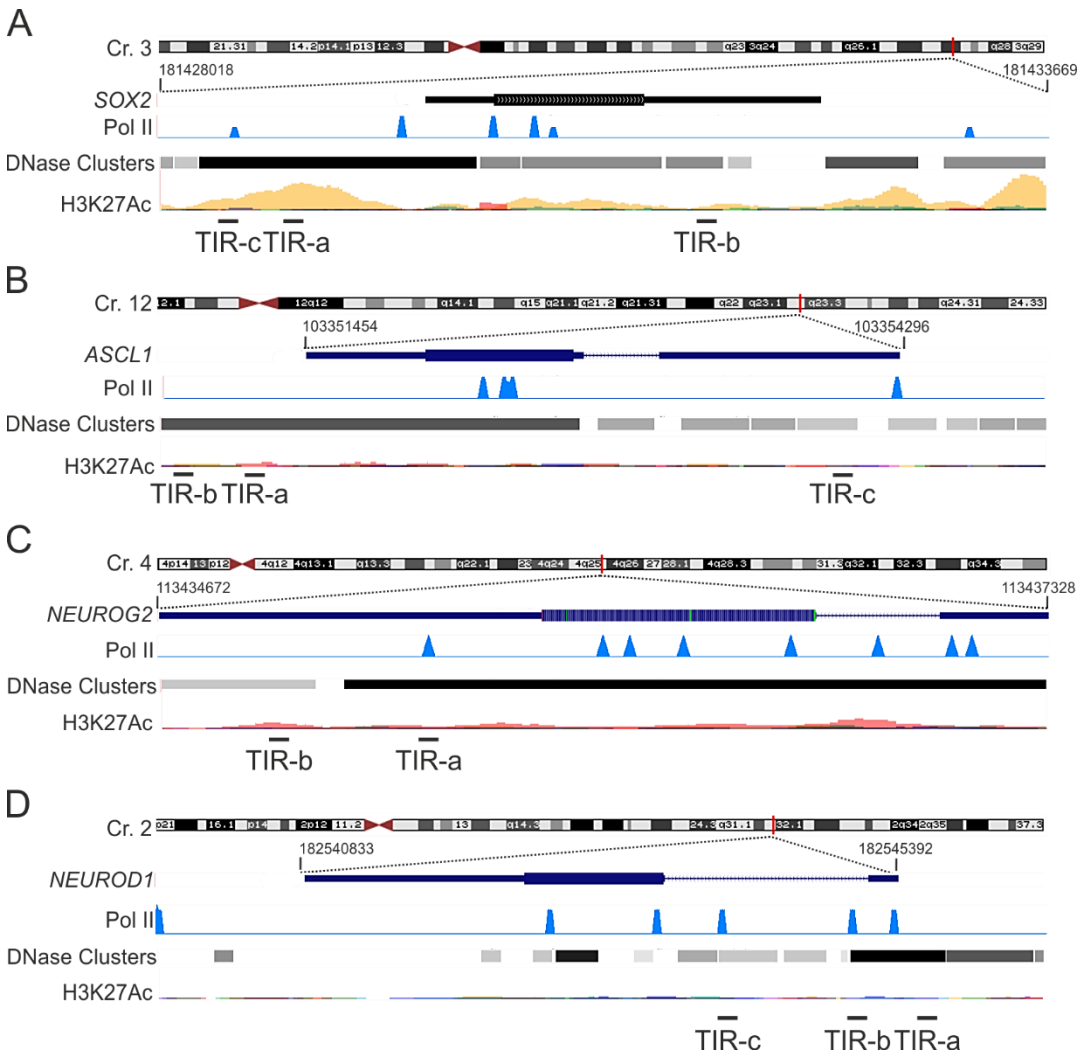


**Figure 51. Schemes of the genes encoding *SOX2* and bHLH factors *ASCL1, NEUROG2* and *NEUROD1*. (A)** *SOX2,* **(B)** *ASCL1*, **(C)** *NEUROG2,* and **(D)** *NEUROD1* genes from the ENCODE for the human genome. Putative TAZ interacting regions (TIR) in the genes were identified taking as reference the regions localized in DNAse-sensitive and H3K27Ac-rich regions, i.e. most likely regulatory promoter regions. Regions sensitive to DNase are represented as dark boxes. RNA Pol II enrichment regions determined by ChIP-seq for RNA polymerase II (Pol II) in CD4 cells (Barski et al., 2007) are indicated in blue.

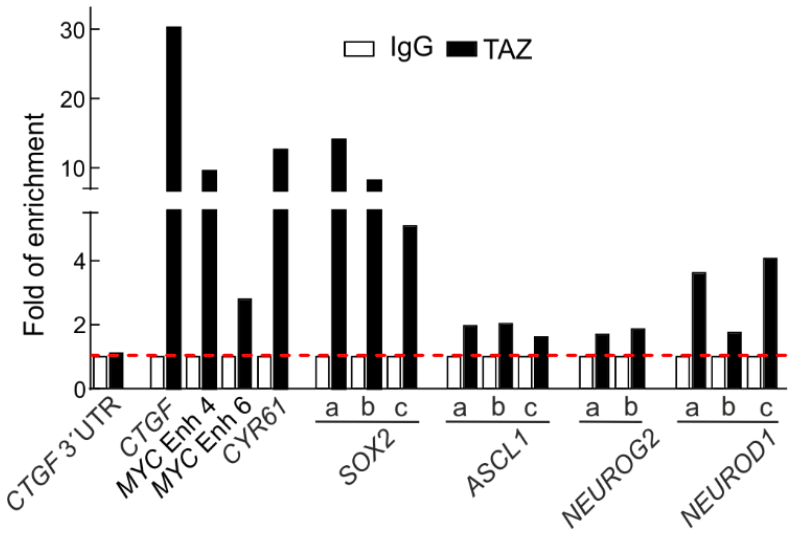


**Figure 52. TAZ recognizes specific regions in *SOX2* and bHLH genes.** ChIP analysis of putative TIRs described in Figure 51 using the anti-TAZ antibody *vs.* a control IgG in ReNcells overexpressing $TAZ^{4SA}$ after 5 days of retroviral transduction. Regions of *CTGF*, *MYC* and *CYR61* were analyzed as positive controls, and a region of *CTGF* (*CTGF* 3´UTR) that does not contain TIR was amplified as negative control.

To evaluate the functionality of the putative TEAD1(a)-binding sequence found in the *SOX2* gene, we next generated a luciferase reporter. Three tandem nucleotide sequences of TEAD1(a)-binding sequence in the *SOX2* gene (5´-CCCCATTCCCATC-3´) were cloned in the promoter region of a luciferase reporter (p29S0D1) as shown in Fig. 53A. Note that only the TEAD1(a)-binding sequence were cloned in the vector, not including other regulatory regions of *SOX2* gene. HEK293T cells were transiently co-transfected with this construct or an empty vector plus a Renilla expression vector (pTK-Renilla) used for normalization and increasing amounts of $TAZ^{4SA}$. Luciferase activity was measured following 24 h after transfection. We found that TAZ overexpression induced luciferase activity in a concentration dependent manner in the reporter carrying TEAD1(a), but not in the negative control (Fig. 53B). To further determine the response of *SOX2*-TEAD1(a) sequence to TAZ in NSPCs, CT or $TAZ^{4SA}$-overexpressing ReNcells were transiently transfected with the empty vector or the TEAD1(a)-luciferase construct. Luciferase activity was measured 24 h after the transient transfection of luciferase constructs. We found a slight non-significant increase in CT ReNcells compared to the control conditions, probably due to the endogenous TAZ in these cells, and a significant increase in luciferase activity in $TAZ^{4SA}$ ReNcells (Fig. 53C). Altogether, these results confirm that TEAD1(a) binding sequence responses to TAZ, indicating that it is probably a proper TEAD1-binding sequence.

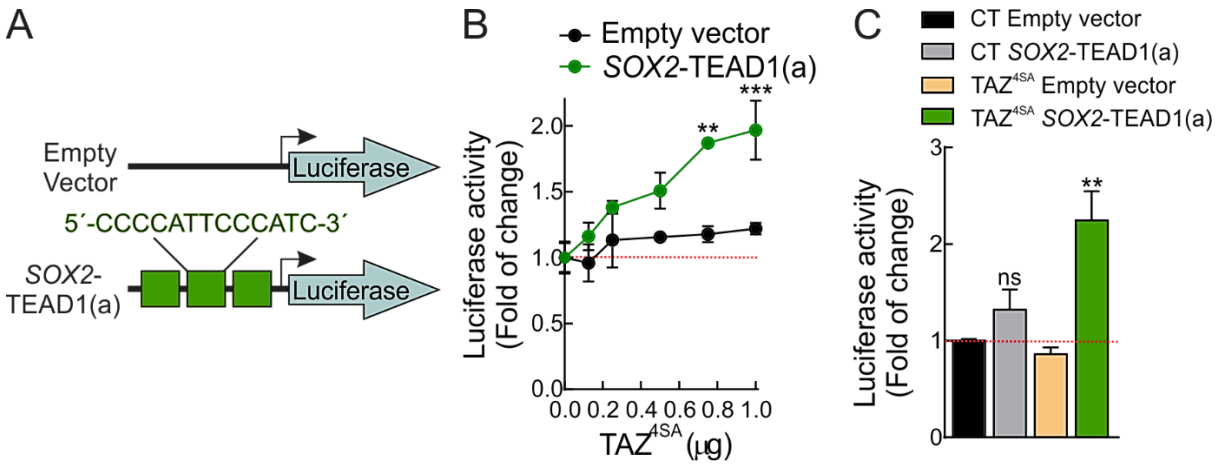


**Figure 53. TEAD1-binding element in the *SOX2* gene responds to TAZ overexpression. (A)** Luciferase reporter construct carrying 3 tandem putative TEAD1(a)-binding sequences from the *SOX2* gene or an empty vector as negative control controlling the expression of luciferase**. (B)** HEK293T cells were co-transfected with the reporters represented in A and increasing amounts of $TAZ^{4SA}$ construct. Values were normalized to pTK-Renilla activity and presented as fold of change. Data are mean ± S.D. (n = 6). Statistical analysis was performed using Student's t test. ** $p \leqslant 0.01$ and *** $p \leqslant 0.001$ *vs.* basal levels. **(C)** ReNcells transducted with retroviral control vector (CT) or retroviral vector encoding constitutive active $TAZ^{4SA}$ were co-transfected with the empty vector or *SOX2*-TEAD1(a) luciferase reporter contruct. Values were normalized to pTK-Renilla activity and presented as fold of change. Data are mean ± S.D. (n = 6). Statistical analysis was performed using Student's *t*-test. ** $p \leqslant 0.01$ *vs.* CT empty vector.

## 7. TAZ expression inversely correlates with the levels of SOX2 and several proneuronal bHLH factors.

Since we found that TAZ co-partners recognize sequences in the regulatory regions of proneurogenic genes, we analyzed the relevance of TAZ in the regulation of their expression. First, we knocked-down TAZ in ReNcells using a lentiviral vector for shTAZ. After 5 days of lentiviral transduction, we found a decrease in TAZ protein levels and its well-known target CTGF (Fig. 54A). TAZ knockdown was accompanied by an increase in the protein levels of SOX2 and NEUROD1 (Fig. 54A). Furthermore, we found a decrease to ~50% in TAZ transcript, *WWTR1*, and ~30% in the *bona fide* targets *CTFG* and *CYR61* (Fig. 54B). Under the same conditions, a significant increase in the transcripts of the proneurogenic factors *SOX2*, *ASCL1*, *NEUROG2* and *NEUROD1* was observed (Fig. 54C).

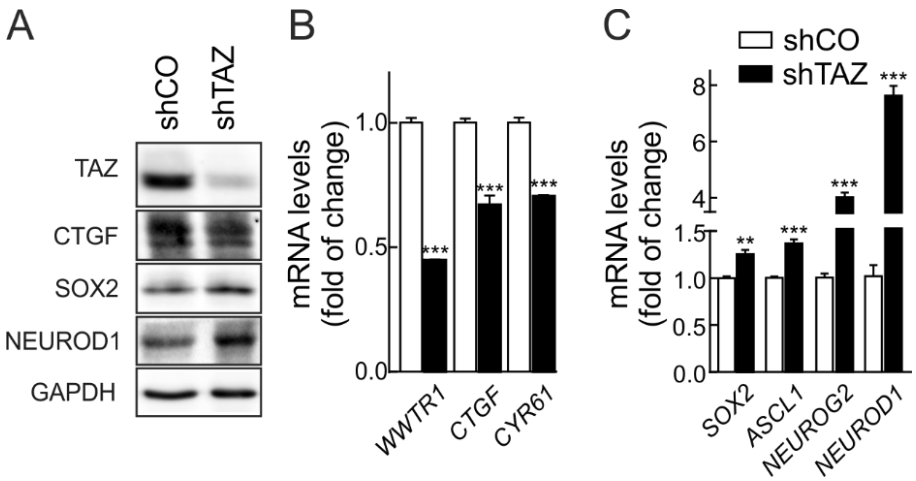


**Figure 54. TAZ depletion favours the expression of SOX2 and several bHLH factors. (A)** Representative immunoblot analysis of TAZ, CTGF, SOX2, NEUROD1 and GAPDH as a loading control in shCO and shTAZ cells after 5 days of lentiviral transduction. **(B)** mRNA levels of *WWTR1* and its targets *CTGF* and *CYR61*. **(C)** mRNA levels of *SOX2*, *ASCL1*, *NEUROG2* and *NEUROD1*. For **B** and **C**, ReNcells were transduced with lentiviral vectors shCO and shTAZ and after 5 days the levels of the indicated transcripts were determined by qRT-PCR and normalized by the geometric mean of *ACTB*, *GAPDH* and *TBP* levels. Data are mean ± S.D. (n = 4). Statistical analysis was performed using a Student's *t*-test. $**p \leqslant 0.01$, $***p \leqslant 0.001$ *vs.* shCO.

Next, we analyzed the protein and transcript levels of the proneurogenic factors in ReNcells transduced with a retroviral vector for expression of active mutant $TAZ^{4SA}$ for 0, 1, 2 and 5 days after transduction under proliferation conditions (Fig. 55A). As expected, we saw a gradual increase of the *bona fide* TAZ target CTGF in parallel to TAZ overexpression (Fig. 55B). At the same time, SOX2 and NEUROD1 levels declined (Fig. 55B). At the transcriptional level, the increase in the TAZ transcript (*WWTR1*) was accompanied by an increase in its positive controls *CTFG* and *CYR61* (Fig. 55C), but also a high decrease in the proneurogenic factors *SOX2*, *ASCL1*, *NEUROG2* and *NEUROD1* (Fig. 55D).

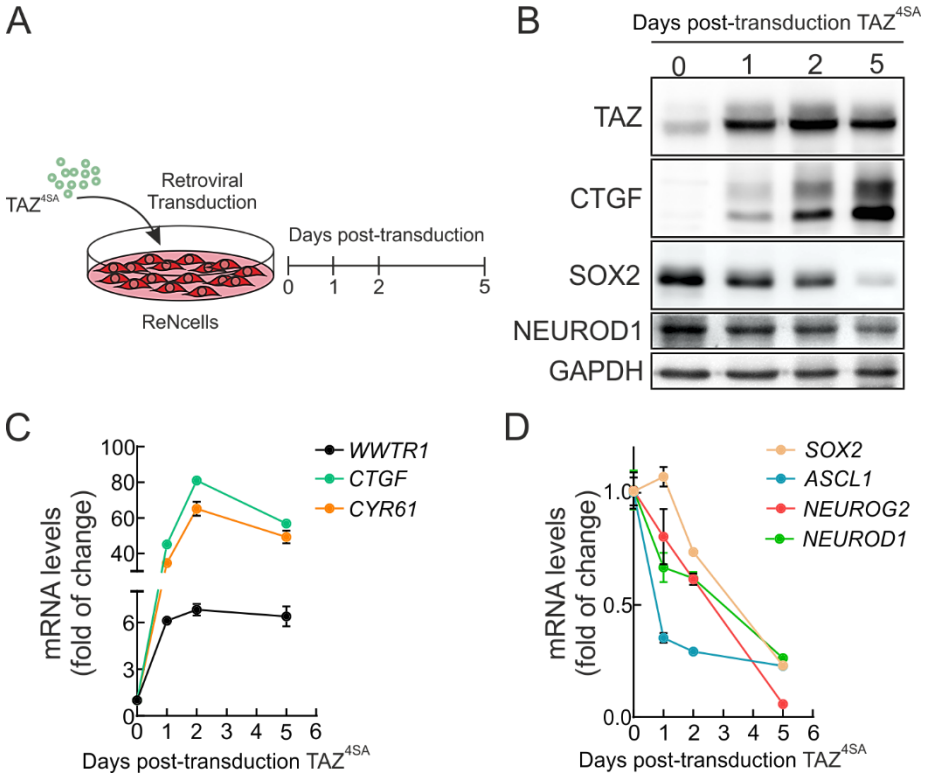


**Figure 55. Upregulation of TAZ decreases the levels of SOX2 and several bHLH factors. (A)** Schematic overview of experimental procedure: ReNcells were transduced with retroviral particles encoding $TAZ^{4SA}$ and the protein and mRNA levels were determined after 0, 1, 2 and 5 days post-transduction. **(B)** Representative immunoblot of TAZ, CTGF, SOX2, NEUROD1 and GAPDH as a loading control in ReNcells transduced with $TAZ^{4SA}$-expressing retrovirus after 0, 1, 2 and 5 days post-transduction. **(C)** mRNA levels of *WWTR1* and its targets *CTGF* and *CYR61*. **(D)** mRNA levels of *SOX2*, *ASCL1*, *NEUROG2* and *NEUROD1*. For **C** and **D**, mRNA levels were determined by qRT-PCR and normalized by the geometric mean of *ACTB*, *GAPDH* and *TBP* levels. Data represent mean ± S.D. (n = 4).

To uncover the effect of TAZ in proneurogenic genes during differentiation, we overexpressed wild type TAZ (TAZ-WT) and constitutively active TAZ ($TAZ^{4SA}$) by retroviral transduction in ReNcells and allow them to grow 5 days under proliferation conditions. Next, we removed the growth factors and analyzed the protein and transcript levels of several proneurogenic factors at 0, 2 and 4 days under differentiation conditions (Fig. 56A). In TAZ overexpressing cells, we found accumulation of TAZ and its target CTGF by immunoblot (Fig. 56B), and *CTGF* and *CYR61* transcripts (Fig. 56C). At the same time points, SOX2 and NEUROD1 protein levels declined (Fig. 56B). On the other hand, the expression of proneurogenic factors increased during differentiation in the control (CT) transduced cells, while *SOX2*, *ASCL1*, *NEUROG2* and *NEUROD1* remained low in TAZ-WT cells and were almost supressed in $TAZ^{4SA}$ cells (Fig. 56D). Together these results strongly suggest that TAZ is a negative regulator of these proneurogenic factors.

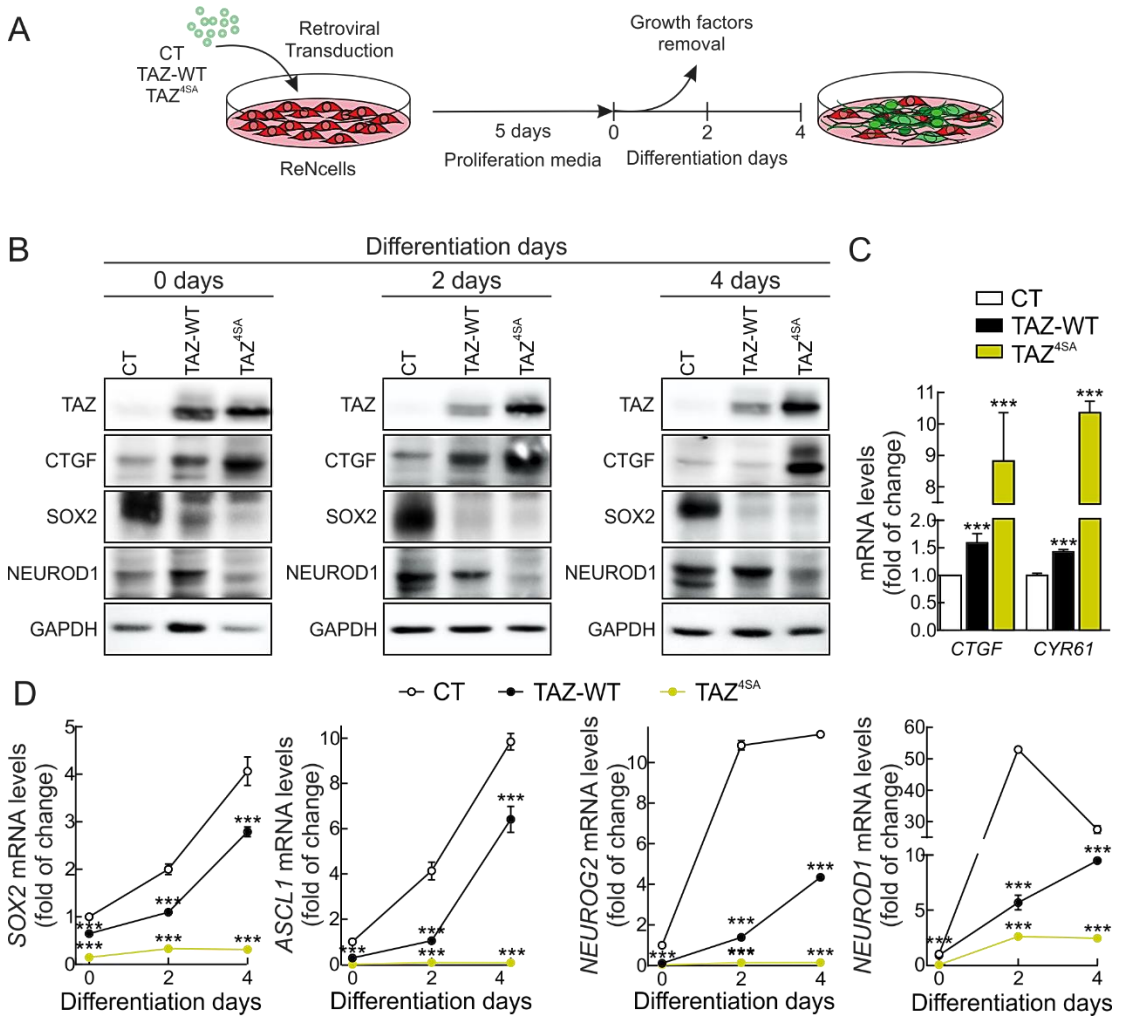


**Figure 56. Overexpression of TAZ decreases the levels of SOX2 and bHLH factors during differentiation.** (**A)** Representative scheme of experimental procedure: ReNcells were transduced with retroviral vector control (CT), TAZ-WT or TAZ$^{4SA}$ and grown for 5 days in proliferative conditions and samples were analyzed at 0, 2 and 4 days in differentiation conditions. **(B)** Representative immunoblot analysis of TAZ, CTGF, SOX2, NEUROD1 and GAPDH as a loading ReNcells CT, TAZ-WT and TAZ$^{4SA}$ at 0, 2 and 4 days of differentiation. **(C)** mRNA levels of *CTGF* and *CYR61*. **(D)** mRNA levels of *SOX2*, *ASCL1*, *NEUROG2* and *NEUROD1*. For **C** and **D**, mRNA levels were determined by qRT-PCR and normalized by the geometric mean of *ACTB*, *GAPDH* and *TBP* levels. Data represent mean ± S.D. (n = 4). Statistical analysis was performed using Student's *t*-test. ***$p \leqslant 0.001$ *vs.* CT.

## 8. TAZ repression of proneurogenic genes is partially TEAD-dependent.

To gain more insight into the implication of TEAD transcription factors in the regulation of proneurogenic factors, we expressed the defective TEAD-binding TAZ mutants. As expected, retroviral overexpression of TAZ-WT and active TAZ$^{4SA}$ led to an increase in the TAZ target CTGF after 5 days (Fig. 57A). At the same time, this CTGF accumulation was partially reverted by the TAZ$^{S51A}$ mutant defective in TEAD-binding (Fig. 57A). Furthermore, SOX2 protein levels decrease in TAZ-WT and even more in TAZ$^{4SA}$ conditions. The mutant TAZ$^{4SA+S51A}$, which disrupted TEAD binding, largely abolished the ability of TAZ to repress SOX2 (Fig. 57A and B). Similar results were observed with NEUROD1

(Fig. 57A and C). Parallel to the increase in TAZ targets (*CTGF* and *CYR61*) in TAZ-WT and TAZ$^{4SA}$ transduced ReNcells (Fig. 57D), we found a decrease at the transcriptional level of *SOX2* and proneural *ASCL1*, *NEUROG2* and *NEUROD1* factors, being this repression almost complete in cells expressing TAZ$^{4SA}$ (Fig. 57E). By contrast, this repression by TAZ$^{S51A}$ and TAZ$^{4SA+S51A}$ was almost absent for *SOX2* and partially reverted for *ASCL1*, *NEUROG2* and *NEUROD1* (Fig. 57E). TAZ can induce itself, making possible that ectopically expressed TAZ might induce endogenous TAZ expression, which is will not be defective in TEAD-binding.

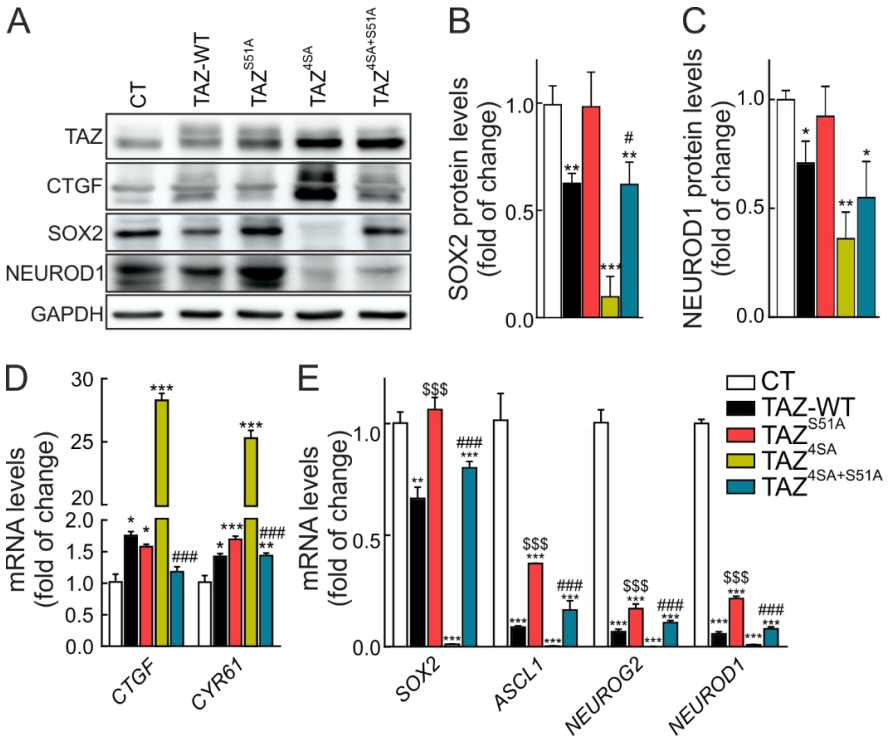


**Figure 57. Downregulation of SOX2 and bHLH factors by TAZ is partially TEAD-dependent. (A)** Representative immunoblots of TAZ, CTGF, SOX2, NEUROD1 and GAPDH as a loading control in ReNcells CT, TAZ-WT, TAZ$^{S51A}$, TAZ$^{4SA}$ and TAZ$^{4SA+S51A}$ after 5 days of retroviral transduction. **(B)** Densitometric quantification of SOX2 protein levels in (A) relative to GAPDH. **(C)** Densitometric quantification of NEUROD1 protein levels in (A) relative to GAPDH. Data are mean ± SEM (n = 4). **(D)** mRNA levels of TAZ targets *CTGF* and *CYR61* **(E)** mRNA levels of *SOX2*, *ASCL1*, *NEUROG2* and *NEUROD1* after 5 days of retroviral transduction. For **D** and **E**, mRNA levels were determined by qRT-PCR and normalized by the geometric mean of *ACTB*, *GAPDH* and *TBP* levels. Data are presented as mean ± S.D. (n = 4). Statistical analysis was performed using Student's *t*-test. $^{*}p \leqslant 0.05$; $^{**}p \leqslant 0.01$, $^{***}p \leqslant 0.001$ *vs.* control conditions. $^{\#}p \leqslant 0.05$; $^{\#\#}p \leqslant 0.01$, $^{\#\#\#}p \leqslant 0.001$ comparing TAZ$^{S51A}$ *vs.* TAZ-WT. $^{\$}p \leqslant 0.05$; $^{\$\$}p \leqslant 0.01$, $^{\$\$\$}p \leqslant 0.001$ comparing TAZ$^{4SA+S51A}$ *vs.* TAZ$^{4SA}$.

To further investigate the role of TEADs in TAZ repression of proneurogenic genes we used ReNcells retrovirally transduced with TAZ$^{4SA}$. In these cells, we performed knockdown of the TEAD isoforms using lentiviral vectors directed to TEAD1/3/4 and TEAD2 (altogether named shTEAD) (Fig. 58A). Depletion of TEADs (Fig. 58B) conducted to lower levels on *CTGF* and *CYR61* transcripts as expected (Fig. 58C), but also to up-regulation of proneurogenic transcripts (Fig. 58D). Altogether, these results suggest that TEADs are involved in the repressive function of TAZ on proneurogenic factors.

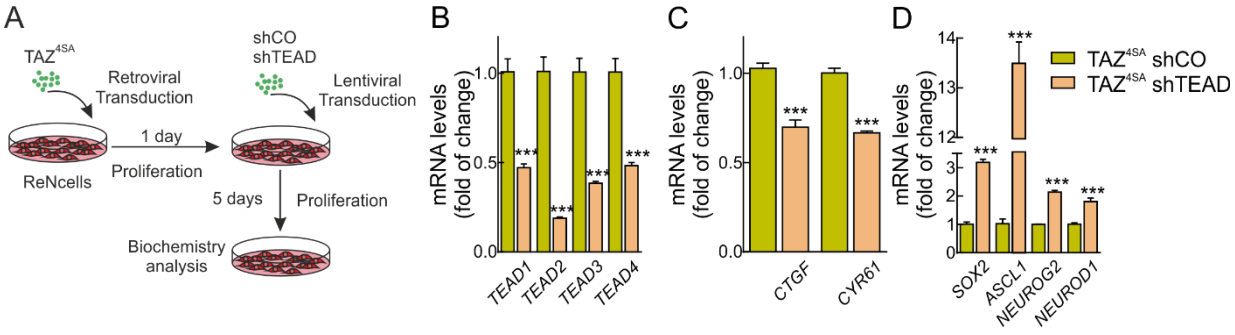


**Figure 58. TEAD knockdown partially recovers the mRNA levels of SOX2 and bHLH factors. (A)** Schematic overview of experimental design: ReNcells were transduced with retroviral vector for overexpression of TAZ$^{4SA}$ and, after 1 days of retroviral transduction, transduced with lentiviral control (shCO) or shTEAD1/3/4 + shTEAD2 (shTEAD) and allowed to grow 5 days under proliferative conditions. **(B)** mRNA levels of *TEAD1*, *TEAD2*, *TEAD3* and *TEAD4*. **(C)** mRNA levels of *CTGF* and *CYR61*. **(D)** mRNA levels of *SOX2*, *ASCL1*, *NEUROG2* and *NEUROD1*. For **B**, **C** and **D**, mRNA levels were determined by qRT-PCR and normalized by the geometric mean of *ACTB*, *GAPDH* and *TBP* levels. Data represent mean ± S.D. (n = 4). Statistical analysis was performed using Student's *t*-test. ***$p \leqslant 0.001$ *vs.* shCO.

## 9. TAZ induces epigenetic changes at the regulatory regions of proneurogenic genes.

We next explored epigenetic mechanisms underlying repression of the proneurogenic genes by TAZ. When CT and TAZ$^{4SA}$-ReNcells were maintained for 5 days in proliferation and 4 additional days in differentiation (Fig. 59A) they presented an increase in the canonical TAZ target CTGF, while SOX2 and NEUROD1 levels were decreased (Fig. 59B). At transcriptional level, TAZ targets *CTGF* and *CYR61* also increased (Fig. 59C) and while proneurogenic transcripts decreased (Fig. 59C). By ChIP-qPCR analysis, we found TAZ enrichment in positive controls and also in the TIRs of proneurogenic genes described in Figure 51, but not in the negative control (*CTGF* 3´UTR) in TAZ$^{4SA}$ cells compared to the control (Fig. 59D). We investigated the recruitment of RNA polymerase II (RNA Pol II) which is engaged together with the transcription machinery to the promoter in the eukaryotic genes (Roeder, 2005; Sandoval et al., 2004). RNA Pol II occupancy was significantly reduced at regulatory regions of proneurogenic genes in TAZ$^{4SA}$-expressing cells compared to control cells, while RNA Pol II levels were higher in *CTGF* and *CYR61* regulatory regions (Fig. 59E).

We then surveyed major histone modifications. Histone 3 (H3) acetylation in the N-terminal Lysine 9, is generally associated with gene activation (Kuo et al., 1996; Strahl and Allis, 2000). ChIP-qPCR assays using anti-acetylated Lys9-H3 antibody (AcH3) indicated that H3 acetylation was increased in TAZ *bona fide* targets *CTGF* and *CYR61*, while it was reduced by TAZ$^{4SA}$ overexpression in proneurogenic genes in the same TIRs, with no changes in the negative control (Fig. 59F). The regulation of histone acetylation suggested the implication of nucleosome remodelling and deacetylase complex (NuRD) (Lai and Wade, 2011). Using ChIP-qPCR assay, we confirmed the enrichment of NuRD subunit chromodomain-helicase-DNA-binding protein 4 (CHD4) in some TIRs of SOX2 and bHLH factors (Fig.

59G). On the basis of these results, we propose that TAZ represses proneurogenic gene expression by changes in histone acetylation and RNA Pol II occupancy at their regulatory regions.

Altogether, our results characterize for the first time TAZ as a master repressor of neuronal differentiation by the transcriptional repression of proneurogenic genes, and this repression is partially TEAD-dependent.

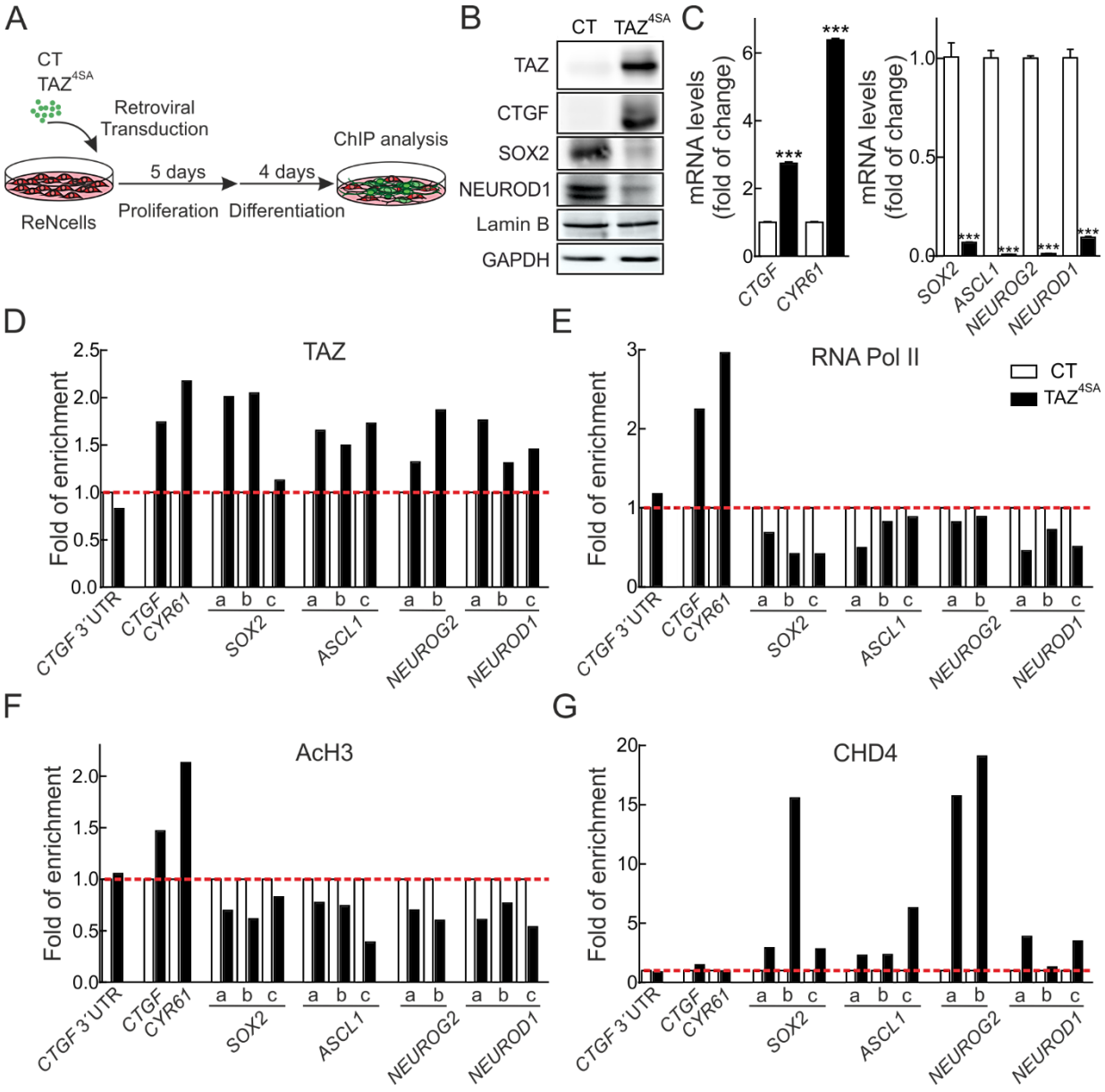


**Figure 59. TAZ recognizes specific regions in *SOX2* and bHLH factors and represses their transcription.** (**A)** Representative scheme of experimental procedure: ReNcells were transduced with retroviral vector control (CT) or TAZ$^{4SA}$ and grown for 5 days in proliferative conditions and 4 days in differentiation conditions. **(B)** Representative immunoblot analysis of TAZ, CTGF, SOX2, NEUROD1 carrying GAPDH and Lamin B as a loading controls in ReNcells CT or expressing TAZ$^{4SA}$. **(C)** mRNA levels of TAZ targets *CTGF* and *CYR61* and *SOX2*, *ASCL1*, *NEUROG2* and *NEUROD1*. mRNA levels were determined by qRT-PCR and normalized by the geometric mean of *ACTB*, *GAPDH* and *TBP* levels. Data are mean ± S.D. (n = 4). Statistical analysis was performed using Student's *t*-test. ***$p \leqslant 0.001$ *vs.* CT. **(D-G)** ChIP analysis of putative TIRs described in Figure 51 using anti-TAZ **(D)**, anti-RNA Pol II **(E)**, anti-AcH3 **(F)** and anti-CHD4 **(G)** antibodies *vs.* a control IgG in ReNcells CT or overexpressing TAZ$^{4SA}$ and normalized relative CT. Regions of *CTGF* and *CYR61* were analyzed as positive controls, and a region of *CTGF* (*CTGF* 3´UTR) that does not contain TIR was used as negative control.

# V. Pathophysiological significance of the axis TAZ/proneurogenic factors in glioblastoma.

## 1. TAZ negatively correlates with the levels of proneurogenic factors in low-grade gliomas and glioblastomas.

To assess the relevance of the TAZ-proneurogenic genes in glioblastomas, we consulted the UCSC Xena platform (http://xena.ucsc.edu/). This platform is a cancer genomics browser for viewing, analysing and visualizing the public data hubs of cancer genomics and clinical data from several projects as The Cancer Genome Atlas (TCGA) or Pan-Cancer Atlas, among others (Goyal, 2019). We analyzed the correlations between expression of TAZ and several proneurogenic genes in 1152 patient samples of lower grade glioma and glioblastoma (GBMLGG). First, we confirmed the positive correlation between TAZ gene expression (*WWTR1*) and its *bona fide* targets *CTGF*, baculoviral IAP repeat containing 5 (*BIRC5)* and *CD44* (Fig. 60A to C). In the same samples, we found that TAZ expression correlates inversely with that of proneurogenic factors *SOX2* (Fig. 61A), *ASCL1* (Fig. 61B), *NEUROG2* (Fig. 61C) and *NEUROD1* (Fig. 61E). Moreover, this negative correlation was also present with several neurogenins (*NEUROG3*) (Fig. 61D) and NEUROD factors (Fig. 61F to H).

Moreover, when we examined the Kaplan-Meier curves of each factor, we found that the higher expression of *WWTR1* and its targets *CTGF*, *BIRC5* and *CD44* was accompanied with poor prognosis (Fig. 62A to D). In accordance with the negative reciprocity with TAZ, high expression levels of proneurogenic genes correlated with a greater life expectancy of the patients (Fig. 63A to H). All in all, this bioinformatics analysis shows for the first time the negative correlation between TAZ and proneurogenic factors in human GBMLGG.

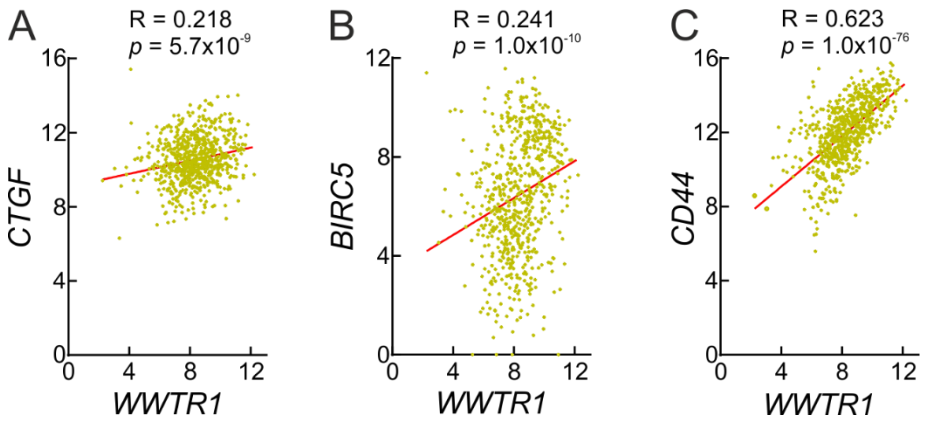


**Figure 60. The expression of *WWTR1* and its targets *CTGF*, *BIRC5* and *CD44* positively correlate in human lower grade gliomas and glioblastomas.** Graph showing positive correlation between expression of *WWTR1* and *CTGF* **(A)**, *BIRC5* **(B)** and *CD44* **(C)** in the TCGA datasets from 1152 patient samples of GBMLGG. Expression levels in A, B and C, expressed as $\log_2(x+1)$ transformed RSEM normalized counts, were directly obtained from the UCSC Xena platform. Pearson's correlation coefficient (R) and p-value were calculated as a function of the t distribution.

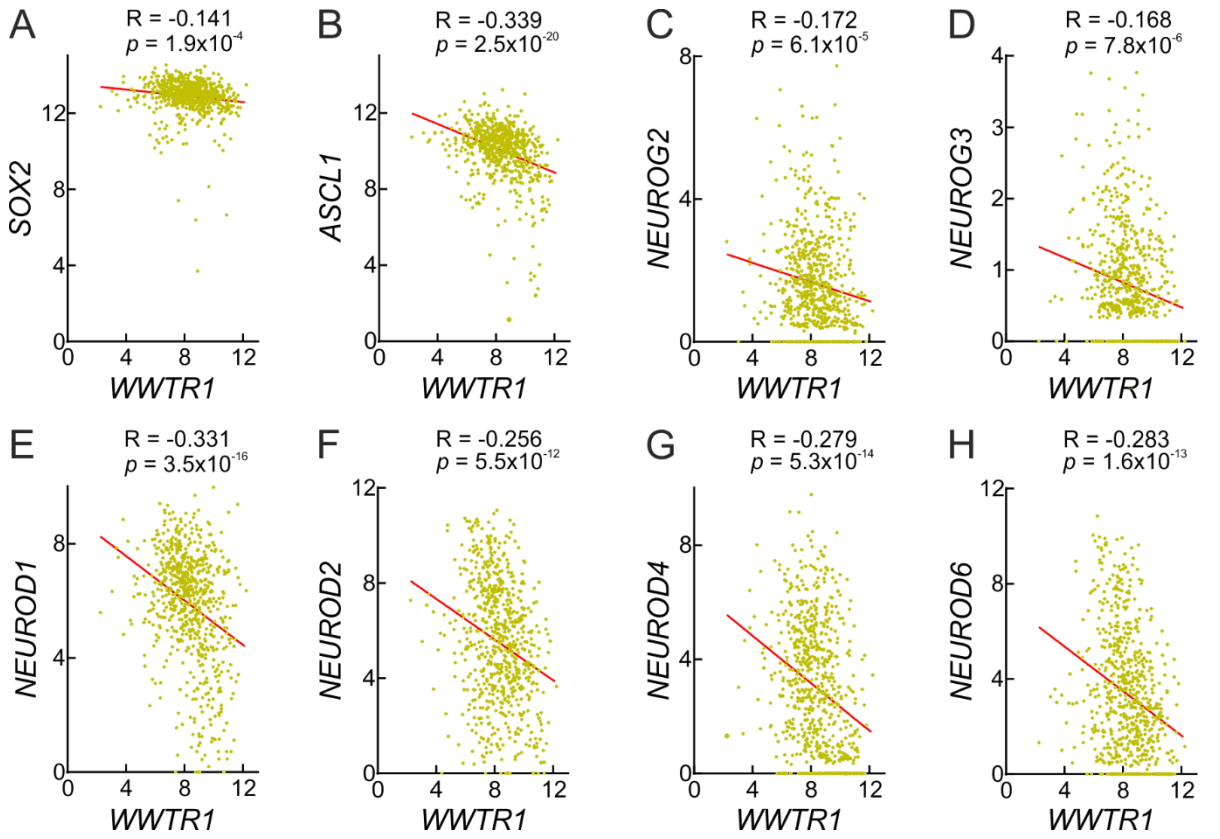


**Figure 61. *WWTR1* expression negatively correlates with proneurogenic genes in human lower grade gliomas and glioblastomas.** Graph showing positive correlation between transcript levels of *WWTR1* and *SOX2* **(A)**, *ASCL1* **(B)**, *NEUROG2* **(C)**, *NEUROG3* **(D)**, *NEUROD1* **(E)**, *NEUROD2* **(F)**, *NEUROD4* **(G)** and *NEUROD6* **(H)** in the TCGA datasets from 1152 patient samples of GBMLGG. Transcript levels, expressed as $\log_2(x+1)$ transformed RSEM normalized counts, were directly obtained from the UCSC Xena platform. Pearson's correlation coefficient (R) and p-value were calculated as a function of the t distribution.

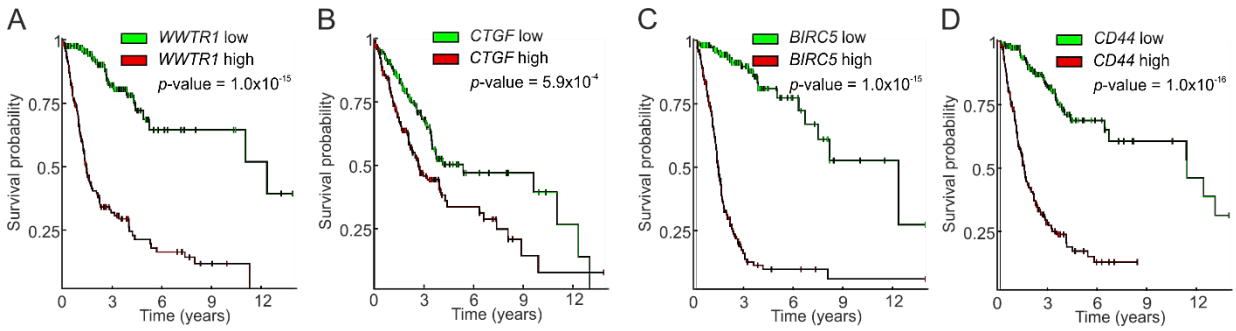


**Figure 62. *WWTR1* and high expression of its targets reduces the life-expectancy in patients with lower grade gliomas and glioblastoma patients.** Kaplan-Meier survival curves of 1152 patients with GBMLGG obtained from the UCSC Xena platform for *WWTR1* **(A)**, *CTGF* **(B)**, *BIRC5* **(C)** and *CD44* **(D)**. Patients were stratified in two groups using Z-score values. Statistically significant differences in survival between groups were calculated using the log-rank test.

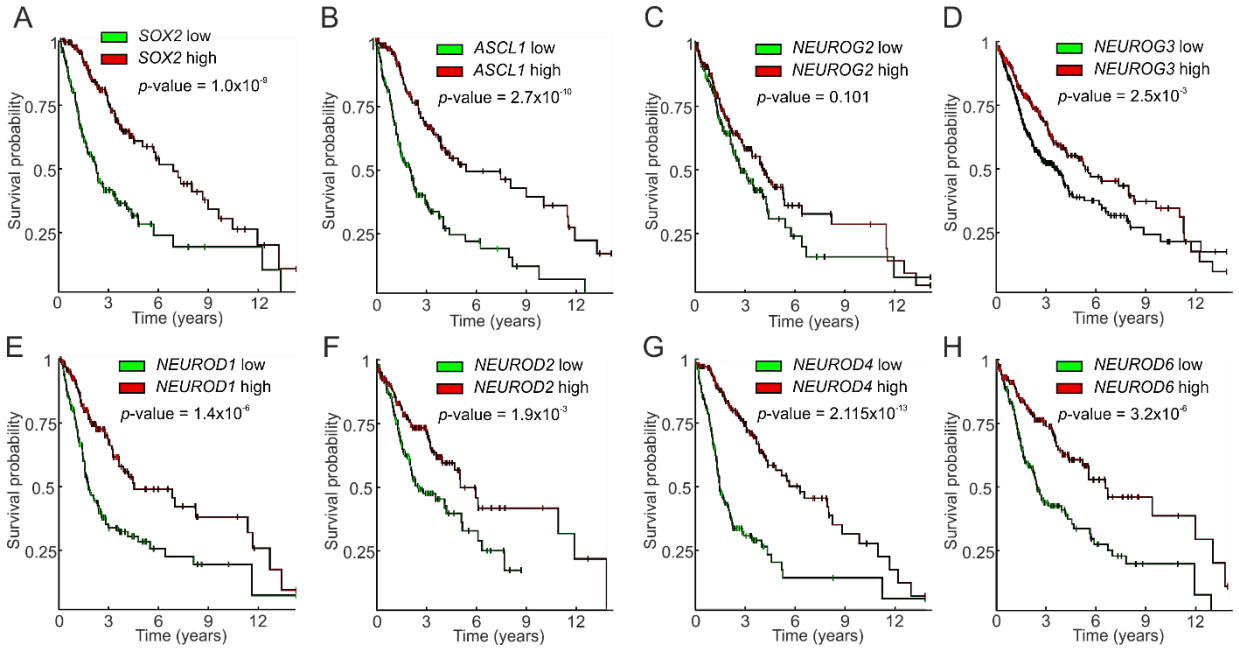


**Figure 63. High expression levels of proneurogenic factors correlate with better life-expectancy in patients with lower grade gliomas and glioblastomas.** Kaplan-Meier survival curves of 1152 patients with GBMLGG obtained from the UCSC Xena platform for *SOX2* **(A)**, *ASCL1* **(B)**, *NEUROG2* **(C),** *NEUROG3* **(D)**, *NEUROD1* **(E)**, *NEUROD2* **(F)**, *NEUROD4* **(G)** and *NEUROD6* **(H)**. Patients were stratified in two groups using Z-score values. Statistically significant differences in survival between groups were calculated using the log-rank test.

## 2. TAZ overexpression favours tumorigenicity of cancer stem cells and represses the expression of proneurogenic factors.

Cancer stem cells (CSCs) are responsible drug resistance and tumour relapse. To gain a more precise insight in the role between TAZ and several proneurogenic genes in cancer, we used the glioblastoma cell line U87-MG which can be grown as glioma stem cells in the appropriate medium as floating neurospheres (Gargini et al., 2015; Gargini et al., 2016; Hardee et al., 2012). This cell line presented high levels of TAZ compared to the human NSPCs cell line ReNcells as determined by immunoblot analysis (Fig. 64A). We next tested the effect of TAZ overexpression by retroviral transduction of U87-MG cells under neurosphere growth conditions. Overexpression of TAZ by retroviral transduction in U87-MG cells (Fig. 64B) led to an increase at the protein level of TAZ-regulated gene CTGF and the transcripts of *CTGF*, *BIRC5* and *CD44* (Fig. 64C). In parallel, a significant down-regulation of *SOX2*, *ASCL1*, *NEUROG2* and *NEUROD1* mRNA levels was observed (Fig. 64D), suggesting that the repressor function TAZ on proneurogenic genes is conserved in this glioma stem cell line.

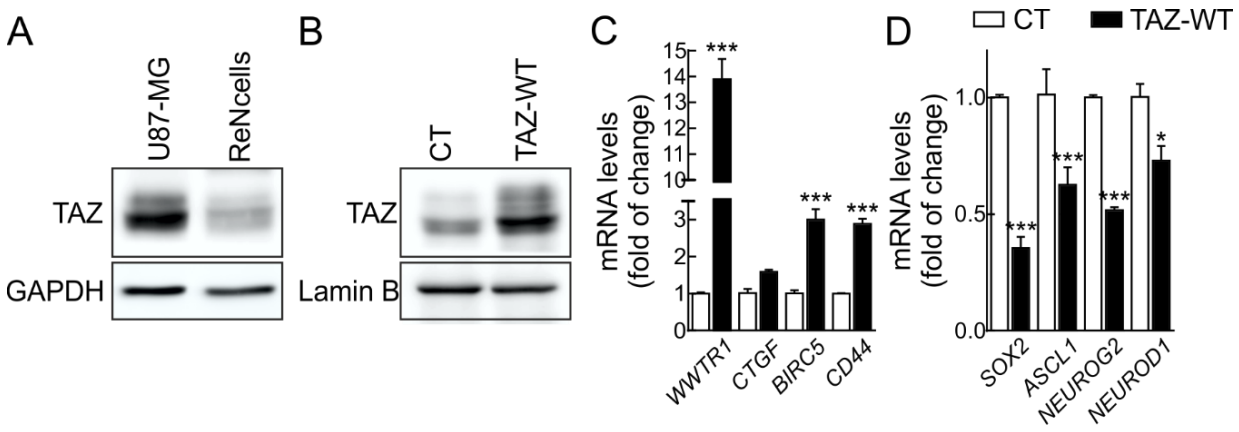


**Figure 64. TAZ overexpression correlates negatively with the levels of proneurogenic transcripts in the glioblastoma cell line U87-MG. (A)** Representative immunoblot of TAZ and GAPDH as a loading control in U87- MG in cancer stem cell (CSC) conditions and ReNcells under proliferative conditions. **(B)** Representative immunoblot analysis of TAZ and Lamin B as a loading control in U87- MG CT and TAZ-WT CSC conditions. **(C)** mRNA levels of *WWTR1* and its targets *CTGF*, *BIRC5* and *CD44* in U87-MG cells CT and TAZ-WT **(D)** mRNA levels of *SOX2* and bHLH factors *ASCL1*, *NEUROG2* and *NEUROD1* in U87-MG cells CT and TAZ-WT. In **C** and **D**, mRNA levels were determined by qRT-PCR and normalized by the geometric mean of *ACTB*, *GAPDH* and *TBP* levels. Data are presented as mean ± S.D. (n = 4). Statistical analysis was performed using Student's *t*-test. *$p \leqslant 0.05$, ***$p \leqslant 0.001$ *vs.* CT.

We found a slight increase to almost 150% compared to the control in the number of secondary neurospheres formed in TAZ-WT-derived cultures (Fig. 65A and B) and a significant increase in the number of cells (Fig. 65C). Even more, when U87-MG cells were injected subcutaneously for xenograft analysis in athymic mice, TAZ overexpression led to a subtle increase in tumour volume compared to the control (Fig. 65D and E). Next, we tested the tumourigenicity of TAZ-overexpressing glioma stem cells by intracranial xenotransplants in athymic mice. The survival rate of mice inoculated with control cells was roughly ~40 days and was decreased to ~30 days in the TAZ overexpressing cells (Fig. 65F). We speculate that the low effect of TAZ overexpression might be due to the fact that glioma stem cells exhibit basally high TAZ levels (Li et al., 2016b) (Fig. 64A).

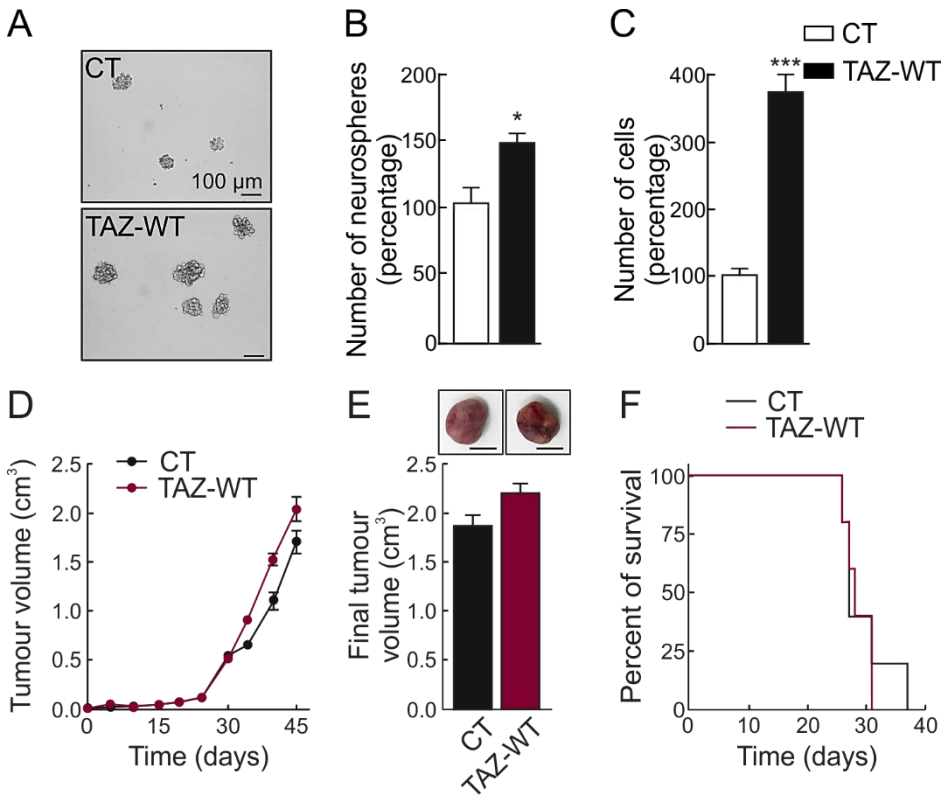


**Figure 65. TAZ overexpression favours cancer stem cell proliferation and tumorigenesis. (A)** Representative images of U-87 MG-derived neurospheres transduced with retroviral control (CT) or encoding human TAZ-WT. **(B)** Quantification of the number of secondary neurospheres as a percentage relative to control. Data are presented as mean ± S.D. (n = 3) *$p \leqslant 0.05$ *vs.* CT according to a Student's t-test. **(C)** Quantification of the number of cells represented as percentage of control. Data are presented as mean ± S.D. (n = 3) ***$p \leqslant 0.001$ *vs.* CT according to a Student's *t*-test. **(D)** Growth curves of subcutaneously xenografted athymic mice with U87-MG cells transduced with empty retrovirus (CT) or a retrovirus expressing *wild-type* TAZ (TAZ-WT) and implanted. Data are presented as mean ± SEM. (n = 4). **(E)** Upper panel, representative tumours of each experimental condition at the end point (scale bar, 1 cm); lower graph, quantification of the final tumour volume. Data are presented as mean ± SEM. (n = 4)**. (F)** Kaplan-Meier survival curves for mice bearing intracranial U87-MG xenografts CT and TAZ-WT (n = 6).

## 3. TAZ-knockdown reduces the tumorigenicity of glioma stem cells and leads to an increase in proneurogenic transcripts.

We next tested the effect of depleting TAZ in U87-MG lentivirally-transduced with shRNA against TAZ for 5 days under neurosphere growth conditions. As shown in Fig, 66, we found that TAZ-knockdown led to a decrease of its target CTGF (Fig. 66A). This decrease was also observed at the transcriptional level with a drastic reduction in *WWTR1* and its targets *CTGF*, *BIRC5* and *CD44* (Fig. 66B). At the same time, TAZ-knockdown correlated with a discrete increase in *SOX2* and *ASCL1* transcripts and a more than 4 folds induction of *NEUROG2* and *NEUROD1* (Fig. 66C). These significant results encouraged us to further confirm them using glioblastoma stem cells obtained from patient explant (GB). TAZ-knockdown in these glioblastoma explant (Fig. 66D and E) led to a decrease in its targets (Fig. 66E) and a significant increase of SOX2 and bHLH factors transcripts (Fig. 66F).

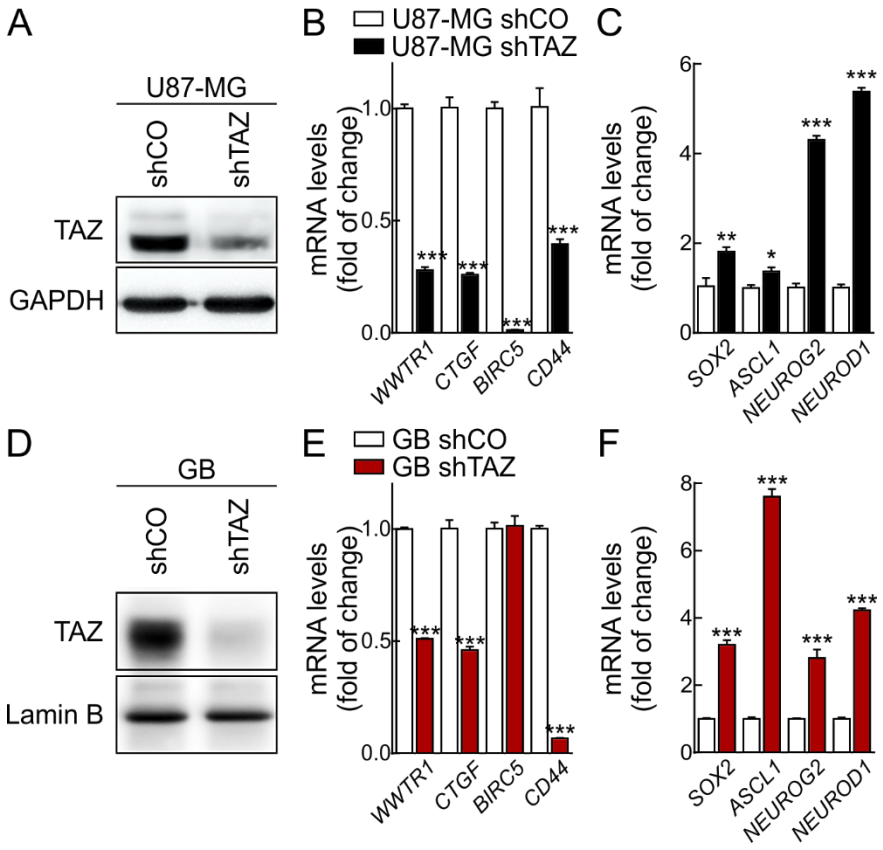


**Figure 66. TAZ depletion favours the expression of *SOX2* and several bHLH factors in the glioblastoma cell line U87-MG and GB. (A)** Representative immunoblot analysis of TAZ and GAPDH as a loading control in U87-MG shCO and shTAZ after 5 days of lentiviral transduction in CSC growth medium. **(B)** mRNA levels of *WWTR1* and its targets *CTGF*, *BIRC5* and *CD44* in U87-MG cells shCO and shTAZ after 5 days of lentiviral transduction. **(C)** mRNA levels of *SOX2* and bHLH factors *ASCL1*, *NEUROG2* and *NEUROD1* in U87-MG cells shCO and shTAZ after 5 days of lentiviral transduction. **(D)** Representative immunoblot analysis of TAZ and Lamin B as a loading control in GB shCO and shTAZ after 5 days of lentiviral transduction in CSC growth medium. **(E)** mRNA levels of *WWTR1* and its targets *CTGF*, *BIRC5* and *CD44* in GB cells shCO and shTAZ after 5 days of lentiviral transduction. **(F)** mRNA levels of *SOX2* and bHLH factors *ASCL1*, *NEUROG2* and *NEUROD1* in GB cells shCO and shTAZ after 5 days of lentiviral transduction. In **B, C, E** and **F**, mRNA levels were determined by qRT-PCR and normalized by the geometric mean of *ACTB*, *GAPDH* and *TBP* levels. Data are presented as mean ± S.D. (n = 4). Statistical analysis was performed using Student's *t*-test. *$p \leqslant 0.05$, **$p \leqslant 0.01$, ***$p \leqslant 0.001$ *vs.* shCO.

We found that U87-MG TAZ-deficient cells showed 10 folds fewer secondary neurospheres (Fig. 67A and B) and lower cell number (Fig. 67C), indicating a deficient proliferative rate compared to control TAZ-expressing cells.

Next, we assessed the tumorigenicity of TAZ-knocked-down glioma stem cells in xenotransplanted athymic mice. The growth of subcutaneous xenografts was substantially reduced by silencing the expression of TAZ in U87-MG cells as determined by the tumour volume (Fig. 67D and E). Very importantly, TAZ-depletion reduced the malignancy of the intracranial tumours and increased the life expectancy of these mice from 40 days in the control cells to more than 70 days in the TAZ-deficient cells (Fig. 67F).

Altogether, our results support a role of this novel TAZ/proneurogenic axis in lower grade gliomas and glioblastomas, unveiling a new pathway to be further explored for therapeutic applications in cancer.

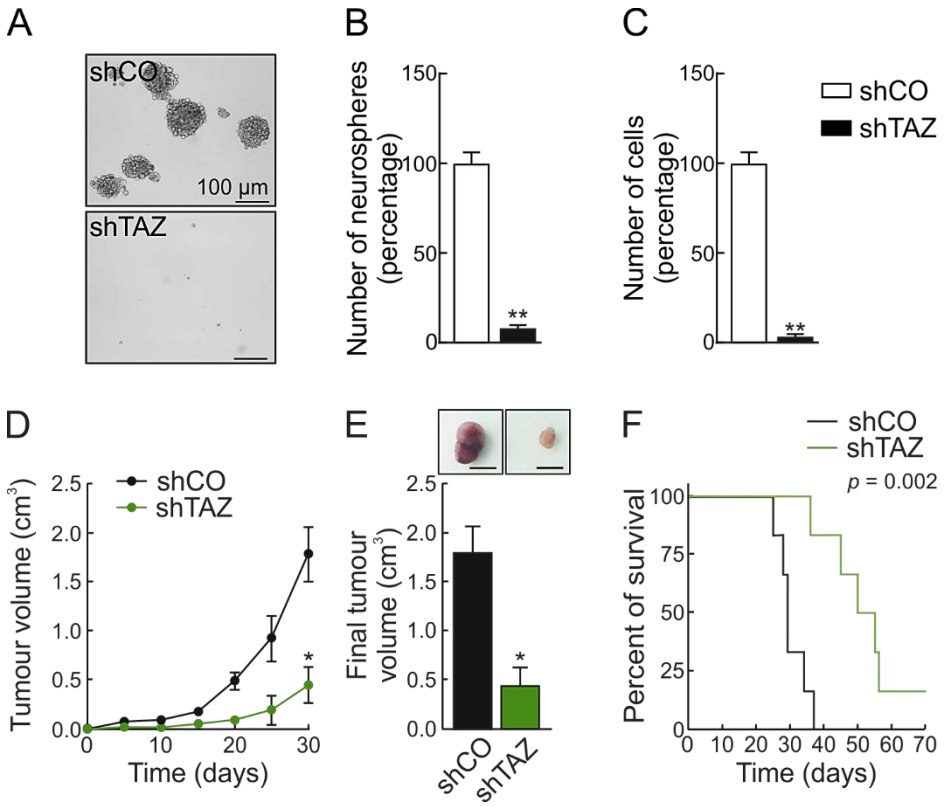


**Figure 67. TAZ-deficiency impairs the tumorigenicity of glioblastoma cancer stem cells. (A)** Representative images of U87-MG- derived neurospheres after 5 days of lentiviral transduction with shCO or human shTAZ. **(B)** Quantification of the number of secondary neurospheres as percentage relative to shCO. Data are presented as mean ± S.D. (n = 3) $^{**}p \leqslant 0.01$ *vs.* shCO according to a Student's t-test. **(C)** Quantification of the number of cells represented as percentage relative to shCO. Data are presented as mean ± S.D. (n = 3) $^{**}p \leqslant 0.01$ *vs.* shCO according to a Student's *t*-test. **(D)** Growth curves of xenograft tumours of U87-MG glioblastoma cells transduced with a lentivirus encoding shCO or human shTAZ and implanted subcutaneously in athymic mice. Data are presented as mean ± SEM (n = 4). $^{*}p \leqslant 0.05$ according to a Student's *t*-test. **(E)** Upper panel, representative tumours of each experimental condition at the end point (scale bar, 1 cm); lower graph, quantification of the final tumour volume. Data are presented as mean ± SEM (n = 4). $^{*}p \leqslant 0.05$ *vs.* shCO according to a Student's *t*-test. **(F)** Kaplan-Meier survival curves for mice bearing intracranial U87-MG xenografts shCO and shTAZ. Log-rank test between shCO and shTAZ is indicated (n = 6).

# DISCUSSION

## 1. NRF2 controls neural stem cell fate at the hippocampus.

Many studies have analyzed the implication of hippocampal adult neurogenesis in synaptic plasticity of the hippocampus and cognitive function (Toda and Gage, 2018), but our study reports a crucial role of transcription factor NRF2 in the mobilization and differentiation of the NSPCs in the hippocampal neurogenic niche of the SGZ (Fig. 68). In the adult, NSPCs give rise to new neurons that integrate in the pre-existing hippocampal neural circuitry at the level of the granular layer (Zhao et al., 2008b) and participate in LTP, which plays a major role in hipocamppal functions related to learning and memory (Garthe et al., 2009; Moser et al., 1998; Whitlock et al., 2006; Nabavi et al., 2014). In fact, depletion of hippocampal neurogenesis results in LTP loss and cognitive impairment (Snyder et al., 2001; Iscru et al., 2013; Saxe et al., 2006). In this study, we measured LTP in the DG, which under physiologic conditions is mainly derived from the born neurons of the adult brain (Wang et al., 2000; Schmidt-Hieber et al., 2004; Snyder et al., 2001; Saxe et al., 2006; Garthe et al., 2009). We describe, for the first time, an impairment in normal LTP linked to NRF2 deficiency. In line with this, Hooper et al described LTP impairment in transgenic mice conditionally overexpressing GSK3β (Hooper et al., 2007) which is a negative regulator of NRF2 (Cuadrado, 2015; Rada et al., 2011; Rada et al., 2012). In other behavioural test aimed at analysis of depression, the forced swimming test, NRF2-deficient mice presented increased immobility without affecting locomotive activity (Martin-de-Saavedra et al., 2013), which is interpreted as the onset and persistence of a depressive-like state (Stone and Lin, 2011; Sun et al., 2011; Serchov et al., 2015). Thus, NRF2 deficiency leads to behavioural and cognitive changes in mice.

Adult hippocampal neurogenesis is highly regulated by extrinsic and intrinsic factors (Cameron and McKay, 1999; Gould et al., 1999; Kempermann and Gage, 1998; Kempermann et al., 1997; Kempermann and Gage, 2002; Mirescu et al., 2004; Gould and Tanapat, 1999; van Praag et al., 1999). A common theme that is nowadays emerging suggests that changes in the intracellular redox status are crucial for the biology of NSPCs (Madhavan, 2015). Recent studies showed an increase in the number of mitochondria and overall production of ROS during mobilization of NSPCs in the SGZ of adult rodents (Walton et al., 2012). Furthermore, Le Belle and colleagues described that NSPCs maintain high ROS levels and are highly responsive to ROS stimulation (Le Belle et al., 2011). Although the authors did not analyze NRF2 directly, a bioinformatics analysis based on previous transcriptomics data sets (Wang et al., 2009; Anantharam et al., 2007) did show changes in the levels of several antioxidant enzymes whose expression is regulated by NRF2. Unfortunately, we could not analyze NRF2 protein levels by immunohistochemistry in the SGZ, because of the low specificity for IHC of available antibodies. Despite of this, we found by immunoblot the absence of NRF2 and the reduction of its transcriptional signature in NSPCs isolated from the SGZ of NRF2 deficiency mice as expected, and, interestingly, NSPCs from either newborn or 3 month-old *Nrf2*$^{-/-}$ mice exhibited a substantially compromised proliferation rate. Our results are in line with a previous study showing that a highly reduced intracellular redox state promotes proliferation and survival (Smith et al., 2000). Neuronal differentiation was also compromised by NRF2

deficiency, while ectopic expression of NRF2 rescued normal neuronal differentiation. Even more, based on EdU assay, NRF2 deficiency altered the physiologic balance between glial and neuronal differentiation of NSPCs, favouring formation of astrocytes. Consistent with this, NRF2 potentiates retinoic acid-induced neuronal differentiation of the SH-SY5Y neuroblastoma cell line (Zhao et al., 2009). By contrast, NRF2 overexpression in differentiating neurons leads to inhibition of neurite outgrowth and arborisation, and electrophysiological maturation (Bell et al., 2015). Thus, NRF2 repression is necessary for neuronal maturation, but NRF2 presence creates the intracellular environment that supports the neural niche.

To further analyze the impact of NRF2 in self-renewal of NSPCs, we used a genetic approach based on lentiviral expression of NRF2 in otherwise deficient NSPCs. Ectopic expression of NRF2 rescued NRF2-deficient NSPCs to cloning and proliferative values similar to those of wild type NSPCs. Additionally, decreasing or increasing NRF2 expression by genetic means was sufficient to significantly suppress or rejuvenate NSPCs properties, respectively. These findings are in line with the data from Coremblum and colleagues, who determined that early postnatal NSPCs express high levels of NRF2, while the NSPCs from aged animals, with lower regenerative capacity, have reduced NRF2. The studies also ascertain that decreasing or increasing NRF2 levels in the young and aged cells respectively, is sufficient to negatively or positively alter the regenerative capacity of NSPCs (Corenblum et al., 2016). Pharmacological induction of NRF2 with resveratrol demonstrated that this compound reverses the decline NSPCs proliferation and neurogenesis induced by ionizing radiation of brain tumours (Prager et al., 2016). Resveratrol also protected hippocampal NSPCs in ethanol-treated rodents (Xu et al., 2015) and in prenatally stressed in rats (Madhyastha et al., 2013).

In order to understand how NRF2 controls the fate of NSPCs, we used the cell pair assay that indicates whether NSC divisions lead to identical siblings with self-renewal capacity or to two different cells, one remaining proliferative and the other entering a differentiation program (Xapelli et al., 2013). The current model of mobilization of the NSPCs establishes that a NSC progenitor will divide symmetrically for several generations to perpetuate the progenitor pool. At the same time, a certain number of asymmetric divisions will lead to a supply of neurons and astrocytes to accommodate specific demands. The last division leads to differentiation of both siblings into astrocytes (Encinas et al., 2011). The fact that the NSPCs pool was exhausted more rapidly in the *Nrf2*$^{-/-}$ mice suggests that either cell-autonomous alterations or the micro-environmental influence leads to the mobilization and terminal differentiation of these neural progenitors. Consistent with this hypothesis, we found an inverse correlation between Ki67-stained progenitors and GFAP-stained astrocytes. Although we cannot discard a micro-environmental influence, our results with the cell pair assay in cell culture, in the absence of other cell types, indicate that NRF2 deficiency leads to cell-autonomous alterations. Indeed, we found that NRF2 deficiency resulted in an increase of asymmetric divisions, leading to the reduction in the number of progenitors. These findings suggest that the exacerbated exhaustion of the NSPCs pool in the *Nrf2*$^{-/-}$ mice is due to an increase in asymmetric divisions, together with imbalance in the cell fate to increase the number of astrocytes and reduce neurons. This hypothesis is consistent with the well reported observation

that NRF2 is required to counterbalance the high levels of intracellular ROS of highly proliferating cells (Schumacker, 2006; Toyokuni et al., 1995; Noble et al., 2003; Rafalski and Brunet, 2011).

The role of NRF2 in neurogenesis has been related to signaling pathways that regulate cell proliferation and differentiation. For example, a functional ARE recognized by NRF2 has been identified in the promoter region of *Notch1* (Wakabayashi et al., 2010; Wakabayashi et al., 2015), the main player of Notch signaling (Engler et al., 2018). In the same way, several studies described the crosstalk between NRF2 and Wnt signaling (Rada et al., 2015; L'Episcopo et al., 2013). In a bidirectional feedback loop, NRF2 deficiency could deregulate Wnt signaling (L'Episcopo et al., 2013) and, on the other hand, activation of Wnt signaling can prevent NRF2 phosphorylation through GSK3β/β-TrCP and its posterior proteasomal degradation, driving to NRF2 accumulation (Rada et al., 2015). Furthermore, NRF2 is linked to the activity of a number of trophic factors including VEGF, PDGF, IGF-1 and TGF-β which are also important for NSPCs (Li et al., 2016a; Ashino et al., 2013; Wiesner et al., 2013; Hsieh, 2012). All these studies point NRF2 as a major regulator of NSPCs fate and function.

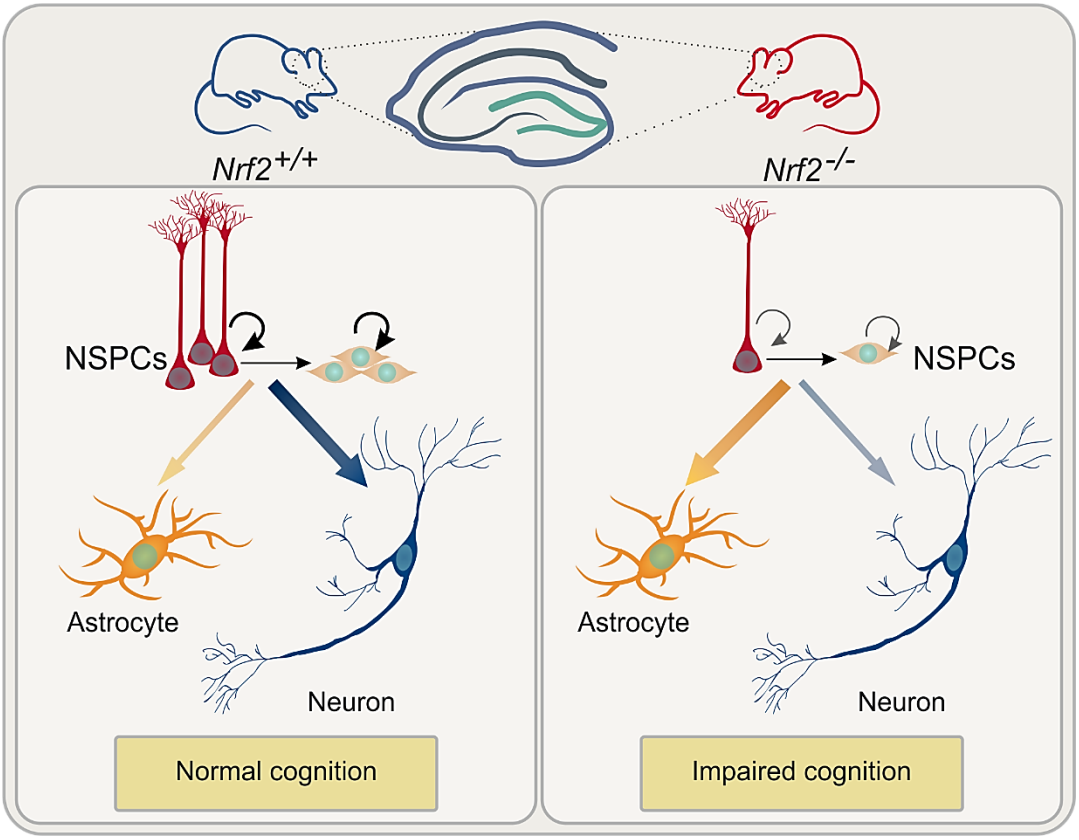


**Figure 68. NRF2 controls the neural stem cell fate in a cell autonomous way.** Absence of NRF2 conducts to an impaired the self-renewal capacity of neural stem/progenitor cells (NSPCs) and an imbalance in astroglial/ neuronal differentiation, impacting the normal hippocampal cognitive function.

## 2. Relevance of NRF2 in neurogenesis in a mouse model of Alzheimer´s disease.

NRF2 orchestrates a symphony of homeostatic responses to multiple stressors that characterize neurodegenerative disease (Deshmukh et al., 2017; Johnson and Johnson, 2015; Ramsey et al., 2007; Sandberg et al., 2014; Pajares et al., 2015). Although it is known that NRF2 and the neurogenic niche of the SGZ losses activity under pathologic conditions such as AD, the molecular mechanisms behind this correlation are largely unknown. For this reason, we recapitulated the main hallmarks of AD pathology, by expressing human $APP^{V717I}$ and $TAU^{P301L}$ in wild type (AT-*Nrf2*$^{+/+}$) or NRF2-knockout (AT-*Nrf2*$^{-/-}$) mice. In fact, we confirmed the presence of the neuropathological hallmarks of AD, TAU-aggregates and amyloid plaques (Goedert et al., 1991; Braak and Braak, 1996) in the hippocampus of these mice.

The absence of NRF2 exacerbated cognitive deficits and impaired LTP in the AT-*Nrf2*$^{-/-}$mice. The fact that memory and learning were severely impaired in these mice as early as 6 months of age suggests that the lack of NRF2 might replicate a prodromal condition of human AD (Wilson et al., 2011). These observations also fit with a previous report showing that NRF2 deficiency exacerbated the deficits in spatial learning and memory, as well as in working and associative memory in the APP/PS1 mouse model of amyloidopathy (Branca et al., 2017). Even more, Kanninen et al., described a memory improvement in these mice after NRF2 lentiviral transduction into the hippocampus and this improvement was associated with a reduction in soluble forms of $A\beta_{1-40}$ and $A\beta_{1-42}$ (Kanninen et al., 2009). Moreover, our AT-*Nrf2*$^{-/-}$mice presented high levels of the soluble Aβ*56 oligomer (Rojo et al., 2017) which has been reported to induce memory impairment in very early in the pathogenesis of AD (Lesne et al., 2013; Lesne et al., 2006).

The fact that at 3 months of age the proteinopathy is similar between AT-*Nrf2*$^{+/+}$ and AT-*Nrf2*$^{-/-}$ mice but the neurogenic niche is highly damaged in AT-*Nrf2*$^{-/-}$ mice suggests that already at this early age there is an attempt of the diseased hippocampus to compensate the ongoing neuronal damage. In fact, the hippocampus of AT-*Nrf2*$^{-/-}$ mice exhibits increased levels of oxidative and pro-inflammatory markers compared to AT-*Nrf2*$^{+/+}$ mice, suggesting that the proteotoxic insult renders these animals more sensitive to oxidative and inflammatory stress (Rojo et al., 2017). These data correlate with previous studies highlighting the implication of persistent oxidative and inflammatory stress in mild cognitive impairment and in AD onset and progression (Gabbita et al., 1998; Nunomura et al., 1999; Pratico, 2008). Another study also supports the impairments in both the proliferative capacity of NSPCs and in the neuronal differentiation early in the AD progression in the APP/PS1 mice (Demars et al., 2010) and in the 3xTg mouse model harbouring human mutant $PS1^{M146V}$, $APP^{KM670/671NL}$ and $TAU^{P301L}$ (Rodriguez et al., 2008a; Hamilton et al., 2010), even preceding cognitive deficits (Lazarov and Marr, 2010; Lazarov and Marr, 2013; Hollands et al., 2016).

Others studies provide evidence of the involvement of NRF2 in neuroprotection both in cell culture of primary postmitotic neurons and in animal models of CNS diseases (Lazarov et al., 2010; Kanninen et al., 2009; Shih et al., 2003; Zhao et al., 2015). Regarding neurogenesis, our results are in

agreement with a previous study showing that up-regulation of NRF2 ameliorated amyloid β-mediated neural stem cell death (Karkkainen et al., 2014). Related to other neurodegenerative disorders, mice submitted to the Parkinsonian toxin 1-methyl-4-phenyl-1,2,3,6-tetrahydropyridine (MPTP) exhibited reduced neurogenesis in the SVZ via impaired NRF2-mediated adaptation to inflammation (L'Episcopo et al., 2013).

The fact that NRF2 possesses both a neuroprotective and a neurogenic function raises the tempting hypothesis that NRF2 up-regulation may be a good possibility to increase the capacity of transplanted NCPCs to preserve the neurogenic functionality of the hippocampus against proteinopathy.

### 3. NRF2 and the Hippo pathway interact through the transcriptional control of the TAZ coding gene *WWTR1*.

The Hippo pathway is a potent regulator of cell proliferation, differentiation, and tissue homeostasis (Misra and Irvine, 2018) and appears to be influenced by the redox status. Thus, Gandhirajan et al., described TAZ as the redox sensor and $H_2O_2$ exposure leads to increased stability and activation of TAZ due to reversible S-glutathionylation at conserved cysteine residues. This suggests that ROS could enhance TAZ protein stability and facilitate tissue repair (Gandhirajan et al., 2016). Because NRF2 is also a potent regulator of cell proliferation and differentiation, and elicits an antioxidant defence, we studied the possible connection between both pathways. We have found that NRF2 regulates the expression of the TAZ coding gene *WWTR1* (Fig. 69).

NRF2 deficiency in NSPCs cultures correlated with low protein and transcript levels of TAZ. As described before, NRF2-deficient NSPCs also present low proliferate rate (Robledinos-Anton et al., 2017). Furthermore, genetic (shRNA and NRF2 overexpression) and chemical (sulforaphane) manipulation of NRF2 in human immortalized NSPCs indicate that the transcript and protein levels of TAZ and TAZ-dependent genes are, at least in part, governed by the levels of NRF2 in neural stem cells (Fig. 69).

We have identified several putative AREs by informatics analysis in the *WWTR1* gene promoter. This analysis was based on the study of other basic region leucine zipper (bZIP)-type transcription factors that also bind AREs, specifically MAFF, MAFK and BACH1 (Katsuoka and Yamamoto, 2016; Jyrkkanen et al., 2011), for which ChIP sequencing data are available in the ENCODE database. The lack of data available for NRF2 binding in ENCODE could be related with the lack of specificity for ChIP analysis of NRF2 antibodies (Lau et al., 2013). Due to the variations within the sequences recognized by bZIP factors (Yamamoto et al., 2006), we compared this information with the human consensus sequence recognized by NRF2 described in the JASPAR database using a Python script. Of note, this script identified with a high relative score the already known AREs in the *HMOX1* and *NQO1* promoters. The most potent ARE in *WWTR1* was located in a DNase-sensitive and H3K27-acetylated region, suggesting that it is accessible to the transcriptional machinery, but was not as potent as the canonical ARE of

*HMOX1* which is rapidly induced upon NRF2 activation. Several studies have analyzed the NRF2 transcriptional signature by microarray or RNA-sequencing approaches (Chorley et al., 2012; Namani et al., 2017). From these studies it is possible to distinguish grades of gene response to NRF2, from the most sensitive genes, related to the classical redox control, to others that require more time and persistent presence of NRF2 for induction. For instance, genes involved in metabolic reprograming or autophagy appear to require persistent exposure to NRF2 (Mitsuishi et al., 2012; Pajares et al., 2016).

The NRF2 and TAZ crosstalk in neurogenesis should be further analyzed. Both proteins have been implicated in neurogenesis in connection with Wnt, Notch and Shh signaling pathways and the mechanistic connection might be at the level of phosphorylation by GSK-3 and subsequent proteasomal degradation (Rada et al., 2011; Huang et al., 2012). GSK3β associates with Axin and APC to make up a complex that targets the transcriptional regulator β-catenin for degradation (Stamos and Weis, 2013). Recent work shows that this complex destabilizes TAZ/β-catenin complexes (Azzolin et al., 2012). Stimulation of cells with Wnt ligands, which inhibits GSK3β activity, increases TAZ and β-catenin levels and nuclear activity. NRF2 also associates with Axin and this complex is destabilized by WNT-3A preventing its GSK3/β-TrCP-dependent proteasomal degradation, leading to increased levels of NRF2 and its transcriptional signature (Rada et al., 2011). Thus, Wnt signaling leads to TAZ and NRF2 accumulation. As described previously, NRF2 is implicated in Notch signaling, regulating *Notch1* gene expression (Wakabayashi et al., 2015; Wakabayashi et al., 2010). Interestingly, Totaro et al. showed that mechano-activation of YAP/TAZ promotes epidermal stemness by inhibiting Notch signaling, a key factor for epidermal differentiation (Totaro et al., 2018; Totaro et al., 2017). Several studies described the functional interplay between Hippo and Hedgehog signaling underlying temporal and spatial control of tissue growth and specification (Cotton et al., 2017; Levasseur et al., 2017). Recent data describe the transcriptional regulation of several Hedgehog signaling components by NRF2 (Martín-Hurtado et al., 2019, *under review*). Thus, in the present study we tested the relationship between two factors implicated in the regulation of signaling pathways related to stem cells properties and function.

The crosstalk between NRF2 and Hippo-pathway has been described with the other major Hippo effector, YAP. Ciamporcero et al found that silencing YAP protein expression reduced NRF2 protein and mRNA expression in bladder cancer cells. On the other hand, NRF2 silencing inhibited YAP expression. Both were involved in cytotoxic drug sensitivity and synergistically reduced the migration of chemoresistant bladder cancer cells (Ciamporcero et al., 2018). While in this study only a correlation between NRF2 and YAP levels was reported, here we have demonstrated the presence of NRF2-binding sequences in the regulatory region of TAZ-encoding gene.

Taken together, our findings provide novel insights into the genomic targets of NRF2. Future work should aim to unravel how the relationship between NRF2 and TAZ contribute to cell proliferation under physiological and pathological conditions such as cancer.

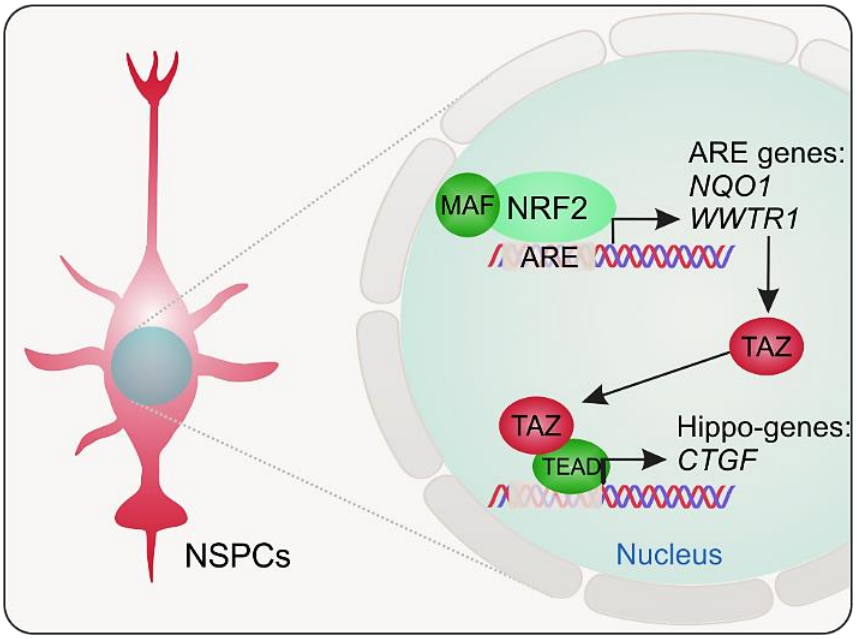


**Figure 69. NRF2 modulates TAZ levels in NSPCs.** NRF2 binds ARE in the promoter regions of its target genes as *NQO1* and in *WWTR1* gene, encoding TAZ. In addition, we show here that NRF2 regulates the expression of *WWTR1* in primary and immortalized NSPCs, that activates a battery of genes, such as *CTGF*, that participate in proliferative responses.

## 4. TAZ is a transcriptional corepressor of neuronal differentiation.

Our study addressed for the first time how the Hippo co-activator TAZ represses the expression of proneurogenic genes (Fig. 70). The transcriptional program underlying neural stem cell differentiation is regulated by largely unknown spatiotemporal patterns of gene expression (Guillemot, 2007; Spitz and Furlong, 2012). The Hippo pathway has been related with the maintenance of the NSPCs pool (Lavado et al., 2018), but the specific role of TAZ in neurogenesis has not been previously addressed. Interestingly, TAZ is implicated in epithelial–mesenchymal transition (EMT) in cancer (Wang et al., 2015b; Li et al., 2015), a process that is critical for neuronal development and the migration of newborn neurons (Kwan et al., 2012).

Based on the data available in the Brain RNA-seq database and our immunofluorescence analysis *in vitro* and *in vivo*, we found that TAZ expression is mostly limited to astrocytes and NSPCs, and decreases along neuronal maturation. Although no previous analysis were focused in TAZ expression in neurogenic niches, our findings are in line with the downregulation of the other Hippo effector, YAP, during neuronal differentiation (Zhang et al., 2012). YAP is also expressed in astrocytes and progenitors, but not in neurons (Huang et al., 2016). However, while we find that TAZ knockdown leads to neuronal differentiation, it is not clear that YAP will do the same. This could be related to different roles of TAZ and YAP or to misleading identification neurons. In fact, Zhang et al. used TUBB3 as a neuronal marker, which it is not specific as it is also expressed in astrocytes and progenitors (Draberova et al., 2008). On the contrary, we used several neuronal markers and astrocytic markers to ensure the proper identification of neurons.

Prompted for our findings, we assessed the presence of TAZ transcriptional co-partners binding sequences in proneurogenic genes. Bioinformatics approaches revealed that the promoters of the proneurogenic genes *SOX2*, *ASCL1*, *NEUROG2* and *NEUROD1* present putative sites for binding to TAZ-transcriptional co-partners. We then uncovered the relationship between TAZ expression and proneurogenic genes by showing TAZ enrichment in their regulatory regions. Furthermore, we ensured the accuracy of these sequences cloning an identified TEAD-binding sequence of *SOX2* in the luciferase reporter and showing a TAZ-dependent response.

The information available about the interaction between TAZ co-partners and proneurogenic genes is very scarce. However, the short half-life of proneurogenic factors indicates the relevance of their transcriptional regulation (Sriuranpong et al., 2002; Ali et al., 2011). It has been described that TAZ co-partner SMAD (Varelas et al., 2008) shares many gene targets with cell-type specific transcription factors that participate in cellular identity (Mullen et al., 2011; Trompouki et al., 2011). Genome-wide experiments demonstrate that the proneural factor ASCL1 assists SMAD3 in binding to a subset of enhancers (Fueyo et al., 2018). Furthermore, Castro et al., described that ASCL1 targets the transcription factors TEAD1, TEAD2 and TAZ using genome-wide analysis of the developing ventral mesencephalon (Castro et al., 2011). Our bioinformatics analysis demonstrated that RUNX1/2- recognizes a sequence in the regulatory regions of proneurogenic genes. Fukui et al., showed that *RUNX1* is down-regulated during neuronal differentiation, while *NEUROG2* is upregulated, but the authors did not establish any further analysis to this correlation (Fukui et al., 2018). Thus, our study establishes for the first time the existence of TAZ-interacting regulatory regions in proneurogenic genes. Furthermore, the upregulation of TAZ repressed the expression of these genes, which was partially recovered by ablation of TAZ-TEAD interaction or TEAD-knockdown. The uncompleted recovery could be: a) because TAZ functional repression is partially TEAD-independent, b) ectopic TAZ upregulates endogenous TAZ, which is not TEAD-binding defective, hiding the TEAD-independent effect. As described in the ENCODE database, the TAZ enhancer regions comprise several TEAD-putative binding sequences. Furthermore, TEAD4 is a target of TAZ (Kim et al., 2015). TEADs are essential for the transcriptional co-activator function of TAZ (Zhang et al., 2009); hence, it would be unexpected that TEAD was also involved in their corepressor function.

Our study shows that the interaction of TAZ with regulatory regions of proneurogenic genes conducts to decreased acetylation of the chromatin and reduced recruitment of RNA polymerase II (RNA Pol II). Of note, the same TAZ-TEAD complex activates genes such as *CTGF* and *CYR61* but suppresses the transcription of others. Enhancer-bound TAZ–TEAD complexes regulate gene transcription by inducing p300-dependent acetylation at lysine 27 of histone H3 (H3K27ac) (Stein et al., 2015), through recruitment of the Mediator complex and induction of transcriptional elongation through the release of RNA polymerase II (Galli et al., 2015). Several recent studies have identified the interaction of TAZ or its *Drosophila* homolog Yki with other regulators of chromatin status as components of the chromatin-remodelling complexes and histone methyltransferase complexes (Basu et al., 2013; Qing et al., 2014;

Skibinski et al., 2014; Oh et al., 2013). In our study, we described that nucleosome remodelling and histone deacetylase (NuRD) complex subunit CHD4 was enriched in the same regulatory regions of proneurogenic factors that were bound by TAZ (Lai and Wade, 2011). Recently, Kim et al., described the interaction between TAZ-paralog YAP with NuRD complex. In this study, the authors showed how the YAP/TEAD recruits the NuRD complex to deacetylate histones and supresses the expression of Trail and DNA Damage Inducible Transcript 4 (DDIT4)-encoding genes to promote cell growth and survival (Kim et al., 2015). The implication of NuRD in transcriptional repression of TAZ/TEAD has also been established by Beyer et al., who described a regulatory complex composed of TAZ/YAP/TEAD, SMAD2/3, and the pluripotency regulator OCT4, that collaborates with NuRD to suppress mesoendoderm genes (Beyer et al., 2013; Totaro et al., 2018). Indeed, TAZ can directly interact with histone deacetylation complex for TAZ/TEAD-induced suppression of ΔNp63 transcription (Valencia-Sama et al., 2015). Together with these studies, our data suggests that TAZ supresses gene expression by directly interacting with the histone deacetylation complex and further affects RNA Pol II recruitment and gene transcription.

It is important to point out the inter-relationship between proneurogenic factors. Although the repressor effect of TAZ on *ASCL1* and *NEUROG2* expression is as strong as on *SOX2* and *NEUROD1*, the enrichment of TAZ in their regulatory regions and the effect in histone acetylation and RNA Pol II recruitment is not as strong. This could be related to the capacity of proneurogenic factors to regulate their own expression. For example, SOX2 can enhance the expression of *ASCL1* and *NEUROG2* by cooperating with RMST (Ng et al., 2013) and POU factors (Lodato et al., 2013) in ESCs and NPCs. NEUROG2 is a pioneer factor that upregulates SOX4, which co-activates *NEUROD1* and *NEUROD4* (Smith et al., 2016). Thus, we speculate that TAZ-dependent repression of a proneurogenic factor presumably would impact the expression of others.

The transcriptional corepressor activity of TAZ opens a new path for understanding the role of TAZ in neural stem cell fate and neuronal reprogramming (Bago et al., 2016; Tang et al., 2017; Dennis et al., 2019). Much work is still needed if we are to obtain a clear and comprehensive understanding of the operational logic focused on the TAZ repressor function in neurogenesis and its possible implication in neural stem cell therapy in neurodegeneration and cancer.

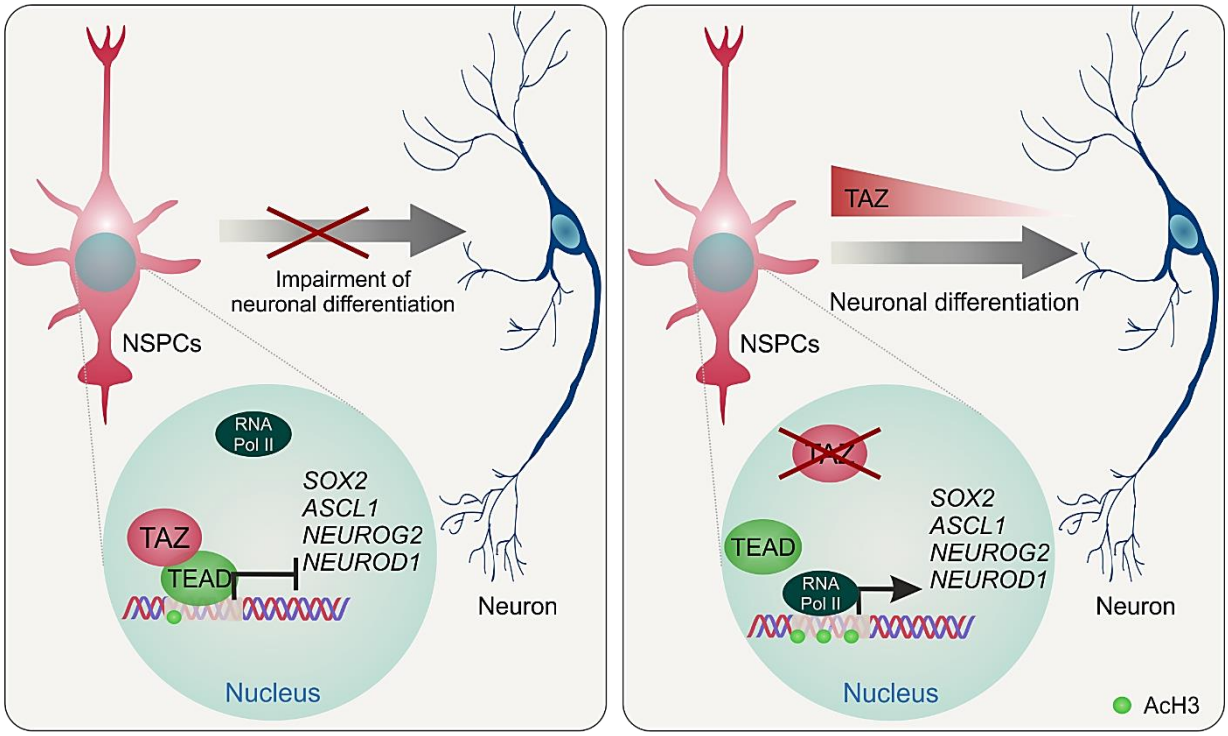


**Figure 70. TAZ represses the program of neuronal differentiation.** In the NSPCs, TAZ represses the expression of proneurogenic factors as SOX2 and bHLH factors ASCL1, NEUROG2 and NEUROD1 by epigenetic changes in the regulatory regions of their encoding genes. During NSPC-neuronal commitment, TAZ levels decrease, allowing the expression of proneurogenic genes and final neuronal differentiation.

## 5. Implications of the novel TAZ/proneurogenic axis in cancer.

There has been disappointingly slow progress in identifying effective therapies for GBM. This is due in part to a lack of understanding of the genes involved in the development of cancer stem cells (CSCs) that participate in the onset and growth of GBM (Chen et al., 2012; Lan et al., 2017).

We investigated the correlation between TAZ and proneurogenic genes in lower grade glioma and glioblastoma patients using the UCSC Xena platform (Goyal, 2019). The correlation between TAZ and its *bona fide* targets was positive, while a tendency to negative correlation was found between TAZ and proneurogenic factors, in line with our previous findings in NSPCs. Furthermore, TAZ and its targets were associated with poor prognosis while high expression of proneurogenic factors was associated with longer patient survival. These findings are in line with the observation that TAZ is generally overexpressed in CSCs and in GBM patients with poor prognosis (Bhat et al., 2011; Yang et al., 2016; Li et al., 2016b). Furthermore, high *WWTR1* levels are predictors of chemoresistance. Indeed, it has been reported that overexpression of TAZ correlated with resistance to the alkylating agent temozolomide, which is the gold standard treatment for gliomas (Tian et al., 2015). Strikingly, ASCL1 is expressed in many gliomas, at low and high levels depending on tumour type (Phillips et al., 2006; Rheinbay et al., 2013; Rousseau et al., 2006; Somasundaram et al., 2005). High ASCL1 expression makes GBM more responsive to Notch inhibition leading to cell cycle exit and neuronal differentiation, and leads to better

overall survival, suggesting that the ASCL1 status should be used to monitor drug responsiveness (Park et al., 2017). Upregulation of another neurogenin, NEUROG1, has been linked to a higher probability of long-term survival of GBM patients (Lu et al., 2016).

To interrogate functional properties of glioblastoma CSCs, we used patient-derived CSC cultures. These cells reflect the properties of primary GBM tumours (Lan et al., 2017; Lee et al., 2006; Meyer et al., 2015; Pollard et al., 2009) following orthotopic xenograftment (Ben-David et al., 2017; Lan et al., 2017). We found that TAZ levels were higher in these cells compared to the non-tumorigenic ReNcell neural stem cell line, further demonstrating an abnormal up-regulation of TAZ in CSCs. Furthermore, CSCs were strictly dependent of TAZ expression to develop spheroids *in vitro*. TAZ silencing in the same cells reduced their tumorigenesis, both in subcutaneous and intracranial xenografts, further demonstrating that TAZ is necessary to maintain CSCs stemness. Consistent with these findings, other studies also showed that TAZ depletion inhibits the proliferation and self-renewal of GBM CSCs (Zhang et al., 2019; Yang et al., 2016).

In this study, we show for the first time that TAZ levels inversely correlate with proneurogenic gene expression in CSCs. It is important to highlight that proneurogenic factors can inhibit tumorigenesis in GBM (Swartling et al., 2014; Swartling et al., 2015; Su et al., 2014). For example, increasing the expression of ASCL1 in GBM CSCs results in suppression of self-renewal, promotion of differentiation and, most significantly, decrease in tumorigenesis (Narayanan et al., 2018; Park et al., 2017; Tang et al., 2017). Introduction of *NEUROG2* or *NEUROD1* in GBMs resulted in cell cycle arrest and massive cell death, and the few surviving cells differentiate into neuron-like cells (Guichet et al., 2013). Recently, Gao et al., supressed CSCs growth by a drug cocktail that upregulates *ASCL1*, *NEUROG2* and *NEUROD1* and reprograms tumour cells into neuronal like cells, suppressing tumour growth and promoting the survival in GBM patient derived xenograft (Gao et al., 2019). Retinoic acid, a neuronal differentiation agent, was assessed for the pro-differentiation and anti-proliferation effects on glioma cells. It induced differentiation and therapy-sensitizing effects, impaired the secretion of angiogenic cytokines, and disrupted CSCs motility (Campos et al., 2010). All these studies highlight the potential of pro-differentiation treatment to target the CSCs in glioblastoma. Thus, we speculate that the tumorigenic function of TAZ could be related, at least partially, to its ability to repress proneurogenic genes and TAZ knockdown could be used as a pro-differentiation cancer cell therapy (Hide et al., 2013).

At this time, no selective TAZ inhibitor is available, but at least as a proof-of concept, we found that genetic knockdown of TAZ drastically increased the expression of proneurogenic genes in gliomas. Although some of caveats exist, TAZ-knockdown or exogenous over-expression of proneurogenic factors may warrant further consideration as a therapeutic approach in glioblastomas.

## 6. Concluding remarks and future perspectives.

Many studies have described that the transcriptional signature of NRF2 is necessary to maintain general homeostasis. In this work, we identified a role of NRF2 in a cell-autonomous regulation of neurogenesis. Recently, the Hippo pathway effectors are receiving attention in the study of cell proliferation and fate under physiologic and pathologic conditions. Here, we described the link between NRF2 and TAZ, opening a new window to understand their implication in stem cell properties. We also identified TAZ as a transcriptional corepressor of the neuronal differentiation program, highlighting the importance of TAZ-knockdown for neural stem cell-based therapy and glioblastoma treatment. Therefore, therapeutic possibilities may arise based on the exploitation of NRF2 and TAZ as crucial regulators of neurogenesis in chronic diseases.

# CONCLUSIONS/ CONCLUSIONES

1. NRF2 controls the proliferation and differentiation of hippocampal neural stem/progenitor cells.
2. NRF2 deficiency impairs hippocampal neurogenesis in a murine model of Alzheimer´s disease.
3. NRF2 recognizes ARE sequences in the promoter region of the TAZ-encoding gene and modulates its expression in neural stem/progenitor cells.
4. TAZ is a transcriptional corepressor of the proneurogenic genes *SOX2*, *ASCL1*, *NEUROG2* and *NEUROD1*, participating in inhibition of neuronal differentiation.
5. The tumorigenic function of TAZ inversely correlates with expression of proneurogenic genes in glioblastoma.

---

1. NRF2 controla la proliferación y diferenciación de las células troncales/progenitores neurales hipocampales.
2. La falta de NRF2 altera la neurogénesis hipocampal en un modelo murino de la enfermedad de Alzhéimer.
3. NRF2 reconoce secuencias ARE en la región promotora del gen que codifica a TAZ y modula su expresión en células troncales/progenitores neurales.
4. TAZ actúa como un corepresor transcripcional de los genes proneurogénicos *SOX2*, *ASCL1*, *NEUROG2* y *NEUROD1*, participando en la inhibición de la diferenciación neuronal.
5. La función tumorigénica de TAZ correlaciona inversamente con la expresión de genes proneurogénicos en glioblastoma.

# REFERENCES

ABERG, M. A., ABERG, N. D., HEDBACKER, H., OSCARSSON, J. & ERIKSSON, P. S. 2000. Peripheral infusion of IGF-I selectively induces neurogenesis in the adult rat hippocampus. *J Neurosci,* 20**,** 2896-903.

ABERG, M. A., ABERG, N. D., PALMER, T. D., ALBORN, A. M., CARLSSON-SKWIRUT, C., BANG, P., ROSENGREN, L. E., OLSSON, T., GAGE, F. H. & ERIKSSON, P. S. 2003. IGF-I has a direct proliferative effect in adult hippocampal progenitor cells. *Mol Cell Neurosci,* 24**,** 23-40.

AIZAWA, K., AGEYAMA, N., YOKOYAMA, C. & HISATSUNE, T. 2009. Age-dependent alteration in hippocampal neurogenesis correlates with learning performance of macaque monkeys. *Exp Anim,* 58**,** 403-7.

ALCANTARA LLAGUNO, S., CHEN, J., KWON, C. H., JACKSON, E. L., LI, Y., BURNS, D. K., ALVAREZ-BUYLLA, A. & PARADA, L. F. 2009. Malignant astrocytomas originate from neural stem/progenitor cells in a somatic tumor suppressor mouse model. *Cancer Cell,* 15**,** 45-56.

ALCANTARA LLAGUNO, S. R. & PARADA, L. F. 2016. Cell of origin of glioma: biological and clinical implications. *Br J Cancer,* 115**,** 1445-1450.

ALI, F., HINDLEY, C., MCDOWELL, G., DEIBLER, R., JONES, A., KIRSCHNER, M., GUILLEMOT, F. & PHILPOTT, A. 2011. Cell cycle-regulated multi-site phosphorylation of Neurogenin 2 coordinates cell cycling with differentiation during neurogenesis. *Development,* 138**,** 4267-77.

ALIC, I., KOSI, N., KAPURALIN, K., GORUP, D., GAJOVIC, S., POCHET, R. & MITRECIC, D. 2016. Neural stem cells from mouse strain Thy1 YFP-16 are a valuable tool to monitor and evaluate neuronal differentiation and morphology. *Neurosci Lett,* 634**,** 32-41.

ALTMAN, J. 1962. Are new neurons formed in the brains of adult mammals? *Science,* 135**,** 1127-8.

ALTMAN J FAU - DAS, G. D. & DAS, G. D. 1965. Autoradiographic and histological evidence of postnatal hippocampal neurogenesis. *J Comp Neurol,* 124**,** 319-35 FAU - Altman, J.

ALTMANN, C., KELLER, S. & SCHMIDT, M. H. H. 2019. The Role of SVZ Stem Cells in Glioblastoma. *Cancers (Basel),* 11.

ALVAREZ-BUYLLA, A. & GARCIA-VERDUGO, J. M. 2002. Neurogenesis in adult subventricular zone. *J Neurosci,* 22**,** 629-34.

AMADOR-ARJONA, A., CIMADAMORE, F., HUANG, C. T., WRIGHT, R., LEWIS, S., GAGE, F. H. & TERSKIKH, A. V. 2015. SOX2 primes the epigenetic landscape in neural precursors enabling proper gene activation during hippocampal neurogenesis. *Proc Natl Acad Sci U S A,* 112**,** E1936-45.

AMADOR-ARJONA, A., ELLIOTT, J., MILLER, A., GINBEY, A., PAZOUR, G. J., ENIKOLOPOV, G., ROBERTS, A. J. & TERSKIKH, A. V. 2011. Primary cilia regulate proliferation of amplifying progenitors in adult hippocampus: implications for learning and memory. *J Neurosci,* 31**,** 9933-44.

AMREIN, I., ISLER, K. & LIPP, H. P. 2011. Comparing adult hippocampal neurogenesis in mammalian species and orders: influence of chronological age and life history stage. *Eur J Neurosci,* 34**,** 978-87.

ANANTHARAM, V., LEHRMANN, E., KANTHASAMY, A., YANG, Y., BANERJEE, P., BECKER, K. G., FREED, W. J. & KANTHASAMY, A. G. 2007. Microarray analysis of oxidative stress regulated genes in mesencephalic dopaminergic neuronal cells: relevance to oxidative damage in Parkinson's disease. *Neurochem Int,* 50**,** 834-47.

APPLE, D. M., FONSECA, R. S. & KOKOVAY, E. 2017. The role of adult neurogenesis in psychiatric and cognitive disorders. *Brain Res,* 1655**,** 270-276.

APREA, J., NONAKA-KINOSHITA, M. & CALEGARI, F. 2014. Generation and characterization of Neurod1-CreER(T2) mouse lines for the study of embryonic and adult neurogenesis. *Genesis,* 52**,** 870-8.

ASHINO, T., YAMAMOTO, M., YOSHIDA, T. & NUMAZAWA, S. 2013. Redox-sensitive transcription factor Nrf2 regulates vascular smooth muscle cell migration and neointimal hyperplasia. *Arterioscler Thromb Vasc Biol,* 33**,** 760-8.

AZZOLIN, L., ZANCONATO, F., BRESOLIN, S., FORCATO, M., BASSO, G., BICCIATO, S., CORDENONSI, M. & PICCOLO, S. 2012. Role of TAZ as mediator of Wnt signaling. *Cell,* 151**,** 1443-56.

BAE, S. J. & LUO, X. 2018. Activation mechanisms of the Hippo kinase signaling cascade. *Biosci Rep,* 38.

BAGO, J. R., SHEETS, K. T. & HINGTGEN, S. D. 2016. Neural stem cell therapy for cancer. *Methods,* 99**,** 37-43.

BAHN, G. & JO, D. G. 2019. Therapeutic Approaches to Alzheimer's Disease Through Modulation of NRF2. *Neuromolecular Med,* 21**,** 1-11.

BARRON, D. A. & KAGEY, J. D. 2014. The role of the Hippo pathway in human disease and tumorigenesis. *Clin Transl Med,* 3**,** 25.

BARSKI, A., CUDDAPAH, S., CUI, K., ROH, T. Y., SCHONES, D. E., WANG, Z., WEI, G., CHEPELEV, I. & ZHAO, K. 2007. High-resolution profiling of histone methylations in the human genome. *Cell,* 129**,** 823-37.

BASU, D., REYES-MUGICA, M. & REBBAA, A. 2013. Histone acetylation-mediated regulation of the Hippo pathway. *PLoS One,* 8**,** e62478.

BASU, S., TOTTY, N. F., IRWIN, M. S., SUDOL, M. & DOWNWARD, J. 2003. Akt phosphorylates the Yes-associated protein, YAP, to induce interaction with 14-3-3 and attenuation of p73-mediated apoptosis. *Mol Cell,* 11**,** 11-23.

BECKERVORDERSANDFORTH, R., ZHANG, C. L. & LIE, D. C. 2015. Transcription-Factor-Dependent Control of Adult Hippocampal Neurogenesis. *Cold Spring Harb Perspect Biol,* 7**,** a018879.

BELL, K. F., AL-MUBARAK, B., MARTEL, M. A., MCKAY, S., WHEELAN, N., HASEL, P., MARKUS, N. M., BAXTER, P., DEIGHTON, R. F., SERIO, A., BILICAN, B., CHOWDHRY, S., MEAKIN, P. J., ASHFORD, M. L., WYLLIE, D. J., SCANNEVIN, R. H., CHANDRAN, S., HAYES, J. D. & HARDINGHAM, G. E. 2015. Neuronal development is promoted by weakened intrinsic antioxidant defences due to epigenetic repression of Nrf2. *Nat Commun,* 6**,** 7066.

BEN-DAVID, U., HA, G., TSENG, Y. Y., GREENWALD, N. F., OH, C., SHIH, J., MCFARLAND, J. M., WONG, B., BOEHM, J. S., BEROUKHIM, R. & GOLUB, T. R. 2017. Patient-derived xenografts undergo mouse-specific tumor evolution. *Nat Genet,* 49**,** 1567-1575.

BENNER, E. J., LUCIANO, D., JO, R., ABDI, K., PAEZ-GONZALEZ, P., SHENG, H., WARNER, D. S., LIU, C., EROGLU, C. & KUO, C. T. 2013. Protective astrogenesis from the SVZ niche after injury is controlled by Notch modulator Thbs4. *Nature,* 497**,** 369-73.

BENRAISS, A., CHMIELNICKI, E., LERNER, K., ROH, D. & GOLDMAN, S. A. 2001. Adenoviral brain-derived neurotrophic factor induces both neostriatal and olfactory neuronal recruitment from endogenous progenitor cells in the adult forebrain. *J Neurosci,* 21**,** 6718-31.

BERGMANN, O., SPALDING, K. L. & FRISEN, J. 2015. Adult Neurogenesis in Humans. *Cold Spring Harb Perspect Biol,* 7**,** a018994.

BERNARDINO, L., AGASSE, F., SILVA, B., FERREIRA, R., GRADE, S. & MALVA, J. O. 2008. Tumor necrosis factor-alpha modulates survival, proliferation, and neuronal differentiation in neonatal subventricular zone cell cultures. *Stem Cells,* 26**,** 2361-71.

BERNINGER, B., COSTA, M. R., KOCH, U., SCHROEDER, T., SUTOR, B., GROTHE, B. & GOTZ, M. 2007. Functional properties of neurons derived from in vitro reprogrammed postnatal astroglia. *J Neurosci,* 27**,** 8654-64.

BERTRAND, N., CASTRO, D. S. & GUILLEMOT, F. 2002. Proneural genes and the specification of neural cell types. *Nat Rev Neurosci,* 3**,** 517-30.

BEYER, T. A., WEISS, A., KHOMCHUK, Y., HUANG, K., OGUNJIMI, A. A., VARELAS, X. & WRANA, J. L. 2013. Switch enhancers interpret TGF-beta and Hippo signaling to control cell fate in human embryonic stem cells. *Cell Rep,* 5**,** 1611-24.

BHAT, K. P., SALAZAR, K. L., BALASUBRAMANIYAN, V., WANI, K., HEATHCOCK, L., HOLLINGSWORTH, F., JAMES, J. D., GUMIN, J., DIEFES, K. L., KIM, S. H., TURSKI, A., AZODI, Y., YANG, Y., DOUCETTE, T., COLMAN, H., SULMAN, E. P., LANG, F. F., RAO, G., COPRAY, S., VAILLANT, B. D. & ALDAPE, K. D. 2011. The transcriptional coactivator TAZ regulates mesenchymal differentiation in malignant glioma. *Genes Dev,* 25**,** 2594-609.

BLALOCK, E. M., GEDDES, J. W., CHEN, K. C., PORTER, N. M., MARKESBERY, W. R. & LANDFIELD, P. W. 2004. Incipient Alzheimer's disease: microarray correlation analyses reveal major transcriptional and tumor suppressor responses. *Proc Natl Acad Sci U S A,* 101**,** 2173-8.

BOEKHOORN, K., TERWEL D FAU - BIEMANS, B., BIEMANS B FAU - BORGHGRAEF, P., BORGHGRAEF P FAU - WIEGERT, O., WIEGERT O FAU - RAMAKERS, G. J. A., RAMAKERS GJ FAU - DE VOS, K., DE VOS K FAU - KRUGERS, H., KRUGERS H FAU - TOMIYAMA, T., TOMIYAMA T FAU - MORI, H., MORI H FAU - JOELS, M., JOELS M FAU - VAN LEUVEN, F., VAN LEUVEN F FAU - LUCASSEN, P. J. & LUCASSEN, P. J. 2006. Improved long-term potentiation and memory in young tau-P301L transgenic mice. *J Neurosci,* 26**,** 3514-23.

BOISSIERE, F., PRADIER, L., DELAERE, P., FAUCHEUX, B., REVAH, F., BRICE, A., AGID, Y. & HIRSCH, E. C. 1996. Regional and cellular presenilin 2 (STM2) gene expression in the human brain. *Neuroreport,* 7**,** 2021-5.

BOLDRINI, M., FULMORE, C. A., TARTT, A. N., SIMEON, L. R., PAVLOVA, I., POPOSKA, V., ROSOKLIJA, G. B., STANKOV, A., ARANGO, V., DWORK, A. J., HEN, R. & MANN, J. J. 2018. Human Hippocampal Neurogenesis Persists throughout Aging. *Cell Stem Cell,* 22**,** 589-599.e5.

BONAGUIDI, M. A., SONG J FAU - MING, G.-L., MING GL FAU - SONG, H. & SONG, H. 2012. A unifying hypothesis on mammalian neural stem cell properties in the adult. *Curr Opin Neurobiol,* 22**,** 754-61 LID - 10.1016/j.conb.2012.03.013 [doi] LID - S0959-4388(12)00051-7 [pii].

BONAGUIDI, M. A., WHEELER, M. A., SHAPIRO, J. S., STADEL, R. P., SUN, G. J., MING, G. L. & SONG, H. 2011. In vivo clonal analysis reveals self-renewing and multipotent adult neural stem cell characteristics. *Cell,* 145**,** 1142-55.

BOTTCHER, R. T. & NIEHRS, C. 2005. Fibroblast growth factor signaling during early vertebrate development. *Endocr Rev,* 26**,** 63-77.

BRAAK, H. & BRAAK, E. 1996. Evolution of the neuropathology of Alzheimer's disease. *Acta Neurol Scand Suppl,* 165**,** 3-12.

BRANCA, C., FERREIRA, E., NGUYEN, T. V., DOYLE, K., CACCAMO, A. & ODDO, S. 2017. Genetic reduction of Nrf2 exacerbates cognitive deficits in a mouse model of Alzheimer's disease. *Hum Mol Genet,* 26**,** 4823-4835.

BRAY, S. & BERNARD, F. 2010. Notch targets and their regulation. *Curr Top Dev Biol,* 92**,** 253-75.

BREUNIG, J. J., SARKISIAN, M. R., ARELLANO, J. I., MOROZOV, Y. M., AYOUB, A. E., SOJITRA, S., WANG, B., FLAVELL, R. A., RAKIC, P. & TOWN, T. 2008. Primary cilia regulate hippocampal neurogenesis by mediating sonic hedgehog signaling. *Proc Natl Acad Sci U S A,* 105**,** 13127-32.

BREUNIG, J. J., SILBEREIS, J., VACCARINO, F. M., SESTAN, N. & RAKIC, P. 2007. Notch regulates cell fate and dendrite morphology of newborn neurons in the postnatal dentate gyrus. *Proc Natl Acad Sci U S A,* 104**,** 20558-63.

BRILL, M. S., NINKOVIC, J., WINPENNY, E., HODGE, R. D., OZEN, I., YANG, R., LEPIER, A., GASCON, S., ERDELYI, F., SZABO, G., PARRAS, C., GUILLEMOT, F., FROTSCHER, M., BERNINGER, B., HEVNER, R. F., RAINETEAU, O. & GOTZ, M. 2009. Adult generation of glutamatergic olfactory bulb interneurons. *Nat Neurosci,* 12**,** 1524-33.

BROOKER, G. J., KALLONIATIS, M., RUSSO, V. C., MURPHY, M., WERTHER, G. A. & BARTLETT, P. F. 2000. Endogenous IGF-1 regulates the neuronal differentiation of adult stem cells. *J Neurosci Res,* 59**,** 332-41.

BROWN, J. P., COUILLARD-DESPRES, S., COOPER-KUHN, C. M., WINKLER, J., AIGNER, L. & KUHN, H. G. 2003. Transient expression of doublecortin during adult neurogenesis. *J Comp Neurol,* 467**,** 1-10.

BURD, G. D. & NOTTEBOHM, F. 1985. Ultrastructural characterization of synaptic terminals formed on newly generated neurons in a song control nucleus of the adult canary forebrain. *J Comp Neurol,* 240**,** 143-52.

CAI, C., TENG, L., VU, D., HE, J. Q., GUO, Y., LI, Q., TANG, X. L., ROKOSH, G., BHATNAGAR, A. & BOLLI, R. 2012. The heme oxygenase 1 inducer (CoPP) protects human cardiac stem cells against apoptosis through activation of the extracellular signal-regulated kinase (ERK)/NRF2 signaling pathway and cytokine release. *J Biol Chem,* 287**,** 33720-32.

CALLUS, B. A., VERHAGEN, A. M. & VAUX, D. L. 2006. Association of mammalian sterile twenty kinases, Mst1 and Mst2, with hSalvador via C-terminal coiled-coil domains, leads to its stabilization and phosphorylation. *Febs j,* 273**,** 4264-76.

CAMERON, H. A. & MCKAY, R. D. 1999. Restoring production of hippocampal neurons in old age. *Nat Neurosci,* 2**,** 894-7.

CAMPOS, B., WAN, F., FARHADI, M., ERNST, A., ZEPPERNICK, F., TAGSCHERER, K. E., AHMADI, R., LOHR, J., DICTUS, C., GDYNIA, G., COMBS, S. E., GOIDTS, V., HELMKE, B. M., ECKSTEIN, V., ROTH, W., BECKHOVE, P., LICHTER, P., UNTERBERG, A., RADLWIMMER, B. & HEROLD-MENDE, C. 2010. Differentiation therapy exerts antitumor effects on stem-like glioma cells. *Clin Cancer Res,* 16**,** 2715-28.

CAO, L., JIAO, X., ZUZGA, D. S., LIU, Y., FONG, D. M., YOUNG, D. & DURING, M. J. 2004. VEGF links hippocampal activity with neurogenesis, learning and memory. *Nat Genet,* 36**,** 827-35.

CAO, X., PFAFF, S. L. & GAGE, F. H. 2008. YAP regulates neural progenitor cell number via the TEA domain transcription factor. *Genes Dev,* 22**,** 3320-34.

CASTRO, D. S., MARTYNOGA, B., PARRAS, C., RAMESH, V., PACARY, E., JOHNSTON, C., DRECHSEL, D., LEBEL-POTTER, M., GARCIA, L. G., HUNT, C., DOLLE, D., BITHELL, A., ETTWILLER, L., BUCKLEY, N. & GUILLEMOT, F. 2011. A novel function of the proneural factor Ascl1 in progenitor proliferation identified by genome-wide characterization of its targets. *Genes Dev,* 25**,** 930-45.

CASTRO, D. S., SKOWRONSKA-KRAWCZYK, D., ARMANT, O., DONALDSON, I. J., PARRAS, C., HUNT, C., CRITCHLEY, J. A., NGUYEN, L., GOSSLER, A., GOTTGENS, B., MATTER, J. M. & GUILLEMOT, F. 2006. Proneural bHLH and Brn proteins coregulate a neurogenic program through cooperative binding to a conserved DNA motif. *Dev Cell,* 11**,** 831-44.

CAVALLARO, M., MARIANI, J., LANCINI, C., LATORRE, E., CACCIA, R., GULLO, F., VALOTTA, M., DEBIASI, S., SPINARDI, L., RONCHI, A., WANKE, E., BRUNELLI, S., FAVARO, R., OTTOLENGHI, S. & NICOLIS, S. K. 2008. Impaired generation of mature neurons by neural stem cells from hypomorphic Sox2 mutants. *Development,* 135**,** 541-57.

CECCHI, G. A., PETREANU, L. T., ALVAREZ-BUYLLA, A. & MAGNASCO, M. O. 2001. Unsupervised learning and adaptation in a model of adult neurogenesis. *J Comput Neurosci,* 11**,** 175-82.

CHAN, E. H., NOUSIAINEN, M., CHALAMALASETTY, R. B., SCHAFER, A., NIGG, E. A. & SILLJE, H. H. 2005. The Ste20-like kinase Mst2 activates the human large tumor suppressor kinase Lats1. *Oncogene,* 24**,** 2076-86.

CHAN, S. W., LIM, C. J., GUO, K., NG, C. P., LEE, I., HUNZIKER, W., ZENG, Q. & HONG, W. 2008. A role for TAZ in migration, invasion, and tumorigenesis of breast cancer cells. *Cancer Res,* 68**,** 2592-8.

CHAN, S. W., LIM, C. J., LOO, L. S., CHONG, Y. F., HUANG, C. & HONG, W. 2009. TEADs mediate nuclear retention of TAZ to promote oncogenic transformation. *J Biol Chem,* 284**,** 14347-58.

CHANDA, S., ANG, C. E., DAVILA, J., PAK, C., MALL, M., LEE, Q. Y., AHLENIUS, H., JUNG, S. W., SUDHOF, T. C. & WERNIG, M. 2014. Generation of induced neuronal cells by the single reprogramming factor ASCL1. *Stem Cell Reports,* 3**,** 282-96.

CHEN, J., LI, Y., YU, T. S., MCKAY, R. M., BURNS, D. K., KERNIE, S. G. & PARADA, L. F. 2012. A restricted cell population propagates glioblastoma growth after chemotherapy. *Nature,* 488**,** 522-6.

CHEN, L., GUERRERO-CAZARES, H., YE, X., FORD, E., MCNUTT, T., KLEINBERG, L., LIM, M., CHAICHANA, K., QUINONES-HINOJOSA, A. & REDMOND, K. 2013. Increased subventricular zone radiation dose correlates with survival in glioblastoma patients after gross total resection. *Int J Radiat Oncol Biol Phys,* 86**,** 616-22.

CHEN, Q., NAKAJIMA, A., CHOI, S. H., XIONG, X. & TANG, Y. P. 2008a. Loss of presenilin function causes Alzheimer's disease-like neurodegeneration in the mouse. *J Neurosci Res,* 86**,** 1615-25.

CHEN, R. H., DING, W. V. & MCCORMICK, F. 2000. Wnt signaling to beta-catenin involves two interactive components. Glycogen synthase kinase-3beta inhibition and activation of protein kinase C. *J Biol Chem,* 275**,** 17894-9.

CHEN, X., XU, H., YUAN, P., FANG, F., HUSS, M., VEGA, V. B., WONG, E., ORLOV, Y. L., ZHANG, W., JIANG, J., LOH, Y. H., YEO, H. C., YEO, Z. X., NARANG, V., GOVINDARAJAN, K. R., LEONG, B., SHAHAB, A., RUAN, Y., BOURQUE, G., SUNG, W. K., CLARKE, N. D., WEI, C. L. & NG, H. H. 2008b. Integration of external signaling pathways with the core transcriptional network in embryonic stem cells. *Cell,* 133**,** 1106-17.

CHORLEY, B. N., CAMPBELL, M. R., WANG, X., KARACA, M., SAMBANDAN, D., BANGURA, F., XUE, P., PI, J., KLEEBERGER, S. R. & BELL, D. A. 2012. Identification of novel NRF2-regulated genes by ChIP-Seq: influence on retinoid X receptor alpha. *Nucleic Acids Res,* 40**,** 7416-29.

CHOWDHRY, S., ZHANG, Y., MCMAHON, M., SUTHERLAND, C., CUADRADO, A. & HAYES, J. D. 2013. Nrf2 is controlled by two distinct beta-TrCP recognition motifs in its Neh6 domain, one of which can be modulated by GSK-3 activity. *Oncogene,* 32**,** 3765-81.

CIAMPORCERO, E., DAGA, M., PIZZIMENTI, S., ROETTO, A., DIANZANI, C., COMPAGNONE, A., PALMIERI, A., ULLIO, C., CANGEMI, L., PILI, R. & BARRERA, G. 2018. Crosstalk between Nrf2 and YAP contributes to maintaining the antioxidant potential and chemoresistance in bladder cancer. *Free Radic Biol Med,* 115**,** 447-457.

CIMADAMORE, F., FISHWICK, K., GIUSTO, E., GNEDEVA, K., CATTAROSSI, G., MILLER, A., PLUCHINO, S., BRILL, L. M., BRONNER-FRASER, M. & TERSKIKH, A. V. 2011. Human ESC-derived neural crest model reveals a key role for SOX2 in sensory neurogenesis. *Cell Stem Cell,* 8**,** 538-51.

CLELLAND, C. D., CHOI, M., ROMBERG, C., CLEMENSON, G. D., JR., FRAGNIERE, A., TYERS, P., JESSBERGER, S., SAKSIDA, L. M., BARKER, R. A., GAGE, F. H. & BUSSEY, T. J. 2009. A functional role for adult hippocampal neurogenesis in spatial pattern separation. *Science,* 325**,** 210-3.

CODEGA, P., SILVA-VARGAS, V., PAUL, A., MALDONADO-SOTO, A. R., DELEO, A. M., PASTRANA, E. & DOETSCH, F. 2014. Prospective identification and purification of quiescent adult neural stem cells from their in vivo niche. *Neuron,* 82**,** 545-59.

COLASANTE, G., RUBIO, A., MASSIMINO, L. & BROCCOLI, V. 2019. Direct neuronal reprogramming reveals unknown functions for known transcription factors. *Front Neurosci,* 13, 283.

CORENBLUM, M. J., RAY, S., REMLEY, Q. W., LONG, M., HARDER, B., ZHANG, D. D., BARNES, C. A. & MADHAVAN, L. 2016. Reduced Nrf2 expression mediates the decline in neural stem cell function during a critical middle-age period. *Aging Cell,* 15**,** 725-36.

COTTON, J. L., LI, Q., MA, L., PARK, J. S., WANG, J., OU, J., ZHU, L. J., IP, Y. T., JOHNSON, R. L. & MAO, J. 2017. YAP/TAZ and Hedgehog Coordinate Growth and Patterning in Gastrointestinal Mesenchyme. *Dev Cell,* 43**,** 35-47.e4.

CREWS, L. & MASLIAH, E. 2010. Molecular mechanisms of neurodegeneration in Alzheimer's disease. *Hum Mol Genet,* 19**,** R12-20.

CREYGHTON, M. P., CHENG, A. W., WELSTEAD, G. G., KOOISTRA, T., CAREY, B. W., STEINE, E. J., HANNA, J., LODATO, M. A., FRAMPTON, G. M., SHARP, P. A., BOYER, L. A., YOUNG, R. A. & JAENISCH, R. 2010. Histone H3K27ac separates active from poised enhancers and predicts developmental state. *Proc Natl Acad Sci U S A,* 107**,** 21931-6.

CUADRADO, A. 2015. Structural and functional characterization of Nrf2 degradation by glycogen synthase kinase 3/beta-TrCP. *Free Radic Biol Med,* 88**,** 147-157.

CUADRADO, A., MANDA, G., HASSAN, A., ALCARAZ, M. J., BARBAS, C., DAIBER, A., GHEZZI, P., LEON, R., LOPEZ, M. G., OLIVA, B., PAJARES, M., ROJO, A. I., ROBLEDINOS-ANTON, N., VALVERDE, A. M., GUNEY, E. & SCHMIDT, H. 2018. Transcription Factor NRF2 as a Therapeutic Target for Chronic Diseases: A Systems Medicine Approach. *Pharmacol Rev,* 70**,** 348-383.

CUADRADO, A., ROJO, A. I., WELLS, G., HAYES, J. D., COUSIN, S. P., RUMSEY, W. L., ATTUCKS, O. C., FRANKLIN, S., LEVONEN, A. L., KENSLER, T. W. & DINKOVA-KOSTOVA,

A. T. 2019. Therapeutic targeting of the NRF2 and KEAP1 partnership in chronic diseases. *Nat Rev Drug Discov,* 18**,** 295-317.

CUI, C. B., COOPER, L. F., YANG, X., KARSENTY, G. & AUKHIL, I. 2003. Transcriptional coactivation of bone-specific transcription factor Cbfa1 by TAZ. *Mol Cell Biol,* 23**,** 1004-13.

CURTIS, M. A., KAM M FAU - NANNMARK, U., NANNMARK U FAU - ANDERSON, M. F., ANDERSON MF FAU - AXELL, M. Z., AXELL MZ FAU - WIKKELSO, C., WIKKELSO C FAU - HOLTAS, S., HOLTAS S FAU - VAN ROON-MOM, W. M. C., VAN ROON-MOM WM FAU - BJORK-ERIKSSON, T., BJORK-ERIKSSON T FAU - NORDBORG, C., NORDBORG C FAU - FRISEN, J., FRISEN J FAU - DRAGUNOW, M., DRAGUNOW M FAU - FAULL, R. L. M., FAULL RL FAU - ERIKSSON, P. S. & ERIKSSON, P. S. 2007. Human neuroblasts migrate to the olfactory bulb via a lateral ventricular. *Science,* 315**,** 1243-9.

DANIELSON, N. B., KAIFOSH, P., ZAREMBA, J. D., LOVETT-BARRON, M., TSAI, J., DENNY, C. A., BALOUGH, E. M., GOLDBERG, A. R., DREW, L. J., HEN, R., LOSONCZY, A. & KHEIRBEK, M. A. 2016. Distinct Contribution of Adult-Born Hippocampal Granule Cells to Context Encoding. *Neuron,* 90**,** 101-12.

DEMARS, M., HU YS FAU - GADADHAR, A., GADADHAR A FAU - LAZAROV, O. & LAZAROV, O. 2010. Impaired neurogenesis is an early event in the etiology of familial Alzheimer's. *J Neurosci Res,* 88**,** 2103-17 LID - 10.1002/jnr.22387 [doi].

DENG, W., AIMONE, J. B. & GAGE, F. H. 2010. New neurons and new memories: how does adult hippocampal neurogenesis affect learning and memory? *Nat Rev Neurosci,* 11**,** 339-50.

DENNIS, C. V., SUH, L. S., RODRIGUEZ, M. L., KRIL, J. J. & SUTHERLAND, G. T. 2016. Human adult neurogenesis across the ages: An immunohistochemical study. *Neuropathol Appl Neurobiol,* 42**,** 621-638.

DENNIS, D. J., HAN, S. & SCHUURMANS, C. 2019. bHLH transcription factors in neural development, disease, and reprogramming. *Brain Res,* 1705**,** 48-65.

DESHMUKH, P., UNNI, S., KRISHNAPPA, G. & PADMANABHAN, B. 2017. The Keap1-Nrf2 pathway: promising therapeutic target to counteract ROS-mediated damage in cancers and neurodegenerative diseases. *Biophys Rev,* 9**,** 41-56.

DICKINSON, B. C., PELTIER, J., STONE, D., SCHAFFER, D. V. & CHANG, C. J. 2011. Nox2 redox signaling maintains essential cell populations in the brain. *Nat Chem Biol,* 7**,** 106-12.

DOETSCH, F. & ALVAREZ-BUYLLA, A. 1996. Network of tangential pathways for neuronal migration in adult mammalian brain. *Proc Natl Acad Sci U S A,* 93**,** 14895-900.

DOETSCH, F., GARCIA-VERDUGO, J. M. & ALVAREZ-BUYLLA, A. 1997. Cellular composition and three-dimensional organization of the subventricular germinal zone in the adult mammalian brain. *J Neurosci,* 17**,** 5046-61.

DRABEROVA, E., DEL VALLE, L., GORDON, J., MARKOVA, V., SMEJKALOVA, B., BERTRAND, L., DE CHADAREVIAN, J. P., AGAMANOLIS, D. P., LEGIDO, A., KHALILI, K., DRABER, P. & KATSETOS, C. D. 2008. Class III beta-tubulin is constitutively coexpressed with glial fibrillary acidic protein and nestin in midgestational human fetal astrocytes: implications for phenotypic identity. *J Neuropathol Exp Neurol,* 67**,** 341-54.

DRAPEAU, E., MAYO, W., AUROUSSEAU, C., LE MOAL, M., PIAZZA, P. V. & ABROUS, D. N. 2003. Spatial memory performances of aged rats in the water maze predict levels of hippocampal neurogenesis. *Proc Natl Acad Sci U S A,* 100**,** 14385-90.

DRISCOLL, I., HOWARD, S. R., STONE, J. C., MONFILS, M. H., TOMANEK, B., BROOKS, W. M. & SUTHERLAND, R. J. 2006. The aging hippocampus: a multi-level analysis in the rat. *Neuroscience,* 139**,** 1173-85.

EHM, O., GORITZ, C., COVIC, M., SCHAFFNER, I., SCHWARZ, T. J., KARACA, E., KEMPKES, B., KREMMER, E., PFRIEGER, F. W., ESPINOSA, L., BIGAS, A., GIACHINO, C., TAYLOR, V., FRISEN, J. & LIE, D. C. 2010. RBPJkappa-dependent signaling is essential for long-term maintenance of neural stem cells in the adult hippocampus. *J Neurosci,* 30**,** 13794-807.

ENCINAS, J. M., MICHURINA TV FAU - PEUNOVA, N., PEUNOVA N FAU - PARK, J.-H., PARK JH FAU - TORDO, J., TORDO J FAU - PETERSON, D. A., PETERSON DA FAU - FISHELL, G., FISHELL G FAU - KOULAKOV, A., KOULAKOV A FAU - ENIKOLOPOV, G. & ENIKOLOPOV, G. 2011. Division-coupled astrocytic differentiation and age-related depletion of neural. *Cell Stem Cell,* 8**,** 566-79 LID - 10.1016/j.stem.2011.03.010 [doi].

ENGLER, A., ZHANG, R. & TAYLOR, V. 2018. Notch and Neurogenesis. *Adv Exp Med Biol,* 1066**,** 223-234.

ENWERE, E., SHINGO, T., GREGG, C., FUJIKAWA, H., OHTA, S. & WEISS, S. 2004. Aging results in reduced epidermal growth factor receptor signaling, diminished olfactory neurogenesis, and deficits in fine olfactory discrimination. *J Neurosci,* 24**,** 8354-65.

ERIKSSON, P. S., PERFILIEVA E FAU - BJORK-ERIKSSON, T., BJORK-ERIKSSON T FAU - ALBORN, A. M., ALBORN AM FAU - NORDBORG, C., NORDBORG C FAU - PETERSON, D. A., PETERSON DA FAU - GAGE, F. H. & GAGE, F. H. 1998. Neurogenesis in the adult human hippocampus. *Nat Med,* 4**,** 1313-7.

ERNST, A., ALKASS, K., BERNARD, S., SALEHPOUR, M., PERL, S., TISDALE, J., POSSNERT, G., DRUID, H. & FRISEN, J. 2014. Neurogenesis in the striatum of the adult human brain. *Cell,* 156**,** 1072-83.

ERNST, A. & FRISEN, J. 2015. Adult neurogenesis in humans- common and unique traits in mammals. *PLoS Biol,* 13**,** e1002045.

FAVARO, R., VALOTTA, M., FERRI, A. L., LATORRE, E., MARIANI, J., GIACHINO, C., LANCINI, C., TOSETTI, V., OTTOLENGHI, S., TAYLOR, V. & NICOLIS, S. K. 2009. Hippocampal development and neural stem cell maintenance require Sox2-dependent regulation of Shh. *Nat Neurosci,* 12**,** 1248-56.

FERRI, A. L., CAVALLARO, M., BRAIDA, D., DI CRISTOFANO, A., CANTA, A., VEZZANI, A., OTTOLENGHI, S., PANDOLFI, P. P., SALA, M., DEBIASI, S. & NICOLIS, S. K. 2004. Sox2 deficiency causes neurodegeneration and impaired neurogenesis in the adult mouse brain. *Development,* 131**,** 3805-19.

FUCCILLO, M., JOYNER, A. L. & FISHELL, G. 2006. Morphogen to mitogen: the multiple roles of hedgehog signalling in vertebrate neural development. *Nat Rev Neurosci,* 7**,** 772-83.

FUEYO, R., IACOBUCCI, S., PAPPA, S., ESTARAS, C., LOIS, S., VICIOSO-MANTIS, M., NAVARRO, C., CRUZ-MOLINA, S., REYES, J. C., RADA-IGLESIAS, A., DE LA CRUZ, X. & MARTINEZ-BALBAS, M. A. 2018. Lineage specific transcription factors and epigenetic regulators mediate TGFbeta-dependent enhancer activation. *Nucleic Acids Res,* 46**,** 3351-3365.

FUKUI, H., RUNKER, A., FABEL, K., BUCHHOLZ, F. & KEMPERMANN, G. 2018. Transcription factor Runx1 is pro-neurogenic in adult hippocampal precursor cells. *PLoS One,* 13**,** e0190789.

FUNA, K. & SASAHARA, M. 2014. The roles of PDGF in development and during neurogenesis in the normal and diseased nervous system. *J Neuroimmune Pharmacol,* 9**,** 168-81.

GABBITA, S. P., LOVELL, M. A. & MARKESBERY, W. R. 1998. Increased nuclear DNA oxidation in the brain in Alzheimer's disease. *J Neurochem,* 71**,** 2034-40.

GAGE, F. H., COATES, P. W., PALMER, T. D., KUHN, H. G., FISHER, L. J., SUHONEN, J. O., PETERSON, D. A., SUHR, S. T. & RAY, J. 1995. Survival and differentiation of adult neuronal progenitor cells transplanted to the adult brain. *Proc Natl Acad Sci U S A,* 92**,** 11879-83.

GAIANO, N. & FISHELL, G. 2002. The role of notch in promoting glial and neural stem cell fates. *Annu Rev Neurosci,* 25**,** 471-90.

GALLI, G. G., CARRARA, M., YUAN, W. C., VALDES-QUEZADA, C., GURUNG, B., PEPE-MOONEY, B., ZHANG, T., GEEVEN, G., GRAY, N. S., DE LAAT, W., CALOGERO, R. A. & CAMARGO, F. D. 2015. YAP Drives Growth by Controlling Transcriptional Pause Release from Dynamic Enhancers. *Mol Cell,* 60**,** 328-37.

GAMBARI, L., LISIGNOLI, G., CATTINI, L., MANFERDINI, C., FACCHINI, A. & GRASSI, F. 2014. Sodium hydrosulfide inhibits the differentiation of osteoclast progenitor cells via NRF2-dependent mechanism. *Pharmacol Res,* 87**,** 99-112.

GANDHIRAJAN, R. K., JAIN, M., WALLA, B., JOHNSEN, M., BARTRAM, M. P., HUYNH ANH, M., RINSCHEN, M. M., BENZING, T. & SCHERMER, B. 2016. Cysteine S-Glutathionylation Promotes Stability and Activation of the Hippo Downstream Effector Transcriptional Co-activator with PDZ-binding Motif (TAZ). *J Biol Chem,* 291**,** 11596-607.

GAO, L., HUANG, S., ZHANG, H., HUA, W., XIN, S., CHENG, L., GUAN, W., YU, Y., MAO, Y. & PEI, G. 2019. Suppression of glioblastoma by a drug cocktail reprogramming tumor cells into neuronal like cells. *Sci Rep,* 9**,** 3462.

GAO, Z., URE, K., ABLES, J. L., LAGACE, D. C., NAVE, K. A., GOEBBELS, S., EISCH, A. J. & HSIEH, J. 2009. Neurod1 is essential for the survival and maturation of adult-born neurons. *Nat Neurosci,* 12**,** 1090-2.

GARGINI, R., CERLIANI, J. P., ESCOLL, M., ANTON, I. M. & WANDOSELL, F. 2015. Cancer stem cell-like phenotype and survival are coordinately regulated by Akt/FoxO/Bim pathway. *Stem Cells,* 33**,** 646-60.

GARGINI, R., ESCOLL, M., GARCIA, E., GARCIA-ESCUDERO, R., WANDOSELL, F. & ANTON, I. M. 2016. WIP Drives Tumor Progression through YAP/TAZ-Dependent Autonomous Cell Growth. *Cell Rep,* 17**,** 1962-1977.

GARTHE, A., BEHR, J. & KEMPERMANN, G. 2009. Adult-generated hippocampal neurons allow the flexible use of spatially precise learning strategies. *PLoS One,* 4**,** e5464.

GEBARA, E., BONAGUIDI, M. A., BECKERVORDERSANDFORTH, R., SULTAN, S., UDRY, F., GIJS, P. J., LIE, D. C., MING, G. L., SONG, H. & TONI, N. 2016. Heterogeneity of Radial Glia-Like Cells in the Adult Hippocampus. *Stem Cells,* 34**,** 997-1010.

GEE, S. T., MILGRAM, S. L., KRAMER, K. L., CONLON, F. L. & MOODY, S. A. 2011. Yes-associated protein 65 (YAP) expands neural progenitors and regulates Pax3 expression in the neural plate border zone. *PLoS One,* 6**,** e20309.

GESCHWIND, D. H. 2003. Tau phosphorylation, tangles, and neurodegeneration: the chicken or the egg? *Neuron,* 40**,** 457-60.

GLEBOVA, N. O. & GINTY, D. D. 2005. Growth and survival signals controlling sympathetic nervous system development. *Annu Rev Neurosci,* 28**,** 191-222.

GOEDERT, M., SISODIA, S. S. & PRICE, D. L. 1991. Neurofibrillary tangles and beta-amyloid deposits in Alzheimer's disease. *Curr Opin Neurobiol,* 1**,** 441-7.

GOEDERT, M. & SPILLANTINI, M. G. 2006. A century of Alzheimer's disease. *Science,* 314**,** 777-81.

GOMEZ, M., GOMEZ, V. & HERGOVICH, A. 2014. The Hippo pathway in disease and therapy: cancer and beyond. *Clin Transl Med,* 3**,** 22.

GOULD, E. 2007. How widespread is adult neurogenesis in mammals? *Nat Rev Neurosci,* 8**,** 481-8.

GOULD, E., REEVES AJ FAU - GRAZIANO, M. S., GRAZIANO MS FAU - GROSS, C. G. & GROSS, C. G. 1999. Neurogenesis in the neocortex of adult primates. *Science,* 286**,** 548-52.

GOULD, E. & TANAPAT, P. 1999. Stress and hippocampal neurogenesis. *Biol Psychiatry,* 46**,** 1472-9.

GOYAL, M. 2019. Genome Databases and Browsers for Cancer. *In:* RANGANATHAN, S., GRIBSKOV, M., NAKAI, K. & SCHÖNBACH, C. (eds.) *Encyclopedia of Bioinformatics and Computational Biology.* Oxford: Academic Press.

GRELAT, A., BENOIT, L., WAGNER, S., MOIGNEU, C., LLEDO, P. M. & ALONSO, M. 2018. Adult-born neurons boost odor-reward association. *Proc Natl Acad Sci U S A,* 115**,** 2514-2519.

GRITTI, A., FROLICHSTHAL-SCHOELLER, P., GALLI, R., PARATI, E. A., COVA, L., PAGANO, S. F., BJORNSON, C. R. & VESCOVI, A. L. 1999. Epidermal and fibroblast growth factors behave as mitogenic regulators for a single multipotent stem cell-like population from the subventricular region of the adult mouse forebrain. *J Neurosci,* 19**,** 3287-97.

GUERRERO-CAZARES, H., GONZALEZ-PEREZ, O., SORIANO-NAVARRO, M., ZAMORA-BERRIDI, G., GARCIA-VERDUGO, J. M. & QUINONES-HINOJOSA, A. 2011. Cytoarchitecture of the lateral ganglionic eminence and rostral extension of the lateral ventricle in the human fetal brain. *J Comp Neurol,* 519**,** 1165-80.

GUICHET, P. O., BIECHE, I., TEIGELL, M., SERGUERA, C., ROTHHUT, B., RIGAU, V., SCAMPS, F., RIPOLL, C., VACHER, S., TAVIAUX, S., CHEVASSUS, H., DUFFAU, H., MALLET, J., SUSINI, A., JOUBERT, D., BAUCHET, L. & HUGNOT, J. P. 2013. Cell death and neuronal differentiation of glioblastoma stem-like cells induced by neurogenic transcription factors. *Glia,* 61**,** 225-39.

GUILLEMOT, F. 2007. Cell fate specification in the mammalian telencephalon. *Prog Neurobiol,* 83**,** 37-52.

GUILLEMOT, F. & ZIMMER, C. 2011. From cradle to grave: the multiple roles of fibroblast growth factors in neural development. *Neuron,* 71**,** 574-88.

GUO, Z., ZHANG, L., WU, Z., CHEN, Y., WANG, F. & CHEN, G. 2014. In vivo direct reprogramming of reactive glial cells into functional neurons after brain injury and in an Alzheimer's disease model. *Cell Stem Cell,* 14**,** 188-202.

GURUSAMY, N., RAY, D., LEKLI, I. & DAS, D. K. 2010. Red wine antioxidant resveratrol-modified cardiac stem cells regenerate infarcted myocardium. *J Cell Mol Med,* 14**,** 2235-9.

HAMILTON, L. K., AUMONT, A., JULIEN, C., VADNAIS, A., CALON, F. & FERNANDES, K. J. 2010. Widespread deficits in adult neurogenesis precede plaque and tangle formation in the 3xTg mouse model of Alzheimer's disease. *Eur J Neurosci,* 32**,** 905-20.

HAN, Y. G., SPASSKY, N., ROMAGUERA-ROS, M., GARCIA-VERDUGO, J. M., AGUILAR, A., SCHNEIDER-MAUNOURY, S. & ALVAREZ-BUYLLA, A. 2008. Hedgehog signaling and primary cilia are required for the formation of adult neural stem cells. *Nat Neurosci,* 11**,** 277-84.

HANSEN, C. G., MOROISHI, T. & GUAN, K. L. 2015. YAP and TAZ: a nexus for Hippo signaling and beyond. *Trends Cell Biol,* 25**,** 499-513.

HARDEE, M. E., MARCISCANO, A. E., MEDINA-RAMIREZ, C. M., ZAGZAG, D., NARAYANA, A., LONNING, S. M. & BARCELLOS-HOFF, M. H. 2012. Resistance of glioblastoma-initiating cells to radiation mediated by the tumor microenvironment can be abolished by inhibiting transforming growth factor-beta. *Cancer Res,* 72**,** 4119-29.

HARTFUSS, E., GALLI, R., HEINS, N. & GOTZ, M. 2001. Characterization of CNS precursor subtypes and radial glia. *Dev Biol,* 229**,** 15-30.

HATAKEYAMA, J., BESSHO, Y., KATOH, K., OOKAWARA, S., FUJIOKA, M., GUILLEMOT, F. & KAGEYAMA, R. 2004. Hes genes regulate size, shape and histogenesis of the nervous system by control of the timing of neural stem cell differentiation. *Development,* 131**,** 5539-50.

HAYES, J. D. & DINKOVA-KOSTOVA, A. T. 2014. The Nrf2 regulatory network provides an interface between redox and intermediary metabolism. *Trends Biochem Sci,* 39**,** 199-218.

HAYES, J. D. & MCMAHON, M. 2009. NRF2 and KEAP1 mutations: permanent activation of an adaptive response in cancer. *Trends Biochem Sci,* 34**,** 176-88.

HE, C. H., GONG, P., HU, B., STEWART, D., CHOI, M. E., CHOI, A. M. & ALAM, J. 2001. Identification of activating transcription factor 4 (ATF4) as an Nrf2-interacting protein. Implication for heme oxygenase-1 gene regulation. *J Biol Chem,* 276**,** 20858-65.

HEINRICH, C., BLUM, R., GASCON, S., MASSERDOTTI, G., TRIPATHI, P., SANCHEZ, R., TIEDT, S., SCHROEDER, T., GOTZ, M. & BERNINGER, B. 2010. Directing astroglia from the cerebral cortex into subtype specific functional neurons. *PLoS Biol,* 8**,** e1000373.

HENG, J. I., NGUYEN, L., CASTRO, D. S., ZIMMER, C., WILDNER, H., ARMANT, O., SKOWRONSKA-KRAWCZYK, D., BEDOGNI, F., MATTER, J. M., HEVNER, R. & GUILLEMOT, F. 2008. Neurogenin 2 controls cortical neuron migration through regulation of Rnd2. *Nature,* 455**,** 114-8.

HENKE, R. M., MEREDITH, D. M., BORROMEO, M. D., SAVAGE, T. K. & JOHNSON, J. E. 2009. Ascl1 and Neurog2 form novel complexes and regulate Delta-like3 (Dll3) expression in the neural tube. *Dev Biol,* 328**,** 529-40.

HEVNER, R. F., HODGE, R. D., DAZA, R. A. & ENGLUND, C. 2006. Transcription factors in glutamatergic neurogenesis: conserved programs in neocortex, cerebellum, and adult hippocampus. *Neurosci Res,* 55**,** 223-33.

HIDE, T., MAKINO, K., NAKAMURA, H., YANO, S., ANAI, S., TAKEZAKI, T., KURODA, J., SHINOJIMA, N., UEDA, Y. & KURATSU, J. 2013. New treatment strategies to eradicate cancer stem cells and niches in glioblastoma. *Neurol Med Chir (Tokyo),* 53**,** 764-72.

HIGGINS, L. G. & HAYES, J. D. 2011. The cap'n'collar transcription factor Nrf2 mediates both intrinsic resistance to environmental stressors and an adaptive response elicited by chemopreventive agents that determines susceptibility to electrophilic xenobiotics. *Chem Biol Interact,* 192**,** 37-45.

HIROTSU, Y., KATSUOKA, F., FUNAYAMA, R., NAGASHIMA, T., NISHIDA, Y., NAKAYAMA, K., ENGEL, J. D. & YAMAMOTO, M. 2012. Nrf2-MafG heterodimers contribute globally to antioxidant and metabolic networks. *Nucleic Acids Res,* 40**,** 10228-39.

HIRRLINGER, P. G., SCHELLER, A., BRAUN, C., QUINTELA-SCHNEIDER, M., FUSS, B., HIRRLINGER, J. & KIRCHHOFF, F. 2005. Expression of reef coral fluorescent proteins in the central nervous system of transgenic mice. *Mol Cell Neurosci,* 30**,** 291-303.

HODGE, R. D., KOWALCZYK, T. D., WOLF, S. A., ENCINAS, J. M., RIPPEY, C., ENIKOLOPOV, G., KEMPERMANN, G. & HEVNER, R. F. 2008. Intermediate progenitors in adult hippocampal neurogenesis: Tbr2 expression and coordinate regulation of neuronal output. *J Neurosci,* 28**,** 3707-17.

HOLLAND, E. C., CELESTINO, J., DAI, C., SCHAEFER, L., SAWAYA, R. E. & FULLER, G. N. 2000. Combined activation of Ras and Akt in neural progenitors induces glioblastoma formation in mice. *Nat Genet,* 25**,** 55-7.

HOLLANDS, C., BARTOLOTTI, N. & LAZAROV, O. 2016. Alzheimer's Disease and Hippocampal Adult Neurogenesis; Exploring Shared. *Front Neurosci,* 10**,** 178 LID - 10.3389/fnins.2016.00178 [doi].

HOOPER, C., KILLICK, R. & LOVESTONE, S. 2008. The GSK3 hypothesis of Alzheimer's disease. *J Neurochem,* 104**,** 1433-9.

HOOPER, C., MARKEVICH, V., PLATTNER, F., KILLICK, R., SCHOFIELD, E., ENGEL, T., HERNANDEZ, F., ANDERTON, B., ROSENBLUM, K., BLISS, T., COOKE, S. F., AVILA, J., LUCAS, J. J., GIESE, K. P., STEPHENSON, J. & LOVESTONE, S. 2007. Glycogen synthase kinase-3 inhibition is integral to long-term potentiation. *Eur J Neurosci,* 25**,** 81-6.

HSIEH, J. 2012. Orchestrating transcriptional control of adult neurogenesis. *Genes Dev,* 26**,** 1010-21.

HUANG, W., LV, X., LIU, C., ZHA, Z., ZHANG, H., JIANG, Y., XIONG, Y., LEI, Q. Y. & GUAN, K. L. 2012. The N-terminal phosphodegron targets TAZ/WWTR1 protein for SCFbeta-TrCP-dependent degradation in response to phosphatidylinositol 3-kinase inhibition. *J Biol Chem,* 287**,** 26245-53.

HUANG, X., LIU, J., KETOVA, T., FLEMING, J. T., GROVER, V. K., COOPER, M. K., LITINGTUNG, Y. & CHIANG, C. 2010. Transventricular delivery of Sonic hedgehog is essential to cerebellar ventricular zone development. *Proc Natl Acad Sci U S A,* 107**,** 8422-7.

HUANG, Z., HU, J., PAN, J., WANG, Y., HU, G., ZHOU, J., MEI, L. & XIONG, W. C. 2016. YAP stabilizes SMAD1 and promotes BMP2-induced neocortical astrocytic differentiation. *Development,* 143**,** 2398-409.

HUFNAGEL, R. B., LE, T. T., RIESENBERG, A. L. & BROWN, N. L. 2010. Neurog2 controls the leading edge of neurogenesis in the mammalian retina. *Dev Biol,* 340**,** 490-503.

IHRIE, R. A. & ALVAREZ-BUYLLA, A. 2011. Lake-front property: a unique germinal niche by the lateral ventricles of the adult brain. *Neuron,* 70**,** 674-86.

IMAYOSHI, I. & KAGEYAMA, R. 2014. bHLH factors in self-renewal, multipotency, and fate choice of neural progenitor cells. *Neuron,* 82**,** 9-23.

IMAYOSHI, I., SHIMOGORI, T., OHTSUKA, T. & KAGEYAMA, R. 2008. Hes genes and neurogenin regulate non-neural versus neural fate specification in the dorsal telencephalic midline. *Development,* 135**,** 2531-41.

ISCRU, E., AHMED, T., COREMANS, V., BOZZI, Y., CALEO, M., CONWAY, E. M., D'HOOGE, R. & BALSCHUN, D. 2013. Loss of survivin in neural precursor cells results in impaired long-term potentiation in the dentate gyrus and CA1-region. *Neuroscience,* 231**,** 413-9.

ITOH, K., CHIBA, T., TAKAHASHI, S., ISHII, T., IGARASHI, K., KATOH, Y., OYAKE, T., HAYASHI, N., SATOH, K., HATAYAMA, I., YAMAMOTO, M. & NABESHIMA, Y. 1997. An Nrf2/small Maf heterodimer mediates the induction of phase II detoxifying enzyme genes through antioxidant response elements. *Biochem Biophys Res Commun,* 236**,** 313-22.

JACQUES, T. S., SWALES, A., BRZOZOWSKI, M. J., HENRIQUEZ, N. V., LINEHAN, J. M., MIRZADEH, Z., C, O. M., NAUMANN, H., ALVAREZ-BUYLLA, A. & BRANDNER, S. 2010. Combinations of genetic mutations in the adult neural stem cell compartment determine brain tumour phenotypes. *Embo j,* 29**,** 222-35.

JESSBERGER, S., CLARK RE FAU - BROADBENT, N. J., BROADBENT NJ FAU - CLEMENSON, G. D., JR., CLEMENSON GD JR FAU - CONSIGLIO, A., CONSIGLIO A FAU - LIE, D. C., LIE DC FAU - SQUIRE, L. R., SQUIRE LR FAU - GAGE, F. H. & GAGE, F. H. 2009. Dentate gyrus-specific knockdown of adult neurogenesis impairs spatial and object. *Learn Mem,* 16**,** 147-54 LID - 10.1101/lm.1172609 [doi].

JHAVERI, D. J., O'KEEFFE, I., ROBINSON, G. J., ZHAO, Q. Y., ZHANG, Z. H., NINK, V., NARAYANAN, R. K., OSBORNE, G. W., WRAY, N. R. & BARTLETT, P. F. 2015. Purification of neural precursor cells reveals the presence of distinct, stimulus-specific subpopulations of quiescent precursors in the adult mouse hippocampus. *J Neurosci,* 35**,** 8132-44.

JIA, Y., CHEN, J., ZHU, H., JIA, Z. H. & CUI, M. H. 2015. Aberrantly elevated redox sensing factor Nrf2 promotes cancer stem cell survival via enhanced transcriptional regulation of ABCG2 and Bcl-2/Bmi-1 genes. *Oncol Rep,* 34**,** 2296-304.

JIN, L. W., SHIE, F. S., MAEZAWA, I., VINCENT, I. & BIRD, T. 2004. Intracellular accumulation of amyloidogenic fragments of amyloid-beta precursor protein in neurons with Niemann-Pick type C defects is associated with endosomal abnormalities. *Am J Pathol,* 164**,** 975-85.

JO, C., GUNDEMIR, S., PRITCHARD, S., JIN, Y. N., RAHMAN, I. & JOHNSON, G. V. 2014. Nrf2 reduces levels of phosphorylated tau protein by inducing autophagy adaptor protein NDP52. *Nat Commun,* 5**,** 3496.

JO, D. G., ARUMUGAM, T. V., WOO, H. N., PARK, J. S., TANG, S. C., MUGHAL, M., HYUN, D. H., PARK, J. H., CHOI, Y. H., GWON, A. R., CAMANDOLA, S., CHENG, A., CAI, H., SONG, W., MARKESBERY, W. R. & MATTSON, M. P. 2010. Evidence that gamma-secretase mediates oxidative stress-induced beta-secretase expression in Alzheimer's disease. *Neurobiol Aging,* 31**,** 917-25.

JOHNSON, D. A. & JOHNSON, J. A. 2015. Nrf2--a therapeutic target for the treatment of neurodegenerative diseases. *Free Radic Biol Med,* 88**,** 253-267.

JYRKKANEN, H. K., KUOSMANEN, S., HEINANIEMI, M., LAITINEN, H., KANSANEN, E., MELLA-AHO, E., LEINONEN, H., YLA-HERTTUALA, S. & LEVONEN, A. L. 2011. Novel insights into the regulation of antioxidant-response-element-mediated gene expression by electrophiles: induction of the transcriptional repressor BACH1 by Nrf2. *Biochem J,* 440**,** 167-74.

KANAI, F., MARIGNANI, P. A., SARBASSOVA, D., YAGI, R., HALL, R. A., DONOWITZ, M., HISAMINATO, A., FUJIWARA, T., ITO, Y., CANTLEY, L. C. & YAFFE, M. B. 2000. TAZ: a novel transcriptional co-activator regulated by interactions with 14-3-3 and PDZ domain proteins. *Embo j,* 19**,** 6778-91.

KANNINEN, K., HEIKKINEN, R., MALM, T., ROLOVA, T., KUHMONEN, S., LEINONEN, H., YLA-HERTTUALA, S., TANILA, H., LEVONEN, A. L., KOISTINAHO, M. & KOISTINAHO, J. 2009. Intrahippocampal injection of a lentiviral vector expressing Nrf2 improves spatial learning in a mouse model of Alzheimer's disease. *Proc Natl Acad Sci U S A,* 106**,** 16505-10.

KANNINEN, K., MALM, T. M., JYRKKANEN, H. K., GOLDSTEINS, G., KEKSA-GOLDSTEINE, V., TANILA, H., YAMAMOTO, M., YLA-HERTTUALA, S., LEVONEN, A. L. & KOISTINAHO, J. 2008. Nuclear factor erythroid 2-related factor 2 protects against beta amyloid. *Mol Cell Neurosci,* 39**,** 302-13.

KARKKAINEN, V., POMESHCHIK Y FAU - SAVCHENKO, E., SAVCHENKO E FAU - DHUNGANA, H., DHUNGANA H FAU - KURRONEN, A., KURRONEN A FAU - LEHTONEN, S., LEHTONEN S FAU - NAUMENKO, N., NAUMENKO N FAU - TAVI, P., TAVI P FAU - LEVONEN, A.-L., LEVONEN AL FAU - YAMAMOTO, M., YAMAMOTO M FAU - MALM, T., MALM T FAU - MAGGA, J., MAGGA J FAU - KANNINEN, K. M., KANNINEN KM FAU - KOISTINAHO, J. & KOISTINAHO, J. 2014. Nrf2 regulates neurogenesis and protects neural progenitor cells against Abeta. *Stem Cells,* 32**,** 1904-16 LID - 10.1002/stem.1666 [doi].

KAROW, M., SANCHEZ, R., SCHICHOR, C., MASSERDOTTI, G., ORTEGA, F., HEINRICH, C., GASCON, S., KHAN, M. A., LIE, D. C., DELLAVALLE, A., COSSU, G., GOLDBRUNNER, R., GOTZ, M. & BERNINGER, B. 2012. Reprogramming of pericyte-derived cells of the adult human brain into induced neuronal cells. *Cell Stem Cell,* 11**,** 471-6.

KATSUOKA, F. & YAMAMOTO, M. 2016. Small Maf proteins (MafF, MafG, MafK): History, structure and function. *Gene,* 586**,** 197-205.

KAUSHIK, A., KELSOE, G. & JATON, J. C. 1995. The nude mutation results in impaired primary antibody repertoire. *Eur J Immunol,* 25**,** 631-4.

KEENE, M. A., CORCES, V., LOWENHAUPT, K. & ELGIN, S. C. 1981. DNase I hypersensitive sites in Drosophila chromatin occur at the 5' ends of regions of transcription. *Proc Natl Acad Sci U S A,* 78**,** 143-6.

KEMPERMANN, G. 2013. Neuroscience. What the bomb said about the brain. *Science,* 340**,** 1180-1.

KEMPERMANN, G. & GAGE, F. H. 1998. Closer to neurogenesis in adult humans. *Nat Med,* 4**,** 555-7.

KEMPERMANN, G. & GAGE, F. H. 2002. Genetic determinants of adult hippocampal neurogenesis correlate with acquisition, but not probe trial performance, in the water maze task. *Eur J Neurosci,* 16**,** 129-36.

KEMPERMANN, G., JESSBERGER, S., STEINER, B. & KRONENBERG, G. 2004. Milestones of neuronal development in the adult hippocampus. *Trends Neurosci,* 27**,** 447-52.

KEMPERMANN, G., KUHN, H. G. & GAGE, F. H. 1997. More hippocampal neurons in adult mice living in an enriched environment. *Nature,* 386**,** 493-5.

KHAIBULLINA, A. A., ROSENSTEIN, J. M. & KRUM, J. M. 2004. Vascular endothelial growth factor promotes neurite maturation in primary CNS neuronal cultures. *Brain Res Dev Brain Res,* 148**,** 59-68.

KHALIFA, J., TENSAOUTI, F., LUSQUE, A., PLAS, B., LOTTERIE, J. A., BENOUAICH-AMIEL, A., URO-COSTE, E., LUBRANO, V. & COHEN-JONATHAN MOYAL, E. 2017. Subventricular zones: new key targets for glioblastoma treatment. *Radiat Oncol,* 12**,** 67.

KHAN, A., FORNES, O., STIGLIANI, A., GHEORGHE, M., CASTRO-MONDRAGON, J. A., VAN DER LEE, R., BESSY, A., CHENEBY, J., KULKARNI, S. R., TAN, G., BARANASIC, D.,

ARENILLAS, D. J., SANDELIN, A., VANDEPOELE, K., LENHARD, B., BALLESTER, B., WASSERMAN, W. W., PARCY, F. & MATHELIER, A. 2018. JASPAR 2018: update of the open-access database of transcription factor binding profiles and its web framework. *Nucleic Acids Res,* 46**,** D260-d266.

KIM, E. J., LEUNG, C. T., REED, R. R. & JOHNSON, J. E. 2007. In vivo analysis of Ascl1 defined progenitors reveals distinct developmental dynamics during adult neurogenesis and gliogenesis. *J Neurosci,* 27**,** 12764-74.

KIM, J. H., YU, S., CHEN, J. D. & KONG, A. N. 2013. The nuclear cofactor RAC3/AIB1/SRC-3 enhances Nrf2 signaling by interacting with transactivation domains. *Oncogene,* 32**,** 514-27.

KIM, M., KIM, T., JOHNSON, R. L. & LIM, D. S. 2015. Transcriptional co-repressor function of the hippo pathway transducers YAP and TAZ. *Cell Rep,* 11**,** 270-82.

KIM, M. K., JANG, J. W. & BAE, S. C. 2018. DNA binding partners of YAP/TAZ. *BMB Rep,* 51**,** 126-133.

KIM, W. Y., WANG, X., WU, Y., DOBLE, B. W., PATEL, S., WOODGETT, J. R. & SNIDER, W. D. 2009. GSK-3 is a master regulator of neural progenitor homeostasis. *Nat Neurosci,* 12**,** 1390-7.

KNOTH, R., SINGEC, I., DITTER, M., PANTAZIS, G., CAPETIAN, P., MEYER, R. P., HORVAT, V., VOLK, B. & KEMPERMANN, G. 2010. Murine features of neurogenesis in the human hippocampus across the lifespan from 0 to 100 years. *PLoS One,* 5**,** e8809.

KOHMAN, R. A. & RHODES, J. S. 2013. Neurogenesis, inflammation and behavior. *Brain Behav Immun,* 27**,** 22-32.

KOJRO, E. & FAHRENHOLZ, F. 2005. The non-amyloidogenic pathway: structure and function of alpha-secretases. *Subcell Biochem,* 38**,** 105-27.

KORNACK, D. R. & RAKIC, P. 2001. Cell proliferation without neurogenesis in adult primate neocortex. *Science,* 294**,** 2127-30.

KRIEGSTEIN, A. & ALVAREZ-BUYLLA, A. 2009. The glial nature of embryonic and adult neural stem cells. *Annu Rev Neurosci,* 32**,** 149-84 LID - 10.1146/annurev.neuro.051508.135600 [doi].

KUHN, H. G., DICKINSON-ANSON, H. & GAGE, F. H. 1996. Neurogenesis in the dentate gyrus of the adult rat: age-related decrease of neuronal progenitor proliferation. *J Neurosci,* 16**,** 2027-33.

KUKEKOV, V. G., LAYWELL, E. D., SUSLOV, O., DAVIES, K., SCHEFFLER, B., THOMAS, L. B., O'BRIEN, T. F., KUSAKABE, M. & STEINDLER, D. A. 1999. Multipotent stem/progenitor cells with similar properties arise from two neurogenic regions of adult human brain. *Exp Neurol,* 156**,** 333-44.

KUO, M. H., BROWNELL, J. E., SOBEL, R. E., RANALLI, T. A., COOK, R. G., EDMONDSON, D. G., ROTH, S. Y. & ALLIS, C. D. 1996. Transcription-linked acetylation by Gcn5p of histones H3 and H4 at specific lysines. *Nature,* 383**,** 269-72.

KUWABARA, T., HSIEH, J., MUOTRI, A., YEO, G., WARASHINA, M., LIE, D. C., MOORE, L., NAKASHIMA, K., ASASHIMA, M. & GAGE, F. H. 2009. Wnt-mediated activation of NeuroD1 and retro-elements during adult neurogenesis. *Nat Neurosci,* 12**,** 1097-105.

KWAK, M. K., ITOH, K., YAMAMOTO, M. & KENSLER, T. W. 2002. Enhanced expression of the transcription factor Nrf2 by cancer chemopreventive agents: role of antioxidant response element-like sequences in the nrf2 promoter. *Mol Cell Biol,* 22**,** 2883-92.

KWAN, K. Y., SESTAN, N. & ANTON, E. S. 2012. Transcriptional co-regulation of neuronal migration and laminar identity in the neocortex. *Development,* 139**,** 1535-46.

KWEIDER, N., FRAGOULIS, A., ROSEN, C., PECKS, U., RATH, W., PUFE, T. & WRUCK, C. J. 2011. Interplay between vascular endothelial growth factor (VEGF) and nuclear factor erythroid 2-related factor-2 (Nrf2): implications for preeclampsia. *J Biol Chem,* 286**,** 42863-72.

L'EPISCOPO, F., TIROLO, C., TESTA, N., CANIGLIA, S., MORALE, M. C., IMPAGNATIELLO, F., PLUCHINO, S. & MARCHETTI, B. 2013. Aging-induced Nrf2-ARE pathway disruption in the subventricular zone drives neurogenic impairment in parkinsonian mice via PI3K-Wnt/beta-catenin dysregulation. *J Neurosci,* 33**,** 1462-85.

LACAR, B., LINKER, S. B., JAEGER, B. N., KRISHNASWAMI, S. R., BARRON, J. J., KELDER, M. J. E., PARYLAK, S. L., PAQUOLA, A. C. M., VENEPALLY, P., NOVOTNY, M., O'CONNOR, C., FITZPATRICK, C., ERWIN, J. A., HSU, J. Y., HUSBAND, D., MCCONNELL, M. J., LASKEN, R. & GAGE, F. H. 2016. Nuclear RNA-seq of single neurons reveals molecular signatures of activation. *Nat Commun,* 7**,** 11022.

LACOMME, M., LIAUBET, L., PITUELLO, F. & BEL-VIALAR, S. 2012. NEUROG2 drives cell cycle exit of neuronal precursors by specifically repressing a subset of cyclins acting at the G1 and S phases of the cell cycle. *Mol Cell Biol,* 32**,** 2596-607.

LAI, A. Y. & WADE, P. A. 2011. Cancer biology and NuRD: a multifaceted chromatin remodelling complex. *Nat Rev Cancer,* 11**,** 588-96.

LAI, D., HO, K. C., HAO, Y. & YANG, X. 2011. Taxol resistance in breast cancer cells is mediated by the hippo pathway component TAZ and its downstream transcriptional targets Cyr61 and CTGF. *Cancer Res,* 71**,** 2728-38.

LAN, X., JORG, D. J., CAVALLI, F. M. G., RICHARDS, L. M., NGUYEN, L. V., VANNER, R. J., GUILHAMON, P., LEE, L., KUSHIDA, M. M., PELLACANI, D., PARK, N. I., COUTINHO, F. J., WHETSTONE, H., SELVADURAI, H. J., CHE, C., LUU, B., CARLES, A., MOKSA, M., RASTEGAR, N., HEAD, R., DOLMA, S., PRINOS, P., CUSIMANO, M. D., DAS, S., BERNSTEIN, M., ARROWSMITH, C. H., MUNGALL, A. J., MOORE, R. A., MA, Y., GALLO, M., LUPIEN, M., PUGH, T. J., TAYLOR, M. D., HIRST, M., EAVES, C. J., SIMONS, B. D. & DIRKS, P. B. 2017. Fate mapping of human glioblastoma reveals an invariant stem cell hierarchy. *Nature,* 549**,** 227-232.

LANGE, C., MIX, E., FRAHM, J., GLASS, A., MULLER, J., SCHMITT, O., SCHMOLE, A. C., KLEMM, K., ORTINAU, S., HUBNER, R., FRECH, M. J., WREE, A. & ROLFS, A. 2011. Small molecule GSK-3 inhibitors increase neurogenesis of human neural progenitor cells. *Neurosci Lett,* 488**,** 36-40.

LAU, A., TIAN, W., WHITMAN, S. A. & ZHANG, D. D. 2013. The predicted molecular weight of Nrf2: it is what it is not. *Antioxid Redox Signal,* 18**,** 91-3.

LAVADO, A., HE, Y., PARE, J., NEALE, G., OLSON, E. N., GIOVANNINI, M. & CAO, X. 2013. Tumor suppressor Nf2 limits expansion of the neural progenitor pool by inhibiting Yap/Taz transcriptional coactivators. *Development,* 140**,** 3323-34.

LAVADO, A., LAGUTIN, O. V., CHOW, L. M., BAKER, S. J. & OLIVER, G. 2010. Prox1 is required for granule cell maturation and intermediate progenitor maintenance during brain neurogenesis. *PLoS Biol,* 8.

LAVADO, A. & OLIVER, G. 2014. Jagged1 is necessary for postnatal and adult neurogenesis in the dentate gyrus. *Dev Biol,* 388**,** 11-21.

LAVADO, A., PARK, J. Y., PARE, J., FINKELSTEIN, D., PAN, H., XU, B., FAN, Y., KUMAR, R. P., NEALE, G., KWAK, Y. D., MCKINNON, P. J., JOHNSON, R. L. & CAO, X. 2018. The Hippo Pathway Prevents YAP/TAZ-Driven Hypertranscription and Controls Neural Progenitor Number. *Dev Cell,* 47**,** 576-591.e8.

LAZAROV, O. & MARR, R. A. 2010. Neurogenesis and Alzheimer's disease: at the crossroads. *Exp Neurol,* 223**,** 267-81.

LAZAROV, O. & MARR, R. A. 2013. Of mice and men: neurogenesis, cognition and Alzheimer's disease. *Front Aging Neurosci,* 5**,** 43.

LAZAROV, O., MATTSON MP FAU - PETERSON, D. A., PETERSON DA FAU - PIMPLIKAR, S. W., PIMPLIKAR SW FAU - VAN PRAAG, H. & VAN PRAAG, H. 2010. When neurogenesis encounters aging and disease. *Trends Neurosci,* 33**,** 569-79 LID - 10.1016/j.tins.2010.09.003 [doi].

LE BELLE, J. E., OROZCO NM FAU - PAUCAR, A. A., PAUCAR AA FAU - SAXE, J. P., SAXE JP FAU - MOTTAHEDEH, J., MOTTAHEDEH J FAU - PYLE, A. D., PYLE AD FAU - WU, H., WU H FAU - KORNBLUM, H. I. & KORNBLUM, H. I. 2011. Proliferative neural stem cells have high endogenous ROS levels that regulate. *Cell Stem Cell,* 8**,** 59-71 LID - 10.1016/j.stem.2010.11.028 [doi].

LEE, J., KOTLIAROVA, S., KOTLIAROV, Y., LI, A., SU, Q., DONIN, N. M., PASTORINO, S., PUROW, B. W., CHRISTOPHER, N., ZHANG, W., PARK, J. K. & FINE, H. A. 2006. Tumor stem cells derived from glioblastomas cultured in bFGF and EGF more closely mirror the phenotype and genotype of primary tumors than do serum-cultured cell lines. *Cancer Cell,* 9**,** 391-403.

LEE, J. H., LEE, J. E., KAHNG, J. Y., KIM, S. H., PARK, J. S., YOON, S. J., UM, J. Y., KIM, W. K., LEE, J. K., PARK, J., KIM, E. H., LEE, J. H., LEE, J. H., CHUNG, W. S., JU, Y. S., PARK, S. H., CHANG, J. H., KANG, S. G. & LEE, J. H. 2018. Human glioblastoma arises from subventricular zone cells with low-level driver mutations. *Nature,* 560**,** 243-247.

LEE, J. M., LI, J., JOHNSON, D. A., STEIN, T. D., KRAFT, A. D., CALKINS, M. J., JAKEL, R. J. & JOHNSON, J. A. 2005. Nrf2, a multi-organ protector? *Faseb j,* 19**,** 1061-6.

LEHTINEN, M. K. & WALSH, C. A. 2011. Neurogenesis at the brain-cerebrospinal fluid interface. *Annu Rev Cell Dev Biol,* 27**,** 653-79.

LEHTINEN, M. K., ZAPPATERRA, M. W., CHEN, X., YANG, Y. J., HILL, A. D., LUN, M., MAYNARD, T., GONZALEZ, D., KIM, S., YE, P., D'ERCOLE, A. J., WONG, E. T., LAMANTIA, A. S. & WALSH, C. A. 2011. The cerebrospinal fluid provides a proliferative niche for neural progenitor cells. *Neuron,* 69**,** 893-905.

LEI, Q. Y., ZHANG, H., ZHAO, B., ZHA, Z. Y., BAI, F., PEI, X. H., ZHAO, S., XIONG, Y. & GUAN, K. L. 2008. TAZ promotes cell proliferation and epithelial-mesenchymal transition and is inhibited by the hippo pathway. *Mol Cell Biol,* 28**,** 2426-36.

LENGLER, J., BITTNER, T., MUNSTER, D., GAWAD AEL, D. & GRAW, J. 2005. Agonistic and antagonistic action of AP2, Msx2, Pax6, Prox1 AND Six3 in the regulation of Sox2 expression. *Ophthalmic Res,* 37**,** 301-9.

LEROY, K., YILMAZ, Z. & BRION, J. P. 2007. Increased level of active GSK-3beta in Alzheimer's disease and accumulation in argyrophilic grains and in neurones at different stages of neurofibrillary degeneration. *Neuropathol Appl Neurobiol,* 33**,** 43-55.

LESNE, S., KOH, M. T., KOTILINEK, L., KAYED, R., GLABE, C. G., YANG, A., GALLAGHER, M. & ASHE, K. H. 2006. A specific amyloid-beta protein assembly in the brain impairs memory. *Nature,* 440**,** 352-7.

LESNE, S. E., SHERMAN, M. A., GRANT, M., KUSKOWSKI, M., SCHNEIDER, J. A., BENNETT, D. A. & ASHE, K. H. 2013. Brain amyloid-beta oligomers in ageing and Alzheimer's disease. *Brain,* 136**,** 1383-98.

LEVASSEUR, A., ST-JEAN, G., PAQUET, M., BOERBOOM, D. & BOYER, A. 2017. Targeted Disruption of YAP and TAZ Impairs the Maintenance of the Adrenal Cortex. *Endocrinology,* 158**,** 3738-3753.

LI, G., BIEN-LY, N., ANDREWS-ZWILLING, Y., XU, Q., BERNARDO, A., RING, K., HALABISKY, B., DENG, C., MAHLEY, R. W. & HUANG, Y. 2009. GABAergic interneuron dysfunction impairs hippocampal neurogenesis in adult apolipoprotein E4 knockin mice. *Cell Stem Cell,* 5**,** 634-45.

LI, L., PAN, H., WANG, H., LI, X., BU, X., WANG, Q., GAO, Y., WEN, G., ZHOU, Y., CONG, Z., YANG, Y., TANG, C. & LIU, Z. 2016a. Interplay between VEGF and Nrf2 regulates angiogenesis due to intracranial venous hypertension. *Scientific Reports,* 6**,** 37338.

LI, W., DONG, S., WEI, W., WANG, G., ZHANG, A., PU, P. & JIA, Z. 2016b. The role of transcriptional coactivator TAZ in gliomas. *Oncotarget,* 7**,** 82686-82699.

LI, W. L., CHU, M. W., WU, A., SUZUKI, Y., IMAYOSHI, I. & KOMIYAMA, T. 2018. Adult-born neurons facilitate olfactory bulb pattern separation during task engagement. *Elife,* 7.

LI, Z., WANG, Y., ZHU, Y., YUAN, C., WANG, D., ZHANG, W., QI, B., QIU, J., SONG, X., YE, J., WU, H., JIANG, H., LIU, L., ZHANG, Y., SONG, L. N., YANG, J. & CHENG, J. 2015. The Hippo transducer TAZ promotes epithelial to mesenchymal transition and cancer stem cell maintenance in oral cancer. *Mol Oncol,* 9**,** 1091-105.

LIE, D. C., COLAMARINO, S. A., SONG, H. J., DESIRE, L., MIRA, H., CONSIGLIO, A., LEIN, E. S., JESSBERGER, S., LANSFORD, H., DEARIE, A. R. & GAGE, F. H. 2005. Wnt signalling regulates adult hippocampal neurogenesis. *Nature,* 437**,** 1370-5.

LIM, F., HERNANDEZ, F., LUCAS, J. J., GOMEZ-RAMOS, P., MORAN, M. A. & AVILA, J. 2001. FTDP-17 mutations in tau transgenic mice provoke lysosomal abnormalities and Tau filaments in forebrain. *Mol Cell Neurosci,* 18**,** 702-14.

LIM, S., BHINGE, A., BRAGADO ALONSO, S., AKSOY, I., APREA, J., CHEOK, C. F., CALEGARI, F., STANTON, L. W. & KALDIS, P. 2017. Cyclin-Dependent Kinase-Dependent Phosphorylation of Sox2 at Serine 39 Regulates Neurogenesis. *Mol Cell Biol,* 37.

LIN, H., ZHU, X., CHEN, G., SONG, L., GAO, L., KHAND, A. A., CHEN, Y., LIN, G. & TAO, Q. 2017. KDM3A-mediated demethylation of histone H3 lysine 9 facilitates the chromatin binding of Neurog2 during neurogenesis. *Development,* 144**,** 3674-3685.

LITHNER, C. U., HEDBERG, M. M. & NORDBERG, A. 2011. Transgenic mice as a model for Alzheimer's disease. *Curr Alzheimer Res,* 8**,** 818-31.

LIU, C., HUANG, W. & LEI, Q. 2011. Regulation and function of the TAZ transcription co-activator. *Int J Biochem Mol Biol,* 2**,** 247-56.

LIU, C. Y., ZHA, Z. Y., ZHOU, X., ZHANG, H., HUANG, W., ZHAO, D., LI, T., CHAN, S. W., LIM, C. J., HONG, W., ZHAO, S., XIONG, Y., LEI, Q. Y. & GUAN, K. L. 2010. The hippo tumor pathway promotes TAZ degradation by phosphorylating a phosphodegron and recruiting the SCF{beta}-TrCP E3 ligase. *J Biol Chem,* 285**,** 37159-69.

LIU, M. L., ZANG, T., ZOU, Y., CHANG, J. C., GIBSON, J. R., HUBER, K. M. & ZHANG, C. L. 2013. Small molecules enable neurogenin 2 to efficiently convert human fibroblasts into cholinergic neurons. *Nat Commun,* 4**,** 2183.

LIU, Z., ZHOU, T., ZIEGLER, A. C., DIMITRION, P. & ZUO, L. 2017. Oxidative Stress in Neurodegenerative Diseases: From Molecular Mechanisms to Clinical Applications. *Oxid Med Cell Longev,* 2017**,** 2525967.

LODATO, M. A., NG, C. W., WAMSTAD, J. A., CHENG, A. W., THAI, K. K., FRAENKEL, E., JAENISCH, R. & BOYER, L. A. 2013. SOX2 co-occupies distal enhancer elements with distinct POU factors in ESCs and NPCs to specify cell state. *PLoS Genet,* 9**,** e1003288.

LU, B., PANG, P. T. & WOO, N. H. 2005. The yin and yang of neurotrophin action. *Nat Rev Neurosci,* 6**,** 603-14.

LU, J., COWPERTHWAITE, M. C., BURNETT, M. G. & SHPAK, M. 2016. Molecular Predictors of Long-Term Survival in Glioblastoma Multiforme Patients. *PLoS One,* 11**,** e0154313.

LUGERT, S., BASAK, O., KNUCKLES, P., HAUSSLER, U., FABEL, K., GOTZ, M., HAAS, C. A., KEMPERMANN, G., TAYLOR, V. & GIACHINO, C. 2010. Quiescent and active hippocampal neural stem cells with distinct morphologies respond selectively to physiological and pathological stimuli and aging. *Cell Stem Cell,* 6**,** 445-56.

LUO, J., DANIELS, S. B., LENNINGTON, J. B., NOTTI, R. Q. & CONOVER, J. C. 2006. The aging neurogenic subventricular zone. *Aging Cell,* 5**,** 139-52.

LUZZATI, F., DE MARCHIS, S., FASOLO, A. & PERETTO, P. 2006. Neurogenesis in the caudate nucleus of the adult rabbit. *J Neurosci,* 26**,** 609-21.

LLEDO, P. M. & SAGHATELYAN, A. 2005. Integrating new neurons into the adult olfactory bulb: joining the network, life-death decisions, and the effects of sensory experience. *Trends Neurosci,* 28**,** 248-54.

MA, Q. 2013. Role of nrf2 in oxidative stress and toxicity. *Annu Rev Pharmacol Toxicol,* 53**,** 401-26.

MA, Q., KINTNER, C. & ANDERSON, D. J. 1996. Identification of neurogenin, a vertebrate neuronal determination gene. *Cell,* 87**,** 43-52.

MADHAVAN, L. 2015. Redox-based regulation of neural stem cell function and Nrf2. *Biochem Soc Trans,* 43**,** 627-31 LID - 10.1042/BST20150016 [doi].

MADHYASTHA, S., SEKHAR, S. & RAO, G. 2013. Resveratrol improves postnatal hippocampal neurogenesis and brain derived neurotrophic factor in prenatally stressed rats. *Int J Dev Neurosci,* 31**,** 580-5.

MAGNUSSON, J. P. & FRISEN, J. 2016. Stars from the darkest night: unlocking the neurogenic potential of astrocytes in different brain regions. *Development,* 143**,** 1075-86.

MALATESTA, P., HARTFUSS, E. & GOTZ, M. 2000. Isolation of radial glial cells by fluorescent-activated cell sorting reveals a neuronal lineage. *Development,* 127**,** 5253-63.

MANORANJAN, B., VENUGOPAL, C., MCFARLANE, N., DOBLE, B. W., DUNN, S. E., SCHEINEMANN, K. & SINGH, S. K. 2012. Medulloblastoma stem cells: where development and cancer cross pathways. *Pediatr Res,* 71**,** 516-22.

MARTIN-DE-SAAVEDRA, M. D., BUDNI, J., CUNHA, M. P., GOMEZ-RANGEL, V., LORRIO, S., DEL BARRIO, L., LASTRES-BECKER, I., PARADA, E., TORDERA, R. M., RODRIGUES, A. L., CUADRADO, A. & LOPEZ, M. G. 2013. Nrf2 participates in depressive disorders through an anti-inflammatory mechanism. *Psychoneuroendocrinology,* 38**,** 2010-22.

MATSUDA, T., IRIE, T., KATSURABAYASHI, S., HAYASHI, Y., NAGAI, T., HAMAZAKI, N., ADEFUIN, A. M. D., MIURA, F., ITO, T., KIMURA, H., SHIRAHIGE, K., TAKEDA, T., IWASAKI, K., IMAMURA, T. & NAKASHIMA, K. 2019. Pioneer Factor NeuroD1 Rearranges Transcriptional and Epigenetic Profiles to Execute Microglia-Neuron Conversion. *Neuron,* 101**,** 472-485.e7.

MCGHEE, J. D., WOOD, W. I., DOLAN, M., ENGEL, J. D. & FELSENFELD, G. 1981. A 200 base pair region at the 5' end of the chicken adult beta-globin gene is accessible to nuclease digestion. *Cell,* 27**,** 45-55.

MCMAHON, M., THOMAS, N., ITOH, K., YAMAMOTO, M. & HAYES, J. D. 2006. Dimerization of substrate adaptors can facilitate cullin-mediated ubiquitylation of proteins by a "tethering" mechanism: a two-site interaction model for the Nrf2-Keap1 complex. *J Biol Chem,* 281**,** 24756-68.

MEMIC, F., KNOFLACH, V., SADLER, R., TEGERSTEDT, G., SUNDSTROM, E., GUILLEMOT, F., PACHNIS, V. & MARKLUND, U. 2016. Ascl1 Is Required for the Development of Specific Neuronal Subtypes in the Enteric Nervous System. *J Neurosci,* 36**,** 4339-50.

MENN, B., GARCIA-VERDUGO, J. M., YASCHINE, C., GONZALEZ-PEREZ, O., ROWITCH, D. & ALVAREZ-BUYLLA, A. 2006. Origin of oligodendrocytes in the subventricular zone of the adult brain. *J Neurosci,* 26**,** 7907-18.

MEYER, M., REIMAND, J., LAN, X., HEAD, R., ZHU, X., KUSHIDA, M., BAYANI, J., PRESSEY, J. C., LIONEL, A. C., CLARKE, I. D., CUSIMANO, M., SQUIRE, J. A., SCHERER, S. W., BERNSTEIN, M., WOODIN, M. A., BADER, G. D. & DIRKS, P. B. 2015. Single cell-derived clonal analysis of human glioblastoma links functional and genomic heterogeneity. *Proc Natl Acad Sci U S A,* 112**,** 851-6.

MICH, J. K., SIGNER, R. A., NAKADA, D., PINEDA, A., BURGESS, R. J., VUE, T. Y., JOHNSON, J. E. & MORRISON, S. J. 2014. Prospective identification of functionally distinct stem cells and neurosphere-initiating cells in adult mouse forebrain. *Elife,* 3**,** e02669.

MING, G. L. & SONG, H. 2011. Adult neurogenesis in the mammalian brain: significant answers and significant questions. *Neuron,* 70**,** 687-702.

MIRESCU, C., PETERS, J. D. & GOULD, E. 2004. Early life experience alters response of adult neurogenesis to stress. *Nat Neurosci,* 7**,** 841-6.

MIRZADEH, Z., MERKLE, F. T., SORIANO-NAVARRO, M., GARCIA-VERDUGO, J. M. & ALVAREZ-BUYLLA, A. 2008. Neural stem cells confer unique pinwheel architecture to the ventricular surface in neurogenic regions of the adult brain. *Cell Stem Cell,* 3**,** 265-78.

MISRA, J. R. & IRVINE, K. D. 2018. The Hippo Signaling Network and Its Biological Functions. *Annu Rev Genet,* 52**,** 65-87.

MITSUISHI, Y., TAGUCHI, K., KAWATANI, Y., SHIBATA, T., NUKIWA, T., ABURATANI, H., YAMAMOTO, M. & MOTOHASHI, H. 2012. Nrf2 redirects glucose and glutamine into anabolic pathways in metabolic reprogramming. *Cancer Cell,* 22**,** 66-79.

MO, J. S., PARK, H. W. & GUAN, K. L. 2014. The Hippo signaling pathway in stem cell biology and cancer. *EMBO Rep,* 15**,** 642-56.

MOECHARS, D., DEWACHTER, I., LORENT, K., REVERSE, D., BAEKELANDT, V., NAIDU, A., TESSEUR, I., SPITTAELS, K., HAUTE, C. V., CHECLER, F., GODAUX, E., CORDELL, B. & VAN LEUVEN, F. 1999. Early phenotypic changes in transgenic mice that overexpress different mutants of amyloid precursor protein in brain. *J Biol Chem,* 274**,** 6483-92.

MOI, P., CHAN, K., ASUNIS, I., CAO, A. & KAN, Y. W. 1994. Isolation of NF-E2-related factor 2 (Nrf2), a NF-E2-like basic leucine zipper transcriptional activator that binds to the tandem NF-E2/AP1 repeat of the beta-globin locus control region. *Proc Natl Acad Sci U S A,* 91**,** 9926-30.

MORENO-JIMENEZ, E. P., FLOR-GARCIA, M., TERREROS-RONCAL, J., RABANO, A., CAFINI, F., PALLAS-BAZARRA, N., AVILA, J. & LLORENS-MARTIN, M. 2019. Adult hippocampal neurogenesis is abundant in neurologically healthy subjects and drops sharply in patients with Alzheimer's disease. *Nat Med,* 25**,** 554-560.

MORRIS, R. 1984. Developments of a water-maze procedure for studying spatial learning in the rat. *J Neurosci Methods,* 11**,** 47-60.

MORRIS, R. G., GARRUD, P., RAWLINS, J. N. & O'KEEFE, J. 1982. Place navigation impaired in rats with hippocampal lesions. *Nature,* 297**,** 681-3.

MORSHEAD, C. M., GARCIA, A. D., SOFRONIEW, M. V. & VAN DER KOOY, D. 2003. The ablation of glial fibrillary acidic protein-positive cells from the adult central nervous system results in the loss of forebrain neural stem cells but not retinal stem cells. *Eur J Neurosci,* 18**,** 76-84.

MOSER, E. I., KROBERT, K. A., MOSER, M. B. & MORRIS, R. G. 1998. Impaired spatial learning after saturation of long-term potentiation. *Science,* 281**,** 2038-42.

MU, Y. & GAGE, F. H. 2011. Adult hippocampal neurogenesis and its role in Alzheimer's disease. *Mol Neurodegener,* 6**,** 85.

MULLEN, A. C., ORLANDO, D. A., NEWMAN, J. J., LOVEN, J., KUMAR, R. M., BILODEAU, S., REDDY, J., GUENTHER, M. G., DEKOTER, R. P. & YOUNG, R. A. 2011. Master transcription factors determine cell-type-specific responses to TGF-beta signaling. *Cell,* 147**,** 565-76.

MURAKAMI, M., NAKAGAWA, M., OLSON, E. N. & NAKAGAWA, O. 2005. A WW domain protein TAZ is a critical coactivator for TBX5, a transcription factor implicated in Holt-Oram syndrome. *Proc Natl Acad Sci U S A,* 102**,** 18034-9.

MURAKAMI, M., TOMINAGA, J., MAKITA, R., UCHIJIMA, Y., KURIHARA, Y., NAKAGAWA, O., ASANO, T. & KURIHARA, H. 2006. Transcriptional activity of Pax3 is co-activated by TAZ. *Biochem Biophys Res Commun,* 339**,** 533-9.

MURAKAMI, S. & MOTOHASHI, H. 2015. Roles of Nrf2 in cell proliferation and differentiation. *Free Radic Biol Med,* 88**,** 168-78.

MURAKAMI, S., SUZUKI, T., HARIGAE, H., ROMEO, P. H., YAMAMOTO, M. & MOTOHASHI, H. 2017. NRF2 Activation Impairs Quiescence and Bone Marrow Reconstitution Capacity of Hematopoietic Stem Cells. *Mol Cell Biol,* 37.

MURPHY, T., DIAS, G. P. & THURET, S. 2014. Effects of diet on brain plasticity in animal and human studies: mind the gap. *Neural Plast,* 2014**,** 563160.

NABAVI, S., FOX, R., PROULX, C. D., LIN, J. Y., TSIEN, R. Y. & MALINOW, R. 2014. Engineering a memory with LTD and LTP. *Nature,* 511**,** 348-52.

NAIT-OUMESMAR, B., DECKER, L., LACHAPELLE, F., AVELLANA-ADALID, V., BACHELIN, C. & BARON-VAN EVERCOOREN, A. 1999. Progenitor cells of the adult mouse subventricular zone proliferate, migrate and differentiate into oligodendrocytes after demyelination. *Eur J Neurosci,* 11**,** 4357-66.

NAKASHIBA, T., CUSHMAN, J. D., PELKEY, K. A., RENAUDINEAU, S., BUHL, D. L., MCHUGH, T. J., RODRIGUEZ BARRERA, V., CHITTAJALLU, R., IWAMOTO, K. S., MCBAIN, C. J., FANSELOW, M. S. & TONEGAWA, S. 2012. Young dentate granule cells mediate pattern separation, whereas old granule cells facilitate pattern completion. *Cell,* 149**,** 188-201.

NAMANI, A., CUI, Q. Q., WU, Y., WANG, H., WANG, X. J. & TANG, X. 2017. NRF2-regulated metabolic gene signature as a prognostic biomarker in non-small cell lung cancer. *Oncotarget,* 8**,** 69847-69862.

NARAYANAN, A., GAGLIARDI, F., GALLOTTI, A. L., MAZZOLENI, S., COMINELLI, M., FAGNOCCHI, L., PALA, M., PIRAS, I. S., ZORDAN, P., MORETTA, N., TRATTA, E., BRUGNARA, G., ALTABELLA, L., BOZZUTO, G., GOROMBEI, P., MOLINARI, A., PADUA, R. A., BULFONE, A., POLITI, L. S., FALINI, A., CASTELLANO, A., MORTINI, P., ZIPPO, A., POLIANI, P. L. & GALLI, R. 2018. The proneural gene ASCL1 governs the transcriptional subgroup affiliation in glioblastoma stem cells by directly repressing the mesenchymal gene NDRG1. *Cell Death Differ*.

NG, S. Y., BOGU, G. K., SOH, B. S. & STANTON, L. W. 2013. The long noncoding RNA RMST interacts with SOX2 to regulate neurogenesis. *Mol Cell,* 51**,** 349-59.

NICOLAS, M. & HASSAN, B. A. 2014. Amyloid precursor protein and neural development. *Development,* 141**,** 2543-8.

NISHIOKA, N., INOUE, K., ADACHI, K., KIYONARI, H., OTA, M., RALSTON, A., YABUTA, N., HIRAHARA, S., STEPHENSON, R. O., OGONUKI, N., MAKITA, R., KURIHARA, H., MORIN-KENSICKI, E. M., NOJIMA, H., ROSSANT, J., NAKAO, K., NIWA, H. & SASAKI, H. 2009. The Hippo signaling pathway components Lats and Yap pattern Tead4 activity to distinguish mouse trophectoderm from inner cell mass. *Dev Cell,* 16**,** 398-410.

NOBLE, M., SMITH, J., POWER, J. & MAYER-PROSCHEL, M. 2003. Redox state as a central modulator of precursor cell function. *Ann N Y Acad Sci,* 991**,** 251-71.

NUNOMURA, A., PERRY, G., PAPPOLLA, M. A., WADE, R., HIRAI, K., CHIBA, S. & SMITH, M. A. 1999. RNA oxidation is a prominent feature of vulnerable neurons in Alzheimer's disease. *J Neurosci,* 19**,** 1959-64.

ODDO, S., CACCAMO, A., KITAZAWA, M., TSENG, B. P. & LAFERLA, F. M. 2003a. Amyloid deposition precedes tangle formation in a triple transgenic model of Alzheimer's disease. *Neurobiol Aging,* 24**,** 1063-70.

ODDO, S., CACCAMO, A., SHEPHERD, J. D., MURPHY, M. P., GOLDE, T. E., KAYED, R., METHERATE, R., MATTSON, M. P., AKBARI, Y. & LAFERLA, F. M. 2003b. Triple-transgenic model of Alzheimer's disease with plaques and tangles: intracellular Abeta and synaptic dysfunction. *Neuron,* 39**,** 409-21.

OH, H., SLATTERY, M., MA, L., CROFTS, A., WHITE, K. P., MANN, R. S. & IRVINE, K. D. 2013. Genome-wide association of Yorkie with chromatin and chromatin-remodeling complexes. *Cell Rep,* 3**,** 309-18.

OKAMOTO, M., INOUE, K., IWAMURA, H., TERASHIMA, K., SOYA, H., ASASHIMA, M. & KUWABARA, T. 2011. Reduction in paracrine Wnt3 factors during aging causes impaired adult neurogenesis. *Faseb j,* 25**,** 3570-82.

OKANO, H. J., PFAFF, D. W. & GIBBS, R. B. 1996. Expression of EGFR-, p75NGFR-, and PSTAIR (cdc2)-like immunoreactivity by proliferating cells in the adult rat hippocampal formation and forebrain. *Dev Neurosci,* 18**,** 199-209.

ORTEGA, F., BERNINGER, B. & COSTA, M. R. 2013a. Primary culture and live imaging of adult neural stem cells and their progeny. *Methods Mol Biol,* 1052**,** 1-11.

ORTEGA, F., GASCON, S., MASSERDOTTI, G., DESHPANDE, A., SIMON, C., FISCHER, J., DIMOU, L., CHICHUNG LIE, D., SCHROEDER, T. & BERNINGER, B. 2013b. Oligodendrogliogenic and neurogenic adult subependymal zone neural stem cells constitute distinct lineages and exhibit differential responsiveness to Wnt signalling. *Nat Cell Biol,* 15**,** 602-13.

ORTIZ-MATAMOROS, A., SALCEDO-TELLO, P., AVILA-MUNOZ, E., ZEPEDA, A. & ARIAS, C. 2013. Role of wnt signaling in the control of adult hippocampal functioning in health and disease: therapeutic implications. *Curr Neuropharmacol,* 11**,** 465-76.

PAGE, K., HOLLISTER, R., TANZI, R. E. & HYMAN, B. T. 1996. In situ hybridization analysis of presenilin 1 mRNA in Alzheimer disease and in lesioned rat brain. *Proc Natl Acad Sci U S A,* 93**,** 14020-4.

PAJARES, M., CUADRADO, A. & ROJO, A. I. 2017. Modulation of proteostasis by transcription factor NRF2 and impact in neurodegenerative diseases. *Redox Biol,* 11**,** 543-553.

PAJARES, M., JIMENEZ-MORENO, N., DIAS, I. H. K., DEBELEC, B., VUCETIC, M., FLADMARK, K. E., BASAGA, H., RIBARIC, S., MILISAV, I. & CUADRADO, A. 2015. Redox control of protein degradation. *Redox Biol,* 6**,** 409-420.

PAJARES, M., JIMENEZ-MORENO, N., GARCIA-YAGUE, A. J., ESCOLL, M., DE CEBALLOS, M. L., VAN LEUVEN, F., RABANO, A., YAMAMOTO, M., ROJO, A. I. & CUADRADO, A. 2016. Transcription factor NFE2L2/NRF2 is a regulator of macroautophagy genes. *Autophagy,* 12**,** 1902-1916.

PAN, D. 2010. The hippo signaling pathway in development and cancer. *Dev Cell,* 19**,** 491-505.

PANALIAPPAN, T. K., WITTMANN, W., JIDIGAM, V. K., MERCURIO, S., BERTOLINI, J. A., SGHARI, S., BOSE, R., PATTHEY, C., NICOLIS, S. K. & GUNHAGA, L. 2018. Sox2 is required for olfactory pit formation and olfactory neurogenesis through BMP restriction and Hes5 upregulation. *Development,* 145.

PARENT, J. M. & MURPHY, G. G. 2008. Mechanisms and functional significance of aberrant seizure-induced hippocampal neurogenesis. *Epilepsia,* 49 Suppl 5**,** 19-25.

PARK, N. I., GUILHAMON, P., DESAI, K., MCADAM, R. F., LANGILLE, E., O'CONNOR, M., LAN, X., WHETSTONE, H., COUTINHO, F. J., VANNER, R. J., LING, E., PRINOS, P., LEE, L., SELVADURAI, H., ATWAL, G., KUSHIDA, M., CLARKE, I. D., VOISIN, V., CUSIMANO, M. D., BERNSTEIN, M., DAS, S., BADER, G., ARROWSMITH, C. H., ANGERS, S., HUANG, X., LUPIEN, M. & DIRKS, P. B. 2017. ASCL1 Reorganizes Chromatin to Direct Neuronal Fate and Suppress Tumorigenicity of Glioblastoma Stem Cells. *Cell Stem Cell,* 21**,** 209-224.e7.

PATASKAR, A., JUNG, J., SMIALOWSKI, P., NOACK, F., CALEGARI, F., STRAUB, T. & TIWARI, V. K. 2016. NeuroD1 reprograms chromatin and transcription factor landscapes to induce the neuronal program. *Embo j,* 35**,** 24-45.

PATON, J. A. & NOTTEBOHM, F. N. 1984. Neurons generated in the adult brain are recruited into functional circuits. *Science,* 225**,** 1046-8.

PATTABIRAMAN, D. R. & WEINBERG, R. A. 2014. Tackling the cancer stem cells - what challenges do they pose? *Nat Rev Drug Discov,* 13**,** 497-512.

PEREZ-MARTIN, M., GRONDONA, J. M., CIFUENTES, M., PEREZ-FIGARES, J. M., JIMENEZ, J. A. & FERNANDEZ-LLEBREZ, P. 2000. Ependymal explants from the lateral ventricle of the adult bovine brain: a model system for morphological and functional studies of the ependyma. *Cell Tissue Res,* 300**,** 11-9.

PHILIPP, M. & CARON, M. G. 2009. Hedgehog signaling: is Smo a G protein-coupled receptor? *Curr Biol,* 19**,** R125-7.

PHILLIPS, H. S., KHARBANDA, S., CHEN, R., FORREST, W. F., SORIANO, R. H., WU, T. D., MISRA, A., NIGRO, J. M., COLMAN, H., SOROCEANU, L., WILLIAMS, P. M., MODRUSAN, Z., FEUERSTEIN, B. G. & ALDAPE, K. 2006. Molecular subclasses of high-grade glioma predict prognosis, delineate a pattern of disease progression, and resemble stages in neurogenesis. *Cancer Cell,* 9**,** 157-73.

PICARD-RIERA, N., DECKER, L., DELARASSE, C., GOUDE, K., NAIT-OUMESMAR, B., LIBLAU, R., PHAM-DINH, D. & BARON-VAN EVERCOOREN, A. 2002. Experimental autoimmune encephalomyelitis mobilizes neural progenitors from the subventricular zone to undergo oligodendrogenesis in adult mice. *Proc Natl Acad Sci U S A,* 99**,** 13211-6.

PINCUS, D. W., GOODMAN, R. R., FRASER, R. A., NEDERGAARD, M. & GOLDMAN, S. A. 1998. Neural stem and progenitor cells: a strategy for gene therapy and brain repair. *Neurosurgery,* 42**,** 858-67; discussion 867-8.

PLEASURE, S. J., COLLINS, A. E. & LOWENSTEIN, D. H. 2000. Unique expression patterns of cell fate molecules delineate sequential stages of dentate gyrus development. *J Neurosci,* 20**,** 6095-105.

POLLARD, S. M., YOSHIKAWA, K., CLARKE, I. D., DANOVI, D., STRICKER, S., RUSSELL, R., BAYANI, J., HEAD, R., LEE, M., BERNSTEIN, M., SQUIRE, J. A., SMITH, A. & DIRKS, P. 2009. Glioma stem cell lines expanded in adherent culture have tumor-specific phenotypes and are suitable for chemical and genetic screens. *Cell Stem Cell,* 4**,** 568-80.

PONTEN, J. & MACINTYRE, E. H. 1968. Long term culture of normal and neoplastic human glia. *Acta Pathol Microbiol Scand,* 74**,** 465-86.

PONTI, G., OBERNIER, K., GUINTO, C., JOSE, L., BONFANTI, L. & ALVAREZ-BUYLLA, A. 2013. Cell cycle and lineage progression of neural progenitors in the ventricular-subventricular zones of adult mice. *Proc Natl Acad Sci U S A,* 110**,** E1045-54.

PRAGER, I., PATTIES, I., HIMMELBACH, K., KENDZIA, E., MERZ, F., MULLER, K., KORTMANN, R. D. & GLASOW, A. 2016. Dose-dependent short- and long-term effects of ionizing irradiation on neural stem cells in murine hippocampal tissue cultures: neuroprotective potential of resveratrol. *Brain Behav,* 6**,** e00548.

PRATICO, D. 2008. Evidence of oxidative stress in Alzheimer's disease brain and antioxidant therapy: lights and shadows. *Ann N Y Acad Sci,* 1147**,** 70-8.

PROZOROVSKI, T., SCHULZE-TOPPHOFF, U., GLUMM, R., BAUMGART, J., SCHROTER, F., NINNEMANN, O., SIEGERT, E., BENDIX, I., BRUSTLE, O., NITSCH, R., ZIPP, F. & AKTAS, O. 2008. Sirt1 contributes critically to the redox-dependent fate of neural progenitors. *Nat Cell Biol,* 10**,** 385-94.

QING, Y., YIN, F., WANG, W., ZHENG, Y., GUO, P., SCHOZER, F., DENG, H. & PAN, D. 2014. The Hippo effector Yorkie activates transcription by interacting with a histone methyltransferase complex through Ncoa6. *Elife,* 3.

QU, Q., SUN, G., LI, W., YANG, S., YE, P., ZHAO, C., YU, R. T., GAGE, F. H., EVANS, R. M. & SHI, Y. 2010. Orphan nuclear receptor TLX activates Wnt/beta-catenin signalling to stimulate neural stem cell proliferation and self-renewal. *Nat Cell Biol,* 12**,** 31-40; sup pp 1-9.

QUINONES-HINOJOSA, A., SANAI, N., SORIANO-NAVARRO, M., GONZALEZ-PEREZ, O., MIRZADEH, Z., GIL-PEROTIN, S., ROMERO-RODRIGUEZ, R., BERGER, M. S., GARCIA-VERDUGO, J. M. & ALVAREZ-BUYLLA, A. 2006. Cellular composition and cytoarchitecture of the adult human subventricular zone: a niche of neural stem cells. *J Comp Neurol,* 494**,** 415-34.

RADA, P., ROJO, A. I., CHOWDHRY, S., MCMAHON, M., HAYES, J. D. & CUADRADO, A. 2011. SCF/{beta}-TrCP promotes glycogen synthase kinase 3-dependent degradation of the Nrf2 transcription factor in a Keap1-independent manner. *Mol Cell Biol,* 31**,** 1121-33.

RADA, P., ROJO, A. I., EVRARD-TODESCHI, N., INNAMORATO, N. G., COTTE, A., JAWORSKI, T., TOBON-VELASCO, J. C., DEVIJVER, H., GARCIA-MAYORAL, M. F., VAN LEUVEN, F., HAYES, J. D., BERTHO, G. & CUADRADO, A. 2012. Structural and functional characterization of Nrf2 degradation by the glycogen synthase kinase 3/beta-TrCP axis. *Mol Cell Biol,* 32**,** 3486-99.

RADA, P., ROJO, A. I., OFFERGELD, A., FENG, G. J., VELASCO-MARTIN, J. P., GONZALEZ-SANCHO, J. M., VALVERDE, A. M., DALE, T., REGADERA, J. & CUADRADO, A. 2015. WNT-3A regulates an Axin1/NRF2 complex that regulates antioxidant metabolism in hepatocytes. *Antioxid Redox Signal,* 22**,** 555-71.

RAFALSKI, V. A. & BRUNET, A. 2011. Energy metabolism in adult neural stem cell fate. *Prog Neurobiol,* 93**,** 182-203.

RAI, K. S., HATTIANGADY, B. & SHETTY, A. K. 2007. Enhanced production and dendritic growth of new dentate granule cells in the middle-aged hippocampus following intracerebroventricular FGF-2 infusions. *Eur J Neurosci,* 26**,** 1765-79.

RAMSEY, C. P., GLASS, C. A., MONTGOMERY, M. B., LINDL, K. A., RITSON, G. P., CHIA, L. A., HAMILTON, R. L., CHU, C. T. & JORDAN-SCIUTTO, K. L. 2007. Expression of Nrf2 in neurodegenerative diseases. *J Neuropathol Exp Neurol,* 66**,** 75-85.

RAPOSO, A., VASCONCELOS, F. F., DRECHSEL, D., MARIE, C., JOHNSTON, C., DOLLE, D., BITHELL, A., GILLOTIN, S., VAN DEN BERG, D. L. C., ETTWILLER, L., FLICEK, P., CRAWFORD, G. E., PARRAS, C. M., BERNINGER, B., BUCKLEY, N. J., GUILLEMOT, F. & CASTRO, D. S. 2015. Ascl1 Coordinately Regulates Gene Expression and the Chromatin Landscape during Neurogenesis. *Cell Rep,* 10**,** 1544-1556.

REYNOLDS, B. A. & WEISS, S. 1992. Generation of neurons and astrocytes from isolated cells of the adult mammalian central nervous system. *Science,* 255**,** 1707-10.

REYNOLDS, B. A. & WEISS, S. 1996. Clonal and population analyses demonstrate that an EGF-responsive mammalian embryonic CNS precursor is a stem cell. *Dev Biol,* 175**,** 1-13.

RHEINBAY, E., SUVA, M. L., GILLESPIE, S. M., WAKIMOTO, H., PATEL, A. P., SHAHID, M., OKSUZ, O., RABKIN, S. D., MARTUZA, R. L., RIVERA, M. N., LOUIS, D. N., KASIF, S., CHI, A. S. & BERNSTEIN, B. E. 2013. An aberrant transcription factor network essential for Wnt signaling and stem cell maintenance in glioblastoma. *Cell Rep,* 3**,** 1567-79.

RICHARDS, L. J., KILPATRICK, T. J. & BARTLETT, P. F. 1992. De novo generation of neuronal cells from the adult mouse brain. *Proc Natl Acad Sci U S A,* 89**,** 8591-5.

ROBLEDINOS-ANTON, N., ROJO, A. I., FERREIRO, E., NUNEZ, A., KRAUSE, K. H., JAQUET, V. & CUADRADO, A. 2017. Transcription factor NRF2 controls the fate of neural stem cells in the subgranular zone of the hippocampus. *Redox Biol,* 13**,** 393-401.

ROCHEFORT, C., GHEUSI, G., VINCENT, J. D. & LLEDO, P. M. 2002. Enriched odor exposure increases the number of newborn neurons in the adult olfactory bulb and improves odor memory. *J Neurosci,* 22**,** 2679-89.

RODRIGUEZ, J. J., JONES VC FAU - TABUCHI, M., TABUCHI M FAU - ALLAN, S. M., ALLAN SM FAU - KNIGHT, E. M., KNIGHT EM FAU - LAFERLA, F. M., LAFERLA FM FAU - ODDO, S., ODDO S FAU - VERKHRATSKY, A. & VERKHRATSKY, A. 2008a. Impaired adult neurogenesis in the dentate gyrus of a triple transgenic mouse. *PLoS One,* 3**,** e2935 LID - 10.1371/journal.pone.0002935 [doi].

RODRIGUEZ, J. J., JONES, V. C., TABUCHI, M., ALLAN, S. M., KNIGHT, E. M., LAFERLA, F. M., ODDO, S. & VERKHRATSKY, A. 2008b. Impaired adult neurogenesis in the dentate gyrus of a triple transgenic mouse model of Alzheimer's disease. *PLoS One,* 3**,** e2935.

RODRIGUEZ, J. J., JONES, V. C. & VERKHRATSKY, A. 2009. Impaired cell proliferation in the subventricular zone in an Alzheimer's disease model. *Neuroreport,* 20**,** 907-12.

ROEDER, R. G. 2005. Transcriptional regulation and the role of diverse coactivators in animal cells. *FEBS Lett,* 579**,** 909-15.

ROJO, A. I., PAJARES, M., GARCIA-YAGUE, A. J., BUENDIA, I., VAN LEUVEN, F., YAMAMOTO, M., LOPEZ, M. G. & CUADRADO, A. 2018. Deficiency in the transcription factor NRF2 worsens inflammatory parameters in a mouse model with combined tauopathy and amyloidopathy. *Redox Biol,* 18**,** 173-180.

ROJO, A. I., PAJARES, M., RADA, P., NUNEZ, A., NEVADO-HOLGADO, A. J., KILLIK, R., VAN LEUVEN, F., RIBE, E., LOVESTONE, S., YAMAMOTO, M. & CUADRADO, A. 2017. NRF2 deficiency replicates transcriptomic changes in Alzheimer's patients and worsens APP and TAU pathology. *Redox Biol,* 13**,** 444-451.

ROJO, A. I., SALINAS, M., MARTIN, D., PERONA, R. & CUADRADO, A. 2004. Regulation of Cu/Zn-superoxide dismutase expression via the phosphatidylinositol 3 kinase/Akt pathway and nuclear factor-kappaB. *J Neurosci,* 24**,** 7324-34.

ROJO DE LA VEGA, M., CHAPMAN, E. & ZHANG, D. D. 2018. NRF2 and the Hallmarks of Cancer. *Cancer Cell,* 34**,** 21-43.

ROJO DE LA VEGA, M., DODSON, M., GROSS, C., MANSOUR, H. M., LANTZ, R. C., CHAPMAN, E., WANG, T., BLACK, S. M., GARCIA, J. G. & ZHANG, D. D. 2016. Role of Nrf2 and Autophagy in Acute Lung Injury. *Curr Pharmacol Rep,* 2**,** 91-101.

ROSS, S. E., GREENBERG, M. E. & STILES, C. D. 2003. Basic helix-loop-helix factors in cortical development. *Neuron,* 39**,** 13-25.

ROUSSEAU, A., NUTT, C. L., BETENSKY, R. A., IAFRATE, A. J., HAN, M., LIGON, K. L., ROWITCH, D. H. & LOUIS, D. N. 2006. Expression of oligodendroglial and astrocytic lineage markers in diffuse gliomas: use of YKL-40, ApoE, ASCL1, and NKX2-2. *J Neuropathol Exp Neurol,* 65**,** 1149-56.

ROY, N. S., WANG S FAU - JIANG, L., JIANG L FAU - KANG, J., KANG J FAU - BENRAISS, A., BENRAISS A FAU - HARRISON-RESTELLI, C., HARRISON-RESTELLI C FAU - FRASER, R. A., FRASER RA FAU - COULDWELL, W. T., COULDWELL WT FAU - KAWAGUCHI, A., KAWAGUCHI A FAU - OKANO, H., OKANO H FAU - NEDERGAARD, M., NEDERGAARD M FAU - GOLDMAN, S. A. & GOLDMAN, S. A. 2000. In vitro neurogenesis by progenitor cells isolated from the adult human. *Nat Med,* 6**,** 271-7.

RUSHMORE, T. H., MORTON, M. R. & PICKETT, C. B. 1991. The antioxidant responsive element. Activation by oxidative stress and identification of the DNA consensus sequence required for functional activity. *J Biol Chem,* 266**,** 11632-9.

RUSHMORE, T. H. & PICKETT, C. B. 1990. Transcriptional regulation of the rat glutathione S-transferase Ya subunit gene. Characterization of a xenobiotic-responsive element controlling inducible expression by phenolic antioxidants. *J Biol Chem,* 265**,** 14648-53.

RYOO, I. G., LEE, S. H. & KWAK, M. K. 2016. Redox Modulating NRF2: A Potential Mediator of Cancer Stem Cell Resistance. *Oxid Med Cell Longev,* 2016**,** 2428153.

SAHAY, A. & HEN, R. 2007. Adult hippocampal neurogenesis in depression. *Nat Neurosci,* 10**,** 1110-5.

SAHAY, A., WILSON DA FAU - HEN, R. & HEN, R. 2011. Pattern separation: a common function for new neurons in hippocampus and. *Neuron,* 70**,** 582-8 LID - 10.1016/j.neuron.2011.05.012 [doi].

SALAH, Z., ALIAN, A. & AQEILAN, R. I. 2012. WW domain-containing proteins: retrospectives and the future. *Front Biosci (Landmark Ed),* 17**,** 331-48.

SANAI, N., ALVAREZ-BUYLLA, A. & BERGER, M. S. 2005. Neural stem cells and the origin of gliomas. *N Engl J Med,* 353**,** 811-22.

SANAI, N., BERGER MS FAU - GARCIA-VERDUGO, J. M., GARCIA-VERDUGO JM FAU - ALVAREZ-BUYLLA, A. & ALVAREZ-BUYLLA, A. 2007. Comment on "Human neuroblasts migrate to the olfactory bulb via a lateral. *Science,* 318**,** 393; author reply 393.

SANAI, N., TRAMONTIN AD FAU - QUINONES-HINOJOSA, A., QUINONES-HINOJOSA A FAU - BARBARO, N. M., BARBARO NM FAU - GUPTA, N., GUPTA N FAU - KUNWAR, S., KUNWAR S FAU - LAWTON, M. T., LAWTON MT FAU - MCDERMOTT, M. W., MCDERMOTT MW FAU - PARSA, A. T., PARSA AT FAU - MANUEL-GARCIA VERDUGO, J., MANUEL-GARCIA VERDUGO J FAU - BERGER, M. S., BERGER MS FAU - ALVAREZ-BUYLLA, A. & ALVAREZ-BUYLLA, A. 2004. Unique astrocyte ribbon in adult human brain contains neural stem cells but lacks. *Nature,* 427**,** 740-4.

SANDBERG, M., PATIL, J., D'ANGELO, B., WEBER, S. G. & MALLARD, C. 2014. NRF2-regulation in brain health and disease: implication of cerebral inflammation. *Neuropharmacology,* 79**,** 298-306.

SANDELIN, A., ALKEMA, W., ENGSTROM, P., WASSERMAN, W. W. & LENHARD, B. 2004. JASPAR: an open-access database for eukaryotic transcription factor binding profiles. *Nucleic Acids Res,* 32**,** D91-4.

SANDOVAL, J., RODRIGUEZ, J. L., TUR, G., SERVIDDIO, G., PEREDA, J., BOUKABA, A., SASTRE, J., TORRES, L., FRANCO, L. & LOPEZ-RODAS, G. 2004. RNAPol-ChIP: a novel application of chromatin immunoprecipitation to the analysis of real-time gene transcription. *Nucleic Acids Res,* 32**,** e88.

SAWAMOTO, K., HIROTA, Y., ALFARO-CERVELLO, C., SORIANO-NAVARRO, M., HE, X., HAYAKAWA-YANO, Y., YAMADA, M., HIKISHIMA, K., TABATA, H., IWANAMI, A., NAKAJIMA, K., TOYAMA, Y., ITOH, T., ALVAREZ-BUYLLA, A., GARCIA-VERDUGO, J. M. & OKANO, H. 2011. Cellular composition and organization of the subventricular zone and rostral migratory stream in the adult and neonatal common marmoset brain. *J Comp Neurol,* 519**,** 690-713.

SAXE, M. D., BATTAGLIA, F., WANG, J. W., MALLERET, G., DAVID, D. J., MONCKTON, J. E., GARCIA, A. D., SOFRONIEW, M. V., KANDEL, E. R., SANTARELLI, L., HEN, R. & DREW, M. R. 2006. Ablation of hippocampal neurogenesis impairs contextual fear conditioning and synaptic plasticity in the dentate gyrus. *Proc Natl Acad Sci U S A,* 103**,** 17501-6.

SCHAFER, F. Q. & BUETTNER, G. R. 2001. Redox environment of the cell as viewed through the redox state of the glutathione disulfide/glutathione couple. *Free Radic Biol Med,* 30**,** 1191-212.

SCHARFMAN, H., GOODMAN, J., MACLEOD, A., PHANI, S., ANTONELLI, C. & CROLL, S. 2005. Increased neurogenesis and the ectopic granule cells after intrahippocampal BDNF infusion in adult rats. *Exp Neurol,* 192**,** 348-56.

SCHMIDT-HIEBER, C., JONAS, P. & BISCHOFBERGER, J. 2004. Enhanced synaptic plasticity in newly generated granule cells of the adult hippocampus. *Nature,* 429**,** 184-7.

SCHUMACKER, P. T. 2006. Reactive oxygen species in cancer cells: live by the sword, die by the sword. *Cancer Cell,* 10**,** 175-6.

SCHWAB, M. H., BARTHOLOMAE, A., HEIMRICH, B., FELDMEYER, D., DRUFFEL-AUGUSTIN, S., GOEBBELS, S., NAYA, F. J., ZHAO, S., FROTSCHER, M., TSAI, M. J. & NAVE, K. A. 2000. Neuronal basic helix-loop-helix proteins (NEX and BETA2/Neuro D) regulate terminal granule cell differentiation in the hippocampus. *J Neurosci,* 20**,** 3714-24.

SEKI, T. & ARAI, Y. 1999. Temporal and spacial relationships between PSA-NCAM-expressing, newly generated granule cells, and radial glia-like cells in the adult dentate gyrus. *J Comp Neurol,* 410**,** 503-13.

SELKOE, D. J. 2001. Alzheimer's disease: genes, proteins, and therapy. *Physiol Rev,* 81**,** 741-66.

SEO, S., HERR, A., LIM, J. W., RICHARDSON, G. A., RICHARDSON, H. & KROLL, K. L. 2005. Geminin regulates neuronal differentiation by antagonizing Brg1 activity. *Genes Dev,* 19**,** 1723-34.

SERCHOV, T., CLEMENT, H. W., SCHWARZ, M. K., IASEVOLI, F., TOSH, D. K., IDZKO, M., JACOBSON, K. A., DE BARTOLOMEIS, A., NORMANN, C., BIBER, K. & VAN CALKER, D. 2015. Increased Signaling via Adenosine A1 Receptors, Sleep Deprivation, Imipramine, and Ketamine Inhibit Depressive-like Behavior via Induction of Homer1a. *Neuron,* 87**,** 549-62.

SHIH, A. Y., JOHNSON, D. A., WONG, G., KRAFT, A. D., JIANG, L., ERB, H., JOHNSON, J. A. & MURPHY, T. H. 2003. Coordinate regulation of glutathione biosynthesis and release by Nrf2-expressing glia potently protects neurons from oxidative stress. *J Neurosci,* 23**,** 3394-406.

SHIN, J., BERG, D. A., ZHU, Y., SHIN, J. Y., SONG, J., BONAGUIDI, M. A., ENIKOLOPOV, G., NAUEN, D. W., CHRISTIAN, K. M., MING, G. L. & SONG, H. 2015. Single-Cell RNA-Seq with Waterfall Reveals Molecular Cascades underlying Adult Neurogenesis. *Cell Stem Cell,* 17**,** 360-72.

SILVA-PALACIOS, A., OSTOLGA-CHAVARRIA, M., ZAZUETA, C. & KONIGSBERG, M. 2018. Nrf2: Molecular and epigenetic regulation during aging. *Ageing Res Rev,* 47**,** 31-40.

SINGH, S. K., HAWKINS, C., CLARKE, I. D., SQUIRE, J. A., BAYANI, J., HIDE, T., HENKELMAN, R. M., CUSIMANO, M. D. & DIRKS, P. B. 2004. Identification of human brain tumour initiating cells. *Nature,* 432**,** 396-401.

SKIBINSKI, A., BREINDEL, J. L., PRAT, A., GALVAN, P., SMITH, E., ROLFS, A., GUPTA, P. B., LABAER, J. & KUPERWASSER, C. 2014. The Hippo transducer TAZ interacts with the SWI/SNF complex to regulate breast epithelial lineage commitment. *Cell Rep,* 6**,** 1059-1072.

SMITH, D. K., YANG, J., LIU, M. L. & ZHANG, C. L. 2016. Small Molecules Modulate Chromatin Accessibility to Promote NEUROG2-Mediated Fibroblast-to-Neuron Reprogramming. *Stem Cell Reports,* 7**,** 955-969.

SMITH, J., LADI, E., MAYER-PROSCHEL, M. & NOBLE, M. 2000. Redox state is a central modulator of the balance between self-renewal and differentiation in a dividing glial precursor cell. *Proc Natl Acad Sci U S A,* 97**,** 10032-7.

SMITH, J. A., DAS, A., RAY, S. K. & BANIK, N. L. 2012. Role of pro-inflammatory cytokines released from microglia in neurodegenerative diseases. *Brain Res Bull,* 87**,** 10-20.

SNYDER, J. S., KEE, N. & WOJTOWICZ, J. M. 2001. Effects of adult neurogenesis on synaptic plasticity in the rat dentate gyrus. *J Neurophysiol,* 85**,** 2423-31.

SOMASUNDARAM, K., REDDY, S. P., VINNAKOTA, K., BRITTO, R., SUBBARAYAN, M., NAMBIAR, S., HEBBAR, A., SAMUEL, C., SHETTY, M., SREEPATHI, H. K., SANTOSH, V., HEGDE, A. S., HEGDE, S., KONDAIAH, P. & RAO, M. R. 2005. Upregulation of ASCL1 and inhibition of Notch signaling pathway characterize progressive astrocytoma. *Oncogene,* 24**,** 7073-83.

SOMMER, L., MA, Q. & ANDERSON, D. J. 1996. neurogenins, a novel family of atonal-related bHLH transcription factors, are putative mammalian neuronal determination genes that reveal progenitor cell heterogeneity in the developing CNS and PNS. *Mol Cell Neurosci,* 8**,** 221-41.

SORRELLS, S. F., PAREDES, M. F., CEBRIAN-SILLA, A., SANDOVAL, K., QI, D., KELLEY, K. W., JAMES, D., MAYER, S., CHANG, J., AUGUSTE, K. I., CHANG, E. F., GUTIERREZ, A. J., KRIEGSTEIN, A. R., MATHERN, G. W., OLDHAM, M. C., HUANG, E. J., GARCIA-VERDUGO, J. M., YANG, Z. & ALVAREZ-BUYLLA, A. 2018. Human hippocampal neurogenesis drops sharply in children to undetectable levels in adults. *Nature,* 555**,** 377-381.

SPALDING, K. L., BERGMANN, O., ALKASS, K., BERNARD, S., SALEHPOUR, M., HUTTNER, H. B., BOSTROM, E., WESTERLUND, I., VIAL, C., BUCHHOLZ, B. A., POSSNERT, G., MASH, D. C., DRUID, H. & FRISEN, J. 2013. Dynamics of hippocampal neurogenesis in adult humans. *Cell,* 153**,** 1219-1227.

SPITZ, F. & FURLONG, E. E. 2012. Transcription factors: from enhancer binding to developmental control. *Nat Rev Genet,* 13**,** 613-26.

SRIURANPONG, V., BORGES, M. W., STROCK, C. L., NAKAKURA, E. K., WATKINS, D. N., BLAUMUELLER, C. M., NELKIN, B. D. & BALL, D. W. 2002. Notch signaling induces rapid degradation of achaete-scute homolog 1. *Mol Cell Biol,* 22**,** 3129-39.

STAMOS, J. L. & WEIS, W. I. 2013. The beta-catenin destruction complex. *Cold Spring Harb Perspect Biol,* 5**,** a007898.

STEEVENS, A. R., SOOKIASIAN, D. L., GLATZER, J. C. & KIERNAN, A. E. 2017. SOX2 is required for inner ear neurogenesis. *Sci Rep,* 7**,** 4086.

STEIN, C., BARDET, A. F., ROMA, G., BERGLING, S., CLAY, I., RUCHTI, A., AGARINIS, C., SCHMELZLE, T., BOUWMEESTER, T., SCHUBELER, D. & BAUER, A. 2015. YAP1 Exerts Its Transcriptional Control via TEAD-Mediated Activation of Enhancers. *PLoS Genet,* 11**,** e1005465.

STEINER, B., KLEMPIN, F., WANG, L., KOTT, M., KETTENMANN, H. & KEMPERMANN, G. 2006. Type-2 cells as link between glial and neuronal lineage in adult hippocampal neurogenesis. *Glia,* 54**,** 805-14.

STEINER, B., KRONENBERG, G., JESSBERGER, S., BRANDT, M. D., REUTER, K. & KEMPERMANN, G. 2004. Differential regulation of gliogenesis in the context of adult hippocampal neurogenesis in mice. *Glia,* 46**,** 41-52.

STONE, E. A. & LIN, Y. 2011. Open-space forced swim model of depression for mice. *Curr Protoc Neurosci,* Chapter 9**,** Unit9.36.

STRAHL, B. D. & ALLIS, C. D. 2000. The language of covalent histone modifications. *Nature,* 403**,** 41-5.

STUPP, R., HEGI, M. E., MASON, W. P., VAN DEN BENT, M. J., TAPHOORN, M. J., JANZER, R. C., LUDWIN, S. K., ALLGEIER, A., FISHER, B., BELANGER, K., HAU, P., BRANDES, A. A., GIJTENBEEK, J., MAROSI, C., VECHT, C. J., MOKHTARI, K., WESSELING, P., VILLA, S., EISENHAUER, E., GORLIA, T., WELLER, M., LACOMBE, D., CAIRNCROSS, J. G. & MIRIMANOFF, R. O. 2009. Effects of radiotherapy with concomitant and adjuvant temozolomide versus radiotherapy alone on survival in glioblastoma in a randomised phase III study: 5-year analysis of the EORTC-NCIC trial. *Lancet Oncol,* 10**,** 459-66.

SU, Z., ZANG, T., LIU, M. L., WANG, L. L., NIU, W. & ZHANG, C. L. 2014. Reprogramming the fate of human glioma cells to impede brain tumor development. *Cell Death Dis,* 5**,** e1463.

SUH, H., CONSIGLIO, A., RAY, J., SAWAI, T., D'AMOUR, K. A. & GAGE, F. H. 2007. In vivo fate analysis reveals the multipotent and self-renewal capacities of Sox2+ neural stem cells in the adult hippocampus. *Cell Stem Cell,* 1**,** 515-28.

SUH, H., DENG, W. & GAGE, F. H. 2009. Signaling in adult neurogenesis. *Annu Rev Cell Dev Biol,* 25**,** 253-75.

SUH, J. H., SHENVI, S. V., DIXON, B. M., LIU, H., JAISWAL, A. K., LIU, R. M. & HAGEN, T. M. 2004. Decline in transcriptional activity of Nrf2 causes age-related loss of glutathione synthesis, which is reversible with lipoic acid. *Proc Natl Acad Sci U S A,* 101**,** 3381-6.

SUN, G. J., SAILOR, K. A., MAHMOOD, Q. A., CHAVALI, N., CHRISTIAN, K. M., SONG, H. & MING, G. L. 2013. Seamless reconstruction of intact adult-born neurons by serial end-block imaging reveals complex axonal guidance and development in the adult hippocampus. *J Neurosci,* 33**,** 11400-11.

SUN, P., WANG, F., WANG, L., ZHANG, Y., YAMAMOTO, R., SUGAI, T., ZHANG, Q., WANG, Z. & KATO, N. 2011. Increase in cortical pyramidal cell excitability accompanies depression-like behavior in mice: a transcranial magnetic stimulation study. *J Neurosci,* 31**,** 16464-72.

SUZUKI, H., CHIBA, T., SUZUKI, T., FUJITA, T., IKENOUE, T., OMATA, M., FURUICHI, K., SHIKAMA, H. & TANAKA, K. 2000. Homodimer of two F-box proteins betaTrCP1 or betaTrCP2 binds to IkappaBalpha for signal-dependent ubiquitination. *J Biol Chem,* 275**,** 2877-84.

SUZUKI, T., MOTOHASHI, H. & YAMAMOTO, M. 2013. Toward clinical application of the Keap1-Nrf2 pathway. *Trends Pharmacol Sci,* 34**,** 340-6.

SWARTLING, F. J., BOLIN, S., PHILLIPS, J. J. & PERSSON, A. I. 2014. Signals that regulate the oncogenic fate of neural stem cells and progenitors. *Exp Neurol,* 260**,** 56-68.

SWARTLING, F. J., CANCER, M., FRANTZ, A., WEISHAUPT, H. & PERSSON, A. I. 2015. Deregulated proliferation and differentiation in brain tumors. *Cell Tissue Res,* 359**,** 225-54.

TAKAYA, K., SUZUKI, T., MOTOHASHI, H., ONODERA, K., SATOMI, S., KENSLER, T. W. & YAMAMOTO, M. 2012. Validation of the multiple sensor mechanism of the Keap1-Nrf2 system. *Free Radic Biol Med,* 53**,** 817-27.

TANG, Y., YU, P. & CHENG, L. 2017. Current progress in the derivation and therapeutic application of neural stem cells. *Cell Death Dis,* 8**,** e3108.

TAVAZOIE, M., VAN DER VEKEN, L., SILVA-VARGAS, V., LOUISSAINT, M., COLONNA, L., ZAIDI, B., GARCIA-VERDUGO, J. M. & DOETSCH, F. 2008. A specialized vascular niche for adult neural stem cells. *Cell Stem Cell,* 3**,** 279-88.

TERWEL, D., LASRADO, R., SNAUWAERT, J., VANDEWEERT, E., VAN HAESENDONCK, C., BORGHGRAEF, P. & VAN LEUVEN, F. 2005. Changed conformation of mutant Tau-P301L underlies the moribund tauopathy, absent in progressive, nonlethal axonopathy of Tau-4R/2N transgenic mice. *J Biol Chem,* 280**,** 3963-73.

THIMMULAPPA, R. K., MAI, K. H., SRISUMA, S., KENSLER, T. W., YAMAMOTO, M. & BISWAL, S. 2002. Identification of Nrf2-regulated genes induced by the chemopreventive agent sulforaphane by oligonucleotide microarray. *Cancer Res,* 62**,** 5196-203.

TIAN, T., LI, A., LU, H., LUO, R., ZHANG, M. & LI, Z. 2015. TAZ promotes temozolomide resistance by upregulating MCL-1 in human glioma cells. *Biochem Biophys Res Commun,* 463**,** 638-43.

TOBIN, M. K., MUSARACA, K., DISOUKY, A., SHETTI, A., BHERI, A., HONER, W. G., KIM, N., DAWE, R. J., BENNETT, D. A., ARFANAKIS, K. & LAZAROV, O. 2019. Human Hippocampal Neurogenesis Persists in Aged Adults and Alzheimer's Disease Patients. *Cell Stem Cell,* 24**,** 974-982.e3.

TODA, T. & GAGE, F. H. 2018. Review: adult neurogenesis contributes to hippocampal plasticity. *Cell Tissue Res,* 373**,** 693-709.

TONG, K. I., KATOH, Y., KUSUNOKI, H., ITOH, K., TANAKA, T. & YAMAMOTO, M. 2006. Keap1 recruits Neh2 through binding to ETGE and DLG motifs: characterization of the two-site molecular recognition model. *Mol Cell Biol,* 26**,** 2887-900.

TONG, K. I., PADMANABHAN, B., KOBAYASHI, A., SHANG, C., HIROTSU, Y., YOKOYAMA, S. & YAMAMOTO, M. 2007. Different electrostatic potentials define ETGE and DLG motifs as hinge and latch in oxidative stress response. *Mol Cell Biol,* 27**,** 7511-21.

TONI, N., LAPLAGNE, D. A., ZHAO, C., LOMBARDI, G., RIBAK, C. E., GAGE, F. H. & SCHINDER, A. F. 2008. Neurons born in the adult dentate gyrus form functional synapses with target cells. *Nat Neurosci,* 11**,** 901-7.

TOTARO, A., CASTELLAN, M., BATTILANA, G., ZANCONATO, F., AZZOLIN, L., GIULITTI, S., CORDENONSI, M. & PICCOLO, S. 2017. YAP/TAZ link cell mechanics to Notch signalling to control epidermal stem cell fate. *Nat Commun,* 8**,** 15206.

TOTARO, A., CASTELLAN, M., DI BIAGIO, D. & PICCOLO, S. 2018. Crosstalk between YAP/TAZ and Notch Signaling. *Trends Cell Biol,* 28**,** 560-573.

TOYOKUNI, S., OKAMOTO, K., YODOI, J. & HIAI, H. 1995. Persistent oxidative stress in cancer. *FEBS Lett,* 358**,** 1-3.

TRIVINO-PAREDES, J., PATTEN, A. R., GIL-MOHAPEL, J. & CHRISTIE, B. R. 2016. The effects of hormones and physical exercise on hippocampal structural plasticity. *Front Neuroendocrinol,* 41**,** 23-43.

TROMPOUKI, E., BOWMAN, T. V., LAWTON, L. N., FAN, Z. P., WU, D. C., DIBIASE, A., MARTIN, C. S., CECH, J. N., SESSA, A. K., LEBLANC, J. L., LI, P., DURAND, E. M., MOSIMANN, C., HEFFNER, G. C., DALEY, G. Q., PAULSON, R. F., YOUNG, R. A. & ZON, L. I. 2011. Lineage regulators direct BMP and Wnt pathways to cell-specific programs during differentiation and regeneration. *Cell,* 147**,** 577-89.

TROPEPE, V., SIBILIA, M., CIRUNA, B. G., ROSSANT, J., WAGNER, E. F. & VAN DER KOOY, D. 1999. Distinct neural stem cells proliferate in response to EGF and FGF in the developing mouse telencephalon. *Dev Biol,* 208**,** 166-88.

TSATMALI, M., WALCOTT, E. C. & CROSSIN, K. L. 2005. Newborn neurons acquire high levels of reactive oxygen species and increased mitochondrial proteins upon differentiation from progenitors. *Brain Res,* 1040**,** 137-50.

UDA, M., ISHIDO, M. & KAMI, K. 2007. Features and a possible role of Mash1-immunoreactive cells in the dentate gyrus of the hippocampus in the adult rat. *Brain Res,* 1171**,** 9-17.

VALENCIA-SAMA, I., ZHAO, Y., LAI, D., JANSE VAN RENSBURG, H. J., HAO, Y. & YANG, X. 2015. Hippo Component TAZ Functions as a Co-repressor and Negatively Regulates DeltaNp63 Transcription through TEA Domain (TEAD) Transcription Factor. *J Biol Chem,* 290**,** 16906-17.

VAN PRAAG, H., CHRISTIE, B. R., SEJNOWSKI, T. J. & GAGE, F. H. 1999. Running enhances neurogenesis, learning, and long-term potentiation in mice. *Proc Natl Acad Sci U S A,* 96**,** 13427-31.

VARELA-NALLAR, L. & INESTROSA, N. C. 2013. Wnt signaling in the regulation of adult hippocampal neurogenesis. *Front Cell Neurosci,* 7**,** 100.

VARELAS, X. 2014. The Hippo pathway effectors TAZ and YAP in development, homeostasis and disease. *Development,* 141**,** 1614-26.

VARELAS, X., SAKUMA, R., SAMAVARCHI-TEHRANI, P., PEERANI, R., RAO, B. M., DEMBOWY, J., YAFFE, M. B., ZANDSTRA, P. W. & WRANA, J. L. 2008. TAZ controls Smad nucleocytoplasmic shuttling and regulates human embryonic stem-cell self-renewal. *Nat Cell Biol,* 10**,** 837-48.

VARELAS, X., SAMAVARCHI-TEHRANI, P., NARIMATSU, M., WEISS, A., COCKBURN, K., LARSEN, B. G., ROSSANT, J. & WRANA, J. L. 2010. The Crumbs complex couples cell density sensing to Hippo-dependent control of the TGF-beta-SMAD pathway. *Dev Cell,* 19**,** 831-44.

VENUGOPAL, R. & JAISWAL, A. K. 1996. Nrf1 and Nrf2 positively and c-Fos and Fra1 negatively regulate the human antioxidant response element-mediated expression of NAD(P)H:quinone oxidoreductase1 gene. *Proc Natl Acad Sci U S A,* 93**,** 14960-5.

VENUGOPAL, R. & JAISWAL, A. K. 1998. Nrf2 and Nrf1 in association with Jun proteins regulate antioxidant response element-mediated expression and coordinated induction of genes encoding detoxifying enzymes. *Oncogene,* 17**,** 3145-56.

VIDAL, M., MORRIS, R., GROSVELD, F. & SPANOPOULOU, E. 1990. Tissue-specific control elements of the Thy-1 gene. *Embo j,* 9**,** 833-40.

VIERBUCHEN, T., OSTERMEIER, A., PANG, Z. P., KOKUBU, Y., SUDHOF, T. C. & WERNIG, M. 2010. Direct conversion of fibroblasts to functional neurons by defined factors. *Nature,* 463**,** 1035-41.

VISVADER, J. E. 2011. Cells of origin in cancer. *Nature,* 469**,** 314-22.

VON OTTER, M., LANDGREN, S., NILSSON, S., ZETTERBERG, M., CELOJEVIC, D., BERGSTROM, P., MINTHON, L., BOGDANOVIC, N., ANDREASEN, N., GUSTAFSON, D. R., SKOOG, I., WALLIN, A., TASA, G., BLENNOW, K., NILSSON, M., HAMMARSTEN, O. & ZETTERBERG, H. 2010. Nrf2-encoding NFE2L2 haplotypes influence disease progression but not risk in Alzheimer's disease and age-related cataract. *Mech Ageing Dev,* 131**,** 105-10.

WAKABAYASHI, N., CHARTOUMPEKIS, D. V. & KENSLER, T. W. 2015. Crosstalk between Nrf2 and Notch signaling. *Free Radic Biol Med,* 88**,** 158-167.

WAKABAYASHI, N., SHIN, S., SLOCUM, S. L., AGOSTON, E. S., WAKABAYASHI, J., KWAK, M. K., MISRA, V., BISWAL, S., YAMAMOTO, M. & KENSLER, T. W. 2010. Regulation of notch1 signaling by nrf2: implications for tissue regeneration. *Sci Signal,* 3**,** ra52.

WALTON, N. M., SHIN, R., TAJINDA, K., HEUSNER, C. L., KOGAN, J. H., MIYAKE, S., CHEN, Q., TAMURA, K. & MATSUMOTO, M. 2012. Adult neurogenesis transiently generates oxidative stress. *PLoS One,* 7**,** e35264.

WANG, H., LEI, Q., OOSTERVEEN, T., ERICSON, J. & MATISE, M. P. 2011. Tcf/Lef repressors differentially regulate Shh-Gli target gene activation thresholds to generate progenitor patterning in the developing CNS. *Development,* 138**,** 3711-21.

WANG, H., LIU, K., GENG, M., GAO, P., WU, X., HAI, Y., LI, Y., LI, Y., LUO, L., HAYES, J. D., WANG, X. J. & TANG, X. 2013. RXRalpha inhibits the NRF2-ARE signaling pathway through a direct interaction with the Neh7 domain of NRF2. *Cancer Res,* 73**,** 3097-108.

WANG, M., LIU, Y., ZOU, J., YANG, R., XUAN, F., WANG, Y., GAO, N. & CUI, H. 2015a. Transcriptional co-activator TAZ sustains proliferation and tumorigenicity of neuroblastoma by targeting CTGF and PDGF-beta. *Oncotarget,* 6**,** 9517-30.

WANG, Q., XU, Z., AN, Q., JIANG, D., WANG, L., LIANG, B. & LI, Z. 2015b. TAZ promotes epithelial to mesenchymal transition via the upregulation of connective tissue growth factor expression in neuroblastoma cells. *Mol Med Rep,* 11**,** 982-8.

WANG, S., SCOTT, B. W. & WOJTOWICZ, J. M. 2000. Heterogenous properties of dentate granule neurons in the adult rat. *J Neurobiol,* 42**,** 248-57.

WANG, X., ZAIDI, A., PAL, R., GARRETT, A. S., BRACERAS, R., CHEN, X. W., MICHAELIS, M. L. & MICHAELIS, E. K. 2009. Genomic and biochemical approaches in the discovery of mechanisms for selective neuronal vulnerability to oxidative stress. *BMC Neurosci,* 10**,** 12.

WAPINSKI, O. L., VIERBUCHEN, T., QU, K., LEE, Q. Y., CHANDA, S., FUENTES, D. R., GIRESI, P. G., NG, Y. H., MARRO, S., NEFF, N. F., DRECHSEL, D., MARTYNOGA, B., CASTRO, D. S., WEBB, A. E., SUDHOF, T. C., BRUNET, A., GUILLEMOT, F., CHANG, H. Y. & WERNIG, M. 2013. Hierarchical mechanisms for direct reprogramming of fibroblasts to neurons. *Cell,* 155**,** 621-35.

WEN, P. H., FRIEDRICH, V. L., JR., SHIOI, J., ROBAKIS, N. K. & ELDER, G. A. 2002. Presenilin-1 is expressed in neural progenitor cells in the hippocampus of adult mice. *Neurosci Lett,* 318**,** 53-6.

WEN, P. Y. & KESARI, S. 2008. Malignant gliomas in adults. *N Engl J Med,* 359**,** 492-507.

WESTERMARK, B., PONTEN, J. & HUGOSSON, R. 1973. Determinants for the establishment of permanent tissue culture lines from human gliomas. *Acta Pathol Microbiol Scand A,* 81**,** 791-805.

WHITLOCK, J. R., HEYNEN, A. J., SHULER, M. G. & BEAR, M. F. 2006. Learning induces long-term potentiation in the hippocampus. *Science,* 313**,** 1093-7.

WIESNER, D., MERDIAN, I., LEWERENZ, J., LUDOLPH, A. C., DUPUIS, L. & WITTING, A. 2013. Fumaric acid esters stimulate astrocytic VEGF expression through HIF-1alpha and Nrf2. *PLoS One,* 8**,** e76670.

WILD, A. C., MOINOVA, H. R. & MULCAHY, R. T. 1999. Regulation of gamma-glutamylcysteine synthetase subunit gene expression by the transcription factor Nrf2. *J Biol Chem,* 274**,** 33627-36.

WILSON, R. S., LEURGANS, S. E., BOYLE, P. A. & BENNETT, D. A. 2011. Cognitive decline in prodromal Alzheimer disease and mild cognitive impairment. *Arch Neurol,* 68**,** 351-6.

WROBEL, C. N., MUTCH, C. A., SWAMINATHAN, S., TAKETO, M. M. & CHENN, A. 2007. Persistent expression of stabilized beta-catenin delays maturation of radial glial cells into intermediate progenitors. *Dev Biol,* 309**,** 285-97.

WU, G., XU, G., SCHULMAN, B. A., JEFFREY, P. D., HARPER, J. W. & PAVLETICH, N. P. 2003. Structure of a beta-TrCP1-Skp1-beta-catenin complex: destruction motif binding and lysine specificity of the SCF(beta-TrCP1) ubiquitin ligase. *Mol Cell,* 11**,** 1445-56.

WU, T., HARDER, B. G., WONG, P. K., LANG, J. E. & ZHANG, D. D. 2015. Oxidative stress, mammospheres and Nrf2-new implication for breast cancer therapy? *Mol Carcinog,* 54**,** 1494-502.

WU, T., ZHAO, F., GAO, B., TAN, C., YAGISHITA, N., NAKAJIMA, T., WONG, P. K., CHAPMAN, E., FANG, D. & ZHANG, D. D. 2014. Hrd1 suppresses Nrf2-mediated cellular protection during liver cirrhosis. *Genes Dev,* 28**,** 708-22.

XAPELLI, S., AGASSE, F., SARDA-ARROYO, L., BERNARDINO, L., SANTOS, T., RIBEIRO, F. F., VALERO, J., BRAGANCA, J., SCHITINE, C., DE MELO REIS, R. A., SEBASTIAO, A. M. & MALVA, J. O. 2013. Activation of type 1 cannabinoid receptor (CB1R) promotes neurogenesis in murine subventricular zone cell cultures. *PLoS One,* 8**,** e63529.

XU, L., YANG, Y., GAO, L., ZHAO, J., CAI, Y., HUANG, J., JING, S., BAO, X., WANG, Y., GAO, J., XU, H. & FAN, X. 2015. Protective effects of resveratrol on the inhibition of hippocampal neurogenesis induced by ethanol during early postnatal life. *Biochim Biophys Acta,* 1852**,** 1298-310.

YAMAMOTO, T., KYO, M., KAMIYA, T., TANAKA, T., ENGEL, J. D., MOTOHASHI, H. & YAMAMOTO, M. 2006. Predictive base substitution rules that determine the binding and transcriptional specificity of Maf recognition elements. *Genes Cells,* 11**,** 575-91.

YANG, R., WU, Y., ZOU, J., ZHOU, J., WANG, M., HAO, X. & CUI, H. 2016. The Hippo transducer TAZ promotes cell proliferation and tumor formation of glioblastoma cells through EGFR pathway. *Oncotarget,* 7**,** 36255-36265.

YANG, X. & XU, T. 2011. Molecular mechanism of size control in development and human diseases. *Cell Res,* 21**,** 715-29.

YASUHARA, T., SHINGO, T. & DATE, I. 2004. The potential role of vascular endothelial growth factor in the central nervous system. *Rev Neurosci,* 15**,** 293-307.

YE, F. & ZHANG, M. 2013. Structures and target recognition modes of PDZ domains: recurring themes and emerging pictures. *Biochem J,* 455**,** 1-14.

YONEYAMA, M., KAWADA, K., GOTOH, Y., SHIBA, T. & OGITA, K. 2010. Endogenous reactive oxygen species are essential for proliferation of neural stem/progenitor cells. *Neurochem Int,* 56**,** 740-6.

YUAN, T. F., GU, S., SHAN, C., MARCHADO, S. & ARIAS-CARRION, O. 2015. Oxidative Stress and Adult Neurogenesis. *Stem Cell Rev,* 11**,** 706-9.

ZECHNER, D., FUJITA, Y., HULSKEN, J., MULLER, T., WALTHER, I., TAKETO, M. M., CRENSHAW, E. B., 3RD, BIRCHMEIER, W. & BIRCHMEIER, C. 2003. beta-Catenin signals regulate cell growth and the balance between progenitor cell expansion and differentiation in the nervous system. *Dev Biol,* 258**,** 406-18.

ZENDER, L., SPECTOR, M. S., XUE, W., FLEMMING, P., CORDON-CARDO, C., SILKE, J., FAN, S. T., LUK, J. M., WIGLER, M., HANNON, G. J., MU, D., LUCITO, R., POWERS, S. & LOWE, S. W. 2006. Identification and validation of oncogenes in liver cancer using an integrative oncogenomic approach. *Cell,* 125**,** 1253-67.

ZHANG, D. D. & HANNINK, M. 2003. Distinct cysteine residues in Keap1 are required for Keap1-dependent ubiquitination of Nrf2 and for stabilization of Nrf2 by chemopreventive agents and oxidative stress. *Mol Cell Biol,* 23**,** 8137-51.

ZHANG, H., DAVIES, K. J. A. & FORMAN, H. J. 2015. Oxidative stress response and Nrf2 signaling in aging. *Free Radic Biol Med,* 88**,** 314-336.

ZHANG, H., DEO, M., THOMPSON, R. C., UHLER, M. D. & TURNER, D. L. 2012. Negative regulation of Yap during neuronal differentiation. *Dev Biol,* 361**,** 103-15.

ZHANG, H., LIU, C. Y., ZHA, Z. Y., ZHAO, B., YAO, J., ZHAO, S., XIONG, Y., LEI, Q. Y. & GUAN, K. L. 2009. TEAD transcription factors mediate the function of TAZ in cell growth and epithelial-mesenchymal transition. *J Biol Chem,* 284**,** 13355-62.

ZHANG, L., CHENG, F., WEI, Y., ZHANG, L., GUO, D., WANG, B. & LI, W. 2019. Inhibition of TAZ contributes radiation-induced senescence and growth arrest in glioma cells. *Oncogene,* 38**,** 2788-2799.

ZHANG, L., YANG, X., YANG, S. & ZHANG, J. 2011. The Wnt /beta-catenin signaling pathway in the adult neurogenesis. *Eur J Neurosci,* 33**,** 1-8.

ZHANG, S., ZHANG, C., SONG, Y., ZHANG, J. & XU, J. 2018. Prognostic role of survivin in patients with glioma. *Medicine (Baltimore),* 97**,** e0571.

ZHANG, Y., CHEN, K., SLOAN, S. A., BENNETT, M. L., SCHOLZE, A. R., O'KEEFFE, S., PHATNANI, H. P., GUARNIERI, P., CANEDA, C., RUDERISCH, N., DENG, S., LIDDELOW, S. A., ZHANG, C., DANEMAN, R., MANIATIS, T., BARRES, B. A. & WU, J. Q. 2014. An RNA-sequencing transcriptome and splicing database of glia, neurons, and vascular cells of the cerebral cortex. *J Neurosci,* 34**,** 11929-47.

ZHANG, Y., SLOAN, S. A., CLARKE, L. E., CANEDA, C., PLAZA, C. A., BLUMENTHAL, P. D., VOGEL, H., STEINBERG, G. K., EDWARDS, M. S., LI, G., DUNCAN, J. A., 3RD, CHESHIER, S. H., SHUER, L. M., CHANG, E. F., GRANT, G. A., GEPHART, M. G. & BARRES, B. A. 2016. Purification and Characterization of Progenitor and Mature Human Astrocytes Reveals Transcriptional and Functional Differences with Mouse. *Neuron,* 89**,** 37-53.

ZHAO, B., YE, X., YU, J., LI, L., LI, W., LI, S., YU, J., LIN, J. D., WANG, C. Y., CHINNAIYAN, A. M., LAI, Z. C. & GUAN, K. L. 2008a. TEAD mediates YAP-dependent gene induction and growth control. *Genes Dev,* 22**,** 1962-71.

ZHAO, C., DENG W FAU - GAGE, F. H. & GAGE, F. H. 2008b. Mechanisms and functional implications of adult neurogenesis. *Cell,* 132**,** 645-60 LID - 10.1016/j.cell.2008.01.033 [doi].

ZHAO, C., TENG, E. M., SUMMERS, R. G., JR., MING, G. L. & GAGE, F. H. 2006. Distinct morphological stages of dentate granule neuron maturation in the adult mouse hippocampus. *J Neurosci,* 26**,** 3-11.

ZHAO, F., WU, T., LAU, A., JIANG, T., HUANG, Z., WANG, X. J., CHEN, W., WONG, P. K. & ZHANG, D. D. 2009. Nrf2 promotes neuronal cell differentiation. *Free Radic Biol Med,* 47**,** 867-79.

ZHAO, X., SUN, G., ZHANG, J., TING, S. M., GONZALES, N. & ARONOWSKI, J. 2015. Dimethyl Fumarate Protects Brain From Damage Produced by Intracerebral Hemorrhage by Mechanism Involving Nrf2. *Stroke,* 46**,** 1923-8.

ZHENG, H., YING, H., YAN, H., KIMMELMAN, A. C., HILLER, D. J., CHEN, A. J., PERRY, S. R., TONON, G., CHU, G. C., DING, Z., STOMMEL, J. M., DUNN, K. L., WIEDEMEYER, R., YOU, M. J., BRENNAN, C., WANG, Y. A., LIGON, K. L., WONG, W. H., CHIN, L. & DEPINHO, R. A. 2008. p53 and Pten control neural and glioma stem/progenitor cell renewal and differentiation. *Nature,* 455**,** 1129-33.

ZHOU, C. J., ZHAO, C. & PLEASURE, S. J. 2004. Wnt signaling mutants have decreased dentate granule cell production and radial glial scaffolding abnormalities. *J Neurosci,* 24**,** 121-6.

ZHU, J., WANG, H., FAN, Y., HU, Y., JI, X., SUN, Q. & LIU, H. 2014. Knockdown of nuclear factor erythroid 2-related factor 2 by lentivirus induces differentiation of glioma stem-like cells. *Oncol Rep,* 32**,** 1170-8.

ZHU, J., WANG, H., SUN, Q., JI, X., ZHU, L., CONG, Z., ZHOU, Y., LIU, H. & ZHOU, M. 2013. Nrf2 is required to maintain the self-renewal of glioma stem cells. *BMC Cancer,* 13**,** 380.

ZIGOVA, T., PENCEA, V., WIEGAND, S. J. & LUSKIN, M. B. 1998. Intraventricular administration of BDNF increases the number of newly generated neurons in the adult olfactory bulb. *Mol Cell Neurosci,* 11**,** 234-45.

ZONG, H., PARADA, L. F. & BAKER, S. J. 2015. Cell of origin for malignant gliomas and its implication in therapeutic development. *Cold Spring Harb Perspect Biol,* 7.

# APPENDICES

# APPENDIX I

**Appendix I.** Script created with Python to compare in human genes the putative AREs, TEAD, SMADs and RUNX- binding sequences with the PSSM and calculate their relative score. In green are the values which have to been changed for each transcription factor. **|Max|** and **|Min|** correspond to absolute value of maximum and minimum calculated from PSSM matrix and **N** correspond to the number of positions of PSSM matrix. PSSM is obtained from the frequency matrix of each transcription factor from JASPAR database.

```
import sys
import re

def Get_PSSM(FileName):
   tmp=(Ihrie and Alvarez-Buylla, 2011)
   MyFile=open(FileName,'r')
   for Nt in ["A","C","G","T"]:
      pos=MyFile.readline()
      tmp[Nt]=pos.strip().split("\t")
   MyFile.close()
   return(tmp)

def Get_Coordin(Coord):
   MyRE=r'(\w*)(chr[0-9XY]{1,2}):(\d+)-(\d+)'
   MyReg=re.compile(MyRE)
   Res=MyReg.search(Coord)
   return(Res.groups())

def Get_MaxScore(Seq,PSSM):
   MaxSc=-100000
   book={}
   for idx in range(len(Seq)-len(PSSM["A"])+1):
      tmpSc=0
      sseq=""
      sequence=[]
      sequence2=[]
      for pos in range(len(PSSM["A"])):
         tmpSc=tmpSc+float(PSSM[Seq[idx+pos]][pos])
         sseq=sseq + Seq[idx+pos]
      if MaxSc<tmpSc:
         MaxSc=tmpSc
         sequence.append(str(tmpSc))
         sequence2.append(sseq)
         book=dict(list(book.items()) + list((dict(zip(sequence,sequence2))).items()))
   return(MaxSc)

def Get_Seq(Seq,PSSM):
   MaxSc=-100000
   book={}
   for idx in range(len(Seq)-len(PSSM["A"])+1):
      tmpSc=0
      sseq=""
      sequence=[]
      sequence2=[]
      for pos in range(len(PSSM["A"])):
         tmpSc=tmpSc+float(PSSM[Seq[idx+pos]][pos])
         sseq=sseq + Seq[idx+pos]
      if MaxSc<tmpSc:
         MaxSc=tmpSc
         sequence.append(str(tmpSc))
         sequence2.append(sseq)
         book=dict(list(book.items()) + list((dict(zip(sequence,sequence2))).items()))
   return(book[str(MaxSc)]))
```

```
def Main(Args):
   PSSM={}
   PSSM=Get_PSSM(Args[1])
   MyFile=open(Args[2],'r')
   for Line in MyFile:
      Fields=Line.strip().split("\t")
      (Name,Chr,Str,End)=Get_Coordin(Fields[0])
      directseq=Fields[1]
      basecomplement={"A":"T":"C":"G","T":"A":"G":"C"}
      rDNAsense=directseq[::-1]
      antisenseDNA=""
      for base in rDNAsense:
         antisenseDNA = antisenseDNA+basecomplement[base]
      MaxScore=Get_MaxScore(Fields[1].upper(),PSSM)
      MaxScore2=Get_MaxScore(antisenseDNA.upper(),PSSM)
      Sequence=Get_Seq(Fields[1].upper(),PSSM)
      Sequence2=Get_Seq(antisenseDNA.upper(),PSSM)
      finded= Fields[1].find(Sequence)
      finded2= antisenseDNA.find(Sequence2)
      if int(Str)>int(End):
         print(Name,"\t",Chr,"\t",str(int(Str)-finded),"\t",str(int(Str)-finded-
N),"\t",
            round(MaxScore,2),"\t",round(MaxScore+|Min|)/(|Max|+|Min|),3),"\t",
            Sequence,"\t", str(finded2+int(End)),"\t", str(finded2+int(End)+N),"\t",

            round(MaxScore2,2),"\t",round(MaxScore2+|Min|)/(|Max|+|Min|),3),"\t",Seque
      nce2)
      else:
         print(Name,"\t",Chr,"\t",str(finded+int(Str)),"\t",str(finded+int(Str)+N),"\t
",
            round(MaxScore,2),"\t",round(MaxScore+|Min|)/(|Max|+|Min|),3),"\t",
            Sequence,"\t",str(int(End)-finded2),"\t",str(int(End)-finded2-N),"\t",
            round(MaxScore2,2),"\t",round(MaxScore2+|Min|)/(|Max|+|Min|),3),"\t",Seque
nce2)
   MyFile.close()

if__name__=='__main__':
   if len(sys.argv)<2:
      print("You must provide the name of the files containing the sequences and
PSSM")
   else:
      Main(sys.argv)
   sys.exit()
```

# APPENDIX II

## Research articles related to the thesis.

- **Robledinos-Antón, N**., Rojo AI., Ferreiro, E., Núñez, Á., Krause, KH., Jaquet, V., Cuadrado, A. Transcription factor NRF2 controls the fate of neural stem cells in the subgranular zone of the hippocampus. Redox Biol. 2017 Jun 27;13:393-401. doi: 10.1016/j.redox.2017.06.010. Impact factor 2017/2018: 7.126.
- Escoll M, Lastra D, Pajares M, **Robledinos-Antón N**, Rojo AI, Fernández-Ginés R, Mendiola M, Martínez-Marín V, Esteban I, Gargini R, and Cuadrado A. Transcription factor NRF2 uses the Hippo pathway effector TAZ to induce tumorigenesis in glioblastomas. *Under review in Cell Reports.* Impact factor 2018: 7.815.
- **Robledinos-Antón, N**., Escoll M., Cuadrado, A. Hippo pathway effector TAZ is a transcriptional corepressor of neuronal differentiation. *In preparation.*

## Reviews.

- Dao VT, Casas AI, Maghzal GJ, Seredenina T, Kaludercic N, **Robledinos-Antón N**, Di Lisa F, Stocker R, Ghezzi P, Jaquet V, Cuadrado A, Schmidt HH. Pharmacology and Clinical Drug Candidates in Redox Medicine. Antioxid Redox Signal. 2015 Nov 10;23(14):1113-29. doi: 10.1089/ars.2015.6430. Epub 2015 Nov 6. Impact factor 2015: 7.093.
- Egea J, Fabregat I, Frapart YM, …, **Robledinos-Antón N**, …, Daiber A. European contribution to the study of ROS: A summary of the findings and prospects for the future from the COST action BM1203 (EU-ROS). Redox Biol. 2017 May 18;13:94-162. doi: 10.1016/j.redox.2017.05.007. Impact factor 2017/2018: 7.126.
- Cuadrado, A., Manda, G., Hassan, A., Alcaraz, MJ., Barbas, C., Daiber, A., Ghezzi, P., León, R., López, MG., Oliva, B., Pajares, M., Rojo, AI, **Robledinos-Antón, N**., Valverde, AM., Guney, E., Schmidt, HHHW. Transcription Factor NRF2 as a Therapeutic Target for Chronic Diseases: A Systems Medicine Approach. Pharmacol Rev. 2018 Apr;70(2):348-383. doi: 10.1124/pr.117.014753. Impact factor 2017/2018: 18.96.
- **Robledinos-Antón N**, Fernández-Ginés R, Manda G and Cuadrado A. Activators and inhibitors of NRF2: a review of its clinical development. Oxid Med Cell Longev. 2019 Jul 14;2019:9372182. doi: 10.1155/2019/9372182. eCollection 2019. Review. Impact factor 2018/2019: 4.868.

## Other research articles published during the PhD.

- Gonzalez-Cano L*, Fuertes-Alvarez S*, **Robledinos-Antón N**, Fariñas I, Marques, M.M, and Marin, M.C. p73 is required for ependymal cell maturation and neurogenic SVZ

cytoarchitecture. Dev Neurobiol. 2015 Oct 20. doi: 10.1002/dneu.22356. Impact factor 2015: 2.259.

- Nayernia, Z., Colaianna, M., **Robledinos-Antón, N**. Gutzwiller, E., Sloan-Béna, F., Stathaki, E., Hibaoui, Y., Cuadrado, A., Hescheler, J., Stasia, MJ., Saric, T., Jaquet, V., Krause, KH. Decreased neural precursor cell pool in NADPH oxidase 2-deficiency: from mouse brain to neural differentiation of patient derived iPSC. Redox Biol. 2017 Apr 24;13:82-93. doi: 10.1016/j.redox.2017.04.026. Impact factor 2017/2018: 7.126.

- Martin-Hurtado A, Martin-Morales R, **Robledinos-Antón N**, Blanco R, Palacios-Blanco I, Lastres-Becker I, Cuadrado A, and Garcia-Gonzalo FR NRF2-dependent gene expression promotes ciliogenesis and Hedgehog signaling. *Under review in Scientific Reports.* Impact factor 2018: 4.525.

Redox Biology 13 (2017) 393–401

Contents lists available at ScienceDirect

Redox Biology

journal homepage: www.elsevier.com/locate/redox

Research paper

# Transcription factor NRF2 controls the fate of neural stem cells in the subgranular zone of the hippocampus

Natalia Robledinos-Antón[a], Ana I. Rojo[a], Elisabete Ferreiro[b], Ángel Núñez[c], Karl-Heinz Krause[d], Vincent Jaquet[d], Antonio Cuadrado[a,*]

[a] Instituto de Investigaciones Biomédicas "Alberto Sols", Faculty of Medicine, Autonomous University of Madrid (UAM), Centro de Investigación Biomédica en Red sobre Enfermedades Neurodegenerativas (CIBERNED), Madrid, Spain
[b] Center for Neuroscience and Cell Biology, Institute for Interdisciplinary Research (IIIUC), University of Coimbra, Portugal
[c] Department of Anatomy, Histology and Neuroscience, Autonomous University of Madrid, Madrid, Spain
[d] Department of Pathology and Immunology, University of Geneva Medical School, 1 rue Michel Servet, 1211 Geneva, Switzerland

ARTICLE INFO

*Keywords:*
Hippocampal neurogenesis
Aging
NRF2
Neural stem cells
Subgranular zone
Oxidative stress

ABSTRACT

Neural stem/progenitor cells (NSPCs) located at the subgranular zone (SGZ) of the hippocampus participate in the maintenance of synaptic networks that ensure cognitive functions during life. Although it is known that this neurogenic niche losses activity with oxidative stress and ageing, the molecular events involved in its regulation are largely unknown. Here, we studied the role of transcription factor Nuclear Factor-Erythroid 2-Related Factor 2 (NRF2) in the control of NSPCs destinies in the SGZ. We first describe that NRF2-knockout (*Nrf2*$^{-/-}$) mice exhibit impaired long term potentiation, a function that requires integrity of the SGZ, therefore suggesting a cognitive deficit that might be linked to hippocampal neurogenesis. Then, we found a reduction in NSCs from birth to adulthood that was exacerbated in *Nrf2*$^{-/-}$ vs. *Nrf2*$^{+/+}$ mice. The clonogenic and proliferative capacity of SGZ-derived NSPCs from newborn and 3-month-old *Nrf2*$^{-/-}$ mice was severely reduced as determined in neurosphere cultures. *Nrf2*-deficiency also impaired neuronal differentiation both the SGZ, and in neurosphere differentiation assays, leading to an abnormal production of astrocytes and oligodendrocytes vs. neurons. Rescue of *Nrf2*$^{-/-}$ NSPCs by ectopic expression of NRF2 attenuated the alterations in clonogenic, proliferative and differentiating capacity of hippocampal NSPCs. In turn, knockdown of the NRF2 gene in wild type NSPCs reproduced the data obtained with *Nrf2*$^{-/-}$ NSPCs. Our findings demonstrate the importance of NRF2 in the maintenance of proper proliferation and differentiation rates of hippocampal NSPCs and suggest that interventions to up-regulate NRF2 might provide a mechanism to preserve the neurogenic functionality of the hippocampus.

## 1. Introduction

Nuclear Factor-Erythroid 2-Related Factor 2 (NRF2) is a transcription factor that regulates homeostatic responses to multiple stressors. Initially connected with biotransformation reactions, it is known to participate in the regulation of hundreds of human genes involved in antioxidant defense, anti-inflammatory response, autophagy, metabolic reprograming of tumor cells, etc. [1–4]. Modulation of the expression of these genes provides a global cellular response to promote cell survival, cell growth, self-renewal, differentiation, proliferation, and increased lifespan, which may be relevant to the function of stem cells [5–7]. NRF2 is expressed in virtually every tissue and promotes survival of stem cells from several origins [8–10]. In the brain, the direct implication of NRF2 in regulation of neural stem cells (NSCs) has been reported only in connection with the normal decline of its activity during aging and the reduction of the NSCs pool at the subventricular zone (SVZ) of the striatum [11].

The adult brain harbors another region of persistent lifelong neurogenesis: the subgranular zone (SGZ) of the *dentate gyrus* (DG) that has been much less explored [12]. This region contains quiescent neural stem cells (NSCs) that on specific demands are mobilized towards generation of rapidly-dividing neural progenitor cells (NPCs), neurons and astrocytes. Newly generated granular neurons are required for the electrophysiological functioning of the perforant path (PP), involved in spatial learning and memory consolidation [13–15]. Progressive loss of neurogenesis at the SGZ has been associated with aging, which also correlates with decline of NRF2 activity [16,17] and with alterations in redox homeostasis. In fact, a relevance of reactive oxygen species (ROS)

* Correspondence to: Instituto de Investigaciones Biomédicas "Alberto Sols", C/ Arturo Duperier 4, 28029 Madrid, Spain.
*E-mail address:* antonio.cuadrado@uam.es (A. Cuadrado).

http://dx.doi.org/10.1016/j.redox.2017.06.010
Received 20 April 2017; Received in revised form 30 May 2017; Accepted 25 June 2017
Available online 27 June 2017

in neural stem/progenitor cell (NSPCs) physiology is suggested by high expression levels of antioxidant genes encoding SOD1, SOD2, GPX, etc. [18]. However, the role of NRF2 in the homeostasis of the neurogenic niche of the SGZ has not been explored.

In this study, we have analyzed the mobilization of the NSPCs pool of the SGZ in *Nrf2*$^{-/-}$ mice at early age and adulthood. We report that exhaustion of NSCs and NPCs of the SGZ pool occurs more rapidly in *Nrf2*-knockout (*Nrf2*$^{-/-}$) mice, when compared to wild type (*Nrf2*$^{+/+}$) mice, which is correlated with the loss of electrophysiological activity of the perforant path.

## 2. Material and methods

### 2.1. Animals

C57BL/6 mouse colonies of the *Nrf2*$^{-/-}$ and *Nrf2*$^{+/+}$ genotypes were established from funders kindly provided by Prof. Masayuki Yamamoto (Tohoku University Graduate School of Medicine, Sendai, Japan) [19]. All the animal procedures were performed according to the protocols approved by the Ethical Committee for Research of the Universidad Autónoma de Madrid, following institutional, Spanish and European guidelines (Boletín Oficial del Estado of 18 March 1988; and 86/609/EEC, 2010/63/EU European Council Directives).

### 2.2. Electrophysiological recordings

Data were obtained from six urethane-anaesthetized (1.6 g/kg i.p.) mice of 6 months of age per group as described in [20]. Briefly, field potentials were recorded through tungsten macroelectrodes (1 MΩ; World Precision Instruments) stereotaxically implanted in the DG (A: -2,3; L: 2; H: 1.5 mm from bregma, according to the Paxinos and Watson Atlas [21]). Twisted bipolar electrodes for electrical stimulation were aimed at the perforant path (A: -2.5; L: 0.5; H: 1.5 mm from bregma) [22]. Baseline recordings were taken with test stimuli (10–50 mA, 0.3 ms, 0.5 Hz) during 15 min before tetanic stimulation consisting of three pulse trains of 10–50 mA, each pulse lasting 0.3 ms and at 50 Hz. Trains lasted 500 ms and the inter-train interval was 2 s. Recording was maintained for 30 min after tetanic stimulation. Field potentials were 0.1 Hz to 1 kHz band-pass filtered, amplified (P15 Amplifier, Grass Co., USA), and digitized at 10 kHz (CED 1401; Cambridge Electronic Design). Signals analysis was carried out with Spike 2 software (Cambridge Electronic Design, Cambridge, UK). Field potential segments of 5 min were analyzed to obtain the response average. The mean average response during the 15 min period before the tetanic stimulation was considered as 100%. Recordings were accepted for analysis when baseline variability was less than 10%.

### 2.3. Immunofluorescence on mouse tissues and stereological analysis

Brain tissue immunofluorescence was performed in 30 μm-thick sections as previously described [2]. Antibodies are described in Suppl. Table S1. Control sections were treated with identical protocol but with the omission of the primary antibody. Cell counts were performed using Fiji Software (http://fiji.sc/Fiji) [23] in 5 sections of the DG separated by 240 μm.

### 2.4. Cell culture and reagents

Human embryonic kidney HEK293T cells were grown in Dulbecco's modified Eagle's medium (DMEM) (Sigma-Aldrich) supplemented with 10% fetal bovine serum (HyClone), 4 mM L-Glutamine (Gibco) and 80 mg/ml gentamicin (Laboratorios Normon). R,S-sulforaphane (SFN; LKT Laboratories, Inc.). Culture of SGZ-derived NSPCs from new-born 0–4 days old pups was described in [24]. For culture of NSPCs from 3-months-old mice, the same protocol was used with the following medium: DMEM/F12/Glutamax, B27 without vitamin A, 20 ng/ml epidermal growth factor (EGF), 20 ng/ml basic fibroblast growth factor (bFGF), 4 μg/ml heparin, and 100 U/ml penicillin/streptomycin.

### 2.5. Immunofluorescence of neurospheres

Neurospheres were adhered to poly-D-lysine-coated coverslips by centrifugation (634*g*, 5 min), and fixed with 4% paraformaldehyde. Then, neurospheres were washed, blocked in PBS containing 0.5% Triton X-100% and 3% bovine serum albumin and incubated overnight (at 4 °C) with the relevant primary antibodies and for 2 h at RT with the appropriate secondary antibodies coupled to Alexa Fluor 488, 594, or 647 (1:500) (Life Technologies-Molecular Probes, Grand Island, NY, USA). Nuclei were stained with DAPI. Images were quantified using Fiji Software (http://fiji.sc/Fiji).

### 2.6. Serial dilution assay

This assay was performed as described in [11]. Briefly, secondary neurospheres were disaggregated with accutase (StemCell Technologies) and seeded into a 96-well plate at 5, 25, 125, 250, 500 and 1000 cells/well dilution. Cells were kept in 5% $CO_2$ and 95% atmospheric air, at 37 °C, in proliferation media, during 7 days, which allowed the formation of tertiary neurospheres. Neurosphere number was determined as de average from 5 wells.

### 2.7. Cell pair assay

As described in [25], a single cell suspension of NSPCs was plated on poly-D-lysine-coated coverslips at a low density (10,000 cells/cm$^2$). Cells were cultured for 24 h in DMEM/F12/Glutamax, B27 (without vitamin A) supplemented with 5 ng/ml or 10 ng/ml EGF and 2.5 or 10 ng/ml bFGF, for pup- or adult-derived neurospheres, respectively. After fixation with 4% PFA, cells were immunostained for SOX2. This assay allowed the quantification of symmetric cell divisions (self-renewal with both SOX2$^+$ siblings) and asymmetric divisions (differentiation with one SOX2$^+$ and one SOX2$^-$ sibling).

### 2.8. Differentiation assays and Sholl analysis

Five-day-old secondary neurospheres were plated on poly-D-lysine-coated coverslips and incubated for 7 days in differentiation media (DMEM/F12-Glutamax, B27 without vitamin A, and 100 U/ml penicillin/streptomycin). Immunostaining and quantification were performed as described above. To quantify neuronal differentiation, Sholl analysis was performed using the Simple neurite tracer plugin (http://homepages.inf.ed.ac.uk/s9808248/imagej/tracer/) and the image processing package Fiji (http://pacific.mpicbg.de/wiki/index.php/Main_Page) in images of differentiated neurospheres immunolabeled for DCX (Santa Cruz).

### 2.9. Production of lentiviral stocks and infection of NSPCs

Recombinant lentiviral stocks were produced in HEK 293 T/17 cells by cotransfecting 10 μg of transfer vector (control plasmid, NFE2L2$^{\Delta ETGE}$ [26], shCO or shNRF2 (shCLN_NM_010902, MISSION shRNA, Sigma)), 6 μg of envelope plasmid pMD2.G (Addgene; deposited by Dr. Didier Trono) and 6 μg of packaging plasmid pSPAX2 (Addgene; deposited by Dr. Didier Trono), using Lipofectamine 2000 Reagent (Invitrogen Life Technologies). After 12 h at 37 °C the medium was replaced with fresh DMEM containing 10% fetal bovine serum. Virus particles were harvested at 24 h and 48 h post-transfection. Adhered NSPCs were incubated with the lentivirus stock for 24 h in DMEM supplemented with 10% FBS and 12 additional hours in proliferation medium. Then, cells were cultured in suspension to allow neurosphere formation.

### 2.10. Immunoblotting

This protocol was performed as described in [1]. Briefly, cells were homogenized in lysis buffer (TRIS pH 7.6 1 M, 400 mM NaCl, 1 mM EDTA, 1 mM EGTA and 1% SDS) and samples heated at 95 °C for 15 min, sonicated and precleared by centrifugation. Primary antibodies used are detailed in Suppl. Table S1.

### 2.11. Quantitative real-time polymerase chain reaction (qRT-PCR)

Total RNA extraction and q-RT-PCR were done as detailed elsewhere [27]. Primer sequences are shown in Suppl. Table S2. All PCRs were performed in triplicate.

### 2.12. Statistical analysis

Data are presented as mean ± SEM. Statistical assessments of differences between groups were analyzed using GraphPad Prism 5 software by one or two-way ANOVA or unpaired Student's *t*-tests, assuming a normal distribution and equal variances as indicated in the legends.

## 3. Results

### 3.1. NRF2 deficiency impairs long term potentiation

Adult *Nrf2*$^{+/+}$ and *Nrf2*$^{-/-}$ mice (6-months old) were examined electrophysiologically for hippocampal long term potentiation (LTP). The synaptic transmission of granule cells of the DG was recorded in response to perforant path (PP) stimulation (Fig. 1A). High frequency stimulation increased the field excitatory post-synaptic potential (fEPSP) in control *Nrf2*$^{+/+}$ mice, but these values were strongly diminished in *Nrf2*$^{-/-}$ mice (Fig. 1B-C), indicating for the first time that NRF2 is required for normal LTP. As the PP is dependent on the activity of excitatory granule neurons of the DG, and these cells are replaced by NSPCs from SGZ [28], we hypothesized that this might be due, at least in part, to impaired hippocampal neurogenesis in *Nrf2*$^{-/-}$ mice.

### 3.2. The clonogenic and proliferative capacity of NSPCs from the SGZ is impaired in NRF2-deficient mice

We first confirmed by qRT-PCR and immunoblotting that NSPCs of the SGZ express NRF2 (Suppl. Fig. 1A-C) and performed immunostaining of the proliferative marker Ki67 in combination with the NSPC marker Nestin to evaluate the number of proliferative NSPCs in the SGZ (Fig. 2A-B). As expected both *Nrf2*$^{+/+}$ and *Nrf2*$^{-/-}$ mice exhibited a drastic reduction of proliferating cells with aging. However the number of proliferating NSPCs was ~50% lower in *Nrf2*$^{-/-}$ mice NSPCs. In order to compare proliferative and clonogenic capacities of NSPCs, we performed neurosphere assays from 3-months old mice. After 5 days in culture the number of cells in the *Nrf2*$^{-/-}$ neurospheres was about ~50% lower compared to *Nrf2*$^{+/+}$ (Fig. 2C). Then, we found that NSPCs from *Nrf2*$^{-/-}$ mice had a lower clonogenic capacity as determined by the number of neurospheres formed after seeding equal amounts of *Nrf2*$^{-/-}$ and *Nrf2*$^{+/+}$ NSPCs (Fig. 2D). In addition, Ki67 immunostaining also demonstrated a reduction in the number of proliferating cells in *Nrf2*$^{-/-}$-derived neurospheres (Fig. 2E-F). In agreement with these results, immunoblot analyses indicated that two proliferative markers, Ki67 and PCNA, were reduced in *Nrf2*$^{-/-}$-derived neurospheres (Suppl. Fig. 2A). Similar results were found in neurosphere cultures established from postnatal (P0-P4) mice (Suppl. Fig. 2B-E). In additional experiments, we analyzed caspase-3 cleavage as a measurement of cell death in the SGZ (data not shown) and neurospheres from both genotypes (Suppl. Fig. 3). We detected very low levels of cleaved caspase-3 by immunohistochemistry or immunoblot, suggesting that NSPCs are not undergoing apoptosis or they do it at undetectable level.

In order to further analyze the involvement of NRF2 in these processes, we rescued NRF2 expression in *Nrf2*$^{-/-}$ NSPCs with a lentiviral vector expressing a constitutively active mutant of NRF2 (NRF2$^{\Delta ETGE}$) [26] (Suppl. Fig. 4A-B). Expression of NRF2 partially improved the clonogenic and proliferative capacity of *Nrf2*$^{-/-}$ NSPCs, leading to increased number of neurospheres as well as of Ki67$^{+}$ cells (Fig. 2G-J). Additionally, we silenced NRF2 with a lentiviral shRNA vector in *Nrf2*$^{+/+}$ NSPCs. Evidence of NRF2-knockdown was provided after induction with the NRF2 activator sulforaphane (SFN) (Suppl. Fig. 4C-D). Knock-down of NRF2 led to a reduction in clonogenic and proliferating capacity of NSPCs (Fig. 2K-N). Taken together these results suggest a cell autonomous need of NRF2 to maintain the clonogenic and proliferative capacity of NSPC pool.

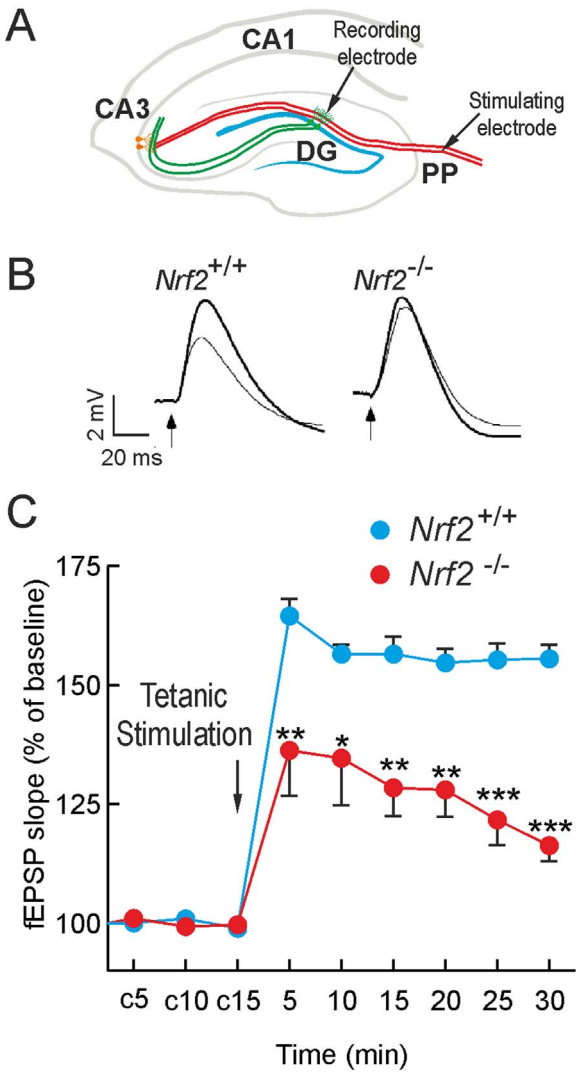


**Fig. 1.** *NRF2 deficiency impairs long term potentiation.* A, upper draw points the positions of the stimulating electrode on the perforant pathway and recording electrode on the granule cell layer: DG, *dentate gyrus*; CA1 and CA3, *Cornu Ammonis* areas 1 and 3, respectively. B, representative responses recorded from *Nrf2*$^{+/+}$ and *Nrf2*$^{-/-}$ mice before (thin line) and after (thick line) high-frequency trains of tetanic stimulation. Calibration: 2 mV, 20 ms. C, LTP of field excitatory postsynaptic potential (fEPSP) in 6-month-old animals before and after tetanic stimulation of the perforant pathway. c5, c10, c15: baseline recordings before tetanic stimulation. Data are mean ± SEM (n = 6). Statistical analysis was performed with two-way ANOVA followed by Bonferroni post-hoc test. **p < 0.01, and ***p < 0.001 comparing *Nrf2*$^{-/-}$ versus *Nrf2*$^{+/+}$ group.

### 3.3. Age-related exhaustion of the NSPCs pool from the SGZ is exacerbated in NRF2-deficient mice

We analyzed by immunostaining with Nestin, SOX2 and GFAP

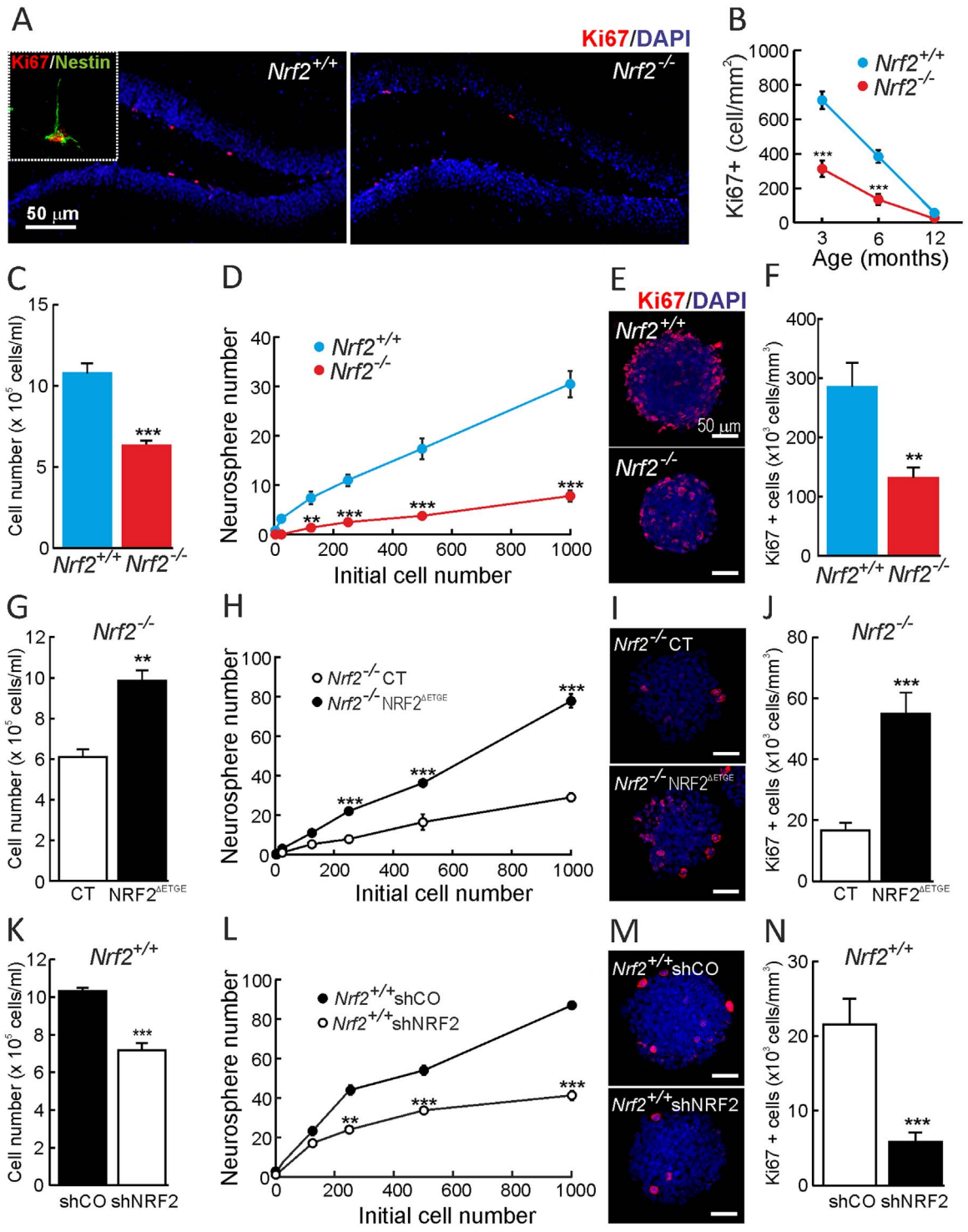


**Fig. 2.** *Impaired proliferative and clonogenic capacity of NSPCs from Nrf2$^{-/-}$ mice.* A, confocal microscope images of Ki67 staining in the SGZ of 3-month-old mice. The green channel for Nestin staining has been removed except in the inset to allow easier visualization of proliferating cells. Nuclei were counterstained with DAPI. B, quantification of Ki67$^+$ cells in 3-, 6- and 12-month-old mice. Data represent mean values ± SEM (n = 4). C, number of cells after 5 days in culture from an initial seeding of 20,000 NSPCs/ml derived from *Nrf2*$^{-/-}$ vs. *Nrf2*$^{+/+}$ 3-month-old mice. D, serial dilution assay of *Nrf2*$^{+/+}$ and *Nrf2*$^{-/-}$ cultures showing the number of neurospheres formed after 7 days (n = 5). E-F, immunofluorescence and quantification of Ki67$^+$ cells, counterstained with DAPI, in neurospheres with similar size (n = 10). G-N, parallel analysis in *Nrf2*$^{-/-}$-derived NSPCs infected with a control vector (CT) or a lentivirus expressing active NRF2$^{\Delta ETGE}$ (G-J), and *Nrf2*$^{+/+}$-derived NSPCs infected with control (shCO) and shNRF2 lentivirus (K-N). Data show mean values ± SEM. **p < 0.01, ***p < 0.001 according to a Student's *t*-test vs. either *Nrf2*$^{-/-}$ (B, C, D, F) or the experimental groups (G,H, J, K, L and N).

antibodies the number of quiescent neural progenitors (QNPs) and amplifying neural progenitors (ANPs), as these cell populations drive NSPCs towards mobilization and differentiation of neural lineages. QNPs were identified as Nestin$^+$/SOX2$^+$/GFAP$^+$ cells and ANPs as Nestin$^+$/SOX2$^+$/GFAP$^-$cells, and were distinguished morphologically: QNPs exhibit a non-branched long neurite across the granular cell layer while ANPs are located at the basis of the granular layer and do not present long neurites (Fig. 3A) [29]. The number of QNPs and ANPs in *Nrf2*$^{+/+}$ mice decreased with aging (Fig. 3B-D). Thus at 15 months of age the number of QNPs and ANPs had decreased to ~50% compared

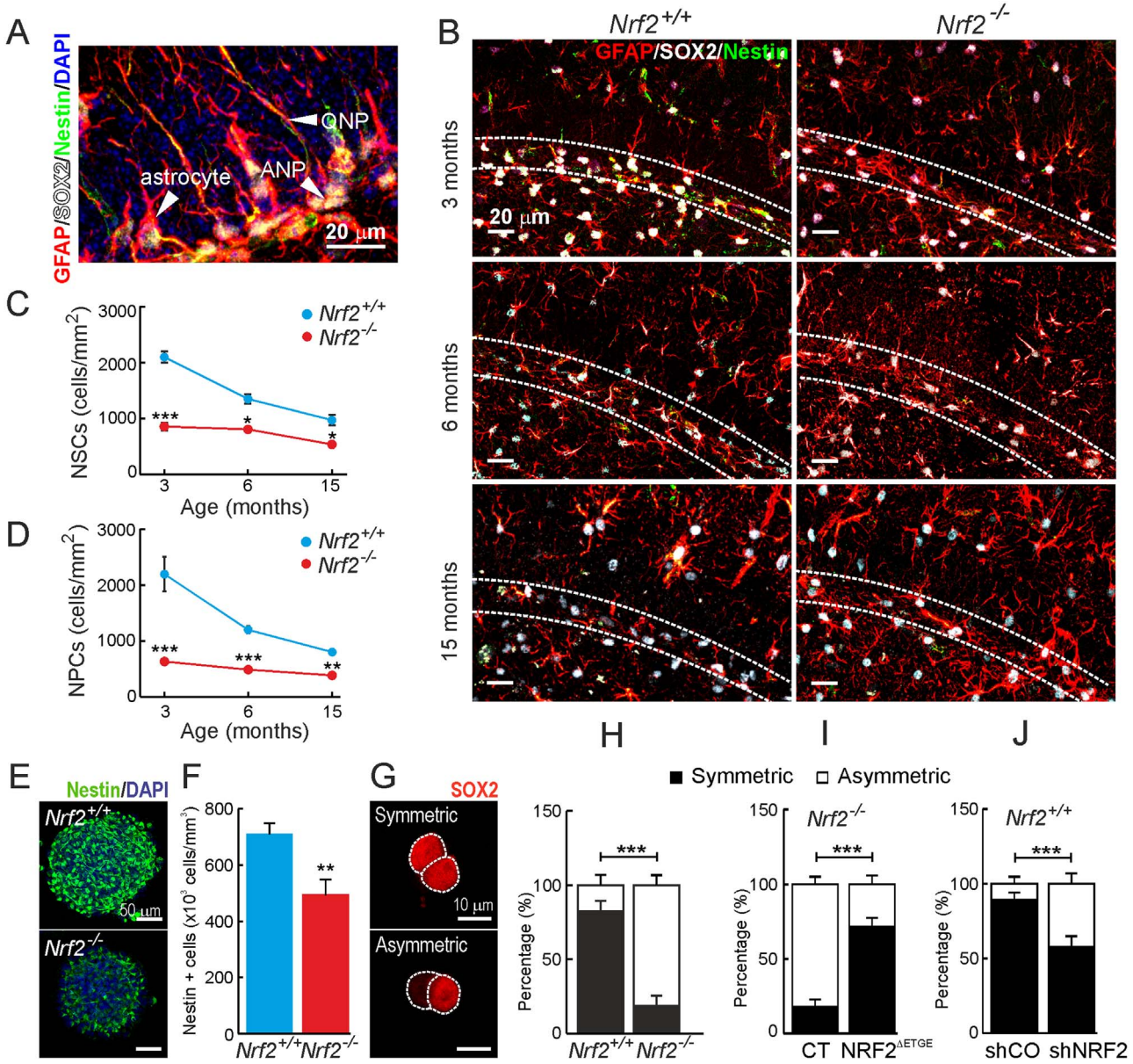


**Fig. 3.** *NRF2-deficiency provokes a drop in the pool of QNPs and ANPs and an increase of asymmetric divisions of NSPCs.* A, confocal image of a SGZ immunostained GFAP/SOX2/Nestin. Arrows point a typical ANP, QNP and astrocyte (see text). B, same staining for 3- (Upper panel), 6- (middle panel) and 15- (low panel) month-old mice. C-D, quantification of QNPs (C) and ANPs (D) in 3-, 6- and 15-month-old mice (n = 3). E-F, nestin immunofluorescence on neurospheres derived from 3-month-old mice (n = 10). G-J, cell pair assay of NSPCs by SOX2 immunofluorescence. G, example of symmetric and asymmetric divisions. Quantification of symmetric and asymmetric divisions in cultures from 3-month-old (H) mice, *Nrf2*$^{-/-}$ NSPCs infected with control or NRF2$^{\Delta ETGE}$ expression lentivirus (I) and *Nrf2*$^{+/+}$ NSPCs infected with control or shRNA lentivirus to knock-down NRF2 (J) (n = 60 pairs). Data show mean values ± SEM.*p < 0.05, **p < 0.01, ***p < 0.001 according to a student's *t*-test vs. either *Nrf2*$^{-/-}$ (C, D, F and H) or the experimental groups (I and J).

to 3 months of age. Importantly, in 3-month-old *Nrf2*$^{-/-}$ mice the amount of these cells was already substantially decreased to ~50%. Accordingly, the number of Nestin$^{+}$ cells was decreased in *Nrf2*$^{-/-}$ neurospheres from newborn (Suppl. Fig. 2F-G) and 3-month-old (Fig. 3E-F) mice.

As these results suggested impaired capacity of QNPs and ANPs to proliferate and differentiate, we further analyzed the number of symmetric and asymmetric divisions in cell culture following staining with SOX2 (Fig. 3G-J). Cells derived from symmetric divisions express SOX2 in both siblings, while in asymmetric divisions only one of the siblings expresses SOX2. As expected ~75% of the *Nrf2*$^{+/+}$ NSPCs derived from symmetric division. However in the *Nrf2*$^{-/-}$ NSPCs symmetric divisions accounted for only ~25% (Fig. 3H). In line with this, the *Nrf2*$^{-/-}$ NSPCs from newborn mice exhibited an increment in asymmetric divisions as compared to control NSPCs (Suppl. Fig. 2H). These data were further confirmed by rescuing *Nrf2*$^{-/-}$ NSPCs with the lentivirus-mediated expression of NRF2$^{\Delta ETGE}$ (Fig. 3I). Moreover, knocking-down NRF2 in *Nrf2*$^{+/+}$ NSPCs resulted in a reduction in symmetric divisions (Fig. 3J). Taken together, these results suggest that NRF2 deficiency limits the self-renewal capacity of the neurogenic niche of the SGZ.

### 3.4. Neuronal differentiation from NSPCs of the SGZ is impaired in NRF2-deficient mice

We analyzed the capacity of the SGZ to produce new neurons using doublecortin (DCX) staining that specifically labels neuroblasts and immature neurons (Fig. 4A-B). In both *Nrf2*$^{+/+}$ and *Nrf2*$^{-/-}$ mice the amount of DCX$^{+}$ cells decreased gradually to ~10% at 12 months of age but the SGZ of *Nrf2*$^{-/-}$ mice presented a lower capacity to generate these neuronal progenitors already at 3 and 6 months of age. These results were also analyzed in neurospheres and again the amount of DCX$^{+}$ cells was substantially decreased to ~20% in newborn (Suppl.

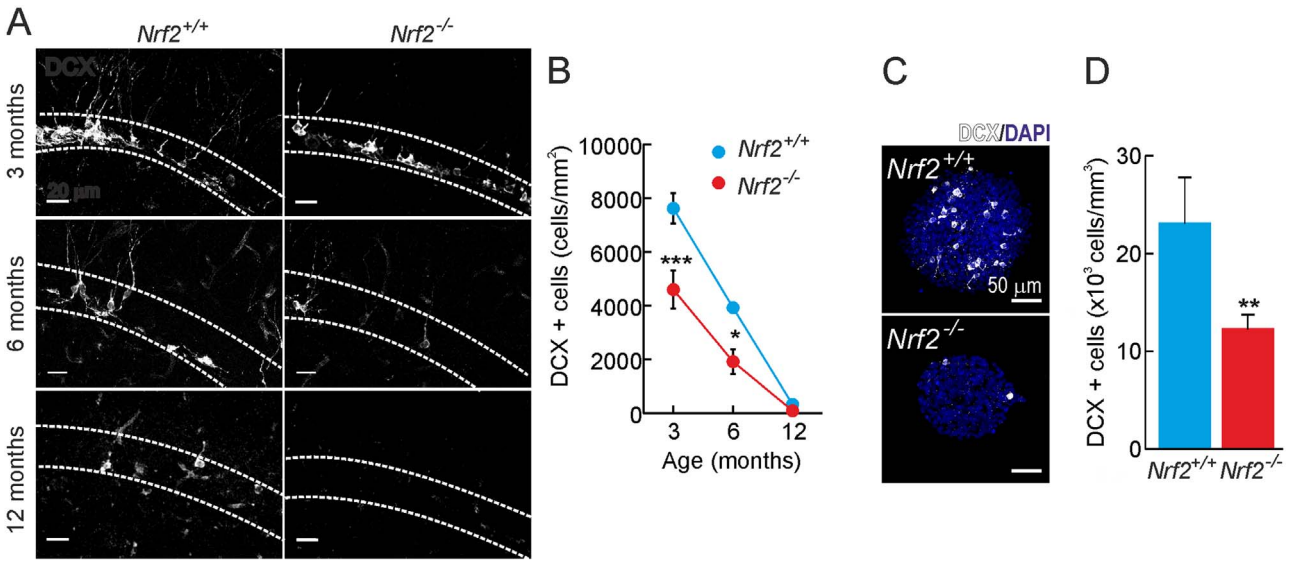


**Fig. 4.** *NRF2-deficiency leads to a reduction of DCX+ cells.* A and B, DCX immunostaining in the SGZ of 3-, 6- and 12-month-old mice (n = 3). C-D, DCX immunofluorescence in neurospheres derived from 3-month-old mice (n = 10). Data represent mean values ± SEM. *p < 0.05, **p < 0.01 and ***p < 0.001 according to a Student's *t*-test vs. the *Nrf2*$^{-/-}$ group.

Fig. 2H-I) and ~50% in 3-month-old *Nrf2*$^{-/-}$ mice (Fig. 4C-D).

Next, we analyzed the differentiation potential of the NSPCs. When plated on poly-D-lysine and grown in the absence of growth factors NSPCs migrate away from the neurosphere core and spread around forming a carpet of cells differentiated to neurons, astrocytes and oligodendrocytes [30]. First, following DCX and DAPI staining, we noted a decrease in the migration distance of cells from newborn (Suppl. Fig. 5A-B) and, more notoriously, from 3-month-old (Fig. 5A-B) *Nrf2*$^{-/-}$ mice. The migration distance was improved by reintroduction of NRF2 expression in *Nrf2*$^{-/-}$ cultures (Fig. 5E-F), and worsened by knock-down of NRF2 in *Nrf2*$^{+/+}$ cultures (Fig. 5H-I). DCX staining in the differentiating cultures indicated impairment in the neuronal differentiation of *Nrf2*$^{-/-}$ neurospheres at birth (Suppl. Fig. 5C) and at 3 months of age (Fig. 5C). Moreover, rescue of NRF2 expression in *Nrf2*$^{-/-}$ cultures led to enhanced neuronal differentiation (Fig. 5G). On the other hand, silencing NRF2 in *Nrf2*$^{+/+}$ neurospheres reduced significantly the percentage of DCX$^{+}$ cells (Fig. 5J). To analyze the maturation of these cells and their capacity to interact with other neurons, we performed a Sholl analysis, that measures the branching complexity, in newborn (Suppl. Fig. 5D) and 3-month-old (Fig. 5D) mice. DCX$^{+}$ cells from *Nrf2*$^{-/-}$ mice showed a decrease in the number of neurite crossings suggesting a reduced maturation compared to those of *Nrf2*$^{+/+}$ mice. All these data suggest that NRF2 is not only important to maintain the NSPCs pool but also to support a proper neuronal differentiation.

### 3.5. NRF2-deficiency impairs the neuron/glia differentiation balance

Astrocyte differentiation in the SGZ was analyzed by GFAP and SOX2 staining (Fig. 6A-B). The *Nrf2*$^{-/-}$ mice exhibited a growing increase in astrocyte abundance at the SGZ for 3, 6 and 15 months of age. When we analyzed the astroglial differentiation in vitro, using GFAP staining, we noted an increase in the number of astrocytes in *Nrf2*$^{-/-}$ vs *Nrf2*$^{+/+}$ cultures, being 20% higher in newborn (Suppl. Fig. 5E-F) and 40% higher in 3-month-old-derived neurospheres (Fig. 6C-D). The increase in astrocytes was also observed *Nrf2*$^{+/+}$ cultures when we silenced NRF2 expression (Fig. 6G-H). Furthermore, recovering NRF2 expression in *Nrf2*$^{-/-}$ cultures resulted in a reduction to 20% of GFAP$^{+}$ cells (Fig. 6E-F). Oligodendrocyte differentiation was analyzed with OLIG2 staining. *Nrf2*$^{-/-}$ neurospheres from newborn (Suppl. Fig. 5G-H) and 3-month-old mice (Fig. 6I-J) exhibited ~2-folds increase in the number of oligodendrocytes. In line with these results, reintroduction of NRF2 in *Nrf2*$^{-/-}$ NSPCs reduced significantly the number of OLIG2-positive cells (Fig. 6K-L) while NRF2 silencing in *Nrf2*$^{+/+}$ cultures resulted in an enrichment in oligodendrocytes under differentiating conditions (Fig. 6M-N). These results could not be replicated in mice (data not shown), in agreement with reports suggesting that NSPCs from the SGZ might not generate oligodendrocytes in vivo [31,32]. All these measurements indicate that NRF2 is a key regulator of the balance between neuronal and glial differentiation.

## 4. Discussion

Here we report for the first time the role of NRF2 in mobilization and differentiation of NSPCs in the SGZ, a neurogenic niche that participates in neurogenesis of the adult hippocampus and therefore has crucial implications in preservation of cognitive functions. SGZ NSPCs appear to have a crucial role in the replacement of new neurons in granule cell layer [33]. These adult-born neurons synaptically integrate in the pre-existing hippocampal neural circuitry and participate in LTP, which plays a role in learning and memory [13,34,35]. In turn, depletion of hippocampal neurogenesis results in LTP loss [36,37].

It has been reported that local induction of oxidative stress during mobilization of neural precursors can occur given the evidence that oxidized DNA and lipids are present in the SGZ of adult rodents [38]. Although the authors did not analyze NRF2 directly, a bioinformatics analysis based on previous transcriptomics data sets [39,40] did show changes in the levels of several antioxidant enzymes whose expression is regulated by NRF2. We could not analyze NRF2 protein levels by immunohistochemistry in the SGZ (data not shown) and, in fact, NRF2 levels were almost undetectable by immunoblotting in NSPCs isolated from the SGZ (Suppl. Fig. 1) and SVZ (data not shown). However, these cells responded to the NRF2 activator SFN indicating that although low, NRF2 is expressed under basal conditions and responds to environmental inducers. To avoid off-target effects of NRF2 activating drugs, we used a genetic approach based on lentiviral reintroduction of NRF2 in NSCs. Ectopic expression of NRF2 rescued otherwise NRF2-deficient NSPCs to cloning and proliferative values, similar to those of wild type NSPCs. Our results are in agreement with a previous study showing that up-regulation of NRF2 ameliorated amyloid β-mediated neural stem cell death [41]. This study also demonstrated that neuronal differentiation of NSPCs is enhanced by NRF2 overexpression [41]. Additionally, we found that decreasing or increasing NRF2 expression by

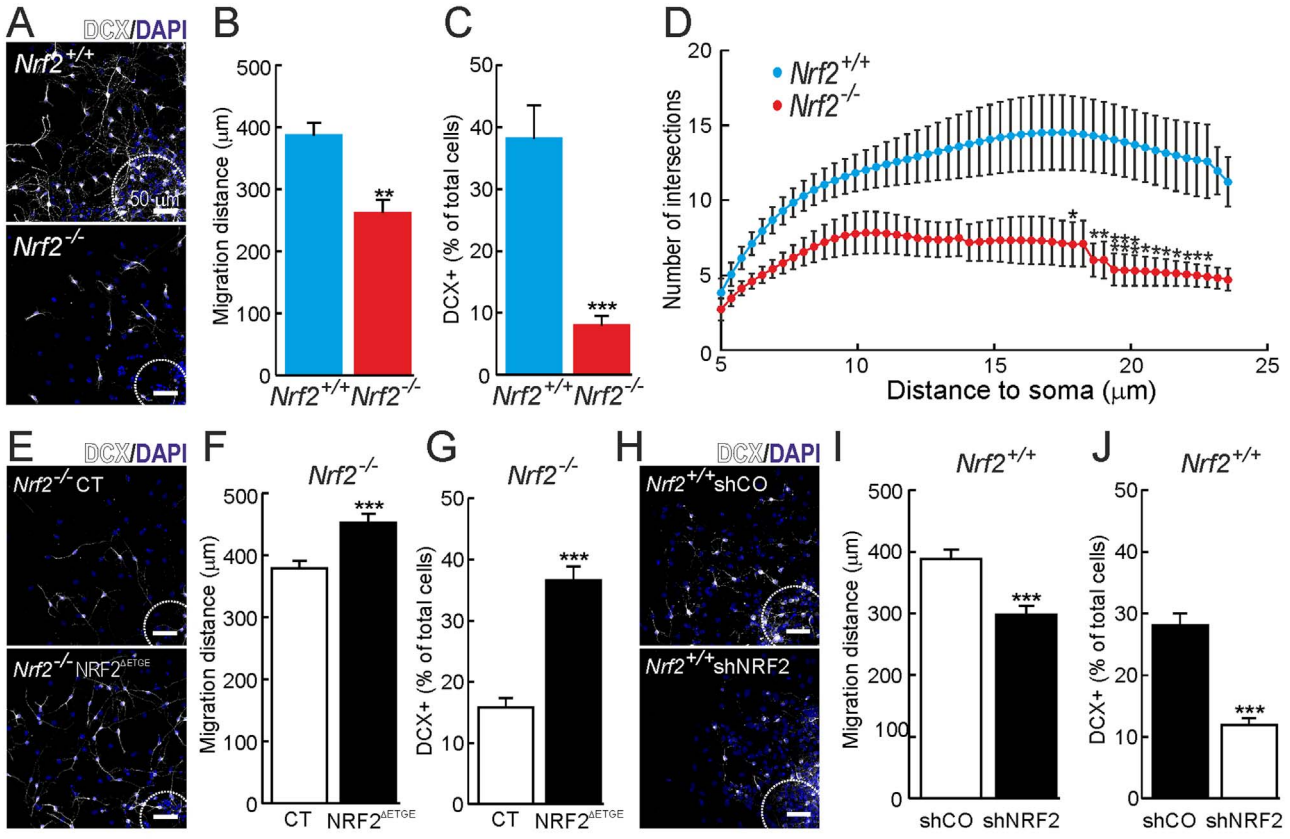


**Fig. 5.** *Role of Nrf2 in the neuronal differentiation of NSPCs.* A, DCX and DAPI staining of neurospheres from 3-months old mice grown under differentiation conditions. B, measurement of the cell migration as determined by distance from the neurosphere edge (dotted line) to DAPI stained nuclei (n = 40). C, quantification of $DCX^+$ cells from neurospheres shown in A (n = 10). D, sholl analysis of the neurons in the differentiated neurospheres derived from 3-months old mice (n = 12). E. DCX and DAPI staining of $Nrf2^{-/-}$ neurospheres rescued by lentiviral expression of $NRF2^{\Delta ETGE}$. F, measurement of their cell migration distance (n = 40). G, quantification of $DCX^+$ cells (n = 10). H-J, parallel analysis in $Nrf2^{+/+}$ neurospheres infected with control of shRNA lentivirus to knockdown NRF2. Data represent mean values ± SEM. *p < 0.05, **p < 0.01 and ***p < 0.001 according to a Student's *t*-test vs. the $Nrf2^{-/-}$ group (B, C and D) or the experimental groups (F, G, I and J).

genetic means was sufficient to significantly suppress or rejuvenate the neurogenic niche of the SGZ. Furthermore, SGZ NSPCs from either new born or 3 month-old $Nrf2^{-/-}$ mice exhibited substantially compromised proliferation and neuronal differentiation. Our results are in line with a previous study showing that a highly reduced intracellular redox state promotes proliferation and survival, whereas a highly oxidized state results in greater differentiation and cell death [42].

In order to understand how NRF2 controls the fate of NSPCs, we used the cell pair assay that indicates whether NCS divisions lead to identical siblings with proliferating capacity (symmetric division) or to two different cells, one retaining proliferation capacity and the other entering a differentiation program (asymmetric division) [25]. The current model of mobilization of the NSPC pool establishes that a NSC progenitor will divide symmetrically for several generations to maintain the progenitor pool. At the same time, a certain number of asymmetric divisions will lead to a supply of neurons as well as astrocytes to accommodate specific demands. The last division leads to differentiation of both siblings into astrocytes [29]. The fact that the NSPC pool was exhausted more quickly in the $Nrf2^{-/-}$ mice suggested that either cell-autonomous alterations or micro-environmental influence leads to the mobilization and terminal differentiation of these neural progenitors. Consistent with this hypothesis, we found an inverse correlation between Ki67-stained progenitors (Fig. 2) and GFAP-stained astrocytes (Fig. 6). Moreover, in the cell pair assay, we found that NRF2 deficiency resulted in an increase of asymmetric divisions, leading to the reduction in the number of progenitors. These findings suggest that the exhaustion of the NSPC pool in the $Nrf2^{-/-}$ mice is due to an increase in asymmetric divisions, together with imbalance in the cell fate to increase the number of astrocytes and reduce neurons. This hypothesis is consistent with the well reported observation that NRF2 is required to counterbalance the high levels of intracellular ROS of highly proliferating cells [43,44]. Furthermore, our study also connects the observed pattern of decline in NSPC function with cognitive impairment.

These results identify for the first time NRF2 as an important factor to prevent the decline in the NSPC pool of the SGZ, during aging, and have important implications towards understanding fundamental aspects of NSPC biology and promising therapeutic interventions in disorders involving hippocampal function.

## Acknowledgements

This work was funded by Grant SAF2016-76520-R of the Spanish Ministry of Economy and Competitiveness. NRA is recipient of a FPU contract of Spanish Ministry of Education Culture and Sports. EF is a recipient a postdoctoral fellowship: SFRH/BPD/86551/2012 (Financiado por Fundos FEDER através do Programa Operacional Factores de Competitividade – COMPETE 2020 e por Fundos Nacionais através da FCT –Fundação para a Ciência e a Tecnologia no âmbito do projecto Estratégico com referência atribuida pelo COMPETE: POCI-01-0145-FEDER-007440). EF enjoyed a short term stay visit at AC's laboratory founded by COST action BM1402 MouseAge.

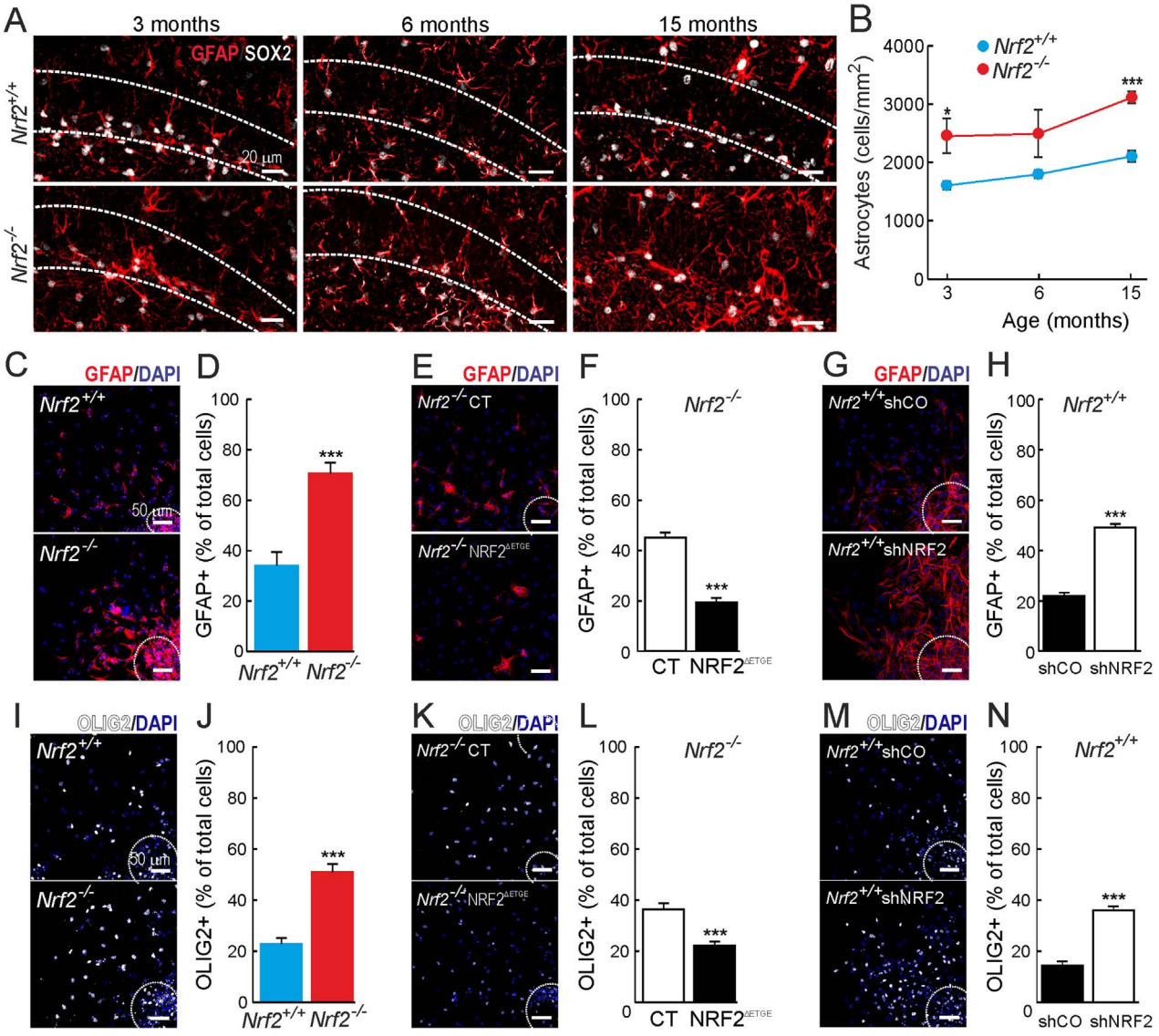


**Fig. 6.** *Nrf2-deficiency leads to an increment in non-neuronal differentiation.* A and B, astrocyte differentiation analyzed in the SGZ of 3-, 6- and 15-months old mice by GFAP/SOX2 immunostaining (n = 3). C-H, astroglial differentiation analyzed by GFAP immunostaining in the neurospheres derived from 3-month-old mice (A and B), *Nrf2*$^{-/-}$ neurospheres derived from control and NRF2$^{\Delta ETGE}$ expressing NCSs (C and D), and *Nrf2*$^{+/+}$ neurospheres derived from control NRF2-knock-down NSPCs (E and F) (n = 10). I-N., oligodendrocyte differentiation analyzed in vitro using Olig2 staining in the differentiated neurospheres derived from 3-month-old mice (I and J), *Nrf2*$^{-/-}$ neurospheres derived from control and NRF2$^{\Delta ETGE}$ expressing NCSs (K and L), and *Nrf2*$^{+/+}$ neurospheres derived from control NRF2-knock-down NSPCs (M and N) (n = 10). Data shown mean values ± SEM. *p < 0.05, **p < 0.01, ***p < 0.001 according to a Student's *t*-test vs. either *Nrf2*$^{-/-}$ group (B, D, J, L and N) or the experimental groups (F, H, P and R).

## Appendix A. Supplementary material

Supplementary data associated with this article can be found in the online version at http://dx.doi.org/10.1016/j.redox.2017.06.010.

## References


[1] M. Pajares, N. Jimenez-Moreno, A.J. Garcia-Yague, M. Escoll, M.L. de Ceballos, F. Van Leuven, A. Rabano, M. Yamamoto, A.I. Rojo, A. Cuadrado, Transcription factor NFE2L2/NRF2 is a regulator of macroautophagy genes, Autophagy 12 (10) (2016) 1902–1916.

[2] A.I. Rojo, N.G. Innamorato, A.M. Martin-Moreno, M.L. De Ceballos, M. Yamamoto, A. Cuadrado, Nrf2 regulates microglial dynamics and neuroinflammation in experimental Parkinson's disease, Glia 58 (5) (2010) 588–598.

[3] A.I. Rojo, P. Rada, M. Mendiola, A. Ortega-Molina, K. Wojdyla, A. Rogowska-Wrzesinska, D. Hardisson, M. Serrano, A. Cuadrado, The PTEN/NRF2 axis promotes human carcinogenesis, Antioxid. Redox Signal. 21 (18) (2014) 2498–2514.

[4] J.D. Hayes, A.T. Dinkova-Kostova, The Nrf2 regulatory network provides an interface between redox and intermediary metabolism, Trends Biochem. Sci. 39 (4) (2014) 199–218.

[5] J. Zhu, H. Wang, Q. Sun, X. Ji, L. Zhu, Z. Cong, Y. Zhou, H. Liu, M. Zhou, Nrf2 is required to maintain the self-renewal of glioma stem cells, BMC Cancer 13 (2013) 380.

[6] I.G. Ryoo, S.H. Lee, M.K. Kwak, Redox modulating NRF2: a potential mediator of cancer stem cell resistance, Oxid. Med. Cell. Longev. 2016 (2016) 2428153.

[7] S. Murakami, H. Motohashi, Roles of Nrf2 in cell proliferation and differentiation, Free Radic. Biol. Med. 88 (Pt B) (2015) 168–178.

[8] N. Gurusamy, D. Ray, I. Lekli, D.K. Das, Red wine antioxidant resveratrol-modified cardiac stem cells regenerate infarcted myocardium, J. Cell. Mol. Med. 14 (9) (2010) 2235–2239.

[9] C. Cai, L. Teng, D. Vu, J.Q. He, Y. Guo, Q. Li, X.L. Tang, G. Rokosh, A. Bhatnagar, R. Bolli, The heme oxygenase 1 inducer (CoPP) protects human cardiac stem cells against apoptosis through activation of the extracellular signal-regulated kinase (ERK)/NRF2 signaling pathway and cytokine release, J. Biol. Chem. 287 (40) (2012) 33720–33732.

[10] L. Gambari, G. Lisignoli, L. Cattini, C. Manferdini, A. Facchini, F. Grassi, Sodium hydrosulfide inhibits the differentiation of osteoclast progenitor cells via NRF2-dependent mechanism, Pharmacol. Res. 87 (2014) 99–112.

[11] M.J. Corenblum, S. Ray, Q.W. Remley, M. Long, B. Harder, D.D. Zhang, C.A. Barnes, L. Madhavan, Reduced Nrf2 expression mediates the decline in neural stem cell function during a critical middle-age period, Aging Cell 15 (4) (2016) 725–736.

[12] P.S. Eriksson, T. Perfilieva E Fau - Bjork-Eriksson, A.M. Bjork-Eriksson T Fau - Alborn, C. Alborn Am Fau - Nordborg, D.A. Nordborg C Fau - Peterson, F.H. Peterson Da Fau - Gage, F.H. Gage, Neurogenesis in the adult human hippocampus, Nat. Med. 4 (11) (1998) 1313–1317.

[13] E.I. Moser, K.A. Krobert, M.B. Moser, R.G. Morris, Impaired spatial learning after saturation of long-term potentiation, Science 281 (5385) (1998) 2038–2042.
[14] N. Madronal, J.M. Delgado-Garcia, A. Fernandez-Guizan, J. Chatterjee, M. Kohn, C. Mattucci, A. Jain, T. Tsetsenis, A. Illarionova, V. Grinevich, et al., Rapid erasure of hippocampal memory following inhibition of dentate gyrus granule cells, Nat. Commun. 7 (2016) 10923.
[15] N. Toni, E.M. Teng, E.A. Bushong, J.B. Aimone, C. Zhao, A. Consiglio, H. van Praag, M.E. Martone, M.H. Ellisman, F.H. Gage, Synapse formation on neurons born in the adult hippocampus, Nat. Neurosci. 10 (6) (2007) 727–734.
[16] J. Meng, Z. Lv, X. Qiao, X. Li, Y. Li, Y. Zhang, C. Chen, The decay of redox-stress response capacity is a substantive characteristic of aging: revising the redox theory of aging, Redox Biol. 11 (2017) 365–374.
[17] N. Kubben, W. Zhang, L. Wang, T.C. Voss, J. Yang, J. Qu, G.H. Liu, T. Misteli, Repression of the antioxidant NRF2 pathway in premature aging, Cell 165 (6) (2016) 1361–1374.
[18] L. Madhavan, V. Ourednik, J. Ourednik, Increased "vigilance" of antioxidant mechanisms in neural stem cells potentiates their capability to resist oxidative stress, Stem Cells 24 (9) (2006) 2110–2119.
[19] K. Itoh, J. Mimura, M. Yamamoto, Discovery of the negative regulator of Nrf2, Keap1: a historical overview, Antioxid. Redox Signal. 13 (11) (2010) 1665–1678.
[20] M. Navarrete, G. Perea, D. Fernandez de Sevilla, M. Gomez-Gonzalo, A. Nunez, E.D. Martin, A. Araque, Astrocytes mediate in vivo cholinergic-induced synaptic plasticity, PLoS Biol. 10 (2) (2012) e1001259.
[21] G. Paxinos, K.B.J. Franklin, The Mouse Brain in Stereotaxic Coordinates, Elsevier Academic Press, Amsterdam; Boston, 2004 (Compact 2nd ed.).
[22] J.L. Trejo, J. Piriz, M.V. Llorens-Martin, A.M. Fernandez, M. Bolos, D. LeRoith, A. Nunez, I. Torres-Aleman, Central actions of liver-derived insulin-like growth factor I underlying its pro-cognitive effects, Mol. Psychiatry 12 (12) (2007) 1118–1128.
[23] J. Schindelin, I. Arganda-Carreras, E. Frise, V. Kaynig, M. Longair, T. Pietzsch, S. Preibisch, C. Rueden, S. Saalfeld, B. Schmid, et al., Fiji: an open-source platform for biological-image analysis, Nat. Methods 9 (7) (2012) 676–682.
[24] L. Bernardino, F. Agasse, B. Silva, R. Ferreira, S. Grade, J.O. Malva, Tumor necrosis factor-alpha modulates survival, proliferation, and neuronal differentiation in neonatal subventricular zone cell cultures, Stem Cells 26 (9) (2008) 2361–2371.
[25] S. Xapelli, F. Agasse, L. Sarda-Arroyo, L. Bernardino, T. Santos, F.F. Ribeiro, J. Valero, J. Braganca, C. Schitine, R.A. de Melo Reis, et al., Activation of type 1 cannabinoid receptor (CB1R) promotes neurogenesis in murine subventricular zone cell cultures, PLoS One 8 (5) (2013) e63529.
[26] P. Rada, A.I. Rojo, S. Chowdhry, M. McMahon, J.D. Hayes, A. Cuadrado, SCF/{beta}-TrCP promotes glycogen synthase kinase 3-dependent degradation of the Nrf2 transcription factor in a Keap1-independent manner, Mol. Cell. Biol. 31 (6) (2011) 1121–1133.
[27] I. Lastres-Becker, N.G. Innamorato, T. Jaworski, A. Rabano, S. Kugler, F. Van Leuven, A. Cuadrado, Fractalkine activates NRF2/NFE2L2 and heme oxygenase 1 to restrain tauopathy-induced microgliosis, Brain J. Neurol. 137 (Pt 1) (2014) 78–91.
[28] G. Kempermann, H. Song, F.H. Gage, Neurogenesis in the adult hippocampus, Cold Spring Harb. Perspect. Biol. 7 (9) (2015) a018812.
[29] J.M. Encinas, N. Michurina Tv Fau - Peunova, J.-H. eunova N Fau - Park, J. Park Jh Fau - Tordo, D.A. Tordo J Fau - Peterson, G. Peterson Da Fau - Fishell, A. Fishell G Fau - Koulakov, G. Koulakov A Fau - Enikolopov, G. Enikolopov, Division-coupled astrocytic differentiation and age-related depletion of neural, Cell Stem Cell 8 (5) (2011) 566–579 (LID - 510.1016/j.stem.2011.1003.1010.).
[30] B.A. Reynolds, S. Weiss, Generation of neurons and astrocytes from isolated cells of the adult mammalian central nervous system, Science 255 (5052) (1992) 1707–1710.
[31] M.A. Bonaguidi, M.A. Wheeler, J.S. Shapiro, R.P. Stadel, G.J. Sun, G.L. Ming, H. Song, In vivo clonal analysis reveals self-renewing and multipotent adult neural stem cell characteristics, Cell 145 (7) (2011) 1142–1155.
[32] S.H. Kang, M. Fukaya, J.K. Yang, J.D. Rothstein, D.E. Bergles, NG2+ CNS glial progenitors remain committed to the oligodendrocyte lineage in postnatal life and following neurodegeneration, Neuron 68 (4) (2010) 668–681.
[33] C. Zhao, F.H. Deng W Fau - Gage, F.H. Gage, Mechanisms and functional implications of adult neurogenesis, Cell 132 (4) (2008) 645–660 (LID - 610.1016/j.cell.2008.1001.1033.
[34] J.R. Whitlock, A.J. Heynen, M.G. Shuler, M.F. Bear, Learning induces long-term potentiation in the hippocampus, Science 313 (5790) (2006) 1093–1097.
[35] S. Nabavi, R. Fox, C.D. Proulx, J.Y. Lin, R.Y. Tsien, R. Malinow, Engineering a memory with LTD and LTP, Nature 511 (7509) (2014) 348–352.
[36] J.S. Snyder, N. Kee, J.M. Wojtowicz, Effects of adult neurogenesis on synaptic plasticity in the rat dentate gyrus, J. Neurophysiol. 85 (6) (2001) 2423–2431.
[37] E. Iscru, T. Ahmed, V. Coremans, Y. Bozzi, M. Caleo, E.M. Conway, R. D'Hooge, D. Balschun, Loss of survivin in neural precursor cells results in impaired long-term potentiation in the dentate gyrus and CA1-region, Neuroscience 231 (2013) 413–419.
[38] N.M. Walton, R. Shin, K. Tajinda, C.L. Heusner, J.H. Kogan, S. Miyake, Q. Chen, K. Tamura, M. Matsumoto, Adult neurogenesis transiently generates oxidative stress, PLoS One 7 (4) (2012) e35264.
[39] X. Wang, A. Zaidi, R. Pal, A.S. Garrett, R. Braceras, X.W. Chen, M.L. Michaelis, E.K. Michaelis, Genomic and biochemical approaches in the discovery of mechanisms for selective neuronal vulnerability to oxidative stress, BMC Neurosci. 10 (2009) 12.
[40] V. Anantharam, E. Lehrmann, A. Kanthasamy, Y. Yang, P. Banerjee, K.G. Becker, W.J. Freed, A.G. Kanthasamy, Microarray analysis of oxidative stress regulated genes in mesencephalic dopaminergic neuronal cells: relevance to oxidative damage in Parkinson's disease, Neurochem. Int. 50 (6) (2007) 834–847.
[41] V. Karkkainen, E. Pomeshchik Y Fau - Savchenko, H. Savchenko E Fau - Dhungana, A. Dhungana H Fau - Kurronen, S. Kurronen A Fau - Lehtonen, N. Lehtonen S Fau - Naumenko, P. Naumenko N Fau - Tavi, A.-L. Tavi P Fau - Levonen, M. Levonen Al Fau - Yamamoto, T. Yamamoto M Fau - Malm, et al., Nrf2 regulates neurogenesis and protects neural progenitor cells against Abeta, Stem Cells 32 (7) (2014) 1904–1916 (LID - 1910.1002/stem.1666).
[42] J. Smith, E. Ladi, M. Mayer-Proschel, M. Noble, Redox state is a central modulator of the balance between self-renewal and differentiation in a dividing glial precursor cell, Proc. Natl. Acad. Sci. USA 97 (18) (2000) 10032–10037.
[43] P.T. Schumacker, Reactive oxygen species in cancer cells: live by the sword, die by the sword, Cancer Cell 10 (3) (2006) 175–176.
[44] S. Toyokuni, K. Okamoto, J. Yodoi, H. Hiai, Persistent oxidative stress in cancer, FEBS Lett. 358 (1) (1995) 1–3.

Cell Reports

# Transcription factor NRF2 uses the Hippo pathway effector TAZ to induce tumorigenesis in glioblastomas

--Manuscript Draft--

| | |
|---|---|
| **Manuscript Number:** | CELL-REPORTS-D-19-00656R1 |
| **Full Title:** | Transcription factor NRF2 uses the Hippo pathway effector TAZ to induce tumorigenesis in glioblastomas |
| **Article Type:** | Research Article |
| **Keywords:** | oxidative stress, cancer stem cells, chemotherapy, glioblastoma |
| **Corresponding Author:** | Antonio Cuadrado<br>Instituto de Investigaciones Biomédicas "Alberto Sols" UAM-CSIC<br>Madrid, SPAIN |
| **First Author:** | Maribel Escoll |
| **Order of Authors:** | Maribel Escoll |
| | Diego Lastra |
| | Marta Pajares |
| | Robledinos-Anton Natalia |
| | Ana I. Rojo |
| | Raquel Fernández-Ginés |
| | Marta Mendiola |
| | Virginia Martínez-Marín |
| | Isabel Esteban |
| | Pilar López-Larrubia |
| | Ricardo Gargini |
| | Antonio Cuadrado |
| **Abstract:** | Transcription factor NRF2 orchestrates a cellular defense against oxidative stress and so far, has been involved in tumor progression by providing a metabolic adaptation to tumorigenic demands and resistance to chemotherapeutics. In this study, we discover that NRF2 also propels tumorigenesis in gliomas and glioblastomas by inducing the expression of the transcriptional co-activator TAZ, a protein of the Hippo signaling pathway that promotes tumor growth. The expression of the genes encoding NRF2 (NFE2L2) and TAZ (WWTR1) showed a positive correlation in 721 gliomas from The Cancer Genome Atlas database. Moreover, NRF2 and TAZ protein levels also correlated in immunohistochemical tissue arrays of glioblastomas. Genetic knock-down of NRF2 decreased, while NRF2 overexpression or chemical activation with sulforaphane, increased TAZ transcript and protein levels. Mechanistically, we identified several NRF2-regulated functional enhancers in the regulatory region of WWTR1. The relevance of the new NRF2/TAZ axis in tumorigenesis was demonstrated in subcutaneous and intracranial grafts. Thus, intracranial inoculation of NRF2-depleted glioma stem cells did not develop tumors as determined by magnetic resonance imaging. Forced TAZ overexpression partly rescued both stem cell growth in neurospheres and tumorigenicity. Hence, NRF2 not only enables tumor cells to be competent to proliferate but it also propels tumorigenesis by activating the TAZ-mediated Hippo transcriptional program. |
| **Suggested Reviewers:** | Donna Zhang<br>University of Arizona<br>dzhang@pharmacy.arizona.edu<br>Expert in NRF2 and cancer |
| | Thomas Kensler |

| | |
|---|---|
| | Johns Hopkins University School of Medicine<br>tkensle1@jhu.edu<br>Expert in NRF2 and cancer |
| | Manuel Serrano<br>Institut de Recerca Biomedica<br>manuel.serrano@irbbarcelona.org<br>Expert in cancer stem cells |
| Opposed Reviewers: | |

UNIVERSIDAD AUTONOMA DE MADRID

**Facultad de Medicina**
**Departamento de Bioquímica**

Editor of Cell Reports

Madrid, 31/7/2019

Dear Dr. Sara Hamilton,

We are submitting the revised version of manuscript entitled "Transcription factor NRF2 uses the Hippo pathway effector TAZ to induce tumorigenesis in glioblastomas" to be considered for publication in Cell Reports.

We have addressed experimentally all reviewers' comments as indicated in the "answer to reviewers" file. We have also included additional data related to magnetic resonance imaging of intracranial grafts. For this reason we have added one more co-author.

We hope that now you find this study suitable for publication in Cell Reports.

Looking forward to hearing from you,

Sincerely,

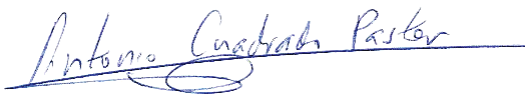

Antonio Cuadrado
Corresponding author

# Transcription factor NRF2 uses the Hippo pathway effector TAZ to induce tumorigenesis in glioblastomas

Maribel Escoll[1,2,3,4], Diego Lastra[1,2,3,4], Marta Pajares[1,2,3,4], Natalia Robledinos-Antón[1,2,3,4], Ana I. Rojo[1,2,3,4], Raquel Fernández-Ginés[1,2,3,4], Marta Mendiola[5], Virginia Martínez-Marín[6], Isabel Esteban[6], Pilar López-Larrubia[4], Ricardo Gargini[7], and Antonio Cuadrado[1,2,3,4]*

[1] Instituto de Investigaciones Biomédicas "Alberto Sols" UAM-CSIC,

[2] Instituto de Investigación Sanitaria La Paz (IdiPaz)

[3] Department of Biochemistry, Faculty of Medicine, Autonomous University of Madrid, Madrid, Spain.

[4] Centro de Investigación Biomédica en Red sobre Enfermedades Neurodegenerativas (CIBERNED), ISCIII, Madrid, Spain.

[5] Laboratory of Pathology and Translational Oncology, Instituto de Investigación Sanitaria La Paz (IdiPaz), Madrid, Spain.

[6] Department of Pathology, Instituto de Investigación Sanitaria La Paz (IdiPaz), Madrid, Spain.

[7] Centro de Biología Molecular "Severo Ochoa" UAM-CSIC, Autonomous University of Madrid, Madrid, Spain.

**Running title:** TAZ mediates NRF2 malignancy in glioblastomas

**Keywords:** oxidative stress, cancer stem cells, chemotherapy, glioblastoma

**DECLARATION OF INTERESTS:** The authors declare no competing interests

*To whom correspondence should be addressed:

Dr. Antonio Cuadrado
Instituto de Investigaciones Biomédicas "Alberto Sols" UAM-CSIC
C/ Arturo Duperier, 4, 28029 Madrid, Spain
Email: antonio.cuadrado@uam.es
Tel: +34915854383/ Fax: +34915854401

**ABSTRACT**

Transcription factor NRF2 orchestrates a cellular defense against oxidative stress and so far, has been involved in tumor progression by providing a metabolic adaptation to tumorigenic demands and resistance to chemotherapeutics. In this study, we discover that NRF2 also propels tumorigenesis in gliomas and glioblastomas by inducing the expression of the transcriptional co-activator TAZ, a protein of the Hippo signaling pathway that promotes tumor growth. The expression of the genes encoding NRF2 (NFE2L2) and TAZ (WWTR1) showed a positive correlation in 721 gliomas from The Cancer Genome Atlas database. Moreover, NRF2 and TAZ protein levels also correlated in immunohistochemical tissue arrays of glioblastomas. Genetic knock-down of NRF2 decreased, while NRF2 overexpression or chemical activation with sulforaphane, increased TAZ transcript and protein levels. Mechanistically, we identified several NRF2-regulated functional enhancers in the regulatory region of WWTR1. The relevance of the new NRF2/TAZ axis in tumorigenesis was demonstrated in subcutaneous and intracranial grafts. Thus, intracranial inoculation of NRF2-depleted glioma stem cells did not develop tumors as determined by magnetic resonance imaging. Forced TAZ overexpression partly rescued both stem cell growth in neurospheres and tumorigenicity. Hence, NRF2 not only enables tumor cells to be competent to proliferate but it also propels tumorigenesis by activating the TAZ-mediated Hippo transcriptional program.

**INTRODUCTION**

Glioblastomas (GBs) are the most common primary malignant brain tumor and remain incurable, with a poor survival rate after diagnosis. They present somatic mutations in receptor tyrosine kinase pathways, p53 and retinoblastoma, that correlate with their anatomopathological classification (Hanif et al., 2017). However, the participation of other effectors in their molecular pathology is less known.

NRF2 (Nuclear factor (erythroid-derived 2)-like 2) is a basic region-leucine zipper transcription factor that forms heterodimers with small musculoaponeurotic fibrosarcoma proteins (MAFs) in the nucleus (Cuadrado et al., 2018). The heterodimer recognizes an enhancer sequence termed antioxidant response element (ARE) that is present in the regulatory regions of more than 200 genes (ARE genes). ARE genes encode a broad network of enzymes involved in phase I, II, and III biotransformation reactions, antioxidant mechanisms encompassing NADPH-, glutathione- and thioredoxin-mediated reactions, lipid and iron catabolism, autophagy gene expression, etc. Through this complex transcriptional network, NRF2 coordinates multifaceted responses to diverse forms of stress for the maintenance of a stable internal environment (Hayes and Dinkova-Kostova, 2014; Lee et al., 2018). It is now accepted that these homeostatic functions provide a growth advantage to cancer cells in the hostile tumor microenvironment and promote cancer progression (DeNicola et al., 2011), metastasis (Wang et al., 2008), and resistance to chemo- and radiotherapy (Namani et al., 2017; Padmanabhan et al., 2006; Sporn and Liby, 2012). Its activity is generally increased in glioblastoma cell lines (Cong et al., 2013) and tumors (Kanamori et al., 2015), and elimination of NRF2 expression inhibits the proliferation and self-renewal of glioma stem cells (Kanamori et al., 2015).

The tumor promoting activity of NRF2 is due to its homeostatic functions. However, high NRF2 expression is observed in embryonic, pluripotent and cancer stem cells (Jia et al., 2015; Wu et al., 2015; Zhu et al., 2014a) in *in vitro* culture, suggesting additional pro-tumorigenic functions. NRF2 controls the expression of the stemness associated protein NOTCH1 (Wakabayashi et al., 2010), while NRF2 inactivation affects stem cell renewal (Jia et al., 2015; Zhu et al., 2014a; Zhu et al., 2013). However, a mechanistic connection between stemness and NRF2 has not been demonstrated yet. Here, we focused on the Hippo pathway effector TAZ (Transcriptional co-activator with PDZ-binding motif). The Hippo pathway is a Ser/Thr phosphorylation-dependent cascade that, through the YAP and TAZ co-activators of TEADs1-4, participates in regulation of organ development, cell proliferation, migration, invasion, and stemness in multiple human cancers (Moroishi et al., 2015). TAZ, encoded by *WWTR1* (WW domain-containing transcription regulator protein 1), is a crucial element of the Hippo signaling pathway. Its expression is elevated in several

tumor types including gliomas (Zhou and Lei, 2016) and correlates with the grade of malignancy, being maximal in glioblastomas (Bhat et al., 2011). Patients with TAZ over-expressing tumors exhibit a poor prognosis, and, in cell models, TAZ promotes tumor progression, while its knockdown prevents proliferation, tumorigenicity and invasion of glioma cells (Bhat et al., 2011). TAZ is exquisitely regulated at the level of protein stability by a wide range of stress signals such as mechanical stress, low energy status, hypoxia and osmotic stress (Dupont et al., 2011; Zhou et al., 2015). These signals activate the Hippo pathway, leading to TAZ phosphorylation and subsequent cytoplasmic retention and degradation (Liu et al., 2010; Yu and Guan, 2013). However, little is known about the regulation of its encoding gene, *WWTR1*, despite it must be crucial in order to sustain high long-term levels of TAZ activity.

In this study, we analyzed if NRF2 might activate the Hippo pathway at the level of TAZ, taking GBs as a model. We report that NRF2 induces the expression of *WWTR1*, which is partly required for its oncogenic activity. Thus, NRF2 delivers a growth, proliferative and survival signal through TAZ in glioblastomas, which is not directly related to redox metabolism or cytoprotection. These results provide a new strategy for targeted glioblastoma therapy at the level of NRF2 by reducing not only its cytoprotective function but also the TAZ-dependent growth and proliferative signature.

## RESULTS

### Analysis of *NFE2L2* and *WWTR1* expression in GBs

We first analyzed the frequency of mutations in the genes *KEAP1*, and *NFE2L2*, encoding the main NRF2 repressor KEAP1 and NRF2, respectively, as well as several other growth-related pathways in 721 brain tumors from The Cancer Genome Atlas (TCGA) database. Only 11 tumors exhibited mutations in *KEAP1* or *NFE2L2* and only 32 in genes of the Hippo pathway (**Fig. 1A**). LGGs exhibited frequent mutations in *IDH1*, encoding Isocitrate Dehidrogenase-1 and *ATRX*, encoding ATP-dependent helicase. By contrast, GBs were prone to mutations in *EGFR*, encoding Epidermal Growth Factor Receptor, and *PTEN*, encoding Phosphatase and Tensin Homolog (**Fig. 1B**). It has been previously reported that LGGs exhibit low NRF2 levels, but the role of this factor in GB is poorly defined. In search for a mechanistic role of NRF2 in GBs, we focused in the Hippo pathway because the lack of frequent mutations might allow unmasking its physiological mechanism of regulation and its pathological subversion. We found a positive correlation in the abundance of *NFE2L2* and *WWTR1* transcripts in both LGGs and GBs (**Fig. 1C and D**). Furthermore, we observed a striking similarity in the prognosis of *NFE2L2* and *WWTR1* overexpressing gliomas.

Besides, high expression of either of them had a bad prognosis with an average of 1.7 years survival in both cases (**Fig. 1E**).

We further investigated NRF2 and TAZ protein levels in a tissue array of 26 histologically-defined GBs, all of which were negative for *IDH1* and *ATFX* mutations (**Supplementary Fig. S1A**). As an additional control of NRF2 activity, we analyzed the downstream regulated gene product NADP(H) quinone oxidoreductase (NQO1). **Fig. 1F** shows three representative GBs with correlatively low, medium and high levels of NRF2, TAZ and NQO1 proteins. Densitometric quantification further demonstrated a statistically significant correlation in the expression of NRF2, TAZ and NQO1 proteins (**Fig. 1G and 1H**). Moreover, there is a positive correlation in the expression of NRF2 and TAZ with the proliferation marker ki67 (**Supplementary Fig. S1A and S1B)**. Considering the strong correlation observed in prognosis, transcript and protein levels, in the following experiments we studied a potential mechanistic connection between NRF2 and TAZ.

**Changes in NRF2 expression modify TAZ levels in tumor explants and cell lines**

Four explants originated from independent GBs were lentivirally-transduced for 7 days with short hairpin RNAs, control (shco) or specific for NRF2 knock-down (shNRF2) (**Fig. 2A and 2B**). Efficient knock-down of NRF2 was confirmed at both the mRNA and protein levels to just 10-20% of its original expression levels. As expected, NRF2 knock-down led to the down-regulation of the *bonafide* NRF2 target NQO1 but, importantly, also led to a decrease of TAZ transcript and protein levels.

We further extended these observations to the GB cell lines U-373 MG and U-87 MG. In agreement with the results obtained in tumor explants, lentiviral knock-down of NRF2 for 7 days in U-373 MG cells led to a reduction of *NQO1*, as a control, as well as *WWTR1* and two of its targets *BIRC5* and *CTGF* (with subtle changes in *CD44*) (**Fig. 2C and 2D**). By contrast, TAZ knock-down reduced the expression of *WWTR1* and its targets but did not have a significant effect on the mRNA levels of *NFE2L2* or *NQO1*. Similar results were found in U-87 MG cells (**Fig. 2E and 2F**). Moreover, a time-course of lentiviral knock-down of NRF2 further demonstrated a progressive reduction in transcript and protein levels of NQO1 as expected but also of TAZ (**Supplementary Fig. S2A and S2B)**. As additional controls, another shNRF2 lentivirus yielded comparable results (**Supplementary Fig. S2C and S2D)** and ectopic expression of NRF2 in the shNRF2-knocked-down cells rescued TAZ levels (**Supplementary Fig. S2E**). These results indicate that NRF2 is required for expression of TAZ.

Then, we used genetic and chemical strategies to upregulate NRF2. Lentiviral over-expression of NRF2 for 4 days led to a modest increase in TAZ and NQO1 mRNA and protein levels in two primary glioblastomas (GB1 and GB3) (Fig. 3A and 3B) and U-373 MG and U-87

MG cells (Supplementary Fig. S3A and S3B). The low effect of NRF2 overexpression might be due to the fact that glioma stem cells exhibit basally high NRF2 levels (Zhu et al., 2014b). Therefore, we analyzed the effect of NRF2 overexpression in the non-tumorigenic ReNcell stem cell line, which exhibits low NRF2 expression (Fig. 3C and Supplementary Fig. S3C). Ectopic expression of NRF2 in these cells led to increased levels of control NQO1 protein and mRNA but also TAZ and its target CTGF (Fig. 3D and 3E).

In order to analyze the temporal changes in the NRF2 and TAZ transcriptional signatures, we treated these cells with the NRF2 activator sulforaphane (SFN, 15 μM). NRF2 was stabilized within the first 3 h of treatment and then slowly decreased to basal levels at 48 h (Fig. 3F). This change correlated with a gradual accumulation of NQO1 and TAZ, first at the transcriptional level and then at the protein level (Fig. 3F, 3G and 3H). Although WWTR1 gene induction was more modest than that for NQO1, at the protein level TAZ also remained significantly elevated for at least 48 h (Fig. 3G). Thereafter, CTGF transcript levels augmented slowly in a fashion consistent with the TAZ increase, further leading to the accumulation of CTGF protein by 48 h (Fig. 3F and 3H). These results suggest a mechanistic connection between NRF2 and the TAZ transcriptional programme. Thus, a first wave of NRF2-dependent transcriptional activation that included NQO1 and TAZ (blue area in Fig. 3H) was followed by a second more modest wave where TAZ levels were high enough to expression of the CTGF gene (green area in Fig 3H).

**The regulation of *WWTR1* by NRF2 is not dependent of the redox state**

NRF2 reinforces the antioxidant defense to tolerate the redox alterations of tumor cells. Therefore, we determined if the reduction of *WWTR1* expression in NRF2-depleted cells could be attributed to a modification of the redox environment. NRF2 was silenced in the four GB explants and the two GB cell lines, and the levels of reactive oxygen species (ROS) were measured with the fluorescent probe hydroethidine (HE) by flow cytometry. As shown in **Fig. 4A**, NRF2-depletion did not increase ROS levels in any of the cell lines analyzed except U-87 MG, and yet there was a drastic reduction of TAZ protein levels, suggesting that the regulation of *WWTR1* by NRF2 is redox-independent. We further analyzed NRF2 knocked-down U-87 MG cells after incubation with the membrane permeable glutathione analog monoethylglutathione (GSH-MEE). The combination of NRF2 silencing and GSH-MEE exposure led to graded levels of HE fluorescence (**Fig. 4B and 4C**), and again TAZ levels were only dependent on NRF2 expression (**Fig. 4D**). These results indicate that NRF2 regulates TAZ by a redox-independent mechanism.

**The *WWTR1* promoter has functional NRF2-binding sites**

We then looked for putative NRF2-regulated AREs in the *WWTR1* gene by using the Encyclopedia of DNA Elements at UCSC (ENCODE)

(http://www.webcitation.org/query?url=https%3A%2F%2Fgenome.ucsc.edu%2F&date=2015-07-29) of the human genome (Feb. 2009). This database contains experimental data from chromatin immunoprecipitation (ChIP) studies of several transcription factors. Although NRF2 is not included, we analyzed three other ARE-binding factors, MAFK, MAFF and BACH1, for which information is available, and retrieved 9 putative ARE candidates according to the consensus sequence for NRF2 binding depicted at the JASPAR database (http://jaspar.genereg.net/) (**Supplementary Table S1A)**. As shown in **Fig. 5A**, some of these AREs are located at transcriptionally active chromatin sites, as determined by the presence of DNAse and acetylation sensitive regions. Additionally, a similar analysis of the YAP coding gene (*YAP1*) evidenced three putative AREs with high score (**Supplementary Table S1A and Supplementary Fig. S4A**) and in fact, YAP was also down-regulated in NRF2-silenced GBMs (**Supplementary Fig. S3B and S4C**). Focusing our study on TAZ, the nine putative AREs of the *WWTR1* gene were further analyzed by ChIP assays for endogenous NRF2 in two glioblastoma explants (**Fig. 5B and Supplemental Table 1B**). To avoid potential unspecific binding, we further confirmed these results with the immunoprecipitation of a V5 tagged-NRF2 construct in HEK293T transfected cells (**Supplemental Fig. 5A**) (McMahon et al., 2003). Immunoprecipitated DNA was analyzed by qRT-PCR with specific primers surrounding the putative AREs (**Supplementary Table S2**). At least 3 of the 9 putative AREs analyzed, termed ARE2, ARE5 and ARE6, exhibited high enrichment although not as strong as the positive controls *HMOX1* and *NQO1* (**Fig. 5B, 5C and Supplementary Table S1B**). No enrichment was detected with specific primers for *ACTB* or for an upstream region of *NQO1* that does not contain an ARE (*NQO1**) (Pajares et al., 2016), carried as negative controls. We chose ARE2, which is located in the 5'-regulatory region, and shows the lowest enrichment of the three AREs in the primary GBs for additional characterization in reporter luciferase assays. Three tandem nucleotide sequences of ARE2-WT or ARE2-mutated in the most conserved T and G residues were cloned in the promoter region of a luciferase reporter (**Fig. 5D**). Because GBs were difficult to transfect, we used U-87 MG and U-373 MG cells. We found that NRF2 interference reduced the luciferase expression of ARE2-WT reporter while the ARE2-mutated reporter did not respond at all **(Fig. 5E)**. Additionally, HEK293T cells transiently co-transfected with these reporters plus increasing amounts of NRF2-$^{\Delta ETGE}$-V5 exhibited increased luciferase activity of ARE2-WT but not ARE2-mutated (**Supplementary Fig. S5B**). Altogether, these results indicate that NRF2 binds and activates specific ARE sequences in the *WWTR1* gene promoter.

**TAZ rescues neurosphere growth of NRF2 knocked-down glioma stem cells**

Cancer stem cells are responsible for anticancer drug resistance and tumor relapse. Two different glioblastoma explants, GB1 and GB3, and both U-373 MG and U-87 MG cell lines can be grown as

glioma stem cells in the appropriate medium as floating spherical colonies, termed neurospheres (Gargini et al., 2015; Gargini et al., 2016; Hardee et al., 2012). Therefore, we next tested the effect of depleting either NRF2 or TAZ under neurosphere growth conditions. Lentiviral knock-down of NRF2 or TAZ yielded GB1 (**Fig. 6A- 6C**), GB3 (**Fig. 6D- 6F**), U-87 MG cells (**Supplementary Fig. S6A and S6B**) and U-373 MG cells (**Supplementary Fig. S6C and S6D**) unable to grow as neurospheres. Moreover, glioma stem cell frequency was decreased as determined in limiting dilution assays (**Supplementary Table S3A)**, demonstrating the importance of both proteins for cancer stem cell growth. In rescue experiments, NRF2 knock-down was combined with ectopic retroviral expression of TAZ in glioblastomas explants GB1 (**Fig. 6G- 6I**), GB3, (**Fig. S6J- 6L**), U-87 MG (**Supplementary Fig. 6E- 6H)** and U-373 MG (**Supplementary Fig. 6I and 6H)**. As shown in **Supplementary Fig. 6F**, overexpression of TAZ led to the induction of the TAZ-regulated genes *BIRC5* and *CD44* despite NRF2-knockdown. Regarding neurosphere growth (**Fig. 6H, 6I, 6K, 6L, Supplementary Fig. 6G- 6J**), TAZ also partially rescued both the number of neurospheres and the number of cells and also, glioma stem cell frequency in limiting dilution assays (**Supplementary Table S3B)**. Altogether, these results point to TAZ as an instrumental effector of NRF2-driven cancer stem cell growth.

**The NRF2/TAZ axis is essential for tumorigenesis of GBs**

We assessed the tumorigenicity of NRF2- or TAZ-knocked down glioma stem cells in xenotransplanted athymic mice. The growth of subcutaneous xenografts was substantially reduced by silencing the expression of either transcription factor in U-87 MG cells (Fig. 7A, and 7B) or U-373 MG cells (Supplementary Fig. S7A and S7B). In mice intracranially inoculated with U-87 MG cells, the survival rate was roughly 30 days and increased up to 40 and 60 days by selective silencing of NRF2 or TAZ, respectively (Fig. 7C).

In order to better reproduce the human pathology, we orthotopically implanted GB3 primary tumor cells and monitored tumor formation in the brain by magnetic resonance imaging (Fig. 7D and 7E). These cells developed tumors that, like in humans, exhibited heterogeneous and diffused borders with peritumoral and systemic brain edema (Supplemental Fig. 7C). Primary GB3 cells developed tumors before 10 days. However, when the same cells were knocked-down for expression of NRF2 or TAZ, they did not generate tumors at least after 30 days (Fig. 7D and 7E).

In additional rescue experiments we tested the relevance of TAZ as an effector of NRF2-mediated tumorigenicity. TAZ over-expression in control cells expressing basal levels of NRF2 did not lead to a statistically significant increase in tumor volume. However, TAZ over-expression restored by 20% the growth of tumors derived from NRF2- knocked-down U-87 MG (Fig. 7F and 7G) and U-373 MG cells (Supplementary Fig. S7D and S7E). In intracranial tumors, mouse life expectancy

decreased from 45 days in the control NRF2-silenced cells to 35 days in the TAZ rescued cells (Fig. 7H). These results indicate that TAZ is one effector of NRF2-induced tumorigenicity in GBs.

**DISCUSSION**

An effective therapy for GB would be possible if its molecular pathology was better known. In the TCGA database we found that somatic mutations in the NRF2 and Hippo pathways are rare (Fig. 1A) whereas EGFR and PTEN mutations are very frequent. However, NRF2 levels were high in these glioma stem cells compared to the non- tumorigenic neural stem cell line ReNcell, therefore demonstrating an abnormal up- regulation of NRF2 in GBs. These results suggest that NRF2 activation might be connected with subversion of signaling pathways that impinge on EGFR or PTEN. We have previously reported that chemical or genetic inhibition of PTEN in prostate and endometrial cancers leads to the activation of NRF2. This is due to the constitutive inhibition of glycogen synthase kinase-3 (GSK-3), thus relieving NRF2 from the GSK3/beta-TrCP ubiquitin-proteasome pathway (Cuadrado, 2015; Rada et al., 2011; Rada et al., 2012).

We also found that the transcript levels of WWTR1 exhibit the same trend as NRF2 to be increased in GBs, suggesting that they might be mechanistically connected. Genetic (shRNA and NRF2 overexpression) and chemical (sulforaphane) manipulation of NRF2 indicated that the transcript and protein levels of TAZ and TAZ-dependent genes are, at least in part, governed by the levels of NRF2. Because TAZ responds to stress signals, we analyzed if the changes in TAZ levels could be attributed to an indirect effect that might result from variations in oxidative stress when NRF2 is silenced. However, under cancer stem cell growth conditions, the depletion of NRF2 did not lead to measurable redox changes except in U-87 MG cells. Although at first glance this finding may seem surprising, it should be noted that up-regulation of NRF2 not only provides redox tolerance, but also a metabolic switch towards the pentose phosphate pathway that leads to NADPH and ribose production as precursors for cell growth and division. This metabolic reprograming may be particularly important in tumors with low growth rate where redox alterations are not so relevant and yet need growth precursors. In any case, the fact that U- 87 MG submitted to GSH-MEE did not alter TAZ levels further suggests that NRF2 can regulate TAZ in a redox-independent manner.

We identified several putative AREs in the WWTR1 gene promoter. The most potent ARE located at a highly DNAse-sensitive and H3K27-acetylated region, suggesting that it is accessible to the transcriptional machinery, but was not as potent as the canonical ARE of HMOX1, which is rapidly induced upon NRF2 activation. Several studies have analyzed the NRF2 transcriptional signature by microarray or RNA-sequencing approaches (Chorley et al., 2012; Namani et al., 2017). From these studies it is possible to distinguish grades of gene response to NRF2, from the most sensitive ones, related to the classical redox control, to others that need more time and persistent presence of

NRF2. For instance, genes involved in metabolic reprograming or autophagy appear to require persistent exposure to NRF2 (Mitsuishi et al., 2012; Pajares et al., 2016). Therefore, we suggest that a low but persistent level of TAZ expression elicited by NRF2 may contribute to promotion of tumorigenesis in GBs. Considering that cell specific epigenetic changes may hinder regulatory sequences, the relevance of this NRF2/TAZ axis needs to be evaluated under the particular conditions of each cellular model.

Glioma stem cells were strictly dependent of NRF2 expression to develop spheroids and tumors, in agreement with a previous study (Ji et al., 2013), as NRF2 knocked-down xenografts exhibited a dramatic reduction in tumor formation following subcutaneous and intracranial inoculation. Interestingly, TAZ overexpression partially restored stem cell growth and tumorigenicity, further demonstrating that TAZ is an effector of NRF2 to support stemness. However, this effect was modest, suggesting the NRF2 uses additional pathways to elicit tumorigenicity. In fact, besides it role in redox regulation, recent studies further suggest that NRF2 regulates pathways involved in tumorigenesis and self-renewal such as Shh ((Jang et al., 2016), Wnt (Rada et al., 2015) and Notch (Wakabayashi et al., 2014).

It would be expected that the Hippo pathway is silent in cancer cells for TAZ to remain transcriptionally active. However, among the 721 gliomas analyzed, only 4.4% exhibited mutations that might potentially inactivate the Hippo pathway (Fig. 1A and (Sanchez-Vega et al., 2018)). Moreover, TAZ expression was increased in these tumors, therefore indicating additional mechanisms for TAZ up-regulation. Our study identifies NRF2 as one such mechanism, hence probably counteracting repressor signals and providing a tumor growth advantage.

An efficient therapy for GBs must consider that high NFE2L2 and WWTR1 levels are predictors of chemoresistance (Rocha et al., 2016; Tian et al., 2015). Indeed, overexpression of NRF2 and TAZ correlated with resistance to the alkylating agent temozolomide, which is the gold standard treatment for gliomas. At this time, no selective NRF2 inhibitor is available, but at least as a proof-of-concept, we found that genetic knock- down of NRF2 drastically reduced TAZ transcriptional signature and stemness in gliomas. Contrary to EGFR and PTEN, the observation that NFE2L2 is not frequently mutated in GBs and that yet NRF2 is strictly necessary to sustain tumorigenesis of glioblastoma stem cells provides a rationale to use drugs that could modulate NRF2 activity as a downstream effector of these mutated genes.

## EXPERIMENTAL PROCEDURES

### Glioma database analyses

LGG and GB datasets were retrieved from The Cancer Genome Atlas (https://www.ncbi.nlm.nih.gov/pubmed/27157931) and analysed for *NFL2L2* and *WWTR1* expression (https://xenabrowser.net/; https://www.ncbi.nlm.nih.gov/pubmed/24120142). Mutations in the Hippo pathway or other signaling genes were also analysed from the TCGA datasets, which were downloaded respectively from cBioPortal (http://www.cbioportal.org/) and TCGA databases (http://tcga-data.nci.nhi.gov/docs/publications/lgggbm_2015), using the UCSC cancer browser.

### Cell culture and reagents

The validated cell lines HEK293T, U-373 MG and U-87 MG were maintained in Dulbecco's Modified Eagle Medium supplemented with 10% fetal bovine serum. Human GBs explants were kindly supplied by Dr Marta Izquierdo (Centro de Biología Molecular "Severo Ochoa" - Autonomous University of Madrid). Most experiments with these explants were performed with GB1 and GB3 because they exhibit the highest proliferative rates. All experiments were conducted under neurosphere culture conditions as described previously (Gargini et al., 2015). Inmortalized human neural stem cells derived from ventral mesencephalon of fetal brain (ReNcell) were plated onto Corning® Matrigel® hESC-Qualified Matrix (CORNING) and maintained in Neurobasal medium (Gibco) containing 2% B27 Supplement (Gibco) (v/v), 20 ng/ml recombinant human EGF (Peprotech), 20 ng/ml recombinant human basic FGF (Peprotech), 100 U/ml Penicillin/Streptomycin (Life Technologies) and 1% Amphotericin b solution (Lonza) in 5% $CO_2$ at 37°C conditions. Sulforaphane (SFN) and GSH-MEE were purchased from Sigma-Aldrich. Limiting dilution assays were performed essentially as described in (Hu and Smyth, 2009). The final data and the statistical significances were calculated using the Extreme Limiting Dilution Analysis (ELDA) software (http://bioinf.wehi.edu.au/software/limdil/ index.html) (Hu and Smyth, 2009).

### Immunoblotting

This protocol was performed as described in (Pajares et al., 2016). Briefly, cells were homogenized in lysis buffer (TRIS pH 7.6 50 mM, 400 mM NaCl, 1 mM EDTA, 1 mM EGTA and 1% SDS) and samples were heated at 95°C for 15 min, sonicated and pre-cleared by centrifugation. Proteins were resolved in SDS-PAGE, transferred to Immobilon-P (Millipore) membranes and proteins of interest were detected with the following primary antibodies: NRF2 (homemade and validated in (Rada et al., 2011)), NQO1 (ab2346, Abcam), GAPDH (CB1001, Merck Millipore), YAP/TAZ (8418, Cell Signaling Techonology); LaminB (sc-6217, Santa Cruz Biotechnology). Proper peroxidase-conjugated secondary antibodies were used for detection by enhanced chemiluminescence (GE

Healthcare).

**Lentiviral and retroviral vector production and infection**

Pseudotyped lentiviral vectors were produced in HEK293T cells transiently co-transfected with 10 μg of the corresponding lentiviral vector pWXL, 6 μg of the packaging plasmid pSPAX2 (12260, Addgene) and 6 μg of the VSV-G envelope protein plasmid pMD2G (12259, Addgene) using Lipofectamine Plus reagent according to the manufacturer's instructions (Invitrogen). Retrovirus supernatant was prepared by transfection of phoenix-Ampho cells (Garry Nolan, Baxter Laboratory in Genetic Pharmacology, Department of Microbiology and Immunology, Stanford University, 450 Serra Mall) with 5 μg of each plasmid using Lipofectamine Plus. Lentiviral vector shRNA control (shco), several shNRF2 and shTAZ were purchased from Sigma-Aldrich (MISSION shRNA). The lentiviral vector pWPXL-NRF2-WT (NRF2) was homemade using as expression vector pWPXL (control) (12257, Addgene). The retroviral vectors used were: pBabePuro (1764, Addgene) and pBabePuroTAZ-WT (TAZ) (generous gift from Kun-Liang Guan). Cells were infected in the presence of 4 μg/ml polybrene (Sigma-Aldrich) and selected with 1 μg/ml puromycin (Sigma-Aldrich).

**Chromatin immunoprecipitation (ChIP) assay**

This protocol was performed as described in (Pajares et al., 2016). Briefly, cells derived from two different glioblastoma explants were grown under stemness conditions and allowed to form neurospheres. Neurospheres were trypsinized and fixed with 1% formaldehyde. For HEK293T, cells were transfected with plasmid pcDNA3-NRF2-$^{\Delta ETGE}$-V5 encoding a NRF2 cDNA that lacks the high-affinity binding site for KEAP1 and contains a V5 tag. DNA complexes were immunoprecipitated with either anti-NRF2 (homemade) and rabbit anti-IgG (ab37415, Abcam) for glioblastoma explants or anti-V5 (37-7500, Invitrogen) and mouse anti-IgG (ab18413, Abcam) antibodies for transfected HEK293T cells. qRT-PCR was performed with the primers shown in **Supplementary Table S2**. Samples from at least 3 independent ChIPs were analyzed.

**Analysis of mRNA levels**

Total RNA extraction and qRT-PCR were done as detailed in (Rojo et al., 2010). Primer sequences are shown in **Supplementary Table S4**. Data analysis was based on the ΔΔCT method, with normalization of the raw data to the housekeeping gene *GAPDH* (Applied Biosystems). All PCRs were performed from triplicate samples.

**Xenograft and intracranial tumorigenicity assays**

Balb/c athymic Nude-Foxn1$^{nu}$ mice (Harlan) were used for the xenograft (eight-week-old males) and intracranial (six-week-old females) tumor assays. U-373 MG or U-87 MG cells ($10^6$ cells in 0.1 ml PBS) were inoculated subcutaneously. For xenografts, tumor growth was examined every 5 days

for up to 65 days. Tumor volume = $\pi/6 \times (\text{mean diameter})^3$ (Escoll et al., 2017). U-87 MG ($10^5$ cells in 2 µl PBS) or GB3 explant glioblastoma cells ($2x10^5$ cells in 2µl PBS with 5 ng/µl recombinant human basic FGF and 5 ng/µl recombinant human EGF, both from Peprotech) were inoculated intracranially at the right hemisphere (1 mm anterior, 1.8 mm lateral to bregma and 3 mm intra-parenchymal). The Intracranial tumor assay protocol was performed as described previously (Gargini et al., 2016).

**Magnetic resonance imaging (MRI)**

MRI experiments were performed on a Bruker AVANCE III system (Bruker Medical GmbH®) using a 7.0-T horizontal superconducting magnet, equipped with a gradient insert (60 mm inner diameter) with a maximum intensity of 360 mT/m and a 1H selective surface coil (23 mm diameter). For assessing the tumor growth, contrast enhanced T1-weighted (CE-T1W) imaging was acquired after the intraperitoneal administration of 0.3M-Gd- diethylenetriaminepentaacetic acid (Magnevist®) at a dose of 0.2 mmol/kg. Images were obtained with a spin-echo sequence and the following parameters: repetition time = 250 ms, echo time = 10 ms, averages = 6, acquisition matrix = 256 × 256, in-plane resolution of 78 × 78 µm2, slice thickness = 1.0 mm and 10 slices in axial orientation (total acquisition time of 4.8 min). For assessing the edema, T2-weighted (T2W) spin-echo images were acquired with a rapid acquisition with relaxation enhancement sequence and the following parameters: repetition time = 2500 ms, echo time = 45 ms, averages = 5, RARE factor = 8, acquisition matrix = 256 × 256, in-plane resolution of 78 × 78 µm2, slice thickness = 1.0 mm and 10 slices in axial orientation (total acquisition time of 5 min). During the procedure, the mice are anesthetized and their vital signs are controlled. Tumor volumes were measured from anatomical CE-T1W images with ImageJ software.

**Immunohistochemistry**

Four µm-thick sections of paraffin-embedded samples of glioblastoma tissue from patients treated at the Instituto de Investigación Sanitaria La Paz (IdiPaz, Madrid, Spain) were arrayed in a collection of three tissue microarray slides. Taken together, these slides encompassed 26 good tumor cores. Sections were deparaffinized and rehydrated in water, and antigen retrieval was carried out by incubation in 1 mM EDTA, 0.05% Tween 20, pH 8.0 at 50°C for 45 min. Endogenous peroxidase and nonspecific antibody reactivity was blocked with peroxidase blocking reagent (Dako) at room temperature for 15 min. The sections were then incubated for 60-90 min at 4°C with the corresponding peroxidase conjugated primary antibodies for NRF2 (PA1-38312, Thermo Fisher Scientific), TAZ (HPA007415, Sigma-Aldrich), NQO1 (ab34173, Abcam), ATRX (DIA-AX1, Dianova), IDH1 (DIA-H09, Dianova), ki67 (M7240, Dako) and developed with 3,3′-diaminobenzidine (DAB). Negative controls with goat serum replacing the primary antibody were

used. The slides were mounted with DPX (VWR International). Detection was performed with the Envision Plus Detection System (Dako). All tumors were negative for IDH1 and ATRX mutations, therefore confirming that according to histological classification they were GBs. Densitometric quantification was done using macros of the ImageJ software.

**Luciferase reporter generation and luciferase assay**

Oligonucleotides with 3 tandem repetitions of the putative ARE2-WT and ARE2-mutaded were cloned as detailed in **Supplementary Table S5** and previously described (Pajares et al., 2018). Cells were transiently transfected with the expression vectors ARE2-WT, ARE2-mutated or positive control ARE-Luc. pTK-Renilla was also transfected as an internal control. Luciferase assays were performed with the Dual- Luciferase Reporter Assay System (Promega, E1910) as previously described (Rada et al., 2012).

**Flow cytometry determination of reactive oxygen species.**

Intracellular reactive oxygen species (ROS) were detected in a FACScan flow cytometer (Becton-Dickinson) with hydroethidine (HE) (ThermoFisher Scientific), which upon oxidation emits orange fluorescence (BP 575/24 nm). Cells were incubated for 1 h at 37°C with 2 μM HE and then detached from the plate, washed once with cold PBS, and analyzed immediately.

**Statistical analyses**

Data are presented as mean ± S.D. (standard deviation) or S.E.M. (standard error of the mean) as indicated in each case. Statistical assessments of differences between groups were analyzed using GraphPad Prism 5 software by the unpaired Student's t-test. For the scatter plots, the Pearson correlation coefficient (R) and the *p*-value associated with this coefficient were analyzed. Statistically significant differences in Kaplan-Meier survival curves were calculated with the log-rank test.

**ACKNOWLEDGEMENTS**

This study was funded by the Spanish Ministry of Economy and Competitiveness (MINECO) under the grant SAF2016-76520-R. ME is recipient of a postdoctoral contract Juan de la Cierva; DL and NRA of a FPU contract of MINECO; MP and RFG of a FPI contracts of Autonomous University of Madrid. RG has been funded by the AECC Scientific Foundation.

**AUTHOR CONTRIBUTIONS**

ME, DL, MP, NRA, AIR and RFG conducted the experiments of molecular biology. MM, VMM and IE conducted tissue arrays. PLL conducted MRI data analysis. RG conducted massive data analysis. ME and AC designed the experiments and wrote the paper.

**REFERENCES**

Bhat, K.P., Salazar, K.L., Balasubramaniyan, V., Wani, K., Heathcock, L., Hollingsworth, F., James, J.D., Gumin, J., Diefes, K.L., Kim, S.H., *et al.* (2011). The transcriptional coactivator TAZ regulates mesenchymal differentiation in malignant glioma. Genes & development *25*, 2594-2609.

Cong, Z.X., Wang, H.D., Wang, J.W., Zhou, Y., Pan, H., Zhang, D.D., and Zhu, L. (2013). ERK and PI3K signaling cascades induce Nrf2 activation and regulate cell viability partly through Nrf2 in human glioblastoma cells. Oncology reports *30*, 715-722.

Cuadrado, A. (2015). Structural and functional characterization of Nrf2 degradation by glycogen synthase kinase 3/beta-TrCP. Free Radic Biol Med *88*, 147-157.

Cuadrado, A., Manda, G., Hassan, A., Alcaraz, M.J., Barbas, C., Daiber, A., Ghezzi, P., Leon, R., Lopez, M.G., Oliva, B., *et al.* (2018). Transcription Factor NRF2 as a Therapeutic Target for Chronic Diseases: A Systems Medicine Approach. Pharmacological reviews *70*, 348-383.

Chorley, B.N., Campbell, M.R., Wang, X., Karaca, M., Sambandan, D., Bangura, F., Xue, P., Pi, J., Kleeberger, S.R., and Bell, D.A. (2012). Identification of novel NRF2-regulated genes by ChIP-Seq: influence on retinoid X receptor alpha. Nucleic Acids Res *40*, 7416-7429.

DeNicola, G.M., Karreth, F.A., Humpton, T.J., Gopinathan, A., Wei, C., Frese, K., Mangal, D., Yu, K.H., Yeo, C.J., Calhoun, E.S., *et al.* (2011). Oncogene-induced Nrf2 transcription promotes ROS detoxification and tumorigenesis. Nature *475*, 106-109.

Dupont, S., Morsut, L., Aragona, M., Enzo, E., Giulitti, S., Cordenonsi, M., Zanconato, F., Le Digabel, J., Forcato, M., Bicciato, S., *et al.* (2011). Role of YAP/TAZ in mechanotransduction. Nature *474*, 179-183.

Escoll, M., Gargini, R., Cuadrado, A., Anton, I.M., and Wandosell, F. (2017). Mutant p53 oncogenic functions in cancer stem cells are regulated by WIP through YAP/TAZ. Oncogene *36*, 3515-3527.

Gargini, R., Cerliani, J.P., Escoll, M., Anton, I.M., and Wandosell, F. (2015). Cancer stem cell-like phenotype and survival are coordinately regulated by Akt/FoxO/Bim pathway. Stem cells (Dayton, Ohio) *33*, 646-660.

Gargini, R., Escoll, M., Garcia, E., Garcia-Escudero, R., Wandosell, F., and Anton, I.M. (2016). WIP Drives Tumor Progression through YAP/TAZ-Dependent Autonomous Cell Growth. Cell reports *17*, 1962-1977.

Hanif, F., Muzaffar, K., Perveen, K., Malhi, S.M., and Simjee Sh, U. (2017). Glioblastoma Multiforme: A Review of its Epidemiology and Pathogenesis through Clinical Presentation and Treatment. Asian Pac J Cancer Prev *18*, 3-9.

Hardee, M.E., Marciscano, A.E., Medina-Ramirez, C.M., Zagzag, D., Narayana, A., Lonning, S.M., and Barcellos-Hoff, M.H. (2012). Resistance of glioblastoma-initiating cells to radiation mediated by the tumor microenvironment can be abolished by inhibiting transforming growth factor-beta. Cancer research *72*, 4119-4129.

Hayes, J.D., and Dinkova-Kostova, A.T. (2014). The Nrf2 regulatory network provides an interface between redox and intermediary metabolism. Trends Biochem Sci *39*, 199-218.

Ji, X.J., Chen, S.H., Zhu, L., Pan, H., Zhou, Y., Li, W., You, W.C., Gao, C.C., Zhu, J.H., Jiang, K., *et al.* (2013). Knockdown of NF-E2-related factor 2 inhibits the proliferation and growth of U251MG human glioma cells in a mouse xenograft model. Oncology reports *30*, 157-164.

Jia, Y., Chen, J., Zhu, H., Jia, Z.H., and Cui, M.H. (2015). Aberrantly elevated redox sensing factor Nrf2 promotes cancer stem cell survival via enhanced transcriptional regulation of ABCG2 and Bcl-2/Bmi-1 genes. Oncology reports *34*, 2296-2304.

Kanamori, M., Higa, T., Sonoda, Y., Murakami, S., Dodo, M., Kitamura, H., Taguchi, K., Shibata, T., Watanabe, M., Suzuki, H., *et al.* (2015). Activation of the NRF2 pathway and its impact on the prognosis of anaplastic glioma patients. Neuro-oncology *17*, 555-565.

Lee, S.B., Sellers, B.N., and DeNicola, G.M. (2018). The Regulation of NRF2 by Nutrient-Responsive Signaling and Its Role in Anabolic Cancer Metabolism. Antioxidants & redox signaling *29*, 1774-1791.

Liu, C.Y., Zha, Z.Y., Zhou, X., Zhang, H., Huang, W., Zhao, D., Li, T., Chan, S.W., Lim, C.J., Hong, W., *et al.* (2010). The hippo tumor pathway promotes TAZ degradation by phosphorylating a phosphodegron and recruiting the SCF{beta}-TrCP E3 ligase. The Journal of biological chemistry *285*, 37159-37169.

McMahon, M., Itoh, K., Yamamoto, M., and Hayes, J.D. (2003). Keap1-dependent proteasomal degradation of transcription factor Nrf2 contributes to the negative regulation of antioxidant response element-driven gene expression. The Journal of biological chemistry *278*, 21592-21600.

Mitsuishi, Y., Taguchi, K., Kawatani, Y., Shibata, T., Nukiwa, T., Aburatani, H., Yamamoto, M., and Motohashi, H. (2012). Nrf2 redirects glucose and glutamine into anabolic pathways in metabolic reprogramming. Cancer cell *22*, 66-79.

Moroishi, T., Hansen, C.G., and Guan, K.L. (2015). The emerging roles of YAP and TAZ in cancer. Nature reviews Cancer *15*, 73-79.

Namani, A., Cui, Q.Q., Wu, Y., Wang, H., Wang, X.J., and Tang, X. (2017). NRF2-regulated metabolic gene signature as a prognostic biomarker in non-small cell lung cancer. Oncotarget *8*, 69847-69862.

Padmanabhan, B., Tong, K.I., Ohta, T., Nakamura, Y., Scharlock, M., Ohtsuji, M., Kang, M.I., Kobayashi, A., Yokoyama, S., and Yamamoto, M. (2006). Structural basis for defects of Keap1 activity provoked by its point mutations in lung cancer. Mol Cell *21*, 689-700.

Pajares, M., Jimenez-Moreno, N., Garcia-Yague, A.J., Escoll, M., de Ceballos, M.L., Van Leuven, F., Rabano, A., Yamamoto, M., Rojo, A.I., and Cuadrado, A. (2016). Transcription factor NFE2L2/NRF2 is a regulator of macroautophagy genes. Autophagy *12*, 1902-1916.

Pajares, M., Rojo, A.I., Arias, E., Diaz-Carretero, A., Cuervo, A.M., and Cuadrado, A. (2018). Transcription factor NFE2L2/NRF2 modulates chaperone-mediated autophagy through the regulation of LAMP2A. Autophagy *14*, 1310-1322.

Rada, P., Rojo, A.I., Chowdhry, S., McMahon, M., Hayes, J.D., and Cuadrado, A. (2011). SCF/{beta}-TrCP promotes glycogen synthase kinase 3-dependent degradation of the Nrf2 transcription factor in a Keap1-independent manner. Molecular and cellular biology *31*, 1121-1133.

Rada, P., Rojo, A.I., Evrard-Todeschi, N., Innamorato, N.G., Cotte, A., Jaworski, T., Tobon-Velasco, J.C., Devijver, H., Garcia-Mayoral, M.F., Van Leuven, F., *et al.* (2012). Structural and functional characterization of Nrf2 degradation by the glycogen synthase kinase 3/beta-TrCP axis. Molecular and cellular biology *32*, 3486-3499.

Rocha, C.R., Kajitani, G.S., Quinet, A., Fortunato, R.S., and Menck, C.F. (2016). NRF2 and glutathione are key resistance mediators to temozolomide in glioma and melanoma cells. Oncotarget *7*, 48081-48092.

Rojo, A.I., Innamorato, N.G., Martin-Moreno, A.M., De Ceballos, M.L., Yamamoto, M., and Cuadrado, A. (2010). Nrf2 regulates microglial dynamics and neuroinflammation in experimental Parkinson's disease. Glia *58*, 588-598.

Sanchez-Vega, F., Mina, M., Armenia, J., Chatila, W.K., Luna, A., La, K.C., Dimitriadoy, S., Liu, D.L., Kantheti, H.S., Saghafinia, S., *et al.* (2018). Oncogenic Signaling Pathways in The Cancer Genome Atlas. Cell *173*, 321-337.e310.

Sporn, M.B., and Liby, K.T. (2012). NRF2 and cancer: the good, the bad and the importance of context. Nature reviews Cancer *12*, 564-571.

Tian, T., Li, A., Lu, H., Luo, R., Zhang, M., and Li, Z. (2015). TAZ promotes temozolomide resistance by upregulating MCL-1 in human glioma cells. Biochemical and biophysical research communications *463*, 638-643.

Wakabayashi, N., Shin, S., Slocum, S.L., Agoston, E.S., Wakabayashi, J., Kwak, M.K., Misra, V., Biswal, S., Yamamoto, M., and Kensler, T.W. (2010). Regulation of notch1 signaling by nrf2: implications for tissue regeneration. Sci Signal *3*, ra52.

Wang, X.J., Sun, Z., Villeneuve, N.F., Zhang, S., Zhao, F., Li, Y., Chen, W., Yi, X., Zheng, W., Wondrak, G.T., *et al.* (2008). Nrf2 enhances resistance of cancer cells to chemotherapeutic drugs, the dark side of Nrf2. Carcinogenesis *29*, 1235-1243.

Wu, T., Harder, B.G., Wong, P.K., Lang, J.E., and Zhang, D.D. (2015). Oxidative stress, mammospheres and Nrf2-new implication for breast cancer therapy? Mol Carcinog *54*, 1494-1502.

Yu, F.X., and Guan, K.L. (2013). The Hippo pathway: regulators and regulations. Genes & development *27*, 355-371.

Zhou, X., and Lei, Q.Y. (2016). Regulation of TAZ in cancer. Protein & cell *7*, 548-561.

Zhou, X., Wang, Z., Huang, W., and Lei, Q.Y. (2015). G protein-coupled receptors: bridging the gap from the extracellular signals to the Hippo pathway. Acta biochimica et biophysica Sinica *47*, 10-15.

Zhu, J., Wang, H., Fan, Y., Hu, Y., Ji, X., Sun, Q., and Liu, H. (2014a). Knockdown of nuclear factor erythroid 2-related factor 2 by lentivirus induces differentiation of glioma stem-like cells. Oncology reports *32*, 1170-1178.

Zhu, J., Wang, H., Ji, X., Zhu, L., Sun, Q., Cong, Z., Zhou, Y., Liu, H., and Zhou, M. (2014b). Differential Nrf2 expression between glioma stem cells and non-stem-like cells in glioblastoma. Oncol Lett *7*, 693-698.

Zhu, J., Wang, H., Sun, Q., Ji, X., Zhu, L., Cong, Z., Zhou, Y., Liu, H., and Zhou, M. (2013). Nrf2 is required to maintain the self-renewal of glioma stem cells. BMC Cancer *13*, 380.

**LEGENDS TO FIGURES**

**Figure 1.** Analysis of *NFE2L2* and *WWTR1* expression in GBs. **(A- E)** Analysis of *NFE2L2* and *WWTR1* expression in 721 gliomas from the TCGA database. **(A)** Analysis of somatic mutations in genes of the Hippo pathway, *KEAP1* and *NFE2L2*. **(B)** Analysis of the most frequent somatic mutations in gliomas. **(C)** *NFE2L2* and *WWTR1* mRNAs are increased in GBs compared to LGGs. *p*-values for differences between groups are indicated in each graph and calculated using Student's t-test. **(D)** Scatter plot showing positive correlation between *NFE2L2* and *WWTR1* expression. The Pearson correlation coefficient (R) and the *p*-value associated with this coefficient are indicated. **(E)** Kaplan-Meier survival curves of patients with gliomas. Patients were stratified in two groups using *NFE2L2* or *WWTR1* Z-score values. Statistically significant differences in survival between groups were calculated using the log-rank test. **(F- H)** NRF2 and TAZ protein levels are positively correlated in GBs. A tissue array of 26 glioblastomas was analyzed. **(F)** Sections of three representative tumors with antibodies against NRF2, TAZ and NQO1 (scale bar, 50 μm). **(G, H)** Scatter plot showing positive correlation between densitometric quantification of DAB-staining (as percentage of area) of NRF2 and TAZ **(G)** or NRF2 and NQO1 **(H)**. The Pearson correlation

coefficient (R) and the *p*-value associated with this coefficient are indicated. See also **Supplementary Figure S1**.

**Figure 2.** NRF2 knocked-down cells exhibit decreased TAZ levels. **(A, B)** Four human glioblastoma explants (GB1, GB2, GB3 and GB4) were transduced with a lentivirus encoding control shRNA (shco) or human shNRF2. **(A)** mRNA levels of *NFE2L2* and *WWTR1* were determined by qRT-PCR and normalized by *GAPDH*. Data are mean ± S.D. (n = 3). Statistical analysis was performed with the Student's t-test. $^{**}p \leqslant 0.01$. **(B)** Representative immunoblot analysis of NRF2, TAZ, NQO1 and GAPDH and LaminB as loading controls (n = 3). **(C, D)**, U-373 MG and **(E, F)** U-87 MG glioblastomas cell lines were transduced with lentiviral vectors containing shcontrol (shco), human shNRF2 or human shTAZ. **(C, E)** mRNA levels of *NFE2L2*, *NQO1*, *WWTR1*, *BIRC5*, *CTGF* and *CD44* were determined by qRT-PCR and normalized by *GAPDH*. Data are mean ± S.D. (n = 3). Statistical analysis was performed with the Student's t-test. $^{**}p \leqslant 0.01$; (NS, indicated not statistically significant). **(D, F)** Representative immunoblot analysis of NRF2, TAZ, NQO1 and GAPDH and LaminB as loading controls (n = 4). Similar results were obtained with a different shNRF2 **(Supplementary Fig. S2)**.

**Figure 3.** Genetic and pharmacological up-regulation of NRF2 increases TAZ levels. **(A, B)** GB1 and GB3 glioblastoma cells were transduced with empty vector or lentiviral vector for overexpression of NRF2. **(A)** Representative immunoblot analysis of NRF2, TAZ, NQO1 and GAPDH as a loading control (n = 3). **(B)** Messenger RNA (mRNA) levels of *WWTR1* were determined by qRT-PCR and normalized by *GAPDH*. Data are presented as mean ± S.D. (n = 3) $^{**}p \leqslant 0.01$ according to a Student's t-test. **(C)** Representative immunoblot analysis of NRF2, TAZ, GAPDH and LaminB as loading controls in ReNcell, GB1 and GB3. **(D, E)** ReNcell were transduced with empty vector or lentiviral vector for overexpression of NRF2. **(D)** Representative immunoblot analysis of NRF2, TAZ, NQO1, CTGF and GAPDH as a loading control (n = 3). **(E)** Messenger RNA (mRNA) levels of *NQO1*, *WWTR1* and *CTGF* were determined by qRT-PCR and normalized by *GAPDH*. Data are presented as mean ± S.D. (n = 3) $^{**}p \leqslant 0.01$ according to a Student's t-test. (**F- H)** ReNcell cells were treated with sulforaphane (SFN) (15 μM) for the indicated times. **(F)** Representative immunoblot analysis of NRF2, TAZ, NQO1, CTGF, GAPDH and LaminB as loading controls (n = 3). **(G)** Densitometric quantification of TAZ levels representative blots from **(F)** relative to GAPDH and LaminB levels. Data are mean ± S.D. (n = 3) $^{*}p \leqslant 0.05$ according to a Student's t-test. **(H)** Messenger RNA (mRNA) levels of *NQO1*, *WWTR1* and *CTGF* were determined by qRT-PCR and normalized by *GAPDH*. Data are presented as mean ± S.D. (n = 3) $^{**}p \leqslant 0.01$ according to a Student's t-test. The blue area represents the wave of NRF2 dependent transcription and the green area depicts a second wave that involves NRF2 and

also TAZ-dependent transcription. The time for transition from one wave to the other was chosen arbitrarily. See also **Supplementary Figure S3**.

**Figure 4.** The regulation of *WWTR1* by NRF2 is not dependent of the redox state. **(A)** U-87 MG and U-373 MG glioblastoma cells and four human glioblastoma explants (GB1, GB2, GB3 and GB4) were transduced with lentiviral vectors containing shcontrol (shco) or human shNRF2 and changes in intracellular ROS were determined by HE staining (n = 3). **(B- D)** U-87 MG glioblastoma cells were transduced with lentiviral vectors containing shco or human shNRF2 and treated with GSH-MEE (10 mM, 16 h). **(B, C)** Flow cytometry analysis of shNRF2-induced intracellular ROS production in HE stained cells. A representative sample of 10,000 cells is shown for each condition. **(D)** Representative immunoblot analysis of NRF2, TAZ and GAPDH as a loading control (n = 3).

**Figure 5.** The *WWTR1* promoter has functional NRF2-binding sites. **(A)** Representative scheme of the gene *WWTR1* encoding TAZ. Regions enriched in acetylated histone H3 lysine 27 (H3K27ac) are shown in blue and regions sensitive to DNase are represented as dark boxes. Experimental sequences reported to bind MAFK, MAFF and BACH1 factors were analyzed for the presence of AREs (ARE 1-9). **(B, C)** ChIP analysis of putative AREs found in **(A)** using the anti-NRF2 antibody vs. a control IgG in glioblastoma explant cells GB1 **(B)** and GB3 **(C)**. **(D)** Luciferase reporter constructs used for assessment of wild type (WT) or mutated ARE2 functionality in pGL3basic vector. **(E)** U-87 MG (left) and U-373 MG (right) glioblastomas cell lines were transduced with lentiviral vectors containing shco and human shNRF2 and transfected with wild type or mutated ARE2. Luciferase activity was measured 24 h after transfection. Luciferase activities were normalized to renilla activity. Results are shown relative to control and are mean ± S.D. (n = 3). $^{**}p \leqslant 0.01$ according to a Student's t-test. See also **Supplementary Table S1, Table S2, Table S5, Supplementary Figure S4** and **Figure S5**.

**Figure 6.** Ectopic expression of TAZ rescues neurosphere growth of NRF2-knocked-down glioma stem cells GB1 **(A- C)** and GB3 **(D- F)** cells were transduced with lentivirus encoding shco, human shNRF2 or human shTAZ. **(A, D)** Representative immunoblot analysis of NRF2, TAZ and GAPDH as a loading control (n = 3). **(B, E)** Representative images of tumor neurosphere formation. Scale bar, 100 μm. **(C, F)** Quantification of the number of secondary neurospheres or the number of cells represented as percentage relative to shco. Data presented mean ± S.D. (n = 3) $^{**}p \leqslant 0.01$ according to a Student's t-test. GB1 **(G- I)** and GB3 **(J, L)** cells were transduced with empty retrovirus as control or a retrovirus expressing TAZ, and then with a lentivirus expressing shco or shNRF2. **(G, J)** Representative immunoblot analysis of NRF2, TAZ and GAPDH as a loading control (n = 3). **(H, K)** Representative images of tumor neurosphere formation. Scale bar, 100 μm.

**(I, L)** Quantification of the number of secondary neurospheres and the number of cells represented as a percentage relative to control-shco. Data are presented as mean ± S.D. (n = 3) **p ⩽ 0.01 according to a Student's t-test. See also **Supplementary Figure S6** and **Supplementary Table S3**.

**Figure 7.** Ectopic expression of TAZ rescues tumorigenesis of NRF2-knocked-down glioma stem cells. **(A, B)** U-87 MG glioblastoma cells were transduced with a lentivirus encoding shco, human shNRF2 or human shTAZ and implanted subcutaneously in athymic mice. **(A)** Growth curves of xenograft tumors. Data are presented as mean ± S.E.M. (n = 4). *$p \leqslant 0.05$ according to a Student's t-test. **(B)** Upper panel, representative tumors of each experimental condition at the end point (scale bar, 1 cm); lower graph, quantification of the final tumor volume. Data are presented as mean ± S.E.M. (n = 4). *$p \leqslant 0.05$ according to a Student's t-test. **(C)** Kaplan-Meier survival curves of mice orthotopically implanted in the brain. Log-rank test between shco and shNRF2 is indicated (n = 6). **(D, E)** GB3 glioblastoma explant cells were transduced with a lentivirus encoding shco, human shNRF2 or human shTAZ and orthotopically implanted in the brain in athymic mice. **(D)** Representative image of T1 MRI of each experimental condition after 10, 20 and 30 days post-surgery. Green arrows indicate the tumor in shco or the injection scar in shNRF2 or shTAZ. **(E)** Growth curves of brain tumors. Data are presented as mean ± S.E.M. (n = 6) **$p \leqslant 0.01$ according to a Student's t-test. **(F, G)** U-87 MG cells were transduced with empty retrovirus or a retrovirus expressing TAZ and then with lentivirus encoding shco or shNRF2 and implanted subcutaneously in athymic mice. **(F)** Growth curves of xenograft tumors. Data are presented as mean ± S.E.M. (n = 4). *$p \leqslant 0.05$ according to a Student's t-test. **(G)** Upper panel, representative tumors of each experimental condition at the end point (scale bar, 1 cm); lower graph, quantification of the final tumor volume. Data are presented as mean ± S.E.M. (n = 4). *$p \leqslant 0.05$ according to a Student's t-test. **(H)** Kaplan-Meier survival curves of mice orthotopically implanted in the brain. Log-rank test between control/shNRF2 and TAZ/shNRF2: $p = 0.056$ (n = 5). See also **Supplementary Fig. S7**.

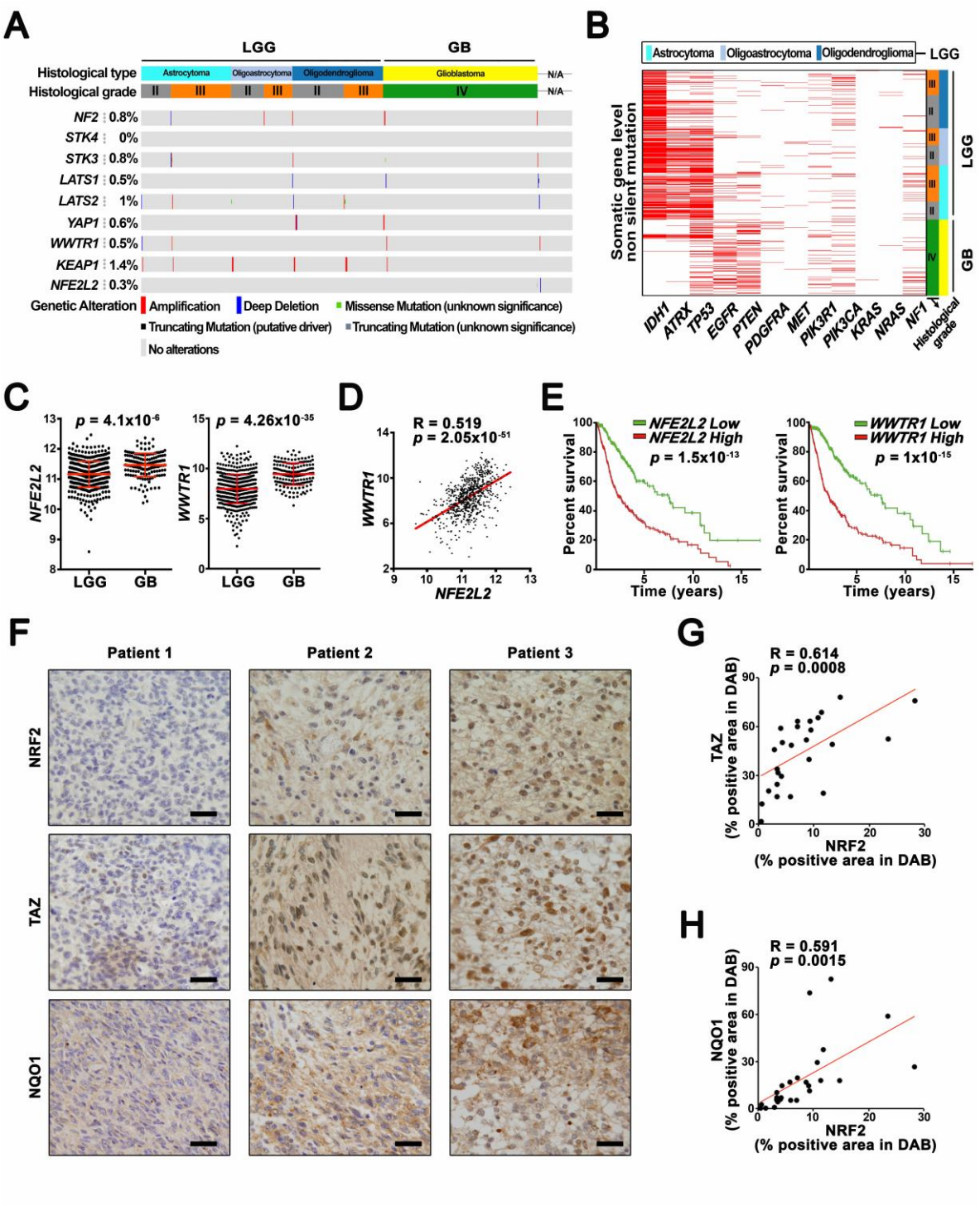
A
LGG
GB
Histological type
Astrocytoma
Oligoastrocytoma
Oligodendroglioma
Glioblastoma
N/A
Histological grade
II
III
IV
NF2 0.8%
STK4 0%
STK3 0.8%
LATS1 0.5%
LATS2 1%
YAP1 0.6%
WWTR1 0.5%
KEAP1 1.4%
NFE2L2 0.3%
Genetic Alteration
Amplification
Deep Deletion
Missense Mutation (unknown significance)
Truncating Mutation (putative driver)
Truncating Mutation (unknown significance)
No alterations
B
Astrocytoma
Oligoastrocytoma
Oligodendroglioma
LGG
Somatic gene level non silent mutation
IDH1
ATRX
TP53
EGFR
PTEN
PDGFRA
MET
PIK3R1
PIK3CA
KRAS
NRAS
NF1
Histological grade
C
p = 4.1x10-6
NFE2L2
LGG
GB
p = 4.26x10-35
WWTR1
LGG
GB
D
R = 0.519
p = 2.05x10-51
WWTR1
NFE2L2
E
NFE2L2 Low
NFE2L2 High
p = 1.5x10-13
Percent survival
Time (years)
WWTR1 Low
WWTR1 High
p = 1x10-15
Percent survival
Time (years)
F
Patient 1
Patient 2
Patient 3
NRF2
TAZ
NQO1
G
R = 0.614
p = 0.0008
TAZ (% positive area in DAB)
NRF2 (% positive area in DAB)
H
R = 0.591
p = 0.0015
NQO1 (% positive area in DAB)
NRF2 (% positive area in DAB)

Figure 1

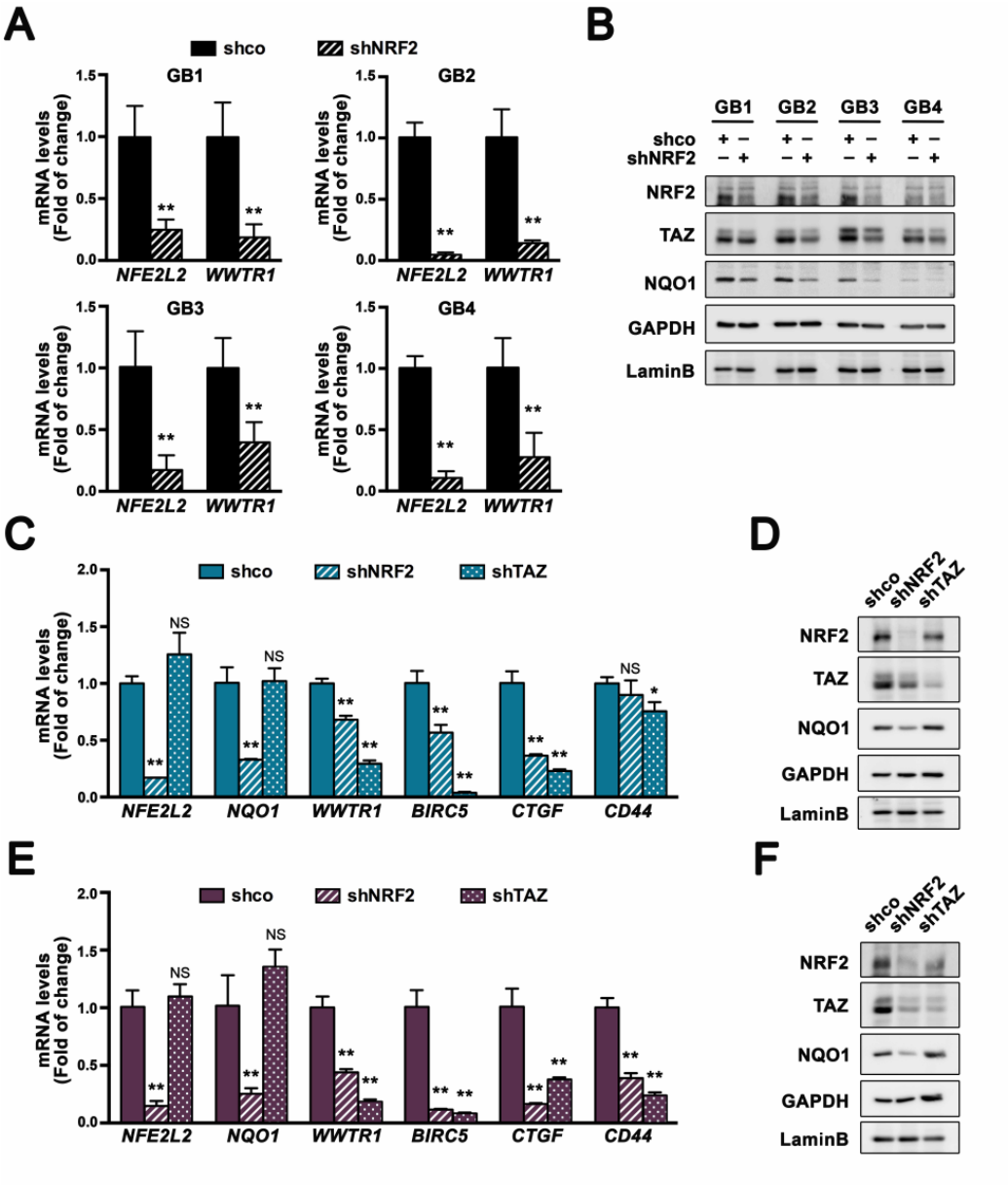
A
shco
shNRF2
GB1
GB2
GB3
GB4
mRNA levels (Fold of change)
NFE2L2
WWTR1
B
GB1
GB2
GB3
GB4
shco
shNRF2
NRF2
TAZ
NQO1
GAPDH
LaminB
C
shco
shNRF2
shTAZ
NS
NFE2L2
NQO1
WWTR1
BIRC5
CTGF
CD44
D
shco
shNRF2
shTAZ
NRF2
TAZ
NQO1
GAPDH
LaminB
E
shco
shNRF2
shTAZ
NS
NFE2L2
NQO1
WWTR1
BIRC5
CTGF
CD44
F
shco
shNRF2
shTAZ
NRF2
TAZ
NQO1
GAPDH
LaminB

Figure 2

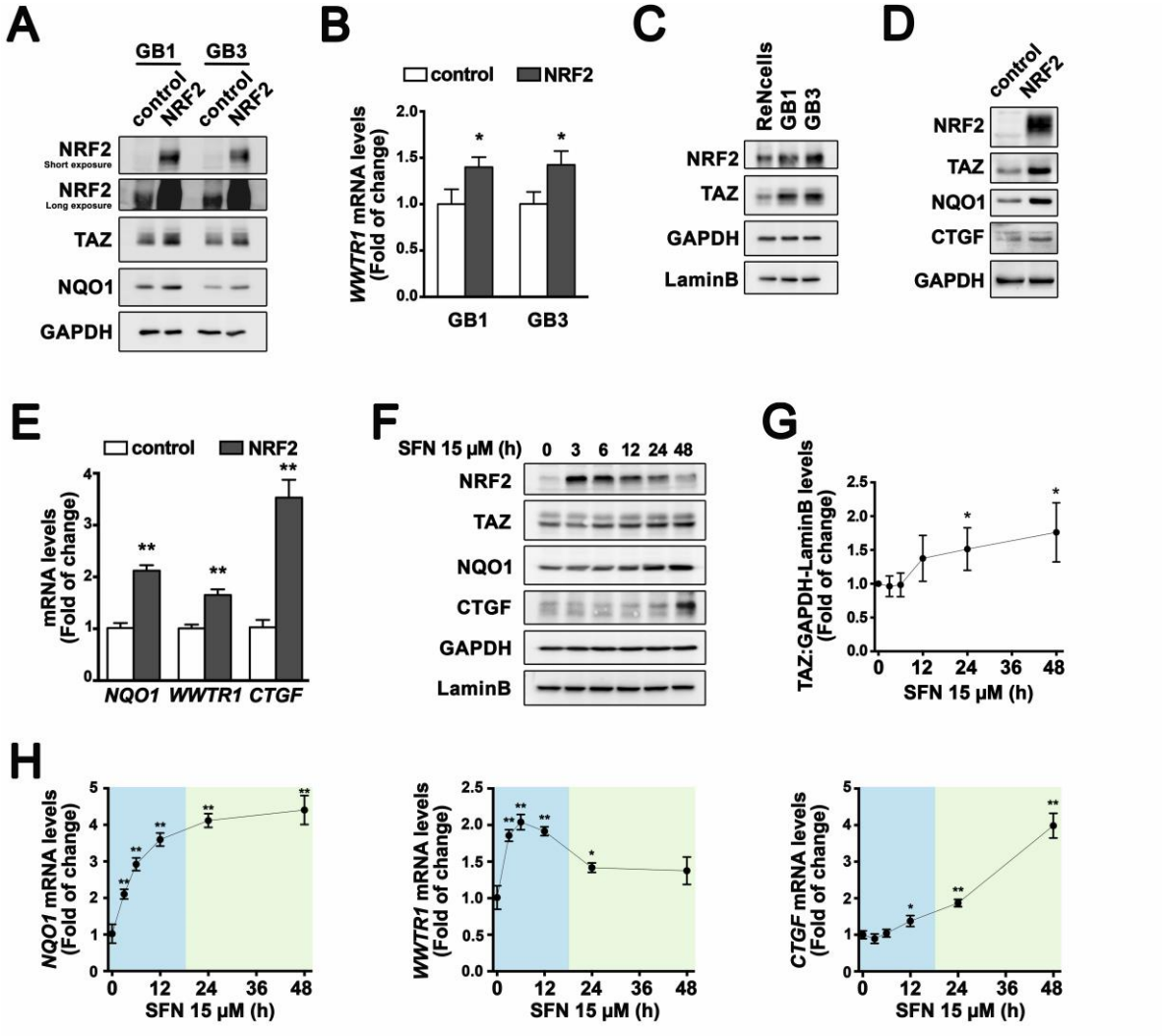
A
GB1
GB3
control
NRF2
control
NRF2
NRF2
Short exposure
NRF2
Long exposure
TAZ
NQO1
GAPDH
B
control
NRF2
WWTR1 mRNA levels
(Fold of change)
GB1
GB3
C
ReNcells
GB1
GB3
NRF2
TAZ
GAPDH
LaminB
D
control
NRF2
NRF2
TAZ
NQO1
CTGF
GAPDH
E
control
NRF2
mRNA levels
(Fold of change)
NQO1
WWTR1
CTGF
F
SFN 15 μM (h)
0
3
6
12
24
48
NRF2
TAZ
NQO1
CTGF
GAPDH
LaminB
G
TAZ:GAPDH-LaminB levels
(Fold of change)
SFN 15 μM (h)
H
NQO1 mRNA levels
(Fold of change)
WWTR1 mRNA levels
(Fold of change)
CTGF mRNA levels
(Fold of change)
SFN 15 μM (h)

Figure 3

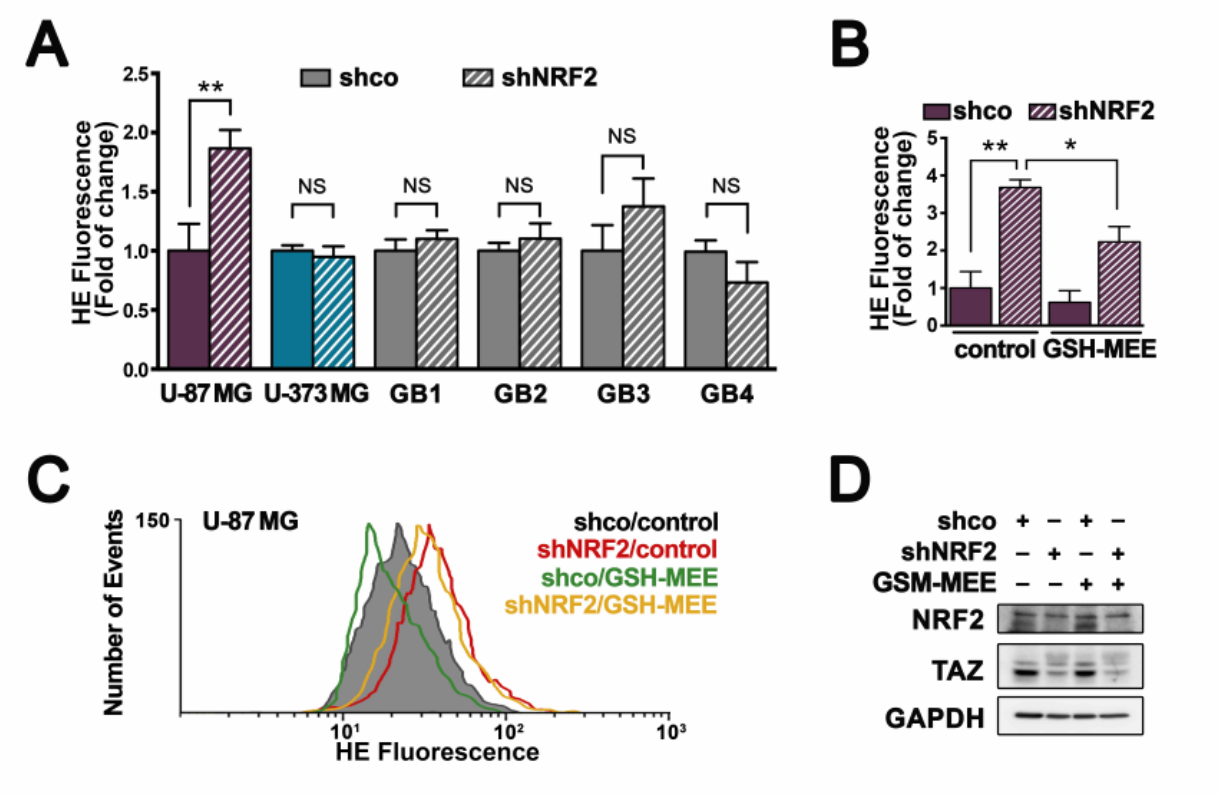
A
shco
shNRF2
HE Fluorescence (Fold of change)
2.5
2.0
1.5
1.0
0.5
0.0
**
NS
NS
NS
NS
NS
U-87 MG
U-373 MG
GB1
GB2
GB3
GB4
B
shco
shNRF2
HE Fluorescence (Fold of change)
5
4
3
2
1
0
**
*
control
GSH-MEE
C
U-87 MG
Number of Events
150
shco/control
shNRF2/control
shco/GSH-MEE
shNRF2/GSH-MEE
10¹
10²
10³
HE Fluorescence
D
shco + − + −
shNRF2 − + − +
GSM-MEE − − + +
NRF2
TAZ
GAPDH

Figure 4

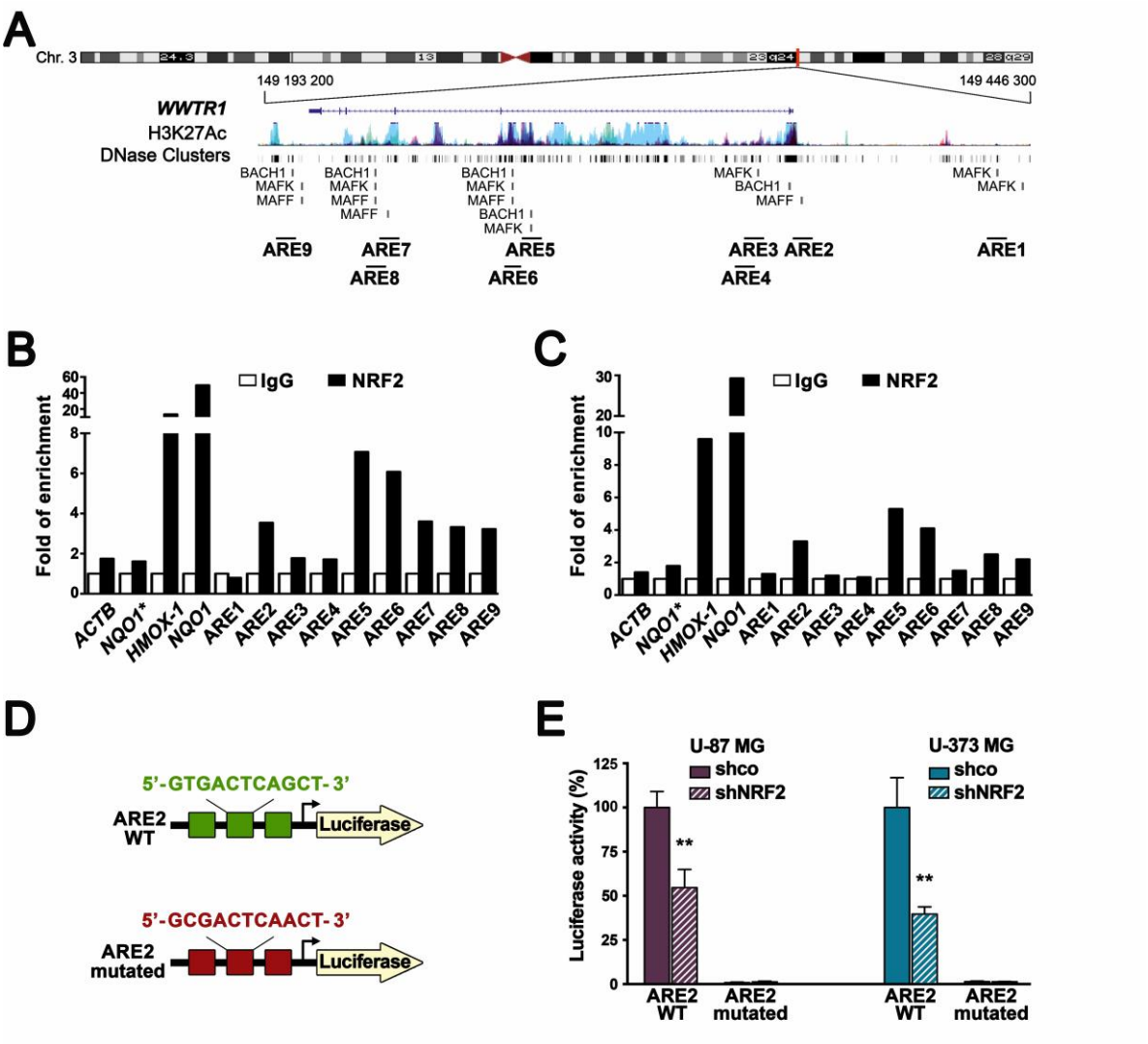
A
Chr. 3
149 193 200
149 446 300
WWTR1
H3K27Ac
DNase Clusters
BACH1
MAFK
MAFF
ARE9
ARE7
ARE8
ARE5
ARE6
ARE3
ARE4
ARE2
ARE1
B
IgG
NRF2
Fold of enrichment
ACTB
NQO1*
HMOX-1
NQO1
ARE1
ARE2
ARE3
ARE4
ARE5
ARE6
ARE7
ARE8
ARE9
C
IgG
NRF2
Fold of enrichment
D
5'-GTGACTCAGCT-3'
ARE2
WT
Luciferase
5'-GCGACTCAACT-3'
ARE2
mutated
Luciferase
E
U-87 MG
shco
shNRF2
U-373 MG
shco
shNRF2
Luciferase activity (%)
**
**
ARE2
WT
ARE2
mutated
ARE2
WT
ARE2
mutated

Figure 5

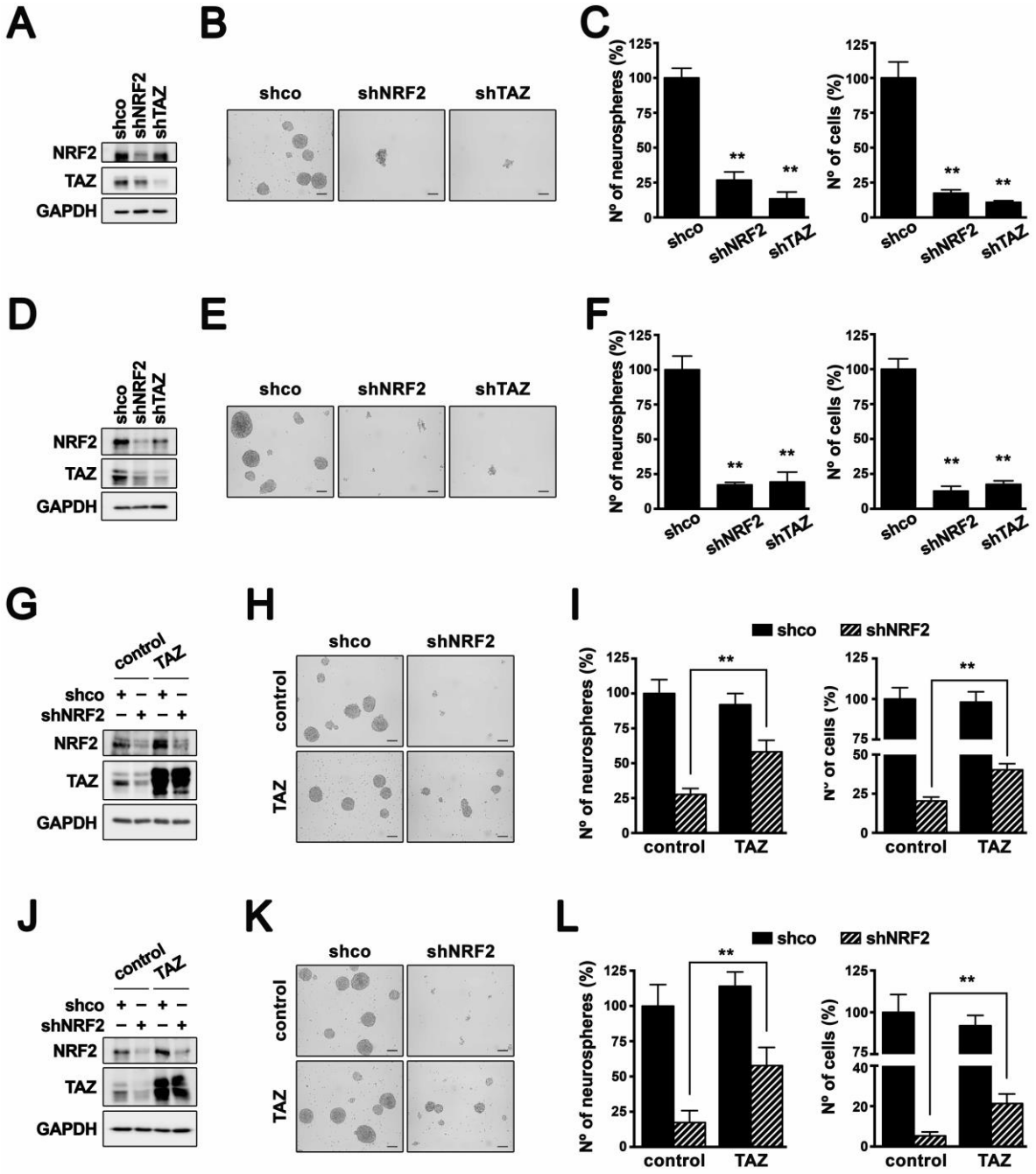
A
shco
shNRF2
shTAZ
NRF2
TAZ
GAPDH
B
shco
shNRF2
shTAZ
C
Nº of neurospheres (%)
Nº of cells (%)
shco
shNRF2
shTAZ
D
E
F
G
control
TAZ
shco + − + −
shNRF2 − + − +
H
I
shco
shNRF2
control
TAZ
J
K
L

Figure 6

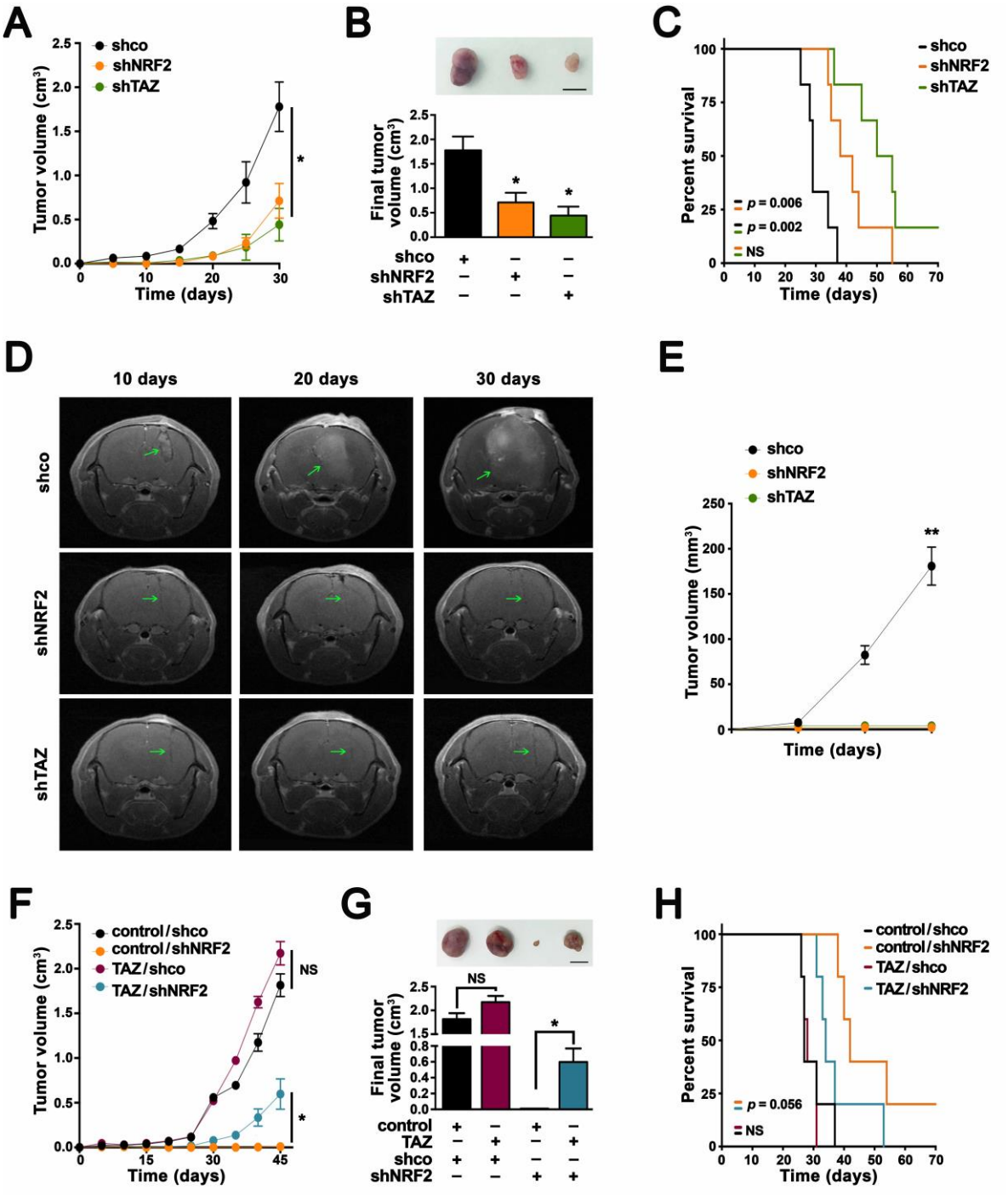
A
shco
shNRF2
shTAZ
Tumor volume (cm³)
Time (days)
B
Final tumor volume (cm³)
shco
shNRF2
shTAZ
C
Percent survival
Time (days)
p = 0.006
p = 0.002
NS
D
10 days
20 days
30 days
shco
shNRF2
shTAZ
E
Tumor volume (mm³)
Time (days)
F
control/shco
control/shNRF2
TAZ/shco
TAZ/shNRF2
Tumor volume (cm³)
Time (days)
NS
G
Final tumor volume (cm³)
control
TAZ
shco
shNRF2
H
Percent survival
Time (days)
p = 0.056
NS

Figure 7

**SUPPLEMENTAL MATERIAL**

**Supplemental Table S1. (A)** Putative Antioxidant Response Elements (AREs) in the *WWTR1* and *YAP1* genes found the ENCODE data base of ChIP data for MAFK/MAFF/BACH1. A bioinformatics analysis was used to identify putative sites with a relative score higher than the 80% (24). The table also shows the max score, the localization in the human genome and ARE sequences with the most relevant bases for binding of the NRF2/MAF heterodimer in bold. The table also shows the negative control ARE (*ACTB* and *NQO1**) and positive control ARE (*HMOX-1* and *NQO1*). **(B)** Independent ChIP assays in GB1, GB3 and HEK293T cells, similar to those shown in **Fig. 5** and **Supplemental Fig. S5**.

**A**

| Gene | Localization of ARE site in the human genomic | Max score | Relative score | Sequence |
|---|---|---|---|---|
| ***WWTR1* ARE1** | chr3: 149435325-149435336 | 11.34 | 0.814 | G**TGC**CAG**AGC**A |
| ***WWTR1* ARE2** | chr3: 149378461-149378450 | 15.97 | 0.925 | G**TGA**CTC**AGC**T |
| ***WWTR1* ARE3** | chr3: 149365723-149365712 | 13.15 | 0.857 | A**TGA**TTA**TGC**A |
| ***WWTR1* ARE4** | chr3: 149365892-149365903 | 13.84 | 0.874 | A**TGT**CTA**AGC**A |
| ***WWTR1* ARE5** | chr3: 149299667-149299656 | 13.44 | 0.864 | A**TGA**GTC**TGC**A |
| ***WWTR1* ARE6** | chr3: 149294176-149294165 | 15.16 | 0.905 | A**TGA**GAC**AGC**A |
| ***WWTR1* ARE7** | chr3: 149258004-149258015 | 13.94 | 0.876 | A**TGA**TGC**AGC**A |
| ***WWTR1* ARE8** | chr3: 149254494-149254483 | 13.36 | 0.862 | C**TGA**CTA**AGC**C |
| ***WWTR1* ARE9** | chr3: 149230221-149230232 | 15.04 | 0.902 | C**TGA**GTG**AGC**G |
| ***ACTB*** | chr7:5570750-5570824 | – | – | None |
| ***NQO1**** | chr16:69763868-69764006 | – | – | None |
| ***HMOX-1*** | chr22:35773158- 35773147 | 18.97 | 0.997 | G**TGA**CTC**AGC**A |
| ***NQO1*** | chr16:69760919-69760908 | 18.97 | 0.997 | G**TGA**CTC**AGC**A |
| ***YAP1* ARE1** | chr11:102009509-102009498 | 11.72 | 0.823 | A**TGA**CTC**AGA**T |
| ***YAP1* ARE2** | chr11:102062347-102062358 | 11.58 | 0.819 | G**TGA**CTC**ATC**T |
| ***YAP1* ARE3** | chr11:102097615-102097626 | 11.58 | 0.819 | G**TGA**CTC**ACC**T |

**B**

| Gene | GB1 | | GB3 | | HEK293T | | | |
|---|---|---|---|---|---|---|---|---|
| | ChIP 2 | | ChIP 2 | | ChIP 2 | | ChIP 3 | |
| | IgG | NRF2 | IgG | NRF2 | IgG | V5 | IgG | V5 |
| ***WWTR1* ARE1** | 1.0 | 1.6 | 1.0 | 1.1 | 1.0 | 2.0 | 1.0 | 1.5 |
| ***WWTR1* ARE2** | 1.0 | 6.1 | 1.0 | 1.9 | 1.0 | 5.7 | 1.0 | 5.4 |
| ***WWTR1* ARE3** | 1.0 | 2.2 | 1.0 | 1.2 | 1.0 | 1.3 | 1.0 | 1.3 |
| ***WWTR1* ARE4** | 1.0 | 1.5 | 1.0 | 0.9 | 1.0 | 1.2 | 1.0 | 1.2 |
| ***WWTR1* ARE5** | 1.0 | 3.5 | 1.0 | 5.1 | 1.0 | 5.5 | 1.0 | 6.1 |
| ***WWTR1* ARE6** | 1.0 | 4.4 | 1.0 | 4.0 | 1.0 | 3.3 | 1.0 | 1.8 |
| ***WWTR1* ARE7** | 1.0 | 2.6 | 1.0 | 1.3 | 1.0 | 2.3 | 1.0 | 2.2 |
| ***WWTR1* ARE8** | 1.0 | 1.5 | 1.0 | 4.1 | 1.0 | 1.6 | 1.0 | 1.3 |
| ***WWTR1* ARE9** | 1.0 | 10.3 | 1.0 | 1.2 | 1.0 | 1.9 | 1.0 | 1.8 |
| ***ACTB*** | 1.0 | 1.6 | 1.0 | 1.1 | 1.0 | 1.1 | 1.0 | 1.3 |
| ***NQO1**** | 1.0 | 2.2 | 1.0 | 1.1 | 1.0 | 2.0 | 1.0 | 1.0 |
| ***HMOX-1*** | 1.0 | 7.6 | 1.0 | 19.3 | 1.0 | 130.4 | 1.0 | 266.2 |
| ***NQO1*** | 1.0 | 32.9 | 1.0 | 79.3 | 1.0 | 39.9 | 1.0 | 58.4 |

**Supplemental Table S2.** Oligonucleotides used for ChIP.

| Gene | Forward Sequence 5´-3´ | Reverse Sequence 5´-3´ |
|---|---|---|
| ***WWTR1* ARE1** | GCACCAGAGGGCATACATCT | AACCACACCATCAGGAAAGC |
| ***WWTR1* ARE2** | AATCCTGTGGGGTGGGTACT | CAGGTACTGCCCGTAAGAGG |
| ***WWTR1* ARE3** | TTCCAGGAAAAACAGGATGG | GAGGCTCCAGAACCTCAATG |
| ***WWTR1* ARE4** | AATGAAGGCTGGGTGTTCAG | TCAAAAACACACCCTCAGCA |
| ***WWTR1* ARE5** | CCTGATTTGGCTCATCTGCT | AGCAGCCATGTGAAAGGTCT |
| ***WWTR1* ARE6** | AGTGAAGCCAGGAAGGAGGT | CACTTCCCAAACCCAGGATA |
| ***WWTR1* ARE7** | TTCCAGCTGTAGGTGCCTTT | CATGAGTCCCTGTGAGCAAA |
| ***WWTR1* ARE8** | ATTCAGCCCTGCTTTTACCC | CCCTCTTTTCTCGTCCCTGT |
| ***WWTR1* ARE9** | CGCGGAGAAATTATCTGCTT | CTTTCTCCTTCCCCCTTCAG |
| ***ACTB*** | CACCCAGCACATTTAGCTAGCTGA | TTCAGAGCAACTGCCCTGAAAGCA |
| ***NQO1**** | TCTCAGTTTTTGCCCTTATTTAA | TAAAAAGTAGAGTGGTTGGAGTGATGACG |
| ***HMOX-1*** | CCCTGCTGAGTAATCCTTTCCCGA | ATGTCCCGACTCCAGACTCCA |
| ***NQO1*** | TGCACCCAGGGAAGTGTGTTGTAT | CCCTTTTAGCCTTGGCACGAAA |

**Supplemental Table S3. (A, B)** Glioma stem cell frequency of GB1 and GB3 cells as determined by limiting dilution analysis. A serial dilution of 16,000 to 60 cells per well were analyzed for neurosphere formation after 5 days. The glioma stem cell frequency was determined by ELDA (n = 8). **(A)** Cells were transduced with lentiviruses encoding shco, human shNRF2 or human shTAZ. **(B)** Cells were transduced with empty retrovirus as control or a retrovirus expressing TAZ, and then with a lentivirus expressing shco or shNRF2. See also **Fig. S6**.

**A**

| Glioma stem cell frecuency | | | | | | |
|---|---|---|---|---|---|---|
| | | | | *p-value* | | |
| | **Lower** | **Estimate** | **Upper** | **shco-shNRF2** | **shco-shTAZ** | |
| **shco** | 2413 | 1538 | 980 | | | **GB1** |
| **shNRF2** | 19123 | 11333 | 6716 | $1.23x10^{-8}$ | | **GB1** |
| **shTAZ** | 23811 | 13705 | 7889 | | $1.08 \times 10^{-9}$ | **GB1** |
| **shco** | 3052 | 1937 | 1229 | | | **GB3** |
| **shNRF2** | 120052 | 39058 | 12708 | $3.48x10^{-10}$ | | **GB3** |
| **shTAZ** | 867335 | 123437 | 17568 | | $1.54 \times 10^{-12}$ | **GB3** |

**B**

| Glioma stem cell frecuency | | | | | | | |
|---|---|---|---|---|---|---|---|
| | | | | *p-value* | | | |
| | **Lower** | **Estimate** | **Upper** | **control/shco control/shNRF2** | **control/shNRF2 TAZ/shNRF2** | **control/shco TAZ/shco** | |
| **control/shco** | 3401 | 2168 | 1382 | | | | **GB1** |
| **control/shNRF2** | 14101 | 8631 | 5283 | $4.51 \times 10^{-5}$ | | | **GB1** |
| **TAZ/shco** | 2490 | 1542 | 955 | | | NS | **GB1** |
| **TAZ/shNRF2** | 6694 | 4255 | 2705 | | 0.04 | | **GB1** |
| **control/shco** | 2244 | 1425 | 905 | | | | **GB3** |
| **control/shNRF2** | 124985 | 40102 | 12867 | $4.87 \times 10^{-13}$ | | | **GB3** |
| **TAZ/shco** | 2691 | 1663 | 1027 | | | NS | **GB3** |
| **TAZ/shNRF2** | 15673 | 8630 | 4752 | | 0.0106 | | **GB3** |

**Supplemental Table S4.** Oligonucleotides used for qRT-PCR.

| Gene | Forward Sequence 5´-3´ | Reverse Sequence 5´-3´ |
|---|---|---|
| ***BIRC5*** | ACCCCGGAGCGGATGG | GCAACCGGACGAATGCTTTT |
| ***CD44*** | ACAAGCACAATCCAGGCAAC | GCTGGTATGAGCTGAGGCTG |
| ***CTGF*** | CTTCTGTGACTTCGGCTCCC | GATGCAGGGAGCACCATCTT |
| ***GAPDH*** | CTCTCTGCTCCTCCTGTTCGAC | TGAGCGATGTGGCTCGGCT |
| ***NFE2L2*** | AAACCAGTGGATCTGCCAAC | GTGACTGAAACGTAGCCGAAGA |
| ***NQO1*** | GTTCATAGGAGAGTTTGCTT | CCTTGCAGAGAGTACATGGA |
| ***WWTR1*** | TTTCCTCAATGGAGGGCCA | GGGTGTTTGTCCTGCGTTTT |
| ***YAP1*** | GAACTGCTTCGGCAGGTGA | GGGCTAACTCCTGACATTTTGG |

**Supplemental Table S5.** Oligonucleotides used for construction of luciferase reporters. Underlined sequences correspond to three putative AREs. Bold letters correspond to mutated nucleotides.

*WWTR1* ARE2-WT:

5′- CTAGTGTGACTCAGCTGGATCCGTGACTCAGCTACGTGAGTGACTCAGCTC -3′

3′- ACACTGAGTCGACCTAGGCACTGAGTCGATGCACTCACTGAGTCGAGAGCT-5′

*WWTR1* ARE2-mutated:

5′- CTAGTG**C**GACTCA**A**CTGGATCCG**C**GACTCA**A**CTACGTGAG**C**GACTCA**A**CTC -3′

3′- AC**G**CTGAGT**T**GACCTAGGC**G**CTGAGT**T**GATGCACTC**G**CTGAGT**T**GAGAGCT-5′

**Supplemental Figure S1. (A)** Sections of three representative tumors with antibodies against IDH1, ATRX and ki67 (scale bar, 50 μm). **(B, C)** Scatter plot showing positive correlation between percentage of positive cell for ki67 and densitometric quantification of DAB-staining (as percentage of area) of NRF2 **(B)** or TAZ **(C)**. The Pearson correlation coefficient (R) and the *p*-value associated with this coefficient are indicated. See also **Fig. 1**.

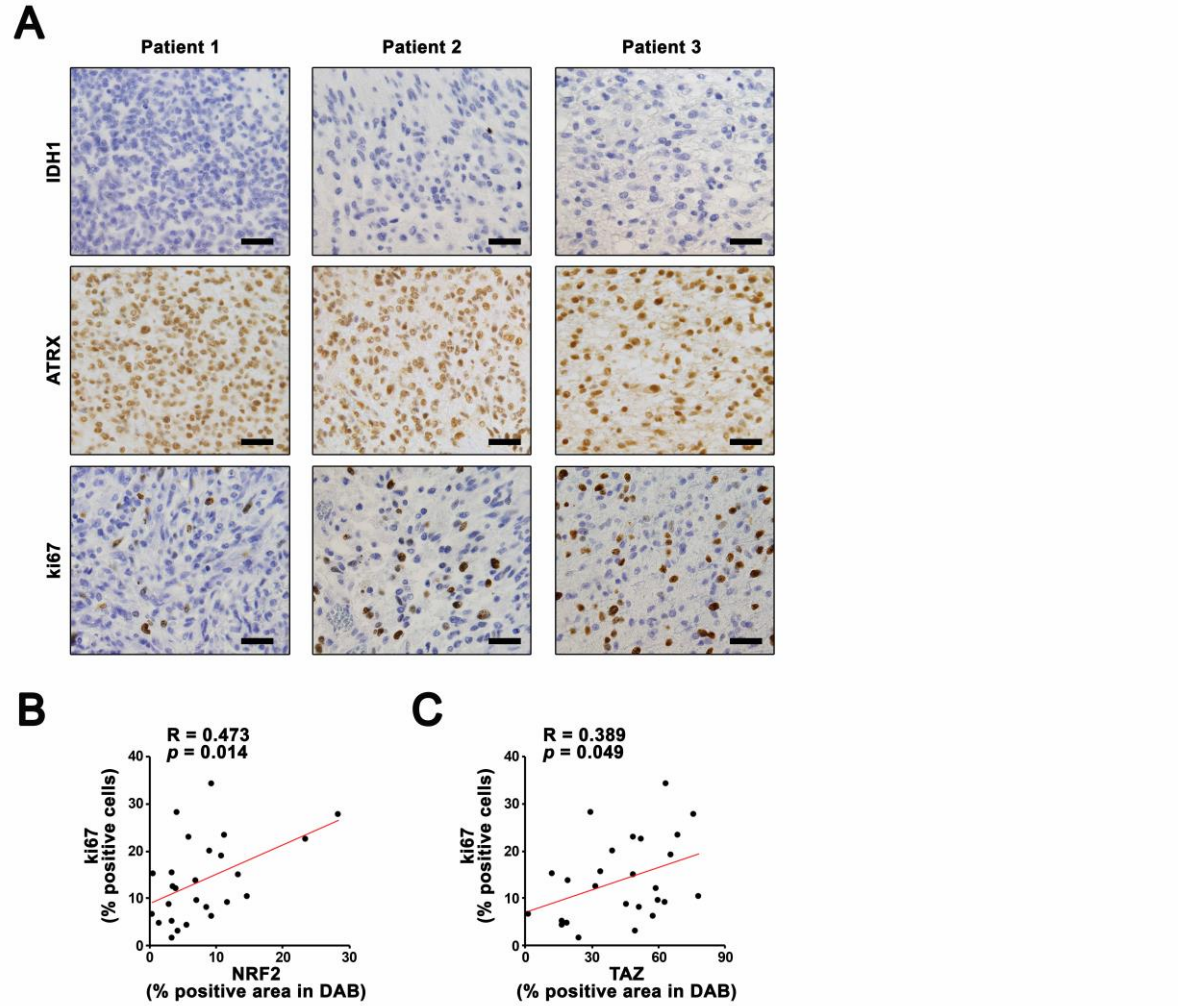

**Supplemental Figure S2. (A, B)** U-87 MG cell lines were transduced for 1, 3 or 5 days with lentivirus encoding shco or shNRF2. **(A)** Messenger RNA (mRNA) levels of *NFE2L2*, *NQO1* and *WWTR1* were determined by qRT-PCR and normalized by *GAPDH*. Data are presented as mean ± S.D. (n = 3) $^{**}p \leqslant 0.01$ according to a Student's t-test. **(B)** Representative immunoblot analysis of NRF2, TAZ, NQO1 and GAPDH as a loading control (n = 3). **(C, D)** U-87 MG cell lines transduced with lentivirus encoding control shRNA (shco) or against NRF2 using two different shNRF2 (shNRF2-1 and shNRF2-2). **(C)** Messenger RNA (mRNA) levels of *NFE2L2* and *WWTR1* were determined by qRT-PCR and normalized by *GAPDH*. Data are presented as mean ± S.D. (n = 3) $^{**}p \leqslant 0.01$ according to a Student's t-test. **(D)** Representative immunoblot analysis of NRF2, TAZ and GAPDH as a loading control (n = 3). **(E)** U-87 MG cells were transduced with lentiviral empty vector (control) or lentiviral vector for expression of NRF2 (NRF2), and then with lentivirus encoding shco or shNRF2. Representative immunoblot analysis of NRF2, TAZ and GAPDH as a loading control (n = 3). See also **Fig. 2**.

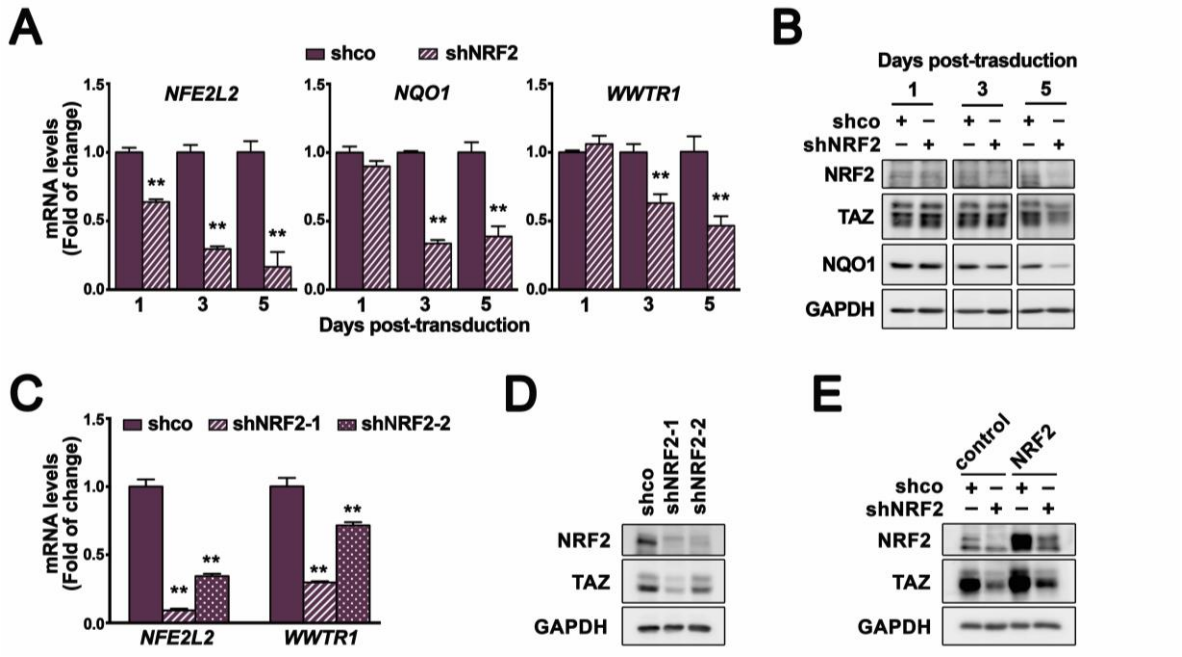

**Supplemental Figure S3**: **(A, B)** U-373 MG and U-87 MG glioblastoma cells were transduced with empty vector or lentiviral vector for overexpression of NRF2. **(A)** Representative immunoblot analysis of NRF2, TAZ, NQO1 and GAPDH as a loading control (n = 3). **(B)** Messenger RNA (mRNA) levels of *WWTR1* were determined by qRT-PCR and normalized by *GAPDH*. Data are presented as mean ± S.D. (n = 3) **p ⩽ 0.01 according to a Student's t-test. **(C)** Representative immunoblot analysis of NRF2, TAZ and GAPDH as a loading control in ReNcell, U-87 MG and U-373 MG. See also **Fig. 3**.

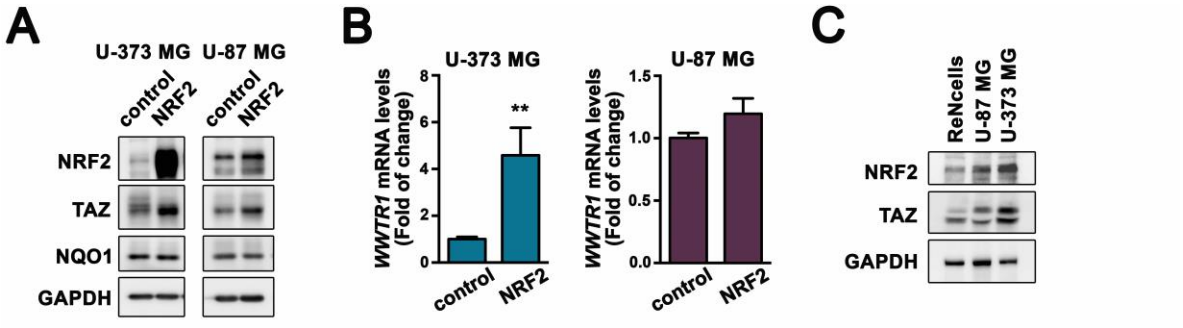

**Supplemental Figure S4: (A)** Representative scheme of the gene *YAP1* encoding YAP. Regions enriched in acetylated histone H3 lysine 27 (H3K27ac) are shown in blue and regions sensitive to DNase are represented as dark boxes. Experimental sequences reported to bind MAFK, MAFF and BACH1 factors were analyzed for the presence of AREs (ARE 1-3). (B, C) GB1 and GB3 were transduced with a lentivirus encoding shco or shNRF2. **(B)** mRNA levels of *WWTR1* and *YAP1* were determined by qRT-PCR and normalized by *GAPDH*. Data are mean ± S.D. (n = 3). Statistical analysis was performed with the Student's t-test. $^{**}p \leqslant 0.01$. **(C)** Representative immunoblot analysis of NRF2, YAP, TAZ and GAPDH and LaminB as loading controls (n = 3). See also **Fig. 5** and **Supplemental Table S1**.

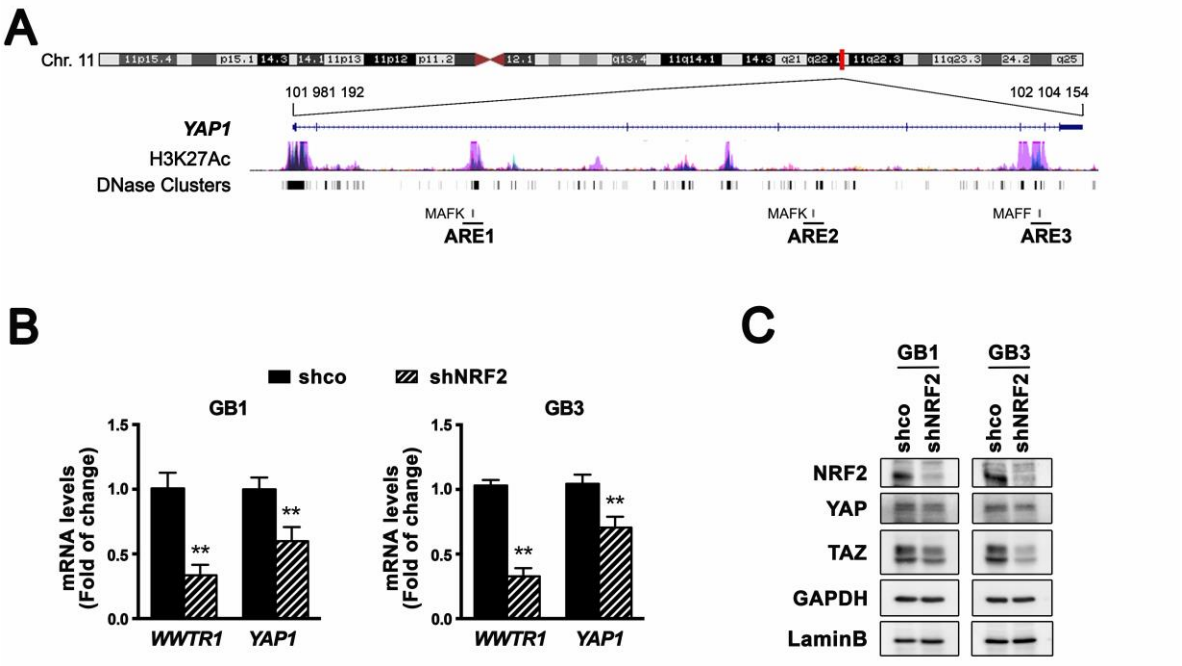

**Supplemental Figure S5. (A)** ChIP analysis of putative AREs found in *WWTR1* using the anti-V5 antibody vs. a control IgG in HEK293T cells overexpressing NRF2-$^{\Delta ETGE}$-V5. **(B)** HEK293T cells were transfected with wild type or mutated ARE2 reporter plus increasing amounts of NRF2-$^{\Delta ETGE}$-V5. Luciferase activity was measured 24 h after transfection. The reporter construct carrying an ARE from *HMOX1* was used as control. Luciferase activities were normalized to renilla activity. Results are shown relative to control and are mean ± S.D. (n = 3). $^{**}p \leqslant 0.01$ according to a Student's t-test. See also **Fig. 5** and **Supplemental Table S1**.

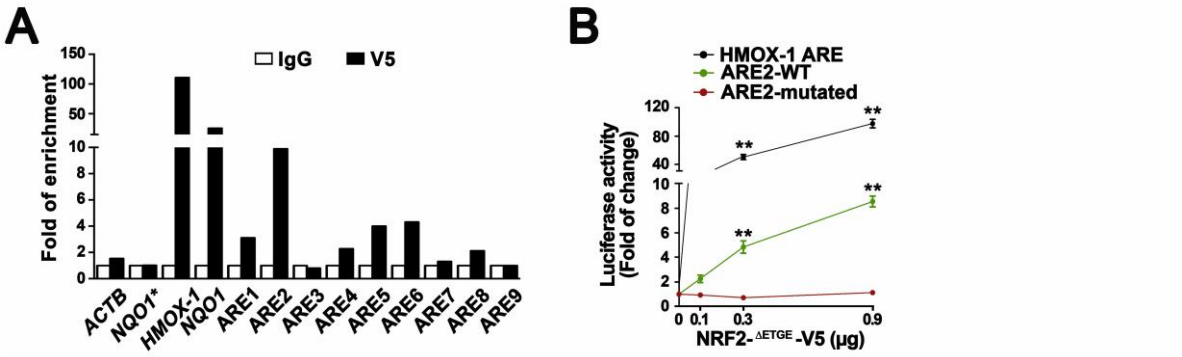

**Supplemental Figure S6.** Ectopic expression of TAZ rescues neurosphere growth of NRF2-knocked-down glioma stem cells U-87 MG **(A, B)** and U-373 MG **(C, D).** Cells were transduced with lentiviruses encoding shco, human shNRF2 or human shTAZ. **(A, C)** Representative images of tumor neurosphere formation. Scale bar, 100 μm. **(B, D)** Quantification of the number of secondary neurospheres or the number of cells represented as percentage relative to shco. Data are presented as mean ± S.D. (n = 3) **p ⩽ 0.01 according to a Student's t-test. U-87 MG **(E- H)** and U-373 MG **(I, J)** cells were transduced with empty retrovirus as control or a retrovirus expressing TAZ, and then with a lentivirus expressing shco or shNRF2. **(E)** Representative immunoblot analysis of NRF2, TAZ and GAPDH as a loading control (n = 3). **(F)** mRNA levels of *BIRC5* and *CD44* were determined by qRT-PCR and normalized by *GAPDH*. Data are presented as mean ± S.D. (n = 3) **p ⩽ 0.01 according to a Student's t-test. **(G, I)** Representative images of tumor neurosphere formation. Scale bar, 100 μm. **(H, J)** Quantification of the number of secondary neurospheres and the number of cells represented as a percentage relative to control-shco. Data are presented as mean ± S.D. (n = 3) **p ⩽ 0.01 according to a Student's t-test. See also **Fig. 6**.

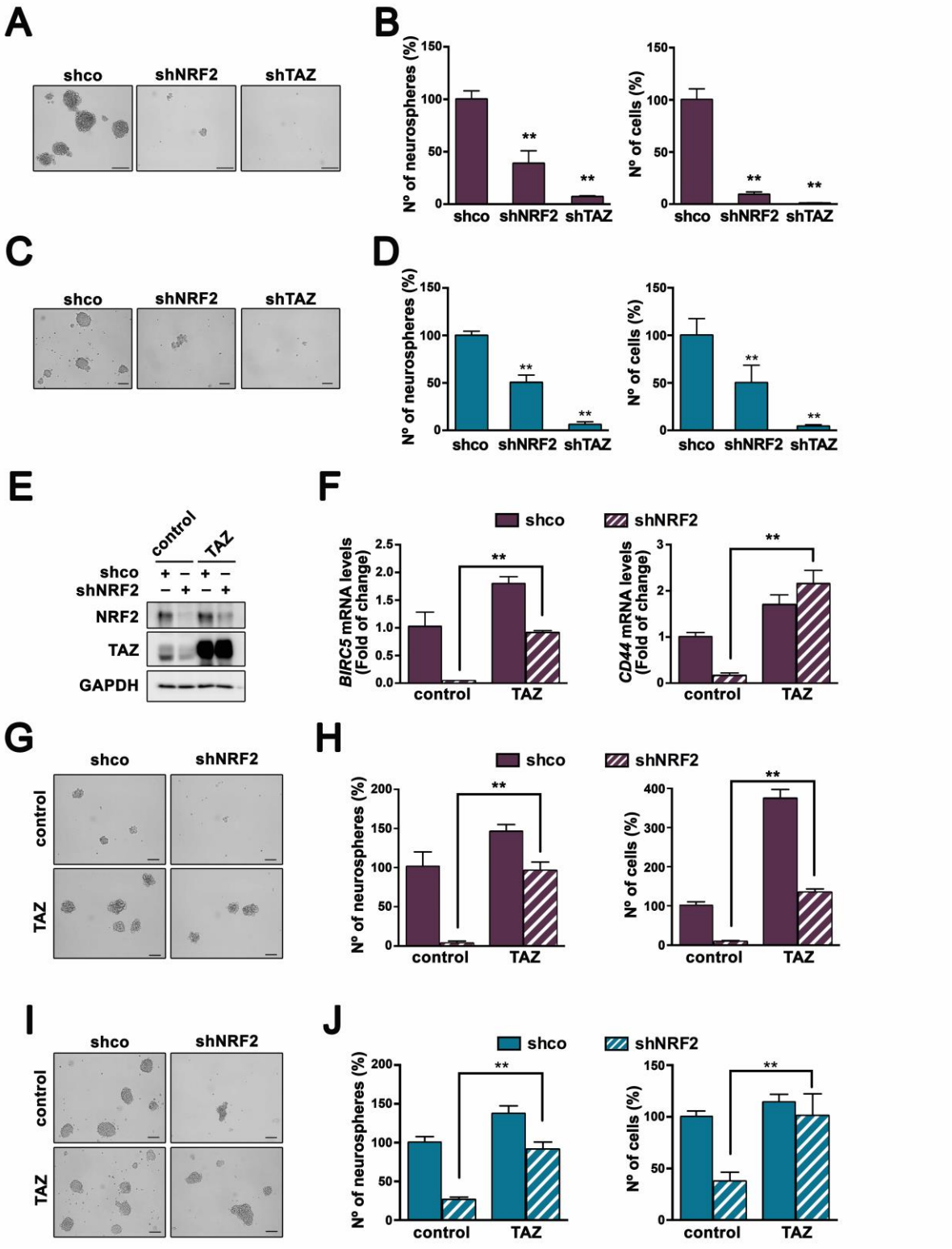
A
shco
shNRF2
shTAZ
B
Nº of neurospheres (%)
Nº of cells (%)
shco shNRF2 shTAZ
C
D
E
control
TAZ
shco
shNRF2
NRF2
TAZ
GAPDH
F
shco
shNRF2
BIRC5 mRNA levels (Fold of change)
CD44 mRNA levels (Fold of change)
control TAZ
G
control
TAZ
H
I
J

**Supplemental Figure S7. (A, B)** U-373 MG glioblastoma cells were transduced with lentivirus shRNA control (shco), human shNRF2 or human shTAZ, and were implanted in nude mice. **(A)** Growth curves of xenograft tumors. The tumor volume was followed-up at the indicated times. Data are presented as mean ± S.E.M. (n = 4). $^{**}p \leqslant 0.01$ according to a Student's t-test. **(B)** Upper panel, representative tumors of each experimental condition at the end point (scale bar, 1 cm); lower graph, quantification of the final tumor volume. Data are presented as mean ± S.E.M. (n = 4). $^{**}p \leqslant 0.01$ according to a Student's t-test. Edema associated with the intracranial tumor formed by GB3. Slices -1, 0 and +1 correspond to three serial sections of the same tumor developed by the shco condition. Slice 0 is also shown in **Fig. 7D**. Representative image of T2 MRI after 10, 20 and 30 days post- surgery. Red arrows indicate edema. **(D, E)** U-373 MG cells were transduced with retrovirus encoding pBabe-puro alone (control) or pBabe-puro-TAZ (TAZ) and then with lentivirus expressing shco or shNRF2 and implanted in athymic mice. **(D)** Growth curves of xenograft tumors. Data are presented as mean ± S.E.M. (n = 4). $p = 0.08$ according to a Student's t-test. **(E)** Upper panel, representative tumors of each experimental condition at the end point (scale bar, 1 cm); lower graph, quantification of the final tumor volume. Data are presented as mean ± S.E.M. (n = 4). $p = 0.08$ according to a Student's t-test. See also **Fig. 7**.

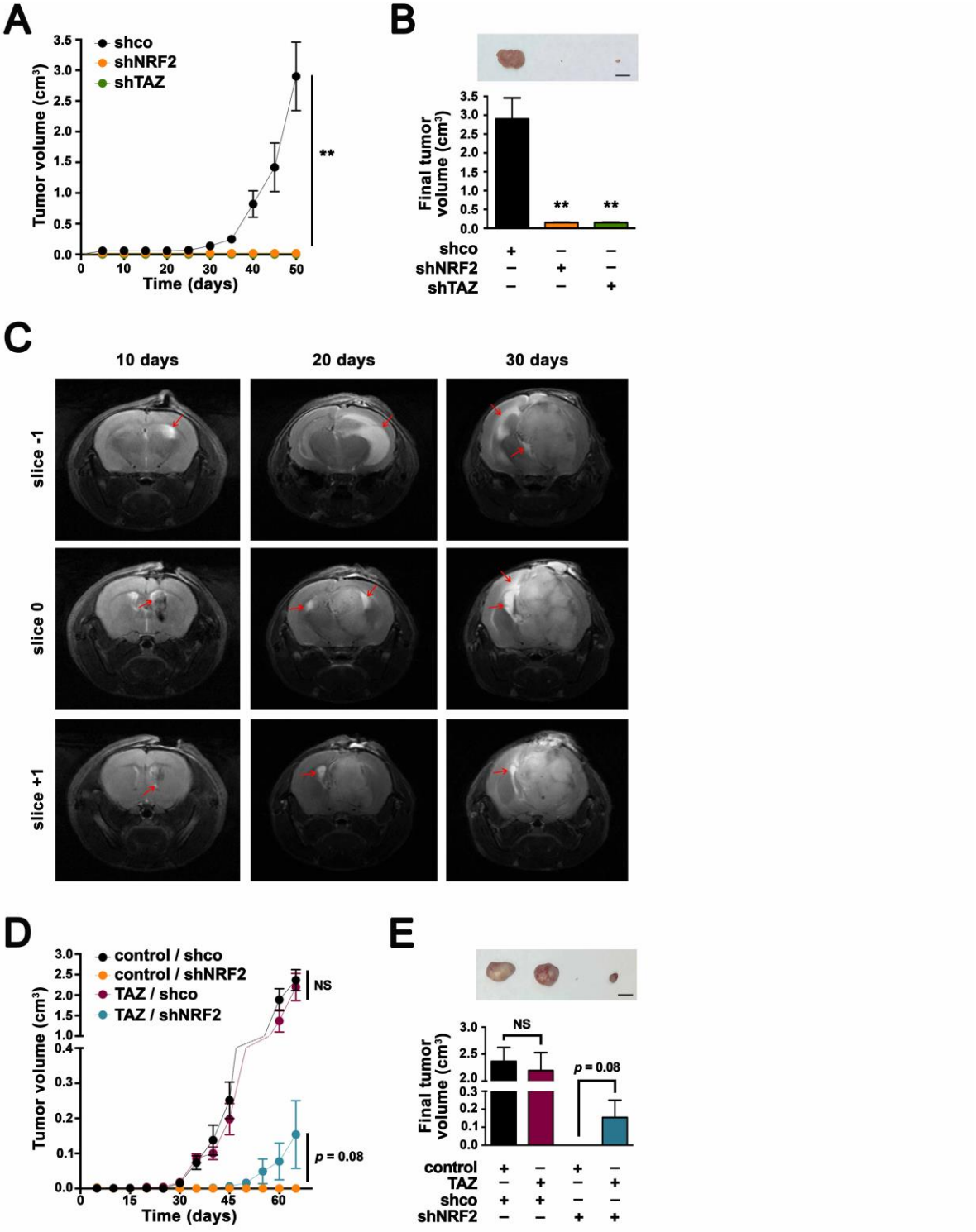
A
shco
shNRF2
shTAZ
Tumor volume (cm³)
Time (days)
**
B
Final tumor volume (cm³)
**
**
shco
shNRF2
shTAZ
C
10 days
20 days
30 days
slice -1
slice 0
slice +1
D
control / shco
control / shNRF2
TAZ / shco
TAZ / shNRF2
Tumor volume (cm³)
Time (days)
NS
p = 0.08
E
Final tumor volume (cm³)
NS
p = 0.08
control
TAZ
shco
shNRF2

## GRAPHICAL ABSTRACT

Scheme showing the main findings of this study: NRF2 induces target genes such as GCLC, NQO1, HMOX1, etc. that in cancer cells may provide a cytoprotective response to stressful signals including radiotherapy and chemotherapy. In addition, we show here that NRF2 also induces the expression of WWTR1, encoding the transcription factor TAZ, that provides direct input into cancer progression by activating a battery of genes that participate in proliferative responses and cancer stem cell renewal. The combined expression of NRF2 and its target TAZ are characteristic of poor prognosis in glioblastomas.

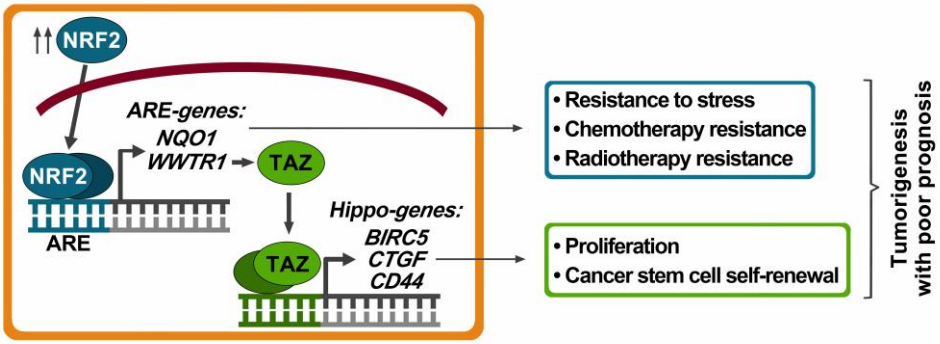

# Hippo pathway effector TAZ is a transcriptional corepressor of neuronal differentiation

Natalia Robledinos-Antón[1], Maribel Escoll[1], and Antonio Cuadrado[1]*

[1] Instituto de Investigaciones Biomédicas "Alberto Sols" UAM-CSIC, Instituto de Investigación Sanitaria La Paz (IdiPaz) and Department of Biochemistry, Faculty of Medicine, Autonomous University of Madrid, Madrid, Spain. Centro de Investigación Biomédica en Red sobre Enfermedades Neurodegenerativas (CIBERNED), ISCIII, Madrid, Spain.

**Running title:** TAZ repress the expression of proneurogenic genes in neural stem cells.

**Keywords:** neural stem cells, neurogenesis, bHLH factors, SOX2, cell therapy

*To whom correspondence should be addressed:

Dr. Antonio Cuadrado
Instituto de Investigaciones Biomédicas "Alberto Sols" UAM-CSIC
C/ Arturo Duperier, 4, 28029 Madrid, Spain
Email: antonio.cuadrado@uam.es
Tel: 34915854383/ Fax: 34915854401

**ABSTRACT**

In this study, we investigated the role of the Hippo pathway effector TAZ in the neuronal specification of NSPCs. We described that TAZ expression in murine neurogenic niches is mainly restricted to NSPCs and absolutely absent in neurons since immature states. We found that TAZ expression declines during neuronal specification of human NSPCs, being neuronal maturation improve by the loss of TAZ in initial NSPCs. Furthermore, TAZ overexpression in hNSPCs impairs their neuronal commitment in, at least in part, TEAD-dependent manner. Indeed, TAZ deletion is accompanied by an increment in the transcripts of SOX2 and proneural bHLH factors ASCL1, NEUROG2 and NEUROD1, meanwhile TAZ overexpression downregulates these transcripts. Basing our studies in bioinformatics analysis, we found that the regulatory regions of the genes encoding SOX2 and proneural bHLH factors ASCL1, NEUROG2 and NEUROD1 present putative sites recognized by TAZ-DNA-binding partners TEAD1/2/3/4 and SMAD 2/3/4. By chromatin immunoprecipitation analysis, we confirmed the enrichment on TAZ in the regulatory regions of these genes. Furthermore, TAZ enrichment in these regions conducts to a reduction in histone acetylation and less recruitment of RNA Pol II. Altogether, our results point TAZ as a transcriptional corepressor of SOX2 and proneural bHLH, thus leading to ablation of neuronal cell fate specification and differentiation.

## INTRODUCTION

The Hippo pathway is a conserved cascade of kinases related to development, differentiation, organ size and regeneration (Mo et al. 2014). In mammals, Hippo pathway comprises the serine/threonine kinases MST1/2 and LATS1/2 and one of its major targets is TAZ (transcriptional coactivator with PDZ binding motif). Activation of Hippo pathway results in TAZ phosphorylation and triggers its inactivation via sequestration by 14-3-3 in cytoplasm or its degradation via ubiquitin-proteasome-dependent manner. When Hippo pathway is inactivated, unphosphorylated TAZ migrates to the nucleus, where it acts as the binding partner of several transcription factors (TFs), mainly TEADs (Chan et al. 2009), but also others as SMADs (Varelas et al. 2008) and RUNX (Cui et al. 2003). Upon its binding to these TFs, hippo transducer TAZ regulates the expression of genes related to cell growth, self-renewal and oncogenic transformation (Chan et al. 2009; H. Zhang et al. 2009). Although TAZ implication in cell proliferation and migration is widely known in cancer (Bhat et al. 2011; M. Wang et al. 2015a), little is known about its role in the neuronal commitment of neural stem/progenitor cells (NSPCs).

These NSPCs are multipotent stem cells which undergo asymmetric division generating neural progenitors and neurons (Taverna et al. 2014). This process involves a number of key factors, including Sex-determining region Y (SRY)-related HMG box 2 (SOX2) and proneural basic helix-loop-helix (bHLH) factors (Ma et al. 1996; Sommer et al. 1996).

SOX2, a member of the SOXB1 family of transcription factors, is expressed in all NSPCs in CNS, playing roles in maintaining NSPCs stemness during development (Cavallaro et al. 2008). SOX2, itself, can induce the conversion of NG2 glia into induced neurons in the adult mouse cerebral cortex (Heinrich et al. 2014). Furthermore, SOX2 marks epigenetically the regulatory regions of proneural bHLH genes, thereby enabling appropriate activation of the differentiation program upon exposure to a neurogenic stimulus (Amador-Arjona et al. 2015; Ng et al. 2013). In vertebrates, bHLH proneural factors comprise among others ASCL1 (Achaete-Scute complex-like 1), Neurogenin-2 (NEUROG2) and NEUROD1. Transient expression of these proneural factors drives neuronal generation from NSPCs (Bertrand et al. 2002). For example, ASCL1 is necessary to induce cell cycle exist and neuronal specification, not only in NSPCs (Wilkinson et al. 2013), but also in somatic non-neural cells (Berninger et al. 2007) (Chanda et al. 2014). Together with Neurogenin-2, ASCL1 regulates the progression of retinal neurogenesis (Hufnagel et al. 2010) and promotes deep-layer neurogenesis in the murine neocortex (Dennis et al. 2017). Neurogenin-2 also regulates cell cycle exit on neuronal progenitors (Lacomme et al. 2012) and initiates a cascade of other critical proneural transcription factors, one of which is NEUROD1. NEUROD1 has been related with terminal differentiation, neuronal maturation and survival (Gao et al. 2009) (Hevner et al. 2006; Pataskar et al. 2016) (Aprea et al. 2014).

Although the function of SOX2 and proneural bHLH factors has been hardly studied in the context of neurogenesis and several of these genes are included in strategies for the conversion of somatic

non-neural cells into neuronal lineage, they are still some questions about their transcriptional activation or inactivation during neuronal commitment.

In this study, we investigated the role of TAZ in the neuronal specification of NSPCs. TAZ deletion is accompanied by an increment in the transcripts of SOX2 and proneural bHLH factors ASCL1, NEUROG2 and NEUROD1, meanwhile TAZ overexpression downregulates these transcripts. By chromatin immunoprecipitation analysis, we confirmed the enrichment on TAZ in the regulatory regions of these genes, conducting to a lower levels of histone acetylation and RNA-polymerase II (RNA Pol II) recruitment. Altogether, our results point TAZ as a transcriptional co-repressor of SOX2 and proneural bHLH, thus leading to ablation of neuronal cell fate specification and differentiation.

## RESULTS

### TAZ expression is absent in mature neurons.

To study the function of TAZ in neurogenesis, we first consulted the Brain RNA-seq database. This database provides the expression levels of numerous genes in the main cell types of human (Y. Zhang et al. 2016) and murine brain (Y. Zhang et al. 2014). We found that *WWTR1* expression, encoding TAZ, is mostly limited to astroglia and endothelial cells and, surprisingly, is low in neurons of either humans (Fig.1A) or mice (Fig. 1B).

These differences prompted us to analyse *WWTR1* expression in the two main murine neurogenic niches: the subventricular zone (SVZ) of the striatum and the subgranular zone (SGZ) of the dentate gyrus (DG), in newborn and 3-, 6-, and 12-months-old mice. We combined TAZ immunostaining with Nestin to identify NSPCs, and DCX to identify neuroblasts and immature neurons. The specificity of anti-TAZ antibody was validated in Fig. S1A-C. As widely reported, the pool of progenitors (Nestin+ cells) greatly declined with aging, both in the SVZ (Fig. 1E and Fig. S1D) and the SGZ (Fig. 1G and Fig. S1E). The number of neuroblasts and immature neurons (DCX+ cells) also decayed with aging in SVZ (Fig. 1F and Fig. S1D) and the SGZ (Fig. 1H and Fig. S1E). More importantly, we found that TAZ-expressing cells also declined parallel to the exhaustion of the pool of progenitors (Fig. S1D and Fig. S1E). Furthermore, in double immunofluorescence assays we found that TAZ is expressed in Nestin+ cells but not in DCX+ cells, both in the SVZ (Fig. 1C) and the SGZ (Fig. 1D) and the pool of double Nestin+/TAZ+ cells (NSPCs expressing TAZ) dramatically declined after 3 months of age in both locations. These results indicate that TAZ expression in murine neurogenic niches is mostly limited to NSPCs and is absent in neurons already from immature stages.

Then, we analyzed the expression of TAZ during differentiation of the human immortalized NSPC line ReNcell. As shown in Fig. 2A, under stem growth conditions (in the presence of growth factors) these cells exhibited the Nestin marker of NSPCs but also expressed TAZ both in the nucleus and cytoplasm (white arrowheads), consistent with our observations in the neurogenic niches. After 7

days in differentiation medium (in the absence of growth factors), many NSPCs were differentiating to immature neurons (DCX+), while others retained the expression of GFAP, marker of both NSPCs and astrocytes. Importantly, DCX+ cells did not express TAZ (Fig. 2B) in agreement with our observations in the murine neurogenic niches (Fig. 1). We also found a progressive loss of Nestin+ NSPCs to ~50%, a progressive increase of DCX+ immature neurons to ~40%, and, more relevant, a decrease in TAZ expression to ~70% that paralleled the loss of NSPCs (Fig. 2C). Additionally, the loss of TAZ+ cells was further correlated with neuronal differentiation because the fraction of Nestin+/TAZ+ cells remained constant while that of DCX+/TAZ+ cells declined (Fig. 2D). This decay was parallel to neuronal maturation, analyzed as neurite length (Fig. 2E and 2F). Moreover, TAZ nuclear expression decreased as neural maturation proceeded (Fig. 2F). These results demonstrate a negative correlation between TAZ expression and exit of stemness towards neuronal differentiation.

**TAZ depletion in neural progenitors favours neuronal differentiation.**

In order to determine if this negative correlation was evidencing a role of TAZ in the control of stemness vs. neuronal differentiation, ReNcells were infected with a control lentivirus (shCO) or with a lentivirus for human TAZ-knockdown (shTAZ) (Fig. S2A), allowed to growth 5 days under proliferative conditions and them grown in differentiation medium for 30 days (Fig. 3A and B). Neuronal differentiation was analyzed with the specific markers DCX (neuroblasts and immature neurons), MAP2 (dendrite marker), TUBB3 (neuronal marker) and TAU (axon marker) (Fig. 3B, C, D). We found that TAZ silencing resulted in an increase in the number neurons as determined by the quantification of DCX+ (Fig. 3B and E), MAP2+ (Fig. 3B and F), TUBB3+ (Fig. 3C and G) and TAU+ (Fig. 3D and H) cells. We next evaluated neuronal complexity and maturation as determined by dendrite length, based on MAP2 staining, and axonal length, based on TAU staining. TAZ-knocked-down cells presented longer dendrites (Fig. 3I) and axons (Fig. 3J) than shCO-infected cells. These results indicate that loss of TAZ favours neuronal differentiation.

**TAZ inhibits neuronal commitment partially in a TEAD-dependent manner.**

As an additional approach, we overexpressed several mutant TAZ versions during 5 days in proliferation medium (Fig. S2B) and analyzed ReNcells differentiation after 30 days in differentiation medium, without growth factors (Fig. 4A and B). Expression of wild type TAZ (TAZ-WT) reduced the neuronal differentiation as determined with the DCX (Fig. 4B and C), MAP2 (Fig. 4B and D) and TAU (Fig. 4B and E) markers. Moreover, expression of the constitutively stable mutant of TAZ ($TAZ^{4SA}$) abolished completely neuronal differentiation (Fig. 4B, C, D and E). Regarding neuronal maturation, we found an impairment in dendrite (MAP2 staining) and axon (TAU) length in TAZ-overexpressing cells,

indicating that TAZ not only diminishes neuronal differentiation, but also affects further stages of neuronal maturation (Fig. 4F and G).

TEAD transcription factors are the main transcriptional co-partners of TAZ. To gain more insight into the implication of TEADs in neuronal commitment, we expressed mutant forms of TAZ defective in the binding to TEAD, were the Ser-51 has been mutated to alanine ($TAZ^{S51A}$) and the constitutively active $TAZ^{4SA+S51A}$ which does not bind 14-3-3 proteins and is not targeted for degradation (H. Zhang et al. 2009). Expression of $TAZ^{S51A}$ partially restored neuronal differentiation as determined with DCX (Fig. 4B and C), MAP2 (Fig. 4B and D) and TAU (Fig.4B and E) immunostaining. Moreover, $TAZ^{4SA+S51A}$, that is not degradable and does not bind TEAD, partially restored neuronal differentiation despite harbouring high TAZ levels (Fig. 4B to E). These findings indicate that TAZ repression of neuronal differentiation is partially TEAD-dependent. These observations were further extended to study the neuronal complexity as described previously. In line with the data on neuronal differentiation, we found that overexpression of TEAD-binding defective TAZ mutants partially restored the dendrite and axonal length (Fig. 4F and G).

**Identification of putative TAZ interacting regions in proneurogenic genes.**

To address why TAZ represses neurogenesis, we first analyzed the possible link between TAZ and transcription factors known to be positive regulators of neurogenesis, such as SOX2 and proneurogenic basic helix-loop-helix factors (bHLH) ASCL1, NEUROG2 and NEUROD1. First, we surveyed the Encyclopedia of DNA Elements at UCSC (ENCODE) of the human genome (Feb. 2009) in search for TAZ-regulated elements. Although TAZ does not bind directly to gene regulatory elements, ENCODE includes information about TAZ co-partners TEAD4, SMAD2 and RUNX. Furthermore, this database also gathers information of DNase hypersensitive areas and acetylation in Lys27 of histone H3 (H3K27Ac), which correlates with open chromatin that characterizes regulatory regions. In addition, we obtained the position specific scoring matrix (PSSM) for the consensus sequence recognize by TAZ co-partners TEAD1, TEAD2 (Fig. S4B and S4C), TEAD3, TEAD4, SMAD2/3/4 and RUNX2 based on the frequency matrix depicted at the JASPAR database. We then compared the regulatory regions retrieved from ENCODE for each gene with the PSSM of the consensus sequence for each transcription factors using a Python-based bioinformatics analysis (Table S10).

Using this script, we obtained a relative score for each sequence and considered those with a relative score higher than 80%. We identified several putative TEADs, SMADs and RUNX binding sites in the gene regulatory regions of *SOX2* and bHLH factors *ASCL1, NEUROG2* and *NEUROD1* (Table S1 to S6). Sequences in the regulatory regions of the *bona fide* TAZ-targets *CTGF* and *CYR61* were analyzed as positive controls (Table S1 to S6).

**TAZ expression inversely correlates with the levels of SOX2 and several proneuronal bHLH factors.**

Since we found that TAZ co-partners recognize sequences in the regulatory regions of proneurogenic genes, we analyzed the relevance of TAZ in the regulation of their expression. First, we knocked-down TAZ in ReNcells using a lentiviral vector for shTAZ. After 5 days of lentiviral transduction, we found a decrease in TAZ protein levels and its well-known target CTGF (Fig. 5A). TAZ knockdown was accompanied by an increase in the protein levels of SOX2 and NEUROD1 (Fig. 5A). Furthermore, we found a decrease to ~50% in TAZ transcript, *WWTR1*, and ~30% in the *bona fide* targets *CTFG* and *CYR61* (Fig. 5B). Under the same conditions, we found a significant increase in the transcripts of the proneurogenic factors *SOX2, ASCL1, NEUROG2* and *NEUROD1* (Fig. 5C).

Next, we analyzed the protein and transcript levels of the proneurogenic factors in ReNcells transduced with a retroviral vector for expression of active mutant $TAZ^{4SA}$ for 1, 2 and 5 days (Fig. S3). As expected, we saw a gradual increase of the bona fide TAZ target CTGF in parallel to TAZ overexpression (Fig. S3A). At the same time, SOX2 and NEUROD1 levels declined (Fig. S3A). At the transcriptional level, the increase in the TAZ transcript (*WWTR1*) was accompanied by an increase in its positive controls *CTFG* and *CYR61* (Fig. S3B), but also a decrease in the proneurogenic factors *SOX2, ASCL1 NEUROG2* and *NEUROD1* (Fig. S3C).

To uncover the effect of TAZ in proneurogenic genes during differentiation, we overexpressed wild type TAZ (TAZ-WT) and constitutively active TAZ ($TAZ^{4SA}$) by retroviral transduction in ReNcells and allow them to grow 5 days under proliferation conditions. Next, we removed the growth factors and analyzed the protein and transcript levels of several proneurogenic factors at 0, 2 and 4 days under differentiation conditions (Fig. S3). In TAZ overexpressing cells, we found accumulation of TAZ and its target CTGF by immunoblot (Fig. S3D), and *CTGF* and *CYR61* transcripts (Fig. S3E). At the same time points, SOX2 and NEUROD1 protein levels declined (Fig. S3D). On the other hand, the expression of proneurogenic factors increased during differentiation in the control (CT) transduced cells, while *SOX2, ASCL1, NEUROG2* and *NEUROD1* remained low in TAZ-WT cells and were almost supressed in $TAZ^{4SA}$ cells (Fig. S3F). Together these results strongly suggest that TAZ is a negative regulator of these proneurogenic factors.

**TAZ repression of proneurogenic genes is partially TEAD-dependent.**

To gain more insight into the implication of TEAD transcription factors in the regulation of proneurogenic factors, we expressed the defective TEAD-binding TAZ mutants. As expected, retroviral overexpression of TAZ-WT and active $TAZ^{4SA}$ led to an increase in the TAZ target CTGF after 5 days (Fig. 5D). At the same time, this CTGF accumulation was partially reverted by the $TAZ^{S51A}$ mutant defective in TEAD-binding (Fig. 57A). Furthermore, SOX2 protein levels decrease in TAZ-WT and even

more in TAZ$^{4SA}$ conditions. The mutant TAZ$^{4SA+S51A}$, which disrupted TEAD binding, largely abolished the ability of TAZ to repress SOX2 (Fig. 5D and E). Similar results were observed with NEUROD1 (Fig. 5D and F). Parallel to the increase in TAZ targets (*CTGF* and *CYR61*) in TAZ-WT and TAZ$^{4SA}$ transduced ReNcells (Fig. 5G), we found a decrease at the transcriptional level of *SOX2* and proneural *ASCL1*, *NEUROG2* and *NEUROD1* factors, being this repression almost complete in cells expressing TAZ$^{4SA}$ (Fig. 5H). By contrast, this repression by TAZ$^{S51A}$ and TAZ$^{4SA+S51A}$ was almost absent for *SOX2* and partially reverted for *ASCL1*, *NEUROG2* and *NEUROD1* (Fig. 5H). As it will be discussed, TAZ can induce itself, making possible that ectopically expressed TAZ might induce endogenous TAZ expression, which is will not be defective in TEAD-binding.

To further investigate the role of TEADs in TAZ repression of proneurogenic genes we used ReNcells retrovirally transduced with TAZ$^{4SA}$. In these cells, we performed knockdown of the TEAD isoforms using lentiviral vectors directed to TEAD1/3/4 and TEAD2 (altogether named shTEAD) (Fig. S4). Depletion of TEADs (Fig. S4D) conducted to lower levels on *CTGF* and *CYR61* transcripts as expected (Fig. S4E), but also to up-regulation of proneurogenic transcripts (Fig. S4F). Altogether, these results suggest that TEADs are involved in the repressive function of TAZ on proneurogenic factors.

**TAZ induces epigenetic changes at the regulatory regions of proneurogenic genes.**

We next explored epigenetic mechanisms underlying repression of the neurogenic genes by TAZ. When CT-ReNcells (CT) and TAZ$^{4SA}$-ReNcells were maintained for 5 days in proliferation and 4 additional days in differentiation (Fig. 6A) they presented and increase in the canonical TAZ target CTGF, while SOX2 and NEUROD1 levels were decreased (Fig. 6B). At transcriptional level, TAZ targets *CTGF* and *CYR61* also increased (Fig. 6C) and while proneurogenic transcripts decreased (Fig. 6D). By ChIP-qPCR analysis, we found TAZ enrichment in positive controls and also in the TAZ-interacting regions (TIRs) of proneurogenic genes described in Figure S5 and Tables S1 to S6, but not in the negative control (CTGF 3´UTR) in TAZ$^{4SA}$ cells compared to the control (Fig. 6E). We investigated the recruitment of RNA polymerase II (RNA Pol II) which is engaged together with the transcription machinery to the promoter in the eukaryotic genes (Roeder 2005) (Sandoval et al. 2004). RNA Pol II occupancy was significantly reduced at regulatory regions of proneurogenic genes in TAZ$^{4SA}$-expressing cells compared to control cells, while RNA Pol II levels were higher in *CTGF* and *CYR61* regulatory regions (Fig. 6F).

We then surveyed major histone modifications. Histone 3 (H3) acetylation in the N-terminal Lysine 9, is generally associated with gene activation (Kuo et al. 1996) (Strahl and Allis 2000). ChIP-qPCR assays using anti-acetylated Lys9-H3 antibody (AcH3) indicated that H3 acetylation was increased in TAZ *bona fide* targets *CTGF* and *CYR61*, while it was reduced by TAZ$^{4SA}$ overexpression in proneurogenic genes in the same TIRs, with no changes in the negative control (Fig. 6G). On the basis of these results, we propose that TAZ represses proneurogenic gene expression by changes in histone acetylation and RNA Pol II occupancy at their regulatory regions.

Altogether, our results characterize for the first time TAZ as a master repressor of neuronal differentiation program, and this repression is partially TEAD-dependent.

## DISCUSSION

Our study addressed for the first time how the Hippo co-activator TAZ represses the expression of proneurogenic genes. The transcriptional program underlying neural stem cell differentiation is regulated by largely unknown spatiotemporal patterns of gene expression (Guillemot 2007) (Spitz and Furlong 2012). The Hippo pathway has been related with the maintenance of the NSPCs pool (Lavado et al. 2018), but the specific role of TAZ in neurogenesis has not been previously addressed. Interestingly, TAZ is implicated in epithelial–mesenchymal transition (EMT) in cancer (Q. Wang et al. 2015b) (Li et al. 2015), a process that is critical for neuronal development and the migration of newborn neurons (Kwan et al. 2012).

Based on the data available in the Brain RNA-seq database and our immunofluorescence analysis in vitro and in vivo, we found that TAZ expression is mostly limited to astrocytes and NSPCs, and decreases along neuronal maturation. Although no previous analysis were focused in TAZ expression in neurogenic niches, our findings are in line with the downregulation of the other Hippo effector, YAP, during neuronal differentiation (H. Zhang et al. 2012). YAP is also expressed in astrocytes and progenitors, but not in neurons (Huang et al. 2016). However, while we find that TAZ knockdown leads to neuronal differentiation, it is not clear that YAP will do the same. This could be related to different roles of TAZ and YAP or to misleading identification neurons. In fact, Zhang et al. used TUBB3 as a neuronal marker, which it is not specific as it is also expressed in astrocytes and progenitors (Draberova et al. 2008). On the contrary, we used several neuronal markers and astrocytic markers to ensure the proper identification of neurons.

Prompted for our findings, we analyzed the presence of TAZ transcriptional co-partners binding sequences in proneurogenic genes. Bioinformatics approaches revealed that the promoters of the proneurogenic genes *SOX2, ASCL1*, *NEUROG2* and *NEUROD1* present putative sites for binding to TAZ-transcriptional co-partners. We then uncovered the relationship between TAZ expression and proneurogenic genes by showing TAZ enrichment in their regulatory regions. Furthermore, we ensured the accuracy of these sequences cloning an identified TEAD-binding sequence of SOX2 in the luciferase reporter and showing a TAZ-dependent response.

The information available about the interaction between TAZ co-partners and proneurogenic genes is very scarce. However, the short half-life of proneurogenic factors indicates the relevance of their transcriptional regulation (Sriuranpong et al. 2002) Ali (Ali et al. 2011). It has been described that TAZ co-partner SMAD (Varelas et al. 2008) shares many gene targets with cell-type specific transcription factors that participate in cellular identity (Mullen et al. 2011) (Trompouki et al. 2011). Genome-wide experiments demonstrate that the proneural factor ASCL1 assists SMAD3 in binding to a subset of

enhancers (Fueyo et al. 2018). Furthermore, Castro et al., described that ASCL1 targets the transcription factors TEAD1, TEAD2 and TAZ using genome-wide analysis of the developing ventral mesencephalon (Castro et al. 2011). Our bioinformatics analysis demonstrated that RUNX1/2- recognizes a sequence in the regulatory regions of proneurogenic genes. Fukui et al., showed that RUNX1 is down-regulated during neuronal differentiation, while NEUROG2 is upregulated, but the authors did not establish any further analysis to this correlation (Fukui et al. 2018). Thus, our study establishes for the first time the existence of TAZ-interacting regulatory regions in proneurogenic genes. Furthermore, the upregulation of TAZ repressed the expression of these genes, which was partially recovered by ablation of TAZ-TEAD interaction or TEAD-knockdown. The uncompleted recovery could be: a) because TAZ functional repression is partially TEAD-independent, b) ectopic TAZ upregulates endogenous TAZ, which is not TEAD-binding defective, hiding the TEAD-independent effect. As described in the ENCODE database, the TAZ enhancer regions comprise several TEAD-putative binding sequences. Furthermore, TEAD4 is a target of TAZ (Kim et al. 2015). TEADs are essential for the transcriptional co-activator function of TAZ (H. Zhang et al. 2009); hence, it would be unexpected that TEAD was also involved in their corepressor function.

Our study shows that the interaction of TAZ with regulatory regions of proneurogenic genes conducts to decreased acetylation of the chromatin and reduced recruitment of RNA Pol II. Of note, the same TAZ-TEAD complex activates genes such as CTGF and CYR61 but suppresses the transcription of others. Enhancer-bound TAZ–TEAD complexes regulate gene transcription by inducing p300-dependent acetylation at lysine 27 of histone H3 (H3K27ac) (Stein et al. 2015), through recruitment of the Mediator complex and induction of transcriptional elongation through the release of RNA polymerase II (Galli et al. 2015). Several recent studies have identified the interaction of TAZ or its Drosophila homolog *Yki* with other regulators of chromatin status as components of the chromatin-remodelling complexes and histone methyltransferase complexes (Basu et al. 2013) (Qing et al. 2014) (Skibinski et al. 2014) (Oh et al. 2013). Recently, Kim et al., described the interaction between TAZ-paralog YAP with the nucleosome remodelling and histone deacetylase (NuRD) complex (Lai and Wade 2011). In this study, the authors showed how the YAP/TEAD recruits the NuRD complex to deacetylate histones and supresses the expression of Trail and DNA Damage Inducible Transcript 4 (DDIT4)-encoding genes to promote cell growth and survival (Kim et al. 2015). The implication of NuRD in transcriptional repression of TAZ/TEAD has also been established by Beyer et al., who described a regulatory complex composed of TAZ/YAP/TEAD, SMAD2/3, and the pluripotency regulator OCT4, that collaborates with NuRD to suppress mesoendoderm genes (Beyer et al. 2013) (Totaro et al. 2018). Indeed, TAZ can directly interact with histone deacetylation complex for TAZ/TEAD-induced suppression of ΔNp63 transcription (Valencia-Sama et al. 2015). Together with these studies, our data suggests that TAZ supresses gene expression by directly interacting with the histone deacetylation complex and further affects RNA Pol II recruitment and gene transcription.

It is important to point out the inter-relationship between proneurogenic factors. Although the repressor effect of TAZ on ASCL1 and NEUROG2 expression is as strong as on SOX2 and NEUROD1, the enrichment of TAZ in their regulatory regions and the effect in histone acetylation and RNA Pol II recruitment is not as strong. This could be related to the capacity of proneurogenic factors to regulate their own expression. For example, SOX2 can enhance the expression of ASCL1 and NEUROG2 by cooperating with RMST (Ng et al. 2013) and POU factors (Lodato et al. 2013) in ESCs and NPCs. NEUROG2 is a pioneer factor that upregulates SOX4, which co-activates NEUROD1 and NEUROD4 (Smith et al. 2016). Thus, we speculate that TAZ-dependent repression of a proneurogenic factor presumably would impact the expression of others.

The transcriptional corepressor activity of TAZ opens a new path for understanding the role of TAZ in neural stem cell fate and neuronal reprogramming (Bago et al. 2016) (Tang et al. 2017) (Dennis et al. 2019). Much work is still needed if we are to obtain a clear and comprehensive understanding of the operational logic focused on the TAZ repressor function in neurogenesis and its possible implication in neural stem cell therapy in neurodegeneration and cancer.

## MATERIALS METHODS

### Brain RNA-seq.

The Brain RNA-seq database of the Stanford University (http://www.brainrnaseq.org/) was analysed for expression of *WWTR1*. Human and mouse data were obtained as described in (Y. Zhang et al. 2014) and (Y. Zhang et al. 2016).

### Animals.

Animals were housed under a 12 h light-dark cycle. Food and water were provided ad libitum and mice were cared according to protocols approved by the Ethics Committee for Research of the Universidad Autónoma de Madrid following institutional, Spanish and European guidelines (RD 53/2013, and ECC 566/2015, 2010/63/UE European Council Directives).

### Cell culture and reagents.

HEK293T were maintained in Dulbecco's Modified Eagle Medium supplemented with 10% fetal bovine serum (Sigma-Aldrich, St. Louis, Missouri, USA), 4 mM L-Glutamine (Gibco) and 80 mg/ml gentamicin (Laboratorios Normon, Madrid, Spain), 100 U/ml penicillin/streptomycin (Life Technologies, Grand Island, NY, USA) and 1% amphotericin B solution (Lonza, Hopkinton, MA, USA) in 5% $CO_2$ at 37 °C conditions. The immortalized human neural stem cell line derived from ventral mesencephalon of fetal brain (ReNcell VM, named in this study ReNcells) was purchased from EMD Millipore (Billerica, MA, USA). ReNcells were plated onto Corning Matrigel hESC-Qualified Matrix (CORNING, Bedford, MA, USA)-coated T75 cell culture flasks (BD Biosciences, San Jose, CA, USA) and maintained in

neurobasal medium (Gibco, Thermo Fisher Scientific, Grand Island, NY, USA) supplemented with 2% (v/v) B27 supplement (Gibco), 20 ng/ml recombinant human epidermal growth factor (Peprotech, NJ, USA), 20 ng/ml recombinant human basic fibroblast growth factor (Peprotech, NJ, USA), 100 U/ml penicillin/streptomycin (Life Technologies, Grand Island, NY, USA) and 1% amphotericin B solution (Lonza, Hopkinton) in 5% $CO_2$ at 37 °C conditions.

**Lentiviral and retroviral vector production and infection.**

Pseudotyped lentiviral vectors were produced in HEK293T cells transiently co-transfected with 10 µg of the corresponding lentiviral vector plasmid, 6 µg of the packaging plasmid pSPAX2 (Addgene Watertown, MA, USA) and 6 µg of the VSV-G envelope protein plasmid pMD2G (Addgene) using Lipofectamine Plus reagent according to the manufacturer's instructions (Invitrogen país). Retrovirus supernatant was prepared by transfection of HEK293T cells with 5 µg of each plasmid using Lipofectamine Plus. Lentiviral vector shRNA control (shco), shTAZ, and several shTEAD2 were purchased from Sigma-Aldrich. Lentiviral vector shTEAD1/3/4 was a generous gift from Prof. Zengqiang Yuan (Chinese Academy of Sciences, Beijing, China). The retroviral vectors used were: pBabePuro (Addgene), pBabePuroTAZ-WT, pBabePuroTAZ$^{S51A}$ (TEAD-binding-defective mutant), pBabePuroTAZ$^{4SA}$ (constitutive active TAZ with all four serine residues in the HxRxxS motif replaced with alanine: S66A, S89A, S117A, and S311A), and pBabePuroTAZ$^{4SA+S51A}$ (generous gifts of Prof. Kun-Liang Guan). Cells were infected in the presence of 4 µg/ml polybrene (Sigma-Aldrich) and selected with 0.5 µg/ml puromycin (Sigma-Aldrich).

**Immunofluorescence.**

Thirty µm-thick coronal murine brain sections were processed for immunofluorescence microscopy as previously described (Robledinos-Anton et al. 2017). Antibodies are shown in Supplementary Table S9. Images were obtained using Leica TCS SP5 confocal microscope and cell counts were performed using FiJi Software (ImageJ). ReNcells VM were adhered on Corning Matrigel hESC-Qualified Matrix coated coverslips, and fixed with 4% paraformaldehyde. Immunofluorescence was performed as described in (Robledinos-Anton et al. 2017). Briefly, cells were washed, blocked in PBS containing 0.5% Triton X-100% and 3% bovine serum albumin and incubated for 16 h at 4 °C with the relevant primary antibodies and for 2 h at room temperature with the appropriate secondary antibodies coupled to Alexa Fluor 488, 555/546, or 647 (1:500) (Life Technologies-Molecular Probes, Grand Island, NY, USA). Nuclei were stained with DAPI. Images were quantified using the Fiji Software (http://fiji.sc/Fiji).

**Differentiation and neuron complexity.**

ReNcell VM were plated after five days of lentiviral/retroviral infection on Corning Matrigel hESC-Qualified Matrix coated coverslips and incubated for 30 days in differentiation medium (Neurobasal medium supplemented with 2% (v/v) B27 supplement and antibiotics). Immunostaining and

quantification were performed as described in (Robledinos-Anton et al. 2017). Primary antibodies are described in Supplementary Table S9. To quantify neuronal complexity, Sholl analysis was performed using the Simple neurite tracer plugin (http://homepages.inf.ed.ac.uk/s9808248/imagej/tracer/); total axonal, dendrite or neurite length were determined using NeuronJ (https://imagescience.org/meijering/software/neuronj/) and the image processing package Fiji (http://pacific.mpicbg.de/wiki/index.php/Main_Page).

**Immunoblotting.**

Immunoblotting was performed as described in (Pajares et al. 2016). Briefly, cells were homogenized in lysis buffer (TRIS pH 7.6 50 mM, 400 mM NaCl, 1 mM EDTA, 1 mM EGTA and 1% SDS) and samples were heated at 95°C for 15 min, sonicated and pre-cleared by centrifugation 10 min at 13,000 rpm. Proteins were resolved in SDS-PAGE, transferred to Immobilon-P (Millipore) membranes and detected with primary antibodies (Supplementary Table S9). Proper peroxidase-conjugated secondary antibodies were used for detection by enhanced chemiluminescence (GE Healthcare, Chicago, Illinois, USA).

**Bioinformatics analysis of response elements for TAZ co-transcription factors.**

Putative TEADs, STATs and SMADs binding domains in *SOX2*, bHLH factor-encoding genes and TAZ-target genes were identified in ENCODE (genome-euro.ucsc.edu) for the human genome taking as a reference the available chromatin immunoprecipitation data for TAZ transcriptional cofactors TEADs and SMADs in DNase-sensitive and H3K27Ac-rich regions. A frequency matrix of the consensus binding sequence of each transcription factor based on the JASPAR database (http://jaspar.genereg.net/) was converted to a position-specific scoring matrix and a script was generated with the Python 3.4 program to scan the promoter sequences with candidate response elements as previously described (Pajares et al. 2016).

**Chromatin immunoprecipitation (ChIP).**

This protocol was performed as described in (Pajares et al. 2016). Briefly, ReNcells were transfected with plasmid CT or pBabePuroTAZ$^{4SA}$ encoding a constitutive activated TAZ (Bhat et al. 2011). The qRT-PCR from immunoprecipitated DNA with antibodies described in Supplementary Table S9. PCR reactions were done with the primers shown in Supplementary Table S7. Samples from 4 independent immunoprecipitations were analyzed.

**Analysis of mRNA levels.**

Total RNA extraction, reverse transcription and quantitative polymerase chain reaction (qRT-PCR) were done as detailed in (Rojo et al. 2010). Primer sequences are shown in Supplementary Table

S8. Data analysis was based on the ΔΔCT method, with normalization of the raw data to the housekeeping gene *GAPDH* (Applied Biosystems). All PCRs were performed from triplicate samples.

**Statistical analysis.**

Data are presented as mean ± S.D. or S.E.M. Statistical assessments of differences between groups were analyzed using GraphPad Prism 5 software by the unpaired Student's t-test. For the scatter plots, the Pearson correlation coefficient (R) and the *p*-value associated with this coefficient were analyzed. Statistically significant differences in Kaplan-Meier survival curves were calculated with the log-rank test.

**ACKNOWLEDGEMENTS**

This study was funded by the Spanish Ministry of Economy and Competitiveness (MINECO) under the grant SAF2016-76520-R. NRA is recipient of a FPU contract of MINECO; ME is recipient of a postdoctoral contract Juan de la Cierva.

**AUTHOR CONTRIBUTIONS**

NRA conducted the experiments of molecular biology. NRA and ME designed the experiments. NRA and AC wrote the paper.

**Competing interests:** The authors declare no competing interests.

**REFERENCES**

Ali, F., et al. (2011), 'Cell cycle-regulated multi-site phosphorylation of Neurogenin 2 coordinates cell cycling with differentiation during neurogenesis', *Development*, 138 (19), 4267-77.

Amador-Arjona, A., et al. (2015), 'SOX2 primes the epigenetic landscape in neural precursors enabling proper gene activation during hippocampal neurogenesis', *Proc Natl Acad Sci U S A*, 112 (15), E1936-45.

Aprea, J., Nonaka-Kinoshita, M., and Calegari, F. (2014), 'Generation and characterization of Neurod1-CreER(T2) mouse lines for the study of embryonic and adult neurogenesis', *Genesis*, 52 (10), 870-8.

Bago, J. R., Sheets, K. T., and Hingtgen, S. D. (2016), 'Neural stem cell therapy for cancer', *Methods*, 99, 37-43.

Barski, A., et al. (2007), 'High-resolution profiling of histone methylations in the human genome', *Cell*, 129 (4), 823-37.

Basu, D., Reyes-Mugica, M., and Rebbaa, A. (2013), 'Histone acetylation-mediated regulation of the Hippo pathway', *PLoS One*, 8 (5), e62478.

Berninger, B., et al. (2007), 'Functional properties of neurons derived from in vitro reprogrammed postnatal astroglia', *J Neurosci*, 27 (32), 8654-64.

Bertrand, N., Castro, D. S., and Guillemot, F. (2002), 'Proneural genes and the specification of neural cell types', *Nat Rev Neurosci*, 3 (7), 517-30.

Beyer, T. A., et al. (2013), 'Switch enhancers interpret TGF-beta and Hippo signaling to control cell fate in human embryonic stem cells', *Cell Rep*, 5 (6), 1611-24.

Bhat, K. P., et al. (2011), 'The transcriptional coactivator TAZ regulates mesenchymal differentiation in malignant glioma', *Genes Dev*, 25 (24), 2594-609.

Castro, D. S., et al. (2011), 'A novel function of the proneural factor Ascl1 in progenitor proliferation identified by genome-wide characterization of its targets', *Genes Dev*, 25 (9), 930-45.

Cavallaro, M., et al. (2008), 'Impaired generation of mature neurons by neural stem cells from hypomorphic Sox2 mutants', *Development,* 135 (3), 541-57.

Cui, C. B., et al. (2003), 'Transcriptional coactivation of bone-specific transcription factor Cbfa1 by TAZ', *Mol Cell Biol,* 23 (3), 1004-13.

Chan, S. W., et al. (2009), 'TEADs mediate nuclear retention of TAZ to promote oncogenic transformation', *J Biol Chem,* 284 (21), 14347-58.

Chanda, S., et al. (2014), 'Generation of induced neuronal cells by the single reprogramming factor ASCL1', *Stem Cell Reports,* 3 (2), 282-96.

Dennis, D. J., Han, S., and Schuurmans, C. (2019), 'bHLH transcription factors in neural development, disease, and reprogramming', *Brain Res,* 1705, 48-65.

Dennis, D. J., et al. (2017), 'Neurog2 and Ascl1 together regulate a postmitotic derepression circuit to govern laminar fate specification in the murine neocortex', *Proc Natl Acad Sci U S A,* 114 (25), E4934-e43.

Draberova, E., et al. (2008), 'Class III beta-tubulin is constitutively coexpressed with glial fibrillary acidic protein and nestin in midgestational human fetal astrocytes: implications for phenotypic identity', *J Neuropathol Exp Neurol,* 67 (4), 341-54.

Fueyo, R., et al. (2018), 'Lineage specific transcription factors and epigenetic regulators mediate TGFbeta-dependent enhancer activation', *Nucleic Acids Res,* 46 (7), 3351-65.

Fukui, H., et al. (2018), 'Transcription factor Runx1 is pro-neurogenic in adult hippocampal precursor cells', *PLoS One,* 13 (1), e0190789.

Galli, G. G., et al. (2015), 'YAP Drives Growth by Controlling Transcriptional Pause Release from Dynamic Enhancers', *Mol Cell,* 60 (2), 328-37.

Gao, Z., et al. (2009), 'Neurod1 is essential for the survival and maturation of adult-born neurons', *Nat Neurosci,* 12 (9), 1090-2.

Guillemot, F. (2007), 'Cell fate specification in the mammalian telencephalon', *Prog Neurobiol,* 83 (1), 37-52.

Heinrich, C., et al. (2014), 'Sox2-mediated conversion of NG2 glia into induced neurons in the injured adult cerebral cortex', *Stem Cell Reports,* 3 (6), 1000-14.

Hevner, R. F., et al. (2006), 'Transcription factors in glutamatergic neurogenesis: conserved programs in neocortex, cerebellum, and adult hippocampus', *Neurosci Res,* 55 (3), 223-33.

Huang, Z., et al. (2016), 'YAP stabilizes SMAD1 and promotes BMP2-induced neocortical astrocytic differentiation', *Development,* 143 (13), 2398-409.

Hufnagel, R. B., et al. (2010), 'Neurog2 controls the leading edge of neurogenesis in the mammalian retina', *Dev Biol,* 340 (2), 490-503.

Kim, M., et al. (2015), 'Transcriptional co-repressor function of the hippo pathway transducers YAP and TAZ', *Cell Rep,* 11 (2), 270-82.

Kuo, M. H., et al. (1996), 'Transcription-linked acetylation by Gcn5p of histones H3 and H4 at specific lysines', *Nature,* 383 (6597), 269-72.

Kwan, K. Y., Sestan, N., and Anton, E. S. (2012), 'Transcriptional co-regulation of neuronal migration and laminar identity in the neocortex', *Development,* 139 (9), 1535-46.

Lacomme, M., et al. (2012), 'NEUROG2 drives cell cycle exit of neuronal precursors by specifically repressing a subset of cyclins acting at the G1 and S phases of the cell cycle', *Mol Cell Biol,* 32 (13), 2596-607.

Lai, A. Y. and Wade, P. A. (2011), 'Cancer biology and NuRD: a multifaceted chromatin remodelling complex', *Nat Rev Cancer,* 11 (8), 588-96.

Lavado, A., et al. (2018), 'The Hippo Pathway Prevents YAP/TAZ-Driven Hypertranscription and Controls Neural Progenitor Number', *Dev Cell,* 47 (5), 576-91.e8.

Li, Z., et al. (2015), 'The Hippo transducer TAZ promotes epithelial to mesenchymal transition and cancer stem cell maintenance in oral cancer', *Mol Oncol,* 9 (6), 1091-105.

Lodato, M. A., et al. (2013), 'SOX2 co-occupies distal enhancer elements with distinct POU factors in ESCs and NPCs to specify cell state', *PLoS Genet,* 9 (2), e1003288.

Ma, Q., Kintner, C., and Anderson, D. J. (1996), 'Identification of neurogenin, a vertebrate neuronal determination gene', *Cell,* 87 (1), 43-52.

Mo, J. S., Park, H. W., and Guan, K. L. (2014), 'The Hippo signaling pathway in stem cell biology and cancer', *EMBO Rep,* 15 (6), 642-56.

Mullen, A. C., et al. (2011), 'Master transcription factors determine cell-type-specific responses to TGF-beta signaling', *Cell,* 147 (3), 565-76.
Ng, S. Y., et al. (2013), 'The long noncoding RNA RMST interacts with SOX2 to regulate neurogenesis', *Mol Cell,* 51 (3), 349-59.
Oh, H., et al. (2013), 'Genome-wide association of Yorkie with chromatin and chromatin-remodeling complexes', *Cell Rep,* 3 (2), 309-18.
Pajares, M., et al. (2016), 'Transcription factor NFE2L2/NRF2 is a regulator of macroautophagy genes', *Autophagy,* 12 (10), 1902-16.
Pataskar, A., et al. (2016), 'NeuroD1 reprograms chromatin and transcription factor landscapes to induce the neuronal program', *Embo j,* 35 (1), 24-45.
Qing, Y., et al. (2014), 'The Hippo effector Yorkie activates transcription by interacting with a histone methyltransferase complex through Ncoa6', *Elife,* 3.
Robledinos-Anton, N., et al. (2017), 'Transcription factor NRF2 controls the fate of neural stem cells in the subgranular zone of the hippocampus', *Redox Biol,* 13, 393-401.
Roeder, R. G. (2005), 'Transcriptional regulation and the role of diverse coactivators in animal cells', *FEBS Lett,* 579 (4), 909-15.
Rojo, A. I., et al. (2010), 'Nrf2 regulates microglial dynamics and neuroinflammation in experimental Parkinson's disease', *Glia,* 58 (5), 588-98.
Sandoval, J., et al. (2004), 'RNAPol-ChIP: a novel application of chromatin immunoprecipitation to the analysis of real-time gene transcription', *Nucleic Acids Res,* 32 (11), e88.
Skibinski, A., et al. (2014), 'The Hippo transducer TAZ interacts with the SWI/SNF complex to regulate breast epithelial lineage commitment', *Cell Rep,* 6 (6), 1059-72.
Smith, D. K., et al. (2016), 'Small Molecules Modulate Chromatin Accessibility to Promote NEUROG2-Mediated Fibroblast-to-Neuron Reprogramming', *Stem Cell Reports,* 7 (5), 955-69.
Sommer, L., Ma, Q., and Anderson, D. J. (1996), 'neurogenins, a novel family of atonal-related bHLH transcription factors, are putative mammalian neuronal determination genes that reveal progenitor cell heterogeneity in the developing CNS and PNS', *Mol Cell Neurosci,* 8 (4), 221-41.
Spitz, F. and Furlong, E. E. (2012), 'Transcription factors: from enhancer binding to developmental control', *Nat Rev Genet,* 13 (9), 613-26.
Sriuranpong, V., et al. (2002), 'Notch signaling induces rapid degradation of achaete-scute homolog 1', *Mol Cell Biol,* 22 (9), 3129-39.
Stein, C., et al. (2015), 'YAP1 Exerts Its Transcriptional Control via TEAD-Mediated Activation of Enhancers', *PLoS Genet,* 11 (8), e1005465.
Strahl, B. D. and Allis, C. D. (2000), 'The language of covalent histone modifications', *Nature,* 403 (6765), 41-5.
Tang, Y., Yu, P., and Cheng, L. (2017), 'Current progress in the derivation and therapeutic application of neural stem cells', *Cell Death Dis,* 8 (10), e3108.
Taverna, E., Gotz, M., and Huttner, W. B. (2014), 'The cell biology of neurogenesis: toward an understanding of the development and evolution of the neocortex', *Annu Rev Cell Dev Biol,* 30, 465-502.
Totaro, A., et al. (2018), 'Crosstalk between YAP/TAZ and Notch Signaling', *Trends Cell Biol,* 28 (7), 560-73.
Trompouki, E., et al. (2011), 'Lineage regulators direct BMP and Wnt pathways to cell-specific programs during differentiation and regeneration', *Cell,* 147 (3), 577-89.
Valencia-Sama, I., et al. (2015), 'Hippo Component TAZ Functions as a Co-repressor and Negatively Regulates DeltaNp63 Transcription through TEA Domain (TEAD) Transcription Factor', *J Biol Chem,* 290 (27), 16906-17.
Varelas, X., et al. (2008), 'TAZ controls Smad nucleocytoplasmic shuttling and regulates human embryonic stem-cell self-renewal', *Nat Cell Biol,* 10 (7), 837-48.
Wang, M., et al. (2015a), 'Transcriptional co-activator TAZ sustains proliferation and tumorigenicity of neuroblastoma by targeting CTGF and PDGF-beta', *Oncotarget,* 6 (11), 9517-30.
Wang, Q., et al. (2015b), 'TAZ promotes epithelial to mesenchymal transition via the upregulation of connective tissue growth factor expression in neuroblastoma cells', *Mol Med Rep,* 11 (2), 982-8.
Wilkinson, G., Dennis, D., and Schuurmans, C. (2013), 'Proneural genes in neocortical development', *Neuroscience,* 253, 256-73.

Zhang, H., et al. (2012), 'Negative regulation of Yap during neuronal differentiation', *Dev Biol,* 361 (1), 103-15.

Zhang, H., et al. (2009), 'TEAD transcription factors mediate the function of TAZ in cell growth and epithelial-mesenchymal transition', *J Biol Chem,* 284 (20), 13355-62.

Zhang, Y., et al. (2014), 'An RNA-sequencing transcriptome and splicing database of glia, neurons, and vascular cells of the cerebral cortex', *J Neurosci,* 34 (36), 11929-47.

Zhang, Y., et al. (2016), 'Purification and Characterization of Progenitor and Mature Human Astrocytes Reveals Transcriptional and Functional Differences with Mouse', *Neuron,* 89 (1), 37-53.

**LEGENDS TO FIGURES**

**Figure 1. TAZ distribution in human and murine brain. (A)** Distribution of *WWTR1* mRNA in cell types isolated from human grey matter from mature brain specimens after removal of meninges and blood clots. For details of human data see (Y. Zhang et al. 2016). **(B)** Analysis of *WWTR1* mRNA expression in glia, neurons and vascular cells isolated from mouse cerebral cortex. *WWTR1* transcript is lower in neurons compared to glia and vascular cells both in human and mice brain. For details of mouse data see (Y. Zhang et al. 2014). In panels A and B, data were obtained from the Brain-RNAseq database. **(C)** TAZ distribution in the subventricular zone (SVZ) neurogenic niche: quantification of the total cell number coexpressing Nestin and TAZ or DCX and TAZ in the SVZ of newborn, 3-, 6- and 12- months old mice. **(D)** TAZ distribution in murine hippocampal neurogenic niche: quantification of the total cell number coexpressing Nestin and TAZ or DCX and TAZ in the subgranular zone (SGZ) neurogenic niche of newborn, 3-, 6- and 12- months old mice. **(E)** Representative immunofluorescence pictures of Nestin and TAZ staining from the neurogenic niche SVZ from the indicated mice, showing TAZ accumulation in Nestin positive cells. **(F)** Representative immunofluorescence pictures from the SVZ neurogenic niche of indicated mice showing immunostaining of neuronal marker Doublecortin (DCX) and TAZ. **(G)** Representative immunofluorescence pictures of Nestin and TAZ staining from the neurogenic niche SGZ from the indicated mice. **(H)** Representative immunofluorescence pictures from the SGZ neurogenic niche of indicated mice showing immunostaining of DCX and TAZ. Nuclei are counterstained with DAPI. White arrowheads indicate TAZ positive cells also delineated with white dotted lines. Yellow arrowheads in G indicate Nestin+ blood vessels, which have not been quantified in this study. Blue dotted lines indicate DCX positive and TAZ negative cells.

**Figure 2. TAZ expression declines during neuronal differentiation. (A)** Representative confocal images of ReNcells immunostained with Nestin and TAZ under proliferative conditions. White arrows indicate TAZ+ cells. **(B)** Representative confocal images of specific neuronal marker DCX, astrocyte and NSPCs marker GFAP with TAZ immunostaining of ReNcells after 7 days of in vitro differentiation. Blue arrows indicate TAZ- cells. **(C)** Quantification of Nestin+, DCX+ and TAZ+ ReNcells during differentiation. **(D)** Percentage of Nestin+/TAZ+ of total Nestin+ cells and DCX+/TAZ+ of total DCX+ ReNcells during differentiation. **(E)** Representative images of DCX+ cells after 3 and 7 days of differentiation. **(F)** Percentage of cells expressing nuclear TAZ (left Y axis) and neurite length (right Y axis) of DCX+ cells during neuronal differentiation, indicating neuronal maturation. Data are mean ± SEM ($n \geq 50$).

**Figure 3. Loss of TAZ favours neuronal differentiation. (A)** Schematic overview of experimental procedure: ReNcells were transduced with lentivirus encoding shcontrol (shCO) or human shTAZ and after 5 days of lentiviral transduction plated under differentiation conditions during 30 days. **(B)**

Representative immunofluorescence confocal images of neuronal markers DCX and MAP2 with TAZ. **(C)** Representative images of TUBB3 immunofluorescence staining. **(D)** Representative image of TAU immunofluorescence staining. Nuclei are counterstained with DAPI. **(E)** Quantification positive DCX cells of cultures described in B. **(F)** Quantification positive MAP2 cells of cultures described in B. **(G)** TUBB3-positive cells quantification of cultures described in C. **(H)** TAU-positive cells quantification from the cultures described in D. **(I)** Neurite length measurements based on MAP2 staining. **(J)** Axonal length measurements of TAU-positive cells. Data are mean ± S.D. (n ≥ 10). Statistical analysis was performed with the Student's t-test. *$p \leqslant 0.05$; **$p \leqslant 0.01$, ***$p \leqslant 0.005$.

**Figure 4. TAZ impairment of neuronal differentiation is partially TEAD-dependent. (A)** Schematic overview of experimental design: ReNcells were transduced with empty vector (CT) or retroviral vector for overexpression of TAZ-WT and TAZ mutants $TAZ^{S51A}$, $TAZ^{4SA}$ and $TAZ^{4SA+S51A}$ and, after 5 days of retroviral transduction, plated under differentiation conditions during 30 days. **(C)** Immunostaining of neuronal markers DCX, MAP2 and TAU. **(D, E, F)** Quantification of DCX+ **(D),** MAP2+ **(E)** and TAU+ **(F)** ReNcells transduced with CT, TAZ-WT, TAZS51A, TAZ4SA and TAZ4SA+S51A after 30 days of differentiation. **(G)** Measurement of dendrite length based on MAP2 staining **(H)** Measurement of axonal length based on TAU staining. Data are mean ± SEM (n ≥ 10). Statistical analysis was performed with the Student's t-test. *p ⩽ 0.05; **p ⩽ 0.01, ***p ⩽ 0.001 vs. CT. #p ⩽ 0.05; ##p ⩽ 0.01, ###p ⩽ 0.001 comparing TAZS51A vs. TAZ-WT. $p ⩽ 0.05; $$p ⩽ 0.01, $$$p ⩽ 0.001 comparing TAZ4SA+S51A vs. TAZ4SA.

**Figure 5. TAZ as a transcriptional repressor of SOX2 and bHLH factors. (A)** Representative immunoblot analysis of TAZ, CTGF, SOX2, NEUROD1 and GAPDH as a loading control in shCO and shTAZ cells after 5 days of lentiviral transduction. **(B)** mRNA levels of *WWTR1* and its targets *CTGF* and *CYR61*. **(C)** mRNA levels of *SOX2, ASCL1, NEUROG2* and *NEUROD1*. **(D)** Representative immunoblots of TAZ, CTGF, SOX2, NEUROD1 and GAPDH as a loading control in ReNcells CT, TAZ-WT, $TAZ^{S51A}$, $TAZ^{4SA}$ and $TAZ^{4SA+S51A}$ after 5 days of retroviral transduction. **(E)** Densitometric quantification of SOX2 protein levels in (A) relative to GAPDH. **(F)** Densitometric quantification of NEUROD1 protein levels in (A) relative to GAPDH. Data are mean ± SEM (n = 4). **(G)** mRNA levels of TAZ targets *CTGF* and *CYR61*. **(H)** mRNA levels of *SOX2, ASCL1, NEUROG2* and *NEUROD1* after 5 days of retroviral transduction. mRNA levels were determined by qRT-PCR and normalized by the geometric mean of *ACTB, GAPDH* and *TBP* levels. Data are presented as mean ± S.D. (n = 4). Statistical analysis was performed using Student's *t*-test. *$p \leqslant 0.05$; **$p \leqslant 0.01$, ***$p \leqslant 0.001$ *vs.* control conditions. $^{\#}p \leqslant 0.05$; $^{\#\#}p \leqslant 0.01$, $^{\#\#\#}p \leqslant 0.001$ comparing $TAZ^{S51A}$ *vs.* TAZ-WT. $^{\$}p \leqslant 0.05$; $^{\$\$}p \leqslant 0.01$, $^{\$\$\$}p \leqslant 0.001$ comparing $TAZ^{4SA+S51A}$ *vs.* $TAZ^{4SA}$.

**Figure 6. TAZ recognizes specific regions in SOX2 and bHLH factors and repress their transcription. (A)** Representative scheme of experimental procedure: ReNcells were transduced with retroviral vector control (CT) or $TAZ^{4SA}$ and grown for 5 days in proliferative conditions and 4 days in differentiation conditions. **(B)** Representative immunoblot analysis of TAZ, CTGF, SOX2, NEUROD1 carrying GAPDH and Lamin B as a loading controls in ReNcells CT or expressing $TAZ^{4SA}$. **(C)** mRNA levels of TAZ targets *CTGF* and *CYR61*. **(D)** mRNA levels of *SOX2, ASCL1, NEUROG2* and *NEUROD1*. For C and D, mRNA levels were determined by qRT-PCR and normalized by the geometric mean of *ACTB, GAPDH* and *TBP* levels. Data are mean ± S.D. (n = 4). Statistical analysis was performed using Student's *t*-test. ***p ⩽ 0.001 vs. CT. **(E)** ChIP analysis of putative TIRs described in Figure S5 using the anti-TAZ antibody vs. a control IgG in ReNcells CT or overexpressing TAZ4SA and normalized relative CT. **(F)** ChIP analysis of putative TIRs described in Figure S5 using the anti-RNA Pol II antibody vs. a control IgG in ReNcells CT or expressing TAZ4SA and normalized relative to CT cells. **(G)** ChIP analysis of putative TIRs described in Figure S5 using the anti-AcH3 antibody vs. a control IgG in ReNcells CT or expressing TAZ4SA and normalized relative to CT. Regions of CTGF and CYR61 were analyzed as positive controls, and a region of CTGF (CTGF 3´UTR) that does not contain TIR was used as negative control**.**

**Supplementary Figure 1. Specificity of TAZ antibody. (A)** Representative confocal images of TAZ immunostaining in CT, TAZ-WT, $TAZ^{S51A}$, $TAZ^{4SA}$ and $TAZ^{4SA+S51A}$, after 5 days of retroviral transduction. **(B)** Representative confocal images of TAZ immunostaining in shCO and shTAZ ReNcells after 5 days of lentiviral transduction. **(C)** Representative immunoblot analysis of TAZ in ReNcells CT, TAZ-WT, $TAZ^{4SA}$ and $TAZ^{4SA+S51A}$, shCO and shTAZ after 5 days of viral transduction, showing a specific band around 50 kDa. **(D)** Quantification of total Nestin, DCX or TAZ positive cells in the neurogenic niche of SVZ of newborn, 3-, 6- and 12-months old mice (n = 5). **(E)** Quantification of total Nestin, DCX or TAZ positive cells in the neurogenic niche of the SGZ of newborn, 3-, 6- and 12-months old mice (n = 5).

**Supplementary Figure 2. (A)** Representative immunoblot analysis of TAZ and GAPDH as a loading control in ReNcells shCO and shTAZ after 5 days of lentiviral transduction used for the differentiation assays in Figure 3. **(B)** Representative immunoblot analysis of TAZ and GAPDH as a loading control in ReNcells CT, TAZ-WT, $TAZ^{S51A}$, $TAZ^{4SA}$ and $TAZ^{4SA+S51A}$ after 5 days of retroviral transduction used in the differentiation assays in Figure 4.

**Supplementary Figure 3. Gradually genetic upregulation of TAZ directly decreases SOX2 and bHLH factors levels. (A)** Representative immunoblot of TAZ, CTGF, SOX2, NEUROD1 and GAPDH as a loading control in ReNcells transduced with $TAZ^{4SA}$-expressing retrovirus after 1, 2 and 5 days post infection. **(B)** mRNA levels of *WWTR1* and its targets *CTGF* and *CYR61*. **(C)** mRNA levels of *SOX2,*

*ASCL1*, *NEUROG2* and *NEUROD1*. **(D)** Representative immunoblot analysis of TAZ, CTGF, SOX2, NEUROD1 and GAPDH as a loading ReNcells CT, TAZ-WT and $TAZ^{4SA}$ at 0, 2 and 4 days of differentiation. **(E)** mRNA levels of *CTGF* and *CYR61*. **(F)** mRNA levels of *SOX2*, *ASCL1*, *NEUROG2* and *NEUROD1*. mRNA levels were determined by qRT-PCR and normalized by the geometric mean of *ACTB*, *GAPDH* and *TBP* levels. Data represent mean ± S.D. ($n \geq 4$). Statistical analysis was performed using Student's *t*-test. ***$p \leqslant 0.001$ vs. CT.

**Supplementary Figure 4. TEADs transcripts expression in ReNcells. (A)** mRNA levels of the different TEADs (1-4) transcripts in ReNcells were determined by qRT-PCR and normalized by *TEAD1*. Data represent mean ± S.D. ($n \geq 8$). **(B)** TEAD2 motif from JASPAR database indicating its binding profile. **(C)** Position specific scoring matrix (PSSM) for TEAD2 PSSM is derived from the frequency matrix available in JASPAR database. **(D)** mRNA levels of *TEAD1*, *TEAD2*, *TEAD3* and *TEAD4*. **(E)** mRNA levels of *CTGF* and *CYR61*. **(F)** mRNA levels of *SOX2*, *ASCL1*, *NEUROG2* and *NEUROD1*. mRNA levels were determined by qRT-PCR and normalized by the geometric mean of *ACTB*, *GAPDH* and *TBP* levels. Data represent mean ± S.D. ($n \geq 4$). Statistical analysis was performed using Student's t-test. ***$p \leqslant 0.001$ vs. shCO.

**Supplementary Figure 5. Schemes of the genes encoding *SOX2* and bHLH factors *ASCL1*, *NEUROG2* and *NEUROD1*. (A)** *SOX2*, **(B)** *ASCL1*, **(C)** *NEUROG2*, and **(D)** *NEUROD1* genes from the ENCODE for the human genome. Putative TAZ interacting regions (TIR) in the genes were identified taking as reference the regions localized in DNAse-sensitive and H3K27Ac-rich regions, i.e. most likely regulatory promoter regions. Regions sensitive to DNase are represented as dark boxes. RNA Pol II enrichment regions determined by ChIP-seq for RNA polymerase II (Pol II) in CD4 cells (Barski et al. 2007) are indicated in blue.

**Figure 1**

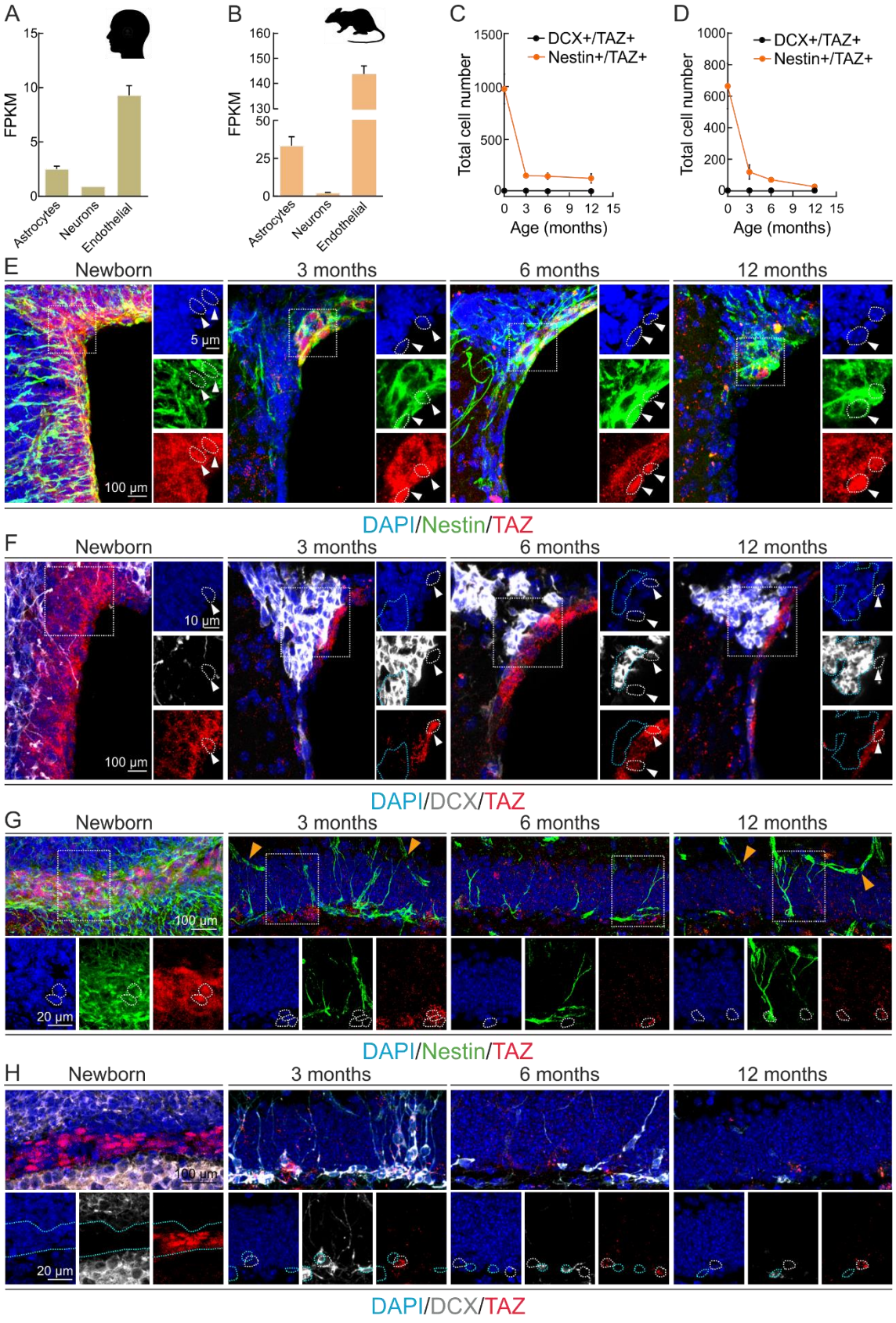
A
FPKM
Astrocytes
Neurons
Endothelial
B
FPKM
Astrocytes
Neurons
Endothelial
C
DCX+/TAZ+
Nestin+/TAZ+
Total cell number
Age (months)
D
DCX+/TAZ+
Nestin+/TAZ+
Total cell number
Age (months)
E
Newborn
3 months
6 months
12 months
5 µm
100 µm
DAPI/Nestin/TAZ
F
Newborn
3 months
6 months
12 months
10 µm
100 µm
DAPI/DCX/TAZ
G
Newborn
3 months
6 months
12 months
100 µm
20 µm
DAPI/Nestin/TAZ
H
Newborn
3 months
6 months
12 months
100 µm
20 µm
DAPI/DCX/TAZ

**Figure 2.**

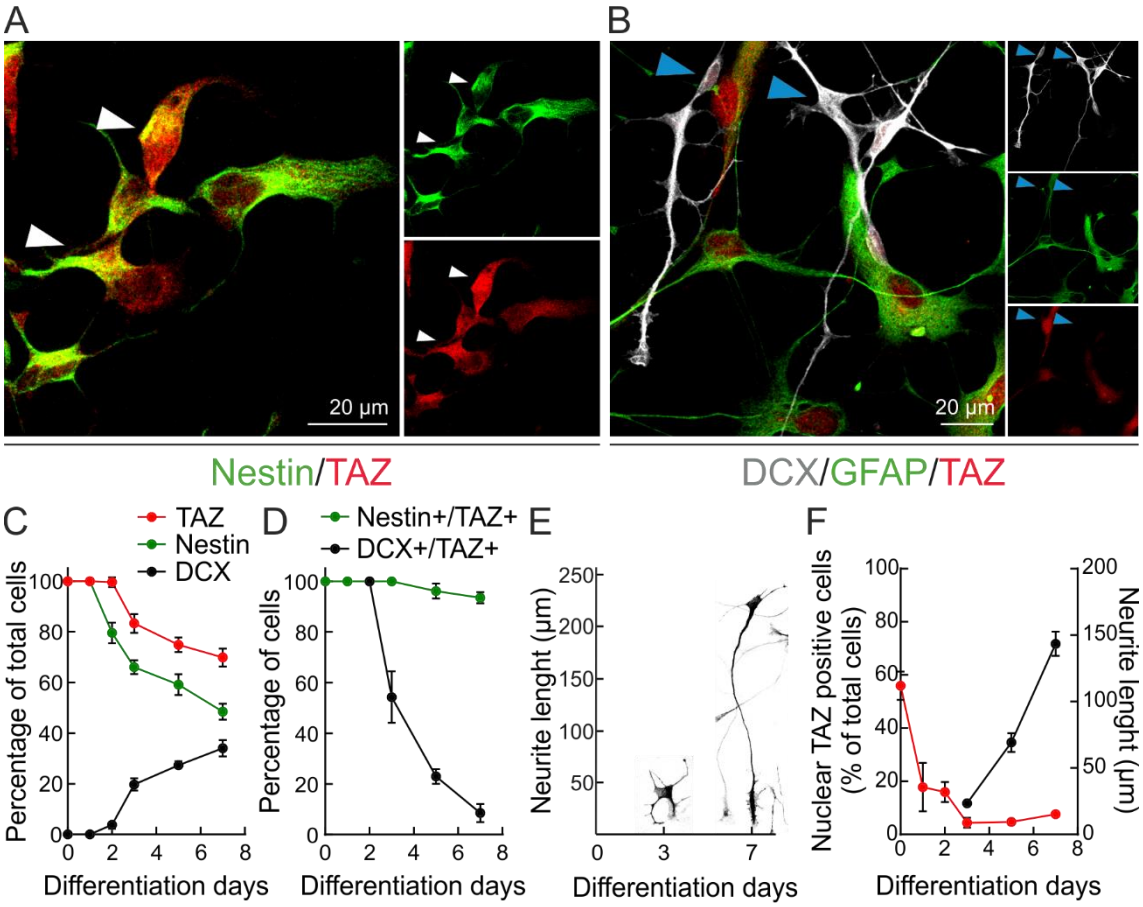
A
B
20 µm
20 µm
Nestin/TAZ
DCX/GFAP/TAZ
C
TAZ
Nestin
DCX
Percentage of total cells
Differentiation days
D
Nestin+/TAZ+
DCX+/TAZ+
Percentage of cells
Differentiation days
E
Neurite lenght (µm)
Differentiation days
F
Nuclear TAZ positive cells (% of total cells)
Neurite lenght (µm)
Differentiation days

**Figure 3.**

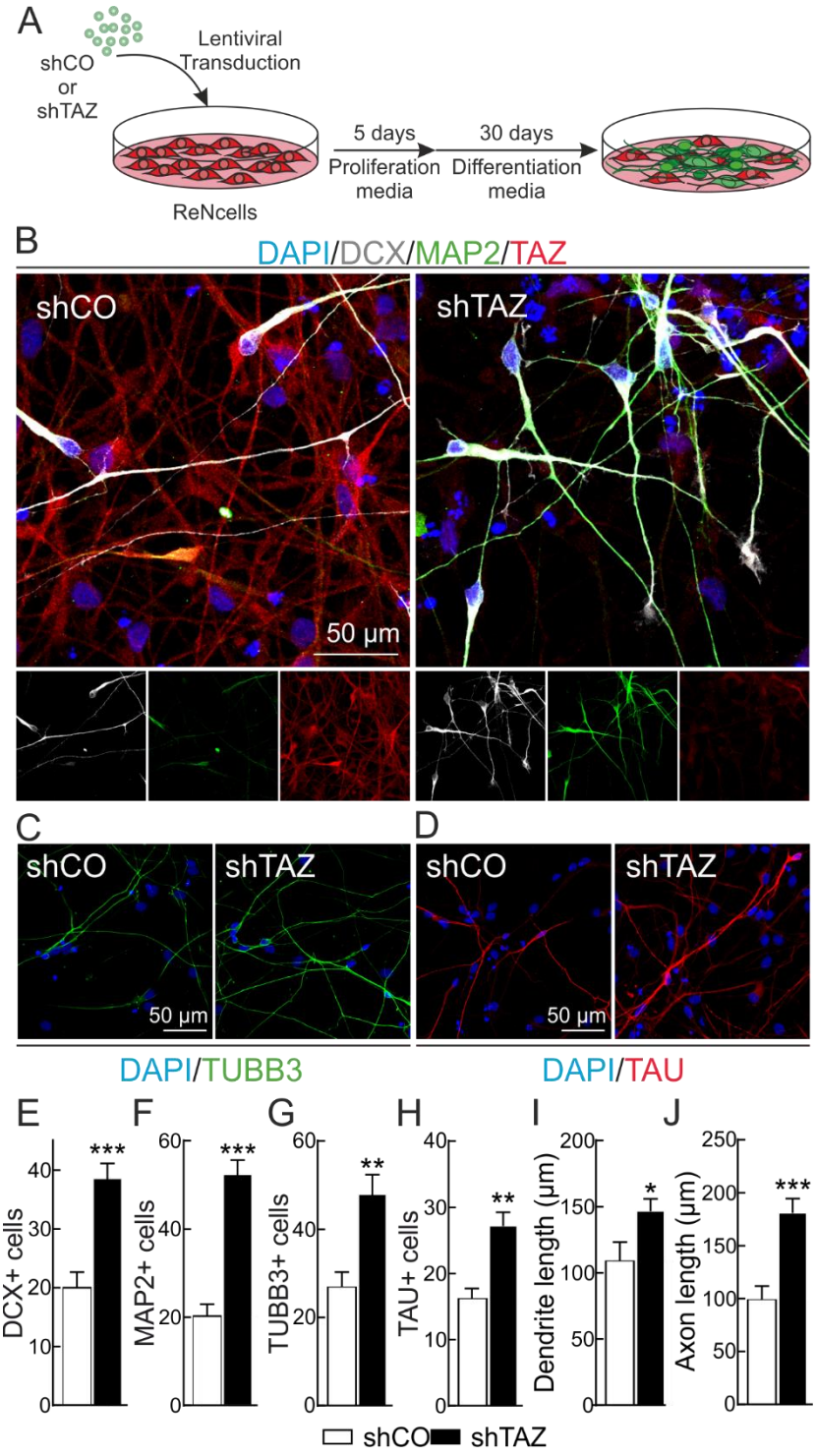
A
shCO
or
shTAZ
Lentiviral
Transduction
ReNcells
5 days
Proliferation
media
30 days
Differentiation
media
B
DAPI/DCX/MAP2/TAZ
shCO
shTAZ
50 µm
C
shCO
shTAZ
50 µm
D
shCO
shTAZ
50 µm
DAPI/TUBB3
DAPI/TAU
E
F
G
H
I
J
DCX+ cells
MAP2+ cells
TUBB3+ cells
TAU+ cells
Dendrite length (µm)
Axon length (µm)
shCO
shTAZ

**Figure 4.**

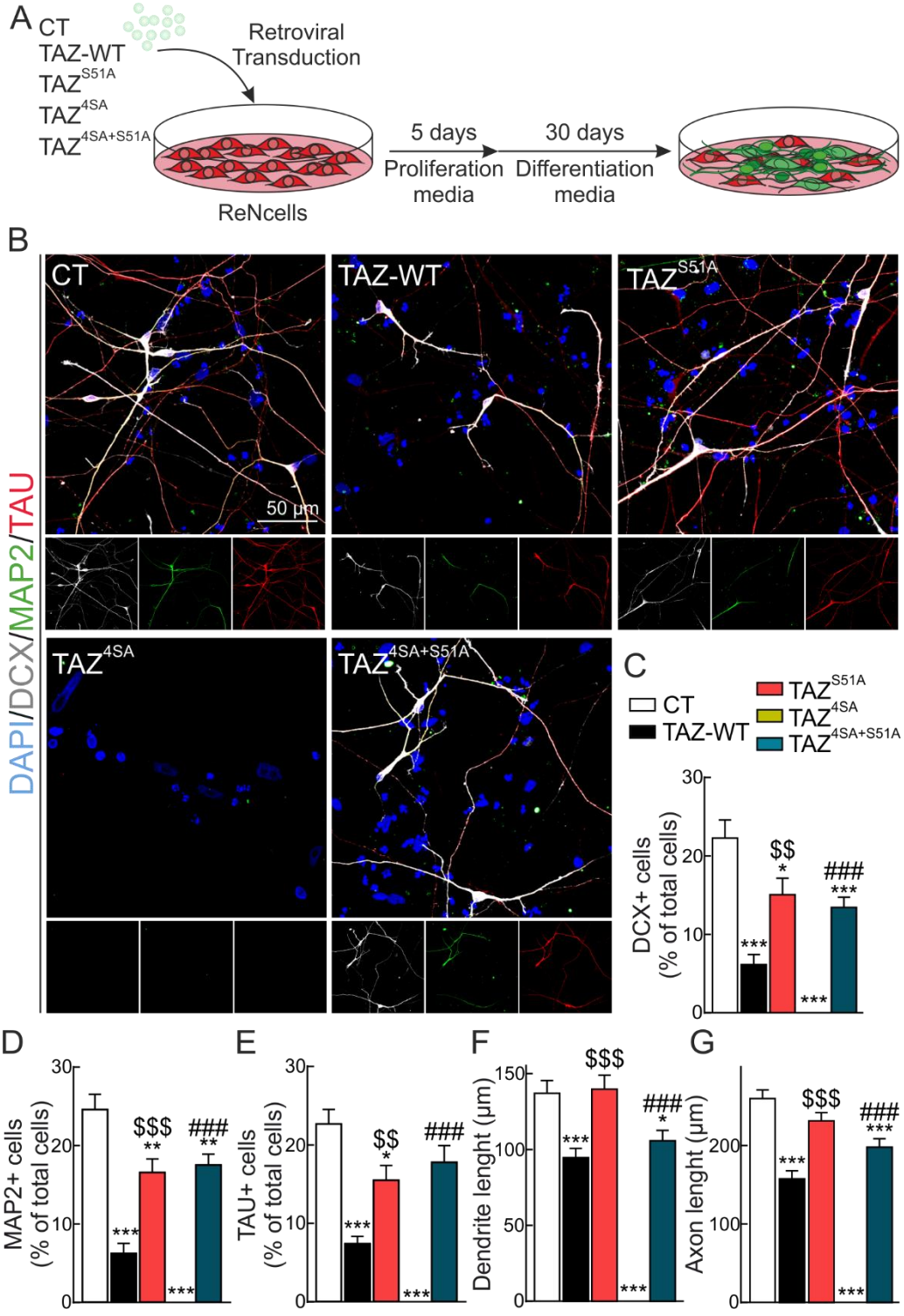
A
CT
TAZ-WT
TAZ S51A
TAZ 4SA
TAZ 4SA+S51A
Retroviral Transduction
ReNcells
5 days
Proliferation media
30 days
Differentiation media
B
CT
TAZ-WT
TAZ S51A
TAZ 4SA
TAZ 4SA+S51A
50 µm
DAPI/DCX/MAP2/TAU
C
CT
TAZ-WT
TAZ S51A
TAZ 4SA
TAZ 4SA+S51A
DCX+ cells (% of total cells)
D
MAP2+ cells (% of total cells)
E
TAU+ cells (% of total cells)
F
Dendrite lenght (µm)
G
Axon lenght (µm)

**Figure 5.**

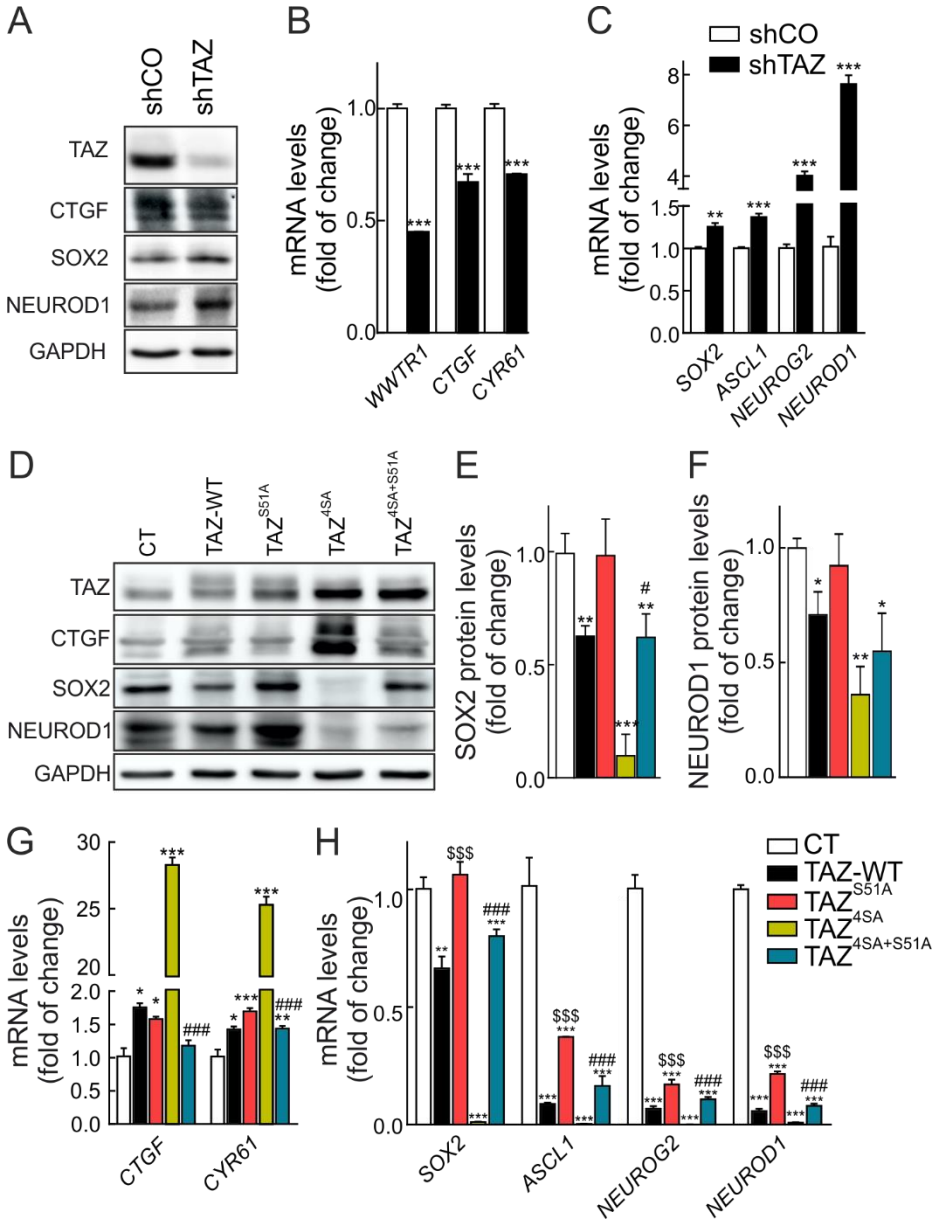
A
shCO
shTAZ
TAZ
CTGF
SOX2
NEUROD1
GAPDH
B
mRNA levels (fold of change)
WWTR1
CTGF
CYR61
C
shCO
shTAZ
mRNA levels (fold of change)
SOX2
ASCL1
NEUROG2
NEUROD1
D
CT
TAZ-WT
TAZ^S51A
TAZ^4SA
TAZ^4SA+S51A
TAZ
CTGF
SOX2
NEUROD1
GAPDH
E
SOX2 protein levels (fold of change)
F
NEUROD1 protein levels (fold of change)
G
mRNA levels (fold of change)
CTGF
CYR61
H
mRNA levels (fold of change)
SOX2
ASCL1
NEUROG2
NEUROD1
CT
TAZ-WT
TAZ^S51A
TAZ^4SA
TAZ^4SA+S51A

**Figure 6.**

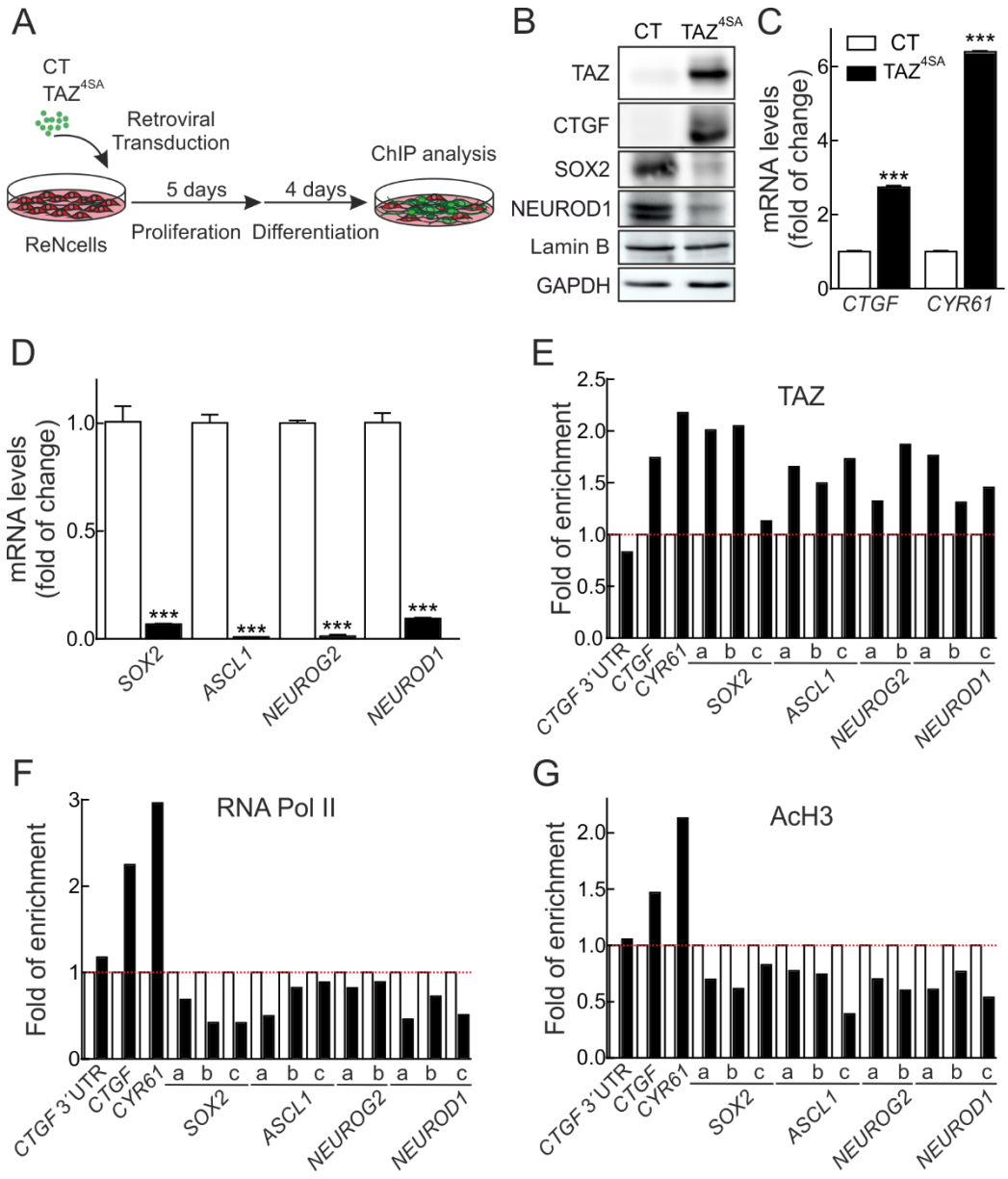
A
CT
TAZ4SA
Retroviral
Transduction
ReNcells
5 days
Proliferation
4 days
Differentiation
ChIP analysis
B
CT
TAZ4SA
TAZ
CTGF
SOX2
NEUROD1
Lamin B
GAPDH
C
CT
TAZ4SA
mRNA levels
(fold of change)
CTGF
CYR61
D
mRNA levels
(fold of change)
SOX2
ASCL1
NEUROG2
NEUROD1
E
TAZ
Fold of enrichment
CTGF 3'UTR
CTGF
CYR61
SOX2
ASCL1
NEUROG2
NEUROD1
F
RNA Pol II
Fold of enrichment
G
AcH3
Fold of enrichment

**Figure S1.**

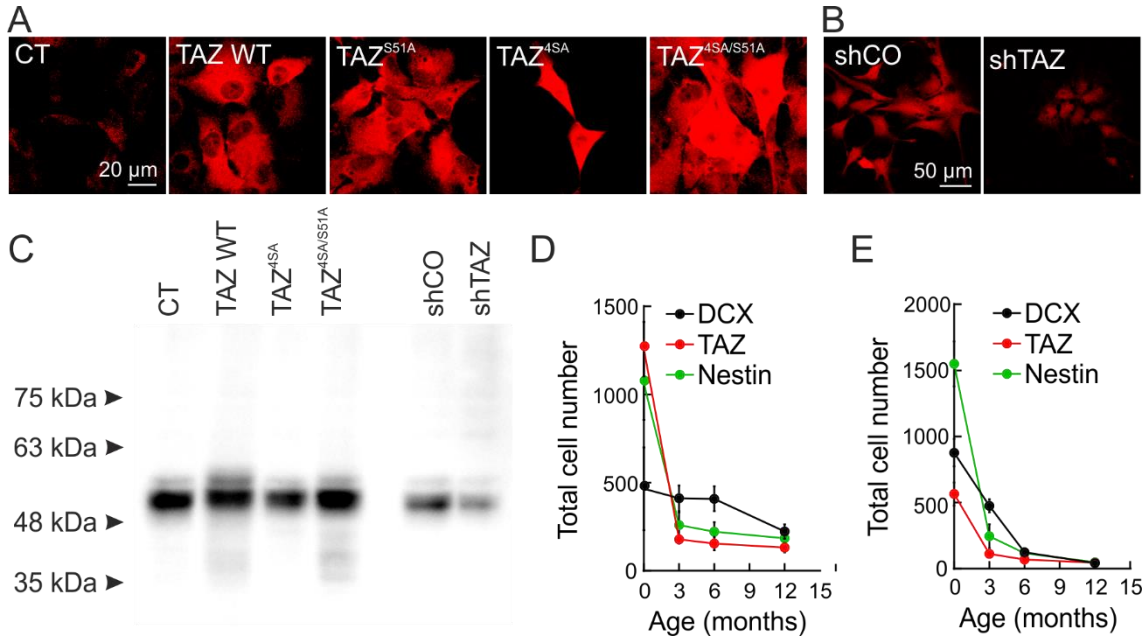


**Figure S2.**

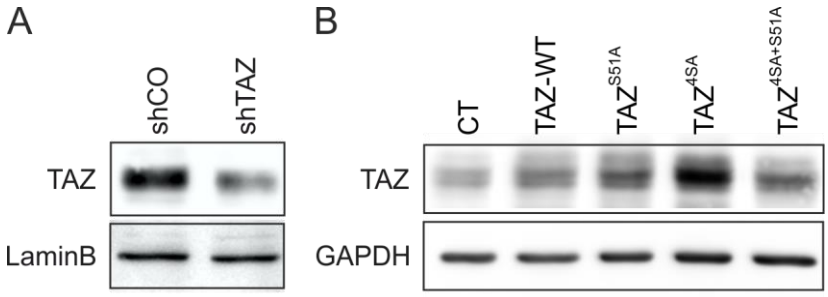

**Figure S3.**

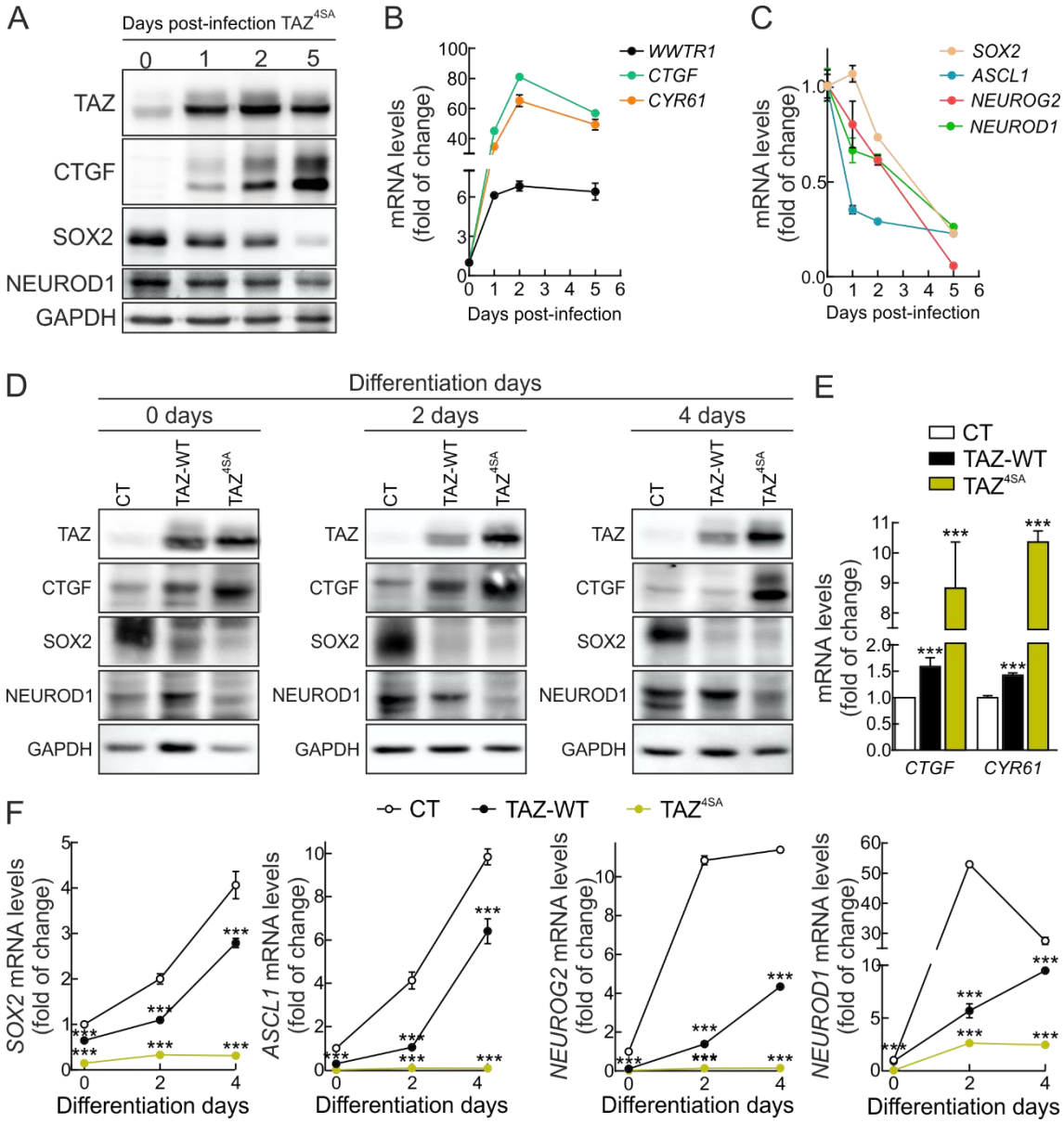
A
Days post-infection TAZ4SA
0 1 2 5
TAZ
CTGF
SOX2
NEUROD1
GAPDH
B
mRNA levels (fold of change)
WWTR1
CTGF
CYR61
Days post-infection
C
mRNA levels (fold of change)
SOX2
ASCL1
NEUROG2
NEUROD1
Days post-infection
D
Differentiation days
0 days
2 days
4 days
CT
TAZ-WT
TAZ4SA
TAZ
CTGF
SOX2
NEUROD1
GAPDH
E
CT
TAZ-WT
TAZ4SA
mRNA levels (fold of change)
CTGF
CYR61
F
CT
TAZ-WT
TAZ4SA
SOX2 mRNA levels (fold of change)
ASCL1 mRNA levels (fold of change)
NEUROG2 mRNA levels (fold of change)
NEUROD1 mRNA levels (fold of change)
Differentiation days

**Figure S4.**

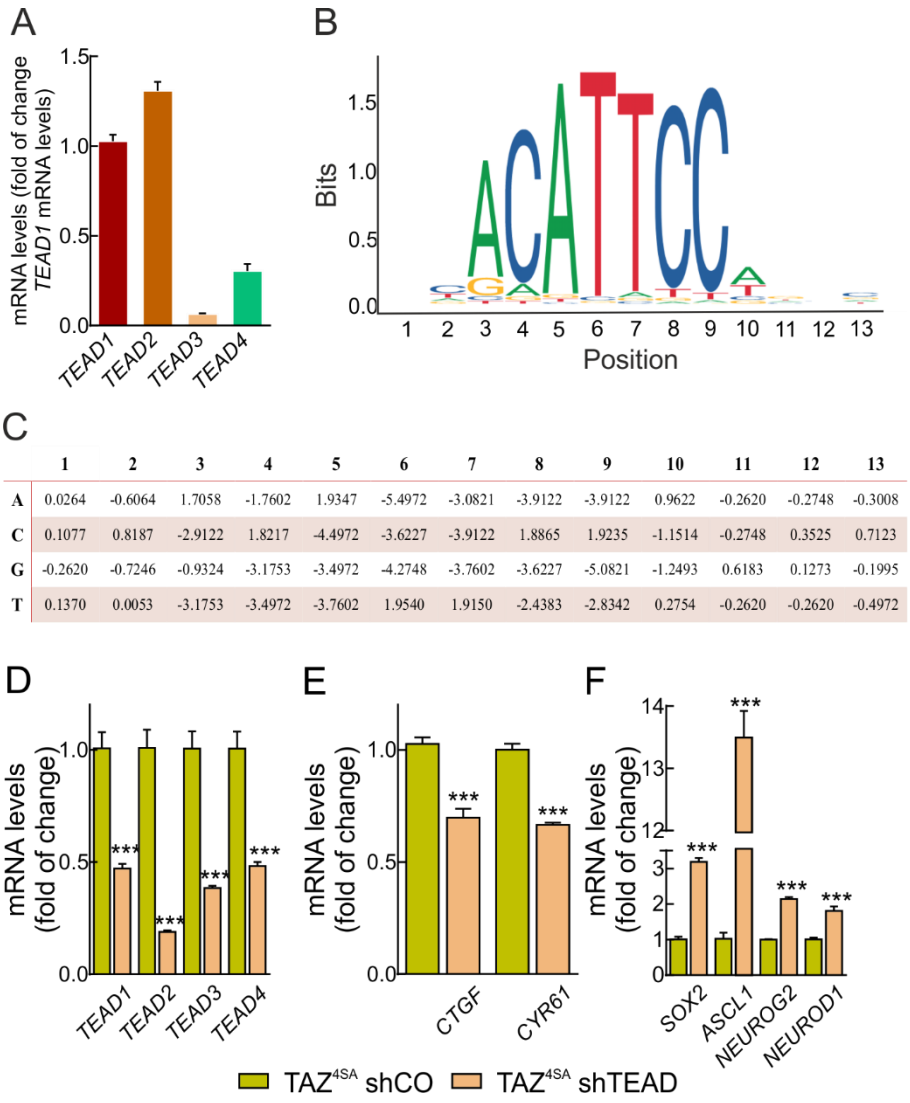


C

| | 1 | 2 | 3 | 4 | 5 | 6 | 7 | 8 | 9 | 10 | 11 | 12 | 13 |
|---|---|---|---|---|---|---|---|---|---|---|---|---|---|
| A | 0.0264 | -0.6064 | 1.7058 | -1.7602 | 1.9347 | -5.4972 | -3.0821 | -3.9122 | -3.9122 | 0.9622 | -0.2620 | -0.2748 | -0.3008 |
| C | 0.1077 | 0.8187 | -2.9122 | 1.8217 | -4.4972 | -3.6227 | -3.9122 | 1.8865 | 1.9235 | -1.1514 | -0.2748 | 0.3525 | 0.7123 |
| G | -0.2620 | -0.7246 | -0.9324 | -3.1753 | -3.4972 | -4.2748 | -3.7602 | -3.6227 | -5.0821 | -1.2493 | 0.6183 | 0.1273 | -0.1995 |
| T | 0.1370 | 0.0053 | -3.1753 | -3.4972 | -3.7602 | 1.9540 | 1.9150 | -2.4383 | -2.8342 | 0.2754 | -0.2620 | -0.2620 | -0.4972 |

**Figure S5.**

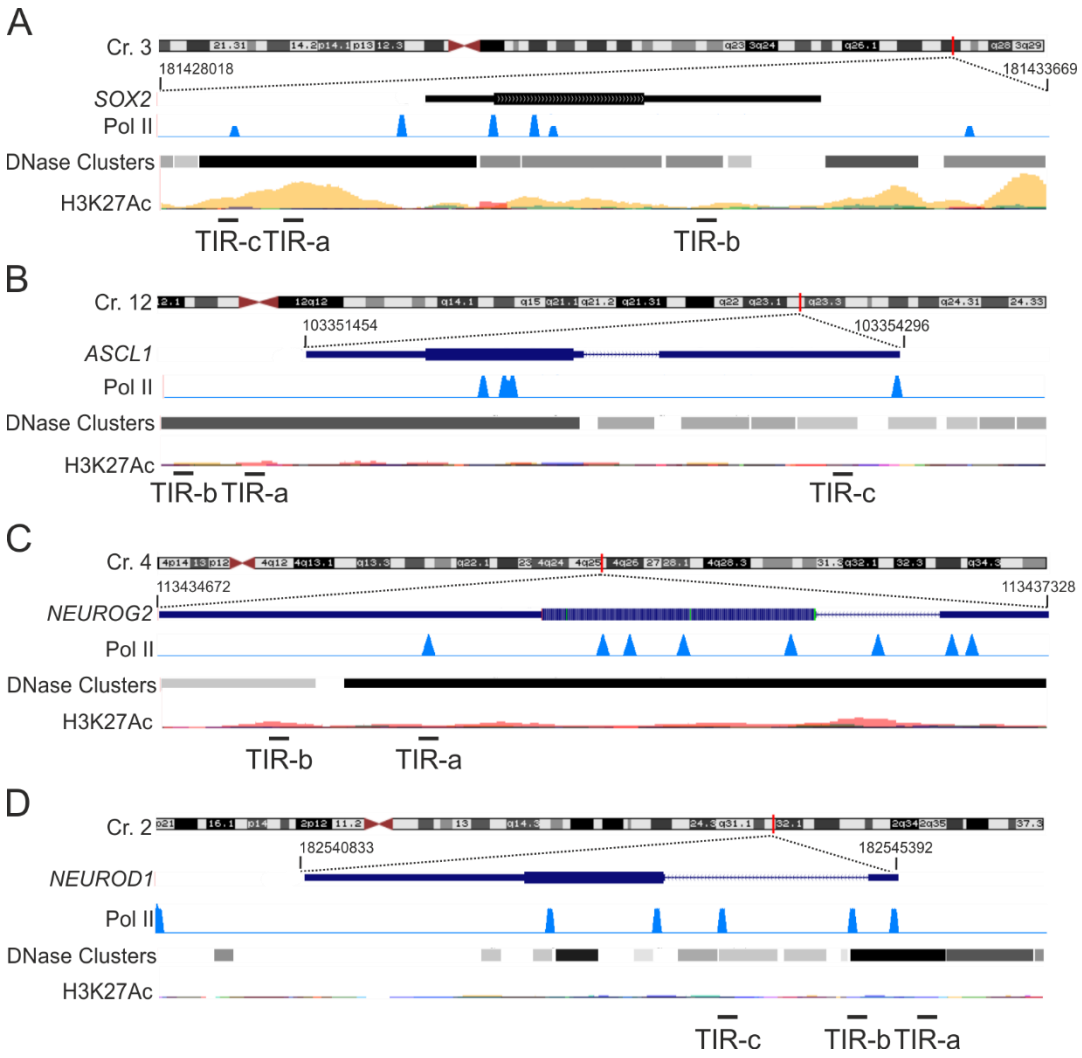
A
Cr. 3
181428018
181433669
SOX2
Pol II
DNase Clusters
H3K27Ac
TIR-c
TIR-a
TIR-b
B
Cr. 12
103351454
103354296
ASCL1
Pol II
DNase Clusters
H3K27Ac
TIR-b
TIR-a
TIR-c
C
Cr. 4
113434672
113437328
NEUROG2
Pol II
DNase Clusters
H3K27Ac
TIR-b
TIR-a
D
Cr. 2
182540833
182545392
NEUROD1
Pol II
DNase Clusters
H3K27Ac
TIR-c
TIR-b
TIR-a

## SUPPLEMENTAL MATERIAL

**Supplemental Table S1.** Putative TEAD1 binding sequences in the promoter regions of SRY-box 2 (SOX2) and bHLH factors genes with a relative score higher than 80%. The table also shows the max score and the localization in the human genome.

| GENE (HUMAN) | LOCALIZATION IN THE HUMAN GENOME | MAX SCORE | RELATIVE SCORE (%) | TEAD1 PUTATIVE BINDING SEQUENCE |
|---|---|---|---|---|
| *CTGF* | chr6:132269288-132269276 | 13.77 | 82.8 | AACATTTCTGAG |
| | chr6:132269659-132269671 | 15.62 | 85.8 | TACATTCTACCT |
| | chr6:132270157-132270169 | 13.62 | 82.5 | TACATTCTGGTG |
| | chr6:132270884-132270872 | 12.97 | 81.5 | GACATTCCAAGA |
| | chr6:132270949-132270961 | 13.1 | 81.7 | CTCATTCCAGCA |
| | chr6:132272609-132272621 | 17.78 | 89.3 | CGCATTCCTCCC |
| *CYR61* | chr1:86046332-86046344 | 16.14 | 86.6 | AGCATTCCTGAG |
| | chr1:86047219-86047207 | 16.2 | 86.7 | TGCATTCCAGCC |
| | chr1:86047721-86047733 | 18.56 | 90.5 | TGCATTCCTCTG |
| | chr1:86048360-86048348 | 14.99 | 84.8 | CACATCCCACCC |
| *SOX2* | chr3:181431413-181431401 | 13.88 | 83 | TCCATTCCCCCG (b) |
| | chr3:181428382-181428394 | 13.77 | 82.8 | AAGATTCCTGAG (c) |
| *ASCL1* | chr12:103349554-103349542 | 13.99 | 83.1 | CACATCCCTGAC (b) |
| *NEUROG2* | chr4:113435415-113435427 | 14.3 | 83.6 | TGCATTCCCCCT (a) |
| *NEUROD1* | chr2:182543940-182543952 | 15.41 | 85.4 | TACATTTCAGCG (c) |
| | chr2:182544023-182544035 | 15.78 | 86 | CACATTCTACTT (c) |

**Supplemental Table S2.** Putative TEAD2 binding sequences in the promoter regions of SRY-box 2 (SOX2) and bHLH factors genes with a relative score higher than 85%. The table also shows the max score and the localization in the human genome.

| GENE (HUMAN) | LOCALIZATION IN THE HUMAN GENOME | MAX SCORE | RELATIVE SCORE (%) | TEAD2 PUTATIVE BINDING SEQUENCE |
|---|---|---|---|---|
| *CTGF* | chr6:132269289-132269276 | 8.66 | 91.1 | AAACATTTCTGAG |
| | chr6:132269658-132269671 | 9.07 | 91.5 | TTACATTCTACCT |
| | chr6:132270885-132270872 | 12.97 | 95.5 | AGACATTCCAAGA |
| | chr6:132270948-132270961 | 10.85 | 93.3 | TCTCATTCCAGCA |
| | chr6:132272599-132272612 | 12.99 | 95.6 | GGACATTCCTCGC |
| *CYR61* | chr1:86046331-86046344 | 10.42 | 92.9 | CAGCATTCCTGAG |
| | chr1:86047220-86047207 | 13.29 | 95.9 | TTGCATTCCAGCC |
| | chr1:86047720-86047733 | 10.16 | 92.6 | CTGCATTCCTCTG |
| | chr1:86048153-86048140 | 10.58 | 93.1 | ATACATTTCTGGC |
| | chr1:86048573-86048560 | 8.39 | 90.8 | TCACAGTCCTGGT |
| | chr1:86049144-86049157 | 11.28 | 93.8 | GGGCATTCCATCC |
| *SOX2* | chr3:181431414-181431401 | 6.99 | 89.3 | GTCCATTCCCCCG (b) |
| | chr3:181428381-181428394 | 8.06 | 90.5 | CAAGATTCCTGAG (c) |
| | chr3:181428844-181428831 | 8.49 | 90.9 | CCCCATTCCCATC (a) |
| *ASCL1* | chr12:103349820-103349833 | 9.6 | 92 | CCACATACCAAGA (a) |
| | chr12:103349555-103349542 | 9.57 | 92 | CCACATCCCTGAC (b) |
| | chr12:103354060-103354047 | 7.77 | 90.1 | CAACATTTCTATA (c) |
| *NEUROG2* | chr4:113435031-113435044 | 5.56 | 87.9 | TTGCATTCAATCA (b) |
| | chr4:113438807-113438794 | 7.65 | 90 | TAACACTCCAACT |
| | chr4:113435345-113435358 | 9.31 | 91.8 | ATACATTTCTTTC (a) |
| *NEUROD1* | chr2:182543939-182543952 | 10.29 | 92.8 | GTACATTTCAGCG (c) |
| | chr2:182544022-182544035 | 9.16 | 91.6 | ACACATTCTACTT (c) |
| | chr2:182544640-182544653 | 8.01 | 90.4 | CCACTTTCCCCCC (b) |
| | chr2:182545564-182545577 | 9.07 | 91.5 | CTCCATTCCGGCC (a) |

**Supplemental Table S3.** Putative TEAD3 binding sequences in the promoter regions of SRY-box 2 (SOX2) and bHLH factors genes with a relative score higher than 90%. The table also shows the max score and the localization in the human genome.

| GENE (HUMAN) | LOCALIZATION IN THE HUMAN GENOME | MAX SCORE | RELATIVE SCORE (%) | TEAD3 PUTATIVE BINDING SEQUENCE |
|---|---|---|---|---|
| ***CTGF*** | chr6:132270622-132270614 | 10.89 | 97.2 | ACATACCG |
| | chr6:132269884-132269892 | 6.86 | 95.2 | GGATTCCG |
| | chr6:132270883-132270875 | 14.08 | 98.7 | ACATTCCA |
| | chr6:132270950-132270958 | 10.59 | 97 | TCATTCCA |
| | chr6:132271352-132271344 | 8.64 | 96.1 | AAATACCT |
| | chr6:132272601-132272609 | 13.43 | 98.4 | ACATTCCT |
| ***CYR61*** | chr1:86046333-86046341 | 12.94 | 98.2 | GCATTCCT |
| | chr1:86047218-86047210 | 13.59 | 98.5 | GCATTCCA |
| | chr1:86047722-86047730 | 12.94 | 98.2 | GCATTCCT |
| | chr1:86048065-86048057 | 10.4 | 96.9 | GCATACCG |
| | chr1:86048501-86048509 | 7.98 | 95.7 | AAATACCG |
| | chr1:86049146-86049154 | 13.59 | 98.5 | GCATTCCA |
| | chr1:86048877-86048869 | 8.64 | 96.1 | AAATACCT |
| ***SOX2*** | chr3:181430473-181430481 | 7.98 | 95.7 | AAATACCG |
| | chr3:181431412-181431404 | 2.17 | 92.9 | CCATTCCC (b) |
| | chr3:181430283-181430291 | 5.92 | 94.7 | GAATGCCT |
| | chr3:181428383-181428391 | 8.01 | 95.8 | AGATTCCT (c) |
| | chr3:181428711-181428703 | 4.13 | 93.8 | GCATCCCA |
| ***ASCL1*** | chr12:103349822-103349830 | 12.2 | 97.8 | ACATACCA (a) |
| | chr12:103350367-103350359 | 7.52 | 95.5 | GGATTCCT |
| ***NEUROG2*** | chr4:113434627-113434619 | 4.54 | 94.1 | AGATGCCA |
| | chr4:113439907-113439899 | 8.17 | 95.8 | GGATTCCA |
| | chr4:113435416-113435424 | 9.23 | 96.4 | GCATTCCC (a) |
| ***NEUROD1*** | chr2:182542983-182542975 | 5.6 | 94.6 | ACATGCCC |
| | chr2:182543732-182543740 | 5.92 | 94.7 | GAATGCCT |
| | chr2:182544713-182544705 | 5.64 | 94.6 | GGATACCT (b) |
| | chr2:182545492-182545484 | 8.16 | 95.8 | GCATGCCG (a) |
| | chr2:182545234-182545242 | 10.04 | 96.8 | GAATTCCT |

**Supplemental Table S4.** Putative TEAD4 binding sequences in the promoter regions of SRY-box 2 (SOX2) and bHLH factors genes with a relative score higher than 90%. The table also shows the max score and the localization in the human genome.

| GENE (HUMAN) | LOCALIZATION IN THE HUMAN GENOME | MAX SCORE | RELATIVE SCORE (%) | TEAD4 PUTATIVE BINDING SEQUENCE |
|---|---|---|---|---|
| ***CTGF*** | chr6:132269659-132269669 | 12.98 | 94.9 | TACATTCTAC |
| | chr6:132270202-132270212 | 12.64 | 94.6 | AACATTCTTC |
| | chr6:132270884-132270874 | 14.12 | 96 | GACATTCCAA |
| | chr6:132272600-132272610 | 14.13 | 96.1 | GACATTCCTC |
| | chr6:132272772-132272762 | 11.87 | 93.8 | AAAATTCTAT |
| ***CYR61*** | chr1:86046332-86046342 | 12.82 | 94.8 | AGCATTCCTG |
| | chr1:86047293-86047303 | 9.02 | 91 | AAAATACTAG |
| | chr1:86047219-86047209 | 13.16 | 95.1 | TGCATTCCAG |
| | chr1:86048500-86048510 | 9.18 | 91.1 | GAAATACCGG |
| | chr1:86049145-86049155 | 13.77 | 95.7 | GGCATTCCAT |
| | chr1:86048878-86048868 | 10.75 | 92.7 | GAAATACCTT |
| ***SOX2*** | chr3:181430472-181430482 | 9.18 | 91.1 | TAAATACCGG |
| | chr3:181431587-181431577 | 8.26 | 0.90.2 | TAAATACTGT |
| | chr3:181430289-181430279 | 8.44 | 90.4 | GGCATTCATG |
| | chr3:181428382-181428392 | 8.78 | 90.8 | AAGATTCCTG (c) |
| ***ASCL1*** | chr12:103349821-103349831 | 12.62 | 94.6 | CACATACCAA (a) |
| | chr12:103353739-103353729 | 12.28 | 94.2 | AGCATTCTAT |
| ***NEUROG2*** | chr4:113434601-113434591 | 11.38 | 93.3 | GAAATTCTTC |
| | chr4:113439588-113439578 | 11.24 | 93.2 | CAAATTCTGT |
| | chr4:113435415-113435425 | 10.91 | 92.9 | TGCATTCCCC (a) |
| ***NEUROD1*** | chr2:182543738-182543728 | 9.05 | 91 | GGCATTCATT |
| | chr2:182543940-182543950 | 8.8 | 90.8 | TACATTTCAG (c) |
| | chr2:182544023-182544033 | 13.72 | 95.6 | CACATTCTAC (c) |
| | chr2:182545233-182545243 | 12.84 | 94.8 | CGAATTCCTC |

**Supplemental Table S5.** Putative SMAD2/3/4 binding sequences in the promoter regions of SRY-box 2 (SOX2) and bHLH factors genes with a relative score higher than 90%. The table also shows the max score and the localization in the human genome.

| GENE (HUMAN) | LOCALIZATION IN THE HUMAN GENOME | MAX SCORE | RELATIVE SCORE (%) | SMAD2/3/4 PUTATIVE BINDING SEQUENCE |
|---|---|---|---|---|
| ***CTGF*** | chr6:132269508-132269521 | 8.17 | 92 | GAGGCTACCACAT |
| | chr6:132270238-132270225 | 8.2 | 92 | TAGTCTATCAACC |
| | chr6:132270384-132270397 | 13.87 | 95.8 | ATGTCTCTCACTC |
| | chr6:132270796-132270809 | 5.12 | 90 | TTGTCTGACTTCT |
| | chr6:132272476-132272489 | 13.97 | 95.9 | CTGGCTGTCTCCT |
| ***CYR61*** | chr1:86046219-86046206 | 14.07 | 96 | GTGTCTGTCTCCC |
| | chr1:86047067-86047080 | 8.74 | 92.4 | CTGCCTGCCACTG |
| | chr1:86048336-86048349 | 7.99 | 91.9 | TTGCCTGGCAGGT |
| | chr1:86049198-86049185 | 8.32 | 92.1 | CTGCCTCTCACA |
| ***SOX2*** | chr3:181431086-181431099 | 6.2 | 90.7 | CCCTCTCACACAT |
| | chr3:181429502-181429515 | 8.17 | 92 | GTGGCTGGCAGGC |
| | chr3:181428859-181428846 | 11.01 | 93.9 | CTGTCTGCCCCCA (a) |
| ***ASCL1*** | chr12:103351454-103351467 | 8.37 | 92.1 | CACTCTCTCACTT |
| | chr12:103350931-103350918 | 7.24 | 91.4 | TTCTCTCTCTCCT |
| ***NEUROG2*** | chr4:113435134-113435121 | 5.98 | 90.5 | CCATCTGTCTCTT |
| | chr4:113436841-113436828 | 10.56 | 93.6 | CTGACTGGCAGCA |
| | chr4:113437328-113437341 | 14.71 | 96.4 | GTGTCTGGCACAC |
| ***NEUROD1*** | chr2:182542551-182542564 | 7.44 | 91.5 | ATGACTCGCTCAT |
| | chr2:182542875-182542862 | 9.08 | 92.6 | ATGTCTTCCACGT |
| | chr2:182543475-182543488 | 10.29 | 93.4 | TTGTCTGCCTCGT |
| | chr2:182544227-182544240 | 7.28 | 91.4 | GGGTCTTCCACCC |
| | chr2:182544628-182544615 | 5.27 | 90.1 | GGGACTCACTCCT (b) |
| | chr2:182545412-182545425 | 6.01 | 90.6 | TCGTCTCCCGCCC |

**Supplemental Table S6.** Putative RUNX2 binding sequences in the promoter regions of SRY-box 2 (SOX2) and bHLH factors genes with a relative score higher than 90%. The table also shows the max score and the localization in the human genome.

| GENE (HUMAN) | LOCALIZATION IN THE HUMAN GENOME | MAX SCORE | RELATIVE SCORE (%) | RUNX2 PUTATIVE BINDING SEQUENCE |
|---|---|---|---|---|
| ***CTGF*** | chr6: 132269512-132269521 | 4.14 | 94.1 | CTACCACAT |
| | chr6: 132270934-132270925 | 6.64 | 95.6 | CAACCACCA |
| | chr6: 132271935-132271926 | 11.74 | 98.6 | CAACCGCAA |
| ***CYR61*** | chr1: 86046444-86046453 | 7.27 | 96 | AGACCGCGA |
| | chr1: 86047194-86047203 | 5.36 | 94.8 | CGACCACAC |
| | chr1: 86047279-86047270 | 12.26 | 99 | AAACCACAA |
| | chr1: 86048526-86048517 | 8.11 | 96.5 | GAACCGCAG |
| ***SOX2*** | chr3: 181430686-181430695 | 6.83 | 95.7 | TACCCGCAG |
| | chr3: 181430914-181430905 | 9.88 | 97.5 | TAACCACAG |
| | chr3: 181431302-181431311 | 9.71 | 97.4 | AAACCGCGA |
| | chr3: 181431473-181431464 | 0.08 | 91.6 | GTACCACTA |
| | chr3: 181430222-181430231 | 2.43 | 93.1 | CCACCGCGG |
| | chr3: 181430304-181430295 | 3.62 | 93.8 | GGACCACAC |
| | chr3: 181428582-181428591 | 6.87 | 95.7 | CCACCACAA |
| | chr3: 181429469-181429460 | 6.06 | 95.2 | ACACCACAC |
| ***ASCL1*** | chr12: 103349919-103349928 | 8.2 | 96.5 | TCACCACAA |
| | chr12:103350513-103350504 | 4.44 | 94.3 | CTACCGCCA |
| | chr12: 103353685-103353694 | 3.78 | 93.9 | AAACCCCAT |
| | chr12: 103353976-103353967 | 9.48 | 97.3 | AAACCACAT |
| ***NEUROG2*** | chr4: 113436266-113436257 | 10.77 | 98.1 | AAACCGCAT |
| | chr4: 113439955-113439964 | 6.08 | 95.2 | TAACCCCAA |
| ***NEUROD1*** | chr2: 182542264-182542255 | 4.84 | 94.5 | ACACCACGA |
| | chr2: 182542484-182542475 | 0.92 | 92.2 | AACCCACTG |
| | chr2: 182543055-182543046 | 4.12 | 94.1 | AACCCACCA |
| | chr2: 182543029-182543038 | 6.77 | 95.7 | AGCCCGCAA |
| | chr2: 182543908-182543899 | 6.64 | 95.6 | CAACCACCA |
| | chr2: 182543847-182543856 | 0.95 | 92.2 | ACACCACTC |
| | chr2: 182544607-182544598 | 1.82 | 92.7 | TTACCGCTC |
| | chr2: 182545639-182545648 | 6.83 | 95.7 | TACCCGCAG |

**Supplemental Table S7.** Oligonucleotides used for ChIP.

| GENE PRODUCT | FORWARD PRIMER (5´- 3´) | REVERSE PRIMER (5´- 3´) |
|---|---|---|
| ***CTGF 3´UTR*** | GGTTTGGCCTAGCACTCCA | TCTGGTGACCTGCTCAATTT |
| ***CTGF*** | TCAGACGGAGGAATGCTGAG | CGAGGCTTTTATACGCTCCG |
| ***CYR61*** | AGCAAACAGCTCACTGCCTT | ATGGTAGTTGGAGGGTCGTG |
| ***SOX2* TIR-a (1)** | CATTTGAAAGCCGCACGACC | ATGCTTCTACTGTCTGCCCC |
| ***SOX2* TIR-a (2)** | ACCGAAACCCTTCTTACGGG | AACCGTAGCAAAGGGGATGC |
| ***SOX2* TIR-a (3)** | GCACGACCGAAACCCTTCTT | TCAACCGTAGCAAAGGGGAT |
| ***SOX2* TIR-b (1)** | AGAGAAAACCTGGGGAGGGT | GCAAAGCTCCTACCGTACCA |
| ***SOX2* TIR-b (2)** | CTGGACTTCTTTTTGGGGGACT | GCAAAGCTCCTACCGTACCA |
| ***SOX2* TIR-c (1)** | ATTACCCTCTTGGGTCCTGG | CAGCGCACACTGGGAGAA |
| ***SOX2* TIR-c (2)** | AAATTACCCTCTTGGGTCCTGG | CACACTGGGAGAAGGCGG |
| ***ASCL1* TIR-a (1)** | TGGGTGCTCACCTCCTATACT | GTGGGATTCACACCTCAGGC |
| ***ASCL1* TIR-a (2)** | TTTGGGTGCTCACCTCCTAT | GGATTCACACCTCAGGCCTTT |
| ***ASCL1* TIR-b** | CGTCATTACTGCCCACCATC | TAAAGGGCCAAGGGGATGAC |
| ***ASCL1* TIR-c (1)** | AGGCCACCAGTTGTACTTCA | TGCCACTTTGAGTTTGGACAG |
| ***ASCL1* TIR-c (2)** | GCCACCAGTTGTACTTCAGCA | GCCACTTTGAGTTTGGACAGTA |
| ***NEUROG2* TIR-a (1)** | TGCAACTGGTTCCTGTGATCT | GCCAGCCATTGCAAATCTGT |
| ***NEUROG2* TIR-a (2)** | TGGTTCCTGTGATCTCTTCACC | CAGCCATTGCAAATCTGTGGA |
| ***NEUROG2* TIR-a (3)** | GGGGAATGCAACTGGTTCCT | ACCAGCAAAATCATTCAGATGC |
| ***NEUROG2* TIR-a (4)** | GCAACTGGTTCCTGTGATCT | TTACCAGCAAAATCATTCAGATGC |
| ***NEUROG2* TIR-b (1)** | AGAGGGGCAGGTTAGAAGTCA | AGCCTAAATTTCCACGCTTGC |
| ***NEUROG2* TIR-b (2)** | TGTTTTGTTAGAGGGGCAGGT | GCCTAAATTTCCACGCTTGCAT |
| ***NEUROD1* TIR-a (1)** | GTCCGCGGAGTCTCTAACTG | ATGCGCCATATGGTCTTCCC |
| ***NEUROD1* TIR-a (2)** | CTAACTGGCGACAGATGGGC | CATTTGTATGCCGCGGAGC |
| ***NEUROD1* TIR-a (3)** | CTGCGGGTAAAAACAGGTCC | ACGTGACCTGCCCATTTGTAT |
| ***NEUROD1* TIR-b (1)** | CCTTGAGTATTCACACCATGGAA | GAGCGGTAACAGGTAGCAGG |
| ***NEUROD1* TIR-b (2)** | TGGATACCTTGAGTATTCACACCA | GGAGCGGTAACAGGTAGCAG |
| ***NEUROD1* TIR-c** | AGCCAGGACAGAAATGGAAGT | TGCCCGACAGGATAATGTGT |

**Supplemental Table S8.** Oligonucleotides used for qRT-PCR.

| GENE PRODUCT | FORWARD PRIMER (5´- 3´) | REVERSE PRIMER (5´- 3´) |
|---|---|---|
| ***ACTB*** | TCCTTCCTGGGCATGGAG | AGGAGGAGCAATGATCTTGATCTT |
| ***ASCL1*** | CATCTCCCCCAACTACTCCA | GAAAGCCATGTCTCTCAGGC |
| ***CTGF*** | CTTCTGTGACTTCGGCTCCC | GATGCAGGGAGCACCATCTT |
| ***CYR61*** | CCAAGAAATCCCCCGAACCA | CGGAACCGCATCTTCACAGT |
| ***GAPDH*** | CTCTCTGCTCCTCCTGTTCGAC | TGAGCGATGTGGCTCGGCT |
| ***NEUROD1*** | GGTGCCTTGCTATTCTAAGACGC | GCAAAGCGTCTGAACGAAGGAG |
| ***NEUROG2*** | ATCCGAGCAGCACTAACACG | GCTGAGGCACAGTTAGAGCC |
| ***SOX2*** | GAGCTTTGCAGGAAGTTTGC | GCAAGAAGCCTCTCCTTGAA |
| ***TBP*** | TGCACAGGAGCCAAGAGTGAA | CACATCACAGCTCCCCACCA |
| ***TEAD1*** | CTGAGTCGCAGTTACCACCA | AGCCTGGAGCCTTTTCAAG |
| ***TEAD2*** | ACATGATGAACAGCGTCCTG | CAGCAGTTCCTGGGTGTCTC |
| ***TEAD3*** | CATCGAGCAGAGCTTCCAG | CGTGCAATCAACTCATTTCG |
| ***TEAD4*** | GCCTTCCACAGTAGCATGG | AAAGCTCCTTGCCAAAACC |
| ***WWTR1*** | TTTCCTCAATGGAGGGCCA | GGGTGTTTGTCCTGCGTTTT |

**Supplemental Table S9.** Primary antibodies.

| Antibody | Reference | Clonality | Isotype | Dilution and application |
|---|---|---|---|---|
| **Acetyl-Histone H3** | Sigma Aldrich. 06-599. | Polyclonal | Rabbit | 1.5 µg (ChIP) |
| **CTGF (L-20)** | Santa Cruz Biotechnology. Sc-14939. | Polyclonal | Goat | 1/2000 (WB) |
| **Doublecortin** | Santa Cruz Biotechnology. Sc-8066. | Polyclonal | Goat | 1/250 (IHC-Fr; ICC/IF) |
| **GAPDH** | Millipore. CB1001. | Monoclonal | Mouse | 1/15000 (WB) |
| **GFAP** | Dako. Z0334. | Polyclonal | Rabbit | 1/200 (IHC-Fr; ICC/IF) |
| **GFAP** | Sigma-Aldrich. G3893. | Monoclonal | Mouse | 1/200 (IHC-Fr; ICC/IF) |
| **IgG2a** | Abcam. Ab18413. | Monoclonal | Mouse | 1/250 (ChIP) |
| **Lamin B** | Santa Cruz Biotechnology. Sc-6217. | Polyclonal | Goat | 1/2000 (WB) |
| **MAP2** | Sigma-Aldrich. M9942. | Monoclonal | Mouse | 1/200 (ICC/IF) |
| **Nestin** | Abcam. Ab11306. | Monoclonal | Mouse | 1/200 (IHC-Fr; ICC/IF) |
| **Nestin** | Novus Biologicals. NB100-1604. | Polyclonal | Chicken | 1/500 (IHC-Fr; ICC/IF) |
| **Nestin (10c2)** | Santa Cruz Biotechnology. Sc-23927. | Monoclonal | Mouse | 1/200 (IHC-Fr; ICC/IF) |
| **NEUROD (A-10)** | Santa Cruz Biotechnology. Sc-46684. | Monoclonal | Mouse | 1/500 (WB) |
| **RNA Pol II (A-10)** | Santa Cruz Biotechnology. Sc-17798. | Monoclonal | Mouse | 3 µg (ChIP) |
| **Rabbit IgG Control** | Abcam. Ab37415. | Polyclonal | Rabbit | 1/100 (ChIP) |
| **SOX2** | R&D Systems. AF2018. | Polyclonal | Goat | 1/500 (IHC-Fr; ICC/IF)<br>1/2000 (WB) |
| **TAZ** | Sigma Aldrich. HPA007415. | Polyclonal | Rabbit | 1/2000 (WB)<br>1/200 (IHC-Fr; ICC/IF)<br>1/100 (ChIP) |
| **Tubulin β class III (TUBB3)** | Sigma-Aldrich. T2200. | Polyclonal | Rabbit | 1/200 (ICC/IF) |
| **V5** | Life Technologies. 37-7500. | Monoclonal | Mouse | 1/2000 (WB) |
| **YAP/TAZ (D24E4)** | Cell Signaling Technology. 8418. | Monoclonal | Rabbit | 1/2000 (WB)<br>1/250 (IHC-Fr; ICC/IF; IHC-P) |

## Graphical abstract.

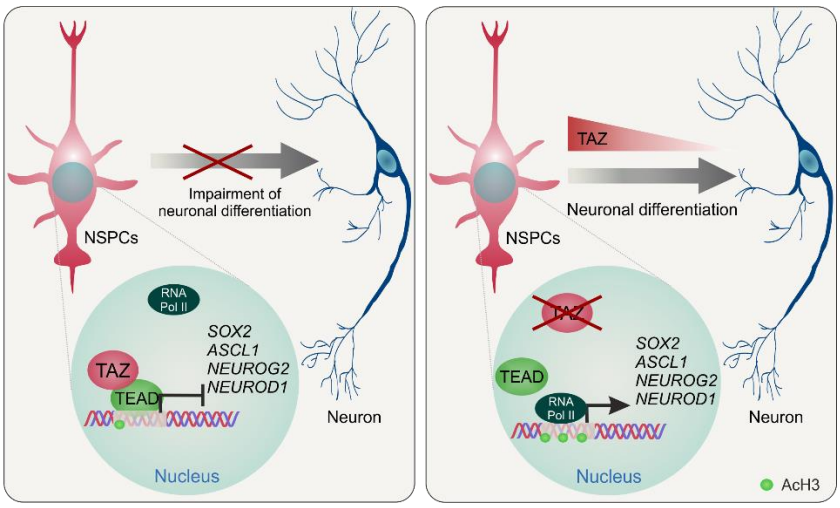

ANTIOXIDANTS & REDOX SIGNALING
Volume 23, Number 14, 2015
DOI: 10.1089/ars.2015.6430

FORUM REVIEW ARTICLE

# Pharmacology and Clinical Drug Candidates in Redox Medicine

V. Thao-Vi Dao,[1] Ana I. Casas,[1] Ghassan J. Maghzal,[2] Tamara Seredenina,[3] Nina Kaludercic,[4] Natalia Robledinos-Anton,[5–8] Fabio Di Lisa,[4,9] Roland Stocker,[2] Pietro Ghezzi,[10] Vincent Jaquet,[3] Antonio Cuadrado,[5–8] and Harald H.H.W. Schmidt[1]

## Abstract

***Significance:*** Oxidative stress is suggested to be a disease mechanism common to a wide range of disorders affecting human health. However, so far, the pharmacotherapeutic exploitation of this, for example, based on chemical scavenging of pro-oxidant molecules, has been unsuccessful. ***Recent Advances:*** An alternative emerging approach is to target the enzymatic sources of disease-relevant oxidative stress. Several such enzymes and isoforms have been identified and linked to different pathologies. For some targets, the respective pharmacology is quite advanced, that is, up to late-stage clinical development or even on the market; for others, drugs are already in clinical use, although not for indications based on oxidative stress, and repurposing seems to be a viable option. ***Critical Issues:*** For all other targets, reliable preclinical validation and drug ability are key factors for any translation into the clinic. In this study, specific pharmacological agents with optimal pharmacokinetic profiles are still lacking. Moreover, these enzymes also serve largely unknown physiological functions and their inhibition may lead to unwanted side effects. ***Future Directions:*** The current promising data based on new targets, drugs, and drug repurposing are mainly a result of academic efforts. With the availability of optimized compounds and coordinated efforts from academia and industry scientists, unambiguous validation and translation into proof-of-principle studies seem achievable in the very near future, possibly leading towards a new era of redox medicine. *Antioxid. Redox Signal.* 23, 1113–1129.

## Introduction

Oxidative stress is the production of reactive oxygen species (ROS) to high nonphysiological concentrations or at nonphysiological locations. Mechanistically, this can lead to DNA damage, lipid peroxidation (72), protein modification, and other pathological effects observed in various chronic disorders, including neurodegenerative, cardiovascular and diabetes-associated renal diseases, and cancer. Many therapeutic attempts to improve patient-relevant outcomes using exogenous small-molecule antioxidants, such as vitamins C and E, have failed (38) or even increased mortality (101) such as in the settings of diabetes mellitus (168, 169).

Possible explanations for this paradox may reside in the lack of specificity of antioxidants towards a certain cellular compartment or tissue, and/or the possibility of generating reductive stress, by increasing levels of reducing agents and therefore disturbing redox homeostasis in the opposite

[1]Cardiovascular Research Institute Maastricht (CARIM), Maastricht University, Maastricht, the Netherlands.
[2]Victor Chang Cardiac Research Institute, and School of Medical Sciences, University of New South Wales, Sydney, Australia.
[3]Department of Pathology and Immunology, Medical School, University of Geneva, Geneva, Switzerland.
[4]Neuroscience Institute, CNR, Padova, Italy.
[5]Centro de Investigación Biomédica en Red sobre Enfermedades Neurodegenerativas (CIBERNED), ISCIII, Madrid, Spain.
[6]Instituto de Investigaciones Biomédicas ''Alberto Sols'' UAM-CSIC, Madrid, Spain.
[7]Instituto de Investigación Sanitaria La Paz (IdiPaz), Madrid, Spain.
[8]Department of Biochemistry, Faculty of Medicine, Autonomous University of Madrid, Madrid, Spain.
[9]Department of Biomedical Sciences, University of Padova, Padova, Italy.
[10]Division of Clinical and Laboratory Investigation, Brighton and Sussex Medical School, Brighton, United Kingdom.

direction. Exogenous antioxidants are also likely to interfere with both disease-triggering and physiological ROS levels. The latter regulate extracellular matrix, control vasomotor activity, are involved in the innate immune response, and promote cell differentiation, proliferation, and migration (4, 10, 161, 163).

Another somewhat indirect type of antioxidant therapeutic strategy that could have fewer side effects relies on the activation of endogenous antioxidant responses. In this context, pharmacological activation of the transcription factor NRF2 is promising therapeutic option currently studied clinically. The conceptual difference between these two antioxidant approaches is broad unspecific scavenging *versus* a localized response at physiological (sub)cellular sites. Only the latter has promise in leaving physiological ROS formation and signaling intact.

Of far broader relevance is a third approach that involves the specific inhibition of the disease-relevant sources of ROS. In this case, the key question is which enzyme to target. Besides NADPH oxidases (NOXs) (10), xanthine oxidase (XO) (96), uncoupled nitric oxide synthase (uc-NOS) (155), and monoamine oxidases (MAOs) (39), other sources such as cytochrome P450 oxidases (44), lipoxygenases (170), and the mitochondrial electron transport chain (134) are all able to generate ROS. Among these, NOXs stand out as their primary function is to produce ROS. All other enzymes do not form ROS as their primary function, but only as a collateral or side product. Examples include uc-NOS, uncoupled mitochondria, and XO. Additional approaches include the inhibition of ROS-toxifying peroxidases, such as myeloperoxidase (MPO), or the functional repair of oxidatively damaged proteins, such as the redox-sensitive soluble guanylate cyclase (sGC), a principle that has already entered the clinic.

We here review the current status and outlook of the most advanced areas in the field of translational redox medicine by focusing on drugs in four categories:

- Activators of endogenous antioxidant defense systems (indirect antioxidants)
- Inhibitors of ROS formation
- Inhibitors of ROS toxification
- Compounds that allow functional repair of ROS-induced damage

## Activators of Antioxidant Defense Systems

The main, if not only, representative members of this group of drugs are nuclear factor (erythroid-derived 2)-like 2 (NRF2) activators. NRF2 is a basic region-leucine zipper (bZIP) transcription factor (Fig. 1A) that forms heterodimers with other bZIP partners, of which the small musculoaponeurotic fibrosarcoma proteins are the best characterized. Together, they recognize an enhancer sequence termed *Antioxidant Response Element (*ARE) that is present in the regulatory regions of over 250 genes (ARE genes), including antioxidant genes such as *HMOX1* (coding heme oxygenase-1) (58). These genes encode enzymes involved in antioxidant reactions, including those driven by glutathione and thioredoxin, generation of nicotinamide adenine dinucleotide phosphate (NADPH), biotransformation, proteostasis, and even DNA repair (58, 90, 135).

The main mechanism of regulation of NRF2 transcriptional activity is through control of protein stabilization by the E3 ligase adapter Kelch-like ECH-associated protein 1

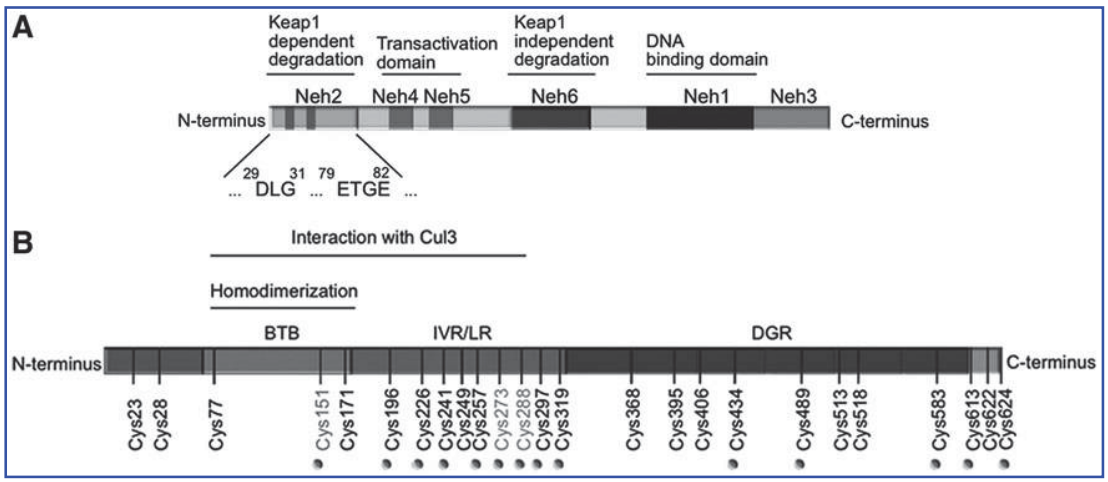


**FIG. 1. Domain structures of NRF2 and KEAP1. (A)** Domain structure of NRF2. NRF2 possesses six highly conserved domains called NRF2-ECH homology (Neh) domains (105). The functional role of each Neh domain is specified. Within the Neh2 domain, the low-affinity (DLG) and high-affinity (ETGE) binding domains to KEAP1 are zoomed in. **(B)** Domain structure of a KEAP1 monomer showing the position of cysteine residues. The N-terminal BTB (bric-a-brac, tramtrack, broad-complex) domain participates in homodimerization and binding to Cul1/Rbx. The C-terminal region, Kelch repeat, DGR domain, contains a WD40 propeller that binds NRF2 at its Neh2 domain. The intervening region connects BTB and DGR domains and is particularly rich in redox-sensitive cysteine residues. C151 is targeted by some electrophiles (tert-butylhydroquinone, diethylmaleate, sulforaphane, and dimethylfumarate; see Fig. 2) disrupting the KEAP1-Cul3 interaction. Other important cysteines are C272 and C288 that react with other compounds (15-deoxy-$\Delta^{12,14}$-prostaglandin $J_2$, 2-cyano-3,12 dioxooleana-1,9 diene-28-imidazolide, ebselen, and cadmium chloride; see Fig. 2) leading to a conformational distortion of the DC domain and altering the KEAP1-NRF2 interaction (147). BTB, (bric-a-brac, tramtrack, broad-complex); DGR, double glycine repeat; DLG, aspartate leucine glycine; ETGE, glutamate, threonine, glycine, glutamate; KEAP1, kelch-like ECH-associated protein 1; Rbx, ring box protein.

(KEAP1). This is a homodimeric zinc (Zn) finger protein that bridges NRF2 with the E3 ligase complex formed by Cullin3 and Rbx proteins (Cul3/Rbx). Under homeostatic conditions, the N-terminal domain of the KEAP1 homodimer binds one molecule of NRF2 at two amino acid sequences of low (aspartate leucine glycine) and high glutamate, threonine, glycine, and glutamate (ETGE) affinity, thus presenting NRF2 to ubiquitination by Cul3/Rbx (152). However, in the presence of ectopic or endogenous electrophiles, KEAP1 is inactivated.

Mechanistically, electrophiles modify sulfhydryl groups of specific redox-sensitive cysteines of KEAP1, including C151, C273, and C288 (Fig. 1B). These modifications of KEAP1 lead to changes in NRF2 recognition, alterations in dimer conformation, or interaction with Cul3/Rbx. As a result, NRF2 escapes KEAP1-dependent degradation, accumulates in the nucleus, and activates ARE genes.

KEAP1 is one of the best-suited proteins to act as an electrophilic/redox sensor as it contains a large number of cysteine residues (27 in the human protein) and can function as an electrophile trap. However, other proteins such as phosphatase and tensin homolog (PTEN), which is mutated in a large number of human tumors, are also redox sensitive (55, 79, 84) and affect NRF2 activity. The catalytic C124 residue of PTEN can be modified through adduct formation with strong electrophiles such as synthetic triterpenoids (2-cyano-3,12-dioxooleana-1,9-dien-28-oic acid-imidazolide; CDDO-Im) (114) and tert-butylhydroquinone (121). This modification results in loss of the PTEN lipid phosphatase activity and yields a more sustained activation of signaling events downstream of phosphoinositide 3-kinase, leading to NRF2 activation by a KEAP1-independent mechanism (117, 118). Thus, electrophilic targeting of NRF2 may involve not only KEAP1 but also other redox-sensitive enzymes. Moreover, KEAP1 interacts with other proteins that also contain the high-affinity binding motif, ETGE (57), such as inhibitor of nuclear factor kappa-B kinase subunit beta and Bcl-2 (78, 109). Hence, some results obtained from KEAP1 mutant or -deficient cells may not be necessarily related to the control of NRF2.

Several groups of electrophilic compounds induce NRF2 in cell culture and less frequently in animals or humans (120) [Fig. 2; for a detailed list of KEAP1 ligands, see refs. (37, 59, 91)]. Many of these compounds are used as nutraceuticals, and for some of them, there is evidence of clinical efficacy. The most successful drug of this type is the ester derivative of fumaric acid, dimethyl fumarate (DMF) (87). DMF crosses the gastrointestinal barrier where it is converted into monomethyl fumarate. The first clinical use of DMF was for the topical treatment of psoriasis in 1994 (5). More recently, an oral formulation of DMF, known as BG12, was commercialized for the treatment of relapsing–remitting multiple sclerosis (14, 76). Other autoimmune diseases such as lupus erythematosus, asthma, and arthritis are under investigation with other formulations of fumarate esters (128, 153).

Other lines of research have focused on targeting NRF2 in degenerative diseases where low-grade chronic inflammation is present. One very potent synthetic triterpenoid, CDDO-methyl ester, bardoxolone methyl, has been studied in great detail for treatment of diabetic nephropathy (157). The initial excitement about this compound was set back by a small yet significant increase in the risk of heart failure. Importantly though, this effect appears not to be related to NRF2 targeting, but rather to alteration of endothelin signaling, leading to reduction in urine volume and sodium excretion in some patients with advanced chronic kidney disease (26). Bardoxolone methyl is now being studied in new indications for pulmonary arterial hypertension, melanoma, and Friedreich's ataxia.

A third NRF2 inducer that has reached the level of clinical studies is the isothiocyanate sulforaphane (SFN) isolated from broccoli sprout extracts. Contrary to DMF and bardoxolone methyl, a drawback of this compound is the absence of a pure formulation that could be used clinically and the lack of commercial value. Nevertheless, SFN provided proof of concept that NRF2 targeting has a therapeutic potential (40, 129, 132). Furthermore, NRF 2 agonists in clinical development are summarized in Table 1.

## Inhibitors of ROS-Forming Enzymes

### *NADPH oxidase inhibitors*

NOXs are transmembrane proteins comprising seven members (NOX1, NOX2, NOX3, NOX4, NOX5, DUOX1, and DUOX2). Each NOX isoform has specific tissue expression and regulation (10, 85). The catalytic core of all NOXs contains four conserved C-terminal NADPH-binding subregions and two flavin adenine dinucleotide (FAD)-binding subregions, as well as four conserved histidine residues, which coordinate two nonidentical iron heme prosthetic groups located between transmembrane domains 3 and 5. They are commonly referred to as the inner and outer heme, depending on their proximity to the cytosol and extracellular space, respectively. NOX activity was first described in neutrophils (7) where it forms superoxide anion radical ($O_2^-$) as part of the phagocytic oxidative burst of the innate immune response (65). All NOX enzymes catalyze the reduction of extracytosolic oxygen (*i.e.*, in phagosomes, endosomes, or the extracellular space) with cytosolic NADPH serving as an electron donor. The activity of most NOX isoforms is tightly regulated: NOX1, NOX2, and NOX3 require the presence of cytosolic proteins, while NOX4 generates ROS in a constitutive manner; NOX5 and DUOX isoforms require increased cellular $Ca^{2+}$ concentrations and binding to N-terminal EF-hand domains for full activity. NOX5 is also a notable exception with respect to preclinical target validation; it is present in several mammals, including humans, but not in mice and rats. Increasing evidence shows that inhibition of NOX activity can be beneficial in multiple models of human diseases [for details, see Casas *et al.* in the same Forum (24)]. In addition, NOX2-derived ROS can have anti-inflammatory effects under certain conditions such as rheumatoid arthritis and multiple sclerosis (67). This provides a rationale for the development of NOX activators. Many advantages and pitfalls of currently available NOX inhibitors have been recently comprehensively reviewed in (4) and (69). In this study, we focus on three chemical compound families, with one compound currently in clinical development (Table 2).

GKT136901 and GKT137831 were developed by GenKyoTex to explore structure–activity relationship along pyrazolopyridine dione compounds (82). These compounds were selected based on oral bioavailability and beneficial pharmacokinetic parameters (4, 70). They block NOX1, NOX4, NOX5, and DUOX (142) activity in the micromolar

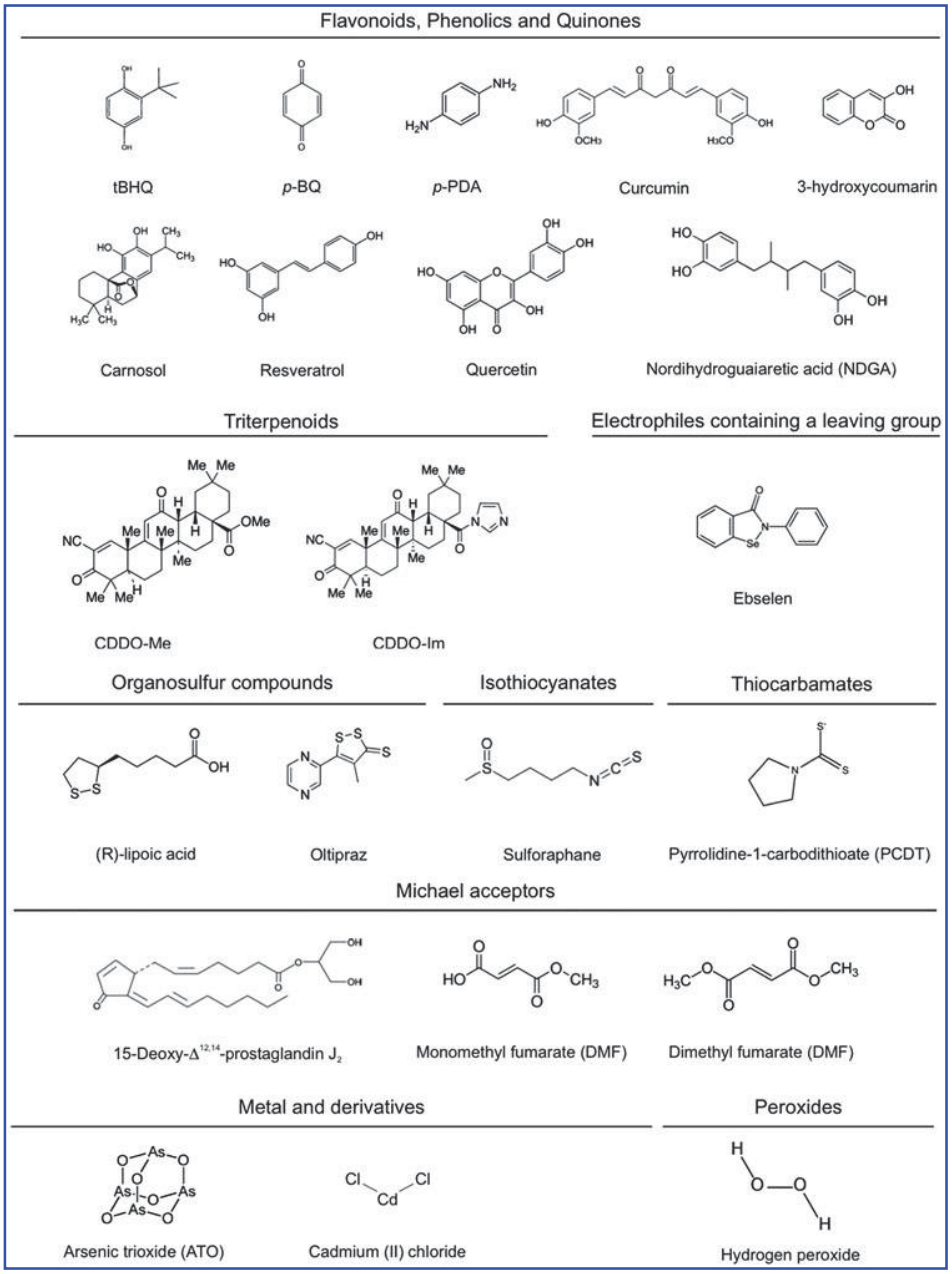


**FIG. 2. Molecular formulas of some common redox-active compounds.** These compounds are capable of modifying protein cysteine thiols by oxidation, reduction, alkylation, and metal chelation and presumably disrupt the KEAP1/NRF2 interaction. The classification has been simplified from Ma *et al.* (91).

range. In terms of off-targets effects, GKT136901 also scavenges peroxynitrite (125), but no interference was identified with other redox-sensitive enzymes, G-protein-coupled receptors, kinases, ion channels, or other enzyme activity (4). However, GKT136901 interacts with Amplex Red fluorescence and dose dependently decreases the signal, thereby complicating the interpretation of *in vitro* results (4). Preclinical results show that GKT137831 reduces glomerular injury and structural changes, as well as macrophage infiltration and proinflammatory transcription factor expression, in models of diabetic nephropathy (54, 70). GKT137831 has entered a clinical study phase II clinical trial, testing its efficacy in diabetic type 2 patients with diabetic nephropathy (50a) (study completed 2015).

Vasopharm developed the triazolo pyrimidine, VAS2870, following a screening approach for NOX2 inhibitors (139, 148). Its derivative, VAS3947, was later generated to slightly improve VAS solubility while keeping a similar NOX inhibitory profile.

Both compounds are able to inhibit different NOX isoforms, such as NOX2 (4), NOX 4, and NOX5 (3, 81), in the micromolar range. Intrathecal injection of VAS2890 significantly reduced cerebral infarct volume and ROS production in a mouse stroke model, suggesting a crucial contribution of one or more NOX enzymes in stroke (Table 2).

However, VAS2870 presents a number of limitations: (i) it blocks NOX2-derived ROS in neutrophils; (ii) its mode of action is independent of NOX2 (50); (iii) it is cytotoxic at low concentrations (171); and (iv) it exerts thioalkylation of cysteine residues *in vitro*, with so far unknown functional relevance (4, 144). In terms of drug development, a proof of principle of VAS compounds in humans is currently unfeasible due to their low solubility and unknown oral pharmacokinetic profile.

Table 1. NRF2 Activators in Clinical Development

| *Compound* | *Chemical characteristics* | *Pathology* | *Outcome* | *Current situation* |
|---|---|---|---|---|
| (DMF) | Methyl ester of fumaric acid | Relapsing–remitting multiple sclerosis | Phase III clinical trial showed that DMF presents anti-inflammatory activity and protects against oxidative injury. Patients have fewer relapses and improved MRI measures of disease activity (75). | TECFIDERA approved in USA, Canada, Australia, Switzerland, and the European Union. |
| | | Rheumatoid Arthritis | Finished last 2010. No data available. | — |
| FP187 | DMF combined with three other fumaric acid esters. Better pharmacological characteristics. | Psoriasis | Still open. No data available. | Phase III clinical trial ongoing. |
| ALKS8700 | Monomethyl fumarate. | — | Evaluate the safety, tolerability, and pharmacokinetics in healthy adults. | Still open, recruiting patients. |
| RTA402 | Acid oleanolic derivate. Semisynthetic triterpenoid. | Type 2 diabetes mellitus. Stage 4 chronic kidney disease. | Phase III clinical trial showed that RTA402 did not reduce the risk of end-stage renal disease or death. High rate of cardiovascular events (34). | Prompted termination of the trial. |
| RTA408 | Next-generation synthetic triterpenoid. | Radiation dermatitis and Friedreich's ataxia. | Phase II clinical trial. | Still open, recruiting patients. |

DMF, dimethyl fumarate; NRF2, nuclear factor (erythroid-derived 2)-like 2.



Table 2. NADPH Oxidase Inhibitors: Chemical Properties and Treatment Indications (4)

| *Compound* | *Chemical structure* | *Drug properties* | *Basic mechanism of action* | *Pathology* |
|---|---|---|---|---|
| GKT136901 | Pyrazolopyridine dione derivate | Peroxynitrite scavenger activity oral administration | NOX1, NOX4, NOX5, DUOX inhibitor | Stroke (unpublished preclinical data) |
| GKT137831 | Pyrazolopyridine dione derivate | Better pharmacokinetic profile than GKT136901 oral administration | NOX1, NOX4, NOX5 inhibitor | Type 2 diabetes mellitus associated with diabetic nephropathy (50a, 70). |
| VAS2870 | Triazolo pyrimidine derivate | Low solubility, poor pharmacokinetic profile. Potential off-target effect leading to thioalkylation of cysteine residues. | NOX2, NOX4, NOX5 inhibitor | Stroke (preclinical data) (81) |
| VAS3947 | Triazolo pyrimidine derivate | Better solubility than VAS2870 with similar NOX inhibitor profile. | NOX2, NOX4, NOX5 inhibitor | — |

NO, nitric oxide; NOX, reduced nicotinamide adenine dinucleotide phosphate oxidase.

Recently, GSK2795039, a novel NOX2 inhibitor, abolished NOX2-induced ROS production in a model of paw inflammation and is protective in an animal model of acute pancreatitis (62). A pharmacokinetic/pharmacodynamic evaluation indicates that GSK2795039 is suitable for *in vivo* use. Further assessment of this compound will provide insights regarding its possible utility for validation of NOX2 as a pharmacological target.

### *XO inhibitors*

Xanthine oxidoreductase (XOR), a 300-kDa homodimer, can exist as an NAD-dependent dehydrogenase (XD) or as an $O_2$-dependent oxidase (XO), depending on the oxidation state of its cysteine thiols (95). XD can be converted into the ROS-generating XO either by formation of intramolecular disulfide bonds (reversible) or by proteolytic cleavage of a loop region connecting the FAD-binding domain and the molybdenum-binding domain (irreversible) (107). While XD depends on $NAD^+$ (31, 140), XO uses $O_2$ as electron acceptor and generates $O_2^-$ and $H_2O_2$ as products (110). As a consequence, XO conversion from XD could be a direct consequence of increased oxidative stress and results in further production of ROS by XO.

XO may contribute to the pathogenesis of various diseases, such as coronary artery disease, type 2 diabetes, and idiopathic dilated cardiomyopathy (21, 22). The XO inhibitor, allopurinol, an analog of hypoxanthine, and its active metabolite, oxypurinol, have been in clinical use for more than 40 years for the treatment of hyperuricemia and gout (41). A recent meta-analysis of 38 clinical trials with allopurinol or oxypurinol in patients with chronic heart failure and coronary artery disease has concluded that XO inhibition improves endothelial function and circulating markers of oxidative stress in patients with, or at risk of, cardiovascular disease (61). Because heterogeneity in those studies made it impossible to come to a conclusion on the effect of XO inhibitors on cardiac outcome, larger prospective multicenter trials are needed (61). Most recently, a study involving 253 high-risk heart failure patients with elevated uric acid levels failed to show improvement with allopurinol in clinical and functional parameters (53).

In 2009, the XOR inhibitor, febuxostat (TEI-6720, TMX-67), was approved by the Food and Drug Administration and marketed for gout (9) as more selective and potent than allopurinol and oxypurinol (110). In contrast to allopurinol, febuxostat has no structural similarity to a purine. Therefore, it has no effects on the activities of other enzymes involved in purine and pyrimidine metabolism, such as guanine deaminase, hypoxanthine-guanine phosphoribosyltransferase, purine nucleoside phosphorylase, orotate phosphoribosyltransferase, and orotidine-5V-monophosphate decarboxylase, compared with allopurinol (166). Contrary to allopurinol and oxypurinol, febuxostat, a potent inhibitor of both XO and XD (146), forms stable long-lasting complexes with the oxidized XOR (111). Its therapeutic application may be useful in cases of allopurinol incompatibility (8). From an experimental point of view, febuxostat may be a superior tool over allopurinol, which may have intrinsic radical scavenging properties that could make it difficult to distinguish between its antioxidant effects and XO inhibition. For example, it was proposed that the protective effects of allopurinol after hypoxia cannot be entirely explained by XO inhibition alone (104).

Another compound used in preclinical studies is BOF-4272 [sodium-8-(3-methoxy-4-phenylsulfinyl-phenyl) pyrazolo[1, 5-a]-1,3,5-triazine-4-olate monohydrate] (112), which specifically inhibits XO-based $O_2^-$ generation (94, 100, 123, 145). However, it could not be tested clinically because of unfavorable pharmacokinetics due to both hepatic metabolism and poor intestinal absorption (108).

Other newly introduced XO inhibitors, such as naphtoflavons, 1,3,5-triazine-based purine analogs, and topiroxostat (FYX-051, 4-[5-pyridin-4-yl-1H-[1, 2, 4] triazol-3-yl]pyridine-2-carbonitrile), are currently being tested in preclinical studies (86, 93, 108, 131). A selection of substances in clinical development is shown in Table 3.

### *MAO inhibitors*

The attention on MAO as a drug target has been driven by the serendipitous discovery of the antidepressant effect of the

Table 3. Monoamine Oxidase and Xanthine Oxidase Inhibitors: Mechanism of Action and Treatment Indications

| *Target* | *Compound* | *Basic mechanism of action* | *Pathology* |
|---|---|---|---|
| MAO | Hydrazines (Phenelzine, isocarboxazid, tranylcypromine) | Nonselective and irreversible MAO inhibitors | Major depressive disorder (130) |
| | Moclobemide, toloxatone, pirlindole | Selective and reversible MAO-A inhibitors | Depression, anxiety (130) |
| | Rasagiline, selegiline | Selective and irreversible MAO-B inhibitors | PD, depression, neurodegenerative diseases (30) |
| | Safinamide | Selective and reversible MAO-B inhibitor | PD (15, 16) |
| XO | Allopurinol and oxypurinol | XOR inhibitor oxypurinol is the active metabolite of allopurinol. | Hyperuricemia and gout (46) cardiovascular disease |
| | Febuxostat | Nonpurine XOR inhibitor. More selective and potent than allopurinol. Do not interfere with other metabolic enzymes. | Hyperuricemia and gout (8) more effective, safe, and well tolerated than allopurinol (8, 27). |
| | BOF-4272 | Inhibits XOR-based superoxide generation. | Impossible for clinical use due to low blood concentrations (112) |
| | Topiroxostat | XOR inhibitor | Hyperuricemia and gout (86, 93, 107) |

PD, Parkinson's Disease; MAO, monoamine oxidase; BOF-4272 sodium,7-[4-(benzenesulfinyl)-3-methoxyphenyl]-1,3,9-triaza-5-azanidabicyclo[4.3.0]nona-3,6,8-trien-2-one; XO, xanthine oxidase; XOR, xanthine oxidoreductase.

antitubercular agent, iproniazid, which was found to act as an MAO inhibitor (35). This observation paved the way to the clinical use of MAO inhibition in depressive disorders (130). Recently, MAO has become also a drug target for ROS-related pathologies. Due to its localization on the outer mitochondrial membrane, $H_2O_2$ and other MAO products [aldehydes and ammonia; for details, see Casas *et al.* in the same Forum (24)] can accumulate in the mitochondria to a significant extent and affect mitochondrial function (73). This can further lead to amplification of oxidative stress and cell damage so that the inhibition of MAO is beneficial in a number of disease models [for details, see Casas *et al.* in the same Forum (24); (11, 17, 18, 36, 73, 74, 98, 136, 156, 165)]. With the possible exception of NOX4 [for details, see Hirschhäuser *et al.* in the same Forum (63)]), MAO is the only known mitochondrial ROS source that can be inhibited pharmacologically without interfering with energy metabolism.

MAO exists in two isoforms, A and B, which generate $H_2O_2$ as a by-product during the oxidative deamination of biogenic monoamines. A wide range of MAO inhibitors are in clinical use, targeting one or both isoforms. Clorgyline is the prototypic MAO-A-specific inhibitor, while deprenyl inhibits MAO-B, and pargyline is nonselective. Recently, other more selective MAO inhibitors have been developed for the treatment of depressive disorders (130). Of those, phenelzine, isocarboxazid, and tranylcypromine are nonselective and irreversible MAO inhibitors, while moclobemide, toloxatone, and pirlindole are MAO-A selective and reversible. Selective and irreversible MAO-B inhibitors, such as selegiline and rasagiline, are widely prescribed for the treatment of affective and neurodegenerative disorders (Table 3), for example, mild symptoms of Parkinson's disease (PD) and associated motor fluctuations (30). Recently, specific and reversible MAO-B inhibitor, safinamide, has been launched in Germany for the treatment of mid- to late-stage PD in combination with levodopa or other PD therapies (15, 16). The therapeutic potential of MAO-B inhibitors is currently being evaluated also for the treatment of Alzheimer's disease. GABA formation from reactive astrocytes is mediated by MAO-B and affects synaptic plasticity, learning, and memory (71). Since astrocytic GABA and MAO-B are upregulated also in postmortem brains of individuals affected by Alzheimer's disease, MAO-B inhibition has been proposed as a potentially effective therapeutic strategy for treating memory impairment in this disease. Indeed, ladostigil, a dual acetylcholine butyrylcholine esterase and brain-selective MAO-A and -B inhibitor, was shown to antagonize scopolamine-induced impairment in spatial memory (66). More recently, a new small-molecule MAO-B inhibitor, EVT 302, is currently in phase IIb clinical trial for the treatment of Alzheimer's disease.

MAO inhibition can also be the result of an off-target effect. For example, the PPAR-gamma agonist, pioglitazone, used for the treatment of type 2 diabetes, specifically inhibits MAO-B in a reversible manner (12), a property that is not shared by other members of the glitazone family, such as troglitazone and rosiglitazone. Importantly, this off-target effect may contribute to the beneficial effects of pioglitazone in diabetic cardiomyopathy.

To date, MAO inhibitors have been used in patients to preserve or increase monoamine levels. It remains to be investigated clinically whether MAO inhibitors modulate oxidative stress-based pathologies and whether their use can be extended to other indications. The most relevant hurdle in the clinical development of MAO inhibitors is represented by a hypertensive reaction occurring when selective MAO-A inhibition is combined with intake of tyramine-rich food, such as aged cheese and alcoholic beverages (43). Tyramine is mostly oxidized by intestinal MAO-A; MAO-A inhibition causes an increase in circulating tyramine, which is taken up by postganglionic sympathetic neurons and induces noradrenaline release. However, MAO-B and reversible MAO-A inhibitors are devoid of this potential risk (167). Other minor contraindications and concerns related to MAO inhibitors are listed in (162).

### *NOS inhibitors*

Nitric oxide (NO) is another ROS, although mostly with beneficial effects. However, under certain conditions, overproduction may cause cell death, for example, in neurotrauma and stroke. Most NOS inhibitors are based on displacing the substrate, arginine, off its binding site. However, none of these has been approved as a drug for any indication. The most dramatic failure was $N^G$-mono-methyl-L-arginine (L-NMMA) in septic shock (89), where L-NMMA resulted in a 10% increase in overall mortality due to a higher proportion of cardiovascular deaths. Another analog, the amidino amino acid N6-(1-iminoethyl)-L-lysine (L-NIL), applied as its 5-tetrazole-amide prodrug (L-NIL-TA, SC-51) was tested to treat asthma. Oral administration of L-NIL-TA reduced exhaled NO levels in both healthy volunteers and asthmatics for at least 72 h without affecting blood pressure and pulse rate, but did not improve respiratory function (56). Finally, GW273629 (3-[[2-[(1-iminoethyl)amino]ethyl] sulfonyl]-L-alanine) was ineffective in the treatment of acute migraine (154).

The most advanced and currently most successful therapeutic approach is to target another and more unique binding site in NOS, the redox-sensitive cofactor, tetrahydrobiopterin (13, 48). Vasopharm's VAS203 has been successfully developed up to phase II for traumatic brain injury (141) (Table 4).

## Inhibitors of ROS Toxification

These inhibitors target enzymes that do not produce ROS but metabolize ROS to other more toxic species. The most prominent example is myeloperoxidase (MPO).

### *MPO inhibitors*

MPO is a heme protein that can use $H_2O_2$ to oxidize $Cl^-$ to the highly reactive hypochlorous acid (HOCl), a potent oxidizing agent, but can also generate free radicals through its catalytic peroxidase cycle (77). Besides the major halide $Cl^-$, MPO can also utilize bromide ($Br^-$) to form brominating species, including hypobromous acid (HOBr) (60).

MPO is abundant in neutrophils and certain macrophages where it plays a role in the innate immune response. MPO-derived oxidants also have the potential to cause host tissue injury *via* initiation of post-translational protein modifications (*i.e.*, chlorination) of proteins (115, 164) and lipid peroxidation (124). As a result, MPO-mediated oxidative damage is thought to contribute to a wide range of chronic inflammatory diseases, including cardiovascular and neuroinflammatory diseases (33, 106). The extracellular $Br^-$ concentration is much lower than that of $Cl^-$ (149). Thus, the physiological relevance of

Table 4. Nitric Oxide Synthase NOS Inhibitors: Mechanism of Action and Treatment Indications

| *Compound* | *Chemical characteristics* | *Basic mechanism of action* | *Pathology* |
|---|---|---|---|
| L-NMMA | Arginine derivate | Nonselective NO synthase inhibitor | Septic shock dramatic failure in clinical trials (89) |
| VAS203 | Tetrahydrobiopterin derivate | Nonselective NO synthase inhibitor | Traumatic brain injury (141) |
| Tilarginine acetate | Arginine derivate | Nonselective NO synthase inhibitor | Cardiogenic shock complicating—acute myocardial infarction (2) |
| L-NIL | Arginine derivate L-NIL-TA and SC-51 prodrug oral administration | Inducible NO synthase inhibitor | Asthma (56) |
| GW273629 | Alanine derivate | Inducible NO synthase inhibitor | Acute migraine (154) |

GW273629, (3-[[2-[(1-iminoethyl)amino]ethyl]sulfonyl]-l-alanine); L-NIL-TA, L-N6-(1-iminoethyl)lysine-5-tetrazole-amide; L-NMMA, 1-(4-aminopentyl)-2-methylguanidine; SC-51, L-N6-(1-iminoethyl)lysine 5-tetrazole amide.

brominating oxidants such as HOBr, although they elicit antimicrobial effects *in vitro* (80, 159), has yet to be determined.

However, complete deficiency of MPO can be detrimental. For example, mice deficient in MPO and the low-density lipoprotein receptor (Ldlr), that is, $Mpo^{-/-}Ldlr^{-/-}$mice, develop larger atherosclerotic lesions compared with $Ldlr^{-/-}$mice (20), and engraftment of bone marrow from $Mpo^{-/-}$mice into $Ldlr^{-/-}$mice increases rather than decreases the size of atherosclerotic lesions (20). Moreover, mice lacking MPO are more susceptible to experimental autoimmune encephalomyelitis, a mouse model of multiple sclerosis (19), and are protected from some features of PD (28). As a result of the implied overall benefit of phagocyte MPO, pharmacological strategies to attenuate MPO-mediated inadvertent oxidant damage aim at partial rather than complete inhibition of the enzyme.

Until recently, no specific MPO inhibitors were described that could be considered drug candidates. Although a number of commercially available compounds, including hydroxamic acids, hydrazines, and hydrazides, were used previously to inhibit the catalytic activity of MPO (92), they are not specific and also inhibit other heme peroxidases.

More recently, AstraZeneca found that 2-thioxanthines are potent and selective suicide inhibitors of MPO. Upon oxidation by MPO compound I, the thioxanthine radical forms an adduct with the heme prosthetic group of the enzyme, resulting in inactivation of MPO (150). These new compounds inhibit MPO activity in plasma, decrease protein chlorination in a mouse model of peritonitis, and elicit a range of beneficial effects in various disease models, without interfering with the killing of bacteria by neutrophils or other peroxidases, for example, thyroid peroxidase or lactoperoxidase activity (150). A number of thioxanthines have yielded positive results in preclinical and clinical studies. For example, the thioxanthine, AZD5904, stopped progression of emphysema and small airway remodeling and partially protected against pulmonary hypertension in a guinea pig model of chronic obstructive pulmonary disease (COPD) induced by exposure to cigarette smoke (29). In addition to AZD5904 entering phase I clinical trials for COPD and multiple sclerosis, AstraZeneca has completed a phase IIA clinical trial with another thioxanthine, AZD3241, in patients with PD (116) (Table 5).

Another small-molecule inhibitor of MPO is INV-315 with a submicromolar $IC_{50}$ [0.9 $\mu$M; (88)]. INV-315 decreases plaque burden and improves endothelial function in apolipoprotein E-deficient mice fed a high-fat diet for 16 weeks, a commonly used mouse model of atherosclerosis (88). However, no direct evidence for MPO inhibition or improved endothelial function was provided in that study. Pfizer, Inc., has also implemented a discovery program targeting MPO in inflammation and has filed patents for 2-thiopyrimidones (Fig. 3), which have a structure that is similar to 2-thioxanthines, suggesting that they may also act as suicide inhibitors by forming adducts with the heme moiety of MPO (23).

### Functional Repair of ROS-Induced Protein Damage

This category of ROS-related drugs does not modulate ROS formation, but corrects some of its functional consequences. In the present review, we focus on NO-cGMP signaling, which appears to be one of the major mechanisms of deregulation initiated by oxidative stress (97). ROS can interfere with NO-cGMP signaling in three manners:

- by uncoupling NOS,
- by chemically scavenging NO, or
- by oxidatively damaging the NO receptor, sGC.

Table 5. Myeloperoxidase Inhibitors: Mechanism of Action and Treatment Indications

| *Compound* | *Chemical characteristics* | *Basic mechanism of action* | *Pathology* |
|---|---|---|---|
| AZD3241 | 2-thioxanthine derivate | MPO inhibitor by forming an adduct with the heme prosthetic group of the enzyme. | Peritonitis (preclinical data) PD (116) |
| AZD5904 | 2-thioxanthine derivate | MPO inhibitor, Similar mechanism of action as AZD3241. | Chronic obstructive pulmonary disease (29) |

MPO, myeloperoxidase.

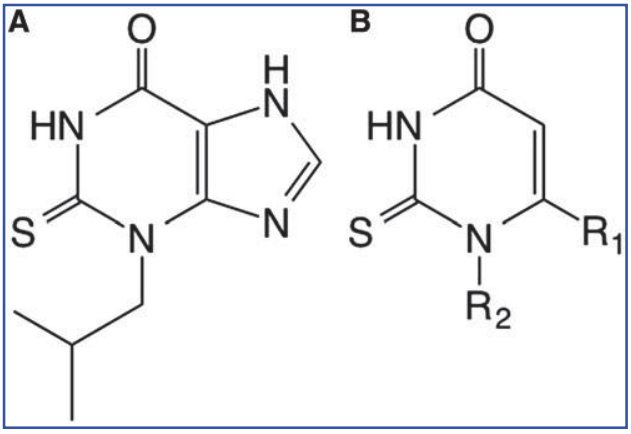


**FIG. 3. Selective myeloperoxidase inhibitors. (A)** Structure of the 2-thioxanthine, TX1 (150). **(B)** Basic structure of 2-thiopyrimidone compounds in development by Pfizer, Inc. R1 is a five- to six-membered aromatic ring with one to three heteroatoms, while R2 is a fully saturated, partially unsaturated of fully unsaturated 1- to 14-membered straight carbon chain.

This essentially leads to four therapeutic options:

- to recouple uc-NOS [*e.g.*, in peripheral arterial disease (Clinical Trials Registry ACTRN12609000882224)]
- to replenish scavenged NO *via* NO donor compounds
- to sensitize sGC for lower NO levels [*e.g.*, in pulmonary arterial hypertension (52) and chronic thromboembolic pulmonary hypertension (51)]
- to (re-)activate oxidatively damaged and heme-free sGC (apo-sGC) (*e.g.*, in calcific aortic valve stenosis [NCT02481258] and neuropathic pain [NCT00799656])

### *NO donors*

For over 100 years, NO-releasing drugs have been in clinical use. However, they have several serious side effects that will most likely lead to their eventual replacement. First, many NO donors are subject to tolerance, leading to loss of efficacy and requiring treatment interruptions. Moreover, they can lead to systemic hypotension and reflex tachycardia. Another concern is the fact that under oxidative stress, additional NO from NO donors leads to a spillover and sGC activation, but may also be metabolized to peroxynitrite. Thus, with NO donors, NO-cGMP signaling is partially and acutely recovered, but this happens at the expense of a chronic buildup of unwanted post-translational modifications such as protein tyrosine nitration (133). In addition, NO-drug hybrid molecules comprising an established drug and an NO-releasing moiety have been developed with the aim to preserve the pharmacological activity of the lead structure and add possibly beneficial effects of NO. Of the many compounds tested and developed, a series of NO-NSAIDs (nonsteroidal anti-inflammatory drugs), nitrosylated adrenoreceptor antagonist moxisylate (S-NO-moxisylate), and latanoprostene bunod (VESNEO®), an NO-donating prostaglandin F2-alpha analog, are currently most advanced. The latter is currently in phase III clinical development for the reduction of intraocular pressure in patients with glaucoma and ocular hypertension. Results from the phase 2b study confirmed that the drug is safe (158). Whether these combinations will not have similar limitations as other NO donors remains to be seen.

### *HNO donors*

Besides classical NO donors and NO-drug hybrid molecules, recent preclinical studies and a phase IIa study reveal the therapeutic potential of an NO-related species, nitroxyl (HNO), which is developed as an HNO-donating drug (CXL-1020) by Cardioxyl, for acute decompensated heart failure therapy (122). However, serious inflammatory irritation at the injection site led to development of a second-generation HNO donor, CXL-1427, which is currently in clinical phase II testing. In contrast to NO donors, HNO donors such as Angeli's Salt/HNO appear to not induce tolerance, at least preclinically (6, 68, 103). Interestingly, HNO seems resistant towards scavenging by superoxide and retains efficacy after repeated infusions (45, 103, 113, 122, 151). However, further proof-of-concept studies need to be performed with safe HNO donors.

### *Recoupling uc-NOS*

Oxidative damage of NOS is seen predominately not only for *NOS3*/eNOS but also for *NOS1*/nNOS (102). For this, two reversible processes are important, the oxidation of the redox-sensitive NOS cofactor, tetrahydrobiopetrin ($BH_4$) (119), and the accumulation of an endogenous antagonist at the arginine substrate binding site, asymmetric-dimethyl-L-arginine (ADMA). ADMA is an independent risk marker, if not a risk factor, for cardiovascular disease states [for details, see Frijhoff *et al.* in the same Forum (47)], which may be mechanistically related to uc-NOS.

To replenish the $BH_4$ binding site, $BH_4$ substitution is an option (143). However, $BH_4$ therapy under oxidative stress may also carry the risk of leading to $BH_2$ accumulation, a $BH_4$ antagonist at the NOS $BH_4$ binding site (13). The so-called salvage pathway recycles oxidized $BH_2$ back to $BH_4$ *via* dihydrofolate reductase (25). Moreover, angiotensin II type 1 receptor blockers and statins may, among other actions, increase the expression of the $BH_4$-forming GTP cyclohydrolase 1 and therefore normalize low $BH_4$ levels (160). High doses of L-arginine may compete off ADMA on eNOS or normalize intracellular ADMA levels. However, a direct antioxidant effect of the guanidine group is also possible (83). Moreover, important differences exist in the bioavailability of arginine in humans *versus* rodents. Hence, L-citrulline, which is absorbed with near 100% bioavailability, may be a better alternative in humans and is subject to ongoing trials (Australian New Zealand Clinical Trials Registry ACTRN12609000882224).

### *sGC stimulators and activators*

Although stimulation and activation of sGC may sound similar, both innovative drug classes display entirely different modes of action and target different redox and disease states of the NO receptor, sGC. sGC stimulators (sGCs) such as riociguat (BAY 63-2521), vericiguat (BAY 1021189), BAY 41-8543, and BAY 60-4552, and YC-1 (49) bind to an allosteric binding site of Fe(II)heme-containing sGC and allosterically sensitize the enzyme for diminished biophase levels of endogenous NO. In a disease condition where biophase levels of NO are diminished, for example, by oxidative stress, higher or physiological increases in cGMP tissue levels can be achieved. Clinical indications may be similar to NO donors, but without the risk of tolerance and protein nitration as an accumulating by-product.

In contrast, sGC activators (sGCa), such as cinaciguat (BAY 58-2667), ataciguat (HMR 1766), and S3448 (126), activate only Fe(III)heme-oxidized or heme-free (apo-)sGC. They do this by either replacing the weakly bound oxidized heme in (apo-)sGC or by directly occupying the orphaned heme pocket in apo-sGC (138).

Otherwise, apo-sGC would be ubiquitinated at the empty heme binding site and degraded (64, 99). Therefore, sGC activators also stabilize apo-sGC. The ratio of oxidized or apo-sGC to Fe(II)-sGC is increased under oxidative stress conditions (42). In a condition where just NO levels are diminished, but Fe(II)sGC is intact, sGCa would be ineffective. Most recently two other sGCa, GlaxoSmithKline's GSK218123A and Boehringher-Ingelheims's Bl 703704, have been tested preclinically in different animal models of hypertension (32) and kidney diseases (137). The possible benefit of this new compound class and precise mechanism of action, as well as safety, need to be further validated.

## Conclusion

In recent years, considerable data have accrued, indicating that disturbances in redox homeostasis are a common mechanism in different cardiovascular, neurological, and metabolic diseases. However, oxidative stress was hitherto not pharmacologically targetable, and the only strategy tested so far, using antioxidants, has been ineffective or even harmful. A possible reason for this is the lack of specificity for disease triggering *versus* physiological ROS that have a signaling, rather than pathological, role. Furthermore, ROS scavenging by antioxidants takes place in all (sub)cellular locations, not just those relevant for the disease. Innovative drugs need to target disease-relevant ROS-producing enzymes, ROS toxifying enzymes, or proteins damaged by ROS. For all of these, small molecules have become available that are able to perturb specific targets and allow for therapeutic proof-of-concept studies.

These include not only new compounds but also some well-characterized drugs, such as allopurinol and MAO isoform-selective inhibitors, which have been clinically used for decades, although not with the purpose to inhibit ROS formation. In addition, sGC stimulators (in the clinic), NOX inhibitor (entering phase III), NOS inhibitors (phase II-III), sGC activators (phase I-II), and superoxide dismutase mimetics such as GC4410 (phase I) [for details, see Schmidt *et al.* in the same Forum (127)] are rapidly gaining relevance. Other possible clinical candidates are, for example, mitochondria targeted antioxidants such as mitoquinone and mito TEMPO [for details, see Schmidt *et al.* in the same Forum (127)].

However, in several cases (*e.g.*, NOX inhibitors), there is an unmet need for isoform-selective drugs. Finally, promising results have been obtained with activators of the transcription factor NRF2, even though in this case the mechanisms are more complex. In particular, one NRF2-activating compound,

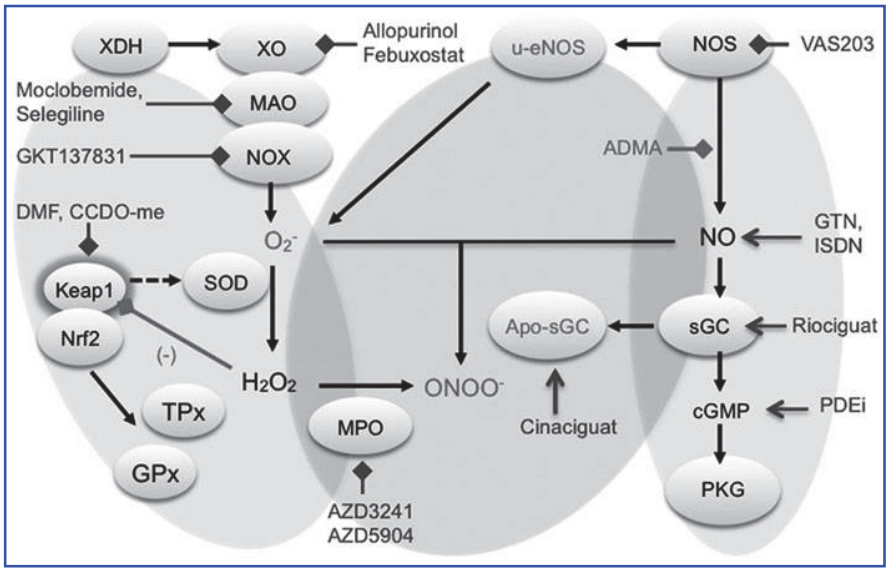


**FIG. 4. Compounds targeting ROS sources, ROS toxifiers, and enzymes damaged by ROS**. The physiologic interaction of NRF2 and KEAP1 underlies a negative feedback mechanism. Disruption of this interaction can be caused by electrophilic compounds, which react with specific cysteines of Keap1. Keap 1 is a sensor for environmental and endogenous reactive oxygen and nitrogen species. In conditions of ROS overload, NRF2 escapes Keap1-dependent degradation, accumulates in the nucleus, and activates ARE genes, leading to activation of glutathione and thioredoxin metabolism, including GPx and TPx. Sources that produce $O_2^-$ are NOX, XO, and MAO. Superoxide anion will be detoxified by SOD to $H_2O_2$ and further by catalase to $H_2O$ or will react with NOS-derived NO to form peroxynitrite (ONOO$^-$). On the other side, NO activates the sGC, which results in cGMP generation and stimulates protein kinase G signaling. The NO production can be reduced by inhibition of NOS with the endogenous L-arginine analog ADMA. In oxidative stress conditions, the sGC heme can be oxidized or removed (apo-sGC), leading to NO unresponsive sGC. Selected inhibitors and activators are indicated with inhibiting or activating *arrows* and *blocks*, respectively. ADMA, asymmetric-dimethyl-L-arginine; ARE, antioxidant responsive element; apo-sGC, heme-free soluble guanylate cyclase; cGMP, cyclic guanosine monophosphate; GPx, glutathione peroxidase; MAO, monoamine oxidases; NO, nitric oxide; NOS, nitric oxide synthase; NOX, nicotinamide adenine dinucleotide phosphate oxidase; ROS, reactive oxygen species; sGC, soluble guanylate cylcase; SOD, superoxide dismutase; TPx, thioredoxin peroxidase; XO, xanthine oxidase.

BG12, is effective and approved for the treatment of multiple sclerosis and, following its success, other NRF2 activators are currently being tested in proof-of-principle studies for various inflammatory diseases (Fig. 4).

### Outlook

New, more specific pharmacological agents and future drugs are likely to transform the field of oxidative stress, with its many potential medical implications. Indirectly acting compounds (*e.g.*, sGCs) have already provided proof of concept. The final breakthrough will be achieved when inhibitors of ROS-forming enzymes will enter evidence-based medicine.

### Acknowledgments

Several authors of this review were supported by the European Cooperation in Science and Technology (COST Action BM1203/EU-ROS). H.H.H.W.S. is the recipient of an ERC Advanced Grant and Marie-Curie IRG and co-leads a EUROSTARS program. R.S. is supported by a Senior Principal Research Fellowship from the National Health and Medical Research Council of Australia N.K. is supported by an EFSD/Sanofi Award.

### Author Disclosure Statement

Vincent Jaquet holds shares in Genkyotex SA and Harald H.H.W. Schmidt in Vasopharm GmbH. For the remaining authors, no competing financial interests exist.

### References

1. This reference has been deleted.
2. Alexander JH, Reynolds HR, Stebbins AL, Dzavik V, Harrington RA, Van de Werf F, and Hochman JS. Effect of tilarginine acetate in patients with acute myocardial infarction and cardiogenic shock: the TRIUMPH randomized controlled trial. *JAMA* 297: 1657–1666, 2007.
3. Altenhofer S, Kleikers PW, Radermacher KA, Scheurer P, Rob Hermans JJ, Schiffers P, Ho H, Wingler K, and Schmidt HH. The NOX toolbox: validating the role of NADPH oxidases in physiology and disease. *Cell Mol Life Sci* 69: 2327–2343, 2012.
4. Altenhofer S, Radermacher KA, Kleikers PW, Wingler K, and Schmidt HH. Evolution of NADPH oxidase inhibitors: selectivity and mechanisms for target engagement. *Antioxid Redox Signal* 23: 406–427, 2015.
5. Altmeyer PJ, Matthes U, Pawlak F, Hoffmann K, Frosch PJ, Ruppert P, Wassilew SW, Horn T, Kreysel HW, Lutz G, *et al.* Antipsoriatic effect of fumaric acid derivatives. Results of a multicenter double-blind study in 100 patients. *J Am Acad Dermatol* 30: 977–981, 1994.
6. Andrews KL, Lumsden NG, Farry J, Jefferis AM, Kemp-Harper BK, and Chin-Dusting JP. Nitroxyl: a vasodilator of human vessels that is not susceptible to tolerance. *Clin Sci (Lond)* 129: 179–187, 2015.
7. Baldrige CW and Gerard RW. The extra respiration of phagocytosis. *Am J Physiol* 103: 235–236, 1932.
8. Becker MA, Schumacher HR, Jr., Wortmann RL, MacDonald PA, Eustace D, Palo WA, Streit J, and Joseph-Ridge N. Febuxostat compared with allopurinol in patients with hyperuricemia and gout. *N Engl J Med* 353: 2450–2461, 2005.
9. Becker MA, Schumacher HR, MacDonald PA, Lloyd E, and Lademacher C. Clinical efficacy and safety of successful longterm urate lowering with febuxostat or allopurinol in subjects with gout. *J Rheumatol* 36: 1273–1282, 2009.
10. Bedard K and Krause KH. The NOX family of ROS-generating NADPH oxidases: physiology and pathophysiology. *Physiol Rev* 87: 245–313, 2007.
11. Bianchi P, Kunduzova O, Masini E, Cambon C, Bani D, Raimondi L, Seguelas MH, Nistri S, Colucci W, Leducq N, and Parini A. Oxidative stress by monoamine oxidase mediates receptor-independent cardiomyocyte apoptosis by serotonin and postischemic myocardial injury. *Circulation* 112: 3297–3305, 2005.
12. Binda C, Aldeco M, Geldenhuys WJ, Tortorici M, Mattevi A, and Edmondson DE. Molecular insights into human monoamine oxidase B inhibition by the glitazone antidiabetes drugs. *ACS Med Chem Lett* 3: 39–42, 2011.
13. Bommel HM, Reif A, Frohlich LG, Frey A, Hofmann H, Marecak DM, Groehn V, Kotsonis P, La M, Koster S, Meinecke M, Bernhardt M, Weeger M, Ghisla S, Prestwich GD, Pfleiderer W, and Schmidt HH. Anti-pterins as tools to characterize the function of tetrahydrobiopterin in NO synthase. *J Biol Chem* 273: 33142–33149, 1998.
14. Bomprezzi R. Dimethyl fumarate in the treatment of relapsing-remitting multiple sclerosis: an overview. *Ther Adv Neurol Disord* 8: 20–30, 2015.
15. Borgohain R, Szasz J, Stanzione P, Meshram C, Bhatt M, Chirilineau D, Stocchi F, Lucini V, Giuliani R, Forrest E, Rice P, and Anand R. Randomized trial of safinamide add-on to levodopa in Parkinson's disease with motor fluctuations. *Mov Disord* 29: 229–237, 2014.
16. Borgohain R, Szasz J, Stanzione P, Meshram C, Bhatt MH, Chirilineau D, Stocchi F, Lucini V, Giuliani R, Forrest E, Rice P, and Anand R. Two-year, randomized, controlled study of safinamide as add-on to levodopa in mid to late Parkinson's disease. *Mov Disord* 29: 1273–1280, 2014.
17. Bortolato M, Chen K, and Shih JC. Monoamine oxidase inactivation: from pathophysiology to therapeutics. *Adv Drug Deliv Rev* 60: 1527–1533, 2008.
18. Brandes RP. Triggering mitochondrial radical release: a new function for NADPH oxidases. *Hypertension* 45: 847–848, 2005.
19. Brennan M, Gaur A, Pahuja A, Lusis AJ, and Reynolds WF. Mice lacking myeloperoxidase are more susceptible to experimental autoimmune encephalomyelitis. *J Neuroimmunol* 112: 97–105, 2001.
20. Brennan ML, Anderson MM, Shih DM, Qu XD, Wang X, Mehta AC, Lim LL, Shi W, Hazen SL, Jacob JS, Crowley JR, Heinecke JW, and Lusis AJ. Increased atherosclerosis in myeloperoxidase-deficient mice. *J Clin Invest* 107: 419–430, 2001.
21. Butler R, Morris AD, Belch JJ, Hill A, and Struthers AD. Allopurinol normalizes endothelial dysfunction in type 2 diabetics with mild hypertension. *Hypertension* 35: 746–751, 2000.
22. Cappola TP, Kass DA, Nelson GS, Berger RD, Rosas GO, Kobeissi ZA, Marban E, and Hare JM. Allopurinol improves myocardial efficiency in patients with idiopathic dilated cardiomyopathy. *Circulation* 104: 2407–2411, 2001.
23. Carpino PA, Conn EL, Dow RL, Dowling MS, Hepworth D, Kung DWS, Orr S, Rocke BN, Ruggeri RB, and Sammons MF. 2-Thiopyrimidinones. edited by USPTO. U.S. Patent 8,835,449: Pfizer Inc.; 2013.
24. Casas A, Dao VT, Daiber A, Maghzal GJ, Di Lisa F, Kaludercic N, Leach S, Jaquet V, Seredenina T, Krause KH, López MG, Stocker R, Ghezzi P, and Schmidt HH. Reactive

oxygen-related diseases: Therapeutic targets and emerging clinical indications. *Antioxid Redox Signal* 23: 1171–1185, 2015.
25. Chalupsky K and Cai H. Endothelial dihydrofolate reductase: critical for nitric oxide bioavailability and role in angiotensin II uncoupling of endothelial nitric oxide synthase. *Proc Natl Acad Sci U S A* 102: 9056–9061, 2005.
26. Chin MP, Reisman SA, Bakris GL, O'Grady M, Linde PG, McCullough PA, Packham D, Vaziri ND, Ward KW, Warnock DG, and Meyer CJ. Mechanisms contributing to adverse cardiovascular events in patients with type 2 diabetes mellitus and stage 4 chronic kidney disease treated with bardoxolone methyl. *Am J Nephrol* 39: 499–508, 2014.
27. Chohan S, Becker MA, MacDonald PA, Chefo S, and Jackson RL. Women with gout: efficacy and safety of urate-lowering with febuxostat and allopurinol. *Arthritis Care Res (Hoboken)* 64: 256–261, 2012.
28. Choi DK, Pennathur S, Perier C, Tieu K, Teismann P, Wu DC, Jackson-Lewis V, Vila M, Vonsattel JP, Heinecke JW, and Przedborski S. Ablation of the inflammatory enzyme myeloperoxidase mitigates features of Parkinson's disease in mice. *J Neurosci* 25: 6594–6600, 2005.
29. Churg A, Marshall CV, Sin DD, Bolton S, Zhou S, Thain K, Cadogan EB, Maltby J, Soars MG, Mallinder PR, and Wright JL. Late intervention with a myeloperoxidase inhibitor stops progression of experimental chronic obstructive pulmonary disease. *Am J Resp Crit Care* 185: 34–43, 2012.
30. Connolly BS and Lang AE. Pharmacological treatment of Parkinson disease: a review. *JAMA* 311: 1670–1683, 2014.
31. Corte ED and Stirpe F. The regulation of rat liver xanthine oxidase. Involvement of thiol groups in the conversion of the enzyme activity from dehydrogenase (type D) into oxidase (type O) and purification of the enzyme. *Biochem J* 126: 739–745, 1972.
32. Costell MH, Ancellin N, Bernard RE, Zhao S, Upson JJ, Morgan LA, Maniscalco K, Olzinski AR, Ballard VL, Herry K, Grondin P, Dodic N, Mirguet O, Bouillot A, Gellibert F, Coatney RW, Lepore JJ, Jucker BM, Jolivette LJ, Willette RN, Schnackenberg CG, and Behm DJ. Comparison of soluble guanylate cyclase stimulators and activators in models of cardiovascular disease associated with oxidative stress. *Front Pharmacol* 3: 128, 2012.
33. Davies MJ, Hawkins CL, Pattison DI, and Rees MD. Mammalian heme peroxidases: from molecular mechanisms to health implications. *Antioxid Redox Signal* 10: 1199–1234, 2008.
34. de Zeeuw D, Akizawa T, Audhya P, Bakris GL, Chin M, Christ-Schmidt H, Goldsberry A, Houser M, Krauth M, Lambers Heerspink HJ, McMurray JJ, Meyer CJ, Parving HH, Remuzzi G, Toto RD, Vaziri ND, Wanner C, Wittes J, Wrolstad D, and Chertow GM. Bardoxolone methyl in type 2 diabetes and stage 4 chronic kidney disease. *N Engl J Med* 369: 2492–2503, 2013.
35. Delay J, Laine B, and Buisson JF. [The action of isonicotinyl-hydrazide used in the treatment of depressive states]. *Ann Med Psychol (Paris)* 110: 689–692, 1952.
36. Di Lisa F, Kaludercic N, Carpi A, Menabo R, and Giorgio M. Mitochondrial pathways for ROS formation and myocardial injury: the relevance of p66(Shc) and monoamine oxidase. *Basic Res Cardiol* 104: 131–139, 2009.
37. Dinkova-Kostova AT, Massiah MA, Bozak RE, Hicks RJ, and Talalay P. Potency of Michael reaction acceptors as inducers of enzymes that protect against carcinogenesis depends on their reactivity with sulfhydryl groups. *Proc Natl Acad Sci U S A* 98: 3404–3409, 2001.
38. Dotan Y, Lichtenberg D, and Pinchuk I. No evidence supports vitamin E indiscriminate supplementation. *Biofactors* 35: 469–473, 2009.
39. Edmondson DE, Mattevi A, Binda C, Li M, and Hubalek F. Structure and mechanism of monoamine oxidase. *Curr Med Chem* 11: 1983–1993, 2004.
40. Egner PA, Chen JG, Zarth AT, Ng DK, Wang JB, Kensler KH, Jacobson LP, Munoz A, Johnson JL, Groopman JD, Fahey JW, Talalay P, Zhu J, Chen TY, Qian GS, Carmella SG, Hecht SS, and Kensler TW. Rapid and sustainable detoxication of airborne pollutants by broccoli sprout beverage: results of a randomized clinical trial in China. *Cancer Prev Res (Phila)* 7: 813–823, 2014.
41. Elion GB. The purine path to chemotherapy. *Science* 244: 41–47, 1989.
42. Evgenov OV, Pacher P, Schmidt PM, Hasko G, Schmidt HH, and Stasch JP. NO-independent stimulators and activators of soluble guanylate cyclase: discovery and therapeutic potential. *Nat Rev Drug Discov* 5: 755–768, 2006.
43. Finberg JP and Gillman K. Selective inhibitors of monoamine oxidase type B and the ''cheese effect.'' *Int Rev Neurobiol* 100: 169–190, 2011.
44. Fleming I, Michaelis UR, Bredenkotter D, Fisslthaler B, Dehghani F, Brandes RP, and Busse R. Endothelium-derived hyperpolarizing factor synthase (Cytochrome P450 2C9) is a functionally significant source of reactive oxygen species in coronary arteries. *Circ Res* 88: 44–51, 2001.
45. Flores-Santana W, Salmon DJ, Donzelli S, Switzer CH, Basudhar D, Ridnour L, Cheng R, Glynn SA, Paolocci N, Fukuto JM, Miranda KM, and Wink DA. The specificity of nitroxyl chemistry is unique among nitrogen oxides in biological systems. *Antioxid Redox Signal* 14: 1659–1674, 2011.
46. Fravel MA and Ernst ME. Management of gout in the older adult. *Am J Geriatr Pharmacother* 9: 271–285, 2011.
47. Frijhoff J, Winyard PG, Zarkovic N, Davies SS, Stocker R, Cheng D, Knight AR, Taylor EL, Oettrich J, Ruskovska T, Gasparovic AC, Cuadrado A, Weber D, Poulsen HE, Grune T, Schmidt HHHW, and Ghezzi P. Clinical relevance of biomarkers of oxidative stress. *Antioxid Redox Signal* 23: 1144–1170, 2015.
48. Frohlich LG, Kotsonis P, Traub H, Taghavi-Moghadam S, Al-Masoudi N, Hofmann H, Strobel H, Matter H, Pfleiderer W, and Schmidt HH. Inhibition of neuronal nitric oxide synthase by 4-amino pteridine derivatives: structure-activity relationship of antagonists of (6R)-5,6,7,8-tetrahydrobiopterin cofactor. *J Med Chem* 42: 4108–4121, 1999.
49. Galle J, Zabel U, Hubner U, Hatzelmann A, Wagner B, Wanner C, and Schmidt HH. Effects of the soluble guanylyl cyclase activator, YC-1, on vascular tone, cyclic GMP levels and phosphodiesterase activity. *Br J Pharmacol* 127: 195–203, 1999.
50. Gatto GJ, Jr., Ao Z, Kearse MG, Zhou M, Morales CR, Daniels E, Bradley BT, Goserud MT, Goodman KB, Douglas SA, Harpel MR, and Johns DG. NADPH oxidase-dependent and -independent mechanisms of reported inhibitors of reactive oxygen generation. *J Enzyme Inhib Med Chem* 28: 95–104, 2013.
50a. Genkyotex Innovation SAS. 2015. Safety and Efficacy of Oral GKT137831 in Patient With Type 2 Diabetes and Albuminuria. National Institutes of Health, USA. https://clinicaltrials.gov/ct2/show/NCT02010242 (last accessed October 29, 2015).

51. Ghofrani HA, D'Armini AM, Grimminger F, Hoeper MM, Jansa P, Kim NH, Mayer E, Simonneau G, Wilkins MR, Fritsch A, Neuser D, Weimann G, and Wang C. Riociguat for the treatment of chronic thromboembolic pulmonary hypertension. *N Engl J Med* 369: 319–329, 2013.
52. Ghofrani HA, Galie N, Grimminger F, Grunig E, Humbert M, Jing ZC, Keogh AM, Langleben D, Kilama MO, Fritsch A, Neuser D, and Rubin LJ. Riociguat for the treatment of pulmonary arterial hypertension. *N Engl J Med* 369: 330–340, 2013.
53. Givertz MM, Anstrom KJ, Redfield MM, Deswal A, Haddad H, Butler J, Tang WH, Dunlap ME, LeWinter MM, Mann DL, Felker GM, O'Connor CM, Goldsmith SR, Ofili EO, Saltzberg MT, Margulies KB, Cappola TP, Konstam MA, Semigran MJ, McNulty SE, Lee KL, Shah MR, and Hernandez AF. Effects of xanthine oxidase inhibition in hyperuricemic heart failure patients: the xanthine oxidase inhibition for hyperuricemic heart failure patients (EXACT-HF) study. *Circulation* 131: 1763–1771, 2015.
54. Gorin Y, Cavaglieri RC, Khazim K, Lee DY, Bruno F, Thakur S, Fanti P, Szyndralewiez C, Barnes JL, Block K, and Abboud HE. Targeting NADPH oxidase with a novel dual Nox1/Nox4 inhibitor attenuates renal pathology in type 1 diabetes. *Am J Physiol Renal Physiol* 308: F1276–87, 2015.
55. Han SJ, Ahn Y, Park I, Zhang Y, Kim I, Kim HW, Ku CS, Chay KO, Yang SY, Ahn BW, Jang DI, and Lee SR. Assay of the redox state of the tumor suppressor PTEN by mobility shift. *Methods* 77–78: 58–62, 2015.
56. Hansel TT, Kharitonov SA, Donnelly LE, Erin EM, Currie MG, Moore WM, Manning PT, Recker DP, and Barnes PJ. A selective inhibitor of inducible nitric oxide synthase inhibits exhaled breath nitric oxide in healthy volunteers and asthmatics. *FASEB J* 17: 1298–1300, 2003.
57. Hast BE, Goldfarb D, Mulvaney KM, Hast MA, Siesser PF, Yan F, Hayes DN, and Major MB. Proteomic analysis of ubiquitin ligase KEAP1 reveals associated proteins that inhibit NRF2 ubiquitination. *Cancer Res* 73: 2199–2210, 2013.
58. Hayes JD and Dinkova-Kostova AT. The Nrf2 regulatory network provides an interface between redox and intermediary metabolism. *Trends Biochem Sci* 39: 199–218, 2014.
59. Hayes JD, McMahon M, Chowdhry S, and Dinkova-Kostova AT. Cancer chemoprevention mechanisms mediated through the Keap1-Nrf2 pathway. *Antioxid Redox Signal* 13: 1713–1748, 2010.
60. Henderson JP, Byun J, Williams MV, Mueller DM, McCormick ML, and Heinecke JW. Production of brominating intermediates by myeloperoxidase. A transhalogenation pathway for generating mutagenic nucleobases during inflammation. *J Biol Chem* 276: 7867–7875, 2001.
61. Higgins P, Dawson J, Lees KR, McArthur K, Quinn TJ, and Walters MR. Xanthine oxidase inhibition for the treatment of cardiovascular disease: a systematic review and meta-analysis. *Cardiovasc Ther* 30: 217–226, 2012.
62. Hirano K, Chen WS, Chueng AL, Dunne AA, Seredenina T, Filippova A, Ramachandran S, Bridges A, Chaudry L, Pettman G, Allan C, Duncan S, Lee KC, Lim J, Ma MT, Ong AB, Ye NY, Nasir S, Mulyanidewi S, Aw CC, Oon PP, Liao S, Li D, Johns DG, Miller ND, Davies CH, Browne ER, Matsuoka Y, Chen DW, Jaquet V, and Rutter AR. Discovery of GSK2795039, a novel small molecule NADPH oxidase 2 inhibitor. *Antioxid Redox Signal* 23: 358–374, 2015.
63. Hirschhäuser C,Bornbaum J, Reis A, Böhme S, Kaludercic N, Menabò R, Di Lisa F, Boengler K, Shah AM, Schulz R, and Schmidt HH. NOX4 in mitochondria: yeast two-hybrid-based interaction with complex I without relevance for basal reactive oxygen species? *Antioxid Redox Signal* 23: 1106–1112, 2015.
64. Hoffmann LS, Schmidt PM, Keim Y, Schaefer S, Schmidt HH, and Stasch JP. Distinct molecular requirements for activation or stabilization of soluble guanylyl cyclase upon haem oxidation-induced degradation. *Br J Pharmacol* 157: 781–795, 2009.
65. Hohn DC and Lehrer RI. NADPH oxidase deficiency in X-linked chronic granulomatous disease. *J Clin Invest* 55: 707–713, 1975.
66. Hong-Qi Y, Zhi-Kun S, and Sheng-Di C. Current advances in the treatment of Alzheimer's disease: focused on considerations targeting Abeta and tau. *Transl Neurodegener* 1: 21, 2012.
67. Hultqvist M, Olofsson P, Wallner FK, and Holmdahl R. Pharmacological potential of NOX2 agonists in inflammatory conditions. *Antioxid Redox Signal* 23: 446–459, 2015.
68. Irvine JC, Kemp-Harper BK, and Widdop RE. Chronic administration of the HNO donor Angeli's salt does not lead to tolerance, cross-tolerance, or endothelial dysfunction: comparison with GTN and DEA/NO. *Antioxid Redox Signal* 14: 1615–1624, 2011.
69. Jaquet V, Scapozza L, Clark RA, Krause KH, and Lambeth JD. Small-molecule NOX inhibitors: ROS-generating NADPH oxidases as therapeutic targets. *Antioxid Redox Signal* 11: 2535–2552, 2009.
70. Jha JC, Gray SP, Barit D, Okabe J, El-Osta A, Namikoshi T, Thallas-Bonke V, Wingler K, Szyndralewiez C, Heitz F, Touyz RM, Cooper ME, Schmidt HH, and Jandeleit-Dahm KA. Genetic targeting or pharmacologic inhibition of NADPH oxidase nox4 provides renoprotection in long-term diabetic nephropathy. *J Am Soc Nephrol* 25: 1237–1254, 2014.
71. Jo S, Yarishkin O, Hwang YJ, Chun YE, Park M, Woo DH, Bae JY, Kim T, Lee J, Chun H, Park HJ, Lee da Y, Hong J, Kim HY, Oh SJ, Park SJ, Lee H, Yoon BE, Kim Y, Jeong Y, Shim I, Bae YC, Cho J, Kowall NW, Ryu H, Hwang E, Kim D, and Lee CJ. GABA from reactive astrocytes impairs memory in mouse models of Alzheimer's disease. *Nat Med* 20: 886–896, 2014.
72. Jomova K and Valko M. Advances in metal-induced oxidative stress and human disease. *Toxicology* 283: 65–87, 2011.
73. Kaludercic N, Carpi A, Nagayama T, Sivakumaran V, Zhu G, Lai EW, Bedja D, De Mario A, Chen K, Gabrielson KL, Lindsey ML, Pacak K, Takimoto E, Shih JC, Kass DA, Di Lisa F, and Paolocci N. Monoamine oxidase B prompts mitochondrial and cardiac dysfunction in pressure overloaded hearts. *Antioxid Redox Signal* 20: 267–280, 2014.
74. Kaludercic N, Takimoto E, Nagayama T, Feng N, Lai EW, Bedja D, Chen K, Gabrielson KL, Blakely RD, Shih JC, Pacak K, Kass DA, Di Lisa F, and Paolocci N. Monoamine oxidase A-mediated enhanced catabolism of norepinephrine contributes to adverse remodeling and pump failure in hearts with pressure overload. *Circ Res* 106: 193–202, 2010.
75. Kappos L, Gold R, Arnold DL, Bar-Or A, Giovannoni G, Selmaj K, Sarda SP, Agarwal S, Zhang A, Sheikh SI, Seidman E, and Dawson KT. Quality of life outcomes with BG-12 (dimethyl fumarate) in patients with relapsing-remitting multiple sclerosis: the DEFINE study. *Mult Scler* 20: 243–252, 2014.
76. Kappos L, Gold R, Miller DH, Macmanus DG, Havrdova E, Limmroth V, Polman CH, Schmierer K, Yousry TA, Yang M, Eraksoy M, Meluzinova E, Rektor I, Dawson KT, San-

drock AW, and O'Neill GN. Efficacy and safety of oral fumarate in patients with relapsing-remitting multiple sclerosis: a multicentre, randomised, double-blind, placebo-controlled phase IIb study. *Lancet* 372: 1463–1472, 2008.
77. Kettle AJ, van Dalen CJ, and Winterbourn CC. Peroxynitrite and myeloperoxidase leave the same footprint in protein nitration. *Redox Rep* 3: 257–258, 1997.
78. Kim JE, You DJ, Lee C, Ahn C, Seong JY, and Hwang JI. Suppression of NF-kappaB signaling by KEAP1 regulation of IKKbeta activity through autophagic degradation and inhibition of phosphorylation. *Cell Signal* 22: 1645–1654, 2010.
79. Kitagishi Y and Matsuda S. Redox regulation of tumor suppressor PTEN in cancer and aging (Review). *Int J Mol Med* 31: 511–515, 2013.
80. Klebanoff SJ. Myeloperoxidase-halide-hydrogen peroxide antibacterial system. *J Bacteriol* 95: 2131–2138, 1968.
81. Kleinschnitz C, Grund H, Wingler K, Armitage ME, Jones E, Mittal M, Barit D, Schwarz T, Geis C, Kraft P, Barthel K, Schuhmann MK, Herrmann AM, Meuth SG, Stoll G, Meurer S, Schrewe A, Becker L, Gailus-Durner V, Fuchs H, Klopstock T, de Angelis MH, Jandeleit-Dahm K, Shah AM, Weissmann N, and Schmidt HH. Post-stroke inhibition of induced NADPH oxidase type 4 prevents oxidative stress and neurodegeneration. *PLoS Biol* 8: pii: e1000479, 2010.
82. Laleu B, Gaggini F, Orchard M, Fioraso-Cartier L, Cagnon L, Houngninou-Molango S, Gradia A, Duboux G, Merlot C, Heitz F, Szyndralewiez C, and Page P. First in class, potent, and orally bioavailable NADPH oxidase isoform 4 (Nox4) inhibitors for the treatment of idiopathic pulmonary fibrosis. *J Med Chem* 53: 7715–7730, 2010.
83. Lass A, Suessenbacher A, Wolkart G, Mayer B, and Brunner F. Functional and analytical evidence for scavenging of oxygen radicals by L-arginine. *Mol Pharmacol* 61: 1081–1088, 2002.
84. Lee SR, Yang KS, Kwon J, Lee C, Jeong W, and Rhee SG. Reversible inactivation of the tumor suppressor PTEN by H2O2. *J Biol Chem* 277: 20336–20342, 2002.
85. Leto TL, Morand S, Hurt D, and Ueyama T. Targeting and regulation of reactive oxygen species generation by Nox family NADPH oxidases. *Antioxid Redox Signal* 11: 2607–2619, 2009.
86. Lim FP and Dolzhenko AV. 1,3,5-Triazine-based analogues of purine: from isosteres to privileged scaffolds in medicinal chemistry. *Eur J Med Chem* 85: 371–390, 2014.
87. Linker RA, Lee DH, Ryan S, van Dam AM, Conrad R, Bista P, Zeng W, Hronowsky X, Buko A, Chollate S, Ellrichmann G, Bruck W, Dawson K, Goelz S, Wiese S, Scannevin RH, Lukashev M, and Gold R. Fumaric acid esters exert neuroprotective effects in neuroinflammation via activation of the Nrf2 antioxidant pathway. *Brain* 134: 678–692, 2011.
88. Liu C, Desikan R, Ying Z, Gushchina L, Kampfrath T, Deiuliis J, Wang A, Xu X, Zhong J, Rao X, Sun Q, Maiseyeu A, Parthasarathy S, and Rajagopalan S. Effects of a novel pharmacologic inhibitor of myeloperoxidase in a mouse atherosclerosis model. *PLoS One* 7: e50767, 2012.
89. Lopez A, Lorente JA, Steingrub J, Bakker J, McLuckie A, Willatts S, Brockway M, Anzueto A, Holzapfel L, Breen D, Silverman MS, Takala J, Donaldson J, Arneson C, Grove G, Grossman S, and Grover R. Multiple-center, randomized, placebo-controlled, double-blind study of the nitric oxide synthase inhibitor 546C88: effect on survival in patients with septic shock. *Crit Care Med* 32: 21–30, 2004.
90. Ma Q. Role of nrf2 in oxidative stress and toxicity. *Annu Rev Pharmacol Toxicol* 53: 401–426, 2013.
91. Ma Q and He X. Molecular basis of electrophilic and oxidative defense: promises and perils of Nrf2. *Pharmacol Rev* 64: 1055–1081, 2012.
92. Malle E, Furtmuller PG, Sattler W, and Obinger C. Myeloperoxidase: a target for new drug development? *Br J Pharmacol* 152: 838–854, 2007.
93. Matsumoto K, Okamoto K, Ashizawa N, and Nishino T. FYX-051: a novel and potent hybrid-type inhibitor of xanthine oxidoreductase. *J Pharmacol Exp Ther* 336: 95–103, 2011.
94. Matsumura F, Yamaguchi Y, Goto M, Ichiguchi O, Akizuki E, Matsuda T, Okabe K, Liang J, Ohshiro H, Iwamoto T, Yamada S, Mori K, and Ogawa M. Xanthine oxidase inhibition attenuates kupffer cell production of neutrophil chemoattractant following ischemia-reperfusion in rat liver. *Hepatology* 28: 1578–1587, 1998.
95. McManaman JL and Bain DL. Structural and conformational analysis of the oxidase to dehydrogenase conversion of xanthine oxidoreductase. *J Biol Chem* 277: 21261–21268, 2002.
96. McNally JS, Davis ME, Giddens DP, Saha A, Hwang J, Dikalov S, Jo H, and Harrison DG. Role of xanthine oxidoreductase and NAD(P)H oxidase in endothelial superoxide production in response to oscillatory shear stress. *Am J Physiol Heart Circ Physiol* 285: H2290–H2297, 2003.
97. Melichar VO, Behr-Roussel D, Zabel U, Uttenthal LO, Rodrigo J, Rupin A, Verbeuren TJ, Kumar HSA, and Schmidt HH. Reduced cGMP signaling associated with neointimal proliferation and vascular dysfunction in late-stage atherosclerosis. *Proc Natl Acad Sci U S A* 101: 16671–16676, 2004.
98. Menazza S, Blaauw B, Tiepolo T, Toniolo L, Braghetta P, Spolaore B, Reggiani C, Di Lisa F, Bonaldo P, and Canton M. Oxidative stress by monoamine oxidases is causally involved in myofiber damage in muscular dystrophy. *Hum Mol Genet* 19: 4207–4215, 2010.
99. Meurer S, Pioch S, Pabst T, Opitz N, Schmidt PM, Beckhaus T, Wagner K, Matt S, Gegenbauer K, Geschka S, Karas M, Stasch JP, Schmidt HH, and Muller-Esterl W. Nitric oxide-independent vasodilator rescues heme-oxidized soluble guanylate cyclase from proteasomal degradation. *Circ Res* 105: 33–41, 2009.
100. Millar TM, Stevens CR, Benjamin N, Eisenthal R, Harrison R, and Blake DR. Xanthine oxidoreductase catalyses the reduction of nitrates and nitrite to nitric oxide under hypoxic conditions. *FEBS Lett* 427: 225–228, 1998.
101. Miller ER, 3rd, Pastor-Barriuso R, Dalal D, Riemersma RA, Appel LJ, and Guallar E. Meta-analysis: high-dosage vitamin E supplementation may increase all-cause mortality. *Ann Intern Med* 142: 37–46, 2005.
102. Miller RT, Martasek P, Roman LJ, Nishimura JS, and Masters BS. Involvement of the reductase domain of neuronal nitric oxide synthase in superoxide anion production. *Biochemistry* 36: 15277–15284, 1997.
103. Miranda KM, Yamada K, Espey MG, Thomas DD, DeGraff W, Mitchell JB, Krishna MC, Colton CA, and Wink DA. Further evidence for distinct reactive intermediates from nitroxyl and peroxynitrite: effects of buffer composition on the chemistry of Angeli's salt and synthetic peroxynitrite. *Arch Biochem Biophys* 401: 134–144, 2002.
104. Moorhouse PC, Grootveld M, Halliwell B, Quinlan JG, and Gutteridge JM. Allopurinol and oxypurinol are hydroxyl radical scavengers. *FEBS Lett* 213: 23–28, 1987.
105. Motohashi H and Yamamoto M. Nrf2-Keap1 defines a physiologically important stress response mechanism. *Trends Mol Med* 10: 549–557, 2004.

106. Nicholls SJ and Hazen SL. Myeloperoxidase and cardiovascular disease. *Arterioscler Thromb Vasc Biol* 25: 1102–1111, 2005.
107. Nishino T. The conversion from the dehydrogenase type to the oxidase type of rat liver xanthine dehydrogenase by modification of cysteine residues with fluorodinitrobenzene. *J Biol Chem* 272: 29859–29864, 1997.
108. Nishino T and Okamoto K. Mechanistic insights into xanthine oxidoreductase from development studies of candidate drugs to treat hyperuricemia and gout. *J Biol Inorg Chem* 20:195–207, 2015.
109. Niture SK and Jaiswal AK. INrf2 (Keap1) targets Bcl-2 degradation and controls cellular apoptosis. *Cell Death Differ* 18: 439–451, 2011.
110. Okamoto K, Eger BT, Nishino T, Kondo S, Pai EF, and Nishino T. An extremely potent inhibitor of xanthine oxidoreductase. Crystal structure of the enzyme-inhibitor complex and mechanism of inhibition. *J Biol Chem* 278: 1848–1855, 2003.
111. Okamoto K, Eger BT, Nishino T, Pai EF, and Nishino T. Mechanism of inhibition of xanthine oxidoreductase by allopurinol: crystal structure of reduced bovine milk xanthine oxidoreductase bound with oxipurinol. *Nucleosides Nucleotides Nucleic Acids* 27: 888–893, 2008.
112. Okamoto K and Nishino T. Mechanism of inhibition of xanthine oxidase with a new tight binding inhibitor. *J Biol Chem* 270: 7816–7821, 1995.
113. Paolocci N, Saavedra WF, Miranda KM, Martignani C, Isoda T, Hare JM, Espey MG, Fukuto JM, Feelisch M, Wink DA, and Kass DA. Nitroxyl anion exerts redox-sensitive positive cardiac inotropy in vivo by calcitonin gene-related peptide signaling. *Proc Natl Acad Sci U S A* 98: 10463–10468, 2001.
114. Pitha-Rowe I, Liby K, Royce D, and Sporn M. Synthetic triterpenoids attenuate cytotoxic retinal injury: cross-talk between Nrf2 and PI3K/AKT signaling through inhibition of the lipid phosphatase PTEN. *Invest Ophthalmol Vis Sci* 50: 5339–5347, 2009.
115. Podrez EA, Abu-Soud HM, and Hazen SL. Myeloperoxidase-generated oxidants and atherosclerosis. *Free Radic Biol Med* 28: 1717–1725, 2000.
116. Posener JA, Hauser RA, Stieber M, Leventer SM, Eketjäll S, Minkwitz MC, Ingersoll EW, and Kugler AR. Safety, tolerability, and pharmacodynamics of AZD3241, a myeloperoxidase inhibitor, in Parkinson's disease [abstract]. *Movement Disord* 29 (Suppl 1): 698, 2014.
117. Rada P, Rojo AI, Chowdhry S, McMahon M, Hayes JD, and Cuadrado A. SCF/{beta}-TrCP promotes glycogen synthase kinase 3-dependent degradation of the Nrf2 transcription factor in a Keap1-independent manner. *Mol Cell Biol* 31: 1121–1133, 2011.
118. Rada P, Rojo AI, Evrard-Todeschi N, Innamorato NG, Cotte A, Jaworski T, Tobon-Velasco JC, Devijver H, Garcia-Mayoral MF, Van Leuven F, Hayes JD, Bertho G, and Cuadrado A. Structural and functional characterization of Nrf2 degradation by the glycogen synthase kinase 3/beta-TrCP axis. *Mol Cell Biol* 32: 3486–3499, 2012.
119. Reif A, Frohlich LG, Kotsonis P, Frey A, Bommel HM, Wink DA, Pfleiderer W, and Schmidt HH. Tetrahydrobiopterin inhibits monomerization and is consumed during catalysis in neuronal NO synthase. *J Biol Chem* 274: 24921–24929, 1999.
120. Rojo AI, Medina-Campos ON, Rada P, Zuniga-Toala A, Lopez-Gazcon A, Espada S, Pedraza-Chaverri J, and Cuadrado A. Signaling pathways activated by the phytochemical nordihydroguaiaretic acid contribute to a Keap1-independent regulation of Nrf2 stability: role of glycogen synthase kinase-3. *Free Radic Biol Med* 52: 473–487, 2012.
121. Rojo AI, Rada P, Mendiola M, Ortega-Molina A, Wojdyla K, Rogowska-Wrzesinska A, Hardisson D, Serrano M, and Cuadrado A. The PTEN/NRF2 axis promotes human carcinogenesis. *Antioxid Redox Signal* 21: 2498–2514, 2014.
122. Sabbah HN, Tocchetti CG, Wang M, Daya S, Gupta RC, Tunin RS, Mazhari R, Takimoto E, Paolocci N, Cowart D, Colucci WS, and Kass DA. Nitroxyl (HNO): a novel approach for the acute treatment of heart failure. *Circ Heart Fail* 6: 1250–1258, 2013.
123. Sanders SA, Eisenthal R, and Harrison R. NADH oxidase activity of human xanthine oxidoreductase—generation of superoxide anion. *Eur J Biochem* 245: 541–548, 1997.
124. Savenkova ML, Mueller DM, and Heinecke JW. Tyrosyl radical generated by myeloperoxidase is a physiological catalyst for the initiation of lipid peroxidation in low density lipoprotein. *J Biol Chem* 269: 20394–20400, 1994.
125. Schildknecht S, Weber A, Gerding HR, Pape R, Robotta M, Drescher M, Marquardt A, Daiber A, Ferger B, and Leist M. The NOX1/4 inhibitor GKT136901 as selective and direct scavenger of peroxynitrite. *Curr Med Chem* 21: 365–376, 2013.
126. Schindler U, Strobel H, Schonafinger K, Linz W, Lohn M, Martorana PA, Rutten H, Schindler PW, Busch AE, Sohn M, Topfer A, Pistorius A, Jannek C, and Mulsch A. Biochemistry and pharmacology of novel anthranilic acid derivatives activating heme-oxidized soluble guanylyl cyclase. *Mol Pharmacol* 69: 1260–1268, 2006.
127. Schmidt HH, Stocker R, Vollbracht C, Paulsen G, Riley D, Daiber A, and Cuadrado A. Antioxidants in translational medicine. *Antioxid Redox Signal* 23: 1130–1143, 2015.
128. Seidel P and Roth M. Anti-inflammatory dimethylfumarate: a potential new therapy for asthma? *Mediators Inflamm* 2013: 875403, 2013.
129. Shiina A, Kanahara N, Sasaki T, Oda Y, Hashimoto T, Hasegawa T, Yoshida T, Iyo M, and Hashimoto K. An open study of sulforaphane-rich broccoli sprout extract in patients with schizophrenia. *Clin Psychopharmacol Neurosci* 13: 62–67, 2015.
130. Shulman KI, Herrmann N, and Walker SE. Current place of monoamine oxidase inhibitors in the treatment of depression. *CNS Drugs* 27: 789–797, 2013.
131. Singh H, Sharma S, Ojha R, Gupta MK, Nepali K, and Bedi PM. Synthesis and evaluation of naphthoflavones as a new class of non purine xanthine oxidase inhibitors. *Bioorg Med Chem Lett* 24: 4192–4197, 2014.
132. Singh K, Connors SL, Macklin EA, Smith KD, Fahey JW, Talalay P, and Zimmerman AW. Sulforaphane treatment of autism spectrum disorder (ASD). *Proc Natl Acad Sci U S A* 111: 15550–15555, 2014.
133. Skatchkov M, Larina LL, Larin AA, Fink N, and Bassenge E. Urinary NItrotyrosine content as a marker of peroxynitrite-induced tolerance to organic NItrates. *J Cardiovasc Pharmacol Ther* 2: 85–96, 1997.
134. Skulachev VP. Role of uncoupled and non-coupled oxidations in maintenance of safely low levels of oxygen and its one-electron reductants. *Q Rev Biophys* 29: 169–202, 1996.
135. Slocum SL and Kensler TW. Nrf2: control of sensitivity to carcinogens. *Arch Toxicol* 85: 273–284, 2011.
136. Sorato E, Menazza S, Zulian A, Sabatelli P, Gualandi F, Merlini L, Bonaldo P, Canton M, Bernardi P, and Di Lisa F. Monoamine oxidase inhibition prevents mitochondrial dys-

function and apoptosis in myoblasts from patients with collagen VI myopathies. *Free Radic Biol Med* 75: 40–47, 2014.
137. Stasch JP, Schlossmann J, and Hocher B. Renal effects of soluble guanylate cyclase stimulators and activators: a review of the preclinical evidence. *Curr Opin Pharmacol* 21c: 95–104, 2015.
138. Stasch JP, Schmidt PM, Nedvetsky PI, Nedvetskaya TY, H S AK, Meurer S, Deile M, Taye A, Knorr A, Lapp H, Muller H, Turgay Y, Rothkegel C, Tersteegen A, Kemp-Harper B, Muller-Esterl W, and Schmidt HH. Targeting the heme-oxidized nitric oxide receptor for selective vasodilatation of diseased blood vessels. *J Clin Invest* 116: 2552–2561, 2006.
139. Stielow C, Catar RA, Muller G, Wingler K, Scheurer P, Schmidt HH, and Morawietz H. Novel Nox inhibitor of oxLDL-induced reactive oxygen species formation in human endothelial cells. *Biochem Biophys Res Commun* 344: 200–205, 2006.
140. Stirpe F and Della Corte E. The regulation of rat liver xanthine oxidase. Conversion in vitro of the enzyme activity from dehydrogenase (type D) to oxidase (type O). *J Biol Chem* 244: 3855–3863, 1969.
141. Stover JF, Belli A, Boret H, Bulters D, Sahuquillo J, Schmutzhard E, Zavala E, Ungerstedt U, Schinzel R, and Tegtmeier F. Nitric oxide synthase inhibition with the antipterin VAS203 improves outcome in moderate and severe traumatic brain injury: a placebo-controlled randomized Phase IIa trial (NOSTRA). *J Neurotrauma* 31: 1599–1606, 2014.
142. Strengert M, Jennings R, Davanture S, Hayes P, Gabriel G, and Knaus UG. Mucosal reactive oxygen species are required for antiviral response: role of Duox in influenza a virus infection. *Antioxid Redox Signal* 20: 2695–2709, 2014.
143. Stroes E, Kastelein J, Cosentino F, Erkelens W, Wever R, Koomans H, Luscher T, and Rabelink T. Tetrahydrobiopterin restores endothelial function in hypercholesterolemia. *J Clin Invest* 99: 41–46, 1997.
144. Sun QA, Hess DT, Wang B, Miyagi M, and Stamler JS. Off-target thiol alkylation by the NADPH oxidase inhibitor 3-benzyl-7-(2-benzoxazolyl)thio-1,2,3-triazolo[4,5-d]pyrimidine (VAS2870). *Free Radic Biol Med* 52: 1897–1902, 2012.
145. Suzuki H, DeLano FA, Parks DA, Jamshidi N, Granger DN, Ishii H, Suematsu M, Zweifach BW, and Schmid-Schonbein GW. Xanthine oxidase activity associated with arterial blood pressure in spontaneously hypertensive rats. *Proc Natl Acad Sci U S A* 95: 4754–4759, 1998.
146. Takano Y, Hase-Aoki K, Horiuchi H, Zhao L, Kasahara Y, Kondo S, and Becker MA. Selectivity of febuxostat, a novel non-purine inhibitor of xanthine oxidase/xanthine dehydrogenase. *Life Sci* 76: 1835–1847, 2005.
147. Takaya K, Suzuki T, Motohashi H, Onodera K, Satomi S, Kensler TW, and Yamamoto M. Validation of the multiple sensor mechanism of the Keap1-Nrf2 system. *Free Radic Biol Med* 53: 817–827, 2012.
148. ten Freyhaus H, Huntgeburth M, Wingler K, Schnitker J, Baumer AT, Vantler M, Bekhite MM, Wartenberg M, Sauer H, and Rosenkranz S. Novel Nox inhibitor VAS2870 attenuates PDGF-dependent smooth muscle cell chemotaxis, but not proliferation. *Cardiovasc Res* 71: 331–341, 2006.
149. Thomas EL, Bozeman PM, Jefferson MM, and King CC. Oxidation of bromide by the human leukocyte enzymes myeloperoxidase and eosinophil peroxidase. Formation of bromamines. *J Biol Chem* 270: 2906–2913, 1995.
150. Tiden AK, Sjogren T, Svensson M, Bernlind A, Senthilmohan R, Auchere F, Norman H, Markgren PO, Gustavsson S, Schmidt S, Lundquist S, Forbes LV, Magon NJ, Paton LN, Jameson GN, Eriksson H, and Kettle AJ. 2-thioxanthines are mechanism-based inactivators of myeloperoxidase that block oxidative stress during inflammation. *J Biol Chem* 286: 37578–37589, 2011.
151. Tocchetti CG, Stanley BA, Murray CI, Sivakumaran V, Donzelli S, Mancardi D, Pagliaro P, Gao WD, van Eyk J, Kass DA, Wink DA, and Paolocci N. Playing with cardiac ''redox switches'': the ''HNO way'' to modulate cardiac function. *Antioxid Redox Signal* 14: 1687–1698, 2011.
152. Tong KI, Padmanabhan B, Kobayashi A, Shang C, Hirotsu Y, Yokoyama S, and Yamamoto M. Different electrostatic potentials define ETGE and DLG motifs as hinge and latch in oxidative stress response. *Mol Cell Biol* 27: 7511–7521, 2007.
153. Tsianakas A, Herzog S, Landmann A, Patsinakidis N, Perusquia Ortiz AM, Bonsmann G, Luger TA, and Kuhn A. Successful treatment of discoid lupus erythematosus with fumaric acid esters. *J Am Acad Dermatol* 71: e15-7, 2014.
154. Van der Schueren BJ, Lunnon MW, Laurijssens BE, Guillard F, Palmer J, Van Hecken A, Depre M, Vanmolkot FH, and de Hoon JN. Does the unfavorable pharmacokinetic and pharmacodynamic profile of the iNOS inhibitor GW273629 lead to inefficacy in acute migraine? *J Clin Pharmacol* 49: 281–290, 2009.
155. Vasquez-Vivar J, Kalyanaraman B, Martasek P, Hogg N, Masters BS, Karoui H, Tordo P, and Pritchard KA, Jr. Superoxide generation by endothelial nitric oxide synthase: the influence of cofactors. *Proc Natl Acad Sci U S A* 95: 9220–9225, 1998.
156. Villeneuve C, Guilbeau-Frugier C, Sicard P, Lairez O, Ordener C, Duparc T, De Paulis D, Couderc B, Spreux-Varoquaux O, Tortosa F, Garnier A, Knauf C, Valet P, Borchi E, Nediani C, Gharib A, Ovize M, Delisle MB, Parini A, and Mialet-Perez J. p53-PGC-1alpha pathway mediates oxidative mitochondrial damage and cardiomyocyte necrosis induced by monoamine oxidase-A upregulation: role in chronic left ventricular dysfunction in mice. *Antioxid Redox Signal* 18: 5–18, 2013.
157. Wang YY, Yang YX, Zhe H, He ZX, and Zhou SF. Bardoxolone methyl (CDDO-Me) as a therapeutic agent: an update on its pharmacokinetic and pharmacodynamic properties. *Drug Des Devel Ther* 8: 2075–2088, 2014.
158. Weinreb RN, Ong T, Scassellati Sforzolini B, Vittitow JL, Singh K, and Kaufman PL. A randomised, controlled comparison of latanoprostene bunod and latanoprost 0.005% in the treatment of ocular hypertension and open angle glaucoma: the VOYAGER study. *Br J Ophthalmol* 99: 738–745, 2015.
159. Weiss SJ, Test ST, Eckmann CM, Roos D, and Regiani S. Brominating oxidants generated by human eosinophils. *Science* 234: 200–203, 1986.
160. Wenzel P, Schulz E, Oelze M, Muller J, Schuhmacher S, Alhamdani MS, Debrezion J, Hortmann M, Reifenberg K, Fleming I, Munzel T, and Daiber A. AT1-receptor blockade by telmisartan upregulates GTP-cyclohydrolase I and protects eNOS in diabetic rats. *Free Radic Biol Med* 45: 619–626, 2008.
161. Williams HC and Griendling KK. NADPH oxidase inhibitors: new antihypertensive agents? *J Cardiovasc Pharmacol* 50: 9–16, 2007.
162. Wimbiscus M, Kostenko O, and Malone D. MAO inhibitors: risks, benefits, and lore. *Cleve Clin J Med* 77: 859–882, 2010.
163. Wingler K, Hermans JJ, Schiffers P, Moens A, Paul M, and Schmidt HH. NOX1, 2, 4, 5: counting out oxidative stress. *Br J Pharmacol* 164: 866–883, 2011.
164. Winterbourn CC and Kettle AJ. Biomarkers of myeloperoxidase-derived hypochlorous acid. *Free Radic Biol Med* 29: 403–409, 2000.

165. Wu JB, Shao C, Li X, Li Q, Hu P, Shi C, Li Y, Chen YT, Yin F, Liao CP, Stiles BL, Zhau HE, Shih JC, and Chung LW. Monoamine oxidase A mediates prostate tumorigenesis and cancer metastasis. *J Clin Invest* 124: 2891–2908, 2014.
166. Yamamoto T, Moriwaki Y, Fujimura Y, Takahashi S, Tsutsumi Z, Tsutsui T, Higashino K, and Hada T. Effect of TEI-6720, a xanthine oxidase inhibitor, on the nucleoside transport in the lung cancer cell line A549. *Pharmacology* 60: 34–40, 2000.
167. Youdim MB and Weinstock M. Therapeutic applications of selective and non-selective inhibitors of monoamine oxidase A and B that do not cause significant tyramine potentiation. *Neurotoxicology* 25: 243–250, 2004.
168. Yusuf S, Dagenais G, Pogue J, Bosch J, and Sleight P. Vitamin E supplementation and cardiovascular events in high-risk patients. The heart outcomes prevention evaluation study investigators. *N Engl J Med* 342: 154–160, 2000.
169. Yusuf S, Sleight P, Pogue J, Bosch J, Davies R, and Dagenais G. Effects of an angiotensin-converting-enzyme inhibitor, ramipril, on cardiovascular events in high-risk patients. The heart outcomes prevention evaluation study investigators. *N Engl J Med* 342: 145–153, 2000.
170. Zhang R, Brennan ML, Shen Z, MacPherson JC, Schmitt D, Molenda CE, and Hazen SL. Myeloperoxidase functions as a major enzymatic catalyst for initiation of lipid peroxidation at sites of inflammation. *J Biol Chem* 277: 46116–46122, 2002.
171. Zielonka J, Cheng G, Zielonka M, Ganesh T, Sun A, Joseph J, Michalski R, O'Brien WJ, Lambeth JD, and Kalyanaraman B. High-throughput assays for superoxide and hydrogen peroxide: design of a screening workflow to identify inhibitors of NADPH oxidases. *J Biol Chem* 289: 16176–16189, 2014.

Address correspondence to:
*Dr. V. Thao-Vi Dao*
*Department of Pharmacology*
*Maastricht University*
*Cardiovascular Research Institute Maastricht (CARIM)*
*Maastricht 6229 ER*
*The Netherlands*

*E-mail:* v.dao@maastrichtuniversity.nl

*Dr. Harald HHW Schmidt*
*Department of Pharmacology*
*Maastricht University*
*Cardiovascular Research Institute Maastricht (CARIM)*
*Maastricht 6229 ER*
*The Netherlands*

*E-mail:* h.schmidt@maastrichtuniversity.nl

Date of first submission to ARS Central, June 24, 2015; date of final revised submission, September 15, 2015; date of acceptance, September 21, 2015.

**Abbreviations Used**

ADMA = asymmetric-dimethyl-L-arginine
apo-sGC = heme-free soluble guanylate cyclase
ARE = antioxidant responsive element
$BH_4$ = tetrahydrobiopterin
bZIP = basic region-leucine zipper
CDDO = 2-cyano-3,12-dioxooleana-1,9-dien-28-oic acid
cGMP = cyclic guanosine monophosphate
COPD = chronic obstructive pulmonary disease
CYBA = cytochrome b alpha subunit
DGR = double glycine repeat
DLG = aspartate leucine glycine.
DMF = dimethyl fumarate
DUOX = dual oxidase
eNOS = endothelial NO synthase
ETGE = glutamate, threonine, glycine, and glutamate
FAD = flavin adenine dinucleotide
GPx = glutathione peroxidase
$H_2O_2$ = hydrogen peroxide
HOBr = hypobromous acid
$IC_{50}$ = half maximal inhibitory concentration
KEAP1 = kelch-like ECH-associated protein 1
LDL = low-density lipoprotein
L-NIL = N6-(1-iminoethyl)-L-lysine
L-NMMA = 1-(4-aminopentyl)-2-methylguanidine
MAO = monoamine oxidases
MPO = myeloperoxidase
NAD = nicotinamide adenine dinucleotide
NADPH = nicotinamide adenine dinucleotide phosphate
NO = nitric oxide
NOS = nitric oxide synthase
NOX = nicotinamide adenine dinucleotide phosphate oxidase
NRF2 = nuclear factor (erythroid-derived 2)-like 2
$O_2^-$ = superoxide anion
PD = Parkinson's disease
PTEN = phosphatase and tensin homolog
Rbx = ring box protein
ROS = reactive oxygen species
SFN = isothiocyanate sulforaphane
sGC = soluble guanylate cyclase
SOD = superoxide dismutase
TPx = thioredoxin peroxidase
uc-NOS = uncoupled nitric oxide synthase
XD = xanthine dehydrogenase
XO = xanthine oxidase
XOR = xanthine oxidoreductase

Redox Biology 13 (2017) 94–162

Contents lists available at ScienceDirect

Redox Biology

journal homepage: www.elsevier.com/locate/redox

Review article

# European contribution to the study of ROS: A summary of the findings and prospects for the future from the COST action BM1203 (EU-ROS)

Javier Egea[a,1], Isabel Fabregat[b,1], Yves M. Frapart[c,1], Pietro Ghezzi[d,1], Agnes Görlach[e,f,1], Thomas Kietzmann[g,1], Kateryna Kubaichuk[g,1], Ulla G. Knaus[h,1], Manuela G. Lopez[a,1], Gloria Olaso-Gonzalez[i,1], Andreas Petry[e,1], Rainer Schulz[j,1], Jose Vina[i,1], Paul Winyard[k,1], Kahina Abbas[c], Opeyemi S. Ademowo[l], Catarina B. Afonso[m], Ioanna Andreadou[n], Haike Antelmann[o], Fernando Antunes[p], Mutay Aslan[q], Markus M. Bachschmid[r], Rui M. Barbosa[s], Vsevolod Belousov[t], Carsten Berndt[u], David Bernlohr[v], Esther Bertrán[b], Alberto Bindoli[w], Serge P. Bottari[x], Paula M. Brito[y,z], Guia Carrara[aa], Ana I. Casas[ab], Afroditi Chatzi[ac], Niki Chondrogianni[ad], Marcus Conrad[ae], Marcus S. Cooke[af], João G. Costa[y,ag], Antonio Cuadrado[ah], Pham My-Chan Dang[ai], Barbara De Smet[aj,aw,cp,cr], Bilge Debelec–Butuner[ak], Irundika H.K. Dias[l], Joe Dan Dunn[al], Amanda J. Edson[am], Mariam El Assar[an], Jamel El-Benna[ai], Péter Ferdinandy[ao,cr], Ana S. Fernandes[ag], Kari E. Fladmark[am], Ulrich Förstermann[ap], Rashid Giniatullin[aq], Zoltán Giricz[ao,cr], Anikó Görbe[ao,cr], Helen Griffiths[l,ar], Vaclav Hampl[as], Alina Hanf[at], Jan Herget[as], Pablo Hernansanz-Agustín[au,av], Melanie Hillion[o], Jingjing Huang[aj,aw,cq,cs], Serap Ilikay[ax], Pidder Jansen-Dürr[ay], Vincent Jaquet[az], Jaap A. Joles[ba], Balaraman Kalyanaraman[bb], Danylo Kaminskyy[bc], Mahsa Karbaschi[af], Marina Kleanthous[bd], Lars-Oliver Klotz[be], Bato Korac[bf], Kemal Sami Korkmaz[bg], Rafal Koziel[ay], Damir Kračun[e], Karl-Heinz Krause[az], Vladimír Křen[bh], Thomas Krieg[bi], João Laranjinha[s], Antigone Lazou[bj], Huige Li[ap], Antonio Martínez-Ruiz[au,bk], Reiko Matsui[r], Gethin J. McBean[bl], Stuart P. Meredith[m], Joris Messens[aw,cs], Verónica Miguel[bm], Yuliya Mikhed[at], Irina Milisav[bn], Lidija Milković[bo], Antonio Miranda-Vizuete[bp], Miloš Mojović[bq], María Monsalve[br], Pierre-Alexis Mouthuy[bs], John Mulvey[bi], Thomas Münzel[at], Vladimir Muzykantov[bt], Isabel T.N. Nguyen[ba], Matthias Oelze[at], Nuno G. Oliveira[y], Carlos M. Palmeira[bu,ct], Nikoletta Papaevgeniou[ad], Aleksandra Pavićević[bq], Brandán Pedre[aw,cs], Fabienne Peyrot[c,bv], Marios Phylactides[bd], Gratiela G. Pircalabioru[bw], Andrew R. Pitt[m], Henrik E. Poulsen[bx,cu,cv], Ignacio Prieto[br], Maria Pia Rigobello[by], Natalia Robledinos-Antón[ah], Leocadio Rodríguez-Mañas[an,bz], Anabela P. Rolo[bu,ct], Francis Rousset[az], Tatjana Ruskovska[cb], Nuno Saraiva[ag], Shlomo Sasson[cc], Katrin Schröder[cd,ce], Khrystyna Semen[bc], Tamara Seredenina[az], Anastasia Shakirzyanova[aq], Geoffrey L. Smith[aa], Thierry Soldati[al], Bebiana C. Sousa[m], Corinne M. Spickett[l], Ana Stancic[bf], Marie José Stasia[cf,cg], Holger Steinbrenner[be], Višnja Stepanić[bo], Sebastian Steven[at], Kostas Tokatlidis[ac], Erkan Tuncay[ch], Belma Turan[ch], Fulvio Ursini[ci], Jan Vacek[cj], Olga Vajnerova[as], Kateřina Valentová[bh], Frank Van Breusegem[aj,cq], Lokman Varisli[ax], Elizabeth A. Veal[ck], A. Suha Yalçın[cl], Olha Yelisyeyeva[bc], Neven Žarković[bs], Martina Zatloukalová[cj], Jacek Zielonka[bb], Rhian M. Touyz[cm,1], Andreas Papapetropoulos[cn,1], Tilman Grune[co,1], Santiago Lamas[bm,1], Harald H.H.W. Schmidt[ab,1], Fabio Di Lisa[cp,*,1], Andreas Daiber[at,ce,**,1]

[a] Institute Teofilo Hernando, Department of Pharmacology, School of Medicine. Univerisdad Autonoma de Madrid, Spain
[b] Bellvitge Biomedical Research Institute (IDIBELL) and University of Barcelona (UB), L'Hospitalet, Barcelona, Spain

[*] Corresponding author at: Universitätsmedizin der Johannes Gutenberg-Universität Mainz, Zentrum für Kardiologie/Kardiologie 1, Langenbeckstr. 1, 55131 Mainz, Germany.
[**] Corresponding author at: Department of Biomedical Sciences, University of Padova, Italy.
*E-mail addresses:* dilisa@bio.unipd.it (F. Di Lisa), daiber@uni-mainz.de (A. Daiber).

http://dx.doi.org/10.1016/j.redox.2017.05.007
Received 5 May 2017; Accepted 8 May 2017
Available online 18 May 2017

[c] LCBPT, UMR 8601 CNRS - Paris Descartes University, Sorbonne Paris Cité, Paris, France
[d] Brighton & Sussex Medical School, Brighton, UK
[e] Experimental and Molecular Pediatric Cardiology, German Heart Center Munich at the Technical University Munich, Munich, Germany
[f] DZHK (German Centre for Cardiovascular Research), partner site Munich Heart Alliance, Munich, Germany
[g] Faculty of Biochemistry and Molecular Medicine, and Biocenter Oulu, University of Oulu, Oulu, Finland
[h] Conway Institute, School of Medicine, University College Dublin, Dublin, Ireland
[i] Department of Physiology, University of Valencia, Spain
[j] Institute of Physiology, JLU Giessen, Giessen, Germany
[k] University of Exeter Medical School, St Luke's Campus, Exeter EX1 2LU, UK
[l] Life & Health Sciences and Aston Research Centre for Healthy Ageing, Aston University, Aston Triangle, Birmingham B4 7ET, UK
[m] School of Life & Health Sciences, Aston University, Aston Triangle, Birmingham B47ET, UK
[n] Laboratory of Pharmacology, Faculty of Pharmacy, National and Kapodistrian University of Athens, Greece
[o] Institute for Biology-Microbiology, Freie Universität Berlin, Berlin, Germany
[p] Departamento de Química e Bioquímica and Centro de Química e Bioquímica, Faculdade de Ciências, Portugal
[q] Department of Medical Biochemistry, Faculty of Medicine, Akdeniz University, Antalya, Turkey
[r] Vascular Biology Section & Whitaker Cardiovascular Institute, Boston University School of Medicine, Boston, MA, USA
[s] Center for Neurosciences and Cell Biology, University of Coimbra and Faculty of Pharmacy, University of Coimbra, Coimbra, Portugal
[t] Molecular technologies laboratory, Shemyakin-Ovchinnikov Institute of Bioorganic Chemistry, Miklukho-Maklaya 16/10, Moscow 117997, Russia
[u] Department of Neurology, Medical Faculty, Heinrich-Heine University, Düsseldorf, Germany
[v] Department of Biochemistry, Molecular Biology and Biophysics, University of Minnesota - Twin Cities, USA
[w] Institute of Neuroscience (CNR), Padova, Italy
[x] GETI, Institute for Advanced Biosciences, INSERM U1029, CNRS UMR 5309, Grenoble-Alpes University and Radio-analysis Laboratory, CHU de Grenoble, Grenoble, France
[y] Research Institute for Medicines (iMed.ULisboa), Faculty of Pharmacy, Universidade de Lisboa, Lisboa, Portugal
[z] Faculdade de Ciências da Saúde, Universidade da Beira Interior, Covilhã, Portugal
[aa] Department of Pathology, University of Cambridge, Cambridge, UK
[ab] Department of Pharmacology & Personalized Medicine, Cardiovascular Research Institute Maastricht (CARIM), Maastricht University, Maastricht, The Netherlands
[ac] Institute of Molecular Cell and Systems Biology, College of Medical Veterinary and Life Sciences, University of Glasgow, University Avenue, Glasgow, UK
[ad] National Hellenic Research Foundation, Institute of Biology, Medicinal Chemistry and Biotechnology, 48 Vas. Constantinou Ave., 116 35 Athens, Greece
[ae] Helmholtz Center Munich, Institute of Developmental Genetics, Neuherberg, Germany
[af] Oxidative Stress Group, Dept. Environmental & Occupational Health, Florida International University, Miami, FL 33199, USA
[ag] CBIOS, Universidade Lusófona Research Center for Biosciences & Health Technologies, Lisboa, Portugal
[ah] Instituto de Investigaciones Biomédicas "Alberto Sols" UAM-CSIC, Instituto de Investigación Sanitaria La Paz (IdiPaz), Department of Biochemistry, Faculty of Medicine, Autonomous University of Madrid. Centro de Investigación Biomédica en Red sobre Enfermedades Neurodegenerativas (CIBERNED), Madrid, Spain
[ai] Université Paris Diderot, Sorbonne Paris Cité, INSERM-U1149, CNRS-ERL8252, Centre de Recherche sur l'Inflammation, Laboratoire d'Excellence Inflamex, Faculté de Médecine Xavier Bichat, Paris, France
[aj] Department of Plant Systems Biology, VIB, 9052 Ghent, Belgium
[ak] Department of Pharmaceutical Biotechnology, Faculty of Pharmacy, Ege University, Bornova, Izmir 35100, Turkey
[al] Department of Biochemistry, Science II, University of Geneva, 30 quai Ernest-Ansermet, 1211 Geneva-4, Switzerland
[am] Department of Molecular Biology, University of Bergen, Bergen, Norway
[an] Fundación para la Investigación Biomédica del Hospital Universitario de Getafe, Getafe, Spain
[ao] Department of Pharmacology and Pharmacotherapy, Medical Faculty, Semmelweis University, Budapest, Hungary
[ap] Department of Pharmacology, Johannes Gutenberg University Medical Center, Mainz, Germany
[aq] A.I. Virtanen Institute for Molecular Sciences, University of Eastern Finland, Kuopio, Finland
[ar] Faculty of Health and Medical Sciences, University of Surrey, Guildford GU2 7XH, UK
[as] Department of Physiology, 2nd Faculty of Medicine, Charles University, Prague, Czech Republic
[at] Molecular Cardiology, Center for Cardiology, Cardiology 1, University Medical Center Mainz, Mainz, Germany
[au] Servicio de Immunología, Hospital Universitario de La Princesa, Instituto de Investigación Sanitaria Princesa (IIS-IP), Madrid, Spain
[av] Departamento de Bioquímica, Facultad de Medicina, Universidad Autónoma de Madrid (UAM) and Instituto de Investigaciones Biomédicas Alberto Sols, Madrid, Spain
[aw] Structural Biology Research Center, VIB, 1050 Brussels, Belgium
[ax] Harran University, Arts and Science Faculty, Department of Biology, Cancer Biology Lab, Osmanbey Campus, Sanliurfa, Turkey
[ay] Institute for Biomedical Aging Research, University of Innsbruck, Innsbruck, Austria
[az] Dept. of Pathology and Immunology, Centre Médical Universitaire, Geneva, Switzerland
[ba] Department of Nephrology & Hypertension, University Medical Center Utrecht, The Netherlands
[bb] Medical College of Wisconsin, Milwaukee, USA
[bc] Danylo Halytsky Lviv National Medical University, Lviv, Ukraine
[bd] Molecular Genetics Thalassaemia Department, The Cyprus Institute of Neurology and Genetics, Nicosia, Cyprus
[be] Institute of Nutrition, Department of Nutrigenomics, Friedrich Schiller University, Jena, Germany
[bf] University of Belgrade, Institute for Biological Research "Sinisa Stankovic" and Faculty of Biology, Belgrade, Serbia
[bg] Department of Bioengineering, Cancer Biology Laboratory, Faculty of Engineering, Ege University, Bornova, 35100 Izmir, Turkey
[bh] Institute of Microbiology, Laboratory of Biotransformation, Czech Academy of Sciences, Videnska 1083, CZ-142 20 Prague, Czech Republic
[bi] Department of Medicine, University of Cambridge, UK
[bj] School of Biology, Aristotle University of Thessaloniki, Thessaloniki 54124, Greece
[bk] Centro de Investigación Biomédica en Red de Enfermedades Cardiovasculares (CIBERCV), Madrid, Spain
[bl] School of Biomolecular and Biomedical Science, Conway Institute, University College Dublin, Dublin, Ireland
[bm] Centro de Biología Molecular "Severo Ochoa" (CSIC-UAM), Madrid, Spain
[bn] University of Ljubljana, Faculty of Medicine, Institute of Pathophysiology and Faculty of Health Sciences, Ljubljana, Slovenia
[bo] Ruđer Bošković Institute, Division of Molecular Medicine, Zagreb, Croatia
[bp] Instituto de Biomedicina de Sevilla, Hospital Universitario Virgen del Rocío/CSIC/Universidad de Sevilla, Sevilla, Spain
[bq] University of Belgrade, Faculty of Physical Chemistry, Studentski trg 12–16, 11000 Belgrade, Serbia
[br] Instituto de Investigaciones Biomédicas "Alberto Sols" (CSIC-UAM), Madrid, Spain
[bs] Laboratory for Oxidative Stress, Rudjer Boskovic Institute, Bijenicka 54, 10000 Zagreb, Croatia
[bt] Department of Pharmacology, Center for Targeted Therapeutics & Translational Nanomedicine, ITMAT/CTSA Translational Research Center University of Pennsylvania The Perelman School of Medicine, Philadelphia, PA, USA
[bu] Center for Neurosciences & Cell Biology of the University of Coimbra, Coimbra, Portugal
[bv] ESPE of Paris, Paris Sorbonne University, Paris, France
[bw] The Research Institute of University of Bucharest, Bucharest, Romania
[bx] Laboratory of Clinical Pharmacology, Rigshospitalet, University Hospital Copenhagen, Denmark
[by] Department of Biomedical Sciences, University of Padova, via Ugo Bassi 58/b, 35131 Padova, Italy
[bz] Servicio de Geriatría, Hospital Universitario de Getafe, Getafe, Spain

[cb] Faculty of Medical Sciences, Goce Delcev University, Stip, Republic of Macedonia
[cc] Institute for Drug Research, Section of Pharmacology, Diabetes Research Unit, The Hebrew University Faculty of Medicine, Jerusalem, Israel
[cd] Institute for Cardiovascular Physiology, Goethe-University, Frankfurt, Germany
[ce] DZHK (German Centre for Cardiovascular Research), partner site Rhine-Main, Mainz, Germany
[cf] Université Grenoble Alpes, CNRS, Grenoble INP, CHU Grenoble Alpes, TIMC-IMAG, F38000 Grenoble, France
[cg] CDiReC, Pôle Biologie, CHU de Grenoble, Grenoble, F-38043, France
[ch] Department of Biophysics, Ankara University, Faculty of Medicine, 06100 Ankara, Turkey
[ci] Department of Molecular Medicine, University of Padova, Padova, Italy
[cj] Department of Medical Chemistry and Biochemistry, Faculty of Medicine and Dentistry, Palacký University, Hnevotinska 3, Olomouc 77515, Czech Republic
[ck] Institute for Cell and Molecular Biosciences, and Institute for Ageing, Newcastle University, Framlington Place, Newcastle upon Tyne, UK
[cl] Department of Biochemistry, School of Medicine, Marmara University, İstanbul, Turkey
[cm] Institute of Cardiovascular and Medical Sciences, University of Glasgow, UK
[cn] Laboratoty of Pharmacology, Faculty of Pharmacy, National and Kapodistrian University of Athens, Greece
[co] German Institute of Human Nutrition, Department of Toxicology, Arthur-Scheunert-Allee 114–116, 14558 Nuthetal, Germany
[cp] Department of Biomedical Sciences and CNR Institute of Neuroscience, University of Padova, Padova, Italy
[cq] Department of Plant Biotechnology and Bioinformatics, Ghent University, 9052 Ghent, Belgium
[cr] Pharmahungary Group, Szeged, Hungary
[cs] Brussels Center for Redox Biology, Structural Biology Brussels, Vrije Universiteit Brussel, 1050 Brussels, Belgium
[ct] Department of Life Sciences of the Faculty of Sciences & Technology of the University of Coimbra, Coimbra, Portugal
[cu] Department of Clinical Pharmacology, Bispebjerg Frederiksberg Hospital, University Hospital Copenhagen, Denmark
[cv] Department Q7642, Rigshospitalet, Blegdamsvej 9, DK-2100 Copenhagen, Denmark

ARTICLE INFO

*Keywords:*
Reactive oxygen species
Reactive nitrogen species
Redox signaling
Oxidative stress
Antioxidants
Redox therapeutics

ABSTRACT

The European Cooperation in Science and Technology (COST) provides an ideal framework to establish multi-disciplinary research networks. COST Action BM1203 (EU-ROS) represents a consortium of researchers from different disciplines who are dedicated to providing new insights and tools for better understanding redox biology and medicine and, in the long run, to finding new therapeutic strategies to target dysregulated redox processes in various diseases. This report highlights the major achievements of EU-ROS as well as research updates and new perspectives arising from its members. The EU-ROS consortium comprised more than 140 active members who worked together for four years on the topics briefly described below. The formation of reactive oxygen and nitrogen species (RONS) is an established hallmark of our aerobic environment and metabolism but RONS also act as messengers via redox regulation of essential cellular processes. The fact that many diseases have been found to be associated with oxidative stress established the theory of oxidative stress as a trigger of diseases that can be corrected by antioxidant therapy. However, while experimental studies support this thesis, clinical studies still generate controversial results, due to complex pathophysiology of oxidative stress in humans. For future improvement of antioxidant therapy and better understanding of redox-associated disease progression detailed knowledge on the sources and targets of RONS formation and discrimination of their detrimental or beneficial roles is required. In order to advance this important area of biology and medicine, highly synergistic approaches combining a variety of diverse and contrasting disciplines are needed.

## 1. Introduction

Andreas Daiber and Fabio Di Lisa.

### 1.1. Mission, structure and major achievements of EU-ROS consortium

The COST Action BM1203 (EU-ROS) is a research consortium of networking supported by the European Cooperation in Science and Technology (COST), which is embedded within the Biomedicine and Molecular Biosciences Domain. It covers areas of basic, preclinical and clinical research in biology, chemistry, physics and medicine, not only on mammalian cells but also plants, bacteria and other organisms. The mission of EU-ROS is to advance the field of redox biology and oxidative stress research by bringing together multi-disciplinary experts by organizing scientific meetings and providing funds for the exchange of researchers between laboratories (for more details see www.eu-ros.eu or www.cost.eu/COST_Actions/bmbs/Actions/BM1203). During the active funding period of EU-ROS (2013–2016) we organized ten major scientific meetings, supported 29 short-term scientific missions for research visits of postdoctoral fellows and Ph.D students, and co-organized three scientific symposia at European conferences of the Society for Free Radical Research Europe (SFRRe). In order to foster the next generation of redox biology scientists we also supported numerous early-stage researchers and invited them either to the six training schools that we (co)organized or to the young investigator sessions at our meetings. Among the major achievements of EU-ROS are three major successful grant applications within the European H2020 funding scheme as well as three major coordinated collections of position papers, reviews and original articles published by our members [1–4]. The “small to medium sized enterprises” (SME) participating in EU-ROS filed three patents with the help of research collaborations established within our consortium. In order to disseminate the collected knowledge to a broader audience of non-expert scientists and the public we also opened a EU-ROS YouTube channel (https://www.youtube.com/channel/UCXFnyGD4uVFUTcLshvDtxcQ). The present collection of research updates and perspectives represents the final dissemination of COST Action BM1203 (EU-ROS).

In order to achieve the scientific objectives, as laid down in the memorandum of understanding of COST Action BM1203, we defined 6 working groups (WG) with elected leaders, each representing a taskforce for a specific area of research or organization/management: WG1 Sources of ROS (Ulla Knaus), WG2 Molecular Mechanisms (Agnes Görlach), WG3 Drugs & Tools (Tamara Seredenina), WG4 Biomarkers (Pietro Ghezzi/Paul Winyard), WG5 Imaging (Yves Frappart) and WG6 Technology Transfer & Funding (Vincent Jaquet).

### 1.2. Redox biology and oxidative stress: the EU-ROS approach

The fact that life requires oxygen, which per se represents a

[1] These authors contributed equally and should be considered joint first or senior authors.

chemically aggressive molecule [5], bears the risk that biomolecules in all aerobic living species on earth are targets of oxidative modifications resulting from uncontrolled formation of reactive oxygen species (ROS[2]) and reactive nitrogen species (RNS[3]). In order to prevent oxidative damage, all aerobic organisms have developed highly efficient antioxidant strategies during evolution. However, these highly reactive species may be generated accidentally as a result of altered metabolism (e.g. during mitochondrial respiration) or can be formed deliberately (e.g. by professional ROS-producing enzymes at sites of inflammation). Hence, it is not surprising that most metabolic diseases, as well as those pathologies associated with low-grade inflammation, display increased patterns of biomarkers of oxidative stress [6]. It is well established that cardiovascular [7–9], neurodegenerative [10,11], metabolic [12,13] and inflammatory diseases [14–16] are associated with increased oxidative stress (some rare immune diseases are linked to insufficient ROS formation [17]). Despite the large body of evidence linking oxidative stress with many common diseases, which is supported by the significant correlation of redox biomarkers with cardiovascular and all-cause mortality [18–20], direct clinical proof is still lacking that oral therapy with antioxidants, such as vitamin C and E, helps to prevent the development or progression of these diseases. Most large-scale antioxidant clinical trials yielded disappointing results regarding all-cause mortality and in some cases oral antioxidants had detrimental effects [21–23] and to this date no “antioxidant” is admitted as a drug for clinical use [24]. More recent reports in publication channels dedicated to the non-expert or public readership highlighted the potential risks associated with excessive oral consumption of antioxidants (see online publications by Mustain [25] and Riley [26]). Antioxidant therapy was also mentioned among “the science myths that will not die” [27]. In contrast, a large number of small to intermediate size cohort studies with short-term and parenteral vitamin C therapy showed highly beneficial effects in various cardiovascular disease settings, and, for vitamin D, positive reports on oral therapy exist [9,19,28]. The most likely explanation for the antioxidant /oxidative stress paradox may be that reactive oxygen and nitrogen species (RONS) are not only injurious (oxidative stress) but also modulate important biological functions (redox signaling). Accordingly, chronic, systemic oral therapy with antioxidants will likely interfere with important ROS-mediated cellular processes, such as stress adaptation by ischemic preconditioning [19,21,28]. Additional reasons for the failure of large trials on oral antioxidant therapy might comprise the pro-oxidant effects of vitamin C and E radicals, reaction kinetics that are too slow, or lack of effective concentrations at sites of RONS formation. It is also possible that the patients included in these trials had already been exposed to drugs with pleiotropic antioxidant effects (e.g. ACE inhibitors or statins) (all reviewed in [19,21,28]). In addition, as shown by the EPIC Norfolk study, large antioxidant clinical trials suffer from suboptimal control of their potential efficacy, such as not measuring the patients’ plasma levels of antioxidants to verify compliance [29]. This study also showed that vitamin C concentrations in the blood inversely correlate with all-cause mortality in healthy volunteers. The inherent problems of vitamin C and E, that were mostly used in clinical trials, were also highlighted by Darley-Usmar and colleagues by a previous review [30]. Moreover, Forman, Davies and Ursini postulated that the nucleophilic tone and para-hormesis (paradoxic oxidative activation of intrinsic defence mechanisms such as the NRF2 pathway) is more important than free radical scavenging properties of antioxidants for their beneficial effects in vivo [31].

This obvious paradox in antioxidant therapy efficacy warrants better understanding of the role of RONS in physiology and pathophysiology. Our consortium put forward the concept that the failure of the traditional antioxidants such as vitamin C and E was predictable considering the above-mentioned limitations, but that excessive formation of RONS (mostly termed “oxidative stress”) plays a role in disease development and progression or, at least, leads to stable biomarkers (e.g. oxidatively modified biomolecules) that can be used for diagnostic aspects in various diseases (reviewed in full detail in the Forum issue by EU-ROS members [2]). In brief, we believe that activation of intrinsic antioxidant processes (e.g. NRF2-dependent pathways), inhibition of disease-relevant sources of RONS (e.g. isoform-specific NOX inhibitors), scavenging of disease-triggering RONS by site- and time-specific antioxidants or even repair of oxidatively inactivated enzymes (the most prominent examples being sGC activators) represent recently clinically established or promising future antioxidant strategies. The main concept of our biomedical approach and working scheme is shown in Fig. 1.1.

The present overview is an interdisciplinary forum of opinions from various experts in the field of redox biology and oxidative stress research participating in EU-ROS. We have separated the present work into 11 sections since the contributions cover a wide range of scientific topics (mammals, worms, bacteria, plants) and even the terminology of RONS varies substantially depending on whether they belong to rather theoretical and basic science oriented disciplines or biomedical and clinical research areas. RONS regulate not only hydrogen sulfide ($H_2S$) but also nitric oxide ($^{\bullet}NO$) and carbon monoxide (CO), thereby affecting all major gasotransmitter systems [33,34]. Also the concept of ROS-induced ROS formation (the crosstalk of different ROS-producing systems) is highlighted in the subsequent sections [35,36]. These direct and indirect mechanisms based upon redox modifications or direct reactions with other messengers (e.g. $^{\bullet}NO$ and $H_2S$) underlie RONS involvement in receptor-dependent signaling pathways, also due to the modulation of expression and activity of transcription factors. The contributions below also highlight how RONS contribute to established signaling pathways by their redox modulation. The interactions of RONS with microparticles [37–39], protein aggregates [40,41] and the gasotransmitter $H_2S$ [33,42] represent important examples that illustrate how RONS as messengers indirectly influence other signaling systems. Therefore, far from being merely biological waste products, RONS represent highly active and tightly regulated signaling molecules.

## 2. Conceptual and mechanistic aspects of ROS and oxidative stress

Ulla G. Knaus (ulla.knaus@ucd.ie).

### 2.1. Background and terminology

“ROS is over”, a statement at the ESF-EMBO meeting (Spain 2015) by Fulvio Ursini, should probably be extended to “Oxidative Stress is over” (Ulla G. Knaus). There is no doubt that ROS exist and that the concept of oxidative stress summarizes certain conditions connected to a variety of diseases. However, the unspecific usage of these blanket terms, especially during recent years, does not adequately reflect the diversity of reactive oxygen metabolites being produced, the intricate regulation of redox signaling and the oxidant-antioxidant balance, or

[2] Throughout this report, the term ROS refers almost exclusively to hydrogen peroxide and superoxide anion radical since both species are involved in redox signaling and are formed by a number of enzymatic sources. Other ROS include the hydroxyl radical or singlet oxygen, which however have most likely no specific roles in redox signaling but rather contribute to unspecific oxidative damage and oxidative stress. A large number of organic peroxides (e.g. lipid peroxides) are also covered by the term ROS but these species are only marginally discussed in the present overview. Other ROS such as hypochlorite are also not in the focus of the present work.

[3] Throughout this report, the term RNS refers almost exclusively to peroxynitrite, peroxynitrous acid and derived free radicals (e.g. hydroxyl radicals and nitrogen dioxide radicals). Peroxynitrite anion has a high specificity for activated thiols and readily reacts with carbon dioxide (the latter supports radical reactions). Peroxynitrous acid also has a high specificity for activated thiols but also reacts with transition metal complexes. RNS also comprises nitric oxide, which upon reaction with oxygen can form nitrogen dioxide radicals or nitrosating species such as $N_2O_3$ and has a high affinity for transition metal complexes such as iron(II), all of which contributes to the potent redox signaling properties of nitric oxide. However, in the context of “oxidation of biomolecules” the term RNS does not refer to nitric oxide due to its weak reactivity towards biomolecules in general.

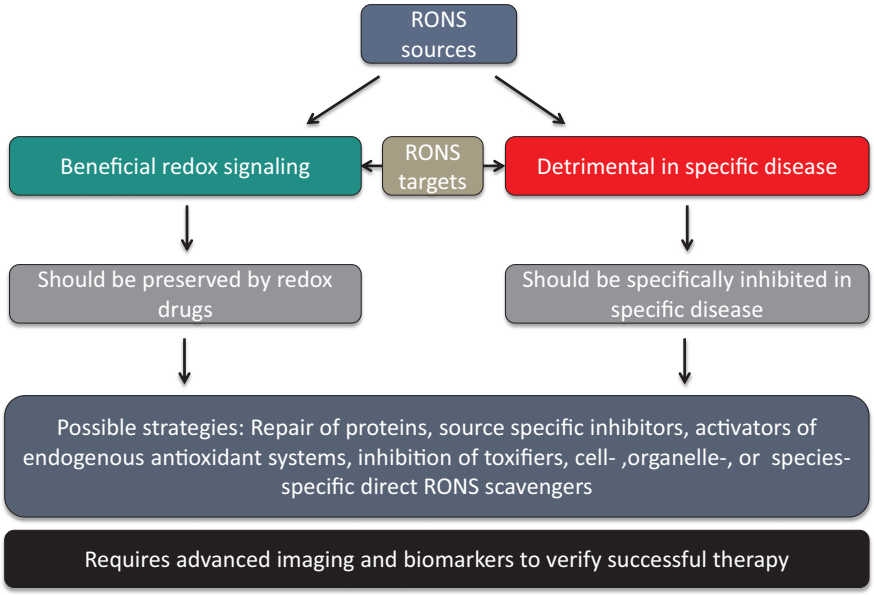


**Fig. 1.1.** The main concept of our biomedical approach and working scheme within the EU-ROS consortium as explained in detail previously [32].

the causality of oxidative modifications versus detrimental outcome in biological systems. “ROS” is discussed below in detail, while oxidative stress is usually defined as an imbalance between production of ROS and antioxidants and the ensuing pathophysiological consequences of increased, unspecified ROS. If the term oxidative stress is used retrospectively via determination of oxidative modifications of proteins, lipids or DNA, it might instead be oxidative damage. Direct measurements of oxidative stress often use oxidized glutathione as readout, but Morgan et al. identified immediate glutathione disulfide removal pathways and antioxidant backup systems that ensured redox homeostasis [43]. In some circumstances oxidative stress is correlated with the presence or upregulation of an enzyme that can (but might not) generate superoxide or hydrogen peroxide, or the presence of cell types that produce these species when activated. However, the outcome in redox biology will always be dependent on the type of oxygen species generated over a certain time period at a certain location. One example is wound healing which requires ROS [44], but may progress to fibrosis when deregulation of the process occurs [45]. Another example is hypoxic tissue reconstitution facilitated by the neutrophil oxidative burst [46] versus neutrophil-mediated tissue injury in other circumstances [47]. What happens when the predominant superoxide source is missing is evident in chronic granulomatous disease (CGD), an inherited immunodeficiency caused by inactivating variants of the NOX2 NADPH oxidase complex. CGD patients present not only with life-threatening infections, but also with hyperinflammation, and *Cybb*$^{-/-}$ (*Nox2*) knockout mice show an increase in proinflammatory mediators and tissue damage in disease models [48–50].

As Carsten Berndt and Marcus Conrad note, ROS, a widely used umbrella term, urgently needs specification. Its use is misleading, as just some of the molecules encompassed under this term are indeed reactive species. This is especially true for the non-radical species, and it is another common misunderstanding that all ROS are radicals. Unlike the hydroxyl radical ($HO^{\bullet}$) or the superoxide anion radical ($O_2^{\bullet-}$) singlet oxygen ($^1O_2$) or hydrogen peroxide ($H_2O_2$) are not radicals, which is underlined by the different reactivities (second order rate constant $M^{-1}\ s^{-1}$) of ROS with a given substrate (methionine) that range from $2\times10^{-2}$ ($H_2O_2$) to $7x10^{9}$ ($HO^{\bullet}$) [51]. Another often neglected fact is the continuous formation of certain reactive species by enzymes under physiological conditions. Ero1α, for instance, generates one $H_2O_2$ molecule following each disulfide bridge formed in the endoplasmic reticulum. Therefore, reactive species cannot be considered solely a phenomenon of damage and disease. These species formed under physiological conditions can contribute to diverse cellular functions. For instance, reversible oxidative posttranscriptional thiol modifications are important during several processes in cells or even whole organisms including embryonic development [52,53]. Moreover, the formation of reactive species at different subcellular sites distinguishes between cellular functions, such as stem cell maintenance or differentiation [54]. Not only posttranslational oxidative modifications, but also damage by certain types of reactive species can be a trigger for specific cellular functions: Ferroptosis after lipid peroxidation was recently shown to specifically impede reprogramming into neurons [55]. For these reasons, it is impossible to measure “ROS”, to induce “ROS”, to inhibit “ROS”, or to accumulate “ROS”. Besides scientific recognition, limited experimental tools are a problem to move research forward (or back) to the specific investigation of specific species. Promising in vivo tools are highly sensitive genetically encoded fluorescence probes [56] and genetic cell and animal models with targeted deficiencies in professional redox enzymes dealing with a select subset of distinct reactive species, such as the ferroptosis regulator glutathione peroxidase 4 [57]. Several research communities focus or have focused on ROS molecules, e.g. the Oxygen Club of California, the Society for Free Radical Research (SFRR), and EU-ROS. Hence, researchers working in the field of redox biology must, whenever possible, discriminate among the different partially reduced forms of oxygen being studied as this will allow us to acknowledge their different chemical features and/or biological functions as well as ultimately help to provide strong and solid mechanistic data on important biological processes.

### 2.2. ROS sources and their activation

There are circumstances where the term “ROS” is unavoidable, mainly due to our inability to exactly measure the species generated in a spatiotemporal manner or to correctly identify or discriminate between species responsible for a certain biological event. Sometimes a mixture of oxygen metabolites is produced as several sources are stimulated or interact with each other. Thus, ROS sources should not be considered isolated enzymatic systems, and biological processes may involve ROS-induced ROS (Andreas Daiber and Matthias Oelze). There is increasing evidence that they can crosstalk with each other via reactive oxygen and nitrogen species signaling [35,58]. The theory of so-called “kindling radicals” or also the “bonfire” hypothesis is based on the formation of a few primary ROS that “inflame” a cascade of ROS

amplification by stimulating the sources of secondary ROS (Fig. 2.1A). This was first described for mitochondria [59] and involves several mitochondrial pores that are required for the release of mitochondrial ROS such as the mitochondrial permeability transition pore, aquaporins or the inner membrane anion channel as well as sources of oxidants (e.g. respiratory complexes, p66shc, monoamine oxidases) [18]. This crosstalk concept can be extended to almost all kinds of sources of oxidants. We have described "redox switches" that lead to uncoupling of endothelial nitric oxide synthase (eNOS), redirecting this enzyme from nitric oxide to superoxide production and thereby changing the entire vascular phenotype from a dilated, anti-thrombotic, anti-inflammatory state to a constricted, thrombotic and inflammatory state (Fig. 2.1B) [18,20,60]. Likewise, initially formed "kindling" ROS easily activate xanthine oxidase by a thiol oxidation-dependent and proteolytic conversion of xanthine dehydrogenase to the oxidase form [60] or activate NADPH oxidases (NOX), either by redox-sensitive activation of protein kinase C and translocation of cytosolic subunits (for NOX1 and NOX2) or by upregulation of all *NOX* isoforms by redox-sensitive transcription factors or changes in mRNA stability [60]. The most important crosstalk between different sources of oxidants was described for mitochondria and NOX, which was reviewed in full detail by us and others [18,58]. We have observed this kind of crosstalk in nitroglycerin-induced endothelial dysfunction and oxidative stress [61], in models of aging-induced vascular dysfunction and oxidative stress [62], as well as

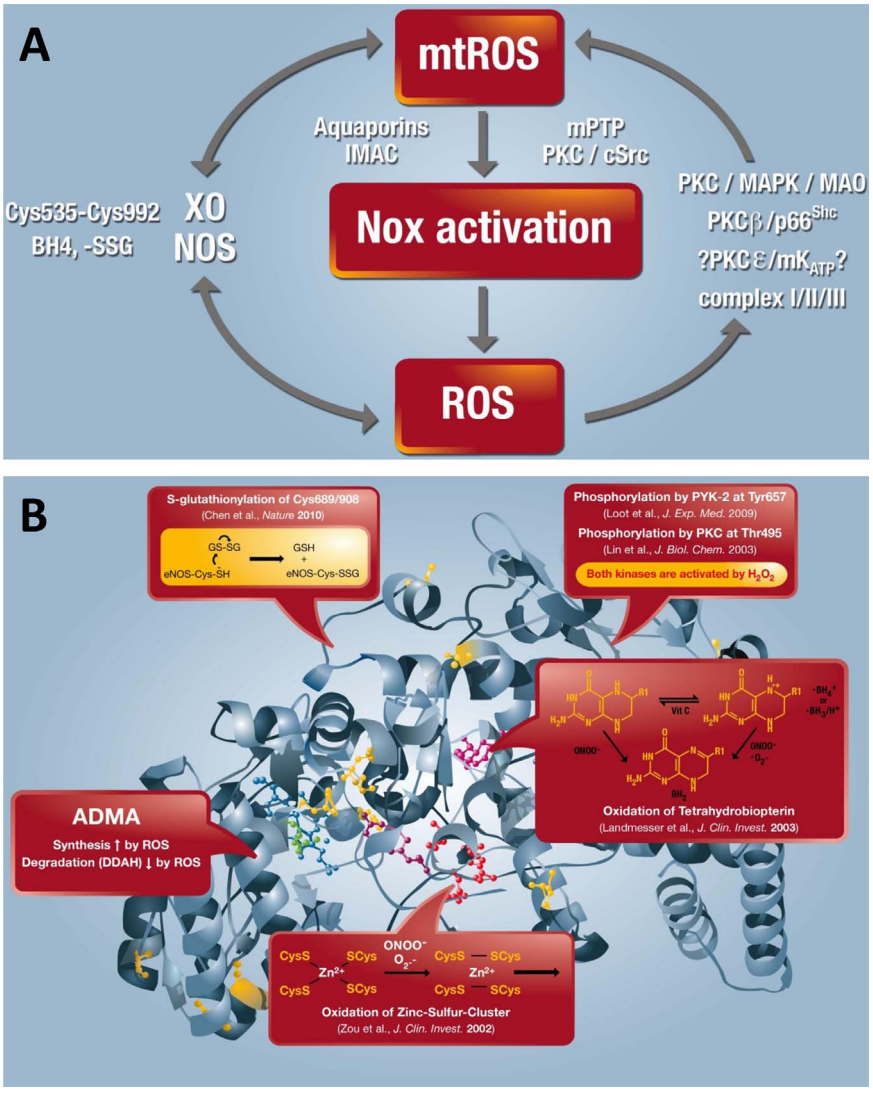


**Fig. 2.1.** (A) Crosstalk between different sources of ROS and RNS (mitochondria, NADPH oxidases, xanthine oxidase and NO synthase). Xanthine oxidase (XO) originates from oxidative stress-mediated conversion of the xanthine dehydrogenase via oxidation of critical thiols in cysteine535/992. NO synthases (mainly eNOS) are uncoupled upon oxidative depletion of tetrahydrobiopterin ($BH_4$), *S*-glutathionylation (-SSG) and other redox switches. Mitochondrial superoxide/hydrogen peroxide formation may be triggered by oxidative stress from all ROS sources (including other damaged/activated mitochondria) via redox-activation of PKC, MAPK, other kinase pathways and potential involvement of redox-sensitive mitochondrial ATP-sensitive potassium channels (mtKATP) with subsequent p66Shc, monoamine oxidase (MAO), respiratory complex activation or impairment of mitochondrial antioxidant defence. Mitochondrial superoxide/ hydrogen peroxide is released to the cytosol via mitochondrial pores and channels (e.g. redox-sensitive mitochondrial permeability transition pore (mPTP), inner membrane anion channel (IMAC) or aquaporins) or by diffusion due to increased mitochondrial permeability under pro-inflammatory conditions. In the cytosol these species (along with released calcium) cause activation of redox-sensitive protein kinases (PKC) and tyrosine kinases (cSrc) with subsequent activation of NADPH oxidases and amplification of the cellular oxidative stress. Modified from [35, 64]. With permission of Elsevier. Copyright 2010 & 2015. (**B**) Redox switches in endothelial nitric oxide synthase (eNOS). X-ray structure of human eNOS with the ironporphyrin (blue), the substrate L-arginine (green), the P450-forming axial iron-thiolate ligand from a cysteine residue (yellow), the cofactor tetrahydrobiopterin ($BH_4$) (purple), the zinc-thiolate complex forming cysteines (red, two from each subunit), and the zinc ion (brown). The boxes represent the "redox switches" in eNOS, such as *S*-glutathionylation, PKC- and protein tyrosine kinase-2 (PYK-2)–dependent phosphorylation, oxidative BH4 depletion, disruption of the zinc-sulfur cluster, as well as asymmetric dimethylarginine (ADMA) synthesis/degradation, all of which contribute to the regulation of its enzymatic activity. GSH, glutathione; GSSG, glutathione disulfide. The crystal structure was rendered from the protein database entry 3NOS (DOI:10.2210/pdb3nos/pdb) using the PyMOL Molecular Graphics System Version 1.2r1 (DeLano Scientific LLC). Adapted from [60]. With permission of Mary Ann Liebert, Inc. Copyright 2014 .

in angiotensin-II induced hypertension and immune cell activation [63]. In conclusion, the redox crosstalk between different sources of oxidants may explain why multiple publications describe different ROS sources as the major pathological trigger in a certain disease (e.g. for the hypertension mitochondrial respiratory chain, NOX1, NOX2, NOX4 and xanthine oxidase) and that pharmacological or genetic blockade of one of these sources was enough to prevent the adverse phenotype [18]. If this concept can be translated to patients, it may be enough to target one specific source of ROS to prevent or retard the progression of a certain disease.

Determination of the ROS source(s) and their interactions is still challenging. The multitude of potential inputs range from NADPH oxidases (NOX1-5, DUOX1-2) and the mitochondrial electron chain, to xanthine oxidase, monoamino oxidase(s), cyclooxygenase(s), lipoxygenase(s), lysyl oxidase(s), cytochrome P450, or MICAL family members, to name a few. In all of the cases, the oxygen metabolite superoxide ($O_2^{\bullet-}$) or $H_2O_2$ is primarily generated as a by-product of key enzymatic reactions of a particular enzyme. NADPH oxidases are the only enzymes solely dedicated to regulate $O_2^-$ (NOX1-3, 5) and $H_2O_2$ (NOX4, DUOX1-2) production [65]. How certain NADPH oxidases can internally convert $O_2^{\bullet-}$ to $H_2O_2$ when using NADPH as the electron donor for the one-electron reduction of molecular oxygen is still unresolved. This feature discriminates the signaling input of NOX4 and DUOX1-2 from other family members due to the diffusibility and longer half-life of $H_2O_2$ versus $O_2^{\bullet-}$ or secondary reactive metabolites.

### 2.3. ROS sources in microbiota

$O_2^{\bullet-}$/ $H_2O_2$ generation by enzymes and their consequences are mainly considered in the context of plant or animal hosts. However, hosts are colonized by an ecological community of commensal, symbiotic and pathogenic microorganisms, collectively termed microbiota. The presence and composition of the microbiota, which includes bacteria, fungi and viruses and resides in biofluids or on epithelial surfaces, is critical for health and disease. Bacteria represent the majority of the human microbiota ($10^{14}$ bacterial cells) with estimates of 1000 or more bacterial species. Bacteria-host interactions in redox biology have been mostly defined by infections, where host defense relies on NOX2-mediated oxidative destruction of pathogens.

Yet an immediate and close relationship exists between commensals, pathogens and host epithelial surfaces, which is best characterized in the intestine. In the gut, feedback communication ensues with bacteria as inducers, targets and producers of ROS (Ulla G. Knaus and Gratiela G. Pircalabioru). The association of germ-free mice with microbiota induced the expression of epithelial DUOX2 [66]. Intestinal pathogens such as *C. jejuni*, *K. pneumoniae*, or L. *monocytogenes* triggered by a yet unknown mechanism the activation of NOX1 and DUOX2, resulting in $O_2^{\bullet-}$ generation and $H_2O_2$ release into the gut lumen [67,68]. Enteropathogenic *E. coli* stimulated a NOX1-mediated pathway that included ASK1, p38 and AFT-2 and culminated in an over 20-fold upregulation of the DUOX2 complex [69]. Others reported that *Lactobacillaceae* activate NOX1, thereby promoting intestinal stem cell proliferation and wound healing responses [70]. While pathogens and segmented filamentous bacteria can gain access to the epithelium, lactobacilli usually colonize the further removed, loose mucus layer. However, any disruption of the barrier including changes in permeability or mucus composition/density will permit the interaction of commensals with host cells and may result in ROS signaling via NOX and/or mitochondria. For example, mitochondrial ROS is required for NLRP3 inflammasome activation by bacteria or bacterial products, and subsequent IL-1β and IL-18 production [71]. The bacteria-host interaction will also initiate release of $H_2O_2$ from the mucosal surface. Uptake of $H_2O_2$ by extracellular bacteria alters their transcriptional program and intrabacterial signaling. Although antioxidant defense genes will be upregulated, Fenton reaction-associated oxidations will decrease phosphotyrosine signaling and alter pathogenicity gene regulation [68,69]. These oxidative modifications reduce the virulence of extracellular bacteria, which can then be eliminated more efficiently by the host.

Certain commensals, in particular *Lactobacillus* and *Lactococcus* strains, use endogenous $H_2O_2$ production as their own means of communication. The bacterial enzymes capable of generating $H_2O_2$ are largely unknown except for L. *acidophilus* [72], although the consequences to host physiology and niche protection have been reported. The antiinflammatory effects of lactobacilli are multifaceted, but lactobacilli-mediated killing of pathogens (e.g. *S. enterica*, *E. coli*) has been firmly associated with their $H_2O_2$ production [73]. Even some catalase-negative pathogens use endogenous $H_2O_2$ production for intra- and inter-bacterial signaling. Aerobic growth of *Streptococcus pneumoniae* leads to pyruvate oxidase (SpxB)-mediated $H_2O_2$ generation, which was required for fatty acid metabolism and inhibited replication of other microorganisms competing for the same environmental niche [74,75]. In conclusion, bacteria need to be considered as endogenous sources and exogenous inducers of $H_2O_2$, thereby propagating intra-and interkingdom signaling.

This connection between bacteria and the host has been studied extensively in the nematode worm *Caenorhabditis elegans* [76–79], but as Elizabeth A. Veal and Antonio Miranda-Vizuete comment, *C. elegans* can serve as a general model for redox biology and has already provided significant new insight into the interplay between ROS, ROS signaling and aging. Notably, genetic studies have failed to show that the ROS-detoxifying activities of any of *C. elegans*' array of ROS-metabolizing enzymes protects against aging. However, these studies have revealed specific roles for several of these proteins in redox signaling, protein homeostasis or regulation of normal physiology. For example, glutathione reductase is essential for cell division during embryonic development [80], thioredoxin reductase or glutathione reductase activity for larval development to reduce disulfide bonds of cuticle components prior to molting [81] and the peroxiredoxin PRDX-2 for regulation of feeding behavior [82] and normal levels of insulin secretion [83]. The causative role of ROS-induced damage in animal aging has also been challenged by the unexpected discovery that increases in ROS can actually promote *C. elegans* longevity (for review see [84]). Nevertheless, stress-activated transcription factors DAF-16 and SKN-1 (orthologous to the mammalian FOXO and NRF2 transcription factors), which promote the expression of a range of defenses, including ROS-detoxifying and phase 2 metabolism enzymes, are vital for survival under stress conditions, during infection and the extended lifespan associated with inhibition of a variety of pathways. As the primary tissue encountering xenobiotics and pathogens that trigger increases in ROS, intestinal levels of these proteins seem particularly important for survival under stress conditions. However, studies with tissue-specific transgenes and RNAi have indicated that cell non-autonomous signals from neurons and germline cells play an important part in regulating these stress defenses (for reviews see [85,86]). Moreover, there is increasing evidence that maintaining *C. elegans* on different strains of *E. coli* can profoundly influence ROS production, redox signaling, metabolism and longevity [87]. *C. elegans* transparency throughout its entire life cycle has enabled the development of a variety of fluorescent redox-sensitive probes that can be employed to monitor in vivo changes in redox status. For example, analysis of animals expressing a genetically encoded peroxide sensor has suggested that peroxide levels are higher during larval development than in adults but rise again following the reproductive period [88]. Recent advances in genome editing tools, NGS approaches to identify mutations obtained by traditional mutagenesis screens, redox proteomics, including OxICAT, metabolomics, and high throughput techniques for genome-wide and tissue-specific RNAi-screening and lifespan analyses have all added to the *C. elegans* toolbox that enhance the power of *C. elegans* as a model to advance the redox biology field. The simplicity, ease of manipulation, microscopic examination, short lifespan and vast range of genetic and post-genomic tools have established *C. elegans* as a powerful model

for providing mechanistic insight into the role of redox changes in normal physiology and disease.

### 2.4. Redox regulation via redox modifications of biomolecules and altered phosphorylation

ROS, in particular $H_2O_2$, participate in redox regulation and signaling responses by modifying proteins, lipids and DNA. An emerging concept is redox control of protein-protein interactions (Andrew R. Pitt and Corinne M. Spickett). Signal transduction via proteins containing redox-sensitive cysteine residues is now a well-established concept, and the list of such proteins is growing rapidly [89]. The cysteine residues involved are most commonly ones with unusually low pKas, which therefore exist as thiolates under physiological conditions [90]. The oxidation of these residues to form a disulfide by reaction with a second, resolving cysteine alters the structure and activity of the protein. A fundamental requirement of redox regulation in signaling is that it must be reversible, and thioredoxin is a central enzyme that mediates the reduction of protein disulfides via formation of an intermolecular disulfide with the target protein. Covalent and non-covalent protein-protein interactions are known to be critical in signaling pathways and are thought to contribute to the commonly observed pleiotrophic effects of ligands and crosstalk between signaling pathways [91]. Advances in proteomic technologies have facilitated studies of the interactomes of an expanding number of proteins. Not surprisingly, these approaches have also been applied to redox proteins, and much attention has focused on members of the thioredoxin family. The covalent interactomes of thioredoxin from *Plasmodium falciparum* and tryparedoxin from *Trypanosoma cruzi* have been reported, driven by the need to identify novel drug targets for protozoan parasites, and in *Escherichia coli*, 268 substrates for Trx were reported from experiments involving strains engineered to optimize trapping of the covalent interaction [92]. The human glutathione-*S*-transferase P interactome has also been reviewed recently, and includes known key players in redox sensing such as STAT3 and NRF2 [93]. There are many reports of interactions of other redox proteins, and in an attempt to bring together all the available information, an “oxidative status interactome map” has been created of known interactions of human cellular-level oxidative status proteins [94]. Although all of these articles report the general interactions of redox-active proteins, the effect of the redox status of the individual proteins on their interactome, especially the non-covalent interactome, has largely been ignored. One study that has addressed this issue investigated the differential interactome of the tumor suppressor PTEN in native (reduced) and reversibly oxidized forms, and reported a number of proteins whose levels changed significantly depending on the redox state, including Anxa2, Trx and Prdx1 [95]. More studies of this kind would help to understand cell redox regulation, and would provide an additional dimension to oxidative status protein mapping.

Oxidative regulation of protein phosphorylation is not only an important part of efficient and essential signal propagation, but can also promote a deregulated state when the reversibility of the oxidation is compromised. This can happen by irreversible overoxidation of cysteines or by irreversible oxidative modification of other amino acids such as methionine or tyrosine. In balanced conditions $H_2O_2$ is required in the endoplasmic reticulum (ER) for oxidative protein folding, while overproduction of ROS results in ER stress. This two edged sword is discussed by Andreas Petry and Agnes Görlach using ER-localized NADPH oxidases as example [96,97]. ER stress activates the unfolded protein response (UPR) in three main steps (or phases). Activation of the Protein Kinase RNA-like Endoplasmic Reticulum Kinase (PERK), which phosphorylates eIF2alpha, results in general inactivation of CAP-dependent translation, despite some specific exceptions such as the transcription factor ATF4. Then, ER stress activates the inositol requiring element 1 (IRE1) – which splices the mRNA of XBP1 – and the transcription factor ATF6. ATF4, ATF6 and XBP1 induce the expression of genes involved in protein folding and degradation in order to reestablish proper protein folding and to remove protein debris. In the later ER stress response, pro-apoptotic proteins are upregulated such as CHOP in order to activate programmed cell death if the cell cannot resume physiological function.

ROS act especially on the phosphorylation status of eIF2alpha since protein phosphatase 1 (PP1), which controls together with GADD34 the dephosphorylation of eIF2alpha, is redox sensitive. $H_2O_2$ is able to oxidize a cysteine close to the catalytic core in a reversible manner resulting in the inactivation of PP1. Sources for ROS in ER stress are Ero1 in the ER or mitochondria, but also NADPH oxidases play a role. NOX1, NOX4 and $p22^{phox}$ were shown to interact with ER proteins such as PDI [98], and NADPH oxidase derived ROS were involved in the ER stress response [99–102]. In response to ER stress due to inhibition of *N*-glycosylation, NOX4 associated with GADD34 thereby oxidizing PP1, extending eIF2alpha phosphorylation and promoting survival of cardiomyocytes [101]. However, other reports showed that 7-keto-cholesterol-induced ER stress in human arterial smooth muscle cells induced NOX4, resulting either directly in cell death [100] or in increased autophagy [99], which demonstrated a pro-apoptotic role for NOX4. In addition, NOX1 and NOX2 can play a pro-apoptotic role in cardiomyocytes [102] and renal cells [103] in response to ER stress. In summary, ROS derived from NADPH oxidases participate in the ER stress response. However, the subsequent outcome seems to be dependent on the cellular context, the stimuli used, the spatial distribution and the type of ROS. It is important to take these parameters into account when analyzing the role of ROS in ER stress and other pathophysiological conditions.

Another enzyme connected to ER stress is neutral sphingomyelinase (N-SMase). Sphingomyelinases (SMases) are categorized into neutral, acid and alkaline subtypes and hydrolyze sphingomyelin to ceramide [104]. Mutay Aslan discusses the accumulating evidence that ceramide induces oxygen species production via the mitochondrial respiratory chain [105,106] and stimulates inducible nitric oxide synthase (NOS2) expression [107]. Indeed, activation of neutral sphingomyelinase (N-SMase) is reported to be involved in various disease pathologies connected to “oxidative stress”. Studies have shown that ischemia reperfusion (IR) injury leads to activation of N-SMase in rat cardiac myocytes [108] and rat liver [109]. Repletion of glutathione (GSH) via *N*-acetylcysteine (NAC) treatment in post-myocardial infarction rat hearts resulted in inhibition of N-SMase and decreased oxidative stress resulting in improved left ventricular function [110]. Similarly, inhibition of N-SMase reduced elevated levels of nitrative and oxidative stress markers in liver IR injury [111].

Neutral SMase is localized in sphingolipid-rich membrane fractions [111], establishing the structural basis for its functional interaction with NOS [112]. Cellular stress responses, which increase N-SMase activity, also affect NOS2 expression and nitric oxide bioavailability. It has been reported that ceramide production by N-SMase is a key mediator in the induction of NOS2. Other studies showed that exogenous ceramide induces NOS2 expression in rat primary astrocytes [113] and reported positive modulation of NOS2 gene expression by SMase and/or ceramide in vascular smooth muscle cells and microglia [114,115]. Neutral SMase inhibition decreased both NOS2 and nitrotyrosine levels in an experimental model of glaucoma [116] and liver IR injury [109]. In summary, studies reveal that cellular stress responses significantly increase N-SMase activity and sphingomyelin/ceramide levels, leading to increased nitrative and oxidative modifications. Inhibition of N-SMase significantly reduced oxidant and nitrative stress markers, which emphasizes the need for future studies evaluating agents blocking N-SMase activity that can facilitate the development of treatment strategies to alleviate inflammation and oxidative injury.

The close relationship between bacteria and host is evident in bacterial toxin production that alters redox regulation in the host and in the response of bacteria to host-derived secondary oxygen metabolites generated as an innate immune response by post-translationally

modifying bacterial proteins for protection and survival. Amanda J. Edson and Kari E. Fladmark discuss how cyanotoxins induce oxidative modifications in the host. The overabundance of cyanobacteria in aquatic ecosystems may result in a large increase in the manufacture and release of cyanotoxins into the aquatic environment, which cause human health implications through biomagnification [117]. A variety of cyanotoxins are produced by a wide range of cyanobacteria including: microcystins [118,119] (MC), nodularin [120] (NOD), and β-*N*-methylamino-L-alanine [121,122] (BMAA). Microcystins and nodularin are potent inhibitors of Ser/Thr protein phosphatases (PP), specifically PP1 and PP2A [118,120] through direct interaction at the catalytic site [123]. Both toxins are cyclic peptides containing several non-proteinogenic amino acids [118,120]. BMAA has been shown to indirectly target PP2A by inhibitory phosphorylation mediated through BMAA activation of the glutamate receptor mGluR5 [124]. However, unlike MC and NOD, BMAA is a non-proteinogenic amino acid with a high degree of structural similarity to simple amino acids allowing it to be misincorporated into proteins leading to an additional toxic effect [121]. MC, NOD, and BMAA exposure of cells has been found to promote protein hyperphosphorylation, increase ROS production, and induce apoptosis [118,120,121,124].

Phosphorylation of proteins including ROS scavenging enzymes may be one of the major mechanisms of ROS induction by cyanotoxins. PP inhibitory action of cyanotoxins will result in broad protein hyperphosphorylation. In addition to ROS induction through PP inhibition, BMAA may also increase ROS through a non-glutamatergic mechanism [122]. $H_2O_2$ accumulation occurs within minutes in MC and NOD-exposed hepatocytes followed by cytoskeletal rearrangement and apoptosis [119,120]. $Ca^{2+}$/calmodulin-dependent protein kinase II (CaMKII) has been shown to be essential in MC- and NOD-induced apoptosis and acts up-stream of $H_2O_2$ accumulation. Inhibition of PP by toxin exposure prevents the dephosphorylation of CaMKII autophosphorylated on Thr287/286 [123] leading to kinase hyper-activation. Rather surprisingly, CaMKII seems to be responsible for all observed MC and NOD-induced phosphorylation supporting its role as a key actor in cytotoxicity. Toxin-induced $H_2O_2$ generation may also amplify CaMKII activity and thereby also $H_2O_2$ generation through specific methionine oxidation of CaMKII [123]. The role of CaMKII in BMAA-induced toxicity remains to be elucidated, however CaMKII is shown to bind to and regulate the directly BMAA targeted mGluR5 receptor [125]. The converging signaling pathways of BMAA, MC and NOD suggest that co-existence of these toxins may increase the environmental risk factor to human health.

### 2.5. Oxidative stress and adaptation processes

Hypochlorous acid (HOCl) is a strong oxidant produced by activated neutrophils that kills pathogenic bacteria. Thus, bacteria have to defend against hypochlorite to maintain the reduced state of their cytoplasm. Gram-negative bacteria utilize glutathione (GSH) as their major thiol-redox buffer, but most Gram-positive bacteria do not produce GSH. Melanie Hillion and Haike Antelmann study redox modifications in Gram-positive bacteria under oxidative stress. Actinomycetes utilize mycothiol (MSH; AcCys-GlcN-myoinositol), which functions in protection against reactive oxygen, nitrogen and electrophilic species, antibiotics and heavy metals [126,127]. Firmicutes bacteria, including *Bacillus* and *Staphylococcus* species produce the redox buffer bacillithiol (BSH; Cys-GlcN-malate). BSH-deficient *Staphylococcus aureus* isolates were more sensitive to antibiotics (fosfomycin and rifampicin) and showed reduced survival in macrophage infection assays [127]. Thus, BSH biosynthesis genes could be drug targets for the development of novel antibiotics to treat *S. aureus* infections. Under conditions of NaOCl stress, BSH plays an important role in the protection and redox regulation of proteins by formation of BSH mixed protein disulfides, termed *S*-bacillithiolation [127]. In *Bacillus subtilis*, *S*-bacillithiolation controls the activity of the organic hydroperoxide repressor OhrR and the methionine synthase MetE [127,128]. *S*-bacillithiolation of the OhrR repressor leads to derepression of the OhrA peroxiredoxin that confers NaOCl resistance. *S*-bacillithiolation of MetE in its Zn-binding active site leads to methionine auxotrophy under oxidative stress. Two bacilliredoxins (BrxA and BrxB) with unusual CGC active site motifs were characterized that function in the reduction of *S*-bacillithiolated OhrR and MetE [129]. De-bacillithiolation results in the formation of bacillithiolated Brx (Brx-SSB) that requires BSH and an uncharacterized BSSB reductase for recycling. However, the bacilliredoxin pathway is redundant with the thioredoxin pathway in vivo for reduction of BSH mixed protein disulfides.

In *Corynebacterium glutamicum*, about 25 *S*-mycothiolated proteins were identified under hypochlorite stress conditions [130]. These include many metabolic enzymes, such as the methionine synthase MetE, the glycogen phosphorylase MalP, the myoinositol-1-phosphate synthase Ino1 and antioxidant enzymes (Tpx, Gpx, MsrA). *S*-mycothiolation of MalP is required for the oxidative stress resistance of *C. glutamicum* and could prevent glycogen degradation under NaOCl stress to save the energy and carbon source. Redox regulation of the thiol peroxidase Tpx, the MSH peroxidase Mpx and the methionine sulfoxide reductase MsrA was recently studied. The mycoredoxin (Mrx1) and thioredoxin (Trx) pathways are both involved in reduction and regeneration of *S*-mycothiolated Mpx and MsrA to restore their enzyme activities for detoxification of peroxides and reduction of methionine sulfoxides [131,132]. In conclusion, *S*-bacillithiolation and *S*-mycothiolation are widespread redox modifications in Gram-positive bacteria that function in redox regulation and thiol-protection under oxidative stress conditions.

Acclimatization of an organism to stress or so-called preconditioning is a modulating response that prevents pathophysiological damage. In plants, waves of calcium and ROS are generated as response to abiotic stress, pathogen infection and mechanical injury. These waves mediate long-distance signaling and systemic cell-to-cell communication [133]. Khrystyna Semen and Olha Yelisyeyeva propose mitochondrial ROS oscillations as a balancing factor in mammalian metabolism. The development of a hormetic reaction (preconditioning or mild stress) represents one approach to increase resistance to oxidative damage and eliminate signs of oxidative stress (OS), which is involved in multiple pathological processes and aging [134,135]. A hormetic reaction is triggered by a mild energy deficit, which precludes some increase in ADP/ATP and $NAD^+$/NADH ratios leading to activation of redox processes and energy function of mitochondria. As a result, mobilization of various metabolic pathways, especially PUFA oxidation, takes place which promotes the flow of succinate into the Krebs cycle, activation of succinate oxidation and monopolization of the respiratory chain by succinate dehydrogenase. Such a metabolic state promotes more diverse shunting of the Krebs cycle with activation of glutamine/glutamate metabolism, the glyoxalate cycle, peroxisomal oxidation and accumulation of succinate. At the same time, activation of transaminase and alcohol dehydrogenase (ALDH2) reactions causes an increased flow of alpha-ketoglutarate and its more efficient oxidation [30,136,137]. Simultaneous activation of pathways related to these two reciprocal mitochondrial substrates serves as an important mechanism involved in the hormetic response. At the cell level that is reflected by the improved interactions between catabolism and anabolism, while excessive flow of electrons in the respiratory chain can be controlled by several mechanisms of “mild uncoupling” including reverse electron transport from Complex II to Complex I, activation of sirtuins (especially SIRT1) and uncoupling proteins. The fine-tuned leak of electrons that occurs with an increase in membrane and ATP potentials is further involved in production of a certain amount of superoxide, hydrogen peroxide and nitric oxide [30,60]. Subsequently these reactive oxygen/nitrogen species function as signaling molecules for multiple pathways, mainly HIF/NRF2/NF-κB and their crosstalk, rather than promote excessive oxidative damage to macromolecules.

Mild prooxidant activity accompanying the formation of a hormetic

response gives rise to the production of metabolic "endogenous" oxygen, which can be readily used either for oxygenase or oxidase reactions, maintenance of $pO_2$ and elimination of hypoxia. Under such circumstances the activity of oxygen dependent enzymes, including those involved in $H_2S$/NO/CO synthesis, is optimized, which promotes activation of $K^+_{ATP}$, BK and TRP channels. In fact, more frequent oscillation of ROS and metabolism dependent $O_2$ promote sustained efficient function of mitochondria, which in turn leads to prolongation of free radical reactions (FRR) and membrane lipid peroxidation in the cell. The oscillatory nature of ROS/$O_2$ and related regulatory substances is the least studied aspect in free radical biology. In our opinion, the most important outstanding questions include the mechanisms of fluctuations of ROS/$O_2$, transcriptional factors and other regulatory substances derived from oxidative modifications of lipid and proteins, their pattern and localization in cell compartments. A better understanding of these mechanisms will promote therapeutic manipulation of ROS generation and thus, the dynamic association of respiratory complexes (supercomplex formation) to maintain optimal energy function of the mitochondria. Energy produced during FRR may play a crucial regulatory role to achieve better self-organization of the metabolism, improved stress resistance and sustained hormetic reactions.

For some diseases, including cardiovascular disease, cancer, or metabolic and neurological pathologies, the involvement of redox deregulation is unquestionable. Fernando Antunes and Paula M. Brito discuss how systems quantitative redox biology may bring us closer to an in depth understanding of "ROS", their effects and therapeutic intervention in disease. Deregulation of reactive oxygen, nitrogen, and sulfur species (RONSS) affects cellular and organismal well being. RONSS target selected proteins either by binding to, or oxidizing metal centers or cysteine residues at the level of specific organs, tissues, cell types, and cellular organelles. These selected proteins constitute redox switches. Most of them are controlled by reversible oxidation and are key players in many signal transduction pathways [138]. The identification of hundreds of redox switches by large scale proteomic analysis [138] has provided new potential therapeutic targets and biomarkers that are yet to be explored. Thus, a critical mass has been reached to implement an ambitious translational redox biomedicine program. Perhaps the most important barrier to the development of such a program is the complexity of RONSS effects, including biphasic curves with narrow concentration ranges that often lead to contradictory conclusions. Such complex behavior is caused by the highly interactive molecular network formed by redox switches. A promising approach to deal with this issue is systems quantitative redox biology [139,140] that integrates the network of redox-regulated pathways and has the potential to predict the behavior of redox networks when interrogated with a pharmaceutical drug. This will help identify redox circuits that are amenable to redox therapeutic interventions without triggering undesired responses by pathways that share the same redox mediators. RONSS generation is tightly controlled with respect to kinetics, concentration and subcellular location [141]; the implications of these observations are that highly targeted redox therapies, as opposed to systemic antioxidant interventions, are key for a viable pharmacological strategy. Recent advances in nanotechnology have provided new tools to deliver drugs to specific therapeutic target locations and have the potential to generate new classes of drugs that contain redox-active molecules or molecules that modulate the levels of RONSS as active pharmaceutical ingredients.

### 2.6. Microparticles and reactive oxygen species

According to Rhian M. Touyz, microparticles, also termed microvesicles, are cell membrane-derived fractions, which are generated from activated cells that undergo stress or injury [37]. Theoretically all cell types are able to generate microparticles, which are detectable in biological fluids. In the circulation the major microparticle subtypes are derived from platelets, neutrophils, erythrocytes and endothelial cells and are measured and phenotyped by specific markers and flow cytometry [37,142]. Microparticles have distinct characteristics: they are 100–1000 nm in diameter, contain features of their parent cells and do not contain nuclear material. Microparticles were first considered as 'plasma dust' representing cell debris; however, it is now clear that these elements are biologically functional and that they are signatures of the cells from which they are derived. Accordingly, microparticles have been considered as biomarkers of various pathologies [37,142,143]. Many pathological states including cardiovascular diseases, kidney disease, cancer, diabetes, thrombosis among others are associated with increased levels of circulating microparticles. In addition, increasing evidence indicates that microparticles themselves can contribute to pathophysiological processes, because they contain proteins, enzymes, nucleic acids, cytoskeletal machinery, specialized lipids and microRNAs, that can be transferred to other cells, thereby initiating signaling events and changes in target cell function [144–146]. Through this mechanism, microparticles also play an important role in cell-cell communication and cross-talk. As such microparticles are now considered not only biomarkers of diseases, but also biovectors. In addition, because microparticles transfer their 'cargo', they have been considered as novel delivery systems for therapeutics [147]. Increased circulating levels of microparticles are found in conditions associated with oxidative stress, including hypertension, diabetes, kidney disease and cancer. Moreover, many of the mechanisms underlying the generation of microparticles involve ROS and many of the effects of microparticles are redox sensitive [148,149]. Formation of microparticles involves lipid oxidation, mitochondrial activation, caspases, calcium signaling and Rho kinase activation, processes linked to increased intracellular ROS bioavailability. Microparticles can possess the enzymatic machinery responsible for ROS formation, including NOX subunits and/or nitric oxide synthase (NOS) and there is growing evidence that microparticles can generate ROS and nitric oxide ($^{\bullet}NO$) [148,149]. Microparticles are supposed to transfer $O_2^{\bullet-}$, $H_2O_2$ and $^{\bullet}NO$ to neighboring cells, and they can stimulate production of ROS in target cells by stimulating cellular oxidases [150]. These processes can be inhibited by ROS scavengers, NOX inhibitors, NOS inhibitors and antioxidants. Hence microparticles are influenced by redox processes and can themselves modulate redox-sensitive signaling pathways [37,148,149]. While it is clear that oxidative stress and microparticle formation are closely linked and that microparticles can act as biovectors influencing cellular redox processes, many of the studies were performed under in vitro conditions in cell-based systems. The pathophysiological significance of these processes in vivo awaits further clarification.

### 2.7. Conclusions

To tackle these questions a multipronged approach is necessary. In depth understanding of the spatiotemporal role of a particular ROS source in vivo can only be achieved by scientific endeavors that combine basic discovery with appropriate animal models. But these studies depend on the development of improved tools for visualization and quantification of the oxygen metabolite generated. In addition, a combination of the expertise of redox biologists, systems biologists, nanotechnologists and clinical scientists will be required to support the successful translation of redox biology knowledge into viable pharmacological treatments and novel diagnostic biomarkers of diseases, which will have a major scientific and socio-economic impact.

## 3. ROS as signaling molecules

Agnes Görlach (goerlach@dhm.mhn.de) and Andreas Petry (petry@dhm.mhn.de).

### 3.1. Introduction

Reactive oxygen species (ROS) in high concentrations have damaging actions, but in lower concentrations they can act as signaling molecules (Fig. 3.1). ROS generated by the activation of enzymes such as NOX, xanthine oxidases, uncoupled NO synthases and other sources such as arachidonic acid metabolizing enzymes, lipoxygenases and cycloxygenases, the cytochrome P450s, peroxidases and other hemoproteins, as well as ROS generated by mitochondria seem to play various roles in the cellular signaling network under different physiological and pathophysiological conditions. Various cellular antioxidant systems oppose ROS load thereby limiting not only cellular damage, but also contributing to ROS-dependent signaling.

### 3.2. Role of ROS in VEGF and TGF signaling

The dual role of ROS as either damaging or signaling molecules is well illustrated in the vascular system. For example, as discussed by María Monsalve and Ignacio Prieto, ROS have been demonstrated to be central in the control of angiogenesis and are required for the induction of endothelial cell migration and proliferation. VEGF-A is the most potent and primary endothelial cell specific angiogenic growth factor and stimulates vascular permeability, endothelial cell proliferation, migration and tube formation, primarily through the VEGF-A receptor 2 (VEGFR-2). ROS work both upstream and downstream of VEGF-A. Exogenous ROS administration induces VEGF-A levels and promotes endothelial migration and proliferation, which can lead to diabetic retinopathy, development of vasa vasorum in atherosclerosis and tumor angiogenesis [151]. ROS-sensitive transcription factors and coactivators have been identified that can directly regulate VEGF-A mRNA levels, such as the hypoxia-inducible factors 1α and 2α (HIF-1α, HIF-2α) [152–154], the transcriptional coactivator peroxisome proliferator γ coactivator 1α (PGC-1α) [155], but also Ref-1, p53, NF-κB and Ets-1 [156].

ROS have also been shown to regulate VEGFR-2 activity and signaling [157]. The antioxidant protein peroxiredoxin II (PrxII) has been found associated with VEGFR-2 and is necessary to prevent its oxidation. VEGFR-2 oxidation renders the receptor insensitive to VEGF-A stimulation [158]. Following VEGFR-2 stimulation and tyrosine phosphorylation, the receptor can be dephosphorylated by several phosphatases such as protein tyrosine phosphatases (PTPs) and density-enhanced phosphatase-1(DEP-1)/CD148 which can be inactivated by ROS [159,160]. Downstream of VEGFR-2, several signaling nodes have also been shown to be ROS sensitive such as PI3K/AKT [161]. Importantly, VEGFR-2 activation can induce ROS production by endothelial cells (EC), and abrogation of VEGFR-2-dependent induction of ROS levels abolishes VEGF-A effects on EC migration and proliferation. It has been amply demonstrated that VEGF-A stimulates ROS production through the activation of NOX enzymes in EC [156]. VEGF-A/VEGFR2-dependent activation of NOX1 has been related to increased angiogenic tube formation of EC [162]. NOX2 knockout mice display impaired neovascularization in hind limb ischemia and their ECs have much reduced VEGF-A induced proliferation and migration [163,164]. In addition, NOX4 siRNA inhibited VEGF-induced EC migration and proliferation [165]. Upon VEGF-A-stimulated receptor phosphorylation, TSAd-dependent Src activation recruits the scaffold protein IQGAP1 that promotes the recruitment of Rac1 and NOX2 to initiate ROS production [166,167]. Furthermore, inhibition of mitochondrial ROS production was sufficient to abrogate VEGF-A and EC migration independent of NOX enzymes [168]. One possible mechanism could be inactivation and transcriptional downregulation of PGC-1α following PI3K/AKT activation in response to growth factor stimulation that results in the enhanced production of mitochondrial ROS required to promote endothelial cell migration [169]. Furthermore, several lines of evidence suggest that NOX enzymes can function downstream of mitochondria. Hence, depletion of mtDNA reduces NOX activity, while induction of mitochondrial dysfunction increases mitochondrial ROS production resulting in the activation of NOX enzymes [58]. Enhanced mitochondrial ROS production was sufficient to recapitulate most if not all the features of diabetic retinopathy, and the underlying mechanism involved was associated with ROS-dependent constitutive activation of VEGFR-2, and reduced sensitivity to VEGF-A stimulation. Importantly, both a mitochondrial targeted antioxidant and a general NOX inhibitor effectively normalized VEGF-A signaling and endothelial tube formation, indicating that both NOX and mitochondrial ROS are functionally co-regulated in this context [170,171].

Other factors that have been identified as potent inducers of ROS belong to the TGF-β family. These cytokines play essential roles in the maintenance of tissue homeostasis, regulation of cell growth, migration and invasion, extracellular matrix remodeling and immune suppression [172]. As Isabel Fabregat points out, deregulation of TGF-β signaling is frequently observed in disease states, such as fibrosis, inflammation and cancer, being considered responsible for part of the sequence of events leading to the end-stage of these diseases [173]. Initial studies in the middle of the 1990s indicated that TGF-β mediates ROS production [174,175] and a NOX activity was suggested to be responsible for the release of $H_2O_2$ [174,176]. Nowadays, NOXs are considered as relevant mediators of TGF-β actions in different cells, contributing to the regulation of growth, death and activation of myofibroblasts, key executers of the fibrotic process. Although different NOXs have been proposed to be modulated by TGF-β, NOX1 and NOX4 appear to be the NOXs most frequently involved in its actions. Under physiological circumstances, NOX4 is transcriptionally upregulated by TGF-β in a Smad-3-dependent manner and is considered a mediator of TGF-β-mediated suppressor effects. In particular, NOX4 is required for TGF-β-induced apoptosis in epithelial cells [177,178]. In contrast, NOX1, activated by TGF-β in a caveolin-1-dependent manner, plays opposite roles, stimulating anti-apoptotic signals and preventing cell death [179]. Deciphering the specific roles of NOX1 and NOX4 in TGF-β actions during tumorigenesis will require further investigations, but current data indicate that overactivation of growth factor signals favor activation of NOX1 and inhibit NOX4 up-regulation, which would prevent cell death [180]. Once cells overcome apoptosis, NOX4 might

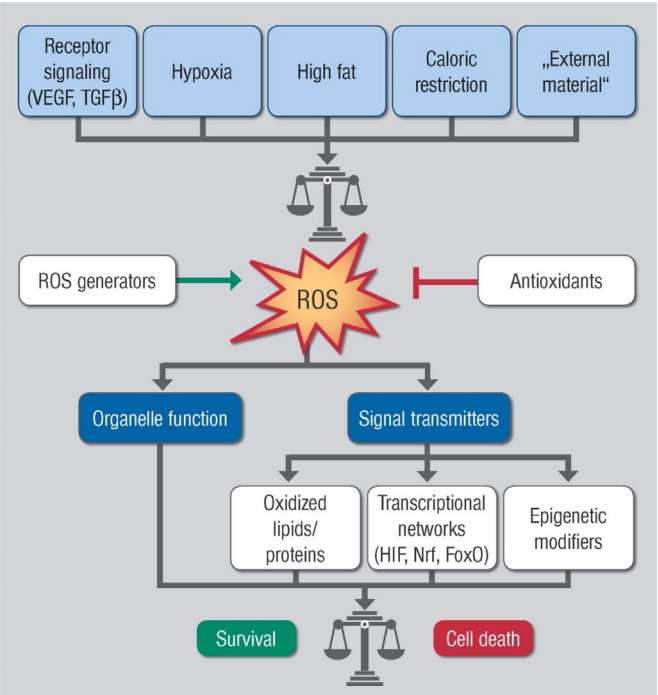


**Fig. 3.1.** Summary scheme of ROS acting as signaling molecules in different disease settings but also in physiological processes.

promote pro-tumorigenic actions of TGF-β, such as epithelial-mesenchymal transitions (EMT), that induce cell migration and invasion [181]. Strong evidence supports a role of NOX4 in mediating TGF-β-induced myofibroblast activation in different models of fibrosis [182,183], as well as in the maintenance of the phenotype of myofibroblasts [184]. NOX4 also mediates TGF-β-induced apoptosis in epithelial cells [178,184], which contributes to the inflammatory process that concurs with increased activation of myofibroblasts and extracellular matrix deposits. These studies provide proof of concept for therapeutic targeting of NOX4 to inhibit TGF-β-induced fibrogenesis. However, further research is required to validate the safety of these inhibitors, at least in those tissues where TGF-β acts as a tumor suppressor factor. In this sense, recent results indicate that knockdown of NOX4 increases proliferation and tumorigenic properties of liver tumor cells [185].

### 3.3. Redox regulation of fundamental cellular processes such as cell death

In a more general way, the dual role of ROS has been associated with different cancer types. As Guia Carrara and Geoffrey L. Smith explain, elevated levels of ROS have been a well established property of most cancers where they contribute to many aspects of tumor development and progression, including cell proliferation, genomic instability, resistance to apoptosis, cell adhesion and motility, and a metabolic shift to glycolysis [186,187]. On the other hand, excess ROS is deleterious to the survival and proliferation of cancer cells. Hence, endogenous antioxidants are also upregulated to detoxify the cell and maintain a delicate balance of elevated intracellular ROS that is beneficial to malignant cells [186,187]. Recently, the Transmembrane Bax Inhibitor-1 Motif-containing (TMBIM) protein family has received increasing attention in relation to its role in cancer, which is supported, for instance, by dysregulation of expression being associated with many cancer types and by the characterization of its multiple functions that constitute important hallmarks of malignancy [188]. The Golgi anti-apoptotic protein (GAAP) is a member of the TMBIM family and is projected by phylogenetic analyses to have originated before the divergence of plants and protozoa about 2000 million years ago [189]. Orthologues of the human GAAP are remarkably conserved at the protein level (e.g. amino acid sequence, length and hydrophobicity profile) throughout eukaryotes, prokaryotes and some poxviruses, in agreement with a highly conserved ancestral structure and function [190–192]. Since the first discovery of this gene in 2002 in camelpox virus [193], several cellular functions and structural properties of GAAPs from various origins have been described. Within eukaryotes, GAAPs regulate $Ca^{2+}$ levels and fluxes from the principal intracellular stores (Golgi and ER), confer resistance to a broad range of apoptotic stimuli and promote cell adhesion and migration via the activation of store-operated $Ca^{2+}$ entry (SOCE) [193-195]. Importantly, these multi-transmembrane proteins were shown recently to form cation-selective ion channels, potentially forming the basis for the modulation of the diverse functions of GAAPs [191]. In view of these functions as important hallmarks of cancer, the effects of human GAAP on ROS homeostasis in the context of cancerous cells were investigated. Significantly greater overall basal ROS levels, and more specifically basal $H_2O_2$, were detected intracellularly in cells over-expressing GAAP. In addition, cells over-expressing GAAP displayed greater invasive capabilities in tissue culture, which was confirmed by the opposite effect upon GAAP knock down by siRNA. Furthermore, the activity of secreted matrix metalloproteinases 2 and 9, which are sensitive to regulation by ROS and play a key role in migration and invasion, was dysregulated in these cells. Although both the mechanistic links between these observations and the contribution of $Ca^{2+}$ remain to be established, ROS appear to be a common factor of importance and relevance in understanding the contribution of GAAP in cancer development. Furthermore, the diverse multifunctional properties of GAAP provide a useful common starting point from which the complex interplay between ROS homeostasis with other important hallmarks of cancer such as cell invasion, migration, and resistance to apoptosis can be studied.

Other cellular structures with a putative relation to ROS are centrosomes. Centrosomes are the microtubule organizing centers (MTOCs) that nucleate and organize microtubules. They have critical roles in various processes, including cell division and polarity. Over 100 years ago, it was claimed that centrosome aberrations may lead to genomic instability and consequently to cancer [196]. As Lokman Varisli and Serap Ilikay summarize, it was reported that genetic manipulations that lead to centrosome amplification can cause tumor development [197]. Consistently, centrosome abnormalities have been observed in many human cancers and in premalignant lesions [198]. Increased centrosome numbers can arise from various mechanisms, such as centrosome overduplication, cell fusions or failures during cytokinesis [199]. However, the causes and mechanisms leading to these effects are not fully understood. In recent years, it was suggested that ROS may be involved in the regulation of centrosome organization. Indeed, various researchers reported that oxidative stress may lead to increases in the number of centrosomes. However, there are contradicting reports in this area. While some researchers reported that oxidative stress can trigger hyperamplification of centrosomes and consequently may promote progression of cancer [200], others suggested that centrosomal abnormalities may contribute to the entry of the cells into senescence, thus preventing proliferation of damaged cells. Consequently, centrosome abnormalities are a part of the defense mechanism that inhibits carcinogenesis [201,202]. On the other hand, it is known that centrosomes are shielded from oxidative stress through their association with peroxiredoxin I (PRX1) during interphase, while this enzyme is inhibited by cyclin-dependent kinase 1 (Cdk1) in mitosis [203]. Moreover, it was reported that the local concentration of $H_2O_2$ around centrosomes is involved in the regulation of centrosomal levels of some cell/centrosome cycle related proteins and also in the regulation of mitotic entry [203]. In concordance, it was shown that reduction of *peri*-centrosomal $H_2O_2$ by centrosome-targeted catalase inhibits entry of cells into mitosis [203]. Consistently, treatment of mitotic cells with $H_2O_2$ causes mitotic slippage and consequently formation of hypertetraploid cells [204]. Although the mechanisms of $H_2O_2$ induced mitotic slippage have not been entirely elucidated, this effect is probably related to exposure of naked centrosomes to $H_2O_2$ without a Prx1 (and probably other antioxidants) shield during mitosis.

### 3.4. Redox regulation involving mitochondria

In mitochondria, the thiol redox conditions are essentially controlled by glutathione and thioredoxin systems. In the latter, a reducing sequence starting with NADPH allows the transfer of electrons to thioredoxin in a process mediated by the mitochondrial selenoenzymes thioredoxin reductases (TrxR2). NADPH is maintained in a reduced form by specific dehydrogenases and by the membrane-bound transhydrogenase. Alberto Bindoli and Maria Pia Rigobello discuss, that TrxR2 is able to reduce, in addition to its specific substrate thioredoxin (Trx2), a large number of different molecules. Thioredoxin is a key component of the thioredoxin system acting as a wide-ranging protein-disulfide reductase and therefore controlling the redox state of different factors [205]. In particular, Trx2 reduces Prx3, which therefore controls the levels of $H_2O_2$. The mitochondrial isoform of cyclophilin (CypD) plays a relevant role in regulating the mitochondrial permeability transition pore [206] and is endowed with redox properties due to the presence of specific cysteine residues [207]. In isolated rat heart mitochondria, the inhibition of TrxR2 with the gold compound auranofin leads to a concomitant oxidation of Trx2, Prx3 and CypD as demonstrated by the redox Western blot technique [208]. Similarly, CEM-R cancer cells incubated with auranofin or other inhibitors of thioredoxin reductase such as ATO (arsenic trioxide) and CNDB (1-chloro-2,4-dinitrobenzene) show also a concurrent oxidation of Trx2, Prx3 and CypD. Both in mitochondria and cancer cells, the addition of $H_2O_2$ leads to an

oxidation pattern similar to that observed after treatment with inhibitors of TrxR2 [208]. In addition, CypD co-immunoprecipitates with both Trx2 and Prx3 [208] indicating a potential cooperation involving these proteins. These results indicate that CypD can act as a redox protein able to modulate the mitochondrial functions such as membrane permeability and that the redox conditions of CypD may be controlled by the thioredoxin system. Of note, Prx3 can act as a sensor of hydrogen peroxide and transduce this oxidation to CypD. This view is further supported by a molecular modeling approach showing a potential interaction of CypD both with Trx2 and Prx3 [208].

As Carlos M. Palmeira and Anabela P. Rolo point out, mitochondria play also an essential role in energy production and cellular homeostasis. Their highly dynamic nature, based on alterations in biogenesis, mitophagy, fusion and fission, allows adjustment of the sequential oxidoreductive reactions in the electron transport chain (ETC) and dissipation of the membrane potential by ATP synthase in response to different environmental cues [209]. Such adaptive processes may involve signaling by ROS and explain how mild levels of mitochondrial-derived ROS trigger a hormetic response resulting in extended lifespan. As ROS are an inevitable by-product of oxidative phosphorylation, alterations in the mitochondrial oxidative rate with a consequent excessive load of ROS, have been traditionally associated with pathological processes such as cancer, diabetes and neurodegeneration. Although in mammals the exact signal released by mitochondria that triggers a hormetic response is still uncertain, more and more studies are addressing ROS as promoters of mitohormesis, as opposed to their pro-aging action due to persistently induced oxidative damage. The concept of mitohormesis proposes that a mild increase in mitochondrial ROS may act as a sublethal trigger of cytoprotective long-lasting metabolic and biochemical changes against larger subsequent stresses [210]. Caloric restriction (CR) has been repeatedly shown to decrease risk- actors for major age-related diseases and to increase lifespan in various organisms. Early on, work in *C. elegans* [211] has shown that reduced glucose availability was linked to an increase in both ROS and catalase activity, ultimately culminating in increased survival rates. Several other studies have further demonstrated that many strategies promoting longevity share a common downstream aspect, that is: increased mitochondrial ROS. Inhibition of the mitochondrial ETC by certain mutations or inactivation of mitochondrial superoxide dismutase increases *C. elegans* lifespan, as reviewed by Dancy et al. [212]. Low doses of rotenone, an inhibitor of complex I, have also been shown to extend the lifespan of *C. elegans* [212] as well as to induce hormesis in primary human fibroblasts, an effect not possible in older cells or with higher concentrations of rotenone [213]. Inhibition of mTORC signaling and the consequent induction of autophagy by caloric restriction or by pharmacological agents has also been found to promote longevity in yeast, worms, flies and mice, as recently reviewed [214]. Further, it has been shown that hearts with impaired mitophagy and consequent accumulation of damaged ROS-forming mitochondria develop cardiomyopathy, which can be surprisingly improved by the ROS-dependent activation of compensatory autophagic pathways of mitochondrial quality control, preventing a vicious cycle of ROS formation and mitochondrial dysfunction [215].

### 3.5. Role of ROS in hypoxia

When oxygen availability is reduced (hypoxia), eukaryotic cells sense this reduction and trigger a series of cellular and systemic responses that facilitate adaptation to hypoxia, including the optimization of oxygen consumption. As Pablo Hernansanz-Agustín and Antonio Martínez-Ruiz explain, some of these responses are mediated through transcriptional regulation by the stabilization of hypoxia-inducible factors (HIFs); however, this mechanism requires at least several hours for activation, and there is crosstalk with ROS signaling (for a recent review, see [216]). Several acute responses operate in minutes in specialized organs in which local temporal changes in the redox state have been implied. One example is the carotid body, which senses variations in blood oxygen to activate the respiratory center. The search for the molecular mechanisms of oxygen sensing in carotid body cells has recently led Fernández-Agüera et al. to propose a fundamental role for mitochondrial complex I in the production of a ROS signal in response to hypoxia [217]. For a long time there has been a debate on whether hypoxia increases or decreases ROS production, with apparently contradictory reports in the literature. This controversy might arise from the ROS source studied, from the cell type, tissue or organism examined, from the techniques used to measure different ROS, and/or from the duration of hypoxia applied in each study. It has recently been shown that several cell types respond to acute hypoxia with a transient increase in superoxide production at the beginning of hypoxia, which has been called a superoxide burst in acute hypoxia [218]. This may explain in part the apparently divergent results found by different groups that have not taken into account the time frame of acute hypoxic ROS production. Molecular mechanisms in acute hypoxia might involve mitochondrial complex I and the mitochondrial sodium/calcium exchanger (NCLX) (Hernansanz-Agustín et al., manuscript under evaluation). Superoxide production in acute hypoxia seems to be a common mechanism for different cell types, but it would elicit different responses in specialized cells and tissues where the adequate components for signal transduction may be present such as cysteine residues sensitive to reversible oxidation. Examples of this are the carotid body cells where localized ROS production inhibits $K^+$ channels [217,219]; or the pulmonary arteries where mitochondrial ROS production may elicit a signal cascade including ceramide production, further ROS production by NADPH oxidases and alterations in ion channel activity [220]. In endothelial cells, by using specialized thiol redox proteomics methods, the reversible oxidation of a range of protein cysteine residues has been observed that could mediate acute responses to hypoxia in these cells [221]. Another molecular example of a hypoxia signal transducer is the $Na^+$,$K^+$ ATPase, with cysteine residues that are sensitive to variations in the oxygen concentration, and that alter the function of the protein (recently reviewed in [222]). In conclusion, ROS production is being increasingly considered as a key signaling event in acute hypoxia, and the molecular mechanisms and functional consequences of this event are currently an active field of research, with implications for molecular physiology and pathology.

An enzyme family that requires oxygen for function, and is thus related to oxygen availability, are $^{\bullet}NO$ synthases. As Damir Kračun and Agnes Görlach discuss, all three family members, endothelial NOS (eNOS), inducible NOS (iNOS) and neuronal NOS (nNOS), catalyze the reaction of $^{\bullet}NO$ production by binding a number of cofactors such as flavin adenine dinucleotide (FAD), flavin mononucleotide (FMN), heme, 5,6,7,8-tetrahydrobiopterin ($BH_4$) and calmodulin to convert L-arginine and $O_2$ to L-citrulline and $^{\bullet}NO$.

The flow of electrons within NOS is tightly regulated. If disturbed, the chemical reduction of oxygen and the generation of $^{\bullet}NO$ are uncoupled and $O_2^{\bullet-}$ is generated from the oxygenase domain. In particular, failure of adequate provision of the cofactor $BH_4$ shifts electrons to molecular oxygen rather than to L-arginine, thus transforming NOS into a pro-oxidant superoxide anion-generating enzyme [223].

Conditions of low oxygen availability have differential effects on $^{\bullet}NO$ levels: decreased, increased and unchanged levels were reported. In some cases, the differences might have been due to different detection methods. Moreover, in several cases, NOS expression levels did not match the $^{\bullet}NO$ levels measured. While several reports showed that NOS expression increased under hypoxia, there was no concomitant increase in $^{\bullet}NO$ levels [224]; recent data indicate that hypoxia leads to uncoupling of NOS, which might explain this observation [225]. Mechanistically, a decrease in $BH_4$ levels observed under hypoxia in vitro and in vivo has been related to this effect. $BH_4$ levels in the endothelium are controlled through *de novo* $BH_4$ synthesis by GTP cyclohydrolase I (GTPCH-1), loss of $BH_4$ by oxidation to 7,8-dihydrobiopterin ($BH_2$), and regeneration of $BH_4$ from $BH_2$ by dihydrofolate

reductase (DHFR) [226]. While GTPCH-1 downregulation under hypoxia was not clearly demonstrated, recent data show that hypoxia can decrease the levels of DHFR, thus diminishing the capacity to recycle $BH_2$ to $BH_4$ [225]. In support of this finding, treatment with folic acid (FA), which has been shown to upregulate DHFR levels under normoxic conditions [227], restored DHFR, $BH_4$, and $^{\bullet}NO$ levels in hypoxic cells [225]. Decreased levels of $BH_4$ and DHFR together with diminished $^{\bullet}NO$ bioavailability were also observed in vivo in mice suffering from chronic hypoxia-induced pulmonary hypertension. While treatment with the biopterin precursor sepiapterin, which needs to be converted to $BH_4$ by DHFR, only marginally affected this disease [228], treatment with FA not only enhanced $^{\bullet}NO$ and BH4 bioavailability but also diminished pulmonary hypertension [225]. Since a decline in DHFR has also been reported to promote angiotensin-II induced hypertension [227], preservation of DHFR levels appears to be an important mechanism to combat uncoupling of NOS and its associated pathologies.

### 3.6. Redox regulation of gene expression via modulation of transcription factors and epigenetic pathways

Conditions of low oxygen are also favorable for stem cell maintenance. As Holger Steinbrenner and Lars-Oliver Klotz point out, adult mammals harbor multipotent somatic stem cells that are capable of replenishing terminally differentiated functional cells for maintenance and regeneration of tissues as well as for adaptation to metabolic demands. Examples include hematopoietic stem cells (HSCs) located in bone marrow, epithelial stem cells in intestinal crypts, and mesenchymal stem cells in adipose tissue and bone marrow. Somatic stem cells in adults are often quiescent but they may temporarily re-enter the cell cycle and proliferate rapidly in response to the appropriate signals. In recent years, it has become increasingly evident that even slight variations in intra- and extracellular levels of ROS may exert a profound impact on the fate and function of stem cells [229,230]. ROS serve as signaling molecules that affect the balance between self-renewal and differentiation of stem cells, their commitment, differentiation and maturation to specialized cell types, and their survival and aging. ROS involved in these processes, such as superoxide and hydrogen peroxide ($H_2O_2$), derive for the most part from the mitochondrial respiratory chain and from membrane-bound NADPH oxidases [229,230]. Transcription factors of the forkhead box, class O (FoxO) family participate in regulating and fine-tuning ROS-modulated cellular differentiation processes, as illustrated by the following examples. FoxOs stimulate the biosynthesis of ROS-reducing proteins located in mitochondria [superoxide dismutase 2 (SOD2), peroxiredoxins 3 and 5], in peroxisomes (catalase), and extracellularly [selenoprotein P (SelP)] [231]. Elevated

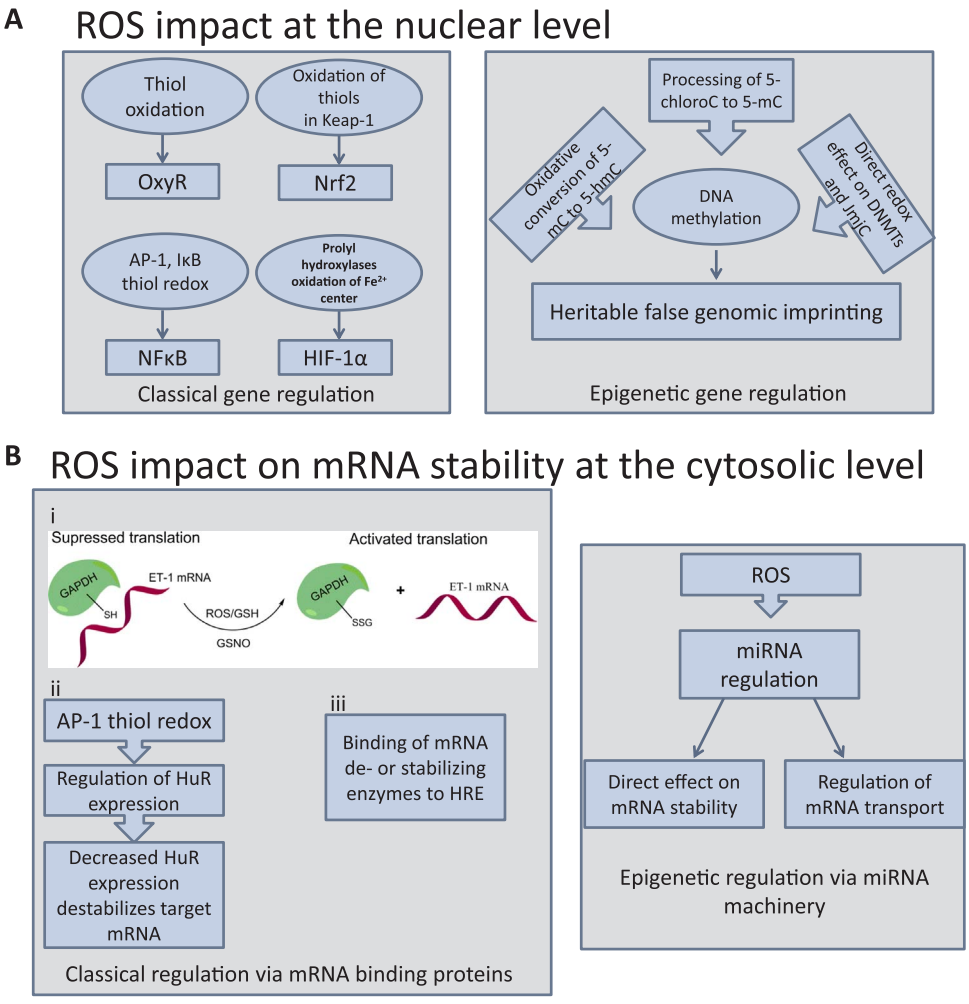


**Fig. 3.2.** (A) Reactive oxygen species can display their regulatory effect on the classical gene regulatory machinery and on epigenetic processes. One of the prominent pathways attributed to oxidative stress is thiol oxidation, which is involved in OxyR, NF-κB and KEAP1 signaling. Oxygen sensing prolyl hydroxylases represent another class of redox-dependent enzymes. For example, epigenetic involvement of ROS has been attributed to oxidative conversion of 5-mC to 5-hmC. (**B**) ROS impact on mRNA stability at the cytosolic level. Reactive oxygen species are involved in GAPDH signaling by directly altering its structure with the help of GSH or *S*-nitrosoglutathione (GSNO), and thus activate translation of endothelin-1 (ET-1) mRNA (i). AP-1 thiol redox regulation directly affects the gene regulating factor HuR by stability of its target mRNAs (ii). ROS have been implicated in the regulation of miRNA pathways, altering mRNA stability and their transport inside the cytosol. HRE means hormone response element. With permission of Elsevier and the authors. Copyright 2015.
Adapted from [238].

circulating levels of SelP may then result, by means of its function as a plasma selenium transporter, in increased biosynthesis and cellular activity of antioxidant and redox state-modulating selenoenzymes such as glutathione peroxidases and thioredoxin reductases [231]. Thus, FoxOs are crucial for cellular stress resistance and longevity. Tightly controlled increases in FoxO expression and activity may balance ROS generation in differentiating cells through an adaptive up-regulation of antioxidant enzymes, which has been well documented for adipogenesis; committed mesenchymal stem cells (preadipocytes) of the subcutaneous adipose tissue may undergo clonal expansion in response to high nutrient intake. This is followed by growth arrest and terminal differentiation into mature lipid-accumulating adipocytes. Adipogenic differentiation of human adipose tissue-derived stem cells has been shown to be associated with elevated ROS generation, and it was stimulated both by exogenous application of $H_2O_2$ and by overexpression of Nox4. During adipogenesis, expression of *FoxO1* and *FoxO3* genes as well as the FOXO target genes coding for catalase and SOD2 were upregulated; silencing of *FoxO1* suppressed adipogenesis [232]. The continuous renewal of the intestinal epithelium represents another example that illustrates the importance of ROS for differentiation processes: stem cells located at the bottom of intestinal crypts are capable of proliferating and differentiating into absorptive and secretory cell types. The switch between cell proliferation and differentiation/growth arrest is typically associated with changes in the intracellular glutathione (GSH/GSSG) and in the extracellular cysteine/cystine redox potentials in the gut: proliferation is fostered in a reducing redox environment, whereas a modest shift towards the oxidation side of the two redox couples favors differentiation. A highly oxidized glutathione redox status, however, associates with cell death [233]. Human intestinal epithelial Caco-2 cells, a commonly used in vitro model for intestinal differentiation, stop proliferation and undergo differentiation into enterocytes/colonocytes following confluency. Differentiation of Caco-2 cells is associated with induction of FoxO1 and SelP [234], an antioxidant protein that was identified as a FoxO1 target gene [235]. Thus, FoxO1-mediated up-regulation of antioxidant enzymes might limit the severity and duration of the redox shift during enterocyte differentiation.

Stem cell differentiation has been also associated with epigenetic alterations. As Alina Hanf and Andreas Daiber summarize, there is a growing body of evidence that ROS/RNS contribute to the regulation of gene expression and genome stability not only by modulation of transcription factors, mRNA stability and DNA damage/repair, but also influence epigenetic pathways by affecting the function or expression of histone and DNA modifying enzymes (Fig. 3.2) [236–238]. For instance, it was shown that oxidative stress alters global histone methylation by attenuating Fe(II)- and α-ketoglutarate-dependent histone demethylase activity of Jumonji C (JmjC) domain-containing enzymes and TET DNA hydroxylases [237,238]. Furthermore, it is well established that levels of HDAC2 are decreased due to inflammation-induced ROS/RNS production in chronic obstructive pulmonary disease (COPD) [239]. Another example is the generation of reactive halogen compounds, such as 5-chlorocytosine, by ROS/RNS, leading to inaccurate methylation by DNA methyltransferase (DNMT) [240]. Adverse redox regulation of epigenetic processes may ultimately result in pathological consequences such as dysfunctional energy metabolism or increased oxidative stress that are associated with cardiovascular pathologies. For instance, hydrogen peroxide ($H_2O_2$) alters the binding of DNA methyl-transferases (DNMTs) to chromatin leading to hypomethylation in atherosclerosis [241,242]. Furthermore, epigenetic silencing of superoxide dismutase 2 (SOD2) by selective hypermethylation of CpG islands in the SOD2 gene is associated with pulmonary arterial hypertension [242,243], and oxidation of HDAC4 by NOX4-mediated ROS production was observed in cardiac hypertrophy [244]. There is experimental evidence that cardiomyocytes of failing hearts undergo significant changes in epigenetic profiles of H3K4 and H3K9 methylation marks that go hand in hand with ROS-induced changes in histone demethylase activity [242,245,246]. This has also been observed in humans with heart failure [247]. Not only histone modifying enzymes but also histone proteins themselves can be directly affected by oxidizing and nitrating agents since exposure to peroxynitrite induces dityrosine formation in histone H2A and H2B leading to structural changes by intra-molecular cross-linking [248,249]. Dityrosine bridge formation represents an irreversible oxidative modification and it may be speculated that histones carrying this modification account for the persistent changes in gene expression observed in various disease states. In conclusion, epigenetic regulation by ROS/RNS in the setting of various oxidative stress-associated disorders may become an attractive target for redox medicine in the near future.

In addition to histone- and DNA-modifying enzymes, microRNAs (miRNAs) have an important impact on the epigenetic landscape. They comprise a large family of conserved, small (19–25 nucleotides (nt) long), non-coding RNAs that regulate gene expression at the post-transcriptional level. miRNAs bind to the 3′-untranslated region (3′-UTR), coding sequences or 5′-untranslated region (5′-UTR) of target messenger RNAs, thus leading to the inhibition of translation or mRNA degradation [250,251]. As Verónica Miguel and Santiago Lamas explain, it has recently been found that miRNAs are able to “fine-tune” the regulation of redox signaling. This may occur by direct interaction with NRF2, the major transcriptional regulator in the defense against ROS [252,253], or its co-regulators Kelch-like ECH-associated protein 1 (KEAP1) and CNC homolog 1 (Bach1), or by controlling the generation of ROS [254]. This new subset of miRNAs, that either regulate redox pathways or are themselves regulated by the cellular redox state, has been termed “redoximiRs” [255]. As pointed out above, fibrosis is an aberrant repair process that results from chronic inflammation and leads to excessive extracellular matrix (ECM) deposition that ultimately impairs organ function [256]. Myofibroblasts are considered the quintessential cell type responsible for ECM accumulation [257]. Fibrosis of major organs including liver, lung, heart, skin and kidney share common molecular mechanisms regarding the genesis of the fibrotic process such as the essential role of the TGF-β pathway [258]. However, major differences exist regarding the cellular origin of myofibroblasts and the role of epithelial-mesenchymal transitions (EMT) in each particular organ [259]. The lack of effective and specific therapeutic alternatives for fibrosis prevention or cure remains a fundamental clinical challenge in all organs. In the last decade, miRNAs have been shown to be modulators of pro- and anti-fibrotic processes in human diseases and this subset of miRNAs are called “fibromiRs” [260,261]. Aberrant expression of fibromiRs drives the initiation and progression of the fibrotic process in response to persistent tissue injury. Moreover, TGF-β signaling through Smad proteins can regulate the transcription of miRNAs by DNA binding or miRNA maturation by associating with the Drosha/DGCR8 complex [262], suggesting a possible link between miRNAs and fibrogenesis. The overlap between the sets of fibromiRs and redoximiRs is now becoming evident and is of potential importance for both mechanistic and translational purposes [263]. Currently several miRNAs pertaining to this intersection have been described and are the objects of intense research, including miR-21 [264–266], miR-29 [267,268], miR-9 [269,270], miR-199 [271] and miR-433 [272]. Of interest, some of these miRNAs, such as miR-21, may regulate metabolic pathways related to fatty acid oxidation, a process that has been proven crucial for the pathogenesis and perpetuation of fibrosis in the kidney [273–275]. Overall, the crosstalk regulation between redox balance and miRNA function appears to be an exciting avenue of research, which may lead to a more profound comprehension of fibrosis and eventually to provide effective therapeutic alternatives.

### 3.7. Redox signaling via RONS-derived electrophiles such as oxidized lipids

Fibrosis and inflammatory diseases have been also associated with lipid oxidation. As Catarina B. Afonso and Corinne M. Spickett discuss, oxidized phospholipids (OxPLs) have a known role in several inflam-

matory diseases such as atherosclerosis and diabetes, but also in neurodegenerative diseases including Alzheimer's and Parkinson's disease. Although they mostly have a pro-inflammatory role, as reviewed recently [276,277], their capacity as anti-inflammatory agents has also been described. The anti-inflammatory activity of OxPLs has been shown to involve several pathways (reviewed in [278]). The mechanisms by which they act include the inhibition of nitric oxide synthesis in macrophages; activation of peroxisome proliferator activated receptors (PPARs), leading to inhibition of major inflammatory pathways (such as the NF-κB and AP-1 signaling pathways); attenuation of dendritic cell activation and maturation, and inhibition of T-cell proliferation and cytotoxicity, which are important in the adaptive immune system. One of the most studied anti-inflammatory mechanisms by which OxPLs act, however, involves the regulation of Toll-like Receptors (TLRs). These receptors are responsible for innate immune responses by recognizing pathogen-associated molecular patterns (PAMPs). The presence of oxidized phospholipids appears to selectively inhibit some proteins of this family (such as TLR2 and TLR4), possibly through binding to assessory proteins important for their activity [278]. However, much research has been performed using specific oxidized phospholipids, and the different phospholipid species could alter the response observed [279]. Also, their anti-inflammatory activity is known to depend on several factors. For example, low concentrations ($< 25$ μM) of the oxPL are thought to be anti-inflammatory, whereas higher concentrations ($> 50$ μM) tend to be pro-inflammatory and cytotoxic [276]. The effects of cell type [280] and the presence of endotoxin [281] have also been reported. The potential of OxPLs for the diagnosis and treatment of inflammatory diseases is evident, but further research is necessary to characterize the relationships fully.

ROS, RNS and lipid peroxidation (LPO) products are not only crucial in regulating cellular signaling processes under physiological and pathophysiological conditions, they are also crucial in the cellular response to materials, acting in turn as chemo-attractants, signaling molecules and agents of degradation [282]. As Pierre-Alexis Mouthuy and Neven Žarković point out, such interactions between cells, materials (or 'scaffolds'), and bioactive molecules can be observed in tissue engineering in order to improve or replace biological tissues in regenerative medicine. In this context, modulation of ROS may have the potential to improve the quality of the engineered constructs. So far, approaches in tissue engineering that target ROS in order to improve cell-material interactions have focused on antioxidant therapies to minimize oxidative stress in cells. However, it is challenging to provide antioxidant concentrations that are physiologically relevant and respond to variations of oxidative stress levels, which may occur during new tissue formation. Thus, recent strategies aim to develop polymeric scaffolds that undergo oxidative degradation and/or release bioactive molecules such as antioxidants in response to the oxidant concentrations [283–285]. On the other hand, considering the multiple roles that oxidants play during the response to biomaterials, pro-oxidant therapies are also becoming attractive for tissue engineering applications. The LPO products, like 4-hydroxynonenal (HNE) known as a "second messenger of free radicals", are particularly interesting candidates to be supplemented as bioactive molecules. Namely, despite being biomarkers of pathological oxidative stress, LPO products have been shown to stimulate cell proliferation and matrix synthesis [286,287]. Compared to ROS and RNS, the LPO products have the advantage of forming rather stable protein adducts. Moreover, their hydrophobicity suggests that their incorporation into a hydrophobic polymer matrix (such as biodegradable polyesters) could lead to a slow and prolonged release, which is desirable for tissue engineering applications. Overall, the existing evidence supports the idea of providing LPO products during tissue engineering in order to stimulate cell infiltration and new tissue formation. Such a novel approach has been proposed as a supplement for a bone regeneration strategy, which is currently being tested using HNE.

Moreover, proteins can be modified by covalent reactions on the nucleophilic residues cysteine, histidine, arginine and lysine, leading to the formation of a wide variety of adducts with oxidized products of lipids. As Bebiana C. Sousa and Corinne M. Spickett explain, even though protein lipoxidation can occur under basal conditions, it is increased and thought to be relevant in pathophysiological conditions [288]. In order to understand their impact on a complex matrix like cells, tissues or body fluids, potentially important protein-lipid adducts are often generated in vitro under controlled conditions [289]. This approach has the advantage of potentially decoding the reactivity of each specific electrophilic lipid species and specific fragmentation patterns of lipoxidation adducts, allowing a targeted analysis in complex biological samples. On the other hand, this strategy also presents some disadvantages, as previously reported by other authors [290,291]. Mass spectrometry (MS)-based analytical approaches are one of the most popular methodologies to study biological systems and are used extensively in the study of protein-lipid adducts. The adducts are detected by MS analysis, often involving liquid-chromatography followed by top-down or bottom-up proteomic strategies. Because the top-down approach requires expensive mass analyzers with high mass accuracy and resolution, the bottom-up approach is the most commonly used. However, it also involves disadvantages; for example, when the aldehydes react with lysine and arginine, this leads to additional difficulties since these modifications may interfere with trypsin digestion, which is typically used in proteomics. Furthermore, stabilization of adducts is required prior to the enzymatic digestion and MS analysis due to their labile nature. Certain MS/MS conditions can cleave labile post-translational modifications during peptide fragmentation, resulting in the neutral loss of the modification. For these reasons, it is advantageous to use enrichment procedures and chemical labeling in order to improve sensitivity and selectivity. Western blot immunoassay using specific or non-specific antibodies can also be performed, followed by in-gel digestion and MS analysis for protein identification. However, the cross-reactivity of some antibodies with different lipids is a major disadvantage. The development of new MS approaches could provide tools to identify and quantify lipid-protein adducts and understand their effects upon oxidative stress and related pathophysiological conditions [292].

### 3.8. Interaction of the gasotransmitter $H_2S$ with ROS and RNS

In recent years, $H_2S$ biology has attracted a lot of attention by unraveling multiple physiological roles for this gasotransmitter, linking it to disease conditions and offering novel translational opportunities, as summarized by Andreas Papapetropoulos (Chair of the COST Action BM1005 (ENOG)). Hydrogen sulfide is generated in mammalian cells by three distinct enzymes: cystathionine-β synthase (CBS), cystathionine-γ lyase (CSE) and 3-mercaptopyruvate sulfotransferase (3MST) [293,294]. Although the exact levels of $H_2S$ in cells remain unknown, they are most likely in the nM range. In addition to free $H_2S$, acid-labile and protein-bound sulfane sulfur pools exist [295]. $H_2S$ is a weak acid and readily ionizes at physiological pH, with 70% of $H_2S$ existing in the anionic sulfide ($HS^-$) form [293]. $H_2S$ is a weaker reductant than cysteine and glutathione. This, in addition to its much lower concentration compared to glutathione and protein thiols, argues against a role for $H_2S$ as a "professional" direct reducing agent in a cellular context. $H_2S$ most likely acts as a signaling molecule boosting endogenous antioxidant mechanisms.

Low levels of $H_2S$ are neuroprotective, cardioprotective, anti-apoptotic and anti-inflammatory [293]. Many of its biological actions have been attributed to its antioxidant properties [293,296]. $H_2S$ impacts on the cellular redox state as it reacts with ROS, inhibits ROS production, activates antioxidant enzymes and upregulates the expression of antioxidant genes. $H_2S$ reacts with ROS/RNS including HOCl, $O_2^{\bullet-}$, $H_2O_2$ and $ONOO^-$ [297]. With the exception of HOCl, the reaction rate constants of $H_2S$ with the above-mentioned oxidants are low, suggesting that they are most likely of little biological significance

[295]. The reaction of $H_2S$ with free radicals can give rise to a number of novel species. Of particular interest is the reaction between $H_2S$ and $^{\bullet}NO$, which generates S/N hybrid species and $HNO^{\bullet}$ [298].

NRF2 is a transcription factor that acts as a major regulator of the cellular defense response to oxidative stress since it is the master transcription factor regulating antioxidant genes [299,300]. NRF2 is found in a complex with Kelch-like ECH-associated protein 1 (KEAP1) in the cytosol that facilitates its degradation through the proteasome pathway. Following exposure to oxidative stress, KEAP1 dissociates from NRF2 allowing it to escape from ubiquitination and enabling translocation to the nucleus where it binds to antioxidant response elements in the promoter region of several genes. Treatment of cells or animals with $H_2S$ donors causes persulfidation of KEAP-1 on cysteine-151, which in turn causes a conformational change in KEAP1 allowing it to dissociate from NRF2 [301]. In addition to NRF2 activation, $H_2S$ donor administration up regulates NRF2 expression [294].

Treatment with $H_2S$ has been shown to be protective against a variety of oxidative stress-related injuries and ROS-induced toxicity [296]. From a mechanistic point of view the protective effects of $H_2S$, in addition to NRF2, have been linked to increased activity of antioxidant enzymes such as superoxide dismutase, catalase and glutathione peroxidase, inhibition of superoxide generation and lipid peroxidation and reduction of NOX expression [296,301]. Moreover, treatment with $H_2S$ donors increases the cellular concentration of reduced glutathione by promoting cysteine and cystine uptake and by upregulating the level of the GSH biosynthetic enzyme γ-glutamylcysteine synthase and GSH reductase; $H_2S$ also increases thioredoxin-1 gene expression [296].

## 4. Redox biomarkers

Paul Winyard (E-mail: p.g.winyard@exeter.ac.uk) and Pietro Ghezzi (E-Mail: P.Ghezzi@bsms.ac.uk).

### 4.1. Introduction

This section will deal with selected redox biomarkers. As the causative molecules of oxidative damage are ROS, one might expect most studies would be performed by measuring ROS, such as the superoxide radical or the hydroxyl radical, (among others) in patients' fluids, just as inflammation researchers measure the level of inflammatory cytokines in disease. However, most ROS are extremely unstable, with half-lives of $10^{-6}$ $-10^{-9}$ s. Also "more long-lived" ROS, such as hydrogen peroxide, have a half-life of less than a millisecond [302]. Therefore, it is difficult to measure them in biological fluids. ROS can be measured during their production in vitro using chemicals (e.g. "spin traps" and "fluorescent probes") to detect them while they are produced, but they cannot be measured in stored plasma or stored culture supernatants. Therefore, we do what is done in high energy physics. Not being able to detect subatomic particles, we can only have a clue of their presence by the traces they leave. The main feature of ROS is their high reactivity, hence the name, and measurement of oxidized macromolecules that can arise by interaction with endogenous ROS can give us an estimate of the production of ROS (Fig. 4.1) [6]. Likewise, upregulation of ROS enzymatic sources or so-called toxifiers (e.g. myeloperoxidase) can also work as biomarkers of oxidative stress.

Measurement of these oxidized molecules can provide three types of biomarkers. Some can be indicators of the production of ROS. An example is *S*-thiolated hemoglobin (whose oxidation, to our knowledge, has no pathogenic role). This is similar to the situation with glycated hemoglobin (HbA1c) in diabetes, a good and stable indicator of how much the organism has been exposed to high blood glucose, but which, unlike blood glucose, has limited functional consequences in vivo. Others are, in effect, biomarkers of oxidative stress, that is, they reflect oxidative damage that may have biological consequences. An example of this type is oxidized DNA metabolites, as they may potentially be responsible for oxidative stress-induced mutagenesis and cancer. A third group of biomarkers consists of oxidized products that have an

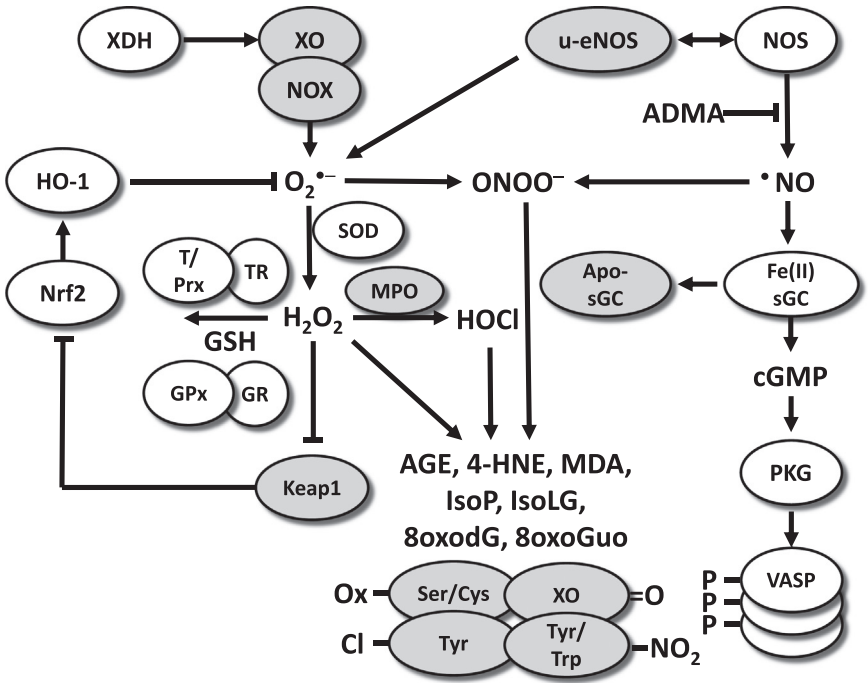


**Fig. 4.1.** Redox pathways associated with putative biomarkers of oxidative stress. The processes that lead to oxidative modifications of proteins, lipids, and nucleotides are highly complex. Enzymes, such as XO, NOX, and NOS, can produce ROS and RNS. These ROS can furthermore serve as substrates for other enzymes to generate additional types of ROS, such as the generation of HOCl from $H_2O_2$ by MPO. Cellular systems and enzymes, including the GSH and thioredoxin system, together with peroxiredoxins (T/Prx), counterbalance the production of ROS. In addition, increased levels of ROS activate NRF2 to transcribe genes that are involved in counteracting these ROS. Oxidative stress affects cGMP signaling through its effects on nitric oxide ($^{\bullet}NO$) production, scavenging, and on the $^{\bullet}NO$ receptor sGC. cGMP, cyclic guanosine monophosphate; GSH, glutathione; $H_2O_2$, hydrogen peroxide; HOCl, hypochlorous acid; MPO, myeloperoxidase; NOS, nitric oxide synthase; NOX, NADPH oxidase; RNS, reactive nitrogen species; ROS, reactive oxygen species; sGC, soluble guanylate cyclase; XO, xanthine oxidase. Adpated from [6]. With permission of Mary Ann Liebert, Inc. Copyright 2015.

intrinsic biological activity, which may propagate some of the consequences of oxidative stress – such as hydroxynonenal, an aldehyde generated by lipid oxidation [303].

This review will deal with different types of stable redox biomarkers that can be used in biological samples from clinical or population-based studies. The biomarkers have been grouped in the subsections below according to their identity as oxidation products of proteins, lipids, or DNA.

### 4.2. Protein oxidation products as redox biomarkers

The following section was composed by Serge P. Bottari, Stuart P. Meredith and Corinne M. Spickett. Biological systems are exposed to various endogenous and exogenous oxidants capable of modifying proteins, which, among other processes, may affect cell signaling pathways [304] and contribute to inflammatory diseases [302]. A number of acute and chronic diseases have been reported to cause, be accompanied by, or be due to, "oxidative stress". This stress can be considered as a deregulation of redox signaling resulting in an excess of ROS, which may be responsible for further complications.

Since the major substrate of the primary ROS, $O_2^{\bullet-}$, in terms of kinetics is $^{\bullet}NO$ (the reaction with $O_2^{\bullet-}$ has a rate constant which is 3–4 times greater than the rate constant for the dismutation of $O_2^{\bullet-}$ catalyzed by SOD), oxidative stress is generally preceded – and accompanied by – an increased generation of RNS, essentially peroxynitrite ($ONOO^-$), which, in the case of excessive concentrations, can cause nitro-oxidative stress [305]. Since RNS can, like ROS, alter proteins, lipids and nucleic acids, RNS may also be involved in pathological mechanisms [306,307]. Interestingly, however, most posttranslational protein modifications due to RNS appear to often be reversible in vivo. Therefore, nitro-oxidation should be considered as a potential therapeutic target, as the modifications involved are modulated primarily by the redox status, $^{\bullet}NO$ and $O_2^{\bullet-}$ fluxes [308], the former being easily manipulable.

The major pathophysiological nitro-oxidative protein modifications elicited by $ONOO^-$ are glutathiolation and *S*-nitrosation of Cys and nitration of Tyr residues. Other modifications are zinc finger oxidation and methionine sulfoxidation. $^{\bullet}NO$ by itself is a major neurotransmitter and an activator of soluble guanylate cyclase. Its reaction with $O_2^{\bullet-}$ therefore has dual consequences: primarily the generation of novel messengers (RNS) and a decreased bioavailability of $^{\bullet}NO$ with direct consequences on its targets [305,307].

Antibody-based methods are among the most common techniques for identifying and quantifying these oxidative post-translational modifications to amino acid residues. The most common techniques (Table 4.1) include ELISA, Western blotting (WB) and immunostaining techniques, such as immunohistochemistry (IHC) and immunocytochemistry (ICC). The accuracy of these techniques relies on the specificity of the available antibodies, but not all antibodies are validated for all procedures [309]. The majority of antibodies against oxidative posttranslational modifications are primarily validated for Western blotting (~75%), with smaller numbers suitable for the other techniques (IHC ~40% and ELISA ~35%), and they are not necessarily interchangeable. Searching on databases such as CiteAb and Biocompare suggests there are more than 500 commercially available antibodies to modified residues (Table 4.1), but on average less than 15% of these have been specifically cited in scientific publications. Some antibodies are more extensively cited and used in different techniques, so selecting the appropriate one is important.

An important issue is the specificity of the antibodies, which may vary according to the immunogen used to generate them, including the carrier. The most commonly used approach is conjugation of the modified residue to either keyhole limpet hemocyanin (KLH) or bovine serum albumin (BSA), but others were produced by immunizing directly with proteins treated with oxidizing, chlorinating or nitrating agents. A limitation of using modified BSA or other proteins is that it generates antibodies to a variety of epitopes on the antigen that may lead to cross reactivity upon translation, especially as most nitrating and chlorinating agents are also oxidizing, so a wide range of oxidative posttranslational modifications result. Even using synthetic modified residues conjugated to a carrier protein, there are likely to be several antibodies to epitopes that do not include the modification site, so purification is required. Thus the resulting polyclonal sera are semi-specific at best; while monoclonal products are better, some cross-reactivity is still possible. For example, limitations of antibodies and antibody-dependent assays for methionine sulfoxide have been reported [310,311]. This indicates the importance of understanding the nature of the antibody being used in order to interpret results correctly, but unfortunately, often little information is available from the supplier. It also suggests the benefit of producing better characterized antibodies, possibly with known sequence specificity in addition to modification specificity.

Among the applications of the above antibodies to immunochemical assays, it is of primary interest to be able to detect and quantify nitro-oxidative "stress" in pathophysiological situations before irreversible oxidative cell damage occurs. Among the nitro-oxidative protein modifications, the most stable and therefore easiest one to investigate is Tyr nitration. Indeed, glutathiolation and *S*-nitrosation, being heavily dependent upon the redox state, can easily be artifactually generated or reduced in biological samples.

In order to achieve monitoring of nitro-oxidative "stress" in pathophysiological situations, Rocha *et al.* developed an ELISA assay for the quantitative determination of nitrated albumin in plasma. Indeed, assaying free or peptide-bound nitroTyr does not reflect nitro-oxidative stress as most of it is of dietary origin [312].

This test allowed Bottari's group to monitor the occurrence of systemic nitro-oxidative "stress" under two conditions which can lead to severe long-term psychomotor retardation: perinatal asphyxia and

**Table 4.1**
Summary of the types of antibodies currently available against oxidatively modified residues.

| Modification | Number of Antibodies | Antibodies Cited | Clonality (mAb: pAb) | Most Common Antigen | Range of Validated Techniques |
|---|---|---|---|---|---|
| 3-Chlorotyrosine | 1 | 1 | 0:1 | 3-Chlorotyrosine (no details) | IA, IHC |
| 3-Nitrotyrosine | 439 | 15 | 129:310 | 3-Nitrotyrosine conjugated to KLH | WB, ELISA, ICC, IF, IHC, IP |
| *S*-nitrosocysteine | 1 | 0 | 0:1 | Recombinant protein | ELISA, WB |
| Cysteine sulfenic Acid | 3 | 3 | 0:3 | Sulfenic acid-cysteine (2-thiodimedone-specific Ig) | WB |
| Cysteine sulfinic acid | 1 | 0 | 0:1 | Cysteine sulfinic acid adducts | ELISA, IHC |
| Cysteine sulfonate | 3 | 3 | 0:3 | Dimedone-modified cysteine conjugated to KLH | WB |
| 5-Hydroxytryptophan | 17 | 1 | 8:9 | Conjugated to bovine serum albumin via a glutaraldehyde linkage | WB, ELISA, ICC, IHC, IF |
| Methionine sulfoxide | 3 | 2 | 0:2 | Protein with methionine sulfoxide modifications | WB |
| Hydroxyproline | 19 | 3 | 0:19 | Conjugated to bovine serum albumin | ELISA, IHC, ICC, WB |
| Carbonyl | 43 | 41 | 27:16 | Conjugated to bovine serum albumin | ELISA, IHC, ICC, WB |

neonatal hypoglycemia [313,314]. Whereas the clinical significance and importance of perinatal asphyxia on neurodevelopmental outcome of severely and even moderately affected newborns is now generally accepted, this has not been the case for neonatal hypoglycemia whose clinical significance is still a matter of intense debate [315–319]. Interestingly, animal models of these two conditions invariably show cerebral insult associated with increased tyrosine nitration both in vitro and in vivo. These observations have been confirmed in postmortem cerebral and medullar tissues of asphyxiated neonates [320,321].

Since high peroxynitrite flux generation has been reported to cause neuronal apoptosis, Wayenberg et al. investigated potential correlations between plasma nitroalbumin levels and other biological and clinical parameters in asphyxiated and hypoglycemic neonates [313]. In perinatal asphyxia, it was found that plasma nitroalbumin concentrations at day 1 to be strongly correlated with the severity of neonatal encephalopathy ($\chi^2$ =7.23; $p < 0.05$) indicating the occurrence of systemic nitro-oxidative stress in these infants. Nitroalbumin levels were also inversely correlated ($p < 0.05$) with Apgar score (a marker for the health of newborns) and arterial blood pH and directly with creatinemia, arterial base deficit and lactacidemia. The latter correlation indicates a correlation between the degree of hypoxia and albumin nitration, whereas the increase in creatinemia is indicative of a decreased glomerular filtration rate, which may reflect afferent arteriolar vasoconstriction. Nitroalbumin levels were back to control levels at day 4 suggesting that this stress was transient [313].

It has been well documented that moderate and severe neonatal encephalopathy are often associated with subsequent periventricular leucomalacia and cerebral palsy, often leading to impaired neurodevelopmental outcome. The data of Wayenberg et al. therefore suggest that increased RNS generation may play a role in hypoxic-ischemic brain injury. Further studies are required to verify whether plasma nitroalbumin may serve as a marker of nitro-oxidative stress in neuroprotective trials.

In neonatal hypoglycemia [314], Wayenberg et al. found an inverse correlation between glycemia and plasma nitroalbumin as early as the first hour of life ($r = -0.35$; $p < 0.02$) and through day 1. Lactacidemia was inversely correlated with nitroalbumin suggesting that lactate may serve as an alternate fuel. Another interesting finding is the strong correlation between nitroalbumin levels and the severity and duration of the hypoglycemic events determined as area-under-the-curve. Similarly, in neonates who had more than 2 hypoglycemic episodes during the first 24 h of life, nitroalbumin levels were still significantly elevated at day 4.

Whereas, as mentioned earlier, the impact of neonatal hypoglycemia on neurodevelopmental outcome is still a matter of debate, our data clearly indicate that severe and repeated hypoglycemic events during the first 24 h of life induce an important and long-lasting systemic nitro-oxidative stress both in preterm and term infants, which may be involved in the cerebral insult responsible for the psychomotor retardation reported by several authors. These observations therefore provide grounds for timely and appropriate management of neonatal hypoglycemia and call for further studies on careful metabolic monitoring and long-term follow-up of the neurodevelopmental outcome of these infants.

In conclusion, plasma nitroalbumin determination provides a highly sensitive and robust marker, which may prove useful for monitoring nitro-oxidative stress and for understanding the involvement and role of redox deregulations and RNS in various pathophysiological conditions.

### 4.3. Lipid oxidation products as redox biomarkers

The following section was composed by Opeyemi S. Ademowo, Irundika Dias and Helen Griffiths. Malondialdehyde (MDA) is the best known and most abundant (10–20 μM in plasma) end-product of the autocatalytic lipid peroxidation chain reaction. In addition to aldehydes, other common cholesterol, phospholipid and polyunsaturated fatty acid peroxidation biomarkers that are formed include ketones such as 4-hydroxynonenal, alcohols such as isoprostanes, hydroperoxides such as 1-palmitoyl-2-(5′-oxo-valeroyl)-*sn*-glycero-3-phosphocholine (POVPC) and cyclic endoperoxides. Polyunsaturated fatty acids (free or in phospholipids) with methylene interrupted unconjugated olefinic bonds are highly susceptible to free radical oxidation and yield hydroperoxide species in situ, which in the case of membranes, are released by phospholipases. Commonly reported examples of oxidized cholesterols (oxysterols) include 6-cholesten-5α-hydroperoxide, 7-ketocholesterol, 7-dehydrocholesterol and 25-hydroxycholesterol [322]. The suitability of these molecules as biomarkers is dependent on their stability, ease of enrichment or separation and accurate detection methods in the presence of several orders of magnitude higher concentrations of the parent lipid. The commonly used thiobarbituric acid-reactive substances (TBARs) assay lacks specificity for MDA measurement in biological materials and is not a method of choice for MDA quantitation [323].

Lipid peroxidation analysis by absorption spectrometry has been superseded by the accurate determination of unmodified or derivatized lipids using chromatographic separation followed by mass spectrometry (MS) methods. Gas and liquid chromatography have been used successfully according to equipment availability, but LC is easier as it does not require the samples to be volatilized. The precision of such methods is achieved by: 1) stability of the analyte; 2) enrichment of the analyte; 3) specific detection by multiple reaction monitoring transitions; 4) the sensitivity of the MS method including variation in dwell time; and 5) the availability of stable isotope standards for the species of interest.

For MDA, the commercial deuterated standard is available to support stable isotope dilution methods; successful derivatization and stabilization in acetone has been achieved using pentafluorobenzylbromide followed by extraction using toluene to remove matrix followed by GC separation to enrich for species of interest [324], and using 3-nitrophenylhydrazine to derivatize followed by LC separation using stable isotope dilution methods to compensate for matrix effects during electrospray ionization [325].

Quantification is typically achieved by selected ion monitoring (SIM) after MS (e.g. of $m/z$ 251 for MDA and $m/z$ 253 for its stable isotope after neutral loss of PFB) and selected reaction monitoring (SRM) by MS/MS of the mass transition (e.g. $m/z$ 251 → $m/z$ 175 for $d_0$-MDA and $m/z$ 253 → $m/z$ 177 for $d_2$-MDA) [324]. By derivatizing MDA, these methods capture the reactive carbonyl prior to sample processing.

Similar to MDA, 4-HNE is highly reactive and MS methods of analysis typically rely on derivatization using PFB to stabilize the reactive carbonyl. After GC separation and analysis by the SIM method, the deuterated analog, HNE-d11, has been successfully used for quantitation [326]. Plasma concentrations of 4HNE are ~100 nM.

Isoprostanes (IsoPs) are stable products of polyunsaturated fatty acid peroxidation. F2-isoP, the most common, is derived from arachidonic acid with a concentration < 0.5 nM in the plasma of healthy human subjects. One LC-MS method using deuterated standardization has been described, despite this method having the potential to be the most sensitive and specific for many different isomeric forms. Solid phase extraction was adopted to remove contaminants and following LC-MS, two MRM transitions were acquired per analyte for quantification and confirmation of IsoPs [327]. The recovery of the spiked standard was 70–120%.

Oxidized cholesterols have biological activity [328] although they are found at very low concentrations in plasma (7-ketocholesterol: < 75 nM). They are often esterified. Some methods describe saponification to release the free oxidized cholesterol as an index of oxidative stress whereas other authors prefer to analyze the biologically active free oxidized forms. Solid phase or liquid-liquid extraction and protein precipitation during sample preparation has proved to be important for sample enrichment. The incorporation of deuterated standards using stable isotope dilution enables absolute recovery to be reported. Using a

monolithic column, efficient chromatographic separation of isomeric oxysterols was achieved; MRM transitions of *m/z* 369/287 enabled specific detection for 7-ketocholesterol with 81–108% recovery [329].

In order to highlight the innovations in the field of lipid peroxidation product analysis by LC, a recent approach for detection of the oxidized phospholipid POVPC has been described that relies on a nanoparticle-based strategy for successful trapping and enrichment of aldehyde-containing oxidized phospholipids [330]. After derivatization of carbonyl containing phospholipids with a bifunctional reagent containing a thiol moiety to bind onto nanoparticles, the derivative and enriched moieties can be released by a reducing agent for analysis by LC-MS/MS. The authors highlight a two-fold improvement in the sensitivity of POVPC detection using nanoparticles.

As LC-MS/MS with SRM methods and deuterated standards become more widely available, a new era of reliable lipid peroxidation analysis will dawn enabling researchers to understand the concentration and species produced in different biological contexts. Improved enrichment techniques that minimize the risk of artefactual oxidation and novel chromatographic materials that can offer improved separation of amphipathic molecules are key to further development in this field.

### 4.4. Nucleic acid oxidation products as redox biomarkers

The following section was composed by Marcus S. Cooke, Mahsa Karbaschi and Henrik E. Poulsen. Nucleic acid oxidation has attracted attention since it was shown that it was one of the most abundant DNA modifications [331]. It also is a pre-mutagenic lesion that induces CG: TA transversion mutations. The guanine moiety is particularly prone to oxidation and is studied as a prototype for both DNA and RNA oxidation. In DNA it can be measured as the nucleoside upon digestion and hydrolysis. The gold standard for measurement is now ultra-high-performance liquid chromatography with tandem mass spectrometry for quantification. The optimum method includes extensive chromatography, isotope dilution with the use of both quantifier and qualified ions [332]. The oxidized nucleosides from both DNA and RNA are excreted into urine and are used as non-invasive biomarkers [6].

Biomonitoring such damage, both in vitro and in vivo, is therefore critical to understanding the mechanisms linking damage with disease, but achieving this can present technical challenges. Blood is a potentially problematic matrix to measure oxidatively generated DNA damage, as it is necessarily invasive (typically ~5 mL is needed); peripheral blood mononuclear cells need to be isolated before analysis or storage, which is a time-consuming process; and artefactual damage occurs when whole blood is frozen without a cryopreservative. To address this, a novel approach has been described that significantly simplifies biomonitoring in vivo: small volumes of whole blood are sufficient (250 μl from a finger prick), which facilitates simple collection and storage without artefacts, together with use in the comet assay without prior isolation of peripheral blood mononuclear cells [333]. Recently, a novel comet assay tank and rack design was described, which exploits holding the slides in a vertical orientation, rather than horizontal [334]. This innovation results in significant improvements in sample throughput (~90% decrease in slide handling time), together with a much smaller footprint, and enhanced cooling. In contrast to blood, urine is non-invasive, although it is also possible to measure biomarkers of oxidative stress in other extracellular matrices [335]. Mass spectrometric approaches remain the gold standard for urinary 8-oxodG analysis, but modifications to a commercially available ELISA for 8-oxo-7,8-dihydro-2'-deoxyguanosine (8-oxodG) have improved its accuracy [336,337]. Most recently, the Cooke laboratory has established an approach that allows genome-wide assessments of DNA.

There are many reports of increased excretion of the guanine nucleoside into urine or elevated tissue levels in many diseases, and this has led many researchers to conclude that nucleic acid oxidation is important in many diseases. Oxidative stress-induced damage to nucleic acids (including DNA, RNA and the corresponding nucleotide pools) has been implicated in the pathogenesis of numerous diseases, including cancer, cardiovascular disease and neurodegenerative disease [338]. However, there is a difference between occurrence and importance, and also there is the problem of whether the lesion causes the disease or is a consequence of the disease. The classic criteria for causation are given by the nine Bradford-Hill criteria [339]: strength, consistency, specificity, temporality, biological gradient, plausibility, coherence, experiment, and analogy. For DNA oxidation there are few publications on the strength (urinary excretion of the oxidized deoxyguaninosine nucleoside (8oxodG)). Consistency is limited and there are only a few existing cohort studies, yet they have shown an association with lung cancer in non-smokers [340] and with breast cancer [341]. These effects are small and probably not important on an individual basis, although they might be important from a public health point of view. There are no important data to evaluate criteria 2,3,4,5. Criterion 6 (plausibility) is provided by the demonstration of GC: TA transversion mutations, even though the quantitative effect is not established. Criterion 7 is partly fulfilled by epidemiological and experimental evidence, and for criterion 8 (experiment) there are data from DNA repair knock-out animals that support the idea that the oxidative modifications are linked to cancer development, or to premature aging [342].

RNA oxidation has only recently attracted attention. The evidence is limited to hemochromatosis [343] and diabetes [344,345]. The data support criterion 1 in that the effects are considerable, but the rest of the criteria are only supported by hypotheses [346].

Beside the Bradford Hill criteria, there are some additional aspects that need to be considered in the context of clinical utility. If a high level of a biomarker is associated with a disease, are there means to reduce the levels and will this either prevent the disease or improve survival of patients with the disease? There are no data on this. Presently, the quest is to identify non-pharmacological or pharmacological means that are non-toxic and that can reduce markers of DNA or RNA oxidation. Hitherto, the only example is blood-letting for the treatment of hemochromatosis that reduces the biomarker for RNA oxidation and also is well established to reduce the morbidity from high body iron [343]. Still, particularly regarding type 2 diabetes, the clear association between morbidity/mortality and the levels of RNA oxidation is very promising with a potential to identify or develop novel treatments for type 2 diabetes.

### 4.5. Conclusion

This comprehensive review has provided a summary of some of the protein-, lipid-, and nucleic acid-based biomarkers of oxidative stress, some of the latest developments in the assay methods by which they may be measured, and some of the applications of these methods in clinical studies. As described above, in general, gas/liquid chromatography-mass spectrometry often provides the platform of choice for the determination of all these types of biomolecules, due to the specificity and sensitivity of this platform. However, this type of platform does not necessarily provide a method that is suitable for large-scale clinical studies because of the relatively high cost of mass spectrometry equipment and, frequently, the relatively high time demands for sample preparation. Even mass spectrometry approaches are not without the dangers of artefacts. It should also be borne in mind that good analytical sensitivity and specificity for a particular biomarker does not necessarily translate into good clinical diagnostic sensitivity and specificity when testing the utility of the biomarker in the diagnosis of a specific human disease.

Immunochemical methods such as ELISAs might provide alternative, high-throughput approaches for the analysis of oxidative stress biomarkers (as described above for a range of protein oxidation products, including 3-nitrotyrosine within the albumin polypeptide backbone). However, great caution should be exercised in relation to the specificity of the antibodies used in ELISAs, and it is evident from Table 4.1 that many commercially available antibodies directed against

protein oxidation products have received limited validation.

One of the challenges in this area is for the "redox biology community" to work together to validate a group of harmonized assays, which will constitute reference standards for oxidative stress biomarkers in clinical studies. An important series of investigations (the National Institute of Environmental Health Biomarkers of Oxidative Stress Study), addressed the question of which assays provide valid read-outs of oxidative stress induced in animal models. The mass spectrometry-based measurement of F2-isoprostanes was identified as a "gold standard" biomarker of free radical damage caused by carbon tetrachloride in rats [347]. A viewpoint regarding the current status of oxidative stress biomarkers as clinically useful tools was provided by a recent review [6]. Visualization of biomarkers measured in various diseases by cluster analysis (Fig. 4.2) shows that the majority of studies have used ROS-induced modifications as markers of oxidative stress [6]. There is also ongoing discussion on whether traditional assays for ROS and RNS detection are still useful in certain setups or should be replaced by more advanced techniques [348–350].

The current review has included some indications as to how oxidative stress biomarkers assays may be applied to medical research studies, but the demonstrated *clinical* value of oxidative stress measures in diagnosis or monitoring in patients has so far been disappointing. In this respect, the challenge is to validate oxidative stress assays in terms of clinical utility – i.e. clinical diagnostic sensitivity and clinical diagnostic specificity. The development of oxidative stress biomarkers needs the substantial further attention of researchers, particularly in relation to the identification of validated biomarkers for the study of: (i) the pharmacodynamics of novel redox-based therapeutics in animal models of disease, (ii) the clinical diagnosis and/or monitoring of human diseases in which oxidative stress is involved, and (iii) clinical trials of novel redox-based therapeutics. As long as the above three areas remain inadequately addressed, we will continue to struggle to translate our increasing understanding of redox biology into advances in human disease therapies based on redox medicine. The studies described above, in relation to nitrated albumin as a biomarker in perinatal asphyxia and neonatal hypoglycemia, begin to take us in the right direction. But the important challenge of identifying reference methods for oxidative stress assays still has some way to go.

## 5. Optimizing ROS detection using EPR or fluorescence: in vivo applications to mammalian cells, tissues and plant biology

Yves M. Frappart (E-mail: yves.frapart@parisdescartes.fr).

### 5.1. Introduction

When oxygen first appeared on Earth, living systems had to adapt to this particular oxidant molecule. This resulted in various reactive oxygen species (ROS: mainly superoxide anion, hydrogen peroxide, but also $^1O_2$, hydroxyl radical) that must be regulated by all aerobic organisms. Due to the regulatory role of ROS and crosstalk between these molecules, their level and localization are therefore critical parameters for biology and medicine. In order for the measurements to be most useful, it often is essential to measure the amount of ROS at particular sites and under appropriate conditions. Specific, sensitive and localized measurements of ROS require special methodologies. As ROS are correlated to oxygen levels, in vivo conditions should be applied to study their biological effects, which is not always possible. Oxygen concentration is therefore a key element in every experiment. There is no gold standard modality to determine, quantify or localize the various ROS species. Scientists who evaluate ROS have to use different modalities, with different qualities and limitations depending on the experimental conditions. Over the last decade, approximately 75% of all reports on ROS have been determined with fluorescence imaging, especially in vitro [355]; almost all the other references have used electron paramagnetic resonance (EPR or electron spin resonance [ESR]) with or without spin trapping for their detection or imaging [356]. Nevertheless other modalities are emerging such as nuclear magnetic resonance imaging (MRI) [357], echography [358] or positron emission tomography [359]. New methodologies such as immuno-spin trapping [360] are also emerging all the time so that it is not possible to give an exhaustive list. Fig. 5.1 shows enzymatic sources of RONS, the reactive species being formed, the potential footprints they leave and imaging techniques that may be applied to measure them

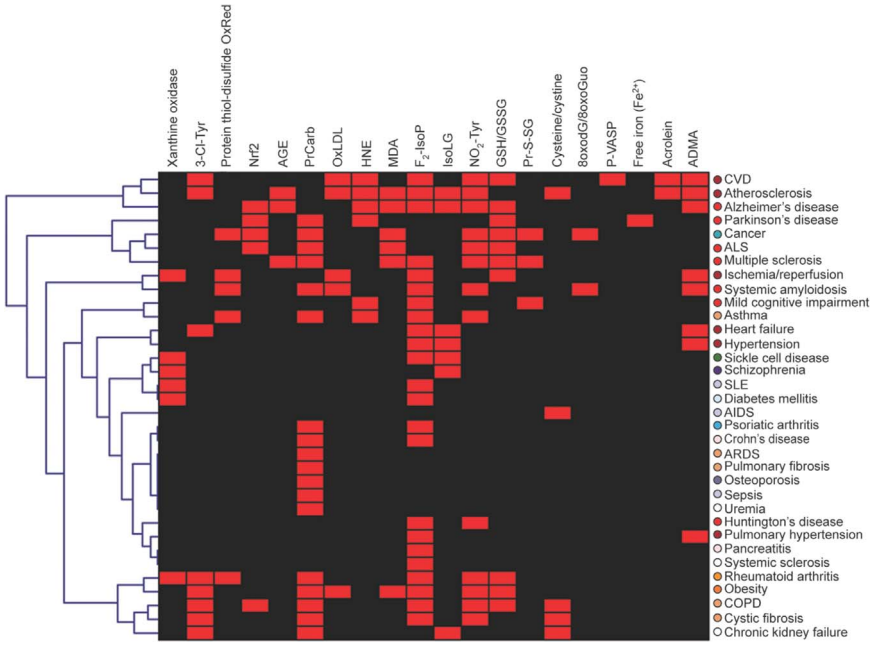


**Fig. 4.2.** Cluster analysis of ROS biomarkers in disease. Different diseases were clustered according to described ROS biomarkers in Refs. [351–353] and studies described in this review. Some disease conditions cluster as might be expected, such as ischemia/reperfusion and heart failure, and amyotrophic lateral sclerosis and multiple sclerosis. A comprehensive analysis of ROS markers and pattern analysis in diseases might uncover common disease mechanisms or new measures of disease progression or treatment outcome. Cluster analysis was performed using Genesis software (https://genome.tugraz.at/genesisclient/genesisclient_description.shtml) as described in Mengozzi et al. [354]. Adpated from [6]. With permission of Mary Ann Liebert, Inc. Copyright 2015.

[361].

Despite its limitation, EPR is still the most suitable technique to detect ROS. EPR can be used in different methodologies such as EPR coupled to spin-trapping. It is the most specific method, as stated by K. Abbas and F. Peyrot.

### 5.2. Spin trapping coupled to EPR is an under used specific method to measure oxidative stress in biological systems

Electron paramagnetic resonance (EPR) is the gold standard to detect paramagnetic species. However, when the aim is the detection of short-lived radicals involved in oxidative stress, such as $O_2^{\bullet-}$ in living systems, direct detection is not possible due to the low sensitivity of the technique. To overcome this limitation, the spin trapping method was introduced in the 1970s. It relies on the specific single-step addition reaction of the radical of interest on an EPR-silent molecule, named the spin trap, which yields a persistent radical, called the spin adduct, the EPR spectrum of which is characteristic of the trapped radical. The most commonly used spin traps for $O_2^{\bullet-}$ in aqueous medium are derivatives of the cyclic nitrone 5,5-dimethyl-1-pyrrolidine *N*-oxide (DMPO, e.g. DEPMPO) (Fig. 5.2). Since its first application to biological systems in 1979, important contributions have been made to improve spin trap structures based on mechanistic analysis of the spin trapping reaction and of the spin adduct decomposition pathways [362,363], but also to improve the methodology by characterizing its limitations, artefacts, and sources of misinterpretations [364–368]. Intracellular detection and quantification are not straightforward, and in vivo detection of $O_2^{\bullet-}$ is impossible with spin traps coupled to EPR. However extracellular detection of $O_2^{\bullet-}$ produced by cells can now be achieved with excellent specificity and satisfactory sensitivity with CD-DIPPMPO, an extracellular spin trap [369]. Spin trapping of NO is based on its high affinity towards ferrous iron and trapping as stable nitrosyl-iron complexes is achieved by either adding iron-diethyldithiocarbamate ($Fe(II)(DETC)_2$) to tissues or isolated cells [63,370], or by measurement of endogenously formed nitrosyl-iron complexes such as Hb-NO [371,372]. Nitrosyl-iron complexes produce typical triplet EPR signals (Fig. 5.2). Though a few spin traps are commercially available, their cost is prohibitive considering that their purity is usually not sufficient for biological studies. Since the quality of the supplies has not improved over the years, there is a need for a greater collaboration between biologists, synthetic chemists, experts in EPR spectroscopy and spin trapping from platforms dedicated to EPR studies of biological systems at national and European levels so that recent advances can be made accessible to all, in order to address questions relative to oxidative stress in biological systems. A few years ago, as Ron Mason was trying to find new accurate ways to use spin trapping in order to determine superoxide levels in living systems, he introduced immuno spin-trapping, which he presented in a recent review [360]. Immuno spin-trapping uses spin-trap antibodies to ensure the detection of the long lived biological species with various methodologies (UV, mass spectrometry, MRI). Spectroscopists can now specifically detect superoxide in vitro; they have therefore moved on to try to overcome the problem in vivo by studying the redox status. Redox status is related to the balance of many biological species (oxidants and reductants or antioxidants).

Despite its hazy definition, the redox status can be used as a tool by biologists in many cases. This kind of measurement is based on the aminoxyl (nitroxide), hydroxyamine redox equilibrium. It is suitable for in vivo imaging [374] and often uses soluble molecular probes. When aminoxyl linked to proteins is used, the redox status and conformational changes can be addressed, as presented by A. Pavićević and M. Zatloukalová: the “Assessment of redox status and conformational changes of proteins using EPR spin labeling”, which gives biologists two important sets of information for their studies. Under different physiological and patho-physiological conditions, proteins undergo various conformational changes, which can be studied with a variety of experimental techniques. One of these techniques is EPR, also known as electron spin resonance spectroscopy (ESR), coupled with the use of paramagnetic compounds called spin labels (SLs). SLs, which are commonly employed for such measurements, are derivatives of cyclic aminoxyl (often addressed as nitroxide) radicals, a class of compounds containing an > N-O$^{\cdot}$ moiety sterically shielded by methyl groups (or other types of groups) attached to the neighboring carbon atoms. In solutions, these molecules are allowed to rotate freely (short rotational correlation time, $\tau_c$), and thus the resulting EPR spectrum is composed of three sharp isotropic lines (for $^{14}N$ nitroxides). However, when molecular motions are restricted (long $\tau_c$) the overall spectral shapes change, i.e. a broadening of the lines occurs due to the anisotropy of hyperfine splitting constants and g-values. If an appropriate SL is attached to a protein, the anisotropic spectra of the immobilized > N-O$^{\cdot}$ moiety provide valuable information about: 1) the hydrophobic/hydrophilic nature of the binding site in the protein; 2) the influence of the local environment induced by various reagents, temperature and pH change, etc.; 3) the binding capacity of the protein; 4) the distances between the active sites of the protein; 5) the folding and unfolding of the protein, which is an especially interesting topic when membrane proteins are studied; 6) the secondary structure of the protein; 7) the dynamics of the protein backbone; and 8) protein-protein and lipid-protein interactions [375,376]. Numerous SLs have been synthesized for this purpose, a few of which are commercially available. Some of the SLs bind non-covalently to the proteins, while others are intended to covalently bind to specific amino acid residues, such as sulfhydryl groups (-SH). The technique involving the application of the latter is known as site-directed spin labeling (SDSL), and is frequently used in synergy with site-directed mutagenesis. Even though the application of SDSL can be beneficial, the use of conventional site-specific spin labels (SSLs) suffers from a number of drawbacks, so the label has to be chosen prudently, and experiments must be planned thoroughly. For instance, the methanethiosulfonate spin label (MTSSL) binds solely to the sulfhydryl group of free cysteine residues. However, it also tends to form dimers, resulting in dipole-dipole interactions, and consequently in the formation of extra spectral features [377]. On the other hand,

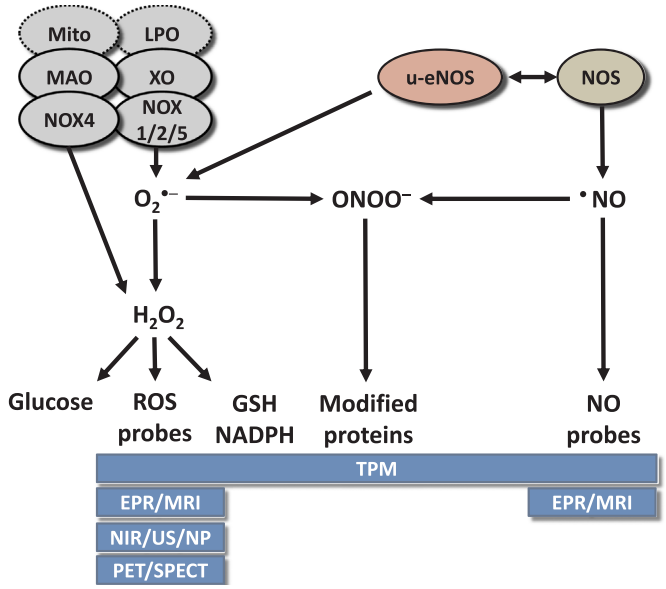


**Fig. 5.1.** Spectrum of different ROS imaging techniques. In the upper part, different sources of ROS are shown: Mitochondria (mito), lipoxygenases (LPO), monoamine oxidase (MAO), nicotinamide adenine dinucleotide phosphate oxidase (NOX4 and NOX 1/2/5), xanthine oxidase (XO), functional nitric oxide synthases (NOS) and dysfunctional / uncoupled eNOS (*u*-eNOS). These result in different types of ROS [including superoxide radical ($O_2^{\bullet-}$), hydrogen peroxide ($H_2O_2$), hypochlorous acid (HOCl, not shown in the scheme), peroxynitrite anion ($ONOO^-$), nitric oxide ($^{\bullet}NO$)] and ROS-induced modifications of GSH, NADPH, proteins, or glucose uptake, which, in turn, are detected by different imaging technologies. Adpated from [361]. With permission of Mary Ann Liebert, Inc. Copyright 2016.

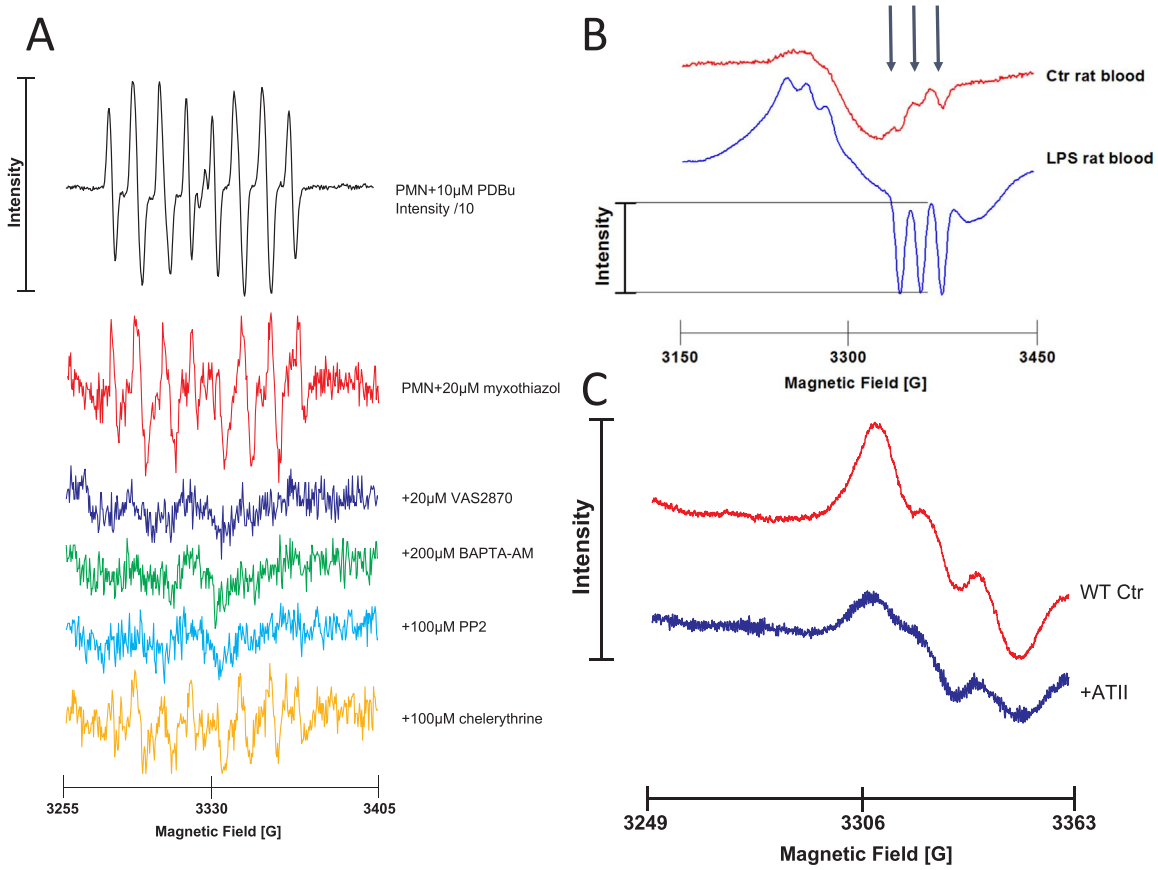


**Fig. 5.2.** (A) Determination of mtROS triggered NADPH oxidase activation in isolated human neutrophils by electron paramagnetic resonance measurement. Freshly isolated human neutrophils ($22x10^6$ PMN/mL) were incubated in PBS with 300 μM $Ca^{2+}/Mg^{2+}$ and 10 mM DEPMPO for 15 min at 37 °C. Activators and inhibitors of phagocytic NOX were added as shown in the figure. The spectrum for phorbol ester (PDBu)-stimulated PMN is displayed at decreased intensity (1/10). All reactions below the red spectrum contained 20 μM myxothiazol. Incubations were with NOX inhibitor (VAS2870), intracellular calcium chelator (BAPTA-AM), cSrc kinase inhibitor (PP2) and PKC inhibitor (chelerythrine). All spectra were recorded at room temperature in 50 μl glass capillaries (Hirschmann Laborgeräte GmbH, Eberstadt, Germany). EPR conditions: $B_0$ = 3300 G, sweep = 150 G, sweep time = 60 s, modulation = 3000 mG, MW power = 10 mW, gain = $9x10^2$ using a Miniscope MS200 from Magnettech (Berlin, Germany). Representative spectra of mixed DEPMPO-OOH˙ and DEPMPO-OH˙ adduct for 2 independent experiments. Spectra were recorded as described previously [373]. With permission of Mary Ann Liebert, Inc. Copyright 2014. (**B**) Whole blood Hb-NO levels were determined by electron paramagnetic resonance spectroscopy as a read-out of iNOS activity in endotoxemic (lipopolysaccharide-treated) rats. The EPR measurements were carried out at 77 K using an X-band table-top spectrometer MS400 (Magnettech, Berlin, Germany). The instrument settings were as follows: 10 mW microwave power, 7000 mG amplitude modulation, 100 kHz modulation frequency, 3300 G center field, 300 G sweep width, 60 s sweep time and 3 scans. With permission of Springer-Verlag Berlin Heidelberg. Copyright 2015. (**C**) Aortic ˙NO formation was measured in untreated control and angiotensin-II infused hypertensive mice by EPR spin trapping using $Fe(DETC)_2$. Each spectrum was measured from one murine aorta. The representative spectra below the bar graph are the mean of all measurements. EPR conditions: $B_0$ = 3276 G, sweep = 115 G, sweep time = 60 s, modulation = 7000 mG, MW power = 10 mW, gain = $9x10^2$ using a Miniscope MS400 from Magnettech (Berlin, Germany). The A23187-stimulated ˙NO signal was absent when the aorta were denuded, L-NAME (200 μM) was added, or when aorta from *eNOS*$^{-/-}$ mice were used (not shown). With permission of Mary Ann Liebert, Inc. Copyright 2014.
(a) Adapted from [63]. (b) Adapted from [371]. (c) Adapted from [63].

maleimido- (MSLs) and 2-iodoacetamido- spin labels (IASLs) need to be incubated with the protein at certain pH values, otherwise they bind not only to –SH, but also to the amino groups.

The protein spin labeling EPR technique has not been used exclusively to study protein conformations and interactions, but has also been applied as a diagnostic tool for various malignancies and benign tumors [378], sepsis [378], diabetes [379], atherosclerosis [379], and cirrhosis [380]. The commonly used methods to detect the aforementioned pathologies include the labeling of blood plasma/serum with 16-doxyl stearic acid (16-DS). 16-DS was chosen due to its high affinity for human serum albumin (HSA). Peptides and metabolites synthesized in the affected organ become attached to HSA, thereby changing its binding capacity and conformation. Such modification is expressed as varied contributions of the unbound, strongly and weakly bound 16-DS to the albumin from the sera of patients, as opposed to healthy individuals. These contributions are calculated using simulation software to decompose EPR spectra, and data are further processed, mainly by neural network software or discriminant analyses. On the other hand, in vitro studies demonstrate that ROS may damage HSA and affect its transport function [381]. Though this methodology offers satisfying accuracy, sensitivity and specificity, and though the procedure seems relatively simple, there are several technical issues that make this diagnostic tool anything but easy. In a recent work by A. Pavićević et al., the analysis of the binding of two spin-labeled fatty acids (SLFAs) to commercial HSA was reported [382]. The obtained data indicate that ethanol, which is extensively used in diagnostic spin labeling protocols, affects the binding of SLFAs to HSA. In order to avoid using ethanol, test tubes should initially be labeled with a small volume of SLFAs dissolved in an organic solvent and left to evaporate. Afterwards, a certain amount of serum should be added and incubated under constant vortexing. The weakness of such an experimental setup is that SLFAs bind to a lower extent to HSA, due to their low water solubility. There are also other difficulties with using 16-DS. One of them is its binding to seven possible sites of HSA; consequently, information about conformational changes cannot be obtained from the specific site. The other issue is that the doxyl group is positioned nearly at the end of the hydrocarbon chain, opposite the carboxylic group. Therefore, anchoring the 16-DS molecule to HSA causes the doxyl moiety to protrude through the albumin's surface [382,383]. Accordingly, 16-DS appears to be an unreliable reporter to

detect local changes in albumin hydrophobic pockets.

Considering all the indicated difficulties, the course of our research was oriented towards estimating the diagnostic potential of other SLs, initially through in vitro studies on purified HSA, and eventually on blood serum samples. The emphasis was on SSLs and SLFAs with a doxyl group attached to the hydrocarbon chain closer to the carboxylic moiety. The preliminary data indicated that the 3-maleimido proxyl (3-MSL) is able to report changes in the cysteine-34 (Cys-34) environment, induced by the binding of fatty acids, warfarin, ibuprofen and benzodiazepines, whose interactions with HSA have been studied exhaustively.

The use of SSLs can also reflect the antioxidant capacity and redox state of HSA (from its free –SH group), since this probe does not bind to the oxidized forms of –SH. The joint electrochemical and EPR study of cytochrome c derivatives indicates that the use of SLs specific for cysteine residues has great potential to estimate the redox state of other proteins bearing free –SH groups as well.

It is very difficult in such innovative methods to reach satisfying accuracy. One way can be to combine multiple methodologies such as “electrochemistry and EPR”. EPR can be completed by electrochemistry to get accurate oxygen concentration information by EPR [384]. Better than adding these methods, one can couple them; this is the proposition of J. Vacek and M. Mojovic that encourages efforts to “couple Electrochemistry and EPR”.

### *5.3. Electrochemistry and EPR to investigate antioxidant and prooxidant systems*

Redox-active and reactive chemical forms directly contribute to homeostasis, the maintenance of a stable internal environment. There is therefore an emphasis on the direct detection and imaging of these chemical entities, among which we classify free radicals, or substances collectively known as RONS as well as an extensive group of antioxidants. Therefore, combining electrochemical methods and EPR spectroscopy represents a highly efficient solution, and both methods can be complementary (thus off-line) or may be applied in situ (i.e. on-line). Electrochemical methods may be used to monitor redox processes; cyclic voltammetry is preferred, or advanced pulse voltammetric techniques, which have a higher sensitivity due to the elimination of capacitive currents [385].

Usually carbon electrodes and anodic voltammetry are used to predict the electron-donor capacity and general reactivity of the examined molecules. The oxidation products can then be identified, which can be further investigated electrochemically, or even isolated and characterized after electrolysis. When interpreting the electrochemical data (voltammograms), we assume that an effective antiradical or antioxidant agent is oxidized at potentials approaching zero, where the electron-donor capacity, and hence its effectiveness, decreases with the increase of anodic potential. Given that many antioxidants are subject to multicomponent (pH-dependent) redox transformations, we always evaluate the potential of the first oxidation peak. Analyses are conveniently performed in an aqueous medium at pH 7.4 in the presence or absence of molecular oxygen, to eliminate artificial effects associated with the spontaneous oxidation of the examined samples. If the redox process is associated with the formation of a radical intermediate, it is practically impossible to detect by electrochemical approaches. For this purpose, EPR spectroscopy, also known as electron spin resonance (ESR) spectroscopy is used [386]. With EPR, we can monitor the absorption of microwave radiation by chemical forms with one or more free electrons, e.g. free radicals, in a strong magnetic field. They can be analyzed using the EPR directly in solution or cell homogenates, in a tissue or even during the anodic reaction on the electrode surface. If the lifetime of the radical forms is too short, the spin-trapping technique is used.

Mojovic et al. present their research on the oxidation of phenolic antioxidants as an example of an effective combination of electrochemical and EPR methods. Although this type of exogenous antioxidant is often perceived sceptically in terms of its biological effect in vivo, a number of these substances are highly effective experimental antioxidants, and in some cases, even chemoprotective agents are fully usable in prophylactic treatments and complementary medicine [387]. One of the most important examples is that of flavonolignans, which are used as hepatoprotectants and antidotes for selected mushroom poisoning. The main example is silybin and its 2,3-dehydroderivative, whose mechanisms of redox transformations and antioxidant effects have been studied [388]. Both of these substances, and also their structural congeners, are characterized by a pleiotropic mode of action, which is partly based on their ability to modulate signaling pathways, or receptor systems in cells (see Section 10.4.2), and also by a combination of their antioxidant vs. prooxidant effects. The antioxidant effect is associated with a relatively high electron-donor capacity, especially for flavonolignan 2,3-dehydroderivatives, and also their metal-chelating capacity. Conversely, pro-oxidant effects are associated with the transition of flavonolignans to reactive aryloxy radical forms or with the formation of highly reactive flavonolignan-metal complexes, which may secondarily generate free radicals through a Fenton-like reaction [389]. Square-wave voltammetry on carbon electrodes [388] was used to investigate the mechanism of redox behavior and analyze the electron-donor capabilities of these substances. EPR spectroscopy was further applied for the direct analysis of aryloxy radicals of flavonolignans that were generated in a strongly alkaline environment according to the methodology developed initially for the purpose of researching flavonol and flavone derivatives [390]. However, aryloxy radicals can also be generated during the electrochemical oxidation of flavonolignans. Their short lifetime, however, makes their identification or further analysis impossible. For this purpose, an in situ spectroelectrochemical technique was developed, where the oxidation of the flavonolignan occurs in the presence of the spin-trap probe 5-*tert*-butoxycarbonyl-5-methyl-1-pyrroline-*N*-oxide (BMPO). The radicals produced during the electrooxidation therefore associate with BMPO and give rise to a stable radical adduct, which can be subsequently quantified by EPR [391]. In addition to the above, we see EPR as an effective tool to analyze metal flavonoid complexes. EPR techniques were applied to the characterization of the highly reactive oxovanadium(IV)/silybin complex, which induces the formation of RONS in the cellular environment [392].

The main prerequisite to combining electrochemical methods and EPR spectroscopy in the study of antioxidant and prooxidant molecules (or molecules which combine both effects) is based on the fact that EPR enables the visualization of free radicals in situ, which are not detectable by electroanalytical approaches. By contrast, EPR exhibits zero interference with the parent forms of the studied species, nor with the final products formed during their redox transformations. Off-line applications of EPR and electroanalysis have recently started to find applications in research of more complex cellular systems and in vivo monitoring and imaging [393]. In the above, in situ approaches (e.g. [391]) were previously only applied in molecular studies with isolated chemical species, whereas future applications clearly point towards the on-line connection of EPR spectroscopy with electroanalysis under more complex (preferably in vivo) conditions. There is clearly potential in the application of implantable microelectrode systems, in the optimization of new technical solutions for spectroelectrochemical instrumentation and in the development of new hybrid techniques based on electrochemical microscopy in combination with EPR imaging approaches.

Applications of electroanalysis in conjunction with EPR spectroscopy are demonstrated here with low-molecular redox-active substances, monomeric flavonolignans, exhibiting an antioxidant effect while under other specific conditions, exhibiting a prooxidant effect. The applicability of the above techniques in research on biopolymers, specifically proteins, is demonstrated in Section 5.2.

As discussed before, fluorescence is the most used methodology,

especially for microscopy. As an example, one can use genetically encoded probes, as proposed by Vsevolod Belousov to detect hydrogen peroxide.

### 5.4. $H_2O_2$ detection using genetically encoded probes and nanoparticles

Out of the many techniques to study redox reactions, imaging using fluorescent genetically encoded biosensors offers the widest set of advantages. First, most importantly, it allows the monitoring of redox events in real time in situ and in vivo. Second, the protein nature of the sensors allows subcellular targeting similar to conventional fluorescent proteins. Recently several technological improvements in the area of redox imaging were achieved.

Since the development of the first genetically encoded redox biosensors, they have all been based on fluorescent proteins with green emission [394]. The development of the first red fluorescent probes for $H_2O_2$, HyPerRed, made multiparameter imaging possible by using co-expression of this sensor with green-emitting probes for $H_2O_2$, GSH/GSSG and pH. Using HyPerRed, ER stress- induced $H_2O_2$ transients in the mitochondrial matrix were detected for the first time within living cells [395]. Interestingly, the increase in $H_2O_2$ was not associated with any detectable increase in the mitochondrial matrix GSSG content. Moreover, no $H_2O_2$ increase was observed in the inter-membrane space or the cytoplasm of the same cells.

Another important direction in the improvement of genetically encoded redox sensors is the expansion of the concentration limits of detection. For example, for $H_2O_2$ signaling studies, it would be important to have a sensor that reflects changes in near-basal concentrations of $H_2O_2$. Although it is not yet clear what the basal concentrations of $H_2O_2$ are, the first successful attempt to make the $H_2O_2$ probes more sensitive has been made recently [396]. The sensor consists of the redox-sensitive fluorescent protein roGFP2 fused to yeast peroxiredoxin Tsa2. This peroxidase has a 100 fold higher reaction rate than OxyR and Orp1 - the domains used in previous $H_2O_2$ sensors, HyPer [397] and Orp1-roGFP2 [398]. The Tsa2 part of the sensor is, however, made non-sensitive to $H_2O_2$. Instead, it brings roGFP2 in close proximity to endogenous Tsa1 incorporating into Tsa1 decamers. Therefore roGFP2 within the probes form redox relays with endogenous Tsa1 rather than with fused Tsa2 inactivated by point mutagenesis. The resulting probe is half-oxidized under basal conditions and sensitive to both increases and decreases in $H_2O_2$. Still some effort has to be made to make roGFP2-Tsp2 functional in cells other than yeast and to improve the reduction speed of the sensor.

One of the basic properties of redox signaling is a high spatio-temporal control over location, and the amounts of the oxidants produced [399]. However, the exact sizes of $H_2O_2$ microdomains are not easy to estimate because of the optical limits of fluorescent microscopy. Super-resolution microscopy becomes a more and more popular instrument to study fine structures in cells, however it has never been used before to study dynamic processes, such as second messenger dynamics and enzymatic activities. Recently, the $H_2O_2$ sensor HyPer2 was successfully used in sub-diffraction microscopy. The exceptional photo stability of the sensor made its use in Stimulated Emission Depletion (STED) microscopy possible. Fused to cytoskeleton structures, HyPer2 was able to resolve the structures with superior resolution and report $H_2O_2$ dynamics in growth factor- stimulated cells. Uneven dynamics of the sensor oxidation between two filaments separated by a distance of 100–200 nm suggests a less than ~100 nm diffusion radius of $H_2O_2$ in the cytoplasm of fibroblasts.

On the other hand, developments have been made in the chemical probes used for detection [400], such as near-infrared sensitive probes [401], biphoton probes or nanoparticles (NPs). According to A. Suha Yalçın, NPs are becoming widely used tools in the field of sensing and imaging. Success in developing different luminescence probes has enabled the monitoring of ROS production both in cells and whole animals [402–404]. Among these are peroxalate-based NPs formulated from peroxalate esters and fluorescent dyes that are used to image $H_2O_2$ in vivo with high specificity and sensitivity. Peroxalate NPs were capable of imaging $H_2O_2$ in the peritoneal cavity of mice during a lipopolysaccharide-induced inflammatory response [402]. The method was further improved by reducing the size of the NPs and modifying their content to detect $H_2O_2$ at physiological concentrations. Chemiluminescent NPs have also been exploited for the in vivo targeting and imaging of tumors and were successfully used to image $H_2O_2$ as a tumor signal molecule [405]. Probes that improve the stability of peroxalates in aqueous systems are sensitive to low concentrations of $H_2O_2$ within the physiological range. Chen et al. [406] have recently developed a novel upconversion luminescence nanoprobe to detect ROS in aqueous solutions, as well as diagnose rheumatoid arthritis and to bioimage ROS in living cells.

### 5.5. High throughput assays for superoxide and hydrogen peroxide for rigorous and specific activity of NADPH oxidases

J. Zielonka and B. Kalyanaraman propose that the combination of fluorescence and EPR spin trapping may yield better results. RONS encompass a range of species displaying oxidizing, nitrating, nitrosating and/or halogenating properties. To better understand the pathophysiological mechanisms of ROS/RNS it is crucial to detect and identify the specific species responsible for a given biological effect and to selectively inhibit the source of its formation. NADPH oxidases are a family of enzymes, the only known function of which is transferring electrons from NADPH to molecular oxygen, and the concomitant generation of $O_2^{\bullet-}$ and $H_2O_2$. NADPH oxidases have been identified as a promising therapeutic target for diseases bearing an oxidative stress component. Despite the wide effort to develop inhibitors of the NOX isoforms, only a limited number of such inhibitors are available. This is due to serious limitations of the assays used to develop NOX inhibitors. Typically, sensitive, but non-selective and artefact-prone assays have been applied for the detection of NOX-derived oxidants, leading to a high rate of false positive hits in high throughput screenings. For example, it has been demonstrated that the L-012 probe to detect superoxide requires one-electron oxidation and may generate superoxide by itself [407]. Also, in many assays horseradish peroxidase (HRP) is used as a catalyst of the oxidation of the probe by NOX-derived $H_2O_2$. The lack of probe selectivity for a specific oxidant and the susceptibility of the HTS assays to peroxidase substrates and inhibitors led to the controversy over the NOX-inhibitory potency of the positive hits selected, including apocynin, VAS2870 and 2-acetylphenothiazine [408].

Recently, Zielonka et al. have developed new assays to monitor the activity of the NADPH oxidases [409] and used them to screen a small library of bioactive compounds for potential NOX2 inhibitors [410]. These assays take advantage of the probes, which react directly with $O_2^{\bullet-}$ or $H_2O_2$ and form easily detectable, fluorescent products. The authors designed and synthesized a cell-impermeable analog of hydroethidine, called hydropropidine ($HPr^+$) to detect NOX2-derived $O_2^{\bullet-}$ [411]. Upon its reaction with superoxide, $HPr^+$ undergoes oxidation to red fluorescent 2-hydroxypropidium whose fluorescence quantum yield can be increased further in the presence of DNA. In order to detect $H_2O_2$ the authors applied coumarin boronic acid (CBA), which upon oxidation forms the blue fluorescent 7-hydroxycoumarin (umbelliferone). Both assays can be carried out in a 384-well plate format, with rapid measurements using a fluorescence plate reader. For the secondary assays, they applied two probes: hydroethidine (HE) for $O_2^{\bullet-}$ and Amplex Red with HRP for $H_2O_2$. HE-based assay was coupled to rapid UHPLC-based detection of 2-hydroxyethidium as a specific product of the reaction of HE with $O_2^{\bullet-}$. The Amplex Red-based assay was used in combination with the fluorescence plate reader. Both secondary (orthogonal) assays can be carried out in a 384-well plate format. All four assays can be used for high throughput monitoring of NOX activity, with the HE assay requiring rapid, microwell plate-compatible UHPLC

instruments. Rapid UHPLC analyses also enable simultaneous monitoring of $O_2^{\bullet-}$ and $H_2O_2$ formation, using a mixture of HE and CBA probes [409,410]. The positive hits identified with these assays can be tested in confirmatory assays, including the measurement of the rates of oxygen consumption by NADPH oxidase in a medium throughput manner using a Seahorse XF96 extracellular flux analyzer and in lower throughput EPR spin trapping of superoxide using DEPPMPO or DIPPMPO cyclic nitrone spin traps.

The newly developed assays provide a framework for reliable measurement of the activity of NADPH oxidases and other cellular sources of $O_2^{\bullet-}$ and $H_2O_2$. Rapid and rigorous detection and quantitation of $O_2^{\bullet-}$ and $H_2O_2$ will lead to better understanding of the chemical biology of $O_2^{\bullet-}$/$H_2O_2$-producing enzymes (e.g. NOX isoforms) and will also help discover specific inhibitors of NOX isoforms.

Most of the time, ROS detection is applied to biomedical science, but very important results can be obtained in plant science, which helps to understand posttranslational modifications, as proposed by B. De Smet, F. Van Breusegem and J. Huang. The oxidation of crucial cysteines to sulfenic acid (SOH), has emerged as a biologically relevant post-translational modification (PTM) with particular importance in redox-mediated signal transduction [412]. Thus, identifying the sulfenome under oxidative stress would allow us to identify key redox-sensors and –transducers [413,414].

### 5.6. Chemical and genetic tools for plant sulfenomics

The oxidation of crucial cysteines to sulfenic acid (SOH), has emerged as a biologically relevant post-translational modification (PTM) with particular importance in redox-mediated signal transduction [412]. Thus, identifying the sulfenome under oxidative stress would allow us to identify key redox-sensors and -transducers [413,414].

Sulfenomic studies have only recently been applied to plants [414–416]. As sulfenic acid is often unstable, its identification was mainly examined on a protein-by-protein-basis. At present, both chemical and genetic approaches are used in plants. The majority of the chemical probes are dimedone derivatives (5,5-dimethyl-1,3-cyclohexanedione), that selectively react with sulfenic acid [417]. The bio-DCP1 probe, which was used in *Medicago truncatula*, is a dimedone analog carrying a biotin affinity tag used for purification [416]. As biotin has many drawbacks, new azido- and alkyne-functionalized dimedone-analogs were developed that allow the addition of biotin post-extraction on the dimedone-tag using click chemistry [415,418]. Their small size and membrane permeability allow the in vivo tagging of sulfenylated proteins. In *Arabidopsis* cells, the DYn-2 probe was used to identify the sulfenome under oxidative stress [415].

The yeast AP-1 (YAP1)-based probe offers a genetic way for the in vivo identification of plant sulfenomes [54,55]. This was first applied in *Medicago truncatula* to identify the sulfenome upon *Medicago truncatula–Sinorhizobium meliloti* symbiosis [416]. Recently, a YAP1C-GS probe has been developed and expressed in *Arabidopsis* cells to reveal the sulfenome under oxidative stress [414].

Using a genetic approach has the advantage that, once the material is transformed, experiments are cost-efficient, allowing multiple repeats and treatments. Additionally, the probe can be targeted to specific tissues or even organelles. On the other hand, chemical probes generate a larger coverage of the sulfenome in a single experiment, as they penetrate whole cells; they do not require transformation and generate stable covalent bonds between the sulfenylated protein and the probes. Another attractive difference is the mode of trapping the sulfenic acid. Whereas the YAP1C genetic probe traps sulfenic acid in its protein context, defined by protein-protein interaction, the chemical probes trap sulfenic acid independently of the protein environment. Another characteristic to consider is that the incubation of the chemical probe can influence the oxidation within a cell, which should not be a problem for the permanently expressed genetic probe, although its expression can act as a scavenger of the oxidized proteins and hence, alter the cell/plant redox state.

As both genetic and chemical probes have specific advantages, the combination of their data obtained with both probes covers the largest part of the plant sulfenome. Current tools are based on protein-identification, rather than on site-identification. Therefore, future research should focus on mapping specific sulfenylation sites. Quantifying the protein sulfenylation, or even the specific cysteine-sulfenylation in response to several elicitors would further improve the sulfenomic approaches and assess the role of cysteine-oxidation upon redox signaling.

### 5.7. Conclusions

As outlined above, imaging ROS is still very challenging, and the choice of the method will largely depend on the experimental conditions. For the selective in vitro specific detection of superoxide on cells, for example, EPR coupled to spin-trapping is the gold standard method. Abbas et al. have recently developed the detection on living cells under conditions close to in vivo conditions. Less selective, but allowing in vivo EPR imaging and protein folding and mobility, EPR can be coupled to spin labeling to allow redox status determination. Coupling to electrochemistry allows the accurate determination of either the oxygen levels, or the anti-oxidant's ability. Genetically encoded biosensors make it possible to determine hydrogen peroxide and open the way to in vivo luminescence bio imaging. Strong efforts are made in chemistry to allow the selective and easy detection of ROS with fluorescent probes, such as nanoparticles. NPs are versatile, and can be used to detect superoxide anion and hydrogen peroxide. EPR and fluorescence can be coupled, as recently proposed by Zielonka et al.; this yields very accurate detection of NADPH oxidase activity, a key enzyme in oxidative stress. Combining different methods can help understand oxidative stress in a post-transcriptional pathway, as proposed by De Smet, Van Breusegem and Huang in plant biology.

There is still no gold standard for ROS detection and imaging. Many methods are under development, and more collaboration between biologists, methodologists of the modality (e.g. fluorescence, EPR) and chemists is needed to make progress and avoid misinterpretations of experiments leading to false conclusions.

## 6. Reactive oxygen and nitrogen species in cardiovascular pathologies

Rainer Schulz (E-mail: rainer.schulz@physiologie.med.uni-giessen.de), Andreas Daiber (E-Mail: daiber@uni-mainz.de) and Fabio Di Lisa (E-mail: fabio.dilisa@gmail.com).

### 6.1. Introduction

In the cardiovascular system, reactive oxygen and nitrogen species (RONS) play an ambivalent role in that small amounts of RONS mediate protective effects (anti-atherosclerotic [Schröder], pro-angiogenesis [Matsui, Bachschmid], endogenous cardioprotection [Andreadou]), while large quantities of RONS cause cell injury eventually leading to loss of viability. RONS-induced cell derangements occur at the level of any organ, including heart [Görbe, Giricz, Ferdinandy] and brain [Casas, Schmidt], especially in the presence of co-morbidities (e.g. diabetes [Schröder; Görbe, Giricz, Ferdinandy]). Furthermore, recent work highlights the contribution of alterations of the intracellular $Zn^{2+}$ pool [Tuncay, Turan] in RONS-induced cell injury. Importantly, the source of RONS due to its cellular (parenchyma [Casas, Schmidt] vs. vasculature [Schröder]) and subcellular localization might contribute to the beneficial [Schröder] or deleterious [Casas, Schmidt] action of RONS. Among the many sources of RONS, a relevant role is played by NADPH oxidases (NOX), uncoupled nitric oxide synthases (NOS) [Li, Förstermann], and various processes in mitochondria. For instance, the

ischemic heart accumulates succinate that upon reperfusion is oxidized causing a burst in ROS formation due to reverse electron transport [Mulvey, Krieg]. Strategies to reduce excessive RONS include administration of antioxidant enzymes (more recently incorporated in endosomes and targeted by antibodies to specific cell types [Muzykantov]) or pharmacological up-regulation of the endogenous antioxidant defense [Lazou]. In addition, an antioxidative effect has been reported for compounds already used in daily practice. This is the case with glucagon-like peptide-1 or DPP4-inhibitors [Steven, Daiber] that abrogate stress-induced blood cell derived RONS. However, antioxidant strategies must be used with caution since they might interfere with endogenous organ protection [Andreadou]. The chapter "Cardiovascular Pathologies" discusses many of the above aspects and is structured according to the importance of RONS in the blood vessels, the heart and the brain (Fig. 6.1).

### 6.2. Oxidative stress and redox processes in atherogenesis and angiogenesis

As pointed out by Katrin Schröder, atherosclerosis is a vascular disease characterized by plaque and neo-intima formation, as well as local inflammation of the vessel wall. The latter is, in part, a consequence of endothelial dysfunction. Monocytes are attracted and adhere at sites of endothelial activation, invade the vessel wall and support a vicious cycle of inflammation and cellular recruitment by processes involving the formation of reactive oxygen and nitrogen species (RONS). Especially the superoxide anion ($O_2^{\bullet-}$) is potentially detrimental for vascular function and promotes atherosclerosis [419]. $O_2^{\bullet-}$ not only limits $^{\bullet}$NO-bioavailability, but also gives rise to $ONOO^-$, which mainly acts as a potent toxic agent. The main source of RONS in the vascular system is the family of NADPH oxidases, whose only known function is the formation of $O_2^{\bullet-}$ and $H_2O_2$. The first NADPH oxidase identified was NOX2, which is the primary NADPH oxidase in macrophages and leukocytes. Its native function is host defense by the massive formation of $O_2^{\bullet-}$, $H_2O_2$ and resulting RONS, in a process termed oxidative burst. Beside the detrimental consequence of massive RONS formation, these species also play an essential role in signal transduction. Recently additional NADPH oxidases have been identified and it is now clear that the number of RONS produced, the site of their formation as well as the type of RONS influences the subsequent signaling. Within the NOX family, NOX4 is an exception as it mainly produces intracellular $H_2O_2$ in a constitutive manner at very low concentrations. NOX4-derived $H_2O_2$ does not influence $^{\bullet}$NO bioavailability, rather it can directly react with proteins in signaling pathways. In fact, NOX4 appears to exert a protective role in the vascular system and prevents vascular inflammation [420]. This protection is, among other mechanisms, mediated by the maintenance of NRF2 expression, which eventually leads to the expression of heme oxygenase-1 (HO-1). Through this pathway, NOX4 favors CO production, which contributes to endothelial quiescence and prevents leukocyte adhesion. The protective role of NOX4 is supported by genetic approaches. *Nox4* deletion has been reported to promote atherosclerosis in both *ApoE*$^{-/-}$ mice and in a model of locally defined atherosclerosis through flow restriction (partial carotid artery ligation with high fat diet) [421]. Similar evidence has been obtained in an LDL receptor knockout mouse [422]. On the other hand, endothelial specific overexpression of *Nox4* protected *ApoE-/-* mice against high fat diet induced atherosclerosis [423]. Notably, *Nox4* expression is reduced in diabetic patients who develop atherosclerotic plaques when compared to diabetic individuals without atherosclerosis [424]. In conclusion, various forms of stress induce an increased expression of *Nox4* that elicits protective mechanisms at least in the vascular system. Importantly, there is evidence that the beneficial role of NOX4 in vascular injury occurs not only in mice, but it may also apply to clinical settings.

Matsui and Bachschmid propose that angiogenesis is redox regulated by the formation of protein glutathione adducts. Oxidative post-translational modification may alter protein functions and mediate cellular signaling. Protein thiols form reversible oxidative modifications including *S*-sulfenylation (-SOH) and *S*-nitrosylation (-SNO) [425], which may react with glutathione (GSH), an abundant intracellular thiol, to form more stable GSH-protein adducts (*S*-glutathionylation) [426]. Protein GSH-adducts can regulate enzyme activity, localization, protein interactions and stability. Various proteins are known to be modified by GSH adducts [427]. GSH adducts can be removed by glutaredoxin-1 (Glrx), a cytosolic thioltransferase that in this way completes the redox signaling cycle. The in vivo role of Glrx and its protein targets in pathophysiology has been explored recently [428–430]. Oxidants are increasingly recognized as factors that promote angiogenesis, and mouse studies revealed that decreasing oxidants may impair ischemic revascularization after hind limb ischemia [164]. Conversely, increasing oxidants by NOX4 or decreasing the antioxidant response by means of *Nrf2* deletion may improve ischemic limb revascularization. These data put forward the concept that oxidants play a protective role in ischemic revascularization, in accordance with multiple reports on ROS conferring beneficial redox

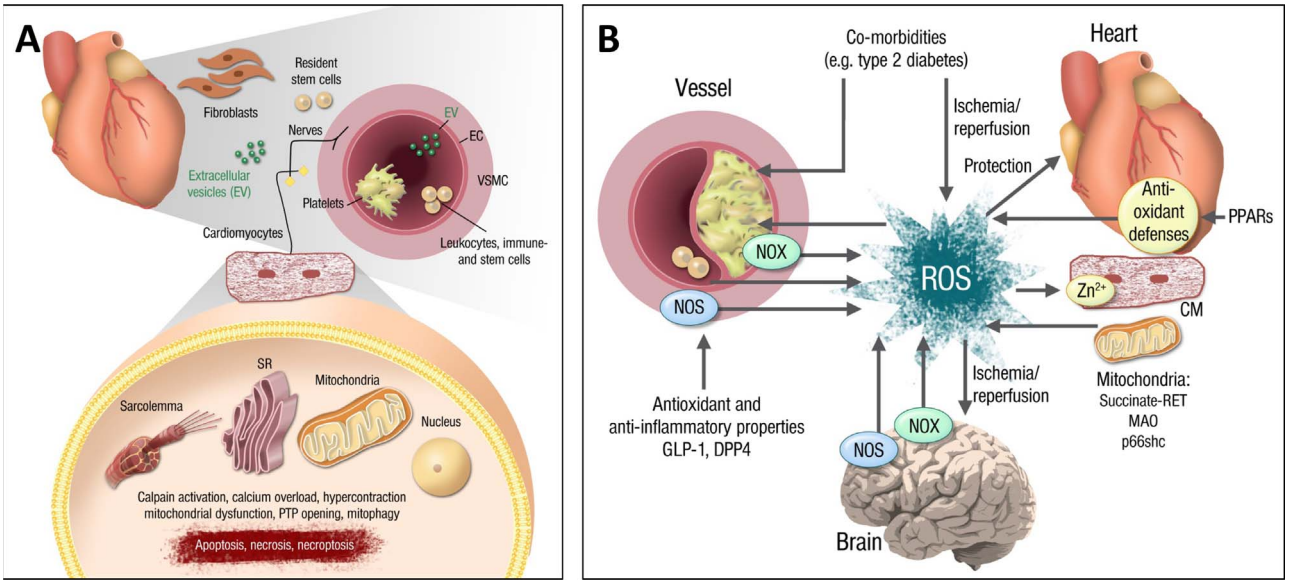


**Fig. 6.1.** Processes contributing to the increase in ROS levels in various tissues. Mitochondrial pathways are highlighted as prominent sources of ROS, especially in the heart. Besides their involvement in tissue injury, ROS have been described also as mediators of cardiac protection against ischemia/reperfusion damage.

signaling in other settings. Glrx is not merely an antioxidant, but obviously also exhibits anti-angiogenic properties. Increased Glrx expression inhibits the angiogenic activity of cultured endothelial cells [431]. Consistent with this finding, Glrx overexpression in vivo also attenuates revascularization after hind limb ischemia [430]. Glrx is known to activate the NF-κB pathway [432]. NF-κB hyper-activation in endothelial cells likely stimulates non-canonical Wnt5a signaling, which induces expression and release of the soluble vascular endothelial growth factor (VEGF) receptor 1 (sFlt-1) into plasma [430]. sFlt-1 is a VEGF decoy receptor, blocking VEGF binding to the proangiogenic VEGF receptor 2. Impaired ischemic revascularization in diabetic mice is associated with elevated levels of sFlt-1 in the ischemic muscle. Because Glrx expression is also NF-κB dependent, proinflammatory conditions such as atherosclerosis [433] and diabetes [432] may increase Glrx leading to impaired or dysregulated angiogenesis. Ablating endogenous Glrx further accelerates ischemic limb revascularization. Hypoxia-inducible factor (HIF-1α), a major angiogenic transcription factor, is stabilized by GSH adducts [428]. In normoxia HIF-1α is hydroxylated and binds to ubiquitin ligase pVHL, which targets HIF-1α to proteasomal degradation. GSH adducts, induced by oxidants or Glrx inhibition, stabilize and activate HIF-1α. As previously reported, nitric oxide-induced *S*-nitrosylation of HIF-1α [434] may also be converted into more stable GSH adducts in the presence of GSH. Watanabe *et al.* confirmed a HIF-1α GSH adduct of $Cys^{520}$ (mouse $Cys^{533}$) by mass spectrometry and demonstrated increased expression of HIF-1α and VEGF-A in ischemic muscle of Glrx KO mice [428]. Increased GSH protein adducts in ischemic limbs are not a hallmark of oxidative stress, but rather contribute to beneficial responses to ischemia through HIF-1α activation. This may be a mechanism by which oxidants promote ischemic revascularization. In summary, Glrx deletion may facilitate revascularization of ischemic muscles not only by means of HIF-1α stabilization, but also by an increase in GSH adducts of other proteins involved in angiogenesis. Therefore, inhibiting Glrx can be a therapeutic strategy to restore circulation in ischemic limbs.

### *6.3. RONS formation in ischemic preconditioning, cardiac cycle, ischemia/reperfusion and cardiomyopathy*

According to Andreadou, low levels of RONS may be associated with beneficial cardioprotection by interventions known as ischemic pre- and post-conditioning (PC, PostC). Cardiac injury associated with post-ischemic reperfusion is contributed mostly by an increased level of reactive oxygen and nitrogen species (RONS), but also by the reduced availability of "beneficial" reactive species such as nitric oxide and intracellular $Ca^{2+}$ overload. These deleterious factors synergize in favoring a prolonged opening of the mitochondrial permeability transition pore (mPTP) that is generally considered as a determining factor in ensuing cell death. However, despite the well-established association between RONS elevation and reperfusion injury of the heart, so far antioxidant treatments have hardly provided any therapeutic benefit in clinical studies of cardiac disease [435,436]. On the other hand, reperfusion injury is greatly reduced by PC and PostC [435,437]. Although the cardioprotective mechanisms triggered by conditioning protocols are still a matter of debate [438], a general consensus exists that RONS play a crucial role. Indeed, while an excessive formation of RONS contributes to irreversible injury, small amounts of RONS contribute to protection, possibly through a redox-dependent activation of protective cytosolic kinases [439]. In this respect RONS share the same paradox with the conditioning phenomena per se, in that a short ischemia/reperfusion episode protects the same as a mild RONS elevation, whereas a prolonged duration of ischemia followed by reperfusion induces injury that largely depends on lethal levels of intracellular RONS [439]. The role of antioxidant compounds in cardioprotection induced by conditioning strategies is an emerging issue, which needs elucidation in order to provide useful information for the translation of the conditioning phenomena in clinical practice [438]. We should mention that PC is mediated in part by a mild formation of RONS, possibly in response to the opening of mitochondrial $K_{ATP}$ channels, and also PostC may lead directly or indirectly to a decrease in RONS [440]. Since the role of antioxidant

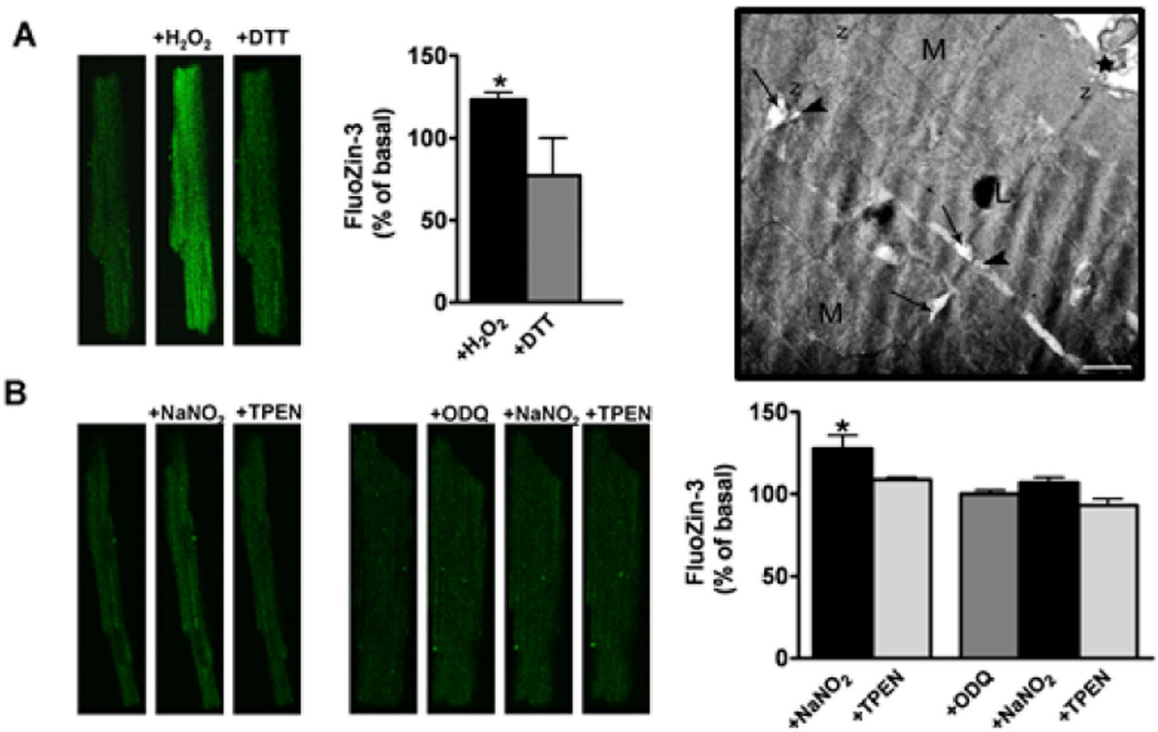


**Fig. 6.2.** The data show marked increases of $[Zn^{2+}]_i$ under either ROS (A) or RNS (B) increases. Bars represent means ( ± ) and *P < 0.05 w.r.t. initial value. **Inset:** Representative electron micrograph images under ZnPT (1-μM) exposure. Magnification: x12,930; bar: 1000 nm; N: nucleus, M: mitochondria, z: Z-line, L: lysosome, arrow: T-tubule, arrow head: sarco/endoplasmic reticulum (SER).

compounds in these conditioning phenomena might differ to some extent, it is important to distinguish their role in pre-and/or postconditioning separately. Several in vivo studies have thus far shown divergent results concerning the role of widely used antioxidants in the prevention and/or abrogation of the beneficial effects of PC in reducing myocardial infarct size. Skyschally et al. [441] demonstrated that the administration of ascorbic acid in pigs abolished the beneficial effect of PC on infarct size possibly due to ROS scavenging [442]. Accordingly, we also showed that in rabbits the antioxidant action of the acute administration of vitamin C, reflected by a decrease in blood and tissue levels of lipid peroxidation products, abolished PC-induced protection [441]. It is worth pointing out that the use of antioxidants is increasing. This is related especially to the commercialization of numerous nutritional supplements or plant extracts containing antioxidant compounds, such as polyphenols and flavonoids that are marketed for the prevention of cardiovascular diseases [443]. Based upon the dependence of endogenous protective mechanisms on ROS generation, it is essential to know the role of all the antioxidant compounds in different physiological and pathological conditions of the cardiovascular system. The complete understanding of redox mechanisms controlling RONS levels in cardiovascular pathophysiology is likely to allow the design of new clinical trials for the use of antioxidants in cardiac diseases.

According to Tuncay and Turan, $Zn^{2+}$ release during the cardiac cycle results in increased intracellular free $Zn^{2+}$($[Zn^{2+}]_i$) levels, and this release is increased in the setting of oxidative stress [444,445]. However, it is not known whether or not there is a direct relationship between the increased production of RONS and $[Zn^{2+}]_i$ changes in cardiomyocytes. Thus, by using confocal microscopy and the specific fluorescence dye FluoZin-3 AM (3 μM), $[Zn^{2+}]_i$ changes were monitored in a H9c2 cardiomyoblast cell-line exposed to RONS. Acute increases in hydrogen peroxide ($H_2O_2$, 100 μM) induced marked increases in $[Zn^{2+}]_i$, which could be reversed by a thiol reducing agent like dithiothreitol (DTT, 500 μM) (Fig. 6.2A). The NO donor $NaNO_2$ (100 μM) induced similar marked increases in $[Zn^{2+}]_i$, which was not observed in the presence of a selective/potent soluble guanylyl cyclase inhibitor like ODQ and was normalized with a heavy-metal $Zn^{2+}$ chelator like TPEN (Fig. 6.2B).

Electron microscopic analysis also demonstrated that increased $[Zn^{2+}]_i$ can induce marked alterations in the ultrastructure of rat cardiomyocytes such as clustering of mitochondria, disruption and damage of myofibrils, enlargement in T-tubules and distortion in the T-tubules (TT) and sarcoplasmic reticulum (SR) intersection (Fig. 6.2, inset). Acute increases in RONS can induce marked elevation of $[Zn^{2+}]_i$ in cardiomyocytes, which may underlie cardiac dysfunction under oxidative stress. In conclusion, in cardiomyocytes, elevated $[Zn^{2+}]_i$ correlates with increased RONS levels.

Mulvey and Krieg highlight the important role of mitochondrial metabolism and RONS formation in myocardial ischemia. RONS have long been known to be key mediators of ischemia/reperfusion (IR) injury, driving not only acute damage but also initiating the pathological cascade that develops over the subsequent weeks and months. This RONS production has generally been assumed to be a non-specific effect of oxygen interacting with a dysfunctional mitochondrial respiratory chain upon its reintroduction to ischemic tissue at reperfusion, a process, which is complex and imprecise. However, recent work from our laboratory shows that contrary to this hypothesis there is in fact a distinct metabolic mechanism responsible [136]. Using an untargeted metabolomic approach, a metabolic hallmark of ischemia was identified from a range of ischemic tissues, which notably included the selective accumulation of succinate. Despite previous descriptions of this in the literature [446], neither the mechanism behind this nor its implications had been characterized. The succinate accumulated during ischemia was found not to originate from normal cardiac metabolism, but rather through aspartate-mediated pathways and reverse action of succinate dehydrogenase (SDH), driven by accumulated ischemic NADH passing electrons through complex I and onto the coenzyme Q (CoQ) pool, which favors the reduction of fumarate by SDH to drive succinate accumulation. Following reperfusion there was then a rapid metabolism of is chemically accumulated succinate, with baseline levels re-established within 5 min [136,447]. RONS generation from electrons stored in the succinate pool is then thought to occur primarily through the reverse action of complex I in a phenomenon known as reverse electron transport (RET) that has been well characterized in vitro but whose importance in vivo has only been recently understood [448]. Importantly, this model provided several testable predictions with regard to the effect of manipulating succinate levels in ischemic tissues and therefore the downstream extent of RONS production and also infarct size as a clinically relevant indicator of IR injury. Decreasing mitochondrial succinate levels during ischemia using either an infusion of the competitive SDH inhibitor dimethyl malonate [136] or sodium malonate [449] resulted in a decrease in RONS production and reduced infarct size in an in vivo mouse model of myocardial IR injury. These could both be brought back to control levels by an infusion of dimethyl succinate. In addition to modulation of mitochondrial metabolism, recent evidence suggests it is also possible to modulate the quantity of RONS produced at reperfusion from the electrons stored in the ischemic succinate pool through inhibition of the active/deactive transition of Complex I. During ischemia, Complex I enters the deactive state but is rapidly reactivated at reperfusion, enabling it to support RONS production by RET [450]. A growing body of evidence suggests a central role for the Cys39 residue found within the ND3 subunit of Complex I, and indeed it has recently been demonstrated using the mitochondria-targeted *S*-nitrosothiol MitoSNO that *S*-nitrosation of this residue can inhibit the active/deactive transition and so allow dissipation of the mitochondrial ischemic succinate pool via alternative pathways to minimize the production of RONS by Complex I [451].

Based on considerations by Görbe, Giricz and Ferdinandy, mitochondrial RONS play an important role in metabolic cardiomyopathies. A growing body of evidence indicates that mitochondrial oxidative stress has a major role in the development of cardiomyopathies in metabolic diseases [452–454]. Cardiac function relies heavily on intact mitochondrial function including mitochondrial biogenesis, fusion, fission, and autophagy-mitophagy. Disturbances in these processes have been linked to increased mitochondrial oxidative stress and the development of metabolic cardiomyopathies. Several oxidative and nitrative stress-related cellular processes have been shown to be deranged in metabolic disorders. In a rat model of hypercholesterolemia enhanced cellular peroxynitrite formation due to an upregulation of NOX4 has been described and discussed as a potential mechanism of cardiovascular complications [455,456] – of note, this finding highlights that NOX4 can play different roles in different organs or disease settings depending on whether it confers beneficial redox signaling or contributes to excessive RONS formation. In the same model, mitochondrial expression of connexin43, which may reduce mitochondrial reactive oxygen species production, was decreased [457]. Evidence obtained in models of metabolic syndrome suggests that mitochondrial oxidative stress is linked to cardiac dysfunction. Indeed, in high-fat diet (HFD)-induced mouse models of metabolic syndrome the elevation in myocardial mitochondrial RONS production was associated with reduced diastolic circumferential strain rate assessed by tagged cardiac magnetic resonance imaging [458]. In addition, in mice, diastolic dysfunction induced by a high-fat high-sucrose (HFHS) diet was accompanied by a 3-fold greater rate of mitochondrial $H_2O_2$ production along with a decrease in both oxygen consumption and ATP synthesis. In this latter model transgenic expression of mitochondria-targeted catalase alleviated oxidative stress and improved diastolic function [459] indicating that mitochondrial ROS formation is causally linked to contractile impairment. This relationship is further supported by pharmacological approaches suggesting that decreasing mitochondrial RONS levels might have a great therapeutic potential – keeping in mind that RONS can also have beneficial effects as discussed for precondi-

tioning phenomena above [438], and therefore the use of antioxidants is always a two-edged sword that needs to be used with great caution. Diabetic mice treated with a mitochondria-targeted antioxidant, Mito-TEMPO, showed preserved heart rates and improved survival after myocardial infarction [460] along with a decrease in mitochondrial RONS generation, apoptosis and myocardial hypertrophy [461]. The latter observations were also obtained *ex vivo* in hyperglycemic cultured cardiomyocytes [461]. Drug candidates other than direct antioxidants have also shown efficacy in the treatment of metabolic cardiomyopathies. Mitochondrial RONS cause opening of the mPTP channels in which cyclophilin D has a major role. A novel inhibitor of cyclophilin D, NIM811, reduced infarct size in diabetic rats [462]. Mitochondrial aldehyde dehydrogenase-2 (ALDH-2), an enzyme responsible for the removal of cardiotoxic aldehydes, is activated by physiological levels of mitochondrial RONS. ALDH-2 overexpression is reported to reduce diabetic cardiomyocyte hypertrophy and contractile dysfunction, while activation of ALDH-2 by Alda-1 has been shown to alleviate high glucose-induced apoptosis and the reduction in mitochondrial membrane potential in H9C2 cells [463]. Although the above reports connect increased mitochondrial RONS production to metabolic cardiomyopathies, a few studies showed a lack of correlation between mitochondrial RONS formation and diabetic cardiomyopathy [464,465]. These findings suggest that mitochondrial oxidative stress might not be present in all models and at all stages of metabolic diseases and that it might not be the common underlying mechanism of metabolic cardiomyopathies, again, warranting caution with the use of antioxidants although the targeted modulation of mitochondrial RONS production and its downstream targets might represent applicable future therapeutic strategies.

### 6.4. RONS formation in cerebral ischemia and stroke

As pointed out by Casas and Schmidt, NADPH oxidase and nitric oxide synthase derived RONS represent potential targets for stroke therapy. Stroke is the leading cause of neurological impairment in industrialized countries, making it the second leading cause of death worldwide and the primary cause of disability. Despite this high medical and social need, no neuroprotective agent is available for clinical therapy and only a single drug reached the market, the antithrombolytic drug rt-PA for ischemic stroke. However, due to its multiple contraindications almost 85% of all stroke patients are excluded from receiving this treatment. RONS have been considered as key players in post-stroke neurodegeneration [466]. Targeting pathologically relevant sources of RONS, such as NOX and NOS, may thus provide promising innovative therapeutic approaches. NADPH oxidases, which include the already mentioned NOX4, constitute the only known enzyme family with the sole function to produce $O_2^{\bullet-}$ and $H_2O_2$. The NOX family consists of seven isoforms: NOX1-5 and the dual oxidases (DUOX 1–2). Due to accessory proteins, each isoform has a distinct quaternary structure, activity regulation, tissue expression and product. Therefore, not all isoforms may contribute equally to ischemic injury [32]. Based on a systematic review and meta-analysis, NOX1 seems to play no role in stroke, neither in infarct size reduction nor in neurological outcome. Similarly, the evidence for NOX2 is extremely contradictory and more or less disproven by a pre-clinical randomized controlled trial with the aim to validate NOX2 as a stroke target. This study turned out negative highlighting a persistent publication bias towards positive findings and the lack of statistical power in many studies [467]. Conversely, brain ischemia is one of the best-validated disease indications for NOX4. Under hypoxic conditions, NOX4 is upregulated leading to oxidative damage, cytotoxicity and neuronal death. Therefore, NOX4 inhibition has been recently considered as a promising target for this pathology. Preclinical results show that NOX inhibition by VAS2870 significantly reduces infarct size and post-stroke RONS formation, suggesting indeed a major contribution of this NOX. Further pre-clinical experiments are being currently conducted using specific NOX4 inhibitors and different animal models of stroke [468]. Similarly, nitric oxide is also considered a member of the RONS family, generated by different NOS isoforms. Studies in mice showed that deletion of neuronal NOS (isoform 1) leads to a significant reduction of post-stroke brain damage, suggesting therapeutic targeting of NOS-1. In fact, it has been recently reported that NOS inhibition (L-NAME) significantly reduces tissue damage and infarct size post-stroke using both in vitro and in vivo ischemia models [469]. However, this was not the case for NOS1-PSD-95 interaction inhibitors, possibly by also interfering with other, protective pathways. Pharmacological targeting of NOX and NOS dependent oxidative stress clearly has neuroprotective effects and reduces infarct volume and RONS production after stroke leading to improved neuronal function and survival. Current and future experiments are aimed at validating these findings in phase II and III clinical trials in other rodent and large animal species for further clinical development as first-in-class neuroprotective treatment of stroke.

### 6.5. Therapeutic targeting of eNOS uncoupling and cardiovascular oxidative stress and inflammation

Based on considerations by Li and Förstermann, pharmacological prevention of eNOS uncoupling is another antioxidant therapeutic strategy that may not interfere with the protective role of redox signaling in the cardiovascular system [9]. Oxidative stress plays a crucial role in the pathogenesis of cardiovascular disease. Among the major producers of RONS, the uncoupled endothelial nitric oxide synthase (eNOS) makes a significant contribution to RONS generation in cardiovascular tissues [470,471]. Under physiological conditions, eNOS produces $^{\bullet}$NO. Endothelium-derived $^{\bullet}$NO has anti-hypertensive, anti-thrombotic and anti-atherosclerotic properties by relaxing blood vessels, inhibiting platelet aggregation/adhesion, preventing leukocyte adhesion/migration, and inhibiting smooth muscle cell proliferation [472]. Under pathological conditions associated with oxidative stress and inflammation, eNOS can be converted from a $^{\bullet}$NO-producing enzyme to a superoxide-generating molecule, a process termed eNOS uncoupling. All cardiovascular risk factors, such as diabetes, hypertension, hypercholesterolemia and smoking, may induce eNOS uncoupling [472]. A number of mechanisms may contribute to eNOS uncoupling [9,473], with deficiency of the eNOS cofactor tetrahydrobiopterin ($BH_4$), deficiency of the eNOS substrate L-arginine, and eNOS *S*-glutathionylation being the most important ones. Peroxynitrite and superoxide can oxidize $BH_4$ to dihydrobiopterin ($BH_2$), leading to $BH_4$ deficiency. A lack of $BH_4$ can also be caused by a reduction of $BH_4$ *de novo* synthesis (e.g. due to down-regulation of the $BH_4$-synthesizing enzyme GTP cyclohydrolase I) or by a decrease of $BH_4$ regeneration from $BH_2$ (e.g. down-regulation of the recycling enzyme dihydrofolate reductase). A recent study demonstrates that $BH_4$-dependent and *S*-glutathionylation-induced eNOS uncoupling are mechanistically independent but functionally linked [474]. L-Arginine deficiency can be caused by inflammation-induced up-regulation of arginases, enzymes that compete with eNOS for the same substrate. By producing superoxide, uncoupled eNOS augments the pre-existing oxidative stress and further enhances eNOS uncoupling, creating a vicious circle. Interestingly, some established cardiovascular drugs (and some other compounds) show the potential to prevent eNOS uncoupling. The recoupling of eNOS may represent pleiotropic effects of these drugs and contribute to their therapeutic benefit. Angiotensin-converting enzyme (ACE) inhibitors, angiotensin II type-1 (AT1) receptor antagonists, statins, the organic nitrate pentaerythritol tetranitrate (PETN), eNOS transcription enhancers and the red wine polyphenol resveratrol have been shown to reverse eNOS uncoupling in disease models by elevating tissue $BH_4$ levels [475,476]. PETN [477] and the AT1 receptor blocker telmisartan [478] additionally prevent eNOS *S*-glutathionylation. Furthermore, arginase inhibition also represents a promising strategy to recouple eNOS [479,480].

As suggested by Muzykantov, the previously described detrimental but also beneficial effects of RONS warrant careful targeting without interfering with the beneficial signaling pathways by using site- and species-specific approaches [9]. Liposomes and other nanocarriers improve the pharmacokinetics of antioxidants including *N*-acetyl cysteine (NAC) and antioxidant enzymes (AOE, i.e. catalase and SOD) and thus help alleviate vascular oxidative stress predominantly via detoxification of extracellular RONS [481]. In order to achieve targeted endothelial interventions, these agents can be conjugated with antibodies to endothelial determinants including cell adhesion molecules ICAM [482] and PECAM [483]. In preclinical studies, diverse formulations of such AOE conjugates (Ab/AOE) show binding to endothelium after *i.v.* injection [482]. Targeting of these formulations qualitatively improves protection of endothelial cells from extracellular RONS [484] and RONS produced inside these cells [485]. As a result, Ab/AOE injected into animals attenuated ischemia-reperfusion injury in lungs of diverse species [486,487], normalized vasoreactivity in angiotensin II-challenged mice [487], inhibited endothelial pro-inflammatory activation caused by cytokines and potentiated the anti-inflammatory effect of NO donors [485]. Further, an indirect inhibitor of NADPH-oxidase loaded in Ab/liposomes accumulated in endothelial cells, inhibited RONS production and provided more potent protection vs. non-targeted counterparts against oxidative stress in mice [488]. Ab/liposomes loaded with EUK-134, a superoxide dismutase/catalase mimetic, bound to endothelial cells and alleviated endotoxin-induced lung inflammation in mice [489]. Likewise, PECAM-targeted nanocarriers loaded with tocopherol and EUK-134 alleviated endothelial inflammatory activation. Encapsulation in polymeric nanocarriers protects AOE from proteases [490]. Modulation of geometry and affinity features of targeted AOE formulations enables their delivery into endothelial endosomes, quenching RONS produced in these vesicles and intercepts pro-inflammatory endothelial signaling and abnormal activation [485]. Endothelial targeting of antioxidants enables anti-inflammatory mechanisms based on interception of endothelial RONS [9]. This drug delivery strategy may find utility in the management of acute vascular oxidative stress and inflammation (Fig. 6.3).

As explained by Lazou, accumulating evidence supports a key role for peroxisome proliferator activated receptors (PPARs) in regulating the redox state in the cardiovascular system through transcriptional or post-translational effects and thereby controls the redox balance in cardiac diseases [491]. PPARs are ligand activated transcription factors that belong to the superfamily of nuclear hormone receptors, with well-documented roles in the transcriptional regulation of cardiac lipid metabolism and energy homeostasis. Their non-metabolic, anti-oxidant, anti-ischemic and anti-inflammatory properties have emerged over the past years and are being actively investigated in relation to cardiac dysfunction. All three PPAR isoforms (α, β/δ, γ) have been implicated in the modulation of oxidative stress, although different mechanisms may be employed by each of them. PPARα and PPARγ function in a similar way towards the modulation of oxidative stress, mostly through the transcriptional regulation of target antioxidant enzymes. PPARα activation via clofibrate diminishes RONS production and lipid peroxidation in rat hearts subjected to acute myocardial ischemia through the upregulation of transcription and activity of antioxidant enzymes such as Cu/Zn-SOD (SOD1), Mn-SOD (SOD2), and catalase in the heart tissue as well as the suppression of AT-1 induced NADPH activity [492]. The PPARα agonist, WY14643, ameliorated oxidative stress in a rat model of IR [493], which is reflected by HO-1 down-regulation post IR in WY14643-treated myocardium. PPARγ agonists like troglitazone, rosiglitazone and pioglitazone induce glutathione peroxidase (GPx 3) in human skeletal muscle cells and thioredoxin in neonatal rat cardiac myocytes [491]. RONS generation was also suppressed in cultured cardiac myocytes treated with a PPARβ/δ agonist due to upregulation of catalase [494]. PPARβ/δ also inhibits RONS generation in vascular muscle cells through inhibition of NADPH oxidases [495]. The effect of PPARβ/δ activation on antioxidant defense may also be attributed to improved mitochondrial biogenesis through regulation of target genes such as PGC-1 and mitofusin 2 [496]. Upregulation and activation of PPARs have been also implicated in the endogenous mechanisms of cardioprotection implying that PPAR activation prior to IR could confer

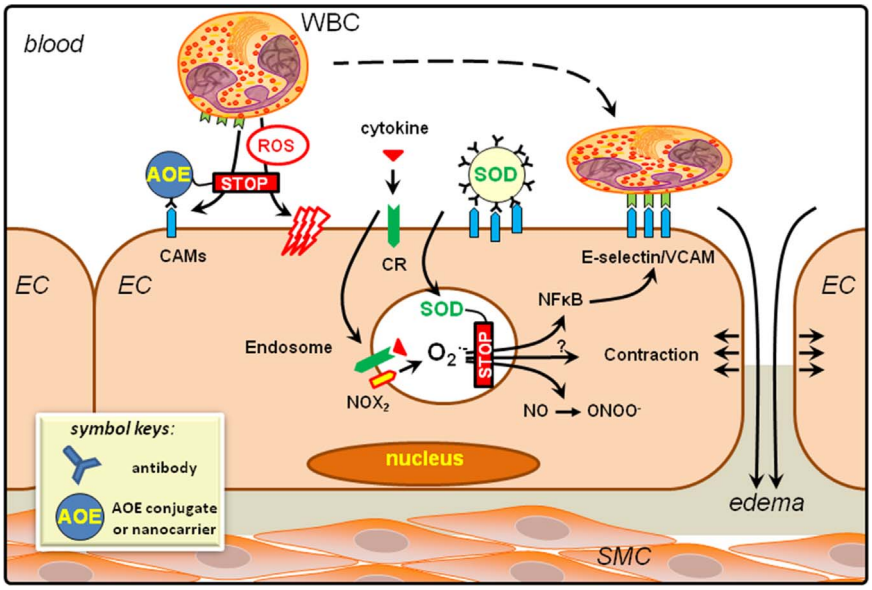


**Fig. 6.3.** Overview on therapeutic options for the improvement of vascular dysfunction. Targeted antioxidant interventions to alleviate pro-inflammatory activation and oxidative stress in endothelial cells. Endothelial ROS from activated NOX2 enzyme in endosomes are formed in response to cytokine binding to the receptors and ignite signaling cascade of transcription factor NFκB. Targeted delivery of antioxidants, antioxidant enzymes (AOE) and inhibitors of ROS production can be achieved using antibodies and other ligands of endothelial surface determinants including cell adhesion molecules PECAM and ICAM. Surface-bound targeted AOE intercept extracellular ROS, whereas targeted formulations using the same ligands configured in a way permitting internalization into the ROS-signaling endosomes allows interception of pro-inflammatory activation manifested among other characteristics by exposure of inducible cell adhesion molecules – E-selectin, VCAM-1, and ICAM-1 - that can be detected using imaging probes conjugated to the ligands of these molecules. With permission of the publisher. 
Adapted from [9].

preconditioning-like protection to the myocardium. Activation of the PPARα isoform results in significant anti-infarct protection, comparable with the effect of classical ischemic preconditioning that appears to involve survival cascades (ERK1/2 and PI3K/Akt), upregulation of eNOS and the opening of mitochondrial KATP channels [497,498]. There are several remaining issues that need to be addressed regarding the biological role of PPARs as regulators of the cardiac redox state, especially regarding the translation of in vitro findings in the in vivo setting. However, the pleiotropic activity of these receptors makes them interesting therapeutic targets for the development of antioxidant strategies that aim to control the intracellular redox balance in various cardiac pathologies, especially linked to dyslipidemia, atherosclerosis, and diabetes, that are frequently associated with cardiovascular disorders.

Steven and Daiber emphasize the importance of the pleiotropic antioxidant, anti-aggregatory and anti-inflammatory potential of established drugs as exemplified by DPP-4 inhibitors and GLP-1 analogs [19]. Glucagon-like peptide-1 (GLP-1) is an incretin hormone and released from L-cells in the intestine after food uptake [499,500]. Its receptor belongs to the family of G-protein-coupled receptors and binding of GLP-1 induces insulin release from beta cells of the pancreas. GLP-1 is involved in glycemic control and due to rapid degradation by the exopeptidase dipeptidyl peptidase-4 (DPP-4) its half-life is below two minutes [501,502]. Accordingly, inhibition of DPP-4 and supplementation of GLP-1 represent new therapeutic targets for the management of diabetes. Besides this first line indication, there are several reports on beneficial effects of DPP-4 inhibition on cardiovascular disease associated with atherosclerosis [503,504], but also with psoriasis [505], hepatic steatosis [506] and stroke [507]. All of these diseases have in common, that inflammation and oxidative stress contribute to their pathophysiology. It was previously shown that DPP-4 inhibition suppresses the proinflammatory phenotype of isolated myelomonocytic cells and proinflammatory cascades in endotoxemic rats [508]. Investigation of the effects of DPP-4 inhibition and GLP-1 supplementation on endotoxemia and septic shock revealed improved survival of septic mice (lipopolysaccharide i.p. injection), even when the therapy with the DPP-4 inhibitor linagliptin or the GLP-1 analog liraglutide was started six hours after induction of endotoxemia [371]. The improvement of mortality is based on the control of the initial inflammatory response, which characterizes LPS-induced endotoxemia. The oxidative burst of inflammatory, myelomonocytic cells, oxidative stress measured by dihydroethidium fluorescence, expression of typical inflammatory genes, as well as vascular infiltration of CD11b+ cells was decreased in endotoxemic animals treated with linagliptin and liraglutide. As a consequence, hemodynamic control was recovered by linagliptin and liraglutide treatment preventing the development of lethal hypotension in the endotoxemic animals, all of which was based on activation of the AMP-dependent protein kinase (AMPK) [371]. Our data suggest that DPP-4 inhibitors and GLP-1 analogs have inhibitory effects on myelomonocytic cells, which in the case of DPP-4 inhibition do not entirely rely on the GLP-1 receptor [372]. Inflammation and hemostasis are subject to a complex interplay in the setting of sepsis. Thrombocytopenia and disseminated intravascular coagulation (DIC), characteristic features leading to end organ damage and death in septic shock, were significantly improved by both drugs [372]. Similar results were obtained in an animal model of experimental thrombosis [509]. Further support of this concept was based on the observation that GLP-1 analogs inhibit platelet activation and aggregation directly via the GLP-1 receptor, which is expressed on murine and human thrombocytes, and by cAMP/adenylyl cyclase signaling [372,509]. In conclusion, sepsis is still a main cause of death all over the world. DPP-4 inhibition and GLP-1 supplementation reduced the mortality in endotoxemic animals by antioxidant, anti-inflammatory and antiaggregatory effects (Fig. 6.4). The potential use of these drugs in patients with sepsis or other inflammatory diseases needs further exploration.

### 6.6. Conclusion

Evidence derived by experimental approaches exploiting powerful tools of molecular and cell biology is rapidly advancing our understanding of redox reactions involved in RONS formation. These molecules, which were once investigated only for their possible involvement in numerous diseases, are now attracting wide interest for their role as intracellular signals, especially those in response to metabolic or mechanical changes. Therefore, besides the well-established notions that high intracellular levels of RONS impair function and viability of practically any cell type, a large body of evidence indicates that ROS are involved in countless physiological processes and trigger powerful mechanisms of protection against cell injury.

In this review section we summarized established concepts and recent advances supporting the dual role of RONS in cardiovascular pathophysiology. These novel findings might support the therapeutic potential of antioxidant interventions and explain the failure of clinical trials using this approach. Indeed, the issues that remain to be elucidated outnumber those that have been clarified.

## 7. ROS and the aging process

Jose Vina (E-mail: Jose. Vina@uv.es) and Gloria Olaso-Gonzalez (E-mail: gloria.olaso@uv.es).

### 7.1. Introduction

The free radical theory of aging postulated by Harman in 1956 has provided a theoretical framework for research oriented toward understanding the mechanisms of aging. This theory states that “aging and

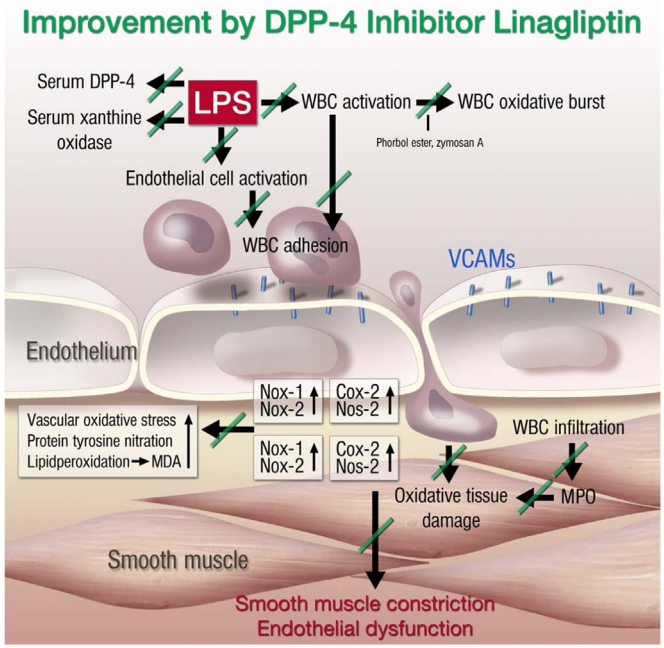


**Fig. 6.4.** Proposed mechanisms of lipopolysaccharide (LPS)-induced vascular dysfunction and improvement by linagliptin therapy. LPS treatment activates white blood cells (WBC, envisaged by increased oxidative burst), increases serum levels of xanthine oxidase (XO), increases DPP-4 serum activity and activates vascular cells (detected by expression of endothelial adhesion molecules and inducible cyclooxygenase [COX-2]). This leads to the infiltration of WBC to the vascular wall (detected by aortic FACS analysis for myelomonocytic cells, inducible nitric oxide synthase [NOS2], NOX2 and myeloperoxidase [MPO] expression) and oxidative damage of the vasculature (NOX1 expression, ROS formation, 3-nitrotyrosine levels and lipidperoxidation by malondialdehyde [MDA]). Finally, the tissue damage results in smooth muscle constriction and endothelial dysfunction. With permission by Oxford University Press. Copyright © 2012. Adopted from [508].

the degenerative diseases associated with it are attributed basically to the deleterious side attacks of free radicals (ROS) on cell constituents and on the connective tissue" [510]. Mitochondria have a major role in ROS production [511]. On the other hand, NADPH oxidases (NOXs) are important enzyme systems involved in inducible ROS formation, since they catalyze the partial reduction of $O_2$ to form ROS. It has been shown that the enhanced expression and/or activity of NOX family members, in particular NOX4, plays an important role in age-associated diseases such as cardiovascular disease, fibrosis, cancer and neurodegenerative diseases like Alzheimer's disease [512,513]. In this situation of misbalance, proteasome-mediated degradation of oxidized proteins is a critical player for protein homeostasis maintenance. Proteasome dysfunction takes place during aging [514]. Proteasome up-regulation in terms of assembly, quantity and function has been achieved through genetic manipulation in animal models. This activation was shown to be successful to decelerate aging progression by enhancing resistance to oxidative stress. However, genetic manipulation is not applicable in humans, so new studies should focus on the identification of nutritional, pharmacological or physiological interventions with proteasome activating properties.

Oxidative stress has been linked with age-associated diseases, but also with a geriatric syndrome characterized by diminished functional reserve and increased vulnerability to low power stressors, i.e. frailty (Fig. 7.1). An association between systemic oxidative stress biomarkers (malondialdehyde, isoprostanes, protein carbonylation and lipoprotein phospholipase A2) and frailty has been reported in the geriatric population [515,516]. Nevertheless, recent data have shown that lower expression of genes related to antioxidant responses to oxidative stress in older people is associated with a higher risk of being frail independently of age and sex (see El Assar et al. contribution, Section 7.6).

In recent years, epidemiological as well as laboratory data have shown that antioxidant supplementation is at least useless if not detrimental in aging [517]. Indeed, antioxidant supplementation did not lower the incidence of many age-associated diseases but, in some cases, increased the risk of death [518].

This has cast doubts on the classical "free radical theory of aging". We thus proposed "the cell signaling disruption theory of aging". This theory postulates that "ROS" cause aging inasmuch as they alter—sometimes irreversibly—the signaling network of the cell. If the cell can cope with the stress caused by relatively mild action of ROS, then adaptation takes place and damage does not occur. If, however, the cell is overwhelmed by the action of radicals, subcellular damage and aging will take place". Indeed, radicals serve as signals and interaction between them is tightly balanced. In this sense, we cannot support the idea of proposing antioxidant supplementation for the general population. It is much better to increase endogenous defenses by nutritional or physiological manipulation than administering antioxidant compounds, such as vitamin C or E. In any case, these considerations do not detract from the free radical theory of aging, which has been extremely useful and has fostered research by providing a general theoretical framework on which many of us have based decades-long experimental research.

### 7.2. NADPH oxidases in aging and age-associated diseases

Pidder Jansen-Dürr and Rafal Koziel summarize that superoxide anions and other ROS can exert beneficial effects under normal conditions through adaptive cellular signaling responses. On the other hand, ROS are able to induce direct damage to biologically sensitive targets like lipids, proteins and nucleic acids, and their overproduction is involved in both chronic diseases and age-related diseases. To date, a variety of different theories of biological aging have been discussed [519,520]; however, many of them describe 'oxidative stress' as the

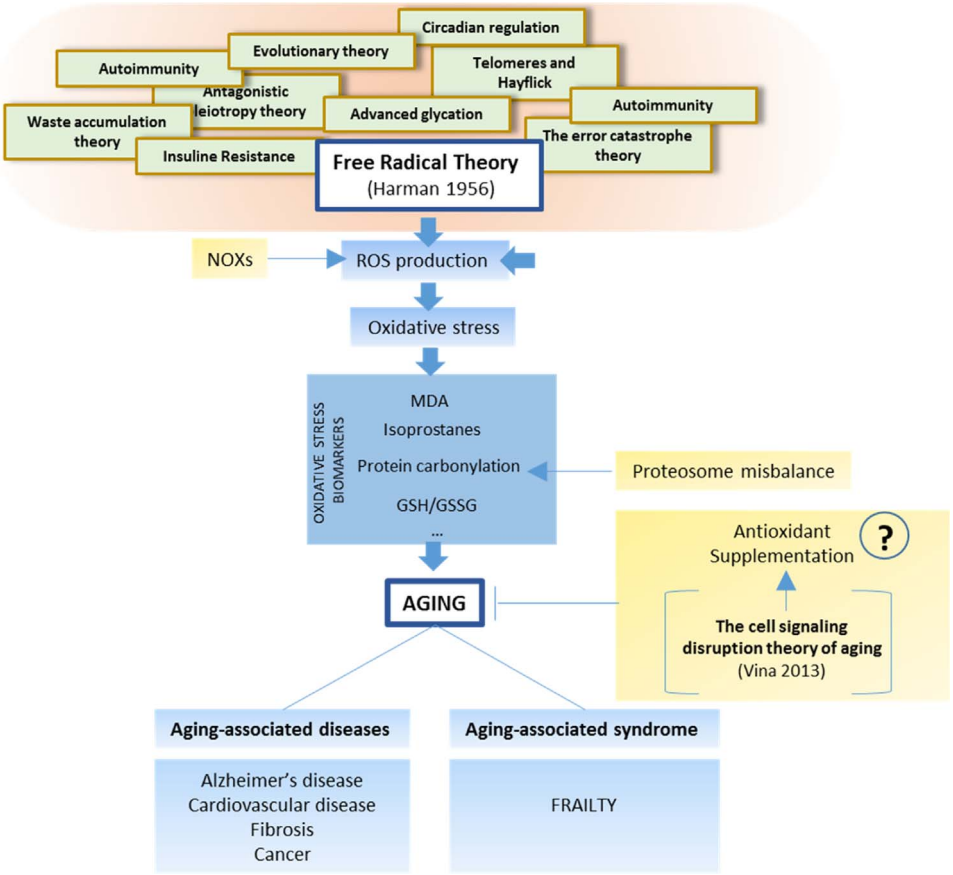


**Fig. 7.1.** Scheme summarizing the main concepts of the free radical theory in aging and development of aging associated diseases and syndromes.

common cause of aging.

The 'free radical theory of aging' predicts the major role of mitochondria-derived ROS in aging [510], however, recent data indicate a key role of other ROS sources in this process. A significant number of enzymatic or chemical processes are capable of producing ROS in vivo; however, the NOXs are the primary enzyme systems involved in inducible ROS formation [65,521,522]. The NOX family of membrane-associated enzymes consists of seven isoforms, Nox1-5 and Duox1-2, and catalyzes the reduction of $O_2$ to form ROS [512,521]. The role and mechanism of the activation of NOXs is isoform type, intracellular localization as well as tissue type specific, and NOX mediated oxidative stress is strongly associated with a variety of human age-related diseases [523](see also below). A growing number of studies indicate that NOX4 is localized to mitochondria in many cell types and promotes aging. We have previously suggested a new pathway by which sustained NOX4 activity decreases mitochondrial function and induces premature senescence in human umbilical vein endothelial cells (HUVEC). NOX4 induced premature senescence by decreasing the concentration and activity of mitochondrial respiratory chain complex I [524,525]. Accordingly, NOX4 knockdown reduced mitochondrial $H_2O_2$ production and markers of oxidative DNA damage, increased the cellular proliferation rate and prolonged the replicative lifespan by more than 2-fold [524,525]. It remains to be shown if increased NOX4 activity contributes to aging of the vasculature in mammals.

The effector role of NOX4, a constitutively active NOX isoform, to drive cellular senescence is conserved for oncogene-induced senescence, a tumor suppressor pathway that restricts the growth of pre-neoplastic cells in mice and humans. Weyemi et al. found that NOX4 is a critical mediator in the oncogenic H-RasV12-induced DNA-damage response and subsequent senescence [526]. H-RasV12 overexpression correlated with increased NOX4 expression, higher ROS levels, DNA damage, histone H2A.X phosphorylation and $p21^{Cip1}$ accumulation. Similar conclusions were reached by Kodama et al. who showed that NOX1- and NOX4-generated ROS play an important role in Ras-induced premature senescence, which may involve the DNA damage response and p38MAPK signaling pathways in primary human lung TIG-3 cells. Both NOXs were upregulated by the Ras oncogene. Ablation of *Nox1* and *Nox4* by small interfering RNAs (siRNAs) blocked the RasV12 senescent phenotype including β-galactosidase activity, growth arrest and accumulation of tumor suppressor proteins such as p53 and p16Ink4a. The involvement of Nox1 in Ras-induced senescence was also confirmed with embryonic fibroblasts derived from *Nox1* knockout mice [527]. Another study suggested an important role of NOX4 in oncogene-independent senescence of hepatocellular carcinoma cells [528].

Of interest is compelling evidence that enhanced expression and/or activity of NOX family members, in particular NOX4, plays an important role in age-associated diseases, including cardiovascular disease, fibrosis and cancer. In the vasculature, NOXs are a major source of ROS and are key players in mediating redox signaling under both physiological and pathological conditions. Cardiovascular disease (CVD) is the leading cause of death, and aging is a major risk factor for CVD development. A substantial number of studies describe the role of NOX4 in the age-related pathology of the cardiovascular system. It was shown that NOX4 has an impact on vasoconstriction, atherosclerosis development, vascular cells hypertrophy, apoptosis and differentiation. One of the major age-related arterial phenotypes thought to be responsible for the development of CVD in older adults is endothelial dysfunction. It was speculated that mitochondrial oxidative stress rises when antioxidants are unable to counteract the ROS produced by NOX4, triggering the aging process of the heart [529]. Wang et al. [530] examined the involvement of NOX in age-associated cardiac remodeling in a rodent model of aging and found that age-dependent increases in blood pressure, cardiomyocyte hypertrophy, coronary artery remodeling and cardiac fibrosis were associated with increased myocardial NOX2 activity. Another study indicates that NOX4 and mitochondrial oxidative stress, but not NOX1 or NOX2, are mediators of CVD in aging mice under hyperlipidemic conditions [531]. Whereas initial results obtained with *Nox4* KO mice did not reveal striking phenotypical differences relative to wild type mice, there is now solid evidence that the absence of NOX4 alters a number of physiological heart parameters (see also above), and increases susceptibility to tissue damage in a mouse model for stroke [532].

A crucial role of NOX4-derived ROS in age-related diseases was also implicated in the initiation, establishment, and development of tissue fibrosis (reviewed in [533]). In particular, strong experimental evidence suggests that pulmonary fibrosis (also referred to as idiopathic pulmonary fibrosis, IPF, for the lack of a well-defined etiology) is caused by excessive NOX4 activity and can be at least partially reverted by targeting the NOX4-NRF2 redox imbalance [534]. On the other hand, work by the Armanios group has established that genetic deficiencies in telomere maintenance systems cause IPF late in life [535], which therefore has been referred to as a "short telomere disease" [536], and the percentage of genetic lesions affecting telomere maintenance in IPF patients is steadily increasing. From these data, it appears conceivable that telomere shortening and activation of NOX enzymes, in particular NOX4, are mechanistically linked; however such links have so far remained elusive. A potential role of NOX2 has been found in age-related neurodegenerative diseases like Alzheimer's disease [513] and Parkinson's disease [537].

The incidence of most cancers increases dramatically with age, indicating that, with a few exceptions, cancer is primarily an age-associated disease. Concerning the role of NOX family members, a dual role in carcinogenesis has been postulated. On the one hand, the function of NOX to mediate oncogene-induced senescence, leading to tumor suppression (see above), indicates that NOX activity restricts tumor growth in some instances. On the other hand, production of ROS by NOX enzymes is essential for signaling pathways driving cell proliferation and survival, indicating that enhanced NOX activity in epithelial cells favors tumorigenesis. This dual role of NOX-derived ROS is best illustrated in prostate cancer, clearly one of the most relevant age-associated malignancies. Analysis of radical prostatectomy tissue samples and benign and malignant prostate epithelial cell lines identified NOX5 as an abundantly expressed NOX isoform and suggested that NOX5-derived ROS and subsequent depletion of PKCζ and JNK inactivation play a critical role in modulating intracellular signaling cascades driving the proliferation and survival of PCa cells [538]. On the other hand, increased expression of *Nox4* in prostate stromal cells (fibroblasts) during their age-associated trans-differentiation to myofibroblasts leads to benign prostate hyperproliferation [539], a condition referred to as "reactive stroma" [540] that is known to favor the emergence of (epithelial) tumor cells in the prostate.

In conclusion, the existing evidence suggests that NOX family members are important drivers of age-associated pathology, and regulating NOX activity/expression and using mitochondrial antioxidants are potential approaches to reducing aging-associated diseases.

### 7.3. Protein aggregates as redox signaling mediators in aging

The aging process and a number of age-associated diseases are accompanied by the accumulation of high-molecular protein aggregates, as reported by Tilman Grune. In the aging process these protein aggregates are often referred to as lipofuscin, ceroid or age associated fluorophores. This material is largely composed of proteins, often amounting to 60–80%. Some of these proteins are oxidized or modified by various reactive metabolites, e.g. carbohydrates forming advanced glycation end products. Various lipids form another major part of such aggregated material. Interestingly, several authors report also the inclusion of various metals in such protein aggregates.

This raised the question, whether included metals are able to trigger metal-catalyzed redox reactions. It could be demonstrated that iron in

protein aggregates is able to catalyze the Fenton-reaction and is only partially chelatable by iron-chelators [541]. Moreover, in the same study it could be demonstrated that in senescent cells protein aggregates contribute to an age-associated shift in the redox-state [541].

Further studies revealed that such protein aggregates do have an active surface. It is likely that due to the reactive surface of the aggregate, e.g. due to reactive hydroperoxides or aldehydes, and due to the hydrophobic patches – a result of the unfolding of the included proteins - protein aggregates can bind cellular proteins. This interactome might either be random or at least partially specific due to the binding of protein-protein-interacting structures. The latter includes certainly the binding of chaperones [542] or proteases designed to degrade unfolded proteins, as in the proteasome [543].

The 20S proteasome is known to be the major intracellular protease responsible for the degradation of damaged and oxidized proteins [543]. On the other hand, it is also the central catalytic part of the ubiquitin-proteasomal-system and, therefore, involved in the degradation of most cytosolic proteins [543]. The proteasome recognizes unfolded protein structures. In the case of protein aggregates this leads to an inhibition of the proteasome upon binding. This was shown in in vitro senescence models [544] or in neurons of Alzheimer's disease patients [545]. Proteasomal inhibition, in turn, leads to a proteasomal mal-performance, leading to disturbances of the regulated turnover of transcription factors, as shown in the case of AP-1 [546], HSF1 and NRF2 [547]. Furthermore, it should be noted that proteasomal inhibition leads also to a vicious cycle in which a reduced level of degradation of newly formed oxidized proteins leads to enhanced protein aggregate formation.

In conclusion, it should be noted that accumulating protein aggregates have multiple pathophysiological effects and cannot be seen as inert waste materials. However, more studies are needed to acquire a more complete scheme of the action of protein aggregates and their contribution to cellular senescence.

### 7.4. Proteasome activation as an anti-aging and anti-aggregation strategy

From the least to the most complex organisms, aging is a natural inevitable process accompanied by several molecular and biochemical failures. As explained by Niki Chondrogianni and Nikoletta Papaevgeniou, damaged and/or wrongly produced macromolecules tend to accumulate and aggregate, resulting in proteostasis impairment that then triggers a cataract of system deficits. Proteasome-mediated degradation is a critical player for protein homeostasis maintenance; proteasomes are large enzymatic complexes that regulate the cellular protein load equilibrium by degrading the unnecessary peptides and proteins. Proteasomal dysfunction is associated with the progression of aging and protein aggregation further aggravates the problem [514]. Consequently, proteasome activation appears to be a promising anti-aging and anti-aggregation approach.

Proteasome up-regulation in terms of assembly, quantity and function has been achieved through genetic manipulation of various catalytic or regulatory subunits or through treatment with specific activating compounds. This activation has been shown to lead to decelerated aging progression and to enhanced longevity. More specifically, overexpression of β1 and β5 catalytic subunits endowed WI38 human fibroblasts with increased resistance to oxidative stress and elongated cellular lifespan [514]. Overexpression of the *pbs-5* subunit (nematode ortholog of β5) in *C. elegans* resulted in increased proteasome content and function that led to enhanced resistance to oxidative stress and extended lifespan in a *daf-16*-, *skn-1*- and *hsf-1*-dependent manner [548]. In accordance, *rpn-6.1* overexpression in *C. elegans* triggered elevated proteasome activities leading to enhanced longevity under conditions of mild heat stress [549]. The positive effect of proteasome activation on longevity was also shown in the fruit fly where overexpression of the RPN11 19S subunit resulted in enhanced proteasome activities and extended lifespan [550]. With regard to compounds, treatment with a pentacyclic triterpenoid, namely 18α-glycyrrhetinic acid, resulted in increased proteasome content and activity both in cellular (human fibroblasts) and organismal (*C. elegans*) models [551,552]. This compound was shown to promote proteasome activation in an NRF2-dependent manner in fibroblasts [551] and a SKN-1-dependent manner in nematodes [552], with elongated lifespan and increased stress resistance as the end result. Finally, rejuvenating and anti-aging properties were attributed to quercetin-mediated proteasome activation in human fibroblasts [553].

Proteasome activation has also been shown to confer protection against the devastating consequences of protein aggregation. Enhancement of proteasome function through *pbs-5* overexpression in nematodes endowed animals with increased survival against expanded polyglutamine and Aβ peptide proteotoxicity [548]. Similarly, *rpn6.1* overexpression conferred proteotoxic stress resistance in a nematode polyglutamine disease model [549], while RPN11 overexpression suppressed the expanded polyglutamine- induced progressive neurodegeneration in fruit flies [550]. Proteasome activation through 18α-glycyrrhetinic acid treatment led to reduced Aβ peptide deposits both in murine neuronal cells and in an Alzheimer's disease nematode model thus resulting in decelerated progression of the disease's phenotype [552]. Likewise, the polyphenol quercetin was found to induce proteasome activity resulting in inhibition of paralysis in a transgenic *C. elegans* strain serving as an animal model for Alzheimer's disease [554].

In conclusion, proteasome activation emerges as a promising strategy in the battle against aging and proteotoxicity. Given that genetic manipulation is not applicable in humans, future studies should focus on the identification of compounds with proteasome activating properties as well as in the elucidation of the involved signals and biochemical pathways.

### 7.5. Free radical theory of aging – dead or alive?

The “free radical theory of aging” was introduced in the early 1950s through the work of Harman [510] and comprises investigations of the role of reactive oxygen species (ROS) formation and mitochondrial function in the aging process and, more recently, the implications of ROS-triggered epigenetic processes and DNA damage for the etiology of aging [555]. Lately, as discussed by Andreas Daiber and Yuliya Mikhed, the field of epigenetics has received considerable attention in the context of aging theories. It has been shown that cellular senescence leads to massive DNA demethylation, causing a state of DNA hypomethylation, particularly in the CpG islands [556] and multiple epigenetic processes are regulated in a redox-dependent manner [238]. Although the lessons learned from animal models of genetic deletion or overexpression of important antioxidant enzymes such as superoxide dismutases, glutathione peroxidases and catalase were rather disappointing, since no clear correlation between life span and the abundance of these antioxidant defense enzymes could be observed, at least some of them (e.g. *Sod1*$^{-/-}$) or double gene ablation combinations showed reduced life expectancy, which would be in line with the “free radical theory of aging” [557,558]. Moreover, the importance of mitochondrial superoxide formation for survival (longevity) is highlighted by the fact that homozygous SOD2 deletion leads to perinatal or neonatal lethality [559] and by the observation that mice deficient in the *p66Shc*$^{-/-}$ gene, a source of mitochondrial ROS formation, display a 30% longer life span [560]. According to more recent data, oxidative stress in general and mitochondrial ROS formation in particular may play an even more important role for the quality of life, healthy aging, or the so-called “healthspan” than for the lifespan per se [561,562]. Healthy aging may be an even more important need and challenge in our aging Western societies, also from an economical point of view considering the tremendous costs associated with our public health systems. The cardiovascular system seems to be an excellent example of this concept. From a mechanistic basis the increasing superoxide formation (coming from gradually increased mitochondrial leakage of

electrons and NADPH oxidase-derived production due to low grade inflammation) with progressing age will lead to antagonization of nitric oxide, a major vasodilator and antiatherothrombotic signaling molecule of the cardiovascular system [555]. Oxidative depletion of nitric oxide bioavailability by superoxide and the reaction product peroxynitrite will lead to impaired cGMP formation, inhibition of prostacyclin synthase by tyrosine nitration and activation of the renin-angiotensin-aldosterone system as well as endothelin-1 signaling, which will lead to a complete switch from a vasculoprotective to a proatherothrombotic phenotype [9]. In support of this concept, genetic deletion of mitochondrial antioxidant enzymes (*Aldh2*$^{-/-}$ and *Sod2*$^{+/-}$) led to an increase in mitochondrial ROS formation, 8-oxoguanine-dependent mitochondrial DNA strand breaks and, most importantly, an impairment of endothelium-dependent and –independent relaxation (vascular function) (Fig. 7.2A-B) [563]. Likewise, genetic deletion of GPx-1 led to an age-dependent impairment of endothelium-dependent and –independent relaxation, increase in oxidative stress markers and eNOS uncoupling as well as aggravation of inflammatory phenotype of the vasculature (summarized in Fig. 7.2C) [62]. Although these animals showed no obvious decrease in lifespan, it may be assumed that the proatherothrombotic and inflammatory phenotype will ultimately lead to increased prevalence of cardiovascular complications as a consequence of the higher burden of oxidative stress, thereby decreasing the healthspan.

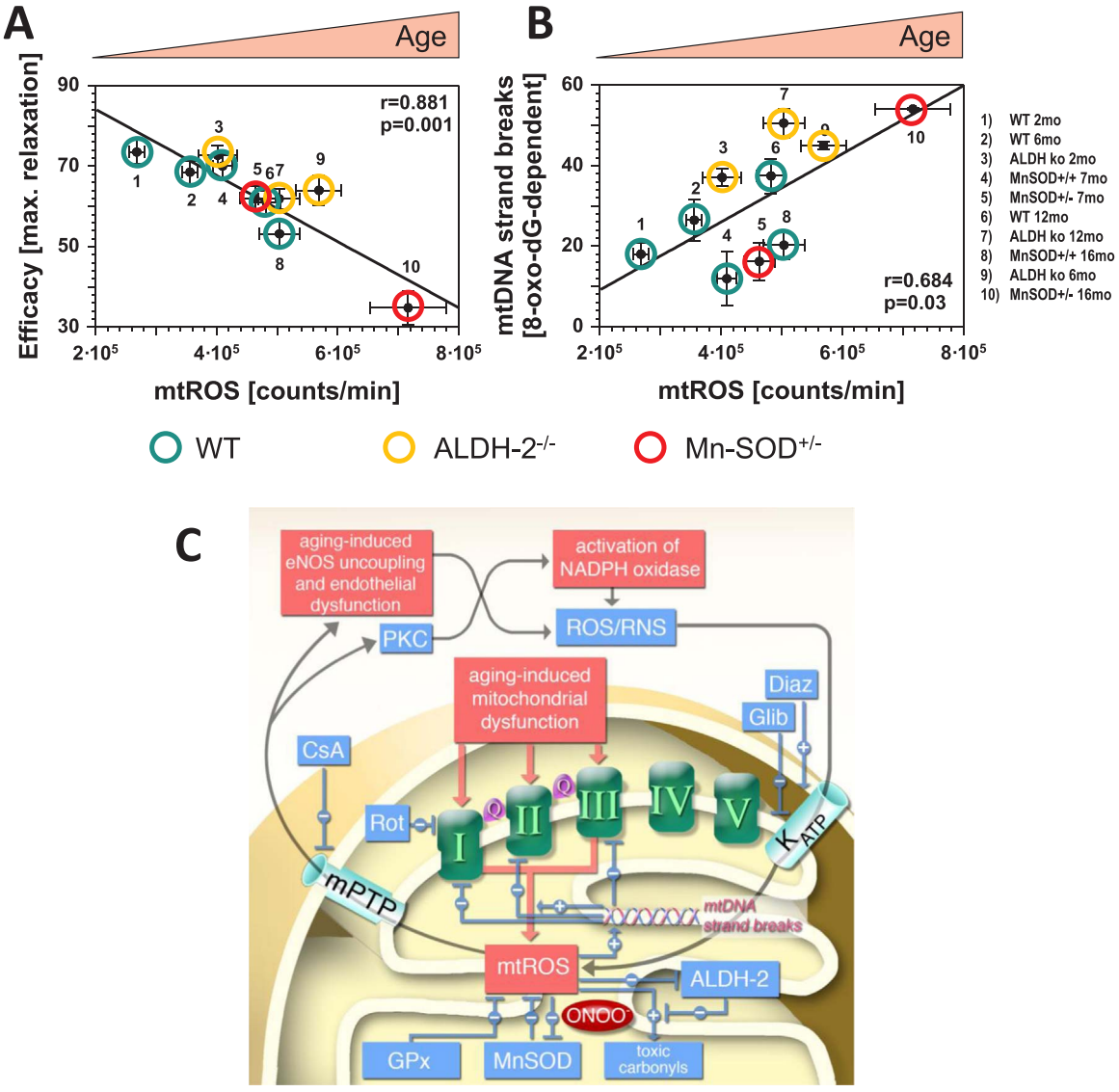


**Fig. 7.2.** Correlations between mitochondrial oxidative stress (mtROS), mitochondrial DNA (mtDNA) damage and vascular (endothelial) function (ACh-induced maximal relaxation). (**A**) mtROS formation was plotted for all age-groups and mouse strains versus the corresponding maximal efficacy in response to acetylcholine (ACh). (**B**) mtROS was plotted for all age-groups and mouse strains versus the corresponding mtDNA damage. ROS were measured using L-012 (100 μM) enhanced chemiluminescence in isolated cardiac mitochondria upon stimulation with succinate (5 mM). r is the correlation coefficient. (**C**) Hypothetic scheme of aging-induced vascular dysfunction and the role of mitochondria in this process. Aging-induced mitochondrial dysfunction triggers mitochondrial reactive oxygen species (mtROS) formation from respiratory complexes I, II, and III (Q = ubiquinone). Break-down of mtROS is catalyzed by glutathione peroxidase (GPx, for $H_2O_2$) or manganese superoxide dismutase (MnSOD), the latter is in turn inhibited by mitochondrial peroxynitrite ($ONOO^-$) formation. mtROS increase the levels of toxic aldehydes and inhibit the mitochondrial aldehyde dehydrogenase (ALDH-2), the detoxifying enzyme of those aldehydes. Increase in mtROS and toxic aldehydes also leads to mtDNA strand breaks which leads to augmented dysfunction in respiratory chain complexes and further increase in mtROS since mtDNA encodes mainly for those respiratory complexes. mtROS also activates mitochondrial permeability transition pore (mPTP), which upon opening releases mtROS to the cytosol leading to protein kinase C (PKC)-dependent NADPH oxidase activation, eNOS uncoupling and finally to endothelial dysfunction [61]. Cytosolic reactive oxygen and nitrogen species (ROS/RNS) in turn were demonstrated to activate $K_{ATP}$ channels, which causes alterations in mitochondrial membrane potential (C) and further augments mtROS levels [564]. Effects of rotenone (Rot), cyclosporine A (CsA), diazoxide (Diaz) and glibenclamide (Glib) have been recently demonstrated in related models of vascular dysfunction and oxidative stress, nitroglycerin-induced nitrate tolerance and angiotensin-II triggered hypertension [61,564]. 
Adopted from [563].

In conclusion, there is solid evidence for the “free radical theory of aging” in experimental studies but translation to the clinical situation requires large scale clinical trials, as currently undertaken by the CHANCES consortium (10,622 individuals) reporting on a clear association between oxidative stress markers and all-cause mortality [565] and the MARK-AGE consortium (3337 individuals) the data of which are currently being prepared for final dissemination [566].

### 7.6. ROS and frailty. Understanding the mechanisms of disability in older people

According to Mariam El Assar and Leocadio Rodríguez-Mañas, frailty is a geriatric syndrome characterized by diminished functional reserve and increased vulnerability to low power stressors. Frailty precedes disability, and, in addition, epidemiological cohorts have demonstrated that the frailty phenotype predicts several outcomes such as falls, hospitalization and mortality [567]. Although the biological determinants of frailty are not well defined, oxidative stress and inflammation have been closely related to aging and seem to be potential drivers of frailty pathogenesis. Inflammation and oxidative stress are closely related processes with crosslinks between their respective signaling pathways. In line with this, observational studies have shown that frailty is associated with different systemic inflammatory biomarkers, including C-reactive protein, and interleukin-6 [568]. Elevated levels of pro-inflammatory cytokines have been shown to be associated with increased risk of morbidity and mortality in frail older subjects. Furthermore, an association between systemic oxidative stress biomarkers (malondialdehyde, isoprostanes, protein carbonylation and lipoprotein phospholipase A2) and frailty has been reported in a geriatric population [515].

The prevalence of chronic diseases such as diabetes, cardiovascular diseases and pulmonary diseases increases with aging. These chronic conditions compromise muscle function, cardiovascular performance and pulmonary function leading to increased vulnerability of the organism when exposed to low intensity stressors. This scenario represents the phenotypic manifestation of frailty. Consistently, all these chronic diseases are associated with a higher risk of frailty in aged populations. The contribution of oxidative stress and reactive oxygen species (ROS) to the decline of different functional systems associated to aging and to age-related chronic diseases has been established [569]. For example, the defective nitric oxide signaling in aged muscle vasculature has been attributed to increased inactivation of this molecule by ROS leading to decreased muscle perfusion. On the other hand, the lung is continuously exposed to oxidative stress while the activity of antioxidant enzymes such as superoxide dismutase and glutathione peroxidase decreases with aging. In addition, the induction of heme oxygenase, which is involved in cellular protection against oxidative stress, is defective in lungs of aged mice, further supporting the involvement of oxidative stress in age-related pulmonary dysfunction.

Since frail older adults have minimal injury resilience and a notably decreased response to stress, the different pathways regulating cellular response to stress (oxidative stress, hypoxia and inflammation among others) stand out as possible players in the development of a frailty phenotype. In this sense, aging, sedentary lifestyle and chronic diseases could cause down-regulation of signaling pathways responsible for the cellular response to oxidative stress, such as NRF2. This results in impaired response to stress and increased oxidative stress leading to a situation of vulnerability to stressors such as frailty. In fact, very recent data obtained by our group have demonstrated that lower expression of genes related to response to oxidative stress in older people is associated with a higher risk of being frail independently of age and sex (El Assar and Rodríguez-Mañas group).

Further investigations are definitely needed to fill the gap of knowledge of this evolving field and provide possible targets for intervention to promote health and independence in the elderly.

## 8. ROS and inflammation in health and disease

Manuela Garcia Lopez (E-mail: manuela.garcia@uam.es) and Javier Egea (E-mail: javier.egea@inv.uam.es).

### 8.1. Introduction

Over the past decade, the study of the biological activity and significance of ROS have gained particular interest from both a physiological and pathological perspective. Since ROS are highly unstable and reactive molecules, they interfere with many cellular processes. ROS react with lipids, nucleic acids and proteins, disrupting their cellular functions. Oxidative stress occurs when the damaging effects of ROS exceed the ability of biological systems to neutralize the oxidizing agents and to repair cellular damage. Physiologically, antioxidant defenses are efficient enough to neutralize the damaging effect of oxidizing molecules. In these conditions, the presence of ROS is important for many physiological cellular processes and they participate as signaling molecules in a wide range of cellular functions. Hence, ROS modulate intracellular transduction pathways and transcriptional factors involved in cell proliferation, differentiation, and maturation [570–572].

Chronic Granulomatous Disease (CGD) is a rare inherited innate immunodeficiency caused by defective NADPH oxidase activity in phagocytes and is recognized as a disease model to understand the pathophysiological consequences of ROS deficiency [22]. CGD patients suffer from life-threatening infections, but an apparent paradox between the absence of ROS production and hyperinflammation is often observed in this disease [32,33]. The key producers of ROS in many cells are the NOX enzymes, of which there are seven members with different tissue distributions and regulatory mechanisms. ROS produced by the isoform NOX2 is essential to organize the response in host defense against pathogens [573].

In the brain, ROS production regulates neuronal development from neuronal precursors [574]. Redox signaling is also required to trigger neuronal differentiation and axon formation [575]. Nitric oxide (˙NO), a diffusible intercellular messenger produced by neuronal nitric oxide synthase (nNOS) exerts a dual regulatory role in neurovascular coupling and neuroenergetics by regulating mitochondrial oxygen consumption [576]. Therefore, ROS act as messengers in the transduction pathways important for synaptic plasticity in the CNS.

The brain is particularly vulnerable to oxidative stress because it consumes a large amount of oxygen, has abundant lipid content, and has little antioxidant activity compared to other organs. The major antioxidants in the brain are ascorbate, glutathione (GSH), and vitamin E in the plasma membrane. GSH production is increased in response to oxidative stress in astrocytes, cells that act as the main supplier of GSH to neurons for antioxidant protection [577]. ROS accumulation in the brain has been associated with the onset of neurodegenerative and psychiatric diseases, whose main consequence is to reduce several neuronal cellular functions. ROS accumulation in neurons and the resulting oxidative stress are responsible for the loss of cognitive and motor functions in several brain diseases.

Oxidative stress and chronic low grade inflammation are interdependent processes that have been implicated in aging and many pathological conditions like cardiovascular disease, neurodegenerative diseases or cancer. Inflammatory cells can release ROS at the site of inflammation increasing oxidative stress, while ROS can initiate intracellular signaling cascades that increase proinflammatory gene expression [47,578].

Chronic inflammation as a consequence of immune failure is often associated with cancer (known as inflammation-induced tumorigenesis). Hence, in different types of cancers, multiple pathways contribute to chronic cytokine release. Hyperinflammation combined with loss of adhesion and the release of angiogenic factors leads to cellular proliferation.

Here we will put forward some examples of how ROS and inflammation can regulate physiological or pathological conditions in different systems.

### 8.2. Dual actions of NOX2-derived ROS

As pointed out by Jamel El-Benna and Pham My-Chan Dang, the production of ROS by NOX2 is essential to mount a rapid response to bacterial and fungal invasion; however, excessive or inappropriate ROS production can induce severe tissue injury that participates in the pathophysiology of acute and chronic inflammatory diseases [579,580]. For several years, NOX2-derived ROS have been considered as pro-inflammatory agents, but recent reports challenged this dogma and suggested that they can also be anti-inflammatory [581].

Under physiological conditions, the objective of ROS production by phagocytes is to kill and eliminate pathogens trapped inside the phagosome [579]. When this goal is successfully achieved, ROS production is terminated and the inflammation is resolved. Thus, the physiological role of transient ROS production is anti-inflammatory as it helps to eliminate inflammation resulting from the infection. In addition to the "direct-ROS-killing effect" during phagocytosis, NOX2-derived ROS can have "paracrine-redox signaling effects" that can modulate the immune response. Indeed, NOX2-derived ROS can dampen T-cell-dependent inflammation through alteration of T-cell membrane oxidation status [582] and of Th17/Treg cell development [583]. The anti-inflammatory role of NOX2-derived ROS is well illustrated in chronic granulomatous disease (CGD) patients who have a genetic defect in one of the NOX2 genes (see Section 8.3). Thus, chronic NOX2 deficiency may cause "ROS-independent" inflammation where ROS are not the causative factor. This "ROS-independent" inflammation is also observed in autoimmune diseases as shown in animal models [581,582,584]. In the presence of high levels of pro-inflammatory mediators (cytokines, TLR agonists, lipid mediators…), NOX2 can be hyper-activated, leading to excessive and prolonged ROS production [583]. This high ROS production is undoubtedly deleterious, as evidenced by the multiple antioxidant strategies that have been developed by the organism to protect against ROS [585]. ROS, particularly the diffusible hydrogen peroxide, can oxidize cellular macromolecules (proteins, lipids, DNA), which leads to tissue injury or to the alteration of cellular functions such as imbalance of intracellular signaling pathways, cytokine production, protease activation and release [585], all of which participate in the "ROS-dependent inflammation." Indeed, inhibition of NOX2 and the use of certain antioxidants protect from inflammation in animal models [586].

### 8.3. Chronic Granulomatous Disease (CGD): implication of NOX2

According to Marie José Stasia, Joe Dan Dunn and Thierry Soldati, CGD is a rare inherited disorder in which phagocytic cells are unable to kill pathogens during an infection. The molecular basis of this disease is the absence of ROS production by the NADPH oxidase complex of phagocytes which is composed of NOX2 and p22phox, also named the membrane flavocytochrome b558, and the cytosolic factors p47phox, p67phox and p40phox. It is a genetically heterogeneous disease with all ethnic groups equally affected. The molecular basis of CGD is characterized by two types of transmission and four main genetic forms. As mentioned earlier, the major genetic form is X-linked CGD caused by mutations in the CYBB gene encoding NOX2. X-CGD accounts for about 70% of the total cases reported to date [587]. The other types of CGD are autosomal recessive forms (AR), characterized by mutations in CYBA, NCF1 and NCF2 encoding p22phox, p47phox and p67phox respectively [588]. Clear information on the severity of CGD according to the genetic forms is difficult to establish. However Kuhns et al. demonstrated a relationship between the presence of residual ROS production and the survival of CGD patients [589]. In addition, mutations affecting the membrane flavocytochrome b558 composed of p22phox and NOX2 seem to be associated with the most severe clinical features of CGD [590]. Indeed, cytochrome b558 is the redox core of the enzyme in which the electron transfer occurs to reduce the molecular oxygen into superoxide.

The soil-dwelling, social amoeba, *Dictyostelium discoideum* (thereafter *Dictyostelium*) is an ideal model organism to determine immunity functions of ROS and the consequences of ROS deficiency, i.e., CGD. *Dictyostelium* amoebae prey on bacteria using phagocytic machinery and intracellular killing mechanisms that are conserved in the immune phagocytes of metazoa, e.g., mammalian macrophages and neutrophils, and are utilized as a model phagocyte to study cell-autonomous immunity [591,592]. Among the conserved machinery are three NOX2 homologs of the NADPH oxidase catalytic subunit (NOX A, B and C), a $p22^{phox}$ homolog, a single, putative NOX-activating protein (NcfA, a homolog of $p67^{phox}$), a secreted myeloperoxidase-like enzyme (PoxA), and enzymes for metabolizing ROS such as superoxide dismutases and catalases [593,594]. *Dictyostelium* also has homologs of STATs, TRAFs, and guanylate-binding proteins, which are regulated by ROS in macrophages [594], and employs autophagy as a defense mechanism against cytosolic bacteria [595], which is activated downstream of ROS in macrophages.

*Dictyostelium* undergoes a developmental cycle during which 100,000 amoebae aggregate to form a multicellular slug that ultimately differentiates into a spore-containing fruiting body. ROS scavengers inhibit the initial aggregation of amoebae, and both NOX-deficient mutants and catalase deficient mutants exhibit defects in fruiting body formation [593,596,597]. The multicellular slug contains specialized sentinel cells (*s*-cells) that serve as its patrolling innate immune system [598]. Like neutrophils, S-cells extrude DNA-based extracellular traps (ETs) via a NOX-dependent mechanism: S-cells from NOX-deficient mutants lose the ability to secrete ETs and to clear bacteria from the slug and subsequent fruiting body [599]. Consequently *Dictyostelium*, on the cusp of multi-cellularity, can be used to model CGD and the influence of NOXs and ETs on the evolution of specialized immune cells and to study the role of ROS in a host-pathogen interaction [600].

CGD patients suffer from recurrent and life threatening infections during early childhood. Phagocytic cells from CGD patients adhere to blood vessels, reach infectious sites by chemotaxis and phagocytose the involved pathogens, but are unable to kill them because of the absence of ROS production by the defective NOX complex. Thus, accumulation of live pathogens in phagocytes, combined with the continuous release of proinflammatory cytokines by these cells, leads to the formation of granulomas in infected tissues. In addition, granuloma formation in hollow organs like the kidneys or the gastrointestinal tract is responsible for obstruction syndromes. Infections can be localized in tissues in direct contact with the environment like the skin, the otorhinolaryngology sphere or, more severely, the lungs. The disease has a more dramatic effect when infections and granulomas are in deep organs such as the brain or the liver. Aspergillosis in the lungs is the first cause of death of CGD patients. One seemingly paradoxical observation that needs to be addressed is: how does the absence of ROS lead to hyperinflammation in CGD? Several hypotheses have been proposed. The oldest one is that efferocytosis by macrophages is reduced in CGD [601]. The overall consequence will be unbalanced neutrophil necrosis, an increase of proteases and toxic oxygen-derived components and release of proinflammatory cytokines, which all contribute to local inflammation. In addition, the absence of ROS production can be responsible for defective activation of genes that regulate NFκB signaling, which is involved in the restriction of the development of inflammatory disorders [602]. Recently, it was shown that ROS deficiency in CGD causes autophagy dysfunction in phagocytes, which contributes to increased production of proinflammatory IL-1β. Indeed, two CGD patients treated with an IL-1 receptor blocker showed rapid and sustained improvement in colitis [603]. Furthermore, defective ATM activation due to the absence of ROS production in a CGD patient was linked to an exacerbation of proinflammatory cytokine release and

apoptosis, which might explain the hyperinflammation in this disease [604].

As components of the phagocytic NOX complex are expressed in cells and tissues other than phagocytes, inactivating mutations in these proteins can have pathophysiological consequences unrelated to immunodeficiency syndromes. ROS production by NOX enzymes controls vascular function via modulation of NO bioactivity. Indeed NOX2 deficiency in CGD patients was related to enhanced arterial dilatation [605]. Violi et al. demonstrated that in vivo platelet activation might be directly associated with NOX2 activity. Thus decreased platelet marker activation correlated with the absence of NOX2 expression found in CGD patients. As NOX2-deficient mice demonstrated impaired memory and synaptic deficit, a role of NOX2 in these processes was proposed [606]. However, clinical studies in children with CGD were rather ambiguous [607,608].

### 8.4. Neuromodulatory actions of nitric oxide

As summarized by J. Laranjinha and R.M. Barbosa, the brain is bioenergetically exigent and, to optimize neuronal function and survival it is equipped with fine mechanisms for a precise spatial and temporal control of cerebral blood flow (CBF) that provides energy substrates according to cellular activity. This process is achieved through neurovascular coupling, an orchestrated intercellular communication among all components of the neurovascular unit (neurons, astrocytes, perycites and microvessels) that results in a rapid and restricted increase in CBF [609]. Yet neuronal energetics is non-linearly coupled to an activity-dependent increase of CBF, i.e. neuronal activity-induced increases in CBF are not accompanied by proportionate increases in oxygen consumption by neuronal mitochondria [610]. Therefore, an activity-dependent CBF increase and oxygen utilization by active neural cells are inextricably linked and establish a functional metabolic axis in the brain termed the “neurovascular-neuroenergetic coupling axis.” This axis incorporates interdependent processes that need to be coordinated in the normal brain. An impaired functionality of the neurovascular-neuroenergetic coupling axis poses a threat to the healthy brain and can prove particularly detrimental for Alzheimer´s disease and the aged brain.

$^{\bullet}$NO, a diffusible intercellular messenger synthesized by the neuron-associated synthase isoform (nNOS), coordinates an integrated regulation of this axis by mediating the neurovascular coupling process and by regulating oxygen utilization by mitochondria. Two lines of reasoning support this hypothesis. The first is based on the in vivo dynamic and simultaneous recordings [611] of $^{\bullet}$NO, oxygen and CBF. It has been shown that upon glutamatergic stimulation of rodent hippocampus, $^{\bullet}$NO synthesized by nNOS associated with the glutamate NMDA receptor diffuses into neighboring vessels and induces an increase of CBF, which couples to neuronal activity by activating soluble guanylate cyclase in smooth muscle cells [612]. The transitory increases of $^{\bullet}$NO and CBF from a basal level are temporarily and spatially coupled with oxygen delivered from the vessels, encompassing a sequence of events consisting of glutamatergic neuronal stimulation, $^{\bullet}$NO transients, CBF increases and oxygen transients. According to the second line of reasoning, the best characterized interaction of $^{\bullet}$NO with the mitochondria is the inhibition of cytochrome *c* oxidase by nanomolar concentrations of $^{\bullet}$NO in competition with oxygen [613]. At physiological oxygen concentrations, NMDA-evoked $^{\bullet}$NO production inhibits hippocampal oxygen consumption at submicromolar concentrations and induces a small difference in the concentration dynamics of $^{\bullet}$NO, reflecting that different states of neuronal activation may lead to different outcomes in terms of metabolic rate [614,615].

### 8.5. Thiol redox homeostasis in astrocytes

According to Gethin J. McBean, several decades of research have led to the conclusion that astrocytes, the so-called ‘metabolic support’ cells of the brain, act as the central supplier of glutathione (γ-glutamyl-cysteinyl-glycine, GSH) for antioxidant protection of neurons. *De novo* synthesis of GSH in astrocytes fulfills the antioxidant capacity of those cells and also provides precursors for GSH synthesis in neurons [616]. Cysteine is the rate-limiting substrate for GSH synthesis and is supplied either by transport from the extracellular medium in the form of cystine into astrocytes using the $x_c^-$ exchanger, or directly into neurons as cysteine via the EAAT3 subtype of the high-affinity glutamate trans-

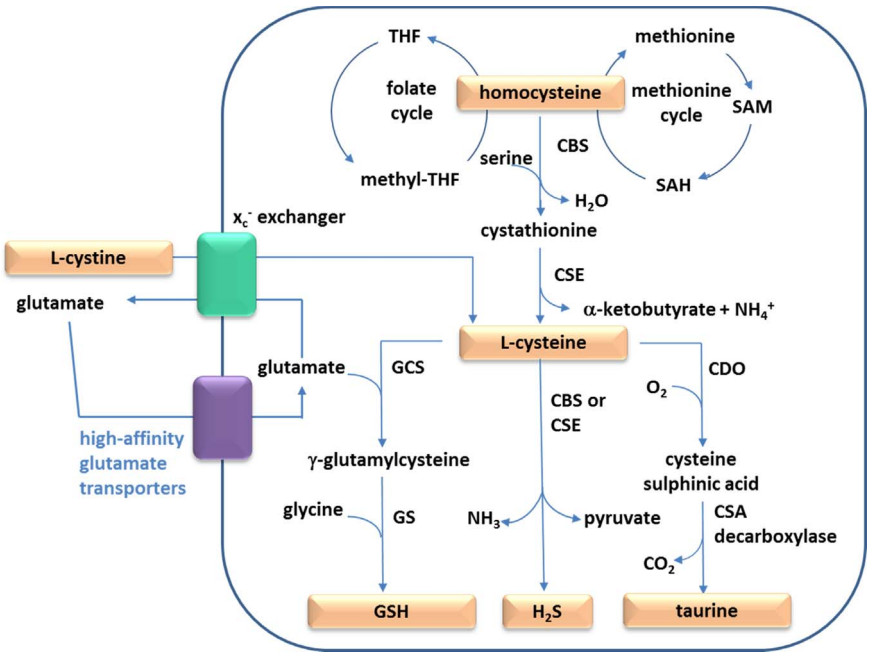


**Fig. 8.1.** Cysteine supply pathways in astrocytes. Cysteine is either taken up in its oxidized form, cystine, from the extracellular medium via the $x_c^-$ cystine-glutamate exchanger, or generated from methionine via the transsulfuration pathway. Cysteine is the immediate precursor for GSH, which is synthesized by the first two enzymes of the γ-glutamyl cycle, as well as taurine and hydrogen sulpfide. CBS, cystathionine-β-synthase; CDO, cysteine dioxygenase; CSA, cysteine sulfinic acid; CSE, cystathionine-γ-lyase; GCS, glutamate cysteine ligase; GS, glutathione synthase; SAH, *S*-adenosylhomocysteine; SAM, *S*-adenosylmethionine.

porter. As the extracellular redox potential dictates a 5:1 ratio of cystine to cysteine, the bulk of uptake takes place into astrocytes. In addition to the $x_c^-$ cystine-glutamate exchanger, cysteine can also be supplied by transsulfuration (TS) from methionine via homocysteine, as shown in Fig. 8.1. In normal astrocytes, the TS pathway supplies up to one third of the cysteine required for GSH, with the majority coming from the extracellular space [577,617].

It is well documented that GSH production in astrocytes is increased in response to oxidative stress. Similarly, upregulation of both the $x_c^-$ exchanger and the TS pathway (via increased expression of the rate-limiting enzyme, cystathionine-γ-lyase (also known as cystathionase; CSE)) occurs following oxidative stress [617,618]. Interestingly, experimentally-induced oxidative stress in primary rat cortical astrocytes shows that the relative contribution of the TS pathway to cysteine for GSH increases to 60%, meaning that, under these conditions, the majority of cysteine for GSH comes from this pathway, rather than the $x_c^-$ exchanger [577]. Pharmacological blockade of the $x_c^-$ cystine-glutamate exchanger in vitro also acts as a signal to upregulate CSE, leading to enhanced synthesis of GSH [577]. It is not clear at present whether the signal to increase flux through the TS pathway occurs in response to a fall in GSH within astrocytes, or to increased oxidative stress, or both. It has been proposed that upregulation of cystine intake under oxidative stress conditions is decoupled from GSH synthesis and, instead, regulates an intracellular-extracellular cysteine-cystine redox cycle [619]. This proposal fits with our results showing that GSH synthesis under oxidative stress conditions increases reliance on the TS pathway. However, further work is required to fully evaluate the interrelationship between these sources of cysteine for GSH, and other important neuroprotective products, for example, taurine and hydrogen sulfide.

Understanding the origin of cysteine for GSH is important for evaluation of the antioxidant capacity of cells in neurodegenerative disease. There are several examples in the literature of up-regulation of the $x_c^-$cystine-glutamate exchanger during neurodegenerative disease [620,621]. Indeed, at first glance, it would appear that the capacity to increase GSH synthesis during neurodegenerative disease-related oxidative stress would be beneficial. However, the downside is that increased capacity of the $x_c^-$cystine-glutamate exchanger is inevitably coupled to the release of glutamate. If this cannot be matched by high-affinity uptake, then the likelihood of glutamate-mediated neurotoxicity threatens neuronal well-being. This situation is well illustrated in the case of glioma/astrocytoma. Here, tumor cells up-regulate the $x_c^-$cystine-glutamate exchanger, but down-regulate the high-affinity glutamate transporters [622]. This imbalance generates the capacity for destruction of neurons and increases the likelihood of epileptiform activity. However, strategies to block the $x_c^-$ exchanger in glioma therapy have been unsuccessful. It is now recognized that drugs that target both the $x_c^-$ exchanger and the TS pathway have greater potential as effective therapeutics [623]. Research is ongoing to fully understand the beneficial potential of the TS pathway in astrocytes, particularly in the context of astrocyte activation and the immune response.

### 8.6. Regulation of the oxidative and inflammatory response by microglial α7 cholinergic receptors

As reported by Manuela G Lopez and Javier Egea, dysfunction of the cholinergic system and mitochondria together with increased oxidative stress and neuroinflammation has been reported during aging and diseases related to age like Alzheimer´s and Parkinson´s disease [624,625]. The α7 acetylcholine nicotinic receptor subtype (α7nAChR) is expressed in neuronal and non-neuronal cells. Wang et al. [626] identified that α7 nAChRs in blood monocytes control inflammation under vagal stimulation and proposed the “cholinergic anti-inflammatory pathway,” which regulates inflammation in the periphery. In the central nervous system, microglia regulate the innate immune response and also express α7 nAChRs; therefore, the role of these receptors in microglial function is being studied.

Primary glial cultures exposed to the α7 nicotinic agonist PNU282987 increased their mitochondrial mass and mitochondrial oxygen consumption without generating oxidative stress. These changes were not seen when the transcriptional factor NRF2 was absent, when the HO-1 enzyme was inhibited and when PGC-1α was silenced. In isolated microglia of adult animals treated with the α7nAChR agonist, a significant increase in mitochondrial mass was also detected. Interestingly, LysMcre-Hmox1$^{\Delta/\Delta}$ animals, which lack HO-1 in microglial cells, and *PGC-1α*$^{-/-}$ animals, which do not express PGC-1α protein, showed lower microglial mitochondrial levels, and treatment with PNU282987 did not change the mitochondrial levels. These results indicate the important function of the α7nAChR/NRF2/HO1 and PGC-1α axis to increase mitochondrial biogenesis and thereby improve the bioenergetic status in microglia [627].

The α7 microglial nicotinic receptor also plays a strategic role in controlling neuroinflammation to afford neuroprotection under brain ischemia conditions as shown in in vitro and in vivo models. Organotypic hippocampal cultures (OHC) exposed to oxygen and glucose deprivation (OGD) elicited cell death. However, the selective α7nAChR agonist PNU282987 incubated post-OGD, reduced cell death, ROS production and TNF-α release. The protective effect of PNU282987 was lost in microglia-depleted OHCs as well as in OHCs from *Nrf2* deficient mice. Administration of the α7nAChR agonist 1 h after induction of photothrombotic stroke in vivo reduced infarct size and improved motor skills in *Hmox1*$^{lox/lox}$ mice that express normal levels of HO-1, but not in *LysMCreHmox1*$^{\Delta/\Delta}$ in which HO-1 expression is inhibited in myeloid cells, including the microglia [628]. These results show that α7 microglial nicotinic receptors play a key role in controlling neuroinflammation and affording neuroprotection under brain ischemia.

Therefore, microglial activation of the α7 nAChR/NRF2/HO-1 axis seems to play an important role in improving microglial bioenergetics and reducing oxidative stress and neuroinflammation [629].

### 8.7. Regulatory mechanisms of ROS in the motor neuron

According to Anastasia Shakirzyanova and Rashid Giniatullin ROS can also regulate neurotransmission at the neuromuscular junction. Curiously, the actions of ROS are remarkably different in the synapses of newborns, adults and old rats [630]. Thus, it has been reported that the inhibitory effect of the diffusible mild oxidant $H_2O_2$ is much stronger in old rats. In newborns tested during the whole first postnatal week, $H_2O_2$ did not affect spontaneous transmitter release from nerve endings and even potentiated the end-plate potentials. The resistance of neonates to $H_2O_2$ inhibition was associated with higher catalase and glutathione peroxidase activities in skeletal muscle. In contrast, the activities of these enzymes were downregulated in old rats. These results indicate that the vulnerability of transmitter release to oxidative damage strongly correlates with aging and might be used as an early indicator of senescence [630]. Consistent with this, it was shown that the concentration of the redox active amino acid homocysteine increases with aging and in many neurodegenerative diseases significantly aggravates ROS-induced depression of transmitter release from motor nerve terminals. This provides a potential mechanism of peripheral impairment in motor neuron diseases associated with hyperhomocysteinemia [631]. Related to this, is has been reported that the co-transmitter ATP, which operates via a ROS-dependent mechanism, activates presynaptic P2Y12 receptors coupled to NOX to generate endogenous ROS and that this signaling complex likely resides in lipid rafts [632].

The association between ROS and motor neuron disease is exemplified in the case of amyotrophic lateral sclerosis (ALS), a neurodegenerative disease characterized by a progressive loss of motor neurons and degradation of the neuromuscular junctions. In ALS, the decline in synaptic function initiates from the presynaptic terminals. Experimental

data have shown that in the neuromuscular junction, a classical model of synaptic transmission, ROS have an inhibitory action on the presynaptic releasing machinery, and it was proposed that the presynaptic sensor of ROS was the SNARE protein Snap25 [633].

### 8.8. Inflammation and ROS in cancer

As explained by Kemal Sami Korkmaz and Bilge Debelec–Butuner, chronic inflammation subsequent to immune failure or insults such as microbial infections is often associated with cancer. The well-known examples come from *Helicobacter pylori* and human papillomavirus infections in stomach and cervix cancers respectively, where multiple pathways synergistically contribute to the activation of cytokine release, that combined with the loss of adhesion and the release of angiogenic factors, may eventually contribute to cellular proliferation, differentiation and tumor progression [634]. Thus, the immune defense mechanisms that play important roles in guarding the organism against environmental insults, might induce malignant growth in these tissues. This event is termed inflammation-induced tumorigenesis.

Toll like receptor (TLR) function is critical for regulation of innate and adaptive immune responses in normal cells and usually necessitates distinguishing the defective functionality of the malignant cells that might influence the sensory ability of the immune defense. Since activation of the pro-survival factors such as NF-κB, ERK and JNK kinases as well as increased levels of IL-6 and IL-12 correlate with highly expressed TLR4 levels in malignant cells [635], these findings indicate the important role of TLRs in chronic inflammation and cancer development.

Interestingly, TLR4 has been associated with metastasis in various types of cancer including the prostate. Highly metastatic human prostate cancer cell lines, PC-3 and DU145, express higher levels of TLR4 [636] compared to RWPE and LNCaP prostate cell lines [634,637,638]. When these cells are treated in vitro with LPS, TNFα is induced, reaching nM concentrations, and proliferation and migration of prostate cancer cells is observed [637,638]. Consistently, the depletion of TLR4 expression inhibits the invasion of these cells and also improves the survival of tumor-bearing animals [636,639], which suggests that the higher TLR4 level or its activation significantly augments tumor cell proliferation upon cytokine exposure. Thus, TLR4 expressed in normal and low-grade tumors could be a contributing factor to chronic inflammation that promotes carcinogenesis.

Nevertheless, the well-known prostate specific and androgen receptor (AR) regulated tumor suppressor NKX3.1 encodes a homeobox protein and facilitates the antioxidant response through transcriptionally upregulating the glutathione peroxidases and peroxiredoxins [640], which leads to subsequent deregulation of the intracellular ROS levels and activation of the DNA damage response.

In addition, the growth rate is metabolically regulated via stress-sensing Sirtuin 1 (SIRT1), an NAD-dependent deacetylase. Under oxidative conditions, such as inflammation, SIRT1 deacetylates a number of transcription factors, including p53, NBS1 and AR, which contribute to the control of the cell cycle, DNA damage response and steroid hormone action in prostate cells respectively. Therefore, SIRT1 has also been linked to tumor cell survival, particularly in prostate cancer, by the deacetylation of AR. Thus, the inflammation induced via TLR4-related cellular mechanisms contributes to the deregulation of the antioxidant response and DNA damage recognition in prostate, where the increased genetic heterogeneity is suppressed via AR, and its deacetylation by activated SIRT1 counteracts the deregulation of cell growth leading to stress tolerance in tumor progression.

### 8.9. Summary and conclusions

In this section we have seen some examples of how ROS formation has regulatory mechanisms that can be implicated in health and disease. ROS formed from NOX, mitochondria, or NO-producing enzymes are not necessarily toxic, but rather compose a network signaling system, known as redox regulation.

In the case of NOX2, we have seen that under physiological conditions ROS production derived from NOX2 may have an anti-inflammatory role when produced in a limited time and space, while a defect in NOX2 can lead to "ROS-independent inflammation." However, when they are overproduced, they become pro-inflammatory as they induce oxidative stress and changes in cell homeostasis during a "ROS-dependent inflammation." While the use of NOX2-deficient mice has advanced our knowledge on the role of NOX2, it is probably not the best approach to determine whether the absence of NOX2 is protective against inflammation, as the deletion of NOX2 inherently leads to a dysregulation of the immune response. A clear example of a human disease related to defects in NOX2 or associated subunits is chronic granulomatous disease [641]; as a consequence of NOX2 deficiency, neutrophil killing is defective due to the extremely low respiratory burst in these cells during phagocytosis [642,643].

ROS generated by NOX enzymes can control vascular function via modulation of NO bioactivity [644]. In the brain, NO can exert a modulatory role both in the neurovascular coupling and in the functionality of energy formation by the mitochondrial respiratory chain. Therefore, neuronal-derived NO can be considered a master regulator of the neurovascular-neuroenergetic coupling axis. Furthermore, dysfunction of the NO-dependent neurovascular and neuroenergetic coupling has been related to the cognitive decline associated with brain aging and Alzheimer´s disease [576].

Besides the regulatory mechanism of neuronal NO, glial cells also play an active role in maintaining the redox balance in the brain. In line with this, astrocytes act as the central supplier of GSH for antioxidant protection of neurons. Cysteine is required to produce GSH in order to control the antioxidant capacity of cells in neurodegenerative disease; therefore, it is now recognized that drugs that target both the $x_c^-$ exchanger and the TS pathway have greater potential as effective therapeutics [623]. On the other hand, in microglial cells, cholinergic stimulation of the α7 nicotinic receptor subtype is being recognized as a target to control neuroinflammation and oxidative stress by inducing hemoxygenase-1 to provide neuroprotection [628].

Homocysteine (HCY) is a pro-inflammatory sulfur-containing redox active endogenous amino acid, whose concentration increases in neurodegenerative disorders including ALS. At the neuromuscular junction, the effect of HCY on oxidative stress-induced impairment of transmitter release was shown to be age-dependent [631]; older rats were more sensitive to the inhibitory effect of $H_2O_2$ than newborns, most probably because the latter have higher levels of antioxidant enzymes. Furthermore, activation of P2Y12 receptors by ATP, which is co-released with ACh at the neuromuscular junction, can induce ROS production by activating NADPH oxidase [632] and thereby control neurotransmission.

Finally, inflammation and oxidative stress can participate in cancer. Activation of pro-inflammatory cascades via TLR4 has been related to highly metastatic tumors [636]. On the other hand, ROS production via NOX2 can regulate inflammation [645]. In line with these observations, it has been reported that NOX activity and expression is associated with tumorigenesis of lung cancer, and that inhibition of NOX function or mRNA expression can significantly block lung cancer formation and invasion [646].

In conclusion, ROS play a Janus-faced role: they can provide physiological actions or contribute to pathogenesis. We have seen in this review that the regulatory actions of ROS are complex and can differ from one cell system to another. Therefore, understanding the fine regulatory mechanisms of ROS in specific cells and tissues will contribute to the identification of precise targets and thus to the development of more efficient therapeutic strategies.

## 9. The emerging roles of redox networks in tumor cell proliferation, hearing loss, neuropsychiatric disorders and cardiovascular pharmacology

Isabel Fabregat (E-mail: ifabregat@idibell.cat) and Santiago Lamas (E-mail: slamas@cbm.csic.es).

### 9.1. Introduction

Our COST Action has invested a significant amount of work and interaction on major biomedical and clinical problems in which ROS have an established role or where significant evidence has been mounted for their participation in the initiation, perpetuation or resolution of the most pressing health challenges in the developed world in the next decade. The focus of this section are the ideas, expertise and studies of the members of the EU-ROS COST Action.

We have grouped the contributions in this sub-section into four major categories: cancer, metabolic diseases, neuropathology and cardiovascular diseases. A summary of these is depicted in Fig. 9.1.

A fundamental problem in cancer biology has to do with the migration of tumor cells to extraneous tissue environments where they may constitute the core of metastatic niches. The role of oxidative stress germane to this phenomenon is far from clear and remains controversial. For example, it has been found that melanoma metastasis may progress by suppressing redox-related effector molecules such as APE1/REF-1 [647] and making melanoma cells less responsive to oxidative-induced DNA damage. In contrast, it has been also reported that oxidative stress may inhibit distant melanoma metastasis in vivo [648]. In a similar vein, the targeting of fundamental endogenous antioxidant systems, such as GSH and thioredoxins, has been proposed as a potential advantageous therapy for cancer and HIV [649]. A more detailed analysis on the molecular mechanisms related to redox responses in the context of cancer cell migration is provided below. Of interest, the cellular and molecular sources responsible for ROS generation have been the object of intense study in pathophysiological settings such as liver fibrosis and carcinogenesis. Here too, the jury is still out regarding the beneficial or detrimental role of NOXs, especially in reference to the apparently opposite effects of NOX1 and NOX4 in liver tumorigenesis, as discussed in the following paragraphs.

The Action has benefited from the work of groups interested in the redox regulation of neurological and psychiatric diseases with a specific emphasis on two relatively unexplored areas: the inner ear and schizophrenia. Of all the NOX isoforms, NOX3 is clearly the most elusive, less studied and even less well understood, primarily due to its restricted topological expression in the inner ear. One of the laboratories involved in this COST action has shed light on the function of NOX3 in balance regulation and hearing function by developing sophisticated mouse models that lend themselves to investigation of this issue. The problem of hearing loss, either genetically based or acquired after environmental exposure to noise or aging, has experienced a recent twist where redox regulation has taken center stage. Indeed, a very captivating report has described that pejvakin, a protein related to peroxisomal function and proliferation, lies at the basis of an inherited sensorineural form of deafness and its lack or malfunction induced by oxidative stress makes the inner ear extremely vulnerable to noise-induced damage [650]. NOX3 is expressed in the cochlea even though mice devoid of it do not show an apparent hearing loss-related phenotype. Whether peroxisomal generation of ROS is connected to NOX3 function is a possibility that remains to be investigated. Another set of diseases where the role of redox regulation is intriguing is in the realm of neuropsychiatry. While a significant amount of evidence regarding the role of oxidative stress has accumulated in neurodegenerative diseases (please see the corresponding section), much less is known in the context of psychoses. In the particular case of schizophrenia, aside from profound alterations in the levels of several neurotransmitters, a disturbed redox homeostasis has been evidenced with a major focus on glutathione regulation. These intriguing findings are discussed below highlighting the major advances and pitfalls in the knowledge of this exciting research avenue.

There is currently little doubt about the relevant role played by oxidative stress in the metabolic syndrome and in particular in type 2 diabetes. Both insulin production, as well as insulin signaling, are redox sensitive processes, highly determined by the levels of $O_2^{\bullet-}$ and $^{\bullet}NO$, and their interplay. Thus, impairment of physiological signaling by ROS/RNS is implicated in the etiopathology of diabetes [651]. Some groups in our COST Action are interested in exploring how the fine tuning of the $O_2^{\bullet-}/^{\bullet}NO$ ratio is regulated and how it affects insulin synthesis and degradation. Furthermore, oxidative stress contributes to pancreatic β

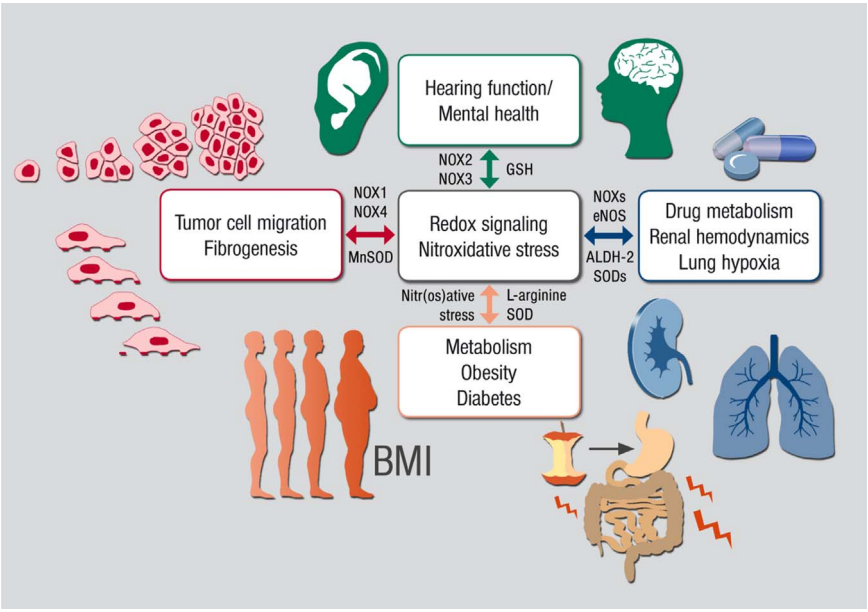


**Fig. 9.1.** Summarizing scheme on the contribution of ROS signaling to different physiological and pathophysiological conditions. This section covers an ample spectrum of disorders with the theme of redox signaling and nitroxidative stress as the common modulator of disturbances related to tumor cell migration, fibrogenesis, hearing loss, neuropsychiatric disorders, metabolic syndrome, drug metabolism, renal hemodynamics and lung hypoxia. In the slide the participation of relevant enzymatic pathways (NOXs, SODs, ALDH-2) are indicated. BMI: body mass index. The rest of the abbreviations are defined in the text.

cell loss, which impairs insulin secretion [652]. Therefore, therapeutic strategies to prevent β cell dysfunction require better knowledge about how to protect them against direct or indirect effects of free radicals and lipid peroxidation. Also relevant is the fact that both insulin sensitivity and metabolic homeostasis depend on the capacity of adipose tissue to take up and utilize excess glucose and fatty acids. This buffering capacity depends on physiological levels of $^{\bullet}NO$, whose function may be altered by excessive formation of $O_2^{\bullet-}$ [653]. Interestingly, recent evidences indicate that redox signaling and oxidative stress may contribute to adipose tissue remodeling and this is a relevant area of research. These new aspects about the relevance of ROS and RNS in the context of metabolic syndromes and diabetes are expanded below highlighting the major challenges addressed by research members within the EU-ROS COST Action.

Cardiovascular physiology and pathophysiology have also been a major object of this COST Action and this is reflected in the present section of this overview. In this section we also include contributions of the COST members related to vascular aspects with a specific focus. One of these is the still unresolved and important problem of toxicity and tolerance derived from the clinical use of organic nitrates. In the last few years new light has been shed upon the molecular mechanisms related to the side effects of nitroglycerin and other nitrates evidencing a major role for mitochondrial dysfunction and disruption of redox homeostasis. A detailed update of the problem is provided in the section that follows. A disturbed vascular redox balance underlies the pathophysiology of important morbid conditions in other organs such as the lung and kidney. In the lung, chronic hypoxic pulmonary hypertension leads to vasoconstriction and vascular remodeling, two phenomena that self-perpetuate the vicious cycle. In the kidney, studies in animals using superoxide dismutase (SOD) mimetics point to an important role of redox dysfunction in the increased vascular resistance associated with chronic kidney disease and open the possibility of therapeutic intervention. Both sets of concepts and data are appropriately discussed below.

### 9.2. Cancer

The following subsections were composed by Esther Bertrán, Isabel Fabregat, Ana Fernandes, and Nuno Saraiva.

#### 9.2.1. Redox regulation of tumor cell migration

Several cellular and extracellular events are involved in ROS production and can directly or indirectly impact on mechanisms involved in different types of cell migration thus contributing to the invasiveness and poor prognosis of several cancers. These mechanisms include invadopodia formation, MMP activation/expression, focal adhesion dynamics, cell-cell contact, cytoskeleton remodeling, and gene expression regulation (Fig. 9.2) [654–656]. In turn, many mechanisms involved in cell migration, such as integrin signaling or $Ca^{2+}$ homeostasis affect ROS production, creating intricate and still poorly understood regulatory mechanisms [656,657]. ROS can act as second-messengers by oxidizing cysteine residues that impose functional changes on cell migration-relevant kinases, phosphatases and transcription factors [658]. The uneven physical and temporal distribution/activity of the elements involved in ROS production (Fig. 9.2) can lead to heterogeneous ROS accumulation within a migrating cell and during the migration process. Several sources may contribute to the generation of ROS (see figure). Their topological distribution influences the localization and oxidative status of many regulatory elements, thus allowing a redox-dependent spatial and temporal regulation of cell migration/adhesion mechanisms. Mitochondrial ROS are associated with the initial ECM contact while a cytosolic ROS increase is involved

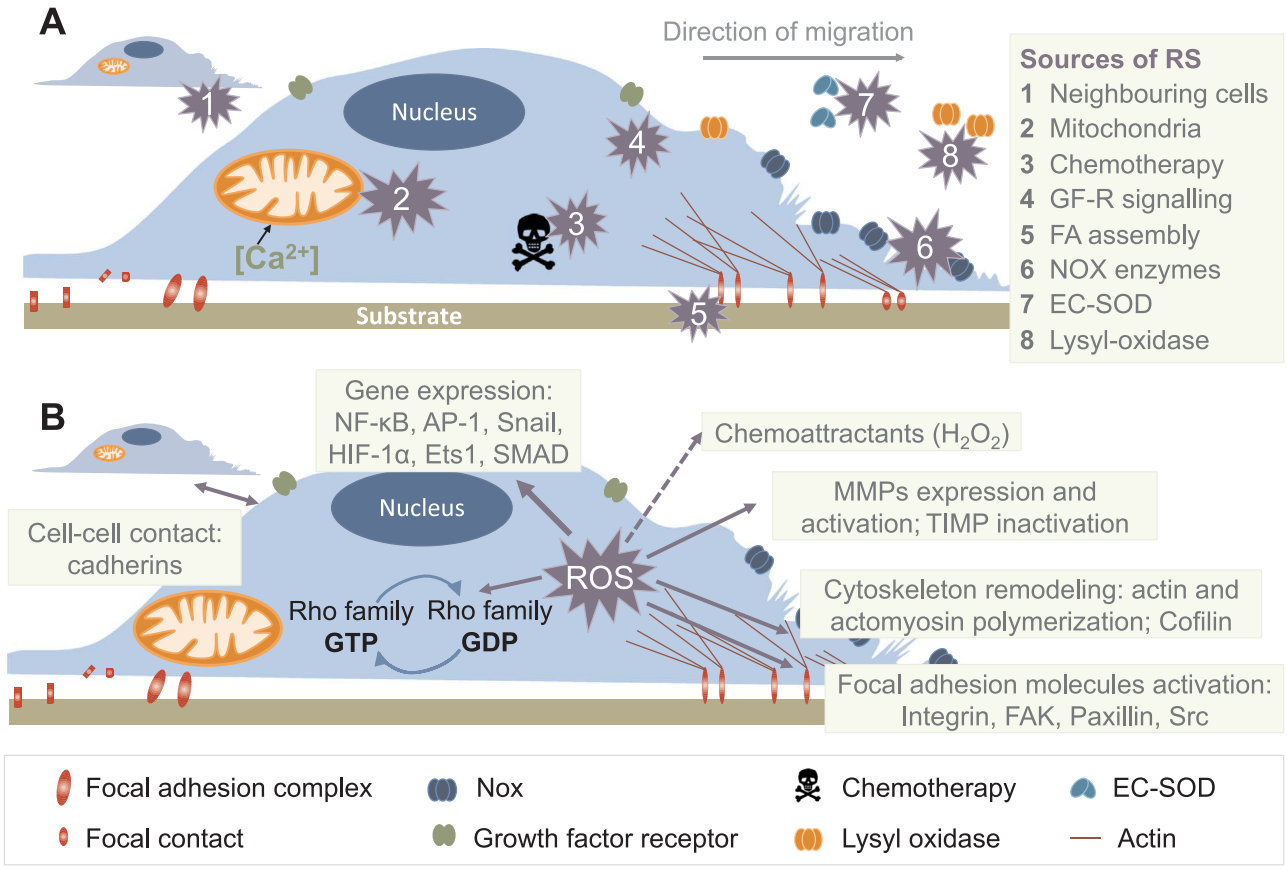


**Fig. 9.2.** ROS and cell migration. (**A**) There are several sources of reactive species (RS) whose subcellular distribution dictates the fate and direction of cell migration. In this cartoon they are indicated by Arabic numbers. (**B**) Key mechanisms involved in the redox-regulation of cell migration. The main effectors participating in cell-cell contact adhesion, gene expression activation, matrix degradation, cytoskeletal remodeling and focal adhesion are indicated.

in cytoskeleton remodeling and NOX-derived ROS are involved in invadopodia formation [186]. Additionally, the existence of an elevated reductive potential as well as strong redox buffers is essential to limit ROS diffusion and maintain a polarized distribution of oxidant intermediates [657]. The final outcome in cell proliferation, migration and adhesion depends on the activation of a series of effectors regulating gene expression, matrix degradation, cytoskeletal remodeling and cell-cell contact adhesion (see figure).

The complexity of mechanisms by which ROS mediate cancer cell migration is still far from being understood. A general pattern of the impact of ROS and antioxidants on tumor metastatic potential is difficult to depict given the inherent differences among cancer types. For example, MnSOD expression may be highly dependent on the primary tissue [659]. Even considering tumors from the same organ of origin, the stage and grade of disease progression may influence intracellular ROS and antioxidant enzyme levels. Most of the previous studies on the influence of ROS in cell migration were performed in cell culture models. However, the activity of antioxidant enzymes varies with the culture conditions and declines after a high number of cell passages. Another aspect that limits the usefulness of cell culture models is their inability to recreate the tumor microenvironment, which includes cancer cells, cancer stem cells and stromal components, such as extracellular matrix, fibroblasts, immune cells, adipocytes, and vascular cells. The analysis of specific subsets of tumor cells is both essential and challenging, since tumors contain different cell types, necrotic material and stroma. Differences between conventional cell culture models and the metastatic microenvironment contribute to the discrepancies observed in the literature, reinforcing the need for more physiologically relevant approaches.

The implementation and standardization of in vivo techniques to measure the levels of specific ROS and their sub-cellular distribution is essential to dissect and confirm several mechanisms by which ROS impact cancer cell migration.

#### 9.2.2. Role of NADPH oxidases in fibrogenesis and cancer

The oxidative stress that takes place during chronic liver diseases is due to increased ROS production, as well as to decreased activity of antioxidant systems. It is not only a consequence of chronic liver injury, but also a significant contributor to excessive tissue remodeling and fibrogenesis. The main source of ROS implicated in liver fibrosis is the NOX family of proteins [523,660]. NOX proteins are also likely to act as a persistent, endogenous source of ROS during Hepatitis C virus (HCV)-induced pathogenesis [661]. These enzymes are expressed in diverse cells and tissues, and their products are essential in several physiological settings [662]. NOX1, NOX2 and NOX4 have been proposed to play essential roles in liver fibrogenesis. Transforming growth factor-beta (TGF-β)-induced activation of hepatic stellate cells (HSC) to myofibroblasts (MFB) is mediated by NOX4-derived ROS [184]. Moreover, NOX1, activated either by TGF-β or other stimuli, promotes myofibroblast proliferation by PTEN inactivation to positively regulate an AKT/FOXO4/p27 signaling pathway [663]. Furthermore, NOX1 activity might further contribute to the inflammatory process that promotes COX-2 expression and prostaglandin synthesis in hepatocytes [664]. Promotion of hepatocyte apoptosis is another crucial event during fibrogenesis since it triggers Kupffer cell and HSC activation by secreting cytokines, chemokines and microparticles. NOX4 is necessary to mediate apoptosis induced by TGF-β [177,184]. However, the pro-apoptotic effect of the cytokine can be attenuated when NOX1 is active [179]. NOX2 is expressed in both endogenous liver cells and bone marrow-derived cells, possibly acting in the process of phagocytosis of dead hepatocytes [665]. The role of NOX in hepatocarcinogenesis is more complex and is still a matter of study in different laboratories. NOX4 may play essential roles mediating TGF-β tumor suppressor functions, in particular its effects on cell death [177,528]. In this sense, recent results indicate that silencing NOX4 in liver tumor cells increases their proliferative and tumorigenic properties [185]. In contrast, NOX1 might control autocrine cell growth of liver tumor cells through regulation of the EGFR pathway [179,666]. In fact, recent studies indicate that NOX1 and NOX4 proteins have opposite prognostic effects in HCC. High NOX1 and low NOX4 expression were independent predictors of both shorter recurrence-free survival and shorter overall survival [667]. In view of the essential roles played by NOX4 in liver fibrosis, recent preclinical studies with a NOX4/1 inhibitor (GKT137831) have demonstrated its efficiency as a potent inhibitor of fibrosis and hepatocyte apoptosis [668], thus paving the way for future translational studies.

### 9.3. Neurological and psychiatric disorders

The following subsections were composed by Vincent Jaquet, Karl-Heinz Krause, Francis Rousset, and Tamara Seredenin.

#### 9.3.1. Redox imbalance in the pathogenesis of schizophrenia

The etiology of schizophrenia is unknown, but it is generally thought that a combination of genetic and environmental factors modulates the disease. A popular theory of schizophrenia involves an imbalance between inhibitory and excitatory neurotransmission. This is evidenced at the neuropathological level by a decrease in number of parvalbumin-positive GABAergic interneurons (PV neurons) and alterations of *N*-methyl-D-aspartate (NMDA) receptor subunits [669]. The molecular mechanisms involved at onset, during psychotic episodes and chronicity of schizophrenia are unknown, but numerous studies in both humans and rodents point towards a contribution of neuroinflammation, increased reactive oxygen species (ROS) generation and dysfunction of redox signaling [670,671].

Most studies using post-mortem analysis of brains of schizophrenic patients indicate (i) increased markers of oxidative modifications of biomolecules, including lipids (4HNE), nucleic acids (8-hydroxydeoxyguanosine) and proteins (carbonylation); (ii) decreased levels of glutathione and enzymes involved in glutathione metabolism, (iii) microgliosis and astrogliosis and increase of microglia activation markers. Rodent models of social isolation and administration of NMDA receptor antagonists recapitulate several neuropathological features (loss of PV neurons and pro-oxidative phenotypes). Several studies have proposed a key role of specific redox systems in the pathogenesis of diseases of the central nervous system (CNS). Low glutathione (GSH) levels are a hallmark of schizophrenia [672]. GSH is a major regulator of intracellular redox homeostasis. Schizophrenic patients show low levels of GSH in blood and in prefrontal cortex, and mice deficient in the Glutamate-Cysteine Ligase gene, the rate-limiting enzyme for GSH synthesis, display behavioral and neurochemical abnormalities commonly associated with schizophrenia [673]. Clinical trials using the general antioxidant agent *N*-acetylcysteine (which can act as a GSH precursor) show promise for treating some features of schizophrenia. Behrens et al. observed an increase in NOX2 activity in neurons following repeated administration of subanesthetic doses of the NMDA receptor antagonist ketamine [674]. Importantly, ketamine administration led to the loss of PV neurons, which could be pharmacologically reversed by administration of the antioxidant apocynin. The efficacy of apocynin was further confirmed in another study using a transgenic model of NMDA receptor hypofunction (Ppp1r2-Cre/fGluN1 knockout mice), which endured social isolation. However, the increase of neuronal oxidation was not changed in NOX2-deficient mice, suggesting that NOX2 is not the main source of ROS in this model [675]. Interestingly PGC-1α – a key regulator of mitochondrial biogenesis and antioxidant response – is enriched in GABAergic interneurons [676]. In this social isolation model, PGC-1α downregulation correlates with increased oxidation in PV interneurons, suggesting a role for mitochondrial ROS [675]. Other studies failed to detect NOX2 in mature neurons, but showed that NOX2 is mainly expressed in microglia and adult neural stem cells in the CNS [677,678]. Microglia are the CNS cell type that expresses the highest levels of proteins

regulating redox dynamics suggesting a prominent role in the CNS redox balance [679]. Further studies assessing microglial perturbations in psychiatric diseases may highlight how redox genes are involved in modulating neuronal activity by pruning synapses and regulating neurogenesis. Altogether, there are strong arguments for redox imbalance in schizophrenia; however, the sources of ROS, redox kinetics, contribution of specific redox pathways and the cell types implicated require further studies.

#### 9.3.2. Role of NOX3 in inner ear pathologies

Research over the last decades has identified a major role for ROS in hearing disorders, including overexposure to noise, ototoxic drugs (e.g. cisplatin) and age-related hearing loss [680]. While the sources of ROS are complex and only partially understood (e.g. mitochondria), there is increasing evidence that activation of NOX enzymes, in particular NOX3, plays a key role in hearing loss. High level and specific expression in the inner ear identifies NOX3 as a prime drug target to combat hearing loss [681]. NOX3 is a multi-subunit NADPH oxidase, functionally and structurally closely related to NOX1 and NOX2. NOX3 is active as a multiprotein complex including the membrane-bound NOX3 and p22phox and the cytosolic subunits NOXO1 and NOXA1. NOX3 is crucial for the formation of otoconia, small proteinaceous carbonate crystals involved in balance [682]. Mice carrying a loss of function mutation within the NOX3 complex – including the common NOX1 to NOX4 subunit $p22^{phox}$, or the cytosolic subunit NOXO1 – have a vestibular phenotype similar to NOX3 mutant mice (referred to as head-tilt mice). However, the role of NOXA1 is less clear and has mostly been addressed in vitro. So far, the physiological relevance of NOX3 expression in the cochlea remains unclear as no hearing phenotype was described for NOX3 loss of function mutant animals. The role of NOX3 in cisplatin induced hearing loss is actually the best documented. An agonist effect of the antineoplastic drug cisplatin on the NADPH oxidase activity of NOX3 was observed in vitro, suggesting a potential role of NOX3 in cochlear damage [683]. Moreover, an increased NOX3 mRNA level has been described in the cochlea of cisplatin treated rats while siRNA against NOX3 were able to prevent cisplatin-mediated hearing loss in this model [684]. Together, it is now accepted that NOX3 is a major source of ROS in the cochlea. However, the role of NOX3 may not be limited to cisplatin-induced ototoxicity. Indeed, oxidative stress is also a major component in other hearing pathologies such as presbycusis, Meniere's disease or noise-induced hearing loss. For these conditions, further experimental confirmation and a deeper confirmation and understanding of the role of NOX3 in hearing loss based on loss of function mutant mice is required. Three mouse models of hearing loss have been successfully developed in one of the laboratories of this COST action – namely noise overexposure, cisplatin and age-related hearing loss models and investigation of the role of NOX3 is currently ongoing through both NOX3 and p22phox mutant mice. In parallel, specific approaches allowing inhibition of pathological NOX3 activity should be developed. At this point, it is difficult to predict whether classical pharmacological approaches, i.e. small molecule NOX3 inhibitors, or rather molecular biology-based therapies, i.e. siRNA-mediated knock-down, will be the ultimate tools for NOX3-targeted therapies.

### 9.4. Metabolic diseases and diabetes

The following subsections were composed by David Bernlohr, Bato Korac, Irina Milisav, Tatjana Ruskovska, Shlomo Sasson, and Ana Stancic.

#### 9.4.1. Importance of setting superoxide/nitric oxide ratio in diabetes. Role of L-arginine

A hallmark of the diabetic state is the increased level of $O_2^{\bullet-}$ in many tissues as a result of hyperglycemia and hyperlipidemia. The high level of $O_2^{\bullet-}$, along with the reduced endogenous synthesis of NO, is responsible for the low bioavailability of NO in diabetic conditions. The product of $O_2^{\bullet-}$/NO interaction, peroxynitrite ($ONOO^-$) and more potent oxidants, deriving from $ONOO^-$, play a significant role in the metabolic complications that accompany diabetes including obesity and insulin resistance. To increase NO bioavailability and/or to simultaneously reduce the $O_2^{\bullet-}$ level in order to improve prediabetic and diabetic states, supplementation with L-arginine, the substrate for NO synthases, as well as mimics of superoxide dismutase (SOD) have been proposed as a potential therapeutic strategy. Several beneficial effects of L-arginine have been observed in diabetes. In the pancreas L-arginine induces β-cell regeneration [685] and positively regulates insulin synthesis and secretion [686]. The favorable effects of L-arginine in obesity and insulin resistance are well-established and could be ascribed to the role of L-arginine in improving fat metabolism, by increasing lipolysis and β-oxidation [687] as well as thermogenesis-related energy expenditure [653,688,689] and insulin sensitivity [687]. It seems likely that all these effects of L-arginine may be related to improved NO bioavailability. An innovative mechanism-based approach for controlling NO and $O_2^{\bullet-}$ levels includes the use of redox-modulating compounds such as selective functional mimics of SOD. SOD mimics were initially designed to scavenge excessive $O_2^{\bullet-}$, but additional data suggest that a decreased formation of peroxynitrite and nitr(os)ative stress and restoration of NO signaling underlie the therapeutic benefits of these agents [690–692]. These compounds show positive effects on insulin sensitivity and metabolic complications in diabetes, in part through the recovery of mitochondrial function [690,692,693]. Altogether, using specific potent redox-active agents to adjust the $O_2^{\bullet-}$/NO ratio seems to have potential in the treatment of

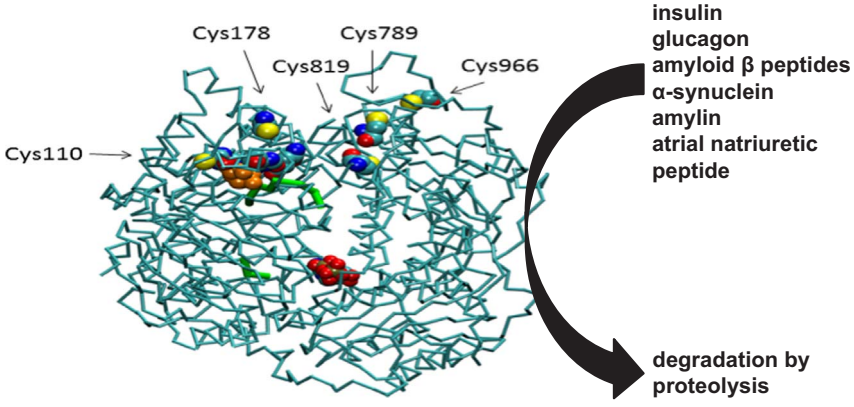


**Fig. 9.3.** Structure of the insulin degrading enzyme complex with amyloid-β, sites of redox regulation and major functions as a peptidase. The structure was displayed by the Visual Molecular Dynamics program [698] from the structure PDB ID: 2G47 [699]. Yellow: the sulfur atoms of cysteines; orange: Glu111; red/gold: ATP, light green: amyloid-β fragment. We acknowledge the help of Jure Stojan to prepare the crystal structure image.

this widespread metabolic disorder. The fact that traditional antioxidants failed to show significant benefits in diabetes emphasizes the importance of the aforementioned approaches.

#### 9.4.2. Regulation of insulin degradation by redox-related pathways

*S*-Nitrosylation (the covalent addition of NO-related species to cysteine residues of target proteins resulting in the formation of nitrosothiols-SNOs) has recently emerged as a relevant mechanism that activates or inhibits protein function, and alters protein conformation, protein aggregation, protein localization and protein-protein interactions [694]. *S*-nitrosylation can affect other post-translational modifications of cysteine thiol groups (like palmitoylation, which is important for protein-membrane associations), bond formations and cellular signal transduction pathways [695,696] Only specific cysteine residues are *S*-nitrosylated, as this depends on the proximity to reactive species, local hydrophobicity and is counterbalanced by denitrosylation enzymes, like the thioredoxin system and protein disulfide isomerases.

Insulin degrading enzyme (IDE) is a zinc metalloprotease that degrades insulin, small peptides and amyloidogenic peptides, like amyloid β peptides, α-synuclein, amylin, and atrial natriuretic peptide (Fig. 9.3) [696]. IDE deficit increases the abundance and signaling of the pancreatic hormones insulin, amylin and glucagon. Increased insulin improves glucose tolerance, increased amylin levels slow postprandial gastric emptying. IDE deficit increases levels of amylin, α-synuclein, and Aβ monomers. These molecules impair the secretory function and survival of pancreatic β cells and neurons through the formation of toxic oligomers. Whereas IDE is expressed in all tissues, the regulation of its levels is an intricate and still unclear process. Cell stress, glucagon and free fatty acids have all been shown to participate [696]. In cells IDE is mostly localized in the cytosol but its presence has also been reported in peroxisomes, mitochondria, cell membranes and extracellular fluids, including cerebrospinal fluid and plasma [696,697].

IDE can be present as a monomer or multimer but it has been shown that dimerization allosterically regulates its catalytic activity [697]. Dimerization and binding with cytoskeletal proteins and ATP enhances the degradation of small peptides, like bradykinin. Aβ-bound IDE structures reveal that the β-strand of amyloidogenic peptides interacts with the door subdomain of IDE, which may explain the affinity of IDE for amyloidogenic peptides.

Exposure of IDE to *S*-nitrosoglutathione can result in the modification of IDE activity through *S*-nitrosylation of at least 5 of its 13 cysteine residues: Cys110, Cys178, Cys819, Cys789 and Cys966 [700]. *S*-nitrosylation of Cys819 promotes nitrosylation of Cys110, which is near the catalytic site that is composed of two glutamates (residues 111 and 189) and a zinc ion coordinated by two histidines (residues 108 and 112). *S*-nitrosylation of Cys110 results in inactivation of IDE. Modification of Cys178 prevents the nitrosothiol formation on Cys110 and buffers the enzyme inhibition. *S*-nitrosylations at Cys789 and Cys966 induce a conformational change that triggers the aggregation of IDE and its inhibition. *S*-nitrosylation of Cys178 protects all of the above mentioned cysteine residues from nitrosylation. The oxidative modifications by $H_2O_2$ resulted in the modifications of the same residues with equal effects on IDE activity. Although these results are from in vitro studies, IDE was exposed to 10–100 μM *S*-nitrosoglutathione or $H_2O_2$, which is in the concentration range of ROS/RNS released under pathophysiological conditions [700]. These modifications were tested for inhibition of Aβ hydrolysis. It has been proposed that the cysteines of IDE act as sensors of environmental ROS/RNS levels through subtle alterations of the protein structure and that IDE function is modulated by the levels of oxidative/nitrosative stress. It is likely that the oxidation of cysteine 178 may result in the protection of the active site under moderate amounts of ROS, while severe oxidative stress inhibits the enzyme. The decreased activity of IDE through *S*-nitrosylation could also reduce the degradation of both insulin and Aβ and contribute to pathological disease conditions in type 2 diabetes and AD. This is supported by findings demonstrating an altered redox state of hippocampal and cortical neurons in both diseases. Indeed, increased levels of glucose result in a significant rise in neuronal reactive nitrogen species similar to the effects of oligomeric Aβ peptides. The high glucose and Aβ oligomers were shown to increase neuronal $Ca^{2+}$ and NO levels in cortico-hippocampal brain slices and in cortical cultures to the $^{\bullet}NO$ levels that could potentially promote *S*-nitrosylation of specific protein thiols in IDE resulting in a reduction or inhibition of its activity [701]. Therefore, increased oxidative/nitrosative stress can contribute to increased Aβ levels, an important pathologic hallmark of AD through the *S*-nitrosylation of IDE. Although IDE is the best characterized enzyme that degrades insulin, reduction in IDE activity in various experimental models does not consistently increase insulin concentrations. Recently the study with the IDE inhibitor that binds to its exosite resulted in increased plasma levels of amylin, but not of insulin [697]. Other regulatory mechanisms and/or IDE substrates may also contribute to glucose homeostasis, development of insulin resistance and diabetes mellitus type 2.

#### 9.4.3. Lipohormesis and lipotoxicity in pancreatic beta cells

Monounsaturated and polyunsaturated fatty acids (MUFA and PUFA, respectively) promote adaptive responses and enhance cell tolerance to lipid overload through induction of cellular defense mechanisms (lipohormesis) that protect cells against lipotoxic effects. Recent lipidomic analysis performed on pancreatic beta cells that were exposed to increasing glucose and palmitic levels revealed extensive remodeling of fatty acids in membrane phospholipids. Particularly, the abundance of PUFA was decreased whereas the content of MUFA increased. These changes were accompanied by non-enzymatic peroxidation of the released PUFA and their transformation to bioactive 4-hydroxyalkenals. This process in beta cells leads to the generation of 4-hydroxynonenal, which activates PPARδ [702–704]. The latter augments the secretion of insulin, which promotes hepatic and peripheral mechanisms that enhance glucose disposal and the incorporation of free fatty acids into triglycerides and their storage in adipose tissues. Excessive and prolonged nutrient overload often interferes with normal cell functions and dysregulates hormonal-mediated inter- and intra-organ metabolic communication networks. In beta cells, hyperglycemia and hyperlipidemia synergistically compromise insulin synthesis, glucose-stimulated insulin secretion and cell survival. The mechanisms underlying these derangements, which characterize the etiology of type 2 diabetes and other manifestations of the metabolic syndrome, have been thoroughly investigated [705]. A central hormetic mechanism is redox-mediated release of KEAP1 from the KEAP1/NRF2 complex, allowing nuclear translocation of NRF2 and its interaction with Antioxidant Response Elements (ARE) in promoters of target genes encoding antioxidant enzymes, ultimately resulting in their activated transcription. Beyond the modification of dietary habits and life style in addition to treatment of the underlying condition, it would be theoretically sound to propose pharmacological approaches with potent oral antioxidants, which are efficiently absorbed, reach the circulation and affect cells, such as beta cells, and protect them against direct and indirect effects of free radicals and lipid peroxidation. However, the prevailing knowledge favors the notion that these oral antioxidants are only effective when triggering intracellular physiological signals related to endogenous protective pathways such as the aforementioned KEAP1/NRF2-ARE axis.

#### 9.4.4. Redox regulation of white adipose tissue remodeling

The white adipose organ features high metabolic activity and endocrine function and regulates whole-body energy homeostasis through the secretion of macronutrients (fatty acids) and adipokines (e.g., adiponectin, resistin). White adipose tissue (WAT) can be anatomically divided into visceral and subcutaneous. It is found distributed broadly in the body and is subject to regulatory cues throughout development and aging. Evolutionarily developed for

effective fat storage in the short periods of food access, as well as for immune surveillance, dysfunctional obese WAT underlies metabolic disorders in the modern era because food is readily and continuously available [706].

In the fed state, insulin mediates the uptake of glucose by adipocytes that is metabolized via the combined actions of glycolysis, TCA cycle and fatty acid biosynthesis to produce precursors utilized for triglyceride biosynthesis. Through these pathways, high nutrient oxidation decreases the adipocyte $NAD^+$/NADH ratio that attenuates the activity of all $NAD^+$ dependent enzymes, including the sirtuins. Sirtuins deacetylate/deacylate both histone and non-histone target proteins regulating their activity and cellular function. SIRT1 is the best studied of all seven mammalian sirtuins. It provides a molecular link between the cellular metabolic status and the adaptive transcriptional response. In the WAT SIRT1 acts through repression of transcriptional activity of the nuclear receptor PPARγ, the master regulator of both lipogenesis and adipogenesis. Calorie restriction increases the adipocyte SIRT1 activity and promotes lipid mobilization, as well as insulin sensitivity and glucose tolerance [707]. Therefore, the adipocyte $NAD^+$/NADH ratio, acts as an important indicator of cellular and whole body energy status, and emerges as one of the key redox regulators of WAT function. SIRT1 also has an important role in the browning of the WAT, a metabolically beneficial WAT remodeling that promotes energy expenditure to combat obesity and diabetes, which might serve as a novel strategy to improve metabolic health. A very recent study reveals that capsaicin (a bioactive compound of red pepper) has the potential to induce increased expression and phosphorylation of SIRT1 in the subcutaneous WAT of mice fed a high fat diet. Activated SIRT1 deacetylates both PPARγ and positive regulatory domain containing 16 (PRDM-16), promotes WAT browning and prevents weight gain. The effect of capsaicin on SIRT1 is mediated by the transient receptor potential cation channel subfamily V 1 (TRPV1), $Ca^{++}$/calmodulin activated protein kinase II and adenosine monophosphate activated kinase (AMPK). In parallel, an increased expression of mitochondrial uncoupling protein 1 (UCP1) was found in the WAT of mice treated with capsaicin, confirming the key role of UCP1 in the browning of WAT [708].

Evolutionarily designed for effective fat storage (and release), the WAT has developed an extraordinary ability for expansion, thus preventing the metabolically detrimental ectopic fat accumulation. As a consequence of nutrient overload, the existing adipocytes enlarge and accumulate triglycerides (a process known as lipogenesis), and/or new adipocytes differentiate from the multipotent mesenchymal stem cells (MSC) to form mature adipocytes (adipogenesis). Adipogenesis, also known as adipose tissue hyperplasia, leads to a metabolically healthy obese WAT phenotype that is characterized by increased secretion of adiponectin and insulin sensitivity, as well as decreased immune cell recruitment, hypoxia and fibrosis. Among the many factors that initiate and regulate adipogenesis, the contribution of ROS has been recognized in the face of NOX4-generated $H_2O_2$. Importantly, ROS depletion with *N*-acetyl-L-cysteine results in abrogation of in vitro adipogenesis [709]. Whereas adipocytes have an extraordinary capacity for fat accumulation (lipogenesis), their growth above the critical volume (hypertrophy) leads to necrotic death and pro-inflammatory remodeling linked to macrophage infiltration and their phenotypic change from M2 (inflammation resolving) to M1 (pro-inflammatory), appearance of crown-like structures, increased angiogenesis and extracellular matrix production, hypoxia, unbalanced production of pro- and anti-inflammatory cytokines, and insulin resistance. Dysfunctional obese WAT exhibits significantly increased protein carbonylation, indicating the central role of excess ROS and oxidative stress in obesity induced insulin resistance [710].

In contrast to the white adipocytes and their function for fat storage, the adipocytes from the brown adipose tissue (BAT) are responsible for energy dissipation in response to cold, exercise or excess calories. The key player in energy dissipation is the inner mitochondrial membrane protein UCP1 that uncouples the electron transport chain (ETC) from ATP biosynthesis, thus dissipating the proton motive force, generating heat, and increasing the rate of substrate oxidation. The recent discovery of metabolically active BAT in human adults has attracted much interest as a potential target for the development of anti-obesity drugs. In addition to the classical white and brown adipocyte phenotype, beige adipocytes (also known as “brite” – short for brown in white, or “brown-like”) have been identified as an inducible form of thermogenic adipocytes. When induced they exhibit high UCP1 expression and energy expenditure. Beige adipocytes express unique genetic signatures that distinguish them from both white and brown adipocytes. In rodents, the brite adipocytes are most abundant in the subcutaneous WAT and are responsible for its browning [711].

Intriguingly, a recent study reveals that UCP1-mediated thermogenesis depends on mitochondrial ROS production. It has been shown in vivo that acute activation of BAT thermogenesis is associated with a substantial increase in mitochondrial superoxide, lipid hydroperoxides and hydrogen peroxide. Pharmacological depletion of mitochondrial ROS inhibits the UCP1 dependent increase in whole-body energy expenditure, confirming the essential role of ROS in the regulation of adipocyte function and metabolism. At the same time, a substantial oxidation and depletion of the cellular and mitochondrial glutathione pool has been demonstrated, as well as an increased global protein sulfenylation, and sulfenylation of UCP1 Cys253 as a redox sensitive site related to thermogenesis [712]. The possible dependence of WAT UCP1 activity on the cellular pro-oxidant state was studied in *Nrf2*$^{-/-}$ mice. The NRF2 transcription factor is a critical regulator of genes involved in detoxification and antioxidant defense. Therefore, *Nrf2*$^{-/-}$ mice are more susceptible to toxicant- and oxidative stress-induced diseases, as well as autoimmune diseases and cancer. Paradoxically, they are also resistant to high fat diet-induced obesity, exhibit improved metabolic profiles, and demonstrate increased energy expenditure in comparison to the wild type mice fed a high fat diet. Such mice also exhibit a concomitant decrease in the GSH/GSSG ratio and up-regulation of UCP1 and other BAT markers in intra-abdominal fat pads [713]. Overall, balanced ROS levels are required for proper WAT function, and both very high and very low levels impede its function and influence whole-body energy homeostasis [714]. Therapeutic control of adipose ROS therefore represents an attractive axis to regulate not only adiposity, but also metabolic healthfulness.

### 9.5. Cardiovascular pathologies

The following subsections were composed by Andreas Daiber, Vaclav Hampl, Jan Herget, Jaap Joles, Thomas Münzel, Isabel Nguyen, and Olga Vajnerova.

#### 9.5.1. Drug-induced oxidative stress – the case of nitroglycerin

Organic nitrate therapy is still a mainstay in the treatment of patients with acute and chronic congestive heart failure, stable coronary artery disease or acute coronary syndrome [715]. However, despite the fact that members of this drug class have been clinically used for more than a century, chronic organic nitrate therapy (especially in the case of nitroglycerin) is associated with a number of serious side effects, including induction of oxidative stress [716] and endothelial and autonomic dysfunction [717], with incomplete understanding of the underlying pathomechanisms. The induction of reactive oxygen and nitrogen species formation by chronic nitroglycerin therapy was shown to largely depend on mitochondrial oxidative metabolism since partial deficiency in MnSOD aggravated nitrate-induced oxidative stress and also the degree of tolerance to the vasodilator activity of nitroglycerin [718]. This was later shown to rely on complex I dysfunction in response to nitroglycerin therapy [719]. The initial formation of mitochondrial reactive oxygen and nitrogen species can also activate secondary sources of oxidants in a crosstalk fashion involving mitochondrial $K_{ATP}$ channels and the permeability transition

pore [61]. This leads to the activation of specific enzymatic "redox switches" in NOXs and eNOS, as recently reviewed [60]. The formation of mitochondrial reactive oxygen and nitrogen species may lead to endothelial dysfunction by the activation of the vascular and phagocytic NOXs through protein kinase C [720] as well as to the uncoupling of eNOS by increased *S*-glutathionylation, inhibitory phosphorylation and oxidative depletion of the eNOS cofactor tetrahydrobiopterin [478]. eNOS uncoupling and oxidative desensitization of the soluble guanylyl cyclase are probably the major enzymatic mechanisms contributing to endothelial dysfunction observed under nitroglycerin therapy, the latter also accounting for impaired nitroglycerin-dependent vasodilation (nitrate tolerance), all of them corrected by co-administration of an activator of soluble guanylyl cyclase [721]. Nitroglycerin-induced endothelial dysfunction but also nitrate tolerance may also rely on direct oxidative break-down of nitric oxide by superoxide leading to the formation of peroxynitrite and significantly increased levels of 3-nitrotyrosine-positive proteins, an effect prevented by the peroxynitrite scavenger hydralazine [722]. Finally, the bioactivation of nitroglycerin largely depends on enzymatic conversion by mitochondrial aldehyde dehydrogenase (ALDH-2) [723], which is a highly redox-regulated enzyme and inactivated by oxidative stress [716]. Hence, nitroglycerin-induced reactive oxygen and nitrogen species formation will ultimately lead to inactivation of the thiol-based enzymatic activity of ALDH-2 contributing to impaired nitroglycerin bioactivation, loss of its vasodilator activity and nitrate tolerance [724]. There is also clinical evidence for nitroglycerin-induced vascular oxidative stress [725] and oxidative DNA damage in patients under chronic nitrate therapy [726]. Very recently, we were able to demonstrate persistent oxidative modifications of DNA and proteins in nitroglycerin-treated rats, even after a 3.5-day nitrate-free interval, which was enough to normalize nitroglycerin responsiveness but not endothelial dysfunction. The latter could be related to endothelial cell death by pro-apoptotic stimuli such as 8-oxoguanine lesions in DNA and 3-nitrotyrosine-positive proteins [727]. Other organic nitrates show similar side effects, such as the activation of NADPH oxidases, increased vascular oxidative stress and severe endothelial dysfunction by chronic isosorbide-5-mononitrate therapy, which was associated with augmented endothelin-1 signaling and eNOS uncoupling [728]. The only exception among the clinically used organic nitrates is pentaerythritol tetranitrate [715,716], which overcomes the typical side effects of nitrovasodilators by mechanisms that are largely based on NRF2-dependent activation of antioxidant enzymes such as heme oxygenase-1 and superoxide dismutase [729,730] as well as beneficial effects on other transcription factor and epigenetic pathways [731,732].

In conclusion, the side effects of chronic therapy with organic nitrates, especially with nitroglycerin, are largely based on oxidative stress and adverse redox regulation. Antioxidant therapy (e.g. by ACE inhibitors or statins) represents a pharmacological tool to overcome these side effects [715–717]. These and other combination therapies with specific antioxidants, inhibitors of relevant sources of oxidants (e.g. inhibitors of NADPH oxidase isoforms) and drugs for repair of oxidative damage (e.g. activators of soluble guanylyl cyclase) need to be explored in the future to increase the therapeutic window of organic nitrates, the oldest drug class in clinical use today.

#### 9.5.2. Regulation of renal hemodynamics in chronic kidney disease

Hypertension and an increased renal vascular resistance (RVR) are inherent to chronic kidney disease (CKD). There is accumulating evidence that oxidative stress is involved in its pathogenesis [733]. Experimental induction of ROS (superoxide and $H_2O_2$) generation in the renal medulla promotes hypertension [734]. Downregulation of the antioxidant enzymes superoxide dismutase (SOD), catalase and glutathione peroxidase in the kidney were found in experimental CKD [735]. Hence, it has been suggested that antioxidant interventions may have beneficial effects on renal hemodynamics in CKD.

Tempol, a SOD-mimetic, has been shown to reduce oxidative injury in cells and animal models. It improved oxidative stress and lowered arterial pressure and RVR in various models of hypertension. However few studies have focused on the effects of Tempol in CKD. Rats undergoing 5/6 renal mass reduction to induce CKD showed an elevated arterial pressure and nitrotyrosine abundance, while urinary $NO_x$ excretion was depressed [736]. The administration of Tempol for one week ameliorated hypertension, reduced the nitrotyrosine abundance and increased $NO_x$ excretion. In spontaneously hypertensive rats (SHR), two weeks of Tempol administration decreased the elevated mean arterial pressure (MAP) and renal excretion of 8-iso-prostaglandin F2α and increased the glomerular filtration rate (GFR) [737], while it had no significant effect on these variables in the normotensive Wistar-Kyoto (WKY) control rats. These findings suggest that oxygen radicals may be involved in the long-term maintenance of hypertension in SHR. Another study found an elevated RVR in SHR compared to WKY rats [738]. When SHR were treated with Tempol the baseline RVR was no longer significantly different from the WKY rats. The additional use of the NO-synthase inhibitor L-NAME did not influence the effects of Tempol on the RVR, suggesting that it has a renal vasodilator effect and that the elevated RVR is unlikely due to ROS-induced quenching of NO.

The two-kidney one-clip model showed an elevated MAP and 8-iso-prostaglandin F2α excretion, which was significantly reduced by the acute administration of Tempol [739]. In the clipped kidney, adding Tempol increased GFR and effective renal plasma flow and reduced RVR compared to their controls. The latter was also found in the non-clipped kidney. This indicates that Tempol is able to have a vasodilating effect via dismutation of the superoxide resulting from angiotensin signaling that is independent of the local perfusion pressure. This supports the role of superoxide during the early stage of renovascular hypertension. In another study the acute effects of the SOD-mimetic on renal hemodynamics were investigated in rats with long-established CKD induced by bilateral 2/3 nephrectomy [740]. Tempol was not able to reduce the increased MAP in the CKD rats, but did lower MAP in age-matched controls with normal kidneys, suggesting that the maintenance of hypertension in this CKD model does not appear to depend on superoxide. As expected, RVR was higher in the CKD rats compared to controls, but the administration of Tempol did not have any significant effect on RVR. This proposes that renal resistance vessels are not sensitive to the renal vasoconstrictor effects of ROS in this model.

These data suggest that although antioxidant therapy can reduce the elevated arterial pressure in the early stages of experimental CKD, it does not appear to be effective once CKD is established. The same concept could be applied to the effects of Tempol on the RVR. In early stages of experimental CKD, prior to the development of renal fibrosis, Tempol can have a vasodilating effect independent of the local perfusion pressure. However, when structural damage occurs to the vascular beds and in their direct proximity, such as in established CKD, the vasodilating effects of Tempol are lost. This suggests that ROS may not be a driving force in the maintenance of disturbed renal hemodynamics in established CKD.

#### 9.5.3. Vascular effects related to chronic hypoxia of lungs and placenta

Oxidative tissue injury participates in the pathogenesis of chronic hypoxic pulmonary hypertension (HPH) [741,742]. HPH is caused by persistent lung hypoxia. It results in an increase in pulmonary vascular resistance to blood flow as a consequence of the sustained increase in the tone of the pulmonary vascular smooth muscle, decreased compliance of pulmonary blood vessels due to fibrosis and muscularization of prealveolar pulmonary arterioles. The severity of HPH is dose dependent. After stabilization it does not progress further. It is fully reversible after several weeks in normoxia. HPH typically appears in residents at high altitudes. It is involved in the pathogenesis of pulmonary hypertension in patients with various lung and heart diseases with alveolar hypoxia.

Two basic mechanisms increase pulmonary vascular resistance in HPH: structural remodeling of the peripheral pulmonary vessel walls

and vasoconstriction. Vasoconstriction plays a pathogenetic role at the onset of HPH and it is related to hypoxia-induced oxidant vascular stress. Superoxide, hydroxyperoxide and peroxynitrite are important vasoactive factors released at the beginning of exposure to chronic hypoxia [743]. Oxidant tissue injury to the pulmonary vascular wall induced by hypoxia is the primary mechanism that triggers vascular remodeling in HPH. Antioxidant treatment at the beginning of hypoxia is more effective in reducing HPH than antioxidant therapy applied in later stages of developed pulmonary hypertension.

For the fetus, the placenta plays a role similar to that of the pulmonary circulation in postnatal life - blood oxygenation and $CO_2$ removal. For this reason, we speculated that the regulatory and pathophysiological mechanisms of the fetoplacental and pulmonary vessels were similar. Indeed, we showed that both acute and chronic hypoxia elevate vascular resistance in the fetoplacental vascular bed, which is similar to pulmonary and in contrast to systemic vascular beds [744]. We have also demonstrated that a well-known state of high oxidative stress, maternal diabetes, causes an increase similar to chronic hypoxia in fetoplacental vascular resistance (preliminary observations). As is the case in the pulmonary circulation, oxidative stress also appears to be a major mechanism of vascular resistance elevation in the fetoplacental circulation.

### 9.6. Conclusions

Redox signaling and oxidative stress constitute fundamental regulatory mechanisms not only in highly prevalent pathologies but also in less explored areas of biomedicine such as those related to fibrosis, cell migration and proliferation, hearing loss, schizophrenic disorders, insulin resistance, drug metabolism, lung hypoxia or renal hemodynamics. In some cases, the underlying molecular mechanisms of this redox sensitivity have been deciphered, in others we are just beginning to open the door. It is clear that the pervading nature of ROS reactivity will continue to offer surprises-and explanations- of complex pathologies such as the ones covered in this section.

## 10. Toxin and bacteria-mediated ROS formation and antioxidant strategies in ROS-related diseases

Thomas Kietzmann (E-mail: Thomas. Kietzmann@oulu.fi) and Kateryna Kubaichuk (E-mail: kateryna.kubaichuk@oulu.fi).

### 10.1. Introduction

Research during the last decade has shown that ROS are important regulators of physiological and pathophysiological processes and not only simply detrimental due to their chemical nature or by causing oxidative stress. This is further supported by findings indicating that redox active compounds are essential components of living organisms. Thereby, recent advances in genomics and proteomics have led to the identification of a “redoxome” consisting of hundreds of proteins involved in redox systems. It comprises enzymes generating RONS such as NADPH oxidases and nitric oxide synthases, redox relays such as peroxiredoxins, thioredoxins and glutaredoxins, enzymes degrading ROS such as superoxide dismutase or catalase, as well as numerous proteins dependent on redox modifications, which are involved in the defense against oxidant, inflammatory and/or proteotoxic stress [745].

Although a number of substances, factors, products of metabolism, and nutrients are important for normal cell biology and redox signaling of all species, toxins are rather important for causing deleterious effects. Since toxins act universally on almost all species, it is conceivable that their action may, at least in part, involve ROS or oxidative stress and that antioxidant defense mechanisms could help to avoid the deleterious effects of toxins.

### 10.2. A toxin and its action via ROS

João G. Costa and Nuno G. Oliveira, discuss how the well-known nephrotoxic food contaminant and animal carcinogen, the mycotoxin ochratoxin A (OTA), appears to act at least partially via ROS and induction of oxidative stress, although different mechanisms of its toxicity have also been pointed out. Furthermore, the OTA actions can be overcome by antioxidant based approaches [746–748] (Fig. 10.1).

OTA increased ROS appear to precede the loss of cell viability particularly in renal cells, indicating that these ROS may contribute to OTA cytotoxicity rather than being a consequence of cell death processes [746,749]. Concomitant with ROS induction, OTA also increased lipid peroxidation, depleted antioxidant enzymes [746–751], induced oxidative stress-related proteins, and caused DNA damage. The latter has also been associated with oxidative DNA damage, as assessed by the formation of 8-oxoguanine or using modified versions of the comet assay (e.g. with FPG) [749,750]. Mechanistically, recent studies propose a pathway in which electrophilic species that directly bind to DNA bases are generated during OTA metabolism [752]. Further, OTA was found to be able to cause nitrosative stress due to stimulation of iNOS-mediated NO formation, which may contribute to the formation of peroxynitrite, nitrogen dioxide, and hydroxyl radicals [753]. Several in vitro and in vivo studies assessed the impact of different antioxidants on the OTA-mediated toxicity and it was found that, in general, antioxidants

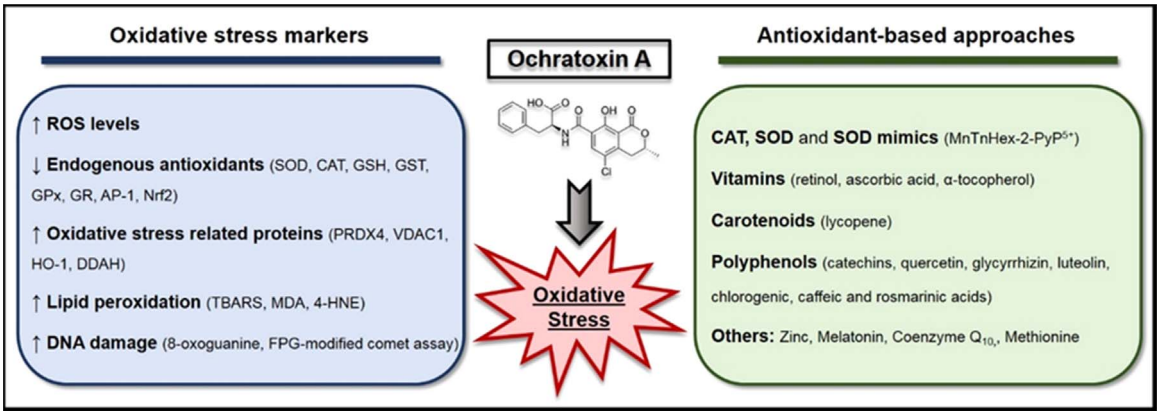


**Fig. 10.1.** Lines of evidence supporting the induction of oxidative stress by Ochratoxin A (OTA). Alterations in biomarkers related with oxidative stress and several antioxidant-based approaches that provide protection against a plethora of OTA-induced toxic effects are indicated. Abbreviations: SOD, superoxide dismutase; CAT, catalase; GSH, glutathione; GST, glutathione *S*-transferase; GPx, glutathione peroxidase; GR, Glutathione reductase; AP-1, activator protein 1; NRF2, nuclear factor E2-related factor 2; PRDX4, peroxiredoxin-4; VDAC1, voltage-dependent anion channel 1; HO-1, heme-oxygenase 1; DDAH, dimethylarginine dimethylaminohydrolase; TBARS, thiobarbituric acid reactive substances; MDA, malondialdehyde; 4-HNE, 4-hydroxynonenal; FPG, formamidopyrimidine DNA glycosylase.

exerted protective effects [746,747,750,751,754].

### 10.3. Are ROS usage and antioxidant reactions conserved?

In order to avoid the life threatening effects of toxins and toxin-induced oxidative stress, both exogenously taken up antioxidants and trace molecules as well as endogenous defense mechanisms contributing to redox regulation with which nature has equipped not only eukaryotes but also prokaryotes and plants, are important to maintain redox status. These systems appear to be quite conserved and, together with the ROS generator sites, they largely contribute to the tightly controlled redox balance.

For example Brandán Pedre and Joris Messens discuss that, *Actinomycetes*, a genus of gram-positive Actinobacteria, possess a low molecular weight thiol molecule, mycothiol (MSH), which serves as a glutathione surrogate [755,756], and they express a mycothiol peroxidase (Mpx) - a glutathione peroxidase-like enzyme. Both, MSH and Mpx are involved in reversibly protecting cysteines from oxidation [130] and controlling the level of ROS [131]. Further, MSH in concert with mycoredoxin-1 [757] and the thioredoxin reduction pathways are alternative routes for the reduction of the different oxidative forms of Mpx. Since thioredoxin can de-mycothiolate Mpx, this indicates the interrelationship between the MSH/mycoredoxin-1 and thioredoxin reduction pathways. Interestingly, this is also seen in the pathogenic Actinobacteria family *Corynebacterium diphtheriae* (Cd), where MSH and thioredoxin can deliver electrons to the methionine sulfoxide reductase A (Cd-MsrA) which stereospecifically reduces Met-S-SO [132], thus controlling sulfur oxidation repair. Thereby, the Cd-MsrA uses a unique intramolecular mycothiol redox relay involving a MSH/mycoredoxin-1 monothiol mechanism, which keeps several MSH-dependent enzymes on track [130–132,757,758]. Interestingly, *Mycobacterium tuberculosis* 1-Cys peroxiredoxin AhpE is reduced by a mycoredoxin-1 dithiol mechanism in addition to the mycothiol/mycoredoxin-1 monothiol mechanism, again indicating that mycothiol-dependent enzymes are promiscuous in the pathway that they use for receiving electrons from NADPH [758]. Overall, it appears that a number of conserved mechanisms are in place to defend against oxidative stress.

Although a variety of microorganisms have well established defense systems against oxidative stress, the gain of compartmentalization in higher organisms created the need to develop an integrated system allowing redox regulation and protection at the same time in each cell compartment. As indicated by Afroditi Chatzi and Kostas Tokatlidis, an excellent example of such cross-talk is the compartment-specific import and folding of proteins in the mitochondrial intermembrane space (IMS) in *Saccharomyces cerevisiae* where potential antioxidant proteins are involved.

The protein import and folding in the IMS relies on the Mia40 pathway [759–761] where Mia40 and Erv1 are key components. Importantly these mechanisms are not restricted to yeast since Mia40 and Erv1 have homologs in almost all organisms including humans. In that system Mia40 functions as a key import receptor in the IMS where it exerts a chaperone-like role recognizing a specific hydrophobic signal of Cys-rich IMS proteins and transfers a disulfide to the substrate [762]. Erv1, on the other hand, is a FAD-linked oxidoreductase that recycles Mia40 to its oxidized state [763]. It was found that the Mia40 pathway is influenced by hydrogen peroxide and that a fraction of Hyr1/Gpx3, a thiol-peroxidase known to act as a redox-transducer in $H_2O_2$ signaling via YAP1 in the cytosol, is localized in the IMS. Additional proteins involved in the antioxidant response, like thioredoxin 1 and thioredoxin reductase1, are also part of the IMS proteome in *S. cerevisiae* [764]. Although these data indicate that the Mia40 oxidative folding in the IMS [765] is associated with antioxidant proteins, its putative links to redox homeostasis and redox signaling are still elusive. However, it is evident that a cross-talk between redox regulation and the oxidative stress response and the IMS oxidative folding pathway exists in higher eukaryotes.

### 10.4. Involvement of ROS and antioxidant mechanisms in human diseases

The existence of rather efficient, and conserved systems involved in both the defense and maintenance of cell, tissue, or organism functionality, indicates that an imbalance in ROS homeostasis is connected with the pathogenesis of frequently occurring diseases.

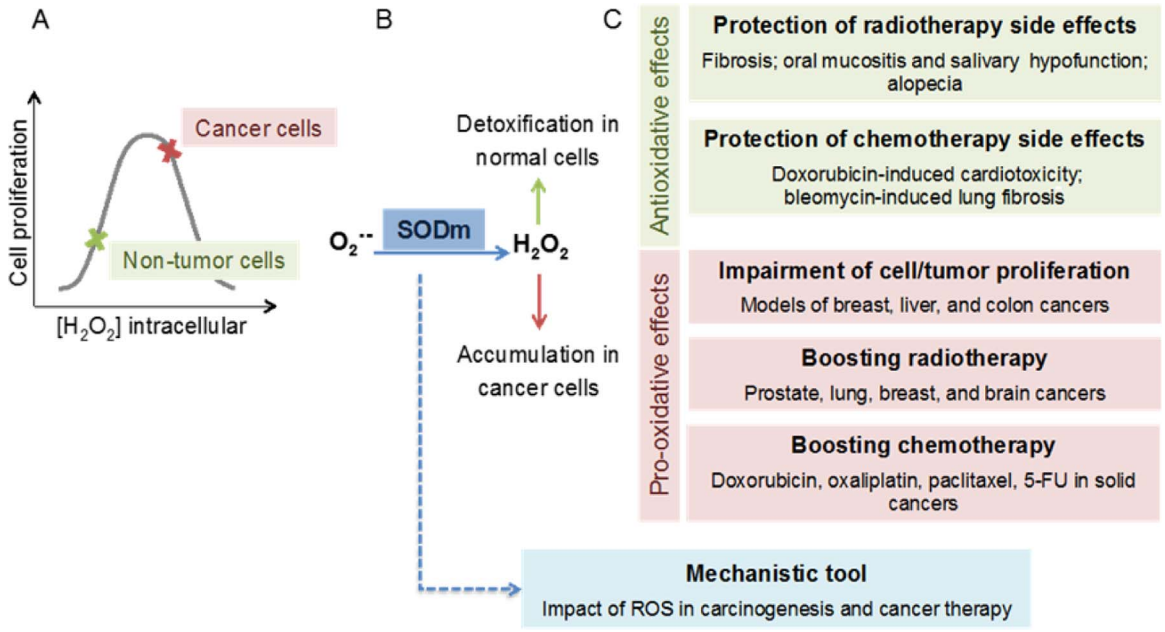


**Fig. 10.2.** SODm in cancer therapy. A. Model proposed to describe the opposite effects of intracellular $H_2O_2$ concentration on the proliferation of cancer and normal cells. B. SODm generate additional intracellular $H_2O_2$, which leads to differential effects in cancer and normal cells. C. Potential applications of SODm in cancer treatment. SODm may protect normal tissues from the adverse side effects of radio and chemotherapy and, conversely, increase the sensitivity of malignant cells to standard radio and chemotherapeutic agents. SODm have also been used as mechanistic tools in the field of redox biology to evaluate the impact of ROS in cancer therapy and in carcinogenesis. (Modified from [768] and book chapter Fernandes et al. Springer International Publishing (2016), Switzerland. DOI 10.1007/978-3-319–30705-3_18).

*10.4.1. ROS and malignant disease*

One example where ROS are considered to be involved is cancer. However, ROS appear to have a dual role; they are often implicated in being the cause of a carcinogenic process, but since the majority of conventional therapies rely also on the increase of ROS they seem to be also of therapeutical benefit causing cancer cell death [766,767].

The intracellular $H_2O_2$ concentration is an important factor for the differential proliferation often observed when comparing cancer and non-cancer cells (Fig. 10.2A) [768]. In general, normal cells do not show high levels of ROS. In contrast, cancer cells with a reduced antioxidant defense and higher instability have usually a higher ROS concentration. This fact can be at least partially be explained by the occurrence of mitochondrial dysfunction, which is associated with an imbalance of the antioxidant defense and an increased production of ROS.

Among the first defenses against ROS is the dismutation of superoxide radicals to hydrogen peroxide and molecular oxygen by SODs; in mitochondria this task is carried out by MnSOD/SOD2. Since mitochondrial dysfunction is a hallmark of cancer, carcinogenesis may be expected to be associated with a dysregulation in the expression of MnSOD. Indeed, numerous reports show that reduced MnSOD contributes to carcinogenesis in many solid tumors [769]. Kateryna Kubaichuk and Thomas Kietzmann discuss the concept that loss of MnSOD leads to a transformed cell type, which was recently supported by findings from cells deficient in MnSOD and in hepatocyte-specific MnSOD knockout mice [770]. The loss of MnSOD in cells caused increased proliferation, reduced apoptosis, decreased contact inhibition and cell adhesion as well as enhanced migration. This was in line with the in vivo findings showing that hepatocyte-specific loss of MnSOD in mice caused liver failure, and initiation of malignant transformation and tumor formation [770].

Mechanistically, these findings could be linked to two pathways: the Wnt/β-catenin pathway and the hypoxia signaling pathway. The Wnt/β-catenin pathway is one of the most important pathways associated with cancer, in particular liver cancer. The Wnt pathway components β-catenin and APC were decreased in MnSOD-deficient HepG2 hepatoma cells as well as in MnSOD deficient mouse livers [770]. This is in line with findings from hepatocyte-specific β-catenin knockout mice, which displayed an increased susceptibility to diethylnitrosamine-induced carcinogenesis [771]. Indeed, induction of HIF-1α, a major regulator of the hypoxia response pathway, was disrupted both in vitro and in vivo due to the loss of MnSOD [770]. Although those data do not unravel all mechanistic aspects of the carcinogenic process in response to MnSOD deficiency, they indicate an intricate interplay between HIF-1α and β–catenin.

Moreover, MnSOD can be regulated by the transcription factor Nuclear factor (erythroid-derived 2)-like 2 (NRF2). As indicated by Natalia Robledinos-Antón and Antonio Cuadrado, NRF2 is of utmost importance and regulates the expression of about 250 genes with homeostatic functions such as those involved in NADPH, glutathione and thioredoxin metabolism, phase II detoxification reactions, inflammation and proteostasis [772,773].

Considering the fact that cancer development is characterized by an altered hypoxia response and malfunctioning of MnSOD, which both can be affected by NRF2, superoxide dismutase mimics (SODm), as well as NRF2 inhibitors, can be considered to be useful in cancer treatment and in other diseases associated with enhanced ROS including cardiovascular, inflammatory, and neurodegenerative disorders [774].

Ana S. Fernandes and Nuno G. Oliveira point out that SODm are synthetic compounds with low molecular weight that mimic the

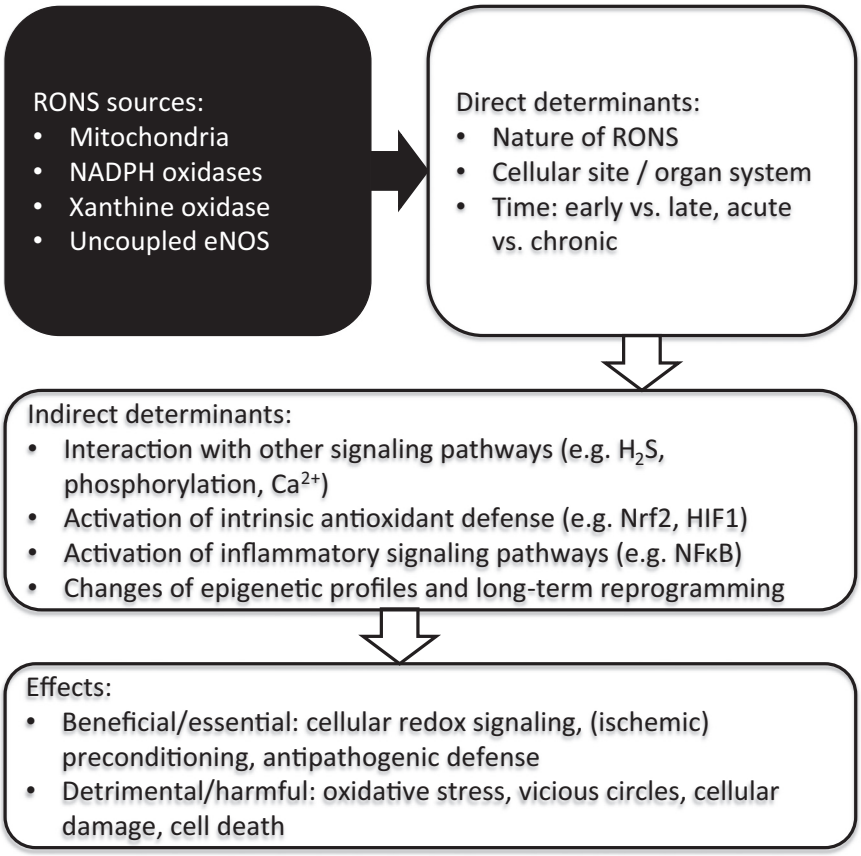


**Fig. 11.1.** Who's the bad guy – or which biological source of RONS formation is the most detrimental one? Likely candidates are mitochondrial RONS formation (mitochondrial superoxide/hydrogen peroxide), NADPH oxidases (Nox1, Nox2, Nox4, in humans also Nox3), uncoupled eNOS (uc-eNOS) or xanthine oxidase (XO). The most challenging task for the future is the discrimination between beneficial and detrimental effects of RONS formation and signaling, which is largely determined by the nature of the involved RONS, as well as the time and place they are formed. This concept was put forward previously [18,21,28,32].

functional properties of SOD enzymes [774,775]. Most SODm are considered polyfunctional antioxidants, rather than specific $O_2^{\bullet-}$ scavengers [775–777]. Along with the disproportionation of $O_2^{\bullet-}$, SODm may react with other reactive species (RS), including peroxynitrite, $CO_3^{\bullet-}$, $H_2O_2$, $^{\bullet}NO_2$ radicals, peroxyl radicals, and alkoxyl radicals [775,776]. Although many compounds with SOD-like activity with distinct chemical structures have been reported, the search for SOD mimics has been mostly focused on complexes that contain a redox-active metal center and rich coordination chemistry [776]. This is the case of Mn(III) porphyrins (MnPs), Mn(II) complexes with cyclic polyamines (aza crown ethers), Mn(III) salen derivatives, and different types of iron and copper complexes [775,776,778,779]. Some non-metallic compounds, such as nitroxides and fullerenes have also been explored as SODm [776,779].

The rationale underling the use of SODm as prospective drugs in cancer treatment is presented in Fig. 10.2. SODm, which lead to an additional amount of $H_2O_2$ (Fig. 10.2B), may reduce cell proliferation and increase the efficacy of chemo- and radiotherapy treatments in cancer cells (pro-oxidative effects).

Conversely, SODm may promote the survival/proliferation of normal cells, protecting them against adverse side effects observed in standard medical treatments for cancer (antioxidant effects) [768,776,778,780]. Finally, SODm can be used to give further mechanistic insights namely to assess the involvement of ROS in carcinogenesis or in cancer therapy (Fig. 10.2).

Mechanistically, SODm can affect redox-based cellular transcriptional activity by affecting reactive thiols of transcription factors (e.g. NF-κB or KEAP1/NRF2) [776,777,780]. In line with this and according to Natalia Robledinos-Antón and Antonio Cuadrado, NRF2 inhibitors are being developed for cancer therapy [781], though a wide range of NRF2 activators is already known. Most activators identified so far target KEAP1 by oxidation or adduct formation [782]. These molecules include allyl sulfides, dithiolethiones, flavonoids, isothiocyanates, polyphenols and terpenoids, etc. Moreover, many of these electrophilic compounds may also react with redox sensitive cysteines located in the catalytic center of several phosphatases, thus up-regulating signaling pathways that further impinge on NRF2 activation. The most successful case reported so far of a drug targeting NRF2 is the ester derivative of fumaric acid, dimethyl fumarate, which is used for treatment of multiple sclerosis.

Ana S. Fernandes and Nuno G. Oliveira explain that although the development of SODm started long ago, none has reached clinical use yet, however, some SODm have been entering phase I/II clinical trials, especially in combination with chemotherapy or radiotherapy regimens. Some examples include MnPs, which are currently being studied for radioprotection in late-stage glioma patients treated with concurrent radiotherapy and temozolamide. In addition, both MnPs and Mn macrocycles are being assessed as radioprotectors in head & neck cancer patients. A different SODm, Mangafodipir, was studied as a protector against oxaliplatin neurotoxicity and FOLFOX6 side effects, while its analog calmangafodipir is being studied in combination with FOLFOX6 in advanced metastatic colorectal cancer [http://clinicaltrials.gov, as of 22nd June 2016].

In summary, there are several therapeutic opportunities for SODm in oncology. These compounds can increase the therapeutic index of chemo- and radiotherapy by boosting the efficacy of such treatments in cancer cells, while counteracting major drug and radiation toxicity issues.

### 10.4.2. ROS and non-malignant disease

Although the above-mentioned SODm may be beneficial in cancer therapy, it is so far unknown whether their antioxidant effect could be of use in other diseases where oxidative stress occurs without proper malignancy. As indicated by Marios Phylactides and Marina Kleanthous, such a disease is β-thalassemia – an autosomal recessive red blood cell disorder characterized by a reduction or complete absence of β-globin chain production, globin chain imbalance and the accumulation of α-globins.

Precipitation and autoxidation of excess α-globins lead to the generation of high levels of ROS as well as the release of free heme and iron. Hemolysis, secondary iron overload, often the result of regular blood transfusions and increased absorption of dietary iron in the gut, as well as ineffective erythropoiesis overwhelm the patients' antioxidant defense systems, giving rise to severe oxidative stress, anemia and secondary complications [783].

Overall, Marios Phylactides and Marina Kleanthous mention that the recurring theme seen in most of the trials involving β-thalassemia patients is an improvement of the oxidant-antioxidant imbalance for the duration of the trial with a decrease of oxidative stress markers (e.g. ROS levels, RBC malondialdehyde concentration, lipid peroxidation) and enhancement of the patients' antioxidant status (e.g. RBC SOD, glutathione peroxidase, reduced glutathione). However, with some rare exceptions [784,785], there is no improvement of the patients' anemia, and no effect on hemoglobin levels. Thus, antioxidant supplements undoubtedly have a beneficial role in the management of β-thalassemia; however, they do not substitute for blood transfusions and iron chelation in patients with the most severe anemia, but they can feature more prominently in milder, transfusion-independent forms of the disease.

Given the central role of ROS in the pathophysiology of the disease, Lidija Milković, and Višnja Stepanić indicate that the use of antioxidants as a means of reducing oxidative damage is an attractive therapeutic option. A wide variety of compounds have been tested in this context without, however, becoming established as an indispensable part of the patients' treatment regime. Some of the antioxidant compounds under investigation are food products or herbal extracts, which are used as supplements or form part of the normal diet (e.g. vitamin E [784,786,787], resveratrol [788], curcuminoids [784,789], *N*-acetylcysteine [785]), CoQ10 [790], green tea [791], fermented papaya preparation [792], or the thistle *Silybum marianum* (L.) extract silymarin [793,794].

The latter appears to be one of the most interesting and, as discussed by Vladimir Kren and Katerina Valentova, silymarin's major active constituent silybin (CAS no. 22888-70-6; syn. silibinin) is a typical radical scavenger per se [795,796]. However, in addition to its radical scavenging activity, this compound selectively interacts with various specific receptors and signaling molecules such as the estrogen receptor [797]. This effect was found to account for the proapoptotic activity of silybin in MCF-7 breast cancer cells [798]. Silybin also targets p53, NF-κB or Wnt/β-catenin signaling in various cancer cells, thus affecting mitogenesis, cell cycle, apoptosis, autophagy, and angiogenesis. Its ability to reverse the P-glycoprotein mediated multi-drug resistance in small lung carcinoma [799] partially explains its chemopreventive and chemoprotective activity [800,801]. Moreover, the ability of silybin to bind to the α-amanitin binding site of RNA polymerase II is probably responsible for its antidote effect in *Amanita* poisoning [802]. Altogether, the role and the mode of action of this traditional and well known chemoprotectant needs to be substantially revised in the future.

### 10.5. ROS, antioxidants and therapeutic options

In addition to the beneficial effects of antioxidant supplements in mild β-thalassemia, their action may not always be a direct antiradical (scavenging) action, as discussed by Lidija Milković and Višnja Stepanić. Although the ability to reduce the amount of ROS in vitro still remains to be an important stage in the evaluation of the antioxidant potency of any new or known compounds [803], this approach is challenged because: i) many known antioxidants do not show direct antiradical activity in vivo and vice versa [31]; ii) proved antioxidants (e.g. flavonoids, PUFAs as part of fish/plant oils) exhibit a dual role acting as antiradical and prooxidant agents simultaneously [804]; and iii) effects of the known antioxidants are mostly related to

their indirect action [31,805].

Hence, more specific therapeutic options need to be used and accordingly first generations of specific compounds (e.g. NOX inhibitors, NRF2 activators, myeloperoxidase inhibitors) are being developed for application in a wide range of diseases including metabolic, fibrotic, and neurodegenerative diseases as well as cancer [32]. The validation of the specificity of these drugs is highly dependent on the availability of specific target engagement and functional assays. Since the redox reactions are complex and often redundant, the careful use of tools for measuring ROS is important to select drugs, identify potential non-specific effects and evaluate their mode of action [806].

Tamara Seredenina and Vincent Jaquet indicate that currently, countless chemical probes are used to detect ROS, all with advantages and limitations; it is therefore advisable to use several of them and it is critical to control the types of ROS with which they react [807]. On this matter, it is worth mentioning the innovative use of the cell-permeable small molecule dihydroethidine as it allows detection of specific oxidants and their quantification both in vitro [808] and in vivo [809,810]. Genetically encoded probes are also great tools for detecting intracellular $H_2O_2$ localization and real time monitoring [56] and may prove essential for redox dynamics; they also allow visualization of the redox state directly in paraformaldehyde fixed tissues [811].

The more specific design of redox active compounds together with the selection of appropriate druggable biological targets should encompass different in silico approaches and in vitro assays for prediction and measurement, respectively, of their various redox activities. In addition to standard cell-free assays that allow evaluation of the antioxidant properties of new compounds [e.g. DPPH scavenging method, Trolox equivalent antioxidant capacity (TEAC) method, ABTS radical cation decolorization assay, Ferric reducing-antioxidant power (FRAP) assay or hydroxyl radical averting capacity (HORAC) method], in vitro models of different cancer and normal cells should be used [812]. In vivo, KO mouse models are to be used to prove the specificity of action of a drug on a given target. They may, according to Danylo Kaminskyy, Khrystyna Semen, and Olha Yelisyeyeva, enable evaluation of a compounds' cytotoxicity and possible selectivity (e.g. toxic to cancer but not to normal cells), pro-oxidative activity (measured as ROS generation), as well as endogenous antioxidative response; whether they are added alone or in combination with known drugs to evaluate any possible synergistic effect.

Despite these advantages and a strong rationale for therapeutic targeting of ROS and redox pathways, it is not known why the antioxidants used so far in clinical trials/therapies did not exert the expected effects [216]. Dose and combination regimen, or duration of treatment, may be partial reasons. Indeed, in those studies high antioxidant doses were usually applied, and some actions such as the prooxidant action of some antioxidants as discussed above have been neglected. Moreover, patients were usually not tested for antioxidant deficiencies and/or compliance as in the EPIC clinical trial [813].

### *10.6. Conclusion*

Altogether, in almost all living organisms ROS cannot simply be considered as detrimental since they contribute to signaling, as well as to maintenance of integrity and homeostasis in different organisms ranging from bacteria to mammals. In the latter, disturbances of ROS homeostasis can contribute to the pathogenesis of several chronic diseases such as atherosclerosis, type II diabetes, and cancer via modulation of diverse processes such as inflammation, and the immune response. The common associated increase in ROS in these diseases points to the therapeutic use of small molecules with antioxidant function; however, so far little or no benefit could be observed from the large scale studies with antioxidant supplementation. Overall, these findings signify that further improvement is needed in our knowledge about ROS, ROS-targets, antioxidants, measurement techniques, and their connection to homeostasis and diseases.

## 11. Concluding remarks

Andreas Daiber and Fabio Di Lisa.

The last decade has witnessed intense research related to the implications of ROS in cellular pathology with special emphasis on the identification of sources, biochemical reactions and cellular effectors responsible for final pathophysiological outcomes. The recognition of RONS as conveyors of physiological signals has added a new level of understanding to their function and has generated contradictory observations regarding the effects of antioxidant molecules, which we are only beginning to unravel. Studies in the context of whole organs both in their healthy and diseased state have expanded the importance of RONS regulation in unpredicted settings. The previous sections highlight some interesting examples of these aspects and also reflects the major achievements of the EU-ROS consortium, evidencing how redox biology is slowly but inexorably evolving towards redox medicine, a concept also put forward in [30,814].

Unfortunately, conclusive and precise answers are still needed and the world of redox biology and medicine still has challenges. The notions on the relevant sources might look obvious, yet it is not clear which are the most important ones under physiological and pathological conditions. In addition, it is not clear how much the various RONS are compartmentalized, especially within a given cell. Thirdly, it is still difficult to monitor RONS formation due to limitations that still affect their assessment. Fourthly, the discussion is open on why and how the same molecules might mediate physiological and pathological events. It is likely that a threshold of RONS levels exists separating beneficial effects from contribution to cell injury. The definition of this threshold, that is likely to be different in healthy and diseased cells, requires quantitative methods that are hardly available. The identification of beneficial levels as opposed to detrimental ones should allow defining and/or predicting the consequences of changes in RONS levels, and how "good" RONS can change into "bad" ones. This last issue is obviously crucial and necessary for the proper translation of experimental findings into clinical settings. This applies not only to the development of focused, if not personalized, therapeutic approaches, but also to diagnostic procedures and disease monitoring. Although providing the correct answers to the above defined questions seems daunting, we hope that future studies and technological advances will clarify the unsolved issues leading to an improved control of cardiac, neurodegenerative, metabolic and inflammatory diseases. These concepts have been laid down by members of the EU-ROS consortium within 3 major coordinated collections of position papers, reviews and original articles published by our members [1–4] (Fig. 11.1).

## Acknowledgements

The EU-ROS consortium (COST Action BM1203) was supported by the European Cooperation in Science and Technology (COST). The present overview represents the final Action dissemination summarizing the major achievements of COST Action BM1203 (EU-ROS) as well as research news and personal views of its members. Some authors were also supported by COST Actions BM1005 (ENOG) and BM1307 (PROTEOSTASIS), as well as funding from the European Commission FP7 and H2020 programmes, and several national funding agencies.

## References

[1] Virtual Collection, Emerging concepts in redox biology and oxidative stress, Redox Biol. (18 articles plus editorial), in: Santiago Lamas, Fabio Di Lisa, Andreas Daiber (eds.). ⟨https://www.journals.elsevier.com/redox-biology/virtual-collections/emerging-conceptsin-redox-biology-and-oxidative-stress-virt⟩.

[2] Forum Issue, Redox medicine, Antioxid. Redox Signal. (9 articles), in: Harald H.H. W. Schmidt, Fabio Di Lisa (eds.) ⟨http://online.liebertpub.com/toc/ars/23/14⟩.

[3] A. Daiber, F. Di Lisa, S. Lamas, Virtual issue by COST action BM1203 (EU-ROS). Emerging concepts in redox biology and oxidative stress, Redox Biol. 8 (2016) 439–441.

[4] Themed issue, Redox biology and oxidative stress in health and disease, Br. J.

Pharmacol. (16 articles), in: Peter Ferdinandy and Andreas Daiber (eds.). ⟨http://onlinelibrary.wiley.com/journal/10.1111/(ISSN)1476–5381/homepage/themed_issues.htm⟩.
[5] O. Augusto, S. Miyamoto, Oxygen radicals and related species, in: K. Pantopoulos, H.M. Schipper (Eds.), Principles of Free Radical Biomedicine, Nova Science Publishers, Inc, 2011.
[6] J. Frijhoff, P.G. Winyard, N. Zarkovic, S.S. Davies, R. Stocker, D. Cheng, A.R. Knight, E.L. Taylor, J. Oettrich, T. Ruskovska, A.C. Gasparovic, A. Cuadrado, D. Weber, H.E. Poulsen, T. Grune, H.H. Schmidt, P. Ghezzi, Clinical relevance of biomarkers of oxidative stress, Antioxid. Redox Signal. 23 (2015) 1144–1170.
[7] K.K. Griendling, G.A. FitzGerald, Oxidative stress and cardiovascular injury: part I: basic mechanisms and in vivo monitoring of ROS, Circulation 108 (2003) 1912–1916.
[8] K.K. Griendling, G.A. FitzGerald, Oxidative stress and cardiovascular injury: part II: animal and human studies, Circulation 108 (2003) 2034–2040.
[9] A. Daiber, S. Steven, A. Weber, V.V. Shuvaev, V.R. Muzykantov, I. Laher, H. Li, S. Lamas, T. Munzel, Targeting vascular (endothelial) dysfunction, Br. J. Pharmacol. (2016), http://dx.doi.org/10.1111/bph.13517.
[10] B.I. Giasson, J.E. Duda, I.V. Murray, Q. Chen, J.M. Souza, H.I. Hurtig, H. Ischiropoulos, J.Q. Trojanowski, V.M. Lee, Oxidative damage linked to neurodegeneration by selective alpha-synuclein nitration in synucleinopathy lesions, Science 290 (2000) 985–989.
[11] H. Ischiropoulos, J.S. Beckman, Oxidative stress and nitration in neurodegeneration: cause, effect, or association? J. Clin. Investig. 111 (2003) 163–169.
[12] A. Ceriello, Oxidative stress and diabetes-associated complications, Endocr. Pract. 12 (Suppl 1) (2006) S60–S62.
[13] J.F. Keaney Jr., J. Loscalzo, Diabetes, oxidative stress, and platelet activation, Circulation 99 (1999) 189–191.
[14] S. Karbach, P. Wenzel, A. Waisman, T. Munzel, A. Daiber, eNOS uncoupling in cardiovascular diseases–the role of oxidative stress and inflammation, Curr. Pharm. Des. 20 (2014) 3579–3594.
[15] C. Szabo, The pathophysiological role of peroxynitrite in shock, inflammation, and ischemia-reperfusion injury, Shock 6 (1996) 79–88.
[16] N.W. Kooy, S.J. Lewis, J.A. Royall, Y.Z. Ye, D.R. Kelly, J.S. Beckman, Extensive tyrosine nitration in human myocardial inflammation: evidence for the presence of peroxynitrite, Crit. Care Med. 25 (1997) 812–819.
[17] G. Aviello, U.G. Knaus, ROS in gastrointestinal inflammation: rescue or Sabotage? Br. J. Pharmacol. (2016), http://dx.doi.org/10.1111/bph.13428.
[18] A. Daiber, F. Di Lisa, M. Oelze, S. Kroller-Schon, S. Steven, E. Schulz, T. Munzel, Crosstalk of mitochondria with NADPH oxidase via reactive oxygen and nitrogen species signalling and its role for vascular function, Br. J. Pharmacol. (2015), http://dx.doi.org/10.1111/bph.13403.
[19] S. Steven, T. Munzel, A. Daiber, Exploiting the pleiotropic antioxidant effects of established drugs in cardiovascular disease, Int. J. Mol. Sci. 16 (2015) 18185–18223.
[20] P. Wenzel, S. Kossmann, T. Munzel, A. Daiber, Redox regulation of cardiovascular inflammation – Immunomodulatory function of mitochondrial and Nox-derived reactive oxygen and nitrogen species, Free Radic. Biol. Med. (2017).
[21] H.H. Schmidt, R. Stocker, C. Vollbracht, G. Paulsen, D. Riley, A. Daiber, A. Cuadrado, Antioxidants in translational medicine, Antioxid. Redox Signal. 23 (2015) 1130–1143.
[22] G. Bjelakovic, D. Nikolova, L.L. Gluud, R.G. Simonetti, C. Gluud, Mortality in randomized trials of antioxidant supplements for primary and secondary prevention: systematic review and meta-analysis, Jama 297 (2007) 842–857.
[23] T. Gori, T. Munzel, Oxidative stress and endothelial dysfunction: therapeutic implications, Ann. Med. 43 (2011) 259–272.
[24] P. Ghezzi, V. Jaquet, F. Marcucci, H.H. Schmidt, The oxidative stress theory of disease: levels of evidence and epistemological aspects, Br. J. Pharmacol. (2016), http://dx.doi.org/10.1111/bph.13544.
[25] P. Mustain Antioxidant Supplements: Too Much of a Kinda Good Thing ⟨https://blogs.scientificamerican.com/food-matters/antioxidant-supplements-too-much-of-a-kinda-good-thing/⟩.
[26] A. Riley Why vitamin pills don't work, and may be bad for you. ⟨http://www.bbc.com/future/story/20161208-why-vitamin-supplements-could-kill-you⟩.
[27] M. Scudellari, The science myths that will not die, Nature 528 (2015) 322–325.
[28] A.F. Chen, D.D. Chen, A. Daiber, F.M. Faraci, H. Li, C.M. Rembold, I. Laher, Free radical biology of the cardiovascular system, Clin. Sci. 123 (2012) 73–91.
[29] K.T. Khaw, S. Bingham, A. Welch, R. Luben, N. Wareham, S. Oakes, N. Day, Relation between plasma ascorbic acid and mortality in men and women in EPIC-Norfolk prospective study: a prospective population study. European prospective investigation into cancer and nutrition, Lancet 357 (2001) 657–663.
[30] A.L. Levonen, B.G. Hill, E. Kansanen, J. Zhang, V.M. Darley-Usmar, Redox regulation of antioxidants, autophagy, and the response to stress: implications for electrophile therapeutics, Free Radic. Biol. Med. 71 (2014) 196–207.
[31] H.J. Forman, K.J. Davies, F. Ursini, How do nutritional antioxidants really work: nucleophilic tone and para-hormesis versus free radical scavenging in vivo, Free Radic. Biol. Med. 66 (2014) 24–35.
[32] A.I. Casas, V.T. Dao, A. Daiber, G.J. Maghzal, F. Di Lisa, N. Kaludercic, S. Leach, A. Cuadrado, V. Jaquet, T. Seredenina, K.H. Krause, M.G. Lopez, R. Stocker, P. Ghezzi, H.H. Schmidt, Reactive oxygen-related diseases: therapeutic targets and emerging clinical indications, Antioxid. Redox Signal. 23 (2015) 1171–1185.
[33] J.T. Hancock, M. Whiteman, Hydrogen sulfide signaling: interactions with nitric oxide and reactive oxygen species, Ann. N. Y. Acad. Sci. 1365 (2016) 5–14.
[34] G.F. Vile, S. Basu-Modak, C. Waltner, R.M. Tyrrell, Heme oxygenase 1 mediates an adaptive response to oxidative stress in human skin fibroblasts, Proc. Natl. Acad. Sci. USA 91 (1994) 2607–2610.
[35] A. Daiber, Redox signaling (cross-talk) from and to mitochondria involves mitochondrial pores and reactive oxygen species, Biochim. Biophys. Acta 1797 (2010) 897–906.
[36] D.B. Zorov, M. Juhaszova, S.J. Sollott, Mitochondrial Reactive Oxygen Species (ROS) and ROS-induced ROS release, Physiol. Rev. 94 (2014) 909–950.
[37] M.C. Larson, C.A. Hillery, N. Hogg, Circulating membrane-derived microvesicles in redox biology, Free Radic. Biol. Med. 73 (2014) 214–228.
[38] S.M. Camus, J.A. De Moraes, P. Bonnin, P. Abbyad, S. Le Jeune, F. Lionnet, L. Loufrani, L. Grimaud, J.C. Lambry, D. Charue, L. Kiger, J.M. Renard, C. Larroque, H. Le Clesiau, A. Tedgui, P. Bruneval, C. Barja-Fidalgo, A. Alexandrou, P.L. Tharaux, C.M. Boulanger, O.P. Blanc-Brude, Circulating cell membrane microparticles transfer heme to endothelial cells and trigger vasoocclusions in sickle cell disease, Blood 125 (2015) 3805–3814.
[39] D. Tsiantoulas, T. Perkmann, T. Afonyushkin, A. Mangold, T.A. Prohaska, N. Papac-Milicevic, V. Millischer, C. Bartel, S. Horkko, C.M. Boulanger, S. Tsimikas, M.B. Fischer, J.L. Witztum, I.M. Lang, C.J. Binder, Circulating microparticles carry oxidation-specific epitopes and are recognized by natural IgM antibodies, J. Lipid Res. 56 (2015) 440–448.
[40] T. Jung, A. Hohn, T. Grune, The proteasome and the degradation of oxidized proteins: part II – protein oxidation and proteasomal degradation, Redox Biol. 2 (2014) 99–104.
[41] F. Kriegenburg, E.G. Poulsen, A. Koch, E. Kruger, R. Hartmann-Petersen, Redox control of the ubiquitin-proteasome system: from molecular mechanisms to functional significance, Antioxid. Redox Signal. 15 (2011) 2265–2299.
[42] F. Sigala, P. Efentakis, D. Karageorgiadi, K. Filis, P. Zampas, E.K. Iliodromitis, G. Zografos, A. Papapetropoulos, I. Andreadou, Reciprocal regulation of eNOS, H2S and CO-synthesizing enzymes in human atheroma: correlation with plaque stability and effects of simvastatin, Redox Biol. 12 (2017) 70–81.
[43] B. Morgan, D. Ezerina, T.N. Amoako, J. Riemer, M. Seedorf, T.P. Dick, Multiple glutathione disulfide removal pathways mediate cytosolic redox homeostasis, Nat. Chem. Biol. 9 (2013) 119–125.
[44] C. Dunnill, T. Patton, J. Brennan, J. Barrett, M. Dryden, J. Cooke, D. Leaper, N.T. Georgopoulos, Reactive oxygen species (ROS) and wound healing: the functional role of ROS and emerging ROS-modulating technologies for augmentation of the healing process, Int. Wound J. 14 (2017) 89–96.
[45] P. Cheresh, S.J. Kim, S. Tulasiram, D.W. Kamp, Oxidative stress and pulmonary fibrosis, Biochim. Biophys. Acta 1832 (2013) 1028–1040.
[46] S.P. Colgan, S.F. Ehrentraut, L.E. Glover, D.J. Kominsky, E.L. Campbell, Contributions of neutrophils to resolution of mucosal inflammation, Immunol. Res. 55 (2013) 75–82.
[47] M. Mittal, M.R. Siddiqui, K. Tran, S.P. Reddy, A.B. Malik, Reactive oxygen species in inflammation and tissue injury, Antioxid. Redox Signal. 20 (2014) 1126–1167.
[48] S. O'Neill, J. Brault, M.J. Stasia, U.G. Knaus, Genetic disorders coupled to ROS deficiency, Redox Biol. 6 (2015) 135–156.
[49] H. Yao, I. Edirisinghe, S.R. Yang, S. Rajendrasozhan, A. Kode, S. Caito, D. Adenuga, I. Rahman, Genetic ablation of NADPH oxidase enhances susceptibility to cigarette smoke-induced lung inflammation and emphysema in mice, Am. J. Pathol. 172 (2008) 1222–1237.
[50] H.Y. Won, E.J. Jang, H.J. Min, E.S. Hwang, Enhancement of allergen-induced airway inflammation by NOX2 deficiency, Immune Netw. 11 (2011) 169–174.
[51] M.J. Davies, Protein oxidation and peroxidation, Biochem. J. 473 (2016) 805–825.
[52] L. Brautigam, L.D. Schutte, J.R. Godoy, T. Prozorovski, M. Gellert, G. Hauptmann, A. Holmgren, C.H. Lillig, C. Berndt, Vertebrate-specific glutaredoxin is essential for brain development, Proc. Natl. Acad. Sci. USA 108 (2011) 20532–20537.
[53] L. Brautigam, L.D. Jensen, G. Poschmann, S. Nystrom, S. Bannenberg, K. Dreij, K. Lepka, T. Prozorovski, S.J. Montano, O. Aktas, P. Uhlen, K. Stuhler, Y. Cao, A. Holmgren, C. Berndt, Glutaredoxin regulates vascular development by reversible glutathionylation of sirtuin 1, Proc. Natl. Acad. Sci. USA 110 (2013) 20057–20062.
[54] T. Prozorovski, R. Schneider, C. Berndt, H.P. Hartung, O. Aktas, Redox-regulated fate of neural stem progenitor cells, Biochim. Biophys. Acta 1850 (2015) 1543–1554.
[55] S. Gascon, E. Murenu, G. Masserdotti, F. Ortega, G.L. Russo, D. Petrik, A. Deshpande, C. Heinrich, M. Karow, S.P. Robertson, T. Schroeder, J. Beckers, M. Irmler, C. Berndt, J.P. Angeli, M. Conrad, B. Berninger, M. Gotz, Identification and successful negotiation of a metabolic checkpoint in direct neuronal reprogramming, Cell Stem Cell 18 (2016) 396–409.
[56] B. Morgan, K. Van Laer, T.N. Owusu, D. Ezerina, D. Pastor-Flores, P.S. Amponsah, A. Tursch, T.P. Dick, Real-time monitoring of basal H2O2 levels with peroxiredoxin-based probes, Nat. Chem. Biol. 12 (2016) 437–443.
[57] J.P. Friedmann Angeli, M. Schneider, B. Proneth, Y.Y. Tyurina, V.A. Tyurin, V.J. Hammond, N. Herbach, M. Aichler, A. Walch, E. Eggenhofer, D. Basavarajappa, O. Radmark, S. Kobayashi, T. Seibt, H. Beck, F. Neff, I. Esposito, R. Wanke, H. Forster, O. Yefremova, M. Heinrichmeyer, G.W. Bornkamm, E.K. Geissler, S.B. Thomas, B.R. Stockwell, V.B. O'Donnell, V.E. Kagan, J.A. Schick, M. Conrad, Inactivation of the ferroptosis regulator Gpx4 triggers acute renal failure in mice, Nat. Cell Biol. 16 (2014) 1180–1191.
[58] S. Dikalov, Cross talk between mitochondria and NADPH oxidases, Free Radic. Biol. Med. 51 (2011) 1289–1301.
[59] D.B. Zorov, C.R. Filburn, L.O. Klotz, J.L. Zweier, S.J. Sollott, Reactive oxygen species (ROS)-induced ROS release: a new phenomenon accompanying induction of the mitochondrial permeability transition in cardiac myocytes, J. Exp. Med. 192 (2000) 1001–1014.
[60] E. Schulz, P. Wenzel, T. Munzel, A. Daiber, Mitochondrial redox signaling: interaction of mitochondrial reactive oxygen species with other sources of oxidative stress, Antioxid. Redox Signal. 20 (2014) 308–324.

[61] P. Wenzel, H. Mollnau, M. Oelze, E. Schulz, J.M. Wickramanayake, J. Muller, S. Schuhmacher, M. Hortmann, S. Baldus, T. Gori, R.P. Brandes, T. Munzel, A. Daiber, First evidence for a crosstalk between mitochondrial and NADPH oxidase-derived reactive oxygen species in nitroglycerin-triggered vascular dysfunction, Antioxid. Redox Signal. 10 (2008) 1435–1447.

[62] M. Oelze, S. Kroller-Schon, S. Steven, E. Lubos, C. Doppler, M. Hausding, S. Tobias, C. Brochhausen, H. Li, M. Torzewski, P. Wenzel, M. Bachschmid, K.J. Lackner, E. Schulz, T. Munzel, A. Daiber, Glutathione peroxidase-1 deficiency potentiates dysregulatory modifications of endothelial nitric oxide synthase and vascular dysfunction in aging, Hypertension 63 (2014) 390–396.

[63] S. Kroller-Schon, S. Steven, S. Kossmann, A. Scholz, S. Daub, M. Oelze, N. Xia, M. Hausding, Y. Mikhed, E. Zinssius, M. Mader, P. Stamm, N. Treiber, K. Scharffetter-Kochanek, H. Li, E. Schulz, P. Wenzel, T. Munzel, A. Daiber, Molecular mechanisms of the crosstalk between mitochondria and NADPH oxidase through reactive oxygen species-studies in white blood cells and in animal models, Antioxid. Redox Signal. 20 (2014) 247–266.

[64] A. Jankovic, A. Korac, B. Buzadzic, V. Otasevic, A. Stancic, A. Daiber, B. Korac, Redox implications in adipose tissue (dys)function – a new look at old acquaintances, Redox Biol. 6 (2015) 19–32.

[65] J.D. Lambeth, A.S. Neish, Nox enzymes and new thinking on reactive oxygen: a double-edged sword revisited, Annu. Rev. Pathol. 9 (2014) 119–145.

[66] F. Sommer, F. Backhed, The gut microbiota engages different signaling pathways to induce Duox2 expression in the ileum and colon epithelium, Mucosal Immunol. 8 (2015) 372–379.

[67] N. Corcionivoschi, L.A. Alvarez, T.H. Sharp, M. Strengert, A. Alemka, J. Mantell, P. Verkade, U.G. Knaus, B. Bourke, Mucosal reactive oxygen species decrease virulence by disrupting campylobacter jejuni phosphotyrosine signaling, Cell Host Microbe 12 (2012) 47–59.

[68] L.A. Alvarez, L. Kovacic, J. Rodriguez, J.H. Gosemann, M. Kubica, G.G. Pircalabioru, F. Friedmacher, A. Cean, A. Ghise, M.B. Sarandan, P. Puri, S. Daff, E. Plettner, A. von Kriegsheim, B. Bourke, U.G. Knaus, NADPH oxidase-derived H2O2 subverts pathogen signaling by oxidative phosphotyrosine conversion to PB-DOPA, Proc. Natl. Acad. Sci. USA 113 (2016) 10406–10411.

[69] G. Pircalabioru, G. Aviello, M. Kubica, A. Zhdanov, M.H. Paclet, L. Brennan, R. Hertzberger, D. Papkovsky, B. Bourke, U.G. Knaus, Defensive mutualism rescues NADPH oxidase inactivation in gut infection, Cell Host Microbe 19 (2016) 651–663.

[70] A.S. Neish, R.M. Jones, Redox signaling mediates symbiosis between the gut microbiota and the intestine, Gut Microbes 5 (2014) 250–253.

[71] A. Rimessi, M. Previati, F. Nigro, M.R. Wieckowski, P. Pinton, Mitochondrial reactive oxygen species and inflammation: molecular mechanisms, diseases and promising therapies, Int. J. Biochem. Cell Biol. 81 (2016) 281–293.

[72] R. Hertzberger, J. Arents, H.L. Dekker, R.D. Pridmore, C. Gysler, M. Kleerebezem, M.J. de Mattos, H(2)O(2) production in species of the Lactobacillus acidophilus group: a central role for a novel NADH-dependent flavin reductase, Appl. Environ. Microbiol. 80 (2014) 2229–2239.

[73] A. Ito, Y. Sato, S. Kudo, S. Sato, H. Nakajima, T. Toba, The screening of hydrogen peroxide-producing lactic acid bacteria and their application to inactivating psychrotrophic food-borne pathogens, Curr. Microbiol. 47 (2003) 231–236.

[74] R. Benisty, A.Y. Cohen, A. Feldman, Z. Cohen, N. Porat, Endogenous H2O2 produced by Streptococcus pneumoniae controls FabF activity, Biochim. Biophys. Acta 1801 (2010) 1098–1104.

[75] C.D. Pericone, K. Overweg, P.W. Hermans, J.N. Weiser, Inhibitory and bactericidal effects of hydrogen peroxide production by Streptococcus pneumoniae on other inhabitants of the upper respiratory tract, Infect. Immun. 68 (2000) 3990–3997.

[76] T.I. Moy, E. Mylonakis, S.B. Calderwood, F.M. Ausubel, Cytotoxicity of hydrogen peroxide produced by Enterococcus faecium, Infect. Immun. 72 (2004) 4512–4520.

[77] E.K. Marsh, R.C. May, Caenorhabditis elegans, a model organism for investigating immunity, Appl. Environ. Microbiol. 78 (2012) 2075–2081.

[78] R. van der Hoeven, K.C. McCallum, D.A. Garsin, Speculations on the activation of ROS generation in C. elegans innate immune signaling, Worm 1 (2012) 160–163.

[79] K.M. Balla, E.R. Troemel, Caenorhabditis elegans as a model for intracellular pathogen infection, Cell Microbiol. 15 (2013) 1313–1322.

[80] J.A. Mora-Lorca, B. Saenz-Narciso, C.J. Gaffney, F.J. Naranjo-Galindo, J.R. Pedrajas, D. Guerrero-Gomez, A. Dobrzynska, P. Askjaer, N.J. Szewczyk, J. Cabello, A. Miranda-Vizuete, Glutathione reductase gsr-1 is an essential gene required for Caenorhabditis elegans early embryonic development, Free Radic. Biol. Med. 96 (2016) 446–461.

[81] J. Stenvall, J.C. Fierro-Gonzalez, P. Swoboda, K. Saamarthy, Q. Cheng, B. Cacho-Valadez, E.S. Arner, O.P. Persson, A. Miranda-Vizuete, S. Tuck, Selenoprotein TRXR-1 and GSR-1 are essential for removal of old cuticle during molting in Caenorhabditis elegans, Proc Natl. Acad. Sci. USA 108 (2011) 1064–1069.

[82] N. Bhatla, H.R. Horvitz, Light and hydrogen peroxide inhibit C. elegans Feeding through gustatory receptor orthologs and pharyngeal neurons, Neuron 85 (2015) 804–818.

[83] M. Olahova, E.A. Veal, A peroxiredoxin, PRDX-2, is required for insulin secretion and insulin/IIS-dependent regulation of stress resistance and longevity, Aging Cell 14 (2015) 558–568.

[84] G.S. Shadel, T.L. Horvath, Mitochondrial ROS signaling in organismal homeostasis, Cell 163 (2015) 560–569.

[85] T.K. Blackwell, M.J. Steinbaugh, J.M. Hourihan, C.Y. Ewald, M. Isik, SKN-1/Nrf, stress responses, and aging in Caenorhabditis elegans, Free Radic. Biol. Med. 88 (2015) 290–301.

[86] L.R. Lapierre, M. Hansen, Lessons from C. elegans: signaling pathways for longevity, Trends Endocrinol. Metab. 23 (2012) 637–644.

[87] F. Cabreiro, D. Gems, Worms need microbes too: microbiota, health and aging in Caenorhabditis elegans, EMBO Mol. Med. 5 (2013) 1300–1310.

[88] D. Knoefler, M. Thamsen, M. Koniczek, N.J. Niemuth, A.K. Diederich, U. Jakob, Quantitative in vivo redox sensors uncover oxidative stress as an early event in life, Mol. Cell 47 (2012) 767–776.

[89] J. Yang, K.S. Carroll, D.C. Liebler, The expanding landscape of the thiol redox proteome, Mol. Cell Proteom. 15 (2016) 1–11.

[90] T.H. Truong, K.S. Carroll, Redox regulation of protein kinases, Crit. Rev. Biochem. Mol. Biol. 48 (2013) 332–356.

[91] J. Westermarck, J. Ivaska, G.L. Corthals, Identification of protein interactions involved in cellular signaling, Mol. Cell Proteom. 12 (2013) 1752–1763.

[92] I.S. Arts, D. Vertommen, F. Baldin, G. Laloux, J.F. Collet, Comprehensively characterizing the thioredoxin interactome in vivo highlights the central role played by this ubiquitous oxidoreductase in redox control, Mol. Cell Proteom. 15 (2016) 2125–2140.

[93] D. Bartolini, F. Galli, The functional interactome of GSTP: a regulatory biomolecular network at the interface with the Nrf2 adaption response to oxidative stress, J. Chromatogr. B Anal. Technol. Biomed. Life Sci. 1019 (2016) 29–44.

[94] P. Zolotukhin, Y. Kozlova, A. Dovzhik, K. Kovalenko, K. Kutsyn, A. Aleksandrova, T. Shkurat, Oxidative status interactome map: towards novel approaches in experiment planning, data analysis, diagnostics and therapy, Mol. Biosyst. 9 (2013) 2085–2096.

[95] I. Verrastro, K. Tveen-Jensen, R. Woscholski, C.M. Spickett, A.R. Pitt, Reversible oxidation of phosphatase and tensin homolog (PTEN) alters its interactions with signaling and regulatory proteins, Free Radic. Biol. Med. 90 (2016) 24–34.

[96] A. Petry, T. Djordjevic, M. Weitnauer, T. Kietzmann, J. Hess, A. Gorlach, NOX2 and NOX4 mediate proliferative response in endothelial cells, Antioxid. Redox Signal. 8 (2006) 1473–1484.

[97] T. Rzymski, A. Petry, D. Kracun, F. Riess, L. Pike, A.L. Harris, A. Gorlach, The unfolded protein response controls induction and activation of ADAM17/TACE by severe hypoxia and ER stress, Oncogene 31 (2012) 3621–3634.

[98] M. Janiszewski, L.R. Lopes, A.O. Carmo, M.A. Pedro, R.P. Brandes, C.X. Santos, F.R. Laurindo, Regulation of NAD(P)H oxidase by associated protein disulfide isomerase in vascular smooth muscle cells, J. Biol. Chem. 280 (2005) 40813–40819.

[99] C. He, H. Zhu, W. Zhang, I. Okon, Q. Wang, H. Li, Y.Z. Le, Z. Xie, 7-Ketocholesterol induces autophagy in vascular smooth muscle cells through Nox4 and Atg4B, Am. J. Pathol. 183 (2013) 626–637.

[100] E. Pedruzzi, C. Guichard, V. Ollivier, F. Driss, M. Fay, C. Prunet, J.C. Marie, C. Pouzet, M. Samadi, C. Elbim, Y. O'Dowd, M. Bens, A. Vandewalle, M.A. Gougerot-Pocidalo, G. Lizard, E. Ogier-Denis, NAD(P)H oxidase Nox-4 mediates 7-ketocholesterol-induced endoplasmic reticulum stress and apoptosis in human aortic smooth muscle cells, Mol. Cell Biol. 24 (2004) 10703–10717.

[101] C.X. Santos, A.D. Hafstad, M. Beretta, M. Zhang, C. Molenaar, J. Kopec, D. Fotinou, T.V. Murray, A.M. Cobb, D. Martin, M. Zeh Silva, N. Anilkumar, K. Schroder, C.M. Shanahan, A.C. Brewer, R.P. Brandes, E. Blanc, M. Parsons, V. Belousov, R. Cammack, R.C. Hider, R.A. Steiner, A.M. Shah, Targeted redox inhibition of protein phosphatase 1 by Nox4 regulates eIF2alpha-mediated stress signaling, EMBO J. 35 (2016) 319–334.

[102] B. Li, J. Tian, Y. Sun, T.R. Xu, R.F. Chi, X.L. Zhang, X.L. Hu, Y.A. Zhang, F.Z. Qin, W.F. Zhang, Activation of NADPH oxidase mediates increased endoplasmic reticulum stress and left ventricular remodeling after myocardial infarction in rabbits, Biochim. Biophys. Acta 1852 (2015) 805–815.

[103] G. Li, C. Scull, L. Ozcan, I. Tabas, NADPH oxidase links endoplasmic reticulum stress, oxidative stress, and PKR activation to induce apoptosis, J. Cell Biol. 191 (2010) 1113–1125.

[104] C. Pavoine, F. Pecker, Sphingomyelinases: their regulation and roles in cardiovascular pathophysiology, Cardiovasc. Res. 82 (2009) 175–183.

[105] S. Corda, C. Laplace, E. Vicaut, J. Duranteau, Rapid reactive oxygen species production by mitochondria in endothelial cells exposed to tumor necrosis factor-alpha is mediated by ceramide, Am. J. Respir. Cell Mol. Biol. 24 (2001) 762–768.

[106] S. Lecour, Van der Merwe, E. Opie, L.H. Sack, M.N. Ceramide, attenuates hypoxic cell death via reactive oxygen species signaling, J. Cardiovasc. Pharmacol. 47 (2006) 158–163.

[107] J.S. Won, Y.B. Im, M. Khan, A.K. Singh, I. Singh, The role of neutral sphingomyelinase produced ceramide in lipopolysaccharide-mediated expression of inducible nitric oxide synthase, J. Neurochem. 88 (2004) 583–593.

[108] O.M. Hernandez, D.J. Discher, N.H. Bishopric, K.A. Webster, Rapid activation of neutral sphingomyelinase by hypoxia-reoxygenation of cardiac myocytes, Circ. Res. 86 (2000) 198–204.

[109] B. Unal, F. Ozcan, H. Tuzcu, E. Kirac, G.O. Elpek, M. Aslan, Inhibition of neutral sphingomyelinase decreases elevated levels of nitrative and oxidative stress markers in liver ischemia-reperfusion injury, Redox Rep. (2016) 1–13.

[110] C. Adamy, P. Mulder, L. Khouzami, N. Andrieu-abadie, N. Defer, G. Candiani, C. Pavoine, P. Caramelle, R. Souktani, P. Le Corvoisier, M. Perier, M. Kirsch, T. Damy, A. Berdeaux, T. Levade, C. Thuillez, L. Hittinger, F. Pecker, Neutral sphingomyelinase inhibition participates to the benefits of N-acetylcysteine treatment in post-myocardial infarction failing heart rats, J. Mol. Cell Cardiol. 43 (2007) 344–353.

[111] H. Sawai, Y.A. Hannun, Ceramide and sphingomyelinases in the regulation of stress responses, Chem. Phys. Lipids 102 (1999) 141–147.

[112] C. Perrotta, E. Clementi, Biological roles of Acid and neutral sphingomyelinases and their regulation by nitric oxide, Physiology 25 (2010) 64–71.

[113] K. Pahan, F.G. Sheikh, M. Khan, A.M. Namboodiri, I. Singh, Sphingomyelinase and ceramide stimulate the expression of inducible nitric-oxide synthase in rat primary astrocytes, J. Biol. Chem. 273 (1998) 2591–2600.

[114] K. Katsuyama, M. Shichiri, F. Marumo, Y. Hirata, Role of nuclear factor-kappaB activation in cytokine- and sphingomyelinase-stimulated inducible nitric oxide synthase gene expression in vascular smooth muscle cells, Endocrinology 139 (1998) 4506–4512.
[115] M.S. Yang, I. Jou, H. Inn-Oc, E. Joe, Sphingomyelinase but not ceramide induces nitric oxide synthase expression in rat brain microglia, Neurosci. Lett. 311 (2001) 133–136.
[116] M. Aslan, G. Basaranlar, M. Unal, A. Ciftcioglu, N. Derin, B. Mutus, Inhibition of neutral sphingomyelinase decreases elevated levels of inducible nitric oxide synthase and apoptotic cell death in ocular hypertensive rats, Toxicol. Appl. Pharmacol. 280 (2014) 389–398.
[117] E. Masseret, S. Banack, F. Boumediene, E. Abadie, L. Brient, F. Pernet, R. Juntas-Morales, N. Pageot, J. Metcalf, P. Cox, W. Camu, French Network on, A. L. S. C. D. Investigation, Dietary BMAA exposure in an amyotrophic lateral sclerosis cluster from southern France, PLoS ONE 8 (2013) e83406.
[118] X. Huang, L. Chen, W. Liu, Q. Qiao, K. Wu, J. Wen, C. Huang, R. Tang, X. Zhang, Involvement of oxidative stress and cytoskeletal disruption in microcystin-induced apoptosis in CIK cells, Aquat. Toxicol. 165 (2015) 41–50.
[119] C. Krakstad, L. Herfindal, B.T. Gjertsen, R. Boe, O.K. Vintermyr, K.E. Fladmark, S.O. Doskeland, CaM-kinaseII-dependent commitment to microcystin-induced apoptosis is coupled to cell budding, but not to shrinkage or chromatin hypercondensation, Cell Death Differ. 13 (2006) 1191–1202.
[120] L.V. Hjornevik, L. Fismen, F.M. Young, T. Solstad, K.E. Fladmark, Nodularin exposure induces SOD1 phosphorylation and disrupts SOD1 co-localization with actin filaments, Toxins 4 (2012) 1482–1499.
[121] O. Okle, K. Stemmer, U. Deschl, D.R. Dietrich, L-BMAA induced ER stress and enhanced caspase 12 cleavage in human neuroblastoma SH-SY5Y cells at low nonexcitotoxic concentrations, Toxicol. Sci. 131 (2013) 217–224.
[122] A.S. Chiu, M.M. Gehringer, N. Braidy, G.J. Guillemin, J.H. Welch, B.A. Neilan, Excitotoxic potential of the cyanotoxin beta-methyl-amino-L-alanine (BMAA) in primary human neurons, Toxicon 60 (2012) 1159–1165.
[123] J.R. Erickson, M.L. Joiner, X. Guan, W. Kutschke, J. Yang, C.V. Oddis, R.K. Bartlett, J.S. Lowe, S.E. O'Donnell, N. Aykin-Burns, M.C. Zimmerman, K. Zimmerman, A.J. Ham, R.M. Weiss, D.R. Spitz, M.A. Shea, R.J. Colbran, P.J. Mohler, M.E. Anderson, A dynamic pathway for calcium-independent activation of CaMKII by methionine oxidation, Cell 133 (2008) 462–474.
[124] M. Arif, S.F. Kazim, I. Grundke-Iqbal, R.M. Garruto, K. Iqbal, Tau pathology involves protein phosphatase 2A in parkinsonism-dementia of Guam, Proc. Natl. Acad. Sci. USA 111 (2014) 1144–1149.
[125] F. Raka, A.R. Di Sebastiano, S.C. Kulhawy, F.M. Ribeiro, C.M. Godin, F.A. Caetano, S. Angers, S.S. Ferguson, Ca(2+)/calmodulin-dependent protein kinase II interacts with group I metabotropic glutamate and facilitates receptor endocytosis and ERK1/2 signaling: role of beta-amyloid, Mol. Brain 8 (2015) 21.
[126] R.C. Fahey, Glutathione analogs in prokaryotes, Biochim. Biophys. Acta 1830 (2013) 3182–3198.
[127] V.V. Loi, M. Rossius, H. Antelmann, Redox regulation by reversible protein S-thiolation in bacteria, Front. Microbiol. 6 (2015) 187.
[128] J.W. Lee, S. Soonsanga, J.D. Helmann, A complex thiolate switch regulates the Bacillus subtilis organic peroxide sensor OhrR, Proc. Natl. Acad. Sci. USA 104 (2007) 8743–8748.
[129] A. Gaballa, B.K. Chi, A.A. Roberts, D. Becher, C.J. Hamilton, H. Antelmann, J.D. Helmann, Redox regulation in Bacillus subtilis: the bacilliredoxins BrxA(YphP) and BrxB(YqiW) function in de-bacillithiolation of S-bacillithiolated OhrR and MetE, Antioxid. Redox Signal. 21 (2014) 357–367.
[130] B.K. Chi, T. Busche, K. Van Laer, K. Basell, D. Becher, L. Clermont, G.M. Seibold, M. Persicke, J. Kalinowski, J. Messens, H. Antelmann, Protein S-mycothiolation functions as redox-switch and thiol protection mechanism in Corynebacterium glutamicum under hypochlorite stress, Antioxid. Redox Signal. 20 (2014) 589–605.
[131] B. Pedre, I. Van Molle, A.F. Villadangos, K. Wahni, D. Vertommen, L. Turell, H. Erdogan, L.M. Mateos, J. Messens, The Corynebacterium glutamicum mycothiol peroxidase is a reactive oxygen species-scavenging enzyme that shows promiscuity in thiol redox control, Mol. Microbiol. 96 (2015) 1176–1191.
[132] M.A. Tossounian, B. Pedre, K. Wahni, H. Erdogan, D. Vertommen, I. Van Molle, J. Messens, Corynebacterium diphtheriae methionine sulfoxide reductase a exploits a unique mycothiol redox relay mechanism, J. Biol. Chem. 290 (2015) 11365–11375.
[133] S. Gilroy, N. Suzuki, G. Miller, W.G. Choi, M. Toyota, A.R. Devireddy, R. Mittler, A tidal wave of signals: calcium and ROS at the forefront of rapid systemic signaling, Trends Plant Sci. 19 (2014) 623–630.
[134] E.J. Calabrese, I. Iavicoli, V. Calabrese, Hormesis: its impact on medicine and health, Hum. Exp. Toxicol. 32 (2013) 120–152.
[135] O. Yelisyeyeva, K. Semen, N. Zarkovic, D. Kaminskyy, O. Lutsyk, V. Rybalchenko, Activation of aerobic metabolism by Amaranth oil improves heart rate variability both in athletes and patients with type 2 diabetes mellitus, Arch. Physiol. Biochem. 118 (2012) 47–57.
[136] E.T. Chouchani, V.R. Pell, E. Gaude, D. Aksentijevic, S.Y. Sundier, E.L. Robb, A. Logan, S.M. Nadtochiy, E.N. Ord, A.C. Smith, F. Eyassu, R. Shirley, C.H. Hu, A.J. Dare, A.M. James, S. Rogatti, R.C. Hartley, S. Eaton, A.S. Costa, P.S. Brookes, S.M. Davidson, M.R. Duchen, K. Saeb-Parsy, M.J. Shattock, A.J. Robinson, L.M. Work, C. Frezza, T. Krieg, M.P. Murphy, Ischaemic accumulation of succinate controls reperfusion injury through mitochondrial ROS, Nature 515 (2014) 431–435.
[137] F. Yin, H. Sancheti, Z. Liu, E. Cadenas, Mitochondrial function in ageing: coordination with signalling and transcriptional pathways, J. Physiol. 594 (2016) 2025–2042.
[138] Y.M. Go, D.P. Jones, The redox proteome, J. Biol. Chem. 288 (2013) 26512–26520.
[139] G.R. Buettner, B.A. Wagner, V.G. Rodgers, Quantitative redox biology: an approach to understand the role of reactive species in defining the cellular redox environment, Cell Biochem. Biophys. 67 (2013) 477–483.
[140] C.S. Pillay, B.D. Eagling, S.R. Driscoll, J.M. Rohwer, Quantitative measures for redox signaling, Free Radic. Biol. Med. 96 (2016) 290–303.
[141] H.S. Marinho, C. Real, L. Cyrne, H. Soares, F. Antunes, Hydrogen peroxide sensing, signaling and regulation of transcription factors, Redox Biol. 2 (2014) 535–562.
[142] R. Rodrigo, M. Libuy, F. Feliu, D. Hasson, Oxidative stress-related biomarkers in essential hypertension and ischemia-reperfusion myocardial damage, Dis. Markers 35 (2013) 773–790.
[143] D. Leonetti, J.M. Reimund, A. Tesse, S. Viennot, M.C. Martinez, A.L. Bretagne, R. Andriantsitohaina, Circulating microparticles from Crohn's disease patients cause endothelial and vascular dysfunctions, PLoS One 8 (2013) e73088.
[144] J. Bhullar, V.M. Bhopale, M. Yang, K. Sethuraman, S.R. Thom, Microparticle formation by platelets exposed to high gas pressures – an oxidative stress response, Free Radic. Biol. Med. 101 (2016) 154–162.
[145] W.Q. Han, F.J. Chang, Q.R. Wang, J.Q. Pan, Microparticles from patients with the acute coronary syndrome impair vasodilatation by inhibiting the Akt/eNOS-Hsp90 signaling pathway, Cardiology 132 (2015) 252–260.
[146] T.N. Pitanga, L. de Aragao Franca, V.C. Rocha, T. Meirelles, V.M. Borges, M.S. Goncalves, L.C. Pontes-de-Carvalho, A.A. Noronha-Dutra, W.L. dos-Santos, Neutrophil-derived microparticles induce myeloperoxidase-mediated damage of vascular endothelial cells, BMC Cell Biol. 15 (2014) 21.
[147] A. Fleury, M.C. Martinez, S. Le Lay, Extracellular vesicles as therapeutic tools in cardiovascular diseases, Front. Immunol. 5 (2014) 370.
[148] D. Burger, D.G. Kwart, A.C. Montezano, N.C. Read, C.R. Kennedy, C.S. Thompson, R.M. Touyz, Microparticles induce cell cycle arrest through redox-sensitive processes in endothelial cells: implications in vascular senescence, J. Am. Heart Assoc. 1 (2012) e001842.
[149] D. Burger, M. Turner, M.N. Munkonda, R.M. Touyz, Endothelial microparticle-derived reactive oxygen species: role in endothelial signaling and vascular function, Oxid. Med. Cell Longev. 2016 (2016) 5047954.
[150] Z. Safiedeen, I. Rodriguez-Gomez, L. Vergori, R. Soleti, D. Vaithilingam, I. Douma, A. Agouni, D. Leiber, S. Dubois, G. Simard, K. Zibara, R. Andriantsitohaina, M.C. Martinez, Temporal cross talk between endoplasmic reticulum and mitochondria regulates oxidative stress and mediates microparticle-induced endothelial dysfunction, Antioxid. Redox Signal. 26 (2017) 15–27.
[151] H. Cai, Hydrogen peroxide regulation of endothelial function: origins, mechanisms, and consequences, Cardiovasc. Res. 68 (2005) 26–36.
[152] H.D. Skinner, J.Z. Zheng, J. Fang, F. Agani, B.H. Jiang, Vascular endothelial growth factor transcriptional activation is mediated by hypoxia-inducible factor 1alpha, HDM2, and p70S6K1 in response to phosphatidylinositol 3-kinase/AKT signaling, J. Biol. Chem. 279 (2004) 45643–45651.
[153] J.H. Ryu, S.H. Li, H.S. Park, J.W. Park, B. Lee, Y.S. Chun, Hypoxia-inducible factor alpha subunit stabilization by NEDD8 conjugation is reactive oxygen species-dependent, J. Biol. Chem. 286 (2011) 6963–6970.
[154] S.A. Patel, M.C. Simon, Biology of hypoxia-inducible factor-2alpha in development and disease, Cell Death Differ. 15 (2008) 628–634.
[155] Z. Arany, S.Y. Foo, Y. Ma, J.L. Ruas, A. Bommi-Reddy, G. Girnun, M. Cooper, D. Laznik, J. Chinsomboon, S.M. Rangwala, K.H. Baek, A. Rosenzweig, B.M. Spiegelman, HIF-independent regulation of VEGF and angiogenesis by the transcriptional coactivator PGC-1alpha, Nature 451 (2008) 1008–1012.
[156] M. Ushio-Fukai, R.W. Alexander, Reactive oxygen species as mediators of angiogenesis signaling: role of NAD(P)H oxidase, Mol. Cell Biochem. 264 (2004) 85–97.
[157] R. Colavitti, G. Pani, B. Bedogni, R. Anzevino, S. Borrello, J. Waltenberger, T. Galeotti, Reactive oxygen species as downstream mediators of angiogenic signaling by vascular endothelial growth factor receptor-2/KDR, J. Biol. Chem. 277 (2002) 3101–3108.
[158] D.H. Kang, D.J. Lee, K.W. Lee, Y.S. Park, J.Y. Lee, S.H. Lee, Y.J. Koh, G.Y. Koh, C. Choi, D.Y. Yu, J. Kim, S.W. Kang, Peroxiredoxin II is an essential antioxidant enzyme that prevents the oxidative inactivation of VEGF receptor-2 in vascular endothelial cells, Mol. Cell 44 (2011) 545–558.
[159] N.K. Tonks, Redox redux: revisiting PTPs and the control of cell signaling, Cell 121 (2005) 667–670.
[160] J. Oshikawa, N. Urao, H.W. Kim, N. Kaplan, M. Razvi, R. McKinney, L.B. Poole, T. Fukai, M. Ushio-Fukai, Extracellular SOD-derived H2O2 promotes VEGF signaling in caveolae/lipid rafts and post-ischemic angiogenesis in mice, PLoS One 5 (2010) e10189.
[161] M.R. Abid, K.C. Spokes, S.C. Shih, W.C. Aird, NADPH oxidase activity selectively modulates vascular endothelial growth factor signaling pathways, J. Biol. Chem. 282 (2007) 35373–35385.
[162] S. Kobayashi, Y. Nojima, M. Shibuya, Y. Maru, Nox1 regulates apoptosis and potentially stimulates branching morphogenesis in sinusoidal endothelial cells, Exp. Cell Res. 300 (2004) 455–462.
[163] M. Ushio-Fukai, Y. Tang, T. Fukai, S.I. Dikalov, Y. Ma, M. Fujimoto, M.T. Quinn, P.J. Pagano, C. Johnson, R.W. Alexander, Novel role of gp91(phox)-containing NAD(P)H oxidase in vascular endothelial growth factor-induced signaling and angiogenesis, Circ. Res. 91 (2002) 1160–1167.
[164] T. Tojo, M. Ushio-Fukai, M. Yamaoka-Tojo, S. Ikeda, N. Patrushev, R.W. Alexander, Role of gp91phox (Nox2)-containing NAD(P)H oxidase in angiogenesis in response to hindlimb ischemia, Circulation 111 (2005) 2347–2355.
[165] S.R. Datla, H. Peshavariya, G.J. Dusting, K. Mahadev, B.J. Goldstein, F. Jiang,

Important role of Nox4 type NADPH oxidase in angiogenic responses in human microvascular endothelial cells in vitro, Arterioscler. Thromb. Vasc. Biol. 27 (2007) 2319–2324.
[166] M. Yamaoka-Tojo, T. Tojo, H.W. Kim, L. Hilenski, N.A. Patrushev, L. Zhang, T. Fukai, M. Ushio-Fukai, IQGAP1 mediates VE-cadherin-based cell-cell contacts and VEGF signaling at adherence junctions linked to angiogenesis, Arterioscler. Thromb. Vasc. Biol. 26 (2006) 1991–1997.
[167] S. Ikeda, M. Yamaoka-Tojo, L. Hilenski, N.A. Patrushev, G.M. Anwar, M.T. Quinn, M. Ushio-Fukai, IQGAP1 regulates reactive oxygen species-dependent endothelial cell migration through interacting with Nox2, Arterioscler. Thromb. Vasc. Biol. 25 (2005) 2295–2300.
[168] Y. Wang, Q.S. Zang, Z. Liu, Q. Wu, D. Maass, G. Dulan, P.W. Shaul, L. Melito, D.E. Frantz, J.A. Kilgore, N.S. Williams, L.S. Terada, F.E. Nwariaku, Regulation of VEGF-induced endothelial cell migration by mitochondrial reactive oxygen species, Am. J. Physiol. Cell Physiol. 301 (2011) C695–C704.
[169] S. Borniquel, N. Garcia-Quintans, I. Valle, Y. Olmos, B. Wild, F. Martinez-Granero, E. Soria, S. Lamas, M. Monsalve, Inactivation of Foxo3a and subsequent down-regulation of PGC-1 alpha mediate nitric oxide-induced endothelial cell migration, Mol. Cell Biol. 30 (2010) 4035–4044.
[170] N. Garcia-Quintans, I. Prieto, C. Sanchez-Ramos, A. Luque, E. Arza, Y. Olmos, M. Monsalve, Regulation of endothelial dynamics by PGC-1alpha relies on ROS control of VEGF-A signaling, Free Radic. Biol. Med. 93 (2016) 41–51.
[171] N. Garcia-Quintans, C. Sanchez-Ramos, I. Prieto, A. Tierrez, E. Arza, A. Alfranca, J.M. Redondo, M. Monsalve, Oxidative stress induces loss of pericyte coverage and vascular instability in PGC-1alpha-deficient mice, Angiogenesis 19 (2016) 217–228.
[172] J. Massague, TGFbeta signalling in context, Nat. Rev. Mol. Cell Biol. 13 (2012) 616–630.
[173] I. Fabregat, J. Moreno-Caceres, A. Sanchez, S. Dooley, B. Dewidar, G. Giannelli, P. Ten Dijke, I.-L. Consortium, TGF-beta signalling and liver disease, FEBS J. 283 (2016) 2219–2232.
[174] A. Sanchez, A.M. Alvarez, M. Benito, I. Fabregat, Apoptosis induced by transforming growth factor-beta in fetal hepatocyte primary cultures: involvement of reactive oxygen intermediates, J. Biol. Chem. 271 (1996) 7416–7422.
[175] V.J. Thannickal, B.L. Fanburg, Activation of an H2O2-generating NADH oxidase in human lung fibroblasts by transforming growth factor beta 1, J. Biol. Chem. 270 (1995) 30334–30338.
[176] B. Herrera, M.M. Murillo, A. Alvarez-Barrientos, J. Beltran, M. Fernandez, I. Fabregat, Source of early reactive oxygen species in the apoptosis induced by transforming growth factor-beta in fetal rat hepatocytes, Free Radic. Biol. Med. 36 (2004) 16–26.
[177] I. Carmona-Cuenca, C. Roncero, P. Sancho, L. Caja, N. Fausto, M. Fernandez, I. Fabregat, Upregulation of the NADPH oxidase NOX4 by TGF-beta in hepatocytes is required for its pro-apoptotic activity, J. Hepatol. 49 (2008) 965–976.
[178] S. Carnesecchi, C. Deffert, Y. Donati, O. Basset, B. Hinz, O. Preynat-Seauve, C. Guichard, J.L. Arbiser, B. Banfi, J.C. Pache, C. Barazzone-Argiroffo, K.H. Krause, A key role for NOX4 in epithelial cell death during development of lung fibrosis, Antioxid. Redox Signal. 15 (2011) 607–619.
[179] J. Moreno-Caceres, J. Mainez, R. Mayoral, P. Martin-Sanz, G. Egea, I. Fabregat, Caveolin-1-dependent activation of the metalloprotease TACE/ADAM17 by TGF-beta in hepatocytes requires activation of Src and the NADPH oxidase NOX1, FEBS J. 283 (2016) 1300–1310.
[180] P. Sancho, E. Bertran, L. Caja, I. Carmona-Cuenca, M.M. Murillo, I. Fabregat, The inhibition of the epidermal growth factor (EGF) pathway enhances TGF-beta-induced apoptosis in rat hepatoma cells through inducing oxidative stress coincident with a change in the expression pattern of the NADPH oxidases (NOX) isoforms, Biochim. Biophys. Acta 1793 (2009) 253–263.
[181] H.E. Boudreau, B.W. Casterline, B. Rada, A. Korzeniowska, T.L. Leto, Nox4 involvement in TGF-beta and SMAD3-driven induction of the epithelial-to-mesenchymal transition and migration of breast epithelial cells, Free Radic. Biol. Med. 53 (2012) 1489–1499.
[182] I. Cucoranu, R. Clempus, A. Dikalova, P.J. Phelan, S. Ariyan, S. Dikalov, D. Sorescu, NAD(P)H oxidase 4 mediates transforming growth factor-beta1-induced differentiation of cardiac fibroblasts into myofibroblasts, Circ. Res. 97 (2005) 900–907.
[183] L. Hecker, R. Vittal, T. Jones, R. Jagirdar, T.R. Luckhardt, J.C. Horowitz, S. Pennathur, F.J. Martinez, V.J. Thannickal, NADPH oxidase-4 mediates myofibroblast activation and fibrogenic responses to lung injury, Nat. Med. 15 (2009) 1077–1081.
[184] P. Sancho, J. Mainez, E. Crosas-Molist, C. Roncero, C.M. Fernandez-Rodriguez, F. Pinedo, H. Huber, R. Eferl, W. Mikulits, I. Fabregat, NADPH oxidase NOX4 mediates stellate cell activation and hepatocyte cell death during liver fibrosis development, PLoS One 7 (2012) e45285.
[185] E. Crosas-Molist, E. Bertran, P. Sancho, J. Lopez-Luque, J. Fernando, A. Sanchez, M. Fernandez, E. Navarro, I. Fabregat, The NADPH oxidase NOX4 inhibits hepatocyte proliferation and liver cancer progression, Free Radic. Biol. Med. 69 (2014) 338–347.
[186] G.Y. Liou, P. Storz, Reactive oxygen species in cancer, Free Radic. Res. 44 (2010) 479–496.
[187] E. Panieri, M.M. Santoro, ROS homeostasis and metabolism: a dangerous liaison in cancer cells, Cell Death Dis. 7 (2016) e2253.
[188] D. Rojas-Rivera, C. Hetz, TMBIM protein family: ancestral regulators of cell death, Oncogene 34 (2015) 269–280.
[189] L. Hu, T.F. Smith, G. Goldberger, LFG: a candidate apoptosis regulatory gene family, Apoptosis 14 (2009) 1255–1265.
[190] G. Carrara, N. Saraiva, C. Gubser, B.F. Johnson, G.L. Smith, Six-transmembrane topology for Golgi anti-apoptotic protein (GAAP) and Bax inhibitor 1 (BI-1) provides model for the transmembrane Bax inhibitor-containing motif (TMBIM) family, J. Biol. Chem. 287 (2012) 15896–15905.
[191] G. Carrara, N. Saraiva, M. Parsons, B. Byrne, D.L. Prole, C.W. Taylor, G.L. Smith, Golgi anti-apoptotic proteins are highly conserved ion channels that affect apoptosis and cell migration, J. Biol. Chem. 290 (2015) 11785–11801.
[192] C. Gubser, D. Bergamaschi, M. Hollinshead, X. Lu, F.J. van Kuppeveld, G.L. Smith, A new inhibitor of apoptosis from vaccinia virus and eukaryotes, PLoS Pathog. 3 (2007) e17.
[193] C. Gubser, G.L. Smith, The sequence of camelpox virus shows it is most closely related to variola virus, the cause of smallpox, J. Gen. Virol. 83 (2002) 855–872.
[194] F. de Mattia, C. Gubser, M.M. van Dommelen, H.J. Visch, F. Distelmaier, A. Postigo, T. Luyten, J.B. Parys, H. de Smedt, G.L. Smith, P.H. Willems, F.J. van Kuppeveld, Human Golgi antiapoptotic protein modulates intracellular calcium fluxes, Mol. Biol. Cell 20 (2009) 3638–3645.
[195] N. Saraiva, D.L. Prole, G. Carrara, B.F. Johnson, C.W. Taylor, M. Parsons, G.L. Smith, hGAAP promotes cell adhesion and migration via the stimulation of store-operated Ca2+ entry and calpain 2, J. Cell Biol. 202 (2013) 699–713.
[196] T. Boveri, Concerning the origin of malignant tumours by Theodor Boveri. Translated and annotated by Henry Harris, J. Cell Sci. 121 (Suppl 1) (2008) S1–S84.
[197] R. Basto, K. Brunk, T. Vinadogrova, N. Peel, A. Franz, A. Khodjakov, J.W. Raff, Centrosome amplification can initiate tumorigenesis in flies, Cell 133 (2008) 1032–1042.
[198] K. Fukasawa, Centrosome amplification, chromosome instability and cancer development, Cancer Lett. 230 (2005) 6–19.
[199] E.A. Nigg, T. Stearns, The centrosome cycle: centriole biogenesis, duplication and inherent asymmetries, Nat. Cell Biol. 13 (2011) 1154–1160.
[200] S. Chae, C. Yun, H. Um, J.H. Lee, H. Cho, Centrosome amplification and multinuclear phenotypes are Induced by hydrogen peroxide, Exp. Mol. Med. 37 (2005) 482–487.
[201] S. Ohshima, Centrosome aberrations associated with cellular senescence and p53 localization at supernumerary centrosomes, Oxid. Med. Cell Longev. 2012 (2012) 217594.
[202] J.A. Manning, S. Kumar, A potential role for NEDD1 and the centrosome in senescence of mouse embryonic fibroblasts, Cell Death Dis. 1 (2010) e35.
[203] J.M. Lim, K.S. Lee, H.A. Woo, D. Kang, S.G. Rhee, Control of the pericentrosomal H2O2 level by peroxiredoxin I is critical for mitotic progression, J. Cell Biol. 210 (2015) 23–33.
[204] S. Ohshima, Abnormal mitosis in hypertetraploid cells causes aberrant nuclear morphology in association with H2O2-induced premature senescence, Cytom. A 73 (2008) 808–815.
[205] A. Bindoli, M.P. Rigobello, Principles in redox signaling: from chemistry to functional significance, Antioxid. Redox Signal. 18 (2013) 1557–1593.
[206] L. Biasutto, M. Azzolini, I. Szabo, M. Zoratti, The mitochondrial permeability transition pore in AD 2016: an update, Biochim. Biophys. Acta 1863 (2016) 2515–2530.
[207] D. Linard, A. Kandlbinder, H. Degand, P. Morsomme, K.J. Dietz, B. Knoops, Redox characterization of human cyclophilin D: identification of a new mammalian mitochondrial redox sensor? Arch. Biochem. Biophys. 491 (2009) 39–45.
[208] A. Folda, A. Citta, V. Scalcon, T. Cali, F. Zonta, G. Scutari, A. Bindoli, M.P. Rigobello, Mitochondrial thioredoxin system as a modulator of cyclophilin D redox state, Sci. Rep. 6 (2016) 23071.
[209] K. Palikaras, N. Tavernarakis, Mitochondrial homeostasis: the interplay between mitophagy and mitochondrial biogenesis, Exp. Gerontol. 56 (2014) 182–188.
[210] M. Ristow, K. Zarse, How increased oxidative stress promotes longevity and metabolic health: the concept of mitochondrial hormesis (mitohormesis), Exp. Gerontol. 45 (2010) 410–418.
[211] T.J. Schulz, K. Zarse, A. Voigt, N. Urban, M. Birringer, M. Ristow, Glucose restriction extends Caenorhabditis elegans life span by inducing mitochondrial respiration and increasing oxidative stress, Cell Metab. 6 (2007) 280–293.
[212] B.M. Dancy, M.M. Sedensky, P.G. Morgan, Effects of the mitochondrial respiratory chain on longevity in C. elegans, Exp. Gerontol. 56 (2014) 245–255.
[213] S. Marthandan, S. Priebe, M. Groth, R. Guthke, M. Platzer, P. Hemmerich, S. Diekmann, Hormetic effect of rotenone in primary human fibroblasts, Immun. Ageing 12 (2015) 11.
[214] D.W. Lamming, Inhibition of the Mechanistic Target of Rapamycin (mTOR)-rapamycin and beyond, Cold Spring Harb. Perspect. Med. 6 (2016).
[215] M. Song, Y. Chen, G. Gong, E. Murphy, P.S. Rabinovitch, G.W. Dorn 2nd., Super-suppression of mitochondrial reactive oxygen species signaling impairs compensatory autophagy in primary mitophagic cardiomyopathy, Circ. Res. 115 (2014) 348–353.
[216] A. Gorlach, E.Y. Dimova, A. Petry, A. Martinez-Ruiz, P. Hernansanz-Agustin, A.P. Rolo, C.M. Palmeira, T. Kietzmann, Reactive oxygen species, nutrition, hypoxia and diseases: problems solved? Redox Biol. 6 (2015) 372–385.
[217] M.C. Fernández-Agüera, L. Gao, P. González-Rodríguez, C.O. Pintado, I. Arias-Mayenco, P. García-Flores, A. García-Pergañeda, A. Pascual, P. Ortega-Sáenz, J. López-Barneo, Oxygen sensing by arterial chemoreceptors depends on mitochondrial complex I signaling, Cell Metab. 22 (2015) 825–837.
[218] P. Hernansanz-Agustin, A. Izquierdo-Alvarez, F.J. Sanchez-Gomez, E. Ramos, T. Villa-Pina, S. Lamas, A. Bogdanova, A. Martinez-Ruiz, Acute hypoxia produces a superoxide burst in cells, Free Radic. Biol. Med. 71 (2014) 146–156.
[219] G. Yuan, C. Vasavda, Y.J. Peng, V.V. Makarenko, G. Raghuraman, J. Nanduri, M.M. Gadalla, G.L. Semenza, G.K. Kumar, S.H. Snyder, N.R. Prabhakar, Protein kinase G-regulated production of H2S governs oxygen sensing, Sci. Signal. 8 (2015) ra37.

[220] L. Moreno, J. Moral-Sanz, D. Morales-Cano, B. Barreira, E. Moreno, A. Ferrarini, R. Pandolfi, F.J. Rupérez, J. Cortijo, M. Sánchez-Luna, E. Villamor, F. Perez-Vizcaíno, A. Cogolludo, Ceramide mediates acute oxygen sensing in vascular tissues, Antioxid. Redox Signal. 20 (2014) 1–14.
[221] A. Izquierdo-Álvarez, E. Ramos, J. Villanueva, P. Hernansanz-Agustín, R. Fernández-Rodríguez, D. Tello, M. Carrascal, A. Martínez-Ruiz, Differential redox proteomics allows identification of proteins reversibly oxidized at cysteine residues in endothelial cells in response to acute hypoxia, J. Proteom. 75 (2012) 5449–5462.
[222] A. Bogdanova, I.Y. Petrushanko, P. Hernansanz-Agustin, A. Martinez-Ruiz, "Oxygen sensing" by Na,K-ATPase: these miraculous thiols, Front. Physiol. 7 (2016) 314.
[223] U. Forstermann, W.C. Sessa, Nitric oxide synthases: regulation and function, Eur. Heart J. 33 (2012) 829–837 (837a-837d).
[224] H.S. Jeffrey Man, A.K. Tsui, P.A. Marsden, Nitric oxide and hypoxia signaling, Vitam. Horm. 96 (2014) 161–192.
[225] K. Chalupsky, D. Kracun, I. Kanchev, K. Bertram, A. Gorlach, Folic acid promotes recycling of tetrahydrobiopterin and protects against hypoxia-induced pulmonary hypertension by recoupling endothelial nitric oxide synthase, Antioxid. Redox Signal. 23 (2015) 1076–1091.
[226] J.K. Bendall, G. Douglas, E. McNeill, K.M. Channon, M.J. Crabtree, Tetrahydrobiopterin in cardiovascular health and disease, Antioxid. Redox Signal. 20 (2014) 3040–3077.
[227] L. Gao, K. Chalupsky, E. Stefani, H. Cai, Mechanistic insights into folic acid-dependent vascular protection: dihydrofolate reductase (DHFR)-mediated reduction in oxidant stress in endothelial cells and angiotensin II-infused mice: a novel HPLC-based fluorescent assay for DHFR activity, J. Mol. Cell Cardiol. 47 (2009) 752–760.
[228] M. Dubois, E. Delannoy, L. Duluc, E. Closs, H. Li, C. Toussaint, A.P. Gadeau, A. Godecke, V. Freund-Michel, A. Courtois, R. Marthan, J.P. Savineau, B. Muller, Biopterin metabolism and eNOS expression during hypoxic pulmonary hypertension in mice, PLoS One 8 (2013) e82594.
[229] C.L. Bigarella, R. Liang, S. Ghaffari, Stem cells and the impact of ROS signaling, Development 141 (2014) 4206–4218.
[230] R.J. Burgess, M. Agathocleous, S.J. Morrison, Metabolic regulation of stem cell function, J. Intern. Med. 276 (2014) 12–24.
[231] L.O. Klotz, C. Sanchez-Ramos, I. Prieto-Arroyo, P. Urbanek, H. Steinbrenner, M. Monsalve, Redox regulation of FoxO transcription factors, Redox Biol. 6 (2015) 51–72.
[232] M. Higuchi, G.J. Dusting, H. Peshavariya, F. Jiang, S.T. Hsiao, E.C. Chan, G.S. Liu, Differentiation of human adipose-derived stem cells into fat involves reactive oxygen species and Forkhead box O1 mediated upregulation of antioxidant enzymes, Stem Cells Dev. 22 (2013) 878–888.
[233] M.L. Circu, T.Y. Aw, Redox biology of the intestine, Free Radic. Res. 45 (2011) 1245–1266.
[234] B. Speckmann, A. Pinto, M. Winter, I. Forster, H. Sies, H. Steinbrenner, Proinflammatory cytokines down-regulate intestinal selenoprotein P biosynthesis via NOS2 induction, Free Radic. Biol. Med. 49 (2010) 777–785.
[235] P.L. Walter, H. Steinbrenner, A. Barthel, L.O. Klotz, Stimulation of selenoprotein P promoter activity in hepatoma cells by FoxO1a transcription factor, Biochem. Biophys. Res. Commun. 365 (2008) 316–321.
[236] A.-M. Baird, K. O'Byrne, S. Gray, Reactive oxygen species and reactive nitrogen species in epigenetic modifications, in: I. Laher (Ed.), Systems Biology of Free Radicals and Antioxidants, Springer Berlin Heidelberg, 2014, pp. 437–455.
[237] Y. Niu, T.L. DesMarais, Z. Tong, Y. Yao, M. Costa, Oxidative stress alters global histone modification and DNA methylation, Free Radic. Biol. Med. 82 (2015) 22–28.
[238] Y. Mikhed, A. Gorlach, U.G. Knaus, A. Daiber, Redox regulation of genome stability by effects on gene expression, epigenetic pathways and DNA damage/repair, Redox Biol. 5 (2015) 275–289.
[239] K. Ito, M. Ito, W.M. Elliott, B. Cosio, G. Caramori, O.M. Kon, A. Barczyk, S. Hayashi, I.M. Adcock, J.C. Hogg, P.J. Barnes, Decreased histone deacetylase activity in chronic obstructive pulmonary disease, N. Engl. J. Med. 352 (2005) 1967–1976.
[240] V. Valinluck, L.C. Sowers, Endogenous cytosine damage products alter the site selectivity of human DNA maintenance methyltransferase DNMT1, Cancer Res. 67 (2007) 946–950.
[241] H.M. O'Hagan, W. Wang, S. Sen, C. Destefano Shields, S.S. Lee, Y.W. Zhang, E.G. Clements, Y. Cai, L. Van Neste, H. Easwaran, R.A. Casero, C.L. Sears, S.B. Baylin, Oxidative damage targets complexes containing DNA methyltransferases, SIRT1, and polycomb members to promoter CpG Islands, Cancer Cell 20 (2011) 606–619.
[242] G.H. Kim, J.J. Ryan, S.L. Archer, The role of redox signaling in epigenetics and cardiovascular disease, Antioxid. Redox Signal. 18 (2013) 1920–1936.
[243] S.L. Archer, G. Marsboom, G.H. Kim, H.J. Zhang, P.T. Toth, E.C. Svensson, J.R. Dyck, M. Gomberg-Maitland, B. Thebaud, A.N. Husain, N. Cipriani, J. Rehman, Epigenetic attenuation of mitochondrial superoxide dismutase 2 in pulmonary arterial hypertension: a basis for excessive cell proliferation and a new therapeutic target, Circulation 121 (2010) 2661–2671.
[244] S. Matsushima, J. Kuroda, T. Ago, P. Zhai, J.Y. Park, L.H. Xie, B. Tian, J. Sadoshima, Increased oxidative stress in the nucleus caused by Nox4 mediates oxidation of HDAC4 and cardiac hypertrophy, Circ. Res. 112 (2013) 651–663.
[245] Q.J. Zhang, H.Z. Chen, L. Wang, D.P. Liu, J.A. Hill, Z.P. Liu, The histone trimethyllysine demethylase JMJD2A promotes cardiac hypertrophy in response to hypertrophic stimuli in mice, J. Clin. Investig. 121 (2011) 2447–2456.
[246] A.B. Stein, T.A. Jones, T.J. Herron, S.R. Patel, S.M. Day, S.F. Noujaim, M.L. Milstein, M. Klos, P.B. Furspan, J. Jalife, G.R. Dressler, Loss of H3K4 methylation destabilizes gene expression patterns and physiological functions in adult murine cardiomyocytes, J. Clin. Investig. 121 (2011) 2641–2650.
[247] R. Kaneda, S. Takada, Y. Yamashita, Y.L. Choi, M. Nonaka-Sarukawa, M. Soda, Y. Misawa, T. Isomura, K. Shimada, H. Mano, Genome-wide histone methylation profile for heart failure, Genes Cells 14 (2009) 69–77.
[248] M.A. Khan, K. Alam, K. Dixit, M.M. Rizvi, Role of peroxynitrite induced structural changes on H2B histone by physicochemical method, Int. J. Biol. Macromol. 82 (2016) 31–38.
[249] M.A. Khan, K. Dixit, S. Jabeen, Moinuddin, K. Alam, Impact of peroxynitrite modification on structure and immunogenicity of H2A histone, Scand. J. Immunol. 69 (2009) 99–109.
[250] V. Ambros, The functions of animal microRNAs, Nature 431 (2004) 350–355.
[251] D.P. Bartel, MicroRNAs: genomics, biogenesis, mechanism, and function, Cell 116 (2004) 281–297.
[252] J.D. Hayes, A.T. Dinkova-Kostova, The Nrf2 regulatory network provides an interface between redox and intermediary metabolism, Trends Biochem. Sci. 39 (2014) 199–218.
[253] A.L. Levonen, B.G. Hill, E. Kansanen, J. Zhang, V.M. Darley-Usmar, Redox regulation of antioxidants, autophagy, and the response to stress: implications for electrophile therapeutics, Free Radic. Biol. Med. 71 (2014) 196–207.
[254] C. Espinosa-Diez, V. Miguel, D. Mennerich, T. Kietzmann, P. Sanchez-Perez, S. Cadenas, S. Lamas, Antioxidant responses and cellular adjustments to oxidative stress, Redox Biol. 6 (2015) 183–197.
[255] X. Cheng, C.H. Ku, R.C. Siow, Regulation of the Nrf2 antioxidant pathway by microRNAs: new players in micromanaging redox homeostasis, Free Radic. Biol. Med. 64 (2013) 4–11.
[256] T.A. Wynn, Common and unique mechanisms regulate fibrosis in various fibroproliferative diseases, J. Clin. Investig. 117 (2007) 524–529.
[257] J.J. Tomasek, G. Gabbiani, B. Hinz, C. Chaponnier, R.A. Brown, Myofibroblasts and mechano-regulation of connective tissue remodelling, Nat. Rev. Mol. Cell Biol. 3 (2002) 349–363.
[258] A. Leask, D.J. Abraham, TGF-beta signaling and the fibrotic response, FASEB J.: Off. Publ. Fed. Am. Soc. Exp. Biol. 18 (2004) 816–827.
[259] B. Hinz, S.H. Phan, V.J. Thannickal, A. Galli, M.L. Bochaton-Piallat, G. Gabbiani, The myofibroblast: one function, multiple origins, Am. J. Pathol. 170 (2007) 1807–1816.
[260] N. Pottier, C. Cauffiez, M. Perrais, P. Barbry, B. Mari, FibromiRs: translating molecular discoveries into new anti-fibrotic drugs, Trends Pharmacol. Sci. 35 (2014) 119–126.
[261] S. O'Reilly, MicroRNAs in fibrosis: opportunities and challenges, Arthritis Res. Ther. 18 (2016) 11.
[262] B.N. Davis, A.C. Hilyard, G. Lagna, A. Hata, SMAD proteins control DROSHA-mediated microRNA maturation, Nature 454 (2008) 56–61.
[263] M. Fierro-Fernandez, V. Miguel, S. Lamas, Role of redoximiRs in fibrogenesis, Redox Biol. 7 (2016) 58–67.
[264] C. Wei, L. Li, I.K. Kim, P. Sun, S. Gupta, NF-kappaB mediated miR-21 regulation in cardiomyocytes apoptosis under oxidative stress, Free Radic. Res. 48 (2014) 282–291.
[265] T. Thum, C. Gross, J. Fiedler, T. Fischer, S. Kissler, M. Bussen, P. Galuppo, S. Just, W. Rottbauer, S. Frantz, M. Castoldi, J. Soutschek, V. Koteliansky, A. Rosenwald, M.A. Basson, J.D. Licht, J.T. Pena, S.H. Rouhanifard, M.U. Muckenthaler, T. Tuschl, G.R. Martin, J. Bauersachs, S. Engelhardt, MicroRNA-21 contributes to myocardial disease by stimulating MAP kinase signalling in fibroblasts, Nature 456 (2008) 980–984.
[266] X. Zhong, A.C. Chung, H.Y. Chen, X.M. Meng, H.Y. Lan, Smad3-mediated upregulation of miR-21 promotes renal fibrosis, J. Am. Soc. Nephrol.: JASN 22 (2011) 1668–1681.
[267] B. Wang, R. Komers, R. Carew, C.E. Winbanks, B. Xu, M. Herman-Edelstein, P. Koh, M. Thomas, K. Jandeleit-Dahm, P. Gregorevic, M.E. Cooper, P. Kantharidis, Suppression of microRNA-29 expression by TGF-beta1 promotes collagen expression and renal fibrosis, J. Am. Soc. Nephrol.: JASN 23 (2012) 252–265.
[268] L. Cushing, P. Kuang, J. Lu, The role of miR-29 in pulmonary fibrosis, Biochem. Cell Biol. Biochim. Biol. Cell 93 (2015) 109–118.
[269] M. Fierro-Fernandez, O. Busnadiego, P. Sandoval, C. Espinosa-Diez, E. Blanco-Ruiz, M. Rodriguez, H. Pian, R. Ramos, M. Lopez-Cabrera, M.L. Garcia-Bermejo, S. Lamas, miR-9-5p suppresses pro-fibrogenic transformation of fibroblasts and prevents organ fibrosis by targeting NOX4 and TGFBR2, EMBO Rep. 16 (2015) 1358–1377.
[270] V. Miguel, O. Busnadiego, M. Fierro-Fernandez, S. Lamas, Protective role for miR-9-5p in the fibrogenic transformation of human dermal fibroblasts, Fibrogenes. Tissue Repair 9 (2016) 7.
[271] Y. Murakami, H. Toyoda, M. Tanaka, M. Kuroda, Y. Harada, F. Matsuda, A. Tajima, N. Kosaka, T. Ochiya, K. Shimotohno, The progression of liver fibrosis is related with overexpression of the miR-199 and 200 families, PloS One 6 (2011) e16081.
[272] C. Espinosa-Diez, M. Fierro-Fernandez, F. Sanchez-Gomez, F. Rodriguez-Pascual, M. Alique, M. Ruiz-Ortega, N. Beraza, M.L. Martinez-Chantar, C. Fernandez-Hernando, S. Lamas, Targeting of gamma-glutamyl-cysteine ligase by miR-433 reduces glutathione biosynthesis and promotes TGF-beta-dependent fibrogenesis, Antioxid. Redox Signal. 23 (2015) 1092–1105.
[273] B.N. Chau, C. Xin, J. Hartner, S. Ren, A.P. Castano, G. Linn, J. Li, P.T. Tran, V. Kaimal, X. Huang, A.N. Chang, S. Li, A. Kalra, M. Grafals, D. Portilla, D.A. MacKenna, S.H. Orkin, J.S. Duffield, MicroRNA-21 promotes fibrosis of the kidney by silencing metabolic pathways, Sci. Transl. Med. 4 (2012) 121ra118.
[274] I.G. Gomez, D.A. MacKenna, B.G. Johnson, V. Kaimal, A.M. Roach, S. Ren,

N. Nakagawa, C. Xin, R. Newitt, S. Pandya, T.H. Xia, X. Liu, D.B. Borza, M. Grafals, S.J. Shankland, J. Himmelfarb, D. Portilla, S. Liu, B.N. Chau, J.S. Duffield, Anti-microRNA-21 oligonucleotides prevent Alport nephropathy progression by stimulating metabolic pathways, J. Clin. Investig. 125 (2015) 141–156.
[275] H.M. Kang, S.H. Ahn, P. Choi, Y.A. Ko, S.H. Han, F. Chinga, A.S. Park, J. Tao, K. Sharma, J. Pullman, E.P. Bottinger, I.J. Goldberg, K. Susztak, Defective fatty acid oxidation in renal tubular epithelial cells has a key role in kidney fibrosis development, Nat. Med. 21 (2015) 37–46.
[276] V.N. Bochkov, O.V. Oskolkova, K.G. Birukov, A.L. Levonen, C.J. Binder, J. Stockl, Generation and biological activities of oxidized phospholipids, Antioxid. Redox Signal. 12 (2010) 1009–1059.
[277] F.H. Greig, S. Kennedy, C.M. Spickett, Physiological effects of oxidized phospholipids and their cellular signaling mechanisms in inflammation, Free Radic. Biol. Med. 52 (2012) 266–280.
[278] C. Mauerhofer, M. Philippova, O.V. Oskolkova, V.N. Bochkov, Hormetic and anti-inflammatory properties of oxidized phospholipids, Mol. Asp. Med. 49 (2016) 78–90.
[279] N. Leitinger, T.R. Tyner, L. Oslund, C. Rizza, G. Subbanagounder, H. Lee, P.T. Shih, N. Mackman, G. Tigyi, M.C. Territo, J.A. Berliner, D.K. Vora, Structurally similar oxidized phospholipids differentially regulate endothelial binding of monocytes and neutrophils, Proc. Natl. Acad. Sci. USA 96 (1999) 12010–12015.
[280] P. Bretscher, J. Egger, A. Shamshiev, M. Trotzmuller, H. Kofeler, E.M. Carreira, M. Kopf, S. Freigang, Phospholipid oxidation generates potent anti-inflammatory lipid mediators that mimic structurally related pro-resolving eicosanoids by activating Nrf2, EMBO Mol. Med. 7 (2015) 593–607.
[281] V.N. Bochkov, A. Kadl, J. Huber, F. Gruber, B.R. Binder, N. Leitinger, Protective role of phospholipid oxidation products in endotoxin-induced tissue damage, Nature 419 (2002) 77–81.
[282] T. Dziubla, D.A. Butterfield, Oxidative Stress and Biomaterials, Academic Press, 2016.
[283] A. Napoli, M. Valentini, N. Tirelli, M. Muller, J.A. Hubbell, Oxidation-responsive polymeric vesicles, Nat. Mater. 3 (2004) 183–189.
[284] P.P. Wattamwar, D. Biswal, D.B. Cochran, A.C. Lyvers, R.E. Eitel, K.W. Anderson, J.Z. Hilt, T.D. Dziubla, Synthesis and characterization of poly(antioxidant beta-amino esters) for controlled release of polyphenolic antioxidants, Acta Biomater. 8 (2012) 2529–2537.
[285] J. Yang, R. van Lith, K. Baler, R.A. Hoshi, G.A. Ameer, A thermoresponsive biodegradable polymer with intrinsic antioxidant properties, Biomacromolecules 15 (2014) 3942–3952.
[286] G. Svegliati Baroni, L. D' Ambrosio, G. Ferretti, P. Biondi, A. Casini, A. Di Sario, S. Saccomanno, A.M. Jezequel, A. Benedetti, F. Orlandi, Proliferation of hepatic stellate cells and lipid peroxidation: changes due to polyphenols, in: P. Gentilini, M.U. Dianzani, (eds). New Trends in Hepatology: the Proceedings of the Annual Meeting of the Italian National Programme on Liver Cirrhosis and Viral Hepatitis, San Miniato (Pisa), Italy, 7–9 January 1996. Dordrecht: Springer Netherlands, 1996, pp. 93–103.
[287] L. Mrakovcic, R. Wildburger, M. Jaganjac, M. Cindric, A. Cipak, S. Borovic-Sunjic, G. Waeg, A.M. Milankovic, N. Zarkovic, Lipid peroxidation product 4-hydroxy-nonenal as factor of oxidative homeostasis supporting bone regeneration with bioactive glasses, Acta Biochim. Pol. 57 (2010) 173–178.
[288] G. Aldini, M.R. Domingues, C.M. Spickett, P. Domingues, A. Altomare, F.J. Sanchez-Gomez, C.L. Oeste, D. Perez-Sala, Protein lipoxidation: detection strategies and challenges, Redox Biol. 5 (2015) 253–266.
[289] F. Magni, C. Galbusera, L. Tremolada, C. Ferrarese, M.G. Kienle, Characterisation of adducts of the lipid peroxidation product 4-hydroxy-2-nonenal and amyloid beta-peptides by liquid chromatography/electrospray ionisation mass spectrometry, Rapid Commun. Mass Spectrom. 16 (2002) 1485–1493.
[290] M. Colzani, G. Aldini, M. Carini, Mass spectrometric approaches for the identification and quantification of reactive carbonyl species protein adducts, J. Proteom. 92 (2013) 28–50.
[291] I. Verrastro, S. Pasha, K.T. Jensen, A.R. Pitt, C.M. Spickett, Mass spectrometry-based methods for identifying oxidized proteins in disease: advances and challenges, Biomolecules 5 (2015) 378–411.
[292] I. Milic, M. Kipping, R. Hoffmann, M. Fedorova, Separation and characterization of oxidized isomeric lipid-peptide adducts by ion mobility mass spectrometry, J. Mass Spectrom. 50 (2015) 1386–1392.
[293] R. Wang, Physiological implications of hydrogen sulfide: a whiff exploration that blossomed, Physiol. Rev. 92 (2012) 791–896.
[294] D.J. Polhemus, D.J. Lefer, Emergence of hydrogen sulfide as an endogenous gaseous signaling molecule in cardiovascular disease, Circ. Res. 114 (2014) 730–737.
[295] O. Kabil, N. Motl, R. Banerjee, H2S and its role in redox signaling, Biochim. Biophys. Acta 1844 (2014) 1355–1366.
[296] Y. Ju, W. Zhang, Y. Pei, G. Yang, H(2)S signaling in redox regulation of cellular functions, Can. J. Physiol. Pharmacol. 91 (2013) 8–14.
[297] Q. Li, J.R. Lancaster Jr., Chemical foundations of hydrogen sulfide biology, Nitric Oxide 35 (2013) 21–34.
[298] M.M. Cortese-Krott, B.O. Fernandez, M. Kelm, A.R. Butler, M. Feelisch, On the chemical biology of the nitrite/sulfide interaction, Nitric Oxide 46 (2015) 14–24.
[299] Q. Ma, Role of nrf2 in oxidative stress and toxicity, Annu. Rev. Pharmacol. Toxicol. 53 (2013) 401–426.
[300] A. Jazwa, A. Cuadrado, Targeting heme oxygenase-1 for neuroprotection and neuroinflammation in neurodegenerative diseases, Curr. Drug Targets 11 (2010) 1517–1531.
[301] Z.Z. Xie, Y. Liu, J.S. Bian, Hydrogen sulfide and cellular redox homeostasis, Oxid. Med. Cell Longev. 2016 (2016) 6043038.
[302] A. Garcia-Garcia, H. Rodriguez-Rocha, N. Madayiputhiya, A. Pappa, M.I. Panayiotidis, R. Franco, Biomarkers of protein oxidation in human disease, Curr. Mol. Med. 12 (2012) 681–697.
[303] H. Esterbauer, R.J. Schaur, H. Zollner, Chemistry and biochemistry of 4-hydroxynonenal, malonaldehyde and related aldehydes, Free Radic. Biol. Med. 11 (1991) 81–128.
[304] S.B. Wall, J.Y. Oh, A.R. Diers, A. Landar, Oxidative modification of proteins: an emerging mechanism of cell signaling, Front. Physiol. 3 (2012) 369.
[305] V. Ullrich, R. Kissner, Redox signaling: bioinorganic chemistry at its best, J. Inorg. Biochem. 100 (2006) 2079–2086.
[306] P. Calcerrada, G. Peluffo, R. Radi, Nitric oxide-derived oxidants with a focus on peroxynitrite: molecular targets, cellular responses and therapeutic implications, Curr. Pharm. Des. 17 (2011) 3905–3932.
[307] S.P. Bottari, Protein tyrosine nitration: a signaling mechanism conserved from yeast to man, Proteomics 15 (2015) 185–187.
[308] A. Daiber, D. Frein, D. Namgaladze, V. Ullrich, Oxidation and nitrosation in the nitrogen monoxide/superoxide system, J. Biol. Chem. 277 (2002) 11882–11888.
[309] C. Houee-Levin, K. Bobrowski, L. Horakova, B. Karademir, C. Schoneich, M.J. Davies, C.M. Spickett, Exploring oxidative modifications of tyrosine: an update on mechanisms of formation, advances in analysis and biological consequences, Free Radic. Res. 49 (2015) 347–373.
[310] N.B. Wehr, R.L. Levine, Wanted and wanting: antibody against methionine sulfoxide, Free Radic. Biol. Med. 53 (2012) 1222–1225.
[311] B. Ghesquiere, K. Gevaert, Proteomics methods to study methionine oxidation, Mass Spectrom. Rev. 33 (2014) 147–156.
[312] B.S. Rocha, B. Gago, R.M. Barbosa, J.O. Lundberg, R. Radi, J. Laranjinha, Intragastric nitration by dietary nitrite: implications for modulation of protein and lipid signaling, Free Radic. Biol. Med. 52 (2012) 693–698.
[313] J.L. Wayenberg, V. Ransy, D. Vermeylen, E. Damis, S.P. Bottari, Nitrated plasma albumin as a marker of nitrative stress and neonatal encephalopathy in perinatal asphyxia, Free Radic. Biol. Med. 47 (2009) 975–982.
[314] J.L. Wayenberg, C. Cavedon, C. Ghaddhab, N. Lefevre, S.P. Bottari, Early transient hypoglycemia is associated with increased albumin nitration in the preterm infant, Neonatology 100 (2011) 387–397.
[315] J.M. Kerstjens, I.F. Bocca-Tjeertes, A.F. de Winter, S.A. Reijneveld, A.F. Bos, Neonatal morbidities and developmental delay in moderately preterm-born children, Pediatrics 130 (2012) e265–e272.
[316] A. Lucas, R. Morley, T.J. Cole, Adverse neurodevelopmental outcome of moderate neonatal hypoglycaemia, BMJ 297 (1988) 1304–1308.
[317] E. Stenninger, R. Flink, B. Eriksson, C. Sahlen, Long-term neurological dysfunction and neonatal hypoglycaemia after diabetic pregnancy, Arch. Dis. Child Fetal Neonatal Ed. 79 (1998) F174–F179.
[318] S. Deshpande, M. Ward Platt, The investigation and management of neonatal hypoglycaemia, Semin. Fetal Neonatal Med. 10 (2005) 351–361.
[319] C.J. McKinlay, J.M. Alsweiler, J.M. Ansell, N.S. Anstice, J.G. Chase, G.D. Gamble, D.L. Harris, R.J. Jacobs, Y. Jiang, N. Paudel, M. Signal, B. Thompson, T.A. Wouldes, T.Y. Yu, J.E. Harding, C.S. Group, Neonatal glycemia and neurodevelopmental outcomes at 2 years, N. Engl. J. Med. 373 (2015) 1507–1518.
[320] F. Groenendaal, H. Lammers, D. Smit, P.G. Nikkels, Nitrotyrosine in brain tissue of neonates after perinatal asphyxia, Arch. Dis. Child Fetal Neonatal Ed. 91 (2006) F429–F433.
[321] F. Groenendaal, J. Vles, H. Lammers, J. De Vente, D. Smit, P.G. Nikkels, Nitrotyrosine in human neonatal spinal cord after perinatal asphyxia, Neonatology 93 (2008) 1–6.
[322] L. Iuliano, Pathways of cholesterol oxidation via non-enzymatic mechanisms, Chem. Phys. Lipids 164 (2011) 457–468.
[323] H.R. Griffiths, L. Moller, G. Bartosz, A. Bast, C. Bertoni-Freddari, A. Collins, M. Cooke, S. Coolen, G. Haenen, A.M. Hoberg, S. Loft, J. Lunec, R. Olinski, J. Parry, A. Pompella, H. Poulsen, H. Verhagen, S.B. Astley, Biomarkers, Mol. Asp. Med. 23 (2002) 101–208.
[324] D. Tsikas, S. Rothmann, J.Y. Schneider, M.T. Suchy, A. Trettin, D. Modun, N. Stuke, N. Maassen, J.C. Frolich, Development, validation and biomedical applications of stable-isotope dilution GC-MS and GC-MS/MS techniques for circulating malondialdehyde (MDA) after pentafluorobenzyl bromide derivatization: mda as a biomarker of oxidative stress and its relation to 15(S)−8-iso-prostaglandin F2alpha and nitric oxide (NO), J. Chromatogr. B Anal. Technol. Biomed. Life Sci. 1019 (2016) 95–111.
[325] C.A. Sobsey, J. Han, K. Lin, W. Swardfager, A. Levitt, C.H. Borchers, Development and evaluation of a liquid chromatography-mass spectrometry method for rapid, accurate quantitation of malondialdehyde in human plasma, J. Chromatogr. B Anal. Technol. Biomed. Life Sci. 1029–1030 (2016) 205–212.
[326] S. Zelzer, H. Mangge, R. Oberreither, C. Bernecker, H.J. Gruber, F. Pruller, G. Fauler, Oxidative stress: determination of 4-hydroxy-2-nonenal by gas chromatography/mass spectrometry in human and rat plasma, Free Radic. Res. 49 (2015) 1233–1238.
[327] C. Chafer-Pericas, L. Rahkonen, A. Sanchez-Illana, J. Kuligowski, I. Torres-Cuevas, M. Cernada, E. Cubells, A. Nunez-Ramiro, S. Andersson, M. Vento, J. Escobar, Ultra high performance liquid chromatography coupled to tandem mass spectrometry determination of lipid peroxidation biomarkers in newborn serum samples, Anal. Chim. Acta 886 (2015) 214–220.
[328] I.H. Dias, M.C. Polidori, H.R. Griffiths, Hypercholesterolaemia-induced oxidative stress at the blood-brain barrier, Biochem. Soc. Trans. 42 (2014) 1001–1005.
[329] C. Helmschrodt, S. Becker, J. Schroter, M. Hecht, G. Aust, J. Thiery, U. Ceglarek, Fast LC-MS/MS analysis of free oxysterols derived from reactive oxygen species in human plasma and carotid plaque, Clin. Chim. Acta 425 (2013) 3–8.
[330] E. Haller, G. Stubiger, D. Lafitte, W. Lindner, M. Lammerhofer, Chemical

recognition of oxidation-specific epitopes in low-density lipoproteins by a nanoparticle based concept for trapping, enrichment, and liquid chromatography-tandem mass spectrometry analysis of oxidative stress biomarkers, Anal. Chem. 86 (2014) 9954–9961.
[331] H. Kasai, P.F. Crain, Y. Kuchino, S. Nishimura, A. Ootsuyama, H. Tanooka, Formation of 8-hydroxyguanine moiety in cellular DNA by agents producing oxygen radicals and evidence for its repair, Carcinogenesis 7 (1986) 1849–1851.
[332] S.T. Rasmussen, J.T. Andersen, T.K. Nielsen, V. Cejvanovic, K.M. Petersen, T. Henriksen, A. Weimann, J. Lykkesfeldt, H.E. Poulsen, Simvastatin and oxidative stress in humans: a randomized, double-blinded, placebo-controlled clinical trial, Redox Biol. 9 (2016) 32–38.
[333] K. Al-Salmani, H.H. Abbas, S. Schulpen, M. Karbaschi, I. Abdalla, K.J. Bowman, K.K. So, M.D. Evans, G.D. Jones, R.W. Godschalk, M.S. Cooke, Simplified method for the collection, storage, and comet assay analysis of DNA damage in whole blood, Free Radic. Biol. Med. 51 (2011) 719–725.
[334] M. Karbaschi, M.S. Cooke, Novel method for the high-throughput processing of slides for the comet assay, Sci. Rep. 4 (2014) 7200.
[335] P.M. Lam, V. Mistry, T.H. Marczylo, J.C. Konje, M.D. Evans, M.S. Cooke, Rapid measurement of 8-oxo-7,8-dihydro-2'-deoxyguanosine in human biological matrices using ultra-high-performance liquid chromatography-tandem mass spectrometry, Free Radic. Biol. Med. 52 (2012) 2057–2063.
[336] P. Rossner Jr., H. Orhan, G. Koppen, K. Sakai, R.M. Santella, A. Ambroz, A. Rossnerova, R.J. Sram, M. Ciganek, J. Neca, E. Arzuk, N. Mutlu, M.S. Cooke, Urinary 8-oxo-7,8-dihydro-2'-deoxyguanosine analysis by an improved ELISA: an inter-laboratory comparison study, Free Radic. Biol. Med. 95 (2016) 169–179.
[337] P. Rossner Jr., V. Mistry, R. Singh, R.J. Sram, M.S. Cooke, Urinary 8-oxo-7,8-dihydro-2'-deoxyguanosine values determined by a modified ELISA improves agreement with HPLC-MS/MS, Biochem. Biophys. Res. Commun. 440 (2013) 725–730.
[338] M.S. Cooke, M.D. Evans, M. Dizdaroglu, J. Lunec, Oxidative DNA damage: mechanisms, mutation, and disease, FASEB J. 17 (2003) 1195–1214.
[339] A.B. Hill, The environment and disease: association or causation? Proc. R. Soc. Med. 58 (1965) 295–300.
[340] S. Loft, P. Svoboda, K. Kawai, H. Kasai, M. Sorensen, A. Tjonneland, U. Vogel, P. Moller, K. Overvad, O. Raaschou-Nielsen, Association between 8-oxo-7,8-dihydroguanine excretion and risk of lung cancer in a prospective study, Free Radic. Biol. Med. 52 (2012) 167–172.
[341] S. Loft, A. Olsen, P. Moller, H.E. Poulsen, A. Tjonneland, Association between 8-oxo-7,8-dihydro-2'-deoxyguanosine excretion and risk of postmenopausal breast cancer: nested case-control study, Cancer Epidemiol. Biomark. Prev. 22 (2013) 1289–1296.
[342] A.E. Hromockyj, A.T. Maurelli, Identification of an Escherichia coli gene homologous to virR, a regulator of Shigella virulence, J. Bacteriol. 171 (1989) 2879–2881.
[343] K. Broedbaek, H.E. Poulsen, A. Weimann, G.D. Kom, E. Schwedhelm, P. Nielsen, R.H. Boger, Urinary excretion of biomarkers of oxidatively damaged DNA and RNA in hereditary hemochromatosis, Free Radic. Biol. Med. 47 (2009) 1230–1233.
[344] H.E. Poulsen, E. Specht, K. Broedbaek, T. Henriksen, C. Ellervik, T. Mandrup-Poulsen, M. Tonnesen, P.E. Nielsen, H.U. Andersen, A. Weimann, RNA modifications by oxidation: a novel disease mechanism? Free Radic. Biol. Med. 52 (2012) 1353–1361.
[345] K. Broedbaek, V. Siersma, T. Henriksen, A. Weimann, M. Petersen, J.T. Andersen, E. Jimenez-Solem, L.J. Hansen, J.E. Henriksen, S.J. Bonnema, N. de Fine Olivarius, H.E. Poulsen, Association between urinary markers of nucleic acid oxidation and mortality in type 2 diabetes: a population-based cohort study, Diabetes Care 36 (2013) 669–676.
[346] H.E. Poulsen, L.L. Nadal, K. Broedbaek, P.E. Nielsen, A. Weimann, Detection and interpretation of 8-oxodG and 8-oxoGua in urine, plasma and cerebrospinal fluid, Biochim. Biophys. Acta 1840 (2014) 801–808.
[347] M.B. Kadiiska, B.C. Gladen, D.D. Baird, D. Germolec, L.B. Graham, C.E. Parker, A. Nyska, J.T. Wachsman, B.N. Ames, S. Basu, N. Brot, G.A. Fitzgerald, R.A. Floyd, M. George, J.W. Heinecke, G.E. Hatch, K. Hensley, J.A. Lawson, L.J. Marnett, J.D. Morrow, D.M. Murray, J. Plastaras, L.J. Roberts 2nd, J. Rokach, M.K. Shigenaga, R.S. Sohal, J. Sun, R.R. Tice, D.H. Van Thiel, D. Wellner, P.B. Walter, K.B. Tomer, R.P. Mason, J.C. Barrett, Biomarkers of oxidative stress study II: are oxidation products of lipids, proteins, and DNA markers of CCl4 poisoning? Free Radic. Biol. Med. 38 (2005) 698–710.
[348] A. Daiber, M. Oelze, S. Steven, S. Kroller-Schon, T. Munzel, Taking up the cudgels for the traditional reactive oxygen and nitrogen species detection assays and their use in the cardiovascular system, Redox Biol. 12 (2017) 35–49.
[349] N.V. Margaritelis, J.N. Cobley, V. Paschalis, A.S. Veskoukis, A.A. Theodorou, A. Kyparos, M.G. Nikolaidis, Principles for integrating reactive species into in vivo biological processes: examples from exercise physiology, Cell Signal. 28 (2016) 256–271.
[350] N.V. Margaritelis, J.N. Cobley, V. Paschalis, A.S. Veskoukis, A.A. Theodorou, A. Kyparos, M.G. Nikolaidis, Going retro: oxidative stress biomarkers in modern redox biology, Free Radic. Biol. Med. 98 (2016) 2–12.
[351] I. Dalle-Donne, R. Rossi, R. Colombo, D. Giustarini, A. Milzani, Biomarkers of oxidative damage in human disease, Clin. Chem. 52 (2006) 601–623.
[352] J. Leiper, M. Nandi, The therapeutic potential of targeting endogenous inhibitors of nitric oxide synthesis, Nat. Rev. Drug Discov. 10 (2011) 277–291.
[353] M. Valko, D. Leibfritz, J. Moncol, M.T. Cronin, M. Mazur, J. Telser, Free radicals and antioxidants in normal physiological functions and human disease, Int. J. Biochem. Cell Biol. 39 (2007) 44–84.
[354] M. Mengozzi, P. Ermilov, A. Annenkov, P. Ghezzi, F. Pearl, Definition of a family of tissue-protective cytokines using functional cluster analysis: a proof-of-concept study, Front. Immunol. 5 (2014) 115.
[355] H. Watanabe, M. Kakihana, S. Ohtsuka, Y. Sugishita, Randomized, double-blind, placebo-controlled study of ascorbate on the preventive effect of nitrate tolerance in patients with congestive heart failure, Circulation 97 (1998) 886–891.
[356] K. Takeshita, T. Ozawa, Recent progress in in vivo ESR spectroscopy, J. Radiol. Res. 45 (2004) 373–384.
[357] M. Yu, R.J. Beyers, J.D. Gorden, J.N. Cross, C.R. Goldsmith, A magnetic resonance imaging contrast agent capable of detecting hydrogen peroxide, Inorg. Chem. 51 (2012) 9153–9155.
[358] J.K. Perng, S. Lee, K. Kundu, C.F. Caskey, S.F. Knight, S. Satir, K.W. Ferrara, W.R. Taylor, F.L. Degertekin, D. Sorescu, N. Murthy, Ultrasound imaging of oxidative stress in vivo with chemically-generated gas microbubbles, Ann. Biomed. Eng. 40 (2012) 2059–2068.
[359] J.T. Jørgensen, M. Persson, J. Madsen, A. Kjær, High tumor uptake of 64Cu: implications for molecular imaging of tumor characteristics with copper-based PET tracers, Nucl. Med. Biol. 40 (2013) 345–350.
[360] R.P. Mason, Imaging free radicals in organelles, cells, tissue, and in vivo with immuno-spin trapping, Redox Biol. 8 (2016) 422–429.
[361] G. Maulucci, G. Bacic, L. Bridal, H.H. Schmidt, B. Tavitian, T. Viel, H. Utsumi, A.S. Yalcin, M. De Spirito, Imaging reactive oxygen species-induced modifications in living systems, Antioxid. Redox Signal. 24 (2016) 939–958.
[362] C. Frejaville, H. Karoui, B. Tuccio, F.L. Moigne, M. Culcasi, S. Pietri, R. Lauricella, P. Tordo, 5-(Diethoxyphosphoryl)−5-methyl-1-pyrroline N-oxide: a new efficient phosphorylated nitrone for the in vitro and in vivo spin trapping of oxygen-centered radicals, J. Med. Chem. 38 (1995) 258–265.
[363] F.A. Villamena, S. Xia, J.K. Merle, R. Lauricella, B. Tuccio, C.M. Hadad, J.L. Zweier, Reactivity of superoxide radical anion with cyclic nitrones: role of intramolecular h-bond and electrostatic effects, J. Am. Chem. Soc. 129 (2007) 8177–8191.
[364] K. Abbas, N. Babić, F. Peyrot, Use of spin traps to detect superoxide production in living cells by electron paramagnetic resonance (EPR) spectroscopy. Methods,109, 2016, 31–43.
[365] N. Beziere, C. Decroos, K. Mkhitaryan, E. Kish, F. Richard, S. Bigot-Marchand, S. Durand, F. Cloppet, C. Chauvet, M.-T. Corvol, F. Rannou, Y. Xu-Li, D. Mansuy, F. Peyrot, Y.-M. Frapart, First combined in vivo X-ray tomography and high-resolution molecular electron paramagnetic resonance (EPR) imaging of the mouse knee joint taking into account the disappearance kinetics of the EPR probe, Mol. Imaging 11 (2012) 220–228.
[366] N. Bézière, M. Hardy, F. Poulhès, H. Karoui, P. Tordo, O. Ouari, Y.-M. Frapart, A. Rockenbauer, J.-L. Boucher, D. Mansuy, F. Peyrot, Metabolic stability of superoxide adducts derived from newly developed cyclic nitrone spin traps, Free Radic. Biol. Med. 67 (2014) 150–158.
[367] F. Leinisch, J. Jiang, E.F. DeRose, V.V. Khramtsov, R.P. Mason, Investigation of spin-trapping artifacts formed by the Forrester-Hepburn mechanism, Free Radic. Biol. Med. 65 (2013) 1497–1505.
[368] S. Pou, M.S. Cohen, B.E. Britigan, G.M. Rosen, Spin-trapping and human neutrophils. Limits of detection of hydroxyl radical, J. Biol. Chem. 264 (1989) 12299–12302.
[369] K. Abbas, M. Hardy, F. Poulhès, H. Karoui, P. Tordo, O. Ouari, F. Peyrot, Detection of superoxide production in stimulated and unstimulated living cells using new cyclic nitrone spin traps, Free Radic. Biol. Med. 71 (2014) 281–290.
[370] A.L. Kleschyov, T. Munzel, Advanced spin trapping of vascular nitric oxide using colloid iron diethyldithiocarbamate, Methods Enzymol. 359 (2002) 42–51.
[371] S. Steven, M. Hausding, S. Kroller-Schon, M. Mader, Y. Mikhed, P. Stamm, E. Zinssius, A. Pfeffer, P. Welschof, S. Agdauletova, S. Sudowe, H. Li, M. Oelze, E. Schulz, T. Klein, T. Munzel, A. Daiber, Gliptin and GLP-1 analog treatment improves survival and vascular inflammation/dysfunction in animals with lipopolysaccharide-induced endotoxemia, Basic Res. Cardiol. 110 (2015) 6.
[372] S. Steven, K. Jurk, M. Kopp, S. Kroller-Schon, Y. Mikhed, K. Schwierczek, S. Roohani, F. Kashani, M. Oelze, T. Klein, S. Tokalov, S. Danckwardt, S. Strand, P. Wenzel, T. Munzel, A. Daiber, Glucagon-like peptide-1 receptor signalling reduces microvascular thrombosis, nitro-oxidative stress and platelet activation in endotoxaemic mice, Br. J. Pharmacol. (2016), http://dx.doi.org/10.1111/bph.13549.
[373] S. Deng, A. Kruger, A.L. Kleschyov, L. Kalinowski, A. Daiber, L. Wojnowski, Gp91phox-containing NAD(P)H oxidase increases superoxide formation by doxorubicin and NADPH, Free Radic. Biol. Med. 42 (2007) 466–473.
[374] P. Kuppusamy, H. Li, G. Ilangovan, A.J. Cardounel, J.L. Zweier, K. Yamada, M.C. Krishna, J.B. Mitchell, Noninvasive imaging of tumor redox status and its modification by tissue glutathione levels, Cancer Res. 62 (2002) 307–312.
[375] L.J. Berliner, From spin-labeled proteins to in vivo EPR applications, Eur. Biophys. J. 39 (2010) 579–588.
[376] J.P. Klare, Site-directed spin labeling EPR spectroscopy in protein research, Biol. Chem. 394 (2013).
[377] C.S. Klug, J.B. Feix, Methods and applications of site-directed spin labeling EPR spectroscopy, Methods Cell Biol. (2008) 617–658.
[378] A. Gurachevsky, S.C. Kazmierczak, A. Jörres, V. Muravsky, Application of spin label electron paramagnetic resonance in the diagnosis and prognosis of cancer and sepsis, Clin. Chem. Lab. Med. 46 (2008).
[379] E.V. Muravskaya, A.G. Lapko, V.A. Muravskii, Modification of transport function of plasma albumin during atherosclerosis and diabetes mellitus, Bull. Exp. Biol. Med. 135 (2003) 433–435.
[380] R. Jalan, K. Schnurr, R.P. Mookerjee, S. Sen, L. Cheshire, S. Hodges, V. Muravsky, R. Williams, G. Matthes, N.A. Davies, Alterations in the functional capacity of albumin in patients with decompensated cirrhosis is associated with increased

mortality, Hepatology 50 (2009) 555–564.
[381] D. Roy, J. Quiles, D.C. Gaze, P. Collinson, J.C. Kaski, G.F. Baxter, Role of reactive oxygen species on the formation of the novel diagnostic marker ischaemia modified albumin, Heart 92 (2006) 113–114.
[382] A.A. Pavićević, A.D. Popović-Bijelić, M.D. Mojović, S.V. Šušnjar, G.G. Bačić, Binding of doxyl stearic spin labels to human serum albumin: an EPR study, J. Phys. Chem. B 118 (2014) 10898–10905.
[383] M.J.N. Junk, H.W. Spiess, D. Hinderberger, The distribution of fatty acids reveals the functional structure of human serum albumin, Angew. Chem. Int. Ed. 49 (2010) 8755–8759.
[384] A. Boutier-Pischon, F. Auger, J.-M. Noël, A. Almario, Y.-M. Frapart, EPR and electrochemical quantification of oxygen using newly synthesized para-silylated triarylmethyl radicals, Free Radic. Res. (2015) 1–8.
[385] J. Li, Y. Liu, E. Kim, J.C. March, W.E. Bentley, G.F. Payne, Electrochemical reverse engineering: a systems-level tool to probe the redox-based molecular communication of biology, Free Radic. Biol. Med. 105 (2017) 110–131.
[386] A. Lund, M. Shiotani, S. Shimada, Principles and Applications of ESR Spectroscopy, Springer Science & Business Media, 2011.
[387] S. Quideau, D. Deffieux, C. Douat-Casassus, L. Pouységu, Plant polyphenols: chemical properties, biological activities, and synthesis, Angew. Chem. Int. Ed. 50 (2011) 586–621.
[388] M. Pyszková, M. Biler, D. Biedermann, K. Valentová, M. Kuzma, J. Vrba, J. Ulrichová, R. Sokolová, M. Mojović, A. Popović-Bijelić, M. Kubala, P. Trouillas, V. Křen, J. Vacek, Flavonolignan 2,3-dehydroderivatives: preparation, antiradical and cytoprotective activity, Free Radic. Biol. Med. 90 (2016) 114–125.
[389] J. Vacek, M. Zatloukalová, T. Desmier, V. Nezhodová, J. Hrbáč, M. Kubala, V. Křen, J. Ulrichová, P. Trouillas, Antioxidant, metal-binding and DNA-damaging properties of flavonolignans: a joint experimental and computational highlight based on 7-O-galloylsilybin, Chem.-Biol. Interact. 205 (2013) 173–180.
[390] J.M. Dimitrić Marković, Z.S. Marković, I.A. Pašti, T.P. Brdarić, A. Popović-Bijelić, M. Mojović, A joint application of spectroscopic, electrochemical and theoretical approaches in evaluation of the radical scavenging activity of 3-OH flavones and their iron complexes towards different radical species, Dalton Trans. 41 (2012) 7295.
[391] R. Sokolová, J. Tarábek, B. Papoušková, J. Kocábová, J. Fiedler, J. Vacek, P. Marhol, E. Vavříková, V. Křen, Oxidation of the flavonolignan silybin. In situ EPR evidence of the spin-trapped silybin radical, Electrochim. Acta 205 (2016) 118–123.
[392] L.G. Naso, E.G. Ferrer, N. Butenko, I. Cavaco, L. Lezama, T. Rojo, S.B. Etcheverry, P.A.M. Williams, Antioxidant, DNA cleavage, and cellular effects of silibinin and a new oxovanadium(IV)/silibinin complex, JBIC J. Biol. Inorg. Chem. 16 (2011) 653–668.
[393] G.P. Kalamkarov, A.E. Bugrova, T.S. Konstantinova, T.F. Shevchenko, [Endogenous content of the nitric oxide in the cell layers of the eye retina], Ross. Fiziol. Zhurnal Im. I. M. Sechenova/Ross. Akad. Nauk 100 (2014) 852–860.
[394] K.A. Lukyanov, V.V. Belousov, Genetically encoded fluorescent redox sensors, Biochim. Et. Biophys. Acta (BBA) – General. Subj. 1840 (2014) 745–756.
[395] Y.G. Ermakova, D.S. Bilan, M.E. Matlashov, N.M. Mishina, K.N. Markvicheva, O.M. Subach, F.V. Subach, I. Bogeski, M. Hoth, G. Enikolopov, V.V. Belousov, Red fluorescent genetically encoded indicator for intracellular hydrogen peroxide, Nat. Commun. 5 (2014).
[396] B. Morgan, K. Van Laer, T.N.E. Owusu, D. Ezerina, D. Pastor-Flores, P.S. Amponsah, A. Tursch, T.P. Dick, Real-time monitoring of basal H2O2 levels with peroxiredoxin-based probes, Nat. Chem. Biol. 12 (2016) 437–443.
[397] V.V. Belousov, A.F. Fradkov, K.A. Lukyanov, D.B. Staroverov, K.S. Shakhbazov, A.V. Terskikh, S. Lukyanov, Genetically encoded fluorescent indicator for intracellular hydrogen peroxide, Nat. Methods 3 (2006) 281–286.
[398] M. Gutscher, M.C. Sobotta, G.H. Wabnitz, S. Ballikaya, A.J. Meyer, Y. Samstag, T.P. Dick, Proximity-based protein thiol oxidation by H2O2-scavenging peroxidases, J. Biol. Chem. 284 (2009) 31532–31540.
[399] N.M. Mishina, P.A. Tyurin-Kuzmin, K.N. Markvicheva, A.V. Vorotnikov, V.A. Tkachuk, V. Laketa, C. Schultz, S. Lukyanov, V.V. Belousov, Does cellular hydrogen peroxide diffuse or act locally? Antioxid. Redox Signal. 14 (2010) 1–7.
[400] Y. Pak, K. Swamy, J. Yoon, Recent progress in fluorescent imaging probes, Sensors 15 (2015) 24374–24396.
[401] Z. Guo, S. Park, J. Yoon, I. Shin, Recent progress in the development of near-infrared fluorescent probes for bioimaging applications, Chem. Soc. Rev. 43 (2013) 16–29.
[402] D. Lee, S. Khaja, J.C. Velasquez-Castano, M. Dasari, C. Sun, J. Petros, W.R. Taylor, N. Murthy, In vivo imaging of hydrogen peroxide with chemiluminescent nanoparticles, Nat. Mater. 6 (2007) 765–769.
[403] S. Santra, J. Xu, K. Wang, W. Tand, Luminescent nanoparticle probes for bioimaging, J. Nanosci. Nanotechnol. 4 (2004) 590–599.
[404] L.M. Uusitalo, N. Hempel, Recent advances in intracellular and in vivo ROS Sensing: focus on nanoparticle and nanotube applications, Int. J. Mol. Sci. 13 (2012) 10660–10679.
[405] W.-G. Choi, S.J. Swanson, S. Gilroy, High-resolution imaging of Ca2+, redox status, ROS and pH using GFP biosensors: imaging of Ca2+, redox, ROS and pH using GFP biosensors, Plant J. 70 (2012) 118–128.
[406] Z. Chen, Z. Liu, Z. Li, E. Ju, N. Gao, L. Zhou, J. Ren, X. Qu, Upconversion nanoprobes for efficiently in vitro imaging reactive oxygen species and in vivo diagnosing rheumatoid arthritis, Biomaterials 39 (2015) 15–22.
[407] J. Zielonka, J.D. Lambeth, B. Kalyanaraman, On the use of L-012, a luminol-based chemiluminescent probe, for detecting superoxide and identifying inhibitors of NADPH oxidase: a reevaluation, Free Radic. Biol. Med. 65 (2013) 1310–1314.
[408] T. Seredenina, G. Chiriano, A. Filippova, Z. Nayernia, Z. Mahiout, L. Fioraso-Cartier, O. Plastre, L. Scapozza, K.-H. Krause, V. Jaquet, A subset of N-substituted phenothiazines inhibits NADPH oxidases, Free Radic. Biol. Med. 86 (2015) 239–249.
[409] J. Zielonka, G. Cheng, M. Zielonka, T. Ganesh, A. Sun, J. Joseph, R. Michalski, W.J. O'Brien, J.D. Lambeth, B. Kalyanaraman, High-throughput assays for superoxide and hydrogen peroxide design of a screening workflow to identify inhibitors of NADPH oxidases, J. Biol. Chem. 289 (2014) 16176–16189.
[410] J. Zielonka, M. Zielonka, L. VerPlank, G. Cheng, M. Hardy, O. Ouari, M.M. Ayhan, R. Podsiadły, A. Sikora, J.D. Lambeth, B. Kalyanaraman, Mitigation of NADPH oxidase 2 activity as a strategy to inhibit peroxynitrite formation, J. Biol. Chem. 291 (2016) 7029–7044.
[411] R. Michalski, J. Zielonka, M. Hardy, J. Joseph, B. Kalyanaraman, Hydropropidine: a novel, cell-impermeant fluorogenic probe for detecting extracellular superoxide, Free Radic. Biol. Med. 54 (2013) 135–147.
[412] C. Waszczak, S. Akter, S. Jacques, J. Huang, J. Messens, F.V. Breusegem, Oxidative post-translational modifications of cysteine residues in plant signal transduction, J. Exp. Bot. 66 (2015) 2923–2934.
[413] J. Cao, M. Ying, N. Xie, G. Lin, R. Dong, J. Zhang, H. Yan, X. Yang, Q. He, B. Yang, The oxidation states of DJ-1 dictate the cell fate in response to oxidative stress triggered by 4-HPR: autophagy or apoptosis? Antioxid. Redox Signal. 21 (2014) 1443–1459.
[414] C. Waszczak, S. Akter, D. Eeckhout, G. Persiau, K. Wahni, N. Bodra, I.V. Molle, B.D. Smet, D. Vertommen, K. Gevaert, G.D. Jaeger, M.V. Montagu, J. Messens, F.V. Breusegem, Sulfenome mining in arabidopsis thaliana, Proc. Natl. Acad. Sci. USA 111 (2014) 11545–11550.
[415] S. Akter, J. Huang, N. Bodra, B.D. Smet, K. Wahni, D. Rombaut, J. Pauwels, K. Gevaert, K. Carroll, F.V. Breusegem, J. Messens, DYn-2 based identification of arabidopsis sulfenomes, Mol. Cell. Proteom. 14 (2015) 1183–1200.
[416] E. Oger, D. Marino, J.-M. Guigonis, N. Pauly, A. Puppo, Sulfenylated proteins in the medicago truncatula–sinorhizobium meliloti symbiosis, J. Proteom. 75 (2012) 4102–4113.
[417] L.V. Benitez, W.S. Allison, The inactivation of the acyl phosphatase activity catalyzed by the sulfenic acid form of glyceraldehyde 3-phosphate dehydrogenase by dimedone and olefins, J. Biol. Chem. 249 (1974) 6234–6243.
[418] Y.H. Seo, K.S. Carroll, Facile synthesis and biological evaluation of a cell-permeable probe to detect redox-regulated proteins, Bioorg. Med. Chem. Lett. 19 (2009) 356–359.
[419] K. Schroder, C. Vecchione, O. Jung, J.G. Schreiber, R. Shiri-Sverdlov, P.J. van Gorp, R. Busse, R.P. Brandes, Xanthine oxidase inhibitor tungsten prevents the development of atherosclerosis in ApoE knockout mice fed a Western-type diet, Free Radic. Biol. Med. 41 (2006) 1353–1360.
[420] K. Schroder, M. Zhang, S. Benkhoff, A. Mieth, R. Pliquett, J. Kosowski, C. Kruse, P. Luedike, U.R. Michaelis, N. Weissmann, S. Dimmeler, A.M. Shah, R.P. Brandes, Nox4 is a protective reactive oxygen species generating vascular NADPH oxidase, Circ. Res. 110 (2012) 1217–1225.
[421] C. Schurmann, F. Rezende, C. Kruse, Y. Yasar, O. Lowe, C. Fork, B. van de Sluis, R. Bremer, N. Weissmann, A.M. Shah, H. Jo, R.P. Brandes, K. Schroder, The NADPH oxidase Nox4 has anti-atherosclerotic functions, Eur. Heart J. 36 (2015) 3447–3456.
[422] H. Langbein, C. Brunssen, A. Hofmann, P. Cimalla, M. Brux, S.R. Bornstein, A. Deussen, E. Koch, H. Morawietz, NADPH oxidase 4 protects against development of endothelial dysfunction and atherosclerosis in LDL receptor deficient mice, Eur. Heart J. 37 (2016) 1753–1761.
[423] S.M. Craige, S. Kant, M. Reif, K. Chen, Y. Pei, R. Angoff, K. Sugamura, T. Fitzgibbons, J.F. Keaney Jr., Endothelial NADPH oxidase 4 protects ApoE-/- mice from atherosclerotic lesions, Free Radic. Biol. Med. 89 (2015) 1–7.
[424] S.P. Gray, E. Di Marco, K. Kennedy, P. Chew, J. Okabe, A. El-Osta, A.C. Calkin, E.A. Biessen, R.M. Touyz, M.E. Cooper, H.H. Schmidt, K.A. Jandeleit-Dahm, Reactive oxygen Species can provide atheroprotection via NOX4-dependent inhibition of inflammation and vascular remodeling, Arterioscler. Thromb. Vasc. Biol. 36 (2016) 295–307.
[425] Y. Wang, J. Yang, J. Yi, Redox sensing by proteins: oxidative modifications on cysteines and the consequent events, Antioxid. Redox Signal. 16 (2012) 649–657.
[426] P. Klatt, S. Lamas, Regulation of protein function by S-glutathiolation in response to oxidative and nitrosative stress, Eur. J. Biochem. 267 (2000) 4928–4944.
[427] J.J. Mieyal, M.M. Gallogly, S. Qanungo, E.A. Sabens, M.D. Shelton, Molecular mechanisms and clinical implications of reversible protein S-glutathionylation, Antioxid. Redox Signal. 10 (2008) 1941–1988.
[428] Y. Watanabe, C.E. Murdoch, S. Sano, Y. Ido, M.M. Bachschmid, R.A. Cohen, R. Matsui, Glutathione adducts induced by ischemia and deletion of glutaredoxin-1 stabilize HIF-1alpha and improve limb revascularization, Proc. Natl. Acad. Sci. USA 113 (2016) 6011–6016.
[429] O.G. Miller, J.B. Behring, S.L. Siedlak, S. Jiang, R. Matsui, M.M. Bachschmid, X. Zhu, J.J. Mieyal, Upregulation of glutaredoxin-1 activates microglia and promotes neurodegeneration: implications for parkinson's disease. Antioxid. Redox Signal., 25, 2016, 967–982.
[430] C.E. Murdoch, M. Shuler, D.J. Haeussler, R. Kikuchi, P. Bearelly, J. Han, Y. Watanabe, J.J. Fuster, K. Walsh, Y.S. Ho, M.M. Bachschmid, R.A. Cohen, R. Matsui, Glutaredoxin-1 up-regulation induces soluble vascular endothelial growth factor receptor 1, attenuating post-ischemia limb revascularization, J. Biol. Chem. 289 (2014) 8633–8644.
[431] A.M. Evangelista, M.D. Thompson, R.M. Weisbrod, D.R. Pimental, X. Tong, V.M. Bolotina, R.A. Cohen, Redox regulation of SERCA2 is required for vascular endothelial growth factor-induced signaling and endothelial cell migration, Antioxid. Redox Signal. 17 (2012) 1099–1108.
[432] S. Hazarika, A.O. Dokun, Y. Li, A.S. Popel, C.D. Kontos, B.H. Annex, Impaired

angiogenesis after hindlimb ischemia in type 2 diabetes mellitus: differential regulation of vascular endothelial growth factor receptor 1 and soluble vascular endothelial growth factor receptor 1, Circ. Res. 101 (2007) 948–956.
[433] M. Okuda, N. Inoue, H. Azumi, T. Seno, Y. Sumi, K. Hirata, S. Kawashima, Y. Hayashi, H. Itoh, J. Yodoi, M. Yokoyama, Expression of glutaredoxin in human coronary arteries: its potential role in antioxidant protection against atherosclerosis, Arterioscler. Thromb. Vasc. Biol. 21 (2001) 1483–1487.
[434] F. Li, P. Sonveaux, Z.N. Rabbani, S. Liu, B. Yan, Q. Huang, Z. Vujaskovic, M.W. Dewhirst, C.Y. Li, Regulation of HIF-1alpha stability through S-nitrosylation, Mol. Cell 26 (2007) 63–74.
[435] P. Pagliaro, F. Moro, F. Tullio, M.G. Perrelli, C. Penna, Cardioprotective pathways during reperfusion: focus on redox signaling and other modalities of cell signaling, Antioxid. Redox Signal. 14 (2011) 833–850.
[436] T. Kalogeris, Y. Bao, R.J. Korthuis, Mitochondrial reactive oxygen species: a double edged sword in ischemia/reperfusion vs preconditioning, Redox Biol. 2 (2014) 702–714.
[437] D.M. Yellon, D.J. Hausenloy, Myocardial reperfusion injury, N. Engl. J. Med. 357 (2007) 1121–1135.
[438] D.J. Hausenloy, D. Garcia-Dorado, H. Erik Botker, S.M. Davidson, J. Downey, F.B. Engel, R. Jennings, S. Lecour, J. Leor, R. Madonna, M. Ovize, C. Perrino, F. Prunier, R. Schulz, J.P. Sluijter, L.W. Van Laake, J. Vinten-Johansen, D.M. Yellon, K. Ytrehus, G. Heusch, P. Ferdinandy, Novel targets and future strategies for acute cardioprotection: position paper of the european society of cardiology working group on cellular biology of the heart. Cardiovasc. Res., 113, 2017, 564-585.
[439] G. Heusch, Molecular basis of cardioprotection: signal transduction in ischemic pre-, post-, and remote conditioning, Circ. Res. 116 (2015) 674–699.
[440] I. Andreadou, E.K. Iliodromitis, D. Farmakis, D.T. Kremastinos, To prevent, protect and save the ischemic heart: antioxidants revisited, Expert Opin. Ther. Targets 13 (2009) 945–956.
[441] K. Tsovolas, E.K. Iliodromitis, I. Andreadou, A. Zoga, M. Demopoulou, K.E. Iliodromitis, T. Manolaki, S.L. Markantonis, D.T. Kremastinos, Acute administration of vitamin C abrogates protection from ischemic preconditioning in rabbits, Pharmacol. Res. 57 (2008) 283–289.
[442] A. Skyschally, R. Schulz, P. Gres, H.G. Korth, G. Heusch, Attenuation of ischemic preconditioning in pigs by scavenging of free oxyradicals with ascorbic acid, Am. J. Physiol. Heart Circ. Physiol. 284 (2003) H698–H703.
[443] C. Local Food-Nutraceuticals, Understanding local Mediterranean diets: a multidisciplinary pharmacological and ethnobotanical approach, Pharmacol. Res. 52 (2005) 353–366.
[444] B. Turan, H. Fliss, M. Desilets, Oxidants increase intracellular free Zn2+ concentration in rabbit ventricular myocytes, Am. J. Physiol. 272 (1997) H2095–H2106.
[445] E. Tuncay, A. Bilginoglu, N.N. Sozmen, E.N. Zeydanli, M. Ugur, G. Vassort, B. Turan, Intracellular free zinc during cardiac excitation-contraction cycle: calcium and redox dependencies, Cardiovasc Res. 89 (2011) 634–642.
[446] O. Pisarenko, I. Studneva, V. Khlopkov, E. Solomatina, E. Ruuge, An assessment of anaerobic metabolism during ischemia and reperfusion in isolated guinea pig heart, Biochim. Biophys. Acta 934 (1988) 55–63.
[447] H. Ashrafian, G. Czibik, M. Bellahcene, D. Aksentijevic, A.C. Smith, S.J. Mitchell, M.S. Dodd, J. Kirwan, J.J. Byrne, C. Ludwig, H. Isackson, A. Yavari, N.B. Stottrup, H. Contractor, T.J. Cahill, N. Sahgal, D.R. Ball, R.I. Birkler, I. Hargreaves, D.A. Tennant, J. Land, C.A. Lygate, M. Johannsen, R.K. Kharbanda, S. Neubauer, C. Redwood, R. de Cabo, I. Ahmet, M. Talan, U.L. Gunther, A.J. Robinson, M.R. Viant, P.J. Pollard, D.J. Tyler, H. Watkins, Fumarate is cardioprotective via activation of the Nrf2 antioxidant pathway, Cell Metab. 15 (2012) 361–371.
[448] E.T. Chouchani, V.R. Pell, A.M. James, L.M. Work, K. Saeb-Parsy, C. Frezza, T. Krieg, M.P. Murphy, A unifying mechanism for mitochondrial superoxide production during ischemia-reperfusion injury, Cell Metab. 23 (2016) 254–263.
[449] L. Valls-Lacalle, I. Barba, E. Miro-Casas, J.J. Alburquerque-Bejar, M. Ruiz-Meana, M. Fuertes-Agudo, A. Rodriguez-Sinovas, D. Garcia-Dorado, Succinate dehydrogenase inhibition with malonate during reperfusion reduces infarct size by preventing mitochondrial permeability transition, Cardiovasc. Res. 109 (2016) 374–384.
[450] N. Gorenkova, E. Robinson, D.J. Grieve, A. Galkin, Conformational change of mitochondrial complex I increases ROS sensitivity during ischemia, Antioxid. Redox Signal. 19 (2013) 1459–1468.
[451] E.T. Chouchani, C. Methner, S.M. Nadtochiy, A. Logan, V.R. Pell, S. Ding, A.M. James, H.M. Cocheme, J. Reinhold, K.S. Lilley, L. Partridge, I.M. Fearnley, A.J. Robinson, R.C. Hartley, R.A. Smith, T. Krieg, P.S. Brookes, M.P. Murphy, Cardioprotection by S-nitrosation of a cysteine switch on mitochondrial complex I, Nat. Med. 19 (2013) 753–759.
[452] Z.V. Varga, Z. Giricz, L. Liaudet, G. Hasko, P. Ferdinandy, P. Pacher, Interplay of oxidative, nitrosative/nitrative stress, inflammation, cell death and autophagy in diabetic cardiomyopathy, Biochim. Biophys. Acta 1852 (2015) 232–242.
[453] O. Pechanova, Z.V. Varga, M. Cebova, Z. Giricz, P. Pacher, P. Ferdinandy, Cardiac NO signalling in the metabolic syndrome, Br. J. Pharmacol. 172 (2015) 1415–1433.
[454] A. Frustaci, J. Kajstura, C. Chimenti, I. Jakoniuk, A. Leri, A. Maseri, B. Nadal-Ginard, P. Anversa, Myocardial cell death in human diabetes, Circ. Res. 87 (2000) 1123–1132.
[455] A. Onody, C. Csonka, Z. Giricz, P. Ferdinandy, Hyperlipidemia induced by a cholesterol-rich diet leads to enhanced peroxynitrite formation in rat hearts, Cardiovasc. Res. 58 (2003) 663–670.
[456] Z.V. Varga, K. Kupai, G. Szucs, R. Gaspar, J. Paloczi, N. Farago, A. Zvara, L.G. Puskas, Z. Razga, L. Tiszlavicz, P. Bencsik, A. Gorbe, C. Csonka, P. Ferdinandy, T. Csont, MicroRNA-25-dependent up-regulation of NADPH oxidase 4 (NOX4) mediates hypercholesterolemia-induced oxidative/nitrative stress and subsequent dysfunction in the heart, J. Mol. Cell Cardiol. 62 (2013) 111–121.
[457] A. Gorbe, Z.V. Varga, K. Kupai, P. Bencsik, G.F. Kocsis, T. Csont, K. Boengler, R. Schulz, P. Ferdinandy, Cholesterol diet leads to attenuation of ischemic preconditioning-induced cardiac protection: the role of connexin 43, Am. J. Physiol. Heart Circ. Physiol. 300 (2011) H1907–H1913.
[458] E.M. Jeong, J. Chung, H. Liu, Y. Go, S. Gladstein, A. Farzaneh-Far, E.D. Lewandowski, S.C. Dudley Jr., Role of mitochondrial oxidative stress in glucose tolerance, insulin resistance, and cardiac diastolic dysfunction, J. Am. Heart Assoc. 5 (2016).
[459] A.L. Sverdlov, A. Elezaby, F. Qin, J.B. Behring, I. Luptak, T.D. Calamaras, D.A. Siwik, E.J. Miller, M. Liesa, O.S. Shirihai, D.R. Pimentel, R.A. Cohen, M.M. Bachschmid, W.S. Colucci, Mitochondrial reactive oxygen species mediate cardiac structural, functional, and mitochondrial consequences of diet-induced metabolic heart disease, J. Am. Heart Assoc. 5 (2016).
[460] M. Luo, X. Guan, E.D. Luczak, D. Lang, W. Kutschke, Z. Gao, J. Yang, P. Glynn, S. Sossalla, P.D. Swaminathan, R.M. Weiss, B. Yang, A.G. Rokita, L.S. Maier, I.R. Efimov, T.J. Hund, M.E. Anderson, Diabetes increases mortality after myocardial infarction by oxidizing CaMKII, J. Clin. Investig. 123 (2013) 1262–1274.
[461] R. Ni, T. Cao, S. Xiong, J. Ma, G.C. Fan, J.C. Lacefield, Y. Lu, S. Le Tissier, T. Peng, Therapeutic inhibition of mitochondrial reactive oxygen species with mito-TEMPO reduces diabetic cardiomyopathy, Free Radic. Biol. Med. 90 (2016) 12–23.
[462] R.C. Sloan, F. Moukdar, C.R. Frasier, H.D. Patel, P.A. Bostian, R.M. Lust, D.A. Brown, Mitochondrial permeability transition in the diabetic heart: contributions of thiol redox state and mitochondrial calcium to augmented reperfusion injury, J. Mol. Cell Cardiol. 52 (2012) 1009–1018.
[463] Y. Guo, W. Yu, D. Sun, J. Wang, C. Li, R. Zhang, S.A. Babcock, Y. Li, M. Liu, M. Ma, M. Shen, C. Zeng, N. Li, W. He, Q. Zou, Y. Zhang, H. Wang, A novel protective mechanism for mitochondrial aldehyde dehydrogenase (ALDH2) in type i diabetes-induced cardiac dysfunction: role of AMPK-regulated autophagy, Biochim. Biophys. Acta 1852 (2015) 319–331.
[464] J.A. Herlein, B.D. Fink, W.I. Sivitz, Superoxide production by mitochondria of insulin-sensitive tissues: mechanistic differences and effect of early diabetes, Metabolism 59 (2010) 247–257.
[465] M.F. Essop, W.Y. Anna Chan, A. Valle, F.J. Garcia-Palmer, E.F. Du Toit, Impaired contractile function and mitochondrial respiratory capacity in response to oxygen deprivation in a rat model of pre-diabetes, Acta Physiol. 197 (2009) 289–296.
[466] K.A. Radermacher, K. Wingler, F. Langhauser, S. Altenhofer, P. Kleikers, J.J. Hermans, M. Hrabe de Angelis, C. Kleinschnitz, H.H. Schmidt, Neuroprotection after stroke by targeting NOX4 as a source of oxidative stress, Antioxid. Redox Signal. 18 (2013) 1418–1427.
[467] P.W. Kleikers, C. Hooijmans, E. Gob, F. Langhauser, S.S. Rewell, K. Radermacher, M. Ritskes-Hoitinga, D.W. Howells, C. Kleinschnitz, H.H. Schmidt, A combined pre-clinical meta-analysis and randomized confirmatory trial approach to improve data validity for therapeutic target validation, Sci. Rep. 5 (2015) 13428.
[468] V.T. Dao, A.I. Casas, G.J. Maghzal, T. Seredenina, N. Kaludercic, N. Robledinos-Anton, F. Di Lisa, R. Stocker, P. Ghezzi, V. Jaquet, A. Cuadrado, H.H. Schmidt, Pharmacology and clinical drug candidates in redox medicine, Antioxid. Redox Signal. 23 (2015) 1113–1129.
[469] C. Kleinschnitz, S. Mencl, P.W. Kleikers, M.K. Schuhmann, G.L. M, A.I. Casas, B. Surun, A. Reif, H.H. Schmidt, NOS knockout or inhibition but not disrupting PSD-95-NOS interaction protect against ischemic brain damage. J. Cereb. Blood Flow Metab., 36, 2016, 1508–12.
[470] H. Li, S. Horke, U. Forstermann, Oxidative stress in vascular disease and its pharmacological prevention, Trends Pharmacol. Sci. 34 (2013) 313–319.
[471] T. Munzel, A. Daiber, V. Ullrich, A. Mulsch, Vascular consequences of endothelial nitric oxide synthase uncoupling for the activity and expression of the soluble guanylyl cyclase and the cGMP-dependent protein kinase, Arterioscler. Thromb. Vasc. Biol. 25 (2005) 1551–1557.
[472] H. Li, S. Horke, U. Forstermann, Vascular oxidative stress, nitric oxide and atherosclerosis, Atherosclerosis 237 (2014) 208–219.
[473] H. Li, U. Forstermann, Prevention of atherosclerosis by interference with the vascular nitric oxide system, Curr. Pharm. Des. 15 (2009) 3133–3145.
[474] M.J. Crabtree, R. Brixey, H. Batchelor, A.B. Hale, K.M. Channon, Integrated redox sensor and effector functions for tetrahydrobiopterin- and glutathionylation-dependent endothelial nitric-oxide synthase uncoupling, J. Biol. Chem. 288 (2013) 561–569.
[475] H. Li, U. Forstermann, Uncoupling of endothelial NO synthase in atherosclerosis and vascular disease, Curr. Opin. Pharmacol. 13 (2013) 161–167.
[476] H. Li, U. Forstermann, Pharmacological prevention of eNOS uncoupling, Curr. Pharm. Des. 20 (2014) 3595–3606.
[477] S. Schuhmacher, M. Oelze, F. Bollmann, H. Kleinert, C. Otto, T. Heeren, S. Steven, M. Hausding, M. Knorr, A. Pautz, K. Reifenberg, E. Schulz, T. Gori, P. Wenzel, T. Munzel, A. Daiber, Vascular dysfunction in experimental diabetes is improved by pentaerithrityl tetranitrate but not isosorbide-5-mononitrate therapy, Diabetes 60 (2011) 2608–2616.
[478] M. Knorr, M. Hausding, S. Kroller-Schuhmacher, S. Steven, M. Oelze, T. Heeren, A. Scholz, T. Gori, P. Wenzel, E. Schulz, A. Daiber, T. Munzel, Nitroglycerin-induced endothelial dysfunction and tolerance involve adverse phosphorylation and S-Glutathionylation of endothelial nitric oxide synthase: beneficial effects of therapy with the AT1 receptor blocker telmisartan, Arterioscler. Thromb. Vasc. Biol. 31 (2011) 2223–2231.
[479] J.H. Kim, L.J. Bugaj, Y.J. Oh, T.J. Bivalacqua, S. Ryoo, K.G. Soucy, L. Santhanam, A. Webb, A. Camara, G. Sikka, D. Nyhan, A.A. Shoukas, M. Ilies,

D.W. Christianson, H.C. Champion, D.E. Berkowitz, Arginase inhibition restores NOS coupling and reverses endothelial dysfunction and vascular stiffness in old rats, J. Appl. Physiol. (1985) 107 (2009) 1249–1257.
[480] N. Xia, S. Horke, A. Habermeier, E.I. Closs, G. Reifenberg, A. Gericke, Y. Mikhed, T. Munzel, A. Daiber, U. Forstermann, H. Li, Uncoupling of endothelial nitric oxide synthase in perivascular adipose tissue of diet-induced obese mice, Arterioscler. Thromb. Vasc. Biol. 36 (2016) 78–85.
[481] R.P. Bowler, J. Arcaroli, J.D. Crapo, A. Ross, J.W. Slot, E. Abraham, Extracellular superoxide dismutase attenuates lung injury after hemorrhage, Am. J. Respir. Crit. Care Med 164 (2001) 290–294.
[482] E.N. Atochina, I.V. Balyasnikova, S.M. Danilov, D.N. Granger, A.B. Fisher, V.R. Muzykantov, Immunotargeting of catalase to ACE or ICAM-1 protects perfused rat lungs against oxidative stress, Am. J. Physiol. 275 (1998) L806–L817.
[483] T.D. Dziubla, V.V. Shuvaev, N.K. Hong, B.J. Hawkins, M. Madesh, H. Takano, E. Simone, M.T. Nakada, A. Fisher, S.M. Albelda, V.R. Muzykantov, Endothelial targeting of semi-permeable polymer nanocarriers for enzyme therapies, Biomaterials 29 (2008) 215–227.
[484] T.D. Sweitzer, A.P. Thomas, R. Wiewrodt, M.T. Nakada, F. Branco, V.R. Muzykantov, PECAM-directed immunotargeting of catalase: specific, rapid and transient protection against hydrogen peroxide, Free Radic. Biol. Med. 34 (2003) 1035–1046.
[485] V.V. Shuvaev, S. Tliba, J. Pick, E. Arguiri, M. Christofidou-Solomidou, S.M. Albelda, V.R. Muzykantov, Modulation of endothelial targeting by size of antibody-antioxidant enzyme conjugates, J. Control Release 149 (2011) 236–241.
[486] B.D. Kozower, M. Christofidou-Solomidou, T.D. Sweitzer, S. Muro, D.G. Buerk, C.C. Solomides, S.M. Albelda, G.A. Patterson, V.R. Muzykantov, Immunotargeting of catalase to the pulmonary endothelium alleviates oxidative stress and reduces acute lung transplantation injury, Nat. Biotechnol. 21 (2003) 392–398.
[487] V.V. Shuvaev, M. Christofidou-Solomidou, F. Bhora, K. Laude, H. Cai, S. Dikalov, E. Arguiri, C.C. Solomides, S.M. Albelda, D.G. Harrison, V.R. Muzykantov, Targeted detoxification of selected reactive oxygen species in the vascular endothelium, J. Pharmacol. Exp. Ther. 331 (2009) 404–411.
[488] E.D. Hood, C.F. Greineder, C. Dodia, J. Han, C. Mesaros, V.V. Shuvaev, I.A. Blair, A.B. Fisher, V.R. Muzykantov, Antioxidant protection by PECAM-targeted delivery of a novel NADPH-oxidase inhibitor to the endothelium in vitro and in vivo, J. Control Release 163 (2012) 161–169.
[489] M.D. Howard, C.F. Greineder, E.D. Hood, V.R. Muzykantov, Endothelial targeting of liposomes encapsulating SOD/catalase mimetic EUK-134 alleviates acute pulmonary inflammation, J. Control Release 177 (2014) 34–41.
[490] T.D. Dziubla, A. Karim, V.R. Muzykantov, Polymer nanocarriers protecting active enzyme cargo against proteolysis, J. Control Release 102 (2005) 427–439.
[491] E. Barlaka, E. Galatou, K. Mellidis, T. Ravingerova, A. Lazou, Role of pleiotropic properties of peroxisome proliferator-activated receptors in the heart: focus on the nonmetabolic effects in cardiac protection, Cardiovasc Ther. 34 (2016) 37–48.
[492] L. Ibarra-Lara, E. Hong, E. Soria-Castro, J.C. Torres-Narvaez, F. Perez-Severiano, L. Del Valle-Mondragon, L.G. Cervantes-Perez, M. Ramirez-Ortega, G.S. Pastelin-Hernandez, A. Sanchez-Mendoza, Clofibrate PPARalpha activation reduces oxidative stress and improves ultrastructure and ventricular hemodynamics in no-flow myocardial ischemia, J. Cardiovasc Pharmacol. 60 (2012) 323–334.
[493] E. Barlaka, V. Ledvenyiova, E. Galatou, M. Ferko, S. Carnicka, T. Ravingerova, A. Lazou, Delayed cardioprotective effects of WY-14643 are associated with inhibition of MMP-2 and modulation of Bcl-2 family proteins through PPAR-alpha activation in rat hearts subjected to global ischaemia-reperfusion, Can. J. Physiol. Pharmacol. 91 (2013) 608–616.
[494] E. Barlaka, A. Gorbe, R. Gaspar, J. Paloczi, P. Ferdinandy, A. Lazou, Activation of PPARbeta/delta protects cardiac myocytes from oxidative stress-induced apoptosis by suppressing generation of reactive oxygen/nitrogen species and expression of matrix metalloproteinases, Pharmacol. Res. 95–96 (2015) 102–110.
[495] H. Lee, S.A. Ham, M.Y. Kim, J.H. Kim, K.S. Paek, E.S. Kang, H.J. Kim, J.S. Hwang, T. Yoo, C. Park, J.H. Kim, D.S. Lim, C.W. Han, H.G. Seo, Activation of PPARdelta counteracts angiotensin II-induced ROS generation by inhibiting rac1 translocation in vascular smooth muscle cells, Free Radic. Res. 46 (2012) 912–919.
[496] J. Liu, P. Wang, J. Luo, Y. Huang, L. He, H. Yang, Q. Li, S. Wu, O. Zhelyabovska, Q. Yang, Peroxisome proliferator-activated receptor beta/delta activation in adult hearts facilitates mitochondrial function and cardiac performance under pressure-overload condition, Hypertension 57 (2011) 223–230.
[497] T. Ravingerova, S. Carnicka, M. Nemcekova, V. Ledvenyiova, A. Adameova, T. Kelly, E. Barlaka, E. Galatou, V.K. Khandelwal, A. Lazou, PPAR-alpha activation as a preconditioning-like intervention in rats in vivo confers myocardial protection against acute ischaemia-reperfusion injury: involvement of PI3K-Akt, Can. J. Physiol. Pharmacol. 90 (2012) 1135–1144.
[498] T. Ravingerova, V. Ledvenyiova-Farkasova, M. Ferko, M. Bartekova, I. Bernatova, O. Pechanova, A. Adameova, F. Kolar, A. Lazou, Pleiotropic preconditioning-like cardioprotective effects of hypolipidemic drugs in acute ischemia-reperfusion in normal and hypertensive rats, Can. J. Physiol. Pharmacol. 93 (2015) 495–503.
[499] L.L. Baggio, D.J. Drucker, Biology of incretins: glp-1 and GIP, Gastroenterology 132 (2007) 2131–2157.
[500] P.K. Lund, R.H. Goodman, P.C. Dee, J.F. Habener, Pancreatic preproglucagon cDNA contains two glucagon-related coding sequences arranged in tandem, Proc. Natl. Acad. Sci. USA 79 (1982) 345–349.
[501] R. Mentlein, B. Gallwitz, W.E. Schmidt, Dipeptidyl-peptidase IV hydrolyses gastric inhibitory polypeptide, glucagon-like peptide-1(7-36)amide, peptide histidine methionine and is responsible for their degradation in human serum, Eur. J. Biochem. 214 (1993) 829–835.
[502] T.J. Kieffer, C.H. McIntosh, R.A. Pederson, Degradation of glucose-dependent insulinotropic polypeptide and truncated glucagon-like peptide 1 in vitro and in vivo by dipeptidyl peptidase IV, Endocrinology 136 (1995) 3585–3596.
[503] J. Matsubara, S. Sugiyama, K. Sugamura, T. Nakamura, Y. Fujiwara, E. Akiyama, H. Kurokawa, T. Nozaki, K. Ohba, M. Konishi, H. Maeda, Y. Izumiya, K. Kaikita, H. Sumida, H. Jinnouchi, K. Matsui, S. Kim-Mitsuyama, M. Takeya, H. Ogawa, A dipeptidyl peptidase-4 inhibitor, des-fluoro-sitagliptin, improves endothelial function and reduces atherosclerotic lesion formation in apolipoprotein E-deficient mice, J. Am. Coll. Cardiol. 59 (2012) 265–276.
[504] Z. Shah, T. Kampfrath, J.A. Deiuliis, J. Zhong, C. Pineda, Z. Ying, X. Xu, B. Lu, S. Moffatt-Bruce, R. Durairaj, Q. Sun, G. Mihai, A. Maiseyeu, S. Rajagopalan, Long-term dipeptidyl-peptidase 4 inhibition reduces atherosclerosis and inflammation via effects on monocyte recruitment and chemotaxis, Circulation 124 (2011) 2338–2349.
[505] T. Nishioka, M. Shinohara, N. Tanimoto, C. Kumagai, K. Hashimoto, Sitagliptin, a dipeptidyl peptidase-IV inhibitor, improves psoriasis, Dermatology 224 (2012) 20–21.
[506] M. Kern, N. Kloting, H.G. Niessen, L. Thomas, D. Stiller, M. Mark, T. Klein, M. Bluher, Linagliptin improves insulin sensitivity and hepatic steatosis in diet-induced obesity, PLoS One 7 (2012) e38744.
[507] V. Darsalia, H. Ortsater, A. Olverling, E. Darlof, P. Wolbert, T. Nystrom, T. Klein, A. Sjoholm, C. Patrone, The DPP-4 inhibitor linagliptin counteracts stroke in the normal and diabetic mouse brain: a comparison with glimepiride, Diabetes 62 (2013) 1289–1296.
[508] S. Kroller-Schon, M. Knorr, M. Hausding, M. Oelze, A. Schuff, R. Schell, S. Sudowe, A. Scholz, S. Daub, S. Karbach, S. Kossmann, T. Gori, P. Wenzel, E. Schulz, S. Grabbe, T. Klein, T. Munzel, A. Daiber, Glucose-independent improvement of vascular dysfunction in experimental sepsis by dipeptidyl-peptidase 4 inhibition, Cardiovasc Res 96 (2012) 140–149.
[509] A. Cameron-Vendrig, A. Reheman, M.A. Siraj, X.R. Xu, Y. Wang, X. Lei, T. Afroze, E. Shikatani, O. El-Mounayri, H. Noyan, R. Weissleder, H. Ni, M. Husain, Glucagon-like peptide 1 receptor activation attenuates platelet aggregation and thrombosis, Diabetes 65 (2016) 1714–1723.
[510] D. Harman, Aging: a theory based on free radical and radiation chemistry, J. Gerontol. 11 (1956) 298–300.
[511] J. Miquel, A.C. Economos, J. Fleming, J.E. Johnson Jr., Mitochondrial role in cell aging, Exp. Gerontol. 15 (1980) 575–591.
[512] P.W. Kleikers, K. Wingler, J.J. Hermans, I. Diebold, S. Altenhofer, K.A. Radermacher, B. Janssen, A. Gorlach, H.H. Schmidt, NADPH oxidases as a source of oxidative stress and molecular target in ischemia/reperfusion injury, J. Mol. Med. 90 (2012) 1391–1406.
[513] L. Park, P. Zhou, R. Pitstick, C. Capone, J. Anrather, E.H. Norris, L. Younkin, S. Younkin, G. Carlson, B.S. McEwen, C. Iadecola, Nox2-derived radicals contribute to neurovascular and behavioral dysfunction in mice overexpressing the amyloid precursor protein, Proc. Natl. Acad. Sci. USA 105 (2008) 1347–1352.
[514] N. Chondrogianni, F.L. Stratford, I.P. Trougakos, B. Friguet, A.J. Rivett, E.S. Gonos, Central role of the proteasome in senescence and survival of human fibroblasts: induction of a senescence-like phenotype upon its inhibition and resistance to stress upon its activation, J. Biol. Chem. 278 (2003) 28026–28037.
[515] C.K. Liu, A. Lyass, M.G. Larson, J.M. Massaro, N. Wang, R.B. D'Agostino Sr., E.J. Benjamin, J.M. Murabito, Biomarkers of oxidative stress are associated with frailty: the Framingham offspring study, Age 38 (2016) 1.
[516] M. Ingles, J. Gambini, J.A. Carnicero, F.J. Garcia-Garcia, L. Rodriguez-Manas, G. Olaso-Gonzalez, M. Dromant, C. Borras, J. Vina, Oxidative stress is related to frailty, not to age or sex, in a geriatric population: lipid and protein oxidation as biomarkers of frailty, J. Am. Geriatr. Soc. 62 (2014) 1324–1328.
[517] M.C. Gomez-Cabrera, M. Ristow, J. Vina, Antioxidant supplements in exercise: worse than useless? Am. J. Physiol. Endocrinol. Metab. 302 (2012) E476–E477 (author reply E478-E479).
[518] Y. Zhang, Y. Ikeno, W. Qi, A. Chaudhuri, Y. Li, A. Bokov, S.R. Thorpe, J.W. Baynes, C. Epstein, A. Richardson, H. Van Remmen, Mice deficient in both Mn superoxide dismutase and glutathione peroxidase-1 have increased oxidative damage and a greater incidence of pathology but no reduction in longevity, J. Gerontol. A Biol. Sci. Med. Sci. 64 (2009) 1212–1220.
[519] K. Jin, Modern biological theories of aging, Aging Dis. 1 (2010) 72–74.
[520] J. Vina, C. Borras, J. Miquel, Theories of ageing, IUBMB Life 59 (2007) 249–254.
[521] K. Bedard, K.H. Krause, The NOX family of ROS-generating NADPH oxidases: physiology and pathophysiology, Physiol. Rev. 87 (2007) 245–313.
[522] M. Geiszt, NADPH oxidases: new kids on the block, Cardiovasc Res 71 (2006) 289–299.
[523] S. Liang, T. Kisseleva, D.A. Brenner, The role of NADPH Oxidases (NOXs) in liver fibrosis and the activation of myofibroblasts, Front. Physiol. 7 (2016) 17.
[524] B. Lener, R. Koziel, H. Pircher, E. Hutter, R. Greussing, D. Herndler-Brandstetter, M. Hermann, H. Unterluggauer, P. Jansen-Durr, The NADPH oxidase Nox4 restricts the replicative lifespan of human endothelial cells, Biochem. J. 423 (2009) 363–374.
[525] R. Koziel, H. Pircher, M. Kratochwil, B. Lener, M. Hermann, N.A. Dencher, P. Jansen-Durr, Mitochondrial respiratory chain complex I is inactivated by NADPH oxidase Nox4, Biochem. J. 452 (2013) 231–239.
[526] U. Weyemi, O. Lagente-Chevallier, M. Boufraqech, F. Prenois, F. Courtin, B. Caillou, M. Talbot, M. Dardalhon, A. Al Ghuzlan, J.M. Bidart, M. Schlumberger, C. Dupuy, ROS-generating NADPH oxidase NOX4 is a critical mediator in oncogenic H-Ras-induced DNA damage and subsequent senescence, Oncogene 31 (2012) 1117–1129.
[527] R. Kodama, M. Kato, S. Furuta, S. Ueno, Y. Zhang, K. Matsuno, C. Yabe-Nishimura, E. Tanaka, T. Kamata, ROS-generating oxidases Nox1 and Nox4 contribute to oncogenic Ras-induced premature senescence, Genes Cells 18 (2013) 32–41.
[528] S. Senturk, M. Mumcuoglu, O. Gursoy-Yuzugullu, B. Cingoz, K.C. Akcali,

M. Ozturk, Transforming growth factor-beta induces senescence in hepatocellular carcinoma cells and inhibits tumor growth, Hepatology 52 (2010) 966–974.
[529] T. Ago, S. Matsushima, J. Kuroda, D. Zablocki, T. Kitazono, J. Sadoshima, The NADPH oxidase Nox4 and aging in the heart, Aging 2 (2010) 1012–1016.
[530] M. Wang, J. Zhang, S.J. Walker, R. Dworakowski, E.G. Lakatta, A.M. Shah, Involvement of NADPH oxidase in age-associated cardiac remodeling, J. Mol. Cell Cardiol. 48 (2010) 765–772.
[531] A.E. Vendrov, K.C. Vendrov, A. Smith, J. Yuan, A. Sumida, J. Robidoux, M.S. Runge, N.R. Madamanchi, NOX4 NADPH oxidase-dependent mitochondrial oxidative stress in aging-associated cardiovascular disease, Antioxid. Redox Signal. 23 (2015) 1389–1409.
[532] C. Kleinschnitz, H. Grund, K. Wingler, M.E. Armitage, E. Jones, M. Mittal, D. Barit, T. Schwarz, C. Geis, P. Kraft, K. Barthel, M.K. Schuhmann, A.M. Herrmann, S.G. Meuth, G. Stoll, S. Meurer, A. Schrewe, L. Becker, V. Gailus-Durner, H. Fuchs, T. Klopstock, M.H. de Angelis, K. Jandeleit-Dahm, A.M. Shah, N. Weissmann, H.H. Schmidt, Post-stroke inhibition of induced NADPH oxidase type 4 prevents oxidative stress and neurodegeneration, PLoS Biol. 8 (2010).
[533] S. Piera-Velazquez, S.A. Jimenez, Role of cellular senescence and NOX4-mediated oxidative stress in systemic sclerosis pathogenesis, Curr. Rheumatol. Rep. 17 (2015) 473.
[534] L. Hecker, N.J. Logsdon, D. Kurundkar, A. Kurundkar, K. Bernard, T. Hock, E. Meldrum, Y.Y. Sanders, V.J. Thannickal, Reversal of persistent fibrosis in aging by targeting Nox4-Nrf2 redox imbalance, Sci. Transl. Med. 6 (2014) 231ra247.
[535] M. Armanios, Telomerase and idiopathic pulmonary fibrosis, Mutat. Res. 730 (2012) 52–58.
[536] S.E. Stanley, I. Noth, M. Armanios, What the genetics "RTEL"ing us about telomeres and pulmonary fibrosis, Am. J. Respir. Crit. Care Med. 191 (2015) 608–610.
[537] W. Zhang, T. Wang, L. Qin, H.M. Gao, B. Wilson, S.F. Ali, W. Zhang, J.S. Hong, B. Liu, Neuroprotective effect of dextromethorphan in the MPTP Parkinson's disease model: role of NADPH oxidase, FASEB J. 18 (2004) 589–591.
[538] M. Holl, R. Koziel, G. Schafer, H. Pircher, A. Pauck, M. Hermann, H. Klocker, P. Jansen-Durr, N. Sampson, ROS signaling by NADPH oxidase 5 modulates the proliferation and survival of prostate carcinoma cells, Mol. Carcinog. 55 (2016) 27–39.
[539] N. Sampson, R. Koziel, C. Zenzmaier, L. Bubendorf, E. Plas, P. Jansen-Durr, P. Berger, ROS signaling by NOX4 drives fibroblast-to-myofibroblast differentiation in the diseased prostatic stroma, Mol. Endocrinol. 25 (2011) 503–515.
[540] G. Ayala, J.A. Tuxhorn, T.M. Wheeler, A. Frolov, P.T. Scardino, M. Ohori, M. Wheeler, J. Spitler, D.R. Rowley, Reactive stroma as a predictor of biochemical-free recurrence in prostate cancer, Clin. Cancer Res 9 (2003) 4792–4801.
[541] A. Hohn, T. Jung, S. Grimm, T. Grune, Lipofuscin-bound iron is a major intracellular source of oxidants: role in senescent cells, Free Radic. Biol. Med. 48 (2010) 1100–1108.
[542] M. Kastle, T. Grune, Interactions of the proteasomal system with chaperones: protein triage and protein quality control, Prog. Mol. Biol. Transl. Sci. 109 (2012) 113–160.
[543] T. Jung, B. Catalgol, T. Grune, The proteasomal system, Mol. Asp. Med. 30 (2009) 191–296.
[544] A. Hohn, T. Jung, S. Grimm, B. Catalgol, D. Weber, T. Grune, Lipofuscin inhibits the proteasome by binding to surface motifs, Free Radic. Biol. Med. 50 (2011) 585–591.
[545] S. Keck, R. Nitsch, T. Grune, O. Ullrich, Proteasome inhibition by paired helical filament-tau in brains of patients with Alzheimer's disease, J. Neurochem. 85 (2003) 115–122.
[546] B. Catalgol, I. Ziaja, N. Breusing, T. Jung, A. Hohn, B. Alpertunga, P. Schroeder, N. Chondrogianni, E.S. Gonos, I. Petropoulos, B. Friguet, L.O. Klotz, J. Krutmann, T. Grune, The proteasome is an integral part of solar ultraviolet a radiation-induced gene expression, J. Biol. Chem. 284 (2009) 30076–30086.
[547] M. Kastle, E. Woschee, T. Grune, Histone deacetylase 6 (HDAC6) plays a crucial role in p38MAPK-dependent induction of heme oxygenase-1 (HO-1) in response to proteasome inhibition, Free Radic. Biol. Med. 53 (2012) 2092–2101.
[548] N. Chondrogianni, K. Georgila, N. Kourtis, N. Tavernarakis, E.S. Gonos, 20S proteasome activation promotes life span extension and resistance to proteotoxicity in Caenorhabditis elegans, FASEB J. 29 (2015) 611–622.
[549] D. Vilchez, I. Morantte, Z. Liu, P.M. Douglas, C. Merkwirth, A.P. Rodrigues, G. Manning, A. Dillin, RPN-6 determines C. elegans longevity under proteotoxic stress conditions, Nature 489 (2012) 263–268.
[550] A. Tonoki, E. Kuranaga, T. Tomioka, J. Hamazaki, S. Murata, K. Tanaka, M. Miura, Genetic evidence linking age-dependent attenuation of the 26S proteasome with the aging process, Mol. Cell Biol. 29 (2009) 1095–1106.
[551] S. Kapeta, N. Chondrogianni, E.S. Gonos, Nuclear erythroid factor 2-mediated proteasome activation delays senescence in human fibroblasts, J. Biol. Chem. 285 (2010) 8171–8184.
[552] N. Papaevgeniou, M. Sakellari, S. Jha, N. Tavernarakis, C.I. Holmberg, E.S. Gonos, N. Chondrogianni, 18alpha-glycyrrhetinic acid proteasome activator decelerates aging and Alzheimer's disease progression in caenorhabditis elegans and neuronal cultures, Antioxid. Redox Signal. 25 (2016) 855–869.
[553] N. Chondrogianni, S. Kapeta, I. Chinou, K. Vassilatou, I. Papassideri, E.S. Gonos, Anti-ageing and rejuvenating effects of quercetin, Exp. Gerontol. 45 (2010) 763–771.
[554] C. Regitz, L.M. Dussling, U. Wenzel, Amyloid-beta (Abeta(1)(-)(4)(2))-induced paralysis in Caenorhabditis elegans is inhibited by the polyphenol quercetin through activation of protein degradation pathways, Mol. Nutr. Food Res. 58 (2014) 1931–1940.
[555] Y. Mikhed, A. Daiber, S. Steven, Mitochondrial oxidative stress, mitochondrial DNA damage and their role in age-related vascular dysfunction, Int. J. Mol. Sci. 16 (2015) 15918–15953.
[556] A.A. Moskalev, A.M. Aliper, Z. Smit-McBride, A. Buzdin, A. Zhavoronkov, Genetics and epigenetics of aging and longevity, Cell Cycle 13 (2014) 1063–1077.
[557] V.I. Perez, A. Bokov, H. Van Remmen, J. Mele, Q. Ran, Y. Ikeno, A. Richardson, Is the oxidative stress theory of aging dead? Biochim. Biophys. Acta 1790 (2009) 1005–1014.
[558] F.L. Muller, M.S. Lustgarten, Y. Jang, A. Richardson, H. Van Remmen, Trends in oxidative aging theories, Free Radic. Biol. Med. 43 (2007) 477–503.
[559] Y. Li, T.T. Huang, E.J. Carlson, S. Melov, P.C. Ursell, J.L. Olson, L.J. Noble, M.P. Yoshimura, C. Berger, P.H. Chan, et al., Dilated cardiomyopathy and neonatal lethality in mutant mice lacking manganese superoxide dismutase, Nat. Genet. 11 (1995) 376–381.
[560] G.G. Camici, F. Cosentino, F.C. Tanner, T.F. Luscher, The role of p66Shc deletion in age-associated arterial dysfunction and disease states, J. Appl. Physiol. 105 (2008) 1628–1631.
[561] D.F. Dai, Y.A. Chiao, D.J. Marcinek, H.H. Szeto, P.S. Rabinovitch, Mitochondrial oxidative stress in aging and healthspan, Longev. Health. 3 (2014) 6.
[562] R.T. Hamilton, M.E. Walsh, H. Van Remmen, Mouse models of oxidative stress indicate a role for modulating healthy aging, J. Clin. Exp. Pathol. Suppl 4 (2012).
[563] P. Wenzel, S. Schuhmacher, J. Kienhofer, J. Muller, M. Hortmann, M. Oelze, E. Schulz, N. Treiber, T. Kawamoto, K. Scharffetter-Kochanek, T. Munzel, A. Burkle, M.M. Bachschmid, A. Daiber, Manganese superoxide dismutase and aldehyde dehydrogenase deficiency increase mitochondrial oxidative stress and aggravate age-dependent vascular dysfunction, Cardiovasc. Res. 80 (2008) 280–289.
[564] A.K. Doughan, D.G. Harrison, S.I. Dikalov, Molecular mechanisms of angiotensin II-mediated mitochondrial dysfunction: linking mitochondrial oxidative damage and vascular endothelial dysfunction, Circ. Res. 102 (2008) 488–496.
[565] B. Schottker, H. Brenner, E.H. Jansen, J. Gardiner, A. Peasey, R. Kubinova, A. Pajak, R. Topor-Madry, A. Tamosiunas, K.U. Saum, B. Holleczek, H. Pikhart, M. Bobak, Evidence for the free radical/oxidative stress theory of ageing from the CHANCES consortium: a meta-analysis of individual participant data, BMC Med. 13 (2015) 300.
[566] M. Capri, M. Moreno-Villanueva, E. Cevenini, E. Pini, M. Scurti, V. Borelli, M.G. Palmas, M. Zoli, C. Schon, A. Siepelmeyer, J. Bernhardt, S. Fiegl, G. Zondag, A.J. de Craen, A. Hervonen, M. Hurme, E. Sikora, E.S. Gonos, K. Voutetakis, O. Toussaint, F. Debacq-Chainiaux, B. Grubeck-Loebenstein, A. Burkle, C. Franceschi, MARK-AGE population: from the human model to new insights, Mech. Ageing Dev. 151 (2015) 13–17.
[567] L. Rodriguez-Manas, L.P. Fried, Frailty in the clinical scenario, Lancet 385 (2015) e7–e9.
[568] H.Y. Lai, H.T. Chang, Y.L. Lee, S.J. Hwang, Association between inflammatory markers and frailty in institutionalized older men, Maturitas 79 (2014) 329–333.
[569] J.M. Argiles, N. Campos, J.M. Lopez-Pedrosa, R. Rueda, L. Rodriguez-Manas, Skeletal muscle regulates metabolism via interorgan crosstalk: roles in health and disease, J. Am. Med Dir. Assoc. 17 (2016) 789–796.
[570] C.K. Sen, L. Packer, Antioxidant and redox regulation of gene transcription, FASEB J. 10 (1996) 709–720.
[571] Y.J. Suzuki, H.J. Forman, A. Sevanian, Oxidants as stimulators of signal transduction, Free Radic. Biol. Med. 22 (1997) 269–285.
[572] F. Esposito, R. Ammendola, R. Faraonio, T. Russo, F. Cimino, Redox control of signal transduction, gene expression and cellular senescence, Neurochem. Res. 29 (2004) 617–628.
[573] W.M. Nauseef, N. Borregaard, Neutrophils at work, Nat. Immunol. 15 (2014) 602–611.
[574] K. Forsberg, A. Wuttke, G. Quadrato, P.M. Chumakov, A. Wizenmann, S. Di Giovanni, The tumor suppressor p53 fine-tunes reactive oxygen species levels and neurogenesis via PI3 kinase signaling, J. Neurosci. 33 (2013) 14318–14330.
[575] K. Wang, T. Zhang, Q. Dong, E.C. Nice, C. Huang, Y. Wei, Redox homeostasis: the linchpin in stem cell self-renewal and differentiation, Cell Death Dis. 4 (2013) e537.
[576] C.F. Lourenco, A. Ledo, C. Dias, R.M. Barbosa, J. Laranjinha, Neurovascular and neurometabolic derailment in aging and Alzheimer's disease, Front. Aging Neurosci. 7 (2015) 103.
[577] G.J. McBean, The transsulfuration pathway: a source of cysteine for glutathione in astrocytes, Amino Acids 42 (2012) 199–205.
[578] S.K. Biswas, Does the interdependence between oxidative stress and inflammation explain the antioxidant paradox? Oxid. Med. Cell Longev. 2016 (2016) 5698931.
[579] W.M. Nauseef, How human neutrophils kill and degrade microbes: an integrated view, Immunol. Rev. 219 (2007) 88–102.
[580] B.M. Babior, Phagocytes and oxidative stress, Am. J. Med. 109 (2000) 33–44.
[581] O. Sareila, T. Kelkka, A. Pizzolla, M. Hultqvist, R. Holmdahl, NOX2 complex-derived ROS as immune regulators, Antioxid. Redox Signal. 15 (2011) 2197–2208.
[582] K.A. Gelderman, M. Hultqvist, J. Holmberg, P. Olofsson, R. Holmdahl, T cell surface redox levels determine T cell reactivity and arthritis susceptibility, Proc. Natl. Acad. Sci. USA 103 (2006) 12831–12836.
[583] J. El-Benna, P.M. Dang, M.A. Gougerot-Pocidalo, Priming of the neutrophil NADPH oxidase activation: role of p47phox phosphorylation and NOX2 mobilization to the plasma membrane, Semin. Immunopathol. 30 (2008) 279–289.
[584] K. Lee, H.Y. Won, M.A. Bae, J.H. Hong, E.S. Hwang, Spontaneous and aging-dependent development of arthritis in NADPH oxidase 2 deficiency through altered differentiation of CD11b+ and Th/Treg cells, Proc. Natl. Acad. Sci. USA 108 (2011) 9548–9553.
[585] W. Droge, Free radicals in the physiological control of cell function, Physiol. Rev. 82 (2002) 47–95.

[586] R. Miesel, M. Kurpisz, H. Kroger, Suppression of inflammatory arthritis by simultaneous inhibition of nitric oxide synthase and NADPH oxidase, Free Radic. Biol. Med. 20 (1996) 75–81.
[587] D. Roos, D.B. Kuhns, A. Maddalena, J. Roesler, J.A. Lopez, T. Ariga, T. Avcin, M. de Boer, J. Bustamante, A. Condino-Neto, G. Di Matteo, J. He, H.R. Hill, S.M. Holland, C. Kannengiesser, M.Y. Koker, I. Kondratenko, K. van Leeuwen, H.L. Malech, L. Marodi, H. Nunoi, M.J. Stasia, A.M. Ventura, C.T. Witwer, B. Wolach, J.I. Gallin, Hematologically important mutations: x-linked chronic granulomatous disease (third update), Blood Cells Mol. Dis. 45 (2010) 246–265.
[588] D. Roos, D.B. Kuhns, A. Maddalena, J. Bustamante, C. Kannengiesser, M. de Boer, K. van Leeuwen, M.Y. Koker, B. Wolach, J. Roesler, H.L. Malech, S.M. Holland, J.I. Gallin, M.J. Stasia, Hematologically important mutations: the autosomal recessive forms of chronic granulomatous disease (second update), Blood Cells Mol. Dis. 44 (2010) 291–299.
[589] D.B. Kuhns, W.G. Alvord, T. Heller, J.J. Feld, K.M. Pike, B.E. Marciano, G. Uzel, S.S. DeRavin, D.A. Priel, B.P. Soule, K.A. Zarember, H.L. Malech, S.M. Holland, J.I. Gallin, Residual NADPH oxidase and survival in chronic granulomatous disease, N. Engl. J. Med. 363 (2010) 2600–2610.
[590] J.M. van den Berg, E. van Koppen, A. Ahlin, B.H. Belohradsky, E. Bernatowska, L. Corbeel, T. Espanol, A. Fischer, M. Kurenko-Deptuch, R. Mouy, T. Petropoulou, J. Roesler, R. Seger, M.J. Stasia, N.H. Valerius, R.S. Weening, B. Wolach, D. Roos, T.W. Kuijpers, Chronic granulomatous disease: the European experience, PLoS One 4 (2009) e5234.
[591] J. Boulais, M. Trost, C.R. Landry, R. Dieckmann, E.D. Levy, T. Soldati, S.W. Michnick, P. Thibault, M. Desjardins, Molecular characterization of the evolution of phagosomes, Mol. Syst. Biol. 6 (2010) 423.
[592] P. Cosson, T. Soldati, Eat, kill or die: when amoeba meets bacteria, Curr. Opin. Microbiol. 11 (2008) 271–276.
[593] B. Lardy, M. Bof, L. Aubry, M.H. Paclet, F. Morel, M. Satre, G. Klein, NADPH oxidase homologs are required for normal cell differentiation and morphogenesis in Dictyostelium discoideum, Biochim. Biophys. Acta 1744 (2005) 199–212.
[594] S. Basu, P. Fey, D. Jimenez-Morales, R.J. Dodson, R.L. Chisholm, dictyBase 2015: expanding data and annotations in a new software environment, Genesis 53 (2015) 523–534.
[595] S.M. Tung, C. Unal, A. Ley, C. Pena, B. Tunggal, A.A. Noegel, O. Krut, M. Steinert, L. Eichinger, Loss of Dictyostelium ATG9 results in a pleiotropic phenotype affecting growth, development, phagocytosis and clearance and replication of Legionella pneumophila, Cell. Microbiol. 12 (2010) 765–780.
[596] G. Bloomfield, C. Pears, Superoxide signalling required for multicellular development of Dictyostelium, J. Cell Sci. 116 (2003) 3387–3397.
[597] M.X. Garcia, H. Alexander, D. Mahadeo, D.A. Cotter, S. Alexander, The Dictyostelium discoideum prespore-specific catalase B functions to control late development and to protect spore viability, Biochim. Biophys. Acta 1641 (2003) 55–64.
[598] G. Chen, O. Zhuchenko, A. Kuspa, Immune-like phagocyte activity in the social amoeba, Science 317 (2007) 678–681.
[599] X. Zhang, O. Zhuchenko, A. Kuspa, T. Soldati, Social amoebae trap and kill bacteria by casting DNA nets, Nat. Commun. 7 (2016) 10938.
[600] X. Zhang, T. Soldati, Of amoebae and men: extracellular DNA traps as an ancient cell-intrinsic defense mechanism, Front. Immunol. 7 (2016) 269.
[601] N. Rieber, A. Hector, T. Kuijpers, D. Roos, D. Hartl, Current concepts of hyperinflammation in chronic granulomatous disease, Clin. Dev. Immunol. 2012 (2012) 252460.
[602] K.L. Brown, J. Bylund, K.L. MacDonald, G.X. Song-Zhao, M.R. Elliott, R. Falsafi, R.E. Hancock, D.P. Speert, ROS-deficient monocytes have aberrant gene expression that correlates with inflammatory disorders of chronic granulomatous disease, Clin. Immunol. 129 (2008) 90–102.
[603] A. de Luca, S.P. Smeekens, A. Casagrande, R. Iannitti, K.L. Conway, M.S. Gresnigt, J. Begun, T.S. Plantinga, L.A. Joosten, J.W. van der Meer, G. Chamilos, M.G. Netea, R.J. Xavier, C.A. Dinarello, L. Romani, F.L. van de Veerdonk, IL-1 receptor blockade restores autophagy and reduces inflammation in chronic granulomatous disease in mice and in humans, Proc. Natl. Acad. Sci. USA 111 (2014) 3526–3531.
[604] C.J. Harbort, P.V. Soeiro-Pereira, H. von Bernuth, A.M. Kaindl, B.T. Costa-Carvalho, A. Condino-Neto, J. Reichenbach, J. Roesler, A. Zychlinsky, B. Amulic, Neutrophil oxidative burst activates ATM to regulate cytokine production and apoptosis, Blood 126 (2015) 2842–2851.
[605] F. Violi, V. Sanguigni, R. Carnevale, A. Plebani, P. Rossi, A. Finocchi, C. Pignata, D. De Mattia, B. Martire, M.C. Pietrogrande, S. Martino, E. Gambineri, A.R. Soresina, P. Pignatelli, F. Martino, S. Basili, L. Loffredo, Hereditary deficiency of gp91(phox) is associated with enhanced arterial dilatation: results of a multicenter study, Circulation 120 (2009) 1616–1622.
[606] K.T. Kishida, C.A. Hoeffer, D. Hu, M. Pao, S.M. Holland, E. Klann, Synaptic plasticity deficits and mild memory impairments in mouse models of chronic granulomatous disease, Mol. Cell Biol. 26 (2006) 5908–5920.
[607] M. Pao, E.A. Wiggs, M.M. Anastacio, J. Hyun, E.S. DeCarlo, J.T. Miller, V.L. Anderson, H.L. Malech, J.I. Gallin, S.M. Holland, Cognitive function in patients with chronic granulomatous disease: a preliminary report, Psychosomatics 45 (2004) 230–234.
[608] T.S. Cole, F. McKendrick, A.J. Cant, M.S. Pearce, C.M. Cale, D.R. Goldblatt, A.R. Gennery, P. Titman, Cognitive ability in children with chronic granulomatous disease: a comparison of those managed conservatively with those who have undergone hematopoietic stem cell transplant, Neuropediatrics 44 (2013) 230–232.
[609] C. Iadecola, Neurovascular regulation in the normal brain and in Alzheimer's disease, Nat. Rev. Neurosci. 5 (2004) 347–360.
[610] M.E. Raichle, M.A. Mintun, Brain work and brain imaging, Annu. Rev. Neurosci. 29 (2006) 449–476.
[611] R.M. Santos, C.F. Lourenco, A.P. Piedade, R. Andrews, F. Pomerleau, P. Huettl, G.A. Gerhardt, J. Laranjinha, R.M. Barbosa, A comparative study of carbon fiber-based microelectrodes for the measurement of nitric oxide in brain tissue, Biosens. Bioelectron. 24 (2008) 704–709.
[612] C.F. Lourenco, R.M. Santos, R.M. Barbosa, E. Cadenas, R. Radi, J. Laranjinha, Neurovascular coupling in hippocampus is mediated via diffusion by neuronal-derived nitric oxide, Free Radic. Biol. Med. 73 (2014) 421–429.
[613] M.W. Cleeter, J.M. Cooper, V.M. Darley-Usmar, S. Moncada, A.H. Schapira, Reversible inhibition of cytochrome c oxidase, the terminal enzyme of the mitochondrial respiratory chain, by nitric oxide. Implications for neurodegenerative diseases, FEBS Lett. 345 (1994) 50–54.
[614] A. Ledo, R. Barbosa, E. Cadenas, J. Laranjinha, Dynamic and interacting profiles of *NO and O2 in rat hippocampal slices, Free Radic. Biol. Med. 48 (2010) 1044–1050.
[615] A. Ledo, R.M. Barbosa, G.A. Gerhardt, E. Cadenas, J. Laranjinha, Concentration dynamics of nitric oxide in rat hippocampal subregions evoked by stimulation of the NMDA glutamate receptor, Proc. Natl. Acad. Sci. USA 102 (2005) 17483–17488.
[616] R. Dringen, B. Pfeiffer, B. Hamprecht, Synthesis of the antioxidant glutathione in neurons: supply by astrocytes of CysGly as precursor for neuronal glutathione, J. Neurosci. 19 (1999) 562–569.
[617] S. Kandil, L. Brennan, G.J. McBean, Glutathione depletion causes a JNK and p38MAPK-mediated increase in expression of cystathionine-gamma-lyase and upregulation of the transsulfuration pathway in C6 glioma cells, Neurochem. Int. 56 (2010) 611–619.
[618] B. Mysona, Y. Dun, J. Duplantier, V. Ganapathy, S.B. Smith, Effects of hyperglycemia and oxidative stress on the glutamate transporters GLAST and system xc- in mouse retinal Muller glial cells, Cell Tissue Res. 335 (2009) 477–488.
[619] A. Banjac, T. Perisic, H. Sato, A. Seiler, S. Bannai, N. Weiss, P. Kolle, K. Tschoep, R.D. Issels, P.T. Daniel, M. Conrad, G.W. Bornkamm, The cystine/cysteine cycle: a redox cycle regulating susceptibility versus resistance to cell death, Oncogene 27 (2008) 1618–1628.
[620] O. Pampliega, M. Domercq, F.N. Soria, P. Villoslada, A. Rodriguez-Antiguedad, C. Matute, Increased expression of cystine/glutamate antiporter in multiple sclerosis, J. Neuroinflamm. 8 (2011) 63.
[621] P. Mesci, S. Zaidi, C.S. Lobsiger, S. Millecamps, C. Escartin, D. Seilhean, H. Sato, M. Mallat, S. Boillee, System xC- is a mediator of microglial function and its deletion slows symptoms in amyotrophic lateral sclerosis mice, Brain 138 (2015) 53–68.
[622] S. Watkins, H. Sontheimer, Unique biology of gliomas: challenges and opportunities, Trends Neurosci. 35 (2012) 546–556.
[623] L. Chen, X. Li, L. Liu, B. Yu, Y. Xue, Y. Liu, Erastin sensitizes glioblastoma cells to temozolomide by restraining xCT and cystathionine-gamma-lyase function, Oncol. Rep. 33 (2015) 1465–1474.
[624] R. Schliebs, T. Arendt, The significance of the cholinergic system in the brain during aging and in Alzheimer's disease, J. Neural Transm. 113 (2006) 1625–1644.
[625] M. McKinney, M.C. Jacksonville, Brain cholinergic vulnerability: relevance to behavior and disease, Biochem. Pharmacol. 70 (2005) 1115–1124.
[626] H. Wang, M. Yu, M. Ochani, C.A. Amella, M. Tanovic, S. Susarla, J.H. Li, H. Wang, H. Yang, L. Ulloa, Y. Al-Abed, C.J. Czura, K.J. Tracey, Nicotinic acetylcholine receptor alpha7 subunit is an essential regulator of inflammation, Nature 421 (2003) 384–388.
[627] E. Navarro, L. Gonzalez-Lafuente, I. Perez-Liebana, I. Buendia, E. Lopez-Bernardo, C. Sanchez-Ramos, I. Prieto, A. Cuadrado, J. Satrustegui, S. Cadenas, M. Monsalve, M.G. Lopez, Heme-oxygenase I and PCG-1alpha regulate mitochondrial biogenesis via microglial activation of Alpha7 nicotinic acetylcholine receptors using PNU282987. Antioxid. Redox Signal., 2016. http://dx.doi.org/10.1089/ars.2016.6698.
[628] E. Parada, J. Egea, I. Buendia, P. Negredo, A.C. Cunha, S. Cardoso, M.P. Soares, M.G. Lopez, The microglial alpha7-acetylcholine nicotinic receptor is a key element in promoting neuroprotection by inducing heme oxygenase-1 via nuclear factor erythroid-2-related factor 2, Antioxid. Redox Signal. 19 (2013) 1135–1148.
[629] J. Egea, I. Buendia, E. Parada, E. Navarro, R. Leon, M.G. Lopez, Anti-inflammatory role of microglial alpha7 nAChRs and its role in neuroprotection, Biochem. Pharmacol. 97 (2015) 463–472.
[630] A. Shakirzyanova, G. Valeeva, A. Giniatullin, N. Naumenko, S. Fulle, A. Akulov, M. Atalay, E. Nikolsky, R. Giniatullin, Age-dependent action of reactive oxygen species on transmitter release in mammalian neuromuscular junctions, Neurobiol. Aging 38 (2016) 73–81.
[631] E. Bukharaeva, A. Shakirzyanova, V. Khuzakhmetova, G. Sitdikova, R. Giniatullin, Homocysteine aggravates ROS-induced depression of transmitter release from motor nerve terminals: potential mechanism of peripheral impairment in motor neuron diseases associated with hyperhomocysteinemia, Front. Cell. Neurosci. 9 (2015) 391.
[632] A. Giniatullin, A. Petrov, R. Giniatullin, The involvement of P2Y12 receptors, NADPH oxidase, and lipid rafts in the action of extracellular ATP on synaptic transmission at the frog neuromuscular junction, Neuroscience 285 (2015) 324–332.
[633] A.R. Giniatullin, F. Darios, A. Shakirzyanova, B. Davletov, R. Giniatullin, SNAP25 is a pre-synaptic target for the depressant action of reactive oxygen species on transmitter release, J. Neurochem. 98 (2006) 1789–1797.
[634] B. Debelec-Butuner, N. Ertunc, K.S. Korkmaz, Inflammation contributes to NKX3.1 loss and augments DNA damage but does not alter the DNA damage response via

increased SIRT1 expression, J. Inflamm. 12 (2015) 12.
[635] S. Zhao, Y. Zhang, Q. Zhang, F. Wang, D. Zhang, Toll-like receptors and prostate cancer, Front. Immunol. 5 (2014) 352.
[636] A. Oblak, R. Jerala, Toll-like receptor 4 activation in cancer progression and therapy, Clin. Dev. Immunol. 2011 (2011) 609579.
[637] S.D. Kundu, C. Lee, B.K. Billips, G.M. Habermacher, Q. Zhang, V. Liu, L.Y. Wong, D.J. Klumpp, P. Thumbikat, The toll-like receptor pathway: a novel mechanism of infection-induced carcinogenesis of prostate epithelial cells, Prostate 68 (2008) 223–229.
[638] B. Debelec-Butuner, C. Alapinar, N. Ertunc, C. Gonen-Korkmaz, K. Yorukoglu, K.S. Korkmaz, TNFalpha-mediated loss of beta-catenin/E-cadherin association and subsequent increase in cell migration is partially restored by NKX3.1 expression in prostate cells, PLoS One 9 (2014) e109868.
[639] H. Yang, H. Zhou, P. Feng, X. Zhou, H. Wen, X. Xie, H. Shen, X. Zhu, Reduced expression of Toll-like receptor 4 inhibits human breast cancer cells proliferation and inflammatory cytokines secretion, J. Exp. Clin. Cancer Res. 29 (2010) 92.
[640] G. Manda, G. Isvoranu, M.V. Comanescu, A. Manea, B. Debelec Butuner, K.S. Korkmaz, The redox biology network in cancer pathophysiology and therapeutics, Redox Biol. 5 (2015) 347–357.
[641] J.A. Winkelstein, M.C. Marino, R.B. Johnston Jr., J. Boyle, J. Curnutte, J.I. Gallin, H.L. Malech, S.M. Holland, H. Ochs, P. Quie, R.H. Buckley, C.B. Foster, S.J. Chanock, H. Dickler, Chronic granulomatous disease. Report on a national registry of 368 patients, Medicine 79 (2000) 155–169.
[642] P.G. Quie, J.G. White, B. Holmes, R.A. Good, In vitro bactericidal capacity of human polymorphonuclear leukocytes: diminished activity in chronic granulomatous disease of childhood, J. Clin. Investig. 46 (1967) 668–679.
[643] B. Holmes, P.G. Quie, D.B. Windhorst, R.A. Good, Fatal granulomatous disease of childhood. An inborn abnormality of phagocytic function, Lancet 1 (1966) 1225–1228.
[644] P.R. Forfia, X. Zhang, F. Ochoa, M. Ochoa, X. Xu, R. Bernstein, P.B. Sehgal, N.R. Ferreri, T.H. Hintze, Relationship between plasma NOx and cardiac and vascular dysfunction after LPS injection in anesthetized dogs, Am. J. Physiol. 274 (1998) H193–H201.
[645] K.L. Singel, B.H. Segal, NOX2-dependent regulation of inflammation, Clin. Sci. 130 (2016) 479–490.
[646] M. Han, T. Zhang, L. Yang, Z. Wang, J. Ruan, X. Chang, Association between NADPH oxidase (NOX) and lung cancer: a systematic review and meta-analysis, J. Thorac. Dis. 8 (2016) 1704–1711.
[647] A. Kaur, M.R. Webster, K. Marchbank, R. Behera, A. Ndoye, C.H. Kugel 3rd, V.M. Dang, J. Appleton, M.P. O'Connell, P. Cheng, A.A. Valiga, R. Morissette, N.B. McDonnell, L. Ferrucci, A.V. Kossenkov, K. Meeth, H.Y. Tang, X. Yin, W.H. Wood 3rd, E. Lehrmann, K.G. Becker, K.T. Flaherty, D.T. Frederick, J.A. Wargo, Z.A. Cooper, M.T. Tetzlaff, C. Hudgens, K.M. Aird, R. Zhang, X. Xu, Q. Liu, E. Bartlett, G. Karakousis, Z. Eroglu, R.S. Lo, M. Chan, A.M. Menzies, G.V. Long, D.B. Johnson, J. Sosman, B. Schilling, D. Schadendorf, D.W. Speicher, M. Bosenberg, A. Ribas, A.T. Weeraratna, sFRP2 in the aged microenvironment drives melanoma metastasis and therapy resistance, Nature 532 (2016) 250–254.
[648] E. Piskounova, M. Agathocleous, M.M. Murphy, Z. Hu, S.E. Huddlestun, Z. Zhao, A.M. Leitch, T.M. Johnson, R.J. DeBerardinis, S.J. Morrison, Oxidative stress inhibits distant metastasis by human melanoma cells, Nature 527 (2015) 186–191.
[649] M. Benhar, I.L. Shytaj, J.S. Stamler, A. Savarino, Dual targeting of the thioredoxin and glutathione systems in cancer and HIV, J. Clin. Investig. 126 (2016) 1630–1639.
[650] S. Delmaghani, J. Defourny, A. Aghaie, M. Beurg, D. Dulon, N. Thelen, I. Perfettini, T. Zelles, M. Aller, A. Meyer, A. Emptoz, F. Giraudet, M. Leibovici, S. Dartevelle, G. Soubigou, M. Thiry, E.S. Vizi, S. Safieddine, J.P. Hardelin, P. Avan, C. Petit, Hypervulnerability to sound exposure through impaired adaptive proliferation of peroxisomes, Cell 163 (2015) 894–906.
[651] L. Rochette, M. Zeller, Y. Cottin, C. Vergely, Diabetes, oxidative stress and therapeutic strategies, Biochim. Biophys. Acta 1840 (2014) 2709–2729.
[652] J. Wang, X. Yang, J. Zhang, Bridges between mitochondrial oxidative stress, ER stress and mTOR signaling in pancreatic beta cells, Cell Signal. 28 (2016) 1099–1104.
[653] A. Jankovic, A. Korac, B. Buzadzic, A. Stancic, V. Otasevic, P. Ferdinandy, A. Daiber, B. Korac, Targeting the nitric oxide/superoxide ratio in adipose tissue: relevance in obesity and diabetes management, Br. J. Pharmacol. (2016), http://dx.doi.org/10.1111/bph.13498.
[654] L. Tochhawng, S. Deng, S. Pervaiz, C.T. Yap, Redox regulation of cancer cell migration and invasion, Mitochondrion 13 (2013) 246–253.
[655] B. Diaz, S.A. Courtneidge, Redox signaling at invasive microdomains in cancer cells, Free Radic. Biol. Med. 52 (2012) 247–256.
[656] L. Goitre, B. Pergolizzi, E. Ferro, L. Trabalzini, S.F. Retta, Molecular crosstalk between integrins and cadherins: do reactive oxygen species set the talk? J. Signal Transduct. 2012 (2012) 807682.
[657] G. Pani, T. Galeotti, P. Chiarugi, Metastasis: cancer cell's escape from oxidative stress, Cancer Metastasis Rev. 29 (2010) 351–378.
[658] W.S. Wu, The signaling mechanism of ROS in tumor progression, Cancer Metastas-. Rev. 25 (2006) 695–705.
[659] V.L. Kinnula, J.D. Crapo, Superoxide dismutases in malignant cells and human tumors, Free Radic. Biol. Med. 36 (2004) 718–744.
[660] E. Crosas-Molist, I. Fabregat, Role of NADPH oxidases in the redox biology of liver fibrosis, Redox Biol. 6 (2015) 106–111.
[661] N.S. de Mochel, S. Seronello, S.H. Wang, C. Ito, J.X. Zheng, T.J. Liang, J.D. Lambeth, J. Choi, Hepatocyte NAD(P)H oxidases as an endogenous source of reactive oxygen species during hepatitis C virus infection, Hepatology 52 (2010) 47–59.
[662] A.I. Evsev'eva, I.V. Abramenko, D.F. Gluzman, G.V. Pisniachevskaia, A.V. Filatov, Immunophenotypic characteristics of lymphocytes in pleural cavity exudates, Vrachebnoe Delo (1989) 34–37.
[663] W. Cui, K. Matsuno, K. Iwata, M. Ibi, M. Matsumoto, J. Zhang, K. Zhu, M. Katsuyama, N.J. Torok, C. Yabe-Nishimura, NOX1/nicotinamide adenine dinucleotide phosphate, reduced form (NADPH) oxidase promotes proliferation of stellate cells and aggravates liver fibrosis induced by bile duct ligation, Hepatology 54 (2011) 949–958.
[664] P. Sancho, P. Martin-Sanz, I. Fabregat, Reciprocal regulation of NADPH oxidases and the cyclooxygenase-2 pathway, Free Radic. Biol. Med. 51 (2011) 1789–1798.
[665] J.X. Jiang, S. Venugopal, N. Serizawa, X. Chen, F. Scott, Y. Li, R. Adamson, S. Devaraj, V. Shah, M.E. Gershwin, S.L. Friedman, N.J. Torok, Reduced nicotinamide adenine dinucleotide phosphate oxidase 2 plays a key role in stellate cell activation and liver fibrogenesis in vivo, Gastroenterology 139 (2010) 1375–1384.
[666] P. Sancho, I. Fabregat, NADPH oxidase NOX1 controls autocrine growth of liver tumor cells through up-regulation of the epidermal growth factor receptor pathway, J. Biol. Chem. 285 (2010) 24815–24824.
[667] S.Y. Ha, Y.H. Paik, J.W. Yang, M.J. Lee, H. Bae, C.K. Park, NADPH oxidase 1 and NADPH oxidase 4 have opposite prognostic effects for patients with hepatocellular carcinoma after hepatectomy, Gut Liver 10 (2016) 826–835.
[668] J.X. Jiang, X. Chen, N. Serizawa, C. Szyndralewiez, P. Page, K. Schroder, R.P. Brandes, S. Devaraj, N.J. Torok, Liver fibrosis and hepatocyte apoptosis are attenuated by GKT137831, a novel NOX4/NOX1 inhibitor in vivo, Free Radic. Biol. Med. 53 (2012) 289–296.
[669] R. Jardri, K. Hugdahl, M. Hughes, J. Brunelin, F. Waters, B. Alderson-Day, D. Smailes, P. Sterzer, P.R. Corlett, P. Leptourgos, M. Debbane, A. Cachia, S. Deneve, Are hallucinations due to an imbalance between excitatory and inhibitory influences on the brain? Schizophr. Bull. 42 (2016) 1124–1134.
[670] M.O. Trepanier, K.E. Hopperton, R. Mizrahi, N. Mechawar, R.P. Bazinet, Postmortem evidence of cerebral inflammation in schizophrenia: a systematic review, Mol. Psychiatry 21 (2016) 1009–1026.
[671] G.E. Hardingham, K.Q. Do, Linking early-life NMDAR hypofunction and oxidative stress in schizophrenia pathogenesis, Nat. Rev. Neurosci. 17 (2016) 125–134.
[672] F. Gu, V. Chauhan, A. Chauhan, Glutathione redox imbalance in brain disorders, Curr. Opin. Clin. Nutr. Metab. Care 18 (2015) 89–95.
[673] P. Steullet, J.H. Cabungcal, A. Kulak, R. Kraftsik, Y. Chen, T.P. Dalton, M. Cuenod, K.Q. Do, Redox dysregulation affects the ventral but not dorsal hippocampus: impairment of parvalbumin neurons, gamma oscillations, and related behaviors, J. Neurosci. 30 (2010) 2547–2558.
[674] M.M. Behrens, S.S. Ali, D.N. Dao, J. Lucero, G. Shekhtman, K.L. Quick, L.L. Dugan, Ketamine-induced loss of phenotype of fast-spiking interneurons is mediated by NADPH-oxidase, Science 318 (2007) 1645–1647.
[675] Z. Jiang, G.R. Rompala, S. Zhang, R.M. Cowell, K. Nakazawa, Social isolation exacerbates schizophrenia-like phenotypes via oxidative stress in cortical interneurons, Biol. Psychiatry 73 (2013) 1024–1034.
[676] E.K. Lucas, S.J. Markwardt, S. Gupta, J.H. Meador-Woodruff, J.D. Lin, L. Overstreet-Wadiche, R.M. Cowell, Parvalbumin deficiency and GABAergic dysfunction in mice lacking PGC-1alpha, J. Neurosci. 30 (2010) 7227–7235.
[677] Z. Nayernia, V. Jaquet, K.H. Krause, New insights on NOX enzymes in the central nervous system, Antioxid. Redox Signal. 20 (2014) 2815–2837.
[678] S. Sorce, M. Nuvolone, A. Keller, J. Falsig, A. Varol, P. Schwarz, M. Bieri, H. Budka, A. Aguzzi, The role of the NADPH oxidase NOX2 in prion pathogenesis, PLoS Pathog. 10 (2014) e1004531.
[679] F. Vilhardt, J. Haslund-Vinding, V. Jaquet, G. McBean, Microglia antioxidant systems and redox signaling. Br. J. Pharmacol., 2016. http://dx.doi.org/10.1111/bph.13426.
[680] R. Kopke, K.A. Allen, D. Henderson, M. Hoffer, D. Frenz, T. Van de Water, A radical demise. Toxins and trauma share common pathways in hair cell death, Ann. N. Y Acad. Sci. 884 (1999) 171–191.
[681] F. Rousset, S. Carnesecchi, P. Senn, K.H. Krause, Nox3-targeted therapies for inner ear pathologies, Curr. Pharm. Des. 21 (2015) 5977–5987.
[682] R. Paffenholz, R.A. Bergstrom, F. Pasutto, P. Wabnitz, R.J. Munroe, W. Jagla, U. Heinzmann, A. Marquardt, A. Bareiss, J. Laufs, A. Russ, G. Stumm, J.C. Schimenti, D.E. Bergstrom, Vestibular defects in head-tilt mice result from mutations in Nox3, encoding an NADPH oxidase, Genes Dev. 18 (2004) 486–491.
[683] B. Banfi, B. Malgrange, J. Knisz, K. Steger, M. Dubois-Dauphin, K.H. Krause, NOX3, a superoxide-generating NADPH oxidase of the inner ear, J. Biol. Chem. 279 (2004) 46065–46072.
[684] D. Mukherjea, S. Jajoo, T. Kaur, K.E. Sheehan, V. Ramkumar, L.P. Rybak, Transtympanic administration of short interfering (si)RNA for the NOX3 isoform of NADPH oxidase protects against cisplatin-induced hearing loss in the rat, Antioxid. Redox Signal 13 (2010) 589–598.
[685] A. Vasilijevic, B. Buzadzic, A. Korac, V. Petrovic, A. Jankovic, B. Korac, Beneficial effects of L-arginine nitric oxide-producing pathway in rats treated with alloxan, J. Physiol. 584 (2007) 921–933.
[686] A.D. Lajoix, H. Reggio, T. Chardes, S. Peraldi-Roux, F. Tribillac, M. Roye, S. Dietz, C. Broca, M. Manteghetti, G. Ribes, C.B. Wollheim, R. Gross, A neuronal isoform of nitric oxide synthase expressed in pancreatic beta-cells controls insulin secretion, Diabetes 50 (2001) 1311–1323.
[687] W.S. Jobgen, S.K. Fried, W.J. Fu, C.J. Meininger, G. Wu, Regulatory role for the arginine-nitric oxide pathway in metabolism of energy substrates, J. Nutr. Biochem. 17 (2006) 571–588.
[688] V. Petrovic, A. Korac, B. Buzadzic, B. Korac, The effects of L-arginine and L-NAME supplementation on redox-regulation and thermogenesis in interscapular brown adipose tissue, J. Exp. Biol. 208 (2005) 4263–4271.

[689] A. Vasilijevic, L. Vojcic, I. Dinulovic, B. Buzadzic, A. Korac, V. Petrovic, A. Jankovic, B. Korac, Expression pattern of thermogenesis-related factors in interscapular brown adipose tissue of alloxan-treated rats: beneficial effect of L-arginine, Nitric Oxide 23 (2010) 42–50.
[690] L.J. Coppey, J.S. Gellett, E.P. Davidson, J.A. Dunlap, D.D. Lund, D. Salvemini, M.A. Yorek, Effect of M40403 treatment of diabetic rats on endoneurial blood flow, motor nerve conduction velocity and vascular function of epineurial arterioles of the sciatic nerve, Br. J. Pharmacol. 134 (2001) 21–29.
[691] V. Otasevic, A. Korac, M. Vucetic, B. Macanovic, E. Garalejic, I. Ivanovic-Burmazovic, M.R. Filipovic, B. Buzadzic, A. Stancic, A. Jankovic, K. Velickovic, I. Golic, M. Markelic, B. Korac, Is manganese (II) pentaazamacrocyclic superoxide dismutase mimic beneficial for human sperm mitochondria function and motility? Antioxid. Redox Signal. 18 (2013) 170–178.
[692] A. Stancic, V. Otasevic, A. Jankovic, M. Vucetic, I. Ivanovic-Burmazovic, M.R. Filipovic, A. Korac, M. Markelic, K. Velickovic, I. Golic, B. Buzadzic, B. Korac, Molecular basis of hippocampal energy metabolism in diabetic rats: the effects of SOD mimic, Brain Res. Bull. 99 (2013) 27–33.
[693] K.L. Hoehn, A.B. Salmon, C. Hohnen-Behrens, N. Turner, A.J. Hoy, G.J. Maghzal, R. Stocker, H. Van Remmen, E.W. Kraegen, G.J. Cooney, A.R. Richardson, D.E. James, Insulin resistance is a cellular antioxidant defense mechanism, Proc. Natl. Acad. Sci. USA 106 (2009) 17787–17792.
[694] K. Wojdyla, A. Rogowska-Wrzesinska, Differential alkylation-based redox proteomics– lessons learnt, Redox Biol. 6 (2015) 240–252.
[695] T. Nakamura, S. Tu, M.W. Akhtar, C.R. Sunico, S. Okamoto, S.A. Lipton, Aberrant protein s-nitrosylation in neurodegenerative diseases, Neuron 78 (2013) 596–614.
[696] H. Im, M. Manolopoulou, E. Malito, Y. Shen, J. Zhao, M. Neant-Fery, C.Y. Sun, S.C. Meredith, S.S. Sisodia, M.A. Leissring, W.J. Tang, Structure of substrate-free human insulin-degrading enzyme (IDE) and biophysical analysis of ATP-induced conformational switch of IDE, J. Biol. Chem. 282 (2007) 25453–25463.
[697] T.B. Durham, J.L. Toth, V.J. Klimkowski, J.X. Cao, A.M. Siesky, J. Alexander-Chacko, G.Y. Wu, J.T. Dixon, J.E. McGee, Y. Wang, S.Y. Guo, R.N. Cavitt, J. Schindler, S.J. Thibodeaux, N.A. Calvert, M.J. Coghlan, D.K. Sindelar, M. Christe, V.V. Kiselyov, M.D. Michael, K.W. Sloop, Dual exosite-binding inhibitors of insulin-degrading enzyme challenge its role as the primary mediator of insulin clearance in vivo, J. Biol. Chem. 290 (2015) 20044–20059.
[698] W. Humphrey, A. Dalke, K. Schulten, VMD: visual molecular dynamics, J. Mol. Graph 14 (33–38) (1996) 27–38.
[699] Y. Shen, A. Joachimiak, M.R. Rosner, W.J. Tang, Structures of human insulin-degrading enzyme reveal a new substrate recognition mechanism, Nature 443 (2006) 870–874.
[700] L.A. Ralat, M. Ren, A.B. Schilling, W.J. Tang, Protective role of Cys-178 against the inactivation and oligomerization of human insulin-degrading enzyme by oxidation and nitrosylation, J. Biol. Chem. 284 (2009) 34005–34018.
[701] M.W. Akhtar, S. Sanz-Blasco, N. Dolatabadi, J. Parker, K. Chon, M.S. Lee, W. Soussou, S.R. McKercher, R. Ambasudhan, T. Nakamura, S.A. Lipton, Elevated glucose and oligomeric beta-amyloid disrupt synapses via a common pathway of aberrant protein S-nitrosylation, Nat. Commun. 7 (2016) 10242.
[702] G. Cohen, Y. Riahi, O. Shamni, M. Guichardant, C. Chatgilialoglu, C. Ferreri, N. Kaiser, S. Sasson, Role of lipid peroxidation and PPAR-delta in amplifying glucose-stimulated insulin secretion, Diabetes 60 (2011) 2830–2842.
[703] G. Cohen, O. Shamni, Y. Avrahami, O. Cohen, E.C. Broner, N. Filippov-Levy, C. Chatgilialoglu, C. Ferreri, N. Kaiser, S. Sasson, Beta cell response to nutrient overload involves phospholipid remodelling and lipid peroxidation, Diabetologia 58 (2015) 1333–1343.
[704] S. Kahremany, A. Livne, A. Gruzman, H. Senderowitz, S. Sasson, Activation of PPARdelta: from computer modelling to biological effects, Br. J. Pharmacol. 172 (2015) 754–770.
[705] G. Maulucci, B. Daniel, O. Cohen, Y. Avrahami, S. Sasson, Hormetic and regulatory effects of lipid peroxidation mediators in pancreatic beta cells, Mol. Asp. Med 49 (2016) 49–77.
[706] P. Zimniak, 4-Hydroxynonenal and fat storage: a paradoxical pro-obesity mechanism? Cell Cycle 9 (2010) 3393–3394.
[707] X. Li, SIRT1 and energy metabolism, Acta Biochim. Biophys. Sin. 45 (2013) 51–60.
[708] P. Baskaran, V. Krishnan, J. Ren, B. Thyagarajan, Capsaicin induces browning of white adipose tissue and counters obesity by activating TRPV1 channel-dependent mechanisms, Br. J. Pharmacol. 173 (2016) 2369–2389.
[709] Y. Kanda, T. Hinata, S.W. Kang, Y. Watanabe, Reactive oxygen species mediate adipocyte differentiation in mesenchymal stem cells, Life Sci. 89 (2011) 250–258.
[710] T. Ruskovska, D.A. Bernlohr, Oxidative stress and protein carbonylation in adipose tissue – implications for insulin resistance and diabetes mellitus, J. Proteom. 92 (2013) 323–334.
[711] S.H. Kim, J. Plutzky, Brown fat and browning for the treatment of obesity and related metabolic disorders, Diabetes Metab. J. 40 (2016) 12–21.
[712] E.T. Chouchani, L. Kazak, M.P. Jedrychowski, G.Z. Lu, B.K. Erickson, J. Szpyt, K.A. Pierce, D. Laznik-Bogoslavski, R. Vetrivelan, C.B. Clish, A.J. Robinson, S.P. Gygi, B.M. Spiegelman, Mitochondrial ROS regulate thermogenic energy expenditure and sulfenylation of UCP1, Nature 532 (2016) 112–116.
[713] K. Schneider, J. Valdez, J. Nguyen, M. Vawter, B. Galke, T.W. Kurtz, J.Y. Chan, Increased energy expenditure, Ucp1 expression, and resistance to diet-induced obesity in mice lacking nuclear factor-erythroid-2-related transcription factor-2 (Nrf2), J. Biol. Chem. 291 (2016) 7754–7766.
[714] J.P. Castro, T. Grune, B. Speckmann, The two faces of reactive oxygen species (ROS) in adipocyte function and dysfunction, Biol. Chem. 397 (2016) 709–724.
[715] T. Munzel, A. Daiber, T. Gori, Nitrate therapy: new aspects concerning molecular action and tolerance, Circulation 123 (2011) 2132–2144.
[716] A. Daiber, T. Munzel, Organic nitrate therapy, nitrate tolerance, and nitrate-induced endothelial dysfunction: emphasis on redox biology and oxidative stress, Antioxid. Redox Signal 23 (2015) 899–942.
[717] T. Munzel, A. Daiber, T. Gori, More answers to the still unresolved question of nitrate tolerance, Eur. Heart J. 34 (2013) 2666–2673.
[718] A. Daiber, M. Oelze, S. Sulyok, M. Coldewey, E. Schulz, N. Treiber, U. Hink, A. Mulsch, K. Scharffetter-Kochanek, T. Munzel, Heterozygous deficiency of manganese superoxide dismutase in mice (Mn-SOD+/-): a novel approach to assess the role of oxidative stress for the development of nitrate tolerance, Mol. Pharmacol. 68 (2005) 579–588.
[719] J.V. Esplugues, M. Rocha, C. Nunez, I. Bosca, S. Ibiza, J.R. Herance, A. Ortega, J.M. Serrador, P. D'Ocon, V.M. Victor, Complex I dysfunction and tolerance to nitroglycerin: an approach based on mitochondrial-targeted antioxidants, Circ. Res. 99 (2006) 1067–1075.
[720] T. Munzel, S. Kurz, S. Rajagopalan, M. Tarpey, B. Freeman, D.G. Harrison, Identification of the membrane bound NADH oxidase as the major source of superoxide anion in nitrate tolerance, Endothelium 3 (Suppl) (1995) s14 (abstract).
[721] A. Jabs, M. Oelze, Y. Mikhed, P. Stamm, S. Kroller-Schon, P. Welschof, T. Jansen, M. Hausding, M. Kopp, S. Steven, E. Schulz, J.P. Stasch, T. Munzel, A. Daiber, Effect of soluble guanylyl cyclase activator and stimulator therapy on nitroglycerin-induced nitrate tolerance in rats, Vasc. Pharmacol. 71 (2015) 181–191.
[722] A. Daiber, M. Oelze, M. Coldewey, K. Kaiser, C. Huth, S. Schildknecht, M. Bachschmid, Y. Nazirisadeh, V. Ullrich, A. Mulsch, T. Munzel, N. Tsilimingas, Hydralazine is a powerful inhibitor of peroxynitrite formation as a possible explanation for its beneficial effects on prognosis in patients with congestive heart failure, Biochem. Biophys. Res. Commun. 338 (2005) 1865–1874.
[723] Z. Chen, J. Zhang, J.S. Stamler, Identification of the enzymatic mechanism of nitroglycerin bioactivation, Proc. Natl. Acad. Sci. USA 99 (2002) 8306–8311.
[724] P. Wenzel, U. Hink, M. Oelze, S. Schuppan, K. Schaeuble, S. Schildknecht, K.K. Ho, H. Weiner, M. Bachschmid, T. Munzel, A. Daiber, Role of reduced lipoic acid in the redox regulation of mitochondrial aldehyde dehydrogenase (ALDH-2) activity. Implications for mitochondrial oxidative stress and nitrate tolerance, J. Biol. Chem. 282 (2007) 792–799.
[725] E. Schulz, N. Tsilimingas, R. Rinze, B. Reiter, M. Wendt, M. Oelze, S. Woelken-Weckmuller, U. Walter, H. Reichenspurner, T. Meinertz, T. Munzel, Functional and biochemical analysis of endothelial (dys)function and NO/cGMP signaling in human blood vessels with and without nitroglycerin pretreatment, Circulation 105 (2002) 1170–1175.
[726] M.G. Andreassi, N. Botto, S. Simi, M. Casella, S. Manfredi, M. Lucarelli, L. Venneri, A. Biagini, E. Picano, Diabetes and chronic nitrate therapy as co-determinants of somatic DNA damage in patients with coronary artery disease, J. Mol. Med. 83 (2005) 279–286.
[727] Y. Mikhed, J. Fahrer, M. Oelze, S. Kroller-Schon, S. Steven, P. Welschof, E. Zinssius, P. Stamm, F. Kashani, S. Roohani, J.M. Kress, E. Ullmann, L.P. Tran, E. Schulz, B. Epe, B. Kaina, T. Munzel, A. Daiber, Nitroglycerin induces DNA damage and vascular cell death in the setting of nitrate tolerance, Basic Res. Cardiol. 111 (2016) 52.
[728] M. Oelze, M. Knorr, S. Kroller-Schon, S. Kossmann, A. Gottschlich, R. Rummler, A. Schuff, S. Daub, C. Doppler, H. Kleinert, T. Gori, A. Daiber, T. Munzel, Chronic therapy with isosorbide-5-mononitrate causes endothelial dysfunction, oxidative stress, and a marked increase in vascular endothelin-1 expression, Eur Heart J. 34 (2013) 3206–3216.
[729] S. Oberle, A. Abate, N. Grosser, H.J. Vreman, P.A. Dennery, H.T. Schneider, D. Stalleicken, H. Schroder, Heme oxygenase-1 induction may explain the antioxidant profile of pentaerythrityl trinitrate, Biochem. Biophys. Res. Commun. 290 (2002) 1539–1544.
[730] M. Oppermann, V. Balz, V. Adams, V.T. Dao, M. Bas, T. Suvorava, G. Kojda, Pharmacological induction of vascular extracellular superoxide dismutase expression in vivo, J. Cell. Mol. Med. 13 (2009) 1271–1278.
[731] A. Pautz, P. Rauschkolb, N. Schmidt, J. Art, M. Oelze, P. Wenzel, U. Forstermann, A. Daiber, H. Kleinert, Effects of nitroglycerin or pentaerithrityl tetranitrate treatment on the gene expression in rat hearts: evidence for cardiotoxic and cardioprotective effects, Physiol. Genom. 38 (2009) 176–185.
[732] Z. Wu, D. Siuda, N. Xia, G. Reifenberg, A. Daiber, T. Munzel, U. Forstermann, H. Li, Maternal treatment of spontaneously hypertensive rats with pentaerythritol tetranitrate reduces blood pressure in female offspring, Hypertension 65 (2015) 232–237.
[733] J.L. Gamboa, F.T. t. Billings, M.T. Bojanowski, L.A. Gilliam, C. Yu, B. Roshanravan, L.J. Roberts 2nd, J. Himmelfarb, T.A. Ikizler, N.J. Brown, Mitochondrial dysfunction and oxidative stress in patients with chronic kidney disease, Physiol. Rep. 4 (2016).
[734] A. Makino, M.M. Skelton, A.P. Zou, R.J. Roman, A.W. Cowley Jr., Increased renal medullary oxidative stress produces hypertension, Hypertension 39 (2002) 667–672.
[735] R.K. Sindhu, A. Ehdaie, F. Farmand, K.K. Dhaliwal, T. Nguyen, C.D. Zhan, C.K. Roberts, N.D. Vaziri, Expression of catalase and glutathione peroxidase in renal insufficiency, Biochim. Biophys. Acta 1743 (2005) 86–92.
[736] N.D. Vaziri, M. Dicus, N.D. Ho, L. Boroujerdi-Rad, R.K. Sindhu, Oxidative stress and dysregulation of superoxide dismutase and NADPH oxidase in renal insufficiency, Kidney Int. 63 (2003) 179–185.
[737] C.G. Schnackenberg, C.S. Wilcox, Two-week administration of tempol attenuates both hypertension and renal excretion of 8-Iso prostaglandin f2alpha, Hypertension 33 (1999) 424–428.
[738] L.T. de Richelieu, C.M. Sorensen, N.H. Holstein-Rathlou, M. Salomonsson, NO-independent mechanism mediates tempol-induced renal vasodilation in SHR, Am. J. Physiol. Ren. Physiol. 289 (2005) F1227–F1234.

[739] G.S. Guron, E.S. Grimberg, S. Basu, H. Herlitz, Acute effects of the superoxide dismutase mimetic tempol on split kidney function in two-kidney one-clip hypertensive rats, J. Hypertens. 24 (2006) 387–394.
[740] D.A. Papazova, A. van Koppen, M.P. Koeners, R.L. Bleys, M.C. Verhaar, J.A. Joles, Maintenance of hypertensive hemodynamics does not depend on ROS in established experimental chronic kidney disease, PLoS One 9 (2014) e88596.
[741] J. Herget, J. Wilhelm, J. Novotna, A. Eckhardt, R. Vytasek, L. Mrazkova, M. Ostadal, A possible role of the oxidant tissue injury in the development of hypoxic pulmonary hypertension, Physiol. Res. 49 (2000) 493–501.
[742] T. Hansen, K.K. Galougahi, D. Celermajer, N. Rasko, O. Tang, K.J. Bubb, G. Figtree, Oxidative and nitrosative signalling in pulmonary arterial hypertension – implications for development of novel therapies, Pharmacol. Ther. 165 (2016) 50–62.
[743] D. Hodyc, E. Johnson, A. Skoumalova, J. Tkaczyk, H. Maxova, M. Vizek, J. Herget, Reactive oxygen species production in the early and later stage of chronic ventilatory hypoxia, Physiol. Res. 61 (2012) 145–151.
[744] V. Jakoubek, J. Bibova, J. Herget, V. Hampl, Chronic hypoxia increases fetoplacental vascular resistance and vasoconstrictor reactivity in the rat, Am. J. Physiol. Heart Circ. Physiol. 294 (2008) H1638–H1644.
[745] B. Gao, A. Doan, B.M. Hybertson, The clinical potential of influencing Nrf2 signaling in degenerative and immunological disorders, Clin. Pharmacol. 6 (2014) 19–34.
[746] E. O'Brien, D.R. Dietrich, Ochratoxin A: the continuing enigma, Crit. Rev. Toxicol. 35 (2005) 33–60.
[747] A. Pfohl-Leszkowicz, R.A. Manderville, Ochratoxin A: an overview on toxicity and carcinogenicity in animals and humans, Mol. Nutr. Food Res 51 (2007) 61–99.
[748] D. Ringot, A. Chango, Y.J. Schneider, Y. Larondelle, Toxicokinetics and toxicodynamics of ochratoxin A, an update, Chem. Biol. Interact. 159 (2006) 18–46.
[749] G.J. Schaaf, S.M. Nijmeijer, R.F. Maas, P. Roestenberg, E.M. de Groene, J. Fink-Gremmels, The role of oxidative stress in the ochratoxin A-mediated toxicity in proximal tubular cells, Biochim. Biophys. Acta 1588 (2002) 149–158.
[750] J.G. Costa, N. Saraiva, P.S. Guerreiro, H. Louro, M.J. Silva, J.P. Miranda, M. Castro, I. Batinic-Haberle, A.S. Fernandes, N.G. Oliveira, Ochratoxin A-induced cytotoxicity, genotoxicity and reactive oxygen species in kidney cells: an integrative approach of complementary endpoints, Food Chem. Toxicol. 87 (2016) 65–76.
[751] M. Marin-Kuan, V. Ehrlich, T. Delatour, C. Cavin, B. Schilter, Evidence for a role of oxidative stress in the carcinogenicity of ochratoxin a, J. Toxicol. 2011 (2011) 645361.
[752] A. Pfohl-Leszkowicz, R.A. Manderville, An update on direct genotoxicity as a molecular mechanism of ochratoxin a carcinogenicity, Chem. Res. Toxicol. 25 (2012) 252–262.
[753] C. Cavin, T. Delatour, M. Marin-Kuan, F. Fenaille, D. Holzhauser, G. Guignard, C. Bezencon, D. Piguet, V. Parisod, J. Richoz-Payot, B. Schilter, Ochratoxin A-mediated DNA and protein damage: roles of nitrosative and oxidative stresses, Toxicol. Sci. 110 (2009) 84–94.
[754] V. Sorrenti, C. Di Giacomo, R. Acquaviva, I. Barbagallo, M. Bognanno, F. Galvano, Toxicity of ochratoxin a and its modulation by antioxidants: a review, Toxins 5 (2013) 1742–1766.
[755] G.L. Newton, N. Buchmeier, R.C. Fahey, Biosynthesis and functions of mycothiol, the unique protective thiol of actinobacteria, Microbiol. Mol. Biol. Rev. 72 (2008) 471–494.
[756] K. Van Laer, C.J. Hamilton, J. Messens, Low-molecular-weight thiols in thiol-disulfide exchange, Antioxid. Redox Signal. 18 (2013) 1642–1653.
[757] K. Van Laer, L. Buts, N. Foloppe, D. Vertommen, K. Van Belle, K. Wahni, G. Roos, L. Nilsson, L.M. Mateos, M. Rawat, N.A. van Nuland, J. Messens, Mycoredoxin-1 is one of the missing links in the oxidative stress defence mechanism of Mycobacteria, Mol. Microbiol. 86 (2012) 787–804.
[758] M. Hugo, K. Van Laer, A.M. Reyes, D. Vertommen, J. Messens, R. Radi, M. Trujillo, Mycothiol/mycoredoxin 1-dependent reduction of the peroxiredoxin AhpE from Mycobacterium tuberculosis, J. Biol. Chem. 289 (2014) 5228–5239.
[759] A. Chacinska, S. Pfannschmidt, N. Wiedemann, V. Kozjak, L.K. Sanjuan Szklarz, A. Schulze-Specking, K.N. Truscott, B. Guiard, C. Meisinger, N. Pfanner, Essential role of Mia40 in import and assembly of mitochondrial intermembrane space proteins, EMBO J. 23 (2004) 3735–3746.
[760] J.M. Herrmann, J. Riemer, Mitochondrial disulfide relay: redox-regulated protein import into the intermembrane space, J. Biol. Chem. 287 (2012) 4426–4433.
[761] M. Naoe, Y. Ohwa, D. Ishikawa, C. Ohshima, S. Nishikawa, H. Yamamoto, T. Endo, Identification of Tim40 that mediates protein sorting to the mitochondrial intermembrane space, J. Biol. Chem. 279 (2004) 47815–47821.
[762] D.P. Sideris, N. Petrakis, N. Katrakili, D. Mikropoulou, A. Gallo, S. Ciofi-Baffoni, L. Banci, I. Bertini, K. Tokatlidis, A novel intermembrane space-targeting signal docks cysteines onto Mia40 during mitochondrial oxidative folding, J. Cell Biol. 187 (2009) 1007–1022.
[763] M. Bien, S. Longen, N. Wagener, I. Chwalla, J.M. Herrmann, J. Riemer, Mitochondrial disulfide bond formation is driven by intersubunit electron transfer in Erv1 and proofread by glutathione, Mol. Cell 37 (2010) 516–528.
[764] F.N. Vogtle, J.M. Burkhart, S. Rao, C. Gerbeth, J. Hinrichs, J.C. Martinou, A. Chacinska, A. Sickmann, R.P. Zahedi, C. Meisinger, Intermembrane space proteome of yeast mitochondria, Mol. Cell Proteom. 11 (2012) 1840–1852.
[765] L. Banci, I. Bertini, C. Cefaro, S. Ciofi-Baffoni, A. Gallo, M. Martinelli, D.P. Sideris, N. Katrakili, K. Tokatlidis, MIA40 is an oxidoreductase that catalyzes oxidative protein folding in mitochondria, Nat. Struct. Mol. Biol. 16 (2009) 198–206.
[766] L. Milkovic, W. Siems, R. Siems, N. Zarkovic, Oxidative stress and antioxidants in carcinogenesis and integrative therapy of cancer, Curr. Pharm. Des. 20 (2014) 6529–6542.
[767] V. Stepanic, A.C. Gasparovic, K.G. Troselj, D. Amic, N. Zarkovic, Selected attributes of polyphenols in targeting oxidative stress in cancer, Curr. Top. Med. Chem. 15 (2015) 496–509.
[768] A. Laurent, C. Nicco, C. Chereau, C. Goulvestre, J. Alexandre, A. Alves, E. Levy, F. Goldwasser, Y. Panis, O. Soubrane, B. Weill, F. Batteux, Controlling tumor growth by modulating endogenous production of reactive oxygen species, Cancer Res. 65 (2005) 948–956.
[769] A.K. Holley, L. Miao, D.K. St Clair, W.H. St Clair, Redox-modulated phenomena and radiation therapy: the central role of superoxide dismutases, Antioxid. Redox Signal. 20 (2014) 1567–1589.
[770] A. Konzack, M. Jakupovic, K. Kubaichuk, A. Gorlach, F. Dombrowski, I. Miinalainen, R. Sormunen, T. Kietzmann, Mitochondrial dysfunction due to lack of manganese superoxide dismutase promotes hepatocarcinogenesis, Antioxid. Redox Signal. 23 (2015) 1059–1075.
[771] X.F. Zhang, X. Tan, G. Zeng, A. Misse, S. Singh, Y. Kim, J.E. Klaunig, S.P. Monga, Conditional beta-catenin loss in mice promotes chemical hepatocarcinogenesis: role of oxidative stress and platelet-derived growth factor receptor alpha/phosphoinositide 3-kinase signaling, Hepatology 52 (2010) 954–965.
[772] J.D. Hayes, A.T. Dinkova-Kostova, The Nrf2 regulatory network provides an interface between redox and intermediary metabolism, Trends Biochem. Sci. 39 (2014) 199–218.
[773] T.H. Rushmore, M.R. Morton, C.B. Pickett, The antioxidant responsive element. Activation by oxidative stress and identification of the DNA consensus sequence required for functional activity, J. Biol. Chem. 266 (1991) 11632–11639.
[774] C. Muscoli, S. Cuzzocrea, D.P. Riley, J.L. Zweier, C. Thiemermann, Z.Q. Wang, D. Salvemini, On the selectivity of superoxide dismutase mimetics and its importance in pharmacological studies, Br. J. Pharmacol. 140 (2003) 445–460.
[775] O. Iranzo, Manganese complexes displaying superoxide dismutase activity: a balance between different factors, Bioorg. Chem. 39 (2011) 73–87.
[776] I. Batinic-Haberle, J.S. Reboucas, I. Spasojevic, Superoxide dismutase mimics: chemistry, pharmacology, and therapeutic potential, Antioxid. Redox Signal. 13 (2010) 877–918.
[777] I. Batinic-Haberle, A. Tovmasyan, I. Spasojevic, An educational overview of the chemistry, biochemistry and therapeutic aspects of Mn porphyrins – from superoxide dismutation to H2O2-driven pathways, Redox Biol. 5 (2015) 43–65.
[778] A.S. Fernandes, J. Costa, J. Gaspar, J. Rueff, M.F. Cabral, M. Cipriano, M. Castro, N.G. Oliveira, Development of pyridine-containing macrocyclic copper(II) complexes: potential role in the redox modulation of oxaliplatin toxicity in human breast cells, Free Radic. Res. 46 (2012) 1157–1166.
[779] G.T. Wondrak, Redox-directed cancer therapeutics: molecular mechanisms and opportunities, Antioxid. Redox Signal. 11 (2009) 3013–3069.
[780] I. Batinic-Haberle, A. Tovmasyan, E.R. Roberts, Z. Vujaskovic, K.W. Leong, I. Spasojevic, SOD therapeutics: latest insights into their structure-activity relationships and impact on the cellular redox-based signaling pathways, Antioxid. Redox Signal. 20 (2014) 2372–2415.
[781] C. Gorrini, I.S. Harris, T.W. Mak, Modulation of oxidative stress as an anticancer strategy, Nat. Rev. Drug Discov. 12 (2013) 931–947.
[782] M.C. Lu, J.A. Ji, Z.Y. Jiang, Q.D. You, The Keap1-Nrf2-ARE pathway as a potential preventive and therapeutic target: an update, Med. Res. Rev. 36 (2016) 924–963.
[783] S. Voskou, M. Aslan, P. Fanis, M. Phylactides, M. Kleanthous, Oxidative stress in beta-thalassaemia and sickle cell disease, Redox Biol. 6 (2015) 226–239.
[784] O.U. Yanpanitch, S. Hatairaktham, R. Charoensakdi, N. Panichkul, S. Fucharoen, S. Srichairatanakool, N. Siritanaratkul, R.W. Kalpravidh, Treatment of beta-thalassemia/hemoglobin E with antioxidant cocktails results in decreased oxidative stress, increased hemoglobin concentration, and improvement of the hypercoagulable state, Oxid. Med. Cell. Longev. 2015 (2015) 537954.
[785] Z.C. Ozdemir, A. Koc, A. Aycicek, A. Kocyigit, N-Acetylcysteine supplementation reduces oxidative stress and DNA damage in children with beta-thalassemia, Hemoglobin 38 (2014) 359–364.
[786] W.P. Pfeifer, G.R. Degasperi, M.T. Almeida, A.E. Vercesi, F.F. Costa, S.T. Saad, Vitamin E supplementation reduces oxidative stress in beta thalassaemia intermedia, Acta Haematol. 120 (2008) 225–231.
[787] L. Tesoriere, D. D'Arpa, D. Butera, M. Allegra, D. Renda, A. Maggio, A. Bongiorno, M.A. Livrea, Oral supplements of vitamin E improve measures of oxidative stress in plasma and reduce oxidative damage to LDL and erythrocytes in beta-thalassemia intermedia patients, Free Radic. Res. 34 (2001) 529–540.
[788] S.S. Franco, L. De Falco, S. Ghaffari, C. Brugnara, D.A. Sinclair, A. Matte, A. Iolascon, N. Mohandas, M. Bertoldi, X. An, A. Siciliano, P. Rimmele, M.D. Cappellini, S. Michan, E. Zoratti, J. Anne, L. De Franceschi, Resveratrol accelerates erythroid maturation by activation of FoxO3 and ameliorates anemia in beta-thalassemic mice, Haematologica 99 (2014) 267–275.
[789] R.W. Kalpravidh, N. Siritanaratkul, P. Insain, R. Charoensakdi, N. Panichkul, S. Hatairaktham, S. Srichairatanakool, C. Phisalaphong, E. Rachmilewitz, S. Fucharoen, Improvement in oxidative stress and antioxidant parameters in beta-thalassemia/Hb E patients treated with curcuminoids, Clin. Biochem. 43 (2010) 424–429.
[790] R.W. Kalpravidh, A. Wichit, N. Siritanaratkul, S. Fucharoen, Effect of coenzyme Q10 as an antioxidant in beta-thalassemia/Hb E patients, Biofactors 25 (2005) 225–234.
[791] S. Ounjaijean, C. Thephinlap, U. Khansuwan, C. Phisalapong, S. Fucharoen, J.B. Porter, S. Srichairatanakool, Effect of green tea on iron status and oxidative stress in iron-loaded rats, Med. Chem. 4 (2008) 365–370.
[792] E. Fibach, E.S. Tan, S. Jamuar, I. Ng, J. Amer, E.A. Rachmilewitz, Amelioration of oxidative stress in red blood cells from patients with beta-thalassemia major and intermedia and E-beta-thalassemia following administration of a fermented papaya preparation, Phytother. Res. 24 (2010) 1334–1338.

[793] H. Darvishi Khezri, E. Salehifar, M. Kosaryan, A. Aliasgharian, H. Jalali, A. Hadian Amree, Potential effects of silymarin and its flavonolignan components in patients with beta-thalassemia major: a comprehensive review in 2015, Adv. Pharmacol. Sci. 2016 (2016) 3046373.
[794] F. Alidoost, M. Gharagozloo, B. Bagherpour, A. Jafarian, S.E. Sajjadi, H. Hourfar, B. Moayedi, Effects of silymarin on the proliferation and glutathione levels of peripheral blood mononuclear cells from beta-thalassemia major patients, Int. Immunopharmacol. 6 (2006) 1305–1310.
[795] D. Biedermann, E. Vavrikova, L. Cvak, V. Kren, Chemistry of silybin, Nat. Prod. Rep. 31 (2014) 1138–1157.
[796] P.F. Surai, Silymarin as a natural antioxidant: an overview of the current evidence and perspectives, Antioxidants 4 (2015) 204–247.
[797] M. Pliskova, J. Vondracek, V. Kren, R. Gazak, P. Sedmera, D. Walterova, J. Psotova, V. Simanek, M. Machala, Effects of silymarin flavonolignans and synthetic silybin derivatives on estrogen and aryl hydrocarbon receptor activation, Toxicology 215 (2005) 80–89.
[798] N. Zheng, P. Zhang, H. Huang, W. Liu, T. Hayashi, L. Zang, Y. Zhang, L. Liu, M. Xia, S. Tashiro, S. Onodera, T. Ikejima, ERalpha down-regulation plays a key role in silibinin-induced autophagy and apoptosis in human breast cancer MCF-7 cells, J. Pharmacol. Sci. 128 (2015) 97–107.
[799] D. Sadava, S.E. Kane, Silibinin reverses drug resistance in human small-cell lung carcinoma cells, Cancer Lett. 339 (2013) 102–106.
[800] R. Agarwal, C. Agarwal, H. Ichikawa, R.P. Singh, B.B. Aggarwal, Anticancer potential of silymarin: from bench to bed side, Anticancer Res. 26 (2006) 4457–4498.
[801] H. Hager, [Problems in the treatment of ocular circulatory disturbances (author's transl)], Klin. Monbl Augenheilkd. 165 (1974) 127–136.
[802] J. Garcia, A.T. Carvalho, D.F. Dourado, P. Baptista, M. de Lourdes Bastos, F. Carvalho, New in silico insights into the inhibition of RNAP II by alpha-amanitin and the protective effect mediated by effective antidotes, J. Mol. Graph. Model. 51 (2014) 120–127.
[803] J. Senkiv, N. Finiuk, D. Kaminskyy, D. Havrylyuk, M. Wojtyra, I. Kril, A. Gzella, R. Stoika, R. Lesyk, 5-Ene-4-thiazolidinones induce apoptosis in mammalian leukemia cells, Eur. J. Med Chem. 117 (2016) 33–46.
[804] O.P. Yelisyeyeva, K.O. Semen, G.V. Ostrovska, D.V. Kaminskyy, T.V. Sirota, N. Zarkovic, D. Mazur, O.D. Lutsyk, K. Rybalchenko, A. Bast, The effect of Amaranth oil on monolayers of artificial lipids and hepatocyte plasma membranes with adrenalin-induced stress, Food Chem. 147 (2014) 152–159.
[805] A. Bast, G.R. Haenen, Ten misconceptions about antioxidants, Trends Pharmacol. Sci. 34 (2013) 430–436.
[806] K. Hirano, W.S. Chen, A.L. Chueng, A.A. Dunne, T. Seredenina, A. Filippova, S. Ramachandran, A. Bridges, L. Chaudry, G. Pettman, C. Allan, S. Duncan, K.C. Lee, J. Lim, M.T. Ma, A.B. Ong, N.Y. Ye, S. Nasir, S. Mulyanidewi, C.C. Aw, P.P. Oon, S. Liao, D. Li, D.G. Johns, N.D. Miller, C.H. Davies, E.R. Browne, Y. Matsuoka, D.W. Chen, V. Jaquet, A.R. Rutter, Discovery of GSK2795039, a novel small molecule NADPH oxidase 2 inhibitor, Antioxid. Redox Signal 23 (2015) 358–374.
[807] G.J. Maghzal, K.H. Krause, R. Stocker, V. Jaquet, Detection of reactive oxygen species derived from the family of NOX NADPH oxidases, Free Radic. Biol. Med. 53 (2012) 1903–1918.
[808] B. Kalyanaraman, B.P. Dranka, M. Hardy, R. Michalski, J. Zielonka, HPLC-based monitoring of products formed from hydroethidine-based fluorogenic probes–the ultimate approach for intra- and extracellular superoxide detection, Biochim. Biophys. Acta 1840 (2014) 739–744.
[809] T. Seredenina, Z. Nayernia, S. Sorce, G.J. Maghzal, A. Filippova, S.C. Ling, O. Basset, O. Plastre, Y. Daali, E.J. Rushing, M.T. Giordana, D.W. Cleveland, A. Aguzzi, R. Stocker, K.H. Krause, V. Jaquet, Evaluation of NADPH oxidases as drug targets in a mouse model of familial amyotrophic lateral sclerosis, Free Radic. Biol. Med. 97 (2016) 95–108.
[810] J. Talib, G.J. Maghzal, D. Cheng, R. Stocker, Detailed protocol to assess in vivo and ex vivo myeloperoxidase activity in mouse models of vascular inflammation and disease using hydroethidine, Free Radic. Biol. Med. 97 (2016) 124–135.
[811] Y. Fujikawa, L.P. Roma, M.C. Sobotta, A.J. Rose, M.B. Diaz, G. Locatelli, M.O. Breckwoldt, T. Misgeld, M. Kerschensteiner, S. Herzig, K. Muller-Decker, T.P. Dick, Mouse redox histology using genetically encoded probes, Sci. Signal. 9 (2016) rs1.
[812] M.N. Alam, N.J. Bristi, M. Rafiquzzaman, Review on in vivo and in vitro methods evaluation of antioxidant activity, Saudi Pharm. J. 21 (2013) 143–152.
[813] A. Agudo, L. Cabrera, P. Amiano, E. Ardanaz, A. Barricarte, T. Berenguer, M.D. Chirlaque, M. Dorronsoro, P. Jakszyn, N. Larranaga, C. Martinez, C. Navarro, J.R. Quiros, M.J. Sanchez, M.J. Tormo, C.A. Gonzalez, Fruit and vegetable intakes, dietary antioxidant nutrients, and total mortality in Spanish adults: findings from the Spanish cohort of the European prospective investigation into cancer and nutrition (EPIC-Spain), Am. J. Clin. Nutr. 85 (2007) 1634–1642.
[814] H. Sies, C. Berndt, D.P. Jones, Oxidative Stress, Ann. Rev. Biochem. (2017), http://dx.doi.org/10.1146/annurev-biochem-061516-045037.

1521-0081/70/2/348–383$35.00
PHARMACOLOGICAL REVIEWS

https://doi.org/10.1124/pr.117.014753
Pharmacol Rev 70:348–383, April 2018

ASSOCIATE EDITOR: MARTIN C. MICHEL

# Transcription Factor NRF2 as a Therapeutic Target for Chronic Diseases: A Systems Medicine Approach

Antonio Cuadrado, Gina Manda, Ahmed Hassan, María José Alcaraz, Coral Barbas, Andreas Daiber, Pietro Ghezzi, Rafael León, Manuela G. López, Baldo Oliva, Marta Pajares, Ana I. Rojo, Natalia Robledinos-Antón, Angela M. Valverde, Emre Guney,[1] and Harald H. H. W. Schmidt[1]

*Centro de Investigación Biomédica en Red Sobre Enfermedades Neurodegenerativas (CIBERNED), Instituto de Investigación Sanitaria La Paz (IdiPaz), Department of Biochemistry and Instituto de Investigaciones Biomédicas Alberto Sols UAM (Autonomous University of Madrid)-CSIC (Centro Superior de Investigaciones Biomédicas), Faculty of Medicine, Autonomous University of Madrid, Madrid, Spain (A.C., M.P., A.I.R., N.R.-A.); Victor Babes National Institute of Pathology, Bucharest, Romania (A.C., G.M.); Department Pharmacology and Personalized Medicine, School for Cardiovascular Medicine, Faculty of Health, Medicine and Life Sciences, Maastricht University, Maastrich, The Netherlands (A.H., H.H.H.W.S.); Instituto Interuniversitario de Investigación de Reconocimiento Molecular y Desarrollo Tecnológico, Universitat Politècnica de València, Universitat de València, Valencia, Spain (M.J.A.); Centre for Metabolomics and Bioanalysis, Facultad de Farmacia, Universidad CEU (Centro de Estudios Universitarios)-San Pablo, Madrid, Spain (C.B.); Center for Cardiology, Cardiology I–Laboratory of Molecular Cardiology, Medical Center of the Johannes Gutenberg University, Mainz, Germany (A.D.); Brighton and Sussex Medical School, Brighton, United Kingdom (P.G.); Instituto Teófilo Hernando y Departamento de Farmacología y Terapéutica, Facultad de Medicina, Universidad Autónoma de Madrid, Madrid, Spain (R.L., M.G.L.); Instituto de Investigación Sanitaria, Servicio de Farmacología Clínica, Hospital Universitario de la Princesa, Madrid, Spain (R.L., M.G.L.); GRIB (Unidad de Investigación en Informática Biomédica), Department of Experimental and Health Sciences, Universitat Pompeu Fabra, Barcelona, Spain (B.O., E.G.); Instituto de Investigaciones Biomédicas Alberto Sols UAM-CSIC and Centro de Investigación Biomédica en Red en Diabetes y Enfermedades Metabólicas Asociadas, Madrid, Spain (A.M.V.); and Structural Bioinformatics Laboratory, Department of Experimental and Health Sciences, Universitat Pompeu Fabra, Barcelona, Spain (E.G.)*



**Address correspondence to:** Dr. Antonio Cuadrado, Instituto de Investigaciones Biomédicas "Alberto Sols" UAM-CSIC, C/ Arturo Duperier 4, 28029 Madrid, Spain. E-mail: antonio.cuadrado@uam.es or Dr. Emre Guney, GRIB, Department of Experimental and Health Sciences, Universitat Pompeu Fabra, Barcelona-08003, Spain. E-mail: emre.guney@upf.edu

This work was supported by Grants SAF2015-71304-REDT, SAF2016-76520-R, SAF2013-4874R, SAF2015-65267-R, and BIO2014-57518 of the Spanish Ministry of Economy and Competiveness; PII4/00372 from the Health Institute Carlos III; PROMETEOII/2014/071 of Generalitat Valenciana; P_37_732/2016 REDBRAIN of the European Regional Development Fund; Competitiveness Operational Program 2014-2020; and the ERC Advanced Grant RadMed 294683 and COST action 15120 OpenMultiMed (H.H.H.W.S.). M.P. is the recipient of a FPU fellowship of Autonomous University of Madrid. E.G. is supported by a European-cofunded Beatriu de Pinos fellowship. R.L. is supproted by the Miguel Servet II fellow (CPII16/00014).

[1]E.G. and H.H.H.W.S. are senior authors who contributed equally to this work.

https://doi.org/10.1124/pr.117.014753.

*Abstract*——**Systems medicine has a mechanism-based rather than a symptom- or organ-based approach to disease and identifies therapeutic targets in a nonhypothesis-driven manner. In this work, we apply this to transcription factor nuclear factor (erythroid-derived 2)–like 2 (NRF2) by cross-validating its position in a protein–protein interaction network (the NRF2 interactome) functionally linked to cytoprotection in low-grade stress, chronic inflammation, metabolic alterations, and reactive oxygen species formation. Multiscale network analysis of these molecular profiles suggests alterations of NRF2 expression and activity as a common mechanism in a subnetwork of diseases (the NRF2 diseasome). This network joins apparently heterogeneous phenotypes such as autoimmune, respiratory, digestive, cardiovascular, metabolic, and neurodegenerative diseases, along with cancer. Importantly, this approach matches and confirms in silico several applications for NRF2-modulating drugs validated in vivo at different phases of clinical development. Pharmacologically, their profile is as diverse as electrophilic dimethyl fumarate, synthetic triterpenoids like bardoxolone methyl and sulforaphane, protein–protein or DNA–protein interaction inhibitors, and even registered drugs such as metformin and statins, which activate NRF2 and may be repurposed for indications within the NRF2 cluster of disease phenotypes. Thus, NRF2 represents one of the first targets fully embraced by classic and systems medicine approaches to facilitate both drug development and drug repurposing by focusing on a set of disease phenotypes that appear to be mechanistically linked. The resulting NRF2 drugome may therefore rapidly advance several surprising clinical options for this subset of chronic diseases.**

## I. Introduction

Life span has almost doubled in the last century, and aging-specific diseases are now becoming prevalent. However, the pathologic mechanisms underlying most of them are poorly understood and treated rather by correcting symptoms or risk factors. Moreover, contrary to a hitherto linear approach that considered one disease, one medicine, chronic diseases demonstrate a high degree of connectedness and a need for more precise, mechanism-based disease definitions rather than the current organ- and symptom-based. After the human genome sequencing and the development of molecular networks, a new concept of disease is thus emerging, in which diseases are diagnosed not only by clinical symptoms, but mainly by the underlying molecular signatures (Goh et al., 2007). The fact that different pathophenotypes have a shared molecular mechanism provides also a rationale toward a new concept of therapy summarized as "several diseases, one medicine" and drug repurposing. Network medicine, i.e., the application of network concepts to the analysis of dynamic connections among diseases and drugs, provides a new opportunity to develop this new approach. Chronic diseases in the elderly are most likely characterized by the loss of homeostasis during aging or as a result of environmental factors, all of them leading to low-grade stress by pathologic formation of reactive oxygen species (ROS), chronic inflammation, and metabolic unbalance. Based on a network medicine approach, in this review we will present extensive evidence indicating that the nuclear factor (erythroid-derived 2)–like

**ABBREVIATIONS:** AD, Alzheimer disease; ALS, amyotrophic lateral sclerosis; AMPK, AMP-activated protein kinase; ARE, antioxidant response element; $\beta$-TrCP, $\beta$-transducin repeat containing E3 ubiquitin protein ligase; bZip, basic region-leucine zipper; CDDO, 2-cyano-3,12-dioxo-oleana-1,9(11)-dien-28-oate; CDDO-Me, CDDO-methyl ester; COPD, chronic obstructive pulmonary disease; CUL3, Cullin 3; DC, dendritic cell; DMF, dimethyl fumarate; EAE, experimental autoimmune encephalomyelitis; ECH, erythroid cell–derived protein with Cap'n'collar homology; GCLC, $\gamma$-glutamyl cysteine ligase catalytic subunit; GCLM, $\gamma$-glutamyl cysteine ligase modulator subunit; GI, gastrointestinal tract; GSH, glutathione; GSK-3, glycogen synthase kinase 3; HFD, high-fat diet; HNSCC, head and neck squamous cell carcinoma; HO-1, heme oxygenase-1; IBD, inflammatory bowel disease; I$\kappa$B, $\kappa$-B inhibitor; IKK, I$\kappa$B kinase; IL, interleukin; KEAP1, kelch-like ECH-associated protein 1; LDL, low-density lipoprotein; LPS, lipopolysaccharide; MAF, musculoaponeurotic fibrosarcoma protein; MMF, monomethyl fumarate; MS, multiple sclerosis; NASH, nonalcoholic steatohepatitis; NF-$\kappa$B, p65 subunit of nuclear factor $\kappa$-light-chain enhancer of activated B cells; NQO1, NADPH:quinone oxidoreductase; NRF2, nuclear factor (erythroid-derived 2)–like 2; PD, Parkinson disease; PI3K, phosphatidylinositol 3-kinase; PPI, protein–protein interaction; PTEN, phosphatase and tensin homolog; RA, rheumatoid arthritis; RBX1, RING-box protein 1; RNS, reactive nitrogen species; ROS, reactive oxygen species; SFN, sulforaphane; SLE, systemic lupus erythematous; SNP, single-nucleotide polymorphism; SQSTM1, sequestosome 1; STAT, signal transducer and activator of transcription; T2DM, type 2 diabetes mellitus; TGF, transforming growth factor; Th, T helper; TNF, tumor necrosis factor; Treg, T regulatory.

2 (NRF2), as the master regulator of multiple cytoprotective responses and a key molecular node within a particular cluster of diseases, provides a new strategy for drug development and repurposing.

## II. From Nuclear Factor (Erythroid-Derived 2)–Like 2 Interactome to Nuclear Factor (Erythroid-Derived 2)–Like 2 Diseasome

### *A. Nuclear Factor (Erythroid-Derived 2)–Like 2 as a Master Regulator of Cellular Homeostasis*

NRF2 is a basic region-leucine zipper (bZip) transcription factor (Fig. 1) that forms heterodimers with small musculoaponeurotic fibrosarcoma protein (MAF) K, G, and F in the nucleus. The heterodimer recognizes an enhancer sequence termed antioxidant response element (ARE) that is present in the regulatory regions of over 250 genes (ARE genes) (Ma, 2013; Hayes and Dinkova-Kostova, 2014). These ARE genes encode a network of cooperating enzymes involved in phase I, II, and III biotransformation reactions and antioxidant mechanisms that generate NADPH, glutathione (GSH), and thioredoxin reactions; lipid and iron catabolism; and interaction with other transcription factors, etc. (Hayes and Dinkova-Kostova, 2014). Recently, NRF2 was also found to regulate the expression of several proteasome subunits and autophagy genes, providing additional interest for its control of proteostasis (Pajares et al., 2015, 2016, 2017; de la Vega et al., 2016).

The great significance of NRF2 from a clinical perspective is that it might be targeted pharmacologically with patient benefit. The main mechanism regulating the transcriptional activity of NRF2 is the control of protein stabilization by the E3 ligase adapter Kelch-like erythroid cell–derived protein with Cap'n'collar homology (ECH)-associated protein 1 (KEAP1) (Fig. 2). KEAP1 is a homodimeric protein that bridges NRF2 with the E3 ligase complex formed by Cullin 3 and RING-box protein 1 (CUL3/RBX1). Under homeostatic conditions, the N-terminal domain of the KEAP1 homodimer binds one molecule of NRF2 at two amino acid sequences with low (aspartate, leucine, and glycine; DLG) and high (glutamate, threonine, glycine, and glutamate; ETGE) affinity, and hence presents NRF2 to ubiquitination by CUL3/RBX1 (Tong et al., 2007) and subsequent degradation by the proteasome. KEAP1 is a redox and electrophile sensor that upon modification of critical cysteines loses its ability to repress NRF2 (Fig. 2; *Biomarkers as Nuclear Factor (Erythroid-Derived 2)–Like 2 Signature and for Monitoring Target Engagement*). An alternative mechanism of regulation of NRF2 stability is the phosphorylation mediated by glycogen synthase kinase 3 (GSK-3) (Fig. 2). This kinase phosphorylates a domain of NRF2 (aspartate, serine, glycine, isoleucine, serine; DSGIS) and hence creates a recognition motif for the E3 ligase adapter $\beta$-transducin

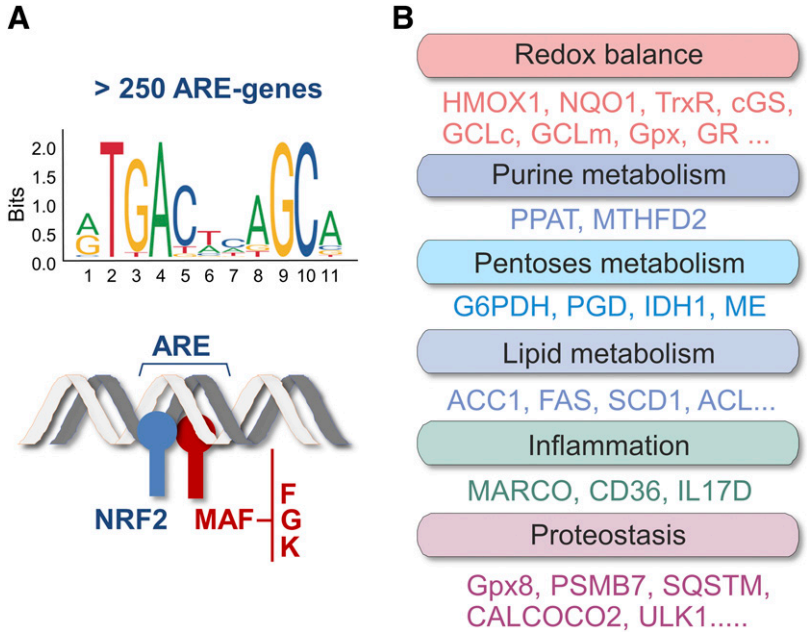


**Fig. 1.** NRF2 as a master regulator of cytoprotective responses. (A) NRF2 heterodimerizes with the members of MAF family through their bZip domain. The heterodimer binds to an enhancer sequence termed ARE that is present in the regulatory regions of over 250 genes (ARE genes). (B) These genes participate in the control of redox metabolism, inflammation, and proteostasis balance, as indicated. The existence of susceptibility SNPs in *NFE2L2*, elevated levels of its target genes in brain necropsies, and positive data from preclinical studies suggests that the imbalance in proteostasis, redox, and inflammatory control may be counterbalanced by NRF2 activation. ACl, ATP citrate lyase; ACC1, acetyl-coenzyme A carboxylase 1; CALCOCO2, calcium binding and coiled-coil domain 2; cGS, c-glutamate cysteine synthetase; FAS, fatty acid synthase; G6PDH, glucose-6-phosphate dehydrogenase; Gpx, glutathione peroxidase; Gpx8, gluthation peroxidase 8; GR, glutathione reductase; HMOX1, heme oxygenase-1; IDH1, isocitrate dehydrogenase 1; ME, malic enzyme; MTHFD2, methylenetetrahydrofolate dehydrogenase 2; PGD, phosphogluconate dehydrogenase; PPAT, phosphoribosyl pyrophosphate amidotransferase; PSMB7, proteasome subunit $\beta$ type-7; SCD1, stearoyl-CoA desaturase; TrxR, thioredoxin reductase; ULK1, unc-51 like autophagy activating kinase 1.

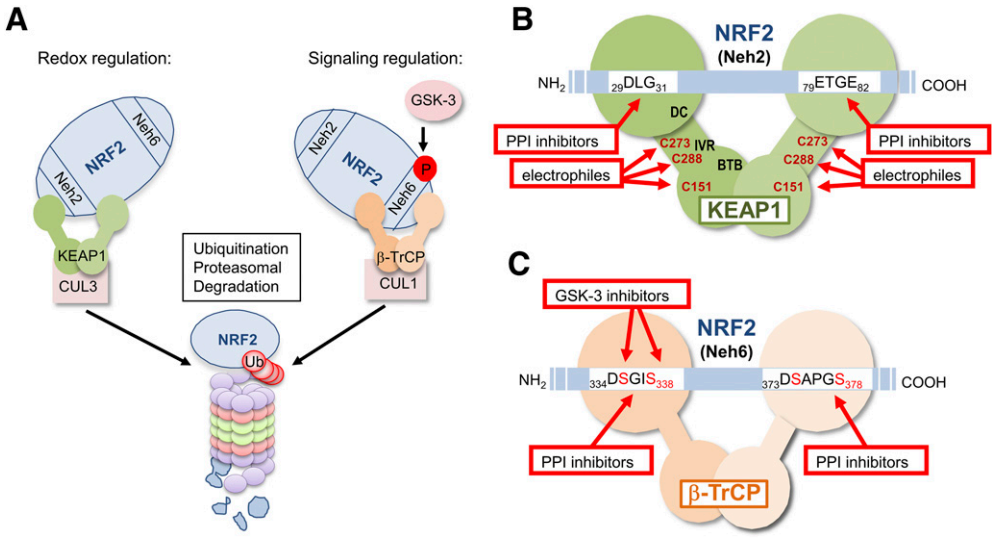


**Fig. 2.** Regulation of NRF2 stability by KEAP1 and β-TrCP and its pharmacological targeting. (A) According to the dual regulation model (Rada et al., 2011), two domains of NRF2, termed Neh2 and Neh6, participate in NRF2 degradation in response to redox and electrophile changes (KEAP1) and to signaling kinases (β-TrCP), respectively. The Neh2 domain binds the E3 ligase adapter KEAP1 that presents NRF2 for ubiquitination to a CUL3/RBX1 complex. The Neh6 domain requires previous phosphorylation by GSK-3 to bind the E3 ligase adapter β-TrCP and subsequent ubiquitination by a CUL1/RBX1 complex (see text for details). (B) Detail of the binding between NRF2 and KEAP1 and current strategies to target this interaction. The KEAP1 homodimer binds NRF2 at two motifs of the Neh2 domain: the low-affinity (29-DLG-31) and the high-affinity (79-ETGE-82) binding sites. Current strategies to disrupt this interaction include the following: electrophiles that alter sulfhydryl groups of cysteines C151, 273, and 288; PPI inhibitors that alter the docking of NRF2 to the DC domain of KEAP1. (C) Hypothetical binding of NRF2 and β-TrCP and suggested strategies to target this interaction. The β-TrCP homodimer binds to the Nhe6 domain at the phospho-motif 334-DSGIS-338 when it is phosphorylated by GSK-3 (Rada et al., 2011, 2012) and at the phospho-motif 373-DSAPGS-378 independently of GSK-3 (Chowdhry et al., 2013). In this figure we postulate that, by analogy with KEAP1, one β-TrCP homodimer interacts with one molecule of NRF2 at the two phospho-motifs, but experimental evidence is still lacking. Two possible strategies to disrupt this interaction include the use of GSK-3 inhibitors and PPI inhibitors.

repeat containing E3 ubiquitin protein ligase (β-TrCP) that presents NRF2 to a CUL1/RBX1 complex, leading to an alternative pathway for ubiquitin-dependent proteasome degradation of NRF2. Therefore, KEAP1 and GSK-3/β-TrCP tightly control NRF2 protein levels in the context of redox homeostasis and cell signaling, respectively (Cuadrado, 2015). Other mechanisms of NRF2 regulation at protein, mRNA, or gene level have been reported (Hayes and Dinkova-Kostova, 2014), but at least these two are amenable to pharmacological regulation.

### *B. Positioning Nuclear Factor (Erythroid-Derived 2)–Like 2 and Its Regulatory Pathway in the Human Interactome and Diseasome*

The gene encoding NRF2, termed *NFE2L2*, is highly polymorphic and presents a mutagenic frequency of 1 per every 72 bp. An excellent review on this topic reported in 2015 up to 18 single-nucleotide polymorphisms (SNPs), most of them in the 5′ regulatory region and in intron 1 (Cho et al., 2015). Several of these SNPs might constitute functional haplotypes that are associated with risk at onset or progression of chronic diseases. Variations in functional haplotypes may have a subtle impact on a proportion of individuals who exhibit clinical symptoms of specific diseases, yet they may have a profound effect at the population level and may define specific strategies to target this gene in precision medicine.

Recent advances in network medicine have provided quantitative tools to characterize how the interplay between genes and their interactions (interactome) is related to pathology (Barabasi et al., 2011; Vidal et al., 2011; Guney et al., 2016), how dysregulated molecular networks are common to various diseases (Menche et al., 2015), and how diseases manifest in particular tissues (Kitsak et al., 2016). To understand the relevance of NRF2 in pathology from the systems medicine perspective, first we have generated the human interactome map. We have integrated and curated information on physical interactions among proteins involved in the NRF2-regulating pathway (Hayes and Dinkova-Kostova, 2014; Cuadrado, 2015). The interaction data have been taken from the recently published human interactome that compiles data across several protein–protein interaction (PPI) resources (Turei et al., 2013; Menche et al., 2015). However, the currently available information for development of the NRF2 interactome is limited by the fact that, because NRF2 is a very short half-life protein, some meaningful interactions may be undetected. Nevertheless, some well-known proteins that physically interact with NRF2 are found in the interactome, including KEAP1, β-TrCP, and MAFs. Another group of NRF2-interacting proteins corresponds to nuclear proteins with functions in regulation of gene expression. These include proteins related with bZip transcription factors, nuclear receptors or coactivators, or proteins involved in histone acetylation. Therefore, the NRF2 interactome evidences additional mechanisms of gene regulation beyond those directly connected to this

transcription factor. NRF2 is phosphorylated at several residues, and therefore it is expected to interact with several kinases that include GSK-3 and several protein kinase C isoforms. These kinases are downstream of some membrane receptors and adapter/scaffold proteins. In addition to this physical interaction, we have identified several biologic functions that are enriched in the NRF2 neighborhood, including metabolic processes, such as biosynthesis of pentose, tetrapyrrole, heme, glucose 6-phospate, cysteine, GSH, glyceraldehyde-3-phosphate, and NADPH. Most of these regulatory proteins do not interact directly with each other but are connected through proteins acting as mediators (Fig. 3; a more detailed description of specific interacting molecules can be found at http://sbi.imim.es/data/nrf2/).

Perturbations of the NRF2 interactome have been reported in several diseases. We have developed a diseasome map by curating a list of 37 NRF2-related diseases based on DisGeNET (Pinero et al., 2017) and GeneCards (Stelzer et al., 2016) databases, as well as knowledge from some studies in animal models. We have also retrieved disease–gene associations for these pathologies using DisGeNET, OMIM, and GWAS databases (Menche et al., 2015) (Table 1). The interactome-based proximity (Guney and Oliva, 2014) of NRF2 to known disease genes for each of the NRF2-related disease phenotypes is shown in Fig. 4. NRF2 is significantly closer to the known disease genes of the digestive system and cancers, such as prostate, liver, and lung neoplasms, compared with randomly selected proteins, highlighting the key functional role of NRF2 in these pathologies. Moreover, NRF2 was found to be proximal to various proteins related to metabolic and cardiovascular diseases, such as diabetes, hyperglycemia, ischemia, middle cerebral artery infarction, and atherosclerosis. Protein interactions of NRF2 also connect it to genes associated to respiratory disorders such as asthma, pulmonary fibrosis, and pulmonary emphysema, as well as to neurodegenerative conditions such as Alzheimer disease (AD), Parkinson disease (PD), and amyotrophic lateral sclerosis (ALS).

The interactome-based proximity therefore offers a perspective on how NRF2 can be linked to various pathologic conditions. The relationships among diseases have been previously summarized as a network, termed diseasome, that is connecting them based on genetic (Goh et al., 2007) and clinical (Hidalgo et al., 2009; Zhou et al., 2014) commonalities. In Fig. 5, we have defined a network of diseases, the NRF2 diseasome, based on shared genes, symptom similarity, and comorbidities. NRF2 appears to connect diseases governed substantially by inflammatory processes, such as acute kidney injury, liver cirrhosis, and atherosclerosis. Furthermore, neurodegenerative diseases such as AD, PD, Huntington's disease, and ALS constitute a cluster consistent with recent studies implicating also NRF2 in neuroinflammatory processes (Rojo et al., 2010; Lastres-Becker et al., 2012, 2014; Jung et al., 2017; Wang et al., 2017b). The regulation of NRF2 by kinase-signaling cascades (Jung et al., 2017) could explain the well-connected cluster of cancers, particularly supporting the involvement of NRF2 in pathologic ROS

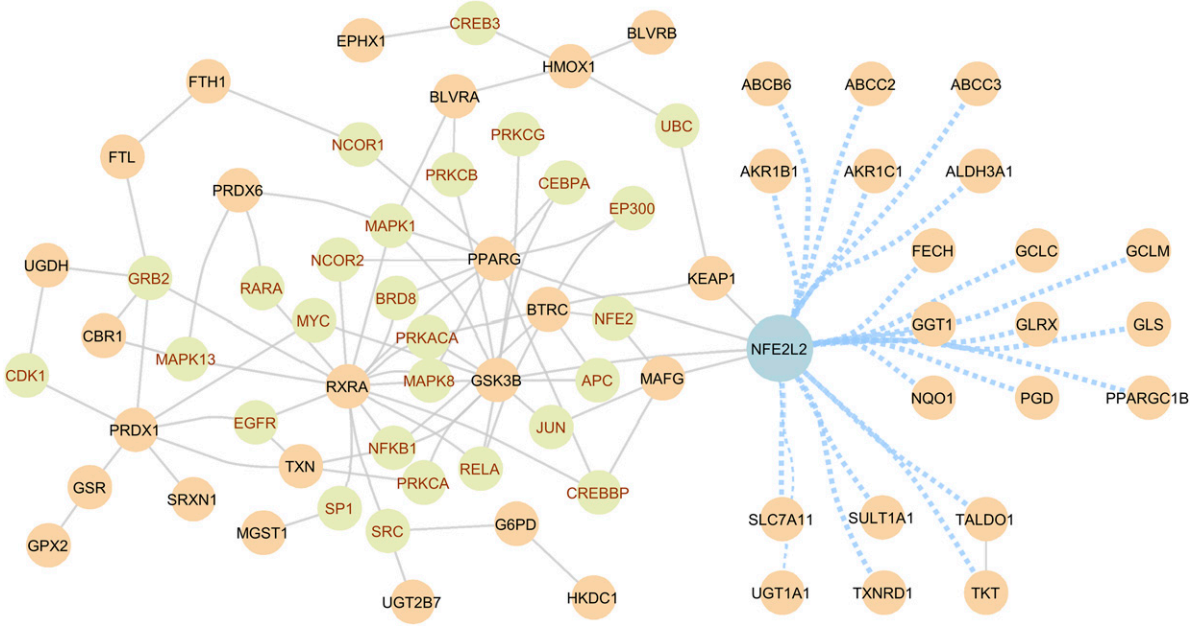


**Fig. 3.** Locating the NRF2 regulatory pathway in the human interactome. NRF2 plays a key role in pathologic ROS formation as well as inflammatory and metabolic responses by coordinating the activity of various proteins. These interactions constitute a molecular interaction network, the NRF2 interactome. The known physical interactions between proteins involved in the NRF2 regulatory pathway (i.e., regulator proteins, brown circles) and the proteins through which they are connected (i.e., mediator proteins, green circles) are shown with a gray link. The regulator proteins that involve more than one mediator protein to connect to NRF2 are shown with a blue link. The regulator proteins are curated from literature, and their interactions are retrieved from various resources, including IntAct, MINT, BioGRID, HPRD, KEGG, and PhosphoSite. The list of all the proteins that interact with NRF2 in the human interactome is available online at http://sbi.imim.es/data/nrf2/.

TABLE 1
Cluster of diseases with evidence of NRF2 association

Disease phenotypes with evidence of genetic association with NRF2 were selected from the DisGeNet database. DisGeNet integrates disease–gene association information from various resources, such as UniProt, ClinVar, GWAS Catalog, and Comparative Toxicogenomics Database and scores disease–gene associations according to the number of resources and publications supporting these associations. The curation of the list was based on the following criteria: 1) only pathophenotypes with more than one citation in Pubmed were selected; 2) the score of reliability was set to a threshold of 0.001; and 3) disease entries with very similar names or overlapping terms were simplified to one single entry.

| Pathophenotype | Reliability Score | Pathophenotype | Reliability Score |
|---|---|---|---|
| Diabetic nephropathy | 0.2016 | Diabetic cardiomyopathy | 0.0803 |
| Liver cirrhosis | 0.2005 | Middle cerebral artery infraction | 0.0800 |
| Nonalcoholic steatohepatitis | 0.2005 | Breast neoplasms | 0.0087 |
| Acute kidney injury | 0.2000 | Vitiligo | 0.0076 |
| Pulmonary fibrosis | 0.2000 | Atherosclerosis | 0.0067 |
| Nonsmall cell lung carcinoma | 0.1252 | Asthma | 0.0043 |
| Squamous cell carcinoma | 0.1243 | Leukemia | 0.0038 |
| Liver neoplasms | 0.1238 | Colon neoplasm | 0.0038 |
| Hyperglycemia | 0.1208 | Gastrointestinal diseases | 0.0029 |
| Drug-induced liver injury | 0.1200 | Parkinson disease | 0.0026 |
| Prostatic neoplasms | 0.1200 | Systemic lupus erythematous nephritis | 0.0026 |
| Chronic obstructive pulmonary disease | 0.0899 | Glioma | 0.0024 |
| Colorectal neoplasms | 0.0847 | Amyotrophic lateral sclerosis | 0.0022 |
| Alzheimer disease | 0.0837 | Ischemia | 0.0016 |
| Type 2 diabetes mellitus | 0.0814 | Pulmonary emphysema | 0.0013 |
| Chronic kidney disease | 0.0808 | Pancreatic neoplasms | 0.0013 |
| Diabetic retinopathy | 0.0805 | Vascular diseases | 0.0013 |
| Huntington's disease | 0.0805 | Sepsis | 0.0013 |

formation underlining colon (Gonzalez-Donquiles et al., 2017) and breast (Lu et al., 2017) tumors.

## III. Target Validation of Nuclear Factor (Erythroid-Derived 2)–Like 2 in Human Disease States

### *A. Key Role of Nuclear Factor (Erythroid-Derived 2)–Like 2 in Resolution of Inflammation*

Persistent inflammation is a hallmark of all pathophenotypes found in the NRF2 diseasome. This is most likely because inflammation is associated with increased local and systemic pathologic formation of reactive oxygen species (ROS). In fact, ROS and reactive nitrogen species (RNS) stimulate and aggravate inflammatory responses that are mechanistically related to the activation of transcription factor, p65 subunit of nuclear factor κ-light-chain enhancer of activated B cells (NF-κB) (Wenzel et al., 2017). Very simplified, in resting immune cells, NF-κB is retained in the cytosol through interaction with the nuclear κ-B inhibitor (IκBα). Pathogen-associated molecular pattern molecules derived from microorganisms as well as damage-associated molecular pattern molecules released in

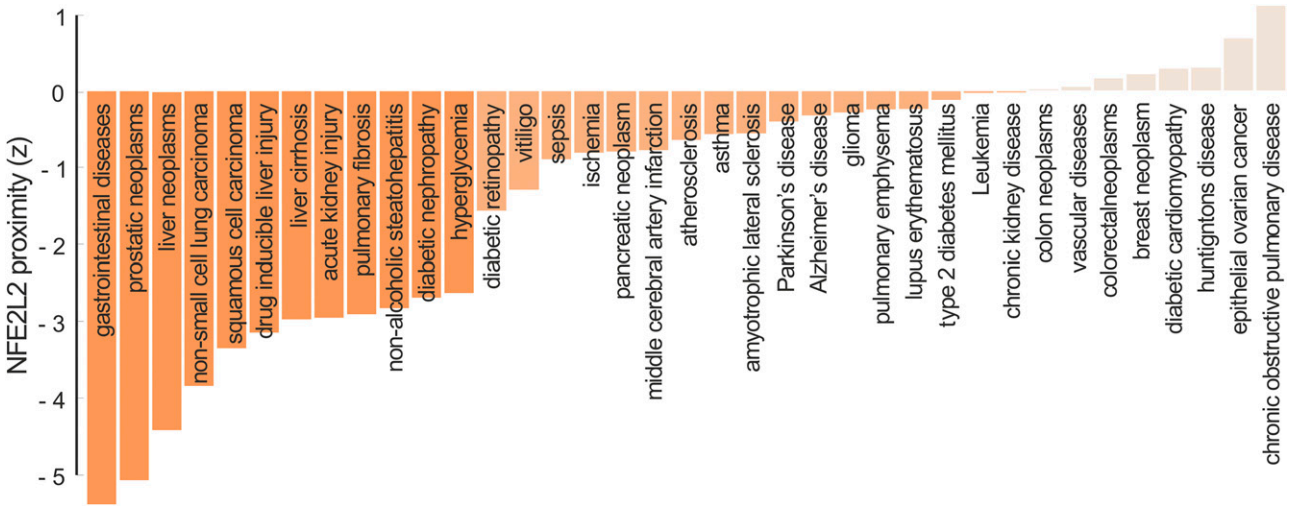


**Fig. 4.** Systems medicine view of NRF2 from the perspective of the human interactome. Diseases are triggered by mutations that perturb proteins and their interactions, affecting a certain neighborhood in the NRF2 interactome. Interactome-based proximity measures the distance of genes to those disease neighborhoods. The bars show the proximity of NRF2 gene (*NFE2L2*) to known disease genes that participate in NRF2-related pathophenotypes. These bars highlight the role of NRF2 in digestive system diseases and cancers. For a given disease, the proximity first calculates the distance from NRF2 to the closest known disease gene and then compares that distance to a random expectation that is estimated using average distances between randomly selected proteins in the interactome. The *z*-score reported by interactome-based proximity corresponds to the significance of the observed distance between NRF2 and the disease genes. A negative value indicates that the observed distance is lower than what would be expected by chance. The bars are colored in varying tones of orange based on the *z*-score: significantly proximal (dark orange), proximal (orange), not proximal (light orange), respectively. The known disease genes are taken from DisGeNet, OMIM, and GWAS Catalog.

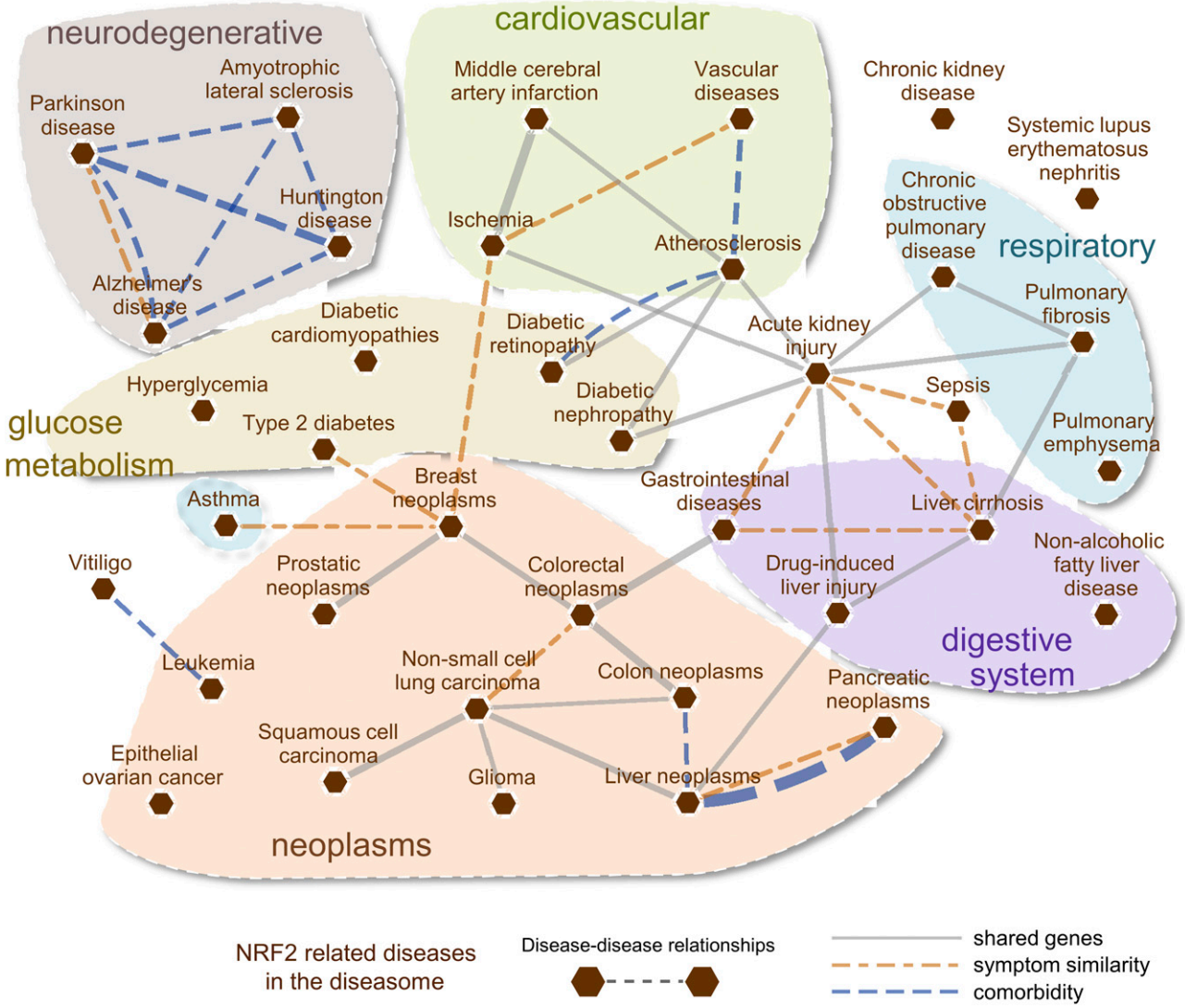


**Fig. 5.** Current status of the NRF2 diseasome. The relationships between diseases are represented as a network in which pathophenotypes are linked by common genetic and clinical descriptors. In the figure, nodes (red hexagons) represent diseases, and the edges are similarities among them based on shared genes, common symptoms, and comorbidities (gray, orange, and blue lines, respectively). The genes and symptoms associated with the diseases are used to identify disease pairs that have a significant genetic and symptomatic overlap calculated using the Jaccard index. Among significant disease–disease connections ($P < 0.05$, assessed by Fisher's exact test based on the observed gene or symptom overlap), only the links that have an elevated overlap and comorbidity are shown to eliminate potentially spurious connections. Accordingly, the diseases that share at least 10% of the disease-associated genes and more than half of the associated symptoms are included in the figure. The comorbidity information is extracted from medical insurance claims, representing disease pairs that tend to occur together in the population (relative risk >2).

response to tissue damage stimulate cognate receptors expressed by immune cells that lead to activation of IκB kinase (IKK)β. This kinase phosphorylates IκBα, targeting it for degradation and allowing nuclear translocation and activation of NF-κB (Napetschnig and Wu, 2013). These events are submitted to redox control through several modes of regulation of IκBα (Bowie and O'Neill, 2000; Morgan and Liu, 2011; Siomek, 2012), but one that has been described recently involves the regulation of IKKβ stability by KEAP1. Just like NRF2, IKKβ possesses an ETGE motif that enables its binding to KEAP for ubiquitination and proteasomal degradation. Therefore, under basal redox conditions, active KEAP1 targets IKKβ for degradation and then IκBα inhibits NF-κB. By contrast, in the presence of ROS, KEAP1 is inhibited and IKKβ is stabilized, phosphorylating IκBα and leading to its degradation and therefore to upregulation of NF-κB (Lee et al., 2009).

Because NRF2 is a master regulator of redox homeostasis, it exerts an indirect control on NF-κB activity. Lipopolysaccharide (LPS) activates simultaneously a fast, proinflammatory NF-κB response and a slow NRF2 response. The NF-κB response is subsequently inhibited when NRF2 is maximally active (Cuadrado et al., 2014). For instance, Ras-related C3 botulinum toxin substrate 1, a small G protein of the Rho family, activated the NF-κB pathway and NRF2 overexpression blocked, whereas NRF2 knockdown enhanced NF-κB–dependent transcription (Cuadrado et al.,

2014). Consistently, in NRF2-deficient (*Nrf2*$^{-/-}$) mice challenged with LPS or tumor necrosis factor (TNF)-$\alpha$, the activity of IKK was exacerbated and led to increased phosphorylation and degradation of I$\kappa$B (Thimmulappa et al., 2006a).

NRF2 also induces an anti-inflammatory phenotype that modulates the functions of CD8$^+$ T cells (Sha et al., 2015) as well as in macrophages and microglia ( Rojo et al., 2010, 2014a; Brune et al., 2013). This is because NRF2 increases cysteine and GSH levels in macrophages through regulation of the cystine/glutamate transporter and the GSH-synthesizing enzyme $\gamma$-glutamyl cysteine ligase modulator and catalytic subunits [$\gamma$-glutamyl cysteine ligase modulator subunit (GCLM) and $\gamma$-glutamyl cysteine ligase catalytic subunit (GCLC)]. Conversely, GSH depletion sensitizes macrophages to NRF2 activation by LPS (Diotallevi et al., 2017). All of these studies point to NRF2 as an anti-inflammatory factor, crucial in controlling the intensity and duration of inflammatory responses (Fig. 6).

NRF2 and NF-$\kappa$B crosstalk through feed forward and feedback mechanisms (Fig. 7). At the transcriptional level, NF-$\kappa$B activates NRF2 expression due to the existence of several functional binding sites in the promoter region of the *NFE2L2* gene, thus inducing a negative feedback loop (Rushworth et al., 2012). Moreover, both NF-$\kappa$B and NRF2 transcription factors require the coactivator CBP/p300, which is a histone acetyltransferase that acetylates and increases the DNA-binding capacity. As such, NF-$\kappa$B overexpression hampers the availability of CBP/p300 for NRF2, hence reducing its transcriptional capacity, whereas NF-$\kappa$B knockdown shows the opposite effect (Liu et al., 2008). Additionally, NF-$\kappa$B may promote interaction of histone deacetylase-3 with MAF proteins, therefore preventing their dimerization with NRF2 (Liu et al., 2008). NF-$\kappa$B binds and translocates KEAP1 to the nucleus, thus favoring NRF2 ubiquitination and degradation in this cellular compartment (Yu et al., 2011). The E3 ligase adapter $\beta$-TrCP tags both I$\kappa$B$\alpha$ (Winston et al., 1999) and NRF2 (Rada et al., 2011, 2012; Cuadrado, 2015) for proteasomal degradation, and therefore it can lead to increased NF-$\kappa$B activity.

The anti-inflammatory activity of NRF2 was thought to rely only on modulation of redox metabolism or crosstalk with NF-$\kappa$B. However, NRF2 can also directly block the transcription of the proinflammatory genes interleukin (IL)-6 and IL-1$\beta$ in macrophages upon exposure to LPS (Kobayashi et al., 2016). LPS exposure or pharmacological activation of NRF2 leads to its binding to the proximal promoters of these proinflammatory genes and blocks the recruitment of RNA pol II. The mechanism appears to be independent of the binding of NRF2 to its well-established ARE enhancer. In other studies, NRF2 could directly regulate the expression of several other macrophage-specific genes, such as macrophage receptor with collagenous structure, a receptor required for bacterial phagocytosis, or CD36, a scavenger receptor for oxidized low-density

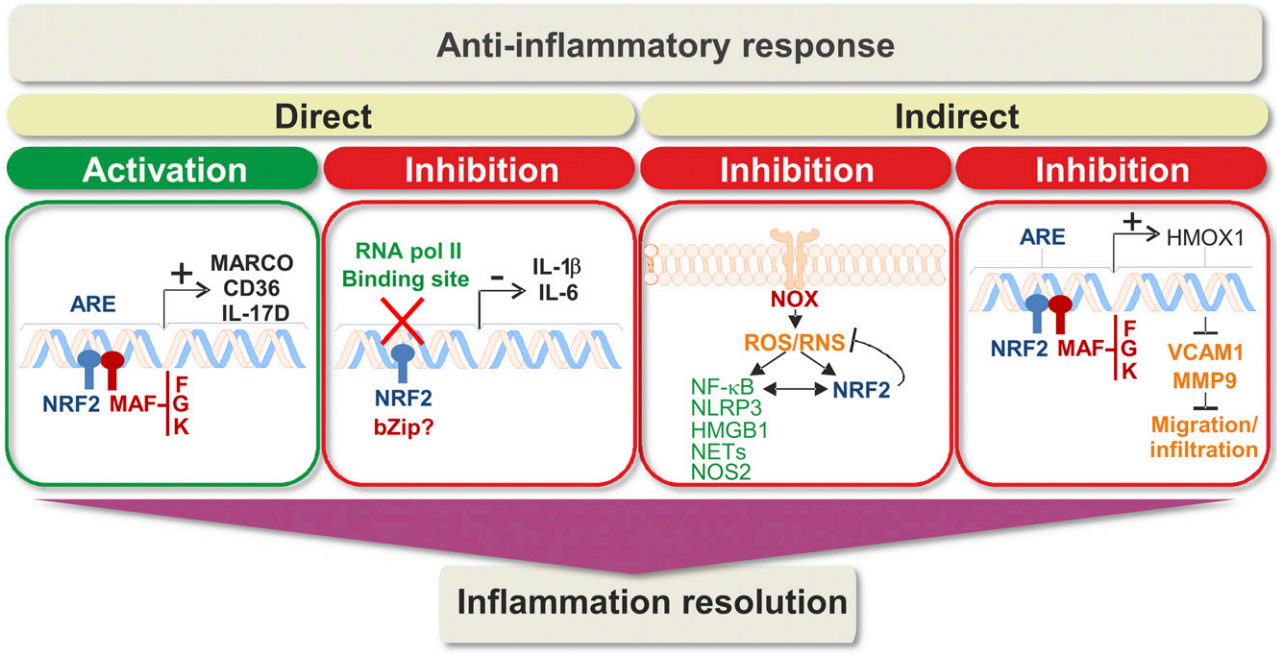


**Fig. 6.** Direct and indirect regulation of inflammation by NRF2. Direct mechanisms of action include transcriptional induction of anti-inflammatory genes as well as transcriptional repression of proinflammatory genes. In the second case, the quotation mark indicates that further work is required to identify the bZip partner of NRF2 in this function, if any. Indirect mechanisms to counteract inflammation involve ROS/RNS modulation and inhibition of migration/infiltration of immune cells. Overall, these pathways lead to an anti-inflammatory response that helps to properly resolve inflammation. The existence of polymorphisms in *NFE2L2* associated with reduced transcriptional activity, the altered levels of target genes in patients, and promising data from preclinical studies support a relevant role of NRF2 in inflammation resolution.

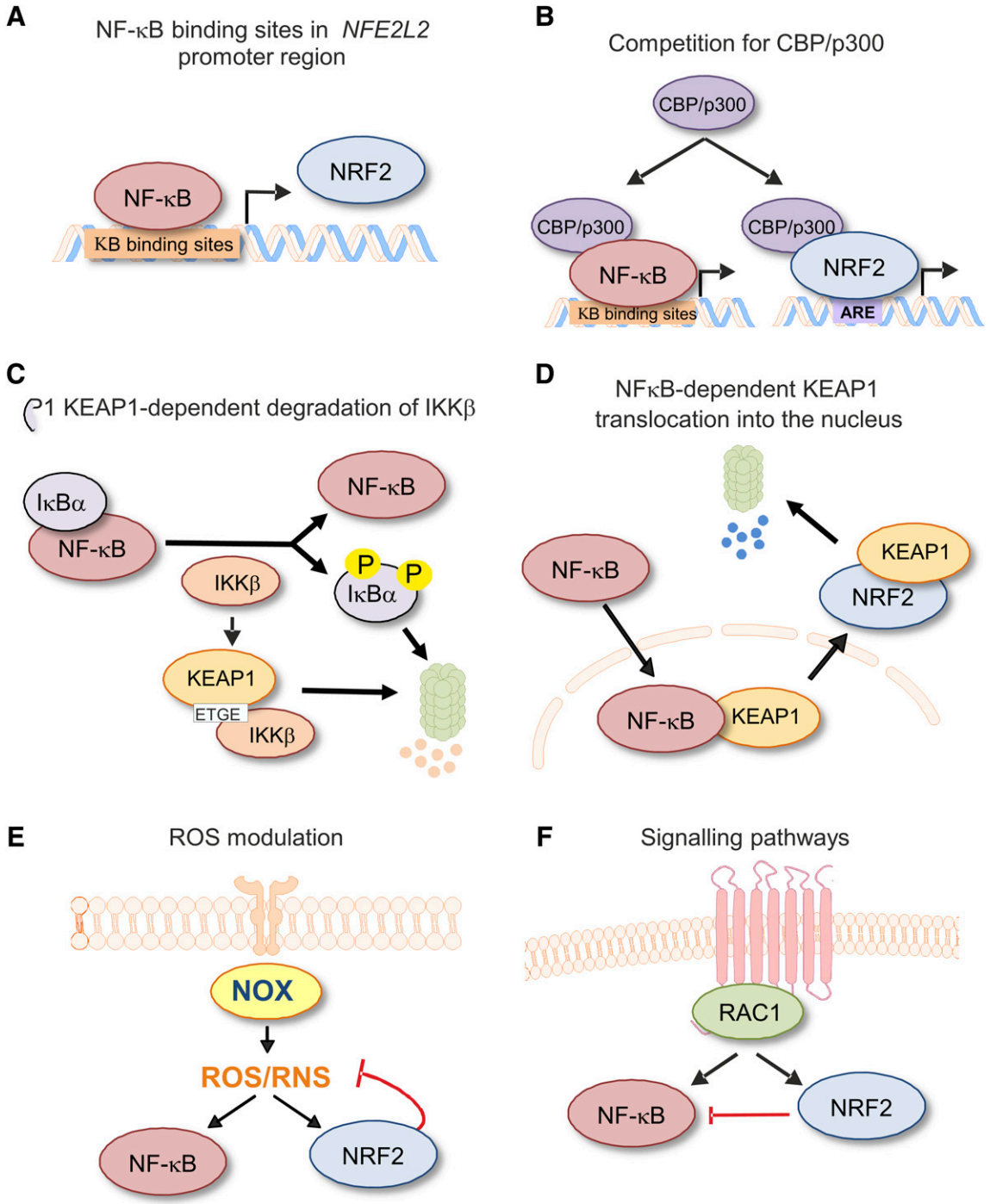


**Fig. 7.** Crosstalk between NF-κB and NRF2 occurs at different levels. (A) Responsive elements have been identified in the promoter region of *NFE2L2*. (B) Both NRF2 and NF-κB transcription factors compete for binding to the transcriptional coactivator CREB-binding protein (CBP/p300). (C) The NF-κB activating kinase IKKβ contains an ETGE motif allowing KEAP1 binding and subsequent ubiquitin–proteasome degradation. (D) NF-κB was reported to bind and translocate KEAP1 to the nucleus, thereby promoting NRF2 degradation. (E) ROS produced during inflammation activate NF-κB and NRF2; finally, NRF2 attenuates ROS and consequently NF-κB activity. (F) Different proinflammatory signals activate the Rho GTPase RAC1, which leads to NF-κB and NRF2 activation. Then NRF2 inhibits RAC1-mediated activation of NF-κB.

lipoprotein (Harvey et al., 2011; Ishii and Mann, 2014). Similarly, the gene encoding the proinflammatory cytokine, IL-17D, contains AREs, and this NRF2–T helper (Th)17 axis seems to confer protection against tumorigenesis and viral infections (Saddawi-Konefka et al., 2016).

Chronic inflammatory processes involve adhesion of leukocytes to the vascular endothelium and infiltration into the damaged tissue. Both processes appear to be modulated by NRF2 together with at least one of its target genes *HMOX1*, coding heme oxygenase-1 (HO-1). The NRF2/HO-1 axis inhibits adhesion of inflammatory

cells to the endothelium by modulating the expression of several cell adhesion molecules such as vascular cell adhesion molecule 1 (Banning and Brigelius-Flohe, 2005; Wenzel et al., 2015). Additionally, NRF2/HO-1 inhibits metalloproteinase-9 in macrophages that are necessary for migration of immune cells within tissues (Bourdonnay et al., 2009).

Numerous preclinical studies have reported that activation of NRF2 by natural compounds (Satoh et al., 2013) or by disrupting its negative regulator KEAP1 leads to potent anti-inflammatory effects in myeloid leukocytes (Kong et al., 2011) and macrophages (Lin et al., 2008). In observational studies, a polymorphism in *NFE2L2* was associated with reduced transcriptional activity correlating with increased risk of inflammatory bowel disease (Arisawa et al., 2008b) and chronic gastritis (Arisawa et al., 2007). One example of the immune modulatory action of NRF2 is provided in the central nervous system. Injured neurons release fractalkine, a chemokine that specifically activates the phosphatidylinositol 3 kinase/AKT (PI3K/AKT) pathway in microglia, resulting in inhibition of GSK-3$\beta$ and upregulation of NRF2 (Lastres-Becker et al., 2014). In this study, necropsies from AD and progressive supranuclear palsy patients exhibited a compensatory increase in fractalkine levels together with upregulated NRF2 protein, suggesting that this pathway contributes to limiting the inflammatory response in the diseased brain.

### *B. Nuclear Factor (Erythroid-Derived 2)–Like 2 in Autoimmune Diseases*

At the periphery of the NRF2 diseasome cluster, we found several autoimmune disease phenotypes, such as vitiligo, asthma, multiple sclerosis (MS), and systemic lupus erythematosus (SLE). Indeed, extensive work in animal models of experimental autoimmune encephalomyelitis (EAE) and rheumatoid arthritis (RA), as well as clinical evidence in MS and psoriasis further points to a role of NRF2 in autoimmune diseases. Oxidative tissue damage and apoptosis may increase the generation of autoantigens, leading to activation of T cells and production of autoantibodies by B cells, e.g., as observed for 3-nitrotyrosine–positive proteins (Thomson et al., 2012). In addition, loss of phase II detoxification enzymes, many of which are transcriptionally regulated by NRF2, results in increased production of reactive intermediates that contribute to formation of haptens or damaged macromolecules that sometimes become immunogenic, increasing hence the pool of autoantigens that trigger autoimmune reactions. Because NRF2-regulated enzymes play a critical role in the detoxification of many chemicals, it is conceivable that NRF2 may be a protective mechanism against the environmental contribution to autoimmune pathogenesis (Ma, 2013). Potential mechanisms for NRF2-mediated regulation of autoimmunity also involve suppression of proinflammatory Th1 and Th17 responses and activation of immunosuppressive T regulatory (Treg) and Th2 ones. There is also increasing evidence that NRF2 may control the differentiation and function of dendritic cells (DCs) and macrophages involved in antigen presentation and regulation of adaptive immune responses. In fact, NRF2 deficiency was shown to alter the function and phenotype of DCs by increasing the expression of costimulatory molecules and consequently the antigen-specific T cell reactivity (Al-Huseini et al., 2013).

MS is a chronic inflammatory disease characterized by infiltration of autoreactive immune cells into the central nervous system. The absence of NRF2 exacerbates the development of EAE, which is a mouse model of MS (Johnson et al., 2010). Part of the effects associated with NRF2 deficiency may be related to the reduced levels of HO-1. Thus, mice with a myeloid-specific HO-1 deficiency exhibited higher incidence of lesions, accompanied by activation of antigen-presenting cells and infiltration of inflammatory Th17 and myelin-specific T cells (Tzima et al., 2009). Knockdown of KEAP1 (Kobayashi et al., 2016) or treatment with a wide range of small molecules that activate NRF2 (Buendia et al., 2016) inhibited the development and severity of disease. NRF2 is strongly upregulated in active MS lesions, and the expression of NRF2-responsive genes is predominantly found in areas of initial myelin destruction (Licht-Mayer et al., 2015). In MS brains, NRF2 and its targets NADPH:quinone oxidoreductase (NQO1) and HO-1 are mainly expressed in infiltrating macrophages and to a lesser extent in astrocytes, most likely as a compensatory response against pathologic ROS formation. In contrast, there is a lack of NRF2 and antioxidant gene expression in oligodendrocytes, and this may underlie their damage and loss in MS (van Horssen et al., 2010). As a consequence of the altered immune and redox homeostasis, HO-1 expression is reduced in peripheral blood mononuclear cells of MS patients and is downregulated during exacerbation of the disease (Fagone et al., 2013). Of note, gene expression profiling in interferon-$\beta$–treated patients identified NRF2 as a potential mediator of long-term antioxidant response and neuronal preservation (Croze et al., 2013).

SLE is underlined by high oxidative environment, deregulated cell death, and defects in removal of dead cells, which leads to cell necrosis as source of autoantigens. Female mice deficient in NRF2 develop with age a multiorgan autoimmune disorder similar to SLE, characterized by increased DNA oxidation, lipid peroxidation, splenocyte apoptosis, presence of antibodies against double-strand DNA and the Smith antigen, along with important tissue damage (vasculitis, glomerulonephritis, hepatitis, and myocarditis) (Li et al., 2004). The fact that only female mice show progression to SLE suggests that female-specific factors may contribute to break immune tolerance to self-antigens

(Li et al., 2004). NRF2 deficiency also results in enhanced proliferative responses of $CD4^+$ T cells, altered $CD4^+/CD8^+$ ratio, and promotion of proinflammatory Th17 in SLE (Ma et al., 2006; Zhao et al., 2016). In fact, NRF2 depletion has been associated with Th17 differentiation and function during development of lupus nephritis, which seems to be mediated by regulation of the suppressor of cytokine signaling 3/phosphorylated signal transducer and activator of transcription (STAT)3 pathway and IL-1$\beta$ signaling (Zhao et al., 2016). In addition, the salivary glands of *Nrf2*$^{-/-}$ mice show intense lymphocyte infiltration, reminiscent of the Sjögren syndrome, which is often associated with SLE (Ma et al., 2006). SLE patients exhibit alterations in repair mechanisms of oxidative DNA damage (Evans et al., 2000), high serum levels of oxidized proteins, apolipoprotein C3 (Morgan et al., 2007), oxidized phospholipids, and autoantibodies against oxidatively modified lipoproteins (Frostegard et al., 2005). NRF2 polymorphisms have not been associated with SLE susceptibility, although the SNP rs35652124 was related to increased risk of nephritis in childhood onset of Mexican females (Cordova et al., 2010).

Rheumatoid arthritis (RA) is a systemic inflammatory disease with a complex but still elusive autoimmune profile, in which neutrophils, macrophages, and lymphocytes are actively recruited and activated in the inflamed joints. This results in increased secretion of proinflammatory mediators such as ROS/RNS, eicosanoids, cytokines (IL-17, TNF-$\alpha$, interferon-$\gamma$, IL-6, and IL-1$\beta$), and catabolic enzymes that trigger hyperproliferation of synovial fibroblasts, joint swelling, and progressive destruction of cartilage and bone (Roberts et al., 2015). Deletion of the NRF2 gene increases vulnerability to joint alterations in experimental RA models. For instance, in mice expressing the T cell receptor KRN and the major histocompatibility complex class II molecule A(g7) (the K/B$\times$N arthritis model), and in antibody-induced arthritis, NRF2 deficiency accelerates the incidence and aggravates the disease course (Maicas et al., 2011; Wu et al., 2016b). NRF2 deficiency dramatically upregulates migration of inflammatory cells, expression of cyclooxygenase-2 and inducible nitric oxide synthase, production of ROS and RNS, and release of proinflammatory cytokines and chemokines. Moreover, NRF2 may be a protective factor for bone metabolism in arthritis (Maicas et al., 2011), and NRF2/HO-1 activation exerts anti-inflammatory and antioxidant effects in animal models of RA and in human synovial fibroblasts (Wu et al., 2016b). It is interesting that antirheumatic gold(I)-containing compounds that stimulate the antioxidant response through activation of NRF2 and upregulation of HO-1 and GCLC proved clinical efficacy in RA (Kobayashi et al., 2016). Moreover, NRF2/HO-1 activation mediates the induction of synovial cell apoptosis and inhibition of proinflammatory cytokine production by cilostazol (Park et al., 2010) as well as the anti-inflammatory effects of $H_2S$ and related compounds, which are able to modify by sulfhydration the cysteine residues of KEAP1 (Wu et al., 2016b). Other drugs that induce NRF2 and HO-1 signaling, such as rebamipide, can divert the differentiation of human and murine $CD4^+$ T cells toward an immunosuppressive Treg phenotype and inhibit the differentiation of $TCD4^+$ cells toward inflammatory Th17 cells through specific inhibition of STAT3 (Moon et al., 2014). Excessive ROS generation within the inflamed synovium appears to contribute to the pathogenesis of RA because patients show a marked increase in ROS formation, lipid peroxidation, protein oxidation, DNA damage, and decrease in the activity of the antioxidant defense mechanisms, all of these contributing to tissue damage and disease progression (Datta et al., 2014). In response to pathologic ROS formation, the NRF2 pathway is activated in synovial cells of RA patients and in joints of antibody-induced arthritic mice, but this response is apparently insufficient to counteract the disease progression (Wu et al., 2016b).

Vitiligo is a skin inflammatory disorder characterized by the accumulation of ROS in the epidermis, which participates in the death of melanocytes. These molecules modify DNA and melanosomal proteins with formation of autoantigens and activation of an autoimmune response against melanocytes (Xie et al., 2016). Genetic studies have revealed associations of NRF2 promoter SNPs with susceptibility to develop vitiligo, such as the SNP at $-650$ position (Guan et al., 2008), whereas the C allele of rs35652124 was shown to be associated with protective effects in a Han Chinese population (Song et al., 2016). NRF2 and its downstream detoxification target genes NQO1, GCLC, and GCLM are upregulated in the epidermis of vitiligo patients, suggesting insufficient activation of this defensive mechanism (Natarajan et al., 2010).

### *C. Nuclear Factor (Erythroid-Derived 2)–Like 2 in Chronic Respiratory Diseases*

The relevance of NRF2 in respiratory diseases was reviewed in 2010 (Cho and Kleeberger, 2010), and in this work we will highlight only the most relevant findings (Fig. 8). Cigarette smoke is a main risk factor for chronic obstructive pulmonary disease (COPD). COPD patients have dysfunctional alveolar macrophages that lead to uncontrolled ROS production, proinflammatory mediators, defective phagocytosis, and an array of metalloproteinases that participate in tissue damage. In fact, the emphysematous lung tissue shows a direct correlation between alveolar macrophage density in the parenchyma and severity of lung destruction (Finkelstein et al., 1995). Impaired phagocytic activity of alveolar macrophages is a major cause of recurrent bacterial and viral infections that cause acute

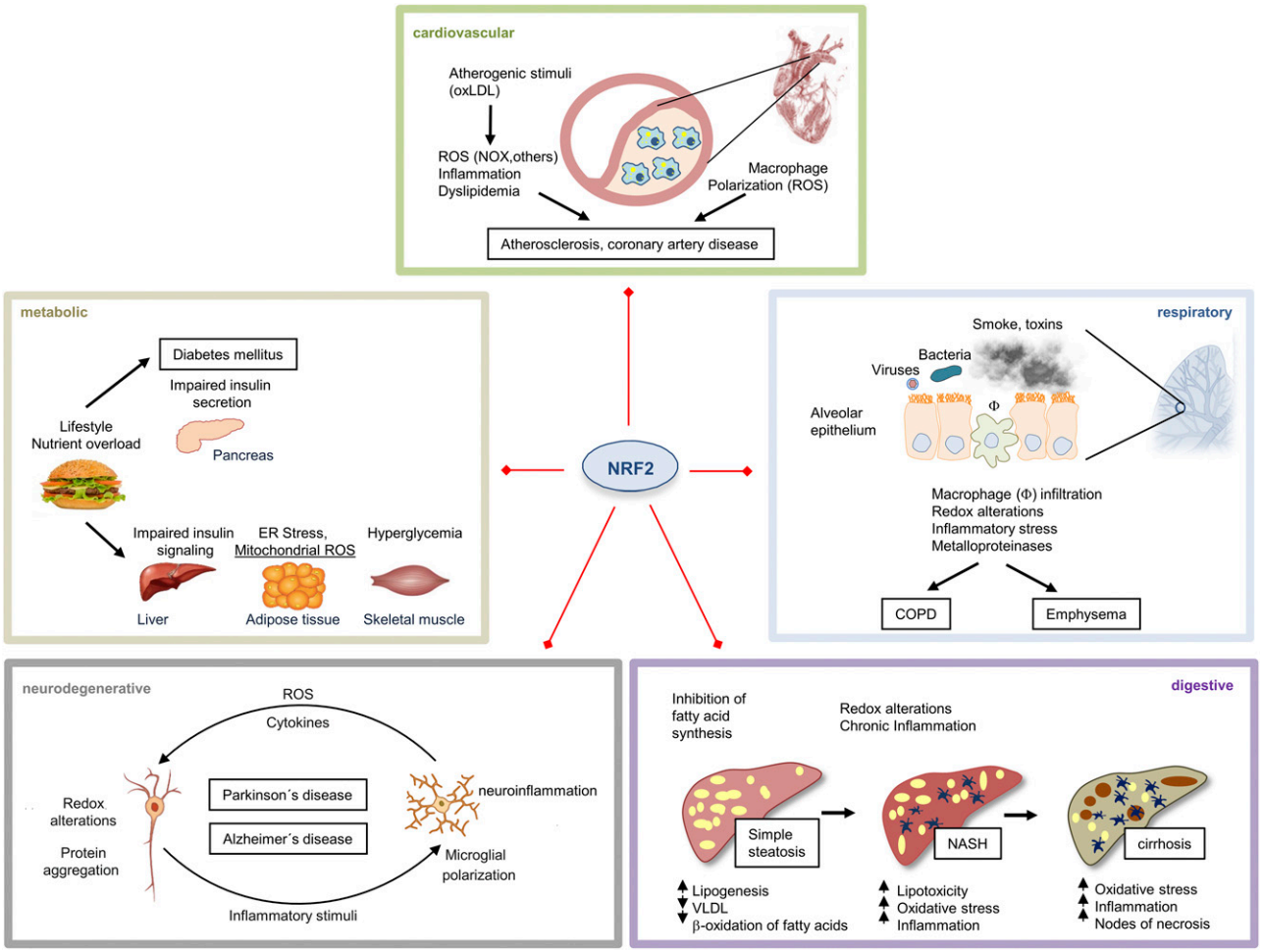


**Fig. 8.** Role of NRF2 in common mechanisms and pathophenotypes of chronic diseases. The picture provides some examples extracted from the NRF2 diseasome cluster of Fig. 5. Common pathomechanisms of these diseases include abnormally high ROS levels and low-grade chronic inflammation that participate in tissue damage. NRF2 provides a cytoprotective signature against these and other tissue-specific alterations by regulating the expression of numerous cytoprotective genes.

exacerbations of COPD and are a major source of morbidity and mortality. *Nrf2*$^{-/-}$ mice exhibit enhanced susceptibility to cigarette smoke-induced emphysema (Rangasamy et al., 2004). Importantly, activation of NRF2 with the isothiocyanate sulforaphane (SFN) restores bacteria recognition and phagocytosis, enhances pulmonary bacterial clearance by alveolar macrophages, and reduces inflammation in wild-type mice, but not in *Nrf2*$^{-/-}$ mice exposed to cigarette smoke (Harvey et al., 2011). In humans, the transcriptional signature of NRF2 is decreased in alveolar macrophages from patients with smoking-related lung emphysema as compared with smoking and nonsmoking patients without emphysema (Goven et al., 2008). Decreased NRF2 expression is associated with increased macrophage expression of the lipid peroxidation product 4-hydroxynonenal. In the *NFE2L2* promoter, a functional haplotype constituted by three SNPs and one triplet repeat, polymorphism that produces low to medium NRF2 expression (Yamamoto et al., 2004), was associated with increased risk to develop COPD (Hua et al., 2010). The low-expressing haplotypes were significant predictors for developing respiratory failure. Thus, the −617A allele of SNP rs6721961 had a significantly higher risk for developing acute lung injury (Marzec et al., 2007).

Pathologic ROS formation may play a role in the pathogenesis of chronic lung fibrosis. An early study demonstrated that pulmonary fibrosis induced by bleomycin is more severe in *Nrf2*$^{-/-}$ than in wild-type mice (Cho et al., 2004). In fact, wild-type mice induced an antioxidant and anti-inflammatory response by upregulating NRF2, and this could not be achieved in the *Nrf2*$^{-/-}$ mice. Later, it was verified that patients with idiopathic pulmonary fibrosis or chronic sarcoidosis/hypersensitivity pneumonitis exhibit increased expression of NRF2 and augmented levels of low-mol. wt. antioxidants in bronchoalveolar lavage fluids, such as uric acid, ascorbic acid, retinol, and $\alpha$-tocopherol, suggesting an unsuccessful adaptive response to the ROS challenge (Markart et al., 2009). Mechanistically, NRF2 deficiency increases myofibroblast differentiation, whereas pharmacological induction of NRF2 with SFN results in lower number of myofibroblasts and

attenuation of the profibrotic effects of transforming growth factor-$\beta$ (TGF-$\beta$) (Artaud-Macari et al., 2013).

### *D. Nuclear Factor (Erythroid-Derived 2)–Like 2 in the Digestive System*

The prominent position of pathophenotypes of the digestive system in the NRF2 diseasome highlights the relevance of the transcriptional signature of NRF2 as a potent adaptive mechanism to chronic oxidative damage and inflammatory stress triggered by xenobiotics. In the gastrointestinal tract (GI), chronic exposure to xenobiotics triggers dysfunctional interactions between the microbiota of the intestinal lumen and the immune system (Aviello and Knaus, 2017). This can lead to chronic diseases of the GI tract, like the inflammatory bowel disease (IBD) phenotypes comprising Crohn's disease and ulcerative colitis, in which there is evidence of activation of a protective NRF2 response. For instance, in colonic tissues from IBD patients, colon epithelial cells responded to inflammatory signals through a NRF2-dependent adaptation that was associated with increased proteasome protein expression (Kruse et al., 2016). Monocyte-derived macrophages from IBD patients evidenced a specific NRF2-dependent gene expression profile that was exacerbated in response to LPS, further suggesting an attempt to attenuate the inflammatory challenge (Baillie et al., 2017). At the genetic level, a particular genotype of the *NFE2L2* gene (−686−684) was associated with the development of ulcerative colitis, especially in females, in a Japanese cohort (Arisawa et al., 2008a). In fact, pathologic processes in the GI are highly dependent on the genetic background of the host in relation with dysfunctional interaction between the microbiota of the intestinal lumen and the immune system (Aviello and Knaus, 2017).

One of the symbiotic effects of the microbiota of the GI is to release moderate amounts of ROS that elicit a cytoprotective response mediated by NRF2 in epithelial colonocytes and infiltrating immune cells (Jones et al., 2015). Moreover, cytoprotective molecules that are under the transcriptional control of NRF2 in eukaryotes can also be produced by commensal bacteria. For instance, the HO-1 homologs in the microbiota may greatly contribute to GI homeostasis, and this can be therapeutically exploited for local delivery of carbon monoxide to the intestine (Onyiah et al., 2014).

The proven involvement of NRF2 in maintaining GI homeostasis makes this transcription factor a promising therapeutic target in IBD. Thus, several chemical compounds and dietary supplements might exhibit beneficial effects, like melatonin, 3-(3-pyridylmethylidene)-2-indolinone, butyrate, *Lactobacillus casei*, L-carnitine, 4-vinyl-2,6-dimethoxyphenol (canolol), lacto-wolfberry (formulated product of wolfberries in skimmed milk), etc. (Orena et al., 2015). Therefore, it is of utmost importance to define the involvement of NRF2 in chronic and acute diseases of the GI tract for better guidance on the therapeutic approach for modulating the NRF2 pathway.

The liver is also a first line of defense against food xenobiotics. Therefore, it is not surprising that the NRF2 diseasome highlights the relevance of this transcription factor in pathophenotypes associated with liver damage. Early work with the *Nrf2*$^{-/-}$ mouse model demonstrated its protective effect against acetaminophen-induced hepatocellular injury, benzo[a]pyrene-induced tumor formation, and Fas- and TNF-$\alpha$–mediated hepatocellular apoptosis (Aleksunes and Manautou, 2007). The higher sensitivity of *Nrf2*$^{-/-}$ mice to chemical toxicity correlated with reduced basal and inducible expression of detoxification enzymes. In humans, the functional haplotype of three NRF2 promoter SNPs that result in reduced NRF2 expression was significantly associated with development of gastric mucosal inflammation, either independently or by interacting with *Helicobacter pylori* infection (Arisawa et al., 2007). Analysis of the transcriptional signature of NRF2 in patients with primary biliary cholangitis indicated that these patients exhibit reduced NRF2 expression together with low levels of HO-1 and GCLC proteins, and these impairments are more advanced in patients with cirrhosis (Wasik et al., 2017).

Pathologic ROS formation is a key mechanism of hepatocellular injury and disease progression in patients with nonalcoholic steatohepatitis (NASH) (Fig. 8). This disease evolves in two phases, one of progressive accumulation of fatty acids in hepatocytes and a second that involves liver injury and inflammatory pathologic ROS formation (Wang et al., 2018). Accordingly, mice fed with a high-fat diet (HFD) developed a simple steatosis, characterized by increased hepatic fat deposition without inflammation or fibrosis, but *Nrf2*$^{-/-}$ mice presented exacerbated hepatic steatosis and substantial inflammation, consistent with NASH (Reccia et al., 2017). It is interesting, however, that the hepatocyte-specific *KEAP1* deletion, while reducing liver steatosis, did not alter inflammation during development of NASH, suggesting a compensatory mechanism (Ramadori et al., 2016). At least in the rat model of NASH, dietary NRF2 activators attenuate the progression of liver fibrosis (Shimozono et al., 2013). Markers of pathologic ROS formation were increased in liver biopsies of NASH patients, and the NRF2 signature was increased, suggesting an attempt to reduce the oxidant and inflammatory burden (Takahashi et al., 2014).

### *E. Nuclear Factor (Erythroid-Derived 2)–Like 2 in the Cardiovascular System*

The NRF2 diseasome cluster points to the high susceptibility of the cardiovascular system to changes in the cellular redox balance and the development of well-known comorbidities like atherosclerosis, hypertension, and diabetes (Griendling and FitzGerald, 2003a,b; Harrison et al., 2003; Jay et al., 2006)

(Fig. 8). A role of NRF2 in preventing these pathophenotypes has been demonstrated in *Nrf2*$^{-/-}$ mice, which exhibit impaired cardiac structure (more remodeling events) and function (less fractional shortening) in response to chronic endurance exercise (Shanmugam et al., 2017a). They are also more susceptible to develop heart failure after myocardial infarction (Strom and Chen, 2017). In contrast, constitutive activation of NRF2 creates a reductive state, characterized by increased cardiac GSH/glutathione disulfide ratio and decreased ROS formation and malondialdehyde levels (Shanmugam et al., 2017b). In humans, microarray analysis in Tako–Tsubo cardiomyopathy indicated an increase in pathologic ROS levels and a compensatory upregulation of NRF2 during the acute phase of this contractile dysfunction (Nef et al., 2008). Recently, systemic inflammation and pathologic ROS formation in hemodialysis patients were associated with downregulation of NRF2 (Pedruzzi et al., 2015), and two promoter polymorphisms (rs35652124 and rs6721961) were associated with increased risk of mortality in these patients (Shimoyama et al., 2014).

One of the most relevant targets of NRF2 in endothelial homeostasis is HO-1, which is usually paralleled by upregulation of ferritin, hence decreasing free iron levels and preventing Fenton-type reactions. Bilirubin, which is generated from the combined activity of HO-1 and biliverdin reductase, is one of the most powerful endogenous antioxidants that scavenges ROS/RNS (Jansen et al., 2010), and is highly efficient in preventing lipid peroxidation in vitro (Stocker et al., 1987). *Hmox1*$^{-/-}$ mice show increased pulmonary hypertension in response to chronic hypoxia (Christou et al., 2000), and pharmacological HO-1 induction improves diabetic complications (Kruger et al., 2006), as well as nitroglycerin-induced vascular dysfunction (nitrate tolerance) (Wenzel et al., 2007). Recently, *Hmox1*$^{-/-}$ mice were shown to display upregulated NADPH oxidase-2, vascular pathologic ROS formation, markers of inflammation, endothelial dysfunction, and higher blood pressure in response to angiotensin-II (Wenzel et al., 2015). In fact, high serum levels of bilirubin are inversely correlated with the incidence of coronary artery disease (Hopkins et al., 1996). Bilirubin prevents the activation of the vascular NADPH oxidase (Kwak et al., 1991), involved in the development of cardiovascular diseases (Griendling and FitzGerald, 2003a,b; Harrison et al., 2003; Jay et al., 2006). Patients suffering from peripheral artery disease, which is a common manifestation of atherosclerosis, present reduced levels of HO-1 (Signorelli et al., 2016).

### *F. Nuclear Factor (Erythroid-Derived 2)–Like 2 in Metabolic Diseases*

Type 2 diabetes mellitus (T2DM) is one of the most common chronic metabolic diseases and is highly underlined in the NRF2 diseasome. Pathologic ROS formation in insulin-sensitive tissues, as well as in pancreas, has been found in T2DM patients, resulting in severe impairment of both insulin secretion by pancreatic $\beta$ cells and insulin action in peripheral tissues (Uruno et al., 2015) (Fig. 8). Likewise, pathologic ROS levels also contribute to the pathogenesis of diabetic complications due to nonenzymatic glycation of proteins. This has been evidenced in diabetic nephropathy, in which the glomeruli exhibit pathologic ROS levels and a compensatory elevation of NRF2 (Jiang et al., 2010). Since 2007, several studies have addressed the role of NRF2 in T2DM and its complications using animal models and cell lines. In vitro studies in human cells reported that NRF2 activation is achieved with acute exposure to high glucose, whereas longer incubation times or oscillating glucose concentration failed to activate NRF2 (Ungvari et al., 2011; Liu et al., 2014). Accordingly, these studies pointed out that NRF2 activation is dependent on glucose concentration and dynamics. In contrast, NRF2 is downregulated in peripheral blood mononuclear cells of prediabetic and diabetic patients, suggesting that NRF2 could be an important therapeutic target (Jimenez-Osorio et al., 2014).

The impact of NRF2 deficiency on hyperglycemia was first shown in *Nrf2*$^{-/-}$ mice, where oxidative and nitrosative alterations were enhanced and led to early-stage renal injury (Yoh et al., 2008). In a subsequent study, streptozotocin-induced diabetic *Nrf2*$^{-/-}$ mice exhibited exacerbated glomerular injury, together with high ROS production and increased expression of the profibrotic markers TGF-$\beta$ and fibronectin (Jiang et al., 2010). In this diabetic model, NRF2 protected against dysfunction of the blood–retina barrier and the progression of diabetic retinopathy (Xu et al., 2014). Likewise, HFD-induced increase in vascular ROS levels was significantly exacerbated in *Nrf2*$^{-/-}$ mice and was accompanied by a severe endothelial dysfunction, as shown by diminished acetylcholine-induced relaxation of aorta and increased expression of intercellular adhesion molecule-1 and TNF-$\alpha$ (Ungvari et al., 2011).

NRF2 plays a complex role in tissue-specific insulin resistance. Thus, HFD-fed *Nrf2*$^{-/-}$ mice displayed better insulin sensitivity due to enhanced insulin signaling in liver and skeletal muscle than their wild-type counterparts, but conversely, these mice developed a severe NASH due to excessive hepatic lipotoxicity linked to pathologic ROS formation (Meakin et al., 2014). Accordingly, this study dissociated hepatic insulin resistance from the development of NASH. In light of these data, a subsequent study demonstrated that the livers of HFD-fed *Nrf2*$^{-/-}$ mice exhibited higher pathologic ROS formation by a significant depletion of GSH due to attenuated expression of the CYP2A5 enzyme (Cui et al., 2013). The knockdown of NRF2 in hepatocytes enhanced the apoptosis induced by palmitate, a fatty acid that is highly elevated in insulin-resistant

obese patients. This effect was correlated with increased production of pathologic ROS, again reinforcing the key role of NRF2 in the progression of NASH (Pilar Valdecantos et al., 2015).

To further examine the role of NRF2 in the metabolic syndrome, NRF2 was ablated in leptin-deficient (ob/ob) mice, a model with an extremely positive energy balance (Xue et al., 2013). Interestingly, global ob/ob/*Nrf2*$^{-/-}$ mice or adipocyte-specific ob/ob/*Nrf2*$^{-/-}$ mice displayed reduced white fat mass, revealing NRF2 as a key player in adipogenesis. These mice had an even more severe metabolic syndrome that was characterized by hyperlipidemia, aggravated insulin resistance, and hyperglycemia, suggesting a mechanistic linkage between the metabolic syndrome and pathologic ROS formation.

Another subset of studies has evaluated the effects of persistent induction of NRF2 in glucose metabolism. Genetic NRF2 induction making use of a hypomorphic allele of *Keap1* (*Keap1*flox/- mutant) decreased blood glucose in the obese diabetic db/db mice by suppressing hepatic glucose 6 phosphatase through the repression of cAMP-CREB signaling in hepatocytes, as well as other gluconeogenic genes, such as peroxisome proliferator-activated receptor coactivator-1$\alpha$ (Uruno et al., 2013). Additionally, enhancement of NRF2 activity in *Keap11*-knocked down mice increased the phosphorylation of AMP-activated protein kinase (AMPK) in the liver, as well as insulin signaling in skeletal muscle, resulting in a substantial improvement of glucose tolerance (Xu et al., 2013). Due to the pleiotropic activities of NRF2 in the context of T2DM, the results of all these and other studies have evidenced the need to design multiple genetic and pharmacological strategies to elucidate the full array of NRF2 functions in tissues involved in the control of whole-body glucose homeostasis.

In addition to diabetic factors like age, body weight, and blood glucose, genetic factors that are linked to NRF2 have been poorly studied in humans. In a Chinese population, the SNP rs6721961 has been associated with pathologic ROS formation and risk of newly diagnosed T2DM and may also contribute to impaired insulin secretory capacity and increased insulin resistance (Wang et al., 2015). The same SNP was associated with diabetes in Mexican mestizo men (Jimenez-Osorio et al., 2017). In a case-control study performed with Han volunteers, a significant difference in genotypic and allelic frequencies of four SNPs of the *NFE2L2* gene was found between T2DM patients with and without complications, including peripheral neuropathy, nephropathy, retinopathy, foot ulcers, and microangiopathy (Xu et al., 2016b).

### *G. Nuclear Factor (Erythroid-Derived 2)–Like 2 in Neurodegenerative Diseases*

The NRF2 diseasome provides evidence of NRF2 involvement in several neurodegenerative diseases, including AD and PD, which represent the most prevalent cognitive and motor disorders of the elderly. In neurodegenerative diseases, the connection between low-grade pathologic ROS formation and proteostasis is particularly relevant because most of these pathophenotypes are characterized by abnormal aggregation of specific proteins (Fig. 8). Evidence pointing to pathologic ROS formation in proteinopathy, as well as NRF2 as regulator of proteasome and autophagy was provided in cellular and animal models (Pajares et al., 2017). Initially, it was reported that the autophagy cargo protein sequestosome 1 (SQSTM1) competes with NRF2 for binding to KEAP1. SQSTM1 takes KEAP1 to the autophagosome degradative pathway, therefore upregulating NRF2 (Komatsu et al., 2010). More recently, it was found that NRF2 regulates the expression of autophagy genes involved in autophagy initiation, cargo recognition, elongation, and autolysosome clearance (Pajares et al., 2016). In this study, amyloidopathy and tauopathy induced by transgene overexpression of human mutant amyloid precursor protein and tau were aggravated in *Nrf2*$^{-/-}$ mice. A connection between NRF2 deficiency and neurodegeneration is supported by a growing body of evidence in animal models (Johnson and Johnson, 2015). The general point of view is that damaged neurons try to activate NRF2-dependent transcription, presumably to increase their own survival. Additionally, upregulation of NRF2 in astrocytes participates in metabolic compensations, including increased supply of GSH for augmenting their proliferative capacity (Bolanos, 2016), whereas NRF2 upregulation in microglia returns this immune cell to a resting state (Rojo et al., 2014a).

Ramsey et al. (2007) evidenced the nuclear localization of NRF2 in dopaminergic neurons of patients with PD. Other studies found that amyloid precursor protein– and tau-injured neurons expressed increased levels of NRF2 and its target SQSTM1, probably as compensatory mechanism to clear these toxic proteins through autophagy (Lastres-Becker et al., 2014; Pajares et al., 2016). In agreement with these results, the levels of HO-1, NQO1, GCLM, and SQSTM1 are increased in AD and PD brains (van Muiswinkel et al., 2004; Cuadrado et al., 2009; Schipper et al., 2009; Lastres-Becker et al., 2016). However, there is some controversy in the field, as Ramsey's study described the accumulation of NRF2 in the cytosol of AD-injured neurons, suggesting an impaired capacity of these neurons to upregulate NRF2 transcriptional activity. In addition, the cytoprotective proteins associated with NRF2 expression, such as NQO1 and SQSTM1, were partly sequestered in Lewy bodies, suggesting impaired neuroprotective capacity of the NRF2 signature in PD patients (Lastres-Becker et al., 2016). One possible explanation for this discrepancy could be that the levels of NRF2 and its target genes might change during ageing and disease progression.

Some SNP haplotypes of *NFE2L2* were associated with decreased risk or delayed onset of ALS, AD, or PD. The onset of ALS was analyzed in two studies regarding three functional promoter SNPs that were previously linked to high gene expression. Interestingly, this haplotype was associated with a 4-year delay in onset of ALS (Bergstrom et al., 2014), but another study did not find a clear association (LoGerfo et al., 2014). Regarding AD, one haplotype allele was associated with 2-year earlier age onset of AD, suggesting that variants of the *NFE2L2* gene may affect AD progression (von Otter et al., 2010b). Genetic association of *NFE2L2* with PD has been analyzed in more detail. Three SNPs in the *NFE2L2* promoter (rs6721961, rs6706649, and rs35652124) were evidenced as protective haplotype in a case-control study (von Otter et al., 2010a). Such haplotype delayed the onset of disease in a Swedish cohort or even reduced the risk of PD in a Polish cohort. These results were supported by four new independent European case-control studies (von Otter et al., 2014), but were not replicated in a Taiwanese population (Chen et al., 2013), suggesting disparity in ethnicities and environmental factors. As an alternative approach, PD cells derived from olfactory mucosa were exposed to smoke extract or pesticide to assess gene–environment interaction, and several SNPs were identified that affect the susceptibility to these toxins (Todorovic et al., 2015). Altogether, it is possible that a slight activation of NRF2, such as that found for some functional haplotypes of the *NFE2L2* gene, should be enough to trigger protective mechanisms in the brain.

## IV. The Kelch-Like ECH-Associated Protein 1 Paradox in Cancer

An apparent dichotomy appears to exist in the role of NRF2 in tumorigenesis and further tumor progression. On one hand, by activating biotransformation reactions, NRF2 protects against chemically induced carcinogenesis. Preclinical studies have demonstrated complete protection against aflatoxin B(1)-induced liver cancer after pharmacological activation of NRF2 in rats (Johnson et al., 2014). In contrast, the protective responses elicited by NRF2 provide a growth advantage in established cancers, and this will be the focus of this section.

Constantly increased levels of ROS can sustain tumorigenesis through alteration of genomic stability, along with activation of specific redox signaling circuits and inflammatory processes that favor survival and proliferation of tumor cells (Reuter et al., 2010). Therefore, upregulation of NRF2 represents a mechanism of adaptation of cancer cells to tolerate high ROS levels that propel tumor progression (Schumacker, 2006) as well as to maintain cancer stem cells that are responsible for tumor relapse and formation of distant metastases (Ryoo et al., 2016). For instance, the NRF2 signature in cancer stem cells from human colorectal tumors pointed out protective mechanisms mediated by high levels of GCLC, glutathione peroxidase, and thioredoxin reductase-1 that underlie the ability of these cells to counteract stressors and chemotherapeutics (Emmink et al., 2013). From this perspective, NRF2 behaves in cancer cells like an oncogene that by inducing chronic activation of ARE-mediated cytoprotective responses affords adaptation to their oxidative environment (Panieri and Santoro, 2016). Several mechanisms of malignant activation of NRF2 have been reported, including somatic mutations, epigenetics, and oncogenic signaling alterations.

Close to 600 somatic mutations have been reported in cancer along the coding sequence of *NFE2L2* (Gao et al., 2017). In Fig. 9, we show the results from a dataset of 10,000 cancer patients (Zehir et al., 2017). In most cases, these mutations alter the interaction of the DLG and ETGE motifs of NRF2 with KEAP1, hence inducing hyperactivation of NRF2 in several solid tumors, including esophagus, skin, lung, and larynx carcinomas (Kim et al., 2010b; Taguchi and Yamamoto, 2017). For instance, in advanced esophageal squamous cancer, gain-of-function mutations of NRF2 were associated with tumor recurrence and poor prognosis due to increased proliferation, attachment-independent survival, and resistance to chemo- and radiotherapy (Shibata et al., 2011). Loss-of-function mutations in the *KEAP1* gene are also frequent in some solid tumors such as lung cancer (Singh et al., 2006). Based on the strong evidence that this pathway regulates $\beta$-TrCP/NRF2, it is strange that disrupting somatic mutations have not been found at the interface between NRF2 and $\beta$-TrCP. This fact suggests that such mutations are not viable for unknown reasons or that the increase in NRF2 levels that would result from the escape of $\beta$-TrCP is not sufficient to drive oncogenicity.

Nonetheless, somatic mutations account for chronic NRF2 activation only in a fraction of cancer patients. At the level of gene expression, it is interesting that an allele of the SNP rs6721961 ($-617C > A$) located at the ARE enhancer of the human NRF2 gene abolished self-induction of NRF2, and this correlated with remarkable survival of these cancer patients (Okano et al., 2013). Epigenetic changes due to promoter hypermethylation of three CpG sites of *KEAP1* have been described in lung tumors, resulting in consequent NRF2 activation that could be reversed by 5-aza-2′-deoxycitydine treatment (Wang et al., 2008). The role of miRNAs in the post-transcriptional regulation of NRF2 levels has been reviewed recently (Kurinna and Werner, 2015). Briefly, miR200a targets the KEAP1 mRNA in human breast cancer cells, leading to its degradation and consequent activation of NRF2 (Eades et al., 2011). In turn, miR28 facilitates the degradation of the NRF2 mRNA (Yang et al., 2011).

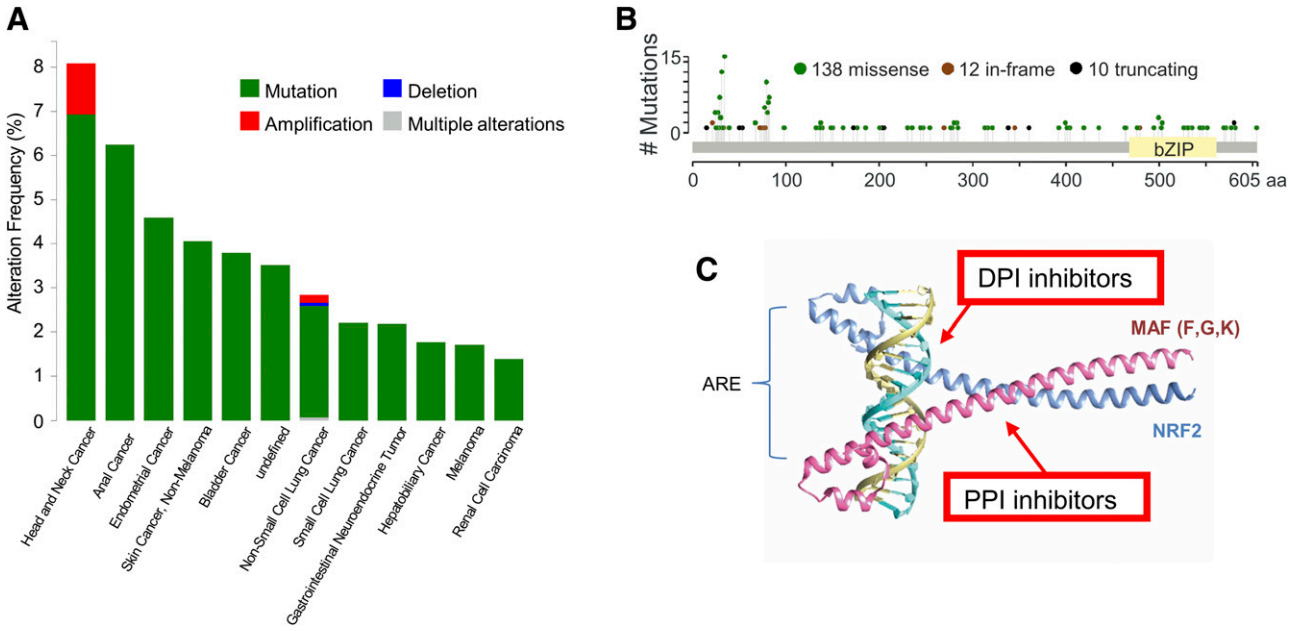


**Fig. 9.** Somatic mutations found in tumors of the MSK-IMPACT Clinical Sequencing Cohort (MSKCC) study (Zehir et al., 2017) and pharmacologic strategies to inhibit NRF2. (A) Percentage of tumors with NRF2 mutations. (B) Distribution of mutations along the NRF2 polypeptide. (C) PyMOL representation of the interaction between the NRF2/MAFF heterodimer and the ARE element. Blue, NRF2; pink, MAFF. The red arrows indicate possible mechanisms of inhibition of NRF2 by small molecules that could target the bZip domains of interaction between NRF2 and MAF proteins (PPI inhibitors) or the interface of interaction of the NRF2-MAF heterodimer with the ARE [DNA–protein interaction (DPI)].

Oncogenes or mutated tumor suppressors may enhance the activation of NRF2 in cancer. Endogenous oncogenic alleles of KRAS, BRAF, or c-MYC upregulate NRF2, presumably through oncogene-mediated ROS generation and consequent chronic inactivation of KEAP1 (DeNicola et al., 2011). The mutated form of the tumor suppressor p53, which sustains the growth of cancer cells by enhancing nutrient uptake and synthesis of building blocks, can also upregulate NRF2, possibly through the crosstalk with the Sp1 transcription factor that binds to the NRF2 promoter (Tung et al., 2015).

The phosphorylation of NRF2 (phospho-NRF2) by various protein kinases is a potential mechanism of activation in 107 hepatocellular carcinomas. Increased levels of phospho-NRF2 were associated with reduced KEAP1 expression and poor 5-year overall survival of patients exhibiting this distinctive phenotype (Chen et al., 2016). Additionally, mutations in the phosphatase and tensin homolog (PTEN) tumor suppressor sustain hyperactive and oncogenic phosphatidylinositol-3-kinase (PI3K)–AKT signaling and consequent increase in NRF2 activity due to the downregulation of the PTEN/GSK-3/$\beta$-TrCP pathway for the proteasomal degradation of NRF2 (Rada et al., 2011, 2012; Cuadrado, 2015). Therapeutic interventions targeting the PTEN/GSK-3/$\beta$-TrCP pathway should take into consideration that GSK-3 may act both as tumor suppressor and tumor promoter, and is also implicated in the generation of cancer stem cells (McCubrey et al., 2014).

Some stress-induced proteins interact with KEAP1 and thus compete with its NRF2 binding in cancer cells. Consequently, NRF2 escapes KEAP1-mediated degradation. One of the NRF2 competitors for KEAP1 binding is the phosphorylated form of the autophagy-adaptor protein SQSTM1 that occurs during selective autophagy used by cancer cells for sustaining their own growth (Shimizu et al., 2016). The cyclin-dependent kinase inhibitor p21 that promotes cell cycle arrest in cancer stem cells was also demonstrated to inhibit the association of NRF2 with KEAP1 through the interaction of its KRR motif with DLG and ETGE motifs in NRF2 (Chen et al., 2009). Recently, it was shown that dipeptidyl-peptidase 3, which bears an ETGE motif, may compete with NRF2 for binding to KEAP1 (Hast et al., 2013). Overexpression of dipeptidyl-peptidase 3, possibly induced by chronic alteration of the redox status, correlates with increased expression of ARE genes and poor prognosis, particularly in estrogen receptor–positive breast cancer (Lu et al., 2017).

NRF2 induces metabolic changes that contribute to cancer progression. For instance, a multiplatform nontargeted metabolomics study identified patterns of metabolite changes in breast tumor samples (Tang et al., 2014). They found that GSH and 3-(4-hydroxyphenyl)lactate were positively correlated with the involvement of BRCA1 in redox homeostasis through interaction with NRF2. Metabolomics studies also indicate that NRF2 can increase aerobic glycolysis in cancer cells to support their high-energy requirements. This occurs through NRF2-mediated induction of Mn-superoxide dismutase expression, leading to elevated mitochondrial production of hydrogen peroxide

and to activation of AMPK. The process is regulated by caveolin-1, which binds directly to both NRF2 and KEAP1, and impedes on NRF2 activation and hence on the glycolytic shift. This is apparently one explanation why glycolytic tumors, which are generally more aggressive, have a caveolin-$1^{low}$/Mn-superoxide $dismutase^{high}$ phenotype (Hart et al., 2016). NRF2 can also drive glucose and glutamine toward anabolic pathways required for tumor cell proliferation (Mitsuishi et al., 2012). In the presence of active PI3K–AKT signaling and loss of KEAP1 activity, NRF2 was shown to induce the shift of glucose metabolism from glycolysis toward anabolic pathways (purine synthesis) in cancer (Mitsuishi et al., 2012; Xu et al., 2016a). This is underlined by NRF2-mediated transcription of genes involved in the pentose phosphate pathway and generation of NADPH (glucose 6 phosphate dehydrogenase; phosphogluconate dehydrogenase, malic enzyme 1, isocitrate dehydrogenase 1, transketolase, and transaldolase), along with genes involved in purine nucleotide synthesis (phosphoribosyl pyrophosphate amidotransferase, methylenetetrahydrofolate dehydrogenase 2).

The fact that activation of NRF2 confers a growth advantage to cancer cells might argue that its pharmacologic activation in chronic diseases presented in this work might imply a high risk of developing cancer. However, it must be considered that the oncogenic activity of NRF2 requires mutations in its gene or in *KEAP1*, which results in very high and persistent induction of NRF2 signaling. This is not the case in pharmacological therapy, in which it is possible to modulate drug dosing and NRF2 activity. Moreover, empirical evidence indicates that subjects enrolled in clinical trials with NRF2 activators do not exhibit increased cancer risk. This is best exemplified in the case of patients with MS, who have been taking the NRF2 activator dimethyl fumarate for several years since it was approved by the regulatory agencies in 2013. Conversely, the use of NRF2 inhibitors in cancer patients might lead to manifestation of the pathophenotypes described in the NRF2 diseasome. This is a possibility that will need further investigation when NRF2 inhibitors reach the clinic.

## V. Nuclear Factor (Erythroid-Derived 2)–Like 2 Drugome

This section attempts to develop a NRF2 drugome that might be useful for future clinical directions to target therapeutically NRF2 centered on the pathophenotypes of the NRF2 diseasome. As stated in Fig. 2B, the pharmacological activation of NRF2 is being pursued for increasing its stability by targeting KEAP1. These strategies are based on the discovery of either electrophile compounds that alter the KEAP1 structure or small molecules that prevent the docking of NRF2 to KEAP1. Although not yet demonstrated empirically, the GSK-3 inhibitors should prevent the recognition of NRF2 by $\beta$-TrCP and some compounds could be discovered to prevent binding of NRF2 to $\beta$-TrCP. The inhibition of NRF2 is being analyzed with compounds that target the bZip dimerization domain to prevent formation of the active NRF2/MAF heterodimer. By comparison with other transcription factors, it might be possible to find small molecules that impede binding of the NRF2/MAF heterodimer to the ARE (Fig. 9C). This section summarizes the most important findings from a translational point of view in both de novo drug discovery and repurposing.

### *A. Electrophilic Nuclear Factor (Erythroid-Derived 2)–Like 2 Inducers*

The majority of known physiologic or pharmacological NRF2 inducers are electrophilic molecules that covalently modify, by oxidation or alkylation, cysteine residues present in the thiol-rich KEAP1 protein (Hur and Gray, 2011; Satoh et al., 2013). KEAP1 is one of the best-suited proteins to act as electrophilic or redox sensor, as it contains 27 cysteine residues in humans and functions as an electrophile trap. The cysteines C151, C273, and C288 of KEAP1 appear to be the most prone to electrophile reaction (Fig. 2B), although there are some specificities (Yamamoto et al., 2008; Saito et al., 2015). Electrophile adducts inhibit KEAP1 in two different ways. One is induction of a conformational change in KEAP1 that will result in loss of its binding capacity to NRF2. The other is the blockade of the interaction between KEAP1 and CUL3/RBX1, resulting in sequestration of KEAP1 with NRF2 and further stabilization of newly synthetized NRF2 (Rachakonda et al., 2008; Baird and Dinkova-Kostova, 2013; Cleasby et al., 2014; Saito et al., 2015).

At least 30 recent patents for NRF2 modulators are indexed in the World International Property Organization. These patents are protecting chalcone derivatives, novel amide triterpenoid derivatives, deuterium-substituted fumarate derivatives, 3-alkylamino-1H-indolyl acrylate derivatives, withanolide, a benzyl derivative containing an activated vinyl group, andrographolide or $[S]^{+}$apomorphine, and sesquiterpene lactone derivative (Sun et al., 2017). Although most of these compounds proved to be useful to some degree from a preclinical proof-of-concept perspective, their clinical value is to date generally very limited. Only a few of them have entered clinical trials, and regulatory bodies, such as Food and Drug Administration or European Medicines Agency, have approved even fewer. We in this study discuss the most developed NRF2 activators along the translational pipeline.

Fumaric acid esters are the most prominent example of a KEAP1 modifier, and dimethyl fumarate (DMF) is to date the only Food and Drug Administration– and European Medicines Agency–approved drug registered as NRF2 activator. The monoester form of DMF,

monomethyl fumarate (MMF), was described as its active metabolite. DMF and MMF are Michael acceptors that directly react with cysteine residues present in KEAP1 (Lin et al., 2011).

DMF and other fumaric acid esters have been used for treating psoriasis for over 50 years, starting at a time when the function of NRF2 was still unknown. This compound was licensed in Europe under the commercial name of Fumaderm. Clinical trials showed a decrease in the psoriasis area and severity index to 50%–80% after 12–16 weeks of DMF therapy (Altmeyer et al., 1994; Mrowietz et al., 1998). More recently, DMF has demonstrated its efficacy in the treatment of adults with moderate to severe chronic plaque psoriasis in a phase III trial (BRIDGE) (Mrowietz et al., 2017). The mechanism of action underlying fumarates in remission of psoriatic lesions includes the decrease in the number of peripheral T cells along with a shift from a Th1 toward a Th2 immune response (Ghoreschi et al., 2011; Tahvili et al., 2015). In another autoimmune disease, SLE, fumaric acid esters have been used as systemic combination therapy in the treatment of severe, extensive, and refractory cutaneous manifestations (Saracino and Orteu, 2017).

DMF was approved in 2013 for the treatment of MS under the commercial name Tecfidera (Xu et al., 2015). The use of DMF in MS patients was propelled by positive results obtained in the MS mouse model of EAE. Significant therapeutic effects on the disease course and histology were associated with a markedly reduced macrophage-mediated inflammation in the spinal cord. Multiplex cytokine analysis in blood evidenced an increase of the anti-inflammatory cytokine IL-10 in DMF-treated animals (Schilling et al., 2006). Moreover, DMF also improved preservation of myelin, axons, and neurons in wild-type, but not in *Nrf2*$^{-/-}$ mice (Ellrichmann et al., 2011). In humans, DMF demonstrated a significant reduction of lesions and annualized relapse rate in MS (Schimrigk et al., 2006). Two phase III clinical trials, DEFINE and CONFIRM, substantiated these results (Fox et al., 2012; Gold et al., 2012). Therefore, DMF is currently used as the first line of treatment of relapsing-remitting MS that cannot be treated by traditional therapies. New formulations of DMF are being tested and patented to improve drug bioavailability and efficacy (Sun et al., 2017). For instance, MMF has been used to develop a second generation of NRF2 inducers as prodrugs (Zeidan et al., 2014). The lead compound ALKS-8700, a 2-(2,5-dioxo-1-pyrrolidinyl)ethyl ester derivative of MMF, is rapidly converted into MMF in the body, hence increasing its bioavailability and reducing gastrointestinal side effects. ALKS-8700 is currently under phase III clinical trial (EVOLVE MS).

DMF and MMF modulate the immune response. For example, they inhibit the maturation of DCs by reducing the release of inflammatory cytokines and hence the ability of DCs to process antigens. Moreover, DMF and MMF activate natural killer cells to lyse DCs and enhance apoptosis of both DCs and T cells (Ghoreschi et al., 2011; Al-Jaderi and Maghazachi, 2015). As such, DMF and MMF impede T cell–mediated autoreactivity. Some studies indicate that DMF also induces type II DCs by triggering GSH depletion, which results in enhanced HO-1 activity and suppression of STAT1 phosphorylation. These classic type II DCs suppress Th1- and Th17-mediated responses in favor of Th2 ones. Furthermore, the increased production of IL-10 by DCs favors the differentiation of $CD4^+$ T cells toward a suppressive Treg phenotype (Ockenfels et al., 1998; Ghoreschi et al., 2011). DMF also inhibits the nuclear translocation of NF-$\kappa$B (Peng et al., 2012) and consequently the production of inflammatory mediators, such as TNF-$\alpha$, IL-1$\beta$, IL-6, chemokines, adhesion molecules, and nitric oxide in microglia and astrocytes (Brennan et al., 2017), as well as in peripheral blood mononuclear cells (Eminel et al., 2017). In addition, DMF exerts antiangiogenic effects that are dependent on the downregulation of vascular endothelial growth factor receptor-2 expression in endothelial cells (Meissner et al., 2011). Recent findings indicated that DMF reduced the number of $CD4^+$, $CD8^+$, Th1, and Th17 cells, whereas the $CD4^+/CD8^+$ ratio and the Th2 subset were increased in the blood of these patients. Interestingly, the inhibitory effects of DMF/MMF on T cell activation were confined mainly to memory T cells (Wu et al., 2017). These immunomodulatory activities of DMF or MMF are important for the protection of oligodendrocytes against ROS-induced cytotoxicity (Scannevin et al., 2012).

Additional mechanisms might explain the inhibition of NF-$\kappa$B independently of NRF2 activation. Thus, DMF may interact with cysteine residues in several proteins that regulate NF-$\kappa$B signaling (Blewett et al., 2016). In addition, DMF inhibits ubiquitin-conjugating enzymes and thus prevents the degradation of the I$\kappa$B repressor of NF-$\kappa$B in response to IL-1$\beta$ or Toll-like receptor agonists (McGuire et al., 2016). Moreover, DMF binds directly to specific cysteine residues in protein kinase C-$\theta$, a key kinase involved in signaling by the T cell receptor (Blewett et al., 2016). In addition, MMF and DMF activate the hydroxycarboxylic acid receptor-2, resulting in inhibition of NF-$\kappa$B and downregulation of proinflammatory cytokines and adhesion molecules (Chen et al., 2014; Gillard et al., 2015) and leading to decreased neutrophil infiltration (Chen et al., 2014). Although these NRF2-independent effects would be relevant in the acute inflammatory phase of EAE, the neuroprotective efficacy of DMF during chronic autoimmune demyelination depends on NRF2 activation (Linker et al., 2011). The clinical benefit of DMF treatment in both *Nrf2*$^{-/-}$ and wild-type mice was associated with a reduction of inflammatory Th1 and Th17 cells, as well as with induction of

anti-inflammatory M2 monocytes. At the same time, decreased expression of CD80 and CD86 costimulatory molecules was observed in wild-type, but not in *Nrf2*$^{-/-}$ mice, indicating that at least these effects were NRF2-dependent (Schulze-Topphoff et al., 2016).

The success of DMF for the treatment of autoimmune diseases indicates that other diseases that share common pathomechanisms underlined by chronic, low-grade inflammation and pathologic ROS formation might benefit from the repositioning of this drug. In a mouse model of Huntington's disease, the survival rate, muscle function, and body weight were preserved with DMF treatment, and this was associated with an increased number of intact neurons (Ellrichmann et al., 2011). Also, in a recent preclinical study of PD, using the $\alpha$-synucleinopathy model of this disease, DMF was neuroprotective in wild-type, but not in *Nrf2*$^{-/-}$ mice due to impaired autophagy induction (Lastres-Becker et al., 2016).

DMF was shown to prevent endothelial dysfunction and cardiovascular pathologic ROS formation and inflammation in diabetic mice (Sharma et al., 2017), and decreased atherosclerosis, kidney dysfunction, and other diabetic complications were reported in apolipoprotein E–deficient mice after streptozotocin injection (Tan et al., 2014). Additionally, several studies indicated that DMF might exert antitumor activity by inhibiting the NF-$\kappa$B pathway, hence adding therapeutic value in the treatment of aggressive cancers (Kastrati et al., 2016). DMF is a relevant example of the drug-repurposing concept within the network pharmacology approach.

Synthetic triterpenoids are derivatives of 2-cyano-3,12-dioxo-oleana-1,9(11)-dien-28-oate (CDDO; bardoxolone, RTA401) that resemble the natural product oleanolic acid. They exhibit Michael acceptor activity through its $\alpha$-$\beta$ unsaturated scaffold and represent the most potent inducers of NRF2 (Sun et al., 2017). They interact with C151 of KEAP1 and impede its interaction with CUL3, hence leading to NRF2 activation (Cleasby et al., 2014). Proof-of-principle studies strongly support the use of synthetic triterpenoids for degenerative diseases and are being the focus of intensive research as antioxidant modulators of inflammation by Reata/Abbott. For instance, CDDO-imidazole (CDDO-Im RTA403) induced in peritoneal neutrophils of wild-type but not *Nrf2*$^{-/-}$ mice the expression of various antioxidant genes (*Hmox1*, *Gclc*, *Gclm*, and *Nqo1*) and attenuated LPS-induced ROS generation and production of proinflammatory cytokines, consequently decreasing mortality (Thimmulappa et al., 2006b). CDDO-ethyl amide (RTA405) and CDDO-CDDO-trifluoethyl amide (RTA 404) had significant effects across all endpoints measured in a toxin-induced PD model (1-methyl-4-phenyl-1,2,3,6-tetrahydropyridine) (Kaidery et al., 2013). In the EAE model of MS, CDDO-CDDO-trifluoethyl amide suppressed inflammation, pathologic ROS formation, and myelin degeneration (Pareek et al., 2011).

CDDO-methyl ester (CDDO-Me, RTA 402) was the first CDDO that reached in clinical trials for the treatment of diabetic nephropathy (Pergola et al., 2011). Although the results of the phase II were very encouraging, CDDO-Me was later withdrawn at phase III (BEACON trial) due to cardiovascular safety issues (Zhang, 2013) that were not related to NRF2 but most likely to an off-target alteration of endothelin signaling (de Zeeuw et al., 2013; Chin et al., 2014). Currently, CDDO-Me is under clinical study as potential treatment of Alport syndrome and pulmonary hypertension (Table 2). In an effort to improve its safety profile, further studies have led to the development of CDDO-difluoropropionamide (RTA-408, omaveloxone), which is currently in phase II trial for the treatment of Friedreich's ataxia, ocular inflammation, and pain after ocular surgery.

Oltipraz is an organosulfur compound that is used as an antischistosomal agent and is currently in phase III trial for the treatment of nonalcoholic steatohepatitis. Advanced clinical trials for the treatment of Huntington's disease are under development with minocycline, an antibiotic that has demonstrated neuroprotective properties due to NRF2 activation (Kuang et al., 2009). Another NRF2 inducer in phase I clinical study for the treatment of acute kidney disease is CXA-10, a nitro fatty acid with anti-inflammatory properties through the activation of NRF2 (Batthyany and Lopez, 2015). Many other NRF2 inducers with the same mechanism of action have been described in the last years (Buendia et al., 2015a,b, 2016), and some are in preclinical studies, such as the compound VEDA-1209, a chalcone derivative with a good anti-inflammatory profile for the treatment of ulcerative colitis.

SFN is an isothiocyanate produced from enzymatic cleavage of the organosulfur compound glucoraphanin, which is present in sprouts of broccoli, cabbage, and other *Brassicacea* plants. The catalytic reaction is driven by the enzyme myrosinase that is found in plants and microbiota of the GI tract (Kensler et al., 2013). More recently, SFN has been obtained by chemical synthesis (Kim et al., 2015). Translation of SFN to the clinic has been achieved by administration of SFN-containing broccoli sprout powder to patients with T2DM (Bahadoran et al., 2012). Broccoli powder decreased plasma malondialdehyde and oxidized low-density lipoprotein (LDL) and increased the total antioxidant capacity. Cardiovascular risk factors such as serum triglycerides, oxidized LDL/LDL ratio, and atherogenic index of plasma (log of triglycerides/high-density lipoprotein ratio) were also reduced. Furthermore, proinflammatory markers such as C-reactive protein and IL-6 were decreased. In a more recent study, SFN administered as concentrated broccoli sprout extract suppressed glucose production from

TABLE 2
Selected NRF2 inducers acting as electrophilic modifiers of KEAP1

The reference corresponds to the code in ClinicalTrials.gov.

| Compound | Disease | Clinical Trial | Reference |
|---|---|---|---|
| Dimethyl fumarate 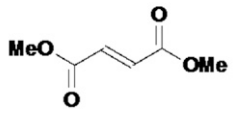 | Multiple sclerosis | Approved | |
| | Psoriasis | Approved | |
| | Rheumatoid arthritis | Phase II | NCT00810836 |
| | Adult brain glioblastoma | Phase I | NCT02337426 |
| | Cutaneous T cell lymphoma | Phase II | NCT02546440 |
| | Obstructive sleep apnea | Phase II | NCT02438137 |
| | Chronic lymphocytic leukemia small lymphocytic lymphoma | Phase I | NCT02784834 |
| ALKS-8700 (MMF-derivate) 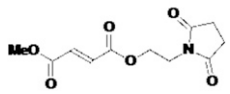 | Multiple sclerosis | Phase III | NCT02634307 |
| CDDO-Me (RTA402) 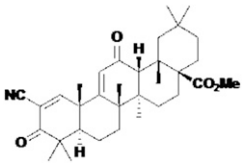 | Diabetic nephropathy | Phase II | NCT00811889 |
| | Chronic kidney disease, T2DM, diabetic nephropathy | Phase III | NCT01351675 |
| | Liver disease | Phase I/II | NCT00550849 |
| | Hepatic impairment | Phase I | NCT01563562 |
| | Advanced solid tumors | Phase I | NCT00529438 |
| | Lymphoid malignancies | | NCT00508807 |
| | Alport syndrome | PhaseII/III | NCT03019185 |
| | Pulmonary hypertension | Phase III | NCT03068130 |
| | Pulmonary arterial hypertension | Phase III | NCT02657356 |
| | Renal insufficiency, T2DM | Phase II | NCT01053936 |
| CDDO-DFPA (RTA-408) 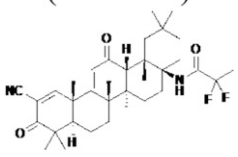 | Mitochondrial myopathy | Phase II | NCT02255422 |
| | Friedreich's ataxia | Phase II | NCT02255435 |
| | Inflammation and pain following ocular surgery | Phase II | NCT02065375 |
| | Corneal endothelial cell loss, ocular pain and inflammation, cataract surgery | Phase II | NCT02128113 |
| | Melanoma | Phase I/II | NCT02259231 |
| | Breast cancer | Phase II | NCT02142959 |
| | Non-small cell lung cancer, melanoma | Phase I | NCT02029729 |
| CXA-10 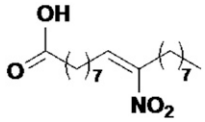 | Acute kidney injury | Phase I | NCT02248051 |
| Minocycline 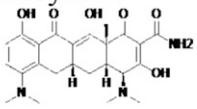 | HD | Phase II/III | NCT00277355 |
| | Intracerebral hemorrhage | Phase I/II | NCT01805895 |
| | Retinitis pigmentosa | Phase I/II | NCT02140164 |
| | Intracerebral hemorrhage | Phase I/II | NCT03040128 |
| Oltipraz 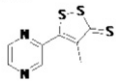 | NASH | Phase III | NCT02068339 |
| | Schistosomiasis | Approved | |
| | Lung cancer | Phase I | NCT00006457 |

(*continued*)

TABLE 2—*Continued*

| Compound | Disease | Clinical Trial | Reference |
|---|---|---|---|
| VEDA-1209 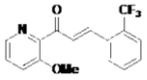 | Ulcerative colitis | Preclinical PK | —— |
| Sulforaphane 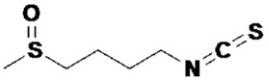 | Cystic fibrosis | Phase II | NCT01315665 |
| | Schizophrenia | Phase II/III | NCT02880462 |
| | | Phase II | NCT02810964 |
| | | Phase II | NCT01716858 |
| | COPD | Phase II | NCT01335971 |
| | Atopic asthmatics | Phase I | NCT01845493 |
| | Autism | Phase II | NCT01474993 |
| | | Phase II | NCT02909959 |
| | | Phase II | NCT02677051 |
| | | Phase II | NCT02654743 |
| | | Phase I/II | NCT02561481 |
| | Healthy | Phase I | NCT01008826 |
| | | Phase I | NCT02023931 |
| | Melanoma | Phase I | NCT01568996 |
| | Asthma | Phase I | NCT01845493 |
| | | Phase I/II | NCT01183923 |
| | Prostate cancer | Phase II | NCT01228084 |
| | Breast cancer | Phase II | NCT00843167 |
| | Lung cancer | Phase II | NCT03232138 |
| | Environmental carcinogenesis | Phase II | NCT01437501 |
| | Alcohol sensitivity | Phase II | NCT01845220 |
| | Aging | Phase II | NCT03126539 |
| | Allergic rhinitis | Phase II | NCT02885025 |
| | *Helicobacter pylori* infection | Phase IV | NCT03220542 |
| | T2DM | Phase II | NCT02801448 |
| | Head and neck squamous cell carcinoma, head and neck cancer, tobacco-related carcinoma | Phase I | NCT03182959 |
| Sulforadex 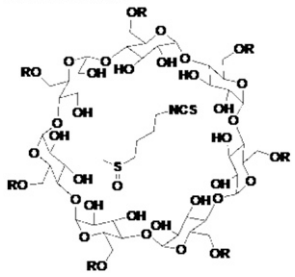 | Subarachnoid hemorrhage | Phase II | NCT02614742 |
| | Breast neoplasm | Phase I/II | NCT02970682 |
| | Prostate cancer | Phase I | NCT02055716 |
| | | | NCT01948362 |
| ITH12674 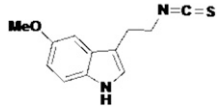 | Brain ischemia | Preclinical PK | — |
| DL-3-n-butylphthalide 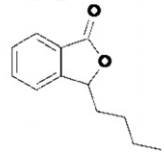 | Alzheimer disease | Phase II | NCT02711683 |
| | Acute ischemic stroke | Phase I/II | NCT02149875 |
| | Vascular cognitive impairment | Phase II/III | NCT02993367 |
| | Cerebrovascular occlusion, collateral blood circulation, anterior cerebral circulation infarction | Phase IV | NCT02594995 |

(*continued*)

TABLE 2—*Continued*

| Compound | Disease | Clinical Trial | Reference |
|---|---|---|---|
| Ursodiol 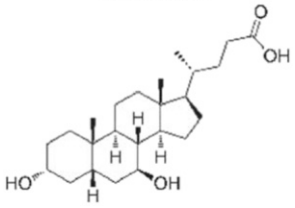 | Cholestasis | Phase II/III | NCT00846963 |
| | HD | Phase I | NCT00514774 |
| | Barrett esophagus, low-grade dysplasia | Phase II | NCT01097304 |
| | Chronic hepatitis C | Phase III | NCT00200343 |
| | T2DM | Phase II | NCT02033876 |
| Resveratrol 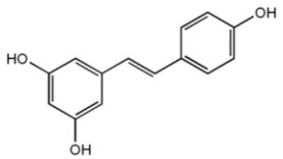 | T2DM | Phase I | NCT01677611 |
| | Colon cancer | Phase I | NCT00256334 |
| | COPD | Phase III | NCT02245932 |
| | Friedreich ataxia | Phase I/II | NCT01339884 |
| | NASH | Phase II/III | NCT02030977 |
| | Non-ischemic cardiomyopathy | Phase III | NCT01914081 |
| | Endometriosis | Phase IV | NCT02475564 |
| | Chronic renal insufficiency | Phase III | NCT02433925 |
| | Metabolic syndrome X | Phase II | NCT02114892 |
| | Chronic subclinic inflammation | Phase III | NCT01492114 |
| | AD | Phase II | NCT01504854 |
| | | Phase III | NCT00743743 |
| Curcumin 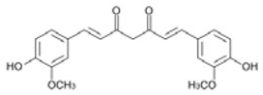 | Colorectal cancer | Phase I | NCT00433576 |
| | HD | Phase III | NCT02336633 |
| | T2DM, cardiovascular risk | Phase IV | NCT01052025 |
| | Schizophrenia, cognition, psychosis | Phase I/II | NCT02104752 |
| | Acute kidney injury, abdominal aortic aneurysm | Phase II/III | NCT01225094 |
| | Chronic kidney diseases, T2DM | Phase II/III | NCT03262363 |
| | AD | Phase I/II | NCT00164749 |
| | Neoplasms | Phase II | NCT02944578 |
| | Crohn's disease | Phase III | NCT02255370 |
| | Chronic schizophrenia | Phase IV | NCT02298985 |
| | Mild cognitive impairment | Phase II | NCT01811381 |
| | Prostate cancer | Phase III | NCT02064673 |
| | Major depression | Phase IV | NCT01750359 |

hepatocytes by nuclear translocation of NRF2 and decreased expression of key enzymes involved in gluconeogenesis. Moreover, SFN reduced fasting blood glucose and glycated hemoglobin in obese patients with T2DM (Axelsson et al., 2017). SFN-induced activation of NRF2 protected renal cells against lupus nephritis by reducing the ROS burden and by inhibiting the NF-$\kappa$B and TGF-$\beta$1 signaling pathways (Jiang et al., 2014a).

In regard to neurodegenerative diseases, it has been shown that SFN crosses the blood brain barrier and provides sufficient cerebral bioavailability to activate the NRF2 signature and to reduce LPS-elicited neuroinflammation, as reflected in the reduction of proinflammatory markers (inducible nitric oxide synthase, IL-6, TNF-$\alpha$) and microgliosis in the hippocampus (Innamorato et al., 2008). SFN also safeguarded dopaminergic neurons against the parkinsonian toxin 1-methyl-4-phenyl-1,2,3,6-tetrahydropyridine and attenuated astrogliosis and microgliosis (Jazwa et al., 2011). In line with these findings, SFN reduced the levels of phosphorylated tau and increased Beclin-1 and LC3-II, suggesting that NRF2 activation might facilitate degradation of this toxic protein through autophagy in the brain (Jo et al., 2014). SFN-treated rats subjected to spinal cord injury had significantly decreased levels of inflammatory cytokines, reduced contusion volume, and improved coordination (Wang et al., 2012). This drug also ameliorated EAE by preserving the blood-brain barrier and by reducing pathologic ROS formation and the number of inflammatory cells (Li et al., 2013). SFN has been used to date in at least 32 clinical studies addressing chronic diseases such as cancer, asthma, chronic kidney disease, T2DM, cystic fibrosis, autism, and schizophrenia (Duran et al., 2016; Houghton et al., 2016) (Table 2).

Altogether, these observations paved the way for the development of other SFN-derived compounds exhibiting an improved pharmacokinetic profile. SFN is an oily substance with low stability in hydrophilic media. Its physicochemical profile prompted Evgen Pharma (Wilmslow, Cheshire, England) to develop a cyclodextrin complex formulation, Sulforadex, which is under phase II clinical trial for the treatment of subarachnoid hemorrhage. SFN was also hybridized with melatonin to generate the ITH12674, a compound that was designed to have a dual drug–prodrug mechanism of action for treatment of brain ischemia (Egea et al., 2015).

Curcumin is the main curcuminoid found in turmeric and has been used for the treatment of obesity, metabolic syndrome, and prediabetes. A nontargeted

metabolomics study to investigate the effects of curcumin on rat liver was conducted by means of gas chromatography with electron impact mass spectrometry. The intermittent intake of curcumin upregulated NRF2 and displayed antioxidant and anti-inflammatory roles in the protection against liver damage (Qiu et al., 2016). Oral consumption of curcumin is effective in lowering serum triglycerides, IL-1$\beta$, IL-4, and vascular endothelial growth factor, and in increasing adiponectin levels in blood. In T2DM patients, curcumin decreases the levels of fasting blood glucose, glycated hemoglobin, serum free fatty acids, triglycerides, and uric acid, and increases the levels of lipoprotein lipase (Na et al., 2013; Chuengsamarn et al., 2014).

Resveratrol is a polyphenol that protects plants against fungal infection and is found in the skin of grapes, red wine, berries, and many other plants. Resveratrol exerts antioxidant properties through activation of NRF2 signaling by downregulating KEAP1 expression and by activating the protein deacetylase sirtuin-1 (Ungvari et al., 2010). In healthy subjects, the dietary administration of resveratrol prevented the elevation in plasma of cholesterol, endotoxins, prooxidants, and inflammatory markers (p47phox, KEAP1, IL-1$\beta$, and TNF-$\alpha$). These events correlated with the elevation of NRF2 activity as determined by enhanced expression of its targets NQO1 and glutathione S-transferase (Ghanim et al., 2011). In T2DM patients, insulin sensitivity was improved after 4 weeks of treatment, as determined by enhanced insulin signaling via AKT, decreased pathologic ROS formation, and reduced levels of glycated hemoglobin (Brasnyo et al., 2011; Bhatt et al., 2012). Overall, resveratrol was reported to prevent major cardiovascular, inflammatory, oxidative, and metabolic complications in hypertension, hypercholesterolemia, atherosclerosis, ischemic heart disease, diabetes, and metabolic syndrome in animal models and patients (Xia et al., 2017).

A problem that is frequently overlooked is the lack of selectivity of electrophilic KEAP1 inhibitors. Electrophiles react with different nucleophiles present in the cell, thus exhibiting off-target and nondesired side effects. For instance, CDDO-Im can interact with more than 500 different targets (Yore et al., 2011). In general, several protein phosphatases contain redox-sensitive cysteines in their catalytic center, and some KEAP1 inhibitors may modify and inactivate these phosphatases, hence disturbing signaling networks. One of these phosphatases is PTEN (Lee et al., 2002; Kitagishi and Matsuda, 2013; Han et al., 2015). The catalytic C124 residue of PTEN can be modified through adduct formation with strong electrophiles such as CDDO-Im (Pitha-Rowe et al., 2009) and tert-butylhydroquinone (Rojo et al., 2014b). Then, the increased activation of the PI3K/AKT pathway involves inhibition of GSK-3 and subsequent stabilization of NRF2 (Fig. 2C) (Rada et al., 2011, 2012). Moreover, KEAP1 interacts with other proteins that also contain the high-affinity binding motif ETGE (Hast et al., 2013), such as Bcl-2 and IKK$\beta$ (Kim et al., 2010a; Cazanave et al., 2014). Therefore, some results obtained from KEAP1-deficient cells may not necessarily be related to NRF2 activation.

### *B. Protein–Protein Interaction Inhibitors for Nuclear Factor (Erythroid-Derived 2)–Like 2 Activation*

To overcome the pitfall of selectivity, a new class of NRF2 inducers that prevent the docking of NRF2 to KEAP1 has emerged (Richardson et al., 2015). The use of PPI inhibitors has been achieved by the prior elucidation of the X-ray crystal structure of KEAP1 (Padmanabhan et al., 2006) bound to a peptide containing the high-affinity binding ETGE motif of NRF2 (Lo et al., 2006). KEAP1 contains a six-bladed $\beta$-propeller with specific hydrophobic and hydrophilic residues that participate in the docking of the ETGE motif that adopts a $\beta$-hairpin structure. Docking is mainly favored by electrostatic interactions between several arginines of KEAP1 and the two glutamates in the ETGE motif (Lo et al., 2006; Padmanabhan et al., 2006). The docking to KEAP1 of the low-affinity DLG motif of NRF2 has also been characterized (Tong et al., 2007). Based on these interactions, peptidomimetic compounds were the first example of PPI inhibitors with significantly improved selectivity over electrophiles (Hu et al., 2013; Marcotte et al., 2013; Winkel et al., 2015). These inhibitors show weak activity in cells, and a new provocative strategy has now been reported based on the use of cyclic peptides. One of these peptides exhibited high-binding affinity for KEAP1 and activation of NRF2 and elicited anti-inflammatory effects in mouse macrophages (Lu et al., 2018).

The discovery of new peptides and small-molecule inhibitors of the KEAP1/NRF2 interaction has been reviewed recently (Abed et al., 2015; Jiang et al., 2016). Briefly, a series of truncated NRF2 peptides was initially evaluated as direct inhibitors of PPI using surface plasmon resonance and fluorescence polarization assays (Hu et al., 2013). The minimal peptide sequence with inhibitory capacity was the 9-mer sequence of LDE-ETGE-FL (Chen et al., 2011; Inoyama et al., 2012). In parallel, Wells and collaborators (Hancock et al., 2013) searched for new putative peptide ligands using a phage display library combined with high-throughput fluorescence polarization assay. They found that hybrid peptides based upon the ETGE motif of NRF2 and SQSTM1 have superior binding activity to KEAP1 compared with either native peptide alone. To facilitate cellular uptake, a peptide was designed with the ETGE motif fused to the cell transduction domain of the HIV-Tat protein and the cleavage sequence of calpain (DEETGE-Cal-Tat). This peptide showed neuroprotective and cognitive-preserving effects in a mouse model of cerebral ischemia (Tu et al., 2015).

TABLE 3
Selected NRF2 inducers acting as NRF2–KEAP1 protein–protein interaction inhibitors

| Compound | Patent | Title | Applicant |
|---|---|---|---|
| Compound 7 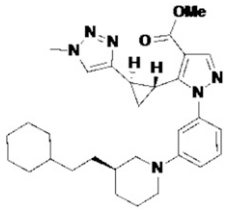 | WO2017060855 | Arylcyclohexyl pyrazoles as NRF2 regulators | GlaxoSmithKline Astex Therapeutics |
| Compound 15 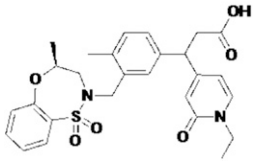 | WO2016/202253 | NRF2 regulators | GlaxoSmithKline Astex Therapeutics, GlaxoSmithKline (China), R&D |
| BM19 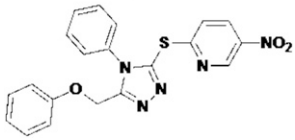 | WO2014/197818 | Small-molecule activators of NRF2 pathway | General Hospital, Regents of the University of California |
| LH601 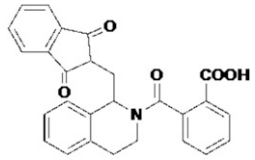 | WO2013/067036 | Direct inhibitors of KEAP1–NRF2 interaction as antioxidant inflammation modulators | Rutgers, The State University of New Jersey, Broad Institute |
| 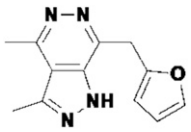 | WO2011/156889 | Novel modulators of NRF2 and uses thereof | TRT Pharma Gerald Batist, Jian Hui Wu |
| AN-465/144580 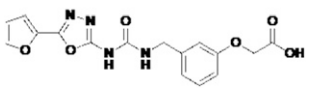 | JP2011/0167537 | KEAP1 protein-binding compound, crystal of complex between the same and KEAP1 protein, and method for producing the same | Toray Industries |

(*continued*)

TABLE 3—*Continued*

| Compound | Patent | Title | Applicant |
|---|---|---|---|
| 3-(2-Oxo-2-phenylethylidene)-2,3,6,7-tetrahydro-1H-pyrazino[2,1-a]isoquinolin-4(11bH)-one (Compound (I)) 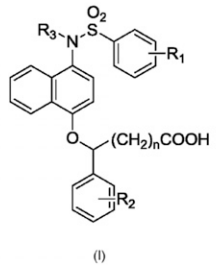 (I) | WO2017124835 | 1-sulfonamido-4-aryloxy compound, and preparation method and medicinal application thereof | China Pharmaceutical University |
| 3-(pyridin-3-ylsulfonyl)-5-(trifluoromethyl)-2H-chromen-2-one (PSTC) 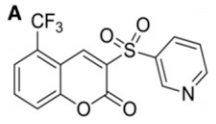 | WO2015/092713 | NRF2 regulators | GlaxoSmithKline Astex Therapeutics Limited |
| Compound 2 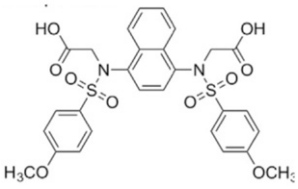 | WO2011156889A1 | Novel regulators of NRF2 and uses thereof | TRT Pharma Gerald Batist, Jian Hui Wu |
| Compound 16 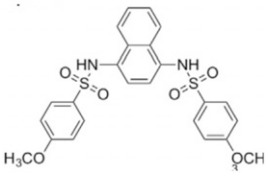 | WO2016/202253 | NRF2 regulators | GlaxoSmithKline Astex Therapeutics, GlaxoSmithKline (China), R&D CO., LTD |

Five families of PPI inhibitors have been described: tetrahydroisoquinoline (Jnoff et al., 2014; Richardson et al., 2015), thiopyrimidine (Marcotte et al., 2013), naphthalene (Jiang et al., 2014b), carbazone (Ranjan et al., 2014), and urea derivatives (Sato et al., 2013). Table 3 compiles recent patents addressing these small molecules. Although these compounds are very promising, it is still needed to demonstrate that they are selective for the KEAP1/NRF2 interaction, because KEAP1 also targets at least Bcl2 and IKK (Kim et al., 2010a; Hast et al., 2013; Cazanave et al., 2014).

From the large number of compounds indexed in the available libraries, the compounds LH601, benzenesulfonyl-pyrimidone 2, N-phenyl-benzenesulfonamide, and a series

of 1,4-diphenyl-1,2,3-triazoles might be very well-suited candidates to inhibit the PPI with KEAP1 (Hu et al., 2013; Jnoff et al., 2014; Bertrand et al., 2015; Wen et al., 2015; Nasiri et al., 2016). These studies described in detail the atomic interaction with KEAP1, the affinity, and the thermodynamics parameters of binding. The therapeutic efficacy of these compounds is to be analyzed in future work in which safety, potency, and blood brain barrier permeability should be addressed.

### *C. Drug Targets Other Than Kelch-Like ECH-Associated Protein 1 for Nuclear Factor (Erythroid-Derived 2)–Like 2 Activation*

Protein kinase GSK-3 phosphorylates the two serine residues in the DSGIS sequence of NRF2 to generate a phosphorylation-dependent degradation motif or phosphodegron (Fig. 2). This phosphodegron is recognized by the E3 ligase adapter $\beta$-TrCP, leading to ubiquitin-dependent proteasomal degradation of NRF2. Therefore, GSK-3 inhibitors should stop NRF2 degradation by preventing the generation of this phosphodegron. GSK-3 is an important kinase in AD and other pathophenotypes. It phosphorylates the cytoskeletal protein tau, facilitating the formation of neurofibrillary tangles, which are pathologic intracellular aggregates that disturb axonal transport and lead to neuronal death (Silva et al., 2014). Therefore, it has been speculated that GSK-3 inhibition might have the double benefit of preventing neurofibrillary tangle formation and NRF2 degradation. Unfortunately, most pipelines for the development of GSK-3 inhibitors have been discontinued due to futility, although in most cases there was not good evidence of target modulation (Palomo and Martinez, 2017).

Conceptually, inhibitors of the $\beta$-TrCP-phosphoNRF2 interaction should also lead to NRF2 activation as they should disrupt this branch of NRF2 degradation (Fig. 2). The molecular interactions between the $\beta$-propeller of $\beta$-TrCP and a peptide containing the NRF2 phosphodegron have been resolved by NMR (Rada et al., 2012). As it happens for KEAP1/EGTE, the most relevant amino acids appear to be several arginine residues of $\beta$-TrCP that interact with the two phosphoserines of the DpSGIpS motif. However, the discovery of small molecules that could inhibit the $\beta$-TrCP-phosphoNRF2 interaction is still to come.

Additional strategies have been developed to inhibit the NRF2 repressor BACH1, a bZip protein that makes heterodimers with MAF proteins and blocks expression of ARE genes. Efficient inhibition of BACH1 by the HPP-4382 compound has been described in vitro (Attucks et al., 2014), but, prior to a full clinical trial, the safety and efficacy profile of HPP-4382 will have to be demonstrated in vivo. Considering that other pathways may also influence NRF2 activity, it is reasonable to speculate that a combinatorial approach will be the best way to activate this transcription factor.

### *D. Nuclear Factor (Erythroid-Derived 2)–Like 2 Inhibitors*

NRF2 has a "dark side" related to its oncogenic activity when constitutively and highly overexpressed. Therefore, NRF2 inhibition has been proposed as a mechanism to sensitize cancer cells to chemotherapeutic drugs or radiotherapy (Milkovic et al., 2017). Two strategies can be envisioned to inhibit NRF2 with small molecules: PPI inhibitors that disrupt the bZip interaction between NRF2 and MAFs, and DNA–protein interaction inhibitors that block binding of NRF2-MAF to the ARE (Fig. 9C). Both strategies are hampered by the need by such drugs to overcome the large free energy of association between protein–protein and, to a lesser extent, protein–DNA interfaces. Nevertheless, such drugs have been found for other bZip transcription factors such as STAT3-STAT3, MYC-MAX, and JUN-FOS (Yap et al., 2011), and new small molecules are being described for NRF2-MAF. For instance, malabaricone-A is a pro-oxidant compound that overcomes leukemia resistance by targeting NRF2 (Manna et al., 2015). Ascorbic acid (vitamin C), a well-known ROS scavenger, was found to sensitize imatinib-resistant cancer cells by decreasing the levels of the NRF2/ARE complex, reducing the expression of the *GCLC* gene and dropping GSH levels (Tarumoto et al., 2004). All-trans-retinoic acid is another example of NRF2 inhibitor that significantly decreases NRF2 activation by potent electrophilic NRF2 inducers in vitro and in vivo. It activates the retinoic acid receptor $\alpha$, which forms a complex with NRF2, hence impeding the binding of the transcription factor to ARE genes (Wang et al., 2007).

Natural products such as brusatol (Ren et al., 2011; Olayanju et al., 2015), ochratoxin A (Tarumoto et al., 2004; Limonciel and Jennings, 2014), and trigonelline (Arlt et al., 2013) have also been found to inhibit NRF2. However, their mechanism of action is not fully understood. In fact, a significant issue related to currently available compounds is the profound off-target effect that they might have. For instance, promising results with brusatol were recently discouraged by the finding that this drug exerts a general and unspecific inhibition of protein synthesis, resulting in the drop of NRF2 levels, but also of many other proteins with rapid turnover (Harder et al., 2017). Similarly, the antiprotozoal agent halofuginone, used in veterinary practice, enhances the chemosensitivity of cancer cells by suppressing NRF2 accumulation, but this effect appears to be indirect by inhibiting prolyl–transfer RNA synthesis that is strongly required for ribosomal translation of NRF2 as well as many other proline-containing proteins (Tsuchida et al., 2017).

A novel approach to identify selective NRF2 inhibitors has been reported recently by the use of quantitative high-throughput screen of small-molecule inhibitors (Singh et al., 2016). The authors identified a first-in class compound, termed ML385, which most likely prevented

the binding of NRF2 to other bZip coactivators. This compound blocked NRF2 transcriptional activity and sensitized KEAP1-deficient cells to carboplatin and other chemotherapeutic drugs. Additional studies are needed to confirm whether ML385 is selective for NRF2 or if it also inhibits other bZip transcription factors.

In light of the highly favorable systemic effects of NRF2 in various tumor pathophenotypes, a specific targeting of NRF2 with small-molecule inhibitors seems to provide an excellent clinical approach. However, it is necessary to determine whether cancer treatment with NRF2 inhibitors increases the risk of other pathophenotypes of the NRF2 diseasome.

### *E. Repurposing Instead of De Novo Drug Discovery and Development*

As previously discussed, numerous compounds are under development to provide a benefit for the pathophenotypes associated with the NRF2 diseasome. An alternative approach is to give drugs that are already in clinical use for a certain pathomechanism a new use for the treatment of other pathomechanisms that are connected to NRF2. This section provides the basis for repositioning some commonly used drugs based on their role in NRF2 regulation.

Metformin is the first-line monotherapy for the T2DM. According to Fig. 6, it provides therapeutic benefit to the NRF2 subcluster of pathophenotypes related to glucose metabolism. In fact, SFN reduces hepatic glucose production and improves glucose control in patients with T2DM (Axelsson et al., 2017). Interestingly, some evidence suggests that metformin may be effective in preventing other nonglycemic pathophenotypes of the NRF2 diseasome, including cardiovascular (Nesti and Natali, 2017), respiratory (Sato et al., 2016), digestive (Bauer and Duca, 2016), neurodegenerative (Markowicz-Piasecka et al., 2017), autoimmune (Schuiveling et al., 2017), and neoplastic (Heckman-Stoddard et al., 2017) disorders. The mechanism of action of metformin is not completely clear, but it involves inhibition of mitochondrial complex I, thus increasing the AMP/ATP ratio (El-Mir et al., 2000; Owen et al., 2000) and leading to activation of the energy sensor AMPK (Hardie, 2004; Rena et al., 2017). Importantly, AMPK activates NRF2 (Wang et al., 2017a; Zhao et al., 2017), and pharmacological targeting of this axis attenuates inflammation after stroke (Wang et al., 2017c) or endotoxin exposure (Ci et al., 2017; Lv et al., 2017). Indeed, metformin activates NRF2 in an AMPK-dependent manner, resulting in inhibition of inflammatory responses in preclinical rodent models of transient global cerebral ischemia (Ashabi et al., 2015; Kaisar et al., 2017). Glucose metabolism and inflammation may not be the only pathomechanisms affected by metformin/NRF2. In fact, other salutary effects have been described for redox (Kocer et al., 2014; Kelleni et al., 2015) and protein homeostasis (Tsai et al., 2017).

Statins prevent and reduce cardiovascular pathophenotypes. In addition to a lipid-lowering effect, statins appear to protect against pathomechanisms associated with the NRF2 network such as inflammatory (Pantan et al., 2016; Wu et al., 2016a; Hwang et al., 2017) and pathologic ROS formation (Abdanipour et al., 2014). They are competitive inhibitors of 3-hydroxy-3-methyl-glutaryl-CoA reductase, which catalyzes the rate-limiting reaction in cholesterol synthesis. Other pleiotropic effects include the upregulation of transcription factor Krüppel-like factor 2, which is induced early during progression of cirrhosis and lessens the development of hepatic vascular dysfunction (Marrone et al., 2015). Recent evidence indicates that at least some statins activate NRF2. In a proteomic study conducted in isolated hepatocytes, high concentrations of simvastatin activated NRF2, probably as a defensive mechanism (Cho et al., 2013). The pretreatment of neural stem cells with lovastatin activated the NRF2 pathway and elicited protection against hydrogen peroxide–induced cell death (Abdanipour et al., 2014). In liver cirrhosis, simvastatin activates an axis formed by Krüppel-like factor 2 and NRF2 to reduce the oxidative burden and inflammatory response of stellate cells, improving liver fibrosis, endothelial dysfunction, and portal hypertension. The mechanism of activation of NRF2 by simvastatin is not completely clear, but it appears to involve elements found in the NRF2 interactome, such as mitogen-activated protein kinase, PI3K/AKT pathways (Jang et al., 2016), and GSK-3 (Lin et al., 2016).

Other cases for drug repurposing can be inferred from the NRF2 interactome of Fig. 4, in particular with signaling kinases. As indicated in Fig. 2C, GSK-3 phosphorylates the Neh6 domain of NRF2, leading to the recognition by $\beta$-TrCP and further ubiquitin-dependent proteasomal degradation. GSK-3 is active in the absence of stimuli and inactive when signaling cascades that activate AKT and other kinases lead to phosphorylation of GSK-3 at its N-terminal pseudosubstrate domain. It follows that medications known to target signaling kinases may be used to upregulate (GSK-3 inhibitors) or downregulate (PI3K/AKT inhibitors) the NRF2 signature.

GSK-3 participates in at least some pathophenotypes found in the NRF2 diseasome such as diabetes and neurodegeneration (Beurel et al., 2015; Maqbool and Hoda, 2017). A broad spectrum of GSK-3 inhibitors has been discovered from natural and synthetic origins (Khan et al., 2017), but probably the best evidence for repurposing a GSK-3 inhibitor to increase NRF2 activity stems from the clinical use of lithium as mood stabilizer (Chiu et al., 2013). Although bipolar disorder and depression are not found at this time in the NRF2 diseasome, it is becoming evident that they exhibit neuroinflammatory and degenerative pathophenotypes that at least in mouse models imply deregulation of

NRF2 (Martin-de-Saavedra et al., 2013; Freitas et al., 2016; Yao et al., 2016).

The NRF2 interactome also provides a justification for the inhibition of NRF2 by cancer drugs that block signaling kinases, thus activating GSK-3. For example, the epidermal growth factor receptor inhibitor erlotinib leads to NRF2 inhibition, participating in tumor cell sensation in nonsmall cell lung cancer (Xiaobo et al., 2016). The kinase cascade inhibitor sorafenib, used in therapy of hepatocellular carcinoma, also leads to inhibition of NRF2 and its downstream targets metallothionein-1 (Houessinon et al., 2016) and methylenetetrahydrofolate dehydrogenase 1 (Lee et al., 2017).

Finally, search for repurposing drugs that might impinge on NRF2 regulation has been done to date in two relevant studies. Using a fluorescence correlation spectroscopy-based screening system, two of 1633 drugs significantly increased NRF2 protein levels in HepG2 cells: chlorophyllin and bonaphton (Yoshizaki et al., 2017). In another study, the connectivity map database that comprises gene expression profiles for human cell lines treated with 1309 agents (Lamb et al., 2006; Iorio et al., 2010) was analyzed (Zhang et al., 2017) in search for potential redox regulators through activation of NRF2 (Xiong et al., 2014). This study found astemizole, a potent antihistamine drug, used in allergic conditions, as a novel NRF2 activator.

## VI. Biomarkers as Nuclear Factor (Erythroid-Derived 2)–Like 2 Signature and for Monitoring Target Engagement

The evaluation of the redox status in patients or population studies is hampered by the short half-life of ROS, in the range of milliseconds or nanoseconds (Ghezzi et al., 2017b). Therefore, biomarkers of pathologic ROS formation are based on measuring the traces left by ROS, which are normally terminal oxidation products of cellular molecules, many of them being nonspecific (Frijhoff et al., 2015). On the contrary, activation of NRF2 and subsequent expression of its target genes is an indirect but reliable estimation of the total exposure of the organism to pathologic ROS formation. Because NRF2 activation is a well-established cellular response to environmental stressors, it has been considered as biomarker of exposure to xenobiotics. In lung, a data mining of several transcription studies followed by Ingenuity pathway analysis reported that the NRF2 signature is upregulated in healthy smokers, therefore suggesting that NRF2-regulated antioxidant genes play a central role in protection against toxic effects of tobacco smoke (Comandini et al., 2010). Similarly, the levels of NQO1, an enzyme regulated by NRF2, were 15-fold higher in liver tissue obtained from acetaminophen-overdosed patients (Aleksunes et al., 2006). The association between disease and nutrition is frequently based on unreliable self-reporting (Archer et al., 2015). Measuring biomarkers of response to nutrients, supposedly having beneficial effects by activating NRF2, could provide a reliable method to validate nutritional studies. However, this possibility is still unexplored.

The changes associated with NRF2 transcription could be useful as biomarker for monitoring the efficacy of drugs aimed at reducing pathologic ROS formation by inhibitors of xanthine oxidase and NADPH oxidase. Similarly, exposure to environmental chemicals could be detected and monitored by defining a global protein and gene expression profile (Ghezzi et al., 2017a). This approach is similar to the use of phase I drug-metabolizing enzymes, in which cytochrome P450, which is induced by various xenobiotics through the Ah receptor, can be used as indicator of marine pollution (Cajaraville et al., 2000). Daily oral administration of fumaric acid esters over 12 weeks was associated with the increased expression of NRF2 target genes in the skin of patients with psoriasis (Onderdijk et al., 2014). Similarly, a fivefold increase in the mRNA level of NQO1 has been reported in peripheral blood mononuclear cells obtained from cancer patients that received a daily dose of CDDO-Me for 3 weeks (Hong et al., 2012).

The use of the transcriptional signature of NRF2 as a biomarker requires a good knowledge of the mechanisms involved in activation of ARE genes, as most of the NRF2 targets are regulated by additional transcription factors. It is therefore important to analyze the expression of several ARE genes. For instance, a study using NRF2 as predictor for response to treatment in lung squamous cell carcinoma has proposed the use of 28 genes to define a NRF2 activation profile (Cescon et al., 2015).

## VII. Conclusions

Systems medicine together with network pharmacology highlights a cluster of chronic disease pathophenotypes in which NRF2 plays a fundamental role. These diseases share common mechanisms, including oxidative, inflammatory, and metabolic alterations. The NRF2 interactome, the NRF2 diseasome, and the NRF2 drugome presented in this work are still in an early stage of development, but they represent a first attempt to structure NRF2 as a common therapeutic and systems medicine approach. The forthcoming refinement of current databases and upcoming clinical outcome data will further improve the accuracy of this new approach to pharmacology and mechanism-based drug repurposing. This paper provides a road map for a comprehensive strategy for drug discovery to activate or inhibit NRF2 and highlights the need of translational efforts toward the development of de novo drugs or the

repurposing of drugs that target NRF2 as a common element in chronic diseases.

**Authorship Contributions**

*Participated in research design:* Cuadrado, Schmidt.

*Wrote or contributed to the writing of the manuscript:* Manda, Oliva, Guney, Alcaraz, Barbas, Valverde, Daiber, Ghezzi, López, León, Pajares, Rojo, Robledinos-Antón, Hassan.

**References**


Abdanipour A, Tiraihi T, Noori-Zadeh A, Majdi A, and Gosaili R (2014) Evaluation of lovastatin effects on expression of anti-apoptotic Nrf2 and PGC-1α genes in neural stem cells treated with hydrogen peroxide. *Mol Neurobiol* **49**:1364–1372.

Abed DA, Goldstein M, Albanyan H, Jin H, and Hu L (2015) Discovery of direct inhibitors of Keap1-Nrf2 protein-protein interaction as potential therapeutic and preventive agents. *Acta Pharm Sin B* **5**:285–299.

Aleksunes LM, Goedken M, and Manautou JE (2006) Up-regulation of NAD(P)H quinone oxidoreductase 1 during human liver injury. *World J Gastroenterol* **12**: 1937–1940.

Aleksunes LM and Manautou JE (2007) Emerging role of Nrf2 in protecting against hepatic and gastrointestinal disease. *Toxicol Pathol* **35**:459–473.

Al-Huseini LM, Aw Yeang HX, Sethu S, Alhumeed N, Hamdam JM, Tingle Y, Djouhri L, Kitteringham N, Park BK, Goldring CE, et al. (2013) Nuclear factor-erythroid 2 (NF-E2) p45-related factor-2 (Nrf2) modulates dendritic cell immune function through regulation of p38 MAPK-cAMP-responsive element binding protein/activating transcription factor 1 signaling. *J Biol Chem* **288**:22281–22288.

Al-Jaderi Z and Maghazachi AA (2015) Vitamin $D_3$ and monomethyl fumarate enhance natural killer cell lysis of dendritic cells and ameliorate the clinical score in mice suffering from experimental autoimmune encephalomyelitis. *Toxins (Basel)* **7**: 4730–4744.

Altmeyer PJ, Matthes U, Pawlak F, Hoffmann K, Frosch PJ, Ruppert P, Wassilew SW, Horn T, Kreysel HW, Lutz G, et al. (1994) Antipsoriatic effect of fumaric acid derivatives: results of a multicenter double-blind study in 100 patients. *J Am Acad Dermatol* **30**:977–981.

Archer E, Pavela G, and Lavie CJ (2015) The inadmissibility of what we eat in America and NHANES dietary data in nutrition and obesity research and the scientific formulation of national dietary guidelines. *Mayo Clin Proc* **90**:911–926.

Arisawa T, Tahara T, Shibata T, Nagasaka M, Nakamura M, Kamiya Y, Fujita H, Hasegawa S, Takagi T, Wang FY, et al. (2007) The relationship between *Helicobacter pylori* infection and promoter polymorphism of the Nrf2 gene in chronic gastritis. *Int J Mol Med* **19**:143–148.

Arisawa T, Tahara T, Shibata T, Nagasaka M, Nakamura M, Kamiya Y, Fujita H, Yoshioka D, Okubo M, Hirata I, et al. (2008a) Nrf2 gene promoter polymorphism and gastric carcinogenesis. *Hepatogastroenterology* **55**:750–754.

Arisawa T, Tahara T, Shibata T, Nagasaka M, Nakamura M, Kamiya Y, Fujita H, Yoshioka D, Okubo M, Sakata M, et al. (2008b) Nrf2 gene promoter polymorphism is associated with ulcerative colitis in a Japanese population. *Hepatogastroenterology* **55**:394–397.

Arlt A, Sebens S, Krebs S, Geismann C, Grossmann M, Kruse ML, Schreiber S, and Schäfer H (2013) Inhibition of the Nrf2 transcription factor by the alkaloid trigonelline renders pancreatic cancer cells more susceptible to apoptosis through decreased proteasomal gene expression and proteasome activity. *Oncogene* **32**: 4825–4835.

Artaud-Macari E, Goven D, Brayer S, Hamimi A, Besnard V, Marchal-Somme J, Ali ZE, Crestani B, Kerdine-Römer S, Boutten A, et al. (2013) Nuclear factor erythroid 2-related factor 2 nuclear translocation induces myofibroblastic dedifferentiation in idiopathic pulmonary fibrosis. *Antioxid Redox Signal* **18**:66–79.

Ashabi G, Khalaj L, Khodagholi F, Goudarzvand M, and Sarkaki A (2015) Pre-treatment with metformin activates Nrf2 antioxidant pathways and inhibits inflammatory responses through induction of AMPK after transient global cerebral ischemia. *Metab Brain Dis* **30**:747–754.

Attucks OC, Jasmer KJ, Hannink M, Kassis J, Zhong Z, Gupta S, Victory SF, Guzel M, Polisetti DR, Andrews R, et al. (2014) Induction of heme oxygenase I (HMOX1) by HPP-4382: a novel modulator of Bach1 activity. *PLoS One* **9**:e101044.

Aviello G and Knaus UG (2017) ROS in gastrointestinal inflammation: rescue or sabotage? *Br J Pharmacol* **174**:1704–1718.

Axelsson AS, Tubbs E, Mecham B, Chacko S, Nenonen HA, Tang Y, Fahey JW, Derry JMJ, Wollheim CB, Wierup N, et al. (2017) Sulforaphane reduces hepatic glucose production and improves glucose control in patients with type 2 diabetes. *Sci Transl Med* **9**:1–12.

Bahadoran Z, Mirmiran P, Hosseinpanah F, Rajab A, Asghari G, and Azizi F (2012) Broccoli sprouts powder could improve serum triglyceride and oxidized LDL/LDL-cholesterol ratio in type 2 diabetic patients: a randomized double-blind placebo-controlled clinical trial. *Diabetes Res Clin Pract* **96**:348–354.

Baillie JK, Arner E, Daub C, De Hoon M, Itoh M, Kawaji H, Lassmann T, Carninci P, Forrest AR, Hayashizaki Y, et al.; FANTOM Consortium (2017) Analysis of the human monocyte-derived macrophage transcriptome and response to lipopolysaccharide provides new insights into genetic aetiology of inflammatory bowel disease. *PLoS Genet* **13**:e1006641.

Baird L and Dinkova-Kostova AT (2013) Diffusion dynamics of the Keap1-Cullin3 interaction in single live cells. *Biochem Biophys Res Commun* **433**:58–65.

Banning A and Brigelius-Flohé R (2005) NF-kappaB, Nrf2, and HO-1 interplay in redox-regulated VCAM-1 expression. *Antioxid Redox Signal* **7**:889–899.

Barabási AL, Gulbahce N, and Loscalzo J (2011) Network medicine: a network-based approach to human disease. *Nat Rev Genet* **12**:56–68.

Batthyany CI and Lopez GV (2015) *Nitroalkene Tocopherols and Analogs Thereof for Use in the Treatment and Prevention of Inflammation Related Conditions*, Complexa, Radnor, PA.

Bauer PV and Duca FA (2016) Targeting the gastrointestinal tract to treat type 2 diabetes. *J Endocrinol* **230**:R95–R113.

Bergström P, von Otter M, Nilsson S, Nilsson AC, Nilsson M, Andersen PM, Hammarsten O, and Zetterberg H (2014) Association of NFE2L2 and KEAP1 haplotypes with amyotrophic lateral sclerosis. *Amyotroph Lateral Scler Frontotemporal Degener* **15**:130–137.

Bertrand HC, Schaap M, Baird L, Georgakopoulos ND, Fowkes A, Thiollier C, Kachi H, Dinkova-Kostova AT, and Wells G (2015) Design, synthesis, and evaluation of triazole derivatives that induce Nrf2 dependent gene products and inhibit the Keap1-Nrf2 protein-protein interaction. *J Med Chem* **58**:7186–7194.

Beurel E, Grieco SF, and Jope RS (2015) Glycogen synthase kinase-3 (GSK3): regulation, actions, and diseases. *Pharmacol Ther* **148**:114–131.

Bhatt JK, Thomas S, and Nanjan MJ (2012) Resveratrol supplementation improves glycemic control in type 2 diabetes mellitus. *Nutr Res* **32**:537–541.

Blewett MM, Xie J, Zaro BW, Backus KM, Altman A, Teijaro JR, and Cravatt BF (2016) Chemical proteomic map of dimethyl fumarate-sensitive cysteines in primary human T cells. *Sci Signal* **9**:rs10.

Bolaños JP (2016) Bioenergetics and redox adaptations of astrocytes to neuronal activity. *J Neurochem* **139** (Suppl 2):115–125.

Bourdonnay E, Morzadec C, Fardel O, and Vernhet L (2009) Redox-sensitive regulation of gene expression in human primary macrophages exposed to inorganic arsenic. *J Cell Biochem* **107**:537–547.

Bowie A and O'Neill LA (2000) Oxidative stress and nuclear factor-kappaB activation: a reassessment of the evidence in the light of recent discoveries. *Biochem Pharmacol* **59**:13–23.

Brasnyó P, Molnár GA, Mohás M, Markó L, Laczy B, Cseh J, Mikolás E, Szijártó IA, Mérei A, Halmai R, et al. (2011) Resveratrol improves insulin sensitivity, reduces oxidative stress and activates the Akt pathway in type 2 diabetic patients. *Br J Nutr* **106**:383–389.

Brennan MS, Matos MF, Richter KE, Li B, and Scannevin RH (2017) The NRF2 transcriptional target, OSGIN1, contributes to monomethyl fumarate-mediated cytoprotection in human astrocytes. *Sci Rep* **7**:42054.

Brüne B, Dehne N, Grossmann N, Jung M, Namgaladze D, Schmid T, von Knethen A, and Weigert A (2013) Redox control of inflammation in macrophages. *Antioxid Redox Signal* **19**:595–637.

Buendia I, Gómez-Rangel V, González-Lafuente L, Parada E, León R, Gameiro I, Michalska P, Laudon M, Egea J, and López MG (2015a) Neuroprotective mechanism of the novel melatonin derivative Neu-P11 in brain ischemia related models. *Neuropharmacology* **99**:187–195.

Buendia I, Michalska P, Navarro E, Gameiro I, Egea J, and León R (2016) Nrf2-ARE pathway: an emerging target against oxidative stress and neuroinflammation in neurodegenerative diseases. *Pharmacol Ther* **157**:84–104.

Buendia I, Navarro E, Michalska P, Gameiro I, Egea J, Abril S, López A, González-Lafuente L, López MG, and León R (2015b) New melatonin-cinnamate hybrids as multi-target drugs for neurodegenerative diseases: Nrf2-induction, antioxidant effect and neuroprotection. *Future Med Chem* **7**:1961–1969.

Cajaraville MP, Bebianno MJ, Blasco J, Porte C, Sarasquete C, and Viarengo A (2000) The use of biomarkers to assess the impact of pollution in coastal environments of the Iberian Peninsula: a practical approach. *Sci Total Environ* **247**: 295–311.

Cazanave SC, Wang X, Zhou H, Rahmani M, Grant S, Durrant DE, Klaassen CD, Yamamoto M, and Sanyal AJ (2014) Degradation of Keap1 activates BH3-only proteins Bim and PUMA during hepatocyte lipoapoptosis. *Cell Death Differ* **21**: 1303–1312.

Cescon DW, She D, Sakashita S, Zhu CQ, Pintilie M, Shepherd FA, and Tsao MS (2015) NRF2 pathway activation and adjuvant chemotherapy benefit in lung squamous cell carcinoma. *Clin Cancer Res* **21**:2499–2505.

Chen H, Assmann JC, Krenz A, Rahman M, Grimm M, Karsten CM, Köhl J, Offermanns S, Wettschureck N, and Schwaninger M (2014) Hydroxycarboxylic acid receptor 2 mediates dimethyl fumarate's protective effect in EAE. *J Clin Invest* **124**:2188–2192.

Chen J, Yu Y, Ji T, Ma R, Chen M, Li G, Li F, Ding Q, Kang Q, Huang D, et al. (2016) Clinical implication of Keap1 and phosphorylated Nrf2 expression in hepatocellular carcinoma. *Cancer Med* **5**:2678–2687.

Chen W, Sun Z, Wang XJ, Jiang T, Huang Z, Fang D, and Zhang DD (2009) Direct interaction between Nrf2 and p21(Cip1/WAF1) upregulates the Nrf2-mediated antioxidant response. *Mol Cell* **34**:663–673.

Chen Y, Inoyama D, Kong AN, Beamer LJ, and Hu L (2011) Kinetic analyses of Keap1-Nrf2 interaction and determination of the minimal Nrf2 peptide sequence required for Keap1 binding using surface plasmon resonance. *Chem Biol Drug Des* **78**:1014–1021.

Chen YC, Wu YR, Wu YC, Lee-Chen GJ, and Chen CM (2013) Genetic analysis of NFE2L2 promoter variation in Taiwanese Parkinson's disease. *Parkinsonism Relat Disord* **19**:247–250.

Chin MP, Reisman SA, Bakris GL, O'Grady M, Linde PG, McCullough PA, Packham D, Vaziri ND, Ward KW, Warnock DG, et al. (2014) Mechanisms contributing to adverse cardiovascular events in patients with type 2 diabetes mellitus and stage 4 chronic kidney disease treated with bardoxolone methyl. *Am J Nephrol* **39**: 499–508.

Chiu CT, Wang Z, Hunsberger JG, and Chuang DM (2013) Therapeutic potential of mood stabilizers lithium and valproic acid: beyond bipolar disorder. *Pharmacol Rev* **65**:105–142.

Cho HY and Kleeberger SR (2010) Nrf2 protects against airway disorders. *Toxicol Appl Pharmacol* **244**:43–56.

Cho HY, Marzec J, and Kleeberger SR (2015) Functional polymorphisms in Nrf2: implications for human disease. *Free Radic Biol Med* **88** (Pt B):362–372.

Cho HY, Reddy SP, Yamamoto M, and Kleeberger SR (2004) The transcription factor NRF2 protects against pulmonary fibrosis. *FASEB J* **18**:1258–1260.
Cho YE, Moon PG, Lee JE, Singh TS, Kang W, Lee HC, Lee MH, Kim SH, and Baek MC (2013) Integrative analysis of proteomic and transcriptomic data for identification of pathways related to simvastatin-induced hepatotoxicity. *Proteomics* **13**: 1257–1275.
Chowdhry S, Zhang Y, McMahon M, Sutherland C, Cuadrado A, and Hayes JD (2013) Nrf2 is controlled by two distinct β-TrCP recognition motifs in its Neh6 domain, one of which can be modulated by GSK-3 activity. *Oncogene* **32**:3765–3781.
Christou H, Morita T, Hsieh CM, Koike H, Arkonac B, Perrella MA, and Kourembanas S (2000) Prevention of hypoxia-induced pulmonary hypertension by enhancement of endogenous heme oxygenase-1 in the rat. *Circ Res* **86**: 1224–1229.
Chuengsamarn S, Rattanamongkolgul S, Phonrat B, Tungtrongchitr R, and Jirawatnotai S (2014) Reduction of atherogenic risk in patients with type 2 diabetes by curcuminoid extract: a randomized controlled trial. *J Nutr Biochem* **25**:144–150.
Ci X, Zhou J, Lv H, Yu Q, Peng L, and Hua S (2017) Betulin exhibits anti-inflammatory activity in LPS-stimulated macrophages and endotoxin-shocked mice through an AMPK/AKT/Nrf2-dependent mechanism. *Cell Death Dis* **8**:e2798.
Cleasby A, Yon J, Day PJ, Richardson C, Tickle IJ, Williams PA, Callahan JF, Carr R, Concha N, Kerns JK, et al. (2014) Structure of the BTB domain of Keap1 and its interaction with the triterpenoid antagonist CDDO. *PLoS One* **9**:e98896.
Comandini A, Marzano V, Curradi G, Federici G, Urbani A, and Saltini C (2010) Markers of anti-oxidant response in tobacco smoke exposed subjects: a data-mining review. *Pulm Pharmacol Ther* **23**:482–492.
Córdova EJ, Velázquez-Cruz R, Centeno F, Baca V, and Orozco L (2010) The NRF2 gene variant, -653G/A, is associated with nephritis in childhood-onset systemic lupus erythematosus. *Lupus* **19**:1237–1242.
Croze E, Yamaguchi KD, Knappertz V, Reder AT, and Salamon H (2013) Interferon-beta-1b-induced short- and long-term signatures of treatment activity in multiple sclerosis. *Pharmacogenomics J* **13**:443–451.
Cuadrado A (2015) Structural and functional characterization of Nrf2 degradation by glycogen synthase kinase 3/β-TrCP. *Free Radic Biol Med* **88** (Pt B):147–157.
Cuadrado A, Martín-Moldes Z, Ye J, and Lastres-Becker I (2014) Transcription factors NRF2 and NF-κB are coordinated effectors of the Rho family, GTP-binding protein RAC1 during inflammation. *J Biol Chem* **289**:15244–15258.
Cuadrado A, Moreno-Murciano P, and Pedraza-Chaverri J (2009) The transcription factor Nrf2 as a new therapeutic target in Parkinson's disease. *Expert Opin Ther Targets* **13**:319–329.
Cui Y, Wang Q, Li X, and Zhang X (2013) Experimental nonalcoholic fatty liver disease in mice leads to cytochrome p450 2a5 upregulation through nuclear factor erythroid 2-like 2 translocation. *Redox Biol* **1**:433–440.
Datta S, Kundu S, Ghosh P, De S, Ghosh A, and Chatterjee M (2014) Correlation of oxidant status with oxidative tissue damage in patients with rheumatoid arthritis. *Clin Rheumatol* **33**:1557–1564.
de la Vega MR, Dodson M, Gross C, Manzour H, Lantz RC, Chapman E, Wang T, Black SM, Garcia JG, and Zhang DD (2016) Role of Nrf2 and autophagy in acute lung injury. *Curr Pharmacol Rep* **2**:91–101.
DeNicola GM, Karreth FA, Humpton TJ, Gopinathan A, Wei C, Frese K, Mangal D, Yu KH, Yeo CJ, Calhoun ES, et al. (2011) Oncogene-induced Nrf2 transcription promotes ROS detoxification and tumorigenesis. *Nature* **475**:106–109.
de Zeeuw D, Akizawa T, Audhya P, Bakris GL, Chin M, Christ-Schmidt H, Goldsberry A, Houser M, Krauth M, Lambers Heerspink HJ, et al.; BEACON Trial Investigators (2013) Bardoxolone methyl in type 2 diabetes and stage 4 chronic kidney disease. *N Engl J Med* **369**:2492–2503.
Diotallevi M, Checconi P, Palamara AT, Celestino I, Coppo L, Holmgren A, Abbas K, Peyrot F, Mengozzi M, and Ghezzi P (2017) Glutathione fine-tunes the innate immune response toward antiviral pathways in a macrophage cell line independently of its antioxidant properties. *Front Immunol* **8**:1239.
Duran CG, Burbank AJ, Mills KH, Duckworth HR, Aleman MM, Kesic MJ, Peden DB, Pan Y, Zhou H, and Hernandez ML (2016) A proof-of-concept clinical study examining the NRF2 activator sulforaphane against neutrophilic airway inflammation. *Respir Res* **17**:89.
Eades G, Yang M, Yao Y, Zhang Y, and Zhou Q (2011) miR-200a regulates Nrf2 activation by targeting Keap1 mRNA in breast cancer cells. *J Biol Chem* **286**: 40725–40733.
Egea J, Buendia I, Parada E, Navarro E, Rada P, Cuadrado A, López MG, García AG, and León R (2015) Melatonin-sulforaphane hybrid ITH12674 induces neuroprotection in oxidative stress conditions by a 'drug-prodrug' mechanism of action. *Br J Pharmacol* **172**:1807–1821.
Ellrichmann G, Petrasch-Parwez E, Lee DH, Reick C, Arning L, Saft C, Gold R, and Linker RA (2011) Efficacy of fumaric acid esters in the R6/2 and YAC128 models of Huntington's disease. *PLoS One* **6**:e16172.
El-Mir MY, Nogueira V, Fontaine E, Avéret N, Rigoulet M, and Leverve X (2000) Dimethylbiguanide inhibits cell respiration via an indirect effect targeted on the respiratory chain complex I. *J Biol Chem* **275**:223–228.
Eminel S, Jin N, Rostami M, Dibbert S, Mrowietz U, and Suhrkamp I (2017) Dimethyl- and monomethylfumarate regulate indoleamine 2,3-dioxygenase (IDO) activity in human immune cells. *Exp Dermatol* **26**:685–690.
Emmink BL, Verheem A, Van Houdt WJ, Steller EJ, Govaert KM, Pham TV, Piersma SR, Borel Rinkes IH, Jimenez CR, and Kranenburg O (2013) The secretome of colon cancer stem cells contains drug-metabolizing enzymes. *J Proteomics* **91**:84–96.
Evans MD, Cooke MS, Akil M, Samanta A, and Lunec J (2000) Aberrant processing of oxidative DNA damage in systemic lupus erythematosus. *Biochem Biophys Res Commun* **273**:894–898.
Fagone P, Patti F, Mangano K, Mammana S, Coco M, Touil-Boukoffa C, Chikovani T, Di Marco R, and Nicoletti F (2013) Heme oxygenase-1 expression in peripheral blood mononuclear cells correlates with disease activity in multiple sclerosis. *J Neuroimmunol* **261**:82–86.
Finkelstein R, Fraser RS, Ghezzo H, and Cosio MG (1995) Alveolar inflammation and its relation to emphysema in smokers. *Am J Respir Crit Care Med* **152**:1666–1672.
Fox RJ, Miller DH, Phillips JT, Hutchinson M, Havrdova E, Kita M, Yang M, Raghupathi K, Novas M, Sweetser MT, et al.; CONFIRM Study Investigators (2012) Placebo-controlled phase 3 study of oral BG-12 or glatiramer in multiple sclerosis. *N Engl J Med* **367**:1087–1097.
Freitas AE, Egea J, Buendia I, Gómez-Rangel V, Parada E, Navarro E, Casas AI, Wojnicz A, Ortiz JA, Cuadrado A, et al. (2016) Agmatine, by improving neuroplasticity markers and inducing Nrf2, prevents corticosterone-induced depressive-like behavior in mice. *Mol Neurobiol* **53**:3030–3045.
Frijhoff J, Winyard PG, Zarkovic N, Davies SS, Stocker R, Cheng D, Knight AR, Taylor EL, Oettrich J, Ruskovska T, et al. (2015) Clinical relevance of biomarkers of oxidative stress. *Antioxid Redox Signal* **23**:1144–1170.
Frostegård J, Svenungsson E, Wu R, Gunnarsson I, Lundberg IE, Klareskog L, Hörkkö S, and Witztum JL (2005) Lipid peroxidation is enhanced in patients with systemic lupus erythematosus and is associated with arterial and renal disease manifestations. *Arthritis Rheum* **52**:192–200.
Gao J, Chang MT, Johnsen HC, Gao SP, Sylvester BE, Sumer SO, Zhang H, Solit DB, Taylor BS, Schultz N, et al. (2017) 3D clusters of somatic mutations in cancer reveal numerous rare mutations as functional targets. *Genome Med* **9**:4.
Ghanim H, Sia CL, Korzeniewski K, Lohano T, Abuaysheh S, Marumganti A, Chaudhuri A, and Dandona P (2011) A resveratrol and polyphenol preparation suppresses oxidative and inflammatory stress response to a high-fat, high-carbohydrate meal. *J Clin Endocrinol Metab* **96**:1409–1414.
Ghezzi P, Floridi L, Boraschi D, Cuadrado A, Manda G, Levic S, D'Acquisto F, Hamilton A, Athersuch TJ, and Selley L (2017a) Oxidative stress and inflammation induced by environmental and psychological stressors: a biomarker perspective. *Antioxid Redox Signal* [published ahead of print].
Ghezzi P, Jaquet V, Marcucci F, and Schmidt HHHW (2017b) The oxidative stress theory of disease: levels of evidence and epistemological aspects. *Br J Pharmacol* **174**:1784–1796.
Ghoreschi K, Brück J, Kellerer C, Deng C, Peng H, Rothfuss O, Hussain RZ, Gocke AR, Respa A, Glocova I, et al. (2011) Fumarates improve psoriasis and multiple sclerosis by inducing type II dendritic cells. *J Exp Med* **208**:2291–2303.
Gillard GO, Collette B, Anderson J, Chao J, Scannevin RH, Huss DJ, and Fontenot JD (2015) DMF, but not other fumarates, inhibits NF-κB activity in vitro in an Nrf2-independent manner. *J Neuroimmunol* **283**:74–85.
Goh KI, Cusick ME, Valle D, Childs B, Vidal M, and Barabási AL (2007) The human disease network. *Proc Natl Acad Sci USA* **104**:8685–8690.
Gold R, Kappos L, Arnold DL, Bar-Or A, Giovannoni G, Selmaj K, Tornatore C, Sweetser MT, Yang M, Sheikh SI, et al.; DEFINE Study Investigators (2012) Placebo-controlled phase 3 study of oral BG-12 for relapsing multiple sclerosis. *N Engl J Med* **367**:1098–1107.
Gonzalez-Donquiles C, Alonso-Molero J, Fernandez-Villa T, Vilorio-Marqués L, Molina AJ, and Martín V (2017) The NRF2 transcription factor plays a dual role in colorectal cancer: a systematic review. *PLoS One* **12**:e0177549.
Goven D, Boutten A, Leçon-Malas V, Marchal-Sommé J, Amara N, Crestani B, Fournier M, Lesèche G, Soler P, Boczkowski J, et al. (2008) Altered Nrf2/Keap1-Bach1 equilibrium in pulmonary emphysema. *Thorax* **63**:916–924.
Griendling KK and FitzGerald GA (2003a) Oxidative stress and cardiovascular injury: part I: basic mechanisms and in vivo monitoring of ROS. *Circulation* **108**: 1912–1916.
Griendling KK and FitzGerald GA (2003b) Oxidative stress and cardiovascular injury: part II: animal and human studies. *Circulation* **108**:2034–2040.
Guan CP, Zhou MN, Xu AE, Kang KF, Liu JF, Wei XD, Li YW, Zhao DK, and Hong WS (2008) The susceptibility to vitiligo is associated with NF-E2-related factor2 (Nrf2) gene polymorphisms: a study on Chinese Han population. *Exp Dermatol* **17**: 1059–1062.
Guney E, Menche J, Vidal M, and Barábasi AL (2016) Network-based in silico drug efficacy screening. *Nat Commun* **7**:10331.
Guney E and Oliva B (2014) Analysis of the robustness of network-based disease-gene prioritization methods reveals redundancy in the human interactome and functional diversity of disease-genes. *PLoS One* **9**:e94686.
Han SJ, Ahn Y, Park I, Zhang Y, Kim I, Kim HW, Ku CS, Chay KO, Yang SY, Ahn BW, et al. (2015) Assay of the redox state of the tumor suppressor PTEN by mobility shift. *Methods* **77–78**:58–62.
Hancock R, Schaap M, Pfister H, and Wells G (2013) Peptide inhibitors of the Keap1-Nrf2 protein-protein interaction with improved binding and cellular activity. *Org Biomol Chem* **11**:3553–3557.
Harder B, Tian W, La Clair JJ, Tan AC, Ooi A, Chapman E, and Zhang DD (2017) Brusatol overcomes chemoresistance through inhibition of protein translation. *Mol Carcinog* **56**:1493–1500.
Hardie DG (2004) The AMP-activated protein kinase pathway–new players upstream and downstream. *J Cell Sci* **117**:5479–5487.
Harrison D, Griendling KK, Landmesser U, Hornig B, and Drexler H (2003) Role of oxidative stress in atherosclerosis. *Am J Cardiol* **91**:7A–11A.
Hart PC, Ratti BA, Mao M, Ansenberger-Fricano K, Shajahan-Haq AN, Tyner AL, Minshall RD, and Bonini MG (2016) Caveolin-1 regulates cancer cell metabolism via scavenging Nrf2 and suppressing MnSOD-driven glycolysis. *Oncotarget* **7**: 308–322.
Harvey CJ, Thimmulappa RK, Sethi S, Kong X, Yarmus L, Brown RH, Feller-Kopman D, Wise R, and Biswal S (2011) Targeting Nrf2 signaling improves bacterial clearance by alveolar macrophages in patients with COPD and in a mouse model. *Sci Transl Med* **3**:78ra32.
Hast BE, Goldfarb D, Mulvaney KM, Hast MA, Siesser PF, Yan F, Hayes DN, and Major MB (2013) Proteomic analysis of ubiquitin ligase KEAP1 reveals associated proteins that inhibit NRF2 ubiquitination. *Cancer Res* **73**:2199–2210.
Hayes JD and Dinkova-Kostova AT (2014) The Nrf2 regulatory network provides an interface between redox and intermediary metabolism. *Trends Biochem Sci* **39**: 199–218.

Heckman-Stoddard BM, DeCensi A, Sahasrabuddhe VV, and Ford LG (2017) Repurposing metformin for the prevention of cancer and cancer recurrence. *Diabetologia* **60**:1639–1647.

Hidalgo CA, Blumm N, Barabási AL, and Christakis NA (2009) A dynamic network approach for the study of human phenotypes. *PLOS Comput Biol* **5**:e1000353.

Hong DS, Kurzrock R, Supko JG, He X, Naing A, Wheler J, Lawrence D, Eder JP, Meyer CJ, Ferguson DA, et al. (2012) A phase I first-in-human trial of bardoxolone methyl in patients with advanced solid tumors and lymphomas. *Clin Cancer Res* **18**:3396–3406.

Hopkins PN, Wu LL, Hunt SC, James BC, Vincent GM, and Williams RR (1996) Higher serum bilirubin is associated with decreased risk for early familial coronary artery disease. *Arterioscler Thromb Vasc Biol* **16**:250–255.

Houessinon A, François C, Sauzay C, Louandre C, Mongelard G, Godin C, Bodeau S, Takahashi S, Saidak Z, Gutierrez L, et al. (2016) Metallothionein-1 as a biomarker of altered redox metabolism in hepatocellular carcinoma cells exposed to sorafenib. *Mol Cancer* **15**:38.

Houghton CA, Fassett RG, and Coombes JS (2016) Sulforaphane and other nutrigenomic Nrf2 activators: can the clinician's expectation be matched by the reality? *Oxid Med Cell Longev* **2016**:7857186.

Hu L, Magesh S, Chen L, Wang L, Lewis TA, Chen Y, Khodier C, Inoyama D, Beamer LJ, Emge TJ, et al. (2013) Discovery of a small-molecule inhibitor and cellular probe of Keap1-Nrf2 protein-protein interaction. *Bioorg Med Chem Lett* **23**: 3039–3043.

Hua CC, Chang LC, Tseng JC, Chu CM, Liu YC, and Shieh WB (2010) Functional haplotypes in the promoter region of transcription factor Nrf2 in chronic obstructive pulmonary disease. *Dis Markers* **28**:185–193.

Hur W and Gray NS (2011) Small molecule modulators of antioxidant response pathway. *Curr Opin Chem Biol* **15**:162–173.

Hwang AR, Han JH, Lim JH, Kang YJ, and Woo CH (2017) Fluvastatin inhibits AGE-induced cell proliferation and migration via an ERK5-dependent Nrf2 pathway in vascular smooth muscle cells. *PLoS One* **12**:e0178278.

Innamorato NG, Rojo AI, García-Yagüe AJ, Yamamoto M, de Ceballos ML, and Cuadrado A (2008) The transcription factor Nrf2 is a therapeutic target against brain inflammation. *J Immunol* **181**:680–689.

Inoyama D, Chen Y, Huang X, Beamer LJ, Kong AN, and Hu L (2012) Optimization of fluorescently labeled Nrf2 peptide probes and the development of a fluorescence polarization assay for the discovery of inhibitors of Keap1-Nrf2 interaction. *J Biomol Screen* **17**:435–447.

Iorio F, Isacchi A, di Bernardo D, and Brunetti-Pierri N (2010) Identification of small molecules enhancing autophagic function from drug network analysis. *Autophagy* **6**:1204–1205.

Ishii T and Mann GE (2014) Redox status in mammalian cells and stem cells during culture in vitro: critical roles of Nrf2 and cystine transporter activity in the maintenance of redox balance. *Redox Biol* **2**:786–794.

Jang HJ, Hong EM, Kim M, Kim JH, Jang J, Park SW, Byun HW, Koh DH, Choi MH, Kae SH, et al. (2016) Simvastatin induces heme oxygenase-1 via NF-E2-related factor 2 (Nrf2) activation through ERK and PI3K/Akt pathway in colon cancer. *Oncotarget* **7**:46219–46229.

Jansen T, Hortmann M, Oelze M, Opitz B, Steven S, Schell R, Knorr M, Karbach S, Schuhmacher S, Wenzel P, et al. (2010) Conversion of biliverdin to bilirubin by biliverdin reductase contributes to endothelial cell protection by heme oxygenase-1-evidence for direct and indirect antioxidant actions of bilirubin. *J Mol Cell Cardiol* **49**:186–195.

Jay D, Hitomi H, and Griendling KK (2006) Oxidative stress and diabetic cardiovascular complications. *Free Radic Biol Med* **40**:183–192.

Jazwa A, Rojo AI, Innamorato NG, Hesse M, Fernández-Ruiz J, and Cuadrado A (2011) Pharmacological targeting of the transcription factor Nrf2 at the basal ganglia provides disease modifying therapy for experimental parkinsonism. *Antioxid Redox Signal* **14**:2347–2360.

Jiang T, Huang Z, Lin Y, Zhang Z, Fang D, and Zhang DD (2010) The protective role of Nrf2 in streptozotocin-induced diabetic nephropathy. *Diabetes* **59**:850–860.

Jiang T, Tian F, Zheng H, Whitman SA, Lin Y, Zhang Z, Zhang N, and Zhang DD (2014a) Nrf2 suppresses lupus nephritis through inhibition of oxidative injury and the NF-κB-mediated inflammatory response. *Kidney Int* **85**:333–343.

Jiang ZY, Lu MC, Xu LL, Yang TT, Xi MY, Xu XL, Guo XK, Zhang XJ, You QD, and Sun HP (2014b) Discovery of potent Keap1-Nrf2 protein-protein interaction inhibitor based on molecular binding determinants analysis [published correction appears in *J Med Chem* (2014) 57:4406]. *J Med Chem* **57**: 2736–2745.

Jiang ZY, Lu MC, and You QD (2016) Discovery and development of Kelch-like ECH-associated protein 1: Nuclear factor erythroid 2-related factor 2 (KEAP1:NRF2) protein-protein interaction inhibitors: achievements, challenges, and future directions. *J Med Chem* **59**:10837–10858.

Jiménez-Osorio AS, González-Reyes S, García-Niño WR, Moreno-Macías H, Rodríguez-Arellano ME, Vargas-Alarcón G, Zúñiga J, Barquera R, Pedraza-Chaverri J, Meza-Espinoza JP, et al. (2017) Corrigendum to "association of nuclear factor-erythroid 2-related factor 2, thioredoxin interacting protein, and heme oxygenase-1 gene polymorphisms with diabetes and obesity in Mexican patients." *Oxid Med Cell Longev* **2017**:7543194.

Jiménez-Osorio AS, Picazo A, González-Reyes S, Barrera-Oviedo D, Rodríguez-Arellano ME, and Pedraza-Chaverri J (2014) Nrf2 and redox status in prediabetic and diabetic patients. *Int J Mol Sci* **15**:20290–20305.

Jnoff E, Albrecht C, Barker JJ, Barker O, Beaumont E, Bromidge S, Brookfield F, Brooks M, Bubert C, Ceska T, et al. (2014) Binding mode and structure-activity relationships around direct inhibitors of the Nrf2-Keap1 complex. *ChemMedChem* **9**:699–705.

Jo C, Gundemir S, Pritchard S, Jin YN, Rahman I, and Johnson GV (2014) Nrf2 reduces levels of phosphorylated tau protein by inducing autophagy adaptor protein NDP52. *Nat Commun* **5**:3496.

Johnson DA, Amirahmadi S, Ward C, Fabry Z, and Johnson JA (2010) The absence of the pro-antioxidant transcription factor Nrf2 exacerbates experimental autoimmune encephalomyelitis. *Toxicol Sci* **114**:237–246.

Johnson DA and Johnson JA (2015) Nrf2–a therapeutic target for the treatment of neurodegenerative diseases. *Free Radic Biol Med* **88** (Pt B):253–267.

Johnson NM, Egner PA, Baxter VK, Sporn MB, Wible RS, Sutter TR, Groopman JD, Kensler TW, and Roebuck BD (2014) Complete protection against aflatoxin B(1)-induced liver cancer with a triterpenoid: DNA adduct dosimetry, molecular signature, and genotoxicity threshold. *Cancer Prev Res (Phila)* **7**:658–665.

Jones RM, Desai C, Darby TM, Luo L, Wolfarth AA, Scharer CD, Ardita CS, Reedy AR, Keebaugh ES, and Neish AS (2015) Lactobacilli modulate epithelial cytoprotection through the Nrf2 pathway. *Cell Reports* **12**:1217–1225.

Jung KA, Lee S, and Kwak MK (2017) NFE2L2/NRF2 activity is linked to mitochondria and AMP-activated protein kinase signaling in cancers through miR-181c/mitochondria-encoded cytochrome c oxidase regulation. *Antioxid Redox Signal* **27**:945–961.

Kaidery NA, Banerjee R, Yang L, Smirnova NA, Hushpulian DM, Liby KT, Williams CR, Yamamoto M, Kensler TW, Ratan RR, et al. (2013) Targeting Nrf2-mediated gene transcription by extremely potent synthetic triterpenoids attenuates dopaminergic neurotoxicity in the MPTP mouse model of Parkinson's disease. *Antioxid Redox Signal* **18**:139–157.

Kaisar MA, Villalba H, Prasad S, Liles T, Sifat AE, Sajja RK, Abbruscato TJ, and Cucullo L (2017) Offsetting the impact of smoking and e-cigarette vaping on the cerebrovascular system and stroke injury: is Metformin a viable countermeasure? *Redox Biol* **13**:353–362.

Kastrati I, Siklos MI, Calderon-Gierszal EL, El-Shennawy L, Georgieva G, Thayer EN, Thatcher GR, and Frasor J (2016) Dimethyl fumarate inhibits the nuclear factor κB pathway in breast cancer cells by covalent modification of p65 protein. *J Biol Chem* **291**:3639–3647.

Kelleni MT, Amin EF, and Abdelrahman AM (2015) Effect of metformin and sitagliptin on doxorubicin-induced cardiotoxicity in rats: impact of oxidative stress, inflammation, and apoptosis. *J Toxicol* **2015**:424813.

Kensler TW, Egner PA, Agyeman AS, Visvanathan K, Groopman JD, Chen JG, Chen TY, Fahey JW, and Talalay P (2013) Keap1-nrf2 signaling: a target for cancer prevention by sulforaphane. *Top Curr Chem* **329**:163–177.

Khan I, Tantray MA, Alam MS, and Hamid H (2017) Natural and synthetic bioactive inhibitors of glycogen synthase kinase. *Eur J Med Chem* **125**:464–477.

Kim JE, You DJ, Lee C, Ahn C, Seong JY, and Hwang JI (2010a) Suppression of NF-kappaB signaling by KEAP1 regulation of IKKbeta activity through autophagic degradation and inhibition of phosphorylation. *Cell Signal* **22**:1645–1654.

Kim T, Kim YJ, Han IH, Lee D, Ham J, Kang KS, and Lee JW (2015) The synthesis of sulforaphane analogues and their protection effect against cisplatin induced cytotoxicity in kidney cells. *Bioorg Med Chem Lett* **25**:62–66.

Kim YR, Oh JE, Kim MS, Kang MR, Park SW, Han JY, Eom HS, Yoo NJ, and Lee SH (2010b) Oncogenic NRF2 mutations in squamous cell carcinomas of oesophagus and skin. *J Pathol* **220**:446–451.

Kitagishi Y and Matsuda S (2013) Redox regulation of tumor suppressor PTEN in cancer and aging (Review). *Int J Mol Med* **31**:511–515.

Kitsak M, Sharma A, Menche J, Guney E, Ghiassian SD, Loscalzo J, and Barabási AL (2016) Tissue specificity of human disease module. *Sci Rep* **6**:35241.

Kobayashi EH, Suzuki T, Funayama R, Nagashima T, Hayashi M, Sekine H, Tanaka N, Moriguchi T, Motohashi H, Nakayama K, et al. (2016) Nrf2 suppresses macrophage inflammatory response by blocking proinflammatory cytokine transcription. *Nat Commun* **7**:11624.

Kocer D, Bayram F, and Diri H (2014) The effects of metformin on endothelial dysfunction, lipid metabolism and oxidative stress in women with polycystic ovary syndrome. *Gynecol Endocrinol* **30**:367–371.

Komatsu M, Kurokawa H, Waguri S, Taguchi K, Kobayashi A, Ichimura Y, Sou YS, Ueno I, Sakamoto A, Tong KI, et al. (2010) The selective autophagy substrate p62 activates the stress responsive transcription factor Nrf2 through inactivation of Keap1. *Nat Cell Biol* **12**:213–223.

Kong X, Thimmulappa R, Craciun F, Harvey C, Singh A, Kombairaju P, Reddy SP, Remick D, and Biswal S (2011) Enhancing Nrf2 pathway by disruption of Keap1 in myeloid leukocytes protects against sepsis. *Am J Respir Crit Care Med* **184**: 928–938.

Kruger AL, Peterson SJ, Schwartzman ML, Fusco H, McClung JA, Weiss M, Shenouda S, Goodman AI, Goligorsky MS, Kappas A, et al. (2006) Up-regulation of heme oxygenase provides vascular protection in an animal model of diabetes through its antioxidant and antiapoptotic effects. *J Pharmacol Exp Ther* **319**: 1144–1152.

Kruse ML, Friedrich M, Arlt A, Röcken C, Egberts JH, Sebens S, and Schäfer H (2016) Colonic lamina propria inflammatory cells from patients with IBD induce the nuclear factor-E2 related factor-2 thereby leading to greater proteasome activity and apoptosis protection in human colonocytes. *Inflamm Bowel Dis* **22**: 2593–2606.

Kuang X, Scofield VL, Yan M, Stoica G, Liu N, and Wong PK (2009) Attenuation of oxidative stress, inflammation and apoptosis by minocycline prevents retrovirus-induced neurodegeneration in mice. *Brain Res* **1286**:174–184.

Kurinna S and Werner S (2015) NRF2 and microRNAs: new but awaited relations. *Biochem Soc Trans* **43**:595–601.

Kwak JY, Takeshige K, Cheung BS, and Minakami S (1991) Bilirubin inhibits the activation of superoxide-producing NADPH oxidase in a neutrophil cell-free system. *Biochim Biophys Acta* **1076**:369–373.

Lamb J, Crawford ED, Peck D, Modell JW, Blat IC, Wrobel MJ, Lerner J, Brunet JP, Subramanian A, Ross KN, et al. (2006) The connectivity map: using gene-expression signatures to connect small molecules, genes, and disease. *Science* **313**: 1929–1935.

Lastres-Becker I, García-Yagüe AJ, Scannevin RH, Casarejos MJ, Kügler S, Rábano A, and Cuadrado A (2016) Repurposing the NRF2 activator dimethyl fumarate as

therapy against synucleinopathy in Parkinson's disease. *Antioxid Redox Signal* **25**: 61–77.
Lastres-Becker I, Innamorato NG, Jaworski T, Rábano A, Kügler S, Van Leuven F, and Cuadrado A (2014) Fractalkine activates NRF2/NFE2L2 and heme oxygenase 1 to restrain tauopathy-induced microgliosis. *Brain* **137**:78–91.
Lastres-Becker I, Ulusoy A, Innamorato NG, Sahin G, Rábano A, Kirik D, and Cuadrado A (2012) α-Synuclein expression and Nrf2 deficiency cooperate to aggravate protein aggregation, neuronal death and inflammation in early-stage Parkinson's disease. *Hum Mol Genet* **21**:3173–3192.
Lee D, Xu IM, Chiu DK, Lai RK, Tse AP, Lan Li L, Law CT, Tsang FH, Wei LL, Chan CY, et al. (2017) Folate cycle enzyme MTHFD1L confers metabolic advantages in hepatocellular carcinoma. *J Clin Invest* **127**:1856–1872.
Lee DF, Kuo HP, Liu M, Chou CK, Xia W, Du Y, Shen J, Chen CT, Huo L, Hsu MC, et al. (2009) KEAP1 E3 ligase-mediated downregulation of NF-kappaB signaling by targeting IKKbeta. *Mol Cell* **36**:131–140.
Lee SR, Yang KS, Kwon J, Lee C, Jeong W, and Rhee SG (2002) Reversible inactivation of the tumor suppressor PTEN by H2O2. *J Biol Chem* **277**:20336–20342.
Li B, Cui W, Liu J, Li R, Liu Q, Xie XH, Ge XL, Zhang J, Song XJ, Wang Y, et al. (2013) Sulforaphane ameliorates the development of experimental autoimmune encephalomyelitis by antagonizing oxidative stress and Th17-related inflammation in mice. *Exp Neurol* **250**:239–249.
Li J, Stein TD, and Johnson JA (2004) Genetic dissection of systemic autoimmune disease in Nrf2-deficient mice. *Physiol Genomics* **18**:261–272.
Licht-Mayer S, Wimmer I, Traffehn S, Metz I, Brück W, Bauer J, Bradl M, and Lassmann H (2015) Cell type-specific Nrf2 expression in multiple sclerosis lesions. *Acta Neuropathol* **130**:263–277.
Limonciel A and Jennings P (2014) A review of the evidence that ochratoxin A is an Nrf2 inhibitor: implications for nephrotoxicity and renal carcinogenicity. *Toxins (Basel)* **6**:371–379.
Lin CH, Lin HI, Chen ML, Lai TT, Cao LP, Farrer MJ, Wu RM, and Chien CT (2016) Lovastatin protects neurite degeneration in LRRK2-G2019S parkinsonism through activating the Akt/Nrf pathway and inhibiting GSK3β activity. *Hum Mol Genet* **25**: 1965–1978.
Lin SX, Lisi L, Dello Russo C, Polak PE, Sharp A, Weinberg G, Kalinin S, and Feinstein DL (2011) The anti-inflammatory effects of dimethyl fumarate in astrocytes involve glutathione and haem oxygenase-1. *ASN Neuro* **3**:75–84.
Lin W, Wu RT, Wu T, Khor TO, Wang H, and Kong AN (2008) Sulforaphane suppressed LPS-induced inflammation in mouse peritoneal macrophages through Nrf2 dependent pathway. *Biochem Pharmacol* **76**:967–973.
Linker RA, Lee DH, Ryan S, van Dam AM, Conrad R, Bista P, Zeng W, Hronowsky X, Buko A, Chollate S, et al. (2011) Fumaric acid esters exert neuroprotective effects in neuroinflammation via activation of the Nrf2 antioxidant pathway. *Brain* **134**: 678–692.
Liu GH, Qu J, and Shen X (2008) NF-kappaB/p65 antagonizes Nrf2-ARE pathway by depriving CBP from Nrf2 and facilitating recruitment of HDAC3 to MafK. *Biochim Biophys Acta* **1783**:713–727.
Liu TS, Pei YH, Peng YP, Chen J, Jiang SS, and Gong JB (2014) Oscillating high glucose enhances oxidative stress and apoptosis in human coronary artery endothelial cells. *J Endocrinol Invest* **37**:645–651.
Lo SC, Li X, Henzl MT, Beamer LJ, and Hannink M (2006) Structure of the Keap1: Nrf2 interface provides mechanistic insight into Nrf2 signaling. *EMBO J* **25**: 3605–3617.
LoGerfo A, Chico L, Borgia L, Petrozzi L, Rocchi A, D'Amelio A, Carlesi C, Caldarazzo Ienco E, Mancuso M, and Siciliano G (2014) Lack of association between nuclear factor erythroid-derived 2-like 2 promoter gene polymorphisms and oxidative stress biomarkers in amyotrophic lateral sclerosis patients. *Oxid Med Cell Longev* **2014**:432626.
Lu K, Alcivar AL, Ma J, Foo TK, Zywea S, Mahdi A, Huo Y, Kensler TW, Gatza ML, and Xia B (2017) NRF2 induction supporting breast cancer cell survival is enabled by oxidative stress-induced DPP3-KEAP1 interaction. *Cancer Res* **77**: 2881–2892.
Lu MC, Jiao Q, Liu T, Tan SJ, Zhou HS, You QD, and Jiang ZY (2018) Discovery of a head-to-tail cyclic peptide as the Keap1-Nrf2 protein-protein interaction inhibitor with high cell potency. *Eur J Med Chem* **143**:1578–1589.
Lv H, Liu Q, Wen Z, Feng H, Deng X, and Ci X (2017) Xanthohumol ameliorates lipopolysaccharide (LPS)-induced acute lung injury via induction of AMPK/GSK3β-Nrf2 signal axis. *Redox Biol* **12**:311–324.
Ma Q (2013) Role of nrf2 in oxidative stress and toxicity. *Annu Rev Pharmacol Toxicol* **53**:401–426.
Ma Q, Battelli L, and Hubbs AF (2006) Multiorgan autoimmune inflammation, enhanced lymphoproliferation, and impaired homeostasis of reactive oxygen species in mice lacking the antioxidant-activated transcription factor Nrf2. *Am J Pathol* **168**:1960–1974.
Maicas N, Ferrándiz ML, Brines R, Ibáñez L, Cuadrado A, Koenders MI, van den Berg WB, and Alcaraz MJ (2011) Deficiency of Nrf2 accelerates the effector phase of arthritis and aggravates joint disease. *Antioxid Redox Signal* **15**:889–901.
Manna A, De Sarkar S, De S, Bauri AK, Chattopadhyay S, and Chatterjee M (2015) The variable chemotherapeutic response of malabaricone-A in leukemic and solid tumor cell lines depends on the degree of redox imbalance. *Phytomedicine* **22**: 713–723.
Maqbool M and Hoda N (2017) GSK3 inhibitors in the therapeutic development of diabetes, cancer and neurodegeneration: past, present and future. *Curr Pharm Des* **23**:4332–4350.
Marcotte D, Zeng W, Hus JC, McKenzie A, Hession C, Jin P, Bergeron C, Lugovskoy A, Enyedy I, Cuervo H, et al. (2013) Small molecules inhibit the interaction of Nrf2 and the Keap1 Kelch domain through a non-covalent mechanism. *Bioorg Med Chem* **21**:4011–4019.
Markart P, Luboeinski T, Korfei M, Schmidt R, Wygrecka M, Mahavadi P, Mayer K, Wilhelm J, Seeger W, Guenther A, et al. (2009) Alveolar oxidative stress is associated with elevated levels of nonenzymatic low-molecular-weight antioxidants in patients with different forms of chronic fibrosing interstitial lung diseases. *Antioxid Redox Signal* **11**:227–240.
Markowicz-Piasecka M, Sikora J, Szydłowska A, Skupień A, Mikiciuk-Olasik E, and Huttunen KM (2017) Metformin - a future therapy for neurodegenerative diseases: theme: drug discovery, development and delivery in Alzheimer's disease: guest editor: Davide Brambilla. *Pharm Res* **34**:2614–2627.
Marrone G, Maeso-Díaz R, García-Cardena G, Abraldes JG, García-Pagán JC, Bosch J, and Gracia-Sancho J (2015) KLF2 exerts antifibrotic and vasoprotective effects in cirrhotic rat livers: behind the molecular mechanisms of statins. *Gut* **64**: 1434–1443.
Martín-de-Saavedra MD, Budni J, Cunha MP, Gómez-Rangel V, Lorrio S, Del Barrio L, Lastres-Becker I, Parada E, Tordera RM, Rodrigues AL, et al. (2013) Nrf2 participates in depressive disorders through an anti-inflammatory mechanism. *Psychoneuroendocrinology* **38**:2010–2022.
Marzec JM, Christie JD, Reddy SP, Jedlicka AE, Vuong H, Lanken PN, Aplenc R, Yamamoto T, Yamamoto M, Cho HY, et al. (2007) Functional polymorphisms in the transcription factor NRF2 in humans increase the risk of acute lung injury. *FASEB J* **21**:2237–2246.
McCubrey JA, Steelman LS, Bertrand FE, Davis NM, Sokolosky M, Abrams SL, Montalto G, D'Assoro AB, Libra M, Nicoletti F, et al. (2014) GSK-3 as potential target for therapeutic intervention in cancer. *Oncotarget* **5**:2881–2911.
McGuire VA, Ruiz-Zorrilla Diez T, Emmerich CH, Strickson S, Ritorto MS, Sutavani RV, Weiβ A, Houslay KF, Knebel A, Meakin PJ, et al. (2016) Dimethyl fumarate blocks pro-inflammatory cytokine production via inhibition of TLR induced M1 and K63 ubiquitin chain formation. *Sci Rep* **6**:31159.
Meakin PJ, Chowdhry S, Sharma RS, Ashford FB, Walsh SV, McCrimmon RJ, Dinkova-Kostova AT, Dillon JF, Hayes JD, and Ashford ML (2014) Susceptibility of Nrf2-null mice to steatohepatitis and cirrhosis upon consumption of a high-fat diet is associated with oxidative stress, perturbation of the unfolded protein response, and disturbance in the expression of metabolic enzymes but not with insulin resistance. *Mol Cell Biol* **34**:3305–3320.
Meissner M, Doll M, Hrgovic I, Reichenbach G, König V, Hailemariam-Jahn T, Gille J, and Kaufmann R (2011) Suppression of VEGFR2 expression in human endothelial cells by dimethylfumarate treatment: evidence for anti-angiogenic action. *J Invest Dermatol* **131**:1356–1364.
Menche J, Sharma A, Kitsak M, Ghiassian SD, Vidal M, Loscalzo J, and Barabási AL (2015) Disease networks: uncovering disease-disease relationships through the incomplete interactome. *Science* **347**:1257601.
Milkovic L, Zarkovic N, and Saso L (2017) Controversy about pharmacological modulation of Nrf2 for cancer therapy. *Redox Biol* **12**:727–732.
Mitsuishi Y, Taguchi K, Kawatani Y, Shibata T, Nukiwa T, Aburatani H, Yamamoto M, and Motohashi H (2012) Nrf2 redirects glucose and glutamine into anabolic pathways in metabolic reprogramming. *Cancer Cell* **22**:66–79.
Moon SJ, Park JS, Woo YJ, Lim MA, Kim SM, Lee SY, Kim EK, Lee HJ, Lee WS, Park SH, et al. (2014) Rebamipide suppresses collagen-induced arthritis through reciprocal regulation of th17/treg cell differentiation and heme oxygenase 1 induction. *Arthritis Rheumatol* **66**:874–885.
Morgan MJ and Liu ZG (2011) Crosstalk of reactive oxygen species and NF-κB signaling. *Cell Res* **21**:103–115.
Morgan PE, Sturgess AD, Hennessy A, and Davies MJ (2007) Serum protein oxidation and apolipoprotein CIII levels in people with systemic lupus erythematosus with and without nephritis. *Free Radic Res* **41**:1301–1312.
Mrowietz U, Christophers E, and Altmeyer P (1998) Treatment of psoriasis with fumaric acid esters: results of a prospective multicentre study: German Multicentre study. *Br J Dermatol* **138**:456–460.
Mrowietz U, Szepietowski JC, Loewe R, van de Kerkhof P, Lamarca R, Ocker WG, Tebbs VM, and Pau-Charles I (2017) Efficacy and safety of LAS41008 (dimethyl fumarate) in adults with moderate-to-severe chronic plaque psoriasis: a randomized, double-blind, Fumaderm®- and placebo-controlled trial (BRIDGE). *Br J Dermatol* **176**:615–623.
Na LX, Li Y, Pan HZ, Zhou XL, Sun DJ, Meng M, Li XX, and Sun CH (2013) Curcuminoids exert glucose-lowering effect in type 2 diabetes by decreasing serum free fatty acids: a double-blind, placebo-controlled trial. *Mol Nutr Food Res* **57**: 1569–1577.
Napetschnig J and Wu H (2013) Molecular basis of NF-κB signaling. *Annu Rev Biophys* **42**:443–468.
Nasiri HR, Linge S, and Ullmann D (2016) Thermodynamic profiling of inhibitors of Nrf2:Keap1 interactions. *Bioorg Med Chem Lett* **26**:526–529.
Natarajan VT, Singh A, Kumar AA, Sharma P, Kar HK, Marrot L, Meunier JR, Natarajan K, Rani R, and Gokhale RS (2010) Transcriptional upregulation of Nrf2-dependent phase II detoxification genes in the involved epidermis of vitiligo vulgaris. *J Invest Dermatol* **130**:2781–2789.
Nef HM, Möllmann H, Troidl C, Kostin S, Böttger T, Voss S, Hilpert P, Krause N, Weber M, Rolf A, et al. (2008) Expression profiling of cardiac genes in Tako-Tsubo cardiomyopathy: insight into a new cardiac entity. *J Mol Cell Cardiol* **44**:395–404.
Nesti L and Natali A (2017) Metformin effects on the heart and the cardiovascular system: a review of experimental and clinical data. *Nutr Metab Cardiovasc Dis* **27**: 657–669.
Ockenfels HM, Schultewolter T, Ockenfels G, Funk R, and Goos M (1998) The antipsoriatic agent dimethylfumarate immunomodulates T-cell cytokine secretion and inhibits cytokines of the psoriatic cytokine network. *Br J Dermatol* **139**: 390–395.
Okano Y, Nezu U, Enokida Y, Lee MT, Kinoshita H, Lezhava A, Hayashizaki Y, Morita S, Taguri M, Ichikawa Y, et al. (2013) SNP (-617C>A) in ARE-like loci of the NRF2 gene: a new biomarker for prognosis of lung adenocarcinoma in Japanese non-smoking women. *PLoS One* **8**:e73794.
Olayanju A, Copple IM, Bryan HK, Edge GT, Sison RL, Wong MW, Lai ZQ, Lin ZX, Dunn K, Sanderson CM, et al. (2015) Brusatol provokes a rapid and transient inhibition of Nrf2 signaling and sensitizes mammalian cells to chemical toxicity: implications for therapeutic targeting of Nrf2. *Free Radic Biol Med* **78**:202–212.

Onderdijk AJ, Balak DM, Baerveldt EM, Florencia EF, Kant M, Laman JD, van IJcken WF, Racz E, de Ridder D, Thio HB, et al. (2014) Regulated genes in psoriatic skin during treatment with fumaric acid esters. *Br J Dermatol* **171**:732–741.

Onyiah JC, Sheikh SZ, Maharshak N, Otterbein LE, and Plevy SE (2014) Heme oxygenase-1 and carbon monoxide regulate intestinal homeostasis and mucosal immune responses to the enteric microbiota. *Gut Microbes* **5**:220–224.

Orena S, Owen J, Jin F, Fabian M, Gillitt ND, and Zeisel SH (2015) Extracts of fruits and vegetables activate the antioxidant response element in IMR-32 cells. *J Nutr* **145**:2006–2011.

Owen MR, Doran E, and Halestrap AP (2000) Evidence that metformin exerts its anti-diabetic effects through inhibition of complex 1 of the mitochondrial respiratory chain. *Biochem J* **348**:607–614.

Padmanabhan B, Tong KI, Ohta T, Nakamura Y, Scharlock M, Ohtsuji M, Kang MI, Kobayashi A, Yokoyama S, and Yamamoto M (2006) Structural basis for defects of Keap1 activity provoked by its point mutations in lung cancer. *Mol Cell* **21**: 689–700.

Pajares M, Cuadrado A, and Rojo AI (2017) Modulation of proteostasis by transcription factor NRF2 and impact in neurodegenerative diseases. *Redox Biol* **11**: 543–553.

Pajares M, Jiménez-Moreno N, Dias IH, Debelec B, Vucetic M, Fladmark KE, Basaga H, Ribaric S, Milisav I, and Cuadrado A (2015) Redox control of protein degradation. *Redox Biol* **6**:409–420.

Pajares M, Jiménez-Moreno N, García-Yagüe AJ, Escoll M, de Ceballos ML, Van Leuven F, Rábano A, Yamamoto M, Rojo AI, and Cuadrado A (2016) Transcription factor NFE2L2/NRF2 is a regulator of macroautophagy genes. *Autophagy* **12**: 1902–1916.

Palomo V and Martinez A (2017) Glycogen synthase kinase 3 (GSK-3) inhibitors: a patent update (2014-2015). *Expert Opin Ther Pat* **27**:657–666.

Panieri E and Santoro MM (2016) ROS homeostasis and metabolism: a dangerous liason in cancer cells. *Cell Death Dis* **7**:e2253.

Pantan R, Tocharus J, Suksamrarn A, and Tocharus C (2016) Synergistic effect of atorvastatin and cyanidin-3-glucoside on angiotensin II-induced inflammation in vascular smooth muscle cells. *Exp Cell Res* **342**:104–112.

Pareek TK, Belkadi A, Kesavapany S, Zaremba A, Loh SL, Bai L, Cohen ML, Meyer C, Liby KT, Miller RH, et al. (2011) Triterpenoid modulation of IL-17 and Nrf-2 expression ameliorates neuroinflammation and promotes remyelination in autoimmune encephalomyelitis. *Sci Rep* **1**:201.

Park SY, Lee SW, Shin HK, Chung WT, Lee WS, Rhim BY, Hong KW, and Kim CD (2010) Cilostazol enhances apoptosis of synovial cells from rheumatoid arthritis patients with inhibition of cytokine formation via Nrf2-linked heme oxygenase 1 induction. *Arthritis Rheum* **62**:732–741.

Pedruzzi LM, Cardozo LF, Daleprane JB, Stockler-Pinto MB, Monteiro EB, Leite M Jr, Vaziri ND, and Mafra D (2015) Systemic inflammation and oxidative stress in hemodialysis patients are associated with down-regulation of Nrf2. *J Nephrol* **28**: 495–501.

Peng H, Guerau-de-Arellano M, Mehta VB, Yang Y, Huss DJ, Papenfuss TL, Lovett-Racke AE, and Racke MK (2012) Dimethyl fumarate inhibits dendritic cell maturation via nuclear factor κB (NF-κB) and extracellular signal-regulated kinase 1 and 2 (ERK1/2) and mitogen stress-activated kinase 1 (MSK1) signaling. *J Biol Chem* **287**:28017–28026.

Pergola PE, Raskin P, Toto RD, Meyer CJ, Huff JW, Grossman EB, Krauth M, Ruiz S, Audhya P, Christ-Schmidt H, et al.; BEAM Study Investigators (2011) Bardoxolone methyl and kidney function in CKD with type 2 diabetes. *N Engl J Med* **365**:327–336.

Pilar Valdecantos M, Prieto-Hontoria PL, Pardo V, Módol T, Santamaría B, Weber M, Herrero L, Serra D, Muntané J, Cuadrado A, et al. (2015) Essential role of Nrf2 in the protective effect of lipoic acid against lipoapoptosis in hepatocytes. *Free Radic Biol Med* **84**:263–278.

Piñero J, Bravo À, Queralt-Rosinach N, Gutiérrez-Sacristán A, Deu-Pons J, Centeno E, García-García J, Sanz F, and Furlong LI (2017) DisGeNET: a comprehensive platform integrating information on human disease-associated genes and variants. *Nucleic Acids Res* **45**:D833–D839.

Pitha-Rowe I, Liby K, Royce D, and Sporn M (2009) Synthetic triterpenoids attenuate cytotoxic retinal injury: cross-talk between Nrf2 and PI3K/AKT signaling through inhibition of the lipid phosphatase PTEN. *Invest Ophthalmol Vis Sci* **50**: 5339–5347.

Qiu P, Man S, Li J, Liu J, Zhang L, Yu P, and Gao W (2016) Overdose intake of curcumin initiates the unbalanced state of bodies. *J Agric Food Chem* **64**: 2765–2771.

Rachakonda G, Xiong Y, Sekhar KR, Stamer SL, Liebler DC, and Freeman ML (2008) Covalent modification at Cys151 dissociates the electrophile sensor Keap1 from the ubiquitin ligase CUL3. *Chem Res Toxicol* **21**:705–710.

Rada P, Rojo AI, Chowdhry S, McMahon M, Hayes JD, and Cuadrado A (2011) SCF/beta-TrCP promotes glycogen synthase kinase 3-dependent degradation of the Nrf2 transcription factor in a Keap1-independent manner. *Mol Cell Biol* **31**:1121–1133.

Rada P, Rojo AI, Evrard-Todeschi N, Innamorato NG, Cotte A, Jaworski T, Tobón-Velasco JC, Devijver H, García-Mayoral MF, Van Leuven F, et al. (2012) Structural and functional characterization of Nrf2 degradation by the glycogen synthase kinase 3/β-TrCP axis. *Mol Cell Biol* **32**:3486–3499.

Ramadori P, Drescher H, Erschfeld S, Schumacher F, Berger C, Fragoulis A, Schenkel J, Kensler TW, Wruck CJ, Trautwein C, et al. (2016) Hepatocyte-specific Keap1 deletion reduces liver steatosis but not inflammation during non-alcoholic steatohepatitis development. *Free Radic Biol Med* **91**:114–126.

Ramsey CP, Glass CA, Montgomery MB, Lindl KA, Ritson GP, Chia LA, Hamilton RL, Chu CT, and Jordan-Sciutto KL (2007) Expression of Nrf2 in neurodegenerative diseases. *J Neuropathol Exp Neurol* **66**:75–85.

Rangasamy T, Cho CY, Thimmulappa RK, Zhen L, Srisuma SS, Kensler TW, Yamamoto M, Petrache I, Tuder RM, and Biswal S (2004) Genetic ablation of Nrf2 enhances susceptibility to cigarette smoke-induced emphysema in mice. *J Clin Invest* **114**:1248–1259.

Ranjan N, Fulcrand G, King A, Brown J, Jiang X, Leng F, and Arya DP (2014) Selective inhibition of bacterial topoisomerase I by alkynyl-bisbenzimidazoles. *MedChemComm* **5**:816–825.

Reccia I, Kumar J, Akladios C, Virdis F, Pai M, Habib N, and Spalding D (2017) Non-alcoholic fatty liver disease: a sign of systemic disease. *Metabolism* **72**:94–108.

Ren D, Villeneuve NF, Jiang T, Wu T, Lau A, Toppin HA, and Zhang DD (2011) Brusatol enhances the efficacy of chemotherapy by inhibiting the Nrf2-mediated defense mechanism. *Proc Natl Acad Sci USA* **108**:1433–1438.

Rena G, Hardie DG, and Pearson ER (2017) The mechanisms of action of metformin. *Diabetologia* **60**:1577–1585.Reuter S, Gupta SC, Chaturvedi MM, and Aggarwal BB (2010) Oxidative stress, inflammation, and cancer: how are they linked? *Free Radic Biol Med* **49**:1603–1616.

Richardson BG, Jain AD, Speltz TE, and Moore TW (2015) Non-electrophilic modulators of the canonical Keap1/Nrf2 pathway. *Bioorg Med Chem Lett* **25**:2261–2268.

Roberts CA, Dickinson AK, and Taams LS (2015) The interplay between monocytes/macrophages and CD4(+) T cell subsets in rheumatoid arthritis. *Front Immunol* **6**: 571.

Rojo AI, Innamorato NG, Martín-Moreno AM, De Ceballos ML, Yamamoto M, and Cuadrado A (2010) Nrf2 regulates microglial dynamics and neuroinflammation in experimental Parkinson's disease. *Glia* **58**:588–598.

Rojo AI, McBean G, Cindric M, Egea J, López MG, Rada P, Zarkovic N, and Cuadrado A (2014a) Redox control of microglial function: molecular mechanisms and functional significance. *Antioxid Redox Signal* **21**:1766–1801.

Rojo AI, Rada P, Mendiola M, Ortega-Molina A, Wojdyla K, Rogowska-Wrzesinska A, Hardisson D, Serrano M, and Cuadrado A (2014b) The PTEN/NRF2 axis promotes human carcinogenesis. *Antioxid Redox Signal* **21**:2498–2514.

Rushworth SA, Zaitseva L, Murray MY, Shah NM, Bowles KM, and MacEwan DJ (2012) The high Nrf2 expression in human acute myeloid leukemia is driven by NF-κB and underlies its chemo-resistance. *Blood* **120**:5188–5198.

Ryoo IG, Lee SH, and Kwak MK (2016) Redox modulating NRF2: a potential mediator of cancer stem cell resistance. *Oxid Med Cell Longev* **2016**:2428153.

Saddawi-Konefka R, Seelige R, Gross ET, Levy E, Searles SC, Washington A Jr, Santosa EK, Liu B, O'Sullivan TE, Harismendy O, et al. (2016) Nrf2 induces IL-17D to mediate tumor and virus surveillance. *Cell Reports* **16**:2348–2358.

Saito R, Suzuki T, Hiramoto K, Asami S, Naganuma E, Suda H, Iso T, Yamamoto H, Morita M, Baird L, et al. (2015) Characterizations of three major cysteine sensors of Keap1 in stress response. *Mol Cell Biol* **36**:271–284.

Saracino AM and Orteu CH (2017) Severe recalcitrant cutaneous manifestations in systemic lupus erythematosus successfully treated with fumaric acid esters. *Br J Dermatol* **176**:472–480.

Sato M, Aoki T, Inoue H, Tanaka T, and Kunishima N (2013) *Keap1 Protein Binding Compound, Cristal of Complex Between the Same and Keap1 Protein, and Method for Producing the Same*, Toray Industries, Tokyo.

Sato N, Takasaka N, Yoshida M, Tsubouchi K, Minagawa S, Araya J, Saito N, Fujita Y, Kurita Y, Kobayashi K, et al. (2016) Metformin attenuates lung fibrosis development via NOX4 suppression. *Respir Res* **17**:107.

Satoh T, McKercher SR, and Lipton SA (2013) Nrf2/ARE-mediated antioxidant actions of pro-electrophilic drugs. *Free Radic Biol Med* **65**:645–657.

Scannevin RH, Chollate S, Jung MY, Shackett M, Patel H, Bista P, Zeng W, Ryan S, Yamamoto M, Lukashev M, et al. (2012) Fumarates promote cytoprotection of central nervous system cells against oxidative stress via the nuclear factor (erythroid-derived 2)-like 2 pathway. *J Pharmacol Exp Ther* **341**:274–284.

Schilling S, Goelz S, Linker R, Luehder F, and Gold R (2006) Fumaric acid esters are effective in chronic experimental autoimmune encephalomyelitis and suppress macrophage infiltration. *Clin Exp Immunol* **145**:101–107.

Schimrigk S, Brune N, Hellwig K, Lukas C, Bellenberg B, Rieks M, Hoffmann V, Pohlau D, and Przuntek H (2006) Oral fumaric acid esters for the treatment of active multiple sclerosis: an open-label, baseline-controlled pilot study. *Eur J Neurol* **13**:604–610.

Schipper HM, Song W, Zukor H, Hascalovici JR, and Zeligman D (2009) Heme oxygenase-1 and neurodegeneration: expanding frontiers of engagement. *J Neurochem* **110**:469–485.

Schuiveling M, Vazirpanah N, Radstake TRDJ, Zimmermann M, and Broen JCA (2017) Metformin, a new era for an old drug in the treatment of immune mediated disease? *Curr Drug Targets* [published ahead of print].

Schulze-Topphoff U, Varrin-Doyer M, Pekarek K, Spencer CM, Shetty A, Sagan SA, Cree BA, Sobel RA, Wipke BT, Steinman L, et al. (2016) Dimethyl fumarate treatment induces adaptive and innate immune modulation independent of Nrf2. *Proc Natl Acad Sci USA* **113**:4777–4782.

Schumacker PT (2006) Reactive oxygen species in cancer cells: live by the sword, die by the sword. *Cancer Cell* **10**:175–176.

Sha LK, Sha W, Kuchler L, Daiber A, Giegerich AK, Weigert A, Knape T, Snodgrass R, Schröder K, Brandes RP, et al. (2015) Loss of Nrf2 in bone marrow-derived macrophages impairs antigen-driven CD8(+) T cell function by limiting GSH and Cys availability. *Free Radic Biol Med* **83**:77–88.

Shanmugam G, Narasimhan M, Conley RL, Sairam T, Kumar A, Mason RP, Sankaran R, Hoidal JR, and Rajasekaran NS (2017a) Chronic endurance exercise impairs cardiac structure and function in middle-aged mice with impaired Nrf2 signaling. *Front Physiol* **8**:268.

Shanmugam G, Narasimhan M, Tamowski S, Darley-Usmar V, and Rajasekaran NS (2017b) Constitutive activation of Nrf2 induces a stable reductive state in the mouse myocardium. *Redox Biol* **12**:937–945.

Sharma A, Rizky L, Stefanovic N, Tate M, Ritchie RH, Ward KW, and de Haan JB (2017) The nuclear factor (erythroid-derived 2)-like 2 (Nrf2) activator dh404 protects against diabetes-induced endothelial dysfunction. *Cardiovasc Diabetol* **16**:33.

Shibata T, Kokubu A, Saito S, Narisawa-Saito M, Sasaki H, Aoyagi K, Yoshimatsu Y, Tachimori Y, Kushima R, Kiyono T, et al. (2011) NRF2 mutation confers malignant potential and resistance to chemoradiation therapy in advanced esophageal squamous cancer. *Neoplasia* **13**:864–873.

Shimizu T, Inoue K, Hachiya H, Shibuya N, Aoki T, and Kubota K (2016) Accumulation of phosphorylated p62 is associated with NF-E2-related factor 2 activation in hepatocellular carcinoma. *J Hepatobiliary Pancreat Sci* **23**:467–471.
Shimoyama Y, Mitsuda Y, Tsuruta Y, Hamajima N, and Niwa T (2014) Polymorphism of Nrf2, an antioxidative gene, is associated with blood pressure and cardiovascular mortality in hemodialysis patients. *Int J Med Sci* **11**:726–731.
Shimozono R, Asaoka Y, Yoshizawa Y, Aoki T, Noda H, Yamada M, Kaino M, and Mochizuki H (2013) Nrf2 activators attenuate the progression of nonalcoholic steatohepatitis-related fibrosis in a dietary rat model. *Mol Pharmacol* **84**:62–70.
Signorelli SS, Li Volsi G, Fiore V, Mangiafico M, Barbagallo I, Parenti R, Rizzo M, and Li Volti G (2016) Plasma heme oxygenase-1 is decreased in peripheral artery disease patients. *Mol Med Rep* **14**:3459–3463.
Silva T, Reis J, Teixeira J, and Borges F (2014) Alzheimer's disease, enzyme targets and drug discovery struggles: from natural products to drug prototypes. *Ageing Res Rev* **15**:116–145.
Singh A, Misra V, Thimmulappa RK, Lee H, Ames S, Hoque MO, Herman JG, Baylin SB, Sidransky D, Gabrielson E, et al. (2006) Dysfunctional KEAP1-NRF2 interaction in non-small-cell lung cancer. *PLoS Med* **3**:e420.
Singh A, Venkannagari S, Oh KH, Zhang YQ, Rohde JM, Liu L, Nimmagadda S, Sudini K, Brimacombe KR, Gajghate S, et al. (2016) Small molecule inhibitor of NRF2 selectively intervenes therapeutic resistance in KEAP1-deficient NSCLC tumors. *ACS Chem Biol* **11**:3214–3225.
Siomek A (2012) NF-κB signaling pathway and free radical impact. *Acta Biochim Pol* **59**:323–331.
Song P, Li K, Liu L, Wang X, Jian Z, Zhang W, Wang G, Li C, and Gao T (2016) Genetic polymorphism of the Nrf2 promoter region is associated with vitiligo risk in Han Chinese populations. *J Cell Mol Med* **20**:1840–1850.
Stelzer G, Rosen N, Plaschkes I, Zimmerman S, Twik M, Fishilevich S, Stein TI, Nudel R, Lieder I, Mazor Y, et al. (2016) The GeneCards suite: from gene data mining to disease genome sequence analyses. *Curr Protoc Bioinformatics* **54**: 1.30.1–1.30.33.
Stocker R, Yamamoto Y, McDonagh AF, Glazer AN, and Ames BN (1987) Bilirubin is an antioxidant of possible physiological importance. *Science* **235**:1043–1046.
Strom J and Chen QM (2017) Loss of Nrf2 promotes rapid progression to heart failure following myocardial infarction. *Toxicol Appl Pharmacol* **327**:52–58.
Sun H, Zhu J, Lin H, Gu K, and Feng F (2017) Recent progress in the development of small molecule Nrf2 modulators: a patent review (2012-2016). *Expert Opin Ther Pat* **27**:763–785.
Taguchi K and Yamamoto M (2017) The KEAP1-NRF2 system in cancer. *Front Oncol* **7**:85.
Tahvili S, Zandieh B, and Amirghofran Z (2015) The effect of dimethyl fumarate on gene expression and the level of cytokines related to different T helper cell subsets in peripheral blood mononuclear cells of patients with psoriasis. *Int J Dermatol* **54**: e254–e260.
Takahashi Y, Kobayashi Y, Kawata K, Kawamura K, Sumiyoshi S, Noritake H, Watanabe S, Chida T, Souda K, Sakaguchi T, et al. (2014) Does hepatic oxidative stress enhance activation of nuclear factor-E2-related factor in patients with nonalcoholic steatohepatitis? *Antioxid Redox Signal* **20**:538–543.
Tan SM, Sharma A, Stefanovic N, Yuen DY, Karagiannis TC, Meyer C, Ward KW, Cooper ME, and de Haan JB (2014) Derivative of bardoxolone methyl, dh404, in an inverse dose-dependent manner lessens diabetes-associated atherosclerosis and improves diabetic kidney disease. *Diabetes* **63**:3091–3103.
Tang X, Lin CC, Spasojevic I, Iversen ES, Chi JT, and Marks JR (2014) A joint analysis of metabolomics and genetics of breast cancer. *Breast Cancer Res* **16**:415.
Tarumoto T, Nagai T, Ohmine K, Miyoshi T, Nakamura M, Kondo T, Mitsugi K, Nakano S, Muroi K, Komatsu N, et al. (2004) Ascorbic acid restores sensitivity to imatinib via suppression of Nrf2-dependent gene expression in the imatinib-resistant cell line. *Exp Hematol* **32**:375–381.
Thimmulappa RK, Lee H, Rangasamy T, Reddy SP, Yamamoto M, Kensler TW, and Biswal S (2006a) Nrf2 is a critical regulator of the innate immune response and survival during experimental sepsis. *J Clin Invest* **116**:984–995.
Thimmulappa RK, Scollick C, Traore K, Yates M, Trush MA, Liby KT, Sporn MB, Yamamoto M, Kensler TW, and Biswal S (2006b) Nrf2-dependent protection from LPS induced inflammatory response and mortality by CDDO-Imidazolide. *Biochem Biophys Res Commun* **351**:883–889.
Thomson L, Tenopoulou M, Lightfoot R, Tsika E, Parastatidis I, Martinez M, Greco TM, Doulias PT, Wu Y, Tang WH, et al. (2012) Immunoglobulins against tyrosine-nitrated epitopes in coronary artery disease. *Circulation* **126**:2392–2401.
Todorovic M, Newman JR, Shan J, Bentley S, Wood SA, Silburn PA, and Mellick GD (2015) Comprehensive assessment of genetic sequence variants in the antioxidant 'master regulator' NRF2 in idiopathic Parkinson's disease. *PLoS One* **10**:e0128030.
Tong KI, Padmanabhan B, Kobayashi A, Shang C, Hirotsu Y, Yokoyama S, and Yamamoto M (2007) Different electrostatic potentials define ETGE and DLG motifs as hinge and latch in oxidative stress response. *Mol Cell Biol* **27**:7511–7521.
Tsai HH, Lai HY, Chen YC, Li CF, Huang HS, Liu HS, Tsai YS, and Wang JM (2017) Metformin promotes apoptosis in hepatocellular carcinoma through the CEBPD-induced autophagy pathway. *Oncotarget* **8**:13832–13845.
Tsuchida K, Tsujita T, Hayashi M, Ojima A, Keleku-Lukwete N, Katsuoka F, Otsuki A, Kikuchi H, Oshima Y, Suzuki M, et al. (2017) Halofuginone enhances the chemosensitivity of cancer cells by suppressing NRF2 accumulation. *Free Radic Biol Med* **103**:236–247.
Tu J, Zhang X, Zhu Y, Dai Y, Li N, Yang F, Zhang Q, Brann DW, and Wang R (2015) Cell-permeable peptide targeting the Nrf2-Keap1 interaction: a potential novel therapy for global cerebral ischemia. *J Neurosci* **35**:14727–14739.
Tung MC, Lin PL, Wang YC, He TY, Lee MC, Yeh SD, Chen CY, and Lee H (2015) Mutant p53 confers chemoresistance in non-small cell lung cancer by upregulating Nrf2. *Oncotarget* **6**:41692–41705.
Türei D, Papp D, Fazekas D, Földvári-Nagy L, Módos D, Lenti K, Csermely P, and Korcsmáros T (2013) NRF2-ome: an integrated web resource to discover protein interaction and regulatory networks of NRF2. *Oxid Med Cell Longev* **2013**: 737591.
Tzima S, Victoratos P, Kranidioti K, Alexiou M, and Kollias G (2009) Myeloid heme oxygenase-1 regulates innate immunity and autoimmunity by modulating IFN-beta production. *J Exp Med* **206**:1167–1179.
Ungvari Z, Bagi Z, Feher A, Recchia FA, Sonntag WE, Pearson K, de Cabo R, and Csiszar A (2010) Resveratrol confers endothelial protection via activation of the antioxidant transcription factor Nrf2. *Am J Physiol Heart Circ Physiol* **299**: H18–H24.
Ungvari Z, Bailey-Downs L, Gautam T, Jimenez R, Losonczy G, Zhang C, Ballabh P, Recchia FA, Wilkerson DC, Sonntag WE, et al. (2011) Adaptive induction of NF-E2-related factor-2-driven antioxidant genes in endothelial cells in response to hyperglycemia. *Am J Physiol Heart Circ Physiol* **300**:H1133–H1140.
Uruno A, Furusawa Y, Yagishita Y, Fukutomi T, Muramatsu H, Negishi T, Sugawara A, Kensler TW, and Yamamoto M (2013) The Keap1-Nrf2 system prevents onset of diabetes mellitus. *Mol Cell Biol* **33**:2996–3010.
Uruno A, Yagishita Y, and Yamamoto M (2015) The Keap1-Nrf2 system and diabetes mellitus. *Arch Biochem Biophys* **566**:76–84.
van Horssen J, Drexhage JA, Flor T, Gerritsen W, van der Valk P, and de Vries HE (2010) Nrf2 and DJ1 are consistently upregulated in inflammatory multiple sclerosis lesions. *Free Radic Biol Med* **49**:1283–1289.
van Muiswinkel FL, de Vos RA, Bol JG, Andringa G, Jansen Steur EN, Ross D, Siegel D, and Drukarch B (2004) Expression of NAD(P)H:quinone oxidoreductase in the normal and Parkinsonian substantia nigra. *Neurobiol Aging* **25**:1253–1262.
Vidal M, Cusick ME, and Barabási AL (2011) Interactome networks and human disease. *Cell* **144**:986–998.
von Otter M, Bergström P, Quattrone A, De Marco EV, Annesi G, Söderkvist P, Wettinger SB, Drozdzik M, Bialecka M, Nissbrandt H, et al. (2014) Genetic associations of Nrf2-encoding NFE2L2 variants with Parkinson's disease: a multicenter study. *BMC Med Genet* **15**:131.
von Otter M, Landgren S, Nilsson S, Celojevic D, Bergström P, Håkansson A, Nissbrandt H, Drozdzik M, Bialecka M, Kurzawski M, et al. (2010a) Association of Nrf2-encoding NFE2L2 haplotypes with Parkinson's disease. *BMC Med Genet* **11**: 36.
von Otter M, Landgren S, Nilsson S, Zetterberg M, Celojevic D, Bergström P, Minthon L, Bogdanovic N, Andreasen N, Gustafson DR, et al. (2010b) Nrf2-encoding NFE2L2 haplotypes influence disease progression but not risk in Alzheimer's disease and age-related cataract. *Mech Ageing Dev* **131**:105–110.
Wang L, Han J, Shan P, You S, Chen X, Jin Y, Wang J, Huang W, Wang Y, and Liang G (2017a) MD2 blockage protects obesity-induced vascular remodeling via activating AMPK/Nrf2. *Obesity (Silver Spring)* **25**:1532–1539.
Wang R, An J, Ji F, Jiao H, Sun H, and Zhou D (2008) Hypermethylation of the Keap1 gene in human lung cancer cell lines and lung cancer tissues. *Biochem Biophys Res Commun* **373**:151–154.
Wang X, Chen H, Liu J, Ouyang Y, Wang D, Bao W, and Liu L (2015) Association between the NF-E2 related factor 2 gene polymorphism and oxidative stress, antioxidative status, and newly-diagnosed type 2 diabetes mellitus in a Chinese population. *Int J Mol Sci* **16**:16483–16496.
Wang X, de Rivero Vaccari JP, Wang H, Diaz P, German R, Marcillo AE, and Keane RW (2012) Activation of the nuclear factor E2-related factor 2/antioxidant response element pathway is neuroprotective after spinal cord injury. *J Neurotrauma* **29**: 936–945.
Wang X, Hausding M, Weng SY, Kim YO, Steven S, Klein T, Daiber A, and Schuppan D (2018) Gliptins suppress inflammatory macrophage activation to mitigate inflammation, fibrosis, oxidative stress, and vascular dysfunction in models of non-alcoholic steatohepatitis and liver fibrosis. *Antioxid Redox Signal*. **28**:87–109.
Wang X, Li M, Cao Y, Wang J, Zhang H, Zhou X, Li Q, and Wang L (2017b) Tenuigenin inhibits LPS-induced inflammatory responses in microglia via activating the Nrf2-mediated HO-1 signaling pathway. *Eur J Pharmacol* **809**:196–202.
Wang XJ, Hayes JD, Henderson CJ, and Wolf CR (2007) Identification of retinoic acid as an inhibitor of transcription factor Nrf2 through activation of retinoic acid receptor alpha. *Proc Natl Acad Sci USA* **104**:19589–19594.
Wang Y, Huang Y, Xu Y, Ruan W, Wang H, Zhang Y, Saavedra JM, Zhang L, Huang Z, and Pang T (2017c) A dual AMPK/Nrf2 activator reduces brain inflammation after stroke by enhancing microglia M2 polarization. *Antioxid Redox Signal* **28**: 141–163.
Wasik U, Milkiewicz M, Kempinska-Podhorodecka A, and Milkiewicz P (2017) Protection against oxidative stress mediated by the Nrf2/Keap1 axis is impaired in primary biliary cholangitis. *Sci Rep* **7**:44769.
Wen X, Thorne G, Hu L, Joy MS, and Aleksunes LM (2015) Activation of NRF2 signaling in HEK293 cells by a first-in-class direct KEAP1-NRF2 inhibitor. *J Biochem Mol Toxicol* **29**:261–266.
Wenzel P, Kossmann S, Münzel T, and Daiber A (2017) Redox regulation of cardiovascular inflammation: immunomodulatory function of mitochondrial and Nox-derived reactive oxygen and nitrogen species. *Free Radic Biol Med* **109**:48–60.
Wenzel P, Oelze M, Coldewey M, Hortmann M, Seeling A, Hink U, Mollnau H, Stalleicken D, Weiner H, Lehmann J, et al. (2007) Heme oxygenase-1: a novel key player in the development of tolerance in response to organic nitrates. *Arterioscler Thromb Vasc Biol* **27**:1729–1735.
Wenzel P, Rossmann H, Müller C, Kossmann S, Oelze M, Schulz A, Arnold N, Simsek C, Lagrange J, Klemz R, et al. (2015) Heme oxygenase-1 suppresses a pro-inflammatory phenotype in monocytes and determines endothelial function and arterial hypertension in mice and humans. *Eur Heart J* **36**:3437–3446.
Winkel AF, Engel CK, Margerie D, Kannt A, Szillat H, Glombik H, Kallus C, Ruf S, Güssregen S, Riedel J, et al. (2015) Characterization of RA839, a noncovalent small molecule binder to Keap1 and selective activator of Nrf2 signaling. *J Biol Chem* **290**:28446–28455.
Winston JT, Strack P, Beer-Romero P, Chu CY, Elledge SJ, and Harper JW (1999) The SCFbeta-TRCP-ubiquitin ligase complex associates specifically with

phosphorylated destruction motifs in IkappaBalpha and beta-catenin and stimulates IkappaBalpha ubiquitination in vitro. *Genes Dev* **13**:270–283.
Wu Q, Wang Q, Mao G, Dowling CA, Lundy SK, and Mao-Draayer Y (2017) Dimethyl fumarate selectively reduces memory T cells and shifts the balance between Th1/Th17 and Th2 in multiple sclerosis patients. *J Immunol* **198**:3069–3080.
Wu W, Zhao L, Yang P, Zhou W, Li B, Moorhead JF, Varghese Z, Ruan XZ, and Chen Y (2016a) Inflammatory stress sensitizes the liver to atorvastatin-induced injury in ApoE-/- mice. *PLoS One* **11**:e0159512.
Wu WJ, Jia WW, Liu XH, Pan LL, Zhang QY, Yang D, Shen XY, Liu L, and Zhu YZ (2016b) S-propargyl-cysteine attenuates inflammatory response in rheumatoid arthritis by modulating the Nrf2-ARE signaling pathway. *Redox Biol* **10**:157–167.
Xia N, Daiber A, Förstermann U, and Li H (2017) Antioxidant effects of resveratrol in the cardiovascular system. *Br J Pharmacol* **174**:1633–1646.
Xiaobo C, Majidi M, Feng M, Shao R, Wang J, Zhao Y, Baladandayuthapani V, Song J, Fang B, Ji L, et al. (2016) TUSC2(FUS1)-erlotinib induced vulnerabilities in epidermal growth factor receptor (EGFR) wildtype non-small cell lung cancer (NSCLC) targeted by the repurposed drug auranofin. *Sci Rep* **6**:35741.
Xie H, Zhou F, Liu L, Zhu G, Li Q, Li C, and Gao T (2016) Vitiligo: how do oxidative stress-induced autoantigens trigger autoimmunity? *J Dermatol Sci* **81**:3–9.
Xiong M, Li B, Zhu Q, Wang YX, and Zhang HY (2014) Identification of transcription factors for drug-associated gene modules and biomedical implications. *Bioinformatics* **30**:305–309.
Xu IM, Lai RK, Lin SH, Tse AP, Chiu DK, Koh HY, Law CT, Wong CM, Cai Z, Wong CC, et al. (2016a) Transketolase counteracts oxidative stress to drive cancer development. *Proc Natl Acad Sci USA* **113**:E725–E734.
Xu J, Donepudi AC, Moscovitz JE, and Slitt AL (2013) Keap1-knockdown decreases fasting-induced fatty liver via altered lipid metabolism and decreased fatty acid mobilization from adipose tissue. *PLoS One* **8**:e79841.
Xu X, Sun J, Chang X, Wang J, Luo M, Wintergerst KA, Miao L, and Cai L (2016b) Genetic variants of nuclear factor erythroid-derived 2-like 2 associated with the complications in Han descents with type 2 diabetes mellitus of Northeast China. *J Cell Mol Med* **20**:2078–2088.
Xu Z, Wei Y, Gong J, Cho H, Park JK, Sung ER, Huang H, Wu L, Eberhart C, Handa JT, et al. (2014) NRF2 plays a protective role in diabetic retinopathy in mice. *Diabetologia* **57**:204–213.
Xu Z, Zhang F, Sun F, Gu K, Dong S, and He D (2015) Dimethyl fumarate for multiple sclerosis. *Cochrane Database Syst Rev* **4**:CD011076.
Xue P, Hou Y, Chen Y, Yang B, Fu J, Zheng H, Yarborough K, Woods CG, Liu D, Yamamoto M, et al. (2013) Adipose deficiency of Nrf2 in ob/ob mice results in severe metabolic syndrome. *Diabetes* **62**:845–854.
Yamamoto T, Suzuki T, Kobayashi A, Wakabayashi J, Maher J, Motohashi H, and Yamamoto M (2008) Physiological significance of reactive cysteine residues of Keap1 in determining Nrf2 activity. *Mol Cell Biol* **28**:2758–2770.
Yamamoto T, Yoh K, Kobayashi A, Ishii Y, Kure S, Koyama A, Sakamoto T, Sekizawa K, Motohashi H, and Yamamoto M (2004) Identification of polymorphisms in the promoter region of the human NRF2 gene. *Biochem Biophys Res Commun* **321**:72–79.
Yang M, Yao Y, Eades G, Zhang Y, and Zhou Q (2011) MiR-28 regulates Nrf2 expression through a Keap1-independent mechanism. *Breast Cancer Res Treat* **129**:983–991.
Yao W, Zhang JC, Ishima T, Dong C, Yang C, Ren Q, Ma M, Han M, Wu J, Suganuma H, et al. (2016) Role of Keap1-Nrf2 signaling in depression and dietary intake of glucoraphanin confers stress resilience in mice. *Sci Rep* **6**:30659.
Yap JL, Worlikar S, MacKerell AD Jr, Shapiro P, and Fletcher S (2011) Small-molecule inhibitors of the ERK signaling pathway: towards novel anticancer therapeutics. *ChemMedChem* **6**:38–48.
Yoh K, Hirayama A, Ishizaki K, Yamada A, Takeuchi M, Yamagishi S, Morito N, Nakano T, Ojima M, Shimohata H, et al. (2008) Hyperglycemia induces oxidative and nitrosative stress and increases renal functional impairment in Nrf2-deficient mice. *Genes Cells* **13**:1159–1170.
Yore MM, Kettenbach AN, Sporn MB, Gerber SA, and Liby KT (2011) Proteomic analysis shows synthetic oleanane triterpenoid binds to mTOR. *PLoS One* **6**:e22862.
Yoshizaki Y, Mori T, Ishigami-Yuasa M, Kikuchi E, Takahashi D, Zeniya M, Nomura N, Mori Y, Araki Y, Ando F, et al. (2017) Drug-repositioning screening for Keap1-Nrf2 binding inhibitors using fluorescence correlation spectroscopy. *Sci Rep* **7**:3945.
Yu M, Li H, Liu Q, Liu F, Tang L, Li C, Yuan Y, Zhan Y, Xu W, Li W, et al. (2011) Nuclear factor p65 interacts with Keap1 to repress the Nrf2-ARE pathway. *Cell Signal* **23**:883–892.
Zehir A, Benayed R, Shah RH, Syed A, Middha S, Kim HR, Srinivasan P, Gao J, Chakravarty D, Devlin SM, et al. (2017) Mutational landscape of metastatic cancer revealed from prospective clinical sequencing of 10,000 patients. *Nat Med* **23**:703–713.
Zeidan TA, Duncan S, Hencken CP, Wynn TA, and Sanrame CN (2014) *Prodrugs of Fumarates and Their Use in Treating Various Diseases*, Alkermes Pharma Ireland, Dublin, Ireland.
Zhang DD (2013) Bardoxolone brings Nrf2-based therapies to light. *Antioxid Redox Signal* **19**:517–518.
Zhang QY, Chu XY, Jiang LH, Liu MY, Mei ZL, and Zhang HY (2017) Identification of non-electrophilic Nrf2 activators from approved drugs. *Molecules* **22**:1–12.
Zhao C, Zhang Y, Liu H, Li P, Zhang H, and Cheng G (2017) Fortunellin protects against high fructose-induced diabetic heart injury in mice by suppressing inflammation and oxidative stress via AMPK/Nrf-2 pathway regulation. *Biochem Biophys Res Commun* **490**:552–559.
Zhao M, Chen H, Ding Q, Xu X, Yu B, and Huang Z (2016) Nuclear factor erythroid 2-related factor 2 deficiency exacerbates lupus nephritis in B6/lpr mice by regulating Th17 cell function. *Sci Rep* **6**:38619.
Zhou X, Menche J, Barabási AL, and Sharma A (2014) Human symptoms-disease network. *Nat Commun* **5**:4212.

Hindawi
Oxidative Medicine and Cellular Longevity
Volume 2019, Article ID 9372182, 20 pages
https://doi.org/10.1155/2019/9372182

*Review Article*

# Activators and Inhibitors of NRF2: A Review of Their Potential for Clinical Development

**Natalia Robledinos-Antón,[1,2] Raquel Fernández-Ginés,[1,2] Gina Manda,[3] and Antonio Cuadrado[1,2,3]**

[1]*Instituto de Investigaciones Biomédicas "Alberto Sols" UAM-CSIC, Instituto de Investigación Sanitaria La Paz (IdiPaz) and Department of Biochemistry, Faculty of Medicine, Autonomous University of Madrid, Madrid, Spain*
[2]*Centro de Investigación Biomédica en Red sobre Enfermedades Neurodegenerativas (CIBERNED), ISCIII, Madrid, Spain*
[3]*Victor Babes National Institute of Pathology, Bucharest, Romania*

Correspondence should be addressed to Antonio Cuadrado; antonio.cuadrado@uam.es

Received 16 January 2019; Revised 26 March 2019; Accepted 16 April 2019; Published 14 July 2019

Academic Editor: Luciano Saso



The transcription factor NRF2 (nuclear factor erythroid 2-related factor 2) triggers the first line of homeostatic responses against a plethora of environmental or endogenous deviations in redox metabolism, proteostasis, inflammation, etc. Therefore, pharmacological activation of NRF2 is a promising therapeutic approach for several chronic diseases that are underlined by oxidative stress and inflammation, such as neurodegenerative, cardiovascular, and metabolic diseases. A particular case is cancer, where NRF2 confers a survival advantage to constituted tumors, and therefore, NRF2 inhibition is desired. This review describes the electrophilic and nonelectrophilic NRF2 activators with clinical projection in various chronic diseases. We also analyze the status of NRF2 inhibitors, which at this time provide proof of concept for blocking NRF2 activity in cancer therapy.

## 1. Introduction

Nuclear factor erythroid 2-related factor 2 (NRF2) is the product of the *NFE2L2* gene and belongs to the cap′n′collar transcription factor family. By sequence homology with other orthologs, the domains termed Neh1-7 have been traditionally allocated in this protein (Figure 1(a)). At the C-terminus, NRF2 contains a basic leucine-zipper (bZip) domain that participates in the formation of heterodimers with other bZip proteins, like small muscle aponeurosis fibromatosis (MAF) K, G, and F [1, 2]. These heterodimers regulate the expression of about 250 human genes that present a regulatory enhancer sequence termed Antioxidant Response Element (ARE; 5′-TGACNNNGC-3′) and participate in multiple homeostatic functions including regulation of inflammation, redox metabolism, and proteostasis [3–6].

From a clinical perspective, it is of utmost importance that NRF2 can be targeted pharmacologically in diseases underlined by oxidative stress and inflammation, such as neurodegenerative, vascular, and metabolic diseases as well as cancer [7, 8]. In models of most chronic diseases, a reinforcement of homeostasis through NRF2 activators provides a beneficial therapeutic effect. In cancer, the pharmacological regulation of NRF2 appears to be context dependent. It is generally accepted that NRF2 inhibitors not only reduce the survival and proliferative advantage of cancer cells but also sensitize tumors to chemo- and radiotherapy [9]. In this review, we describe the pharmacological activators of NRF2 that are in several stages of pharmacological development for the treatment of several chronic diseases. The most developed compounds activate NRF2 by preventing its degradation by KEAP1-dependent mechanisms. We also discuss

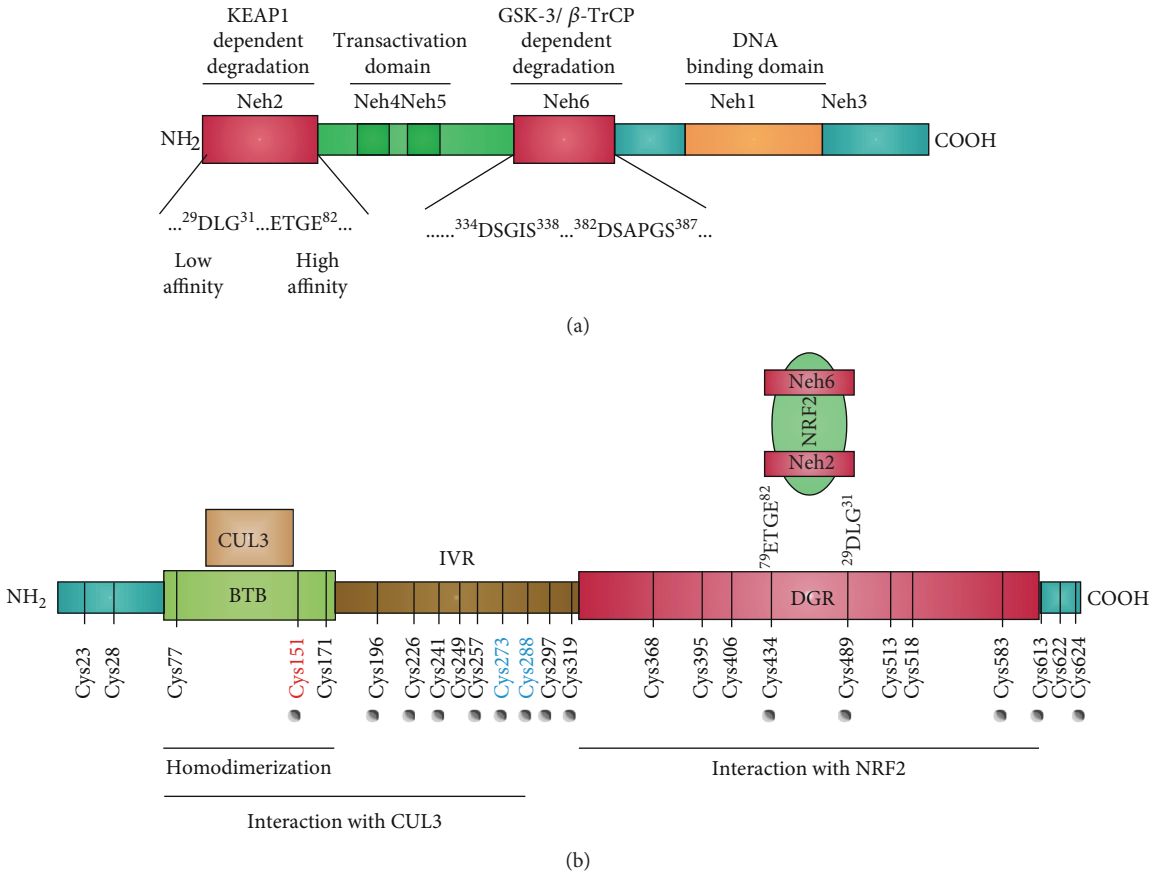


Figure 1: Domain structures of NRF2 and KEAP1. (a) Domain structure of NRF2. NRF2 possesses six highly conserved domains called NRF2-ECH homology (Neh) domains [167]. The functional role of each Neh domain is specified. Within the Neh2 domain, the low-affinity (DLG) and high-affinity (ETGE) binding domains to KEAP1 are zoomed in. (b) Domain structure of a KEAP1 monomer showing the position of cysteine residues. The N-terminal BTB (bric-a-brac, tramtrack, broad complex) domain participates in homodimerization and binding to CUL3/RBX1. The C-terminal region, DGR (double glycine repeat) domain, contains a double glycine repeat called Kelch repeat that binds NRF2-Neh2 domain. The intervening region (IVR/LR) connects BTB and DGR domains and is particularly rich in redox-sensitive cysteine residues. Red and blue cysteine residues in KEAP1 are the most relevant for electrophile reactivity. This figure has been modified and extended from [168] to highlight the degradation domains in NRF2 and the cysteines of KEAP1.

the current state of NRF2 inhibitors which may be highly relevant for cancer therapeutics although at this time they are still in early phases of development.

## 2. Physiologic Regulation of NRF2

NRF2 is ubiquitously and constitutively expressed by cells, thus ensuring their prompt protective response to oxidative, inflammatory, and metabolic stresses. Under normal physiological conditions, NRF2 has a rapid turnover and presents a half-life of about 20-30 min due to its constant degradation by the ubiquitin proteasome system [10, 11]. Therefore, under nonstressed conditions, low NRF2 levels provide basal expression of its target genes.

The main control of NRF2 stability is exerted by the E3 ligase adapter Kelch-like ECH-associated protein 1 (KEAP1). KEAP1 is a homodimer protein that comprises three functional domains (Figure 1(b)): a broad complex, tramtrack, bric-a-brac (BTB) homodimerization domain, an intervening region (IVR), and a C-terminal Kelch domain with a double glycine repeat (DGR). The Kelch domain binds to the Neh2 domain of NRF2 at two amino acid sequences: DLG and ETGE. Experiments based on isothermal calorimetry have led to the conclusion that the ETGE motif exhibits about one hundred times higher affinity for KEAP1 than the DLG motif [12]. KEAP1 presents NRF2 for ubiquitination by the E3 ligase complex formed by Cullin3 and RBX1 proteins (CUL3/RBX1) [13], resulting in subsequent NRF2 degradation by the proteasome 26S [2, 14].

KEAP1 contains 27 cysteine residues in humans, converting this protein in a redox sensor for endogenous and environmental oxidative signals as well as for electrophilic reactions [15]. Under redox-challenging conditions, the cellular redox buffers comprising glutathione (GSH), thioredoxin, etc. maintain low intracellular levels of reactive oxygen species (ROS) and glutathionylated proteins. However, ROS oxidize thiols and induce glutathionylation and alkylation of macromolecules, therefore having the capacity to modify KEAP1 cysteines [16]. From a pharmacological perspective, electrophile reaction with some cysteines of KEAP1 leads to the formation of adducts that prevent the ubiquitination NRF2, resulting in its stabilization, nuclear

translocation, and transcriptional induction of NRF2-target genes [7, 8].

An alternative mechanism for proteasomal degradation of NRF2 is mediated by the glycogen synthase kinase 3 (GSK-3) and the E3 ligase adapter $\beta$-TrCP. GSK-3$\alpha$ and $\beta$ are serine/threonine protein kinases involved in several signaling pathways such as receptor tyrosine kinase, WNT, and Hedgehog that influence cell division, survival, and development [17, 18]. GSK-3$\alpha$ and $\beta$ are maintained in an inactive state under normal conditions due to their inhibition by AKT-mediated phosphorylation at their N-terminal pseudosubstrate domain or by sequestration in protein complexes. However, in the absence of receptor signaling, active GSK-3 phosphorylates NRF2 at the Neh6 domain (DSGIS). This phosphodomain recruits $\beta$-TrCP, which recognizes pSGIpS, and the CUL1/RBX1 complex for ubiquitin-proteasome degradation [19]. $\beta$-TrCP also recognizes another motif in the Neh6 domain of NRF2 (DSAPGS) which appears to be constitutively phosphorylated in a GSK-3-independent manner [20]. Additional degradative systems are able to regulate NRF2 at posttranscriptional level, such as the inositol-requiring enzyme (IRE1)/E3 ubiquitin ligase synoviolin (HRD1) [21].

NRF2 can be regulated at the transcriptional level. The *NFE2L2* gene promoter presents several regulatory sequences: (a) one xenobiotic response element (XRE; 5′-TA/TGCG TGA/C-3′) at -712 and two XRE-like sequences at +755 and +850 that are recognized by the transcription factor Aryl Hydrocarbon Receptor (AHR) [22]; (b) two ARE-like sequences at -492 (AREL1; TGACTCCGC) and -754 pb (AREL2; TGACTGTGGC), which allow NRF2 autoregulation [23]; (c) one 12-O-tetradecanoylphorbol-13-acetate-response element (TRE) (TGCGTCA) at +267 to +273 pb that is activated by the oncogenic KRAS [24], BRAF, and MYC [25] hence being critically involved in carcinogenesis; (d) one NF-$\kappa$B binding site that responds to inflammatory stimuli [26]; and (e) epigenetic changes such as promoter methylation, microRNAs including miR-144 [27], miR-28 [28], miR-98-5p [29], and long noncoding RNA deregulation [30] that contribute to changes in expression of the NRF2-coding gene.

## 3. Pharmacologic Activators of NRF2

The so-called "NRF2 activators" should be more precisely termed "KEAP1 inhibitors" as their molecular target is in fact KEAP1 [31]. These compounds can be classified as electrophiles, protein-protein interaction (PPI) inhibitors, and multitarget drugs (Figure 2).

*3.1. Electrophilic Compounds.* Most pharmacological NRF2 activators are electrophilic molecules that covalently modify cysteine residues present in the thiol-rich KEAP1 protein by oxidation or alkylation [32–34]. Many cysteines of KEAP1 are modified by different electrophiles [35–37]. Cysteines Cys-151, Cys-273, and Cys-288 [38, 39] appear to be the most susceptible to electrophile reaction [40, 41]. Other sensitive cysteines are Cys-226, Cys-434, and Cys-613. This "cysteine-code" controls KEAP1 activity when the protective response mediated by NRF2 is needed. Selected electrophilic activators of NRF2 that are in various stages of clinical development are presented in Table 1.

One mechanism of KEAP1 inhibition is the sequestration in complexes with NRF2 that cannot be ubiquitinated. Modifications of several cysteines in KEAP1 generate a nonfunctional closed state with both Neh2 motifs (DLG and ETGE) of NRF2 interacting with the KEAP1 dimer but not leading to ubiquitination. As a result, free KEAP1 is not regenerated at a sufficient rate and newly synthesized NRF2 escapes KEAP1-mediated ubiquitination and subsequent degradation [42].

Another mechanism of KEAP1 inhibition is related to its interaction with the CUL3/RBX1 complex, required for NRF2 ubiquitination. Cys-151 located at the BTB domain influences the interaction of KEAP1 with CUL3. The crystal structure of the BTB domain bound to the pentacyclic triterpenoid 2-cyano-3,12-dioxo-oleana-1,9(11)-dien-28-oate (bardoxolone, CDDO, RTA401) indicates that adduct formation with Cys-151 most likely disrupts the interaction between KEAP1 and CUL3 [43–45]. As a result, KEAP1 is clogged in a NRF2 bound conformation, and newly formed NRF2 escapes ubiquitination. Synthetic triterpenoids have been derived from the natural compound oleanolic acid to provide them with strong Michael acceptor reactivity. This is achieved mainly through the addition of enone and ciano groups to the A ring and another enone group to the C ring [46, 47]. Bardoxolone methyl (CDDO-Me or RTA 402) reached clinical trials for the treatment of advanced chronic kidney disease (CKD) and type 2 diabetes mellitus [48]. Although phase II clinical trials demonstrated long-term increment in glomerular filtration, CDDO-Me was halted at phase III due to cardiovascular safety issues [49]. A new phase II clinical trial has recently started recruiting patients with rare chronic kidney diseases to better define the safety and efficacy profiles of CDDO-Me. Currently, CDDO-Me is also under clinical study for the Alport syndrome and pulmonary hypertension. In an effort to improve the safety profile, a second-generation difluoromethyl acetamide derivative of bardoxolone methyl, called RTA-408 (Omaveloxone), is now under clinical investigation in phase II clinical trials for Friedreich's ataxia, ocular inflammation, and pain after ocular surgery [50]. Recently, a preclinical study evaluated RTA-408 for diabetic wound recovery and pointed NRF2 upregulation as responsible for the observed improvement in regenerative capacity [51].

The most successful NRF2 activator to date is the fumaric acid ester dimethyl fumarate (DMF) (BG-12 or Tecfidera, from Biogen) that has been approved in 2013 by FDA for relapsing-remitting multiple sclerosis (MS) [52–55]. Previously, DMF was authorized for the treatment of psoriasis [56]. DMF was shown to reduce the number of peripheral T cells, $CD8^+$ cells being more sensitive to DMF than $CD4^+$ cells [57, 58]. DMF also reduces total B lymphocyte counts, especially memory B cells, along with a decrease in granulocyte-macrophage colony-stimulating factor, IL-6, and TNF-$\alpha$ production, leading to an anti-inflammatory shift in B cell responses [59, 60]. The DMF-induced activation of NRF2 in the central nervous system was described

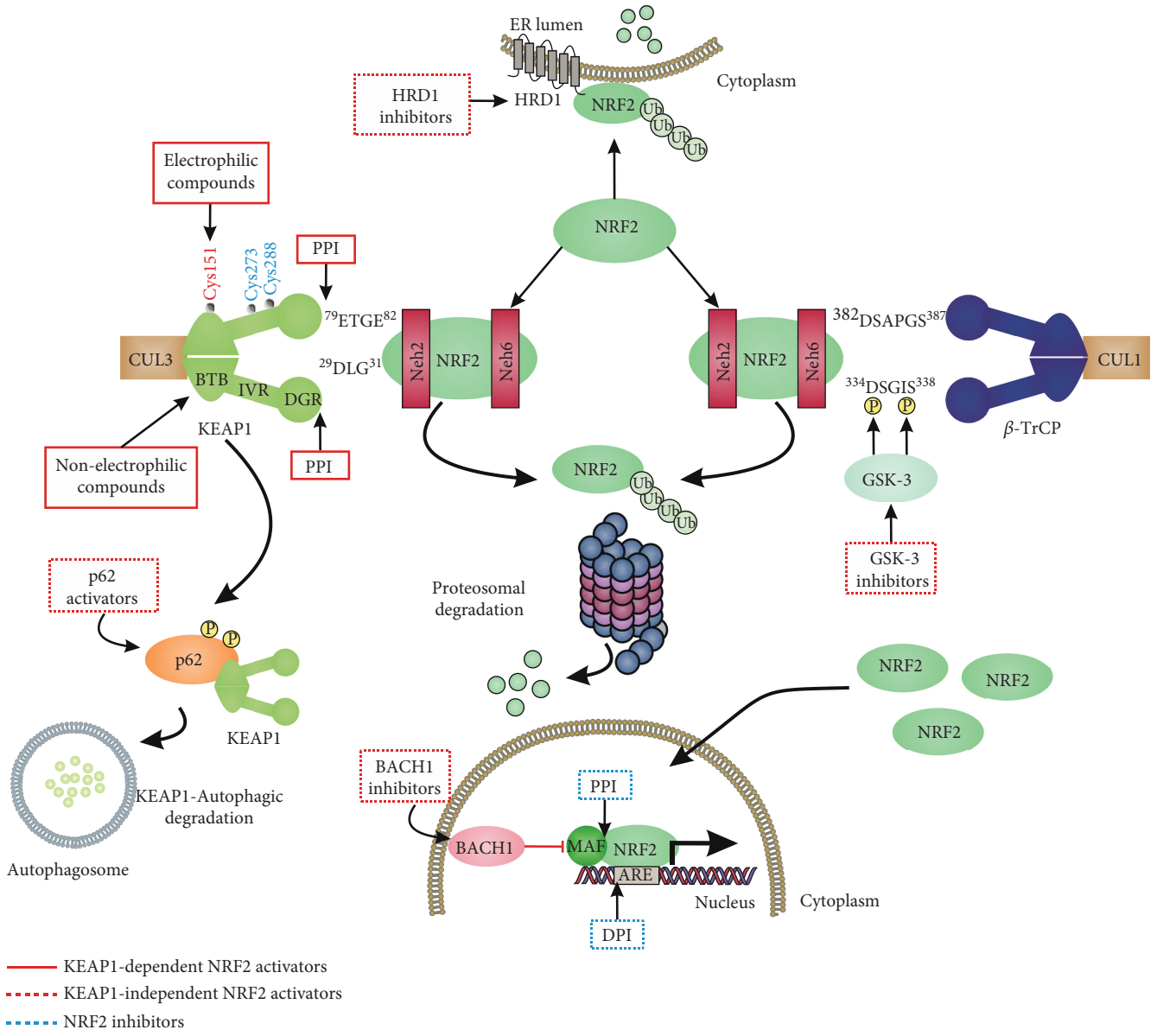


Figure 2: Summary of the pharmacological strategies to modulate NRF2 activity.

in the MS mice model of experimental allergic encephalomyelitis [61]. In this model, DMF-dependent NRF2 activation correlated with an improvement in the clinical course of MS, favored axon preservation, and increased astrocyte activation. These beneficial effects of DMF did not occur in NRF2-null mice, hence indicating that DMF was acting mainly by targeting the NRF2 pathway. DMF is mostly converted to monomethyl fumarate (MMF) by intestinal esterases, and only a small fraction is found in blood conjugated with glutathione [62]. Therefore, an oral formulation of a monomethyl fumarate (MMF) derivative, diroximel fumarate (2-(2,5-dioxo-1-pyrrolidinyl)ethyl ester; ALKS-8700; Alkermes) which exhibits improved bioavailability and efficacy, is currently under phase III trial for MS [63, 64]. However, the biological effects of these fumaric acid esters are not fully characterized and KEAP1/NRF2-independent effects are being described. For instance, it has been reported that DMF and MMF activate the nicotinic receptor hydroxycarboxylic acid receptor 2, which is expressed in immune cells and gut epithelial cells, resulting in NRF2-independent anti-inflammatory responses [65].

Oltipraz (4-methyl-5(pyrazinyl-2)-1-2-dithiole-3-thione) is a NRF2 inducer that enhances GSH biosynthesis and phase II detoxification enzymes, such as NQO1. Oltipraz is a promising chemopreventive agent [66] under phase III clinical trial for the treatment of nonalcoholic fatty liver disease.

Ursodiol (ursodeoxycholic acid) is an FDA-approved drug for the treatment of primary biliary cirrhosis. Although its cytoprotective mechanisms have not been elucidated yet, several research groups suggested that the upregulation of NRF2 by ursodiol induces detoxification and antioxidant mechanisms that play a role in its therapeutic efficacy [67, 68].

Several natural compounds have been identified as electrophilic NRF2 inducers, including sulforaphane, curcumin,

Table 1: Selected electrophilic activators of NRF2 under clinical development.

| Compound | Type | Mechanism of action | Disease | Clinical trial | ClinicalTrials.gov identifier |
|---|---|---|---|---|---|
| Bardoxolone-methyl (CDDO-Me) 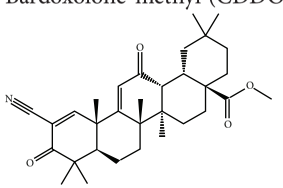 | Synthetic triterpenoids | Electrophilic modification of KEAP1-Cys-151 | Diabetic nephropathy | Phase II | NCT00811889 |
| | | | IgA nephropathy<br>CKD associated with type 1 diabetes<br>Focal segmental glomerulosclerosis<br>Autosomal dominant polycystic kidney | Phase II | NCT03366337 |
| | | | Chronic kidney disease<br>Type 2 diabetes<br>Diabetic nephropathy | Phase III | NCT01351675 |
| | | | Liver disease | Phase I/II | NCT00550849 |
| | | | Hepatic impairment<br>Healthy | Phase I | NCT01563562 |
| | | | Advanced solid tumors lymphoid malignancies | Phase I | NCT00529438<br>NCT00508807 |
| | | | Alport syndrome | Phase II/III cardinal | NCT03019185 |
| | | | Pulmonary hypertension | Phase III RANGER | NCT03068130 |
| | | | Pulmonary arterial hypertension | Phase III | NCT02657356 |
| | | | Renal insufficiency, chronic<br>Diabetes mellitus, type 2 | Phase II | NCT01053936 |
| RTA-408 (omaveloxolone) 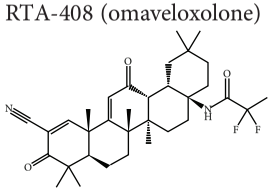 | Synthetic triterpenoids | Electrophilic modification of KEAP1-Cys-151 | Mitochondrial myopathy | Phase II | NCT02255422 |
| | | | Friedreich's ataxia | Phase II | NCT02255435 |
| | | | Inflammation and pain following ocular surgery | Phase II | NCT02065375 |
| | | | Corneal endothelial cell loss<br>Ocular pain<br>Ocular inflammation<br>Cataract surgery | Phase II | NCT02128113 |
| | | | Melanoma | Phase I/II | NCT02259231 |
| | | | Breast cancer | Phase II | NCT02142959 |
| Dimethyl fumarate 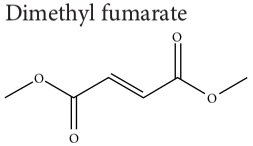 | Fumaric acid ester | Electrophilic modification of KEAP1-Cys-151 | Multiple sclerosis | *Approved* | |
| | | | Psoriasis | *Approved* | |
| | | | Rheumatoid arthritis | Phase II | NCT00810836 |
| | | | Adult brain glioblastoma | Phase I | NCT02337426 |
| | | | Cutaneous T cell lymphoma | Phase II | NCT02546440 |
| | | | Obstructive sleep apnea | Phase II | NCT02438137 |
| | | | Chronic lymphocytic leukemia<br>Small lymphocytic lymphoma | Phase I | NCT02784834 |

Table 1: Continued.

| Compound | Type | Mechanism of action | Disease | Clinical trial | ClinicalTrials.gov identifier |
|---|---|---|---|---|---|
| ALKS-8700 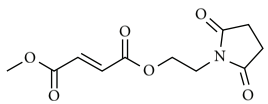 | Fumaric acid ester (MMF-derivate) | Electrophilic modification of KEAP1-Cys-151 | Multiple sclerosis | Phase III | NCT02634307 |
| Oltipraz 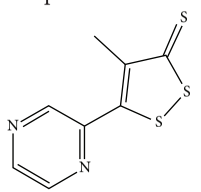 | Organosulfur compound | Electrophilic modification of KEAP1-Cys-151 | Nonalcoholic steatohepatitis | Phase III | NCT02068339 |
| | | | Schistosomiasis | *Approved* | |
| | | | Lung cancer | Phase I | NCT00006457 |
| Ursodiol 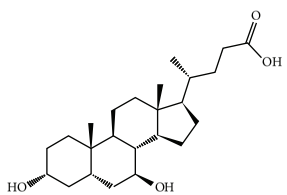 | Biliary acid | Electrophilic modification of KEAP1-Cys-151 | Cholestasis | Phase II/III | NCT00846963 |
| | | | Diarrhea | Phase IV | NCT02748616 |
| | | | Cholelithiasis | Phase III | NCT02721862 |
| | | | Primary biliary cirrhosis | Phase IV | NCT01510860 |
| | | | Barrett esophagus Low-grade dysplasia | Phase II | NCT01097304 |
| | | | Chronic hepatitis C | Phase III | NCT00200343 |
| | | | Type 2 diabetes mellitus | Phase II | NCT02033876 |
| Sulforaphane 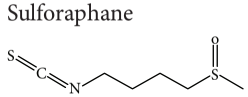 | Isothiocyanate | Electrophilic modification of KEAP1-Cys-151 | Schizophrenia | Phase II/III | NCT02880462 |
| | | | | Phase II | NCT02810964 |
| | | | | Phase II | NCT01716858 |
| | | | COPD | Phase II | NCT01335971 |
| | | | Atopic asthmatics | Phase I | NCT01845493 |
| | | | Autism spectrum disorder | Phase II | NCT01474993 |
| | | | | Phase II | NCT02909959 |
| | | | | Phase II | NCT02677051 |
| | | | | Phase II | NCT02654743 |
| | | | | Phase I/II | NCT02561481 |
| | | | Healthy | Phase I | NCT01008826 |
| | | | | Phase I | NCT02023931 |
| | | | Melanoma | Phase I | NCT01568996 |
| | | | Asthma | Phase I | NCT01845493 |
| | | | | Phase I/II | NCT01183923 |
| | | | Prostate cancer | Phase II | NCT01228084 |

Table 1: Continued.

| Compound | Type | Mechanism of action | Disease | Clinical trial | ClinicalTrials.gov identifier |
|---|---|---|---|---|---|
| | | | Breast cancer | Phase II | NCT00843167 |
| | | | Lung cancer | Phase II | NCT03232138 |
| | | | Environmental carcinogenesis | Phase II | NCT01437501 |
| | | | Alcohol sensitivity | Phase II | NCT01845220 |
| | | | Aging | Phase II | NCT03126539 |
| | | | Rhinitis, allergic | Phase II | NCT02885025 |
| | | | Helicobacter pylori infection | Phase IV | NCT03220542 |
| | | | Diabetes mellitus, noninsulin-dependent | Phase II | NCT02801448 |
| Sulforadex (SFX-01) 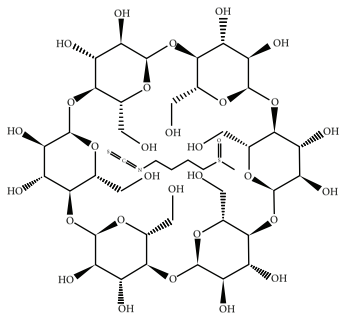 | Sulforaphane/alpha-cyclodextrin complex | Electrophilic modification of KEAP1-Cys-151 | Subarachnoid haemorrhage | Phase II | NCT02614742 |
| | | | Breast neoplasm | Phase I/II | NCT02970682 |
| | | | Prostate cancer | Phase I | NCT02055716<br>NCT01948362 |
| ITH12674 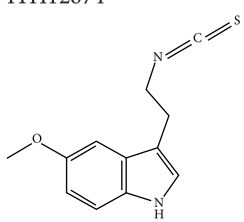 | Melatonin-sulforaphane hybrid | Electrophilic modification of KEAP1-Cys-151 | Brain ischemia | Preclinical PK | No clinical trials available |
| Curcumin 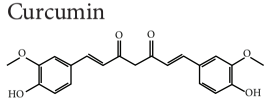 | Stilbene | Electrophilic modification of KEAP1-Cys-151 | Type 2 diabetes<br>Prediabetes<br>Insulin resistance<br>Cardiovascular risk | Phase IV | NCT01052025 |
| | | | Schizophrenia<br>Cognition<br>Psychosis | Phase I/II | NCT02104752 |
| | | | Acute kidney injury<br>Abdominal aortic aneurysm | Phase II/III | NCT01225094 |

Table 1: Continued.

| Compound | Type | Mechanism of action | Disease | Clinical trial | ClinicalTrials.gov identifier |
|---|---|---|---|---|---|
| | | | Chronic kidney diseases<br>Diabetes mellitus, type 2<br>Polymorphism | Phase II/III | NCT03262363 |
| | | | Alzheimer's disease | Phase I/II | NCT00164749 |
| | | | Neoplasms | Phase II | NCT02944578 |
| | | | Crohn's disease | Phase III | NCT02255370 |
| | | | Chronic schizophrenia | Phase IV | NCT02298985 |
| | | | Mild cognitive impairment | Phase II | NCT01811381 |
| | | | Prostate cancer | Phase III | NCT02064673 |
| | | | Major depression | Phase IV | NCT01750359 |
| Resveratrol 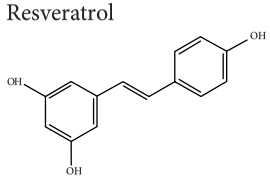 | (*E*)-Stilbene derivate | Electrophilic modification of KEAP1-Cys-151 | Type 2 diabetes | Phase I | NCT01677611 |
| | | | Colon cancer | Phase I | NCT00256334 |
| | | | COPD | N/A | NCT02245932 |
| | | | Friedreich ataxia | Phase I/II | NCT01339884 |
| | | | Nonalcoholic fatty liver | Phase II/III | NCT02030977 |
| | | | Nonischemic cardiomyopathy | Phase III | NCT01914081 |
| | | | Endometriosis | Phase IV | NCT02475564 |
| | | | Chronic renal insufficiency | Phase III | NCT02433925 |
| | | | Metabolic syndrome X | Phase II | NCT02114892 |
| | | | Chronic subclinical inflammation<br>Redox status | Phase III | NCT01492114 |
| | | | Alzheimer's disease | Phase II | NCT01504854 |
| | | | | Phase III | NCT00743743 |
| | | | Huntington disease | Phase III | NCT02336633 |
| CXA-10 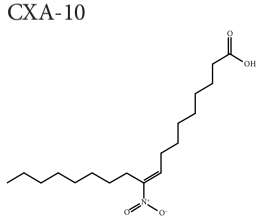 | Nitro-fatty acid (NFA) | Electrophilic modification of KEAP1-Cys-273 and Cys-288 | Acute kidney injury | Phase I | NCT02248051 |
| | | | Pulmonary arterial hypertension (PAH) | Phase II | NCT03449524 |
| | | | Primary focal segmental glomerulosclerosis (FSGS) | Phase II | NCT03422510 |

resveratrol, quercetin, genistein, and more recently andrographolide [69]. For instance, sulforaphane (SFN), an isothiocyanate found in cruciferous vegetables, has been successfully used for the treatment of patients with type II diabetes mellitus [70, 71]. Due to the capacity of SFN to cross the blood-brain barrier, it protects against neurodegenerative disorders as demonstrated in murine models of disease. Regarding acute brain damage, SFN was shown to exert protective effects in hypoxic-ischemic injury in rats by reducing the infarct ratio and by upregulating NRF2 and HO-1 [72, 73]. In neurodegenerative disease models, SFN proved protective capacity against the neurotoxic $A\beta_{1\text{-}42}$ peptide in neuronal cells [74]. *In vivo*, SFN ameliorated cognitive impairment in an acute mouse model of Alzheimer disease (AD) [75]. In Parkinson disease (PD), SFN protected dopaminergic cells against the cytotoxic effects of 6-hydroxydopamine [76]. In the 1-methyl-4-phenyl-1,2,3,6-tetrahydropyridine mouse model of PD, SFN counteracted astrogliosis and microgliosis and reduced the death of dopaminergic neurons [77–79]. To improve the stability of SFN, Evgen Pharma has developed a cyclodextrin formulation, SFX-01, which is under phase II clinical trial for the treatment of subarachnoid haemorrhage. A hybrid molecule of SFN and melatonin (ITH12674) was designed to have a dual "drug-prodrug" mechanism of action for the treatment of brain ischemia [80].

Another natural compound that modifies Cys-151 in KEAP1 and has also ROS-scavenging activity is curcumin, a linear diarylheptanoid present in turmeric (*Curcuma longa*) [81]. It has been used for the treatment of obesity, metabolic syndrome, and prediabetes [82–84]. Furthermore, curcumin has been shown to suppress the deleterious action of carcinogens by activating NRF2 [85, 86].

9-Nitro-octadec-9-enoic acid (OA-$NO_2$) is a nitro-fatty acid with anti-inflammatory properties. OA-$NO_2$ reacts with several cysteine residues of KEAP1, but mainly with Cys-273 and Cys-288, and its activity seems to be independent of Cys-151 [36]. CXA-10 (10-nitro-9(E)-octadec-9-enoic acid) is an isomer of OA-$NO_2$ which has proven efficacy the uni-nephrectomized deoxycorticosterone acetate-high salt mouse model of CKD [87] and is under several phase I clinical trials for the treatment of this disease [88] and under phase II trials for the treatment of pulmonary arterial hypertension and primary focal segmental glomerulosclerosis.

The list of electrophilic compounds able to interact with KEAP1 is continuously growing. For instance, some compounds like 15-deoxy-$\Delta$12,14-prostaglandin $J_2$ interact with Cys-273 and Cys-288 of the KEAP1 homodimer [40]. This prostaglandin has a cyclopentenone core that is able to modify covalently Cys-273 and induce NRF2 in models of ureteral obstruction [89], hepatic ischemia-reperfusion injury [90], and atherosclerosis [91]. However, its clinical use is still far from being demonstrated. In a recent study, the metabolite itaconate was described as a NRF2 activator that alkylates cysteines 151, 257, 288, 273, and 297 of KEAP1. A cell-permeable itaconate derivate, 4-octyl itaconate, protects against lipopolysaccharide cytotoxicity, thus providing an anti-inflammatory response. Furthermore, this compound is a more potent NRF2 activator than DMF [92]. Some other examples are *tert*-butylhydroquinone [93], diethyl maleate [94], TFM-735 [95], and nitric oxide [96]. However, most of these compounds have not evolved beyond proof-of-concept experiments, and a long way needs to be covered to characterize their pharmacodynamic properties, clinical safety profile, and efficacy in noncommunicable diseases.

*3.2. Protein-Protein Interaction Inhibitors of the KEAP1-NRF2 System.* Protein-protein interaction (PPI) inhibitors interfere with the docking of NRF2 to the Kelch propeller of KEAP1 and provide more selectivity over electrophilic compounds which may eventually form adducts with redox-sensitive cysteines other than those in KEAP1 [97]. Based on the X-ray crystal structure of KEAP1 [98], small PPI inhibitors have been designed to impede the binding of the ETGE motif to KEAP1 [99]. The ETGE motif adopts a $\beta$-hairpin structure that docks to the Kelch propeller of KEAP1 through specific hydrophobic and electrostatic interactions [98, 99]. A similar strategy is devised to prevent the interaction of the low-affinity DLG motif which is required for correct lysine ubiquitination in NRF2 [13].

The first PPI inhibitors of KEAP1 were designed from a series of truncated NRF2 peptides [100, 101]. Some selected peptides are shown in Table 2. It was found that the minimal binding sequence of NRF2 required for docking to KEAP1 is the 9-mer sequence LDEETGEFL [100–102]. A related peptide was designed to increase cell penetrance by adding the Tat sequence of the human immunodeficiency virus and the cleavage sequence of calpain (-Cal-Tat). This peptide demonstrated neuroprotection and cognition-preserving effects in a mouse model of cerebral ischemia [103]. Moreover, hybrid peptides based on both the region of interaction between KEAP1 and NRF2 (ETGE motif) and with the region of interaction between KEAP1 and p62/Sequestosome-1 (SQSTM1) exhibited superior binding activity compared to either native peptide alone [104]. Due to unfavorable drug-like properties, such as low oral bioavailability and cellular permeability of peptides, research has been lately focused on the development of small molecules. However, a cyclic peptide was used recently to improve KEAP1 binding and NRF2 accumulation in cells [105].

Current PPI inhibitors are tetrahydroisoquinoline [97, 106], thiopyrimidine [107], naphthalene [108], carbazone [109], and urea derivatives [110]. Recently, the naphthalene-based nonelectrophilic PPI inhibitors were modified to develop nonnaphthalene heterocyclic scaffold based on 1,4-isoquinoline that avoids the carcinogenic and mutagenic properties of naphthalenes [111]. Some patents addressing these small molecules are presented in Table 3.

Several PPI inhibitors with improved selectivity over electrophiles have been identified through screening of small molecule libraries. These compounds include SRS-5, benzenesulfonyl-pyrimidone 2, N-phenyl-benzenesulfonamide, and a series of 1,4-diphenyl-1,2,3-triazole [106, 112–115]. Recently, a new protocol for identifying reversible modifiers of the NRF2/KEAP1 interaction was proposed [116]. The biochemical assays comprised time-resolved fluorescence resonance energy transfer as primary screening tool, surface plasmon resonance to evaluate the affinity of KEAP1

Table 2: Selected peptides acting as NRF2-KEAP1 protein-protein interaction inhibitors.

| Sequence | Mechanism of action | Reference |
|---|---|---|
| LDEETGEFL-NH2 | Binding to KEAP1-Kelch domain | [100, 101] |
| DEETGE-CAL-Tat ($NH_2$-RKKRRQRRR-PLFAERLDEETGEFLPN$H_2$) | | [103] |
| Ac-DPETGEL-OH | | [102] |
| FITC$\beta$-DEETGEF-OH | | [102] |
| FITC-$\beta$-LDEETGEFL-OH | | [102] |
| Ac-DEETGEF-OH | | [102] |
| Ac-DPETGEL-OH | | [102] |
| FITC-LDEETGEFL-$NH_2$ | | [100] |
| FAM-LDEETGEFL-$NH_2$ | | [108] |
| LQLDEETGEFLPIQGK(MR121)-OH | | [107] |
| Ac-LDEETGEFL-$NH_2$ | | [100, 101] |
| Ac-DPETGEL-$NH_2$ | | [104] |
| Ac-NPETGEL-OH | | [104] |
| St-DPETGEL-OH | | [104] |
| YGRKKRRQRRRLQLDEETGEFLPIQ | | [162] |
| c[GQLDPETGEFL] | | [105] |

binders, and $^1$H-$^{15}$N heteronuclear single-quantum coherence nuclear magnetic resonance assay to further analyze the binding mode. This protocol will help in identifying and improving the properties of reversible binders to KEAP1.

*3.3. Other Mechanism of NRF2 Activation.* The phosphorylation of NRF2 by GSK-3 leads to its ubiquitination by the E3 ligase $\beta$-TrCP and subsequent proteasomal degradation. An aberrant activity of GSK-3 is linked with several pathologies such as AD, cardiovascular diseases, or cancer among others [117–120]. Therefore, several clinical trials are now focused on GSK-3 inhibitors for the treatment of several pathologies [121]. For instance, the GSK-3-inhibitor Tideglusib, a thiadiazolidinone compound, was studied in phase II trials for AD in the ARGO study [122]. Another inhibitor is Enzastaurin which is intended for the treatment of solid and hematological cancers. Although Enzastaurin provided promising results at the preclinical level, treatment failed in phase II and III trials [123, 124]. GSK-3-dependent NRF2 phosphorylation was shown to be inhibited by nordihydroguaiaretic acid [125]. This compound and its derivative terameprocol are in phase I and II clinical trials for the treatment of several types of cancers, such as gliomas and leukemias (Table 4) [126].

Focusing on E3 ubiquitin ligase $\beta$-TrCP, it would be possible to develop small molecules able to disrupt the docking of NRF2 to $\beta$-TrCP, hence opening a new way regarding KEAP1-independent activators of NRF2 [127]. A novel E3 ubiquitin ligase linked to KEAP1-independent NRF2 degradation is HRD1 [21]. HRD1-dependent NRF2 degradation has been described in the context of cirrhotic liver. HRD1 is a transcriptional target of X-box-binding protein 1 (XBP1) that is upregulated upon activation of the inositol-requiring enzyme 1 (IRE1) during endoplasmic reticulum (ER) stress related to cirrhotic conditions. Inhibitors of HRD1 and IRE1 restore the NRF2 response in liver cirrhosis [21].

Several proteins contain a (E/S)TGE motif that resembles the high-affinity ETGE motif of NRF2. The motif confers to these proteins the ability to compete with NRF2 for KEAP1 binding, leading to a noncanonical mechanism of NRF2 stabilization [128]. Proteins containing the (E/S)TGE motif are dipeptidyl peptidase 3, Partner and Localizer of BRCA2, and SQSTM1/p62. SQSTM1/p62, a protein that transports specific cargos to the autophagosome, including KEAP1, sustains NRF2 stabilization and translocation to the nucleus [129–131]. Compounds which elevate SQSTM1/p62 levels, like rapamycin [132] and trehalose [133], are being therefore studied in several phase II and III trials in connection with diabetes mellitus, systemic lupus erythematosus, and autosomal dominant polycystic kidney disease.

Another way to inhibit the transcriptional activity of NRF2 is to impede its interaction with critical components in the nucleus. BTB domain and CNC homolog 1 (BACH1) is a transcriptional repressor which belongs to the cap′n′ collar, b-Zip family. BACH1 competes in the nucleus with NRF2 to form heterodimers with small MAF proteins and blocks therefore the expression of ARE genes [134]. A recent study characterized the HPP-4382 compound as an inhibitor of BACH1 repression activity *in vitro* [135].

All these alternative mechanisms for NRF2 stabilization and activation suggest that a combinatorial pharmaceutical approach will be the best way to activate the cytoprotective responses mediated by NRF2.

## 4. Pharmacologic Inhibitors of NRF2

The implication of NRF2 in cancer is still controversial. Several studies described that NRF2 knockout mice are more susceptible to chemically induced carcinogenesis, pointing NRF2 as a potential tumor suppressor that limits carcinogenesis [136, 137]. On the other hand, NRF2 is overexpressed in many types of tumors, and it has been related to poor disease prognosis because it confers a survival and growth advantage to cancer cells, along with resistance to chemo- and radiotherapy [138–140]. Altogether, these results suggest a protective role of NRF2 in the first steps of cancer, but in advanced stages, NRF2 overexpression helps cancer cells to adapt to the tumorigenic demands. Cancer cells are "addicted" to NRF2 and resist treatment with chemotherapy or radiotherapy [141, 142]. Therefore, it is reasonable to assume that NRF2 inhibitors should sensitize tumor cells to anticancer therapies. In all cases, the mechanism of inhibition is either unknown or not specific, and therefore, NRF2 inhibitors are still far from being translated from bench to bedside.

*4.1. Agonists of Nuclear Receptors.* Ligands of the glucocorticoid receptor such as dexamethasone [143] and clobetasol propionate [144] inhibit NRF2 by blocking its transcriptional activity or preventing its nuclear translocation. All-*trans*-retinoic acid and bexarotene, agonists of the retinoic acid receptor-$\alpha$ and retinoid X receptor-$\alpha$, inhibit the transcriptional activity of NRF2 [145, 146]. Retinoid X receptor-$\alpha$

Table 3: Selected small molecule activators of NRF2 acting as NRF2-KEAP1 protein-protein interaction inhibitors.

| Compound | Type | Ref. | Patent |
|---|---|---|---|
| (SRS)-5 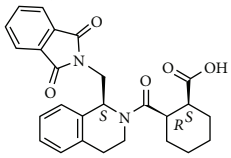 | 1,2,3,4-Tetrahydroisoquinoline core | [112] | WO2013/067036 |
| Cpd 15 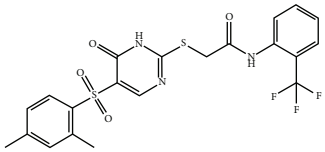 | Benzenesulfonyl-pyrimidone | [107] | WO2016/202253 |
| Cpd 16 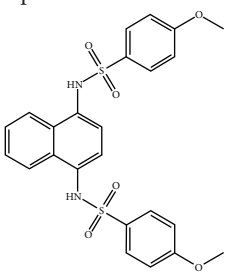 | 1,4-Diaminonaphthalene core | [107] | WO2016/202253 |
| Compound 2 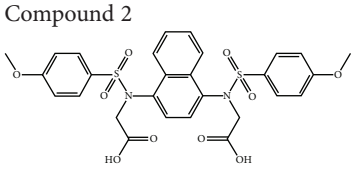 | 1,4-Diaminonaphthalene core | [163] | CN105566241A |
| 3-(Pyridin-3-ylsulfonyl)-5-(trifluoromethyl)-2H-chromen-2-one (PSTC) 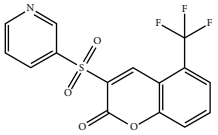 | Sulfonyl coumarins | [164] | WO2015/092713 |
| AN-465/144580 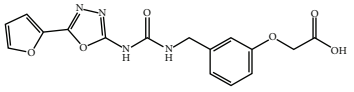 | Other structure classes | [165] | JP2011/0167537 |
| Compound 7 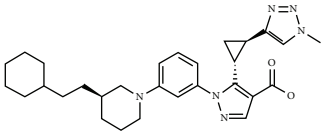 | Arylcyclohexyl pyrazoles | [166] | WO2017060855 |

appears to bind to the Neh7 domain of NRF2 preventing binding to the ARE enhancer [146]. The pharmacological value of this mechanism of NRF2 inhibition is limited by the multiple effects that are expected through the regulation of these nuclear receptors.

*4.2. Natural Compounds.* Several compounds of natural origin have been reported to inhibit NRF2. The quassinoid brusatol, extracted from *Brucea javanica*, inhibits the NRF2 transcriptional signature and sensitizes tumors and cancer cell lines to several chemotherapeutics [147]. However, its mechanism of action is not specific as it blocks protein translation, hence affecting other short-lived proteins as well [148–150].

The flavonoids luteolin [151] and wogonin [152] were reported to inhibit NRF2 and sensitize cells to anticancer drugs by increasing the instability to its transcript. However, later studies also indicated that these compounds may elicit NRF2 activation [153]. Therefore, their value as NRF2 inhibitor is highly controversial.

Table 4: Selected KEAP1-independent activators of NRF2.

| Compound | Mechanism of action | Disease | Clinical trial | ClinicalTrials.gov identifier |
|---|---|---|---|---|
| Tideglusib 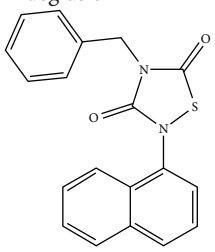 | GSK-3 inhibition | Autism spectrum disorders | Phase II | NCT02586935 |
| | | Myotonic dystrophy 1 | Phase II | NCT02858908 |
| | | Alzheimer's disease | Phase II | NCT01350362 |
| Nordihydroguaiaretic acid (NDGA) 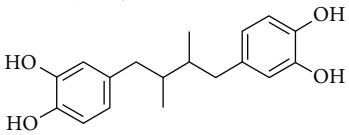 | GSK-3 inhibition | Prostate cancer | Phase II | NCT00678015 |
| | | | Phase I | NCT00313534 |
| | | Brain and central nervous system tumors | Phase I/II | NCT00404248 |
| Terameprocol (NDGA derivative) 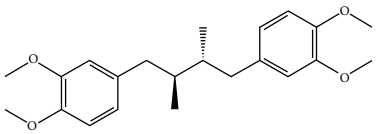 | GSK-3 inhibition | High-grade glioma | Phase I | NCT02575794 |
| | | Leukemias<br>Acute myeloid leukemia (AML)<br>Acute lymphocytic leukemia (ALL) | Phase I | NCT00664677 |
| | | Refractory solid tumors<br>Lymphoma | Phase I | NCT00664586 |
| Enzastaurin 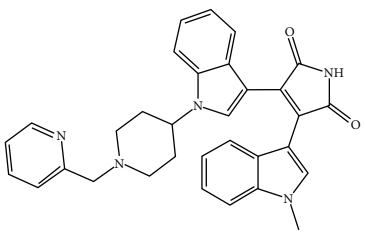 | GSK-3 inhibition | Diffuse large B cell lymphoma | Phase III | NCT03263026 |
| | | Solid tumor<br>Lymphoma, malignant | Phase I | NCT01432951 |
| LS-102 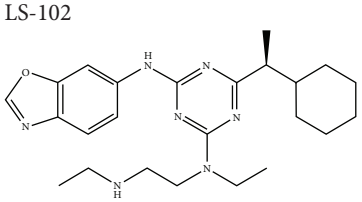 | HRD1 inhibition | — | — | No clinical trials available |
| Rapamycin 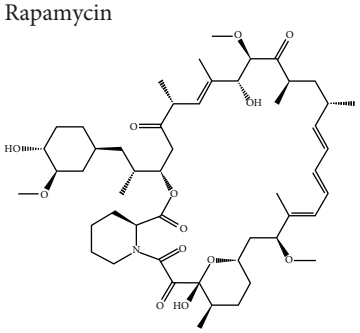 | p62/SQSTM1 activation | Diabetes mellitus, type 1 | Phase III | NCT01060605 |
| | | Systemic lupus erythematosus (SLE) | Phase II | NCT00779194 |
| | | Autosomal dominant polycystic kidney disease | Phase II/III | NCT00920309 |

Table 4: Continued.

| Compound | Mechanism of action | Disease | Clinical trial | ClinicalTrials.gov identifier |
|---|---|---|---|---|
| HPP-4382 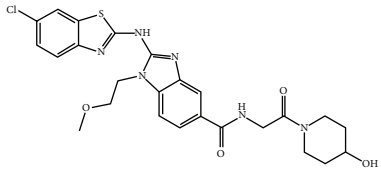 | BACH1 inhibition | — | — | No clinical trials available |

Other natural compounds such the mycotoxin ochratoxin A [154] and the coffee alkaloid trigonelline [155] prevent the nuclear translocation of NRF2. In leukemic cells, malabaricone-A, a plant-derived prooxidant, effectively inhibits NRF2 transcriptional activity as reflected by a reduction in HO-1 protein levels and leads to ROS accumulation and subsequent cell apoptosis [156]. Ascorbic acid, a well-known ROS scavenger, was found to sensitize imatinib-resistant cancer cells by decreasing the levels of the NRF2/ARE complex, hence reducing the expression of Glutamate-Cysteine Ligase Catalytic Subunit and dropping GSH levels [157]. In general, the main concern with these compounds is that their selectivity for NRF2 inhibition has not been conclusively demonstrated.

*4.3. Other Approaches.* The lack of knowledge about the fine structure of NRF2 hampers a straightforward strategy for the *in silico* analysis of small molecules that might dock to relevant domains of interaction with MAF proteins, ARE enhancer, etc. Therefore, a high-throughput screening was used which is helping in the identification of NRF2 inhibitors but still not providing selectivity [158]. A first-in-class compound, termed ML385, was found after the screening of a chemical library of 400,000 molecules. ML385 blocks NRF2 transcriptional activity and sensitizes KEAP1-deficient cells to carboplatin and other chemotherapeutics. ML385 interacts with the DNA-binding domain of NRF2 and most likely prevents the binding of NRF2 to AREs. However, given the similarity between AREs and other enhancers such as AP1, additional studies are needed to clearly establish if ML385 is selective for NRF2 or if it also inhibits other bZip transcription factors involved in chemoresistance.

Halofuginone, a synthetic derivate of febrifugine that is used in veterinary medicine, blocked the chemoresistance and radioresistance of cancer cells in parallel to the decrease of NRF2 protein levels [159]. It was found that halofuginone induces amino acid starvation resulting in global inhibition of protein synthesis.

Another compound, AEM1, decreased the expression of NRF2-controlled genes and sensitized KEAP1-deficient A549 lung tumor cells to various chemotherapeutic agents [160]. Although it seems that the anticancer effect of AEM1 is restricted to cell lines harboring mutations which render NRF2 constitutively active, the selectivity for NRF2 inhibition is not demonstrated yet.

In HeLa cells transfected with an ARE-driven luciferase reporter, a pyrazolyl hydroxamic acid, termed 4f, inhibited NRF2, reduced cell proliferation of myeloid cell lines, and increased apoptosis of acute myeloid leukemia cells [161]. Most likely, 4f altered the BCL2/BAX ratio and induced mitochondria-dependent apoptosis.

## 5. Conclusions

The NRF2/KEAP1 system represents a very promising pharmacological target to control common pathologic mechanisms of many chronic diseases characterized by low-grade oxidative stress and inflammation. A plethora of NRF2 activators, mostly of electrophilic nature, have been identified and a few are under clinical development. The pleiotropic effects of NRF2 on cell physiology together with potential off-target effects exerted by some NRF2 activators explain why drug development is moving slowly. The field of NRF2 inhibitors that may have a huge impact on cancer therapy is less advanced. Future work should be directed towards finding compounds with a good pharmacokinetic/pharmacodynamic profile for specific diseases.

## Abbreviations

AD: Alzheimer's disease
AHR: Aryl hydrocarbon receptor
BACH1: BTB domain and CNC homolog 1
BTB: Bric-a-brac, tramtrack, broad complex
$\beta$-TrCP: Beta-transducin repeat-containing E3 ubiquitin protein ligase
CUL3: Cullin3
DMF: Dimethyl fumarate
DRG: Double glycine repeat
GSH: Glutathione
GSK-3: Glycogen synthase kinase
IVR: Intervening region
KEAP1: Kelch-like ECH-associated protein 1
MMF: Monomethyl fumarate
MS: Multiple sclerosis
*NFE2L2*: Gene encoding NRF2
NRF2: Nuclear factor erythroid 2-related factor 2
PD: Parkinson's disease
PPI: Protein-protein interaction
RBX1: RING-box protein 1
ROS: Reactive oxygen species
SFN: Sulforaphane
SQSTM1: Sequestosome-1
XRE: Xenobiotic response element.

## Conflicts of Interest

The authors declare that there is no conflict of interest regarding the publication of this paper.

## Acknowledgments

This work was supported by grants SAF2016-76520-R of the Spanish Ministry of Economy and Competitiveness, B2017/BMD-3827 of the Autonomous Community of Madrid, and P_37_732/2016 REDBRAIN of the European Regional Development Fund; Competitiveness Operational Program 2014-2020. NRA and RFG are recipients of FPU and FPI contracts, respectively, of the Spanish Ministry of Economy and Competitiveness.

## Supplementary Materials

Overview of the strategies aimed at pharmacologic regulation of NRF2. KEAP1-dependent and KEAP1-independent strategies to activate NRF2 are included in red boxes. The current strategies for inhibition of NRF2 are indicated in the grey boxes. PPI: protein-protein interaction inhibitor; DPI: DNA-protein interaction inhibitor. *(Supplementary Materials)*

## References

[1] Q. Ma, "Role of nrf2 in oxidative stress and toxicity," *Annual Review of Pharmacology and Toxicology*, vol. 53, no. 1, pp. 401–426, 2013.

[2] J. D. Hayes and A. T. Dinkova-Kostova, "The Nrf2 regulatory network provides an interface between redox and intermediary metabolism," *Trends in Biochemical Sciences*, vol. 39, no. 4, pp. 199–218, 2014.

[3] M. Pajares, N. Jiménez-Moreno, Á. J. García-Yagüe et al., "Transcription factor NFE2L2/NRF2 is a regulator of macroautophagy genes," *Autophagy*, vol. 12, no. 10, pp. 1902–1916, 2016.

[4] M. Pajares, A. Cuadrado, and A. I. Rojo, "Modulation of proteostasis by transcription factor NRF2 and impact in neurodegenerative diseases," *Redox Biology*, vol. 11, pp. 543–553, 2017.

[5] M. R. de la Vega, M. Dodson, C. Gross et al., "Role of Nrf2 and autophagy in acute lung injury," *Current Pharmacology Reports*, vol. 2, no. 2, pp. 91–101, 2016.

[6] M. Pajares, N. Jiménez-Moreno, I. H. K. Dias et al., "Redox control of protein degradation," *Redox Biology*, vol. 6, pp. 409–420, 2015.

[7] A. Cuadrado, A. I. Rojo, G. Wells et al., "Therapeutic targeting of the NRF2 and KEAP1 partnership in chronic diseases," *Nature Reviews Drug Discovery*, vol. 18, no. 4, pp. 295–317, 2019.

[8] A. Cuadrado, G. Manda, A. Hassan et al., "Transcription factor NRF2 as a therapeutic target for chronic diseases: a systems medicine approach," *Pharmacological Reviews*, vol. 70, no. 2, pp. 348–383, 2018.

[9] M. Rojo de la Vega, E. Chapman, and D. D. Zhang, "NRF2 and the hallmarks of cancer," *Cancer Cell*, vol. 34, no. 1, pp. 21–43, 2018.

[10] M. McMahon, N. Thomas, K. Itoh, M. Yamamoto, and J. D. Hayes, "Redox-regulated turnover of Nrf2 is determined by at least two separate protein domains, the redox-sensitive Neh2 degron and the redox-insensitive Neh6 degron," *Journal of Biological Chemistry*, vol. 279, no. 30, pp. 31556–31567, 2004.

[11] Y. Katoh, K. Iida, M. I. Kang et al., "Evolutionary conserved N-terminal domain of Nrf2 is essential for the Keap1-mediated degradation of the protein by proteasome," *Archives of Biochemistry and Biophysics*, vol. 433, no. 2, pp. 342–350, 2005.

[12] K. I. Tong, Y. Katoh, H. Kusunoki, K. Itoh, T. Tanaka, and M. Yamamoto, "Keap1 recruits Neh2 through binding to ETGE and DLG motifs: characterization of the two-site molecular recognition model," *Molecular and Cellular Biology*, vol. 26, no. 8, pp. 2887–2900, 2006.

[13] K. I. Tong, B. Padmanabhan, A. Kobayashi et al., "Different electrostatic potentials define ETGE and DLG motifs as hinge and latch in oxidative stress response," *Molecular and Cellular Biology*, vol. 27, no. 21, pp. 7511–7521, 2007.

[14] T. Suzuki, H. Motohashi, and M. Yamamoto, "Toward clinical application of the Keap1-Nrf2 pathway," *Trends in Pharmacological Sciences*, vol. 34, no. 6, pp. 340–346, 2013.

[15] V. Sihvola and A. L. Levonen, "Keap1 as the redox sensor of the antioxidant response," *Archives of Biochemistry and Biophysics*, vol. 617, pp. 94–100, 2017.

[16] R. Holland, A. E. Hawkins, A. L. Eggler, A. D. Mesecar, D. Fabris, and J. C. Fishbein, "Prospective type 1 and type 2 disulfides of Keap1 protein," *Chemical Research in Toxicology*, vol. 21, no. 10, pp. 2051–2060, 2008.

[17] E. M. Hur and F. Q. Zhou, "GSK3 signalling in neural development," *Nature Reviews Neuroscience*, vol. 11, no. 8, pp. 539–551, 2010.

[18] K. P. Hoeflich, J. Luo, E. A. Rubie, M. S. Tsao, O. Jin, and J. R. Woodgett, "Requirement for glycogen synthase kinase-3$\beta$ in cell survival and NF-$\kappa$B activation," *Nature*, vol. 406, no. 6791, pp. 86–90, 2000.

[19] A. Cuadrado, "Structural and functional characterization of Nrf2 degradation by glycogen synthase kinase 3/$\beta$-TrCP," *Free Radical Biology & Medicine*, vol. 88, pp. 147–157, 2015.

[20] S. Chowdhry, Y. Zhang, M. McMahon, C. Sutherland, A. Cuadrado, and J. D. Hayes, "Nrf2 is controlled by two distinct $\beta$-TrCP recognition motifs in its Neh6 domain, one of which can be modulated by GSK-3 activity," *Oncogene*, vol. 32, no. 32, pp. 3765–3781, 2013.

[21] T. Wu, F. Zhao, B. Gao et al., "Hrd1 suppresses Nrf2-mediated cellular protection during liver cirrhosis," *Genes & Development*, vol. 28, no. 7, pp. 708–722, 2014.

[22] W. Miao, L. Hu, P. J. Scrivens, and G. Batist, "Transcriptional regulation of NF-E2 p45-related factor (NRF2) expression by the aryl hydrocarbon receptor-xenobiotic response element signaling pathway: direct cross-talk between phase I and II drug-metabolizing enzymes," *Journal of Biological Chemistry*, vol. 280, no. 21, pp. 20340–20348, 2005.

[23] M. K. Kwak, K. Itoh, M. Yamamoto, and T. W. Kensler, "Enhanced expression of the transcription factor Nrf2 by cancer chemopreventive agents: role of antioxidant response element-like sequences in the nrf2 promoter," *Molecular and Cellular Biology*, vol. 22, no. 9, pp. 2883–2892, 2002.

[24] S. Tao, S. Wang, S. J. Moghaddam et al., "Oncogenic KRAS confers chemoresistance by upregulating NRF2," *Cancer Research*, vol. 74, no. 24, pp. 7430–7441, 2014.

[25] G. M. DeNicola, F. A. Karreth, T. J. Humpton et al., "Oncogene-induced Nrf2 transcription promotes ROS detoxification and tumorigenesis," *Nature*, vol. 475, no. 7354, pp. 106–109, 2011.

[26] S. A. Rushworth, L. Zaitseva, M. Y. Murray, N. M. Shah, K. M. Bowles, and D. J. MacEwan, "The high Nrf2 expression in human acute myeloid leukemia is driven by NF-κB and underlies its chemo-resistance," *Blood*, vol. 120, no. 26, pp. 5188–5198, 2012.

[27] C. Sangokoya, M. J. Telen, and J. T. Chi, "microRNA miR-144 modulates oxidative stress tolerance and associates with anemia severity in sickle cell disease," *Blood*, vol. 116, no. 20, pp. 4338–4348, 2010.

[28] M. Yang, Y. Yao, G. Eades, Y. Zhang, and Q. Zhou, "MiR-28 regulates Nrf2 expression through a Keap1-independent mechanism," *Breast Cancer Research and Treatment*, vol. 129, no. 3, pp. 983–991, 2011.

[29] X. Sun, X. Li, S. Ma, Y. Guo, and Y. Li, "MicroRNA-98-5p ameliorates oxygen-glucose deprivation/reoxygenation (OGD/R)-induced neuronal injury by inhibiting Bach1 and promoting Nrf2/ARE signaling," *Biochemical and Biophysical Research Communications*, vol. 507, no. 1-4, pp. 114–121, 2018.

[30] F. P. Fabrizio, A. Sparaneo, D. Trombetta, and L. A. Muscarella, "Epigenetic versus genetic deregulation of the KEAP1/NRF2 axis in solid tumors: focus on methylation and noncoding RNAs," *Oxidative Medicine and Cellular Longevity*, vol. 2018, Article ID 2492063, 21 pages, 2018.

[31] S. Magesh, Y. Chen, and L. Hu, "Small molecule modulators of Keap1-Nrf2-ARE pathway as potential preventive and therapeutic agents," *Medicinal Research Reviews*, vol. 32, no. 4, pp. 687–726, 2012.

[32] W. Hur and N. S. Gray, "Small molecule modulators of antioxidant response pathway," *Current Opinion in Chemical Biology*, vol. 15, no. 1, pp. 162–173, 2011.

[33] T. Satoh, S. R. McKercher, and S. A. Lipton, "Nrf2/ARE-mediated antioxidant actions of pro-electrophilic drugs," *Free Radical Biology & Medicine*, vol. 65, pp. 645–657, 2013.

[34] A. J. Wilson, J. K. Kerns, J. F. Callahan, and C. J. Moody, "Keap calm, and carry on covalently," *Journal of Medicinal Chemistry*, vol. 56, no. 19, pp. 7463–7476, 2013.

[35] M. H. L. Wong, H. K. Bryan, I. M. Copple et al., "Design and synthesis of irreversible analogues of bardoxolone methyl for the identification of pharmacologically relevant targets and interaction sites," *Journal of Medicinal Chemistry*, vol. 59, no. 6, pp. 2396–2409, 2016.

[36] E. Kansanen, G. Bonacci, F. J. Schopfer et al., "Electrophilic nitro-fatty acids activate NRF2 by a KEAP1 cysteine 151-independent mechanism," *Journal of Biological Chemistry*, vol. 286, no. 16, pp. 14019–14027, 2011.

[37] S. Fourquet, R. Guerois, D. Biard, and M. B. Toledano, "Activation of NRF2 by nitrosative agents and $H_2O_2$ involves KEAP1 disulfide formation," *Journal of Biological Chemistry*, vol. 285, no. 11, pp. 8463–8471, 2010.

[38] A. L. Levonen, A. Landar, A. Ramachandran et al., "Cellular mechanisms of redox cell signalling: role of cysteine modification in controlling antioxidant defences in response to electrophilic lipid oxidation products," *Biochemical Journal*, vol. 378, no. 2, pp. 373–382, 2004.

[39] N. Wakabayashi, A. T. Dinkova-Kostova, W. D. Holtzclaw et al., "Protection against electrophile and oxidant stress by induction of the phase 2 response: fate of cysteines of the Keap1 sensor modified by inducers," *Proceedings of the National Academy of Sciences of the United States of America*, vol. 101, no. 7, pp. 2040–2045, 2004.

[40] T. Yamamoto, T. Suzuki, A. Kobayashi et al., "Physiological significance of reactive cysteine residues of Keap1 in determining Nrf2 activity," *Molecular and Cellular Biology*, vol. 28, no. 8, pp. 2758–2770, 2008.

[41] R. Saito, T. Suzuki, K. Hiramoto et al., "Characterizations of three major cysteine sensors of Keap1 in stress response," *Molecular and Cellular Biology*, vol. 36, no. 2, article MCB.00868-15, 2015.

[42] L. Baird, D. Lleres, S. Swift, and A. T. Dinkova-Kostova, "Regulatory flexibility in the Nrf2-mediated stress response is conferred by conformational cycling of the Keap1-Nrf2 protein complex," *Proceedings of the National Academy of Sciences of the United States of America*, vol. 110, no. 38, pp. 15259–15264, 2013.

[43] A. Cleasby, J. Yon, P. J. Day et al., "Structure of the BTB domain of Keap1 and its interaction with the triterpenoid antagonist CDDO," *PLoS One*, vol. 9, no. 6, article e98896, 2014.

[44] T. Iso, T. Suzuki, L. Baird, and M. Yamamoto, "Absolute amounts and status of the Nrf2-Keap1-Cul3 complex within cells," *Molecular and Cellular Biology*, vol. 36, no. 24, pp. 3100–3112, 2016.

[45] S. Dayalan Naidu, A. Muramatsu, R. Saito et al., "C151 in KEAP1 is the main cysteine sensor for the cyanoenone class of NRF2 activators, irrespective of molecular size or shape," *Scientific Reports*, vol. 8, no. 1, p. 8037, 2018.

[46] A. T. Dinkova-Kostova, K. T. Liby, K. K. Stephenson et al., "Extremely potent triterpenoid inducers of the phase 2 response: correlations of protection against oxidant and inflammatory stress," *Proceedings of the National Academy of Sciences of the United States of America*, vol. 102, no. 12, pp. 4584–4589, 2005.

[47] K. T. Liby and M. B. Sporn, "Synthetic oleanane triterpenoids: multifunctional drugs with a broad range of applications for prevention and treatment of chronic disease," *Pharmacological Reviews*, vol. 64, no. 4, pp. 972–1003, 2012.

[48] P. E. Pergola, P. Raskin, R. D. Toto et al., "Bardoxolone methyl and kidney function in CKD with type 2 diabetes," *The New England Journal of Medicine*, vol. 365, no. 4, pp. 327–336, 2011.

[49] D. D. Zhang, "Bardoxolone brings Nrf2-based therapies to light," *Antioxidants & Redox Signaling*, vol. 19, no. 5, pp. 517-518, 2013.

[50] D. R. Lynch, J. Farmer, L. Hauser et al., "Safety, pharmacodynamics, and potential benefit of omaveloxolone in Friedreich ataxia," *Annals of Clinical Translational Neurology*, vol. 6, no. 1, pp. 15–26, 2019.

[51] P. S. Rabbani, T. Ellison, B. Waqas et al., "Targeted Nrf2 activation therapy with RTA 408 enhances regenerative capacity of diabetic wounds," *Diabetes Research and Clinical Practice*, vol. 139, pp. 11–23, 2018.

[52] Z. Xu, F. Zhang, F. Sun, K. F. Gu, S. Dong, and D. He, "Dimethyl fumarate for multiple sclerosis," *Cochrane Database of Systematic Reviews*, vol. 4, article CD011076, 2015.

[53] S. Schimrigk, N. Brune, K. Hellwig et al., "Oral fumaric acid esters for the treatment of active multiple sclerosis: an

open-label, baseline-controlled pilot study," *European Journal of Neurology*, vol. 13, no. 6, pp. 604–610, 2006.

[54] R. Gold, L. Kappos, D. L. Arnold et al., "Placebo-controlled phase 3 study of oral BG-12 for relapsing multiple sclerosis," *The New England Journal of Medicine*, vol. 367, no. 12, pp. 1098–1107, 2012.

[55] R. J. Fox, D. H. Miller, J. T. Phillips et al., "Placebo-controlled phase 3 study of oral BG-12 or glatiramer in multiple sclerosis," *The New England Journal of Medicine*, vol. 367, no. 12, pp. 1087–1097, 2012.

[56] S. Hoxtermann, C. Nuchel, and P. Altmeyer, "Fumaric acid esters suppress peripheral CD4- and CD8-positive lymphocytes in psoriasis," *Dermatology*, vol. 196, no. 2, pp. 223–230, 1998.

[57] E. A. Mills, M. A. Ogrodnik, A. Plave, and Y. Mao-Draayer, "Emerging understanding of the mechanism of action for dimethyl fumarate in the treatment of multiple sclerosis," *Frontiers in Neurology*, vol. 9, no. 5, 2018.

[58] M. Ghadiri, A. Rezk, R. Li et al., "Dimethyl fumarate-induced lymphopenia in MS due to differential T-cell subset apoptosis," *Neurology - Neuroimmunology Neuroinflammation*, vol. 4, no. 3, article e340, 2017.

[59] R. Li, A. Rezk, M. Ghadiri et al., "Dimethyl fumarate treatment mediates an anti-inflammatory shift in B cell subsets of patients with multiple sclerosis," *Journal of Immunology*, vol. 198, no. 2, pp. 691–698, 2017.

[60] M. D. Smith, K. A. Martin, P. A. Calabresi, and P. Bhargava, "Dimethyl fumarate alters B-cell memory and cytokine production in MS patients," *Annals of Clinical Translational Neurology*, vol. 4, no. 5, pp. 351–355, 2017.

[61] R. A. Linker, D. H. Lee, S. Ryan et al., "Fumaric acid esters exert neuroprotective effects in neuroinflammation via activation of the Nrf2 antioxidant pathway," *Brain*, vol. 134, no. 3, pp. 678–692, 2011.

[62] S. Dibbert, B. Clement, T. Skak-Nielsen, U. Mrowietz, and M. Rostami-Yazdi, "Detection of fumarate-glutathione adducts in the portal vein blood of rats: evidence for rapid dimethylfumarate metabolism," *Archives of Dermatological Research*, vol. 305, no. 5, pp. 447–451, 2013.

[63] H. Sun, J. Zhu, H. Lin, K. Gu, and F. Feng, "Recent progress in the development of small molecule Nrf2 modulators: a patent review (2012-2016)," *Expert Opinion on Therapeutic Patents*, vol. 27, no. 7, pp. 763–785, 2017.

[64] T. A. Zeidan, S. Duncan, C. P. Hencken, T. A. Wynn, and C. N. Sanrame, *Prodrugs of fumarates and their use in treating various diseases*, Alkermes Pharma Ireland Limited, 2014.

[65] F. von Glehn, R. P. C. Dias-Carneiro, A. S. Moraes et al., "Dimethyl fumarate downregulates the immune response through the HCA2/GPR109A pathway: implications for the treatment of multiple sclerosis," *Multiple Sclerosis and Related Disorders*, vol. 23, pp. 46–50, 2018.

[66] T. W. Kensler, G. S. Qian, J. G. Chen, and J. D. Groopman, "Translational strategies for cancer prevention in liver," *Nature Reviews Cancer*, vol. 3, no. 5, pp. 321–329, 2003.

[67] K. Okada, J. Shoda, K. Taguchi et al., "Ursodeoxycholic acid stimulates Nrf2-mediated hepatocellular transport, detoxification, and antioxidative stress systems in mice," *American Journal of Physiology-Gastrointestinal and Liver Physiology*, vol. 295, no. 4, pp. G735–G747, 2008.

[68] K. Kawata, Y. Kobayashi, K. Souda et al., "Enhanced hepatic Nrf2 activation after ursodeoxycholic acid treatment in patients with primary biliary cirrhosis," *Antioxidants & Redox Signaling*, vol. 13, no. 3, pp. 259–268, 2010.

[69] D. P. W. Wong, M. Y. Ng, J. Y. Leung et al., "Regulation of the NRF2 transcription factor by andrographolide and organic extracts from plant endophytes," *PLoS One*, vol. 13, no. 10, article e0204853, 2018.

[70] Z. Bahadoran, P. Mirmiran, F. Hosseinpanah, A. Rajab, G. Asghari, and F. Azizi, "Broccoli sprouts powder could improve serum triglyceride and oxidized LDL/LDL-cholesterol ratio in type 2 diabetic patients: a randomized double-blind placebo-controlled clinical trial," *Diabetes Research and Clinical Practice*, vol. 96, no. 3, pp. 348–354, 2012.

[71] A. S. Axelsson, E. Tubbs, B. Mecham et al., "Sulforaphane reduces hepatic glucose production and improves glucose control in patients with type 2 diabetes," *Science Translational Medicine*, vol. 9, no. 394, article eaah4477, 2017.

[72] Z. Ping, W. Liu, Z. Kang et al., "Sulforaphane protects brains against hypoxic-ischemic injury through induction of Nrf2-dependent phase 2 enzyme," *Brain Research*, vol. 1343, pp. 178–185, 2010.

[73] J. Zhao, N. Kobori, J. Aronowski, and P. K. Dash, "Sulforaphane reduces infarct volume following focal cerebral ischemia in rodents," *Neuroscience Letters*, vol. 393, no. 2-3, pp. 108–112, 2006.

[74] H. M. Park, J. A. Kim, and M. K. Kwak, "Protection against amyloid beta cytotoxicity by sulforaphane: role of the proteasome," *Archives of Pharmacal Research*, vol. 32, no. 1, pp. 109–115, 2009.

[75] H. V. Kim, H. Y. Kim, H. Y. Ehrlich, S. Y. Choi, D. J. Kim, and Y. S. Kim, "Amelioration of Alzheimer's disease by neuroprotective effect of sulforaphane in animal model," *Amyloid*, vol. 20, no. 1, pp. 7–12, 2013.

[76] J. M. Han, Y. J. Lee, S. Y. Lee et al., "Protective effect of sulforaphane against dopaminergic cell death," *The Journal of Pharmacology and Experimental Therapeutics*, vol. 321, no. 1, pp. 249–256, 2007.

[77] A. Jazwa, A. I. Rojo, N. G. Innamorato, M. Hesse, J. Fernández-Ruiz, and A. Cuadrado, "Pharmacological targeting of the transcription factor Nrf2 at the basal ganglia provides disease modifying therapy for experimental parkinsonism," *Antioxidants & Redox Signaling*, vol. 14, no. 12, pp. 2347–2360, 2011.

[78] A. Tarozzi, C. Angeloni, M. Malaguti, F. Morroni, S. Hrelia, and P. Hrelia, "Sulforaphane as a potential protective phytochemical against neurodegenerative diseases," *Oxidative Medicine and Cellular Longevity*, vol. 2013, Article ID 415078, 10 pages, 2013.

[79] C. A. Houghton, R. G. Fassett, and J. S. Coombes, "Sulforaphane and other nutrigenomic Nrf2 activators: can the clinician's expectation be matched by the reality?," *Oxidative Medicine and Cellular Longevity*, vol. 2016, Article ID 7857186, 17 pages, 2016.

[80] J. Egea, I. Buendia, E. Parada et al., "Melatonin-sulforaphane hybrid ITH12674 induces neuroprotection in oxidative stress conditions by a 'drug-prodrug' mechanism of action," *British Journal of Pharmacology*, vol. 172, no. 7, pp. 1807–1821, 2015.

[81] Sreejayan and M. N. A. Rao, "Nitric oxide scavenging by curcuminoids," *The Journal of Pharmacy and Pharmacology*, vol. 49, no. 1, pp. 105–107, 1997.

[82] P. Qiu, S. Man, J. Li et al., "Overdose intake of curcumin initiates the unbalanced state of bodies," *Journal of Agricultural and Food Chemistry*, vol. 64, no. 13, pp. 2765–2771, 2016.

[83] L. X. Na, Y. Li, H. Z. Pan et al., "Curcuminoids exert glucose-lowering effect in type 2 diabetes by decreasing serum free fatty acids: a double-blind, placebo-controlled trial," *Molecular Nutrition & Food Research*, vol. 57, no. 9, pp. 1569–1577, 2013.

[84] S. Chuengsamarn, S. Rattanamongkolgul, B. Phonrat, R. Tungtrongchitr, and S. Jirawatnotai, "Reduction of atherogenic risk in patients with type 2 diabetes by curcuminoid extract: a randomized controlled trial," *The Journal of Nutritional Biochemistry*, vol. 25, no. 2, pp. 144–150, 2014.

[85] H. Hatcher, R. Planalp, J. Cho, F. M. Torti, and S. V. Torti, "Curcumin: from ancient medicine to current clinical trials," *Cellular and Molecular Life Sciences*, vol. 65, no. 11, pp. 1631–1652, 2008.

[86] E. Balogun, M. Hoque, P. GONG et al., "Curcumin activates the haem oxygenase-1 gene via regulation of Nrf2 and the antioxidant-responsive element," *The Biochemical Journal*, vol. 371, no. 3, pp. 887–895, 2003.

[87] C. M. Arbeeny, H. Ling, M. M. Smith et al., "CXA-10, a nitrated fatty acid, is renoprotective in deoxycorticosterone acetate-salt nephropathy," *The Journal of Pharmacology and Experimental Therapeutics*, vol. 369, no. 3, pp. 503–510, 2019.

[88] C. I. Batthyany and G. V. Lopez, *Nitroalkene tocopherols and analogs thereof for use in the treatment and prevention of inflammation related conditions*, Complexa Inc., 2015.

[89] L. Nilsson, F. Palm, and R. Nørregaard, "15-Deoxy-$\Delta^{12,14}$-prostaglandin $J_2$ exerts antioxidant effects while exacerbating inflammation in mice subjected to ureteral obstruction," *Mediators of Inflammation*, vol. 2017, Article ID 3924912, 10 pages, 2017.

[90] K. Chen, J. J. Li, S. N. Li et al., "15-Deoxy-$\Delta^{12,14}$-prostaglandin $J_2$ alleviates hepatic ischemia-reperfusion injury in mice via inducing antioxidant response and inhibiting apoptosis and autophagy," *Acta Pharmacologica Sinica*, vol. 38, no. 5, pp. 672–687, 2017.

[91] J. Lu, S. Guo, X. Xue et al., "Identification of a novel series of anti-inflammatory and anti-oxidative phospholipid oxidation products containing the cyclopentenone moiety *in vitro* and *in vivo*: implication in atherosclerosis," *Journal of Biological Chemistry*, vol. 292, no. 13, pp. 5378–5391, 2017.

[92] E. L. Mills, D. G. Ryan, H. A. Prag et al., "Itaconate is an anti-inflammatory metabolite that activates Nrf2 via alkylation of KEAP1," *Nature*, vol. 556, no. 7699, pp. 113–117, 2018.

[93] X. J. Wang, J. D. Hayes, L. G. Higgins, C. R. Wolf, and A. T. Dinkova-Kostova, "Activation of the NRF2 signaling pathway by copper-mediated redox cycling of para- and ortho-hydroquinones," *Chemistry & Biology*, vol. 17, no. 1, pp. 75–85, 2010.

[94] J. M. Lee, J. D. Moehlenkamp, J. M. Hanson, and J. A. Johnson, "Nrf2-dependent activation of the antioxidant responsive element by tert-butylhydroquinone is independent of oxidative stress in IMR-32 human neuroblastoma cells," *Biochemical and Biophysical Research Communications*, vol. 280, no. 1, pp. 286–292, 2001.

[95] C. Higashi, A. Kawaji, N. Tsuda et al., "The novel Nrf2 inducer TFM-735 ameliorates experimental autoimmune encephalomyelitis in mice," *European Journal of Pharmacology*, vol. 802, pp. 76–84, 2017.

[96] T. Suzuki and M. Yamamoto, "Stress-sensing mechanisms and the physiological roles of the Keap1-Nrf2 system during cellular stress," *Journal of Biological Chemistry*, vol. 292, no. 41, pp. 16817–16824, 2017.

[97] B. G. Richardson, A. D. Jain, T. E. Speltz, and T. W. Moore, "Non-electrophilic modulators of the canonical Keap1/Nrf2 pathway," *Bioorganic & Medicinal Chemistry Letters*, vol. 25, no. 11, pp. 2261–2268, 2015.

[98] B. Padmanabhan, K. I. Tong, T. Ohta et al., "Structural basis for defects of Keap1 activity provoked by its point mutations in lung cancer," *Molecular Cell*, vol. 21, no. 5, pp. 689–700, 2006.

[99] S. C. Lo, X. Li, M. T. Henzl, L. J. Beamer, and M. Hannink, "Structure of the Keap1:Nrf2 interface provides mechanistic insight into Nrf2 signaling," *The EMBO Journal*, vol. 25, no. 15, pp. 3605–3617, 2006.

[100] D. Inoyama, Y. Chen, X. Huang, L. J. Beamer, A. N. T. Kong, and L. Hu, "Optimization of fluorescently labeled Nrf2 peptide probes and the development of a fluorescence polarization assay for the discovery of inhibitors of Keap1-Nrf2 interaction," *Journal of Biomolecular Screening*, vol. 17, no. 4, pp. 435–447, 2012.

[101] Y. Chen, D. Inoyama, A. N. T. Kong, L. J. Beamer, and L. Hu, "Kinetic analyses of Keap1-Nrf2 interaction and determination of the minimal Nrf2 peptide sequence required for Keap1 binding using surface plasmon resonance," *Chemical Biology & Drug Design*, vol. 78, no. 6, pp. 1014–1021, 2011.

[102] R. Hancock, H. C. Bertrand, T. Tsujita et al., "Peptide inhibitors of the Keap1-Nrf2 protein-protein interaction," *Free Radical Biology & Medicine*, vol. 52, no. 2, pp. 444–451, 2012.

[103] J. Tu, X. Zhang, Y. Zhu et al., "Cell-permeable peptide targeting the Nrf2-Keap1 interaction: a potential novel therapy for global cerebral ischemia," *The Journal of Neuroscience*, vol. 35, no. 44, pp. 14727–14739, 2015.

[104] R. Hancock, M. Schaap, H. Pfister, and G. Wells, "Peptide inhibitors of the Keap1-Nrf2 protein-protein interaction with improved binding and cellular activity," *Organic & Biomolecular Chemistry*, vol. 11, no. 21, pp. 3553–3557, 2013.

[105] M. C. Lu, Q. Jiao, T. Liu et al., "Discovery of a head-to-tail cyclic peptide as the Keap1-Nrf2 protein-protein interaction inhibitor with high cell potency," *European Journal of Medicinal Chemistry*, vol. 143, pp. 1578–1589, 2018.

[106] E. Jnoff, C. Albrecht, J. J. Barker et al., "Binding mode and structure-activity relationships around direct inhibitors of the Nrf2-Keap1 complex," *ChemMedChem*, vol. 9, no. 4, pp. 699–705, 2014.

[107] D. Marcotte, W. Zeng, J. C. Hus et al., "Small molecules inhibit the interaction of Nrf2 and the Keap1 Kelch domain through a non-covalent mechanism," *Bioorganic & Medicinal Chemistry*, vol. 21, no. 14, pp. 4011–4019, 2013.

[108] Z.-Y. Jiang, M. C. Lu, L.–. L. Xu et al., "Discovery of potent Keap1-Nrf2 protein-protein interaction inhibitor based on molecular binding determinants analysis," *Journal of Medicinal Chemistry*, vol. 57, no. 6, pp. 2736–2745, 2014.

[109] N. Ranjan, G. Fulcrand, A. King et al., "Selective inhibition of bacterial topoisomerase I by alkynyl-bisbenzimidazoles," *MedChemComm*, vol. 5, no. 6, pp. 816–825, 2014.

[110] M. Sato, T. Aoki, H. Inoue et al., "Keap1 protein binding compound, cristal of complex between the same and Keap1 protein, and method for producing the same," TORAY INDUSTRIES Inc., 2013.

[111] B. G. Richardson, A. D. Jain, H. R. Potteti et al., "Replacement of a naphthalene scaffold in Kelch-like ECH-associated protein 1 (KEAP1)/nuclear factor (erythroid-derived 2)-like 2 (NRF2) inhibitors," *Journal of Medicinal Chemistry*, vol. 61, no. 17, pp. 8029–8047, 2018.

[112] L. Hu, S. Magesh, L. Chen et al., "Discovery of a small-molecule inhibitor and cellular probe of Keap1-Nrf2 protein-protein interaction," *Bioorganic & Medicinal Chemistry Letters*, vol. 23, no. 10, pp. 3039–3043, 2013.

[113] X. Wen, G. Thorne, L. Hu, M. S. Joy, and L. M. Aleksunes, "Activation of NRF2 signaling in HEK293 cells by a first-in-class direct KEAP1-NRF2 inhibitor," *Journal of Biochemical and Molecular Toxicology*, vol. 29, no. 6, pp. 261–266, 2015.

[114] H. C. Bertrand, M. Schaap, L. Baird et al., "Design, synthesis, and evaluation of triazole derivatives that induce Nrf2 dependent gene products and inhibit the Keap1-Nrf2 protein-protein interaction," *Journal of Medicinal Chemistry*, vol. 58, no. 18, pp. 7186–7194, 2015.

[115] H. R. Nasiri, S. Linge, and D. Ullmann, "Thermodynamic profiling of inhibitors of Nrf2:Keap1 interactions," *Bioorganic & Medicinal Chemistry Letters*, vol. 26, no. 2, pp. 526–529, 2016.

[116] A. Bresciani, A. Missineo, M. Gallo et al., "Nuclear factor (erythroid-derived 2)-like 2 (NRF2) drug discovery: biochemical toolbox to develop NRF2 activators by reversible binding of Kelch-like ECH-associated protein 1 (KEAP1)," *Archives of Biochemistry and Biophysics*, vol. 631, pp. 31–41, 2017.

[117] C. Hooper, R. Killick, and S. Lovestone, "The GSK3 hypothesis of Alzheimer's disease," *Journal of Neurochemistry*, vol. 104, no. 6, pp. 1433–1439, 2008.

[118] T. Silva, J. Reis, J. Teixeira, and F. Borges, "Alzheimer's disease, enzyme targets and drug discovery struggles: from natural products to drug prototypes," *Ageing Research Reviews*, vol. 15, pp. 116–145, 2014.

[119] J. Luo, "Glycogen synthase kinase 3$\beta$ (GSK3$\beta$) in tumorigenesis and cancer chemotherapy," *Cancer Letters*, vol. 273, no. 2, pp. 194–200, 2009.

[120] H. Lal, F. Ahmad, J. Woodgett, and T. Force, "The GSK-3 family as therapeutic target for myocardial diseases," *Circulation Research*, vol. 116, no. 1, pp. 138–149, 2015.

[121] A. P. Saraswati, S. M. Ali Hussaini, N. H. Krishna, B. N. Babu, and A. Kamal, "Glycogen synthase kinase-3 and its inhibitors: potential target for various therapeutic conditions," *European Journal of Medicinal Chemistry*, vol. 144, pp. 843–858, 2018.

[122] S. Lovestone, M. Boada, B. Dubois et al., "A phase II trial of tideglusib in Alzheimer's disease," *Journal of Alzheimer's Disease*, vol. 45, no. 1, pp. 75–88, 2015.

[123] T. Bourhill, A. Narendran, and R. N. Johnston, "Enzastaurin: a lesson in drug development," *Critical Reviews in Oncology/-Hematology*, vol. 112, pp. 72–79, 2017.

[124] G. Lombardi, A. Pambuku, L. Bellu et al., "Effectiveness of antiangiogenic drugs in glioblastoma patients: a systematic review and meta-analysis of randomized clinical trials," *Critical Reviews in Oncology/Hematology*, vol. 111, pp. 94–102, 2017.

[125] A. I. Rojo, O. N. Medina-Campos, P. Rada et al., "Signaling pathways activated by the phytochemical nordihydroguaiaretic acid contribute to a Keap1-independent regulation of Nrf2 stability: role of glycogen synthase kinase-3," *Free Radical Biology & Medicine*, vol. 52, no. 2, pp. 473–487, 2012.

[126] V. Palomo and A. Martinez, "Glycogen synthase kinase 3 (GSK-3) inhibitors: a patent update (2014-2015)," *Expert Opinion on Therapeutic Patents*, vol. 27, no. 6, pp. 657–666, 2017.

[127] P. Rada, A. I. Rojo, N. Evrard-Todeschi et al., "Structural and functional characterization of Nrf2 degradation by the glycogen synthase kinase 3/$\beta$-TrCP axis," *Molecular and Cellular Biology*, vol. 32, no. 17, pp. 3486–3499, 2012.

[128] B. E. Hast, D. Goldfarb, K. M. Mulvaney et al., "Proteomic analysis of ubiquitin ligase KEAP1 reveals associated proteins that inhibit NRF2 ubiquitination," *Cancer Research*, vol. 73, no. 7, pp. 2199–2210, 2013.

[129] A. Jain, T. Lamark, E. Sjøttem et al., "*p62/SQSTM1* is a target gene for transcription factor NRF2 and creates a positive feedback loop by inducing antioxidant response element-driven gene transcription," *Journal of Biological Chemistry*, vol. 285, no. 29, pp. 22576–22591, 2010.

[130] A. Lau, X. J. Wang, F. Zhao et al., "A noncanonical mechanism of Nrf2 activation by autophagy deficiency: direct interaction between Keap1 and p62," *Molecular and Cellular Biology*, vol. 30, no. 13, pp. 3275–3285, 2010.

[131] M. Komatsu, H. Kurokawa, S. Waguri et al., "The selective autophagy substrate p62 activates the stress responsive transcription factor Nrf2 through inactivation of Keap1," *Nature Cell Biology*, vol. 12, no. 3, pp. 213–223, 2010.

[132] S. Sarkar and D. C. Rubinsztein, "Small molecule enhancers of autophagy for neurodegenerative diseases," *Molecular BioSystems*, vol. 4, no. 9, pp. 895–901, 2008.

[133] Y. Mizunoe, M. Kobayashi, Y. Sudo et al., "Trehalose protects against oxidative stress by regulating the Keap1-Nrf2 and autophagy pathways," *Redox Biology*, vol. 15, pp. 115–124, 2018.

[134] S. Dhakshinamoorthy, A. K. Jain, D. A. Bloom, and A. K. Jaiswal, "Bach1 competes with Nrf2 leading to negative regulation of the antioxidant response element (ARE)-mediated NAD(P)H:quinone oxidoreductase 1 gene expression and induction in response to antioxidants," *Journal of Biological Chemistry*, vol. 280, no. 17, pp. 16891–16900, 2005.

[135] O. C. Attucks, K. J. Jasmer, M. Hannink et al., "Induction of heme oxygenase I (HMOX1) by HPP-4382: a novel modulator of Bach1 activity," *PLoS One*, vol. 9, no. 7, article e101044, 2014.

[136] M. Ramos-Gomez, P. M. Dolan, K. Itoh, M. Yamamoto, and T. W. Kensler, "Interactive effects of *nrf2* genotype and oltipraz on benzo[*a*]pyrene-DNA adducts and tumor yield in mice," *Carcinogenesis*, vol. 24, no. 3, pp. 461–467, 2003.

[137] C. Xu, M. T. Huang, G. Shen et al., "Inhibition of 7,12-dimethylbenz(*a*)anthracene-induced skin tumorigenesis in C57BL/6 mice by sulforaphane is mediated by nuclear factor E2-related factor 2," *Cancer Research*, vol. 66, no. 16, pp. 8293–8296, 2006.

[138] L. M. Solis, C. Behrens, W. Dong et al., "Nrf2 and Keap1 abnormalities in non-small cell lung carcinoma and association with clinicopathologic features," *Clinical Cancer Research*, vol. 16, no. 14, pp. 3743–3753, 2010.

[139] T. Shibata, T. Ohta, K. I. Tong et al., "Cancer related mutations in NRF2 impair its recognition by Keap1-Cul3 E3 ligase and promote malignancy," *Proceedings of the National*

*Academy of Sciences of the United States of America*, vol. 105, no. 36, pp. 13568–13573, 2008.

[140] T. Ohta, K. Iijima, M. Miyamoto et al., "Loss of Keap1 function activates Nrf2 and provides advantages for lung cancer cell growth," *Cancer Research*, vol. 68, no. 5, pp. 1303–1309, 2008.

[141] L. Milkovic, N. Zarkovic, and L. Saso, "Controversy about pharmacological modulation of Nrf2 for cancer therapy," *Redox Biology*, vol. 12, pp. 727–732, 2017.

[142] H. Kitamura and H. Motohashi, "NRF2 addiction in cancer cells," *Cancer Science*, vol. 109, no. 4, pp. 900–911, 2018.

[143] S. H. Ki, I. J. Cho, D. W. Choi, and S. G. Kim, "Glucocorticoid receptor (GR)-associated SMRT binding to C/EBP$\beta$ TAD and Nrf2 Neh4/5: role of SMRT recruited to GR in GSTA2 gene repression," *Molecular and Cellular Biology*, vol. 25, no. 10, pp. 4150–4165, 2005.

[144] E. J. Choi, B. J. Jung, S. H. Lee et al., "A clinical drug library screen identifies clobetasol propionate as an NRF2 inhibitor with potential therapeutic efficacy in KEAP1 mutant lung cancer," *Oncogene*, vol. 36, no. 37, pp. 5285–5295, 2017.

[145] X. J. Wang, J. D. Hayes, C. J. Henderson, and C. R. Wolf, "Identification of retinoic acid as an inhibitor of transcription factor Nrf2 through activation of retinoic acid receptor alpha," *Proceedings of the National Academy of Sciences of the United States of America*, vol. 104, no. 49, pp. 19589–19594, 2007.

[146] H. Wang, K. Liu, M. Geng et al., "RXR$\alpha$ inhibits the NRF2-ARE signaling pathway through a direct interaction with the Neh7 domain of NRF2," *Cancer Research*, vol. 73, no. 10, pp. 3097–3108, 2013.

[147] D. Ren, N. F. Villeneuve, T. Jiang et al., "Brusatol enhances the efficacy of chemotherapy by inhibiting the Nrf2-mediated defense mechanism," *Proceedings of the National Academy of Sciences of the United States of America*, vol. 108, no. 4, pp. 1433–1438, 2011.

[148] B. Harder, W. Tian, J. J. la Clair et al., "Brusatol overcomes chemoresistance through inhibition of protein translation," *Molecular Carcinogenesis*, vol. 56, no. 5, pp. 1493–1500, 2017.

[149] S. Vartanian, T. P. Ma, J. Lee et al., "Application of mass spectrometry profiling to establish brusatol as an inhibitor of global protein synthesis," *Molecular & Cellular Proteomics*, vol. 15, no. 4, pp. 1220–1231, 2016.

[150] J. Zhu, H. Wang, F. Chen et al., "An overview of chemical inhibitors of the Nrf2-ARE signaling pathway and their potential applications in cancer therapy," *Free Radical Biology & Medicine*, vol. 99, pp. 544–556, 2016.

[151] X. Tang, H. Wang, L. Fan et al., "Luteolin inhibits Nrf2 leading to negative regulation of the Nrf2/ARE pathway and sensitization of human lung carcinoma A549 cells to therapeutic drugs," *Free Radical Biology & Medicine*, vol. 50, no. 11, pp. 1599–1609, 2011.

[152] Y. Zhong, F. Zhang, Z. Sun et al., "Drug resistance associates with activation of Nrf2 in MCF-7/DOX cells, and wogonin reverses it by down-regulating Nrf2-mediated cellular defense response," *Molecular Carcinogenesis*, vol. 52, no. 10, pp. 824–834, 2013.

[153] A. K. Pandurangan, S. K. Ananda Sadagopan, P. Dharmalingam, and S. Ganapasam, "Luteolin, a bioflavonoid inhibits Azoxymethane-induced colorectal cancer through activation of Nrf2 signaling," *Toxicology Mechanisms and Methods*, vol. 24, no. 1, pp. 13–20, 2014.

[154] A. Limonciel and P. Jennings, "A review of the evidence that ochratoxin A is an Nrf2 inhibitor: implications for nephrotoxicity and renal carcinogenicity," *Toxins*, vol. 6, no. 1, pp. 371–379, 2014.

[155] A. Arlt, S. Sebens, S. Krebs et al., "Inhibition of the Nrf2 transcription factor by the alkaloid trigonelline renders pancreatic cancer cells more susceptible to apoptosis through decreased proteasomal gene expression and proteasome activity," *Oncogene*, vol. 32, no. 40, pp. 4825–4835, 2013.

[156] A. Manna, S. de Sarkar, S. de, A. K. Bauri, S. Chattopadhyay, and M. Chatterjee, "The variable chemotherapeutic response of Malabaricone-A in leukemic and solid tumor cell lines depends on the degree of redox imbalance," *Phytomedicine*, vol. 22, no. 7-8, pp. 713–723, 2015.

[157] T. Tarumoto, T. Nagai, K. Ohmine et al., "Ascorbic acid restores sensitivity to imatinib via suppression of Nrf2-dependent gene expression in the imatinib-resistant cell line," *Experimental Hematology*, vol. 32, no. 4, pp. 375–381, 2004.

[158] A. Singh, S. Venkannagari, K. H. Oh et al., "Small molecule inhibitor of NRF2 selectively intervenes therapeutic resistance in KEAP1-deficient NSCLC tumors," *ACS Chemical Biology*, vol. 11, no. 11, pp. 3214–3225, 2016.

[159] K. Tsuchida, T. Tsujita, M. Hayashi et al., "Halofuginone enhances the chemo-sensitivity of cancer cells by suppressing NRF2 accumulation," *Free Radical Biology & Medicine*, vol. 103, pp. 236–247, 2017.

[160] M. J. Bollong, H. Yun, L. Sherwood, A. K. Woods, L. L. Lairson, and P. G. Schultz, "A small molecule inhibits deregulated NRF2 transcriptional activity in cancer," *ACS Chemical Biology*, vol. 10, no. 10, pp. 2193–2198, 2015.

[161] J. Zhang, L. Su, Q. Ye et al., "Discovery of a novel Nrf2 inhibitor that induces apoptosis of human acute myeloid leukemia cells," *Oncotarget*, vol. 8, no. 5, pp. 7625–7636, 2017.

[162] R. Steel, J. Cowan, E. Payerne, M. A. O'Connell, and M. Searcey, "Anti-inflammatory effect of a cell-penetrating peptide targeting the Nrf2/Keap1 interaction," *ACS Medicinal Chemistry Letters*, vol. 3, no. 5, pp. 407–410, 2012.

[163] Z. Y. Jiang, L.–. L. Xu, M. C. Lu et al., "Structure-activity and structure-property relationship and exploratory in vivo evaluation of the nanomolar Keap1-Nrf2 protein-protein interaction inhibitor," *Journal of Medicinal Chemistry*, vol. 58, no. 16, pp. 6410–6421, 2015.

[164] J. G. Yonchuk, J. P. Foley, B. J. Bolognese et al., "Characterization of the potent, selective Nrf2 activator, 3-(pyridin-3-ylsulfonyl)-5-(trifluoromethyl)-2H-chromen-2-one, in cellular and in vivo models of pulmonary oxidative stress," *The Journal of Pharmacology and Experimental Therapeutics*, vol. 363, no. 1, pp. 114–125, 2017.

[165] H.-P. Sun, Z.-Y. Jiang, M.-Y. Zhang et al., "Novel protein–protein interaction inhibitor of Nrf2–Keap1 discovered by structure-based virtual screening," *MedChemComm*, vol. 5, no. 1, pp. 93–98, 2014.

[166] T. G. Davies, W. E. Wixted, J. E. Coyle et al., "Monoacidic inhibitors of the Kelch-like ECH-associated protein 1: nuclear factor erythroid 2-related factor 2 (KEAP1:NRF2) protein-protein interaction with high cell potency identified by fragment-based discovery," *Journal of Medicinal Chemistry*, vol. 59, no. 8, pp. 3991–4006, 2016.

[167] K. Itoh, N. Wakabayashi, Y. Katoh et al., "Keap1 represses nuclear activation of antioxidant responsive elements by Nrf2 through binding to the amino-terminal Neh2 domain," *Genes & Development*, vol. 13, no. 1, pp. 76–86, 1999.

[168] K. Taguchi, H. Motohashi, and M. Yamamoto, "Molecular mechanisms of the Keap1-Nrf2 pathway in stress response and cancer evolution," *Genes to Cells*, vol. 16, no. 2, pp. 123–140, 2011.

# p73 is Required for Ependymal Cell Maturation and Neurogenic SVZ Cytoarchitecture

**L. Gonzalez-Cano,[1†] S. Fuertes-Alvarez,[1] N. Robledinos-Anton,[1] A. Bizy,[3] A. Villena-Cortes,[2] I. Fariñas,[3] M.M. Marques,[4] Maria C. Marin[1,2]**

[1] Instituto De Biomedicina (IBIOMED) and Departamento de Biologia Molecular, Universidad de Leon, Campus De Vegazana, Leon 24071, Spain

[2] Departamento De Biologia Molecular, Universidad de Leon, Campus De Vegazana, Leon 24071, Spain

[3] Departamento De Biologia Celular and CIBERNED, Universidad De Valencia, Burjassot 46100, Spain

[4] Instituto De Desarrollo Ganadero and Departamento De Produccion Animal, University of Leon, Campus De Vegazana, 24071 Leon, Spain

*Received 19 June 2015; revised 30 September 2015; accepted 15 October 2015*

**ABSTRACT: The adult subventricular zone (SVZ) is a highly organized microenvironment established during the first postnatal days when radial glia cells begin to transform into type B-cells and ependymal cells, all of which will form regenerative units, pinwheels, along the lateral wall of the lateral ventricle. Here, we identify p73, a p53 homologue, as a critical factor controlling both cell-type specification and structural organization of the developing mouse SVZ. We describe that p73 deficiency halts the transition of the radial glia into ependymal cells, leading to the emergence of immature cells with abnormal identities in the ventricle and resulting in loss of the ventricular integrity. p73-deficient ependymal cells have noticeably impaired ciliogenesis and they fail to organize into pinwheels, disrupting SVZ niche structure and function. Therefore, p73 is essential for appropriate ependymal cell maturation and the establishment of the neurogenic niche architecture. Accordingly, lack of p73 results in impaired neurogenesis. Moreover, p73 is required for translational planar cell polarity establishment, since p73 deficiency results in profound defects in cilia organization in individual cells and in intercellular patch orientation. Thus, our data reveal a completely new function of p73, independent of p53, in the neurogenic architecture of the SVZ of rodent brain and in the establishment of ependymal planar cell polarity with important implications in neurogenesis.**

 Develop Neurobiol 76: 730–747, 2016

***Keywords:*** **p73; ciliogenesis; ependymal cells; neurogenic pinwheel; planar cell polarity**

## INTRODUCTION

Maintenance of neural stem cell (NSC) capacity to self-renew is dependent upon intrinsic regulatory networks and extrinsic cues within the NSC niches (Miller and Gauthier-Fisher, 2009). The members of the p53 family of tumor suppressor genes, *TP53, TP63*, and *TP73*, are important players in NSC biology (Killick et al., 2011). In particular, TP73 is deeply involved in NSC maintenance and organization of the sub-ventricular zone (SVZ) germinal

*Correspondence to*: Dr. M. C. Marin (carmen.marin@unileon.es).

Contract grant sponsor: Spanish Ministerio de Ciencia e Innovación; contract grant number: SAF2012-36143.

Contract grant sponsor: Junta de Castilla y Leon; contract grant numbers: LE015A10-2; LE310U14.

L. Gonzalez-Cano and S. Fuertes-Alvarez contributed equally to this work.

[†]*Present address:* Luxembourg Centre for Systems Biomedicine (LCSB), University of Luxembourg, Esch-Belval, Luxembourg.

Additional Supporting Information may be found in the online version of this article.

Published online 31 October 2015 in Wiley Online Library (wileyonlinelibrary.com).
DOI 10.1002/dneu.22356

center (Agostini et al., 2010; Fujitani et al., 2010; Gonzalez-Cano et al., 2010; Talos et al., 2010) and regulates the balance between symmetric and asymmetric cell divisions of NSC (Gonzalez-Cano et al., 2013). The hydrocephalus phenotype of *Trp73*−/− mice (p73KO from now on) (Yang et al., 2000) suggested a possible p73 role in ependymal ciliary function that might be linked to its regulation of the neurogenic environment. However, this has never been addressed.

The architecture of the SVZ is established during the first postnatal days when a select group of radial glia cells (RGCs) begins to transform into NSC (Merkle et al., 2004), while other subpopulation gives rise to ependymal cells (ECs). ECs will form pinwheel structures with B-cells (NSC) intercalated among them. B-cells have a small apical surface with a single primary cilium contacting the ventricle and large basal process contacting blood vessels, and exhibit ultrastructural characteristics and markers of astroglial cells, including GFAP and GLAST expression (Ihrie and Alvarez-Buylla, 2011). The apical processes of the B-cells form the core of the pinwheel, which itself is formed by multi and bi-ciliated ECs (Mirzadeh et al., 2008). This highly organized microenvironment is necessary for maintaining NSC self-renewal and differentiation capacity as well as the neurogenic niche homeostasis (Lim et al., 2000; Chmielnicki et al., 2004; Ramirez-Castillejo et al., 2006; Andreu-Agullo et al., 2009).

Multiciliated ECs have a prominent role in the maintenance of the neurogenic niche, since they induce neurogenesis and suppress gliogenesis by secreting the bone morphogenetic protein (BMP) inhibitor, Noggin (Lim et al., 2000; Chmielnicki et al., 2004). ECs are defined as large-apical surface multiciliated cells that express S100ß and Vimentin (Spassky et al., 2005; Raponi et al., 2007; Mirzadeh et al., 2008; Pastrana et al., 2009). ECs are generated from RG in a multistep process orchestrated by the primary cilium and its basal body apparatus (Spassky et al., 2005). RG planar cell polarity (PCP) is first established during perinatal development when the primary cilium migrates toward the rostral end. Later on, from P5 until P20, cilia clusters in maturing ECs become densely packed, with basal bodies aligned and positioned as a patch on the downstream side of the EC apical surface with respect to the direction of cerebrospinal fluid (CSF) flow (Bayly and Axelrod, 2011). Thus, EC cilia display two types of PCP: rotational PCP (rPCP) which refers to the parallel alignment of the basal bodies within each multi-ciliated cell and translational PCP (tPCP), defined by the basal body cluster anterior position on the cell apical surface (Mirzadeh et al., 2010). Both forms of polarity correlate with the onset of coordinated cilia beating in a uniform direction (Hirota et al., 2010).

Defects in cilia are associated with a range of human diseases, such as primary ciliary dyskinesia or hydrocephaly (Badano et al., 2006; Kishimoto and Sawamoto, 2012). In the brain, EC cilia are required for CSF circulation and neurogenesis (Boutin et al., 2014). Disruption in PCP establishment results in dysfunctions of ependymal cilia and their directional beating. Thus, the identification of the main players in EC maturation and PCP establishment might have important therapeutic implications.

Here we describe that p73 deficiency impairs ependymal cell maturation and ciliogenesis, as well as their organization in neurogenic pinwheel structures. Moreover, lack of p73 dramatically alters the establishment of PCP and affects the neurogenic capacity of the germinal center, independently of p53.

## MATERIAL AND METHODS

### Mice Husbandry, Genotyping, and BrdU Treatment

Housing and animal experiments were conducted in agreement with European and Spanish regulations on the protection of animals used for scientific purposes (Council Directive 2010/63/UE and RD 53/2013, respectively) with the appropriate institutional committee approval. Mice heterozygous for *Trp73* on a mixed background C57BL/6 x 129/svJae (Yang et al., 2000) were backcrossed to C57BL/6, at least five times, to enrich for C57BL/6 background. Heterozygous animals were crossed to obtain the p73KO mice. C57BL/6 p53 knockout mice (p53KO) were previously described (Donehower et al., 1992). To generate the double p73;p53 knock-out mice (DKO), heterozygous *Trp73*+/− animals were crossed with p53KO mice, obtaining the double heterozygous mice, *Trp73*+/−; *Tp53*+/−. Then, double heterozygous were inter-crossed to originate the DKO animals. Genotyping of adult animals was performed by PCR analysis as described before (Yang et al., 2000; Flores et al., 2005). The thymidine analogue BrdU (Sigma, St. Louis, MO) was administered intraperitoneal (90 mg $kg^{-1}$) in pulse injections every 2 h, during 8 h. Male and female mice were used in the experiments.

### Immunohistochemistry

Animals were fully anesthetized using an analgesic/anesthetic mixture of medetomidine hydrochloride (Domtor®, Orion Corporation, Espoo, Finlandia) and ketamine (Imalgene® 500, Merial, Duluth, GA). Medetomidine (1 mg $kg^{-1}$)/ketamine (75 mg $kg^{-1}$) euthanasic mixture

**Table 1 Primary Antibodies Used for Immunohistochemistry**

| Antibody | Host | Dilution | Manufacturer, Catalog Number |
|---|---|---|---|
| BrdU | Mouse | 1:200 | Dako,·M0744 |
| BrdU | Mouse | 1:500 | BD Biosciences,·347583 |
| ß-Catenin | Rabbit | 1:100 | Cell signaling,·9587 |
| ß-Catenin | Mouse | 1:100 | BD Biosciences, 610153 |
| Dcx | Goat | 1:150 | Santa Cruz Biotech,·SC8066 |
| GFAP | Chicken | 1:500 | Chemicon,·Ab5541 |
| GLAST | Rabbit | 1:100 | Tocris, 2064 |
| IB4 | Mouse | 1:20 | Sigma,·L2140 |
| Ki67 | Rabbit | 1:100 | Abcam,·ab15580 |
| s100ß | Rabbit | 1:100 | Dako,·Z0311 |
| Ac-Tubulin | Mouse | 1:1000 | Sigma,·T6793 |
| $\gamma$-Tubulin | Goat | 1:200 | Santa Cruz Biotech,·SC7396 |
| Vimentin | Guinea Pig | 1:500 | Fitzgerald,·20R-VP004 |

was prepared in phosphate buffer saline (PBS) and injected intraperitoneally. Animals were euthanized in agreement with European and Spanish regulations by transcardial perfusion with 0.1*M* PBS supplemented with 1% heparin until the drained blood became clear, and then with ~20–40 mL of fresh 4% paraformaldehyde (PFA) in 0.1*M* PBS, depending of the age of the animal.

After perfusion, brains were dissected and post-fixed overnight (o/n) in fresh 4% PFA in PBS solution at 4°C. For cryopreservation, samples were incubated for 24 h in 30% sucrose/PBS solution. Samples were then frozen in dry ice and stored at −80°C. A 30-μm-thick coronal sections were prepared using a Microm HM450 sliding microtome (Thermo Scientific, Walthman, MA) and stored in PBS supplemented with 0.05% sodium azide at 4°C. BrdU and Ki67 staining required antigen retrieval for which sections were incubated in 2N HCl for 15 min at 37°C. Then, sections were washed and stained according to the published protocol (Gonzalez-Cano et al., 2010). Sections were incubated with the indicated antibodies (Table 1). Confocal microscopy images were obtained with Nikon Eclipse TE2000 confocal microscope (Nikon, Chiyoda-Tokyo, Japan) and Olympus FluoView FV10i Confocal Laser Scanning Microscope (Olympus, Shinjuku-Tokyo, Japan). Figures show single level representative pictures.

## Isolation and Immunostaining of SVZ Wholemounts

Wholemounts of the lateral wall of the ventricles were dissected from 7, 15, and 160 postnatal day mice. Animals were anesthetized and euthanized in agreement with European and Spanish regulations and the brain was dissected and placed in cold 0.1*M* PBS. Dissection of the WMs was made under the stereomicroscope as described (Mirzadeh et al., 2010). WMs were transferred ventricle side up to a 24-well plate with 4%PFA/0.1% Triton-X100 (Tx100), fixed o/n at 4°C and stored in 0.1M PBS at 4°C.

WMs were incubated for 2 h at room temperature in blocking buffer (0.1M PBS/10% NDS/0.5% Tx100). Then, sections were incubated for 48 h at 4°C with the appropriate primary antibodies (Table 1) diluted in blocking buffer. Immunofluorescent detections were carried out with Alexa Fluor (Invitrogen, Carlsbad, CA) or DyLight (Pierce, Whaltman, MA) and Cy2, Cy3, and Cy5 (Jackson ImmunoResearch Laboratories, West Grove, PA) conjugated secondary antibodies. DAPI (1 μg $mL^{-1}$) was used for nuclear counterstaining. Samples were analysed in an Olympus FluoView FV10i confocal laser scanning microscope (Olympus, Shinjuku-Tokyo, Japan). Images were acquired and processed using FV10-ASW 2.1 viewer software.

## Scanning Electron Microscopy (SEM)

Lateral wall isolated from P7 and P15 mice were fixed with 0.1*M* PBS/2% glutaraldehyde, pH 7.2–7.4 at 4°C. Then, samples were dehydrated through a series of aqueous ethanol solutions (30, 70, 90, 96, and 100% ethanol) and finally dried with liquid $CO_2$ (critical point at 8°C). To obtain SEM images, samples were covered with a cycle of evaporation of gold atoms induced by argon in vacuum conditions (0.05–0.07 mbar). SEM images were obtained using a JEOL Scanning Electron Microscope (JEOL, Akishima-Tokyo, Japan). Images of the wholemounts were acquired every 0.5 μm and maximum projection of three to five consecutive Z levels are shown.

## Image Data Quantification and Statistical Analyses

For all the analyses, at least three independent mice from each genotype were considered. Analysis of SVZ coronal sections was performed considering anterior, medial and posterior sections. For each section, Z-stacks (20 μm) from at least six dorso-ventral regions along the wall of the ventricle were acquired. To determine the numbers of positive

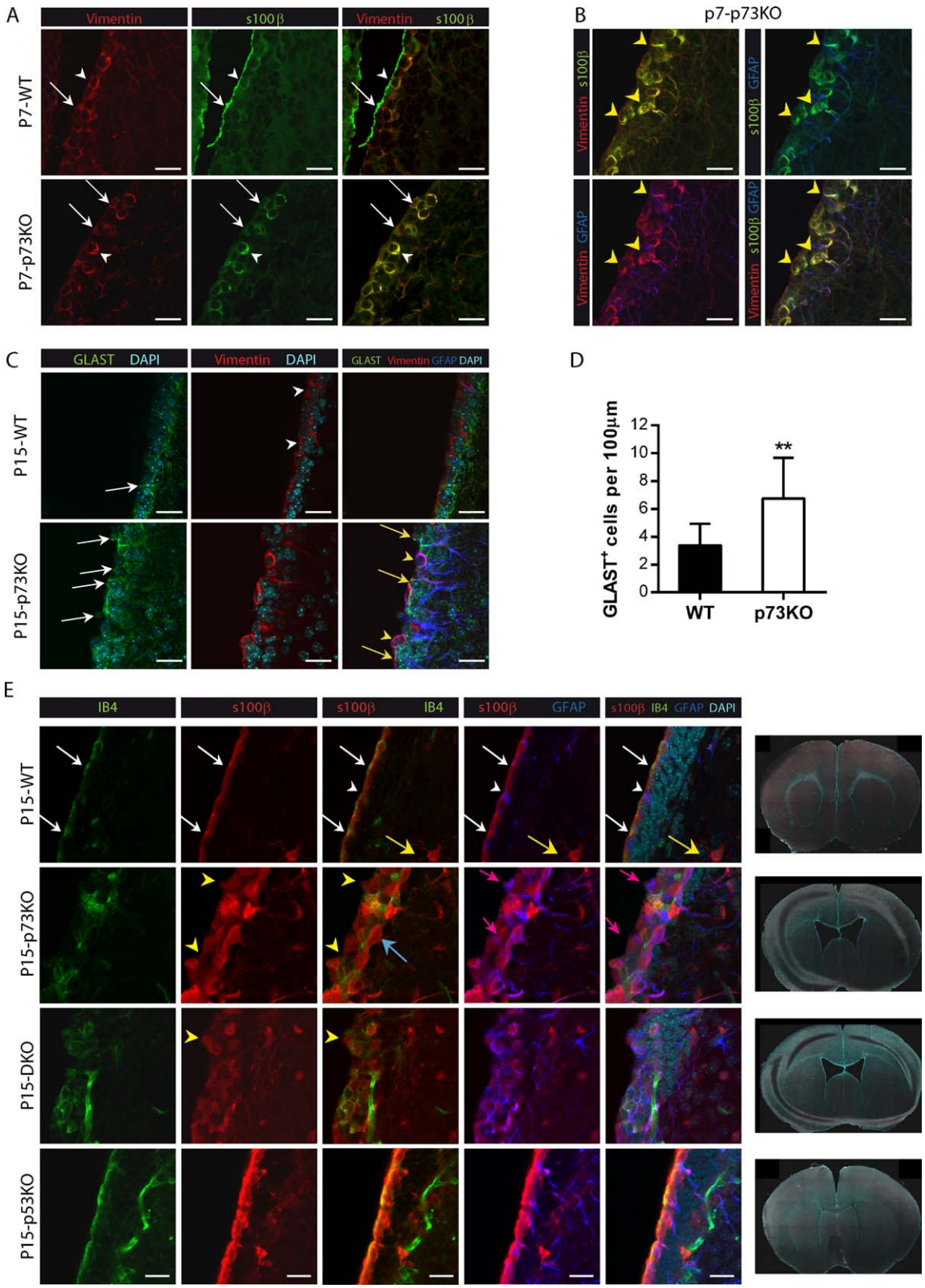
A
Vimentin
s100β
Vimentin s100β
P7-WT
P7-p73KO
B
p7-p73KO
Vimentin s100β
s100β GFAP
Vimentin GFAP
Vimentin s100β GFAP
C
GLAST DAPI
Vimentin DAPI
GLAST Vimentin GFAP DAPI
P15-WT
P15-p73KO
D
GLAST+ cells per 100µm
12
10
8
6
4
2
0
**
WT
p73KO
E
IB4
s100β
s100β IB4
s100β GFAP
s100β IB4 GFAP DAPI
P15-WT
P15-p73KO
P15-DKO
P15-p53KO

**Figure 1.**

cells, images were counted approximately every 7 μm ensuring that different cells were considered. The percentage of positive or double positive cells was calculated relative to the total number of nuclei (DAPI staining) at each Z level. When comparing the number of B cells versus GFAP positive cells, the number of GFAP and positive cells was first determined independently. Then, the percentage of GFAP/Ki67 cells out of the GFAP positive was calculated. Quantification of GLAST cells refers to the number of positive cells touching the ventricle relative to the analyzed lateral wall length (linear measurement = 130 $\mu$m).

Wholemount image analysis was performed counting four non overlapping fields (130 $\mu$m × 130 $\mu$m) of every specified region and genotype. Images of the WM were acquired every 0.5 μm and maximum projections of three to five consecutive Z levels are shown. In some cases, due to the cell heterogeneity depending on the region and the genotype, data are presented relative to the total surface analysed.

A customized software developed by Wimasis (Wimasis GmbH, Munich, Germany) was used to determine cell areas, percentage of cell polarization and angle displacement. Ten independent representative images per genotype were analyzed. For cell polarization analysis, the contours of ependymal cells and BB patches were defined and the relative distance between the geometric center of the apical cell surface and the BB cluster centroid was determined and divided by the cell radio. Angle displacement was determined relative to a reference angle for each microscopy field by drawing a vector from the cell center to the cluster centroid (Boutin et al., 2014).

Comparison of the cellular populations that constitute the SVZ was carried out using a Kruskal–Wallis test together with Dunn's multiple comparisons test. For all the other analyses, Mann–Whitney non-parametric tests were performed. Angle displacements were compared by circular statistical analysis. Data were graphically represented using Oriana software (Kovach Computing Services, Anglesey, Wales) and Watson's $U^2$ test was performed. Differences were considered significant when $P < 0.05$ ($^*P < 0.05$, $^{**}P < 0.01$, $^{***}P < 0.001$) and all data are reported as mean ± standard deviation of the mean (SD).

## RESULTS

### p73 Deficiency Alters RG Cells Transition into ECs, Generating Immature Cells with Abnormal Identities and Resulting in Loss of Ventricular Integrity

ECs are generated from RGCs during perinatal development. This ependymal layer is crucial for the SVZ germinal center organization and function. Thus, to address whether p73 deficiency affected the maturation and organization of the EC layer, we analyzed P7 and P15 coronal sections using EC markers (Vimentin and S100$\beta$) together with GFAP. In P7-wild type (WT) mice [Fig. 1(A)], most of the ependymal-Vimentin$^+$/S100$\beta^+$ cells already formed a mono-stratified epithelium lining the ventricle, although there were areas that remained pseudo-stratified at this stage (white arrows). In the absence of p73, formation of the monostratified epithelium looked halted and chains of S100$\beta^+$/Vimentin$^+$ cells appeared to progress inwards with remarkable separations between the cells [Fig. 1(A), white arrows]. In WT ECs Vimentin and S100$\beta$ proteins did not have the same cellular localization, with S100$\beta$ being expressed mostly at the apical surface (white arrowheads). On the contrary, in p73KO ECs these proteins co-localized (white arrowhead) also coinciding with GFAP expression around the cell soma and radial extensions [Fig. 1(B), yellow arrowheads].

Many of these triple positive cells (S100$\beta$/Vimentin/GFAP) were contacting the ventricle and could

**Figure 1** Lack of p73 results in a defective ependymal cell layer and loss of ventricular integrity. (A,B) Expression of Vimentin (A,B, red), S100$\beta$ (A, B, green), and GFAP (B, blue) in confocal images of brain coronal sections from P7 WT and p73KO mice. Mono- or pseudo-stratified ependymal layers are indicated by white arrows. Colocalization of S100$\beta^+$/Vimentin$^+$ is indicated by white arrowheads (A) and S100ß$^+$/Vimentin$^+$/GAFP$^+$ by yellow arrowheads (B). (C) Analysis of GLAST (green), Vimentin (red), and GFAP (blue) expression in P15 mice after RGC transition into ependymal cells. Vimentin$^+$ cells are indicated by white arrowheads. Different stages of RGCs transition were detected: immature GLAST$^+$-RGCs (white arrows), RGCs in transition GLAST$^+$/Vimentin$^+$ (yellow arrows) and aberrant GLAST$^+$/Vimentin$^+$/GFAP$^+$ cells (yellow arrowheads). (D) Quantification of GLAST$^+$ cells touching the lateral wall of the ventricule of SVZ. (E) Coronal sections of P15 WT, p73KO, p53KO, and DKO mice were stained with the indicated antibodies and the LW of the lateral ventricle was analyzed by confocal microscopy. WT LW showed a mono-stratified epithelium of ependymal S100$\beta^+$/IB4$^+$ cells (red/green, white arrows), with some S100ß$^+$/GFAP$^+$ positive mature astrocytes in the striatum (yellow arrows) and a few GFAP$^+$/S100$\beta^-$ B-cells (white arrowheads). TP73 defective cells formed a pseudo-stratified and discontinuous layer (yellow arrowheads) with S100$\beta^+$/GFAP$^+$ cells (pink arrows) with periventricular soma and long RG-like striatal processes. Some S100$\beta^+$ ependymal cells were IB4$^-$ (blue arrows). Tile scan of coronal sections images (×10) from WT, p73KO, p5KO, and DKO mice. Scale bars: 20 $\mu$m. [Color figure can be viewed in the online issue, which is available at wileyonlinelibrary.com.]

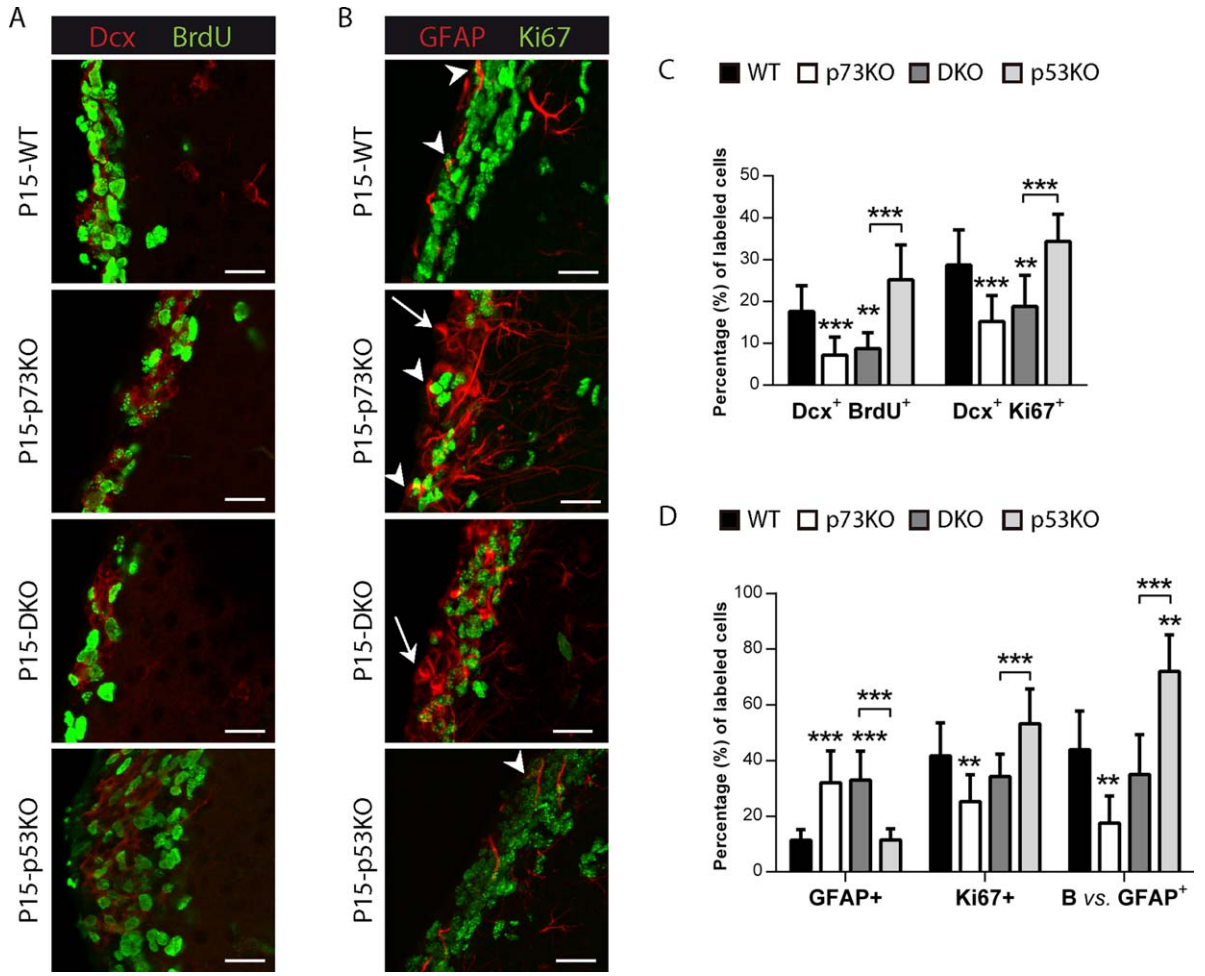


**Figure 2** p73 deficiency affects proliferating neuroblasts and neural stem cells, even in the absence of p53. Coronal sections of P15 WT, p73KO, p53KO, and DKO mice were stained with the indicated antibodies and the LW of the lateral ventricle was analyzed by confocal microscopy (A, B) and cellular populations were quantified (C, D). (A, C) p73 loss resulted in less proliferating neuroblasts [Doublecortin ($Dcx^+$)/$BrdU^+$ (red/green)], even in the absence of p53. (B, D) Mice lacking p73 had more non proliferating astrocytes indicated by white arrows ($GFAP^+$, red), but a reduced proportion of B-cells, indicated by white arrowheads ($GFAP^+$/$Ki67^+$, red/green). Scale bars: 20 $\mu$m. [Color figure can be viewed in the online issue, which is available at wileyonlinelibrary.com.]

correspond with immature cells in a transitional state from RGCs to ECs [Fig. 1(B)]. To address this, we analyzed expression and localization of the RGC marker GLAST, together with Vimentin, at a stage were RG transition into ECs has just been completed (P15) (Lavado and Oliver, 2011). As previously described (Mirzadeh et al., 2008), $GLAST^+$-RGCs were mostly absent from the ventricle wall in P15 WT brains and $Vimentin^+$-ECs lacked GLAST expression [Fig. 1(C), white arrowheads]. However, p73KO brains had significantly more $GLAST^+$-RGCs that remained in contact with the ventricle [Fig. 1(C,D), white arrows]. Moreover, many of these cells expressed Vimentin in their processes ($Vimentin^+$/$GLAST^+$ cells, yellow arrows). This pattern of marker expression strongly suggests an immature phenotype in the p73KO brains. We also detected an aberrant triple positive population ($Vimentin^+$/$GLAST^+$/$GFAP^+$) in P15-p73KO mice [Fig. 1(C), yellow arrowheads]. This population most likely represent an intermediate cellular state during RG transformation into $GFAP^+$ astrocytes and B cells (Spassky et al., 2005), indicating that p73 might be required for RGCs cell fate determination.

To further study the effect of p73 deficiency on ependymal cell maturation and morphology, P15 coronal sections were stained with antibodies against S100ß (also expressed by mature GFAP-astrocytes) and isolectin B4 (IB4), which also labels endothelial cells. At this stage, WT mice already exhibited an

organized and continuous mono-stratified epithelium of mature ECs ($S100\beta^+/IB4^+$) [Fig. 1(E), white arrows] with few B-cells ($GFAP^+/S100\beta^-$) contacting the ventricle (white arrowheads) and some mature $GFAP^+/S100\beta^+/IB4^-$ astrocytes only in the striatum (yellow arrows). In contrast, lack of p73, resulted in a pseudo-stratified and discontinuous ependyma with scattered $S100\beta^+$-ECs [Fig. 1(E), yellow arrowheads]. It is worth noticing that not all $S100\beta^+$-ECs were positive for IB4 (blue arrow) but, in turn, p73KO brains had abundant $GFAP^+/S100\beta^+$ cells, some of which were in contact with the ventricle (pink arrow), suggesting either an incomplete maturation or an astrocytic nature. p73-deficient ependymal layer had gaps, invaginations, and "bumps" [Fig. 1(E), yellow arrowheads and Supporting Information Fig. 1], indicating that lack of p73 compromises ependymal barrier integrity. Defects in the ependymal barrier have been associated to hydrocephalus (Jimenez et al, 2014), a condition observed in the p73KO mice (Yang et al., 2000). However, it has been proposed that hydrocephalus in p73KO could be the result of induced apoptosis associated to an exacerbated p53 activity, due to the lack of the prosurvival DNp73 isoform (Pozniak et al., 2002; Lee et al., 2004). To address this possibility, even though the number of $S100\beta^+$ cells was not lower in p73KO SVZ than in WT brains (data not shown), we analyzed coronal sections from p53 knock-out (p53KO) and double mutant p73KO/p53KO (DKO) brains. DKO, like p73KO, showed severe hydrocephalus and enlarged ventricles [Fig. 1(E)], suggesting that p73-loss has a dominant effect. Consistently, DKO also had numerous $S100\beta^+$ ECs, some of which were $IB4^+$, but these ECs did not form a monostratified epithelium [Fig. 1(E)] demonstrating that p53 abolishment did not restore the phenotype. Moreover, DKO mice, but not the single p53KO, displayed defective ependymal layers [Fig. 1(E), yellow arrowheads].

It has been reported that disruption of the mature ependyma disturbs neurogenic activity (Jimenez et al., 2014). Mature ECs create a permissive neurogenic environment by secreting Noggin (Lim et al., 2000). Noggin and S100ß expression co-localized within the ependymal layer in WT mice (Supporting Information Fig. 1). However, in the p73KO, Noggin was detected throughout the SVZ and did not completely match the $S100\beta^+$ expressing cells, highlighting the lack of appropriate organization and maturation of ECs (Supporting Information Fig. 1). This finding not only was consistent with the idea that p73 is required for the transition of RG into the different cell types that comprise the SVZ but, more importantly, it also suggested possible defects in the neurogenic environment of this region in p73-defective mice. To address this, we analyzed the different cellular populations that constitute the SVZ. P15 brain coronal sections were first stained against Doublecortin (Dcx), combined with the proliferation markers Ki67 or BrdU to quantify the proliferating neuroblasts [Fig. 2(A–C)]. It has been published that p53KO mice had more proliferating neuroblasts than WT (Ferrón et al., 2009). However, we observed that, lack of p73, alone or in the context of p53KO (DKO), resulted in a significant reduction of the proliferating neuroblasts compared to WT or p53KO, respectively [Fig. 2(C)], indicating that p73 deficiency leads to a reduction in neurogenesis in the SVZ, despite p53 absence. However, p53 ablation in the context of p73 deficiency (DKO) did not elevate the number of proliferating neuroblasts, indicating that p73 effect was not due to enhanced neuroblast cell death resultant from p53 compensatory activation.

RGC will also give raise to neural stem cells (B-cell) and astrocytes. Thus, we next analyzed these populations: astrocytes (non-proliferative GFAP cells) and B-cells, identified as the subpopulation of proliferating astrocytes (GFAP/Ki67 double positive) in the SVZ (Merkle et al., 2004). Strikingly, lack of p73 gave raise to $GFAP^+$ cells that had a periventricular cell soma in contact with the ventricle, $GFAP^+$ filaments that formed tangles surrounding the nucleus, and long $GFAP^+$ processes that extended across the striatum towards the pial surface, altogether resembling the morphology of RG cells [Fig. 2(B), white arrows]. However, most of these $GFAP^+$ cells were non-proliferating cells [Fig. 2(B,D), white arrows], discarding their possible identity as B-cells. While 43.86% of $GFAP^+$ cells represented B-cells in the WT, only 17.56% of $GFAP^+$ cells were B-cells in p73KO. Moreover, p73 deficiency, alone or in the context of p53 ablation (DKO), resulted in significant reduction in the proportion of B-cells in the SVZ compared to WT and p53KO, respectively [Fig. 2(D)], suggesting a p73 requirement for adult neural stem cells establishment and maintenance.

Altogether the alterations in the p73KO SVZ indicate that p73 loss results in an aberrant maturation of the ECs, affecting the SVZ environment, which might cause, at least in part, the impaired neurogenic capacity of the germinal centers, independently of p53.

## p73 is Essential for the Ependymal Cell Assembly into Neurogenic SVZ Pinwheels

EC generation involves the transformation of monociliated RGCs into multiciliated ECs during the first

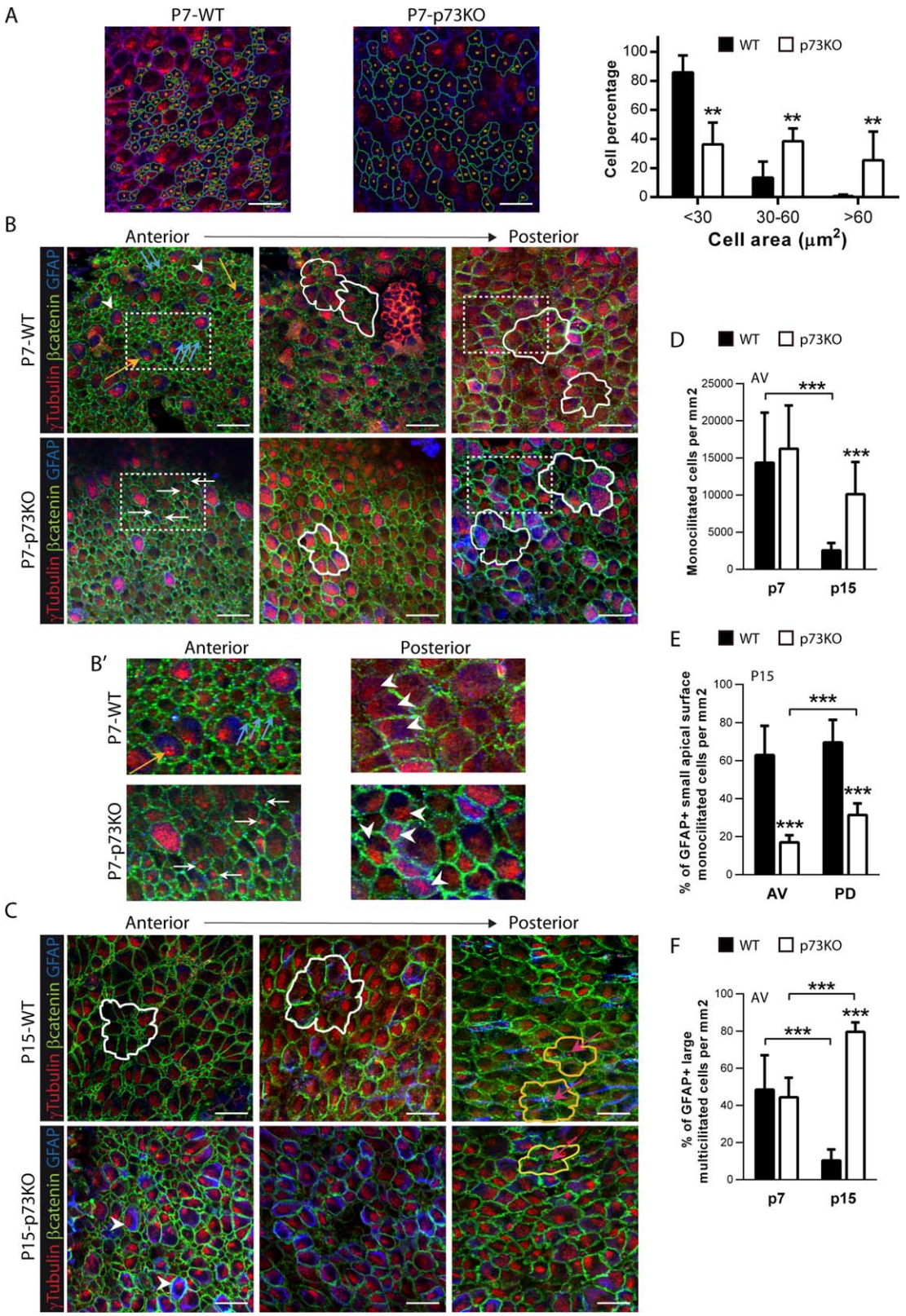
A
P7-WT
P7-p73KO
WT
p73KO
Cell percentage
100
80
60
40
20
0
**
**
**
<30
30-60
>60
Cell area (μm²)
B
Anterior
Posterior
P7-WT
P7-p73KO
γTubulin βcatenin GFAP
B′
Anterior
Posterior
P7-WT
P7-p73KO
C
Anterior
Posterior
P15-WT
P15-p73KO
γTubulin βcatenin GFAP
D
WT
p73KO
AV
***
***
Monocilitated cells per mm2
25000
20000
15000
10000
5000
0
p7
p15
E
WT
p73KO
P15
***
***
***
% of GFAP+ small apical surface monocilitated cells per mm2
100
80
60
40
20
0
AV
PD
F
WT
p73KO
AV
***
***
***
% of GFAP+ large multicilitated cells per mm2
100
80
60
40
20
0
p7
p15

**Figure 3.**

postnatal days (P0-P15) (Spassky et al., 2005). Within the first postnatal week, RGCs gradually increase their apical surfaces and upon reaching certain size, multiply the number of basal bodies (BB) to develop clusters of motile cilia (Mirzadeh et al., 2010). To analyze this maturation, P7-WT and p73KO mice wholemounts dissections were stained with $\gamma$-tubulin to label the cilia basal bodies (BBs), and $\beta$-catenin to delimit the cell membrane, and the apical cell surface size was quantified [Fig. 3(A)]. Most of the mono-BB cells in WT mice were small cells with an apical surface $\leq$25 $\mu m^2$ corresponding to B-cells and RGCs according to Mirzadeh et al. (2010). WT mice also had mono-BB cells with expanded apical surface, between 30 and 60 $\mu m^2$, which are RGCs in transition (Mirzadeh et al., 2010), but we rarely detected mono-BB cells with an apical surface bigger than 60 $\mu m^2$. However, in p73KO mice the percentages of mono-BB cells with intermediate size or with apical surfaces bigger than 60 $\mu m^2$ were significantly higher [Fig. 3(A)]. The later cells correspond, most likely, to abnormal stages of RGC transitioning into ECs.

The neurogenic capacity of the rodents SVZ is dependent upon ependymal cells integrity and their capacity to assemble into the unique structures that define this region: the pinwheels (Kuo et al., 2006; Paez-Gonzalez 2011). Multi and bi-ciliated ECs surround mono-ciliated $GFAP^+$-B-cells forming pinwheels in which the apical processes of the neural stem cells constitute the core of the structure (Mirzadeh et al., 2008). To address whether p73-deficiency affected SVZ cytoarchitecture, P7 and P15 wholemounts were stained with $\gamma$-tubulin, $\beta$-catenin and GFAP antibodies to identify ventricle-contacting monociliated $GFAP^+$-neural stem cells (B-cells) and multiciliated $GFAP^-$ ECs [Fig. 3(B–D)].

P7-WT AV region showed mono-BB cells which do not express GFAP and correspond to RGCs [Fig. 3(B, B')], blue arrows] and RGCs with extended apical surface and $\gamma$-tubulin stainings marks like dense punctuated deposits known as deuterosomes (Spassky et al., 2005) [Fig. 3(B, B'), yellow arrows]. There were also cells with multiple BBs, which are sparse and randomly oriented in the apical surface, that correspond to immature multiciliated cells [Fig. 3(B), white arrowheads].

Toward posterior regions, WT-ECs seemed to be organizing into pinwheel structures, with immature large $GFAP^+$-multi BB cells surrounding groups of small mono-BB cells (pre-pinwheels) [Fig. 3(B), white lines], confirming the gradual transformation of the lateral ventricle wall in WT mice. The maturing p73KO-ECs were arranged into aberrant structures, with many intermediate-size mono-BB cells in the core, but without a pre-pinwheel organization [Fig. 3(B), white lines]. Moreover, while in the WT brains neighbors cells have begun to coordinate their BB clusters [Fig. 3(B') white arrowheads], in p73KO the cells do not show any coordinated orientation at this stage (white arrowheads). Nevertheless, p73 deficient mice did not show significant differences in the number of total mono-BB cells [Fig. 3(D)], neither in multi-BB cells (WT $32.83 \pm 12.45$ vs. p73KO $22.02 \pm 8.086$; $p = 0.0734$).

P15-WT mice [Fig. 3(C)] showed a progressive maturation with pre-pinwheel patterns (white lines) at AV zone and pinwheels (yellow lines) in PD regions, very similar to those described in the adult mice (Mirzadeh et al., 2008). The monociliated cells at the pinwheel core had a small apical surface with long $GFAP^+$ processes oriented tangentially to the epithelial surface, what identified them as B-cells [Fig. 3(C), pink arrows]. Surprisingly, P15-p73KO SVZ lacked this cytoarchitecture [Fig. 3(C)]. First, the number of total monociliated cells was significantly higher in p73KO than in the WT [Fig. 3(D)]. However, $62.9\% \pm 15.4\%$ of monociliated cells in WT were $GFAP^+$ B-cells, while in p73KO only $17.0\% \pm 3.8\%$ (AV region) and $31.4\% \pm 6.1\%$ (PD region) expressed this marker [Fig. 3(E)], indicating that p73 deficient monociliated cells were not *bona-fide* B-cells. As we progressed toward the posterior regions, a more organized distribution was observed,

**Figure 3** Lack of p73 delays the establishment of the lateral ventricle wall cytoarchitecture and the organization of ependymal cells into pinwheels. Confocal Z-stacks images of lateral ventricle wall whole-mounts from the indicated age and phenotype immunostained for $\beta$-catenin (green), $\gamma$-tubulin (red), and GFAP (blue). (A) Confocal images of P7 WT and p73KO SVZ with trace of the cell contour (green) and quantification of mono- basal body (BB) cell size. (B, B') In P7 mice, RGCs are identified by the presence of a single BB and small apical surface (blue arrows). Immature multiciliated cells are shown by either yellow arrows (cells with deuterosomes) or by white arrowheads (cells with multiple BB covering the apical surface). The orientation of RGCs and multi-BB cells is indicated by white arrows and white arrowheads, respectively. (B, C) In P7 and P15 mice white and yellow lines mark pre-pinwheels and pinwheels respectively, and pink arrows indicate pinwheel core cells. (D–F) Quantification of the indicated populations at anterior-ventral (AV) and posterior-dorsal (PD) regions in P7 and P15 mice. The images represent Z-stacks (20 $\mu$m) from at least 6 dorso-ventral regions. Scale bars: 20 $\mu$m. [Color figure can be viewed in the online issue, which is available at wileyonlinelibrary.com.]

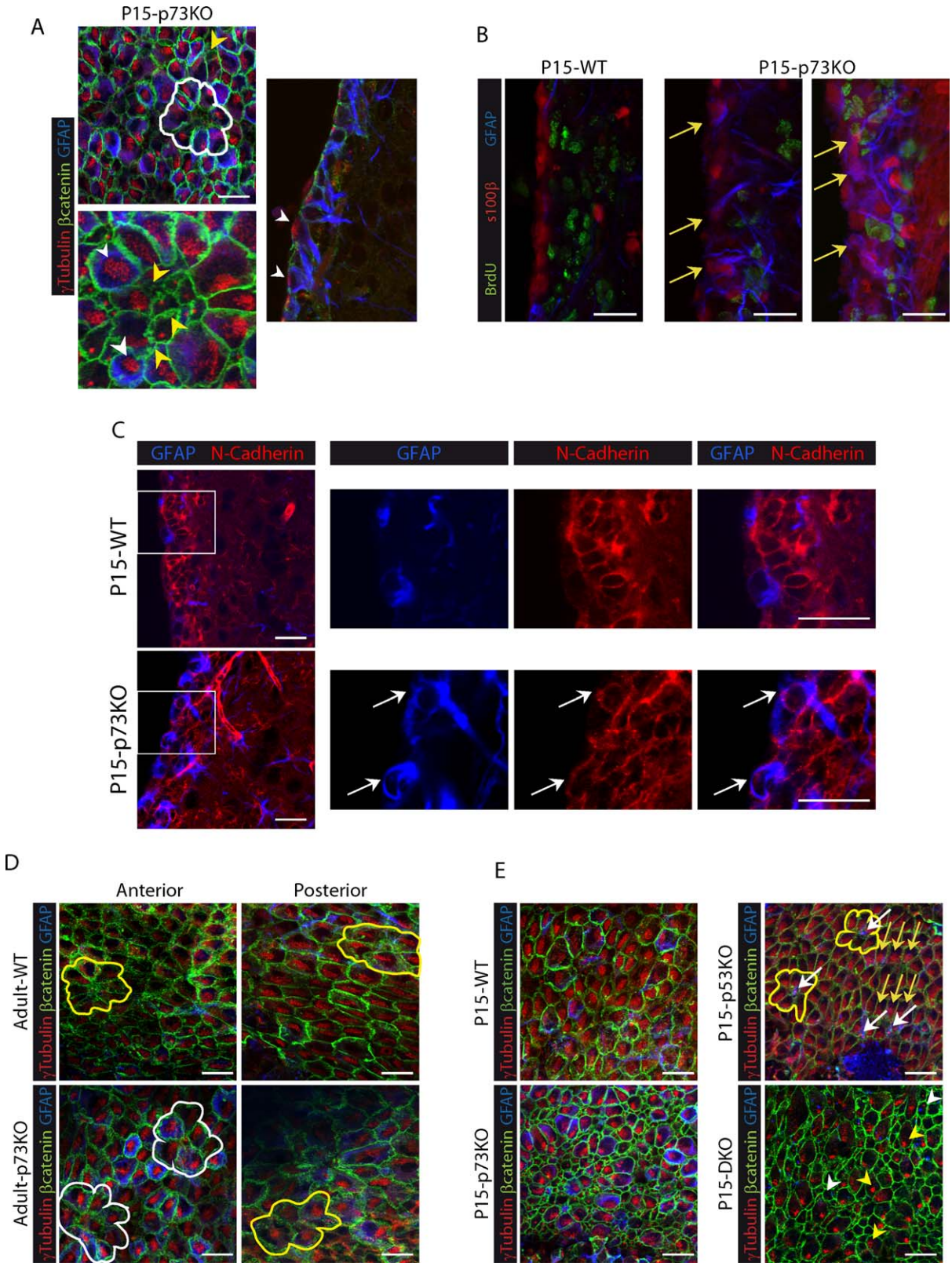
A
P15-p73KO
γTubulin βcatenin GFAP
B
P15-WT
P15-p73KO
BrdU s100β GFAP
C
GFAP N-Cadherin
GFAP
N-Cadherin
GFAP N-Cadherin
P15-WT
P15-p73KO
D
Anterior
Posterior
Adult-WT
Adult-p73KO
γTubulin βcatenin GFAP
E
P15-WT
P15-p73KO
P15-p53KO
P15-DKO
γTubulin βcatenin GFAP

**Figure 4.**

but structures resembling pinwheel patterns were seldom detected [yellow lines and pink arrows]. In the absence of p73, it is noteworthy that, a significant number of large-surface multi-BB cells touching the ventricle, which by definition are ECs (Spassky et al., 2005), were GFAP$^+$, even at P15 [Fig. 3(C,F), white arrowheads]. These large multiciliated-GFAP$^+$ cells [Fig. 4(A), white arrowheads] seemed to correspond with the previously described cells contacting the ventricle that coexpressed S100$\beta$, Vimentin and GFAP, some of which were also GLAST$^+$ [Fig. 1(B,C), yellow arrowheads]. These cells had an aberrant membrane morphology with waves and pleats [Fig. 4(A), yellow arrowheads], suggesting that the intercellular junctions at the apical surface of these cells might be affected.

It has been reported that p73KO brains suffer ependymal denudation (Medina-Bolivar et al., 2014). This process triggers neighboring astrocytes to proliferate and form a superficial cell layer covering the denuded ventricular surface (Roales-Buján et al., 2012). The reactive astrocytes found at the denuded ventricular walls resemble the ependymal cells in several aspects, like the expression of vimentin, but maintain specific differences like lack of N-cadherin expression and absence of cilia (Roales-Buján et al., 2012). Thus, we sought to determine whether the GFAP-expressing cells in p73KO VZ/SVZ were indeed, reactive astrocytes. We analyzed the proliferation capacity of S100$\beta^+$/GFAP$^+$ cells, since remodeling astrocytes have been shown to express proliferative markers (Kuo et al., 2006; Luo et al., 2008), and found that most of the S100$\beta^+$/GFAP$^+$ cells in the p73KO SVZ were nonproliferating BrdU$^-$-cells [Fig. 4(B), yellow arrows]. Furthermore, the cells lining the ventricles in p73 deficient mice, including the GFAP$^+$ cells, expressed N-cadherin at the lateral plasma membrane [Fig. 4(C), white arrows]. A similar phenotype was observed in DKO mice (Supporting Information Fig.2). Moreover, the presence of BB clusters in these GFAP$^+$ cells revealed their fate as multicilliated ependymal cells [Fig. 4(A), white arrowheads]. Altogether, our data is consistent with a defect in RGC maturation and the presence of aberrant and immature multiciliated-ECs in p73KO VZ/SVZ, rather than with the presence of remodeling astrocytes. It is meaningful that adult p73KO maintained the observed phenotype in adulthood with the presence of multiple large-surface ependymal cells with BBs clusters and altered membrane junctions [Fig. 4(D)]. Adult p73KO multiciliated cells had strong GFAP expression and very condensed basal bodies clusters forming mainly pre-pinwheel structures [Fig. 4(D) white lines] and only a small number of pinwheels (yellow line). Thus, in the absence of p73, EC maturation is halted, with the immature ECs remaining in the lateral ventricle. These data confirm that p73 deficiency results in a deregulation of the transition process from RGC to ependymal and B-cells, leading to the emergence of aberrant cells not capable of assemble into neurogenic structures.

To further address whether p53 function played a relevant role on neurogenic pinwheel organization, we performed a comparative study of wholemounts from the four genotypes at P15, since the DKO mice do not survive any longer. p53 deficient brains displayed an organized VZ with mature multiciliated ECs and monociliated GFAP$^+$-B cells forming pinwheels [Fig. 4(E), yellow lines]. Thus, lack of p53 did not affect the cytoarchitecture of the lateral ventricle wall, despite the numerous B-cells touching the ventricle [Fig. 4(E), white arrows]. Strikingly, DKO mice were very similar to p73KO, with numerous monociliated cells with expanded apical surface, some of them GFAP$^+$ [Fig. 4(E), white arrowhead].

**Figure 4** p73 deficiency results in immature and aberrant multiciliated ependymal cells that persist in adulthood, independently of p53. (A) Magnification of confocal WMs Z-stacks micrographs (left) and coronal section (right) from P15 p73KO mice immunostained for $\beta$-catenin (green), $\gamma$-tubulin (red), and GFAP (blue). Yellow arrowheads indicate multiciliated cells with aberrant membrane morphology, while multiciliated cells with abnormal identities (GFAP$^+$) are marked by white arrowheads. (B) Confocal images of brain coronal section from WT and p73KO mice. Inmunostaining for BrdU (green), S100$\beta$ (red), and GFAP (blue) indicate that most of the S100$\beta^+$/GFAP$^+$ cells in the p73KO SVZ were non-proliferating cells (BrdU$^-$) (yellow arrows). (C) Confocal images and magnifications of P15 coronal sections immunostained for N-Cadherin (red), and GFAP (blue). White arrows indicate N-cadherin$^+$/GFAP$^+$ cell touching the ventricle. (D) Analysis of lateral ventricle wall whole-mounts of the indicated phenotypes at P160 (D) and P15 (E) immunostained for $\beta$-catenin (green), $\gamma$-tubulin (red), and GFAP (blue). Pinwheel structures are marked by white lines and pre-pinwheel structures by yellow lines. (E) Wholemount analysis of P15 mice from the four genotypes. While p53KO mice presented pinwheel structures (yellow lines) with B cells (white arrows), DKO mice showed aberrant expanded apical surface monociliated GFAP$^+$ cells (white arrowheads) and cells with deuterosomes (yellow arrowheads), but not organized structures. Yellow arrows follow basal body polarization of ependymal cells. Scale bars: 20 $\mu$m. [Color figure can be viewed in the online issue, which is available at wileyonlinelibrary.com.]

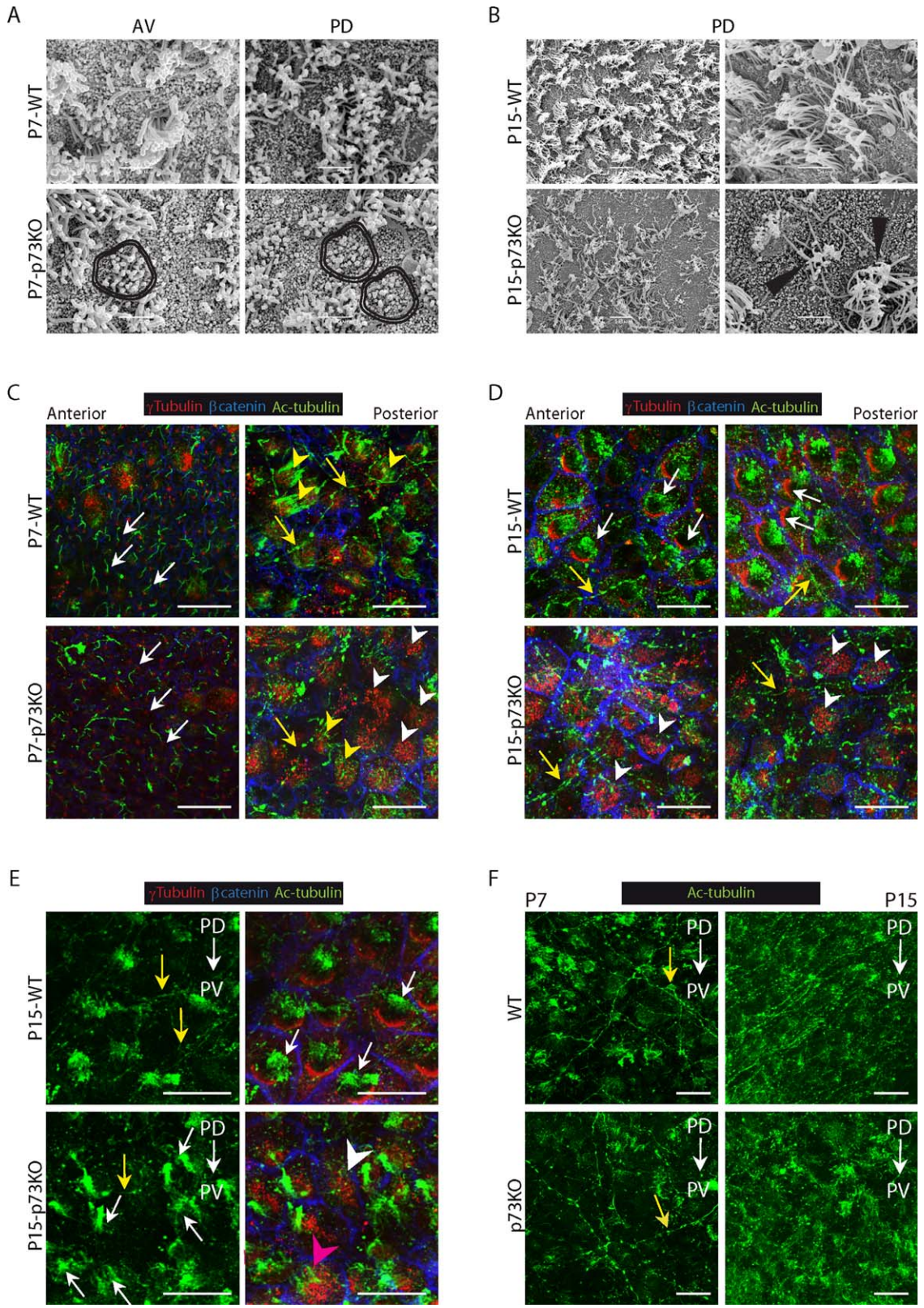
A
AV
PD
P7-WT
P7-p73KO
B
PD
P15-WT
P15-p73KO
C
Anterior
γTubulin βcatenin Ac-tubulin
Posterior
P7-WT
P7-p73KO
D
Anterior
γTubulin βcatenin Ac-tubulin
Posterior
P15-WT
P15-p73KO
E
γTubulin βcatenin Ac-tubulin
PD
PV
P15-WT
P15-p73KO
F
P7
Ac-tubulin
P15
PD
PV
WT
p73KO

**Figure 5.**

Moreover, many multiciliated cells still had deuterosomes, with no detectable polarization, characteristic of immature ECs [yellow arrowheads]. These results demonstrate that while p73 function is required for the establishment of SVZ architecture while p53 is not essential for these processes.

## Lack of p73 Impairs Ciliogenesis and Planar Cell Polarity Establishment

To address whether lack of p73 affected the genesis and organization of ependymal cilia, we performed a comparative study of P7 and P15 WT and p73KO mice using SEM. It has been described that cilia tufts appear around P5 and reach their mature density by P10 (Tissir et al., 2010). Accordingly, P7-WT AV regions displayed some monociliated cells [Supporting Information Fig. 3(A), black arrows; Fig. 5(A),] and abundant multiciliated cells [Supporting Information Fig. 3(A,B)] covering most of the ventricular surface. At the same stage, p73KO showed an immature phenotype with many monociliated cells [Supporting Information Fig. 3(A,B), black arrows] and less cilia tufts [Supporting Information Fig. 3(A,B)]. Moreover, it is noteworthy the presence of cells with cilia of different sizes distributed through the whole apical surface [Fig. 5(A), double line]. As reported (Spassky et al., 2005), we observed that by P15 mature ECs dominate the VZ displaying compacted cilia clusters on the apical surface which have begun to be coordinately oriented [Fig. 5(B)]. In contrast, cilia tufts in p73KO cells displayed an abnormal organization and, in some cases, the individual cilia within a given cell did not point to the same direction and some cilia seem to be angled or even truncated [Fig. 5(B), black triangles]. This data suggests that in the p73KO mice the cilia fail to form normally.

We found intriguing that while the SEM analysis revealed less cilia covered area in p73KO lateral ventricle wall [Fig. 5(B)], our previous en-face whole-mount staining of the walls of the lateral ventricle (Fig. 3) demonstrated that there were no differences in the number of total multiciliated cells in the p73KO, as accounted by the presence of BB clusters. Thus, we hypothesized that p73-deficient VZ ependymal cells had BB clusters, but lacked cilia due to a defect in the ciliogenesis process. To address this, we analyzed wholemounts of P7 and P15 SVZ stained for acetylated tubulin (Ac-tubulin) which marks ependymal long motile cilia and RGCs short primary cilia. At P7 anterior regions, WT mice displayed RGCs with a primary cilium associated to a single basal body [Fig. 5(C), white arrows], while at posterior regions, ECs have long cilia tufts emanating from BBs patches (yellow arrowheads). The majority, although not all, p73-deficient RGCs had a primary cilium associated to a basal body [Fig.5(C), white arrows]. However, many ECs had BB clusters that lacked cilia (white arrowheads). Few p73KO ECs had BB patches with associated cilia, but in these cases, the EC displayed disorganized cilia of different lengths [Fig.5(C), yellow arrowheads], similar to those observed by SEM [Fig. 5(A), double lines].

P15 WT ECs displayed densely packed BB clusters, all associated to cilia tufts [Fig. 5(D,E), white arrows]. The cilia dysfunction was patent in p73KO at this stage where many of the large surface cells had disorganized BB clusters that were not associated with cilia [Fig. 5(D,E), white arrowheads]. Ac-tubulin antibodies also stained some long and slender processes with varicosities [Fig. 5(C–F), yellow arrows], corresponding with supra-ependymal axons (Tong et al., 2014). Supra-ependymal axons run parallel to the anterior–posterior axis (PD→AD) of the lateral ventricle on the dorsal V-SVZ and along the dorso-ventral axis (PD→PV) of the WT mice. Surprisingly, the lateral ventricular wall of the P7-p73KO mice had a less dense network of supra-ependymal axons which lack direction [Fig. 5(F) and

**Figure 5** Lack of p73 alters motile cilia generation and planar cell polarity establishment during the transformation of monociliated RG into ependymal cells. SEM analysis of WT and p73KO lateral ventricle wall wholemounts at P7 (A) and P15 (B). (A) P7-p73KO mice displayed aberrant groups of cilia of different length (double lines). Scale bar: 5 $\mu$m (B) P15 WT PD region showed organized multiciliated cells while in p73KO the cells had angled and truncated cilia (black triangles). Scale bar: 5 and 10 $\mu$m. (C–F) Confocal Z-stacks images of WMs immunostained for $\gamma$-tubulin (red), $\beta$-catenin (blue) and Ac-tubulin (green) from P7 (C, F) and P15 (D–F) mice. (C) At P7 RGCs had a primary cilium associated to a single basal body (white arrows) and immature ECs had long cilia emanating from basal bodies patches (yellow arrowheads). Most p73KO ECs had multiple basal bodies but lacked motile cilia (white arrowheads) and only few displayed cilia, but disorganized and of different lengths (yellow arrowheads). (D,E) Mature WT-EC showed characteristic oriented basal bodies patches associated to cilia tufts (white arrows). ECs in p73KO had non oriented BB clusters either associated to disorganized cilia (pink arrowhead) or without cilia (white arrowheads). (F) Comparison of the supra-ependymal axons (C-F, yellow arrows) network between WT and p73KO mice. AV: anterior-ventral; PD: posterior-dorsal. PD→AD: anterior-posterior axis. PD→PV: dorso-ventral axis. Scale bar: 20 $\mu$m. [Color figure can be viewed in the online issue, which is available at wileyonlinelibrary.com.]

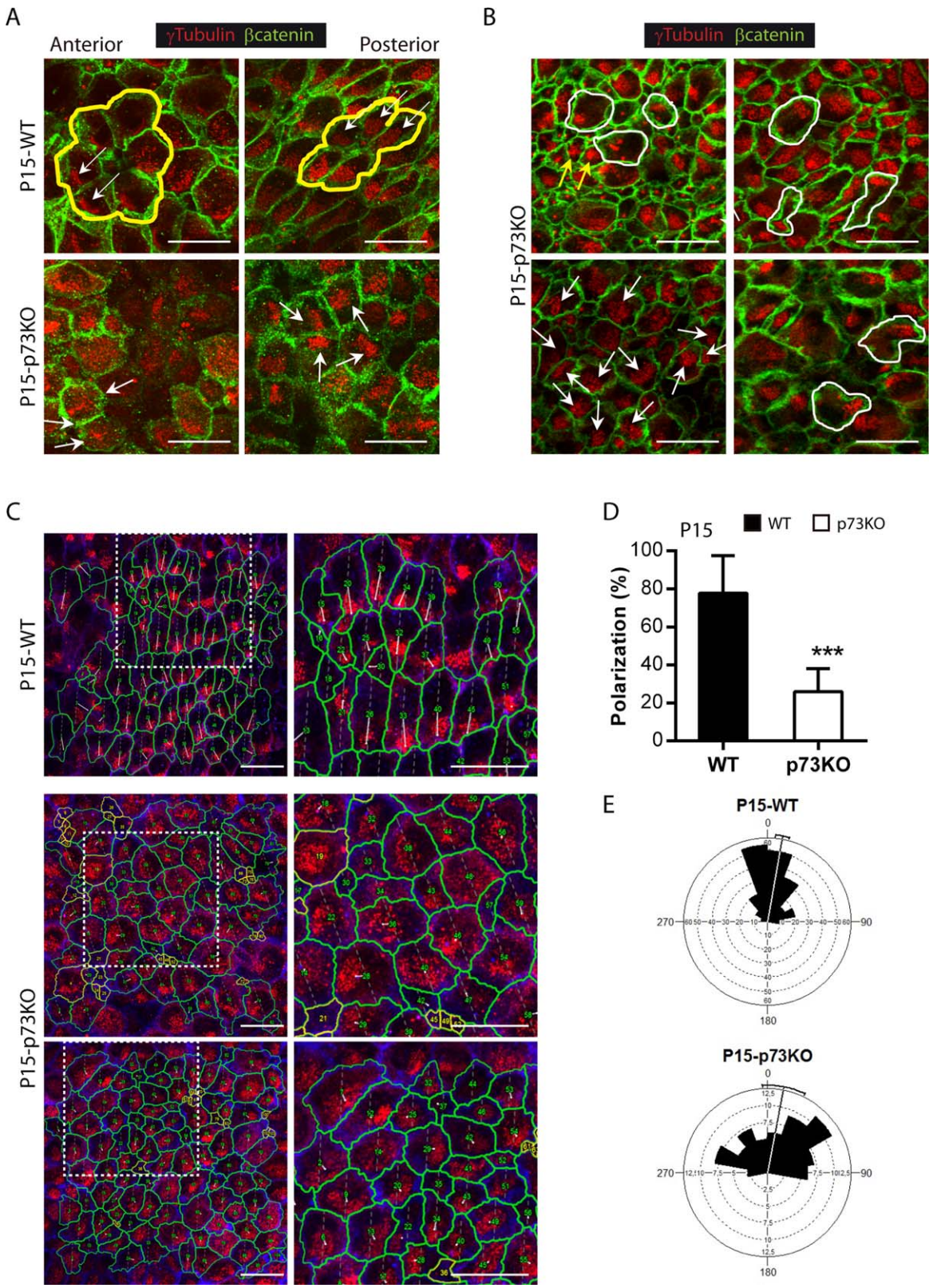
A
Anterior
γTubulin βcatenin
Posterior
P15-WT
P15-p73KO
B
γTubulin βcatenin
P15-p73KO
C
P15-WT
P15-p73KO
D
P15
WT
p73KO
Polarization (%)
100
80
60
40
20
0
***
WT
p73KO
E
P15-WT
P15-p73KO
0
90
180
270

**Figure 6.**

Supporting Information Fig.4(A), yellow arrows]. This was also evident at P15 stage where a fine and organized network of supra-ependymal axons running on a dorso-ventral direction was observed in the WT mice [Fig. 5(F) and Supporting Information Fig. 4(B), yellow arrows]), whereas p73-deficient mice showed a less dense and disorganized network, presumably contributing to their neurogenic deficiency.

Our results confirmed that p73 deficiency results in defective ciliogenesis during the transition from monociliated RGCs into multiciliated ECs. A correlation between defective ciliogenesis and alterations in ependymal planar polarization has been previously reported (Mirzadeh et al., 2010). In agreement, throughout this work we had detected, in p73KO cells, irregularities in the position of BBs on the apical surface of the cells, i.e., defects in translational cell polarity (tPCP). For example, while neighboring RGCs in P7-WT mice had their cilia BB displaced to the same side of the apical surface [Fig. 3(B'), blue arrows], neighboring p73KO-RGCs had their cilia positioned on opposite sides [Fig. 3(B'), white arrows], suggesting that p73 deficiency affected RGCs primary cilium polarization. Most multiciliated P15 WT ECs were polarized at tissue level (tPCP established), since they had their BB patches compacted and clustered on the "downstream" side of the apical cell surface, with respect to the direction of CSF flow, and cilia tufts following the same orientation [Fig. 5(D,E), white arrows]. However, in p73-deficient cells most BB clusters were not polarized [Fig. 5(D), white arrowheads), independently of the presence of cilia tufts [Fig. 5(E), white arrows, pink arrowhead] or its absence [white arrowheads], suggesting that p73 effect on tPCP was upstream of ciliogenesis.

Moreover, WT ECs that conform a pinwheel structure had their BB clusters polarized with a similar orientation [Fig. 6(A), yellow lines and white arrows,]. That was not the case in p73KO ECs, which had their BBs either distributed throughout the apical surface, or oriented following different directions [Fig.6 (A,B), white arrows). Moreover, they display different arrays of cilia cluster distribution: some cells had very tightly compacted basal bodies [Fig. 6(B), yellow arrows], others formed more than one cluster located on one side of the apical surface, or even in two opposing poles [white lines]. Altogether, suggesting that p73 is essential to organize BB in individual cells and also for intercellular BB patch orientation. To further address p73 requirement for the establishment of tPCP we quantify the degree of cluster polarization relative to the apical surface. For this purpose we use a program generated by Wimasis® to calculate the polarization ratio [Fig. 6(C,D)]. We measured the relative distance between the geometric center of the apical surface and the BB cluster centroid (Boutin et al., 2014). We observed significant differences between WT ECs, with a mean polarization ratio of $77.72 \pm 19.77$, and p73KO cells with a ratio of $25.99 \pm 12.13$ [Fig. 6(D)], indicating that p73 is essential to organize translational polarity at single cell level. Furthermore, we asked whether p73 deficiency affected the coordination of BB patches displacement at tissue level by drawing a vector from the cell center to the cluster centroid (Boutin et al., 2014). Vectors of neighbor WT ECs had similar direction, but in p73KO ECs they were more divergent [Fig. 6(C), white lines]. Calculation of the angle of displacement [Fig. 6(E)] indicated that the angular deviation of individual vectors from the mean was $\pm 35.76°$ in the WT while the p73 deficient cells displayed a significantly higher deviation, with a mean of $\pm 57.83°$ (Watson's U2 test $p < 0.005$). Altogether, our data strongly support the hypothesis that p73 is essential to translational PCP.

## DISCUSSION

The appropriate functioning of ependymal cells is fundamental to create and maintain the neurogenic

**Figure 6** Lack of p73 impairs translational planar cell polarity in ependymal cells. Confocal Z-stacks images of lateral ventricle wall wholemounts from the indicated age and phenotype immunostained for $\beta$-catenin (green, A, B or blue, C) and $\gamma$-tubulin (red). (A) P15-WT ECs, but not the p73KO, were organized in pinwheel structures (yellow lines) and displayed translational PCP with cilia patches clustered on the "downstream" side of the apical cell surfaces, and oriented with respect to the direction of CSF flow (white arrows). (B) p73KO multiciliated ECs had the basal bodies distributed throughout the apical surface (white arrows) and showed different cilia clusters distribution: e.g. BB patches compacted very tightly (yellow arrows) or multiple clusters (white lines). (C) Trace of the cell contour (green) and magnifications of the white line inserts (right panels). Lines from the cell center to the BB centroid show BB cluster's angle displacement. Scale bar: 20 $\mu$m. (D) Quantification of BB polarization (the relative distance between the geometric center of the apical surface and the BB cluster centroid) (E) Angular distribution of vectors of BB displacement around the mean. In WT, the majority of vectors were closely distributed showing the coordination of BB displacement among neighbor cells. In the absence of p73, this coordination is lost, leading to a broader distribution. [Color figure can be viewed in the online issue, which is available at wileyonlinelibrary.com.]

milieu of the germinal niche in the SVZ of rodent brain (Lledo et al., 2008). In this regard, since p73 is expressed in the ependymal cells (Hernandez-Acosta et al., 2011; Medina-Bolivar et al., 2014), we hypothesized that p73 had a possible role in EC biology. In agreement with our hypothesis, ependymal cell denudation in p73 deficient mice has recently been described (Medina-Bolivar et al 2014), although the nature of the ECs defects have not been described.

Our results indicated that p73 ablation did not result in less S100$\beta^+$ cells, but rather in ECs immaturity with the consequent cellular disorganization in the VZ and loss of brain ventricular integrity. One of the hallmarks of the p73 deficient brain is the presence of immature ECs that express GFAP and had the basal bodies clustered in deuterosomes. These immature ECs fail to organize into neurogenic pinwheels, disrupting p73KO-SVZ cytoarchitecture and thus, niche structure and function (Kokovay et al., 2012). These features are maintained in the adult p73KO VZ, suggesting that the EC maturation was halted and confirming that p73 deficiency results in a deregulation of the transition process from RGC to ependymal and B-cells, leading to the emergence of aberrant cells with abnormal intermediate identities within the lateral wall of the ventricle. p73 deficient ependymal cells had an aberrant membrane morphology with pleats and invaginations that could be the cause of their failure in establishing appropriate cell to cell adhesions. This p73KO phenotype was also detected in the absence of p53 (DKO mice), suggesting that p73-deficient effect is not due to an enhanced cell death resultant from p53 compensatory activation in the absence of the anti-apoptotic DNp73. Indeed, the ependymal layer in the absence of p73, including in DKO, is pseudostratified and discontinuous indicating p73 requirement for brain ventricular integrity. In this regard, studies have demonstrated that ependymal cell–cell adhesion regulates NSC activation under physiological and regenerative conditions (Porlan et al., 2014). Thus, lack of cellular contacts in the p73KO SVZ could lead to activation and subsequent depletion of the normally quiescent NSCs.

In P15 p73KO mice we detect monociliated cells (accounted by BB staining) that cannot be identified as bona fide B1-cells (neural stem cells). These cells resemble the monociliated-small apical surface radial glial cells observed in WT brains at early immature stages (P7) that did not yet display GFAP expression. It is possible that in the absence of p73, only few RGC are capable to progress into functional neural stem cells (GFAP expressing B1-cells), leading to a diminished neural stem cell population in the SVZ. This lack of an appropriate pool of neural stem cells could be the underlying mechanism of the impaired neurogenic capacity in p73KO mice brain. This suggests that p73 is not only essential for neural stem cell maintenance (Agostini et al., 2010; Fujitani et al., 2010; Gonzalez-Cano et al., 2010; Talos et al., 2010), but also for the *de novo* generation of neural stem cells during the postnatal generation of the neurogenic niche in mice SVZ. In agreement with impaired neurogenic function, p73KO lateral wall had a less dense network of supra-ependymal axons, known to directly interact with NSCs to regulate neurogenesis (Tong et al., 2014). These axons normally encircle the base of ependymal cilia tufts; therefore, their reduction could be secondary to abnormal cilia generation and growth. It has been proposed that glutamate provided by these axons may supplement metabolic pathways in multiciliated ECs in order to fuel the energy demand of the ciliary beating (Robinson et al., 1996). Consistent with p73 requirement for the maintenance of the neurogenic niche function, our analysis revealed that p73KO mice had significantly less proliferating neuroblasts and B cells than WT mice. This effect it not due to p53-induced cell death since DKO mice also showed a significant reduction in these cellular populations in the SVZ. These results support an impairment of neurogenesis and probably a decrease in the number of new neurons that migrate to the OB. Thus, p73 deficiency has a profound effect on SVZ maintenance and neurogenesis.

The most striking alteration of the p73KO brain is the profound defects in ECs planar cell polarity. Our data strongly suggest that p73 is necessary for the primary cilia organization in RGCs, which orchestrates the planar polarized architecture of both radial glia and their progeny ependymal cells (Mirzadeh et al., 2010), and also for the establishment of ependymal tPCP. Moreover, in the absence of p73 many ECs had basal body clusters but lacked cilia, or the number of total cilia tufts was lower, indicating that p73 deficiency alters or delays ciliogenesis.

We demonstrate that p73 function is necessary to organize the basal bodies within individual cells and, even though it is not required for basal body cluster displacement from the center, it is essential for intercellular patch orientation, since the p73KO cells did not have a common direction of displacement. Lack of basal body cluster orientation in p73KO ECs was independent of the presence of cilia tufts, suggesting that p73 effect on PCP is upstream of ciliogenesis. This is in agreement with reported observations that support the notion that PCP signaling influences cilium, while definitive evidence for regulation of PCP signaling by cilium is still missing (Gray et al., 2011). Many PCP

core regulator genes like *Cadherin EGF LAG Seven-Pass G-Type 1-3 (Celsr 1-3), Frizzled Class Receptor 3 (Fzd3), Van Gogh like1-2 (Vangl1-2)* and *Dishevelled1-3 (Dvl1-3*) or *Non-Muscle Myosin* II (*NMII*) have also been implicated in cilia development and function (Ibañez-Tallon, et al. 2004; Lechtreck et al., 2008; Guirao et al., 2010; Hirota et al., 2010; Ohata et al., 2014). However, the mechanism of p73 regulation of PCP remains elusive.

Our results show that lack of p73 results in profound defects in the timing of ependymal cell maturation, and in the establishment of planar cell polarity, altogether affecting the correct assembly of the neurogenic cytoarchitecture of the SVZ germinal center. These alterations could be the subjacent mechanisms that lead to the hydrocephalus and defective neurogenic capacity of the p73 deficient mice, highlighting the important role of p73 in brain development and brain homeostasis.

## ACKNOWLEDGMENTS

The authors thank Dr. Luis Fernando de la Fuente Crespo (Departamento de Produccion Animal, Universidad de Leon) for the advice with the statistical analysis.

## REFERENCES

Agostini M, Tucci P, Chen H, Knight RA, Bano D, Nicotera P, McKeon F, et al. 2010. P73 regulates maintenance of neural stem cell. Biochem Biophys Res Commun 403:13–17.

Andreu-Agullo C, Morante-Redolat JM, Delgado AC, Farinas I. 2009. Vascular niche factor PEDF modulates notch-dependent stemness in the adult subependymal zone. Nat Neurosci 12:1514–1523.

Badano JL, Mitsuma N, Beales PL, Katsanis N. 2006. The ciliopathies: an emerging class of human genetic disorders. Annu Rev Genomics Hum Genet 7:125–148.

Bayly R, Axelrod JD. 2011. Pointing in the right direction: New developments in the field of planar cell polarity. Nat Rev Genet 12:385–391.

Boutin C, Labedan P, Dimidschstein J, Richard F, Cremer H, Andre P, Yang Y, Montcouquiol M, Goffinet AM, Tissir F. 2014. A dual role for planar cell polarity genes in ciliated cells. Proc Natl Acad Sci U S A 111:E3129–E3138.

Chmielnicki E, Benraiss A, Economides AN, Goldman SA. 2004. Adenovirally expressed noggin and brain-derived neurotrophic factor cooperate to induce new medium spiny neurons from resident progenitor cells in the adult striatal ventricular zone. J Neurosci 24:2133–2142.

Donehower LA, Harvey M, Slagle BL, McArthur MJ, Montgomery CA Jr, Butel JS Bradley A. 1992. Mice deficient for p53 are developmentally normal but susceptible to spontaneous tumours. Nature 356:215–221.

Ferrón SR, Marqués-Torrejón MA, Mira H, Flores I, Taylor K, Blasco MA, Fariñas I. 2009. Telomere shortening in neural stem cells disrupts neuronal differentiation and neuritogenesis. J Neurosci 29(46):14394–14407.

Flores ER, Sengupta S, Miller JB, Newman JJ, Bronson R, Crowley D, Yang A, et al. 2005. Tumor predisposition in mice mutant for p63 and p73: Evidence for broader tumor suppressor functions for the p53 family. Cancer Cell 7: 363–373.

Fujitani M, Cancino GI, Dugani CB, Weaver IC, Gauthier-Fisher A, Paquin A, Mak TW, et al. 2010. TAp73 acts via the bHLH Hey2 to promote long-term maintenance of neural precursors. Curr Biol 20:2058–2065.

Gonzalez-Cano L, Herreros-Villanueva M, Fernandez-Alonso R, Ayuso-Sacido A, Meyer G, Garcia-Verdugo JM, Silva A, et al. 2010. P73 deficiency results in impaired self renewal and premature neuronal differentiation of mouse neural progenitors independently of P53. Cell Death Dis 1:e109.

Gonzalez-Cano L, Hillje AL, Fuertes-Alvarez S, Marques MM, Blanch A, Ian RW, Irwin MS, et al. 2013. Regulatory feedback loop between TP73 and TRIM32. Cell Death Dis 4:e704.

Gray RS, Roszko I, Solnica-Krezel L. 2011. Planar cell polarity: Coordinating morphogenetic cell behaviors with embryonic polarity. Dev Cell 21:120–133.

Guirao B, Meunier A, Mortaud S, Aguilar A, Corsi JM, Strehl L, Hirota Y, et al. 2010. Coupling between hydrodynamic forces and planar cell polarity orients mammalian motile cilia. Nat Cell Biol 12:341–350.

Hernandez-Acosta NC, Cabrera-Socorro A, Morlans MP, Delgado FJ, Suarez-Sola ML, Sottocornola R, Lu X, Gonzalez-Gomez M, Meyer G. 2011. Dynamic expression of the p53 family members p63 and p73 in the mouse and human telencephalon during development and in adulthood. Brain Res 1372:29–40.

Hirota Y, Meunier A, Huang S, Shimozawa T, Yamada O, Kida YS, Inoue M, et al. 2010. Planar polarity of multiciliated ependymal cells involves the anterior migration of basal bodies regulated by non-muscle myosin II. Development 137:3037–3046.

Ihrie RA, Alvarez-Buylla A. 2011. Lake-front property: a unique germinal niche by the lateral ventricles of the adult brain. Neuron 70:674–686.

Jimenez AJ, Domínguez-Pinos MD, Guerra MM, Fernández-Llebrez P, Pérez-Fígares JM. 2014. Structure and function of the ependymal barrier and diseases associated with ependyma disruption. Tissue Barriers 2:e28426.

Killick R, Niklison-Chirou M, Tomasini R, Bano D, Rufini A, Grespi F, Velletri T, et al. 2011. P73: A multifunctional protein in neurobiology. Mol Neurobiol 43:139–146.

Kishimoto N, Sawamoto K. 2012. Planar polarity of ependymal cilia. Differentiation 83:S86–S90.

Kokovay E, Wang Y, Kusek G, Wurster R, Lederman P, Lowry N, Shen Q, et al. 2012. VCAM1 is essential to maintain the structure of the SVZ niche and acts as an environmental sensor to regulate SVZ lineage progression. Cell Stem Cell 11:220–230.

Kuo CT, Mirzadeh Z, Soriano-Navarro M, Rasin M, Wang D, Shen J, Sestan N, et al. 2006. Postnatal deletion of Numb/Numblike reveals repair and remodeling capacity in the subventricular neurogenic niche. Cell 127:1253–1264.

Lavado A, Oliver G. 2011. Six3 is required for ependymal cell maturation. Development 138:5291–5300.

Lechtreck KF, Delmotte P, Robinson ML, Sanderson MJ, Witman GB. 2008. Mutations in hydin impair ciliary motility in mice. J Cell Biol 180:633–643.

Lee AF, Ho DK, Zanassi P, Walsh GS, Kaplan DR, Miller FD. 2004. Evidence that DeltaNp73 promotes neuronal survival by p53-dependent and p53-independent mechanisms. J Neurosci 24:9174–9184.

Lim DA, Tramontin AD, Trevejo JM, Herrera DG, Garcia-Verdugo JM, Alvarez-Buylla A. 2000. Noggin antagonizes BMP signaling to create a niche for adult neurogenesis. Neuron 28:713–726.

Lledo PM, Merkle FT, Alvarez-Buylla A. 2008. Origin and function of olfactory bulb interneuron diversity. Trends Neurosci 31:392–400.

Luo J, Shook BA, Daniels SB, Conover JC. 2008. Subventricular zone-mediated ependyma repair in the adult mammalian brain. J Neurosci 28:3804–3813.

Medina-Bolivar C, Gonzalez-Arnay E, Talos F, Gonzalez-Gomez M, Moll UM, Meyer G. 2014. Cortical hypoplasia and ventriculomegaly of p73-deficient mice: Developmental and adult analysis. J Comp Neurol 522:2663–2679.

Merkle FT, Tramontin AD, Garcia-Verdugo JM, Alvarez-Buylla A. 2004. Radial glia give rise to adult neural stem cells in the subventricular zone. Proc Natl Acad Sci USA 101:17528–17532.

Miller FD, Gauthier-Fisher A. 2009. Home at last: Neural stem cell niches defined. Cell Stem Cell 4:507–510.

Mirzadeh Z, Han YG, Soriano-Navarro M, Garcia-Verdugo JM, Alvarez-Buylla A. 2010. Cilia organize ependymal planar polarity. J Neurosci 30:2600–2610.

Mirzadeh Z, Merkle FT, Soriano-Navarro M, Garcia-Verdugo JM, Alvarez-Buylla A. 2008. Neural stem cells confer unique pinwheel architecture to the ventricular surface in neurogenic regions of the adult brain. Cell Stem Cell 3:265–278.

Ohata S, Nakatani J, Herranz-Perez V, Cheng J, Belinson H, Inubushi T, Snider WD, et al. 2014. Loss of dishevelleds disrupts planar polarity in ependymal motile cilia and results in hydrocephalus. Neuron 83:558–571.

Paez-Gonzalez P, Abdi K, Luciano D, Liu Y, Soriano-Navarro M, Rawlins E, Bennett V, Garcia-Verdugo JM, Kuo CT. 2011. Ank3-dependent SVZ niche assembly is required for the continued production of new neurons. Neuron 71:61–75.

Pastrana E, Cheng LC, Doetsch F. 2009. Simultaneous prospective purification of adult subventricular zone neural stem cells and their progeny. Proc Natl Acad Sci U S A 106:6387–6392.

Porlan E, Marti-Prado B, Morante-Redolat JM, Consiglio A, Delgado AC, Kypta R, Lopez-Otin C, et al. 2014. MT5-MMP regulates adult neural stem cell functional quiescence through the cleavage of N-cadherin. Nat Cell Biol 16:629–638.

Pozniak CD, Barnabe-Heider F, Rymar VV, Lee AF, Sadikot AF, Miller FD. 2002. p73 is required for survival and maintenance of CNS neurons. J Neurosci 22:9800–9809.

Ramirez-Castillejo C, Sanchez-Sanchez F, Andreu-Agullo C, Ferron SR, Aroca-Aguilar JD, Sanchez P, Mira H, et al. 2006. Pigment epithelium-derived factor is a niche signal for neural stem cell renewal. Nat Neurosci 9:331–339.

Raponi E, Agenes F, Delphin C, Assard N, Baudier J, Legraverend C, Deloulme JC. 2007. S100B expression defines a state in which GFAP-expressing cells lose their neural stem cell potential and acquire a more mature developmental stage. Glia 55:165–177.

Roales-Buján R, Páez P, Guerra M, Rodríguez S, Vío K, Ho-Plagaro A, García-Bonilla M, et al. 2012. Astrocytes acquire morphological and functional characteristics of ependymal cells following disruption of ependyma in hydrocephalus. Acta Neuropathol 124:531–546.

Robinson SR, Noone DF, O'Dowd BS. 1996. Ependymocytes and supra-ependymal axons in rat brain contain glutamate. Glia 17:345–348.

Spassky N, Merkle FT, Flames N, Tramontin AD, Garcia-Verdugo JM, Alvarez-Buylla A. 2005. Adult ependymal cells are postmitotic and are derived from radial glial cells during embryogenesis. J Neurosci 25:10–18.

Talos F, Abraham A, Vaseva AV, Holembowski L, Tsirka SE, Scheel A, Bode D, et al. 2010. p73 is an essential regulator of neural stem cell maintenance in embryonal and adult CNS neurogenesis. Cell Death Differ 17:1816–1829.

Tissir F, Qu Y, Montcouquiol M, Zhou L, Komatsu K, Shi D, Fujimori T, et al. 2010. Lack of cadherins Celsr2 and Celsr3 impairs epen6dymal ciliogenesis, leading to fatal hydrocephalus. Nat Neurosci 13:700–707.

Tong CK, Chen J, Cebrian-Silla A, Mirzadeh Z, Obernier K, Guinto CD, Tecott LH, et al. 2014. Axonal control of the adult neural stem cell niche. Cell Stem Cell 14:500–511.

Yang A, Walker N, Bronson R, Kaghad M, Oosterwegel M, Bonnin J, Vagner C, et al. 2000. P73-deficient mice have neurological, pheromonal and inflammatory defects but lack spontaneous tumours. Nature 404:99–103.

Redox Biology 13 (2017) 82–93

Contents lists available at ScienceDirect

Redox Biology

journal homepage: www.elsevier.com/locate/redox

Research Paper

# Decreased neural precursor cell pool in NADPH oxidase 2-deficiency: From mouse brain to neural differentiation of patient derived iPSC

Zeynab Nayernia[a], Marilena Colaianna[a], Natalia Robledinos-Antón[e], Eveline Gutzwiller[a], Frédérique Sloan-Béna[f], Elisavet Stathaki[f], Yousef Hibaoui[b], Antonio Cuadrado[e], Jürgen Hescheler[c], Marie-José Stasia[d], Tomo Saric[c], Vincent Jaquet[a], Karl-Heinz Krause[a,*]

[a] Department of Pathology and Immunology, University of Geneva Medical School, 1-rue Michel Servet, 1211 Geneva, Switzerland
[b] Department of Genetic Medicine and Development, University of Geneva Medical School, 1 rue Michel Servet, 1211 Geneva, Switzerland
[c] Center for Physiology and Pathophysiology, Institute for Neurophysiology, Medical Faculty, University of Cologne, Cologne 50931, Germany
[d] Université Grenoble Alpes, Techniques de l'Ingénierie Médicale et de la Complexité- Grenoble, F38000 Grenoble, France
[e] Instituto de Investigaciones Biomédicas "Alberto Sols", Faculty of Medicine, Autonomous University of Madrid (UAM), Centro de Investigación Biomédica en Red sobre Enfermedades Neurodegenerativas (CIBERNED), Madrid, Spain
[f] Hôpitaux Universitaires de Genève HUG, Laboratoires de Cytogénétique Constitutionnelle, Service de Médecine Génétique, Geneva, Switzerland

ARTICLE INFO

*Key words:*
NOX2
Reactive oxygen species
Adult neurogenesis
in vitro neural differentiation
Neural stem/progenitor cells
Induced pluripotent stem cells (iPSC)

ABSTRACT

There is emerging evidence for the involvement of reactive oxygen species (ROS) in the regulation of stem cells and cellular differentiation. Absence of the ROS-generating NADPH oxidase NOX2 in chronic granulomatous disease (CGD) patients, predominantly manifests as immune deficiency, but has also been associated with decreased cognition. Here, we investigate the role of NOX enzymes in neuronal homeostasis in adult mouse brain and in neural cells derived from human induced pluripotent stem cells (iPSC). High levels of NOX2 were found in mouse adult neurogenic regions. In NOX2-deficient mice, neurogenic regions showed diminished redox modifications, as well as decrease in neuroprecursor numbers and in expression of genes involved in neural differentiation including *NES*, *BDNF* and *OTX2*. iPSC from healthy subjects and patients with CGD were used to study the role of NOX2 in human in vitro neuronal development. Expression of NOX2 was low in undifferentiated iPSC, upregulated upon neural induction, and disappeared during neuronal differentiation. In human neurospheres, NOX2 protein and ROS generation were polarized within the inner cell layer of rosette structures. NOX2 deficiency in CGD-iPSCs resulted in an abnormal neural induction in vitro, as revealed by a reduced expression of neuroprogenitor markers (*NES*, *BDNF*, *OTX2*, *NRSF/REST*), and a decreased generation of mature neurons. Vector-mediated NOX2 expression in NOX2-deficient iPSCs rescued neurogenesis. Taken together, our study provides novel evidence for a regulatory role of NOX2 during early stages of neurogenesis in mouse and human.

## 1. Introduction

There is increasing evidence for the role of reactive oxygen species (ROS) in developmental processes, such as cardiomyogenesis [33,7,8], hematopoiesis [48,49], and neurogenesis [14,30,42,54,59,66,67]. This role of ROS might at least in part be due to a regulatory role in stem cell homeostasis and differentiation. Several redox-sensitive signaling pathways have been described, including $H_2O_2$-dependent protein phosphatase inhibition, as well as redox-regulation of transcription factors and ion channels [19].

There is a wide range of possible cellular sources of ROS, including mitochondria, xanthine oxidase, lipoxygenase, cyclooxygenases, cytochrome P450, nitric oxide synthase and peroxisomes [23]. In addition to these systems that produce ROS as a side reaction, there is the NOX family of NADPH oxidases (NOXs), for which production of ROS is the main biological function [3,32]. Enzymes of the NOX family include the phagocyte NAPDH oxidase NOX2, as well as more recently discovered isoforms (NOX1, NOX3-5, and DUOX1-2). NOXs are highly regulated enzymes, with some of the isoforms (NOX1-NOX4) functioning in a subunit-dependent manner. For example, NOX2 functions as a complex containing at least five subunits ($p22^{phox}$, $p47^{phox}$, $p67^{phox}$ and $p40^{phox}$, and small Rac GTPases) [29]. Loss of function mutations in any of the constituents of the NOX2 complex leads to the genetic disorder chronic granulomatous disease (CGD). CGD patients predominantly show an

* Correspondence to: Dept. of Pathology and Immunology, Centre Médical Universitaire, 1, rue Michel-Servet, CH-1211 Geneva 4, Switzerland.
*E-mail address:* Karl-Heinz.Krause@unige.ch (K.-H. Krause).

http://dx.doi.org/10.1016/j.redox.2017.04.026
Received 8 February 2017; Received in revised form 19 April 2017; Accepted 20 April 2017
Available online 24 April 2017

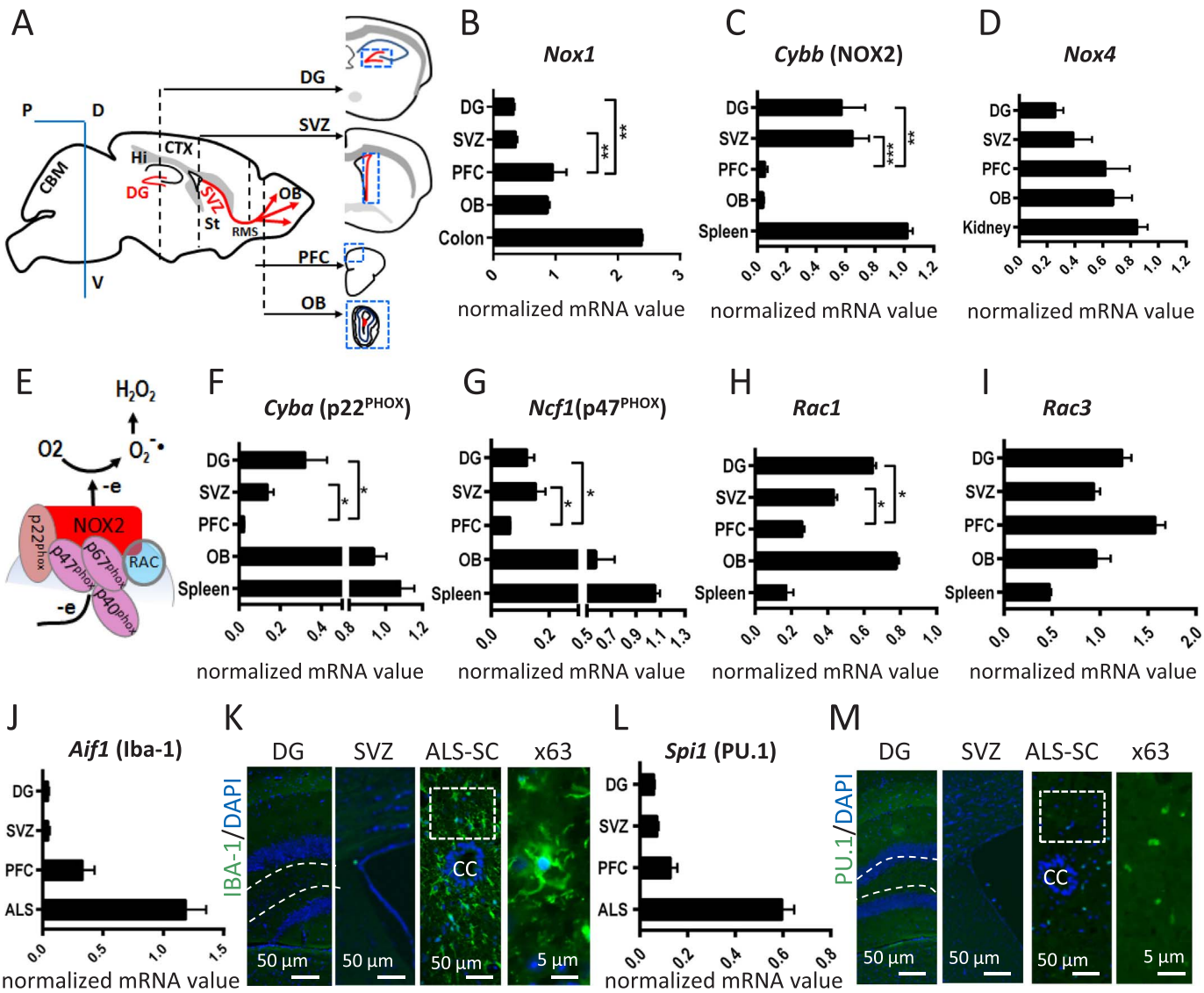


**Fig. 1.** NOX2 and subunits, but not microglia markers, are expressed in neurogenic regions of the mouse brain. (A) Schematic representation of micro-dissected adult mouse brain areas (dashed blue lines) including the neurogenic regions dentate gyrus (DG) and subventricular zone (SVZ) and the non-neurogenic regions olfactory bulb (OB) and prefrontal cortex (PFC). CBM: cerebellum, Hi: hippocampus, St: striatum, RMS: rostral migratory stream. (B-D, F-I) mRNA expression of NOX isoforms and NOX subunits in micro-dissected brain regions. The following murine tissues were used as positive control; colon (*Nox1*), spleen (*Nox2*), and kidney (*Nox4*). (E) Schematic representation of the *Nox2* complex including its subunits *Cyba* ($p22^{phox}$), *Ncf1* ($p47^{phox}$), *Ncf2* ($p67^{phox}$), *Ncf4* ($p40^{phox}$) and *Rac*. (J, L): expression of microglia markers *Aif-1* (IBA-1) and *Spi-1* (PU.1), in different brain regions as assessed by RT-qPCR (J, L) or by immunofluorescence (K, M). ALS = spinal cord of mice overexpressing $SOD1^{G93A}$ mutant (a model for amyotrophic lateral sclerosis, ALS) served as a positive control for high levels of microglial gene expression [51]. For RT-qPCR, expression values were normalized to housekeeping genes and data are shown as mean ± SEM. Statistics were done by Student's *t*-test from $n = 6$. $^{*}P < 0.05$, $^{**}P < 0.01$, $^{***} < 0.001$.

immunological phenotype, including susceptibility to infection, hyper inflammation and autoimmunity [55]. However, there is also evidence for a role of NOX2 in the physiological function of the central nervous system (CNS): NOX2-deficient mice [26] and CGD patients [45] have a discreet, but consistently observed cognitive impairment. Thus, the question to which extent NOX2 plays a role in the physiological function of the CNS is pertinent.

Basically there are two main concepts to explain how ROS might be involved in the physiological function of the CNS: modulation of the function of mature neurons [12,24,25,27,31,43,4,52,58,61] versus impact on neural development and neurogenesis [14,30,31,59]. These two concepts are not mutually exclusive and the nature of ROS regulation might depend on the brain area and neural cell types. For instance, RNAseq studies in the murine cerebral cortex demonstrate that under physiological conditions, NOX2 is mostly expressed in microglia, while NOX4 is mostly found in endothelial cells [68]. However, several recent publications suggest that NOX2 is highly expressed in neural progenitor cells (NPCs) in murine adult neurogenic regions: the subventricular zone (SVZ) of the lateral ventricle and the dentate gyrus (DG) of the mouse hippocampus [30,60,67]. These regions contain adult neural stem cells (NSCs) and differentiate into neural progenitors which migrate, mature and are finally integrated into various brain regions. Adult neurogenesis is not only involved in brain repair, but regulates several physiological functions, in particular memory [13].

A recent review on the role of redox environment in neurogenic development [44] summarized the present knowledge as follows. The cellular redox state during neurogenesis and neural differentiation controls specific mechanism of lineage progression through control of signal transduction and transcriptional regulation. More specifically, redox-dependent mechanisms regulate NSC proliferation, cell cycle exit, and differentiation into mature neurons and glia. Oxidizing species accumulate during early stages of differentiation, while a reductive environment persists during terminally differentiated neural cells. The

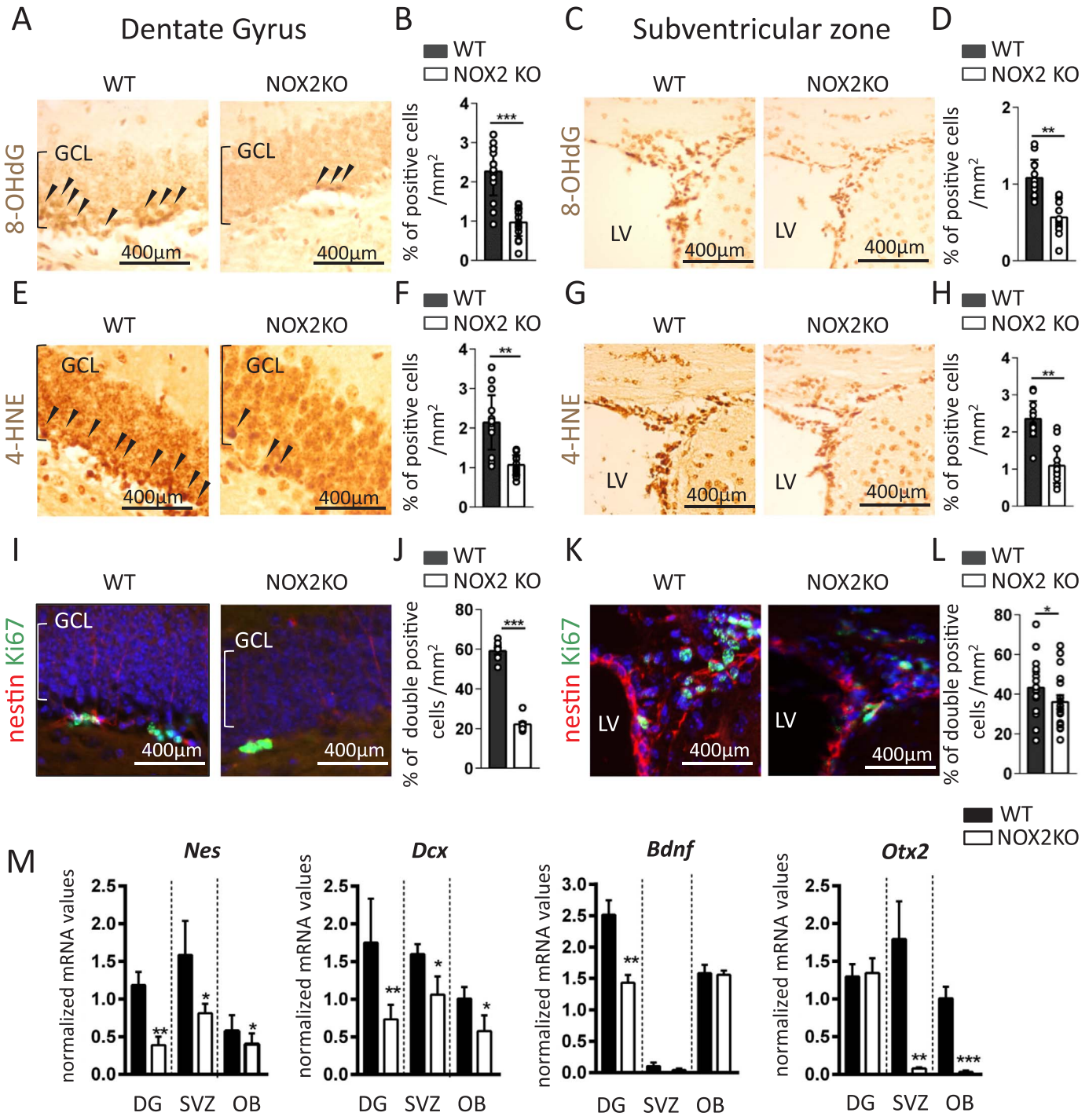


**Fig. 2.** Decreased oxidative modifications and proliferating neuroprecursor cells in neurogenic brain regions of NOX2-deficient mice. Oxidative modifications of DNA (8-hydroxydeoxyguanosine, 8-OHdG in Figure A, C) and lipids (4-hydroxynonenal; 4-HNE in Figure E, G) were detected using DAB immunohistochemistry in sections of the neurogenic mouse brain regions. The SVZ and DG from wild type (WT) and NOX2-knock-out mice were analyzed. Arrows in panel A and E indicate intensely stained cells in the subgranular zone (SGZ) of the dentate gyrus. (B, D, F and H) Quantification of 8-OHdG and 4-HNE DAB staining are shown as bar graphs as % of positive cells per analyzed area as analyzed by Metamorph software (see Material and Methods). Immunofluorescence staining of proliferating progenitor cells in DG (I) and SVZ (K) of wild type and NOX2 KO mice. IF markers: Nestin (red); Ki67 (green); DAPI (blue). Quantification of immunofluorescence staining (% of double-positive cells/total cells) in the DG (J) and SVZ (L). Data are shown as mean ± SEM. Statistics were performed using Student's *t*-test from 8 animals per condition. (M) RT-qPCR analysis of *Nes* (nestin), neuroblast marker *Dcx* (doublecortin), *Bdnf* (brain derived neurotrophic factor) and *Otx2* transcription factor in neural stem/progenitor cells of DG and SVZ. Data are shown as mean ± SEM. Statistics done by Student's *t*-test from n =7. *P < 0.05, **P < 0.01, *** < 0.001.

generation of certain neurotrophic growth factors also appears to be under redox control [47]. For example, there is a redox-regulation of brain-derived neurotrophic factor BDNF [39,53], which contributes to the self-renewal and survival of neural stem/progenitor cells during neurogenesis, influencing memory and cognition [46,5,64]. These findings on the role of redox-dependent processes in neurogenesis raise the question whether NOX enzymes play a role during early stages of neural differentiation.

While hitherto the study of neurodevelopmental processes was mostly restricted to animal models, the availability of human pluripotent stem cells provides now powerful tools to study the mechanisms underlying cellular decisions during neural differentiation in a human

system [15,56]. And, while there are many fundamental developmental mechanisms shared between mice and humans, there are also considerable differences. For example, preclinical mouse studies did not predict the teratogenicity of thalidomide while transcriptomic and proteomic investigation of the compound using human embryonic stem cells (hESCs) clearly indicated that thalidomide impacts several key developmental human genes at clinically relevant concentrations [40]. This could be due to differences in the metabolism of the compounds.

In this study we have investigated the role of NOX2 during neurogenesis in mice and in human induced pluripotent stem cells (hiPSCs). For this purpose, we investigated brains from NOX2-deficient mice, as well as in NPCs and neurons differentiated from iPSCs derived from NOX2-deficient and $p22^{phox}$-deficient CGD patients. We show that NOX2 is highly expressed in neurogenic regions of the mouse brain, as well as in NPCs derived from hiPSCs. NOX2 deficiency or inhibition decreases oxidative modifications in neural stem/precursor cells, reduces the size of the neuroprogenitor pool, and impacts down-stream neural differentiation. Correction of NOX2 expression in CGD-hiPSCs was associated with the restoration of the expression to near normal levels of crucial genes involved in neurogenesis. Our results provide further evidence for a role of NOX2 in neurogenesis, unrelated to the well-known function of the enzyme in inflammation and host defense.

## 2. Results

### 2.1. NOX expression and activity in neurogenic regions of the adult mouse brain

To examine the expression and function of NOX enzymes and their subunits in neurogenic regions [1], we first investigated the subventricular zone (SVZ) and the dentate gyrus (DG) isolated from adult mouse brain (see Material and methods). In the SVZ, proliferating NPCs are lining the lateral ventricles from where they migrate towards the olfactory bulb and differentiate into granular interneuron cells [35,36,38]. In the DG of the hippocampus, the sub-granular zone (SGZ) contains precursor cells, which proliferate and migrate along the granular cell layer to differentiate into hippocampal granule cells [9,2,28] (Fig. 1A).

We studied the expression of the different NOX isoforms in microdissected neurogenic regions (see *Methods*) (Fig. 1B-D and Fig. S1D and S1E). NOX1 and NOX4 expression was relatively low in neurogenic brain regions, but showed higher levels in the prefrontal cortex (PFC) and the olfactory bulb (OB). No relevant expression in neurogenic regions was observed for *Nox3* and the two *Duox* genes (Fig. S1D). In contrast, *Cybb* (NOX2) was markedly higher in both neurogenic regions as compared to PFC and OB (Fig. 1C). Similarly, *Cyba* ($p22^{phox}$) and *Ncf1* ($p47^{phox}$) as well as GTPase Rac1were significantly higher expressed in DG, SVZ and the olfactory bulb (Figs. 1F, 1G and 1H), while there was no distinct pattern for *Ncf4* ($p40^{phox}$) and *Ncf2* ($p67^{phox}$) or for other GTPase Rac isoforms including Rac2 and Rac3 (Figs. 1H and 1I, and Fig. S1E). Note that the NOX2 enrichment in the neurogenic regions is considerable as it approaches levels comparable to those observed in spleen.

The CNS phagocyte microglia is the most relevant NOX2 expressing cells in the brain and its presence might provide an explanation for the high NOX2 levels observed in neurogenic regions [50]. We therefore investigated microglia markers in the SVZ and the DG. The microglia marker *Aif1* (IBA-1) was expressed only at very low levels in neurogenic regions (Figs. 1J and 1K). Similarly, the transcription factor *Spi1* (PU.1) which is highly expressed in microglia and other types of phagocytes [3] was found at only very low levels in neurogenic regions (Figs. 1L and 1M).

To assess the relative contribution of NOX2-derived ROS in murine neurogenic areas, we investigated the levels and localization of oxidative modifications of DNA (8-OHdG; 8-hydroxyguanosine) and of lipids (4-HNE; 4-hydroxynonenal). Analysis of both markers revealed elevated staining localizing to cells within SVZ and DG (Fig. 2A-H). In the granular cell layer of the DG, the staining intensity of 8-OHdG was strongest in the lower layer, i.e. the SGZ, which is enriched in proliferating NPCs (Figs. 2A and 2B, arrow heads).

Staining for 8-OHdG and 4-HNE was markedly decreased in NOX2-deficient mice as compared to wild-type DG (Figs. 2A and 2E, left vs. right panels) and SVZ (Figs. 2C and 2G, left vs. right panels). Quantification of staining showed lower levels of 8-OHdG (Figs. 2B and 2D) and 4-HNE (Figs. 2F and 2H) in NOX2-deficient mice suggesting that NOX2 contributes to oxidative modifications in specific subsets of cells of SVZ and DG. Thus, a significant fraction of oxidative modifications in the neurogenic areas can most likely be attributed to NOX2-derived ROS. The residual oxidative modifications might be due to low levels of other NOX isoforms (see Fig. S1D) or to distinct cellular sources, such as mitochondria and xanthine oxidase.

In order to assess proliferation in NOX2 deficient mice, we analyzed the proportion of nestin and Ki-67 double positive cells in the DG (Figs. 2I and 2J) and the SVZ (Figs. 2K and 2L). As shown in Fig. 2I-L, the proportion of nestin-Ki67 positive cells is significantly lower in the DG and the SVZ from NOX2-deficient mice suggesting that NOX2 deficiency is associated with a reduced proliferation of NPCs in adult neurogenic regions.

We next analyzed mRNA levels of a panel of neuronal and neural stem/progenitor markers [41] using qPCR in the two neurogenic regions as well as in the OB, which is the projection zone of SVZ. These results showed a clear impact of NOX2-deficiency: mRNA levels for nestin (expressed in NSCs and NPCs), doublecortin (*Dcx*) (expressed in young migrating neurons), *BDNF* (a soluble factor regulating neurogenesis), *Otx2* (neurogenesis transcription factor), as well as *NeuN* (marker of mature neurons) were significantly decreased in NOX2-deficient regions (Fig. 2M and S1F)[34]. Note, however, that there were regional differences. While *Otx2* was massively decreased in the SVZ of NOX2-deficient mice, there was no impact on expression in the DG. Conversely, while there was a significant decrease of BDNF in the DG of NOX2-deficient mice, BDNF was below detection levels in the SVZ (as described previously [20] (Fig. 2M). No impact of NOX2 deficiency was observed on mRNA levels of the glutamatergic marker *mGluR*, as well as the GABAergic markers *Calb1* (*Calbindin)* and *Gad67* (Fig. 2G). Interestingly, in the OB global neuronal and NPC markers (*Nestin*, *Otx2*, *Dcx*, *NeuN*) were also decreased, despite the fact that NOX2 levels in this region are low (Fig. 2M and S1F). Taken together these results demonstrate a functional impact of NOX2 deficiency not only on neural stem/precursor cells as well but also on the olfactory bulb, a mature neural region.

### 2.2. Proliferation deficit of NPCs derived from the neurogenic niche of NOX2 deficient mice

To asses further whether NOX2 affects the stemness of NPCs, we isolated NPCs from the neurogenic niches of WT and NOX2-deficient pups (P0 to P4). Relatively high level expression of NOX2 was observed in the dissected regions (Fig. S2A) but, unlike the adult neurogenic niches, the microglia markers IBA-1 and PU.1 were present (Fig. S2B; note, however, that the microglia markers disappeared during neurosphere formation, Fig. S2C). The dissected tissues were dissociated into single cells and allowed to proliferate and form primary neurospheres [33] (Fig. 3A, B). A serial dilution assay [11] indicated a decrease in the number of formed neurospheres after 7 days at every dilution tested in the NOX2-deficient cultures, (Fig. 3C). To analyze the cellular composition of the neurospheres, we performed immunocytochemical staining for nestin. The number of nestin-positive cells was strikingly reduced in NOX2-deficient neurospheres (Fig. 3D, E), strengthening the idea of a decreased NSC pool in the absence of NOX2. The proliferation rate of NSCs was evaluated using EdU pulse labeling assay. A decrease in the percentage of EdU-positive cells in NOX2-deficient neurospheres was observed at 2, 4 and 8 h after incubation with EdU compared to WT

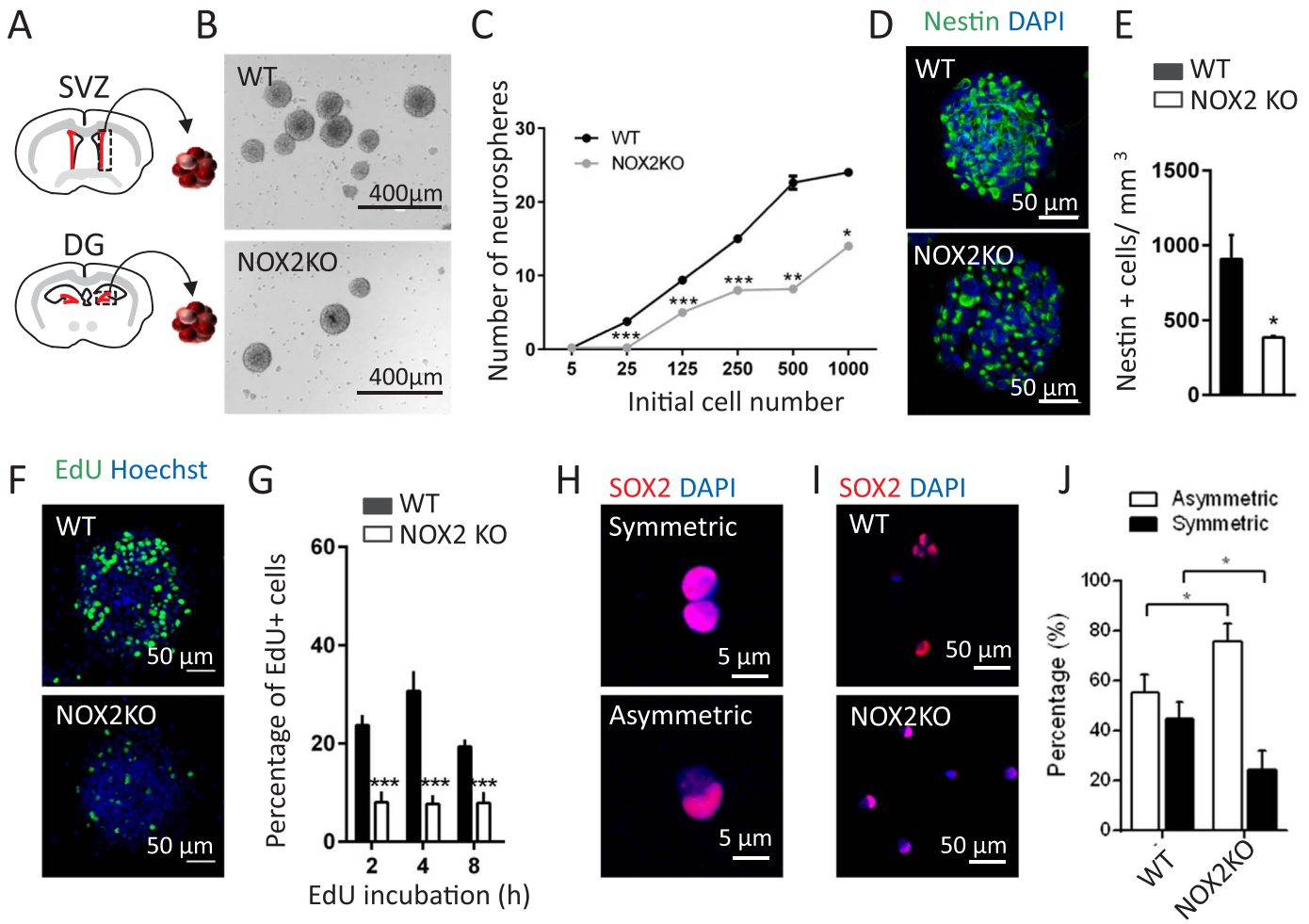


**Fig. 3.** Impaired proliferation and altered balance in symmetric/asymmetric divisions of NSCs from NOX2-deficient mice. (A) Schematic representation of generation of neurospheres from subventricular zone (SVZ) and dentate gyrus (DG). (B) Light microscope pictures of the neurospheres derived from the SVZ of WT and NOX2-deficient mice (NOX2-KO). (C) Dilution assay and quantification of neurosphere generation as a function of the initial number of seeded cells demonstrates decreased proliferation of NOX2-deficient neural stem/precursor cells. (D) Immunostaining of nestin within neurospheres. (E) Quantification of nestin-staining in neurospheres (n = 6) from D. (F) Representative image of EdU-labeled cells in neurospheres after 8 h of incubation from WT and NOX-deficient mice; (G) Quantification of EdU incorporation after incubation of neurospheres during 2, 4 and 8 h. (H) Cell pair assay with SOX2 staining allows visualizing symmetric and asymmetric division of the cells; (I) representative image of SOX2 staining of WT and NOX2-deficient neurospheres (J). Quantification of symmetric and asymmetric divisions in neurospheres from WT and NOX2-KO as percentage of dividing cells. Data were analyzed by Student's *t*-test and shown as mean values ± SEM.*P < 0.05, **P < 0.01, *** < 0.001.

neurospheres (Figs. 3F and 3G). The decreased number of proliferative cells could be caused by an imbalance in the symmetric/asymmetric divisions. An increase of asymmetric divisions would lead to a decrease in the pool of undifferentiated NSCs and to an increase in the number of differentiated cells. To analyze this, we performed the cell-pair assay, showing that asymmetric divisions (Fig. 3H-J) are more prominent in NOX2-deficient cultures suggesting that lack of NOX2 leads to a bias towards asymmetric cell divisions.

Taken together, these results suggest that NOX2 deficiency diminishes self-renewal of NPCs through symmetric divisions, affecting the maintenance of stem cells pool.

### 2.3. Immunolocalization of NOX2 in Macaca fascicularis brain

To our knowledge, there are no useful antibodies to perform immunohistochemistry of NOX2 in mouse tissues (available antibodies lack specificity and sensitivity). However, there are very good immunohistochemistry-compatible antibodies against human NOX2. In particular, there is the monoclonal 7D5 antibody, which has also been shown to specifically recognize NOX2 in other primates [65]. We therefore performed immunohistochemistry of the DG in the Macaca fascicularis (macaque) brain (Fig. S3). DCX immunostaining (young migrating neurons) showed a moderately intense, but clearly discernable staining in the DG, with a preferential staining of the SGZ (Fig. S3A). Immunostaining of NOX2 revealed a remarkably intense staining throughout the granular cell layer (GCL). A weaker staining of NOX2 could also be found in some adjacent areas. Although the exact nature of these NOX2-expressing cells is unknown, immunohistochemistry in the macaque brain confirms that the high expression of NOX2 in the DG is not limited to rodents, but is also observed in primates.

### 2.4. Role of NOX2 during neural differentiation of human iPSCs

To study the effect of NOX2 deficiency on human neurogenesis, we generated iPSCs from two different types of CGD patients, X-linked NOX2-deficient patient (X°-CGD) and an autosomal-recessive $p22^{phox}$-deficient patient (AR-22°-CGD) [6]. Two iPSC lines from healthy donors (control-iPSCs) and the human ESC line H1 (H1-hESCs) were used as control lines. As expected for cells that have acquired a pluripotent state, these iPSCs showed typical morphology of hPSC colonies, expressed markers of pluripotent cells and differentiated in vivo and in vitro into the lineages derived from three embryonic germ-layers mesoderm, ectoderm and endoderm (Fig. S4). We also confirmed that, like the parental fibroblasts, the X°-CGD-iPSCs harbored the nonsense

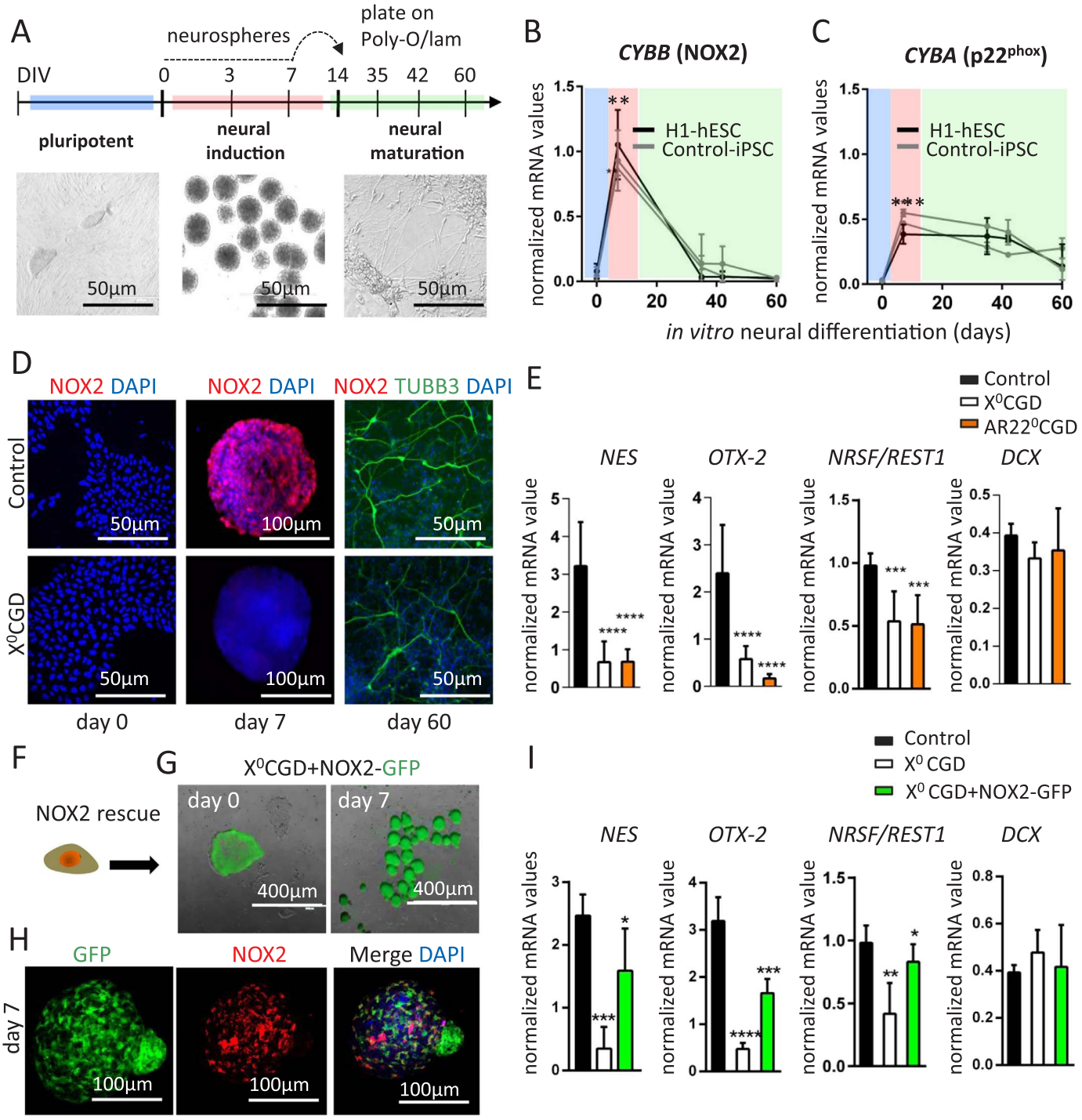


**Fig. 4.** NOX2 impacts early human neural differentiation **in vitro.** (A) Schematic representation of in vitro neural differentiation of human PSCs: undifferentiated pluripotent stage (blue), neural induction in neurosphere culture (pink) neural maturation on poly L-ornithine/laminin (green). DIV = days of in vitro. (B) Expression of *CYBB* (NOX2; B) and its subunit *CYBA* ($p22^{phox}$; C) was assessed in control hiPSCs (C3, C4 lines) and human ESC line H1 (H1-hESCs) at the undifferentiated pluripotent stage (blue bar: day 0), after neural induction (red bar: day 7) and during neuronal maturation (green bar: day 7–60). (D) Immunostaining demonstrates the absence of NOX2 protein in the pluripotent stage (day 0), the presence of NOX2 protein during the neural induction phase (day 7), and the absence of NOX2 protein in beta 3 tubulin-positive neurons (day 60). (E) Quantitative RT-PCR expression of a NPC marker nestin (*NES)*, transcription factors involved in neural fate and differentiation (*OTX2* and *NRSF/REST1)* and a gene involved in neurodevelopment (*DCX)* in neurospheres derived from control-iPSCs, X°-CGD-iPSCs and AR-22°-iPSCs (n = 8). (F) Schematic representation of NOX2 rescue in the X°-CGD-iPSC line using a lentiviral vector expressing *NOX2* and GFP. (G) High expression of GFP in pluripotent colonies (day 0) and in neurospheres (day 7) derived from X°-CGD + NOX2-GFP-iPSC lines. (H) In neurospheres derived from the X°-CGD + NOX2-GFP-iPSC line (day 7), the GFP fluorescence (green) and positive NOX2 immunostaining (red) are observed. (I) Expression of *NES*, *OTX2*, *NRSF/REST* and *DCX* in neurospheres derived from X°-CGD + NOX2-GFP-iPSCs. Data are shown as mean ± SEM, $n = 9$. Statistical analyses were done by one-way ANOVA followed by multiple comparisons Tukey's test. $^{*}P < 0.05$, $^{**}P < 0.01$, $^{***} < 0.001$, $^{****} < 0.0001$. (For interpretation of the references to color in this figure legend, the reader is referred to the web version of this article.)

mutation (**C**gA→**T**gA) at the position 469 of exon 5 of the *CYBB* (*NOX2)* gene leading to the absence of NOX2 mRNA and protein. The mutation was absent in the iPSC control lines and present in all the X°CGD-iPSC lines (Fig. S6A). Among the three CGD iPSC lines, one had large copy number variations detected by CGH array and was therefore excluded from further experiments (Fig. S5).

Based on the mouse data obtained in the first part of this study, we examined a possible role of NOX2 in neural differentiation of the

described iPSC lines, as well as the human embryonic pluripotent stem cell line H1-hESCs (for protocol see Fig. 4A). We first investigated the temporal expression pattern of *CYBB* (NOX2*)* and *CYBA* ($p22^{phox}$) by quantitative RT-PCR (qRT-PCR) upon neural induction and neuronal differentiation of control-iPSCs and H1-hESCs (Figs. 4B and 4C). As shown in Fig. 4B, *CYBB* and *CYBA* expression was very low in undifferentiated control-iPSCs and H1-hESCs. Upon neural induction into NPCs, the expression of both genes was strongly increased. In contrast to *CYBB* which expression returns to baseline levels in neurons (Fig. 4B), *CYBA* expression remains high (Fig. 4C). These results were also confirmed at the protein level showing (i) high expression of NOX2 in the NPCs and (ii) t absence of NOX2 protein in undifferentiated iPSC and in neurons. As expected, NOX2 protein was undetectable in X°-CGD-iPSC-derived NPCs (Fig. 4D).

### 2.5. Neurogenesis impairment in NPCs derived from X°-CGD-iPSCs and AR-22°-iPSCs

To investigate a possible functional impact of NOX2 deficiency on early stage of neural induction, we measured by q-RT-PCR the expression of neural progenitor markers in neurospheres derived from control-iPSCs, X°-CGD-iPSCs and AR-22°-iPSCs. Corroborating our observations in the mouse brain, NOX2 deficiency was associated with a 4-fold decrease of *NES* (Nestin) in NPCs (Fig. 4E). This was associated with a decrease of the expression of transcription factors involved in neural fate and differentiation such as *OTX2* and *NRSF/REST1* (Fig. 4E). However, no difference in the expression of *DCX* was found between NPCs derived from control-iPSCs, X°-CGD-iPSCs and AR-22°-iPSCs (Fig. 4E).

To provide additional support for NOX2 involvement in the defective neurogenesis of X°-CGD-iPSCs, we performed a rescue of NOX2 expression in X°-CGD-iPSCs providing an isogenic iPSC-based model. For this, X°-CGD-iPSCs were transduced with a lentiviral vector carrying human *CYBB (NOX2)* cDNA and GFP as selection marker (Fig. S6A). GFP-positive cells were selected by flow cytometry sorting and induced to differentiate into neurospheres (Fig. 4G). The obtained rescue line will be referred to as X°-CGD + hNOX2. At the undifferentiated pluripotent stage, X°-CGD + hNOX2 expressed mRNA for *CYBB* (*NOX2)* (Fig. S6B), but no NOX2 immunoreactivity was observed (not shown). This is possibly explained by the absence of $p22^{phox}$ in undifferentiated human PSCs (Fig. 4C), and the fact that NOX2 requires $p22^{phox}$ for protein stability. However, upon differentiation of PSCs towards neurospheres, $p22^{phox}$ expression increases (Fig. 4C), which stabilizes the NOX2 protein and hence allows its detection (Fig. 4D). Accordingly, a clear NOX2 staining could be observed in neurospheres derived from the X°-CGD + hNOX2-iPSCs (Fig. 4H). Importantly, NOX2 rescue in neurospheres derived from X°-CGD-C6 + hNOX2-iPSCs increased the expression of the neural markers *NES*, *OTX2*, and *NRSF/REST1* (Fig. 4I), indicative of an improved neurogenesis.

### 2.6. Localization and activity of NOX2 in neural rosettes derived from PSCs

In order to identify which type of cells are expressing NOX2 during neural induction, we used a co-immunostaining for NOX2 and the NPC marker nestin in neurospheres derived from control and X°-CGD-iPSCs [21]. Within neurospheres, we observed a clear population of cells with nuclei-rich regions positive for both nestin and NOX2 (Fig. 5A), with NOX2 staining occurring mostly in cell bodies, and nestin staining extending to neurites (Fig. 5A, right panel). As expected, NOX2 was not expressed in the X°-CGD neurospheres (Fig. 4A, lower panel, and Fig. 5B). Interestingly, the number of nestin and Ki67 double positive cells was lower in X°-CGD than in control neurospheres (Figs. 5C and 5D) while the fraction of young migratory -DCX-positive neurons was similar in both groups (Figs. 5E and 5F).

To further investigate cellular localization of NOX2, we generated neurospheres from H1-hESCs. Basically we observed two different types of rosettes in neurospheres derived from H1-hESCs: poly-rosette neurospheres (Fig. 5G) and mono-rosette neurospheres (Fig. 5I). NOX2 staining was observed in inner cell layers of these rosettes (Figs. 5H and 5J), which represent the in vitro analogue of the neural tube, where neurogenesis is initiated [10,16]. To verify whether NOX2 is functional, we used two different probes to detect ROS, namely CellROX and nitroblue tetrazolium (NBT). Fig. 5K shows an example of CellROX visualization in a poly-rosette neurosphere. Intense red fluorescence indicates ROS generation, which was observed in the center of the rosettes (Fig. 5K, left panel). After addition of the NOX inhibitor diphenyleneiodonium (DPI), the red fluorescence of CellROX decreased (Figs. 5K and 5L), compatible with the concept that NOX2 is the source of ROS generation. A blue formazan precipitate corresponding to NBT reduction was observed in two different mono-rosette neurospheres, and was absent in rosettes pre-treated with DPI (Figs. 5M and 5N). Note that addition of DPI to neurospheres would not remove already established NBT precipitates.

### 2.7. Altered maturation of NPCs derived from NOX2-deficient iPSCs into neurons

Given the impact of NOX2 deficiency on differentiation of iPSCs into NPCs, we further studied the effect of NOX2 deficiency on later stages of neural differentiation (Fig. 6). For this purpose, NPCs were plated on polyornithin/laminin-coated dishes (at day 0) and allowed to mature for 60 days. The expression of neuronal markers (*TUBB3*, *MAP2* and *BDNF*) was analyzed by RT-qPCR at different time points of neural differentiation (Figs. 6A, 6C and 6E) and by immunofluorescence staining at day 60 of neuronal differentiation (Figs. 6F, 6J, 6M, and 6P). Interestingly, neurons derived from X°-CGD-iPSCs and AR-22°-CGD-iPSCs expressed lower levels of neuronal markers (*TUBB3*, *MAP2* and *BDNF*) than those derived from control-iPSCs (Figs. 6A, 6C and 6E). Consistent with these results, upon neuronal differentiation, X°-CGD-iPSCs and AR-22°-CGD-iPSCs generated less β3-tubulin positive cells and MAP2-positive cells (Figs. 6B and 6D). Quantification of neurite branching from soma of MAP2-positive neurons at day 60 of differentiation showed that the mean number of branches was lower in neurons derived from X°-CGD-iPSCs and AR-22°-CGD-iPSCs compared to those derived from control-iPSCs (Figs. 6F and 6G), which translates into a reduced length of neurites in neurons derived from X°-CGD-iPSCs and AR-22°-CGD-iPSCs (Fig. 6H).

Considering that an impaired maturation could explain the cognitive impairment observed in CGD patients, we investigated the expression of both pre- and post-synaptic markers of neurons by RT-qPCR and by immunofluorescence analysis. As shown, no difference in *SYN1*, *SNAP25* and *PSD95* expression was found in neurons derived from X°-CGD-iPSCs, AR-22°-CGD-iPSCs and control-iPSCs (Fig. 6I). In line with this, the density of synapsin punctae was similar in neurons derived from X°-CGD-iPSCs, AR-22°-CGD-iPSCs and control-iPSCs (Figs. 6J and 6K).

In order to determine if the reduced number of neurons generated from X°-CGD-iPSCs, AR-22°-CGD-iPSCs is associated with a gliogenic shift, we analyzed the expression of astroglial (*S100B* and *GFAP*) and oligodendroglial markers (*OLIG1* and *OLIG2*) by RT-qPCR upon neuronal differentiation of these iPSCs. Interestingly, no difference in the expression of *GFAP* and *S100B* as well as in the number of GFAP-positive cells was observed upon neuronal differentiation of X°-CGD- and AR-22°-CGD-iPSCs (Figs. 6L, 6M and 6N). By contrast, upon neuronal differentiation both X°-CGD- and AR-22°-CGD-iPSCs showed a reduced expression of *OLIG1* and *OLIG2* as well as a reduced number of OLIG2-positive cells (Figs. 6O, 6P and 6Q). Collectively, our results suggest that NOX2 deficiency is associated with a reduced generation of neurons and oligodendroglial cells with no impact in the number of astroglial cells.

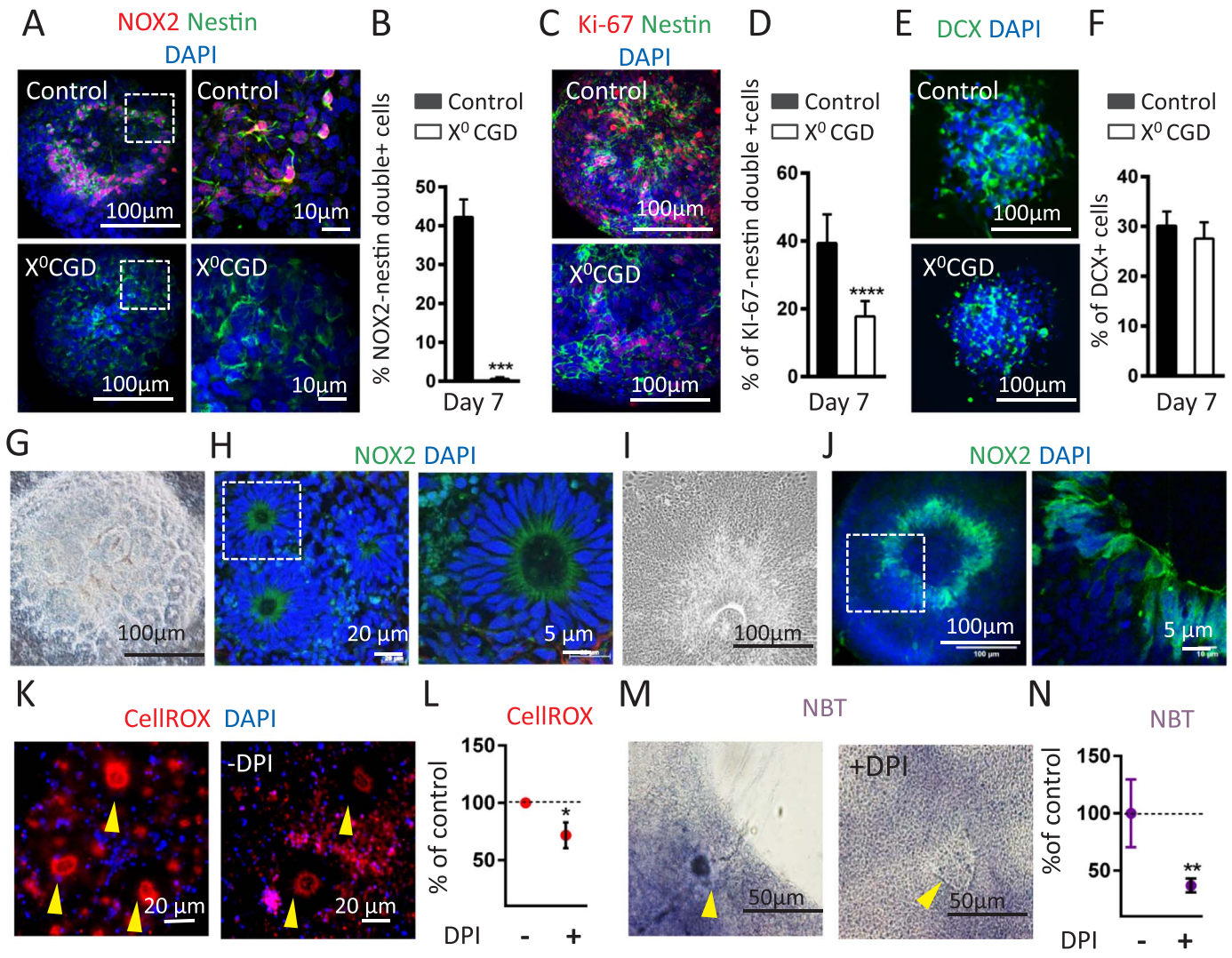


**Fig. 5.** NOX2 localization and activity in NPCs derived from iPSCs Immunofluorescence images (A) and quantification (B) of NOX2 (red) and the NPC marker nestin (green) in neurospheres (day7) of control and X°-CGD-iPSCs. Images in panel (A) are shown at lower (left) and higher (right) magnifications. (C) Co-staining of neurospheres with the proliferation marker Ki-67 and the NPC marker nestin. (D) Quantification of percentage of Ki67-nestin double positive cells. Immunostaining images (E) and quantification (F) of the early neuronal marker DCX (n = 6). Formation of multiple small rosettes (G) and single large rosettes (I) in neurospheres (day 7) derived from H1-hESCs (light microscopy). (H, J) NOX2 immunostaining in the two distinct types of rosette structures (right panels: higher magnification). (K, M) ROS production was visualized in neural rosette structures by using CellROX and NBT (yellow arrows). Generation of ROS was decreased in presence of 10uM DPI (flavoprotein inhibitor), arrows in yellow, suggesting NOX2 as a main source of ROS generation in rosettes (right panels in K and M). (L and M) Dot plot graph demonstrating ROS measurement in neural rosettes using DPI (flavoprotein inhibitor) (n = 5). Statistics were done Student's *t*-test. $^{*}P < 0.05$, $^{**}P < 0.01$, *** < 0.001, **** < 0.0001. (For interpretation of the references to color in this figure legend, the reader is referred to the web version of this article.)

## 3. Discussion

In this study, we show that the ROS-generating enzyme NOX2 is highly expressed in neurogenic regions of the mouse and macaque brain, as well as in neurally differentiated human iPS cells. Using NOX2-deficient mice and iPSC from NOX2-deficient patients, we demonstrate that NOX2 is functionally relevant in nestin positive NPCs and their proliferation.

To our knowledge, this is the first article that presents the role of NOX2 during neural differentiation by using human NOX2 deficient-iPSC lines. Two previous studies have investigated the role of ROS, and to some extent NOX, in NPCs. Le belle et al. has described the presence of NOX2 in the SVZ and a role of ROS in the self-renewal and multipotency of mouse NSCs. However, the conclusions of this study was mostly based on the use of non-specific inhibitors [14,30]. have shown NOX2-dependent regulation of proliferation and signaling in adult mouse hippocampal precursor (AHP) cells and decrease NPC proliferation NOX2-deficient adult mouse dentate gyrus [14,30].

Our study provides several novel and relevant elements: i) we investigated all NOX isoforms and demonstrate that only NOX2 mRNA is specifically enriched in the DG and SVZ; ii) we excluded the possibility that the presence of NOX2 in neurogenic regions is due to microglia; iii) by demonstrating decreased oxidative modifications in neurogenic regions of NOX2-deficient animals, we demonstrated that NOX2 is functional in neurogenic regions; iv) we detected region-specific role of NOX2, which mediates BDNF generation in the dentate gyrus, but Otx2 expression in the subventricular zone and olfactory bulb.

The role of human NOX2 was studied using iPSC from two different patients, one with X-linked *CYBB* (NOX2) deficiency, and one with autosomal *CYBA* ($p22^{phox}$) deficiency. As discussed in the introduction, $p22^{phox}$ is an obligatory subunit of the NOX2 complex, but in addition, it is also part of the NOX1, NOX3, and NOX4 complex [3]. Globally speaking, the results obtained with the two different types of CGD iPSCs were similar. However, the results obtained with the $p22^{phox}$ deficient cells (AR-22°) were more pronounced than the one observed with the NOX2-deficient cells. Thus, we cannot exclude a small contribution of NOX1, NOX3, or NOX4 to ROS generation in neurogenesis. Note, that in

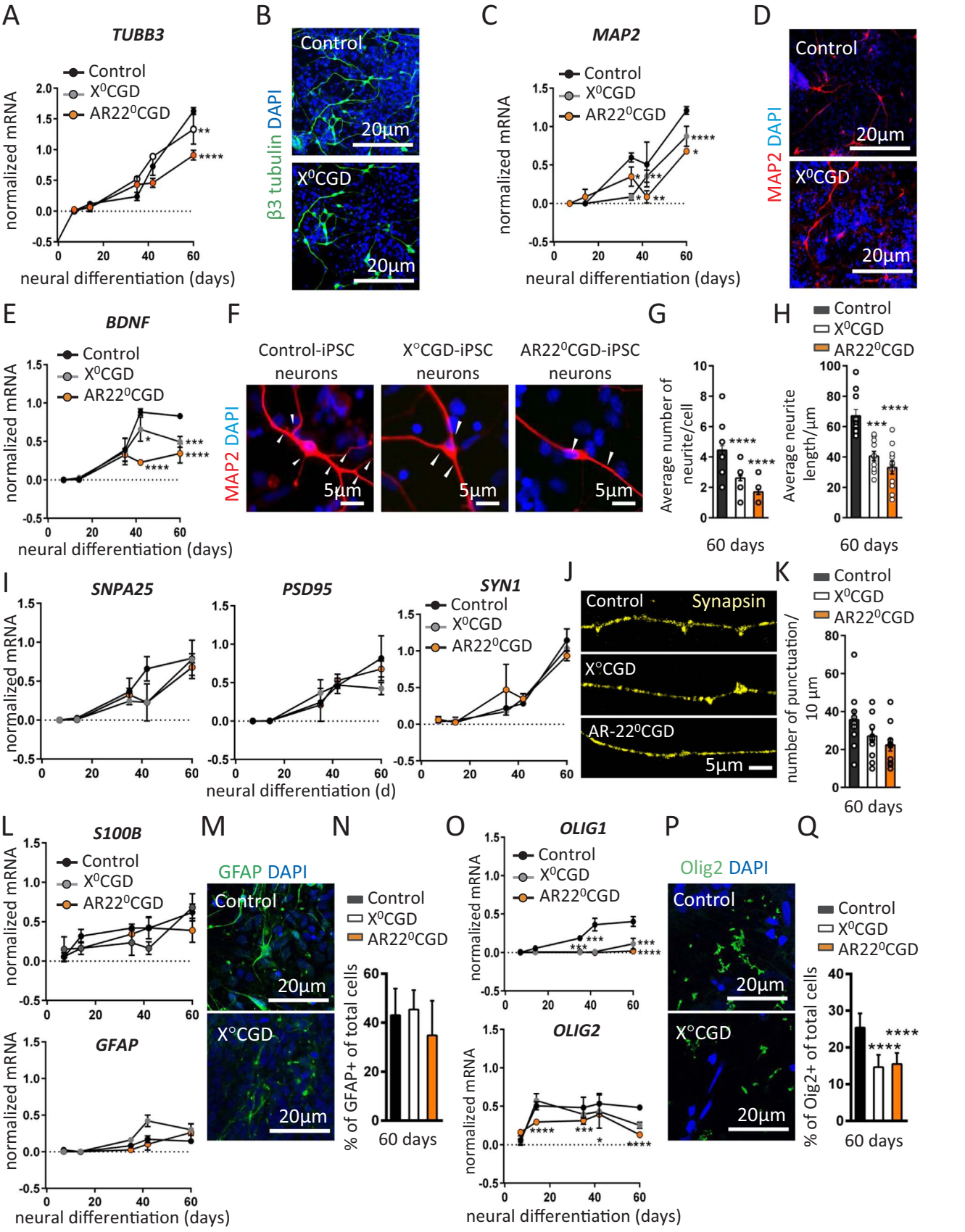


(caption on next page)

**Fig. 6.** *In vitro* neuronal maturation of control and CGD iPSC. Control iPSCs, X°-CGD-iPSCs and AR-22°-iPSCs were assessed by RT-qPCR analysis and immunofluorescent staining. Expression of the neuronal marker, β3-tubulin (A, B), and the mature neuronal marker *MAP2* (C, D), and brain derived neurotrophic factor *BDNF* (E). (F) Representative images and quantitative analysis of neurite number (G) and neurite length (H) from MAP2 positive neurons at day 60 of differentiation (n = 7). (I) Analysis of synaptic markers *SNPA25*, *PSD95* and *SYN1* by RT-qPCR in neurons derived from control and CGD-iPSCs, and immunostaining of synapsin (J) and quantification of the number of synapsin punctuations/10 μm (K, n = 4) at day 60 of differentiation. Analysis of glial markers S100B and GFAP (astrocytes, L, M, N), Olig1 and Olig2 (oligodendrocytes, O, P,Q) by RT-qPCR and immunostaining after 60 days of neural differentiation of control, $X^0$-CGD- and AR-$22^0$-CGD iPSC lines (n = 4 for RT-qPCR and n = 5 for immunofluorescence). Data are shown as mean ± SEM. Statistics were done by one-way ANOVA followed by multiple comparison Tukey's *test.* *P < 0.05, **P < 0.01, *** < 0.001, **** < 0.000.

contrast to the rapid down-regulation of NOX2 during neuronal differentiation of human ESCs and iPSCs, there was a persistence of $p22^{phox}$ expression, possibly compatible with a role of other NOX enzymes during later stages of neuronal differentiation.

Also, a role for microglia during neurogenesis is emerging [50]. Thus a likely explanation for the presence of NOX2 in neurogenic zones would be the presence of microglia, a CNS phagocyte which typically expresses the phagocyte NADPH oxidase NOX2 [12,18,31,42,54,63]. However, the following arguments plead against a microglial localization of NOX2 in neurogenic regions: i) NOX2-rich neurogenic regions of the adult mouse brain contained only very low amounts of microglia; ii) in vitro neuroectodermal differentiation of iPSCs is NOX2-regulated, but no microglia (of mesodermal origin) is present under these conditions; and iii) immunofluorescence staining shows NOX2 within rosette-like structures, which are analogous to the neural tube [16,17], and it co-localization with the NPC marker nestin. Interestingly, the presence of NOX2 appears to be required for symmetric divisions, which might not be an independent effect, but rather a mechanism that contributes to the maintenance of the physiological number of proliferating NSC. In the absence of this NOX2-driven oxidizing environment there is a decrease in the neuroprecursor pool.

Eventually, at the final stage of neural maturation, NOX2 appears to be strongly down-regulated. This corroborates RNAseq data from a mature neuronal region (cortex) where NOX2 is almost exclusively detected in microglia and completely absent in mature neurons [68]. However our data do not formally exclude the possibility that low level NOX2 expression may be present in neuronal subpopulations or at specific developmental stages (for review see [42].

We observed particularities associated with the NOX2 expression in neurogenic regions which merit discussion: i) NOX2 expression is not accompanied by a detectable expression of the transcription factors PU.1, which is one of the main known transcription factors driving NOX2 expression in leukocytic cells [57]. This suggests a PU.1-independent NOX2 expression in NPCs and the presence of alternative transcriptional regulation of NOX2. ii) The expression levels of several cytoplasmic NOX2 subunits (in particular $p67^{phox}$, $p40^{phox}$) were below detection threshold. Yet, our data show that NOX2 is functional in mouse and human NSCs/NPCs: NOX2 deficiency has a marked impact on NSC/NPC proliferation and gene expression and NOX2 expression is associated with ROS generation in neurogenic regions. Based on our present knowledge of NOX2 biochemistry, it seems unlikely that NSCs/NPCs exhibit a subunit-independent ROS generation by NOX2, but rather that low level and/or intermittent expression of subunits suffices to activate NOX2 in NSCs/NPCs; iii) the expression of the Rac GTPase isoforms in the neurogenic regions of the mouse brain is also unique as compared with other NOX2 expressing tissues. As expected, the neutrophil-typical Rac2 is virtually absent. However, in addition to Rac1, which is typically associated with NOX2 in macrophages, neurogenic regions also express high levels of the neuronal Rac3 [37]. Thus, it is tempting to speculate that Rac3 might be implicated in NOX2 activity in NSC/NPC.

In human phagocytes, activation of NOX2 is a tightly regulated system which responds to specific stimuli and rapidly deactivates once the relevant stimulus has disappeared. For the time being, we do not have evidence that NOX2 in NSCs behaves in a similar way. Indeed, under our experimental conditions, NOX2 appears to be active without addition of a specific stimulus (data not shown). However, we observed NOX2 activity in NSCs/NPCs within the neurogenic niche, where various growth factors are released which contributes to the control of the NSC/NPC system. Indeed, there is evidence for activation and/or enhanced expression of NOX2 by neural growth factors such as FGF2 [14], BDNF [53] and VEGF [31]. For example, NOX2 expression is decreased in neurogenic regions of VEGF-deficient mice [31]. In addition, there appears to be a feed-forward mechanism through a redox-sensitive activation of the respective growth factor receptors by NOX2 [62]. Thus, although we do not have experimental evidence for a receptor-dependent activation of NOX2 in neural precursors, our data certainly do not exclude this possibility.

Deficiency of NOX2 leads to a moderate decrease in cognitive function in man [45] and mice [26]. Given recent results that connect adult neurogenesis and learning [46,5,64], it is possible that the defective neurogenesis caused by NOX2 deficiency plays a causal role in the decreased cognition observed in CGD. This is also particularly relevant with respect to BDNF, which is thought to play a role in learning [22] and was found in our study to be decreased in human and mouse carrying NOX2-loss of function mutations. Future studies are needed to address whether learning associated neurogenesis is indeed decreased in CGD mice.

These results likely explain a hitherto poorly understood phenotype of NOX2-deficient CGD patients. It also adds a new level of complexity to the concept of NOX2 as a drug target for the treatment of oxidative stress diseases of the CNS.

## Author contributions

Z.N. conceived the study, designed and performed experiments, analyzed the data and wrote the manuscript. M.C. performed the dissection of the neurogenic regions of adult mouse. N.R.A. performed mouse neurospheres experiments under A.C supervision. E.G. performed several immunohistochemical analyses on human iPSCs. F.S.B and E.S performed the array-CGH for iPSC characterization. Y.H. provided the human primers as well as useful experience in handling and experimenting with iPSC. M.J.S. diagnosed and characterized the mutation of CGD patients. T.S. and J.H. generated the iPSC lines from CGD fibroblasts. KHK, VJ, conceived the study, wrote and edited the manuscript. All authors read and approved the final manuscript.

## Acknowledgment

This study was supported by the Swiss National Foundation (SNF) grant number 31003A-160220/1, European Community's Framework Programme (FP7/2007–2013) under grant 278611 (Neurinox), Swiss State Secretariat for Education and Innovation C13.0142, German Federal Ministry for Education and Research (Bundesministerium( für Bildung und Forschung, BMBF; grant number 01GN0824), Ministry for Innovation, Science und Research of the State of North Rhine-Westphalia (323-400-010-13), and Köln Fortune Programs of the Medical Faculty of the University of Cologne, Germany. Natalia Robledinos-Anton was supported by a grant from the COST action EUROS BM1203 and the program for training university lecturers (FPU14/01073) from Spanish Ministry of Education. The authors would like to thank Eric Rouiller from the University of Fribourg (Laboratory of Neurophysiology, Fribourg, Switzerland) for kindly donating *Macaca fascicularis* brain samples for NOX2 analysis. The authors would also like to thank the collaborators in human genetics, genomic platform, flow cytometry and bioimaging core facility, Yves Alexandre Cambet at

READS units at the University of Geneva. We are grateful to Olivier Plastre, Stéphanie Sgroi and Christophe Delgado for technical help. The authors would also like to thank Michel Dubois-Dauphin for discussions.

## Appendix A. Supporting information

Supplementary data associated with this article can be found in the online version at http://dx.doi.org/10.1016/j.redox.2017.04.026.

## References

[1] J. Altman, G.D. Das, Autoradiographic and histological evidence of postnatal hippocampal neurogenesis in rats, J. Comp. Neurol. 124 (1965) 319–335.
[2] J. Altman, G.D. Das, Autoradiographic and histological studies of postnatal neurogenesis. I. A longitudinal investigation of the kinetics, migration and transformation of cells incorporating tritiated thymidine in neonate rats, with special reference to postnatal neurogenesis in some brain regions, J. Comp. Neurol. 126 (1966) 337–389.
[3] K. Bedard, K.H. Krause, The NOX family of ROS-generating NADPH oxidases: physiology and pathophysiology, Physiol. Rev. 87 (2007) 245–313.
[4] C. Betzen, R. White, C.M. Zehendner, E. Pietrowski, B. Bender, H.J. Luhmann, C.R. Kuhlmann, Oxidative stress upregulates the NMDA receptor on cerebrovascular endothelium, Free Radic. Biol. Med. 47 (2009) 1212–1220.
[5] M. Blurton-Jones, M. Kitazawa, H. Martinez-Coria, N.A. Castello, F.J. Muller, J.F. Loring, T.R. Yamasaki, W.W. Poon, K.N. Green, F.M. LaFerla, Neural stem cells improve cognition via BDNF in a transgenic model of Alzheimer disease, Proc. Natl. Acad. Sci. USA 106 (2009) 13594–13599.
[6] J. Brault, E. Goutagny, N. Telugu, K. Shao, M. Baquie, V. Satre, C. Coutton, D. Grunwald, J.P. Brion, V. Barlogis. et al. Optimized Generation of Functional Neutrophils and Macrophages from Patient-Specific Induced Pluripotent Stem Cells: Ex Vivo Models of X(0)-Linked, AR22(0)- and AR47(0)- Chronic Granulomatous Diseases. BioResearch open access 3, 2014, pp. 311–326.
[7] M. Buggisch, B. Ateghang, C. Ruhe, C. Strobel, S. Lange, M. Wartenberg, H. Sauer, Stimulation of ES-cell-derived cardiomyogenesis and neonatal cardiac cell proliferation by reactive oxygen species and NADPH oxidase, J. Cell Sci. 120 (2007) 885–894.
[8] J.R. Burgoyne, H. Mongue-Din, P. Eaton, A.M. Shah, Redox signaling in cardiac physiology and pathology, Circ. Res. 111 (2012) 1091–1106.
[9] H.A. Cameron, R.D. McKay, Restoring production of hippocampal neurons in old age, Nat. Neurosci. 2 (1999) 894–897.
[10] S.M. Chambers, C.A. Fasano, E.P. Papapetrou, M. Tomishima, M. Sadelain, L. Studer, Highly efficient neural conversion of human ES and iPS cells by dual inhibition of SMAD signaling, Nat. Biotechnol. 27 (2009) 275–280.
[11] M.J. Corenblum, S. Ray, Q.W. Remley, M. Long, B. Harder, D.D. Zhang, C.A. Barnes, L. Madhavan, Reduced Nrf2 expression mediates the decline in neural stem cell function during a critical middle-age period, Aging Cell 15 (2016) 725–736.
[12] A. Coyoy, M. Olguin-Albuerne, P. Martinez-Briseno, J. Moran, Role of reactive oxygen species and NADPH-oxidase in the development of rat cerebellum, Neurochem. Int. 62 (2013) 998–1011.
[13] W. Deng, J.B. Aimone, F.H. Gage, New neurons and new memories: how does adult hippocampal neurogenesis affect learning and memory? Nat. Rev. Neurosci. 11 (2010) 339–350.
[14] B.C. Dickinson, J. Peltier, D. Stone, D.V. Schaffer, C.J. Chang, Nox2 redox signaling maintains essential cell populations in the brain, Nat. Chem. Biol. 7 (2011) 106–112.
[15] R. Dolmetsch, D.H. Geschwind, The human brain in a dish: the promise of iPSC-derived neurons, Cell 145 (2011) 831–834.
[16] Y. Elkabetz, G. Panagiotakos, G. Al Shamy, N.D. Socci, V. Tabar, L. Studer, Human ES cell-derived neural rosettes reveal a functionally distinct early neural stem cell stage, Genes Dev. 22 (2008) 152–165.
[17] Y. Elkabetz, L. Studer, Human ESC-derived neural rosettes and neural stem cell progression, Cold Spring Harb. Symp. Quant. Biol. 73 (2008) 377–387.
[18] M.T. Fischer, R. Sharma, J.L. Lim, L. Haider, J.M. Frischer, J. Drexhage, D. Mahad, M. Bradl, J. van Horssen, H. Lassmann, NADPH oxidase expression in active multiple sclerosis lesions in relation to oxidative tissue damage and mitochondrial injury, Brain 135 (2012) 886–899.
[19] H.J. Forman, F. Ursini, M. Maiorino, An overview of mechanisms of redox signaling, J. Mol. Cell. Cardiol. (2014).
[20] R.P. Galvao, J.M. Garcia-Verdugo, A. Alvarez-Buylla, Brain-derived neurotrophic factor signaling does not stimulate subventricular zone neurogenesis in adult mice and rats, J. Neurosci. 28 (2008) 13368–13383.
[21] A.V. Gilyarov, Nestin in central nervous system cells, Neurosci. Behav. Physiol. 38 (2008) 165–169.
[22] A. Gomez-Palacio Schjetnan, M.L. Escobar-Rodriguez, [Memory coding and retention: brain-derived neurotrophic factor (BDNF) in synaptic plasticity], Rev. De. Neurol. 45 (2007) 409–417.
[23] K.M. Holmstrom, T. Finkel, Cellular mechanisms and physiological consequences of redox-dependent signalling, Nat. Rev. Mol. Cell Biol. 15 (2014) 411–421 (LID −410.1038/nrm3801)(doi).
[24] S.K. Hota, K.B. Hota, D. Prasad, G. Ilavazhagan, S.B. Singh, Oxidative-stress-induced alterations in Sp factors mediate transcriptional regulation of the NR1 subunit in hippocampus during hypoxia, Free Radic. Biol. Med. 49 (2010) 178–191.
[25] A.T. Huddleston, W. Tang, H. Takeshima, S.L. Hamilton, E. Klann, Superoxide-induced potentiation in the hippocampus requires activation of ryanodine receptor type 3 and ERK, J. Neurophysiol. 99 (2008) 1565–1571.
[26] K.T. Kishida, C.A. Hoeffer, D. Hu, M. Pao, S.M. Holland, E. Klann, Synaptic plasticity deficits and mild memory impairments in mouse models of chronic granulomatous disease, Mol. Cell. Biol. 26 (2006) 5908–5920.
[27] K.T. Kishida, M. Pao, S.M. Holland, E. Klann, NADPH oxidase is required for NMDA receptor-dependent activation of ERK in hippocampal area CA1, J. Neurochem. 94 (2005) 299–306.
[28] H.G. Kuhn, H. Dickinson-Anson, F.H. Gage, Neurogenesis in the dentate gyrus of the adult rat: age-related decrease of neuronal progenitor proliferation, J. Neurosci. 16 (1996) 2027–2033.
[29] J.D. Lambeth, T. Kawahara, B. Diebold, Regulation of Nox and Duox enzymatic activity and expression, Free Radic. Biol. Med. 43 (2007) 319–331.
[30] J.E. Le Belle, N.M. Orozco, A.A. Paucar, J.P. Saxe, J. Mottahedeh, A.D. Pyle, H. Wu, H.I. Kornblum, Proliferative neural stem cells have high endogenous ROS levels that regulate self-renewal and neurogenesis in a PI3K/Akt-dependant manner, Cell Stem Cell 8 (2011) 59–71.
[31] A. Lelli, A. Gervais, C. Colin, C. Cheret, C. Ruiz de Almodovar, P. Carmeliet, K.H. Krause, S. Boillee, M. Mallat, The NADPH oxidase Nox2 regulates VEGFR1/CSF-1R-mediated microglial chemotaxis and promotes early postnatal infiltration of phagocytes in the subventricular zone of the mouse cerebral cortex, Glia 61 (2013) 1542–1555.
[32] T.L. Leto, S. Morand, D. Hurt, T. Ueyama, Targeting and regulation of reactive oxygen species generation by Nox family NADPH oxidases, Antioxid. Redox Signal 11 (2009) 2607–2619.
[33] J. Li, M. Stouffs, L. Serrander, B. Banfi, E. Bettiol, Y. Charnay, K. Steger, K.H. Krause, M.E. Jaconi, The NADPH oxidase NOX4 drives cardiac differentiation: role in regulating cardiac transcription factors and MAP kinase activation, Mol. Biol. Cell 17 (2006) 3978–3988.
[34] P.M. Lledo, M. Alonso, M.S. Grubb, Adult neurogenesis and functional plasticity in neuronal circuits, Nat. Rev. Neurosci. 7 (2006) 179–193.
[35] C. Lois, A. Alvarez-Buylla, Proliferating subventricular zone cells in the adult mammalian forebrain can differentiate into neurons and glia, Proc. Natl. Acad. Sci. USA 90 (1993) 2074–2077.
[36] C. Lois, A. Alvarez-Buylla, Long-distance neuronal migration in the adult mammalian brain, Science 264 (1994) 1145–1148.
[37] A.M. Lorincz, G. Szarvas, S.M. Smith, E. Ligeti, Role of Rac GTPase activating proteins in regulation of NADPH oxidase in human neutrophils, Free Radic. Biol. Med. 68C (2013) 65–71.
[38] M.B. Luskin, Restricted proliferation and migration of postnatally generated neurons derived from the forebrain subventricular zone, Neuron 11 (1993) 173–189.
[39] M.P. Mattson, S. Maudsley, B. Martin, A neural signaling triumvirate that influences ageing and age-related disease: insulin/igf-1, BDNF and serotonin, Ageing Res. Rev. 3 (2004) 445–464.
[40] K. Meganathan, S. Jagtap, V. Wagh, J. Winkler, J.A. Gaspar, D. Hildebrand, M. Trusch, K. Lehmann, J. Hescheler, H. Schluter, et al., Identification of thalidomide-specific transcriptomics and proteomics signatures during differentiation of human embryonic stem cells, PloS One 7 (2012) e44228.
[41] G.L. Ming, H. Song, Adult neurogenesis in the mammalian brain: significant answers and significant questions, Neuron 70 (2011) 687–702.
[42] Z. Nayernia, V. Jaquet, K.H. Krause, New Insights on NOX Enzymes in the Central Nervous System, Antioxid. Redox Signal. (2014).
[43] M. Olguin-Albuerne, J. Moran, ROS produced by NOX2 control in vitro development of cerebellar granule neurons development, ASN Neuro 7 (2015).
[44] E.A. Ostrakhovitch, O.A. Semenikhin, The role of redox environment in neurogenic development, Arch. Biochem. Biophys. 534 (2013) 44–54 (LID -10.1016/j.abb.2012.1008.1002)(doi) (LID - S0003-9861)(1012)(00301-00303)(pii).
[45] M. Pao, E.A. Wiggs, M.M. Anastacio, J. Hyun, E.S. DeCarlo, J.T. Miller, V.L. Anderson, H.L. Malech, J.I. Gallin, S.M. Holland, Cognitive function in patients with chronic granulomatous disease: a preliminary report, Psychosomatics 45 (2004) 230–234.
[46] D. Park, A.P. Xiang, F.F. Mao, L. Zhang, C.G. Di, X.M. Liu, Y. Shao, B.F. Ma, J.H. Lee, K.S. Ha, et al., Nestin is required for the proper self-renewal of neural stem cells, Stem Cells 28 (2010) 2162–2171.
[47] A. Petry, M. Weitnauer, A. Gorlach, Receptor activation of NADPH oxidases, Antioxid. Redox Signal. 13 (2010) 467–487.
[48] C. Piccoli, A. D'Aprile, M. Ripoli, R. Scrima, L. Lecce, D. Boffoli, A. Tabilio, N. Capitanio, Bone-marrow derived hematopoietic stem/progenitor cells express multiple isoforms of NADPH oxidase and produce constitutively reactive oxygen species, Biochem. Biophys. Res. Commun. 353 (2007) 965–972.
[49] C. Piccoli, R. Ria, R. Scrima, O. Cela, A. D'Aprile, D. Boffoli, F. Falzetti, A. Tabilio, N. Capitanio, Characterization of mitochondrial and extra-mitochondrial oxygen consuming reactions in human hematopoietic stem cells. Novel evidence of the occurrence of NAD(P)H oxidase activity, J. Biol. Chem. 280 (2005) 26467–26476.
[50] K. Sato, Effects of Microglia on Neurogenesis, Glia 63 (2015) 1394–1405.
[51] T. Seredenina, Z. Nayernia, S. Sorce, G.J. Maghzal, A. Filippova, S.C. Ling, O. Basset, O. Plastre, Y. Daali, E.J. Rushing, et al., Evaluation of NADPH oxidases as drug targets in a mouse model of familial amyotrophic lateral sclerosis, Free Radic. Biol. Med. 97 (2016) 95–108.
[52] F. Serrano, N.S. Kolluri, F.B. Wientjes, J.P. Card, E. Klann, NADPH oxidase immunoreactivity in the mouse brain, Brain Res. 988 (2003) 193–198.
[53] X. Song, B. Zhou, P. Zhang, D. Lei, Y. Wang, G. Yao, T. Hayashi, M. Xia, S. Tashiro, S. Onodera, et al., Protective Effect of Silibinin on Learning and Memory

Impairment in LPS-Treated Rats via ROS-BDNF-TrkB Pathway, Neurochem. Res. 41 (2016) 1662–1672.
[54] S. Sorce, K.H. Krause, NOX enzymes in the central nervous system: from signaling to disease, Antioxid. Redox Signal 11 (2009) 2481–2504.
[55] M.J. Stasia, X.J. Li, Genetics and immunopathology of chronic granulomatous disease, Semin. Immunopathol. 30 (2008) 209–235.
[56] J.L. Stein, L. de la Torre-Ubieta, Y. Tian, N.N. Parikshak, I.A. Hernandez, M.C. Marchetto, D.K. Baker, D. Lu, C.R. Hinman, J.K. Lowe, et al., A quantitative framework to evaluate modeling of cortical development by neural stem cells, Neuron 83 (2014) 69–86.
[57] S. Suzuki, A. Kumatori, I.A. Haagen, Y. Fujii, M.A. Sadat, H.L. Jun, Y. Tsuji, D. Roos, M. Nakamura, PU.1 as an essential activator for the expression of gp91(phox) gene in human peripheral neutrophils, monocytes, and B lymphocytes, Proc. Natl. Acad. Sci. USA 95 (1998) 6085–6090.
[58] M.V. Tejada-Simon, F. Serrano, L.E. Villasana, B.I. Kanterewicz, G.Y. Wu, M.T. Quinn, E. Klann, Synaptic localization of a functional NADPH oxidase in the mouse hippocampus, Mol. Cell. Neurosci. 29 (2005) 97–106.
[59] M. Tsatmali, E.C. Walcott, K.L. Crossin, Newborn neurons acquire high levels of reactive oxygen species and increased mitochondrial proteins upon differentiation from progenitors, Brain Res. 1040 (2005) 137–150.
[60] H.L. Vieira, P.M. Alves, A. Vercelli, Modulation of neuronal stem cell differentiation by hypoxia and reactive oxygen species, Progress. Neurobiol. 93 (2011) 444–455.
[61] X. Wang, E.K. Michaelis, Selective neuronal vulnerability to oxidative stress in the brain, Front. Aging Neurosci. 2 (2010) 12.
[62] J.F. Woolley, A. Corcoran, G. Groeger, W.D. Landry, T.G. Cotter, Redox-regulated growth factor survival signaling, Antioxid. Redox Signal. 19 (2013) 1815–1827.
[63] D.C. Wu, D.B. Re, M. Nagai, H. Ischiropoulos, S. Przedborski, The inflammatory NADPH oxidase enzyme modulates motor neuron degeneration in amyotrophic lateral sclerosis mice, Proc. Natl. Acad. Sci. USA 103 (2006) 12132–12137.
[64] A.G. Xuan, D.H. Long, H.G. Gu, D.D. Yang, L.P. Hong, S.L. Leng, BDNF improves the effects of neural stem cells on the rat model of Alzheimer's disease with unilateral lesion of fimbria-fornix, Neurosci. Lett. 440 (2008) 331–335.
[65] A. Yamauchi, L. Yu, A.J. Potgens, F. Kuribayashi, H. Nunoi, S. Kanegasaki, D. Roos, H.L. Malech, M.C. Dinauer, M. Nakamura, Location of the epitope for 7D5, a monoclonal antibody raised against human flavocytochrome b558, to the extracellular peptide portion of primate gp91phox, Microbiol. Immunol. 45 (2001) 249–257.
[66] M. Yoneyama, K. Kawada, Y. Gotoh, T. Shiba, K. Ogita, Endogenous reactive oxygen species are essential for proliferation of neural stem/progenitor cells, Neurochem. Int. 56 (2010) 740–746.
[67] T.F. Yuan, S. Gu, C. Shan, S. Marchado, O. Arias-Carrion, Oxidative Stress and Adult Neurogenesis, Stem Cell Rev. 11 (2015) 706–709.
[68 Y. Zhang, K. Chen, S.A. Sloan, M.L. Bennett, A.R. Scholze, S. O'Keeffe, H.P. Phatnani, P. Guarnieri, C. Caneda, N. Ruderisch, et al., An RNA-sequencing transcriptome and splicing database of glia, neurons, and vascular cells of the cerebral cortex, J. Neurosci.: Off. J. Soc. Neurosci. 34 (2014) 11929–11947.

# NRF2-dependent gene expression promotes ciliogenesis and Hedgehog signaling

Ana Martin-Hurtado[1-2], Raquel Martin-Morales[1-2], Natalia Robledinos-Antón[1-3], Ruth Blanco[1-3], Ines Palacios-Blanco[1-2], Isabel Lastres-Becker[1-3], Antonio Cuadrado[1-3] & Francesc R. Garcia-Gonzalo[1-2,*]

[1]Alberto Sols Biomedical Research Institute UAM-CSIC and Department of Biochemistry, School of Medicine, Autonomous University of Madrid (UAM), Madrid, Spain; [2]La Paz University Hospital Research Institute (IdiPAZ), Madrid, Spain; [3]Centro de Investigación Biomédica en Red sobre Enfermedades Neurodegenerativas (CIBERNED), ISCIII, Madrid, Spain.

*To whom correspondence should be addressed: Francesc R. Garcia-Gonzalo, Departamento de Bioquímica (Lab C-11), Facultad de Medicina UAM, C/Arzobispo Morcillo 4, 28029 Madrid, Spain. Tel. (+34) 91 497 5447; FAX: (+34) 91 497 5353; Email: francesc.garcia@uam.es.

---

The transcription factor NRF2 is a master regulator of cellular antioxidant and detoxification responses, but it also regulates other processes such as autophagy and pluripotency. In human embryonic stem cells (hESCs), NRF2 antagonizes neuroectoderm differentiation, which only occurs after NRF2 is repressed via a Primary Cilia-Autophagy-NRF2 (PAN) axis. However, the functional connections between NRF2 and primary cilia, microtubule-based plasma membrane protrusions that function as cellular antennae, remain poorly understood. For instance, nothing is known about whether NRF2 affects cilia, or whether cilia regulation of NRF2 extends beyond hESCs. Here, we show that NRF2 and primary cilia reciprocally regulate each other. First, we demonstrate that fibroblasts lacking primary cilia have higher NRF2 activity, which is rescued by autophagy-activating mTOR inhibitors, indicating that the PAN axis also operates in differentiated cells. Furthermore, we show that NRF2 controls cilia formation and function. NRF2-null cells grow fewer and shorter cilia and display impaired Hedgehog signaling, a cilia-dependent pathway. These defects are not due to increased oxidative stress or ciliophagy, but rather to NRF2 promoting expression of multiple ciliogenic and Hedgehog pathway genes. Among these, we focused on GLI2 and GLI3, the transcription factors controlling Hh pathway output. Both their mRNA and protein levels are reduced in NRF2-null cells, consistent with their gene promoters containing consensus ARE sequences predicted to bind NRF2. Moreover, GLI2 and GLI3 fail to accumulate at the ciliary tip of NRF2-null cells upon Hh pathway activation. Given the importance of NRF2 and ciliary signaling in human disease, our data may have important biomedical implications.

## INTRODUCTION

Primary cilia are microtubule-based plasma membrane protrusions that function as cell type-specific antennae by accumulating signal receptors and transducers. Structurally, the ciliary membrane is undergirded by the ciliary shaft, or axoneme, consisting of nine microtubule pairs emanating from the basal body, a membrane-anchored centriole[1,2].

The presence of primary cilia is cell cycle and cell type-dependent[3,4]. In the cell cycle, cilia form during G1/G0 and disassemble before mitosis[3]. Moreover, specific transcription factors (e.g. RFX1-4, FOXJ1) promote ciliogenic gene expression in a cell type-specific manner[4,5]. Ciliogenesis and ciliary maintenance critically depend on a bidirectional trafficking system, known as intraflagellar transport (IFT), that moves cargoes up and down the axoneme[1,2]. To do this, cargoes bind adaptors such as IFT-B and IFT-A complexes, which in turn associate to microtubule motors moving toward (heterotrimeric kinesin-2) or from (cytoplasmic dynein-2) the ciliary tip.

In mammals, the complete absence of cilia is embryonic lethal, as seen in mice lacking essential ciliogenic genes such as *Ift88* and *Kif3a* [6,7]. Less severe congenital ciliary defects lead to ciliopathies, a diverse group of human diseases causing blindness, cystic kidneys, obesity, sterility, polydactyly and brain malformations, among other symptoms[1]. Cilia defects acquired later in life are associated with ailments such as cancer and neurodegeneration[8-11].

Disruption of Hedgehog (Hh) signaling, a cilia-dependent pathway controlling multiple aspects of embryogenesis and adult stem cell function[7], explains many (but not all) ciliopathy symptoms and cilia-dependent cancers. Hh ligands, such as Sonic Hedgehog (SHH), act in paracrine fashion by binding to Patched (PTCH1), a ciliary transmembrane protein. Ligand binding prevents PTCH1 from opposing the ciliary accumulation of Smoothened (SMO), a seven transmembrane protein whose activation displaces another G protein-coupled receptor, GPR161, from cilia. This in turn lowers cAMP levels and PKA activity at the basal body, affecting phosphorylation of GLI2 and GLI3, the zinc finger transcription factors mediating Hh pathway output. This promotes GLI2 and GLI3 accumulation at the ciliary tip, where they dissociate from SUFU, a pathway repressor. From the ciliary tip, GLI2 and GLI3 travel to the ciliary base to meet different fates: GLI2 is processed into a transcriptional activator and translocates to the nucleus to activate target genes, whereas GLI3 is fully degraded in the proteasome, abolishing its basal activity as a transcriptional repressor. Thus, by promoting GLI2 activation and GLI3 non-repression, Hh ligands stimulate expression of target genes, including *Ptch1* and *Gli1*, another activating GLI [7].

Primary cilia also modulate mTOR signaling and autophagy[12-17]. In the kidney, mechanosensory cilia in tubular epithelial cells respond to fluid flow by repressing mTOR, thereby promoting autophagy and reducing cell volume, a homeostatic mechanism perturbed in polycystic kidney disease[13,15,18,19]. Similar pathways occur in other cell types, such as fibroblasts and radial glia[16,17]. During human embryonic stem cell (hESC) differentiation, cell fate choice between mesendoderm and neuroectoderm is also controlled by cilium-dependent autophagy[12]. In the first stages of neuroectoderm progenitor specification, cell cycle lengthening allows cilia to emerge during G1. Cilia in turn activate autophagy, resulting in the inactivation of NRF2, which antagonizes neuroectoderm differentiation. Whether this so-called Primary Cilium-Autophagy-NRF2 (PAN) axis is conserved in other cell types, and whether mTOR is involved in it, has not been addressed[12].

NRF2 (nuclear factor erythroid 2-related factor 2), encoded by the *Nfe2l2* gene, is a basic region-leucine zipper (bZip) transcription factor best known as a master regulator of cellular antioxidant and detoxification responses[20]. Under normal conditions, NRF2 binding to KEAP1 targets the former for ubiquitin-dependent proteasome degradation. By modifying cysteine residues in KEAP1, oxidative stress, or electrophilic compounds like dimethyl fumarate (DMF), an FDA-approved drug for treatment of multiple sclerosis, disrupt KEAP1-NRF2 binding, leading to NRF2 accumulation[20]. NRF2 then

translocates to the nucleus and activates expression of its multiple target genes by binding to antioxidant response elements (AREs) in their enhancer regions[20]. Many of these genes encode detoxification enzymes, such as heme oxygenase-1 (*Hmox1*) or the catalytic (*Gclc*) and modulatory (*Gclm*) subunits of glutamate-cysteine ligase, which catalyzes the first step in the biosynthesis of glutathione, a major cellular scavenger of reactive oxygen species (ROS)[20]. NRF2 also targets autophagy genes, which contribute to stress tolerance. Hence, NRF2 is both a regulator of autophagy and an autophagy-regulated protein[12,21,22].

Likewise, primary cilia both control and are controlled by autophagy[12,14,23,24]. A cilia-specific form of autophagy, termed ciliophagy, plays a key role in lung damage caused by cigarette smoke. HDAC6, a histone deacetylase and ubiquitin-binding autophagy receptor, plays a key role in both ciliophagy and aggrephagy, the autophagic clearance of protein aggregates[23,25,26]. Moreover, autophagy promotes ciliogenesis and lengthens cilia by removing an inhibitory protein, OFD1, from the basal body vicinity [24].

In view of these reciprocal cilia-autophagy and NRF2-autophagy connections, we wondered whether analogous reciprocal relationships exist between cilia and NRF2. Indeed, we find that fibroblasts lacking cilia have increased NRF2 activity, which we rescue with mTOR inhibitors. Conversely, NRF2-null cells have defects in ciliogenesis and Hh signaling. These defects, rather than being caused by changes in redox stress or ciliophagy, are due to NRF2 promoting expression of multiple ciliogenic and Hh pathway genes.

## RESULTS

### Primary cilia downregulate NRF2 transcriptional activity via mTOR

Cells lacking KIF3A, a kinesin-2 subunit, or IFT88, an IFT-B complex component, are completely incapable of growing cilia and are commonly used to study the effects of cilia ablation[1,6,7,27]. We confirmed this using both *Kif3a*$^{-/-}$ and *Ift88*$^{-/-}$ mouse embryonic fibroblasts (MEFs). After 24 hours of starvation, most wild type MEFs displayed primary cilia, in which both axoneme (acetylated α-tubulin, AcTub) and ciliary membrane (ARL13B) markers are seen to emerge from the γ-tubulin-positive basal bodies. In contrast, *Kif3a*$^{-/-}$ and *Ift88*$^{-/-}$ MEFs failed to grow any cilia under the same conditions (Fig.1a).

To test whether cilia regulate NRF2 activity in MEFs, we measured mRNA levels of heme oxygenase-1 (*Hmox1*) and glutamate-cysteine ligase catalytic subunit (*Gclc*), two well-established transcriptional NRF2 targets[20], in *Kif3a*$^{-/-}$, *Ift88*$^{-/-}$ and their respective littermate control MEFs (Fig.1b-c). We tested this in presence or absence of DMF, a known NRF2 activator[20]. Both with and without DMF, cilia-null MEFs displayed consistently higher *Hmox1* and *Gclc* mRNA levels, an effect that was more obvious and significant in presence of DMF (Fig.1b-c). As expected, DMF raised *Hmox1* and *Gclc*, but to a lesser extent in cilia-null MEFs (Fig.1b-c). Since these results were observed for both *Kif3a* and *Ift88* MEFs, this suggests that cilia downregulate NRF2 transcriptional activity. Accordingly, another NRF2 target gene, NADPH quinone oxidoreductase-1 (*Nqo1*), was also upregulated, together with *Hmox1*, in both *Kif3a*$^{-/-}$ and *Ift88*$^{-/-}$ MEFs, and this upregulation was enhanced by another NRF2 activator, sulforaphane (Supplementary Fig.S1a-b)[20]. Furthermore, *Hmox1* protein levels were also increased in *Ift88*$^{-/-}$ MEFs, and the effect was clearer in sulforaphane-treated cells (Supplementary Fig.S1c).

To see if this increase in NRF2 activity was due to increased NRF2 protein levels, we analyzed the latter by Western blot in *Kif3a*$^{+/+}$ and *Kif3a*$^{-/-}$ MEFs treated or not with DMF. Relative to α-tubulin, NRF2 protein levels were strongly upregulated by DMF in both *Kif3a*$^{+/+}$ and *Kif3a*$^{-/-}$ MEFs, without obvious differences between cell types (Fig.1d). Hence, the effect of KIF3A on NRF2 activity is not due to changes in NRF2 protein levels.

Since primary cilia downregulation of NRF2 during neuroectoderm differentiation is mediated by autophagy, we next tested whether mTOR inhibitors, which are widely used to activate autophagy, could restore normal NRF2 activity in *Kif3a*$^{-/-}$ MEFs[12,28]. For this, we used both Torin-1 and rapamycin, an ATP-competitive and an allosteric mTOR inhibitor, respectively[29]. Indeed, gene expression of both *Hmox1* and *Gclc* returned to wild type levels upon treatment of *Kif3a*$^{-/-}$ MEFs with either Torin-1 or rapamycin (Fig.1e-f).

To assess whether changes in autophagic flux may explain the mTOR-dependent effects of cilia on NRF2 activity, we used Western blot to look at the relative levels of LC3-I and LC3-II in presence or absence of chloroquine, an autophagolysosome blocker. It is well-established that, during autophagy, LC3-I is conjugated to phosphatidylethanolamine, thus generating LC3-II and tethering it to autophagosomes, which evolve into autophagolysosomes where LC3-II is degraded. Based on this, the chloroquine-induced increase in LC3-II levels (normalized as LC3-II/LC3-I ratio) is a widely accepted measure of autophagic flux. In starved and DMF-treated *Kif3a*$^{+/+}$ MEFs, we saw a clear chloroquine-induced increase in the LC3-II/LC3-I ratio, indicating active autophagy (Fig.1g). Under the same conditions, autophagic flux in *Kif3a*$^{-/-}$ MEFs was reduced by more than 30% relative to the *Kif3a*$^{+/+}$ control. This reduction, however, was rescued by both Torin-1 and rapamycin, in whose presence autophagic flux in *Kif3a*$^{-/-}$ MEFs was even higher than that in *Kif3a*$^{+/+}$ cells (Fig.1g). Since autophagy flux in these cells shows a strong inverse correlation with NRF2 target expression, these data are consistent with primary cilia downregulating NRF2 by promoting autophagy.

Intriguingly, this correlation did not clearly extend to NRF2 protein levels, even though quantitation of NRF2/Tubulin ratios showed a slight increase in *Kif3a*$^{-/-}$ relative to *Kif3a*$^{+/+}$ MEFs, an increase that was no longer seen when *Kif3a*$^{-/-}$ MEFs were treated with mTOR inhibitors (Fig.1h). However, to what extent this modest increase in NRF2 protein might explain the observed increase in NRF2 transcriptional activity remains unclear.

Altogether, these data suggest that the PAN axis described in differentiating hESCs is also operative in more differentiated cell types, such as MEFs.

**Ciliary repression of NRF2 does not involve Hh signaling**

Since primary cilia are required for vertebrate Hh signaling, we also tested whether Hh pathway alterations might be involved in the higher NRF2 activity of *Kif3a*$^{-/-}$ MEFs. In these cells, lack of cilia prevents proteolytic processing of GLI transcription factors[7]. Since GLI3 is processed into a transcriptional repressor (GLI3R) in a constitutive and cilia-dependent manner, *Kif3a*$^{-/-}$ MEFs fail to form GLI3R, leading to higher unstimulated expression of Hh target genes *Gli1* and *Ptch1* (Supplementary Fig.S2a).

KIF3A and cilia are also required for GLI2 processing, which forms a transcriptional activator (GLI2A) only upon Hh pathway stimulation. Hence, *Kif3a*$^{-/-}$ MEFs fail to form GLI2A and do not induce target gene expression in response to Hh pathway agonists. Nevertheless, Hh target gene expression can be stimulated in these cells by transfecting them with a constitutively active, oncogenic allele of GLI2 known as GLI2ΔN [27]. Indeed, transient expression of GLI2ΔN activated Hh target expression in *Kif3a*$^{+/+}$ and, even more so, in *Kif3a*$^{-/-}$ MEFs, where GLI3R does not counteract its effect (Supplementary Fig.S2a).

However, despite strongly activating Hh signaling in *Kif3a*$^{+/+}$ and *Kif3a*$^{-/-}$ MEFs, GLI2ΔN had no effect on *Hmox1* and *Gclc* gene expression, indicating that NRF2 activity is not affected by GLI2ΔN-induced Hh pathway activation (Supplementary Fig.S2b).

Thus, GLI2 activation does not mediate the effects of cilia on NRF2. Nor does GLI2 inhibition, as GLI2 is transcriptionally inactive in unstimulated MEFs, as confirmed by our observation that GLI2 inhibitor

GANT61 does not lower Hh target expression in MEFs not treated with Hh pathway agonists (data not shown)[30].

Having ruled out GLI2, it was still possible that cilia repress NRF2 activity by promoting GLI3R synthesis. If this were the case, then GLI3R expression in *Kif3a*$^{-/-}$ MEFs should lower NRF2 activity, restoring it to normal. However, this is not the case (Supplementary Fig.S2c-d).

Overall, these data indicate that the negative impact of cilia on NRF2 activity is not related to Hh signaling.

**Ciliogenesis is reduced in NRF2-null cells**

We next wondered whether NRF2 affects cilia in addition to being affected by them. To test this, we first looked at ciliogenesis in *Nfe2l2*$^{+/+}$ and *Nfe2l2*$^{-/-}$ MEFs. Although *Nfe2l2*$^{-/-}$ MEFs generated cilia that appeared normal by ARL13B, AcTub and γ-tubulin staining (Fig.2a), the percentage of such cells displaying primary cilia was reduced in half relative to *Nfe2l2*$^{+/+}$ cells (Fig.2b). Moreover, cilia in *Nfe2l2*$^{-/-}$ MEFs were on average 15-20% shorter than control cilia (Fig.2c). Primary *Nfe2l2*$^{-/-}$ MEFs displayed similar ciliogenic defects, excluding MEF immortalization as their cause (Supplementary Fig.S3).

We then examined whether NRF2 affects ciliogenesis *in vivo*. Since NRF2-null mice are viable and develop normally, we reasoned their embryonic cilia cannot be strongly perturbed[31]. In contrast, adult NRF2-null mice have phenotypes that could potentially be explained by ciliogenic defects. In particular, both NRF2 and cilia play important roles in the hippocampus, affecting cognitive functions[11,32,33]. Thus, we decided to look at hippocampal cilia in coronal sections of three month-old *Nfe2l2*$^{+/+}$ and *Nfe2l2*$^{-/-}$ mouse brains. Moreover, since NRF2 plays a prominent role in astrocytes[34-36], and ARL13B specifically labels astrocytic cilia in adult mouse brain[37,38], we focused our study on this cell type, which can be readily identified with the GFAP marker[38]. In both *Nfe2l2*$^{+/+}$ and *Nfe2l2*$^{-/-}$ hippocampus, ARL13B$^{+}$ cilia were indeed only seen in close association with GFAP$^{+}$ astrocytes, confirming the above reports (Fig.2c)[37,38]. In control sections, about 50% of such GFAP$^{+}$ cells contained a primary cilium, but this percentage was reduced to about 10% in equivalent *Nfe2l2*$^{-/-}$ sections (Fig.2c-d).

Thus, our data suggest that NRF2 is required for optimal ciliogenesis both *in vitro* and *in vivo*.

**Hh signaling is reduced in NRF2-null cells**

Since Hh signaling is cilia-dependent, we next examined Hh pathway responsiveness in *Nfe2l2*$^{-/-}$ MEFs. To do this, we used Smoothened agonist (SAG), a well-established Hh pathway activator[39]. While SAG strongly induced Hh target genes *Gli1* and *Ptch1* in *Nfe2l2*$^{+/+}$ cells, this response was much attenuated in *Nfe2l2*$^{-/-}$ MEFs, even if still significant (Fig.3a). Very similar results were obtained in primary MEFs, confirming defective Hh responsiveness is not related to MEF immortalization (Supplementary Fig.S4). Moreover, differences in SAG responsiveness were also seen by Western blot of GLI1, whose protein levels were strongly upregulated by SAG in *Nfe2l2*$^{+/+}$ MEFs but much less so in *Nfe2l2*$^{-/-}$ MEFs (Fig.3b). Thus, NRF2-null cells display defects in both ciliogenesis and Hh signaling.

**ROS, HDAC6, mTOR and PKA inhibitors do not rescue Hh signaling in NRF2-null cells**

We then asked whether increased oxidative stress in absence of NRF2 was the cause for the sharp decrease in Hh signaling. To address this, we used N-acetyl-cysteine (NAC), a glutathione precursor that promotes ROS scavenging, thereby reducing oxidative stress[40]. NAC treatment of *Nfe2l2*$^{-/-}$ MEFs did not affect their poor SAG responsiveness relative to wild type cells, indicating that the antioxidant functions of NRF2 are not the main reason why it promotes Hh signaling (Fig.4).

Another possible explanation for the effect of NRF2 on cilia and Hh signaling is that NRF2 affects ciliophagy, which critically depends on HDAC6, a protein that is upregulated in *Nfe2l2*$^{-/-}$ cells and

functions as both a protein deacetylase and a ubiquitin-binding autophagy receptor[23,25,26]. If increased HDAC6-dependent ciliophagy was the cause of *Nfe2l2*$^{-/-}$ MEFs displaying ciliogenic and Hh signaling defects, then Tubastatin A, an HDAC6 inhibitor that blocks ciliophagy, should improve Hh responses in these cells[23,41]. However, this is not the case (Fig.4).

Since PKA, by promoting generation of GLI repressors at the expense of GLI activators, is a negative regulator of Hh signaling, we also tested whether a PKA inhibitor, H89, restored high Hh responsiveness in *Nfe2l2*$^{-/-}$ MEFs[42]. The lack of such restoration indicates that NRF2 is required downstream of PKA in the Hh pathway (Fig.4).

Lastly, given that NRF2 promotes autophagy[21,22], we tested whether autophagy stimulation with mTOR inhibitor Torin-1 improved Hh signaling in *Nfe2l2*$^{-/-}$ MEFs, but it did not (Fig.4).

Hence, oxidative stress, HDAC6-dependent ciliophagy, overactive PKA or reduced autophagy do not appear to explain the cilia and Hh phenotypes of *Nfe2l2*$^{-/-}$ MEFs.

**Ciliogenic and Hh pathway gene expression is reduced in NRF2-null cells**

NRF2 is a transcription factor with hundreds of known target genes, so we reasoned that its effects on cilia and Hh signaling might be mediated by changes in gene expression. To test this, we first looked at mRNA levels of ciliogenic genes in *Nfe2l2*$^{+/+}$ and *Nfe2l2*$^{-/-}$ MEFs. These genes encode proteins such as ciliary microtubule motors (*Dync2h1*) and components of intraflagellar transport complexes IFT-B (*Ift74*, *Ift88*, *Ift172*) and IFT-A (*Ift140*). Interestingly, expression of all IFT and motor genes analyzed was significantly lower in *Nfe2l2*$^{-/-}$ relative to *Nfe2l2*$^{+/+}$ MEFs, regardless of whether or not cells were treated with SAG (Fig.5a). Similar results were obtained in primary MEFs (Supplementary Fig.S5a).

*Nfe2l2*$^{-/-}$ MEFs show a two-fold reduction in ciliogenesis (Fig.2b), yet their Hh responsiveness is lower by at least 4-fold (Fig.3a). This suggested that the remaining cilia in *Nfe2l2*$^{-/-}$ MEFs are not fully functional regarding Hh signal transduction. This, we hypothesized, might be due to defects in gene expression of Hh pathway components. To test this, we measured mRNA levels for several Hh pathway mediators, including positive regulators SMO, GLI2 and IFT27, and negative regulators GLI3, SUFU and GPR161[7]. All of them were significantly downregulated in *Nfe2l2*$^{-/-}$ MEFs independently of Hh pathway activation (Fig.5b). Similar reductions in Hh pathway gene expression were observed in primary MEFs (Supplementary Fig.S5b).

Additionally, we measured gene expression of RFX transcription factors, some of which promote ciliogenesis by binding to X-box motifs in the regulatory regions of many ciliary genes[1,4,5]. Interestingly, two of them were significantly reduced (*Rfx5* and *Rfx7*), one was strongly upregulated (*Rfx8*) and three were unaffected (*Rfx1*, *Rfx2*, *Rfx3*) in *Nfe2l2*$^{-/-}$ MEFs (Supplementary Fig.S6a). For *Rfx4*, absence of NRF2 made no difference in immortalized MEFs, yet it upregulated expression about 100-fold in primary MEFs (Supplementary Fig.S6b). However, as interesting as these changes may be, they seem to bear little or no relationship with our observed ciliogenic and Hh defects, as will be discussed later.

In contrast, the widespread reduction in ciliogenic and Hh pathway gene expression shown in Fig.5a-b is likely to be a major cause of the ciliogenic and Hh signaling defects of *Nfe2l2*$^{-/-}$ MEFs.

**DMF does not increase basal levels of ciliogenesis and Hh responsiveness**

Since NRF2 loss in *Nfe2l2*$^{-/-}$ MEFs causes a reduction in ciliogenesis and Hh signaling, we wondered whether higher NRF2 levels would have the opposite effect, increasing ciliogenesis and Hh pathway output. To test this, we treated *Nfe2l2*$^{+/+}$ MEFs (and *Nfe2l2*$^{-/-}$ MEFs as a negative control) with DMF, which raises NRF2 protein levels (Fig.1c)[20]. DMF treatment did not significantly increase ciliogenesis in either *Nfe2l2*$^{+/+}$ or *Nfe2l2*$^{-/-}$ MEFs, nor did it affect ciliary length (Supplementary Fig.S7a-b). Likewise, Hh responsiveness was not enhanced by DMF (Supplementary Fig.S7c). Thus, it appears that

basal NRF2 levels are not limiting for ciliogenesis or Hh signaling in MEFs, at least under our study conditions.

**DMF stimulates ciliogenic gene expression**

Even though DMF did not enhance ciliogenesis or Hh signaling, its upregulation of NRF2 protein levels might still cause an increase in NRF2-dependent gene expression. We therefore tested if DMF affects expression of some of the ciliogenic and Hh pathway genes from Fig.S5. Interestingly, DMF caused a significant increase in *Dync2h1* and *Ift88* mRNA levels in *Nfe2l2*$^{+/+}$ but not *Nfe2l2*$^{-/-}$ MEFs, indicating that the effect depends on NRF2 (Supplementary Fig.S8a). As for Hh pathway genes, we checked mRNA levels of *Smo*, *Gli2* and *Gli3*. Although we did not see any significant DMF-induced increase for any of these genes in control or NRF2-null MEFs, in the former there was a consistent upward trend, which might merit further study (Supplementary Fig.S8b). Altogether, these experiments suggest that NRF2 levels in control cells may be limiting for the expression of some genes but not for others.

**Identification of putative AREs in ciliogenic and Hh pathway genes**

Given the effects of NRF2 upon ciliogenic and Hh pathway gene expression, we reasoned that some of these genes might be direct targets of NRF2. If so, they should contain ARE sequences in their regulatory regions. To assess this possibility, we analyzed the promoter regions of all ciliogenic and Hh pathway genes whose expression we found reduced in NRF2-null cells. Promoter sequences of the human genes were compared with consensus ARE sequences from the JASPAR database, as previously described[22].

Remarkably, many of these genes contain putative ARE sequences with high scores relative to the consensus (Fig.5c). In particular, two genes (*GLI2* and *GLI3*) contain putative AREs with relative scores higher than 0.99, indicating a virtually perfect match with the consensus. Six other genes (*IFT172*, *IFT140*, *IFT88*, *GPR161*, *PTCH1*, and *IFT27*) contain putative AREs with scores above 0.9, whereas *IFT74* has one above 0.8. In contrast, no putative AREs with scores above 0.8 were found in the promoter regions of *DYNC2H1*, *GLI1*, *SUFU* and *SMO*.

Altogether, our bioinformatic analysis supports the idea that some ciliogenic and/or Hh pathway genes are direct NRF2 transcriptional targets.

**GLI2 and GLI3 ciliary localization and protein levels are reduced in NRF2-null cells**

Of all the Hh pathway genes whose expression is reduced in NRF2-null cells, GLI2 and GLI3 are potentially the most significant, as they act downstream of all others, directly controlling Hh target gene expression[7]. We therefore looked at GLI2 and GLI3 proteins in *Nfe2l2*$^{-/-}$ MEFs. Both GLI2 and GLI3 are known to accumulate at the ciliary tip upon Hh pathway activation[7,43]. This accumulation is important for GLI2 to be processed into the transcriptionally active GLI2A, and for GLI3 to stop being processed into a repressor, GLI3R, and undergo full proteasomal degradation instead[7,44-46]. Thus, failure of GLI2 and/or GLI3 to accumulate at the ciliary tip might well explain the low Hh responsiveness of *Nfe2l2*$^{-/-}$ MEFs. To test this hypothesis, we performed immunofluorescence for GLI2 and GLI3 in *Nfe2l2* MEFs treated with either vehicle or SAG. In *Nfe2l2*$^{+/+}$ MEFs, SAG induced a strong accumulation of both GLI2 and GLI3 at the ciliary tip. By contrast, their accumulation in SAG-treated *Nfe2l2*$^{-/-}$ MEFs was strongly and significantly reduced (Fig.6a-d).

Western blot analysis of GLI2 and GLI3 confirmed a strong reduction in the overall basal levels of these proteins, especially of their proteolytically processed lower molecular weight forms (Fig.6e-f). Moreover, *Nfe2l2*$^{-/-}$ MEFs appeared to react differently to SAG than *Nfe2l2*$^{+/+}$ MEFs. In control cells, as previously shown, SAG did not affect the pattern of GLI2 bands[47], but caused a marked reduction in GLI3 levels[48]. On the other hand, *Nfe2l2*$^{-/-}$ MEFs responded to SAG by reducing the processed forms of GLI2 while having only a modest effect on GLI3 (Fig.6e-f). Together with the immunofluorescence data, these results suggest that GLI2 and GLI3 ciliary accumulation, processing and protein levels are abnormal in NRF2-null cells.

Finally, we also carried out immunofluorescence and Western blot with IFT88 and SMO antibodies. Despite the observed lower mRNA levels in *Nfe2l2*$^{-/-}$ MEFs relative to control (Fig.5a-b), we saw no such differences in either ciliary IFT88 intensity (Supplementary Fig.S9a-b), ciliary SMO intensity with or without SAG (Supplementary Fig.S9c-d), or total levels of these proteins as seen by Western blot in presence or absence of DMF (Supplementary Fig.S9e). This might reflect compensatory mechanisms that maintain protein homeostasis despite altered mRNA levels.

## DISCUSSION

In pluripotent hESCs, cell fate choice between mesendoderm and ectoderm lineages depends on the PAN axis, whereby early emergence of cilia in some cells stimulates autophagy, thereby downregulating NRF2 activity and committing those cells to neuroectoderm[12]. Here, we have shown data suggesting that the PAN axis is also at work in more differentiated cell types, including fibroblasts. In support of this, NRF2 transcriptional activity is higher in cells unable to grow cilia (Fig.1a-c), whose autophagic flux is reduced (Fig.1g). Moreover, mTOR inhibitors, which raise autophagic flux in cilia-null cells (Fig.1g), fully rescue the abnormal NRF2 activity of these cells (Fig.1e-f).

If the PAN axis is not restricted to hESCs, then what is its biological role beyond early embryogenesis? In stem cells, it may control cell fate choices in a similar way to what it does in hESCs, except that the relevant NRF2 target genes would differ in each case (in hESCs it promotes expression of pluripotency genes OCT4 and NANOG, which are epigenetically silenced in more differentiated cells[12]).

In terminally differentiated cells, the PAN axis might convey information about ciliary integrity or stress. Since genetic deletion of cilia reduces autophagy and raises NRF2 activity, something similar might occur by accidental or stress-induced cilia ablation or damage. If so, this would trigger NRF2-dependent cytoprotective responses, which might include cilia regeneration, consistent with our data that NRF2 promotes ciliogenic gene expression. Consistent with this, NRF2 plays a protective role in cigarette smoke-induced harm to airway cilia[23]. Also, flow sensation in renal mechanosensory cilia represses mTOR to promote autophagy and reduce cell size[13,15]. Thus, it would be interesting to test whether mechanical stress in renal cilia also modulates NRF2 activity. If so, this could have important implications, as disruption of this ciliary pathway causes polycystic kidney disease (PKD), the most common ciliopathy[19]. The fact that NRF2 dysregulation is involved in kidney cystogenesis in a mouse cancer model supports a potential connection between NRF2 and PKD[49].

Mechanistically, many questions remain concerning how the PAN axis works. Our data indicate that GLI-dependent Hh signaling is not involved (Supplementary Fig.S2), but how cilia control autophagy and NRF2 remains poorly understood. For instance, our evidence shows cilia downregulate NRF2 activity but not its protein levels (Fig.1d,h). Since NRF2 is often regulated through protein stability[50], this raises the question of how cilia affect NRF2 in MEFs, and whether this mechanism also applies to hESCs, where NRF2 protein levels were not assessed[12].

We have also found that NRF2-null cells grow fewer and shorter cilia than normal (Fig.2), and display poor Hh signaling, a cilia-dependent pathway (Fig.3). We investigated several possible causes for these effects. Hh responsiveness in *Nfe2l2*$^{-/-}$ MEFs was not improved by NAC, which acts in oxidatively stressed cells by replenishing their levels of glutathione, a major cellular antioxidant and ROS scavenger (Fig.4)[40]. This largely rules out oxidative stress as a significant cause of Hh signaling defects in our model. And since Hh defects arise, at least partly, from ciliogenic defects, the lack of Hh signaling rescue by NAC also suggests, indirectly, that oxidative stress does not explain reduced ciliation in *Nfe2l2*$^{-/-}$ MEFs. Tubastatin A, an HDAC6 inhibitor, also failed to even partially rescue Hh signaling (Fig.4). Thus, ciliophagy, the HDAC6-dependent autophagic resorption of cilia, does not account for the Hh defects either[23]. Likewise, lack of rescue by Torin-1 shows that mTOR is not involved in poor Hh responsiveness in *Nfe2l2*$^{-/-}$ MEFs, indicating that NRF2 affects cilia through mechanisms distinct from how cilia affect NRF2 (Fig.4). We also failed to rescue Hh signaling with H89, a PKA inhibitor

(Fig.4). Since PKA acts as a Hh pathway repressor downstream of SMO but upstream of GLI2 and GLI3, these data pointed to Hh signaling disruption downstream of SMO and PKA[7].

We then discovered that multiple ciliogenic and Hh pathway mRNAs are expressed at lower levels in *Nfe2l2*$^{-/-}$ MEFs (Fig.5a-b). These moderate but highly significant reductions in gene expression, when combined, likely account for the ciliogenic and Hh defects of *Nfe2l2*$^{-/-}$ cells.

The evidence for this is particularly strong for the Hh pathway. GLI2 and GLI3 transcription factors are the main controllers of Hh target gene expression (as GLI1 is a Hh target gene whose expression is almost negligible before pathway stimulation)[7]. Hh pathway stimulation alters the transcriptional activities of GLI2 and GLI3, turning the former into an activator (GLI2A) and preventing the latter from turning into a repressor (GLI3R), its fate under basal conditions[7]. For these changes to occur, GLI2 and GLI3 need to accumulate at the ciliary tip, but this accumulation is strongly reduced in *Nfe2l2*$^{-/-}$ MEFs (Fig.6a-d)[7,44-46]. In addition, GLI2 and GLI3 protein levels are strongly reduced in these mutants (Fig.6e-f), as are their mRNAs (Fig.5b). These changes in GLI2 and GLI3 can readily explain the observed Hh defects. And since GLI2 and GLI3 act downstream from SMO, GPR161, IFT27 and SUFU in the Hh pathway[7], the lower mRNA expression observed for the latter genes is likely to be of little consequence in terms of Hh pathway output (Fig.5b). In fact, despite the lower mRNA levels in *Nfe2l2*$^{-/-}$ MEFs, SMO protein levels and SAG-induced cilia translocation appear unaffected in these cells (Supplementary Fig.S9c-e).

Regarding ciliogenesis, it is less clear which genes and their products are responsible for the observed defects. In principle, each of the genes studied in Fig.5a might account for these defects, as they are all important in the process. Moreover, since our analysis was far from exhaustive, many other ciliogenic genes might be affected in NRF2-null cells. Since IFT88 is absolutely required for ciliogenesis (Fig.1a), we tested the role of IFT88 protein in the ciliogenic defects of *Nfe2l2*$^{-/-}$ MEFs. Intriguingly, neither total nor ciliary IFT88 protein levels were visibly affected in mutant relative to control MEFs (Supplementary Fig.S9a-b). This might indicate that compensatory mechanisms operate in *Nfe2l2*$^{-/-}$ MEFs to keep IFT88 and SMO protein levels constant, despite lowered mRNA levels.

Some RFX transcription factors promote ciliogenesis by stimulating expression of ciliogenic genes such as the ones in Fig.5a, so a reduction in one or more pro-ciliogenic RFX factors could neatly explain why NRF2-null MEFs grow fewer and shorter cilia. RFX1-4 are well established pro-ciliogenic factors[4], but none of them was reduced in *Nfe2l2*$^{-/-}$ MEFs. Instead, we found reductions in *Rfx5* and *Rfx7* (Supplementary Fig.S6). RFX5 and RFX7 constitute a distinct RFX subfamily and both play important roles in immunity[4,5,51], yet only RFX7 has recently been linked to ciliogenesis in the neural tube[52]. Whether RFX7 contributes to the ciliogenic phenotype of NRF2-null cells remains unaddressed.

Unlike *Rfx5* and *Rfx7*, we found elevated levels of *Rfx4* and *Rfx8* in NRF2-null MEFs. This, however, cannot explain the ciliogenic defects, which were seen in both primary and immortalized *Nfe2l2*$^{-/-}$ MEFs (Fig.2a-c and Supplementary Fig.S3), whereas *Rfx4* upregulation only occurred in the former (Supplementary Fig.S6b). Additionally, higher RFX4 levels would be expected to upregulate ciliogenic genes, not reduce them. Virtually nothing is known about RFX8, except that it belongs to the same RFX subfamily as RFX4 [4,5].

Since NRF2 stimulates its target genes by binding to ARE sequences in their promoters, we performed a bioinformatic search for putative ARE sequences in the human promoters of the ciliogenic and Hh pathway genes whose expression we found reduced in *Nfe2l2*$^{-/-}$ MEFs (Fig.5c). Remarkably, the top two hits from this analysis were *GLI2* and *GLI3*, whose promoters each contain a perfect match with the consensus ARE sequence (relative score = 0.997). Together with the data presented above, this suggests that *GLI2* and *GLI3* may be direct NRF2 targets, although this awaits experimental demonstration. Putative ARE sequences with relative scores in the 0.81-0.98 range were also found in *IFT172*, *IFT140*, *IFT88*, *IFT74*, *GPR161*, *PTCH1* and *IFT27*. Consistent with these data, *Ift74*, *Ift27* and *Gpr161*

promoter sequences were pulled down with NRF2 in a ChIP-seq study in sulforaphane-treated cells[53]. The presence of putative AREs in *PTCH1* (but not *GLI1*) promoter raises the possibility that NRF2 directly upregulates Hh targets. If so, we would expect lower basal *PTCH1* levels in unstimulated NRF2-null MEFs, which we did not detect. However, since basal *PTCH1* levels are very low, detecting such a reduction, if it exists, could be very challenging. Using cells with higher basal *PTCH1* levels could clarify this issue.

Since genetic deletion of NRF2 reduces ciliogenic and Hh pathway gene expression, we also tested whether NRF2 stabilization by DMF had the opposite effect. Interestingly, ciliogenic genes *Dync2h1* and *Ift88* were both significantly upregulated in DMF-treated *Nfe2l2*$^{+/+}$ but not *Nfe2l2*$^{-/-}$ MEFs (Supplementary Fig.S8a). This confirms that these genes are positively regulated by NRF2. In these experiments, we also tested expression of *Gli2*, *Gli3* and *Smo*. Although the data pointed in the same direction, DMF did not cause any statistically significant changes in the expression of these genes (Supplementary Fig.S8b). Likewise, DMF did not increase ciliogenesis or Hh responsiveness above basal levels, indicating that NRF2 levels in these cells are not limiting for these processes (Supplementary Fig.S7).

Beyond the mechanistic details, our work raises an important question: what is the biological significance of NRF2 affecting ciliogenesis and Hh signaling? Severe ciliogenesis and Hh signaling disruptions in mouse embryos lead to embryonic lethality and malformations[7,54]. In contrast, *Nfe2l2*$^{-/-}$ mice are viable, have no malformations, and do fairly well unless exposed to stress[31,55]. Hence, cilia and Hh signaling cannot be severely perturbed in *Nfe2l2*$^{-/-}$ mouse embryos. Together with our data, this suggests that NRF2 affects ciliogenesis and Hh signaling in a manner dependent on cell type, tissue and developmental stage. Comprehensive spatiotemporal studies can shed light on this issue.

Our data so far show that NRF2 affects ciliogenesis in both embryonic fibroblasts and hippocampal astrocytes, so one might expect NRF2-null mice to have cilia or Hh-dependent phenotypes related to these cell types. In this regard, we have recently reported defects in hippocampal neurogenesis in NRF2-null mice, a process where cilia and Hh signaling also play important roles[32,56-58]. Thus, neurogenesis defects in the NRF2-null hippocampus may well be related to defective ciliation. If so, this might involve astrocyte cilia, but maybe also neuronal cilia, which are not labeled by ARL13B and thus were not visualized in our study[37,38].

The reasons why NRF2 affects ciliogenesis in some cell types more than others remain a mystery. Cell type-specific compensatory mechanisms may exist, which could act at many levels, such as gene expression, protein stability or enzyme activity, to name a few. Redundancy is another possibility: NFE2L1/NRF1, an NRF2-related transcription factor, acts redundantly with NRF2 during mouse development[59]. Thus, our data might be explained by NRF1 compensating for NRF2 loss in some cell types but not others. If so, one would expect *Nfe2l1-Nfe2l2* double knockout mice to display cilia and Hh-related phenotypes. These embryos are delayed, show signs of massive oxidative stress and apoptosis, and die at midgestation, too early to assess for all but the most drastic defects in cilia and Hh signaling[1,7,59]. On the other hand, NRF1 is expressed ubiquitously, and *Nfe2l1-Nfe2l2* double mutant MEFs show markedly higher apoptosis and stress sensitivity than *Nfe2l2*$^{-/-}$ MEFs, demonstrating that NRF1 is present and functional in the latter[59,60]. Therefore, cilia and Hh defects in *Nfe2l2*$^{-/-}$ MEFs are unlikely to be explained by lack of NRF1 function in these cells. Still, factors other than NRF1 might act redundantly with NRF2.

Another possible *in vivo* meaning of the NRF2-Hh connection is that Hh signaling participates in NRF2-dependent cytoprotective responses. Since NRF2 promotes Hh signaling, stress-induced NRF2 stabilization might enhance Hh signaling, which might protect cells from damage in some way. Although Hh signaling stimulation by oxidative stress and cytoprotective effects of Hh signaling are both reported in the literature[61-66], our data showed no enhancement of Hh responsiveness by DMF, as mentioned above (Supplementary Fig.S7c). This, however, does not rule out that Hh responses play

cytoprotective roles *in vivo*, particularly in cell types where basal NRF2 protein levels are low relative to what cells need for optimal Hh responsiveness.

Here, we have established a clear connection between NRF2, expression of ciliogenic and Hh pathway genes, and the processes controlled by these genes. The physiopathological contexts where changes in NRF2 activity affect cilia and Hh signaling remain to be elucidated.

## METHODS

### Reagents, plasmids and antibodies

*Reagents*: Torin-1 (ApexBio, 250nM), Rapamycin (Fisher Bioreagents, 200nM), dimethyl fumarate (Sigma, 20µM), Chloroquine (Acros Organics, 10 µM), SAG (Cayman, 200nM), R,S-Sulforaphane (LKT Laboratories, 15µM), N-acetyl-L-cysteine (Alfa Aesar, 3mM), H89 dihydrochloride (BioVision, 10µM) and Tubastatin A (Cayman, 10µM). *Plasmids*: pcDNA3.1-mGli2ΔN and pcDNA3.1-hGLI3R were kind gifts of Drs. Victor L. Ruiz-Perez and Elisa Martí, respectively[67]. *Antibodies*: Acetylated α-Tubulin (Sigma, T7451, 1:10,000), GLI1 (Cell Signaling, L42B10, 1:1,000), GFAP (Sigma, G3893, 1:200), HMOX1 (Enzo Life Sciences, 1:2,000), SMO (Proteintech 66851-1-Ig, WB: 1:1000) GAPDH (Proteintech, 60004-1-Ig, 1:1,000), β-Actin (Proteintech, 66009-1-Ig, 1:5,000) and α-Tubulin (Proteintech, 66031-1-Ig, 1:1,000) were from mouse. GLI2 (R&D systems, AF3635, WB: 0.1µg/ml, IF: 1µg/ml), GLI3 (R&D systems, AF3690, WB: 1µg/ml, IF: 5µg/ml), Lamin B (Santa Cruz, sc-6217, 1:5,000) and γ-Tubulin (Santa Cruz, sc-7396, 1:200) were from goat. ARL13B (Proteintech, 17711-1-AP, 1:200), LC3B (Cell Signaling Technology, #2775, 1:2000), SMO (Abcam, ab38686, IF: 1:1000), IFT88 (Proteintech, 13967-1-AP, WB: 1:1000, IF: 1/100) and NRF2 (described in [21], 1:5,000) were from rabbit. Due to their initial low specificity (see Fig.3b and Supplementary Fig.S11), NRF2 antibodies were repeatedly incubated with membranes from NRF2-null cells, which led to greater specificity towards NRF2, as seen in Fig.1d, Fig.1h and Supplementary Fig.S11. Secondary antibodies were from donkey (Thermofisher, AlexaFluor 488, 555 or 647-conjugated) or from goat (Thermofisher, HRP-conjugated).

### Animals

Colonies of *Nfe2l2*$^{+/+}$ and *Nfe2l2*$^{-/-}$ C57BL/6 mice were established from funders kindly provided by Prof. Masayuki Yamamoto[68]. Animal procedures were performed according to protocols approved by the Ethical Committee for Research of the Spanish National Research Council (CSIC), in accordance with institutional, Spanish and European guidelines (*Boletín Oficial del Estado*, 18 March 1988; and European Council Directives 86/609/EEC and 2003/65/EC).

### Cell culture

*Kif3a*$^{+/+}$, *Kif3a*$^{-/-}$, *Ift88*$^{+/+}$ and *Ift88*$^{-/-}$ MEFs have been reported elsewhere[69]. *Nfe2l2*$^{+/+}$ and *Nfe2l2*$^{-/-}$ littermate MEFs were derived from E11.5 mouse embryos and immortalized with SV40 large T antigen using previously described protocols[43]. All MEFs were grown in DMEM medium supplemented with 10% fetal bovine serum at 37ºC and 5% $CO_2$ in a humidified atmosphere. All cell lines were mycoplasma-free, as ascertained by regular tests. To induce ciliogenesis and for drug treatments, MEFs were starved for 24 hours in OptiMEM medium (Thermofisher). For autophagy flux analysis, cells were starved for 4 hours in Earle's Balanced Salts Solution (EBSS, Sigma).

### RT-qPCR

Total cellular RNA was extracted using GeneJET RNA purification kit (Thermofisher) and reverse transcribed with MMLV Reverse Transcriptase (Promega) using oligo-$dT_{18}$. Quantitative real time PCR was performed using PowerUp SYBR Green Master Mix (Thermofisher) and the primer pairs listed in Supplementary Fig.S10. Reactions were run on an Applied Biosystems StepOne Real Time PCR System and data analyzed using $\Delta\Delta C_t$ method with β-Actin as control gene.

**Western blot and quantitation**

Total cell lysates were prepared in buffer containing 50mM Tris-HCl pH 7.5, 150mM NaCl, 1% IGEPAL CA-630 and protease inhibitor cocktail (Thermofisher). Lysates were centrifuged at 20,000 x g for 10 min at 4ºC to obtain postnuclear supernatants, whose protein concentrations were equalized after measuring them with Pierce BCA Protein Assay kit. Samples were then processed for SDS-PAGE, run in 4-20% Novex Tris-Glycine gels (Thermofisher) and transferred to nitrocellulose membranes for immunostaining. Results were visualized using ECL chemiluminescence reagents and captured on either X-ray film or using an MF-ChemiBIS 3.2 system (DNR Bio-Imaging Systems). Images were then cropped and their brightness and contrast adjusted using Adobe Photoshop. Uncropped and unadjusted images are shown in Supplementary Fig. S11. For band quantitation, Fiji (Image J) software was used. Briefly, 8-bit grayscale images of blots were inverted and average pixel intensity measured for all bands of interest and their corresponding backgrounds. Total pixel intensity of each band was then obtained by multiplying average pixel intensity by pixel number. To this value, total pixel intensity of an equally-sized background area was subtracted in order to obtain the specific band signal, which was expressed as a ratio to the control band. For autophagy flux calculation, basal LC3B-II/I ratio was subtracted from the same ratio in presence of chloroquine, and the resulting difference was normalized relative to control sample.

**Immunofluorescence and quantitation**

Cultured cells were grown on coverslips, fixed 5 min at RT in PBS with 4% paraformaldehyde, then 3 min at -20ºC in freezer-cold methanol. Cells were blocked and permeabilized in blocking solution (PBS + 0.1% Triton X100 + 2% donkey serum + 0.02% sodium azide) for 30-60 min at RT before proceeding with standard immunostaining procedures and imaging with a Nikon 90i fluorescence microscope. All cilia quantitations were performed with the aid of Fiji (Image J) software. For percent ciliation, one or more coverslips per condition were examined in each independent experiment. For each coverslip, seven representative cell fields were used to count cilia (identified by ARL13B and γ-Tubulin costaining), whose number was divided by total cells (DAPI-labeled nuclei). For length measurements, cilia were identified as above and their length measured in the ARL13B channel. For ciliary intensity measurements, unsaturated 8-bit images were used. Total signal in the region of interest (ciliary tip region for GLI2-3 or whole cilium for IFT88 and SMO) was obtained for the relevant channel as the product of average pixel intensity and pixel number in the region. Background signal was likewise measured near each region of interest and subtracted from total signal to obtain the specific signal. For *in vivo* studies, 30 µm-thick coronal brain sections of 3-month-old mice were obtained and processed as previously described[32]. Five hippocampal sections were imaged for each mouse using a Leica TCS SP5 confocal microscope. For quantitation, Fiji was used to count cilia, identified as rod-shaped ARL13B$^+$ structures, and GFAP$^+$ astrocytes. Since ARL13B$^+$ cilia were only seen in close association with astrocytes, which is consistent with reports indicating that ARL13B is an astrocytic ciliary marker in adult brain[37,38], we plotted data as percentage of GFAP$^+$ astrocytes carrying ARL13B$^+$ cilia.

**Bioinformatics**

Putative ARE sequence identification was performed as previously described[22]. Briefly, we first identified putative AREs in the promoter regions of our genes of interest using the Encyclopedia of DNA Elements at UCSC (ENCODE) of the human genome (Feb. 2009), based on the ChIP data available for ARE-binding transcription factors BACH1 and MAFK. Subsequently, using a Python-based script, these putative AREs were compared with the position-specific scoring matrix (PSSM) derived from the frequency matrix of the consensus ARE sequence recognized by NRF2, obtained from JASPAR database. We considered only putative AREs with a relative score higher than 80% [22].

**Statistical analysis**

GraphPad Prism 7 software was used to graph and statistically analyze data. The specific details of each experiment are provided in the corresponding figure legends.

**Data availability**

The datasets generated during the current study are available from the corresponding author on reasonable request.

**REFERENCES**


1 Reiter, J. F. & Leroux, M. R. Genes and molecular pathways underpinning ciliopathies. *Nat Rev Mol Cell Biol* **18**, 533-547, doi:10.1038/nrm.2017.60 (2017).

2 Garcia-Gonzalo, F. R. & Reiter, J. F. Scoring a backstage pass: mechanisms of ciliogenesis and ciliary access. *J Cell Biol* **197**, 697-709, doi:10.1083/jcb.201111146 (2012).

3 Wang, L. & Dynlacht, B. D. The regulation of cilium assembly and disassembly in development and disease. *Development* **145**, doi:10.1242/dev.151407 (2018).

4 Choksi, S. P., Lauter, G., Swoboda, P. & Roy, S. Switching on cilia: transcriptional networks regulating ciliogenesis. *Development* **141**, 1427-1441, doi:10.1242/dev.074666 (2014).

5 Sugiaman-Trapman, D. *et al.* Characterization of the human RFX transcription factor family by regulatory and target gene analysis. *BMC Genomics* **19**, 181, doi:10.1186/s12864-018-4564-6 (2018).

6 Marszalek, J. R., Ruiz-Lozano, P., Roberts, E., Chien, K. R. & Goldstein, L. S. Situs inversus and embryonic ciliary morphogenesis defects in mouse mutants lacking the KIF3A subunit of kinesin-II. *Proc Natl Acad Sci U S A* **96**, 5043-5048 (1999).

7 Bangs, F. & Anderson, K. V. Primary Cilia and Mammalian Hedgehog Signaling. *Cold Spring Harb Perspect Biol* **9**, doi:10.1101/cshperspect.a028175 (2017).

8 Eguether, T. & Hahne, M. Mixed signals from the cell's antennae: primary cilia in cancer. *EMBO Rep* **19**, doi:10.15252/embr.201846589 (2018).

9 Hu, L., Wang, B. & Zhang, Y. Serotonin 5-HT6 receptors affect cognition in a mouse model of Alzheimer's disease by regulating cilia function. *Alzheimers Res Ther* **9**, 76, doi:10.1186/s13195-017-0304-4 (2017).

10 Kaliszewski, M., Knott, A. B. & Bossy-Wetzel, E. Primary cilia and autophagic dysfunction in Huntington's disease. *Cell Death Differ* **22**, 1413-1424, doi:10.1038/cdd.2015.80 (2015).

11 Armato, U., Chakravarthy, B., Pacchiana, R. & Whitfield, J. F. Alzheimer's disease: an update of the roles of receptors, astrocytes and primary cilia (review). *Int J Mol Med* **31**, 3-10, doi:10.3892/ijmm.2012.1162 (2013).

12 Jang, J. *et al.* Primary Cilium-Autophagy-Nrf2 (PAN) Axis Activation Commits Human Embryonic Stem Cells to a Neuroectoderm Fate. *Cell* **165**, 410-420, doi:10.1016/j.cell.2016.02.014 (2016).

13 Orhon, I. *et al.* Primary-cilium-dependent autophagy controls epithelial cell volume in response to fluid flow. *Nat Cell Biol* **18**, 657-667, doi:10.1038/ncb3360 (2016).

14 Pampliega, O. *et al.* Functional interaction between autophagy and ciliogenesis. *Nature* **502**, 194-200, doi:10.1038/nature12639 (2013).

15 Boehlke, C. *et al.* Primary cilia regulate mTORC1 activity and cell size through Lkb1. *Nat Cell Biol* **12**, 1115-1122, doi:10.1038/ncb2117 (2010).

16 Foerster, P. *et al.* mTORC1 signaling and primary cilia are required for brain ventricle morphogenesis. *Development* **144**, 201-210, doi:10.1242/dev.138271 (2017).

17 Struchtrup, A., Wiegering, A., Stork, B., Ruther, U. & Gerhardt, C. The ciliary protein RPGRIP1L governs autophagy independently of its proteasome-regulating function at the ciliary base in mouse embryonic fibroblasts. *Autophagy* **14**, 567-583, doi:10.1080/15548627.2018.1429874 (2018).

18 Grantham, J. J., Geiser, J. L. & Evan, A. P. Cyst formation and growth in autosomal dominant polycystic kidney disease. *Kidney Int* **31**, 1145-1152 (1987).

19 Bergmann, C. *et al.* Polycystic kidney disease. *Nat Rev Dis Primers* **4**, 50, doi:10.1038/s41572-018-0047-y (2018).

20 Cuadrado, A. *et al.* Transcription Factor NRF2 as a Therapeutic Target for Chronic Diseases: A Systems Medicine Approach. *Pharmacol Rev* **70**, 348-383, doi:10.1124/pr.117.014753 (2018).
21 Pajares, M. *et al.* Transcription factor NFE2L2/NRF2 modulates chaperone-mediated autophagy through the regulation of LAMP2A. *Autophagy* **14**, 1310-1322, doi:10.1080/15548627.2018.1474992 (2018).
22 Pajares, M. *et al.* Transcription factor NFE2L2/NRF2 is a regulator of macroautophagy genes. *Autophagy* **12**, 1902-1916, doi:10.1080/15548627.2016.1208889 (2016).
23 Lam, H. C. *et al.* Histone deacetylase 6-mediated selective autophagy regulates COPD-associated cilia dysfunction. *J Clin Invest* **123**, 5212-5230, doi:10.1172/JCI69636 (2013).
24 Tang, Z. *et al.* Autophagy promotes primary ciliogenesis by removing OFD1 from centriolar satellites. *Nature* **502**, 254-257, doi:10.1038/nature12606 (2013).
25 Lee, J. Y. *et al.* HDAC6 controls autophagosome maturation essential for ubiquitin-selective quality-control autophagy. *EMBO J* **29**, 969-980, doi:10.1038/emboj.2009.405 (2010).
26 Pandey, U. B. *et al.* HDAC6 rescues neurodegeneration and provides an essential link between autophagy and the UPS. *Nature* **447**, 859-863, doi:10.1038/nature05853 (2007).
27 Wong, S. Y. *et al.* Primary cilia can both mediate and suppress Hedgehog pathway-dependent tumorigenesis. *Nat Med* **15**, 1055-1061, doi:10.1038/nm.2011 (2009).
28 Kim, Y. C. & Guan, K. L. mTOR: a pharmacologic target for autophagy regulation. *J Clin Invest* **125**, 25-32, doi:10.1172/JCI73939 (2015).
29 Thoreen, C. C. *et al.* An ATP-competitive mammalian target of rapamycin inhibitor reveals rapamycin-resistant functions of mTORC1. *J Biol Chem* **284**, 8023-8032, doi:10.1074/jbc.M900301200 (2009).
30 Lauth, M., Bergstrom, A., Shimokawa, T. & Toftgard, R. Inhibition of GLI-mediated transcription and tumor cell growth by small-molecule antagonists. *Proc Natl Acad Sci U S A* **104**, 8455-8460, doi:10.1073/pnas.0609699104 (2007).
31 Chan, K., Lu, R., Chang, J. C. & Kan, Y. W. NRF2, a member of the NFE2 family of transcription factors, is not essential for murine erythropoiesis, growth, and development. *Proc Natl Acad Sci U S A* **93**, 13943-13948 (1996).
32 Robledinos-Anton, N. *et al.* Transcription factor NRF2 controls the fate of neural stem cells in the subgranular zone of the hippocampus. *Redox Biol* **13**, 393-401, doi:10.1016/j.redox.2017.06.010 (2017).
33 Sterpka, A. & Chen, X. Neuronal and astrocytic primary cilia in the mature brain. *Pharmacol Res* **137**, 114-121, doi:10.1016/j.phrs.2018.10.002 (2018).
34 Chen, P. C. *et al.* Nrf2-mediated neuroprotection in the MPTP mouse model of Parkinson's disease: Critical role for the astrocyte. *Proc Natl Acad Sci U S A* **106**, 2933-2938, doi:10.1073/pnas.0813361106 (2009).
35 Gan, L., Vargas, M. R., Johnson, D. A. & Johnson, J. A. Astrocyte-specific overexpression of Nrf2 delays motor pathology and synuclein aggregation throughout the CNS in the alpha-synuclein mutant (A53T) mouse model. *J Neurosci* **32**, 17775-17787, doi:10.1523/JNEUROSCI.3049-12.2012 (2012).
36 Liddell, J. R. Are Astrocytes the Predominant Cell Type for Activation of Nrf2 in Aging and Neurodegeneration? *Antioxidants (Basel)* **6**, doi:10.3390/antiox6030065 (2017).
37 Kasahara, K., Miyoshi, K., Murakami, S., Miyazaki, I. & Asanuma, M. Visualization of astrocytic primary cilia in the mouse brain by immunofluorescent analysis using the cilia marker Arl13b. *Acta Med Okayama* **68**, 317-322, doi:10.18926/AMO/53020 (2014).
38 Sipos, E., Komoly, S. & Acs, P. Quantitative Comparison of Primary Cilia Marker Expression and Length in the Mouse Brain. *J Mol Neurosci* **64**, 397-409, doi:10.1007/s12031-018-1036-z (2018).
39 Chen, J. K., Taipale, J., Young, K. E., Maiti, T. & Beachy, P. A. Small molecule modulation of Smoothened activity. *Proc Natl Acad Sci U S A* **99**, 14071-14076, doi:10.1073/pnas.182542899 (2002).
40 Rushworth, G. F. & Megson, I. L. Existing and potential therapeutic uses for N-acetylcysteine: the need for conversion to intracellular glutathione for antioxidant benefits. *Pharmacol Ther* **141**, 150-159, doi:10.1016/j.pharmthera.2013.09.006 (2014).

41 Butler, K. V. *et al.* Rational design and simple chemistry yield a superior, neuroprotective HDAC6 inhibitor, tubastatin A. *J Am Chem Soc* **132**, 10842-10846, doi:10.1021/ja102758v (2010).
42 Chijiwa, T. *et al.* Inhibition of forskolin-induced neurite outgrowth and protein phosphorylation by a newly synthesized selective inhibitor of cyclic AMP-dependent protein kinase, N-[2-(p-bromocinnamylamino)ethyl]-5-isoquinolinesulfonamide (H-89), of PC12D pheochromocytoma cells. *J Biol Chem* **265**, 5267-5272 (1990).
43 Garcia-Gonzalo, F. R. *et al.* Phosphoinositides Regulate Ciliary Protein Trafficking to Modulate Hedgehog Signaling. *Dev Cell* **34**, 400-409, doi:10.1016/j.devcel.2015.08.001 (2015).
44 Kim, J., Kato, M. & Beachy, P. A. Gli2 trafficking links Hedgehog-dependent activation of Smoothened in the primary cilium to transcriptional activation in the nucleus. *Proc Natl Acad Sci U S A* **106**, 21666-21671, doi:10.1073/pnas.0912180106 (2009).
45 Santos, N. & Reiter, J. F. A central region of Gli2 regulates its localization to the primary cilium and transcriptional activity. *J Cell Sci* **127**, 1500-1510, doi:10.1242/jcs.139253 (2014).
46 Tukachinsky, H., Lopez, L. V. & Salic, A. A mechanism for vertebrate Hedgehog signaling: recruitment to cilia and dissociation of SuFu-Gli protein complexes. *J Cell Biol* **191**, 415-428, doi:10.1083/jcb.201004108 (2010).
47 Li, J., Wang, C., Pan, Y., Bai, Z. & Wang, B. Increased proteolytic processing of full-length Gli2 transcription factor reduces the hedgehog pathway activity in vivo. *Dev Dyn* **240**, 766-774, doi:10.1002/dvdy.22578 (2011).
48 Wang, B., Fallon, J. F. & Beachy, P. A. Hedgehog-regulated processing of Gli3 produces an anterior/posterior repressor gradient in the developing vertebrate limb. *Cell* **100**, 423-434 (2000).
49 Adam, J. *et al.* Renal cyst formation in Fh1-deficient mice is independent of the Hif/Phd pathway: roles for fumarate in KEAP1 succination and Nrf2 signaling. *Cancer Cell* **20**, 524-537, doi:10.1016/j.ccr.2011.09.006 (2011).
50 Cuadrado, A. Structural and functional characterization of Nrf2 degradation by glycogen synthase kinase 3/beta-TrCP. *Free Radic Biol Med* **88**, 147-157, doi:10.1016/j.freeradbiomed.2015.04.029 (2015).
51 Castro, W. *et al.* The transcription factor Rfx7 limits metabolism of NK cells and promotes their maintenance and immunity. *Nat Immunol* **19**, 809-820, doi:10.1038/s41590-018-0144-9 (2018).
52 Manojlovic, Z., Earwood, R., Kato, A., Stefanovic, B. & Kato, Y. RFX7 is required for the formation of cilia in the neural tube. *Mech Dev* **132**, 28-37, doi:10.1016/j.mod.2014.02.001 (2014).
53 Chorley, B. N. *et al.* Identification of novel NRF2-regulated genes by ChIP-Seq: influence on retinoid X receptor alpha. *Nucleic Acids Res* **40**, 7416-7429, doi:10.1093/nar/gks409 (2012).
54 Garcia-Gonzalo, F. R. *et al.* A transition zone complex regulates mammalian ciliogenesis and ciliary membrane composition. *Nat Genet* **43**, 776-784, doi:10.1038/ng.891 (2011).
55 Chan, K., Han, X. D. & Kan, Y. W. An important function of Nrf2 in combating oxidative stress: detoxification of acetaminophen. *Proc Natl Acad Sci U S A* **98**, 4611-4616, doi:10.1073/pnas.081082098 (2001).
56 Amador-Arjona, A. *et al.* Primary cilia regulate proliferation of amplifying progenitors in adult hippocampus: implications for learning and memory. *J Neurosci* **31**, 9933-9944, doi:10.1523/JNEUROSCI.1062-11.2011 (2011).
57 Berbari, N. F. *et al.* Hippocampal and cortical primary cilia are required for aversive memory in mice. *PLoS One* **9**, e106576, doi:10.1371/journal.pone.0106576 (2014).
58 Rhee, S., Kirschen, G. W., Gu, Y. & Ge, S. Depletion of primary cilia from mature dentate granule cells impairs hippocampus-dependent contextual memory. *Sci Rep* **6**, 34370, doi:10.1038/srep34370 (2016).
59 Leung, L., Kwong, M., Hou, S., Lee, C. & Chan, J. Y. Deficiency of the Nrf1 and Nrf2 transcription factors results in early embryonic lethality and severe oxidative stress. *J Biol Chem* **278**, 48021-48029, doi:10.1074/jbc.M308439200 (2003).
60 Uhlen, M. *et al.* Proteomics. Tissue-based map of the human proteome. *Science* **347**, 1260419, doi:10.1126/science.1260419 (2015).

61 Das, S. *et al.* Loss of Merlin induces metabolomic adaptation that engages dependence on Hedgehog signaling. *Sci Rep* **7**, 40773, doi:10.1038/srep40773 (2017).
62 Chen, K. Y., Chiu, C. H. & Wang, L. C. Anti-apoptotic effects of Sonic hedgehog signalling through oxidative stress reduction in astrocytes co-cultured with excretory-secretory products of larval Angiostrongylus cantonensis. *Sci Rep* **7**, 41574, doi:10.1038/srep41574 (2017).
63 Dai, R. L. *et al.* Sonic hedgehog protects cortical neurons against oxidative stress. *Neurochem Res* **36**, 67-75, doi:10.1007/s11064-010-0264-6 (2011).
64 He, W. *et al.* Sonic hedgehog promotes neurite outgrowth of cortical neurons under oxidative stress: Involving of mitochondria and energy metabolism. *Exp Cell Res* **350**, 83-90, doi:10.1016/j.yexcr.2016.11.008 (2017).
65 Kaushal, J. B., Popli, P., Sankhwar, P., Shukla, V. & Dwivedi, A. Sonic hedgehog protects endometrial hyperplasial cells against oxidative stress via suppressing mitochondrial fission protein dynamin-like GTPase (Drp1). *Free Radic Biol Med* **129**, 582-599, doi:10.1016/j.freeradbiomed.2018.10.427 (2018).
66 Lin, E. H. *et al.* Hedgehog pathway maintains cell survival under stress conditions, and drives drug resistance in lung adenocarcinoma. *Oncotarget* **7**, 24179-24193, doi:10.18632/oncotarget.8253 (2016).
67 Alvarez-Medina, R., Cayuso, J., Okubo, T., Takada, S. & Marti, E. Wnt canonical pathway restricts graded Shh/Gli patterning activity through the regulation of Gli3 expression. *Development* **135**, 237-247, doi:10.1242/dev.012054 (2008).
68 Itoh, K., Mimura, J. & Yamamoto, M. Discovery of the negative regulator of Nrf2, Keap1: a historical overview. *Antioxidants & redox signaling* **13**, 1665-1678, doi:10.1089/ars.2010.3222 (2010).
69 Kodani, A., Salome Sirerol-Piquer, M., Seol, A., Garcia-Verdugo, J. M. & Reiter, J. F. Kif3a interacts with Dynactin subunit p150 Glued to organize centriole subdistal appendages. *EMBO J* **32**, 597-607, doi:10.1038/emboj.2013.3 (2013).

## ACKNOWLEDGEMENTS

We thank members of the Garcia-Gonzalo and Cuadrado labs for helpful suggestions and Drs. Victor L. Ruiz-Perez, Elisa Martí, Masayuki Yamamoto and Bruno Sainz for sharing reagents, mice or equipment. This work was supported by European Regional Development Fund (ERDF)-cofunded grants from the Spanish Ministry of Economy and Competitiveness (MINECO) to FRGG (SAF2015-66568-R and RYC2013-14887) and to AC and ILB (SAF2016-76520-R). AMH was supported by an ERDF-cofunded predoctoral contract from the Community of Madrid government. RMM, NRA and RB were supported by predoctoral grants from MINECO.

## AUTHOR CONTRIBUTIONS

ILB, AC and FRGG designed the study. AMH, RMM, NRA, RB and IPB performed the experiments. All authors contributed to analyzing the results. ILB, AC and FRGG supervised the work. FRGG wrote the manuscript with help from AC, ILB, NRA and AMH.

## ADDITIONAL INFORMATION

**Supplementary information** accompanies this paper (Supplementary Figures S1-S11).

**Competing interests:** The authors declare no competing interests.

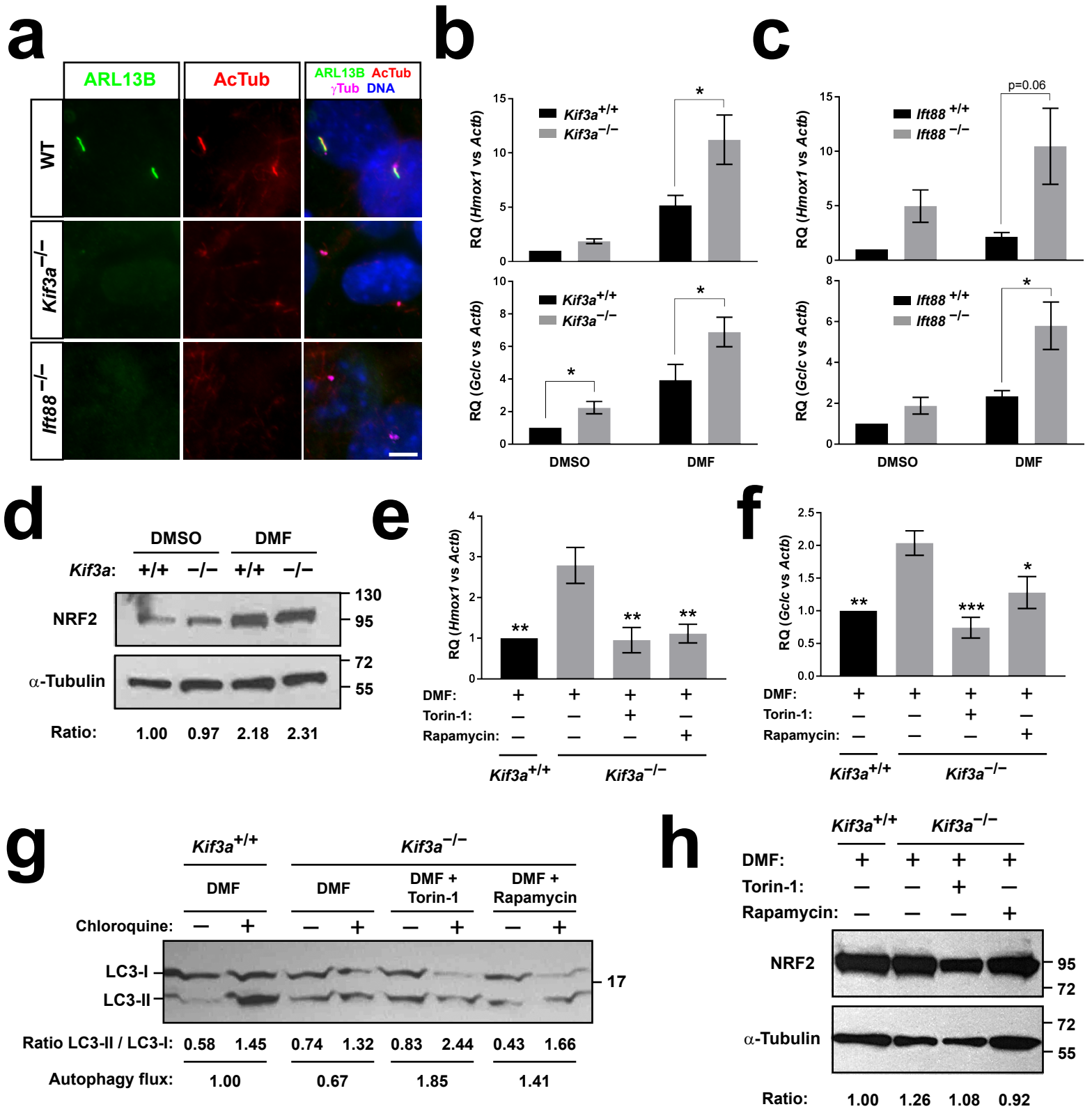


**Figure 1. Primary cilia downregulate NRF2 activity via mTOR.** (**a**) Representative immunofluorescence images of ARL13B, acetylated α-Tubulin (AcTub) and γ-Tubulin (γTub) in control (*Kif3a*$^{+/+}$, WT), *Kif3a*$^{-/-}$ and *Ift88*$^{-/-}$ MEFs starved 24h to induce ciliogenesis. Nuclei were counterstained with DAPI. Scale bar, 5μm. (**b**) Expression of NRF2 target genes *Hmox1* and *Gclc* was analyzed by RT-qPCR in *Kif3a*$^{+/+}$ and *Kif3a*$^{-/-}$ MEFs starved for 24h and then treated for 6h in starvation medium with vehicle (DMSO) or 20mM dimethyl fumarate (DMF), as indicated. Data are β-Actin (Actb)-normalized relative mRNA levels (mean ± SEM, n=4 independent experiments). (**c**) Same as in b using *Ift88*$^{+/+}$ and *Ift88*$^{-/-}$ MEFs (mean ± SEM, n=3 independent experiments). (**d**) *Kif3a* MEFs treated as in b were analyzed by Western blot with antibodies against NRF2 and α-Tubulin, as loading control. Molecular weight markers in kilodaltons are on the right. Quantitation of NRF2/Tubulin band intensity ratio is shown below. The compared bands were both in the same gel and blot. See methods for details. Uncropped blots are shown in Supplementary Fig.S11. (**e-f**) *Hmox1* and *Gclc* were analyzed as in b in *Kif3a* MEFs treated with DMF (20mM), Torin-1 (250nM) or Rapamycin (200nM), as indicated. Data shown as in b (mean ± SEM, n=6 independent experiments). (**g**) *Kif3a* MEFs were serum-starved for 24h and then incubated for 4h in Earle's balanced salt solution (EBSS) with or without 10μM Chloroquine and analyzed by Western blot with anti-LC3 antibodies. Each sample's LC3-II/LC3-I ratio is shown below, together with relative autophagy flux (LC3 ratio increase by Chloroquine, normalized to control). (**h**) *Kif3a* MEFs treated as in e-f were analyzed by Western blot and quantitated as in d. ------Statistical analysis in b-c and e-f: two-way ANOVA followed by Tukey's multiple comparisons test. Asterisks indicate p<0.05 (*), p<0.01 (**) or p<0.001 (***).

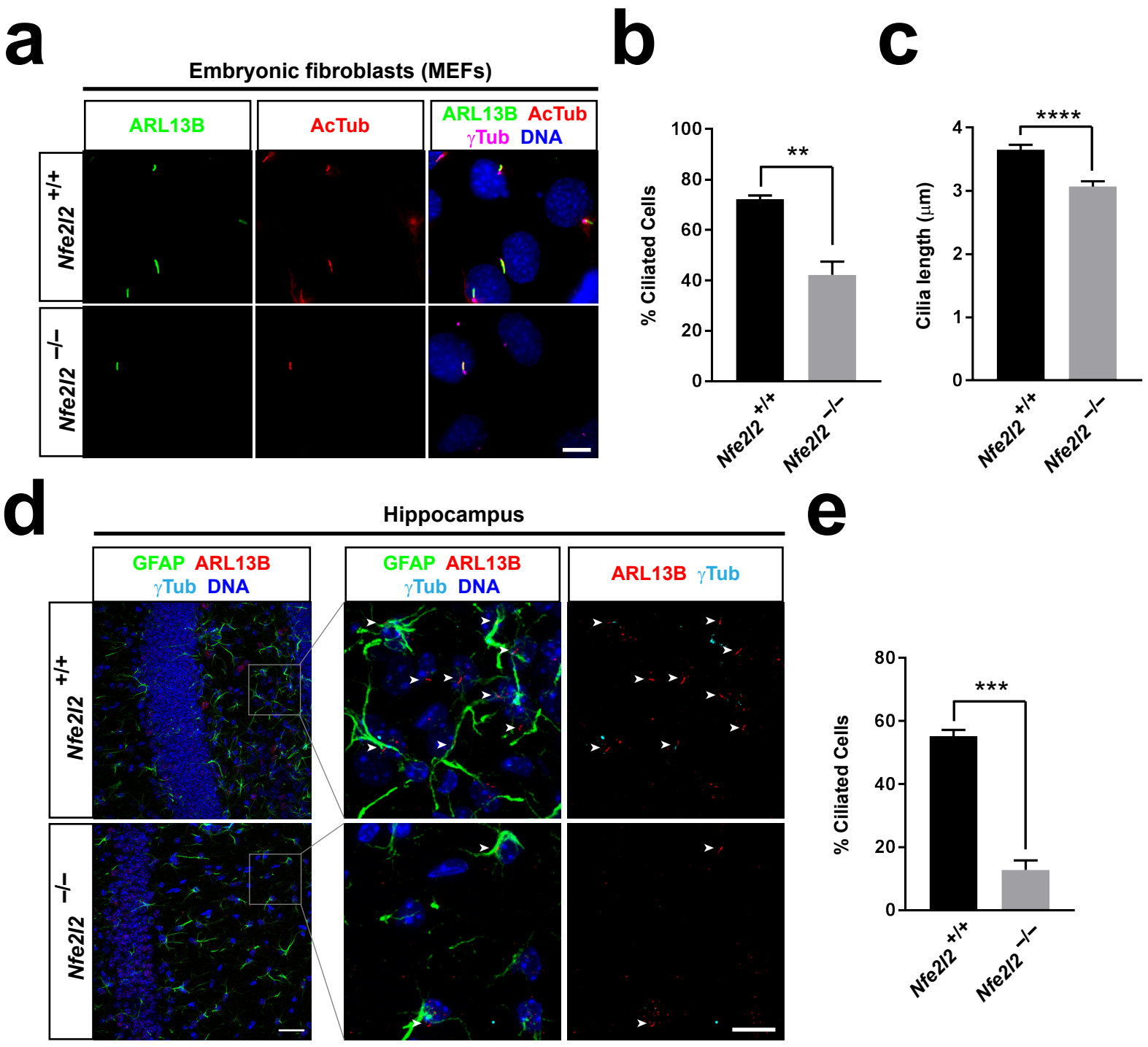


**Figure 2. Ciliogenesis is reduced in NRF2-null cells**. **(a)** Representative immunofluorescence images for ARL13B, acetylated α-tubulin (AcTub) and γ-tubulin (γTub) in *Nfe2l2*$^{+/+}$ and *Nfe2l2*$^{-/-}$ littermate MEFs starved 24h to induce ciliogenesis. Nuclei were counterstained with DAPI. Scale bar, 10μm. **(b)** Quantitation of percentage of ciliated cells in a (mean ± SEM of n=3 independent experiments). **(c)** Quantitation of cilia length in a (mean ± SEM of n=81-85 cilia measured per condition). **(d)** Representative immunofluorescence images for ARL13B, γ-tubulin and astrocyte marker GFAP in hippocampus of 3-month old *Nfe2l2*$^{+/+}$ and *Nfe2l2*$^{-/-}$ mice. Nuclei were counterstained with DAPI. Boxed region in left is magnified on the right. Arrowheads point to cilia. Scale bars, 25μm (left) and 10μm (right).**(d)** Quantitation of percentage of ciliated cells from c (mean ± SEM, n=3 mice). Asterisks in b, c and e: statistical significance in unpaired two-tailed t-tests with p<0.01(**), p<0.001 (***) or p<0.0001 (****).

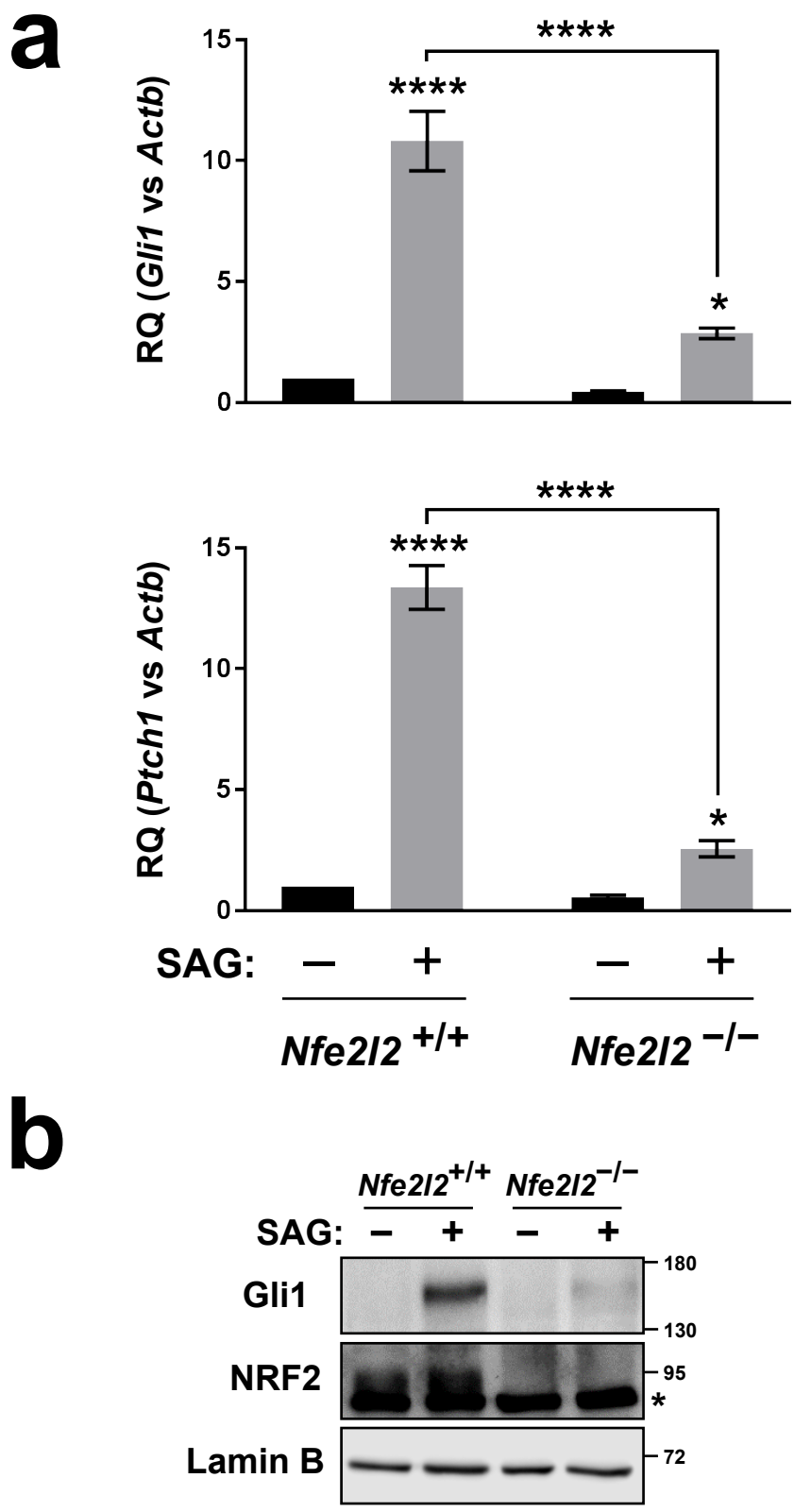


**Figure 3. Hh signaling is reduced in NRF2-null cells**. **(a)** *Nfe2l2* $^{+/+}$ and *Nfe2l2* $^{-/-}$ MEFs were starved 24h in presence of DMSO or SAG (200nM) and expression of Hh target genes *Gli1* (top) and *Ptch1* (bottom) was analyzed by RT-qPCR. Data shown as β-actin (*Actb*)-normalized relative mRNA levels (mean ± SEM, n=8-9). Statistical analysis: two-way ANOVA followed by Tukey's multiple comparisons tests. Asterisks: $p<0.05$ (*) or $p<0.0001$ (****). **(b)** *Nfe2l2* MEFs treated as in a were analyzed by Western blot with antibodies for GLI1, NRF2 and Lamin-B as loading control. Molecular weight markers in kilodaltons are shown on the right. Asterisk denotes non-specific band. Uncropped blots are shown in Supplementary Fig.S11.

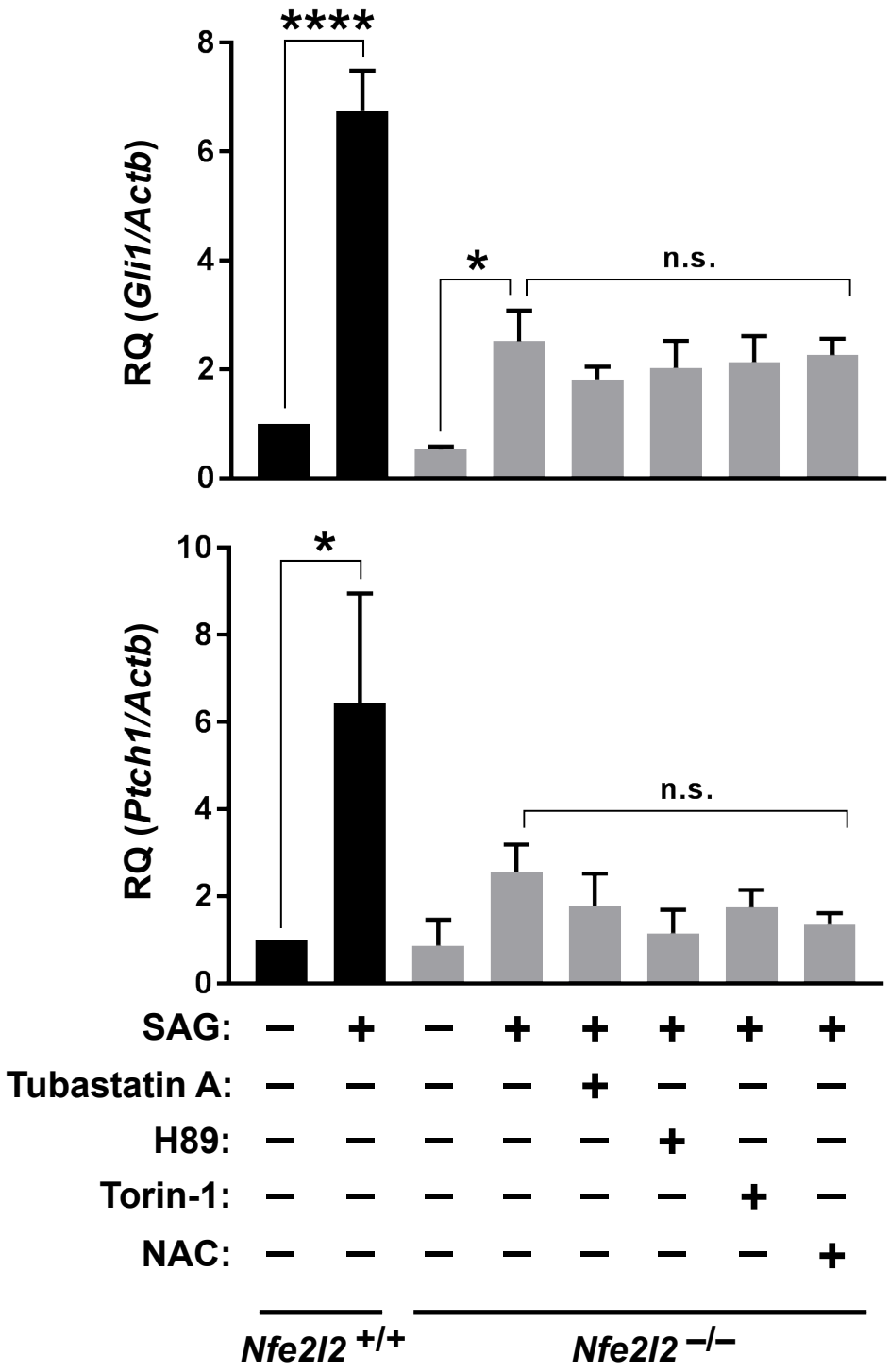


**Figure 4. Hh signaling defects in NRF2-null cells are not rescued by HDAC6, PKA, mTOR or ROS inhibitors**. *Nfe2l2* $^{+/+}$ and *Nfe2l2* $^{-/-}$ MEFs were starved 24h in presence of DMSO (vehicle), SAG (200nM), Tubastatin A (10μM), H89 (10μM), Torin-1 (250nM) or NAC (3mM), as indicated, and expression of Hh target genes *Gli1* and *Ptch1* was analyzed by RT-qPCR. Data displayed as β-actin-normalized relative mRNA levels (mean ± SEM of n=5 independent experiments). Statistical analysis: one-way ANOVA followed by Tukey's multiple comparisons tests. Significance: $p<0.05$ (*), $p<0.0001$ (****) or not significant (n.s.).

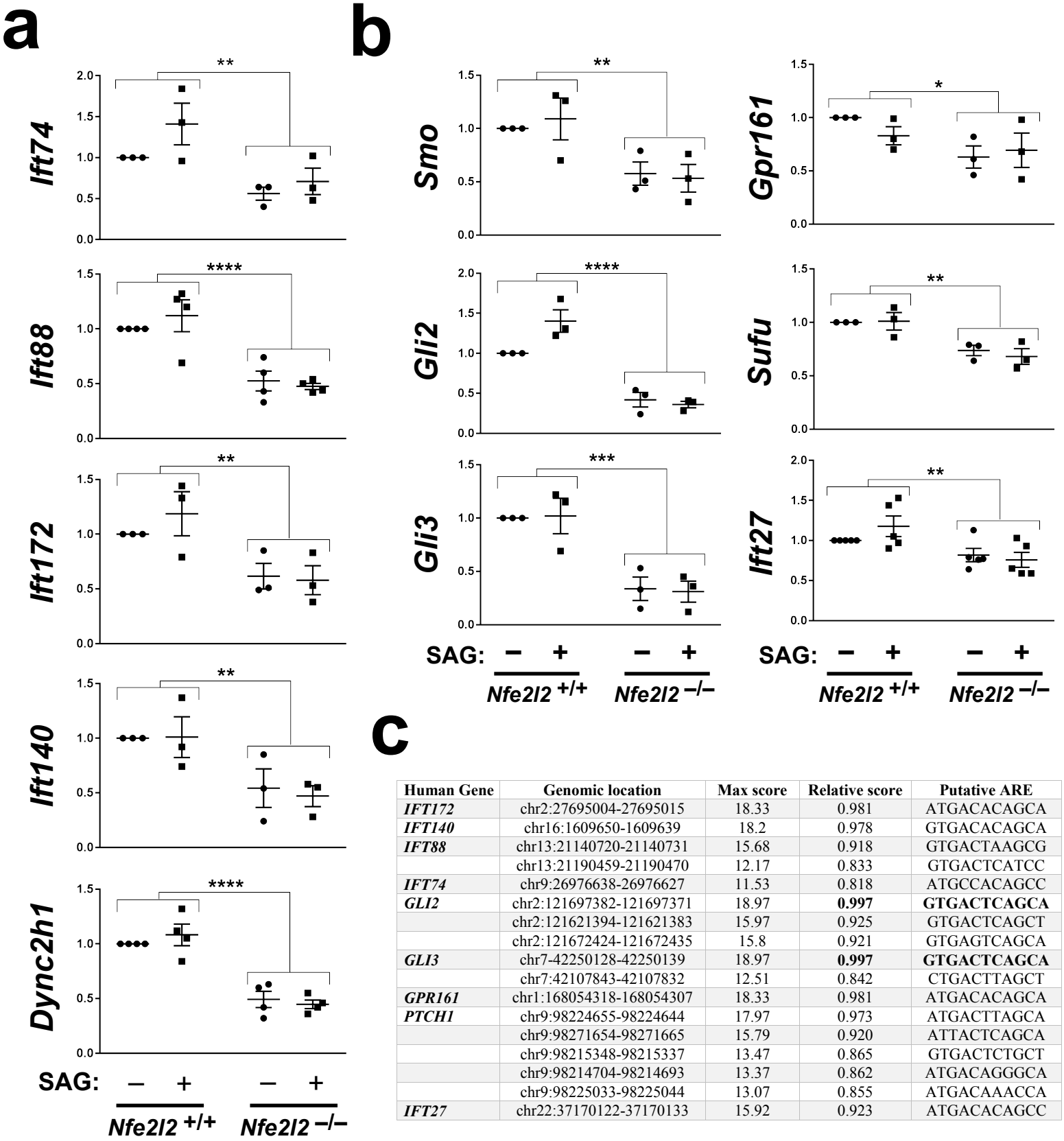


c

| Human Gene | Genomic location | Max score | Relative score | Putative ARE |
|---|---|---|---|---|
| ***IFT172*** | chr2:27695004-27695015 | 18.33 | 0.981 | ATGACACAGCA |
| ***IFT140*** | chr16:1609650-1609639 | 18.2 | 0.978 | GTGACACAGCA |
| ***IFT88*** | chr13:21140720-21140731 | 15.68 | 0.918 | GTGACTAAGCG |
| | chr13:21190459-21190470 | 12.17 | 0.833 | GTGACTCATCC |
| ***IFT74*** | chr9:26976638-26976627 | 11.53 | 0.818 | ATGCCACAGCC |
| ***GLI2*** | chr2:121697382-121697371 | 18.97 | **0.997** | **GTGACTCAGCA** |
| | chr2:121621394-121621383 | 15.97 | 0.925 | GTGACTCAGCT |
| | chr2:121672424-121672435 | 15.8 | 0.921 | GTGAGTCAGCA |
| ***GLI3*** | chr7-42250128-42250139 | 18.97 | **0.997** | **GTGACTCAGCA** |
| | chr7:42107843-42107832 | 12.51 | 0.842 | CTGACTTAGCT |
| ***GPR161*** | chr1:168054318-168054307 | 18.33 | 0.981 | ATGACACAGCA |
| ***PTCH1*** | chr9:98224655-98224644 | 17.97 | 0.973 | ATGACTTAGCA |
| | chr9:98271654-98271665 | 15.79 | 0.920 | ATTACTCAGCA |
| | chr9:98215348-98215337 | 13.47 | 0.865 | GTGACTCTGCT |
| | chr9:98214704-98214693 | 13.37 | 0.862 | ATGACAGGGCA |
| | chr9:98225033-98225044 | 13.07 | 0.855 | ATGACAAACCA |
| ***IFT27*** | chr22:37170122-37170133 | 15.92 | 0.923 | ATGACACAGCC |

**Figure 5. Ciliogenic and Hh pathway gene expression is reduced in NRF2-null cells**. **(a)** *Nfe2l2* $^{+/+}$ and *Nfe2l2* $^{-/-}$ MEFs were starved 24h in presence of DMSO or SAG (200nM) and expression of the indicated ciliogenic genes was analyzed by RT-qPCR. **(b)** Expression of the indicated Hh pathway genes was analyzed as in a. All data in a-b shown as β-actin-normalized relative mRNA levels (mean ± SEM of n=3-5 independent experiments). Statistical analysis: two-way ANOVA. Significance between genotypes: p<0.01 (**) or p<0.0001 (****). SAG treatment did not cause significant differences. **(c)** Putative ARE sequences were identified for the human ciliogenic and Hh pathway genes indicated on the left. Table shows genomic location and sequences of these putative AREs, as well as maximum and relative scores (see methods for details). Only sequences with relative score above 0.8 were considered as hits. No such hits were found for for *DYNC2H1*, *SMO*, *SUFU* or *GLI1*.

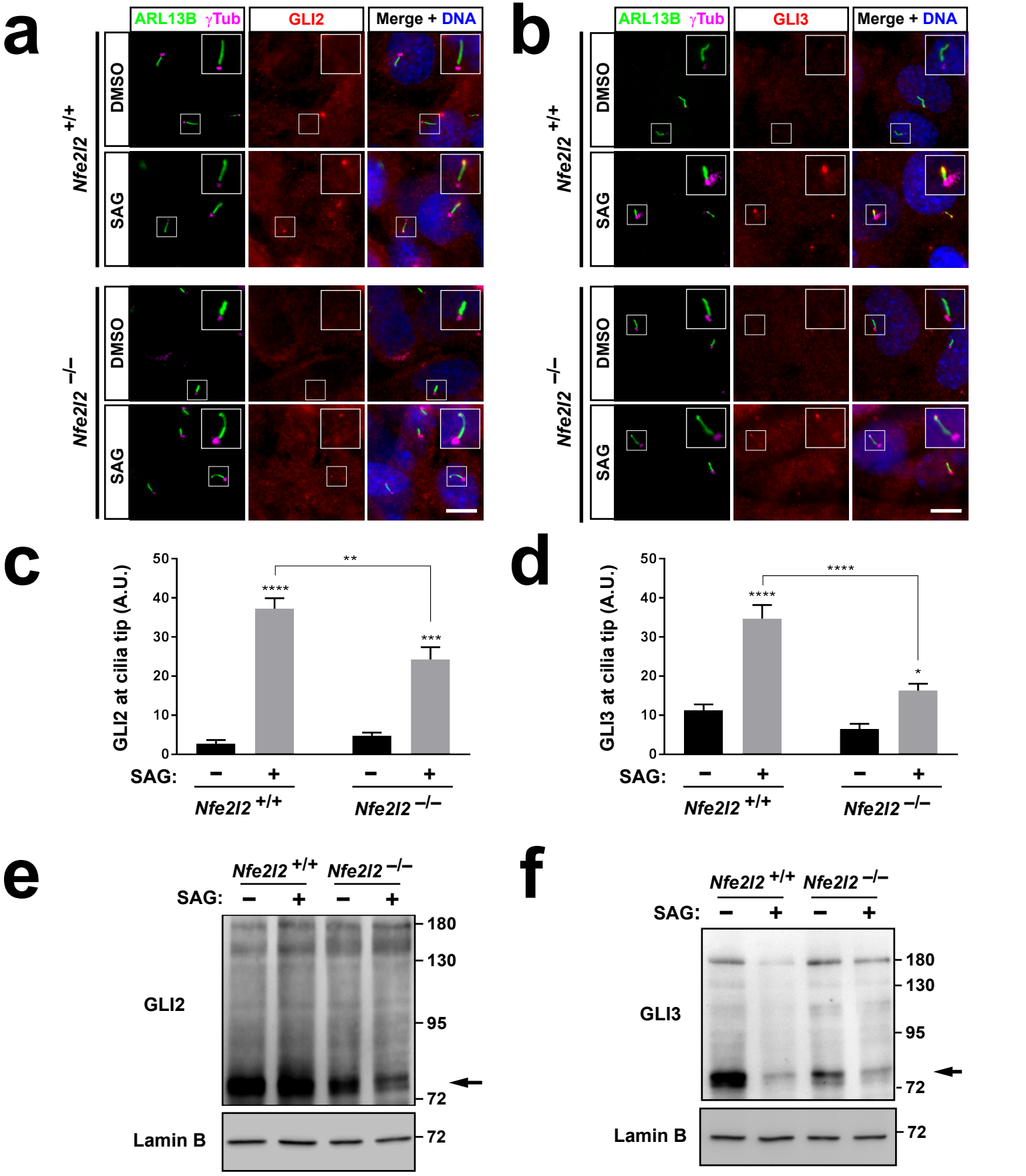


**Figure 6. GLI2 and GLI3 ciliary tip accumulation and protein levels are reduced in NRF2-null cells**. **(a-b)** Representative immunofluorescence images for ARL13B, γ-tubulin and GLI2 (a) or GLI3 (b) in *Nfe2l2*$^{+/+}$ and *Nfe2l2*$^{-/-}$ littermate MEFs starved 24h in presence of DMSO (vehicle) or SAG (200nM). Nuclei were counterstained with DAPI. Top right of each image shows magnification of boxed area. Scale bars, 10μm. **(c-d)** Quantification of GLI2 (c) or GLI3 (d) signal intensity at ciliary tip from a-b. Data are mean ± SEM of at least 40 cilia per condition (A.U.: arbitrary units). Statistical analysis: two-way ANOVA followed by Tukey's multiple comparisons tests. Asterisks: p<0.05 (*), p<0.01 (**), p<0.001 (***) or p<0.0001 (****). **(e-f)** *Nfe2l2* $^{+/+}$ and *Nfe2l2* $^{-/-}$ MEFs were treated as in a-b and analyzed by Western blot with GLI2 (e) and GLI3 (f) antibodies. Most GLI2 and GLI3 are found in their processed forms (arrows), whose levels are reduced in mutant MEFs (and by SAG treatment for GLI3, as expected). Lamin B was used as loading control. Molecular weight markers in kDa are on the right.